MICROBIAL ECOLOGY IN RESERVOIRS AND LAKES

EDITED BY: Haihan Zhang, Raju Sekar and Petra M. Visser
PUBLISHED IN: Frontiers in Microbiology

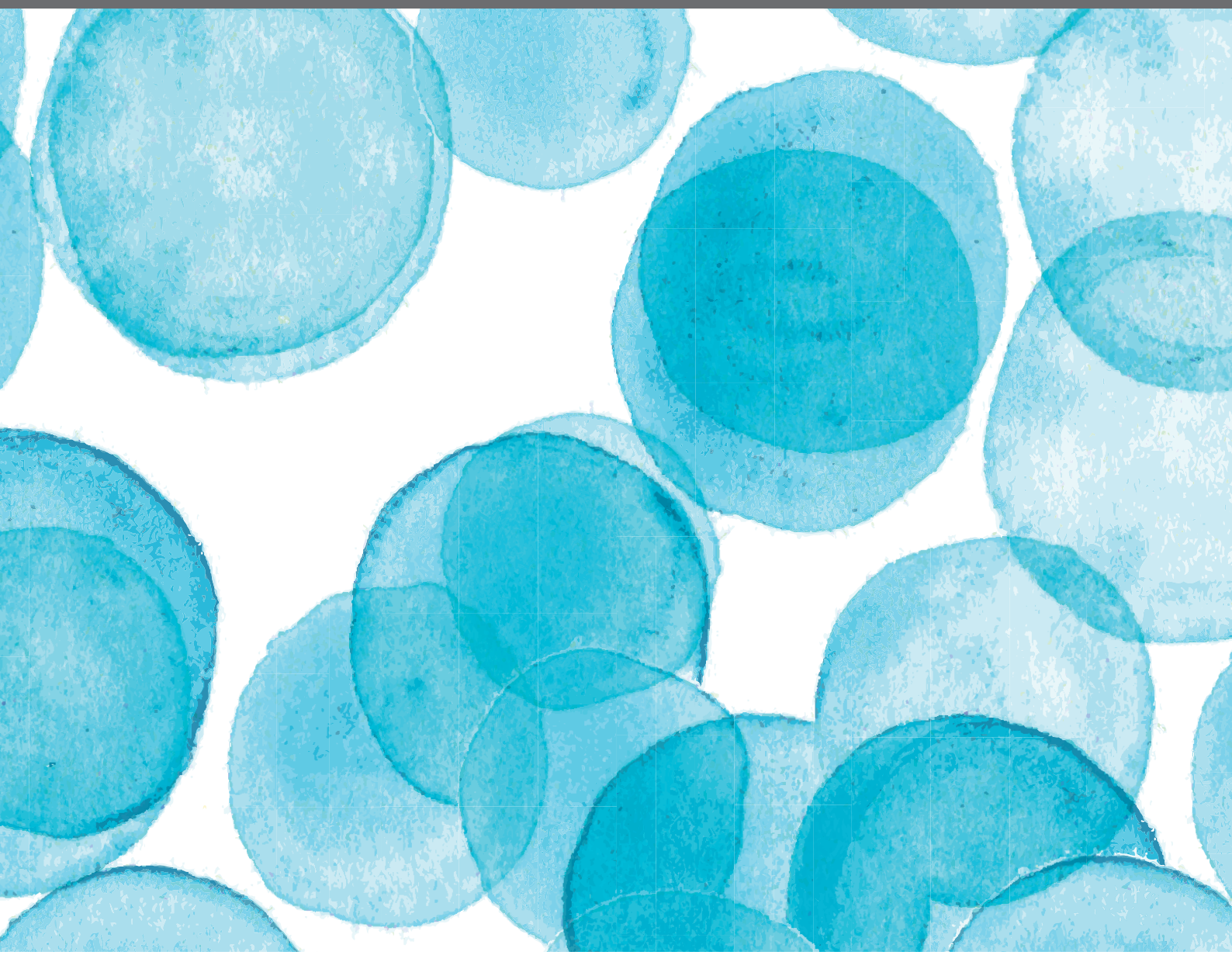

frontiers Research Topics

Frontiers eBook Copyright Statement

The copyright in the text of individual articles in this eBook is the property of their respective authors or their respective institutions or funders. The copyright in graphics and images within each article may be subject to copyright of other parties. In both cases this is subject to a license granted to Frontiers.

The compilation of articles constituting this eBook is the property of Frontiers.

Each article within this eBook, and the eBook itself, are published under the most recent version of the Creative Commons CC-BY licence. The version current at the date of publication of this eBook is CC-BY 4.0. If the CC-BY licence is updated, the licence granted by Frontiers is automatically updated to the new version.

When exercising any right under the CC-BY licence, Frontiers must be attributed as the original publisher of the article or eBook, as applicable.

Authors have the responsibility of ensuring that any graphics or other materials which are the property of others may be included in the CC-BY licence, but this should be checked before relying on the CC-BY licence to reproduce those materials. Any copyright notices relating to those materials must be complied with.

Copyright and source acknowledgement notices may not be removed and must be displayed in any copy, derivative work or partial copy which includes the elements in question.

All copyright, and all rights therein, are protected by national and international copyright laws. The above represents a summary only. For further information please read Frontiers' Conditions for Website Use and Copyright Statement, and the applicable CC-BY licence.

ISSN 1664-8714
ISBN 978-2-88963-943-4
DOI 10.3389/978-2-88963-943-4

About Frontiers

Frontiers is more than just an open-access publisher of scholarly articles: it is a pioneering approach to the world of academia, radically improving the way scholarly research is managed. The grand vision of Frontiers is a world where all people have an equal opportunity to seek, share and generate knowledge. Frontiers provides immediate and permanent online open access to all its publications, but this alone is not enough to realize our grand goals.

Frontiers Journal Series

The Frontiers Journal Series is a multi-tier and interdisciplinary set of open-access, online journals, promising a paradigm shift from the current review, selection and dissemination processes in academic publishing. All Frontiers journals are driven by researchers for researchers; therefore, they constitute a service to the scholarly community. At the same time, the Frontiers Journal Series operates on a revolutionary invention, the tiered publishing system, initially addressing specific communities of scholars, and gradually climbing up to broader public understanding, thus serving the interests of the lay society, too.

Dedication to Quality

Each Frontiers article is a landmark of the highest quality, thanks to genuinely collaborative interactions between authors and review editors, who include some of the world's best academicians. Research must be certified by peers before entering a stream of knowledge that may eventually reach the public - and shape society; therefore, Frontiers only applies the most rigorous and unbiased reviews.
Frontiers revolutionizes research publishing by freely delivering the most outstanding research, evaluated with no bias from both the academic and social point of view. By applying the most advanced information technologies, Frontiers is catapulting scholarly publishing into a new generation.

What are Frontiers Research Topics?

Frontiers Research Topics are very popular trademarks of the Frontiers Journals Series: they are collections of at least ten articles, all centered on a particular subject. With their unique mix of varied contributions from Original Research to Review Articles, Frontiers Research Topics unify the most influential researchers, the latest key findings and historical advances in a hot research area! Find out more on how to host your own Frontiers Research Topic or contribute to one as an author by contacting the Frontiers Editorial Office: researchtopics@frontiersin.org

MICROBIAL ECOLOGY IN RESERVOIRS AND LAKES

Topic Editors:
Haihan Zhang, Xi'an University of Architecture and Technology, China
Raju Sekar, Xi'an Jiaotong-Liverpool University, China
Petra M. Visser, University of Amsterdam, Netherlands

Citation: Zhang, H., Sekar, R., Visser, P. M., eds. (2020). Microbial Ecology in Reservoirs and Lakes. Lausanne: Frontiers Media SA. doi: 10.3389/978-2-88963-943-4

Table of Contents

frontiers in Microbiology

EDITORIAL
published: 26 June 2020
doi: 10.3389/fmicb.2020.01348

Editorial: Microbial Ecology in Reservoirs and Lakes

Haihan Zhang[1,2]*, *Raju Sekar*[3] and *Petra M. Visser*[4]

[1] Shaanxi Key Laboratory of Environmental Engineering, Key Laboratory of Northwest Water Resource, Environment and Ecology, Ministry of Education, Xi'an University of Architecture and Technology, Xi'an, China, [2] School of Environmental and Municipal Engineering, Xi'an University of Architecture and Technology, Xi'an, China, [3] Department of Biological Sciences, Xi'an Jiaotong-Liverpool University, Suzhou, China, [4] Department of Freshwater and Marine Ecology, Institute for Biodiversity and Ecosystem Dynamics, University of Amsterdam, Amsterdam, Netherlands

Keywords: reservoirs, lakes, surface water, sediments, DNA sequencing, CARD-FISH, ARGs, freshwater

Editorial on the Research Topic

Microbial Ecology in Reservoirs and Lakes

In freshwater ecosystems, microbes play major roles in global energy fluxes and diverse biogeochemical (C, N, P, S, and other elements) cycling pathways of deep reservoirs and shallow lakes (Liu et al., 2015, 2019; Savvichev et al., 2018). Compared to oligotrophic, stable deep ocean ecosystems, these freshwater bodies host distinct microbial communities that are associated with water and sediments (Hutchins and Fu, 2017). The aquatic microbial populations in freshwater and oceans may be largely driven by changes in the nutritional status of the water bodies due to variations in the hydrological regime and climate change (He et al., 2015; Beall et al., 2016; Hayden and Beman, 2016). Recently, thanks to the fast development of high-throughput sequencing technology (Shade et al., 2012) and bioinformatics combined with functional genomics (Berg et al., 2016), an unexpected diversity of functional microbes was unveiled in reservoirs and lakes (Preheim et al., 2016; Xue et al., 2018; Yan et al., 2020).

The Frontiers Research Topic—*Microbial Ecology in Reservoirs and Lakes*—invited contributions in the following areas: (a) Relationship between water quality parameters and microbial community composition; (b) Functional microbial communities in water and sediments; (c) Effects of hydrological regimes (e.g., thermal stratification, rainstorm, water level) on dynamics of microbial communities; and (d) Algal blooms and their interactions with other microbial communities. Finally, special emphasis was placed on modeling of ecosystem-based water quality data and microbial community composition using DNA sequencing techniques.

A total of 21 articles have been published in this Research Topic and combined in this e-book to highlight the new findings on diverse aspects and recent advances in microbial ecology (e.g., community diversity and distribution of prokaryotes and eukaryotes in various freshwater environments, quantification of microbes that are associated with blooms, antibiotic resistance, and fecal contaminations). The research reported in these articles was carried out in eutrophic, mesotrophic, and oligotrophic reservoirs and lakes located in different regions of China, Canada, Japan, Europe, and the USA. The aim of this Editorial article is to summarize the new findings reported in these articles, to broaden our understanding of the composition, diversity, abundance, dynamics, and function of microbes in freshwater ecosystems.

In this topic, Shen et al. used metagenomics workflow to reveal the relationships between the trophic status and planktonic microbiota in freshwater lakes on Yun-Gui Plateau, China. The microbial communities in the eutrophic and mesotrophic-oligotrophic lake ecosystems showed a large difference in community structure. The authors addressed that the overall differences in the genetic potential for elemental cycling and metabolic functions were closely correlated to the

OPEN ACCESS

Edited by:
Jonathan P. Zehr, University of California, Santa Cruz, United States

Reviewed by:
George S. Bullerjahn, Bowling Green State University, United States

***Correspondence:**
Haihan Zhang
zhanghaihan@xauat.edu.cn

Specialty section:
This article was submitted to Aquatic Microbiology, a section of the journal Frontiers in Microbiology

Received: *10 April 2020*
Accepted: *26 May 2020*
Published: *26 June 2020*

Citation:
Zhang H, Sekar R and Visser PM (2020) Editorial: Microbial Ecology in Reservoirs and Lakes. Front. Microbiol. 11:1348. doi: 10.3389/fmicb.2020.01348

divergence of the microbial community. Wu Y.-F. et al. employed high-throughput sequencing to investigate microbial succession during anaerobic decomposition of *Microcystis* on eutrophic sediments collected from Mei Liang Bay of Lake Taihu. The results showed that addition of *Microcystis* to the sediment induced phylogenetic clustering and structure instability of the sediment microbial community. Cruaud et al. showed that eukaryotic microbial communities had clear seasonal patterns in a Canadian river which were likely caused by the changes of environmental conditions. At the same time, a probable contribution of the bacterial community to the temporal distributions of the protist community structure was supported by potential interplays with the bacterial community composition.

The distribution of kinetoplastids in deep water layers during summer stratification was revealed using group-specific catalyzed reporter deposition and fluorescence *in situ* hybridization (CARD-FISH) probes and 18S rRNA gene sequencing by Mukherjee et al.. The results indicated that kinetoplastids were widely distributed in deep waters. Unexpectedly, the authors found the presence of diplonemids, a sister group of kinetoplastids. Colombet et al. reported the discovery of "Aster-Like Nanoparticles (ALNs)" in pelagic environments. This study shows that ALNs are novel and abundant in aquatic ecosystems and that not all virus-like particles detected in aquatic systems are necessarily viruses. Moreover, the study concluded that there may be more unknown ecologically important ultra-small particles in the aquatic systems. Cai et al. studied variations of δ^{15}NPN and δ^{15}NTDN during thermal stratification and their relationships with the environmental factors and phytoplankton in Lianhe Reservoir, China. The results revealed that δ^{15} NPN and δ^{15} NTDN changed with seasonal thermal cycling; moreover, cell density was the main factor that regulated the nitrogen stable isotope distribution. Davenport et al. undertook a meta-transcriptomic approach to reveal the temporal changes in the metabolic functions of *Microcystis* spp. During the bloom periods, the results demonstrated that there was different gene expression patterns between samples collected during the day or night. Besides, the partition of *Microcystis* gene expression depended on both circadian regulation and changes in environmental physico-chemical factors.

To better understand the spatial and seasonal variations of picophytoplankton communities in aquatic ecosystems, Shi et al. performed high-throughput sequencing to study the abundance and diversity of photosynthetic picoeukaryotes (PPEs) and phycoerythrin-rich picocyanobacteria (PE-cells) in Lake Fuxian, China. *Synechococcus* was the major PE-cell type, with a relatively similar abundance throughout the year, except for a decrease in summer. The authors showed that seasonal changes significantly influenced the composition, diversity, and abundance of PPE -cells. Jiang et al. analyzed the microbiota and their relationships with temperature changes and other environmental variables within a decadal period in five alpine lakes using 16S rRNA gene deep-amplicon sequencing. The results revealed that temperature, nutrients, and dissolved organic carbon had a significant effect on the bacterial community composition. Bomberg et al. investigated the composition and the metabolic features of the microbial communities in water bodies separated by permafrost collected in the area of Kangarlussuaq, Western Greenland. This study showed that highly diverse microbial communities existed in different cold Greenlandic aqueous environments, and showed clear patterns in the microbial communities according to habitats, with unique metabolic characteristics.

Wu K. et al. investigated the potential drivers of the relative abundance of bacterial communities and their relationship with water-depth in Lake Lugu located in Southwest China. The results showed that water depth was the most important factor that affected the relative abundance of 11 dominant bacterial species. Meanwhile, other physical, chemical, and biological variables also had a greater impact on the abundance of some bacterial species.

Fang et al. used high-throughput approaches to investigate the dynamics of antibiotic resistance genes (ARGs) in relationship with the microbial communities and environmental patterns in a subtropical urban reservoir in China by high-frequency sampling. The results indicated that the bacterial community had a seasonal pattern, while the ARGs composition did not change seasonally; moreover, the bacterial abundance and the community diversity were much more strongly correlated with environmental factors than ARGs. Palacin-Lizarbe et al. quantified guilds of four genes related to the N-transformation pathway in benthic habitats of 11 mountain lakes in Spain to reveal the effects of nitrogen deposition on microbial-driven patterns in oligotrophic freshwater ecosystems. They pointed out that those microbes of different gene types live in different water-depth layers leading to two different responses to high atmospheric N deposition in oligotrophic lakes of different trophic status.

Nakatsu et al. studied the impact of riverine microbial impact on Lake Michigan. The study assessed if Grand Calumet River was a source of bacterial contamination at different sites in Lake Michigan, and whether the feces associated bacteria in the samples were related to the pathogen indicator species *Escherichia coli*. The results showed that there were significant differences in bacterial communities at different sites, and environmental factors had a significant effect on this difference. At the same time, there was a significant positive correlation between fecal-related bacteria and pathogen-indicator organisms. Vadde et al. evaluated the most suitable microbial source tracking qPCR assays for detecting host-associated fecal pollution across the Tiaoxi River in the Taihu watershed. Their experiments indicated that several locations in the Tiaoxi River are heavily polluted by fecal contamination and this correlated well with the land-use patterns. Moreover, Xu et al. collected historical data of harmful algal blooms (HABs) events that occurred in the Bei Bu Gulf in China, and investigated the pattern of HABs in order to predict the future trends. This paper confirmed that over the past several years, HABs became progressively worse. Liu et al. evaluated the effects of different DNA extraction kits on the abundance and distribution of rare and abundant plankton taxa in the surface layers of a reservoir. Their experiment showed that the use of different DNA extraction kits had

greater impact on rare taxa than on abundant taxa. Besides, different DNA extraction kits had their own advantages when studying different microbes. Furthermore, Monchamp et al. used high-throughput sequencing approaches to study the diversity and composition of non-photosynthetic cyanobacteria (NCY) in sediment cores of 10 lakes of the European peri-Alpine region. The authors found that different lake had different NCY communities, while there was no significant change in the diversity of NCY combinations within and between lakes over the past 100 years. In seven European perialpine lakes, Okazaki et al. investigated the richness and composition of CL500-11(Phylum Chloroflexi) by means of CARD-FISH. This paper explored a wide habitat range of CL500-11 in ultra-oligotrophic lakes or mesotrophic lakes. In summary, we expect that these papers will stimulate new discussions and investigations on the microbial ecology of freshwater reservoirs and lakes. The results will improve our understanding of the molecular microbial ecological characteristics of freshwater ecosystems. From a more applied perspective, it also shows the basic database for environmental and water resource management to increase the health status of reservoirs and lakes by using some artificial strengthening technologies (e.g., water lifting aerators) to enhance the microbial community metabolic activity in drinking water reservoirs ecosystems, and supply cleaner and healthier drinking water for consumers.

AUTHOR CONTRIBUTIONS

All authors listed have made a substantial, direct and intellectual contribution to the work, and approved it for publication.

FUNDING

Research and the preparation of this manuscript were made possible by the support from the National Natural Science Foundation of China (Grant Nos. 51978561; 51979217), and the International Science and Technology Cooperation Program in Shaanxi Province (Grant No. 018KW-011). RS would like to acknowledge the Key Program Special Fund in Xi'an Jiaotong-Liverpool University (XJTLU; Grant No. KSF-E-20) and Natural Science Foundation of the Jiangsu Higher Education Institutions of China (Grant No. 13KJB180022) for financial support.

ACKNOWLEDGMENTS

We would like to thank the Editorial Office staff of Frontiers in Microbiology for their initial invitation and great support of this Research Topic. We are grateful to all reviewers for their insightful comments and valuable suggestions to these manuscripts. We are also thankful to the additional editors for handling some of the manuscripts and chief editors for making final decisions on the manuscripts.

REFERENCES

Beall, B. F. N., Twiss, M. R., Smith, D. E., Oyserman, B. O., Rozmarynowycz, M. J., Binding, C. E., et al. (2016). Ice cover extent drives phytoplankton and bacterial community structure in a large north-temperate lake: implications for a warming climate. *Environ. Microbiol.* 18, 1704–1719. doi: 10.1111/1462-2920.12819

Berg, J. S., Michellod, D., Pjevac, P., Martinez-Perez, C., Buckner, C. R. T., and Hach, P. F. (2016). Intensive cryptic microbial iron cycling in the low iron water column of the meromictic Lake Cadagno. *Environ. Microbiol.* 18, 5288–5302. doi: 10.1111/1462-2920.13587

Hayden, C. J., and Beman, J. M. (2016). Microbial diversity and community structure along a lake elevation gradient in Yosemite National Park, California, USA. *Environ. Microbiol.* 18, 1782–1791. doi: 10.1111/1462-2920.12938

He, R., Wooller, M. J., Pohlman, J. W., Tiedje, J. M., and Leigh, M. B. (2015). Methane-derived carbon flow through microbial communities in arctic lake sediments. *Environ. Microbiol.*17, 3233–3250. doi: 10.1111/1462-2920.12773

Hutchins, D. A., and Fu, F. X. (2017). Microorganisms and ocean global change. *Nat. Biotechnol.* 2, 1–11. doi: 10.1038/nmicrobiol.2017.58

Liu, L. M., Chen, H. H., Liu, M., Yang, J. R., Xiao, P., Wilkinson, D. M., et al. (2019). Response of the eukaryotic plankton community to the cyanobacterial biomass cycle over 6 years in two subtropical reservoirs. *ISME J.* 13, 2196–2208. doi: 10.1038/s41396-019-0417-9

Liu, L. M., Yang, J., Yu, Z., and Wilkinson, D. M. (2015). The biogeography of abundant and rare bacterioplankton in the lakes and reservoirs of China. *ISME J.* 9, 2068–2077. doi: 10.1038/ismej.2015.29

Preheim, S. P., Olesen, S. W., Spencer, S. J., Materna, A., Varadharajan, C., Blackburn, M., et al. (2016). Surveys, simulation and single-cell assays relate function and phylogeny in a lake ecosystem. *Nat. Biotechnol.* 1:16130. doi: 10.1038/nmicrobiol.2016.130

Savvichev, A. S., Babenko, V. V., Lunina, O. N., Letarova, M. A., Boldyreva, D. I., Veslopolova, E. F., et al. (2018). Sharp water column stratification with an extremely dense microbial population in a small meromictic lake, Trekhtzvetnoe. *Environ. Microbiol.* 20, 3784–3797. doi: 10.1111/1462-2920.14384

Shade, A., Read, J. S., Youngblut, N. D., Fierer, N., Knight, R., Kratz, T. K., et al. (2012). Lake microbial communities are resilient after a whole-ecosystem disturbance. *ISME J.* 6, 2153–2167. doi: 10.1038/ismej.2012.56

Xue, Y. Y., Chen, H. H., Yang, J. R., Liu, M., Huang, B. Q., and Yang, J. (2018). Distinct patterns and processes of abundant and rare eukaryotic plankton communities following a reservoir cyanobacterial bloom. *ISME J.* 12, 2263–2277. doi: 10.1038/s41396-018-0159-0

Yan, M. M., Chen, S. N., Huang, T. L., Li, B. Q., Li, N., Liu, K. W., et al. (2020). Community compositions of phytoplankton and eukaryotes during the mixing periods of a drinking water reservoir: dynamics and interactions. *Int. J. Environ. Res. Public Health* 17:1128. doi: 10.3390/ijerph17041128

Conflict of Interest: The authors declare that the research was conducted in the absence of any commercial or financial relationships that could be construed as a potential conflict of interest.

Copyright © 2020 Zhang, Sekar and Visser. This is an open-access article distributed under the terms of the Creative Commons Attribution License (CC BY). The use, distribution or reproduction in other forums is permitted, provided the original author(s) and the copyright owner(s) are credited and that the original publication in this journal is cited, in accordance with accepted academic practice. No use, distribution or reproduction is permitted which does not comply with these terms.

frontiers in Microbiology

ORIGINAL RESEARCH
published: 27 November 2018
doi: 10.3389/fmicb.2018.02891

The Broad Habitat Spectrum of the CL500-11 Lineage (Phylum Chloroflexi), a Dominant Bacterioplankton in Oxygenated Hypolimnia of Deep Freshwater Lakes

Yusuke Okazaki[1,2], Michaela M. Salcher[3], Cristiana Callieri[4] and Shin-ichi Nakano[1]*

[1] Center for Ecological Research, Kyoto University, Otsu, Japan, [2] Bioproduction Research Institute, National Institute of Advanced Industrial Science and Technology, Tsukuba, Japan, [3] Limnological Station, Institute of Plant and Microbial Biology, University of Zurich, Zurich, Switzerland, [4] CNR-IRSA Institute of Water Research, Microbial Ecology Group, Verbania, Italy

OPEN ACCESS

Edited by:
Raju Sekar, Xi'an Jiaotong-Liverpool University, China

Reviewed by:
Hugo Sarmento, Universidade Federal de São Carlos, Brazil
Hiroyuki Imachi, Japan Agency for Marine-Earth Science and Technology, Japan

***Correspondence:**
Yusuke Okazaki
okazaki.yusuke.e31@kyoto-u.jp

Specialty section:
This article was submitted to Aquatic Microbiology, a section of the journal Frontiers in Microbiology

Received: *08 August 2018*
Accepted: *12 November 2018*
Published: *27 November 2018*

Citation:
Okazaki Y, Salcher MM, Callieri C and Nakano S (2018) The Broad Habitat Spectrum of the CL500-11 Lineage (Phylum Chloroflexi), a Dominant Bacterioplankton in Oxygenated Hypolimnia of Deep Freshwater Lakes. Front. Microbiol. 9:2891. doi: 10.3389/fmicb.2018.02891

CL500-11 (phylum *Chloroflexi*) is one of the most ubiquitous and abundant bacterioplankton lineages in deep freshwater lakes inhabiting the oxygenated hypolimnion. While metagenomics predicted possible eco-physiological characteristics of this uncultured lineage, no consensus on their ecology has so far been reached, partly because their niche is not clearly understood due to a limited number of quantitative field observations. This study investigated the abundance and distribution of CL500-11 in seven deep perialpine lakes using catalyzed reporter deposition-fluorescence *in situ* hybridization (CARD-FISH). Samples were taken vertically (5–12 depths in each lake) and temporally (in two lakes) at the deepest point of the lakes located in Switzerland, Italy, and Austria with varying depth, trophic state, mixing regime, and water retention time. The results showed a dominance of CL500-11 in all the lakes; their proportion to total prokaryotes ranged from 4.3% (Mondsee) to 24.3% (Lake Garda) and their abundance ranged from 0.65×10^5 (Mondsee) to 1.77×10^5 (Lake Garda) cells mL^{-1}. By summarizing available information on CL500-11 occurrence to date, we demonstrated their broad habitat spectrum, ranging from ultra-oligotrophic to meso-eutrophic lakes, while low abundances or complete absence was observed in lakes with shallow depth, low pH, and/or short water retention time (<1 year). Together with available metagenomic and geochemical evidences from literatures, here we reviewed potential substrates supporting growth of CL500-11. Overall, the present study further endorsed ubiquity and quantitative significance of CL500-11 in deep freshwater systems and narrowed the focus on their physiological characteristics and ecological importance.

Keywords: bacterioplankton, CL500-11, CARD-FISH, perialpine lakes, oxygenated hypolimnion

INTRODUCTION

In thermally stratified lakes, the water layer below the thermocline is defined as hypolimnion. In deep lakes this large volume of water is generally oxygenated throughout the year due to (i) winter vertical mixing, (ii) downward intrusion of oxygenated cold water from rivers (Ambrosetti et al., 2010), and (iii) low oxygen consumption due to their oligo- to mesotrophic conditions. In those lakes, the oxygenated hypolimnion accounts for the major parts in volume, and thus, their microbial composition is of significant importance in overall biogeochemical processes.

The CL500-11 lineage (phylum *Chloroflexi,* class *Anaerolineae*) is one of the most abundant microbial groups in oxygenated hypolimnia. After its first discovery by 16S rRNA gene cloning-sequencing as a dominant bacterioplankton lineage in a deep sample (500 m) from Crater Lake (United States) (Urbach et al., 2001), their 16S rRNA gene sequences have been reported from global deep freshwater lakes (Okazaki et al., 2013). Subsequently, catalyzed reporter deposition-fluorescence *in situ* hybridization (CARD-FISH) revealed a dominance of CL500-11 in the hypolimnia of Lake Biwa (Japan, 16.5% of the total bacterioplankton in maximum) (Okazaki et al., 2013), Lake Michigan (United States, 18.1%) (Denef et al., 2016), six deep Japanese lakes (3.9–25.9% in each lake) (Okazaki et al., 2017), and Lake Zurich (Switzerland, 11%) (Mehrshad et al., 2018). Despite their high abundances in deep water layers, CL500-11 were barely detected in the epilimnia during the stratification period, indicating their specificity to the hypolimnion (Okazaki et al., 2013, 2017; Okazaki and Nakano, 2016). Cells of CL500-11 are vibrioid and relatively larger (1–2 μm length) than average prokaryotes in the water column (Okazaki et al., 2013, 2017; Denef et al., 2016; Mehrshad et al., 2018), suggesting their contribution in biomass is even higher than in abundance. Monthly profiles taken for almost 2 years in Lake Biwa revealed a recurrent annual turnover of CL500-11 population, in which their dominance was only observed during stratification and discontinued in the following winter mixing period (Okazaki et al., 2013). This dynamic population succession suggests ecological and biogeochemical significance of CL500-11 in deep lakes' ecosystems.

The proposed ubiquity and numerical dominance of CL500-11 in the deep oxygenated hypolimnion was recently challenged by CARD-FISH reports of low abundances or even complete absence in several lakes and reservoirs (Okazaki et al., 2017; Mehrshad et al., 2018). However, factors driving their distribution pattern and defining their ecological niche have not yet been clearly understood, although various environmental parameters including the lake trophic state, hypolimnetic temperature, oxygen concentration, and water retention time of the lakes, have been examined (Okazaki et al., 2017). Several metagenome-assembled genomes (MAGs) allowed insights in the eco-physiology of CL500-11, by which they were characterized as aerobic heterotrophs, harboring genes for flagellar motility and xanthorhodopsins, and potentially utilizing nitrogen-rich dissolved organic matter (DOM) and exogenous reduced sulfur compounds (Denef et al., 2016; Mehrshad et al., 2018). However, no consensus on their ecological niche has been reached so far, ultimately owing to a lack of cultivated representatives, but also because of a limited number of quantitative field observations, which is required to understand their lifestyle and interpret metagenomic implications.

The European perialpine lakes are potentially major habitats for CL500-11 since many of them are deep and oligo- to mesotrophic in general with an oxygenated hypolimnion. In fact, 16S rRNA sequences of CL500-11 have been retrieved from Lake Geneva (Humbert et al., 2009) and Lake Zurich (Van den Wyngaert et al., 2011; Mehrshad et al., 2018) which are perialpine lakes. Although CARD-FISH has been commonly employed to quantitatively investigate bacterioplankton communities in perialpine lakes (Salcher, 2013; Salcher et al., 2015; Callieri et al., 2016; Shabarova et al., 2017; Hernández-Avilés et al., 2018; Neuenschwander et al., 2018) quantification of CL500-11 was unprecedented in these lakes, until a recent report from Lake Zurich (Mehrshad et al., 2018). To fill these gaps, the present study aims to measure the abundances of CL500-11 in seven deep perialpine lakes by means of CARD-FISH. The results revealed their broad habitat spectrum and quantitative significance, and together with latest information from literatures, here we review possible eco-physiological characteristics of CL500-11.

MATERIALS AND METHODS

Collection of Water Samples and Environmental Measurements

Water samples were taken at a pelagic station in the deepest area of seven perialpine lakes with a variety of sizes, depths and trophic states (**Table 1**). Single vertical samples were collected from Lake Como (5 depths), Iseo (5 depths), Garda (5 depths), Thun (9 depths), and Mondsee (12 depths) during summer stratification, while time-series samples were taken from Lake Zurich (9 depths at biweekly) and Maggiore (4 or 5 depths at once or twice a month) to cover the whole stratification period. Samples for cell counting and CARD-FISH were fixed with 2% formaldehyde immediately after the collection and kept at 4°C in the dark until further processing. Total prokaryotic abundance was determined by enumeration of 4′,6-di-amino-2-phenylindole (DAPI) stained cells (Porter and Feig, 1980). The prokaryotic abundances in Lake Maggiore were determined in the integrated 0–20 m (epilimnetic) and 20–350 m (hypolimnetic) as described previously (Bertoni et al., 2010; Hernández-Avilés et al., 2012). Vertical profiles of water temperature, pH, and dissolved oxygen concentration were determined *in situ* with a multiparameter probe at the time of sampling. Chemical parameters of the sampled waters were determined following the standard methods by APHA and AWWA (2005) for Lake Maggiore, Como, Iseo, and Garda, and by the International Organization for Standardization (ISO 13395:1996, 11732:2005, and 15681-2:2003) for the other lakes.

CARD-FISH Analysis

CARD-FISH for CL500-11 cells was performed as described by Okazaki et al. (2013) using the same probe CLGNS-584 (5′-GCCGACTTGCCCAACCTC-3′) and helper CLGNS-567h

TABLE 1 | Limnological characteristics of the study sites.

Lake	Country	Latitude (N)	Longitude (E)	Max. depth (m)	Surface area (km^2)	Water volume ($10^6 m^3$)	Surface elevation (m)	Water retention time (y)	Trophic state	Sampling date
Zurich	Switzerland	47°15′	8°41′	136	88	4300	406	1.4	Mesotrophic	2015.1.7–2015.12.16 (Biweekly)
Maggiore	Italy/ Switzerland	45°48′	8°39′	370	213	37900	193	4.1	Oligo-mesotrophic	2011.3.8–2012.1.12 (Once or twice a month)
Como	Italy	46°00′	9°15′	410	146	22500	198	4.5	Mesotrophic	2011.7.12
Iseo	Italy	45°44′	10°04′	251	62	7600	186	4.1	Meso-eutrophic	2011.7.11
Garda	Italy	45°42′	10°43′	350	368	48900	65	26.6	Oligo-mesotrophic	2011.9.26
Thun	Switzerland	46°41′	7°43′	217	48	6500	558	1.8	Oligotrophic	2010.7.12
Mondsee	Austria	47°50′	13°20′	68	14	520	481	1.8	Mesotrophic	2016.9.14

(5′-CTACACGCCCTTTACGCC-3′) set, which have been demonstrated to produce consistent results with the 16S rRNA gene amplicon sequencing analyses (Denef et al., 2016; Okazaki et al., 2017). The specificity of the probe was reconfirmed using the TestProbe 3.0 tool[1] against the SILVA (Quast et al., 2013) SSU 132 Ref NR99 database (includes only non-redundant, high-quality, nearly full-length 16S rRNA gene sequences). The result indicated that the two CL500-11 16S rRNA gene sequences in the database (accession numbers = AF316759 and HM8566384) were exclusively targeted by the probe. Further, inspection against the SILVA SSU 132 Parc database (includes all available sequences containing relatively shorter and lesser quality ones) demonstrated that all the 60 probe-targeted sequences in the database were closely related to AF316759 or HM8566384 (identity > 97%; **Supplementary Table S1**), except one sequence (identity = 95.9%) that presumably contains erroneous bases as it is a raw output from the error-prone 454 sequencing platform (KM133681). These results collectively support the specificity of the probe CLGNS-584 in the latest 16S rRNA gene database.

The hybridization was performed at 35°C and the optimum formamide concentration in the hybridization buffer was determined as 40% by testing a series of formamide concentration (5% interval) to obtain the best stringency (that is, highest concentration without signal loss). A previous study that separately investigated the optimum formamide concentration for the same probe also supported 40% to archive the best stringency (Mehrshad et al., 2018). At least 1000 DAPI-positive cells and corresponding FISH-positive cells were counted in each sample using an automated high-throughput microscopy (Zeder and Pernthaler, 2009), which has been widely applied to quantifications of FISH-positive bacterioplankton cells in freshwater systems (Salcher et al., 2011, 2015; Shabarova et al., 2017; Neuenschwander et al., 2018). The abundance of CL500-11 were calculated by multiplying their relative proportions (determined by CARD-FISH) with the total prokaryotic abundances (determined by DAPI-counts).

[1]https://www.arb-silva.de/search/testprobe/

Data Analysis

Chemical measurements were collected from literatures for lakes where CARD-FISH on CL500-11 has been carried out previously. However, not every parameter was available in all lakes. To compare values among the lakes, the maximum and minimum of total nitrogen and phosphorus recorded in each lake were used. The relationships between CL500-11 abundance (the maximum value recorded in each lake) and limnological or chemical properties of the lakes were statistically inspected by the Spearman's rank test using the R 3.4.3 software (R Core Team, 2017). The values used for the analysis and the sources for the data are summarized in **Supplementary Table S2**.

RESULTS AND DISCUSSION

The vertical profile of temperature and dissolved oxygen indicated that the oxygenated (dissolved oxygen > 5 mg L^{-1}) hypolimnion (the water layer below the thermocline) was present in all lakes, though the deeper hypolimnion (150–251 m) was anoxic in Lake Iseo and oxygen depletion in the bottom layer was observed in Lake Zurich and Mondsee (**Figure 1**). Total prokaryotic abundances ranged from 0.2×10^6 (Lake Maggiore) to 5.2×10^6 (Mondsee) cells mL^{-1} in the epilimnia, and 0.1×10^6 (Lake Maggiore) to 3.2×10^6 (Mondsee) cells mL^{-1} in the hypolimnia of the seven lakes (**Figure 2**). The CL500-11 cells detected by CARD-FISH were of the same size and shape (vibrioid, 1–2 μm length; **Figure 3**) as previously described (Okazaki et al., 2013, 2017; Denef et al., 2016; Mehrshad et al., 2018), indicating universality of their cell morphology. High proportions of CL500-11 were observed in the oxygenated hypolimnia of all investigated lakes; the maximum value recorded in each lake was 4.3% (Mondsee), 8.8% (Como and Iseo), 16.5% (Thun), 17.8% (Zurich), 19.8% (Maggiore), and 24.3% (Garda), resulted in their calculated abundances from 0.65×10^5 (Mondsee) to 1.77×10^5 (Garda)

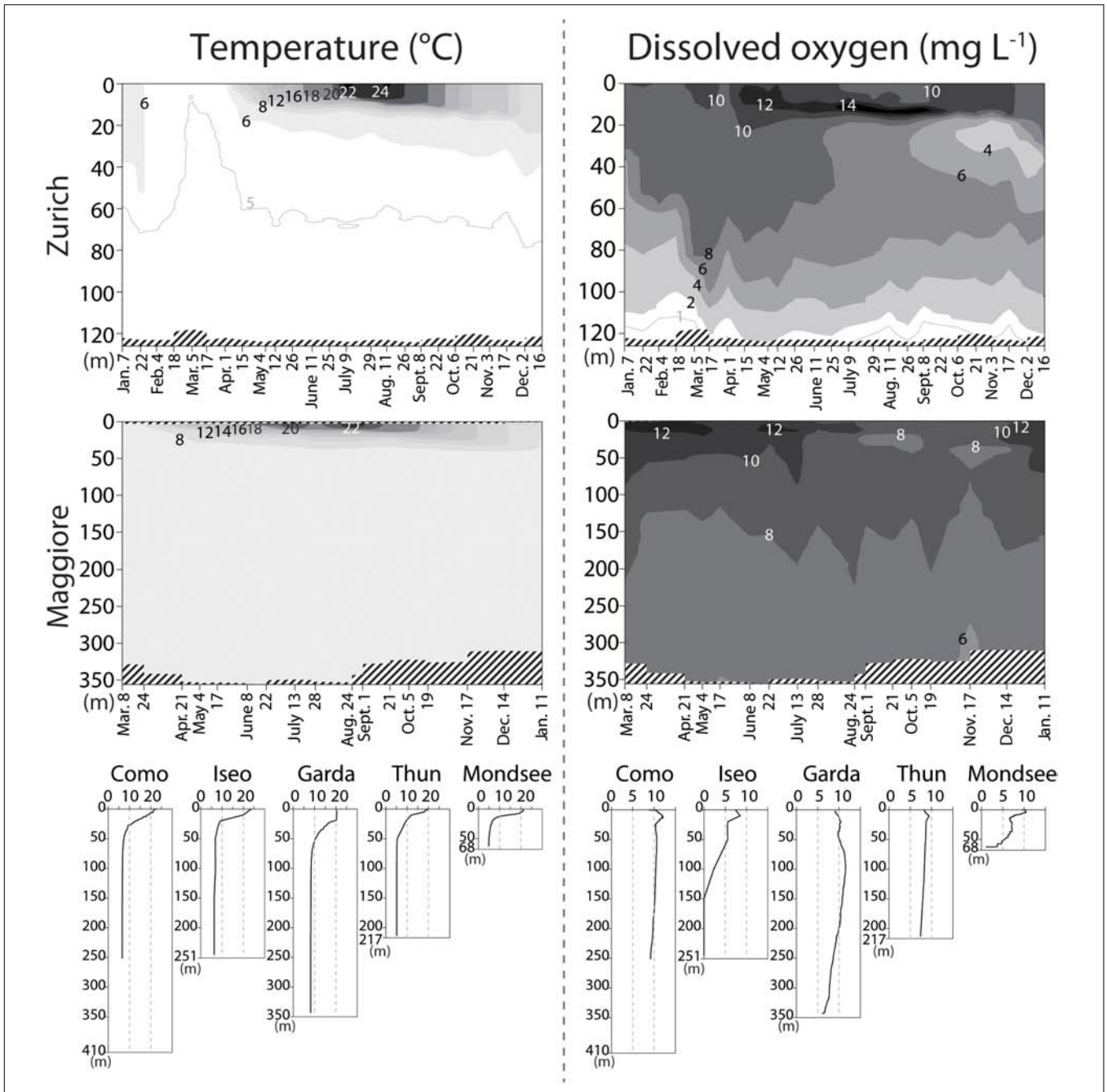

FIGURE 1 | Profiles of the temperature (left panels; °C) and dissolved oxygen (right panels; mg L^{-1}) measured *in situ*. The vertical axes indicate water depth. For Lake Zurich and Maggiore, the sampling dates are indicated in the horizontal axes, and spatio-temporal measurements are shown by contours. Shaded areas indicate missing measurements.

cells mL^{-1} (**Figure 4**). These are within the range of previously reported values in other lakes (**Figure 5**).

The Oxygenated Hypolimnion as Preferred Habitat for CL500-11

The vertical distribution of CL500-11 showed a virtual absence in the epilimnion during the stratification period (**Figure 4**), thus further underpinning their prior adaptation to the hypolimnion environment. They were also not abundant in either anoxic bottom layers or in the transition zone between oxic and suboxic layers, as observed in Lake Zurich, Iseo, and Mondsee (**Figures 1**, **4**), supporting the predictions from MAGs that CL500-11 are strict aerobes (Denef et al., 2016; Mehrshad et al., 2018). The time-series sampling in Lake Zurich and Maggiore revealed dynamic spatio-temporal successions of CL500-11

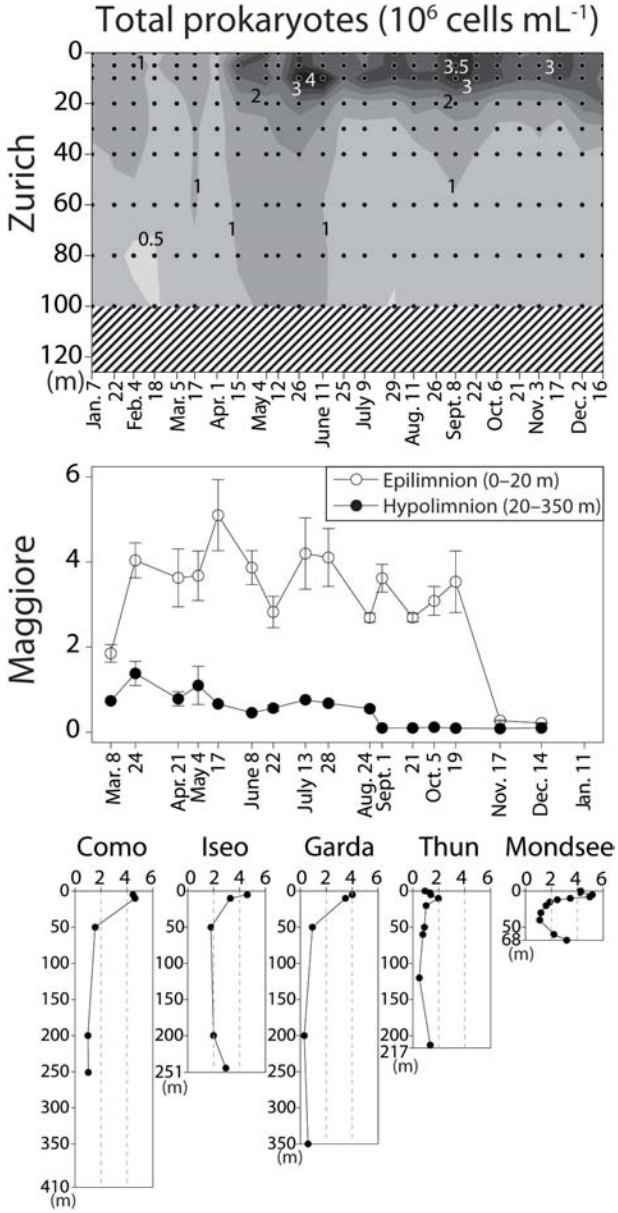

FIGURE 2 | Total prokaryotic abundance determined by enumeration of DAPI-stained cells (10^6 cells mL^{-1}). The vertical axes indicate water depth. For Lake Zurich, spatio-temporal measurement is shown by contours. Dots indicate sampling depths and dates, shaded areas missing measurements. The data for Lake Maggiore were measured in an integrated sample for epilimnetic (0–20 m) and hypolimnetic (20–350 m) water (see main text for detail). Error bars indicate standard error.

(**Figure 4**). Notably, the high-resolution sampling in Lake Zurich (fortnightly sampling of 9 depths) revealed that the water layers with absence and dominance of CL500-11 were clearly separated by the thermocline that was deepening with season (**Figures 1**, **4**). This indicates that CL500-11 do not survive for long times in the epilimnion. Although the cause of CL500-11 mortality in the epilimnion is unknown, it might be possible that physico-chemical conditions there, such as high water temperature and light radiation, are lethal for these bacteria.

In Lake Biwa, CL500-11 abundances decreased below detection limit during the winter mixing period (Okazaki et al., 2013). On the contrary, the spatio-temporal profiles in Lake Zurich and Maggiore showed low but still detectable numbers (1.5–4.1% of all prokaryotes) of CL500-11 prevailed throughout the winter mixing (**Figure 4**), in line with reported CL500-11 at the end of the spring mixing period in the dimictic Lake Michigan (Denef et al., 2016). They might be present throughout winter mixing in Lake Garda as well, as a recent study detected *Anaerolineae*-related 16S rRNA sequences in the lake throughout the mixing period for two consecutive years (Salmaso et al., 2018). Since the abundance of CL500-11 showed decreasing trends during winter mixing (**Figure 4**), the mixed water column is likely a suboptimum habitat for them, and thus, their survival during winter mixing period may be a vital factor as it determines their initial abundance at the onset of the next stratification phase. It is notable that *in situ* metatranscriptome data from Lake Michigan showed that many CL500-11 genes, including rhodopsins and genes for oxidative stress response mechanisms, were expressed more in the surface water during the mixing period than in the hypolimnion (Denef et al., 2016). This suggests that CL500-11 can potentially front the mixing event and optimize their survival mechanisms until the onset of the next stratification phase. If the mixing disturbance is a non-preferred event for CL500-11, water depth might be one of the determinants for their abundance during the mixing period. Likely in deep lakes,—due to a higher volumetric hypolimnion-to-epilimnion ratio, the mixing disturbance is less intense, resulting in less exposure to light and higher concentrations of hypolimnion-originated dissolved substances and biota, including CL500-11 themselves. Indeed, positive correlations (Spearman's coefficients, $p < 0.05$) were observed between CL500-11 cell density and the maximum depth or water volume of a lake (**Table 2**). This "dilution effect" might be one of the reasons for the absence of CL500-11 during the winter mixing period in Lake Biwa (Okazaki et al., 2013), as the lake has relatively shallow depth (73 m) at the sampling site, compared to those in Lake Maggiore (350 m), Zurich (136 m), Michigan (110 m), and Garda (350 m).

Possible Substrates Supporting Growth of CL500-11

Despite the exclusive occurrence of CL500-11 in oxygenated hypolimnia, the result of the present study, together with previous reports of CL500-11 occurrence (**Supplementary Table S2**), revealed a broad habitat spectrum of CL500-11 (**Table 3**). CL500-11 have been detected in oxygenated hypolimnia of lakes and reservoirs located across the globe, with a variety in origin, trophic state, hypolimnetic temperature, surface area, depth, mixing regime, and water retention time (**Table 3** and **Supplementary Table S2**). Moreover, most of the investigated environmental parameters, including trophic load of the lakes (i.e., total nitrogen and phosphorus), did not show significant correlations with CL500-11 abundances (**Table 2**). Indeed, the dominance of CL500-11 was observed in both ultra-oligotrophic

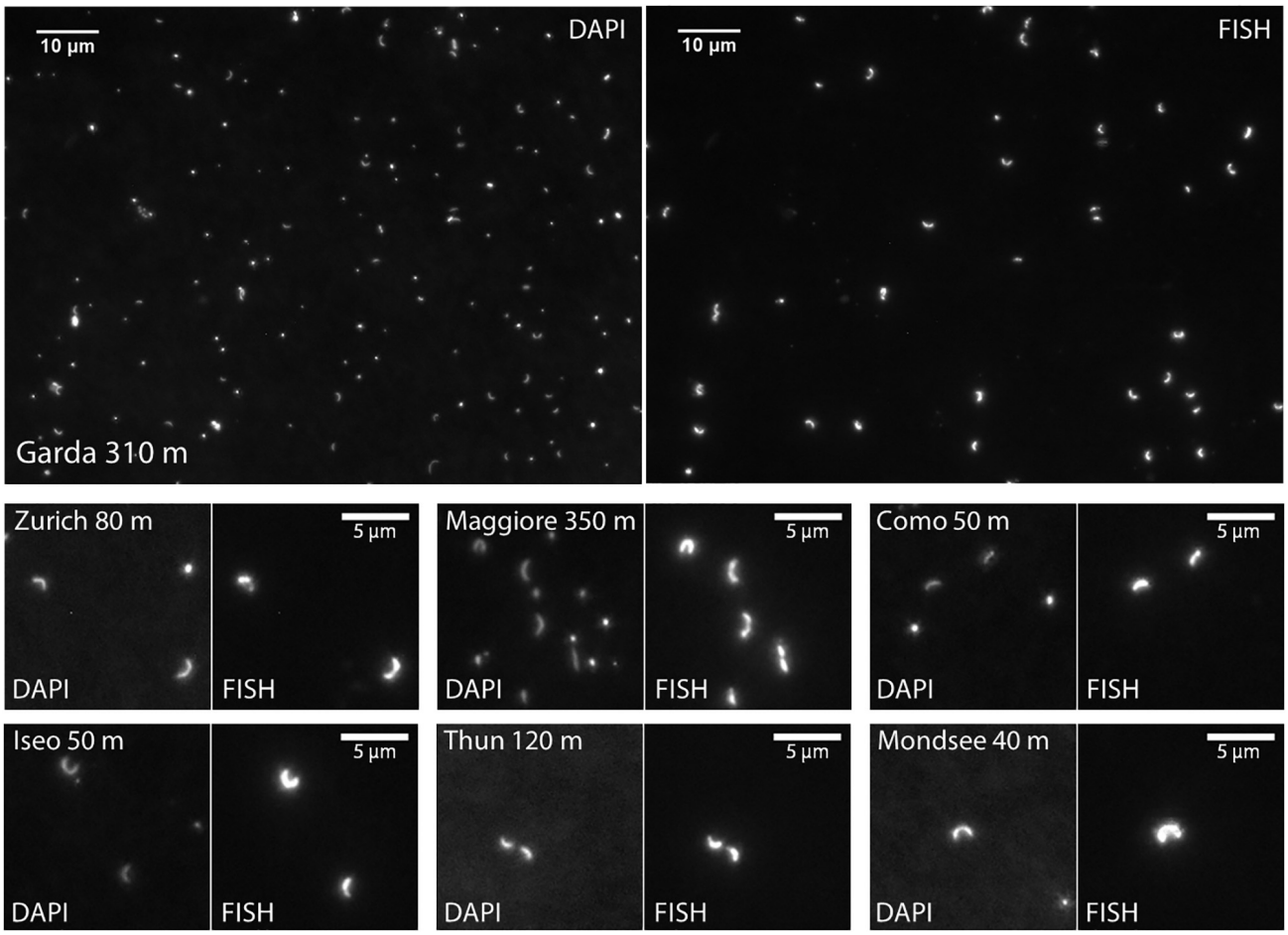

FIGURE 3 | Microscopic images of CL500-11 cells detected by CARD-FISH. In each panel, DAPI-stained cells and the corresponding FISH-positives were shown in the left and right side, respectively. A whole microscopic field was shown for the sample taken from 310 m in Lake Garda, where the highest proportion of CL500-11 cells was recorded. For the other lakes, enlarged images were shown. The samples taken on December were used for the images from Lake Zurich and Maggiore.

Crater Lake (Urbach et al., 2001) and meso-eutrophic Lake Iseo (**Figure 4**). These facts suggest that substrates supporting growth of CL500-11 are ubiquitously present in oxygenated hypolimnia of freshwater systems.

High numbers of CL500-11 were observed in broad layers of hypolimnion; for instance, they accounted for >5% of all prokaryotes from 50 to 350 m in Lake Garda and from 50 to 213 m in Lake Thun (**Figure 4**). In line with previous observations (Okazaki et al., 2013, 2017), all of the observed CL500-11 cells were planktonic, i.e., not particle-associated (**Figure 3**). Since all samples were taken at pelagic stations, terrestrial input is likely less important for CL500-11 growth than autochthonous resources produced within the lake. Consequently, CL500-11 are likely depending on autochthonous DOM distributed in the whole hypolimnion. In freshwater systems, refractory DOM accumulating in the water column can be more than a 100 years old (Goldberg et al., 2015) and old substrates can still potentially be bioavailable (Guillemette et al., 2017). Assuming that DOM supporting CL500-11 growth would accumulate in the water column over a year, one may expect that lakes with longer water retention time would show higher abundances of CL500-11 due to higher concentrations of the DOM. However, no significant relationship between CL500-11 abundances and water retention times was detected (**Table 2**), i.e., high abundances were also observed in lakes with short water retention times, including Lake Zurich (1.4 years) and Thun (1.8 years) (**Table 1** and **Figure 4**). It is thus likely that the resources for CL500-11 growth do not accumulate in the water column over a year but likely turnover within an annual timescale. This is in accordance with a stable isotope analysis in Lake Biwa (Maki et al., 2010) reporting that semi-labile autochthonous DOM, originally generated and accumulated in the epilimnion, was transported to the whole hypolimnion during winter mixing where it was slowly being consumed during the subsequent stratification period. Besides, CL500-11 were not abundant in two artificial reservoirs (Římov and T) with water retention times of around 0.3 years (**Figure 5** and **Supplementary Table S2**), supporting the hypothesis that a water retention time of more than a year is required to maintain a stable population of CL500-11.

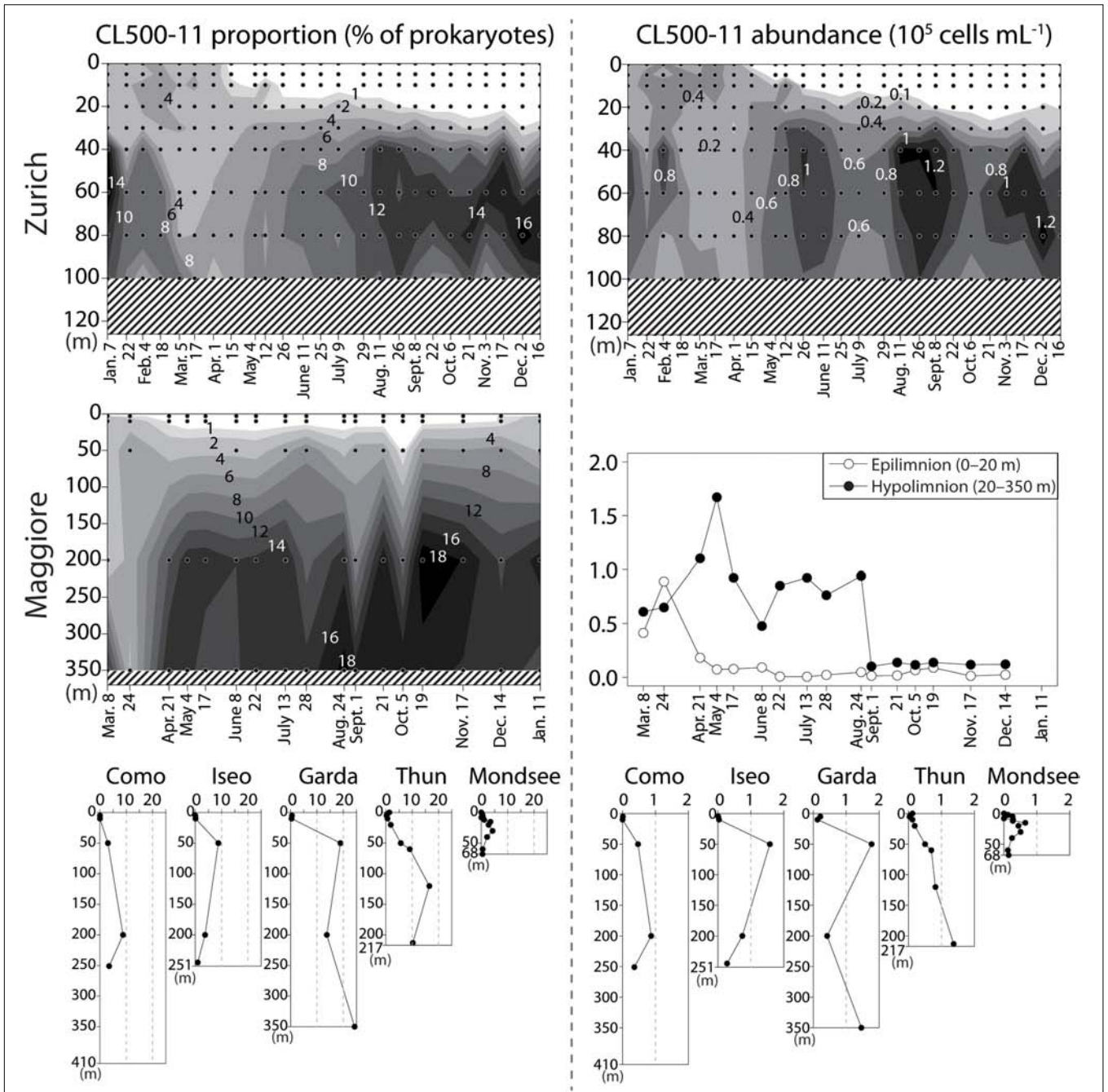

FIGURE 4 | Proportions of CL500-11 in percentage of total prokaryotes (FISH-positive vs. DAPI-stained cells) (**left**; %) and their absolute abundances (**right**; 10^5 cells mL^{-1}) generated by multiplying relative proportions with total prokaryotic abundances (**Figure 2**). The vertical axes indicate water depth. For Lake Zurich and Maggiore, spatio-temporal measurements are shown by contours. Dots indicate sampling depths and dates, shaded areas missing measurements. In Lake Maggiore, since total prokaryotic abundances were determined in the integrated epilimnetic (0–20 m) and hypolimnetic (20–350 m) samples (**Figure 2**), the averaged percentage for each layer was used to generate average CL500-11 abundances for epi- and hypolimnion.

The seasonal profiles of Lake Zurich (**Figure 4**) and Biwa (Okazaki et al., 2013) indicate that the abundance of CL500-11 increases toward the end of the stratification period, implying that their resources for growth are continuously supplied in the hypolimnion in these lakes till the end of the stratification period. These facts evoke an additional hypothesis that CL500-11 utilize substrates secondary produced *in situ* by microbial processes (Ogawa et al., 2001; Jiao and Zheng, 2011; Guillemette and del Giorgio, 2012). Indeed, studies have demonstrated that, similar to marine systems (Timko et al., 2015b; Shen and Benner, 2018), DOM is more photo-labile in the hypolimnion than in the epilimnion (Hayakawa et al., 2016; Yamada et al., 2018),

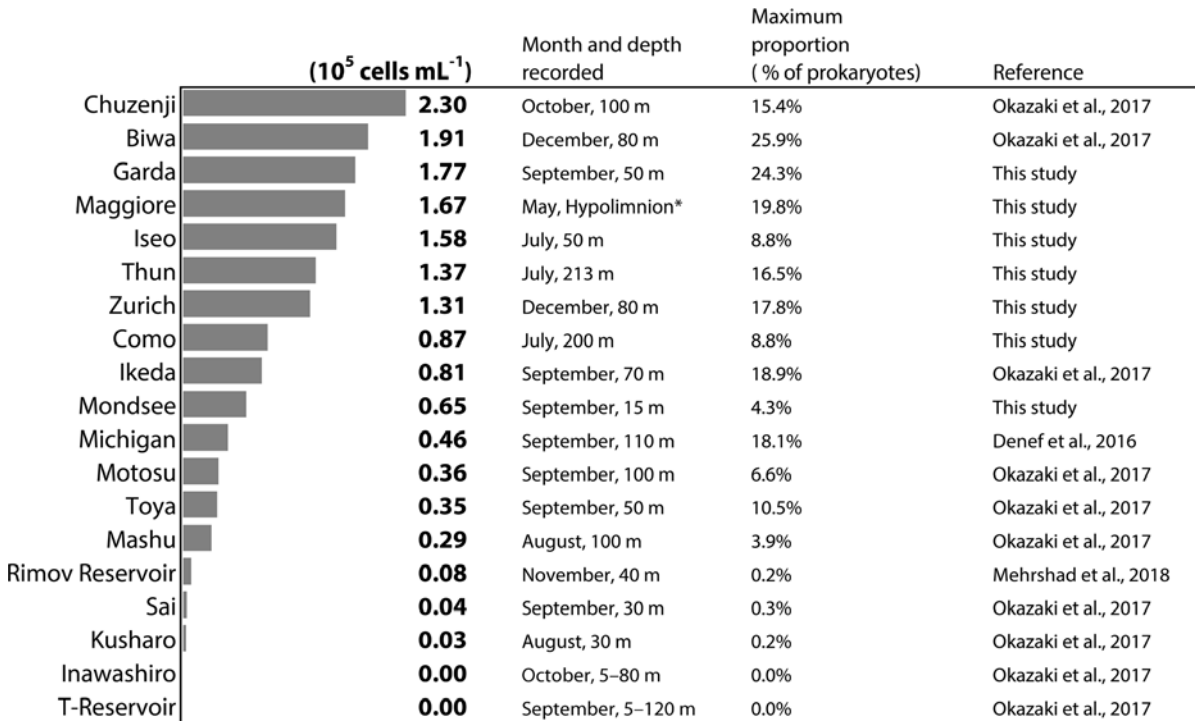

FIGURE 5 | Maximum abundance of CL500-11 recorded by CARD-FISH analyses in each lake. *Bacterial abundance in the hypolimnion of Lake Maggiore was determined using an integrated sample from 20 to 350 m.

TABLE 2 | The Spearman's coefficients (ρ) and the corresponding *p*-values between the CL500-11 maximum abundance and environmental measurements in each lake.

	Surface area	Surface elevation	Water retention time	Maximum depth	Water volume	Hypolimnetic temperature during stratification	pH (min)	pH (max)	TN (min)	TN (max)	TP (min)*	TP (max)
p-value	0.136	0.459	0.657	**0.025**	**0.034**	0.107	**0.004**	0.251	0.270	0.432	0.104	**0.022**
ρ	0.355	−0.181	0.109	0.512	0.488	0.381	0.631	0.277	0.284	0.204	0.385	0.520

*The original data used for the statistics are available in **Supplementary Table S2**. p-values lower than 0.05 are shown in bold. For pH, TN, and TP, minimum (min) and maximum (max) values recorded in each lake were separately used. *TP measurements below detection limits were replaced with the value of the detection limit.*

suggesting that a part of hypolimnetic DOM is produced *in situ* and distinct from DOM produced and accumulated in the epilimnion, which likely consist of already-photobleached substrates such as carboxylic acids (Bertilsson and Tranvik, 2000). Correspondingly, a low number of transporters for carboxylic acids was found in CL500-11 MAGs compared to other freshwater microbes (Denef et al., 2016), pointing to a non-preferred utilization of these photobleached compounds. On the other hand, CL500-11 MAGs harbor a high number of transporters for di- and oligopeptide, as well as transporters for spermidine/putrescein, and branched-chain amino acids (Denef et al., 2016; Mehrshad et al., 2018). Such nitrogen-rich, protein-like DOM can be originated from remnants of bacterial cell walls (McCarthy et al., 1998; Nagata et al., 2003) and membranes (Tanoue et al., 1995), and consumption of such DOM by the microbial community in the oxygenated hypolimnion have been suggested by DOM profiling by stoichiometry (Kim et al., 2006) and by excitation and emission matrices (Thottathil et al., 2013; Hayakawa et al., 2016) in Lake Biwa. One CL500-11 MAG also included a transporter for *N*-acetylglucosamine, a breakdown product of bacterial cell walls (Denef et al., 2016; Mehrshad et al., 2018). Moreover, a study has reported 16S rRNA gene sequences of CL500-11 from an actively growing prokaryotic community in *N*-acetylglucosamine-enriched lake water (Tada and Grossart, 2014). These data collectively lead to the speculation that CL500-11 are scavenging cell wall compounds or other cellular remnants released *in situ* by grazing or viral lysis of other prokaryotes (Nagata et al., 2003; Middelboe and Jørgensen, 2006; Eckert et al., 2013), which can be continuously produced in the water column of hypolimnion.

Potential Limiting Factors for the Distribution of CL500-11

Besides the two artificial reservoirs discussed above, low abundances of CL500-11 in the oxygenated hypolimnion during

TABLE 3 | The range of environmental measurements of the lakes where CL500-11 were detected.

Region	Asia, Europe, North America, South America
Lake origin	Glacial, Caldera, Tectonic, Dammed, Artificial reservoir
Trophic state	Oligotrophic to meso-eutrophic
Surface area (km^2)	2.06–82097
Surface elevation (m)	60–2357
Water retention time (y)	0.3–330
Maximum depth (m)	43–1637
Water volume (10^6 m^3)	34.5–23615000
Mixing regime	Dimictic, Monomictic, Meromictic**
Occurrence of anoxic bottom layer	Yes and No
Hypolimnetic temperature during stratification* (°C)	3.8–10.9
pH*	6.8–9.9
TN* ($\mu g\ L^{-1}$)	60–2002
TP* ($\mu g\ L^{-1}$)	2.55–45

*The data for each lake are available in **Supplementary Table S2**. *Lakes only with cloning/amplicon sequencing were not included for these parameters. **The upper hypolimnion was oxygenated in these meromictic lakes.*

the stratified period were also found in previously investigated Lake Kusshoro and Inawashiro (Okazaki et al., 2017) (**Figure 5**), despite their relatively high maximum depth (118 and 94 m, respectively), large surface area (79.6 and 103.3 km^2), and long water retention time (12 and 5.4 years) (**Supplementary Table S2**). It is notable that these lakes receive inflows influenced by volcanic activities and were acidic (pH < 5.0) until 30 years ago, followed by neutralization with pH ranges of 7–7.5 and 6.6–7, respectively, to date (Oyama et al., 2014; Sutani et al., 2014). Further, we have recently noticed an absence of CL500-11 in the water column of Lake Tazawa, a deep (423 m), slightly acidic (pH < 6) oligotrophic freshwater lake, which receives acidic volcanic inflow as well (Okazaki et al., unpublished data). The statistical test also supported a positive relationship (p = 0.004) between CL500-11 abundances and minimum recorded pH in a lake (**Table 2**). Although the direct factor affecting CL500-11 in low pH condition is unknown, it is likely that they cannot survive in lakes affected by acidic volcanic inflow. In addition to anion and cation concentrations, pH may affect photo-liability and colloidal size of DOM (Pace et al., 2012; Timko et al., 2015a). These factors may be critical for CL500-11 survival, in accordance to other studies that identified pH as master driver for the distribution of different microbial lineages (Lindstrom et al., 2005; Newton et al., 2011).

In Lake Maggiore, severe drops in the total prokaryotic abundance were observed in September in the hypolimnion and in November in the epilimnion (**Figure 2**), which resulted in a drastic decline of the CL500-11 population in September as well (**Figure 4**). Such dynamics in abundance might be attributable to top-down control, namely grazing and viral lysis, yet unfortunately, no data is available for the viral and predators' communities during the study period. Recent observations reported hypolimnion-specific heterotrophic nanoflagellate communities (Mukherjee et al., 2015, 2017) that might be grazing on CL500-11. Larger mixotrophic flagellates and ciliates may also be the major predator of CL500-11, as they can efficiently graze bacterioplankton of this size as well (Posch et al., 1999). It is likely that CL500-11 are also lysed by specific viruses, since virus-host interactions are more specific than size-selective prey-predator interactions. The diversity of grazers and viruses in oxygenated hypolimnia remains largely unexplored, and the main mortality agents for CL500-11 are yet-to-be identified. Future studies should pay more attention to understand mechanisms behind CL500-11 population dynamics and the turnover of organic matter via CL500-11.

CONCLUSION

Overall, the quantitative investigation of CL500-11 in perialpine lakes further endorsed ubiquity and quantitative significance of this bacterioplankton lineage in global deep freshwater systems (**Figures 4**, **5** and **Table 3**). Our results as well as metagenomic and geochemical insights from literatures allowed to hypothesize possible characteristics of substrates supporting CL500-11 growth, most likely nitrogen-rich autochthonous DOM ubiquitously available in the hypolimnion that may turnover within an annual timescale. CL500-11 may either directly utilize DOM derived from the epilimnion transferred by winter vertical mixing, or depend on DOM secondary produced *in situ*, for example, cellular debris from other microbes. We further suggest that shallow depth, low pH, and short water retention time would limit CL500-11 dominance. However, eco-physiological mechanisms and consequences of these findings and assumptions are still mostly unknown or lack direct evidences, and there still remain unexplored factors potentially controlling CL500-11 dynamics such as grazing and viral infection. These subjects need further verification in future studies.

Not only their importance in ecosystem and biogeochemical cycling, but also their evolutionary and biogeographic backgrounds are intriguing topics for debate, given that CL500-11 is the sole bacterioplankton lineage affiliated with *Chloroflexi* dominating in freshwater systems and exclusively inhabiting the oxygenated hypolimnion. Although the ecology of CL500-11 has been gradually understood by the growing number of researches, there may be still many remarkable characteristics yet-to-be discovered. For instance, a recent metagenomic study revealed that CL500-11 are present even in the brackish Caspian Sea, and identified at least three species in four investigated lakes based on average nucleotide identities of MAGs, for which a candidate genus Profundisolitarius was proposed (Mehrshad et al., 2018). Continuous efforts should be made to uncover the ecology of this enigmatic bacteria by further field explorations and meta-omics surveys, along with the ultimate challenge toward their isolation and cultivation (Salcher and Šimek, 2016).

AUTHOR CONTRIBUTIONS

YO conceived the study. MS and CC collected the samples and field measurements. YO and MS performed CARD-FISH. YO, MS, CC, and SN wrote the manuscript.

FUNDING

This study was supported by JSPS KAKENHI (15J00971 and 18J00300) and by The Kyoto University Foundation Overseas' Research Fellowship. Samples and abiotic data from Mondsee were provided by Bettina Sonntag and Barbara Kammerlander in the course of the Austrian Science Fund (FWF) project I2238-B25.

ACKNOWLEDGMENTS

We thank Eugen Loher and Thomas Posch for help with sampling of Lake Zurich and the Water Supply Company Zurich for the provision of chemical data. Samples from Lake Thun were taken by Tanja Shabarova, abiotic data was provided by Markus Zeh (BVE-AWA Bern). We also thank Mario Contesini for sampling Lake Maggiore, Como, Garda and Iseo and Salvador Hernández-Avilés for filter preparation, in the course of CIPAIS project.

SUPPLEMENTARY MATERIAL

The Supplementary Material for this article can be found online at: https://www.frontiersin.org/articles/10.3389/fmicb.2018.02891/full#supplementary-material

TABLE S1 | List of the 60 sequences in the SILVA SSU 132 Parc database that perfectly match the probe CLGNS_584. Nucleotide identities to the two CL500-11 sequences in the SILVA SSU 132 Ref NR99 database (AF316759 and HM856384) are shown in the second and third columns. The other columns are retrieved from the output of the TestProbe 3.0 tool.

TABLE S2 | Summarized information for lakes where CL500-11 were investigated or detected. The first sheet contains lakes where CL500-11 have been enumerated with CARD-FISH, and the second sheet includes lakes where 16S rRNA sequences of CL500-11 have been retrieved. The references for the data are summarized in the third sheet.

REFERENCES

Ambrosetti, W., Barbanti, L., and Carrara, E. A. (2010). Mechanisms of hypolimnion erosion in a deep lake (Lago Maggiore, N. Italy). *J. Limnol.* 69:3. doi: 10.4081/jlimnol.2010.3

APHA, and AWWA (2005). *Standard Methods for the Examination of Water and Wastewater*. Washington, DC: American Public Health Association.

Bertilsson, S., and Tranvik, L. J. (2000). Photochemical transformation of dissolved organic matter in lakes. *Limnol. Oceanogr.* 45, 753–762. doi: 10.4319/lo.2000.45.4.0753

Bertoni, R., Callieri, C., Corno, G., Rasconi, S., Caravati, E., and Contesini, M. (2010). Long-term trends of epilimnetic and hypolimnetic bacteria and organic carbon in a deep holo-oligomictic lake. *Hydrobiologia* 644, 279–287. doi: 10.1007/s10750-010-0150-x

Callieri, C., Hernández-Avilés, S., Salcher, M. M., Fontaneto, D., and Bertoni, R. (2016). Distribution patterns and environmental correlates of Thaumarchaeota abundance in six deep subalpine lakes. *Aquat. Sci.* 78, 215–225. doi: 10.1007/s00027-015-04183

Denef, V. J., Mueller, R. S., Chiang, E., Liebig, J. R., and Vanderploeg, H. A. (2016). Chloroflexi CL500-11 populations that predominate deep-lake hypolimnion bacterioplankton rely on nitrogen-rich dissolved organic matter metabolism and c 1 compound oxidation. *Appl. Environ. Microbiol.* 82, 1423–1432. doi: 10.1128/AEM.03014-15

Eckert, E. M., Baumgartner, M., Huber, I. M., and Pernthaler, J. (2013). Grazing resistant freshwater bacteria profit from chitin and cell-wall-derived organic carbon. *Environ. Microbiol.* 15, 2019–2030. doi: 10.1111/1462-2920.12083

Goldberg, S. J., Ball, G. I., Allen, B. C., Schladow, S. G., Simpson, A. J., Masoom, H., et al. (2015). Refractory dissolved organic nitrogen accumulation in high-elevation lakes. *Nat. Commun.* 6:6347. doi: 10.1038/ncomms7347

Guillemette, F., Bianchi, T. S., and Spencer, R. G. M. (2017). Old before your time: ancient carbon incorporation in contemporary aquatic foodwebs. *Limnol. Oceanogr.* 62, 1682–1700. doi: 10.1002/lno.10525

Guillemette, F., and del Giorgio, P. A. (2012). Simultaneous consumption and production of fluorescent dissolved organic matter by lake bacterioplankton. *Environ. Microbiol.* 14, 1432–1443. doi: 10.1111/j.1462-2920.2012.02728.x

Hayakawa, K., Kojima, R., Wada, C., Suzuki, T., Sugiyama, Y., Kumagai, T., et al. (2016). Distribution and characteristics of ultraviolet absorption and fluorescenceof dissolved organic matter in a large lake (Lake Biwa, Japan). *J. Great Lakes Res.* 42, 571–579. doi: 10.1016/j.jglr.2016.02.006

Hernández-Avilés, J. S., Bertoni, R., Macek, M., and Callieri, C. (2012). Why bacteria are smaller in the epilimnion than in the hypolimnion? A hypothesis comparing temperate and tropical lakes. *J. Limnol.* 71:10. doi: 10.4081/jlimnol.2012.e10

Hernández-Avilés, J. S., Callieri, C., Bertoni, R., Morabito, G., Leoni, B., Lepori, F., et al. (2018). Prokaryoplankton and phytoplankton community compositions in five large deep perialpine lakes. *Hydrobiologia* 824:71. doi: 10.1007/s10750-018-3586-z

Humbert, J.-F., Dorigo, U., Cecchi, P., Le Berre, B., Debroas, D., and Bouvy, M. (2009). Comparison of the structure and composition of bacterial communities from temperate and tropical freshwater ecosystems. *Environ. Microbiol.* 11, 2339–2350. doi: 10.1111/j.1462-2920.2009.01960.x

Jiao, N., and Zheng, Q. (2011). The microbial carbon pump: from genes to ecosystems. *Appl. Environ. Microbiol.* 77, 7439–7444. doi: 10.1128/AEM.05640-11

Kim, C., Nishimura, Y., and Nagata, T. (2006). Role of dissolved organic matter in hypolimnetic mineralization of carbon and nitrogen in a large, monomictic lake. *Limnol. Oceanogr.* 51, 70–78. doi: 10.4319/lo.2006.51.1.0070

Lindstrom, E. S., Kamst-Van Agterveld, M. P., and Zwart, G. (2005). Distribution of typical freshwater bacterial groups is associated with pH, temperature, and lake water retention time. *Appl. Environ. Microbiol.* 71, 8201–8206. doi: 10.1128/AEM.71.12.8201-8206.2005

Maki, K., Kim, C., Yoshimizu, C., Tayasu, I., Miyajima, T., and Nagata, T. (2010). Autochthonous origin of semi-labile dissolved organic carbon in a large monomictic lake (Lake Biwa): carbon stable isotopic evidence. *Limnology* 11, 143–153. doi: 10.1007/s10201-009-0299-z

McCarthy, M. D., Hedges, J. I., and Benner, R. (1998). Major bacterial contribution to marine dissolved organic nitrogen. *Science* 281, 231–234. doi: 10.1126/science.281.5374.231

Mehrshad, M., Salcher, M. M., Okazaki, Y., Nakano, S., Šimek, K., Andrei, A.-S., et al. (2018). Hidden in plain sight—highly abundant and diverse planktonic freshwater Chloroflexi. *Microbiome* 6:176. doi: 10.1186/s40168-018-0563-8

Middelboe, M., and Jørgensen, N. O. G. (2006). Viral lysis of bacteria: an important source of dissolved amino acids and cell wall compounds. *J. Mar. Biol. Assoc.* 86, 605–612. doi: 10.1017/S0025315406013518

Mukherjee, I., Hodoki, Y., and Nakano, S. (2015). Kinetoplastid flagellates overlooked by universal primers dominate in the oxygenated hypolimnion of Lake Biwa, Japan. *FEMS Microbiol. Ecol.* 91:fiv083. doi: 10.1093/femsec/fiv083

Mukherjee, I., Hodoki, Y., and Nakano, S. (2017). Seasonal dynamics of heterotrophic and plastidic protists in the water column of Lake Biwa, Japan. *Aquat. Microb. Ecol.* 80, 123–137. doi: 10.3354/ame01843

Nagata, T., Meon, B., and Kirchman, D. L. (2003). Microbial degradation of peptidoglycan in seawater. *Limnol. Oceanogr.* 48, 745–754. doi: 10.4319/lo.2003.48.2.0745

Neuenschwander, S. M., Ghai, R., Pernthaler, J., and Salcher, M. M. (2018). Microdiversification in genome-streamlined ubiquitous freshwater Actinobacteria. *ISME J.* 12, 185–198. doi: 10.1038/ismej.2017.156

Newton, R. J., Jones, S. E., Eiler, A., McMahon, K. D., and Bertilsson, S. (2011). A guide to the natural history of freshwater lake bacteria. *Microbiol. Mol. Biol. Rev.* 75, 14–49. doi: 10.1128/MMBR.00028-10

Ogawa, H., Amagai, Y., Koike, I., Kaiser, K., and Benner, R. (2001). Production of refractory dissolved organic matter by bacteria. *Science* 292, 917–920. doi: 10.1126/science.1057627

Okazaki, Y., Fujinaga, S., Tanaka, A., Kohzu, A., Oyagi, H., and Nakano, S. (2017). Ubiquity and quantitative significance of bacterioplankton lineages inhabiting the oxygenated hypolimnion of deep freshwater lakes. *ISME J.* 11, 2279–2293. doi: 10.1038/ismej.2017.89

Okazaki, Y., Hodoki, Y., and Nakano, S. (2013). Seasonal dominance of CL500-11 bacterioplankton (phylum Chloroflexi) in the oxygenated hypolimnion of Lake Biwa. Japan. *FEMS Microbiol. Ecol.* 83, 82–92. doi: 10.1111/j.1574-6941.2012.01451.x

Okazaki, Y., and Nakano, S.-I. (2016). Vertical partitioning of freshwater bacterioplankton community in a deep mesotrophic lake with a fully oxygenated hypolimnion (Lake Biwa, Japan). *Environ. Microbiol. Rep.* 8, 780–788. doi: 10.1111/1758-2229.12439

Oyama, Y., Yamada, H., Wakana, I., and Takahashi, M. (2014). Neutralization of lake onneto, Japan. *Jpn. J. Limnol.* 76, 45–50. doi: 10.3739/rikusui.76.45

Pace, M. L., Reche, I., Cole, J. J., Fernández-Barbero, A., Mazuecos, I. P., and Prairie, Y. T. (2012). pH change induces shifts in the size and light absorption of dissolved organic matter. *Biogeochemistry* 108, 109–118. doi: 10.1007/s10533-011-9576-0

Porter, K. G., and Feig, Y. S. (1980). The use of DAPI for identifying and counting aquatic microflora1. *Limnol. Oceanogr.* 25, 943–948. doi: 10.4319/lo.1980.25.5.0943

Posch, T., Simek, K., Vrba, J., Pernthaler, J., Nedoma, J., Sattler, B., et al. (1999). Predator-induced changes of bacterial size-structure and productivity studied on an experimental microbial community. *Aquat. Microb. Ecol.* 18, 235–246. doi: 10.3354/ame018235

Quast, C., Pruesse, E., Yilmaz, P., Gerken, J., Schweer, T., Yarza, P., et al. (2013). The SILVA ribosomal RNA gene database project: improved data processing and web-based tools. *Nucleic Acids Res.* 41, D590–D596. doi: 10.1093/nar/gks1219

R Core Team (2017). *R: A Language and Environment for Statistical Computing*. Vienna: R Foundation Statistical Computating.

Salcher, M., and Šimek, K. (2016). Isolation and cultivation of planktonic freshwater microbes is essential for a comprehensive understanding of their ecology. *Aquat. Microb. Ecol.* 77, 183–196. doi: 10.3354/ame01796

Salcher, M. M. (2013). Same same but different: ecological niche partitioning of planktonic freshwater prokaryotes. *J. Limnol.* 73, 74–87. doi: 10.4081/jlimnol.2014.813

Salcher, M. M., Neuenschwander, S. M., Posch, T., and Pernthaler, J. (2015). The ecology of pelagic freshwater methylotrophs assessed by a high-resolution monitoring and isolation campaign. *ISME J.* 9, 2442–2453. doi: 10.1038/ismej.2015.55

Salcher, M. M., Pernthaler, J., and Posch, T. (2011). Seasonal bloom dynamics and ecophysiology of the freshwater sister clade of SAR11 bacteria "that rule the waves" (LD12). *ISME J.* 5, 1242–1252. doi: 10.1038/ismej.2011.8

Salmaso, N., Albanese, D., Capelli, C., Boscaini, A., Pindo, M., and Donati, C. (2018). Diversity and cyclical seasonal transitions in the bacterial community in a large and deep perialpine lake. *Microb. Ecol.* 76, 125–143. doi: 10.1007/s00248-017-1120-x

Shabarova, T., Kasalický, V., Šimek, K., Nedoma, J., Znachor, P., Posch, T., et al. (2017). Distribution and ecological preferences of the freshwater lineage LimA (genus Limnohabitans) revealed by a new double hybridization approach. *Environ. Microbiol.* 19, 1296–1309. doi: 10.1111/1462-2920.13663

Shen, Y., and Benner, R. (2018). Mixing it up in the ocean carbon cycle and the removal of refractory dissolved organic carbon. *Sci. Rep.* 8:2542. doi: 10.1038/s41598-018-20857-5

Sutani, D., Utsumi, M., Kato, Y., and Sugiura, N. (2014). Estimation of the changes in phytoplankton community composition in a volcanic acidotrophic Lake, Inawashiro, Japan. *Jpn. J. Water Treat. Biol.* 50, 53–69. doi: 10.2521/jswtb.50.53

Tada, Y., and Grossart, H.-P. (2014). Community shifts of actively growing lake bacteria after N-acetyl-glucosamine addition: improving the BrdU-FACS method. *ISME J.* 8, 441–454. doi: 10.1038/ismej.2013.148

Tanoue, E., Nishiyama, S., Kamo, M., and Tsugita, A. (1995). Bacterial membranes: possible source of a major dissolved protein in seawater. *Geochim. Cosmochim. Acta* 59, 2643–2648. doi: 10.1016/0016-7037(95)00134-4

Thottathil, S. D., Hayakawa, K., Hodoki, Y., Yoshimizu, C., Kobayashi, Y., and Nakano, S. (2013). Biogeochemical control on fluorescent dissolved organic matter dynamics in a large freshwater lake (Lake Biwa, Japan). *Limnol. Oceanogr.* 58, 2262–2278. doi: 10.4319/lo.2013.58.6.2262

Timko, S. A., Gonsior, M., and Cooper, W. J. (2015a). Influence of pH on fluorescent dissolved organic matter photo-degradation. *Water Res.* 85, 266–274. doi: 10.1016/j.watres.2015.08.047

Timko, S. A., Maydanov, A., Pittelli, S. L., Conte, M. H., Cooper, W. J., Koch, B. P., et al. (2015b). Depth-dependent photodegradation of marine dissolved organic matter. *Front. Mar. Sci.* 2:66. doi: 10.3389/fmars.2015.00066

Urbach, E., Vergin, K. L., Young, L., Morse, A., Larson, G. L., and Giovannoni, S. J. (2001). Unusual bacterioplankton community structure in ultra-oligotrophic Crater Lake. *Limnol. Oceanogr.* 46, 557–572. doi: 10.4319/lo.2001.46.3.0557

Van den Wyngaert, S., Salcher, M. M., Pernthaler, J., Zeder, M., and Posch, T. (2011). Quantitative dominance of seasonally persistent filamentous cyanobacteria (*Planktothrix rubescens*) in the microbial assemblages of a temperate lake. *Limnol. Oceanogr.* 56, 97–109. doi: 10.4319/lo.2011.56.1.0097

Yamada, E., Ueda, T., Tanaka, T., Fujii, K., Mizuguchi, H., and Fuse, Y. (2018). Effects of photoirradiation on the characteristics of dissolved organic matter in Lake Biwa and its surrounding rivers. *J. Environ. Saf.* 9, 23–32. doi: 10.11162/daikankyo.E17RP1101

Zeder, M., and Pernthaler, J. (2009). Multispot live-image autofocusing for high-throughput microscopy of fluorescently stained bacteria. *Cytometry A.* 75, 781–788. doi: 10.1002/cyto.a.20770

Conflict of Interest Statement: The authors declare that the research was conducted in the absence of any commercial or financial relationships that could be construed as a potential conflict of interest.

Copyright © 2018 Okazaki, Salcher, Callieri and Nakano. This is an open-access article distributed under the terms of the Creative Commons Attribution License (CC BY). The use, distribution or reproduction in other forums is permitted, provided the original author(s) and the copyright owner(s) are credited and that the original publication in this journal is cited, in accordance with accepted academic practice. No use, distribution or reproduction is permitted which does not comply with these terms.

frontiers in Microbiology

ORIGINAL RESEARCH
published: 14 January 2019
doi: 10.3389/fmicb.2018.03344

Long Term Diversity and Distribution of Non-photosynthetic Cyanobacteria in Peri-Alpine Lakes

Marie-Eve Monchamp[1,2], *Piet Spaak*[1,2] *and Francesco Pomati*[1,2]*

[1] Department of Aquatic Ecology, Swiss Federal Institute of Aquatic Science and Technology, Eawag, Dübendorf, Switzerland, [2] Swiss Federal Institute of Technology, Institute of Integrative Biology, Zurich, Switzerland

The phylum Cyanobacteria comprises a non-photosynthetic lineage. The diversity and distribution of non-photosynthetic cyanobacteria (NCY) across aquatic environments are currently unknown, including their ecology. Here, we report about composition and phylogenetic diversity of two clades of NCY in ten lakes of the European peri-Alpine region, over the past ∼100 years. Using 16S rDNA sequences obtained from dated sediment cores, we found almost equal proportion of taxa assigned to Melainabacteria and the deepest-branching group Sericytochromatia (ML635J-21) (63 total detected taxa). The topology of our reconstructed phylogenies reflected evolutionary relationships expected from previous work, that is, a clear separation between the deepest branching Sericytochromatia, the Melainabacteria, and the photosynthetic cyanobacteria clades. While different lakes harbored distinct NCY communities, the diversity of NCY assemblages within and between lakes (alpha and beta diversity) did not significantly change over the last century. This is in contrast with what was previously reported for photosynthetic cyanobacteria. Unchanged community phylogenetic similarity over geographic distance indicated no dispersal limitation of NCY at the regional scale. Our results solicit studies linking in-lake environmental factors to the composition of these microorganisms' communities, whose assembly appeared not to have been influenced by large-scale anthropogenic environmental changes. This is the first attempt to study the diversity and distribution of NCY taxa across temperate lakes. It provides a first step towards understanding their distribution and ecological function in pelagic aquatic habitats, where these organisms seem to be prevalent.

Keywords: Melainabacteria, ML635J-21, Sericytochromatia, metabarcoding, sedimentary DNA, distance-decay relationship, meta-community, Anthropocene

OPEN ACCESS

Edited by:
Petra M. Visser, University of Amsterdam, Netherlands

Reviewed by:
Yonghui Zeng, Aarhus University, Denmark
Nico Salmaso, Fondazione Edmund Mach, Italy
Anne D. Jungblut, Natural History Museum, United Kingdom

***Correspondence:**
Francesco Pomati
Francesco.Pomati@eawag.ch

Specialty section:
This article was submitted to Aquatic Microbiology, a section of the journal Frontiers in Microbiology

Received: *19 September 2018*
Accepted: *27 December 2018*
Published: *14 January 2019*

Citation:
Monchamp M-E, Spaak P and Pomati F (2019) Long Term Diversity and Distribution of Non-photosynthetic Cyanobacteria in Peri-Alpine Lakes. Front. Microbiol. 9:3344. doi: 10.3389/fmicb.2018.03344

INTRODUCTION

Cyanobacteria are a highly diverse group of gram-negative prokaryotes that have colonized a wide range of environments, from desert crusts to fresh and marine waters, and from the tropics to the poles (Whitton and Potts, 2002). They have played a crucial role in modifying the Earth's atmosphere through the process of oxygenic photosynthesis, which enabled the evolution of life in more complex forms (Fischer et al., 2016b). Cyanobacteria have been studied for decades, and their diversity has been described both morphologically (Rippka et al., 1979; Komárek et al., 2014) and genetically (Shih et al., 2013). Cyanobacteria are often considered a nuisance in aquatic ecosystems as they can form large blooms and decrease water quality, ecosystem functions and ecosystem services (Rigosi et al., 2014).

With the development of molecular techniques allowing the investigation of non-cultivable organisms, an unexpected diversity of cyanobacteria was unveiled in many ecosystems (Sogin et al., 2006; Di Rienzi et al., 2013; Soo et al., 2014; Meola et al., 2015). Genome sequencing recently revealed important information about a clade of non-photosynthetic prokaryotes closely related to the Cyanobacteria. The name Melainabacteria was proposed (Di Rienzi et al., 2013), because several representatives of this group have been found in aphotic environments. They were first thought to constitute a sister-phylum of the Cyanobacteria (Di Rienzi et al., 2013), but additional genomic information confirmed the position of Melainabacteria as a sister-clade of photosynthetic cyanobacteria and as part of the same phylum (Soo et al., 2014). Based on genomic evidence, a re-classification has been proposed for the phylum Cyanobacteria, with the class-level lineages Oxyphotobacteria (all cyanobacteria capable of photosynthesis) and Melainabacteria, as well as a third class called ML635J-21 (Soo et al., 2014), for which the name Sericytochromatia was recently proposed (Soo et al., 2017). Sericytochromatia is the most basal lineage and forms a paraphyletic group that is the ancestor of both Melainabacteria and photosynthetic cyanobacteria (Fischer et al., 2016a; Soo et al., 2017). After diverging from Melainabacteria, the Oxyphotobacteria developed oxygenic photosynthesis around 2.4–2.35 billion years ago based on molecular clock estimates (see Shih et al., 2016; Soo et al., 2017) and geological data (Fischer et al., 2016a).

For ease of discussion, we hereafter refer to class Oxyphotobacteria as photosynthetic cyanobacteria, and we use the nomenclature proposed by (Soo et al., 2014, 2017) for the class Melainabacteria, wherein the following orders are included: Gastranaerophilales (YS2), Obscuribacterales (mle1-12), Caenarcaniphilales (ACD20), and Vampirovibrionales (SM1D11). Because there is only a hand-full of Melainabacteria and Sericytochromatia sequenced genomes (Soo et al., 2017), the metabolism, functions, and ecological role of these organisms are not fully known. Representatives of Melainabacteria and Sericytochromatia have been found both in photic and aphotic environments, such as subsurface ground water (Di Rienzi et al., 2013), lake water and algal biofilms (Soo et al., 2017; Salmaso et al., 2018), marine and lacustrine sediment (Ley et al., 2005), animal and human feces (Soo et al., 2014) and guts (Ley et al., 2005). A list of non-photosynthetic cyanobacteria (NCY) representatives with their associated environments is presented in **Table 1**.

All sequenced genomes of Melainabacteria confirm that they completely lack the photosynthesis apparatus, supporting the hypothesis that the acquisition of the photosystem in photosynthetic cyanobacteria happened after divergence from the non-photosynthetic Melainabacteria (Soo et al., 2014, 2017). All representatives of Melainabacteria are thought to be able to perform fermentation and some are thought to be capable of anaerobic and aerobic respiration (Di Rienzi et al., 2013; Soo et al., 2014, 2017). Some Melainabacteria in the Caenarcaniphilales, Vampirovibrionales, and Obscuribacterales orders are also capable of aerobic respiration under both high and low oxygen conditions (Soo et al., 2017). This ability has been acquired after the evolution of oxygenic photosynthesis in the sister-clade photosynthetic cyanobacteria (Shih et al., 2016; Soo et al., 2017). The Gastranaerophilales are found in human and other animal guts and although their exact role is unknown, they are thought to have a beneficial effect for their hosts by aiding digestion and as a source of vitamins B and K (Di Rienzi et al., 2013). Some Gastranaerophilales are flagellated, but other representatives appear to have only a subset of the necessary genes for encoding a functional flagellum (Soo et al., 2014). The Gastranaerophilales and Caenarcaniphilales seem to lack the genes for anaerobic and aerobic respiration, suggesting that they support their metabolism by fermentation only (Soo et al., 2014). *Vampirovibrio chlorellavorus* (previously assigned to genus *Bdellovibrio*) is a predatory bacterium that was originally described in 1972, and which was first suggested being a member of the Deltaproteobacteria (Gromov and Mamkaeva, 1972). This bacterium was recently isolated from a 36-year old co-culture sample of *Chlorella vulgaris* lyophilised cells (NCBI 11383) (Coder and Starr, 1978) and whole genome sequencing confirmed the position of *Vampirovibrio* in the class Melainabacteria (order Vampirovibrionales) part of phylum Cyanobacteria (Soo et al., 2015). *V. chlorellavorus* predates on *Chlorella* cells and, consistently with other classes of Melainabacteria, it lacks the genes for carbon fixation and photosynthesis (Soo et al., 2014).

In this study, we used a dataset consisting of 16S rDNA sequences obtained from high-throughput amplicon sequencing of samples collected in sediment cores from ten lakes, spanning ∼100 years (from ∼1900 to present), to study the diversity and distribution of NCY over the Anthropocene in the European peri-Alpine region. Lake sediments are well known to constitute rich archives of information about freshwater pelagic communities, in terms of both species resting stages and biomolecules (Gregory-Eaves and Beisner, 2011). Sedimentary DNA (sedDNA) in particular has been instrumental in reconstructing past community composition of various plankton forms, such as bacteria, phyto- and zooplankton, as well as microbial eukaryotes (Domaizon et al., 2017). Cyanobacteria were found to be well preserved in deep hard-water lakes (Domaizon et al., 2013; Monchamp et al., 2016). We have demonstrated previously that the reconstruction of cyanobacterial community structure and phylogenetic diversity using sedDNA, amplification, and sequencing relates almost 1:1 to pelagic microscopic counts from lakes over the past 40 years (Monchamp et al., 2016). Here, we used 16S rDNA sequences from sedimentary archives to investigate changes in NCY prevalence and community composition over time across our panel of ten lakes. Since we were only interested in the diversity of environmentally associated NCY, we present the composition of all groups of NCY, but exclude the gut-associated Gastranaerophilales order from the diversity analyses. Additionally, we tested for changes in community similarity across lakes and geographic distances to infer patterns of NCY dispersal at the regional scale. Results are discussed in comparison with previously observed community changes in photosynthetic cyanobacterial assemblages in the same lake samples (Monchamp et al., 2018a).

TABLE 1 | List of Melainabacteria and Sericytochromatia representatives and the type of environment in which they have been found.

Class	Order	Environment	Reference
Melainabacteria	Gastranaerophilales	Human fecal samples	Qin et al., 2010; Soo et al., 2014
	Gastranaerophilales	Koala fecal samples	Soo et al., 2014
	Gastranaerophilales	Soil sample	McGorum et al., 2015
	Obscuribacterales	Activated sludge from a batch (aerobic) reactor performing enhanced biological phosphorus removal (EBPR)	Soo et al., 2014
	Obscuribacterales	Plant washing; horse ileal content; soil sample	McGorum et al., 2015
	Obscuribacterales	Aquifer	Wrighton et al., 2012; Di Rienzi et al., 2013
	Caenarcaniphilales	Anaerobic reactor treating a high-strength organic wastewater	Soo et al., 2014
	Caenarcaniphilales	Freshwater lakes (epilimnion)	Soo et al., 2017; Salmaso et al., 2018
	Vampirovibrionales Vampirovibrionales	*Chlorella vulgaris* culture *Chlorella* in commercial ponds	Soo et al., 2015; Ganuza et al., 2016
	Vampirovibrionales	Multiisolate	Soo et al., 2017
Sericytochromatia (ML635J-21)	NA	Plant washing; soil sample; marine and lacustrine sediments	McGorum et al., 2015
	NA	Freshwater lakes (epilimnion) marine surface water samples (uncultured marine bacteria)	Gies et al., 2014; Salmaso et al., 2018
	NA	Subsurface groundwater	Soo et al., 2017

MATERIALS AND METHODS

Data Collection

We used the high-throughput MiSeq (Illumina) data from (Monchamp et al., 2018a), consisting of 16S rDNA cyanobacterial sequences obtained from sequencing of 107 DNA samples spanning over ∼100 years of sedimentary archives from 10 lakes located around the European Alps (**Supplementary Tables S1, S2**). These lakes have been chosen based on their geographic location, their eutrophication history, and because they cover a wide gradient of trophic levels and morphological characteristics (**Supplementary Table S1**). History of these lakes is well known due to monitoring programs carried out by various governmental and institutional agencies over the last two to six decades (Monchamp et al., 2018a). The lakes are located at altitudes between 194 and 463 m above sea level (mean = 369, median = 400.5), with differences between altitudes of less than 300m. Therefore, relative to their environmental change history and physico-chemical properties, we did not consider altitude as an important factor for our study. Due to the natural formation of annual varves over the last century in the deep hard-water lakes studied, dating could be performed at high (yearly) temporal resolution in most cases. In addition, the cores were dated based on lead and cesium radioisotope (^{210}Pb, ^{137}Cs) measurements (see Monchamp et al., 2018a).

The study is based on environmental DNA, i.e., both extracellular and intracellular DNA that is preserved in lake sediments. The raw sequences are publically available in the European Nucleotide Archive repository; https://www.ebi.ac.uk/ena under the project number PRJEB21329. The amplified region of approximately 400 bp in length (range = 370–415 bp, mean = 386.2 bp) covers part of the V3–V4 regions of the 16S gene. A large proportion of the sequences (almost 20%) were classified as part of the Cyanobacteria phylum, but did not belong to photosynthetic cyanobacteria. These sequences were highly related to the Melainabacteria and ML635J-21 (Sericytochromatia) groups in the Greengenes database (DeSantis et al., 2006). Here, we used this subset of sequence data to investigate the alpha and beta diversity of NCY in the ten lakes.

All details related to sediment sampling, sample processing, DNA extraction, PCR amplification, and sequencing are described in our previous work (Monchamp et al., 2016, 2018a). One or two cores from each lake were opened longitudinally and sediment samples were collected at various depths based on the age models. Sediments were then transferred to a clean lab facility where DNA was extracted using the PowerSoil DNA Isolation Kit (Mo Bio Laboratories). We performed two DNA extractions per layer and pooled the two extracts to increase homogeneity of sampling. This pooled sedDNA was used in PCR reactions (three separate PCR per sample) using the pair of cyanobacteria-specific primers CYA359-F and CYA784-R (Nübel et al., 1997; DeSantis et al., 2006) attached to individual tags of 10–12 nucleotides (Monchamp et al., 2018a). The purified extracts were then pooled in equimolar concentration in a single library which was sent to the sequencing facility (Fasteris, Geneva, Switzerland) for adaptor ligation and sequencing on an Illumina MiSeq platform.

Sequence Data Processing

Briefly, the raw 16S rDNA sequences were quality controlled using the workflow developed at the Genetic Diversity Centre, ETH Zürich as described elsewhere (Monchamp et al., 2016, 2018a). After quality filtering, primer trimming and size selection, the amplicons were clustered into operational taxonomic units (OTUs) following the UPARSE workflow (Edgar, 2013), based on an abundance threshold of 5, and a minimum sequence similarity of 97%. The taxonomic assignment of OTUs was done with a confidence threshold of 89% based on the Greengenes database (DeSantis et al., 2006; Monchamp et al., 2016) using PyNAST (McDonald et al., 2012). The latter database was chosen because it was found to comprise a broad range of representatives in phylum

Cyanobacteria, including the NCY groups (Monchamp et al., 2016). The alignment was finally imported in FastTree (Price et al., 2010) to infer a phylogeny based on maximum-likelihood.

The reference OTUs FASTA sequences, the tree file, and the taxonomic assignment file were imported in the software R (R Development Core Team, 2016) version 3.3.2, using the package "phyloseq" in Bioconductor (McMurdie and Holmes, 2013). The dataset was filtered to retain only the NCY OTUs. Of these, twenty-nine were assigned to the deepest-branching clade Sericytochromatia, thirty OTUs were assigned to Melainabacteria (two Vampirovibrionales, six Obscuribacterales, and twenty-two Gastranaerophilales), and four NCY OTUs were not assigned to a class. The trees in **Figures 1**, **2** are representations of all of the NCY OTUs recovered (63 in total). The phylogeny was inferred based on neighbor joining with bootstrap analysis (100 replicates) using the alignment program MAFFT (Katoh and Standley, 2013) and visualized and annotated with the online program iTOL (Letunic and Bork, 2016). OTUs that were found in less than two samples over the whole dataset were excluded from the diversity analyses to reduce biases associated to rare taxa and to possible sequencing errors.

A small number of physiological traits have been previously attributed to Melainabacteria and Sericytochromatia based on genome sequencing and analysis (Di Rienzi et al., 2013; Soo et al., 2014, 2017). We added information about respiration, photosynthesis, motility, and known predatory behavior to the phylogenetic tree of OTUs for reference (**Figure 1**). Note that this list of traits is an extrapolation of the information based on genome sequencing of a small subset of Melainabacteria representatives, thus the definitive presence or absence of the listed traits in the OTUs found in the present study cannot be confirmed.

Compositional and Phylogenetic Diversity Analyses

For the diversity analyses, we used all OTUs assigned to Sericytochromatia, as well as the Melainabacteria representatives that are generally associated with environmental samples [i.e., the orders Vampirovibrionales (SM1D11) and Obscuribacterales (mle1-12)]. We excluded the order Gastranaerophilales that is associated with gut samples as it was considered irrelevant to the present study aiming at describing the diversity of NCY lake communities. Our dataset did not include representatives of the Caenarcaniphilales order.

Using this reduced dataset, we assessed the diversity and community composition of NCY within and across the 10 peri-Alpine lakes over ∼100 years. In order to estimate indices of alpha and beta diversity that can be used for comparisons, samples were rarefied to even sequencing depth (201 reads per sample) using the *rarefy_even_depth* function in "phyloseq." This coverage retained a high number of samples, and was sufficient to cover a high percentage of OTU richness in the majority of samples (**Supplementary Table S3** and **Supplementary Figure S1**). We used linear ordinary least square (OLS) regression to determine the significance of variation in the log-transformed rarefied OTU richness over time within the lakes. Hierarchical clustering of taxa for pattern detection was performed by calculating Euclidian distances on OTU prevalence in the lakes over time. The dendrogram was constructed by average linkage method and the color-coded image map produced in CIMminer (Weinstein et al., 1997).

For calculating beta diversity between communities across all lakes and between time periods, the rarefied samples were binned into 10-year blocks (to accommodate for the number of samples available at given years and the dating precision). A distance matrix based on phylogenetic dissimilarity (Unifrac distances) across all samples at each period was calculated. The "adonis" function in the "vegan" package (Oksanen et al., 2013) was used to apply PERMANOVA (Anderson, 2001) to verify temporal and spatial (lake and region) effects on the dissimilarity between groups. If a lake sediment core was sampled at two depths that were grouped in the same period of time (e.g., years 1992 and 1997), the pairwise distance between the two samples was excluded from the dissimilarity estimation (to remove the internal turnover effect within lakes). We used the package "Imap" version 1.32 for producing a matrix of pairwise geographic distances between lakes (**Supplementary Table S2**). This distance matrix was used for assessing the distance-decay relationship for all community phylogenies in each decade over the twentieth century. For comparison with the photosynthetic cyanobacteria communities, we used data from (Monchamp et al., 2018a,b). The data was insufficient to estimate the distance-decay relationship between NCY communities in the 1900s and the 2010s. Because the assumption of independence is violated when using multiple pairwise comparisons, the significance of the distance-decay curves at each time period was assessed by a Mantel (Mantel, 1967) permutational test (with 999 repetitions) between distance matrices using the package "ade4" for R.

RESULTS

Composition and Phylogenetic Diversity of Non-photosynthetic Cyanobacteria

Our rarefied dataset of Sericytochromatia and Melainabacteria comprised of 63 taxa distributed in 66 samples. The neighbor joining tree of all 16S rDNA reference sequences (OTUs) recovered from the sediments of the ten peri-Alpine lakes is shown in **Figure 1**. The two lineages Sericytochromatia and Melainabacteria are well supported by the bootstrap values. **Figure 2** shows the same phylogeny as in **Figure 1** together with a table showing the distribution of the OTUs in each lake.

Richness Change Over Time

All the following analyses are based on the reduced dataset where the gut-associated lineage Gastranaerophilales, not considered relevant for the present environmental survey, was excluded. They comprised about 1/3 of all NCY taxa so, after exclusion of Gastranaerophilales, the final rarefied data comprised 40 taxa in 66 samples. The majority of OTUs (30) were assigned to class Sericytochromatia, and the Melainabacteria OTUs mostly belonged to the Obscuribacterales order (5 OTUs). A single

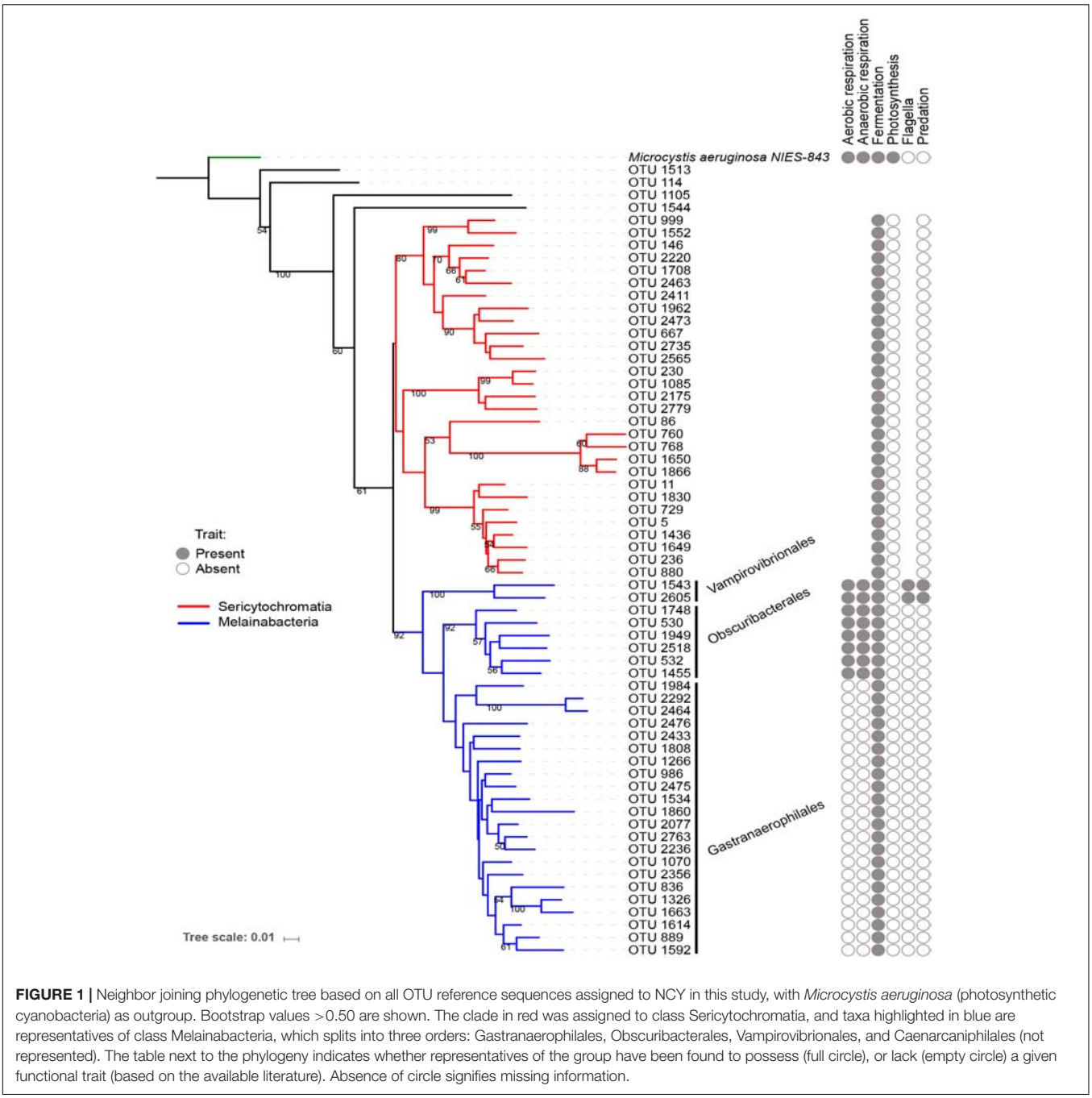

FIGURE 1 | Neighbor joining phylogenetic tree based on all OTU reference sequences assigned to NCY in this study, with *Microcystis aeruginosa* (photosynthetic cyanobacteria) as outgroup. Bootstrap values >0.50 are shown. The clade in red was assigned to class Sericytochromatia, and taxa highlighted in blue are representatives of class Melainabacteria, which splits into three orders: Gastranaerophilales, Obscuribacterales, Vampirovibrionales, and Caenarcaniphilales (not represented). The table next to the phylogeny indicates whether representatives of the group have been found to possess (full circle), or lack (empty circle) a given functional trait (based on the available literature). Absence of circle signifies missing information.

OTU was assigned to Vampirovibrionales, and four OTUs were not assigned to a class. The richness of environmentally associated NCY OTUs did not increase significantly over the last century across the studied lakes (n = 66, p > 0.3; **Figure 3**). Lake Annecy was the only exception where the richness of NCY increased significantly over time (R^2 = 0.86, p = 0.003, n = 7).

Temporal Changes in OTU Prevalence

Clustering of NCY OTUs highlights five groups (**Figure 4**). Cluster I comprises of four OTUs that were prevalent in the lakes at all time-periods. Representatives of this cluster are all affiliated to class Sericytochromatia. Cluster II shows a large number of OTUs that appear to be randomly distributed and that were never found in high prevalence across the ten lakes. Cluster III comprises of rare and isolated OTUs, and cluster IV highlights a group of OTUs that were generally more prevalent in older times compared to the last 3–4 decades. Most of the latter OTUs were also found in recent sediment, but they were less common across the region. They are mainly representatives of the Sericytochromatia class, and one OTU is assigned

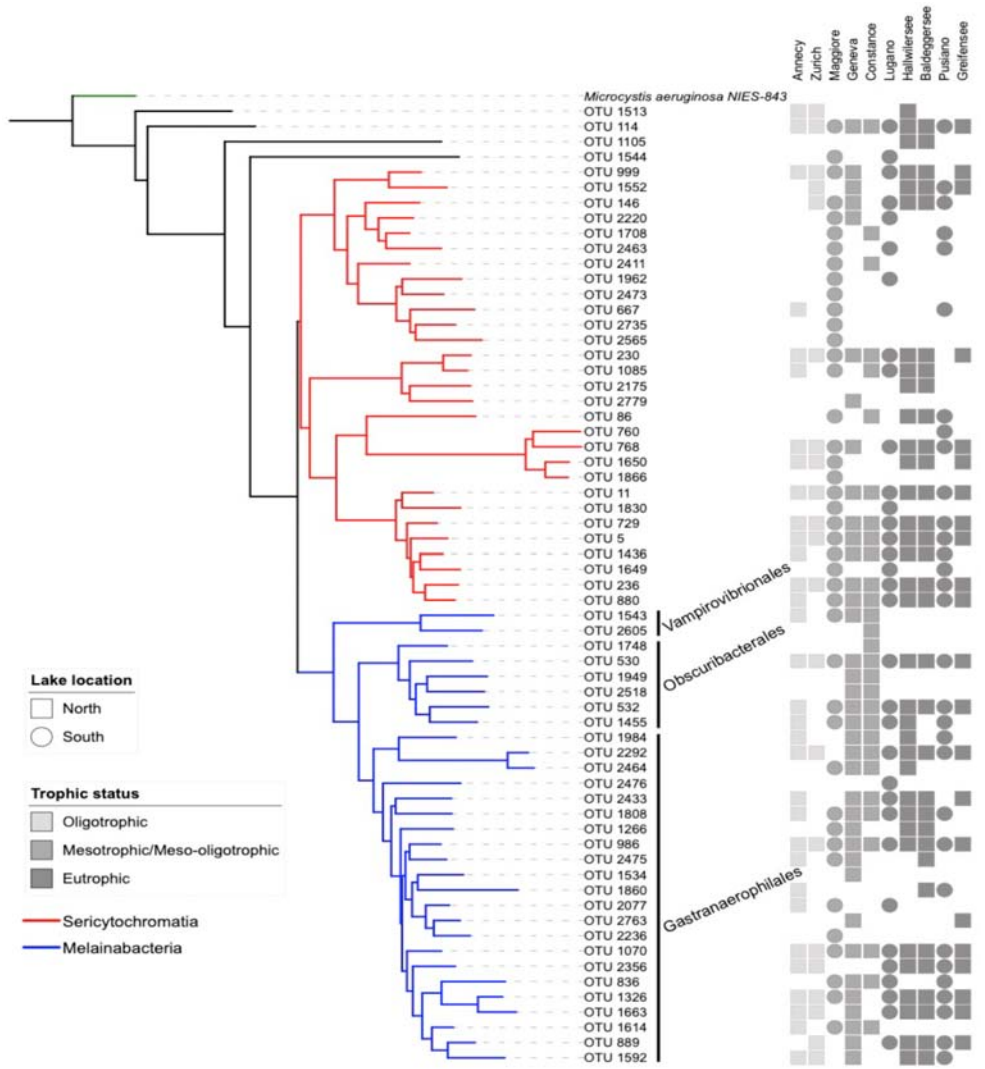

FIGURE 2 | Neighbor joining phylogenetic tree based on all OTU reference sequences assigned to NCY in this study (same as **Figure 1**), with *M. aeruginosa* (photosynthetic cyanobacteria) as outgroup. The table next to the phylogeny summarizes the OTU composition in each lake (detected; full shape, not detected; no shape). The shades of gray refer to the lake's trophic status and the shapes refer to the location of the lakes relative to the Alpine mountain range (square; north, circles; south).

to Obscuribacterales. Finally, cluster V is composed of two Sericytochromatia representatives, and one unidentified OTU, which is most likely associated with class Sericytochromatia (ML635J-21) considering its position in the phylogeny (see OTU 114 in **Figure 1**). Interestingly, OTUs in Cluster V show the opposite pattern observed in Cluster IV: they became more common across the region since the 1940s (**Figure 4**).

Temporal and Regional Change in Similarity

Between-lake phylogenetic similarity (based on Unifrac distances) in NCY communities at each decade between the 1940s and 1970s was mostly stable, with a slight increase starting from the 1980s onward (**Figure 5**). PERMANOVA, however, did not support a temporal effect over the NCY assemblages during the time span covered by our analysis (i.e., 1940s−2000s; **Table 2**). Interestingly, no significant discrimination of community similarity was detected in NCY assemblages also north–south of the Alps. PERMANOVA supported a lake effect in phylogenetic community similarity, suggesting a significant lake-specificity of NCY communities (**Table 2**). The community Unifrac similarity values obtained for each pairwise set of samples plotted against geographic distance revealed no significant distance-decay curve at all time-periods in NCY communities (**Figure 6A**). The relationship across all pairs of communities at each decade was additionally tested using compositional similarity (Jaccard distances based on presence-absence of OTUs) (**Figure 6B**).

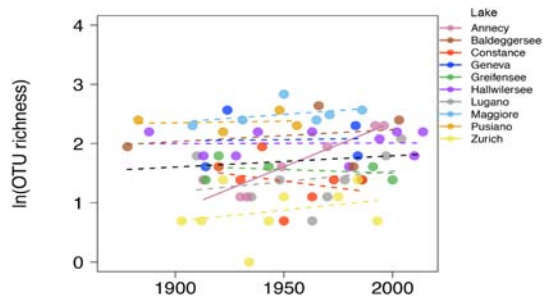

FIGURE 3 | Natural log-transformed OTU richness of NCY associated with environmental samples over time in the ten lakes. The dashed lines show the non-significant linear fit for each lake, and the full line (Lake Annecy only) shows a significant OLS fit (R^2 = 0.862, p = 0.003, n = 7). The OLS fit over all observations (n = 66) is not significant at the p = 0.05 level (black dashed line).

Also in this latter case, there was no significant relationship between compositional similarity in NCY and geographic distance.

DISCUSSION

Little is known about the recently discovered clades of NCY in nature. The class Sericytochromatia is the least understood since only three genomes have been sequenced (Soo et al., 2017). The ecological function and the niche occupied by NCY are currently unknown. As reviewed in the introduction, it appears that NCY might be present in both photic and aphotic habitats, with no clear associations between clades and particular environments. Both Melainabacteria and Sericytochromatia have been found in surface waters, including lakes, and algal biofilms (Quast et al., 2013; Gies et al., 2014; Soo et al., 2017; Salmaso et al., 2018). It appears plausible that, like photosynthetic cyanobacteria, Melainabacteria and Sericytochromatia are aquatic life forms. In this study, we found members of NCY at every depth of the sediment cores and in all the peri-Alpine lakes investigated. It could be hypothesized that these organisms are also able to thrive in sediment layers, given their ability to grow under anoxic conditions (Soo et al., 2017). We, however, consider the possibility that this organisms' habitat is actually the sediment

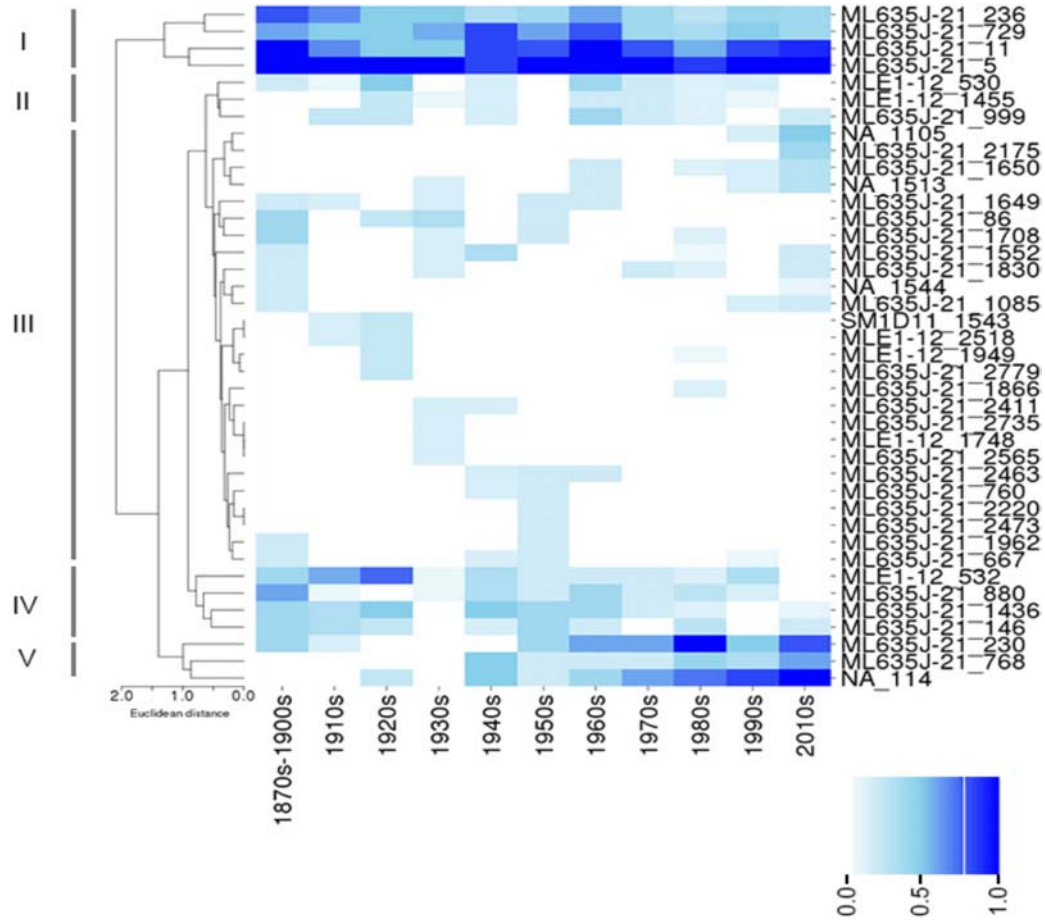

FIGURE 4 | Color-coded map showing the prevalence (i.e., the proportion of lakes where an OTU was found at a given time period) of Sericytochromatia (ML635J-21), Obscuribacterales, and Vampirovibrionales in the lakes between the 1870s and the 2010s. Hierarchical clustering was based on Euclidian distances based on prevalence of OTUs and revealed five main clusters: I–V (see section "Results"). The absence of an OTU at a given time period is depicted by a white box, and the gradient of color is proportional to the prevalence of an OTU in the group of lakes sampled at a given time period.

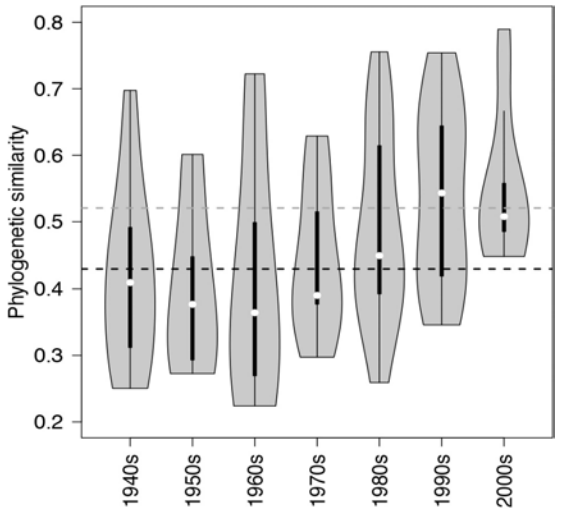

FIGURE 5 | Violin plots showing the probability density of phylogenetic similarities (overall range, interquartile ranges and median – based on Unifrac) among lake communities of NCY at each decade from the 1940s to the 2000s. The horizontal dashed lines, representing the mean similarity value across all observations for each group of cyanobacteria (black for photosynthetic cyanobacteria from Monchamp et al. (2018a); dark gray for NCY), are shown for reference.

quite unlikely, given the documented presence of NCY in aquatic environments (**Table 1**). For example, recent evidence suggests that NCY tend to be more prevalent during summer and autumn in the deep, peri-Alpine, and meso-oligotrophic lake Garda (Salmaso et al., 2018). More explorative studies and genome sequencing are needed to shed light on the actual ecology of these bacteria. Here, we consider sediment layers as archives for bacteria living in the lake water and we discuss our findings in terms of changes in NCY assemblages over time.

The topology of our reconstructed phylogenetic tree (**Figure 1**) reflected the relationships among taxa that were expected from previous work (Di Rienzi et al., 2013; Soo et al., 2014, 2017; Fischer et al., 2016a): we found a clear separation between the Sericytochromatia, Melainabacteria, and photosynthetic cyanobacteria. The number of NCY OTUs recovered from the sedimentary archive of peri-Alpine lakes was much lower in comparison to the richness of photosynthetic cyanobacteria determined previously in the same lakes (Monchamp et al., 2018a). Most of the OTUs were assigned to the deepest-branching paraphyletic group, the Sericytochromatia, and to the Melainabacteria order Gastranaerophilales. As mentioned earlier, the latter OTUs were not retained for further analysis because of their association mostly with guts and feces samples (Di Rienzi et al., 2013; Quast et al., 2013). Gastranaerophilales diversity and distribution in our samples also appears to be purely random, suggesting that their presence in lakes might be the result of release from local point sources, for example via run-off from land, wastewater, or excretions by wild animals and livestock in the lake watershed.

Our results describing the long-term composition and phylogenetic diversity of NCY assemblages in peri-Alpine lakes represent the earliest attempt to explore the distribution of these microorganisms across large spatial and temporal scales, and to investigate their change over broad environmental gradients. Our studied lakes have in fact been characterized by a well-documented history of climate warming and eutrophication, which have led to significant changes in the composition and assembly of photosynthetic cyanobacterial communities (Monchamp et al., 2018a,b). Unlike photosynthetic cyanobacteria, which have increased their diversity at the local and regional scale over the past century (Monchamp et al., 2018a), the richness of environmentally associated NCY did not significantly increase over time, with the exception of Lake Annecy. We have no information to interpret the interesting pattern detected in Lake Annecy. We have no evidence for methodological biases specific for this lake, and neither for directional environmental drivers that are unique to Lake Annecy, which was the most pristine lake in our dataset and it has been impacted by only weak anthropogenic changes over the past century (Monchamp et al., 2018a). No change in community structure, however, suggests that NCY live in a relatively stable lake environment, either in terms of species composition (if they depend on other organisms for growth) or in terms of water physics and chemistry. This is a puzzle, given the evidence for seasonality in NCY dynamics in Lake Garda (Salmaso et al., 2018), and the clear changes in trends and seasonality of lake environments over the past century (Adrian et al., 2009; Smith and Schindler, 2009; Rigosi et al., 2014; Salmaso et al., 2015; Yankova et al., 2017; Monchamp et al., 2018a).

Our results suggest that NCY communities are not shaped by the same environmental drivers as photosynthetic cyanobacteria, and that their composition is most likely lake-dependent (**Table 2**). We have previously observed that, in the same lakes,

TABLE 2 | Test of the effects of temporal and spatial factors on community phylogenetic similarities of NCY and photosynthetic cyanobacteria [the latter from Monchamp et al. (2018a,b)], determined by PERMANOVA*.

	Non-photosynthetic cyanobacteria			Photosynthetic cyanobacteria		
	DF	*Pseudo-F*	*p*	*DF*	*Pseudo-F*	*p*
Temporal (decades)	8	1.2031	0.211	7	1.7684	**0.001**
Regional (north-south)	1	1.8719	0.1042	1	3.381	**0.0004**
Local (lake)	9	3.6927	**0.0001**	9	2.6669	**0.001**

*p-Values are based on 9,999 permutations, bold face indicates statistical significance ($p < 0.05$), DF, degree of freedom. Samples dated to years between the 1940s and the 2010s were used. *PERMANOVA, Permutational Multivariate Analysis of Variance using Distance Matrices.*

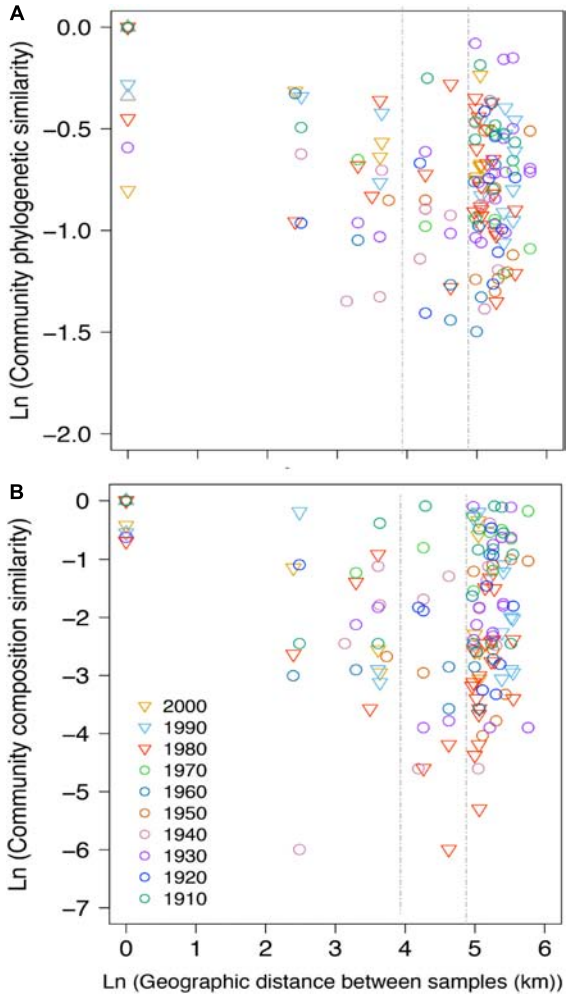

FIGURE 6 | Distance-decay plot showing the natural log-transformed pairwise **(A)** phylogenetic distances (based on Unifrac) calculated among all pairwise communities of NCY and **(B)** community composition similarity (based on Jaccard) at each decade (color-coded) between the 1910s to the 2000s (insufficient pairwise comparisons for the 1900s and 2010s). Each point represents the pairwise natural log-transformed distance between communities plotted against the natural log-transformed geographic distance. A null geographic distance signifies that the pairwise phylogenetic similarity was calculated between samples from the same lake corresponding to the same time-period. The two vertical dashed lines mark 50 and 130 km distances for reference. The absolute geographic distances between lakes (in km) are shown in **Supplementary Table S2**.

the richness and composition of photosynthetic cyanobacterial assemblages were significantly explained by the interaction between warming and eutrophication, with climate change being the strongest driver (Monchamp et al., 2018a,b). PERMANOVA confirmed that photosynthetic cyanobacterial phylogenetic diversity is strongly influenced by temporally changing drivers (Monchamp et al., 2018a,b), and suggest that both local (lake) and regional (north–south) environments play a significant role in shaping composition of these assemblages (**Table 2**). NCY communities did not show significant temporal dynamics at the decadal scale, and therefore no signs of correlation with temporally changing environmental conditions (**Table 2**). Similarly, we found no significant effect of regional drivers, like climatic difference between north and south of the Alps (**Table 2**). We found, however, a significant lake effect on the phylogenetic distance estimated between each pair of NCY communities. Since we did not detect dispersal limitation between lakes, neither for NCY (**Figure 6**) nor photosynthetic cyanobacteria (**Supplementary Figure S2**; Monchamp et al., 2018b), our results suggest that local features of lakes are important determinants of community structure in Sericytochromatia and Melainabacteria.

We can only speculate about what the above-mentioned lake features could be. If we assume that NCY thrive in the water-column, as suggested by previous work (Salmaso et al., 2018), it is possible that lake depth, volume, retention time, mixing regime, trophic state and/or catchment characteristics are important factors influencing the composition and diversity of these microorganisms' communities. Between-lake phylogenetic similarity (based on Unifrac distances) in NCY communities was higher than the average similarity estimated between lakes for photosynthetic cyanobacterial communities (**Figure 5**; Monchamp et al., 2018a). This could indicate that within-lake factors have, however, a weaker effect on the community composition of NCY than they have on photosynthetic cyanobacterial community change. Understanding of environmental factors driving the diversity and distribution of NCY strongly requires follow up surveys, such as the monitoring of several lakes of different characteristics over depth profiles, and during seasonal succession (Salmaso et al., 2018). It has been suggested that the scale of sampling might be relevant to determine the relative influence of local factors versus environmental gradients (Martiny et al., 2006). Extending our survey of NCY diversity to a larger region might also reveal patterns associated with changes in climate that could not emerge from our peri-Alpine study, or of other environmental gradients that may have played a significant role in the establishment of NCY clades in different lakes and regions. Another important aspect that could not be addressed in our study is the abundance of NCY in lakes, to evaluate their importance for microbial ecosystem functioning.

CONCLUSION

Eutrophication and climate warming have been strong environmental drivers during the Anthropocene, impacting lake ecosystem processes (Adrian et al., 2009; Smith and Schindler, 2009) and cyanobacterial community assembly (O'Neil et al., 2012; Rigosi et al., 2014; Huisman et al., 2018; Monchamp et al., 2018a,b). Our study suggests that NCY communities have been unaffected by large-scale anthropogenic environmental change. The lack of decay in phylogenetic similarity over time and over geographic distance across lake communities suggests temporally stable communities with no limitation to dispersal at the regional (peri-Alpine) scale. This is consistent with most reports about microbial dispersal, which rarely showed evidence for geographic distance-decay patterns at the local

(0–100 km) and regional (101–5,000 km) scales (Hanson et al., 2012). As previously reported (Monchamp et al., 2018b), the dissimilarity of communities over geographic distance was also non-significant in photosynthetic cyanobacterial assemblages (**Supplementary Figure S2**). Being temporally stable and lake specific, NCY assemblages could perhaps be used in future studies as an internal lake reference, to which compare patterns of other ecological communities under suspected environmental forcing.

Our study represents an initial exploratory survey of the composition and diversity of ecologically unknown clades of NCY. Our results uncover the diversity of these currently cryptic organisms, which might play a role in lake biogeochemistry. High-throughput sequencing of environmental DNA has the potential to illuminate the ecological niche of these understudied and uncultivable groups of NCY, at the local as well as over large geographic scales. In combination with genome sequencing, diversity surveys and possibly outdoors experiments will help gain understanding on the ecology, evolution and function of these microbes in their natural environment.

AUTHOR CONTRIBUTIONS

M-EM, FP, and PS designed the study. M-EM performed the sampling, laboratory work, and data analysis. M-EM and FP wrote the manuscript, which was reviewed and commented by PS.

FUNDING

This work was supported by the Swiss Enlargement Contribution; project IZERZ0 – 142165, "CyanoArchive" to PS, in the framework of the Romanian-Swiss Research Programme.

ACKNOWLEDGMENTS

High-throughput sequencing was performed at Fasteris sequencing company in Geneva (Switzerland). We thank Jean-Claude Walser (Genetic Diversity Centre, ETH Zürich) for bioinformatics support, and Marco Thali (Eawag) for his help with the sequencing library preparation. We thank Alois Zwyssig, Alfred Lück, Adrian Gilli, Patrick Turko, Nathalie Dubois, and Andrea Lami for help in the field, and Isabelle Domaizon and Cécile Chardon for providing sedimentary DNA samples from lakes Geneva and Annecy. We also thank the three referees for their constructive comments.

SUPPLEMENTARY MATERIAL

The Supplementary Material for this article can be found online at: https://www.frontiersin.org/articles/10.3389/fmicb.2018.03344/full#supplementary-material

REFERENCES

Adrian, R., O'reilly, C. M., Zagarese, H., Baines, S. B., Hessen, D. O., Keller, W., et al. (2009). Lakes as sentinels of climate change. *Limnol. Oceanogr.* 54, 2283–2297. doi: 10.4319/lo.2009.54.6_part_2.2283

Anderson, M. J. (2001). A new method for non parametric multivariate analysis of variance. *Austral Ecol.* 26, 32–46.

Coder, D. M., and Starr, M. P. (1978). Antagonistic association of the chlorellavorus bacterium (*"Bdellovibrio chlorellavorus"*) with *Chlorella vulgaris*. *Curr. Microbiol.* 1, 59–64. doi: 10.1007/BF02601710

DeSantis, T. Z., Hugenholtz, P., Larsen, N., Rojas, M., Brodie, E. L., Keller, K., et al. (2006). Greengenes, a chimera-checked 16S rRNA gene database and workbench compatible with ARB. *Appl. Environ. Microbiol.* 72, 5069–5072. doi: 10.1128/AEM.03006-05

Di Rienzi, S. C., Sharon, I., Wrighton, K. C., Koren, O., Hug, L. A., Thomas, B. C., et al. (2013). The human gut and groundwater harbor non-photosynthetic bacteria belonging to a new candidate phylum sibling to Cyanobacteria. *eLife* 2:e01102. doi: 10.7554/eLife.01102

Domaizon, I., Savichtcheva, O., Debroas, D., Arnaud, F., Villar, C., Pignol, C., et al. (2013). DNA from lake sediments reveals the long-term dynamics and diversity of *Synechococcus* assemblages. *Biogeosci. Discuss.* 10, 2515–2564. doi: 10.5194/bgd-10-2515-2013

Domaizon, I., Winegardner, A., Capo, E., Gauthier, J., and Gregory-Eaves, I. (2017). DNA-based methods in paleolimnology: new opportunities for investigating long-term dynamics of lacustrine biodiversity. *J. Paleolimnol.* 58, 1–21. doi: 10.1007/s10933-017-9958-y

Edgar, R. C. (2013). UPARSE: highly accurate OTU sequences from microbial amplicon reads. *Nat. Methods* 10, 996–998. doi: 10.1038/nmeth.2604

Fischer, W. W., Hemp, J., and Johnson, J. E. (2016a). Evolution of oxygenic photosynthesis. *Annu. Rev. Earth Planet. Sci.* 44, 647–683. doi: 10.1146/annurev-earth-060313-054810

Fischer, W. W., Hemp, J., and Valentine, J. S. (2016b). How did life survive Earth's great oxygenation? *Curr. Opin. Chem. Biol.* 31, 166–178. doi: 10.1016/j.cbpa.2016.03.013

Ganuza, E., Sellers, C. E., Bennett, B. W., Lyons, E. M., and Carney, L. T. (2016). A novel treatment protects Chlorella at commercial scale from the predatory bacterium *Vampirovibrio chlorellavorus*. *Front. Microbiol.* 7:848. doi: 10.3389/fmicb.2016.00848

Gies, E. A., Konwar, K. M., Thomas Beatty, J., and Hallam, S. J. (2014). Illuminating microbial dark matter in meromictic Sakinaw Lake. *Appl. Environ. Microbiol.* 80, 6807–6818. doi: 10.1128/AEM.01774-14

Gregory-Eaves, I., and Beisner, B. E. (2011). Palaeolimnological insights for biodiversity science: an emerging field. *Freshw. Biol.* 56, 2653–2661. doi: 10.1111/j.1365-2427.2011.02677.x

Gromov, B. V., and Mamkaeva, K. A. (1972). Electron microscopic study of parasitism by *Bdellovibrio chlorellavorus* bacteria on cells of the green alga *Chlorella vulgaris*. *Tsitologiia* 14, 256–260.

Hanson, C. A., Fuhrman, J. A., Horner-Devine, M. C., and Martiny, J. B. H. (2012). Beyond biogeographic patterns: processes shaping the microbial landscape. *Nat. Rev. Microbiol.* 10, 497–506. doi: 10.1038/nrmicro2795

Huisman, J., Codd, G. A., Paerl, H. W., Ibelings, B. W., Verspagen, J. M. H., and Visser, P. M. (2018). Cyanobacterial blooms. *Nat. Rev. Microbiol.* 16, 471–483. doi: 10.1038/s41579-018-0040-1

Katoh, K., and Standley, D. M. (2013). MAFFT multiple sequence alignment software version 7: improvements in performance and usability. *Mol. Biol. Evol.* 30, 772–780. doi: 10.1093/molbev/mst010

Komárek, J., Kaštovský, J., Mareš, J., and Johansen, J. R. (2014). Taxonomic classification of cyanoprokaryotes (cyanobacterial genera) 2014, using a polyphasic approach. *Preslia* 86, 295–335.

Letunic, I., and Bork, P. (2016). Interactive Tree Of Life (iTOL): an online tool for phylogenetic tree display and annotation. *Nucleic Acids Res.* 44, 242–245. doi: 10.1093/nar/gkw290

Ley, R. E., Backhed, F., Turnbaugh, P., Lozupone, C. A., Knight, R. D., and Gordon, J. I. (2005). Obesity alters gut microbial ecology. *Proc. Natl. Acad. Sci. U.S.A.* 102, 11070–11075. doi: 10.1073/pnas.0504978102

Mantel, N. (1967). The detection of disease clustering and a generalized regression approach. *Cancer Res.* 13, 209–220.

Martiny, J. B., Bohannan, B. J. M., Brown, J. H., Colwell, R. K., Fuhrman, J. A., Green, J. L., et al. (2006). Microbial biogeography: putting microorganisms on the map. *Nat. Rev. Microbiol.* 4, 102–112. doi: 10.1038/nrmicro1341

McDonald, D., Price, M. N., Goodrich, J., Nawrocki, E. P., Desantis, T. Z., Probst, A., et al. (2012). An improved Greengenes taxonomy with explicit ranks for ecological and evolutionary analyses of bacteria and archaea. *ISME J.* 6, 610–618. doi: 10.1038/ismej.2011.139

McGorum, B. C., Pirie, R. S., Glendinning, L., Mclachlan, G., Metcalf, J. S., Banack, S. A., et al. (2015). Grazing livestock are exposed to terrestrial cyanobacteria. *Vet. Res.* 46, 1–10. doi: 10.1186/s13567-015-0143-x

McMurdie, P. J., and Holmes, S. (2013). Phyloseq: an R package for reproducible interactive analysis and graphics of microbiome census data. *PLoS One* 8:e61217. doi: 10.1371/journal.pone.0061217

Meola, M., Lazzaro, A., and Zeyer, J. (2015). Bacterial composition and survival on Sahara dust particles transported to the European alps. *Front. Microbiol.* 6:1454. doi: 10.3389/fmicb.2015.01454

Monchamp, M.-E., Spaak, P., Domaizon, I., Dubois, N., Bouffard, D., and Pomati, F. (2018a). Homogenization of lake cyanobacterial communities over a century of climate change and eutrophication. *Nat. Ecol. Evol.* 2, 317–324. doi: 10.1038/s41559-017-0407-0

Monchamp, M.-E., Spaak, P., and Pomati, F. (2018b). High dispersal levels and lake warming are emergent drivers of cyanobacterial community assembly over the Anthropocene in peri-Alpine lakes. *bioRxiv* [Preprint]. doi: 10.1101/419762

Monchamp, M.-E., Walser, J.-C., Pomati, F., and Spaak, P. (2016). Sedimentary DNA reveals cyanobacteria community diversity over 200 years in two peri-alpine lakes. *Appl. Environ. Microbiol.* 82, 6472–6482. doi: 10.1128/AEM.02174-16

Nübel, U., Garcia-Pichel, F., and Muyzer, G. (1997). PCR primers to amplify 16S rRNA genes from cyanobacteria. *Appl. Environ. Microbiol.* 63, 3327–3332.

Oksanen, J., Blanchet, F. G., Kindt, R., Legendre, P., Minchin, P. R., O'hara, R. B., et al. (2013). *vegan: Community Ecology Package. R Package Version 2.0-10*. Available at: http://CRAN.R-project.org/package=vegan

O'Neil, J. M., Davis, T. W., Burford, M. A., and Gobler, C. J. (2012). The rise of harmful cyanobacteria blooms: the potential roles of eutrophication and climate change. *Harmful Algae* 14, 313–334. doi: 10.1016/j.hal.2011.10.027

Price, M. N., Dehal, P. S., and Arkin, A. P. (2010). FastTree 2 – approximately maximum-likelihood trees for large alignments. *PLoS One* 5:e9490. doi: 10.1371/journal.pone.0009490

Qin, J., Li, R., Raes, J., Arumugam, M., Burgdorf, S., Manichanh, C., et al. (2010). A human gut microbial gene catalog established by metagenomic sequencing. *Nature* 464, 59–65. doi: 10.1038/nbt.3353

Quast, C., Pruesse, E., Yilmaz, P., Gerken, J., Schweer, T., Yarza, P., et al. (2013). The SILVA ribosomal RNA gene database project: improved data processing and web-based tools. *Nucleic Acids Res.* 41, 590–596. doi: 10.1093/nar/gks1219

R Development Core Team (2016). *R: A Language and Environment for Statistical Computing*. Vienna: R Foundation for Statistical Computing.

Rigosi, A., Carey, C. C., Ibelings, B. W., and Brookes, J. D. (2014). The interaction between climate warming and eutrophication to promote cyanobacteria is dependent on trophic state and varies among taxa. *Limnol. Oceanogr.* 59, 99–114. doi: 10.4319/lo.2014.59.1.0099

Rippka, R., Deruelles, J., Waterbury, J. B., Herdman, M., and Stanier, R. Y. (1979). Generic assignments, strain histories and properties of pure cultures of cyanobacteria. *J. Gen. Microbiol.* 111, 1–61. doi: 10.1099/00221287-111-1-1

Salmaso, N., Albanese, D., Capelli, C., Boscaini, A., Pindo, M., and Donati, C. (2018). Diversity and cyclical seasonal transitions in the bacterial community in a large and deep perialpine lake. *Microb. Ecol.* 76, 125–143. doi: 10.1007/s00248-017-1120-x

Salmaso, N., Capelli, C., Shams, S., and Cerasino, L. (2015). Expansion of bloom-forming *Dolichospermum lemmermannii* (Nostocales, Cyanobacteria) to the deep lakes south of the Alps: colonization patterns, driving forces and implications for water use. *Harmful Algae* 50, 76–87. doi: 10.1016/j.hal.2015.09.008

Shih, P. M., Hemp, J., Ward, L. M., Matzke, N. J., and Fischer, W. W. (2016). Crown group Oxyphotobacteria postdate the rise of oxygen. *Geobiology* 15, 19–29. doi: 10.1111/gbi.12200

Shih, P. M., Wu, D., Latifi, A., Axen, S. D., Fewer, D. P., Talla, E., et al. (2013). Improving the coverage of the cyanobacterial phylum using diversity-driven genome sequencing. *Proc. Natl. Acad. Sci. U.S.A.* 110, 1053–1058. doi: 10.1073/pnas.1217107110

Smith, V. H., and Schindler, D. W. (2009). Eutrophication science: where do we go from here? *Trends Ecol. Evol.* 24, 201–207. doi: 10.1016/j.tree.2008.11.009

Sogin, M. L., Morrison, H. G., Huber, J. A., Mark Welch, D., Huse, S. M., Neal, P. R., et al. (2006). Microbial diversity in the deep sea and the underexplored "rare biosphere". *Proc. Natl. Acad. Sci. U.S.A.* 103, 12115–12120. doi: 10.1073/pnas.0605127103

Soo, R. M., Hemp, J., Parks, D. H., Fischer, W. W., and Hugenholtz, P. (2017). On the origins of oxygenic photosynthesis and aerobic respiration in Cyanobacteria. *Science* 355, 1436–1440. doi: 10.1126/science.aal3794

Soo, R. M., Skennerton, C. T., Sekiguchi, Y., Imelfort, M., Paech, S. J., Dennis, P. G., et al. (2014). An expanded genomic representation of the phylum Cyanobacteria. *Genome Biol. Evol.* 6, 1031–1045. doi: 10.1093/gbe/evu073

Soo, R. M., Woodcroft, B. J., Parks, D. H., Tyson, G. W., and Hugenholtz, P. (2015). Back from the dead; the curious tale of the predatory cyanobacterium *Vampirovibrio chlorellavorus*. *PeerJ* 3:e968. doi: 10.7717/peerj.968

Weinstein, J. N., Myers, T. G., O'connor, P. M., Friend, S. H., Fornace, A. J., Kohn, K. W., et al. (1997). An information-intensive approach to the molecular pharmacology of cancer. *Science* 275, 343–349. doi: 10.1126/science.275.5298.343

Whitton, B. A., and Potts, M. (2002). *The Ecology of Cyanobacteria: Their Diversity in Time and Space*. New York, NY: KluwerAcademic Publishers. doi: 10.1007/0-306-46855-7

Wrighton, K. C., Thomas, B. C., Sharon, I., Miller, C. S., Castelle, C. J., Verberkmoes, N. C., et al. (2012). Fermentation, hydrogen, and sulfer metabolism in multiple uncultivated bacterial phyla. *Science* 337, 1661–1665. doi: 10.1126/science.1224041

Yankova, Y., Neuenschwander, S., Köster, O., and Posch, T. (2017). Abrupt stop of deep water turnover with lake warming: drastic consequences for algal primary producers. *Sci. Rep.* 7:13770. doi: 10.1038/s41598-017-13159-9

Conflict of Interest Statement: The authors declare that the research was conducted in the absence of any commercial or financial relationships that could be construed as a potential conflict of interest.

Copyright © 2019 Monchamp, Spaak and Pomati. This is an open-access article distributed under the terms of the Creative Commons Attribution License (CC BY). The use, distribution or reproduction in other forums is permitted, provided the original author(s) and the copyright owner(s) are credited and that the original publication in this journal is cited, in accordance with accepted academic practice. No use, distribution or reproduction is permitted which does not comply with these terms.

frontiers in Microbiology

ORIGINAL RESEARCH
published: 11 March 2019
doi: 10.3389/fmicb.2019.00454

Rare Plankton Subcommunities Are Far More Affected by DNA Extraction Kits Than Abundant Plankton

*Min Liu[1,2], Yuanyuan Xue[1,2] and Jun Yang[1]**

[1] Aquatic EcoHealth Group, Key Laboratory of Urban Environment and Health, Institute of Urban Environment, Chinese Academy of Sciences, Xiamen, China, [2] University of Chinese Academy of Sciences, Beijing, China

Advances in high-throughput sequencing technologies allow a more complete study of microbial plankton community composition and diversity, especially in the rare microbial biosphere. The DNA extraction of plankton is a key step for such studies; however, little is known about its influences on the abundant or rare microbial biosphere. Our aim was to quantify the influences of different DNA extraction kits on abundant and rare plankton in the surface waters of a reservoir and provide a reference for the comparisons between microbial community studies with different extraction methods. We evaluated the influence of five common commercial kits on DNA quality, microbial community diversity and composition, and the reproducibility of methods using both 16S and 18S rRNA genes amplicon sequencing. Our data showed that results of Fast DNA Spin Kit for Soil (MPF) had higher α diversity for bacteria and high DNA quality, indicating that it is the most suitable approach for bacterioplankton diversity study. However, DNeasy Blood & Tissue Kit (QD) and QIAamp DNA Mini Kit (QQ) methods could produce results that are easier to replicate for bacteria and eukaryotes, respectively, and were more comparable between studies. The use of different DNA extraction kits had larger influence on the rare taxa compared with abundant taxa. Therefore, the comparability between studies that employed different extraction methods can be improved by removing low-abundance or less-representative OTUs. Collectively, this study provides a comprehensive assessment of the biases associated with DNA extraction for plankton communities from a freshwater reservoir. Our results may guide researchers in experimental design choices for DNA-based ecological studies in aquatic ecosystem.

Keywords: DNA extraction, high-throughput sequencing, plankton, species diversity, community composition

OPEN ACCESS

Edited by:
Raju Sekar,
Xi'an Jiaotong-Liverpool University, China

Reviewed by:
Jian Yang,
China University of Geosciences, China
Yusuke Okazaki,
National Institute of Advanced Industrial Science and Technology (AIST), Japan

****Correspondence:***
Jun Yang
jyang@iue.ac.cn

Specialty section:
This article was submitted to Aquatic Microbiology, a section of the journal Frontiers in Microbiology

Received: *25 October 2018*
Accepted: *20 February 2019*
Published: *11 March 2019*

Citation:
Liu M, Xue Y and Yang J (2019) Rare Plankton Subcommunities Are Far More Affected by DNA Extraction Kits Than Abundant Plankton. Front. Microbiol. 10:454. doi: 10.3389/fmicb.2019.00454

INTRODUCTION

Recently, with the rapid development of sequencing technology DNA-based experiments have become routinely used to study the microbial community in various ecosystems (Shendure et al., 2017; Sinha et al., 2017; Knight et al., 2018). Microorganisms in aquatic ecosystems (i.e., oceans, rivers, lakes and reservoirs) which are some of the most studied ecosystems for their high microbial diversity, play key roles in biogeochemical processes (Liu et al., 2015; Sunagawa et al., 2015; Xue et al., 2018). Numerous studies have shown DNA-based approaches may provide unprecedented

insight into the dynamics of microbial communities, and reveal general principles about their ecology and mechanisms of community assembly. However, several technical limitations are still underexplored in acquiring the DNA from water samples and constitute a key constraint to the accuracy of the new findings (Deiner et al., 2015; Walden et al., 2017).

Generally, different DNA extraction methods are recommended based on the origin of the samples as there is not a single superior method which can be applied across all samples and microbes (Kuhn et al., 2017; Sinha et al., 2017; Walden et al., 2017). Studies have showed suitable extraction methods for specific samples such as human fecal (Costea et al., 2017), soil protist (Santos et al., 2015, 2017) and fish (Eichmiller et al., 2016). The variable structure of microbial cell walls can lead to a misrepresentation of specific microbial taxa, increasing the difficulty of data comparison between studies (Cabeen and Jacobs-Wagner, 2005; Santos et al., 2017). So far, few researches have evaluated the influences of different extraction methods on bacterial and eukaryotic plankton communities, respectively (Eland et al., 2012; Albertsen et al., 2015; Li et al., 2015; McCarthy et al., 2015; Walden et al., 2017). Further, we have very limited knowledge how DNA extraction methods influence the plankton community of bacteria and eukaryotes together, with an emphasis on the comparison between abundant and rare plankton.

An important aspect that should be considered is the influence of DNA extraction methods on the rare biosphere of the microbial community. The study of these rare taxa has become a very active research area, due to the development of fast and cheap high-throughput sequencing and their important and unknown ecological roles (Sogin et al., 2006; Pedrós-Alió, 2012; Liu et al., 2015, 2017, 2019; Lynch and Neufeld, 2015; Xue et al., 2018). However, until now, only a few studies have evaluated the influences of DNA extraction kits on rare taxa (**Supplementary Table S1**). Limited studies have showed that kits contamination of different methods may be different and would have a high influence on microbial samples with low biomass (Salter et al., 2014; Velásquez-Mejía et al., 2018). To better compare results collected from different research groups or studies, the evaluation of the influence of DNA extraction methods on taxa in different relative abundances is an urgent call.

The reproducibility of each DNA extraction method is another important aspect which should be considered and assessed. The reproducibility has a very important role in comparing data from different studies, labs, or even within the same study (Zhou et al., 2011; Sinha et al., 2017). Here we collected one surface water sample from a subtropical reservoir, and systematically tested how distinct DNA extraction methods influence on the taxa in different relative abundances (i.e., rare and abundant taxa), instead of the effect of downstream analysis (i.e., PCR, primer choice, DNA sequencing platform, and bioinformatics). Additionally, sequencing depth was also considered to better estimate the reproducibility of each DNA extraction method.

The aim of this study was to inform the experimental design by quantifying the relative influence of DNA extraction on plankton taxa with different relative abundances, and to provide a reference for the comparison of different studies on microbial plankton communities, instead of obtain the "best" protocols for aquatic microbiome studies. We compared five commonly used DNA extraction kits, using the 16S rRNA and 18S rRNA gene amplicon sequences data as the readout, and evaluated taxonomic variability of both bacterial and microeukaryotic plankton. Specifically, we assessed: (i) the influence of DNA extractions on the bacterial and eukaryotic diversity; (ii) the influence of DNA extraction kits on plankton community composition based on different distances; (iii) the similarity of community composition detected from the replicate extractions, which indicates the reproducibility of each method.

MATERIALS AND METHODS

Experimental Design

Water samples (upper 50 cm, 15 litter) were collected by a 5-L polymethyl methacrylate sampler in Tingxi Reservoir (24°48′N, 118°08′E) on July 26, 2016. Then all waters were put into a 20-L PVC bottle and transferred to the laboratory as soon as possible. The samples were first filtered through a 200 μm pore-size sieve to remove debris, large metazoans and grains. Then plankton communities (500 mL water) were collected on each 0.22 μm pore-size polycarbonate filter (47 mm diameter, Millipore, Billerica, MA, United States). The water was well mixed in the 20-L PVC bottle before filtering to keep the uniformity of each filtered sample. The filters were then stored at −80°C until DNA extraction.

Five commercial DNA extraction kits from three companies which are commonly used to extract DNA from environmental samples (Lear et al., 2018), were evaluated in this study (**Table 1**). Commercial DNA extraction kits were used in this study for their standardized application in multiple-labs (Renshaw et al., 2015; Walden et al., 2017). The DNA extractions were carried out in triplicate for each kit, and subsequent analyses were performed on the 15 individual extracts. All triplicates were taken from the same water and same bottle (20-L PVC bottle). Negative control extractions, where new membranes without plankton samples were added, were also performed for each method in triplicate. Each membrane or filter represents one replication. We mostly followed the instructions of manufacturers but introduced changes to improve the comparability among different DNA extraction kits. For MBS kit, to make it comparable to other DNA extraction kits, instead of filtering by Sterivex^{TM} filter unit, the filtered membrane was cut into small pieces and put into a sterilization centrifuge tube. Then we added the 0.9 mL of solution ST1B, vortexed as instruction and followed by adding 0.9 mL of ST2. After incubation at 90°C for 5 min, the mixtures were cooled at room temperature for 2 min. Next, the mixtures were vortexed at maximum speed for 5 min. After this, the lysate was added into the 5 mL PowerWater® Sterivex^{TM} glass Bead Tube. The other steps followed the manufacturer instructions to extract the DNA. The extracted DNA was quantified by a NanoDrop 1000 spectrophotometer (Thermo Fisher Scientific, Pittsburgh, PA, United States) and stored at −20°C until further use. Extracts were considered to contain sufficiently pure genomic DNA when their A260/A280 nm ratio was between 1.8

TABLE 1 | The five common DNA extraction kits used in this study.

Extraction kits	Abbreviation	Lysis method	Company	Headquarter address
PowerWater DNA isolation kit	MB	Mechanical, chemical	MoBio Laboratories Inc.	Carlsbad, CA, United States
PowerWater® Sterivex™ DNA isolation kit	MBS	Mechanical, chemical	MoBio Laboratories Inc.	Carlsbad, CA, United States
Fast DNA spin kit for soil	MPF	Mechanical, chemical	MP Biomedicals	Santa Ana, CA, United States
DNeasy blood and tissue kit	QD	Heat, chemical, enzymatic	Qiagen	Hilden, Germany
QIAamp DNA mini kit	QQ	Heat, chemical	Qiagen	Hilden, Germany

and 2.0. Otherwise, the extracted DNA included proteins, phenols or other contaminants (Hermans et al., 2018).

PCR Amplification and Illumina Sequencing

We used primer pairs targeting the V3-V4 variable region of 16S rRNA gene in bacteria (341F, 5′-CCTAYGGGRBGCASCAG-3′; 806R, 5′-GGACTACNNGGGTATCTAAT-3′) (Yu et al., 2005; Sundberg et al., 2013; Guo et al., 2018) and the V9 variable region of the 18S rRNA gene in eukaryotes (1380F, 5′-CCCTGCCHTTTGTACACAC-3′; 1510R, 5′-CCTTCYGCAGGTTCACCTAC-3′) (Amaral-Zettler et al., 2009; Liu et al., 2017; Xue et al., 2018). Each DNA sample and negative control were run in triplicate. Each DNA sample was individually PCR-amplified in 30 μL reactions included an initial denaturation at 98°C for 1 min, followed by 30 cycles of 10 s at 98°C, 30 s at 50°C, and 30 s at 72°C. At the end of the amplification, the amplicons were subjected to final 5 min extension at 72°C. The 30 μL PCR mixture included 15 μL of Phusion® High-Fidelity PCR Master Mix (New England Biolabs, Beverly, MA, United States); 0.2 μM of forward and reverse primers, and about 10 ng template DNA for both bacteria and eukaryotes. The triplicate PCR products were mixed in equimolar amounts and were confirmed after running in 1% agarose gel. Then the PCR products were isolated from the gel and purified with GeneJET Gel Extraction Kit (Thermo Fisher Scientific, Hudson, NH, United States). Sequencing libraries were constructed using NEB Next Ultra DNA Library Prep Kit for Illumina (New England Biolabs, Ipswich, MA, United States) following manufacturer's instructions, and barcodes were added. The library quality was estimated on the Qubit 2.0 Fluorometer (Thermo Fisher Scientific, Waltham, MA, United States) and Agilent Bioanalyzer 2100 system (Agilent Technologies, Palo Alto, CA, United States). At last, the library was sequenced on the Illumina MiSeq platform (Illumina, Inc., San Diego, CA, United States) using a 250 bp paired-end protocol (Liu et al., 2017).

Bioinformatics

Paired-end reads were merged by using FLASH (Magoč and Salzberg, 2011) and then assigned to each sample according to the unique barcodes. Sequence data were processed using quantitative insights into microbial ecology (QIIME v.1.8.0) software following standard protocols: maximum number of consecutive low-quality base = 3; minimum of continuous high-quality base = 75% of total read length; maximum number of ambiguous bases = 0 (Caporaso et al., 2010). Chimeric sequences were identified by UCHIME and discarded before further analysis (Edgar et al., 2011). Quality-filtered sequences were then assigned to operational taxonomic units (OTUs) at 97% level of sequence similarity by using the pick_otus.py. The 97% threshold has been widely used for both of bacteria and eukaryotes (Henderson et al., 2013; Liu et al., 2015, 2017; Dai et al., 2016; Hermans et al., 2018; Xue et al., 2018). There is no general agreement on a standard definition to classify the eukaryotes into OTUs at species level. We selected 97% threshold for eukaryotic plankton to facilitate comparisons between studies because many previous studies used this threshold to define OTUs (Liu et al., 2017; Xue et al., 2018). Further, our previous study (Liu et al., 2017) found that the choice of different thresholds (97% vs. 99%) had no apparent effect on overall results and general conclusions in plankton community ecology. Sequences were taxonomically classified by the RDP classifier using the 80% confidence threshold against the Silva 123 for bacteria (Quast et al., 2013) and PR^2 for eukaryotes (Guillou et al., 2013), respectively. For bacteria, all eukaryota, chloroplasts, archaea, mitochondria, unknown sequences and singleton OTUs were excluded. For eukaryotes, unassigned and singleton OTUs were excluded. Finally, sequences data were normalized to 41,744 and 121,146 sequences per sample using the "sub.sample" command in MOTHUR v.1.33.3 (Schloss et al., 2009) for bacteria and eukaryotes, respectively.

All raw sequences from this study have been submitted to the National Center for Biotechnology Information (NCBI) Sequence Read Archive (SRA) database under the BioProject number PRJNA474064 and the accession number SRP149868.

Definition of Rare and Abundant Plankton

In order to evaluate the effects of DNA extraction kits on taxa in different relative abundances, we expanded the classification of microbial taxa based on the detected sequences and their relative abundance. This followed the definition of abundant (1%) and rare (0.01%) biosphere in previous studies (Pedrós-Alió, 2012; Liu et al., 2015; Xue et al., 2018). All OTUs were artificially defined and grouped into 6 exclusive categories following previous studies (Dai et al., 2016; Xue et al., 2018; Liu et al., 2019): (i) the OTUs with a relative abundance always ≥1% in all replicates were regarded as always abundant taxa (AT); (ii) the OTUs with a relative abundance greater than 0.01% in all replicates and ≥1% in some replicates but never rare (<0.01%) were regarded as conditionally abundant taxa (CAT); (iii) the OTUs with a relative abundance varying from rare (<0.01%) to abundant (≥1%) were regarded as conditionally rare and abundant taxa (CRAT); iv) the OTUs with relative abundance between 0.01% and 1% in all

replicates were regarded as moderate taxa (MT); v) the OTUs with a relative abundance <0.01% in some replicates but never ≥1% in all replicates were regarded as conditionally rare taxa (CRT); (vi) the OTUs with a relative abundance always <0.01% in all replicates were regarded as always rare taxa (RT).

Data Analyses

Rarefaction curves, and α-diversity indices were computed by MOTHUR v.1.33.3 (Schloss et al., 2009). The non-parametric Kruskal-Wallis test was used to evaluate the influences of DNA extraction kits on α-diversity indices and the quality and quantity of DNA by SPSS 22.0 (IBM Corp., Armonk, NY, United States).

Four dissimilarity matrices (Bray-Curtis, Jaccard, weighted unifrac and unweighted unifrac) within and between DNA extraction kits were calculated with the relative abundance-based OTUs of bacteria and eukaryotes. Analysis of similarities (ANOSIM) was used to estimate the significant differences among different DNA extraction kits. Complete separation is suggested by $R = 1$, with $R = 0$ representing no separation (Clarke and Gorley, 2015). We used the adonis function (vegan R packages) to run a PERMANOVA on the Bray-Curtis dissimilarity profiles using 10,000 permutations for assessing the effect of DNA extraction methods (Anderson, 2001). Similarity of percentages analysis (SIMPER) analysis was performed with PAST (Paleontological Statistics, version 3.01) software to identify the contribution of each OTU to the community dissimilarity (Hammer et al., 2001). The Bray-Curtis dissimilarity was used as the distance for ANOSIM, PERMANOVA and SIMPER analyses.

The reproducibility of each DNA extraction kit, evaluating the difference between plankton community compositions among triplicates within each DNA kit, was quantified by computing the average dissimilarity of each set of three replicates, using four dissimilarity matrices. The lower the dissimilarity measure, the more consistent that method was predicted to be. In addition, we randomly selected subsets of cleaned sequences (10,000, 20,000, 30,000, and 40,000 for bacteria; 10,000, 20,000, 30,000, 40,000, 50,000, 60,000, 70,000, 80,000, 90,000, and 100,000 for eukaryotes) from each replicate to estimate the influence of sequencing depth on the reproducibility. The one-way ANOVA was used to test the significant difference for reproducibility of DNA extraction kits.

A Venn diagram was constructed using the "Venn Diagram" package to compare the number of OTUs detected by using different DNA extraction kits. The "Niche breadth" approach of Levins (1968) was used to evaluate DNA extraction kits preference by the formula:

$$B_j = \frac{1}{\sum_{i=1}^{N} P_{ij}^2} \quad (1)$$

where B_j indicates the number of DNA extraction kits which the OTU occurred and P_{ij} represents the percentage of individuals belonging to species j present in a given DNA extraction kit *i*. Phylotypes characteristic of specific DNA extraction kit were identified using indicator species analysis (ISA). Those indicator OTUs with a *P*-value <0.05 and phylotypes with indicator values >50, were considered valid (Dufrene and Legendre, 1997). A heat map of the 20 most abundant OTUs and high-rank taxa was made using the "pheatmap" package in the R environment.

RESULTS

Effect of Extraction Kits on Plankton DNA Quality and Quantity

Although the DNA purity of the same filtered samples had no significant difference across different DNA extraction kits, the DNA concentrations varied greatly (**Supplementary Figure S1**). The DNA purity ranged from 1.90 to 2.15. The best results were obtained using PowerWater DNA Isolation Kit (MB) (mean, 1.97), PowerWater® Sterivex™ DNA Isolation Kit (MBS) (1.95) and Fast DNA Spin Kit for soil (MPF) (1.93). The highest DNA concentration was obtained using Fast DNA Spin Kit for soil (MPF) (mean ± s.e., 64.80 ± 1.12 ng/μL), and PowerWater DNA Isolation Kit (MB) (15.85 ± 2.90 ng/μL) produced the lowest yield of DNA. Overall, MPF can maximize DNA concentration and purity. All negative extraction controls yielded DNA below the limit of detection.

Effect of Extraction Kits on Plankton Richness and α-Diversity

Most of the microbial plankton taxa had been recovered, as indicated by the species accumulation curves (**Figure 1A**), although no single replicate sample achieved a full saturation in the rarefaction curves. The sequencing depth for eukaryotic plankton (121,146) was higher than that of bacteria (41,744). Distinct influences of DNA extraction kits on α-diversity indices were observed for bacteria and eukaryotes (**Figure 1B**). For bacteria, only observed OTU number and Shannon-Wiener index had significant differences among DNA extraction kits ($P < 0.05$). MB showed the lowest OTU number (2005 ± 235) and Shannon-Wiener (4.34 ± 0.02), however the highest values of OTU number (3027 ± 19) and Shannon-Wiener (4.89 ± 0.12) were obtained from MPF. For eukaryotes, no significant difference was found for any α-diversity index among five different DNA extraction kits.

Reproducibility and Comparability of DNA Extraction Kits

To evaluate the effects of extraction kits on rare and abundant microbial taxa, we defined and grouped all OTUs into six exclusive categories based on their ranges of the relative abundance in 15 replicate samples (**Supplementary Figure S2**). Rare taxa had the highest OTUs number for both bacteria (86.62%) and eukaryotes (80.75%), whereas abundant taxa had the lowest OTUs number for both bacteria (0.04%) and eukaryotes (0%). For bacteria, conditionally abundant taxa showed the highest sequence number (42.65%), while the lowest sequence number was found in conditionally rare and abundant taxa (1.32%). For eukaryotes, conditionally abundant taxa also showed the highest sequence number (57.71%), while the lowest sequence number was found in abundant taxa (0%).

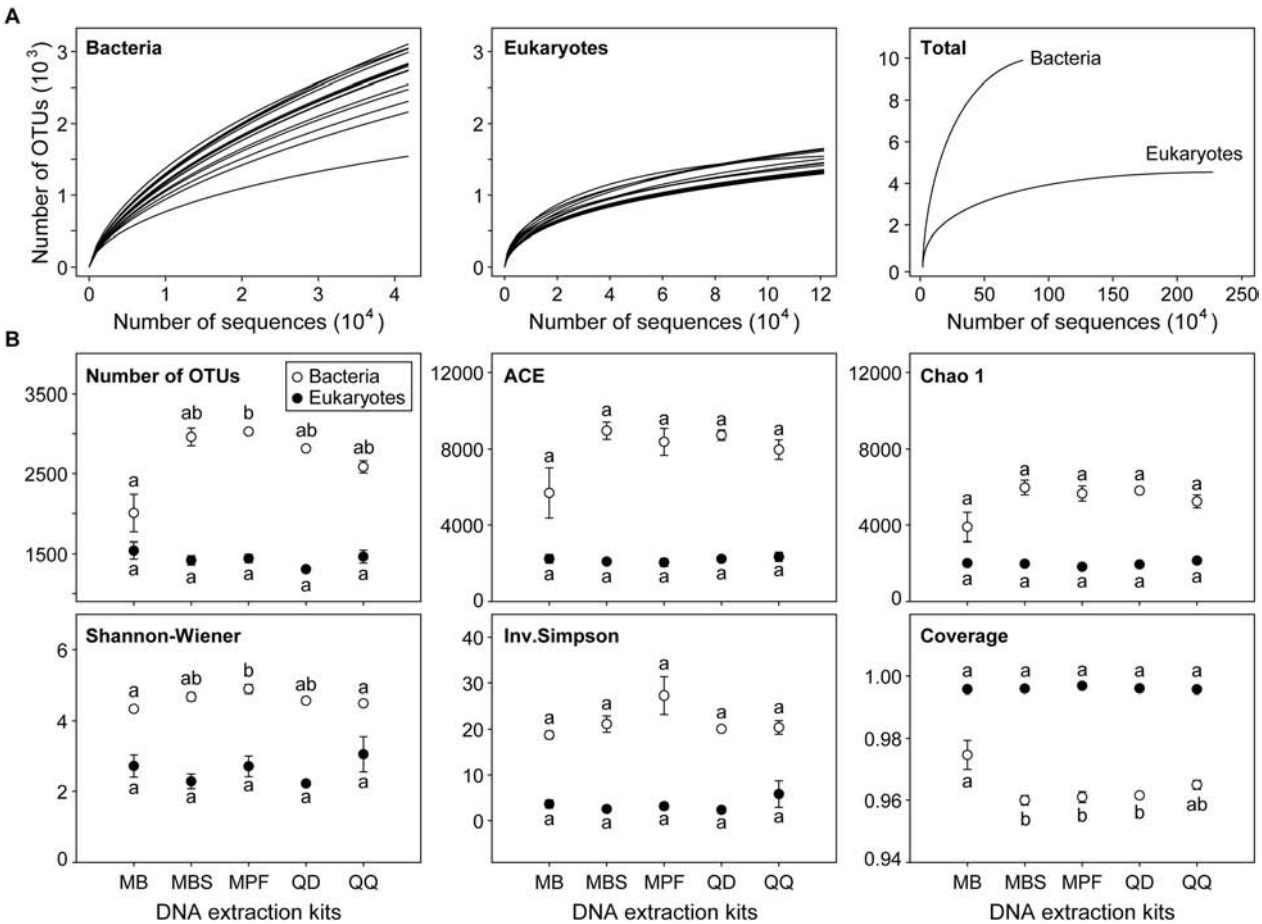

FIGURE 1 | The effect of DNA extraction kits on α-diversity of both bacterial and eukaryotic plankton. **(A)** Rarefaction curves of each single community and the combined communities for bacteria and eukaryotes, respectively. **(B)** Comparison of community diversity parameters. The OTUs were defined at 97% sequence similarity level. All data are means ± standard error ($n = 3$). Significant difference ($P < 0.05$) is indicated by different letters of the alphabet, and the significance is calculated by non-parametric Kruskal-Wallis test.

Community dissimilarity can be mainly due to the differences of DNA extraction methods (**Figure 2A** and **Supplementary Figures S3A–S5A**). The reproducibility of each DNA extraction kit showed significant difference ($P < 0.05$). QD and QQ exhibited the highest consistency for bacteria (0.62) and eukaryotes (0.76), respectively (**Figure 2B**). Different DNA extractions showed distinct patterns of consistency along relative abundance ranks (**Figure 2** and **Supplementary Figures S3–S5**). Interestingly, RT, CRT and CRAT had lower consistency compared with AT, CAT and MT categories for both bacteria and eukaryotes (**Figure 2B**), indicating that DNA extractions have the larger effects on taxa with the lower relative abundance. In general, the higher the average between-replicate dissimilarity was, the larger the standard error of the dissimilarity was estimated (**Figure 2** and **Supplementary Figures S3–S5**). Furthermore, we did not find that the sequencing depth showed any significant influence on the reproducibility of each DNA extraction kit for eukaryotes from 10,000 to 100,000 sequences (**Supplementary Figure S6**). For bacterial community, however, the reproducibility of both QD and QQ was significant higher for 40,000 sequencing depth than 10,000 sequencing depth ($P < 0.05$), while sequencing depth exhibited no significant effect on the reproducibility of three other DNA extraction kits from 10,000 to 40,000 sequences (**Supplementary Figure S6**).

Effects of Extraction Kits on Community Composition

Four kinds of distance indices were considered to compare the community differences among the DNA extraction kits based on the variation of OTUs along relative abundance ranks, and in general they produced similar results (**Figures 2C** and **Supplementary Figures S3C–S5C**). For both bacteria and eukaryotes, most of the community differences were from rare taxa. By contrast, abundant, conditionally abundant, and moderate taxa showed higher similarity and higher consistency among different DNA extraction kits. In addition, two non-parametric multivariate statistical tests (ANOSIM and Adonis) showed that these observed differences were statistically significant (**Table 2**). Furthermore, the SIMPER analysis showed

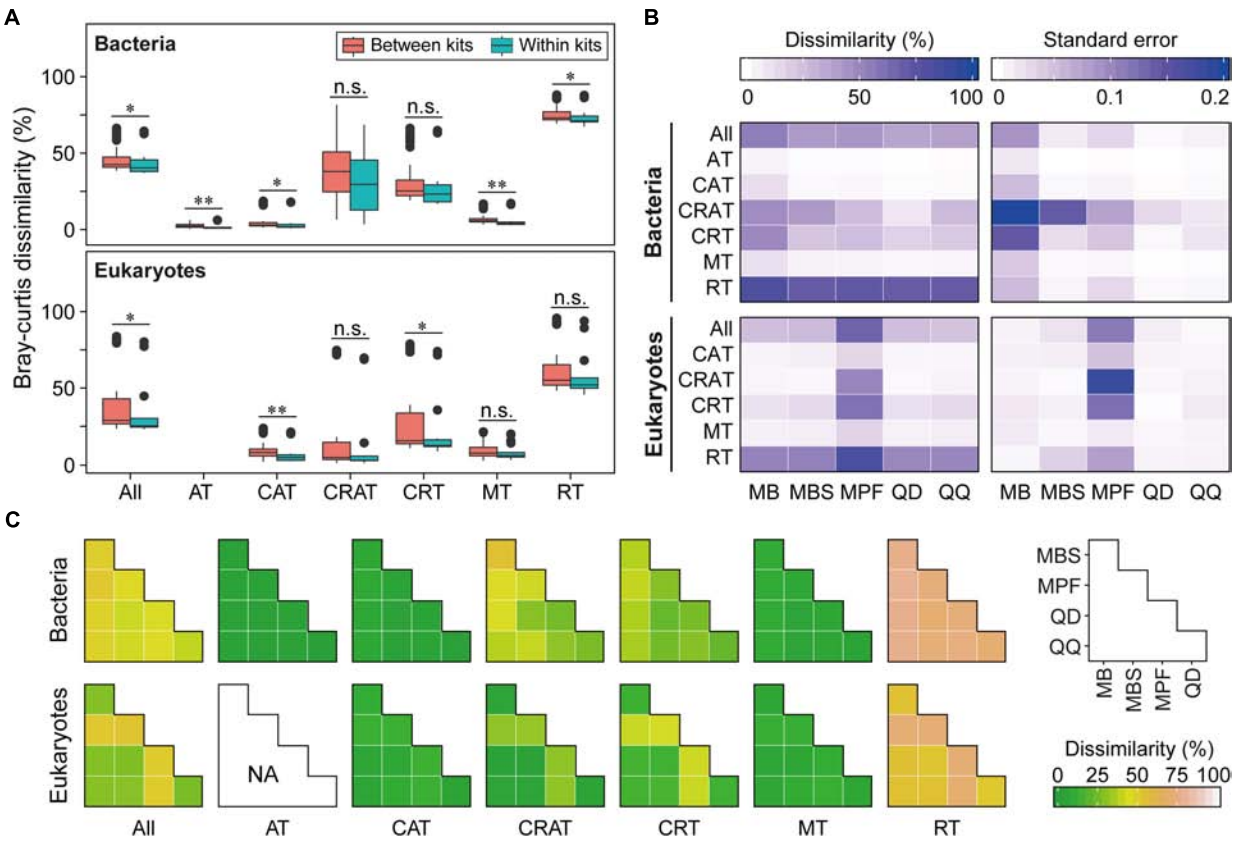

FIGURE 2 | The effect of DNA extraction kits on community composition of both bacterial and eukaryotic plankton based on Bray-Curtis dissimilarity. **(A)** The overview of pairwise Bray-Curtis dissimilarity of bacterial and eukaryotic plankton communities based on five different DNA extraction kits, respectively. Statistical analysis is non-parametric Mann-Whitney *U* test. $*P < 0.05$, $**P < 0.01$, n.s. $P > 0.05$. **(B)** Variation in the community composition of six OTUs categories produced by three replicates within the DNA extractions kits. The data were expressed as mean Bray-Curtis dissimilarity (left) and its standard error (right), with a more dark blue indicating a more dissimilar or larger variation. **(C)** Pairwise Bray-Curtis dissimilarity of bacterial and eukaryotic plankton communities between different DNA extraction kits. Note that no always abundant taxa (AT) was identified for eukaryotic plankton in this study. AT, always abundant taxa; CAT, conditionally abundant taxa; CRAT, conditionally rare and abundant taxa; CRT, conditionally rare taxa; MT, moderate taxa; RT, always rare taxa.

TABLE 2 | Analysis of similarity (ANOSIM) and permutational multivariate analysis of variance (PERMANOVA) for comparisons of microbial plankton communities among five different DNA extraction kits based on Bray-Curtis dissimilarity.

Category	ANOSIM				PERMANOVA			
	Bacteria		Eukaryotes		Bacteria		Eukaryotes	
	R	*P*-value	R	*P*-value	R^2	*P*-value	R^2	*P*-value
All	**0.34**	**0.004**	**0.32**	**0.001**	**0.33**	**0.006**	**0.37**	**0.002**
AT	**0.48**	**0.001**	–	–	**0.50**	**0.009**	–	–
CAT	**0.40**	**0.001**	**0.51**	**0.001**	0.30	0.318	**0.54**	**0.001**
CRAT	**0.26**	**0.008**	**0.32**	**0.002**	0.40	0.073	**0.37**	**0.002**
CRT	**0.28**	**0.005**	**0.33**	**0.003**	0.33	0.150	**0.38**	**0.005**
MT	**0.58**	**0.001**	**0.18**	**0.040**	**0.39**	**0.016**	0.35	0.241
RT	**0.35**	**0.001**	**0.26**	**0.002**	**0.31**	**0.003**	**0.34**	**0.002**

Bold font indicates the significance at $P < 0.05$. Values show the R and R^2 values for ANOSIM and PERMANOVA, respectively. The operational taxonomic units (OTUs) were defined at 97% sequence similarity threshold. The ANOSIM statistic compares the mean of ranked dissimilarities among groups to the mean of ranked dissimilarities within groups. An R value close to "1" suggests dissimilarity between groups, while an R value near "0" suggests an even distribution of high and low ranks within and between groups. Negative R values indicate that dissimilarities are greater within groups than between groups. AT, always abundant taxa; CAT, conditionally abundant taxa; CRAT, conditionally rare and abundant taxa; CRT, conditionally rare taxa; MT, moderate taxa; RT, always rare taxa. Note that no always abundant taxa (AT) was identified for eukaryotic plankton in this study.

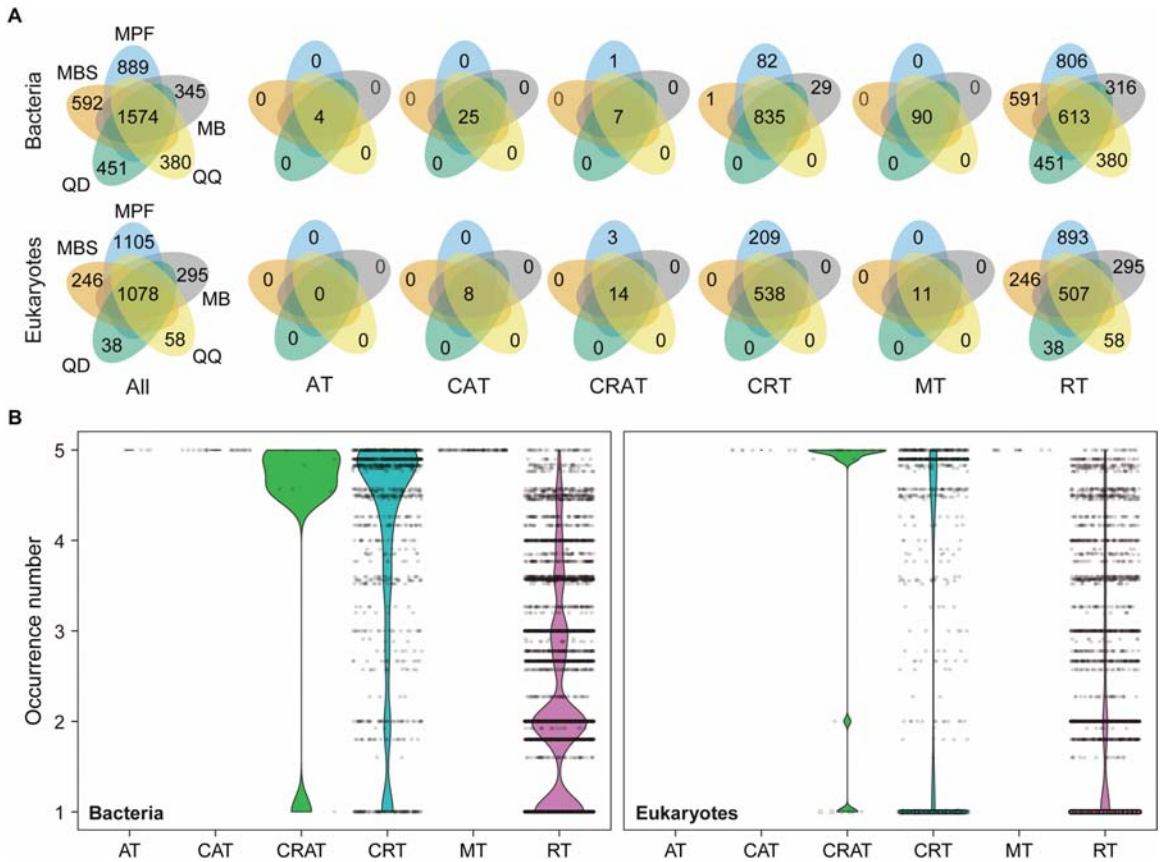

FIGURE 3 | The effect of DNA extraction kits on the OTUs occurrence. **(A)** Venn diagram showing the number of OTUs that shared and unique by different DNA extraction kits. **(B)** The occurrence (that is, the number of DNA extraction kits where an OTU was found) based on niche breadth analysis for all the bacterial and eukaryotic OTUs, respectively. AT, always abundant taxa; CAT, conditionally abundant taxa; CRAT, conditionally rare and abundant taxa; CRT, conditionally rare taxa; MT, moderate taxa; RT, always rare taxa.

that RT and CRT accounted for the largest contribution for community differences for both bacteria (69.62% for RT, 27.86% for CRT) and eukaryotes (59.56% for RT, 38.24% for CRT) (**Supplementary Figure S7**).

The influence of DNA extraction kits on community composition was identified at both OTU and higher taxonomic levels (**Figures 3**, **4**). At OTU level, significant differences were found for specific taxa. First, regardless the microbial plankton types, most of the unique OTUs for each method belonged to the rare taxa (**Figure 3A**). In total, 15% bacterial OTUs and 23% eukaryotic OTUs were identified in at least four extraction kits, and less than 60% OTUs were found in no more than two methods for both bacteria and eukaryotes (**Figure 3B**). Second, indicator OTUs were identified for each DNA extraction kit (**Supplementary Table S2**). For bacteria, the numbers of indicator OTUs among kits were 1 for MB, 0 for MBS, 6 for MPF, 0 for QD, and 2 for QQ methods. For eukaryotes, the numbers of indicator OTUs were 4 for MB, 0 for MBS, 13 for MPF, 0 for QD, and 7 for QQ methods. At last, only 4 (Actinobacteria, Cyanobacteria, Proteobacteria, Bacteroidetes) of 20 most abundant OTUs were significantly different among DNA extraction kits for bacteria, whereas no difference was identified for eukaryotic plankton (**Figure 4A**). At high-rank taxa level, no any significant difference was found for bacteria, while both Rhodophyta and Centroheliozoa were significantly different among five DNA extraction kits for eukaryotes (**Figure 4B**).

Finally, to improve data comparability, we removed singleton sequences and OTUs with less and equal to 5, 10, 50, 100, 500 sequences. We found that the larger number of sequences removed, the lower the community dissimilarity (**Figure 5A**) and the higher overlap of the OTUs (**Figure 5B**) for both bacteria and eukaryotes. This indicates that the low-abundance taxa had significant contribution to the community dissimilarity.

DISCUSSION

With the development of high-throughput technologies of target genes, researchers can now directly quantify the rare biosphere, which play very important ecological and biogeochemical roles in various ecosystems (Sogin et al., 2006; Pedrós-Alió, 2012; Liu et al., 2015, 2019; Lynch and Neufeld, 2015; Xue et al., 2018). However, great caution is needed when using DNA-based sequencing technologies for describing and

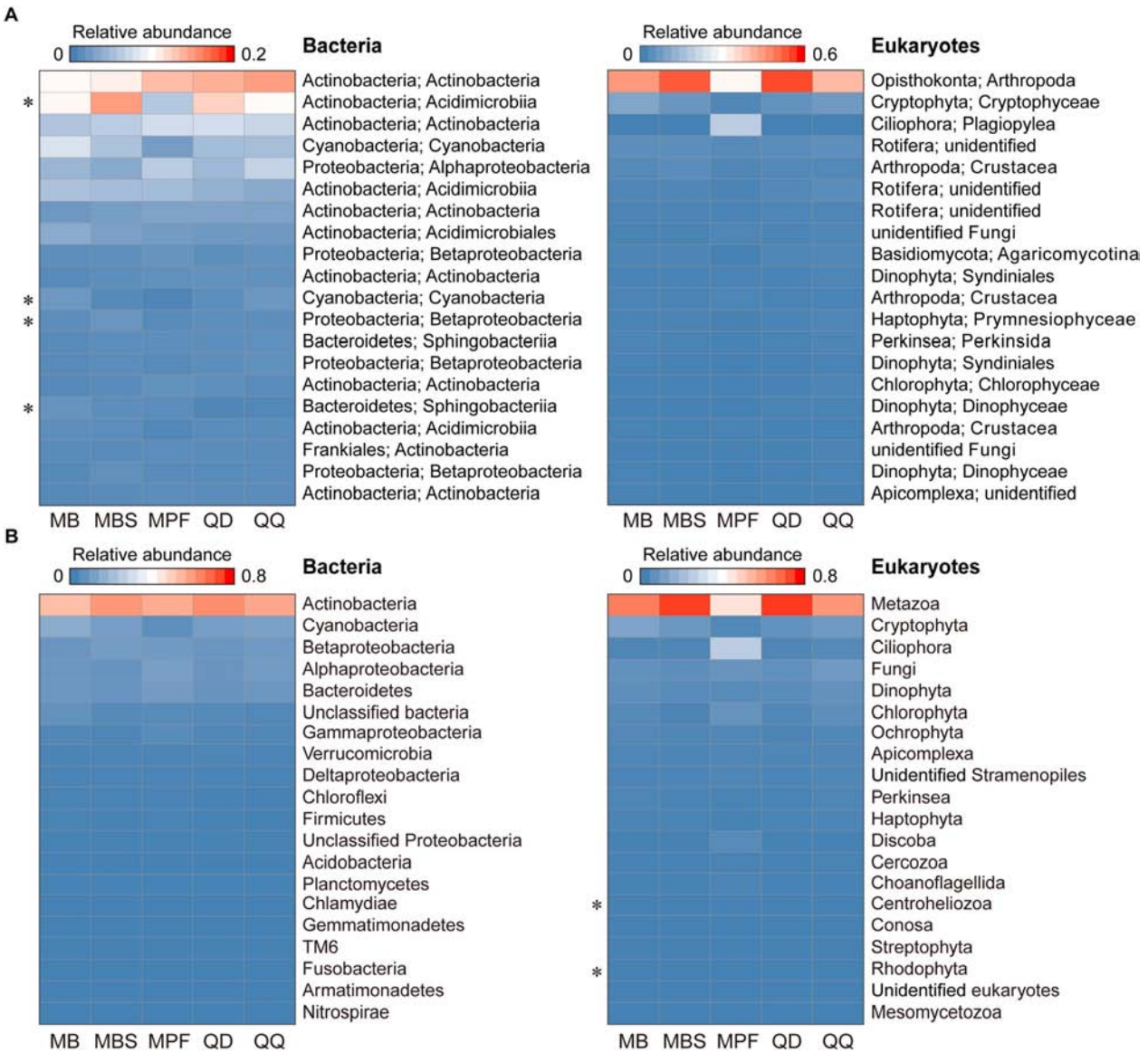

FIGURE 4 | The effect of DNA extraction kits on the community composition. **(A)** Heat map of 20 most abundant OTUs in bacterial and eukaryotic plankton dataset. **(B)** Variation of main high-rank taxa of bacterial and eukaryotic plankton within each of DNA extraction kit. Statistical analysis is non-parametric Kruskal-Wallis test. $^*P < 0.05$. Each OTU or high-rank taxon is in a row, and color intensity indicates its average relative abundance of each DNA extraction kit ($n = 3$).

characterizing the diversity and composition of microbial community. The aim of this study is to comprehensively and systematically understand how low-abundance taxa were influenced by different DNA extraction kits. Here, we compared the variations of plankton communities from a single water sample using five of the most commonly used DNA extraction kits. We found that different DNA extraction kits had distinct influences on the alpha-diversity, community composition and specific taxa for both bacteria and eukaryotes. Specifically, low-abundance taxa were greatly affected by different DNA extraction kits. We also found that the community composition reproducibility varied among the DNA extraction kits.

The alpha-diversity of a microbial community could be influenced by DNA extraction kits to different degrees. Previous studies have found that the choice of DNA extraction methods could affect the alpha-diversity of bacterial communities from kick-net, leaf litter, soil and water (Purswani et al., 2011; Deiner et al., 2015; Hermans et al., 2018). However, no significant difference in alpha-diversity was obtained for eukaryotic (animal, fungal and plant) communities from soil and water samples (Hermans et al., 2018). Another study showed that no significant differences were found among DNA extraction kits when assessing diversity of eukaryotic microalgae from freshwater by using denaturant gradient gel electrophoresis (Eland et al., 2012). Compared with the previous studies mentioned above,

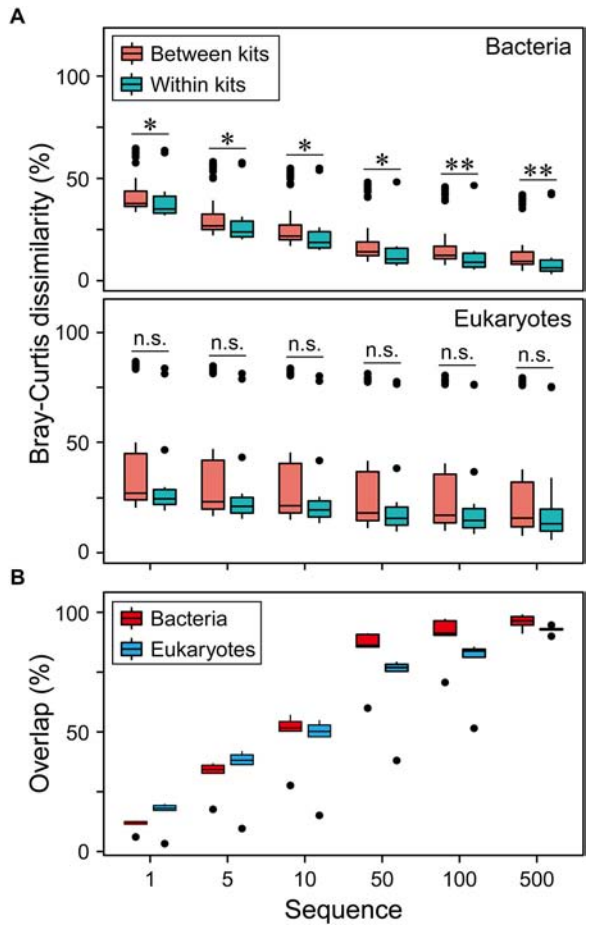

FIGURE 5 | Effects of data preprocessing on resolving the differences of microbial communities. **(A)** The overview of pairwise Bray-Curtis dissimilarity of bacterial and eukaryotic plankton communities based on five different DNA extraction kits after the OTUs with < = 1, 5, 10, 50, 100, 500 sequences were removed. For bacteria, linear regression resulted in a significant pattern for between kits (R^2 = 0.19, P < 0.01) and within kits (R^2 = 0.14, P < 0.01). For eukaryotes, linear regression resulted in a significant pattern only for between kits (R^2 = 0.01, P < 0.01). **(B)** The overlap of three replicates of bacterial and eukaryotic plankton communities based on five different DNA extraction kits after the OTUs with < = 1, 5, 10, 50, 100, 500 sequences were removed. Linear regression resulted in a significant correlation for bacteria (R^2 = 0.37, P < 0.01) and eukaryotes (R^2 = 0.45, P < 0.01).

sequencing depths were higher in this study. Our results indicated that the alpha-diversity of bacteria was significantly affected by different DNA extraction kits, whereas there was no significant influence on the alpha-diversity of eukaryotic plankton community.

Additionally, significant differences were found for specific taxa at OTU or phylum level for both bacteria and eukaryotes. Previous studies have shown the preference in extraction specific taxa such as cyanobacteria, Excavata, Cercozoa and Amoebozoa (Singh et al., 2011; Santos et al., 2017). The differences in community composition detected may partly be due to the distinct susceptibility of bacterial and eukaryotic cell wall to different lysis methods or beads of different materials and sizes (Bürgmann et al., 2001; Fredricks et al., 2005; Henderson et al., 2013; Velásquez-Mejía et al., 2018). Mechanical lysis is suitable for bacteria attributed to its harder lysing cells, whereas direct lysis of cells based on bead-beating protocols is considered to be more suited to the detection of microeukaryotes, as these cells often have fortified cell walls or very resilient cell membranes (Santos et al., 2017; Hermans et al., 2018). Otherwise, even for bacteria, methods without a bead beating or enzymatic treatment step generally extracted less DNA from Gram-positive bacteria (Knudsen et al., 2016). Other factors such as sample type or origin (Knudsen et al., 2016), inherent specimen properties (Knudsen et al., 2016; Sinha et al., 2017), primer choice (Albertsen et al., 2015) and bioinformatics protocol choices (Sinha et al., 2017) can also influence the outcome of microbial community analysis. It is difficult to find a single extraction method for all circumstances. Our results highlighted that it is important to design specific DNA extraction method to target particular taxonomic groups.

Previous studies have found the influence of DNA extraction kits on the whole or abundant taxa in microbial communities (Knudsen et al., 2016; Sinha et al., 2017; Hermans et al., 2018), however, the influence of extraction methods on low-abundance taxa were not comprehensively and systematically evaluated. Recently, Weiss et al. (2014) found that DNA extraction kits had significant influence on the resulting microbial community profile of low-biomass samples. Our results indicated that low-abundance taxa were largely influenced by the DNA extraction kits, and offered further evidence supporting that plankton taxa in different relative abundances were disproportionately influenced. One explanation for the results is that as the number of "true" taxa becomes less, the potential for contaminants occupying a larger fraction of the sequences will become greater (Weiss et al., 2014). Another explanation for this is that some of the community differences between DNA extraction kits may be actually "real" chance differences between replicate samples. It's possible that some replicate samples may not contain any individuals of a very rare taxon, despite the fact that we mixed the water before filtering. In addition, the differences in microbial communities may also come from the amplicon sequencing-based detection method, as its influence on analyzing microbial community composition (Zhou et al., 2011). To be conservative, it is ideal to adopt a single DNA extraction method for increasing the comparability of different studies. Our results indicate that we can improve the community comparisons between studies that employed different extraction methods with an exception of RT and CRT for their large contributions to community differences among different DNA extraction kits.

Consistency of generating OTU profiles is highly desirable in order to facilitate assessments and comparisons of plankton species diversity and distribution across space and time. Reproducibility is a crucial issue for the study of microbial community ecology. Sample processing steps, from sampling to downstream data analysis, can introduce some biases; such biases can skew data sets by introducing changes in the relative abundances observed, and they can affect the variation among replicates (Zhou et al., 2011; Costea et al., 2017; Pollock et al., 2018; Velásquez-Mejía et al., 2018). The differences in the replicates for each DNA extraction kit are likely the result of

DNA extraction and sequencing depth, because other sample process steps should influence all our replicate samples in a similar way (Velásquez-Mejía et al., 2018). Similarly, Zhou et al. (2011) found a reliable diversity comparison across different samples by removing less-representative OTUs for bacteria (e.g., OTUs present only in 1 or 2 of the 14 tag sequence data sets). Our result supported this finding and further demonstrated that the taxa in different relative abundance showed distinct patterns of reproducibility. This could be explained by the high OTUs overlap between replicate samples when low-abundance OTUs were removed from the dataset (**Figure 5**). In addition, sequencing depth should also be considered, because the percentage of shared OTUs increased as the sequencing depth increase (Liu et al., 2017). However, sequencing depth only exhibited a significant and minor influence on the results of QD and QQ for bacteria, with no significant influence identified for other DNA extraction methods (**Supplementary Figure S6**). There are also some limitations in this research that need for further study. For example, the technical replicates should be increased to better estimate the background noise level (Zhou et al., 2011). Sample handling environment, and bioinformatics should also be considered for their important influence on the community composition (Costea et al., 2017; Sinha et al., 2017).

CONCLUSION

In conclusion, DNA extraction methods had an influence on the results of downstream microbial community analyses, including relative abundances of specific community members for both bacteria and eukaryotes at OTU and higher taxonomic levels. The rare plankton subcommunities are far more affected by DNA extraction kits than the abundant plankton. Every extraction kit was effective, though each showed its own strengths and weaknesses in observing special taxonomic community profiles. MPF produced higher α diversity for bacteria and high quality and yield of DNA, therefore it is the most suitable DNA methods for bacterial plankton diversity study. While QD and QQ methods could produce results that are easier to replicate for bacteria and eukaryotes, respectively. Moreover, our results highlight that the comparability between studies that employed different extraction methods can be improved by removing low-abundance OTUs for their larger contribution to community variation. There is no doubt that the efforts to assess bias within labs as proposed here, and guidelines for best practices across labs, will facilitate comparative studies to characterize microbial communities from multiple sampling surveys and various environments.

DATA AVAILABILITY

The datasets generated for this study can be found in National Center for Biotechnology Information (NCBI) Sequence Read Archive (SRA) database, BioProject number PRJNA474064 and the accession number SRP149868.

AUTHOR CONTRIBUTIONS

JY designed the research. ML and YX performed the experiments. ML and JY analyzed the data and wrote the manuscript. All authors have significantly contributed to the writing of the manuscript.

FUNDING

This work was funded by the Strategic Priority Research Program of the Chinese Academy of Sciences (XDA23040302), the National Natural Science Foundation of China (91851104 and 31672312), and the Xiamen Municipal Bureau of Science and Technology (3502Z20172024).

ACKNOWLEDGMENTS

We are very grateful to Prof. David M. Wilkinson for his valuable comments on an earlier version of the manuscript. We thank our two reviewers for insightful comments who helped in improving the clarity of this paper. The research was also supported by the Wuhan Branch, Supercomputing Center, Chinese Academy of Sciences, China.

SUPPLEMENTARY MATERIAL

The Supplementary Material for this article can be found online at: https://www.frontiersin.org/articles/10.3389/fmicb.2019.00454/full#supplementary-material

REFERENCES

Albertsen, M., Karst, S. M., Ziegler, A. S., Kirkegaard, R. H., and Nielsen, P. H. (2015). Back to basics-the influence of DNA extraction and primer choice on phylogenetic analysis of activated sludge communities. *PLoS One* 10:e0132783. doi: 10.1371/journal.pone.0132783

Amaral-Zettler, L. A., McCliment, E. A., Ducklow, H. W., and Huse, S. M. (2009). A method for studying protistan diversity using massively parallel sequencing of V9 hypervariable regions of small-subunit ribosomal RNA genes. *PLoS One* 4:e6372. doi: 10.1371/journal.pone.0006372

Anderson, M. J. (2001). A new method for non-parametric multivariate analysis of variance. *Austral Ecol.* 26, 32–46. doi: 10.1111/j.1442-9993.2001.01070.pp.x

Bürgmann, H., Pesaro, M., Widmer, F., and Zeyer, J. (2001). A strategy for optimizing quality and quantity of DNA extracted from soil. *J. Microbiol. Methods* 45, 7–20. doi: 10.1016/S0167-7012(01)00213-5

Cabeen, M. T., and Jacobs-Wagner, C. (2005). Bacterial cell shape. *Nat. Rev. Microbiol.* 3, 601–610. doi: 10.1038/nrmicro1205

Caporaso, J. G., Kuczynski, J., Stombaugh, J., Bittinger, K., Bushman, F. D., Costello, E. K., et al. (2010). QIIME allows analysis of high-throughput community sequencing data. *Nat. Methods* 7, 335–336. doi: 10.1038/nmeth.f.303

Clarke, K. R., and Gorley, R. N. (2015). *PRIMER v7: User Manual/Tutorial*. Plymouth: PRIMER-E Ltd.

Costea, P. I., Zeller, G., Sunagawa, S., Pelletier, E., Alberti, A., Levenez, F., et al. (2017). Towards standards for human fecal sample processing in metagenomic studies. *Nat. Biotechnol.* 35, 1069–1076. doi: 10.1038/nbt.3960

Dai, T., Zhang, Y., Tang, Y., Bai, Y., Tao, Y., Huang, B., et al. (2016). Identifying the key taxonomic categories that characterize microbial community diversity using full-scale classification: a case study of microbial communities in the sediments of Hangzhou Bay. *FEMS Microbiol. Ecol.* 92:fiw150. doi: 10.1093/femsec/fiw150

Deiner, K., Walser, J. C., Mächler, E., and Altermatt, F. (2015). Choice of capture and extraction methods affect detection of freshwater biodiversity from environmental DNA. *Biol. Conserv.* 183, 53–63. doi: 10.1016/j.biocon.2014.11.018

Dufrene, M., and Legendre, P. (1997). Species assemblages and indicator species: the need for a flexible asymmetrical approach. *Ecol. Monogr.* 67, 345–366. doi: 10.2307/2963459

Edgar, R. C., Haas, B. J., Clemente, J. C., Quince, C., and Knight, R. (2011). UCHIME improves sensitivity and speed of chimera detection. *Bioinformatics* 27, 2194–2200. doi: 10.1093/bioinformatics/btr381

Eichmiller, J. J., Miller, L. M., and Sorensen, P. W. (2016). Optimizing techniques to capture and extract environmental DNA for detection and quantification of fish. *Mol. Ecol. Resour.* 16, 56–68. doi: 10.1111/1755-0998.12421

Eland, L. E., Davenport, R., and Mota, C. R. (2012). Evaluation of DNA extraction methods for freshwater eukaryotic microalgae. *Water Res.* 46, 5355–5364. doi: 10.1016/j.watres.2012.07.023

Fredricks, D. N., Smith, C., and Meier, A. (2005). Comparison of six DNA extraction methods for recovery of fungal DNA as assessed by quantitative PCR. *J. Clin. Microbiol.* 43, 5122–5128. doi: 10.1128/JCM.43.10.5122-5128.2005

Guillou, L., Bachar, D., Audic, S., Bass, D., Berney, C., Bittner, L., et al. (2013). The Protist Ribosomal Reference database (PR2): a catalog of unicellular eukaryote small sub-unit rRNA sequences with curated taxonomy. *Nucleic Acids Res.* 41, D597–D604. doi: 10.1093/nar/gks1160

Guo, Y. Y., Liu, M., Liu, L. M., Liu, X., Chen, H. H., and Yang, J. (2018). The antibiotic resistome of free-living and particle-attached bacteria under a reservoir cyanobacterial bloom. *Environ. Int.* 117, 107–115. doi: 10.1016/j.envint.2018.04.045

Hammer, Ø., Harper, D. A. T., and Ryan, P. D. (2001). PAST: paleontological statistics software package for education and data analysis. *Palaeontol. Electron.* 4, 1–9.

Henderson, G., Cox, F., Kittelmann, S., Vahideh, H. M., Zethof, M., Noel, S. J., et al. (2013). Effect of DNA extraction methods and sampling techniques on the apparent structure of cow and sheep rumen microbial communities. *PLoS One* 8:e74787. doi: 10.1371/journal.pone.0074787

Hermans, S. M., Buckley, H. L., and Lear, G. (2018). Optimal extraction methods for the simultaneous analysis of DNA from diverse organisms and sample types. *Mol. Ecol. Resour.* 18, 557–569. doi: 10.1111/1755-0998.12762

Knight, R., Vrbanac, A., Taylor, B. C., Aksenov, A., Callewaert, C., Debelius, J., et al. (2018). Best practices for analysing microbiomes. *Nat. Rev. Microbiol.* 16, 410–422. doi: 10.1038/s41579-018-0029-9

Knudsen, B. E., Lasse, B., Munk, P., Oksana, L., Priemé, A., Aarestrup, F. M., et al. (2016). Impact of sample type and DNA isolation procedure on genomic inference of microbiome composition. *mSystems* 1:e00095-16. doi: 10.1128/mSystems.00095-16

Kuhn, R., Böllmann, J., Krahl, K., Bryant, I. M., and Martienssen, M. (2017). Comparison of ten different DNA extraction procedures with respect to their suitability for environmental samples. *J. Microbiol. Methods* 143, 78–86. doi: 10.1016/j.mimet.2017.10.007

Lear, G., Dickie, I., Banks, J., Boyer, S., Buckley, H. L., Buckley, T. R., et al. (2018). Methods for the extraction, storage, amplification and sequencing of DNA from environmental samples. *New Z. J. Ecol.* 42, 1A–50A. doi: 10.20417/nzjecol.42.9

Levins, R. (1968). *Evolution in Changing Environments*. Princeton, NJ: Princeton University Press.

Li, P., Yang, S. F., Lv, B. B., Zhao, K., Lin, M. F., Zhou, S., et al. (2015). Comparison of extraction methods of total microbial DNA from freshwater. *Genet. Mol. Res.* 14, 730–738. doi: 10.4238/2015.January.30.16

Liu, L. M., Liu, M., Wilkinson, D. M., Chen, H. H., Yu, X. Q., and Yang, J. (2017). DNA metabarcoding reveals that 200-μm-size-fractionated filtering is unable to discriminate between planktonic microbial and large eukaryotes. *Mol. Ecol. Resour.* 17, 991–1002. doi: 10.1111/1755-0998.12652

Liu, L. M., Yang, J., Yu, Z., and Wilkinson, D. M. (2015). The biogeography of abundant and rare bacterioplankton in the lakes and reservoirs of china. *ISME J.* 9, 2068–2077. doi: 10.1038/ismej.2015.29

Liu, M., Liu, L. M., Chen, H. H., Yu, Z., Yang, J. R., Xue, Y. Y., et al. (2019). Community dynamics of free-living and particle-attached bacteria following a reservoir *Microcystis* bloom. *Sci. Total Environ.* 660, 501–511. doi: 10.1016/j.scitotenv.2018.12.414

Lynch, M. D., and Neufeld, J. D. (2015). Ecology and exploration of the rare biosphere. *Nat. Rev. Microbiol.* 13, 217–229. doi: 10.1038/nrmicro3400

Magoč, T., and Salzberg, S. L. (2011). FLASH: fast length adjustment of short reads to improve genome assemblies. *Bioinformatics* 27, 2957–2963. doi: 10.1093/bioinformatics/btr507

McCarthy, A., Chiang, E., Schmidt, M. L., and Denef, V. J. (2015). RNA preservation agents and nucleic acid extraction method bias perceived bacterial community composition. *PLoS One* 10:e0121659. doi: 10.1371/journal.pone.0121659

Pedrós-Alió, C. (2012). The rare bacterial biosphere. *Annu. Rev. Mar. Sci.* 4, 449–466. doi: 10.1146/annurev-marine-120710-100948

Pollock, J., Glendinning, L., Wisedchanwet, T., and Watson, M. (2018). The madness of microbiome: attempting to find consensus "best practice" for 16S microbiome studies. *Appl. Environ. Microb.* 84, e2627–e2617. doi: 10.1128/AEM.02627-17

Purswani, J., Martín-Platero, A. M., Reboleiro-Rivas, P., González-López, J., and Pozo, C. (2011). Comparative analysis of microbial DNA extraction protocols for groundwater samples. *Anal. Biochem.* 416, 240–242. doi: 10.1016/j.ab.2011.05.024

Quast, C., Pruesse, E., Yilmaz, P., Gerken, J., Schweer, T., Yarza, P., et al. (2013). The SILVA ribosomal RNA gene database project: improved data processing and web-based tools. *Nucleic Acids Res.* 41, D590–D596. doi: 10.1093/nar/gks1219

Renshaw, M. A., Olds, B. P., Jerde, C. L., McVeigh, M. M., and Lodge, D. M. (2015). The room temperature preservation of filtered environmental DNA samples and assimilation into a phenol–chloroform–isoamyl alcohol DNA extraction. *Mol. Ecol. Resour.* 15, 168–176. doi: 10.1111/1755-0998.12281

Salter, S. J., Cox, M. J., Turek, E. M., Calus, S. T., Cookson, W. O., Moffatt, M. F., et al. (2014). Reagent and laboratory contamination can critically impact sequence-based microbiome analyses. *BMC Biol.* 12:87. doi: 10.1186/s12915-014-0087-z

Santos, S. S., Nielsen, T. K., Hansen, L. H., and Winding, A. (2015). Comparison of three DNA extraction methods for recovery of soil protist DNA. *J. Microbiol. Methods* 115, 13–19. doi: 10.1016/j.mimet.2015.05.011

Santos, S. S., Nunes, I., Nielsen, T. K., Jacquiod, S., Hansen, L. H., and Winding, A. (2017). Soil DNA extraction procedure influences protist 18S rRNA gene community profiling outcome. *Protist* 168, 283–293. doi: 10.1016/j.protis.2017.03.002

Schloss, P. D., Westcott, S. L., Ryabin, T., Hall, J. R., Hartmann, M., Hollister, E. B., et al. (2009). Introducing mothur: open-source, platform-independent, community-supported software for describing and comparing microbial communities. *Appl. Environ. Microb.* 75, 7537–7541. doi: 10.1128/AEM.01541-09

Shendure, J., Balasubramanian, S., Church, G. M., Gilbert, W., Rogers, J., Schloss, J. A., et al. (2017). DNA sequencing at 40: past, present and future. *Nature* 550, 345–353. doi: 10.1038/nature24286

Singh, S. P., Rastogi, R. P., Häder, D. P., and Sinha, R. P. (2011). An improved method for genomic DNA extraction from cyanobacteria. *World J. Microb. Biotechnol.* 27, 1225–1230. doi: 10.1007/s11274-010-0571-8

Sinha, R., Abu-Ali, G., Vogtmann, E., Fodor, A. A., Ren, B., Amir, A., et al. (2017). Assessment of variation in microbial community amplicon sequencing by the microbiome quality control (MBQC) project consortium. *Nat. Biotechnol.* 35, 1077–1086. doi: 10.1038/nbt.3981

Sogin, M. L., Morrison, H. G., Huber, J. A., Mark Welch, D., Huse, S. M., Neal, P. R., et al. (2006). Microbial diversity in the deep sea and the under explored "rare biosphere". *Proc. Natl. Acad. Sci. U.S.A.* 103, 12115–12120. doi: 10.1073/pnas.0605127103

Sunagawa, S., Coelho, L. P., Chaffron, S., Kultima, J. R., Labadie, K., Salazar, G., et al. (2015). Structure and function of the global ocean microbiome. *Science* 348:1261359. doi: 10.1126/science.1261359

Sundberg, C., Al-Soud, W. A., Larsson, M., Alm, E., Yekta, S. S., Svensson, B. H., et al. (2013). 454 pyrosequencing analyses of bacterial and archaeal richness in

21 full-scale biogas digesters. *FEMS Microbiol. Ecol.* 85, 612–626. doi: 10.1111/1574-6941.12148

Velásquez-Mejía, E. P., de la Cuesta-Zuluaga, J., and Escobar, J. S. (2018). Impact of DNA extraction, sample dilution, and reagent contamination on 16S rRNA gene sequencing of human feces. *Appl. Microbiol. Biotechnol.* 102, 403–411. doi: 10.1007/s00253-017-8583-z

Walden, C., Carbonero, F., and Zhang, W. (2017). Assessing impacts of DNA extraction methods on next generation sequencing of water and wastewater samples. *J. Microbiol. Methods* 141, 10–16. doi: 10.1016/j.mimet.2017.07.007

Weiss, S., Amir, A., Hyde, E. R., Metcalf, J. L., Song, S. J., and Knight, R. (2014). Tracking down the sources of experimental contamination in microbiome studies. *Genome Biol.* 15:564. doi: 10.1186/s13059-014-0564-2

Xue, Y. Y., Chen, H. H., Yang, J. R., Liu, M., Huang, B. Q., and Yang, J. (2018). Distinct patterns and processes of abundant and rare eukaryotic plankton communities following a reservoir cyanobacterial bloom. *ISME J.* 12, 2263–2277. doi: 10.1038/s41396-018-0159-0

Yu, Y., Lee, C., Kim, J., and Hwang, S. (2005). Group-specific primer and probe sets to detect methanogenic communities using quantitative real-time polymerase chain reaction. *Biotechnol. Bioeng.* 89, 670–678. doi: 10.1002/bit.20347

Zhou, J., Wu, L., Deng, Y., Zhi, X., Jiang, Y., Tu, Q., et al. (2011). Reproducibility and quantitation of amplicon sequencing-based detection. *ISME J.* 5, 1303–1313. doi: 10.1038/ismej.2011.11

Conflict of Interest Statement: The authors declare that the research was conducted in the absence of any commercial or financial relationships that could be construed as a potential conflict of interest.

Copyright © 2019 Liu, Xue and Yang. This is an open-access article distributed under the terms of the Creative Commons Attribution License (CC BY). The use, distribution or reproduction in other forums is permitted, provided the original author(s) and the copyright owner(s) are credited and that the original publication in this journal is cited, in accordance with accepted academic practice. No use, distribution or reproduction is permitted which does not comply with these terms.

frontiers in Microbiology

ORIGINAL RESEARCH
published: 13 March 2019
doi: 10.3389/fmicb.2019.00451

Historical Occurrence of Algal Blooms in the Northern Beibu Gulf of China and Implications for Future Trends

Yixiao Xu[1,2], *Teng Zhang*[1,2] *and Jin Zhou*[3]*

[1] *Key Laboratory of Environment Change and Resources Use in Beibu Gulf, Ministry of Education, Guangxi Teachers Education University, Nanning, China,* [2] *Guangxi Key Laboratory of Earth Surface Processes and Intelligent Simulation, Guangxi Teachers Education University, Nanning, China,* [3] *Division of Ocean Science and Technology, Graduate School at Shenzhen, Tsinghua University, Shenzhen, China*

Large-scale harmful algal blooms (HABs) occur in the coastal waters of the northern Beibu Gulf, China, and have deleterious effects on the marine ecosystem. The frequency, duration, and extent of HAB events in this region have increased over the last 30 years. However, the underlying causes of HABs and their likely future trends are unclear. To investigate, we evaluated historical data for temporal trends of HABs in the Beibu Gulf, and association with environmental factors as possible drivers. The results confirmed that HAB events had increased in frequency, from 6 reported events during the period 1985–2000, to 13 during 2001–2010, and 20 during 2011–2017. We also found that the geographic scale of algal blooms had increased from tens of km^2 to hundreds of km^2. There were temporal changes in HAB trigger species: prior to 2000, the cyanobacteria *Microcystis aeruginosa* was the dominant species, while during the period 2001–2010, blooms of cyanobacteria, dinoflagellates, and diatoms co-occurred, and during 2011–2017, the haptophyte *Phaeocystis globosa* became the dominant algal bloom species. Principal component analysis and variation partitioning analysis indicated that nutrient discharge, industrial development, and human activities were the key drivers of HAB events, and redundancy analysis showed that variation in the algal community tended to be driven by nutrient structure. Other factors, such as shipping activities and mariculture, also contributed to HAB events and algal succession, especially to *P. globosa* blooms. We speculated that the increasing severity of algal blooms in the northern Beibu Gulf reflects a more complex aquatic environment and highlights the damaging effects of anthropogenic inputs, urbanization development, and an expanding industrial marine-economy on the marine ecosystem. This research provides more insight into the increase of HABs and will aid their management in the Beibu Gulf.

Keywords: algal blooms, Beibu Gulf, occurrence trend, *Phaeocystis globosa*, marine pollution, management

OPEN ACCESS

Edited by:
Haihan Zhang,
Xi'an University of Architecture and Technology, China

Reviewed by:
Jianjun Wang,
Nanjing Institute of Geography and Limnology (CAS), China
Patricia M. Glibert,
University of Maryland Center for Environmental Science (UMCES), United States
Renata Medina-Silva,
Pontifícia Universidade Católica do Rio Grande do Sul, Brazil

***Correspondence:**
Jin Zhou
zhou.jin@sz.tsinghua.edu.cn

Specialty section:
This article was submitted to Aquatic Microbiology, a section of the journal Frontiers in Microbiology

Received: *02 December 2018*
Accepted: *20 February 2019*
Published: *13 March 2019*

Citation:
Xu Y, Zhang T and Zhou J (2019) Historical Occurrence of Algal Blooms in the Northern Beibu Gulf of China and Implications for Future Trends. Front. Microbiol. 10:451. doi: 10.3389/fmicb.2019.00451

INTRODUCTION

Phytoplankton are a fundamental component of the marine ecosystem, playing multiple roles in nutrient cycling, and supporting global biological and geochemical processes (Lindh et al., 2013). However, excessive propagation of phytoplankton may cause an ecological phenomenon called harmful algal blooms (HABs). Some algal species that cause HABs produce toxins which lead to

the human poisoning syndromes called paralytic shellfish poisoning, diarrhetic shellfish poisoning, amnesic shellfish poisoning, neurotoxic shellfish poisoning, and ciguatera fish poisoning. In other cases, non-toxic, high-biomass HABs can kill fish and marine organisms through both physical and chemical mechanisms, and can also induce hypoxia or anoxia, killing marine life at multiple trophic levels (Heisler et al., 2008).

HABs have significantly increased throughout the world's coastal oceans over the last century mostly due to seawater eutrophication and climate change (Anderson et al., 2012; Glibert et al., 2018). China is also challenged by eutrophication and recurrent, large, and diversified algal blooms including red tides, green tides, and brown tides in coastal waters (Yu and Liu, 2016; Yi et al., 2018). The most persistent and damaging HABs occur in the Bohai Sea, Changjiang River estuary, and the coastal waters of the South China Sea (Tang et al., 2006; Yu and Liu, 2016; Zhou et al., 2017).

The semi-enclosed body of water of the northern Beibu Gulf is in southwest China, northwest of the South China Sea. Algal blooms in the region are fairly new to scientists and the public, as it is often thought of as the last "clean ocean" and one of the most abundant fishing grounds in Chinese coastal waters (Chen et al., 2011; Zhong, 2015). It was thus a shock to the local government and even to HAB scientists when *Phaeocystis globosa* blooms almost blocked the cooling waters used for a nuclear power station in Fangchenggang (Cao et al., 2017; Gong et al., 2018), covered waters near the nuclear station, and broke out simultaneously across the whole coast of the northern Beibu Gulf (Kaiser et al., 2013; Lai et al., 2014; Luo et al., 2016). Against this background, our study reviewed algal blooms from 1980s to 2017, and analyzed their frequency, duration, geographical distribution, and associated physicochemical parameters in the Beibu Gulf, and aimed to speculate on future trends in HABs occurrence to improve mitigation and management of future HABs in the region.

MATERIALS AND METHODS

Study Area

The northern Beibu Gulf (20° 58′-22° 50′ N, 107° 29′-110° 20′ E) (**Figure 1**) covers an area of 130,000 km^2, with an average water depth of 38 m and a 1,629 km coastline (Chen et al., 2011; Li et al., 2014b). Tieshan, Lianzhou, Qinzhou, Fangchenggang, and Zhenzhu bays lie from East to West, with Weizhou Island offshore (**Figure 1**). The climate is tropical monsoon, with prevailing southwest winds in summer and northeast winds in winter, and an average annual seawater temperature of 24.5°C. The warm wet weather, in conjunction with abundant nutrient input from coastal rivers, such as the Nanliujiang and Qinjiang rivers, creates one of the most abundant fishing grounds in China (Chen et al., 2011).

Data

Algal blooms recorded between 1985 and 2017 in the northern Beibu Gulf were collected from published literature, online media, monitoring station reports, and personal observations. Information including location, causative organism, taxonomy, and bloom area were extracted from these raw algal bloom data and are summarized in **Table 1**. Data sources are summarized in **Table 2** and are provided as **Supplements 1–15**: (1) population;

FIGURE 1 | Location of the study area.

TABLE 1 | Details and sources of historical algal bloom data (1985–2017).

Date	Location	Causative organism	Taxonomy	Area (km^2)	References
June 1985	Weizhou Island	*Trichodesmium erythraeum*	Cyanophyta, Cyanophyceae	—	Liang and Qian, 1991
March 1995	Lianzhou Bay	*Microcystis* sp.	Cyanophyta, Chroococcophyceae	≤10	Wei and He, 1998; Li et al., 2014a
Apr 1995	Beihai Port	*Microcystis aeruginosa*	Cyanophyta, Chroococcophyceae	—	Beihai Yearbook Editorial Committee, 1997
Nov 1995	Beihai Port	*Microcystis aeruginosa*	Cyanophyta, Chroococcophyceae	—	Beihai Yearbook Editorial Committee, 1997
Dec 1999	Weizhou Island	*Microcystis aeruginosa*	Cyanophyta, Chroococcophyceae	>50	Southland Morning Post, 2002; Qiu et al., 2005
May 2000	Weizhou Island	*Microcystis aeruginosa*	Cyanophyta, Chroococcophyceae	3	China Ocean Yearbook Editorial Committee, 2002
May 2001	Weizhou Island	—	—	20	China Ocean Yearbook Editorial Committee, 2003; Luo et al., 2016
May, 2002	Weizhou Island	—	—	5	Beihai Yearbook Editorial Committee, 2003; Marine Environmental Monitoring Center of Beihai Guangxi, 2006
June, 2002	Weizhou Island	*Trichodesmium hildebrandtii*	Cyanophyta, Cyanophyceae	20	Beihai Yearbook Editorial Committee, 2003
June 2003	Weizhou Island	*Microcystis flos-aquae*	Cyanophyta, Chroococcophyceae	20	Marine Environmental Monitoring Center of Beihai Guangxi, 2006
July 2003	Weizhou Island	*Trichodesmium erythraeum*	Cyanophyta, Cyanophyceae	10	China Ocean Yearbook Editorial Committee, 2004; China Oceanic Information Network, 2011
Feb 2004	Beihai	*Microcystis flos-aquae*	Cyanophyta, Chroococcophyceae	40	Marine Environmental Monitoring Center of Beihai Guangxi, 2006
Mar, 2004	Weizhou Island	*Microcystis flos-aquae*	Cyanophyta, Chroococcophyceae	2	Marine Environmental Monitoring Center of Beihai Guangxi, 2006
June 2004	Weizhou Island	*Trichodesmium erythraeum*	Cyanophyta, Cyanophyceae	40	Beihai Chorography Office, 2005; Li et al., 2009
May 2005	Weizhou Island	—	—	250	Tong, 2006
Apr 2008	Weizhou Island	*Noctiluca scintillans*	Dinophyta, Dinophyceae	0.025	State Oceanic Administration People's Republic of China, 2009
Apr 2008	Qinzhou Bay	*Noctiluca scintillans*	Dinophyta, Dinophyceae	0.0001	State Oceanic Administration People's Republic of China, 2009
July 2009	Lianzhou Bay	*Skeletonema costatum*	Bacillariophyta, Mediophyceae	—	Li et al., 2011
May 2010	Beibu Gulf	*Guinardia flaccida*	Bacillariophyta, Coscinodiscophyceae	150	Dou et al., 2015
Apr 2011	Qinzhou Bay	*Noctiluca scintillans*	Dinophyta, Dinophyceae	1.2	Southland Morning Post, 2015; Luo et al., 2016
Nov 2011	Beihai, Qinzhou, Fangcheng	*Phaeocystis globosa*	Haptophyta, Prymnesiophyceae	10	News China, 2011; Beihai Chorography Editorial Committee, 2012
Feb, 2012	Lianzhou Bay	*Guinardia flaccida*	Bacillariophyta, Coscinodiscophyceae	—	Li et al., 2015b
Jan–Dec 2013	Beibu Gulf (12 small blooms)	—	—	—	Southland Morning Post, 2015
Feb–Mar 2014	Tieshan Port-Shatian Port	*Phaeocystis globosa*	Haptophyta, Prymnesiophyceae	—	Li et al., 2015a
Feb–Mar 2014	Lianzhou Bay- Beihai	*Phaeocystis globosa*	Haptophyta, Prymnesiophyceae	—	Li et al., 2015a
Jan 2015	Almost entire northern Beibu Gulf coast	*Phaeocystis globosa*	Haptophyta, Prymnesiophyceae	—	Southland Morning Post, 2015
Feb 2017	Qinzhou Bay	*Phaeocystis globosa*	Haptophyta, Prymnesiophyceae	—	Author's observation
Mar 2017	Almost entire Weizhou Island coast	*Phaeocystis globosa*	Haptophyta, Prymnesiophyceae	—	Author's observation

TABLE 2 | Supplements, data sources, authors and data for (1) population, (2) gross industrial output value, (3) gross domestic product, (4) consumption of chemical fertilizers, (5) Guangxi seawater cultured areas, (6) Guangxi artificially cultured products, (7) Guangxi seawater aquatic products, (8) Guangxi marine related GDP, (9) Fishing boats in the northern Beibu Gulf of China from 2001 to 2010, (10–14) seawater nutrient content of NO_3, NO_2, NH_4, PO_4, S_iO_3, dissolved inorganic nitrogen (DIN), and Chemical Oxygen Demand (COD) in Tieshan Bay, Lianzhou Bay, Qinzhou Bay, Fangcheng Bay and the northern Beibu Gulf of China from 1983 to 2015, and (15) areas of five classification of summer seawater quality between 2010 and 2016 in the northern Beibu Gulf.

Supplements	Data sources	Authors	Data
Supplement 1	1989–2016 Guangxi Statistical Yearbook	China Statistics Press	Population (10^4 persons) for Nanning, Beihai, Qinzhou, and Fangchenggang from 1988 to 2015.
Supplement 2	1989–2016 Guangxi Statistical Yearbook	China Statistics Press	Gross industrial output value (10^8 Yuan) for Nanning, Beihai, Qinzhou, and Fangchenggang from 1988 to 2015.
Supplement 3	1989–2016 Guangxi Statistical Yearbook	China Statistics Press	Gross domestic product (10^8 Yuan) for Nanning, Beihai, Qinzhou and Fangchenggang from 1988 to 2015.
Supplement 4	1989–2016 Guangxi Statistical Yearbook	China Statistics Press	Consumption of chemical fertilizers (10^4 tons) for Nanning, Beihai, Qinzhou, and Fangchenggang from 1988 to 2015.
Supplement 5	1994–2007 Guangxi Statistical Yearbook	China Statistics Press	Guangxi seawater cultured areas (10^3 hectares) from 1978 to 2006.
Supplement 6	1994–2016 Guangxi Statistical Yearbook	China Statistics Press	Guangxi artificially cultured products (10^4 tons) from 1978 to 2015.
Supplement 7	1992–2017 Guangxi Statistical Yearbook	China Statistics Press	Guangxi seawater aquatic products (10^4 tons) from 1978 to 2015.
Supplement 8	2007–2016 Guangxi Marine Economic Statistics Bulletin	Department of Ocean and Fisheries of Guangxi Zhuang Autonomous Region	Guangxi marine related GDP (10^9 Yuan) from 2007 to 2016.
Supplement 9	Scientific publication	(Lan and Li, 2013)	Fishing boats in the northern Beibu Gulf of China from 2001 to 2010.
Supplement 10	Scientific publication	See **Supplementary Table 1**	Seawater nutrient content in Tieshan Bay, Guangxi from 1983 to 2012.
Supplement 11	Scientific publication	See **Supplementary Table 2**	Seawater nutrient content in Lianzhou Bay, Guangxi from 1991 to 2015.
Supplement 12	Scientific publication	See **Supplementary Table 3**	Seawater nutrient content in Qinzhou Bay, Guangxi from 1983 to 2015.
Supplement 13	Scientific publication	See **Supplementary Table 4**	Seawater nutrient content in Fangcheng Bay, Guangxi from 1983 to 2015.
Supplement 14	Scientific publication	See **Supplementary Table 5**	Seawater nutrient content in the northern Beibu Gulf, China from 1983 to 2015.
Supplement 15	2014-2016 Guangxi Marine Environmental Quality Bulletin	Department of Ocean and Fisheries of Guangxi Zhuang Autonomous Region	Areas of five classification of summer seawater quality between 2010 and 2016 in the northern Beibu Gulf (km^2).

(2) gross industrial output value; (3) gross domestic product; (4) consumption of chemical fertilizers; (5) Guangxi seawater cultured areas; (6) Guangxi artificially cultured products; (7) Guangxi seawater aquatic products; (8) Guangxi marine related GDP; (9) fishing boats in the northern Beibu Gulf of China from 2001 to 2010; (10–14) seawater nutrient content of NO_3, NO_2, NH_4, PO_4, S_iO_3, dissolved inorganic nitrogen (DIN), and Chemical Oxygen Demand (COD) in Tieshan Bay from 1983 to 2012, in Qinzhou Bay, Fangcheng Bay and the northern Beibu Gulf of China from 1983 to 2015, and in Lianzhou Bay from 1991 to 2015; and (15) areas of five classification of summer seawater quality between 2010 and 2016 in the northern Beibu Gulf. Among them, (1), (4–9) were defined as human activity, (2,3) as industrial development, (5–8) as mariculture, and (10–15) as environmental factors.

The seawater quality data containing the five classifications of summer seawater quality from 2010 to 2016 came from the 2014–2016 marine environmental quality bulletin of Guangxi, released by the Department of Ocean and Fisheries of the Guangxi Zhuang Autonomous Region. It was examined and classified according to the seawater quality standard of China (GB3097-1997), and was categorized from I to IV, where Grade I is defined as high quality seawater for ocean fishing, and marine nature reserves that contain rare and endangered marine organisms. Grade II is used for aquaculture, bathing beaches, and seawater activity areas with direct human contact, and also for industrial water use in relation to human consumption. Grade III is defined as general industrial water and coastal scenic areas, while Grade IV represents the worst quality seawater used for harbor and ocean engineering operations.

Statistical Analysis

We used one-way ANOVA in SPSS (v. 13.0) (Chicago, Illinois, USA) to evaluate differences in environmental parameters during three time periods (1985–2000; 2001–2010; and 2011–2017) at the $p < 0.05$ or $p < 0.01$ level. Correlations between HAB outbreaks and physicochemical factors based on euclidean distance were calculated using principal component analysis and visualized using R software (v2.15.1, www.r-project.org). The relationship between the environmental factors, human

activities, and HAB events from 1985 to 2017 was measured using multivariate correlation analysis (redundancy analysis), which was performed using the Canoco software package for Windows (v4.5) (Ithaca, New York, USA) with Monte Carlo permutation tests (499 permutations) (Terbraak and Smilauer, 2002; Legendre et al., 2011). HAB-causing species and environmental parameters used in the redundancy analysis were normalized through a logarithmic transformation ($\log_{10}$ (n+1)). We used variation partitioning analysis (VPA) to analyze the relative contribution of multiple parameters (industrial development, ID; environmental factors, EF; and human activities, HA) to HAB variation. The data came from **Table 2** as defined in Data section. These data were ($\log_2$ (x+1)) transformed for standardization. VPA was performed using the VEGAN package in R.

RESULTS

Historical HAB Events

There were 39 algal bloom events from 1985 to 2017, 15.4% occurred during the period 1985–2000, 33.3% during 2001–2010, and 51.3% during 2011–2017 (**Figures 2A,B**). The maximum area of algal blooms increased from >50 km^2 in the 1990s to 250 km^2 in the 2000s, and then HABs covered almost the entire coast between 2011 and 2017 (**Table 1**). Unfortunately, the area values between 2012 and 2017, when HABs became widespread, are not available. HAB duration was relatively short, occurring over days during the period 1985–2000; however, they typically occurred for weeks in the latter periods (**Table 1**).

Prior to 2000, HABs tended to occur at Beihai Port, Lianzhou Bay, and Weizhou Island; during the period 2001–2010, 70% of HABs occurred at Weizhou Island; and after 2011, HABs occurred at a greater number of sites, including along the coasts of Tieshan, Beihai, Qinzhou, Fangchenggang, and Weizhou Island (**Figure 2C**).

The causative microalgae included the cyanobacteria *Trichodesmium erythraeum* and *Microcystis* spp., with *M. aeruginosa* as the dominant species during the period 1985–2000. Blooms of cyanobacteria *T. hildebrandtii*, *T. erythraeum*, and *M. flos-aquae*, dinoflagellate *Noctiluca scintillans,* and diatoms *Skeletonema costatum* and *Guinardia flaccida* co-occurred without an obviously dominant species for the period 2001–2010. Between 2011 and 2017, the haptophyte *P. globosa* was the major species in blooms, particularly in the past 5 years (**Table 1**). We noticed that 4 of the 39 algal bloom events were associated with mortality of marine organisms such as fish and shrimp, and were attributed to *T. erythraeum* blooms in May 2001, July 2003, and June 2004 around Weizhou Island, and a *N. scintillans* bloom in Qinzhou in April 2011 (China Ocean Yearbook Editorial Committee, 2003, 2004; Beihai Chorography Office, 2005; State Oceanic Administration People's Republic of China, 2009; Luo et al., 2016).

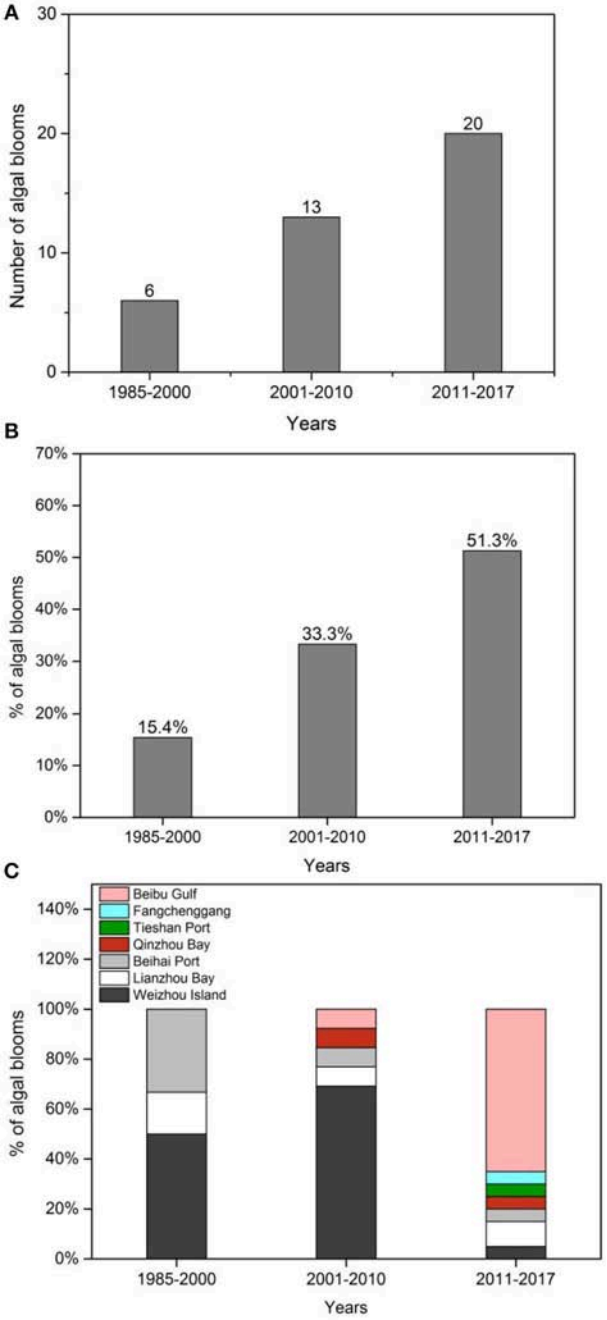

FIGURE 2 | Number **(A)** and proportion (%) **(B)** of algal blooms reported in the northern Beibu Gulf of China from 1985–2017; **(C)** proportion (%) of algal blooms at different locations in the northern Beibu Gulf of China from 1985 to 2017.

Industrial Development and Human Activities

Nanning, Qinzhou, Beihai, and Fangchenggang are the main districts in the Beibu Gulf Economic Zone. During the period 1980s−2015, across the districts there were 3.2–68.0, 98.1–22,703.3, 113.4–868.0, and 15.2-20,733.3-fold increases in population, gross industrial output value, gross domestic product, and fertilizer, respectively (**Figures 3A–D**). Nevertheless, these parameters were quite stable until the 1990s, when the substantial increases started. Although Nanning and Qinzhou generally reached much higher values than Beihai and

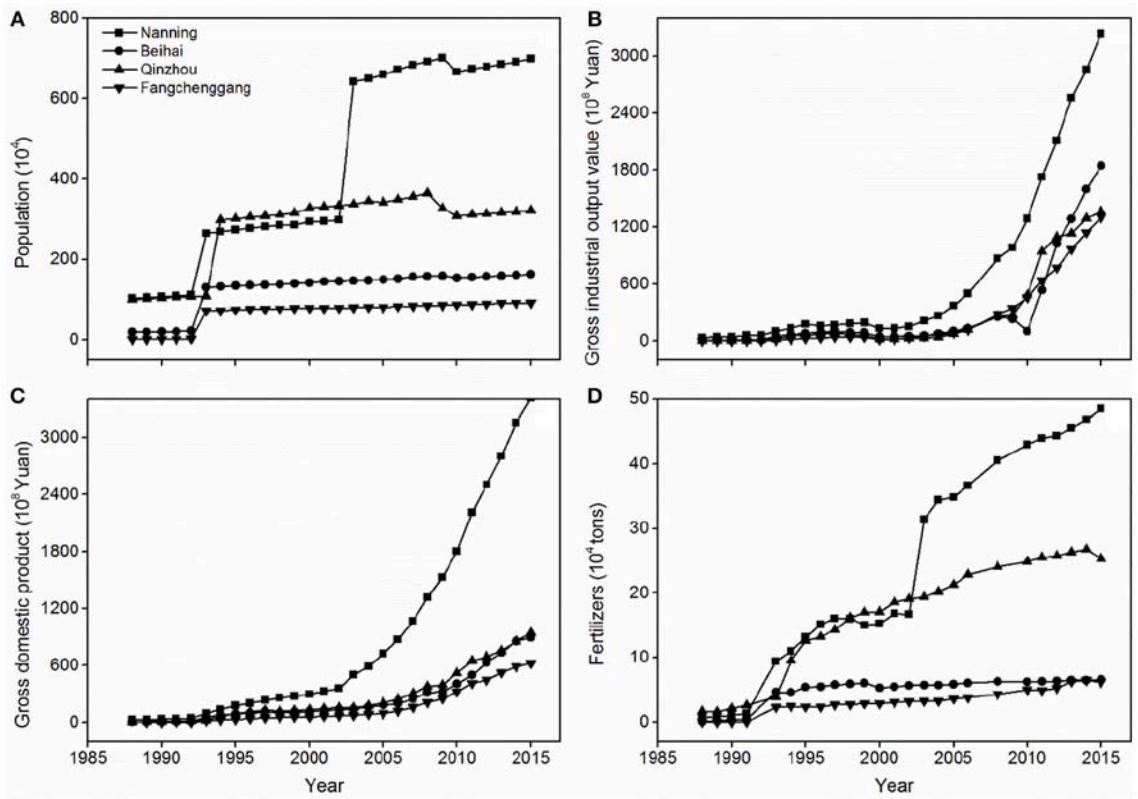

FIGURE 3 | Time-series plots of **(A)** population (10^4), **(B)** gross industrial output value (10^8 Yuan), **(C)** gross domestic product (10^8 Yuan), and **(D)** fertilizers (10^4 tons) in four key regions of the Guangxi Beibu Gulf Economic Zone.

Fangchenggang since the 2000s, all maximum fold increases were found in Fangchenggang due to its small initiating values in the 1980s.

The seawater cultured area increased 33.6-fold from 1978 to 2006; artificially cultured products and seawater aquatic products increased by 2,607.9- and 21.7-fold, respectively, from 1978 to 2015 (**Figures 4A–C**), with these parameters exhibiting a significant increase after the 1990s. There was an associated 3.9-fold increase in marine related GDP from 2007 to 2016 across the region (**Figure 4D**). Shipping transport in the northern Beibu Gulf intensified, with increases in the number of fishing boats (from 500 in 2001 to 3,850 in 2010) and effluent (3.74-fold increase from 2001 to 2010) (**Figure 5**).

Environmental Factors

We found significant increases in the levels of DIN, NO_3, NO_2, NH_4, and PO_4 ($p < 0.05$) in the study region (**Figure 6**). From 1980 to 2010, there were 17.9-, 12.7-, 33.5-, and 1.5-fold increases in average DIN, NO_3, NO_2, and NH_4 in the northern Beibu Gulf, respectively (**Table 3**). From 1990 to 2010, average PO_4 increased almost 2-fold, and there were no significant differences in concentrations of SiO_3 and COD ($p > 0.05$), although both were lowest in the 1980s (**Figure 6**, **Table 3**). Maximum concentrations of SiO_3 in the northern Beibu Gulf increased from 81.0 μM in the 1980s to 113.0 μM in the 1990s, and to 167.1 μM in the 2000s, while maximum COD increased from 2.7 mg/L in the 1980s to 7.5 mg/L in 2010s (**Figure 6**).

There was a deterioration in summer seawater quality between 2009 and 2016, with a generally increasing trend in the area of seawater with quality ranked in the lowest category (Grade IV), quality worse than Grade IV, and quality lower than Grade I during 2011–2015 (**Figure 7**).

Correlation Between Influencing Factors and HAB Events

We found there were temporal trends in multiple factors influencing HAB events (**Figure 8A**): between 1985 and 2000, there was an association with NH_4^+, seawater aquatic products, and marine related GDP value; while between 2001 and 2010, there was an association with artificially cultured products, fertilizer use, gross domestic product, and C-N-P-Si sources (such as COD, NO_3, PO_4, and SiO_3). Between 2011 and 2017 there was an association between HAB events and NO_3, NO_2, COD, PO_4, fishing activities, seawater quality, population number, industrial development, and mariculture.

For simplification, we used nutrients as the target in the redundancy analysis, and found that there was temporal variation in the dominant phytoplankton species (**Figure 8B**). Succession of algae tended to be driven by N and P content, and the two

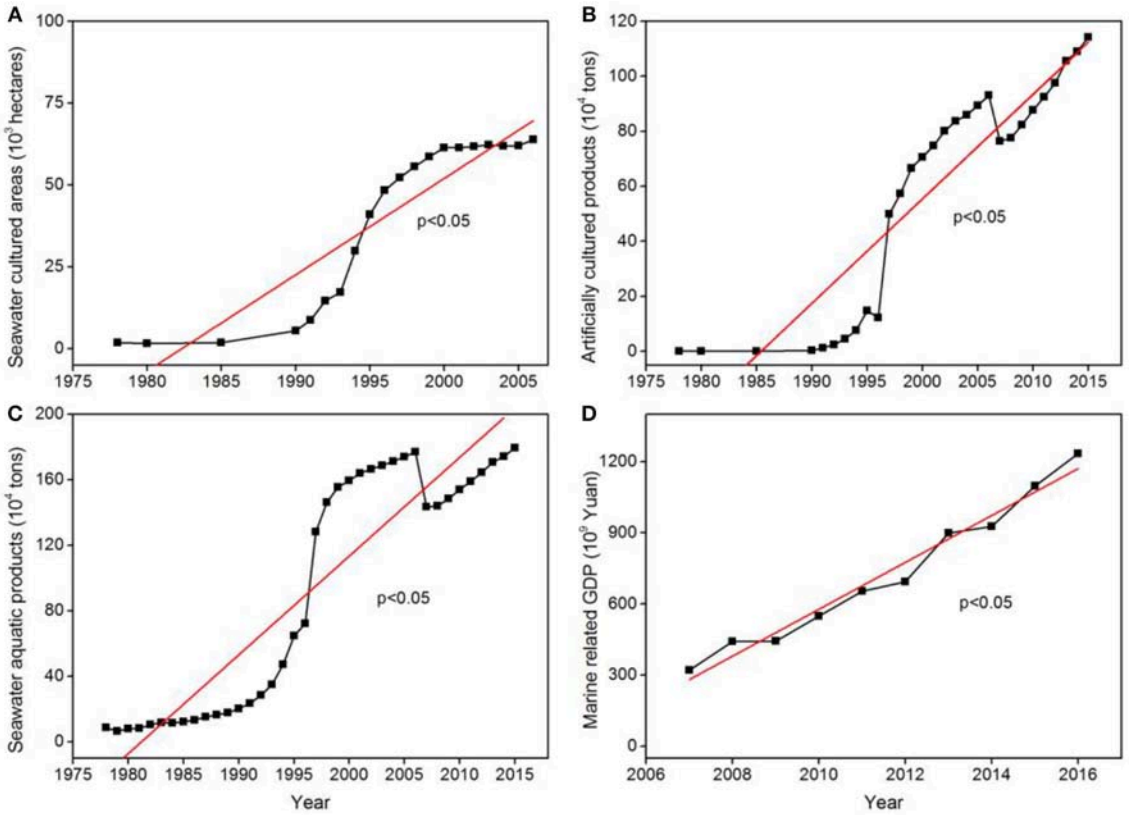

FIGURE 4 | Time-series plots of **(A)** seawater cultured areas (10^3 hectares), **(B)** artificially cultured products (10^4 tons), **(C)** seawater aquatic products (10^4 tons), and **(D)** marine related GDP (10^9 Yuan) in the northern Beibu Gulf. Red line denotes change in trend. For $p<0.05$, at the 0.05 level, the slope is significantly different from zero; for $p > 0.05$, at the 0.05 level, the slope is not significantly different from zero.

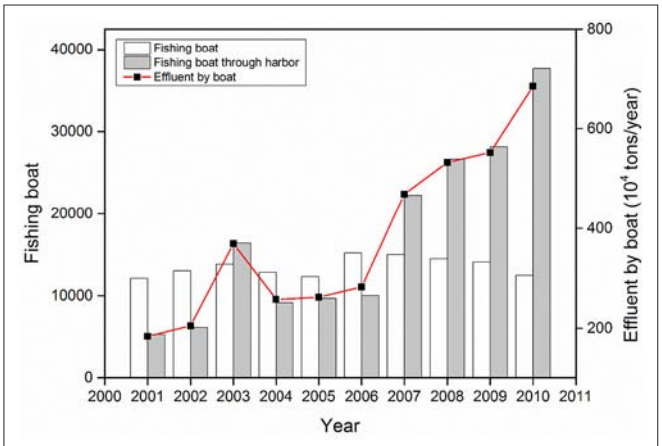

FIGURE 5 | Number of fishing boats and harbored fishing boats, and amount of effluent produced by boat in the northern Beibu Gulf of China from 2001 to 2010.

dominant species in earlier years, *M. aeruginosa* and *M. flos-aquae*, showed a preference for high levels of NH_4. Two species prominent from 2001 to 2010, *S. costatum* and *G. flaccida*, were closely associated with SiO_3 and COD. Other dominant species, *Trichodesmium* spp. and *N. scintillans* showed association with high levels of NO_3 and PO_4, and we found that DIN and PO_4 influenced *P. globosa* abundance.

VPA showed that when combined, ID, EF, and HA explained 65.7% of the variation in HAB outbreaks (**Figure 9**), whereas independently, ID, EF, and HA explained 14.7% ($p < 0.05$), 20.6% ($p < 0.05$), and 13.2% ($p < 0.05$) of the variation, respectively. Interactions between ID and EF, EF and HA, and HA and ID explained 7.1, 4.9, and 5.2% of variation, respectively. Overall 34.3% of variation in HAB events was not explained by these parameters.

DISCUSSION

Similar to many coastal regions globally, HABs in the northern Beibu Gulf have significantly increased in frequency, duration, geographical distribution, and degree of harm in recent decades (Anderson et al., 2002; Heisler et al., 2008). However, compared with already developed Chinese coastal areas such as the Bohai estuary and Changjiang River Estuary, there was an ∼ 10–15 year lag for the remarkable breakout of HABs in the northern Beibu Gulf (Luo et al., 2016; Yu and Liu, 2016; Song et al., 2018). Most anthropogenic activities surveyed in this study increased substantially by the late 1990s, when HAB frequency started to

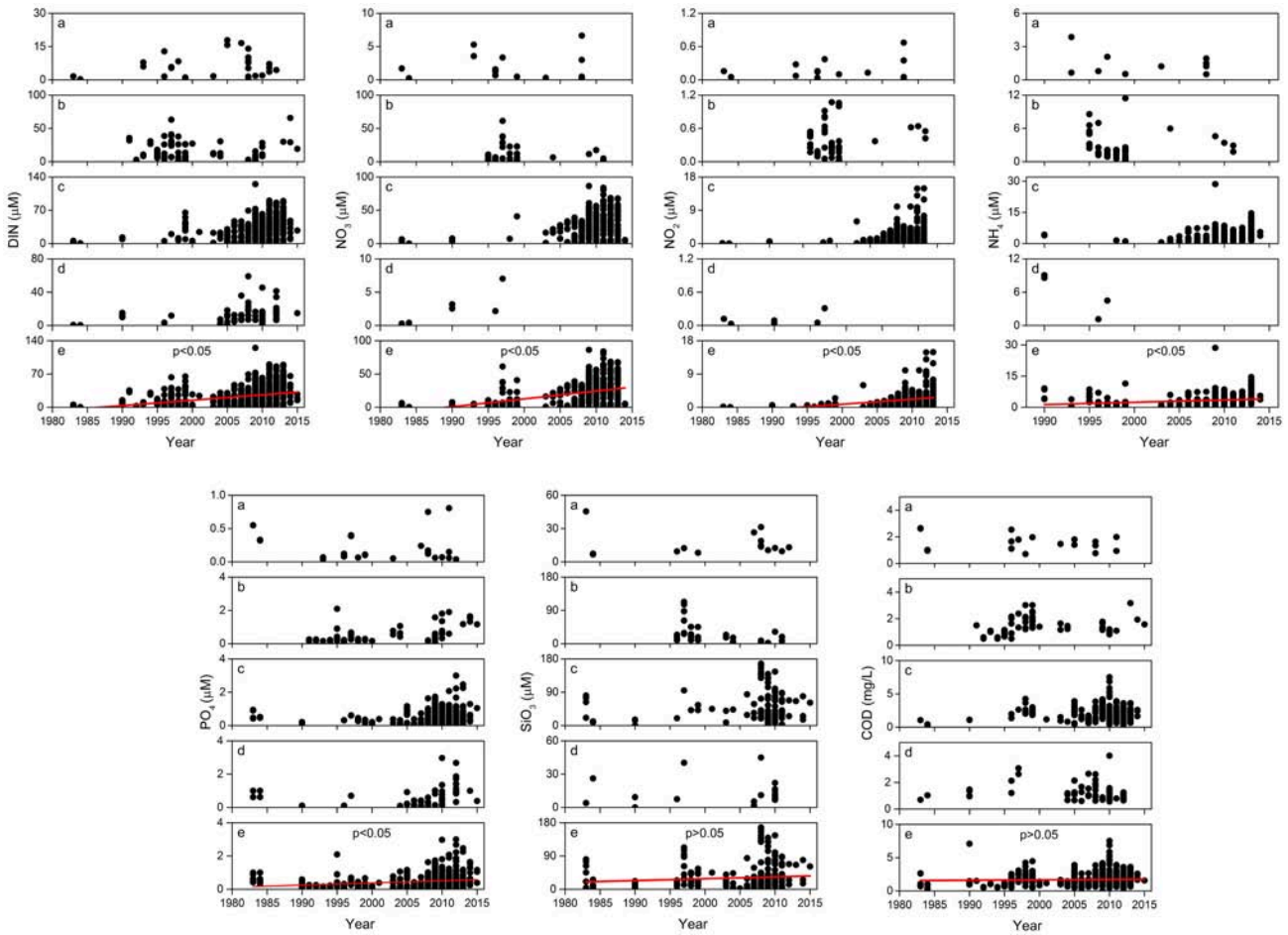

FIGURE 6 | Temporal changes in seawater nutrient content between 1980 and 2015 in (a) Tieshan Bay; (b) Lianzhou Bay; (c) Qinzhou Bay; (d) Fangcheng Bay; and, (e) Beibu Gulf, where $n = 697$, 456, 453, 442, 708, 278, and 560 for linear fit of DIN, NO_3, NO_2, NH_4, PO_4, SiO_3, and COD, respectively, and the red line denotes the long term trend. For $p < 0.05$, at the 0.05 level, the slope is significantly different from zero; for $p > 0.05$, at the 0.05 level, the slope is not significantly different from zero.

TABLE 3 | Long term trend in seawater nutrient (μM) and COD (mg/L) content in the northern Beibu Gulf. Data are means ±SD.

Year	DIN	NO_3	NO_2	NH_4	PO_4	SiO_3	COD
1980s	1.7 ± 1.9	2.1 ± 2.4	0.07 ± 0.05	1.5 ± 0.4	0.6 ± 0.2	23.5 ± 28.5	1.2 ± 0.9
1990s	14.2 ± 13.8	9.3 ± 11.9	0.37 ± 0.39	2.7 ± 2.5	0.3 ± 0.3	28.2 ± 27.5	1.8 ± 1.0
2000s	19.4 ± 17.8	20.4 ± 16.5	1.72 ± 1.66	2.7 ± 2.8	0.4 ± 0.4	31.4 ± 38.6	1.8 ± 1.0
2010s	29.9 ± 21.9	26.5 ± 20.2	2.43 ± 2.55	4.0 ± 2.9	0.6 ± 0.5	33.6 ± 29.6	1.6 ± 1.0

increase exponentially. It is thus likely anthropogenic activities play crucial roles in the occurrence of HABs in the region. Similar increases in HAB frequencies linked to anthropogenic activities, population, and industrial development were reported as early as 1976–1986 in Tolo Harbor, Hong Kong and 1965–1976 in the Seto Inland Sea of Japan (Lam and Ho, 1989; Okaichi, 1989). We thus speculate that the trend in HAB events in the northern Beibu Gulf is extremely likely to follow HAB patterns in already polluted coastal waters and will therefore further intensify if HAB mitigation and management strategies are not carried out in the near future.

Among the locations, Weizhou Island was the algal blooms hot spot prior to 2010, but blooms occurrences near the island subsequently declined while blooms increased in nearshore waters along the entire Beibu Gulf coast. The volcanic Weizhou Island is a natural source of trace metals such as iron and manganese, and nutrients N and P (Li and Lai, 2007), and the southwest monsoon in the Indian Ocean, which brings high temperatures and strong rainfall to the region, washes terrestrial nutrients into the nearshore waters, which fuels algal blooms. Nutrient-rich seawater passes through the Qiongzhou Strait in the northern Beibu Gulf all year round and elicited a stronger

effect on HABs at Weizhou Island than in the bays of Beihai, Qinzhou, and Fangcheng, because summer seawater upwelling delivers abundant nutrients to the sea surface near the island (Yang et al., 2006; Shi, 2014). Most HABs occur at the southern part of Weizhou Island which is the main location for industrial and mariculture activities, and has a dense population that has

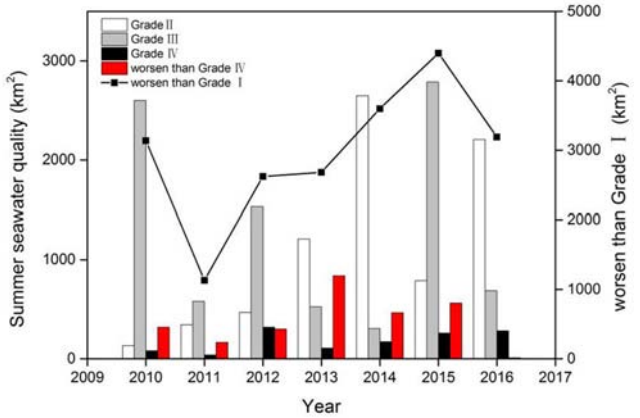

FIGURE 7 | Summer seawater quality between 2009 and 2016 in the northern Beibu Gulf. Seawater quality is categorized from I–IV, where Grade I is defined as high quality seawater for ocean fishing, marine nature reserves that contain rare and endangered marine organism, while Grade IV represent the worst quality seawater used for harbor and ocean engineering operations.

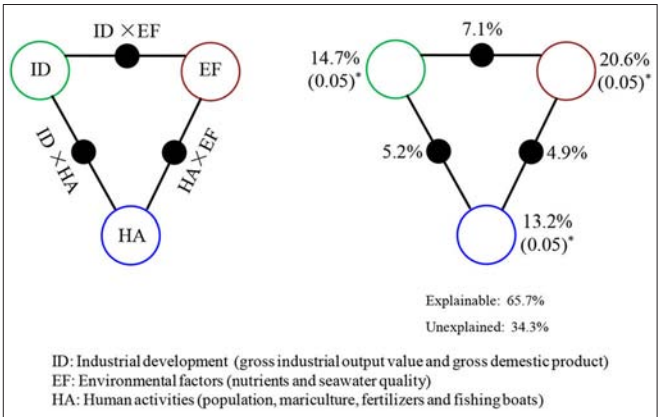

FIGURE 9 | Variation partitioning analysis (VPA) of HAB events explained by multiple influencing factors including industrial development, ID; environmental factors, EF; and human activities, HA. The angles and sides of the triangles represent the variation explained by each single factor and by the combination of any two factors, respectively.

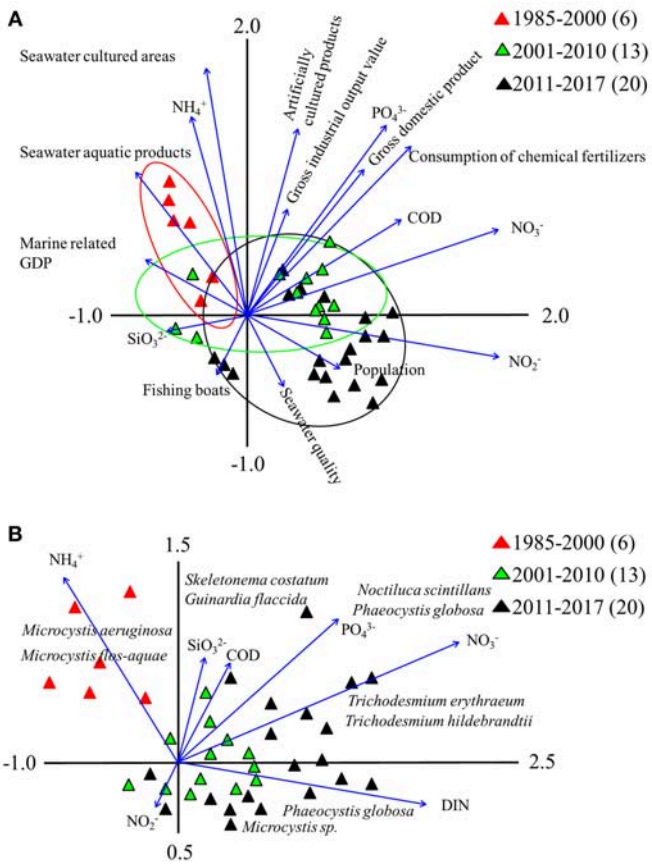

FIGURE 8 | Principal component analysis **(A)** and redundancy analysis **(B)** of industrial development, environmental factors, human activities and HAB events at sampling stations from 1985 to 2017 in the study region. Arrow length indicates importance of each factor in HAB events.

polluted the coastline (Qiu et al., 2005; He et al., 2013; Li et al., 2014a; Dou et al., 2015). Finally, the nutrient structure in Weizhou Island has changed from N limitation (N:P = 4.1) in the beginning of the 1990s (Wei et al., 2005) to P limitation (N:P = 38.1) in the late 2000s (Sun et al., 2010; He et al., 2013), which may partly explain the decline in HABs after the 2000s.

There were also changes in the ratios of Si:N:P in the northern Beibu Gulf over the study period, the N:P ratio increased from 2.9 to 6.5 in the 1980s to 24.8 to 202.6 in the 1990s in Qinzhou Bay (Wei et al., 2002a), similar trends have been recorded in Tieshan Bay and Lianzhou Bay (Wei et al., 2002b; Lan et al., 2014; Yang et al., 2015). These shifts from N limitation to N abundance, with relative sufficiency of Si, and P limitation (Wu, 2014; Wang F. et al., 2015; Yang et al., 2015) are likely to have changed algal species composition in marine ecosystems (Glibert, 2017). This may explain the recent dominance of *Phaeocystis* blooms in the region, in accordance with the substantial N requirements of *P. globosa* to support its proliferation and sustained blooms (Xu et al., 2003; Zheng, 2014; Gong et al., 2018).

Temporal shifts in dominant HAB species driven by nutrient conditions have been widely seen in Chinese waters. Changjiang River estuary, the most notable HAB area in China, has experienced an obvious change of dominant blooming microalgae from diatoms to noxious or toxic dinoflagellates in the last 30 years (Yang et al., 2015; Yu et al., 2017). This shift was thought to be largely driven by the increasing ratio of DIN:P and high DIN, which increased 4-fold from 20.5 μM in the 1960s to 80.0 μM in the 2000s (Ye et al., 2004; Wang and Cao, 2012; Yu et al., 2017). During 2009–2016, the proportion of dinoflagellate blooms has also risen to as high as 79% on the south China coast, induced by changes in seawater temperature, DIN, and P concentration (Yi et al., 2018). Changes in phytoplankton communities may also relate to climate change (Hallegraeff, 2010; Wells and Karlson, 2018), which needs to be investigated in the future for the northern Beibu Gulf.

The haptophyte *Phaeocystis* forms massive HABs in many parts of the world, from tropical and subtropical to Arctic and Antarctic oceans (Long et al., 2007; Smith et al., 2017). This bloom is recognized both as a nuisance and as an ecologically important phytoplankton, with production of haemolytic substances in relation to the risk of marine life and human health, as well as dimethylsulfide (DMS) involved in the biological regulation of the climate (Medlin and Zingone, 2007; Wang S. et al., 2015). So far, six *Phaeocystis* species have been clearly defined, and only three of them, *P. globosa*, *P. pouchetii*, and *P. antarctica*, were described to date as bloom forming species (Schoemann et al., 2005; Medlin and Zingone, 2007). However, in Chinese seawaters *P. globosa* is the only bloom causing organism within this genus to date, with its blooms first documented from Oct 1997-Feb 1998 in southeast China, covering thousands of km^2 in the coastal waters of Fujian and Guangdong (Chen et al., 1999; Qi et al., 2002). It then frequently appeared in southern coastal areas (Hainan, Hong Kong, and Guangdong), and Bohai and Yellow River estuaries from 2000 to 2009 (Qi et al., 2002; Li et al., 2012). Blooms of *P. globosa* started to occur from 2011 in the northern Beibu Gulf and have continued breaking out in recent years (**Table 1**). *Phaeocystis* has a complex polymorphic life cycle alternating between flagellated cells and colonies enclosed in an exopolysaccharide matrix (Rousseau et al., 2013), protecting it from predators, enhanced UVB, and viral and bacterial infections (Brussaard et al., 2005; Kennedy et al., 2012). Interestingly, *Phaeocystis* develops blooms in the colonial form, particularly in waters with abundant nitrates, phosphate, and urea (Schoemann et al., 2005; Wang et al., 2007; Liang et al., 2018). In addition to the advantages of colony morphology, another competitive advantage of *P. globosa* in the northern Beibu Gulf may be its environmental adaptations, such as high tolerance of varied environmental light, preference for high temperatures and flexible nutrient uptake strategy (Schoemann et al., 2005; Xu et al., 2017).

Both abiotic and biotic factors affect the formation and duration of HAB events (Smith et al., 1999; Lewitus et al., 2012; Smetacek, 2012; Smida et al., 2012). In this study, about 65.7% of HAB variation was explained by human activity factors, environmental factors, and industrial development, indicating that these parameters are dominant determinants of HAB formation. Our findings support the previous viewpoint that abiotic factors are the main drivers affecting algal bloom formation and community structure (Worden et al., 2015). On the other hand, we note that 34.3% of HAB variation was not explained by the data measured, which indicates that other abiotic (water chemistry and hydrodynamics) and/or biotic (algal species interactions, viral lysis, reactive oxygen species abundance, and fungal and zooplankton predation) factors that were not included in this analysis may be important drivers of HAB events (Sun et al., 2017; Karasiewicz et al., 2018; Zhang et al., 2018). Further investigation of the interactions among algae, bacteria, viruses, and ciliates, particularly their network relationship over longer time scales, is needed to better characterize the underlying mechanisms driving the increases in HAB events and phytoplankton community variation in the northern Beibu Gulf.

CONCLUSION

Algal blooms in the northern Beibu Gulf have intensified over the past three decades, likely as a result of anthropogenic influences. Continuing economic and industrial development, as well as a rising human population in the region, will lead to further increases in HAB events in the future. Thus, HAB mitigation strategies should include: (1) an increase in the number of buoys and automatic monitoring stations along the northern Beibu Gulf coast; (2) the development of satellite remote sensing, *in situ* cell observations, and computer modeling to predict bloom events; (3) reductions in nutrient discharge and/or improved management for N/P removal; and, (4) the creation of a science-based ecological management plan to perform the ecophysiological and toxicological characterization of regional algal bloom species. There should be government-level efforts to enrich database records of HAB events and analyze the key environmental

drivers of HABs to improve the sustainable development of this region.

AUTHOR CONTRIBUTIONS

YX and TZ collect the data and designed the experiments. YX and JZ contributed to the analyses work. The manuscript was first written by YX and TZ, and then improved by YX and JZ.

FUNDING

This work was funded by the National Natural Science Foundation of China (41506137, 41661021 and 41361022), Natural Science Foundation of Guangxi (2016GXNSFBA380037 and 2016JJF15001), the Opening Foundation of Key Laboratory of Environment Change and Resources Use in Beibu Gulf Ministry of Education (Guangxi Teachers Education University), and the Guangxi Key Laboratory of Earth Surface Processes and Intelligent Simulation (Guangxi Teachers Education University) (GTEU-KLOP-K1805).

SUPPLEMENTARY MATERIAL

The Supplementary Material for this article can be found online at: https://www.frontiersin.org/articles/10.3389/fmicb.2019.00451/full#supplementary-material

REFERENCES

Anderson, D. M., Alpermann, T. J., Cembella, A. D., Collos, Y., Masseret, E., and Montresor, M. (2012). The globally distributed genus *Alexandrium*: multifaceted roles in marine ecosystems and impacts on human health. *Harmful Algae* 14, 10–35. doi: 10.1016/j.hal.2011.10.012

Anderson, D. M., Glibert, P. M., and Burkholder, J. M. (2002). Harmful algal blooms and eutrophication: nutrient sources, composition, and consequences. *Estuaries* 25, 704–726.

Beihai Chorography Editorial Committee (2012). *2012 Beihai Yearbook*. Nanning: Guangxi People's Publishing House. 350 (in Chinese).

Beihai Chorography Office (2005). *2005 Beihai Yearbook*. Nanning: Guangxi People's Publishing House. 314 (in Chinese).

Beihai Yearbook Editorial Committee (1997). *1997 Beihai Yearbook*. Nanning: Guangxi People's Publishing House. 183 (in Chinese).

Beihai Yearbook Editorial Committee (2003). *2003 Beihai Yearbook*. Nanning: Guangxi People's Publishing House. 217 (in Chinese).

Brussaard, C. P. D., Kuipers, B., and Veldhuis, M. J. W. (2005). A mesocosm study *Phaeocystis globosa* population dynamics I. Regulatory role of viruses in bloom control. *Harmful Algae* 4, 859–874. doi: 10.1016/j.hal.2004.12.015

Cao, X., Yu, Z., and Qiu, L. (2017). Field experiment and emergent application of modified clays for *Phaeocystis globosa* blooms mitigation. *Oceanol. Et Limnologia Sin.* 48, 753–759 (in Chinese). doi: 10.11693/hyhz20170200026

Chen, J., Xu, N., Jiang, T., Wang, Y., Wang, C., and Qi, Y. (1999). A report of *phaeocystis globosa* bloom in coastal water of southeast China. *J. Jinan Univer.* 20, 124–129 (in Chinese).

Chen, Z., Cai, W., Xu, S., Huang, Z., and Qiu, Y. (2011). Risk assessment of coastal ecosystem in Beibu Gulf, Guangxi of South China. *Chinese J. Appl. Ecol.* 22, 2977–2986. doi: 10.13287/j.1001-9332.2011.0416

China Ocean Yearbook Editorial Committee (2002). *2001 China Ocean Yearbook*. Beijing: China Ocean Press, 372 (in Chinese).

China Ocean Yearbook Editorial Committee (2003). *2002 China Ocean Yearbook*. Beijing: China Ocean Press, 181 (in Chinese).

China Ocean Yearbook Editorial Committee (2004). 2003 China Ocean Yearbook. Beijing: China Ocean Press, 213 (in Chinese).

China Oceanic Information Network (2011). *2003 Marine Environmental Quality Bulletin of Guangxi: Red Tides*. Available online at: http://www.nmdis.org.cn/gongbao/nrhuanjing/nryanhai/nr2003/nr03guangxi/201107/t20110729_18394.html (Accessed Mar 1, 2019). (in Chinese).

Dou, Y., Gao, J., Shi, X., Chen, R., and Zhou, W. (2015). Outbreak frequency and factors influencing red tides in nearshore waters of the South China Sea from 2000 to 2013. *J. Hydroecol.* 36, 31–27 (in Chinese). doi: 10.15928/j.1674-3075.2015.03.005

Glibert, P. M. (2017). Eutrophication, harmful algae and biodiversity—Challenging paradigms in a world of complex nutrient changes. *Mar. Poll. Bull.* 124, 591–606. doi: 10.1016/j.marpolbul.2017.04.027

Glibert, P. M., Al-Azri, A., Icarus Allen, J., Bouwman, A. F., Beusen, A. H. W., Burford, M. A., et al. (2018). "Key questions and recent research advances on harmful algal blooms in relation to nutrients and eutrophication," in *Global Ecology and Oceanography of Harmful Algal Blooms*, eds P. M. Glibert, E. Berdalet, M. A. Burford, G. C. Pitcher, and M. Zhou (Cham: Springer), 229–259. doi: 10.1007/978-3-319-70069-4_12

Gong, B., Wu, H., Ma, J., Luo, M., and Li, X. (2018). The algae community in taxon Haptophyceae at the early bloom stage of *Phaeocystis globosa* in Northern Beibu Gulf in winter. *BioRxiv [preprint]*. doi: 10.1101/492454

Hallegraeff, G. M. (2010). Ocean climate change, phytoplankton community responses, and harmful algal blooms: a formidable predictive challenge. *J. Phycol.* 46, 220–235. doi: 10.1111/j.1529-8817.2010.00815.x

He, B., Li, G., Wei, M., and Tan, Q. (2013). Relationship between the seasonality of seawater N:P ratio and the structure of plankton on the reefs of Weizhou Island, northern South China Sea. *J. Trop. Oceano.* 32, 64–72 (in Chinese). doi: 10.3969/j.issn.1009-5470.2013.04.010

Heisler, J., Glibert, P. M., Burkholder, J. M., Anderson, D. M., Cochlan, W., Dennison, W. C., et al. (2008). Eutrophication and harmful algal blooms: a scientific consensus. *Harmful Algae* 8, 3–13. doi: 10.1016/j.hal.2008.08.006

Kaiser, D., Unger, D., Qiu, G., Zhou, H., and Gan, H. (2013). Natural and human influences on nutrient transport through a small subtropical Chinese estuary. *Sci Total. Environ.* 450–451, 92–107. doi: 10.1016/j.scitotenv.2013.01.096

Karasiewicz, S., Breton, E., Lefebvre, A., Fariñas, T. H., and Lefebvre, S. (2018). Realized niche analysis of phytoplankton communities involving HAB: *Phaeocystis* spp. as a case study. *Harmful Algae* 72, 1–13. doi: 10.1016/j.hal.2017.12.005

Kennedy, F., McMinn, A., and Martin, A. (2012). Effect of temperature on the photosynthetic efficiency and morphotype of *Phaeocystis antarctica*. *J. Exp. Marine Biol. Ecol.* 429, 7–14. doi: 10.1016/j.jembe.2012.06.016

Lai, J., Jiang, F., Ke, K., Xu, M., Lei, F., and Chen, B. (2014). Nutrients distribution and trophic status assessment in the northern Beibu Gulf, China. *Chin. J. Oceanol. Limnol.* 32, 1128–1144. doi: 10.1007/s00343-014-3199-y

Lam, C. W., and Ho, K. (1989). "Red tides in Tolo Harbour, Hong Kong," in *Red tides, Biology Environmental Science and Toxicology*, eds T. Okaichi, D. M. Anderson, and T. Nemoto (New York, NY: Elsevier), 49–52.

Lan, W., and Li, T. (2013). Problems and countermeasures of marine ecosystem Qinzhou Bay. *Environ. Sci. Manage.* 38, 118–122 (in Chinese). doi: 10.3969/j.issn.1673-1212.2013.01.029

Lan, W., Li, T., and Han, L. (2014). Distribution and seasonal variation of nutrition in the adjacent waters of Tieshangang bay in Guangxi. *Marine Sci.* 38, 63–69 (in Chinese). doi: 10.11759/hykx20100812001

Legendre, P., Oksanen, J., and Braak, C. J. F. T. (2011). Testing the significance of canonical axes in redundancy analysis. *Method. Ecol. Evol.* 2, 269–277. doi: 10.1111/j.2041-210X.2010.00078.x

Lewitus, A. J., Horner, R. A., Caron, D. A., Garcia-Mendoza, E., Hickey, B. M., Hunter, M., et al. (2012). Harmful algal blooms along the North American west coast region: history, trends, causes, and impacts. *Harmful Algae* 19, 133–159. doi: 10.1016/j.hal.2012.06.009

Li, B., Lan, W., Li, T., and Li, M. (2015a). Variation of environmental factors during *Phaeocystis globosa* blooms and its implications for the bloom decay.

Chinese J. Ecol. 34, 1351–1358 (in Chinese). doi: 10.13292/j.1000-4890.20150311.050

Li, F., and Lai, C. (2007). Investigations on red tide in the sea area of Guangxi and countermeasures. *Environ. Sci. Manage.* 32, 76–109 (in Chinese). doi: 10.3969/j.issn.1673-1212.2007.09.023

Li, S., Xu, S., Liang, M., and He, G. (2014b). Research on marine environmental protection and the management of the Beibu Gulf in Guangxi. *J. Qinzhou Univer.* 29, 1-5 (in Chinese).

Li, T., Lan, W., Lu, Y., and Xie, X. (2015b). Application of automatic monitoring buoy in early warning for algal blooms in offshore area. *Marine Forecasts* 32, 70–78 (in Chinese). doi: 10.11737/j.issn.1003-0239.2015.01.011

Li, T., Li, Y., Lai, C., Ning, Y., and Lu, Y. (2011). Analyze red tide with automatic monitoring system of water quality in Lianzhou Gulf. *Environ. Monitor. China* 27, 32–35 (in Chinese). doi: 10.3969/j.issn.1002-6002.2011.04.008

Li, X., Zhang, J., and Liu, G. (2009). Studies of a *Trichodesmium erythraeum* red tide in sea area near Weizhou Island Guangxi. *Guangxi Sci.* 16, 188–192 (in Chinese). doi: 10.13656 /j.cnki.gxkx.2009.02.017

Li, Y., Shen, P., Huang, L., and Qi, Y. (2012). Taxonomy and phylogenetics of genus *Phaeocystis*: Research progress. *Chin. J. Ecol.* 31, 745–754 (in Chinese). doi: 10.13292/j.1000-4890.2012.0153

Li,. S., Dai, Z., Ge, Z., Xie, H., and Huang, H. (2014a). Research on the changes of the ecological environment disasters along the northern Beibu Gulf. *J. Catastrophol.* 29, 43–47 (in Chinese). doi: 10.3969/j.issn.1000-811X.2014.04. 009

Liang, D., Wang, X., and Wang, Y. (2018). Effects of different nitrogen on the growth and the formation of colony in *phaeocystis globosa*. *Adv. Marine Sci.* 36, 272–278 (in Chinese). doi: 10.3969/j.issn.1671-6647.2018.02.012

Liang, S., and Qian, H. (1991). Relationship between harmful algal blooms and monsoon transform in the north of South China Sea. *Res. Dev. South China Sea* 3, 1–5 (in Chinese).

Lindh, M. V., Riemann, L., Baltar, F., Romero-Oliva, C., Salomon, P. S., Granéli, E., et al. (2013). Consequences of increased temperature and acidification on bacterioplankton community composition during a mesocosm spring bloom in the Baltic Sea. *Environ. Microbiol. Rep*. 5, 252–262. doi: 10.1111/1758-2229.12009

Long, J. D., Frischer, M. E., and Robertson, C. Y. (2007). A *phaeocystis globosa* bloom associated with upwelling in the subtropical South Atlantic Bight. *J. Plankton Res.* 29, 769–774. doi: 10.1093/plankt/fbm058

Luo, J., Li, T., and Lan, W. (2016). Evolution trend and prevention strategy of algae bloom in the Beibu Gulf. *Environ. Protec.* 20, 40–42 (in Chinese). doi: 10.14026/j.cnki.0253-9705.2016.20.008

Marine Environmental Monitoring Center of Beihai Guangxi (2006). *2001-2005 Report on Coastal Seawater Quality of Guangxi* (in Chinese).

Medlin, L., and Zingone, A. (2007). A taxonomic review of the genus *phaeocystis*. *Biogeochemistry* 83, 3–18. doi: 10.1007/s10533-007-9087-1

News China (2011). *Red tide appears in part of Beibu Gulf of Guangxi*. Available online at: http://news.xinhuanet.com/fortune/2011-11/10/c_111158418.htm (Accessed May 12, 2018). (in Chinese).

Okaichi, T. (1989). "Red tide problems in the Seto Inland Sea, Japan," in *Red tides, Biology Environmental Science and Toxicology*, eds T. Okaichi, D. M. Anderson, and T. Nemoto (New York, NY: Elsevier),137–142.

Qi, Y., Xu, N., Wang, Y., Lu, S., and Chen, J. (2002). Progress of studies on red tide in China—Studies on *Phaeocystis globosa* red tide and its DMS (DMSP) production. *China Basic Sci.* 4, 23–27 (in Chinese). doi: 10.3969/j.issn.1009-2412.2002.04.005

Qiu, S., Lai, T., and Zhuang, J. (2005). A case analysis of the *Microcystis aeruginosa* red tide occurring in the sea field of Nanwan harbor, Weizhou Island. *Guangxi Sci.* 12, 330–333 (in Chinese). doi: 10.13656/j.cnki.gxkx.2005.04.026

Rousseau, V., Lantoine, F., Rodriguez, F., LeGall, F., Chrétiennot-Dinet, M., and Lancelot, C. (2013). Characterization of *Phaeocystis globosa* (Prymnesiophyceae), the blooming species in the Southern North Sea. *J. Sea. Res.* 76, 105–113. doi: 10.1016/j.seares.2012.07.011

Schoemann, V., Becquevort, S., Stefels, J., Rousseau, V., and Lancelot, C. (2005). *Phaeocystis* blooms in the global ocean and their controlling mechanisms: a review. *J. Sea Res.* 53, 43–66. doi: 10.1016/j.seares.2004.01.008

Shi, M. (2014). Study comments on circulation in Beibu Gulf. *Guangxi Sci.* 21, 313–324 (in Chinese). doi: 10.13656/j.cnki.gxkx.2014.04.001

Smetacek, V. (2012). Making sense of ocean biota: how evolution and biodiversity of land organisms differ from that of the plankton. *J. Biosci.* 37, 589–607. doi: 10.1007/s12038-012-9240-4

Smida, D. B., Sahraoui, I., Mabrouk, H. H., and Hlaili Sakka, A. (2012). Seasonal dynamics of genus *Alexandrium* (potentially toxic dinoflagellate) in the lagoon of Bizerte (North of Tunisia) and controls by the abiotic factors. *Cri. Rev. Biol.* 335, 406–416. doi: 10.1016/j.crvi.2012.04.007

Smith, V. H., Tilman, G. D., and Nekola, J. C. (1999). Eutrophication: impacts of excess nutrient inputs on freshwater, marine, and terrestrial ecosystems. *Environ. Pollut*. 100, 179–196.

Smith, W. O., Jr, McGillicuddy., D. J, Jr.,Olson, E. B., Kosnyrev, V., et al. (2017). Mesoscale variability in intact and ghost colonies of *Phaeocystis antarctica* in the Ross Sea: Distribution and abundance. *J. Marine Syst.* 166, 97–107. doi: 10.1016/j.jmarsys.2016.05.007

Song, N., Wang, N., Wu, N., and Lin, W. (2018). Temporal and spatial distribution of harmful algal blooms in the Bohai Sea during 1952∼2016 based on GIS. *China Environ. Sci.* 38, 1142–1148 (in Chinese). doi: 10.19674/s.cnki.issn1000-6923.2018.0136

Southland Morning Post (2002). *Red Tides Invade Twice, The Clean Sea may Disappear, the Beibu Gulf of Guangxi is in Emergency*. Available online at: http://news.sina.com.cn/c/2002-05-17/0908578104.html (Accessed May, 12 2018). (in Chinese).

Southland Morning Post (2015). *High Frequency of Red Tides Occur in Beibu Gulf, With 18 Red Tides in 20 Years*. Available at: http://gx.people.com.cn/n/2015/1222/c179430-27371761-2.html (Accessed May 12, 2018). (in Chinese).

State Oceanic Administration People's Republic of China (2009). *2008 Marine Environmental Quality Bulletin of Guangxi: Ocean Disastar*. Available online at: http://www.coi.gov.cn/gongbao/nrhuanjing/nryanhai/nr2008/nr08guangxi/201107/t20110729_17976.html (Accessed May 12, 2018). (in Chinese).

Sun, J. Y., Song, Y., Ma, Z. P., Zhang, H. J., Yang, Z. D., Cai, Z. H., et al. (2017). Fungal community dynamics during a marine dinoflagellate (*Noctiluca scintillans*) bloom. *Mar. Environ. Res.* 131, 183–194. doi: 10.1016/j.marenvres.2017.10.002

Sun, Y., Chen, B., Ma, Z., and Yu, W. (2010). Assessment and cause analysis of eutrophication in the adjacent sea areas of south subtropical islands. *Mar. Sci. Bull.* 29, 572–576 (in Chinese). doi: 10.3969/j.issn.1001-6392.2010.05.017

Tang, D., Di, B., Wei, G., Ni, I., Oh, I. S., and Wang, S. (2006). Spatial, seasonal and species variations of harmful algal blooms in the South Yellow Sea and East China Sea. *Hydrobiologia* 568, 245–253. doi: 10.1007/s10750-006-0108-1

Terbraak, C. J. F., and Smilauer, P. (2002). *Canoco Reference Manual and Canodraw for Windows User's Guide: Software for Canonical Community Ordination (version 4. 5)*. New York, NY: Microcomputer Power.

Tong, M. (2006). Classfication, Grading and Risk Assessment System of Harmful Algal Blooms in Coastal China. [master's thesis]. Jinan University, 64 (in Chinese).

Wang, F., Lin, Y., Cao, W., Zhang, W., Zheng, L., Yang, W., et al. (2015). The relationship between nutrients and phytoplankton community structure in northern Beibu Gulf. *J. Trop. Oceano.* 34, 73–85 (in Chinese). doi: 10.11978/2014134

Wang, J., and Cao, J. (2012). Variation and effect of nutrient on phytoplankton community in Changjiang Estuary during last 50 years. *Marine Environ. Sci.* 31, 310–315 (in Chinese). doi: 10.3969/j.issn.1007-6336.2012.03.002

Wang, S., Elliott, S., Maltrud, M., and Cameron-Smith, P. (2015). Influence of explicit *Phaeocystis* parameterizations on the global distribution of marine dimethyl sulfide. *J. Geophys. Res.* 120, 2158–2177. doi: 10.1002/2015JG003017

Wang, Y., Qi, Y., and Li, S. (2007). Nutritional requirements for the growth of *Phaeocystis globosa* scherffel. *Acta Hydrobiol. Sinica* 31, 24–29 (in Chinese). doi: 10.3321/j.issn:1000-3207.2007.01.004

Wei, M., and He, B. (1998). A study on eutrophication and red tide formation in Lianzhou Bay. *Tropic Oceanol.* 17, 65–72 (in Chinese).

Wei, M., Lai, T., and He, B. (2002a). Change trend of the chemical items in Qinzhou Bay in the last twenty yearsINutrient condition in usual discharged period. *Mar. Environ. Sci.* 21, 49–52 (in Chinese). doi: 10.3969/j.issn.1007-6336.2002.03.011

Wei, M., Lai, T., and He, B. (2002b). Development trend of the water quality conditions in the Tieshangang Bay. *Mar. Sci. Bull.* 21, 69–74 (in Chinese). doi: 10.3969/j.issn.1001-6392.2002.05.010

Wei, M., Li, G., He, B., and Liang, W. (2005). Preliminory study of the relatioship between plankton and environmental factors in the coral reef system around Weizhou Island. *Trans. Oceanol. Limnol.* 2, 34–39 (in Chinese). doi: 10.3969/j.issn.1003-6482.2005.02.006

Wells, M. L., and Karlson, B. (2018). "Harmful algal blooms in a changing ocean," in *Global Ecology and Oceanography of Harmful Algal Blooms*, eds P. M. Glibert, E. Berdalet, M. A. Burford, G. C. Pitcher, and M. Zhou (Cham: Springer), 77–90. doi: 10.1007/978-3-319-70069-4_5

Worden, A. Z., Follows, M. J., Giovannoni, S. J., Wilken, S., Zimmerman, A. E., and Keeling, P. J. (2015). Rethinking the marine carbon cycle: factoring in the multifarious lifestyles of microbes. *Science* 347:1257594. doi: 10.1126/science.1257594

Wu, M. (2014). *The Distribution Feature of Nutrients and the Study of their Influence on Ecosystem in the Northern Beibu Gulf. [master's thesis]*. Xiamen University, 115 (in Chinese).

Xu, N., Huang, B., Hu, Z., Tang, Y., Duan, S., and Zhang, C. (2017). Effects of temperature, salinity, and irradiance on the growth of harmful algal bloom species *Phaeocystis globosa* Scherffel (Prymnesiophyceae) isolated from the South China Sea. *Chin. J. Oceanol. Limnol.* 35, 557–565. doi: 10.1007/s00343-017-5352-x

Xu, N., Qi, Y., Chen, J., Huang, W., Lv, S., and Wang, Y. (2003). Analysis on the cause of *Phaeocystis globosa* Scherffel red tide. *Acta Sci. Circumstan.* 23, 113–118 (in Chinese). doi: 10.13671/j.hjkxxb.2003.01.022

Yang, J., Zhang, R., Zhao, Z., Weng, S., and Li, F. (2015). Temporal and spatial distribution characteristics of nutrients in the coastal seawater of Guangxi Beibu Gulf during the past 25 years. *Ecol. Environ. Sci.* 24, 1493–1498 (in Chinese). doi: 10.16258/j.cnki.1674-5906.2015.09.011

Yang, S., Chen, B., and Li, P. (2006). A study of the characteristics of water transport from the South China Sea into Beibu Bay via the Qiongzhou Stratit in summer in terms of temperature and salinity data. *Trans. Oceanol. Limnol.* 1, 1–7 (in Chinese). doi: 10.3969/j.issn.1003-6482.2006.01.001

Ye, S., Ji, H., Cao, L., and Huang, X. (2004). Red tides in the Yangtze River Estuary and adjacent sea areas: causes and mitigation. *Marine Sci.* 28, 26–31 (in Chinese). doi: 10.3969/j.issn.1000-3096.2004.05.006

Yi, B., Chen, K., Zhou, J., and, L.ü, Y. (2018). Characteristics of red tide in coastal region of south China from 2009 to 2016. *Transact. Oceanol. Limnol.* 2, 23–31 (in Chinese). doi: 10.13984/j.cnki.cn37-1141.2018.02.004

Yu, R., and Liu, D. (2016). Harmful algal blooms in the coastal waters of China: Current situation, long-term changes and prevention strategies. *Chinese Acad. Sci.* 31, 1167–1174 (in Chinese). doi: 10.16418/j.issn.1000-3045.2016.10.005

Yu, R., Zhang, Q., Kong, F., Zhou, Z., Chen, Z., Zhao, Y., et al. (2017). Status, impacts and long-term changes of harmful algal blooms in the sea area adjacent to the Changjiang River estuary. *Oceanol. Et Limnol. Sin.* 48, 1178–1186 (in Chinese). doi: 10.11693/hyhz20170900247

Zhang, H., Wang, Y., Chen, S., Zhao, Z., Feng, J., Zhang, Z., et al. (2018). Water bacterial and fungal community compositions associated with urban lakes, Xi'an, China. *Int. J. Environ. Res. Public. Health.* 15:E469. doi: 10.3390/ijerph15030469

Zheng, B. (2014). *Ecological Studies on Plankton in Northern Beibu Gulf*. [master's thesis]. Xiamen University, 201 (in Chinese).

Zhong, C. (2015). Protect the last clean ocean in China: Beibu Gulf. *Contemporary Guangxi*, 14:40 (in Chinese).

Zhou, Z., Yu, R., and Zhou, M. (2017). Resolving the complex relationship between harmful algal blooms and environmental factors in the coastal waters adjacent to the Changjiang River estuary. *Harmful Algae* 62, 60–72. doi: 10.1016/j.hal.2016.12.006

Conflict of Interest Statement: The authors declare that the research was conducted in the absence of any commercial or financial relationships that could be construed as a potential conflict of interest.

Copyright © 2019 Xu, Zhang and Zhou. This is an open-access article distributed under the terms of the Creative Commons Attribution License (CC BY). The use, distribution or reproduction in other forums is permitted, provided the original author(s) and the copyright owner(s) are credited and that the original publication in this journal is cited, in accordance with accepted academic practice. No use, distribution or reproduction is permitted which does not comply with these terms.

frontiers in Microbiology

ORIGINAL RESEARCH
published: 24 April 2019
doi: 10.3389/fmicb.2019.00699

Quantification of Microbial Source Tracking and Pathogenic Bacterial Markers in Water and Sediments of Tiaoxi River (Taihu Watershed)

*Kiran Kumar Vadde[1], Alan J. McCarthy[2], Rong Rong[1] and Raju Sekar[1]**

[1] Department of Biological Sciences, Xi'an Jiaotong-Liverpool University, Suzhou, China, [2] Microbiology Research Group, Institute of Integrative Biology, University of Liverpool, Liverpool, United Kingdom

Taihu Lake is one of the largest freshwater lakes in China, serving as an important source of drinking water; >60% of source water to this lake is provided by the Tiaoxi River. This river faces serious fecal contamination issues, and therefore, a comprehensive investigation to identify the sources of fecal contamination was carried out and is presented here. The performance of existing universal (BacUni and GenBac), human (HF183-Taqman, HF183-SYBR, BacHum, and Hum2), swine (Pig-2-Bac), ruminant (BacCow), and avian (AV4143 and GFD) associated microbial source tracking (MST) markers was evaluated prior to their application in this region. The specificity and sensitivity results indicated that BacUni, HF183-TaqMan, Pig-2-Bac, and GFD assays are the most suitable in identifying human and animal fecal contamination. Therefore, these markers along with marker genes specific to selected bacterial pathogens were quantified in water and sediment samples of the Tiaoxi River, collected from 15 locations over three seasons during 2014 and 2015. Total/universal *Bacteroidales* markers were detected in all water and sediment samples (mean concentration 6.22 $\log_{10}$ gene copies/100 ml and 6.11 $\log_{10}$ gene copies/gram, respectively), however, the detection of host-associated MST markers varied. Human and avian markers were the most frequently detected in water samples (97 and 89%, respectively), whereas in sediment samples, only human-associated markers were detected more often (86%) than swine (64%) and avian (8.8%) markers. The results indicate that several locations in the Tiaoxi River are heavily polluted by fecal contamination and this correlated well with land use patterns. Among the five bacterial pathogens tested, *Shigella* spp. and *Campylobacter jejuni* were the most frequently detected pathogens in water (60% and 62%, respectively) and sediment samples (91% and 53%, respectively). Shiga toxin-producing *Escherichia coli* (STEC) and pathogenic *Leptospira* spp. were less frequently detected in water samples (55% and 33%, respectively) and sediment samples (51% and 13%, respectively), whereas *E. coli* O157:H7 was only detected in sediment samples (11%). Overall, the higher prevalence and concentrations of *Campylobacter jejuni*, *Shigella* spp., and STEC, along with the MST marker detection at a number of locations in the Tiaoxi River, indicates poor water quality and a significant human health risk associated with this watercourse.

Keywords: fecal pollution, Taihu watershed, Tiaoxi River, microbial source tracking (MST), pathogens, qPCR quantification

OPEN ACCESS

Edited by:
David A. Walsh,
Concordia University, Canada

Reviewed by:
Asli Aslan,
Georgia Southern University, United States
Jincai Ma,
Jilin University, China

***Correspondence:**
Raju Sekar
Sekar.Raju@xjtlu.edu.cn

Specialty section:
This article was submitted to Aquatic Microbiology, a section of the journal Frontiers in Microbiology

Received: *14 November 2018*
Accepted: *20 March 2019*
Published: *24 April 2019*

Citation:
Vadde KK, McCarthy AJ, Rong R and Sekar R (2019) Quantification of Microbial Source Tracking and Pathogenic Bacterial Markers in Water and Sediments of Tiaoxi River (Taihu Watershed). Front. Microbiol. 10:699. doi: 10.3389/fmicb.2019.00699

GRAPHICAL ABSTRACT | Tracking fecal contamination and pathogens in watersheds using molecular methods.

INTRODUCTION

Fecal contamination of drinking water sources, harvestable shellfish, and recreational waters is a major concern of public health, as it promotes human exposure to pathogenic microorganisms (Napier et al., 2017). Therefore, continuous monitoring and proper protection of these waters are required. Traditionally, fecal indicator bacteria (FIB) have been used to monitor pollution in environmental waters and to assess the associated public health risks (Griffith et al., 2009). There are several limitations to using FIB for microbial water quality monitoring, as these bacteria can persist and replicate outside of the host (Byappanahalli et al., 2003) and there can also be a poor correlation between FIB and pathogen presence (Ahmed et al., 2013). The major limiting factor, however, is that FIB detection does not indicate the source or origin of fecal contamination (Field and Samadpour, 2007), which is crucial for the characterization of a public health risk and the implementation of remediation measures. Therefore, microbial source tracking (MST) techniques have been developed over the last decade to unequivocally identify the sources and origins of fecal pollution. Both library-dependent (LD-MST) and library-independent MST (LI-MST) methods are available for identifying the source of fecal pollution, although LD-MST methods have several limitations in correctly assigning fecal contamination to host-specific sources (Harwood et al., 2003; Field and Samadpour, 2007). However, quantitative PCR (qPCR) based LI-MST techniques have proven to be widely applicable in the study of fecal contamination in environmental samples, because they can accurately quantify the host-specific MST target sequences (Layton et al., 2006; Kildare et al., 2007). Among the LI-MST methods, *Bacteroidales* are often used as the target, as they are obligate anaerobic bacteria found in the human and animal gut at higher levels than *E. coli* (Bernhard and Field, 2000); host-associated *Bacteroidales* 16S rRNA gene markers have been developed for different hosts to discriminate between human and other animal fecal sources in the environment (Kildare et al., 2007; Shanks et al., 2008; Mieszkin et al., 2009; Raith et al., 2013; Green et al., 2014). It has recently been reported that avian feces could be better distinguished from other fecal sources by targeting bacterial taxonomic groups such as *Helicobacter* spp., rather than *Bacteroidales* 16S rRNA (Green et al., 2012).

Previous reports specified that geographical differences could significantly affect the performance of these MST assays and recommended proper assessment prior to field application at new study areas (Reischer et al., 2013; Odagiri et al., 2015; Boehm et al., 2016). In China, studies on qPCR based MST assays to monitor fecal pollution are very limited (Jia et al., 2014; He et al., 2016; Fan et al., 2017). He et al. (2016) validated five MST and four mitochondrial DNA fecal source tracking (FST) markers for their applicability to study fecal pollution in the Taihu Lake watershed. They reported that mitochondrial DNA based human FST methods were superior (though slight cross-reactivity was observed with pig fecal samples, the primary livestock in the Taihu watershed) to those *Bacteroidales* based MST (BacH, HF183 SYBR) assays tested, but the most widely used MST makers, such as HF183 Taqman and BacHum qPCR assays were not included. They also reported that the Pig-2-Bac assay (*Bacteroidales* based) showed a higher accuracy than other mitochondrial DNA based swine FST markers. Jia et al. (2014) used swine specific *Bacteroidales* assay (Pig-2-Bac) to assess the levels of swine fecal pollution in the Hongqi River, and Fan et al. (2017) developed two new assays based on genome fragment enrichment (GFE) targeting *Bacteroidales*-like sequences present in pig fecal samples. Although MST methods provide information on the source of fecal pollution, they do not provide evidence for, or confirm the presence of, bacterial pathogens. Determining the correlation between MST data and direct pathogen detection has been addressed in relatively few cases (Ridley et al., 2014; Bradshaw et al., 2016; Steele et al., 2018). The correlation of MST markers with pathogen presence in environmental samples has provided

mixed results in MST field studies (Tambalo et al., 2012; Marti et al., 2013). Field studies to evaluate the correlation of MST marker and pathogens presence in a watershed are important for the assessment of the associated public health risk, have not previously been carried out in the Taihu watershed region.

Taihu Lake, one of the top five freshwater lakes in China, serves as a very important source of water supply, aquaculture, tourism, flood protection, and transportation. The Taihu watershed, located in southeast Jiangsu province and the Yangtze River basin, is one of the most populated regions of China, with a population density of 1,200 people per km^2 and annual production of approximately six million pigs and/or chickens (Qin et al., 2007). It is reported that decline in the water quality of Taihu Lake is due to pollutants such as untreated sewage, animal and industrial waste inputs from rivers associated with the volume of river discharge entering the lake (Zhang Y. et al., 2016). Inputs from rivers are the main route of contaminants and nutrients, to the detriment of the ecological health of the lake (Saxena et al., 2015). Currently, more than 200 rivers are connected to Taihu Lake but there are only 13 primary inflow rivers (Zhang Y. et al., 2016). Tiaoxi River contributes approximately 60% of the total source water to Taihu Lake, significantly driving the water quality status of Taihu Lake (Zhang Y. et al., 2016).

Here, we report the results of a comprehensive evaluation of existing general and host-specific MST qPCR markers, using fecal samples collected from the Taihu watershed region, in order to identify the most suitable MST qPCR assays for detecting host associated fecal pollution across this large and important water catchment. Secondly, this study reports the presence and abundance of MST and pathogenic bacterial gene markers in the Tiaoxi River water and sediment samples, in order to assess the fecal contamination of this river and to characterize correlations across the FIB, MST, and specific bacterial pathogens markers.

MATERIALS AND METHODS

Overview of the Study Area

The mainstream of the Tiaoxi River is 158 km in length consisting of the Eastern, Western, Southern, and Northern Tiaoxi Rivers (Zhang Y. et al., 2016). The Tiaoxi River flows in northern Zhejiang province covering the upstream agricultural areas and the downstream urban cities of the northern Zhejiang Province. It has been estimated that the river collects water from one million inhabitants residing in the moderately sized cities of Zhejiang Province (Zhang Y. et al., 2016). Poultry is a common livestock in Zhejiang province, and waste disposal is an issue (Zheijiang, 2016). Excluding poultry, pigs comprise more than 90% of the remaining livestock population in this region (NBSC, 2015). It has been reported that the Tiaoxi River is severely polluted by various sources such as farmlands, domestic sewage, and industrial waste, subsequently affecting the Taihu Lake water quality (Hagedorn and Liang, 2011; Lv et al., 2015).

Evaluation of Existing MST Markers for Applicability in Taihu Watershed

Selection of MST qPCR Assays and Fecal Sampling

The preliminary selection of MST assays for this study was based on the identity of the livestock population in Zhejiang Province and as per the data released by the National Bureau of Statistics, PR China in 2015 (NBSC, 2015). The MST assays developed and designed elsewhere were selected to validate their applicability; the details of the MST assays are provided in **Supplementary Table S1**. To determine the specificity and sensitivity of host-associated MST qPCR markers, individual and composite fecal and wastewater samples were used as target sources (Ahmed et al., 2016b). In total, 61 fresh individual and composite fecal samples, collected from various hosts in Huzhou (Zhejiang province) and Suzhou (Jiangsu province), were tested. The details of the collection of fecal and wastewater samples and preparation of composite fecal samples are provided in **Supplementary Note S1**. Individual fecal samples from animal hosts representing pigs, chickens, dogs, and cows (n = 10 for each) and composite fecal sources from ducks and geese (n = 3 pooled samples, each pooled sample was prepared from five individual fecal samples) were collected from farms, pet stores and the backyards of households located near the Taihu Lake/Tiaoxi River watershed region in the Huzhou area. All fecal samples were transported to the laboratory on ice and stored at −20°C within 6 h of collection. Primary effluents (500 ml; n = 6) were collected from a wastewater treatment plant (WWTP) located in Suzhou and brought to the laboratory on ice. Biomass from primary influents was collected by centrifugation at 4,000 × g for 10 min at 4°C, and DNA was extracted immediately. Ethical approval for handling fecal samples in this study was acquired from Xi'an Jiaotong-Liverpool University (XJTLU) Research Ethics Committee.

DNA Extraction and qPCR Assay Conditions

DNA extraction from the fecal/sewage samples was performed using the PowerFecal® DNA isolation kit that uses Inhibitor Removal Technology® (IRT) (MoBio, Carlsbad, CA, United States), following the manufacturer's instructions. The quality and quantity of extracted DNA was confirmed by NanoDrop ND 2000C (Thermo Fisher Scientific., United States) and extracts were stored at −20°C prior to further analysis. Further quality assurance of extracted DNA samples and the details of plasmid standard construction for MST qPCR assays are provided in **Supplementary Note S2**.

All qPCR reactions (20 μl) were performed in triplicate and the reaction mixture for all Taqman chemistry-based qPCR assays included 10 μl of TaqMan Environmental Master Mix 2.0 (Applied Biosystems, Foster City, CA, United States), 2 μl of the probe/primer set with a final concentration as shown in **Supplementary Table S1** and 8 μl of the 10-fold diluted target DNA template. For the two SYBR Green chemistry based qPCR assays (HF183 SYBR and GFD), the reaction mixture contained 10 μl of SYBR Green Master Mix 2.0 (Thermo Scientific, United States), 2 μl of primer mixture and 8 μl of the 10-fold diluted target DNA templates as stated above. The correct amplification products for these SYBR Green assays were chosen

based on the melting curve analysis as described previously (Seurinck et al., 2005; Green et al., 2012).

qPCR Performance Characteristics and Data Analysis

For each MST assay, the limit of detection (LOD) was determined from the standard curve. The lowest concentration of standard gene copies that could be confidently detected in all triplicates was considered as the LOD (Schriewer et al., 2013; Ahmed et al., 2016a). All the qPCR results were normalized to gene copies/ng of DNA and the samples considered positive if the concentrations were above the LOD. The interpretation of the qPCR assay results was as stated in the previous studies (Ahmed et al., 2016b; Nshimyimana et al., 2017). Sensitivity and specificity of all qPCR assays were determined as described previously (Ahmed et al., 2013). The statistical and qPCR data analyses were carried out using either Microsoft Excel or SPSS version 22.0. The linear regression analysis was performed using Microsoft Excel; the statistical significance in the abundance of Bac-Uni and GenBac3 markers of fecal and sewage samples was determined using SPSS 22.0 (IBM Inc., Chicago, IL, United States).

Quantification of MST and Pathogenic Bacterial Gene Markers in Tiaoxi River Water and Sediment Samples

Sample Collection and Processing

Initially, 25 sampling locations were selected covering the East and West, and junctions of the Tiaoxi River with other tributaries, extending to approximately 100 km of the mainstream river (**Figure 1**); samples were collected from these locations in three seasons (autumn 2014, winter, and summer 2015). Locations comprising domestic, agricultural, and industrial areas were selected for sampling and the land use pattern of the sampling locations was reported in our previous study (Vadde et al., 2018); the details are also provided in **Supplementary Table S2**. Water samples were collected in sterile 5 L polypropylene containers and sediments were collected using a sediment sampler; the samples in triplicate were transferred to sterile 50 ml tubes. Water and sediment samples were transported to the laboratory on ice and were processed within 8 h. Sediment samples were frozen at −20°C and the water samples (250 ml) were filtered through 0.22 μm polycarbonate membrane filters (Millipore, United Kingdom) and stored at −20°C prior to DNA extraction. The DNA was extracted from membrane filters (water samples) and sediment samples using PowerSoil DNA Isolation Kit (MoBio Inc., Carlsbad, CA, United States) as per the manufacturer's instructions.

Enumeration of Fecal Coliforms

The current study incorporates microbiological assessment data published in our previous study (Vadde et al., 2018). The enumeration of fecal coliforms (FC) was carried out by standard membrane filtration technique (APHA, 2005) using mFC agar (Difco, Germany) according to the manufacturer's instructions. The FC count data were used for initial assessment of fecal pollution at the Tiaoxi River and to prioritize the locations for further quantification of MST and pathogenic bacterial gene markers at these locations.

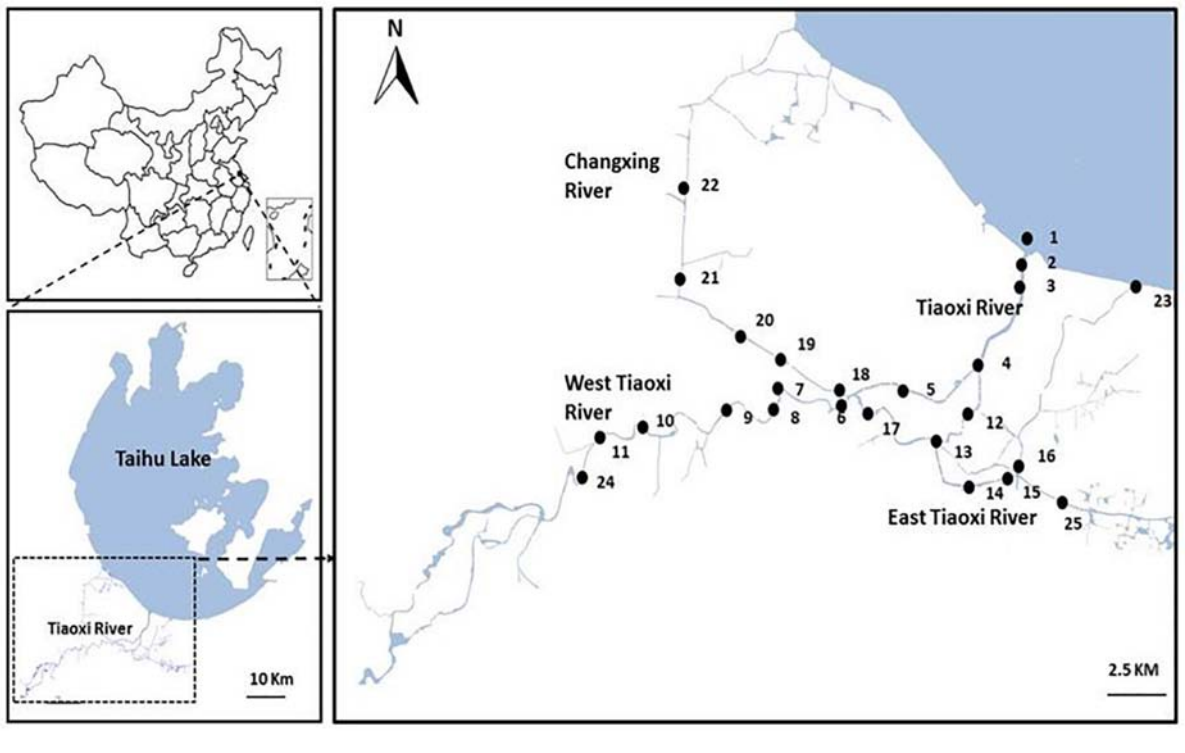

FIGURE 1 | Map of the sampling locations selected for the current study in Tiaoxi River (Taihu watershed).

Quantification of MST and Pathogenic Bacterial Gene Markers by qPCR

As validated in this study, four previously designed qPCR assays targeting total, human, swine, and avian associated fecal sources were selected for their quantification in water and sediment samples of the Tiaoxi River (**Table 1**). Three TaqMan assays (BacUni, HF183 Taqman, and Pig-2-Bac) were selected for detection of the total, human and swine associated *Bacteroidale*s, and one SYBR green-GFD assay was selected for detection of avian associated fecal markers (Kildare et al., 2007; Mieszkin et al., 2009; Green et al., 2012, 2014). In addition, five qPCR assays targeting *stx2, eae, LipL32, ipaH*, and *mapA* genes of the specific pathogenic bacteria were selected for this study (**Table 1**). Two qPCR assays targeting the *eae* gene specific for *E. coli* O157:H7 (Ibekwe et al., 2002) and *stx2* gene specific for Shiga toxin producing *E. coli* (Beutin et al., 2008) were applied using SYBR Green chemistry. Three assays targeting the *LipL32* gene specific for pathogenic *Leptospira* sp. (Stoddard et al., 2009), *ipaH* gene specific for *Shigella* spp. (Wang et al., 2007) and *mapA* gene specific for *Campylobacter jejuni* (Best et al., 2003) used TaqMan chemistry.

All qPCR reactions were run in triplicate with a final reaction volume of 20 μL. A seven-point 10-fold serially diluted recombinant plasmid DNA with a target sequence was used to generate the standard curve (range 10^1 to 10^7 copies/reaction) in each qPCR assay. All the TaqMan qPCR assays (20 μl of master mix), contained 10 μl of TaqMan Environmental Master Mix 2.0 (Applied Biosystems, United Kingdom), 2 μL of template DNA, 6 μl nuclease-free water and 2 μL of primers and probes at the final concentrations shown in **Table 1**. SYBR Green assays (20 μl of master mix) contained 10 μl of SYBR Green PCR Master Mix (Thermo Fisher Technologies, Foster City, CA, United States), 7.0 μL nuclease-free water, 2 μL of template DNA and 1 μL of primer mixture with a final concentration as in **Table 1**. Prior to quantification, the absence of PCR inhibitors was analyzed in at least 10% of DNA samples by applying the BacUni qPCR assay that amplifies the 16S rRNA gene of *Bacteroidales* (Odagiri et al., 2015). The accuracy and efficiency of the standard curves were determined by including a positive control of 10^3 copies of the plasmid standard as the unknown in each assay (Oster et al., 2014).

Data Processing and Statistical Analyses

All the qPCR assay results were processed based on the Minimum Information for Publication of Quantitative Real-Time PCR Experiments (MIQE) guidelines (Bustin et al., 2009); if the R^2 or efficiencies were not achieved by any assay, the samples were tested again. The details of the LOD, limit of quantification (LOQ), and final assessment of qPCR results for each of the MST and pathogen quantification assays are provided in **Supplementary Information**. For statistical analysis, the concentrations of FC, MST markers, and genes of pathogenic bacteria were log transformed and non-detects

TABLE 1 | List of primers and probes used for quantification of MST markers and genes of pathogenic bacteria.

Target source/ organism	Assay	Primer/probe	Concentration	Oligonucleotide sequence (5′–3′)	Annealing temperature (°C)	References
Total *Bacteroidales*	BacUni	BacUni-520F	400 nM	CGTTATCCGGATTTATTGGGTTTA	60	Kildare et al., 2007
		BacUni-690R1	400 nM	CAATCGGAGTTCTTCGTGATATCTA		
		BacUni656P	80 nM	FAM-TGGTGTAGCGGTGAAA-MGB		
Human associated *Bacteroidales*	HF183	HF183F	1000 nM	ATCATGAGTTCACATGTCCG	60	Green et al., 2014
		BacR287R	1000 nM	CTTCCTCTCAGAACCCCTATCC		
		BacP234P	80 nM	FAM-CTAATGGAACGCATCCC-MGB		
Swine associated *Bacteroidales*	Pig-2-Bac	Pig-2-Bac41F	300 nM	GCATGAATTTAGCTTGCTAAATTTGAT	60	Mieszkin et al., 2009
		Pig-2-Bac163R	300 nM	ACCTCATACGGTATTAATCCGC		
		Pig-2-Bac113P	200 nM	VIC-TCCACGGGATAGCC-MGB		
Avian associated Marker	GFD	GFD-F	100 nM	TCGGCTGAGCACTCTAGGG	57	Green et al., 2012
		GFD-R	100 nM	GCGTCTCTTTGTACATCCCA		
C. jejuni	*mapA*	mapA F	400 nM	CTGGTGGTTTTGAAGCAAAGATT	60	Best et al., 2003
		mapA R	400 nM	CAATACCAGTGTCTAAAGTGCGTTTAT		
		mapA P	80 nM	FAM-TTGAATTCCAACATCGCTAATGTATA AAAGCCCTTT-TAMRA		
Pathogenic *Leptospira* spp.	*LipL32*	LipL32F	300 nM	AAG CAT TAC CGC TTG TGG TG	60	Stoddard et al., 2009
		LipL32R	300 nM	GAA CTC CCA TTT CAG CGA TT		
		LipL32P	200 nM	FAM-AAAGCCAGGACAAGCGCCG-BHQ1		
Shigella spp.	*ipaH*	ipaH F	400 nM	CTTGACCGCCTTTCCGATA	64	Oster et al., 2014
		ipaH R	400 nM	AGCGAAAGACTGCTGTCGAAG-		
		ipaH P	80 nM	FAM-AAC AGG TCG CTG CAT GGC TGG AA-TAMRA		
E. coli (STEC)	*stx2*	Stx2F	200 nM	CAGGCAGATACAGAGAGAATTTCG	61	Beutin et al., 2008
		Stx2R	200 nM	CCGGCGTCATCGTATACACA		
E. coli O157:H7	*eae*	eae-F	200 nM	GTAAGTTACACTATAAAAGCACCGTCG	56	Ibekwe et al., 2002
		eae-R	200 nM	TCTGTGTGGATGGTAATAAATTTTTG		

were assigned as 0 (Bradshaw et al., 2016). The data were not normally distributed (based on Kolmogorov–Smirnov test) after transformation, therefore Kruskal–Wallis non-parametric ANOVA with Dunn's post-test was used for determining statistical significance among different sampling locations. The correlation among FC, MST markers and genes of pathogenic bacteria in water samples was analyzed by Spearman's coefficient correlation.

RESULTS

Evaluation of Existing MST Makers for Applicability in Taihu Watershed

Quality Assurance of Fecal DNA and Performance Characteristics of MST qPCR Assays

Reliable quantification and specific detection of genetic markers by qPCR poses many challenges, therefore assays should be carefully designed and optimized to obtain maximum achievable specificity and sensitivity (Bustin et al., 2009). The quality assurance of fecal/sewage DNA was assessed by the BacUni assay and the results showed that all the fecal/sewage DNA had matching concentrations (based on mean Cp and percentage of coefficient of variation) of BacUni markers in the two different dilutions tested (1:10 and 1:100), indicating the absence or negligible amounts of PCR inhibitors. Therefore, all further assays were performed with 1:10 diluted DNA extracts. The Cp mean values for the BacUni marker in 1:10 and 1:100 diluted human fecal samples are provided in **Supplementary Table S3**.

The amplification efficiencies of all MST qPCR assays tested were in the range 86–102% and the correlation coefficient (r^2) values were $\geq$0.98. The detailed performance characteristics of all the qPCR assays are provided in the **Supplementary Table S4**; all of the values were within the limits recommended in the MIQE guidelines (Bustin et al., 2009). All of the qPCR standards were re-analyzed to determine the master standard curve with standardized slope, amplification efficiencies, and correlation coefficient (r^2) values. The details of master standard curves and LOD for each tested MST assay are presented in **Table 2**.

TABLE 2 | Performance characteristics of MST qPCR assays tested using fecal and sewage samples.

Assay	Slope	y-intercept	R^2	Efficiency	LOD* (gc/rxn)
BacUni	−3.32	43.3	0.99	100.0	24.5
GenBac3	−3.27	40.3	0.99	101.8	14.1
BacHum	−3.26	38.4	0.99	102	36.8
HF183 Taqman	−3.37	39.6	0.99	99.7	11.5
HumM2	−3.34	42.2	0.99	98.9	75
HF183 SYBR	−3.3	36.2	0.99	100.9	10
Pig-2-Bac	−3.27	41.1	0.99	102	30
BacCow	−3.31	41.6	0.99	100.3	100
AV4143	−3.5	43	0.99	93	10
GFD	−3.41	36.9	0.99	96	11.3

**LOD, limit of detection.*

TABLE 3 | Performance of human-associated *Bacteroidales* MST assays on fecal and sewage samples.

Source	No. of samples tested	BacHum		HF183 Taqman		HF183 SYBR		Hum2	
		No. of positive samples (%)	Mean (±SD[a]) concentration (log_{10} gene copies per ng)	No. of positive samples (%)	Mean (±SD) concentration (log_{10} gene copies per ng)	No. of positive samples (%)	Mean (±SD) concentration (log_{10} gene copies per ng)	No. of positive samples (%)	Mean (±SD) concentration (log_{10} gene copies per ng)
Human	10	6 (60)	3.98 (±0.75)	6 (60)	4.51 (±0.78)	7 (70)	3.99 (±0.81)	7 (70)	3.28 (±0.31)
Sewage	5	5 (100)	2.41 (±0.69)	5 (100)	2.73 (±0.25)	5 (100)	1.46 (±0.72)	1 (20)	1.76
Pig	10	0 (0)	0	0 (0)	0	0	0	2 (20)	2.46 (±1.20)
Chicken	10	6 (60)	2.53 (±0.37)	7 (70)	3.22 (±0.3)	7 (70)	2.18 (±0.45)	4 (40)	2.03 (±0.73)
Cow	10	1 (10)	1.8	0 (0)	0	3 (30)	1.38 (±0.48)	2 (20)	2.12 (±0.93)
Dog	10	2 (20)	1.75 (±0.47)	2 (20)	1.36 (0.52)	2 (20)	1.43 (±0.12)	1 (10)	2.24
Duck*	3	0 (0)	0	0 (0)	0	1 (33)	1.41	0 (0)	0
Goose*	3	0 (0)	0	0 (0)	0	1 (33)	1.68	1 (33)	1.97
Target			3.19 (±1.11)		3.63 (±1.25)		2.72 (±0.93)		2.52 (±1.07)
Non-target			2.14 (±1.07)		2.5 (±1.31)		1.62 (±0.33)		2.16 (±0.19)
Sensitivity		73.3%		73.3%		80%		53.3%	
Specificity		80.4%		80.4%		69.5%		78.2%	

**Composite fecal samples. [a]SD, standard deviation.*

TABLE 4 | Performance of animal associated MST assays on fecal samples.

Source	No. of samples tested	Pig-2-Bac		BacCow		AV4143		GFD	
		No. of positive samples (%)	Mean (±SD) concentration (log_{10} gene copies per ng)	No. of positive samples (%)	Mean (±SD) concentration (log_{10} gene copies per ng)	No. of positive samples (%)	Mean (±SD) concentration (log_{10} gene copies per ng)	No. of positive samples (%)	Mean (±SD) concentration (log_{10} gene copies per ng)
Human	10	0 (0)	0	0 (0)	0	1 (10)	1.7	0 (0)	0
Pig	10	9 (90)	3.03 (±0.59)	2 (20)	2.52 (±0.89)	0 (0)	0	0 (0)	0
Chicken	10	0 (0)	0	2 (20)	2.32 (±0.77)	10 (100)	4.13 (±0.49)	7 (70)	2.20 (±0.19)
Cow	10	2 (20)	1.70 (±0.84)	10 (100)	4.3 (±0.65)	2 (20)	1.3 (±086)	1 (10)	1.2
Dog	10	0 (0)	0	0 (0)	0	0 (0)	0	3 (30)	1.3 (±0.40)
Target			3.03 (±0.59)		4.30 (±0.65)		4.13 (±0.49)		2.20 (±0.19)
Non-target			1.70 (±0.84)		2.42 (±0.14)		1.5 (±0.2)		1.25 (±0.07)
Sensitivity		90%		100%		100%		70%	
Specificity		95%		77.5%		95%		92.50%	

Performance of Universal and Human *Bacteroidales* Assays

Both BacUni and GenBac3 assays, targeting universal/general *Bacteroidales*, exhibited 100% sensitivity to fecal and sewage samples as they amplified DNA from all the samples. The mean concentration of these markers in fecal and sewage samples is given in **Supplementary Table S5**. Comparatively, BacUni showed slightly higher total *Bacteroidales* concentrations [copies per nanogram (ng) of DNA] than the GenBac3 assay in all of the tested samples.

Among the four human-associated assays tested, the HF183 SYBR marker was the most sensitive but showed high cross-reactivity (**Table 3**). It was found in 80% of human origin samples (7/10 human feces and 5/5 sewage samples) at an average concentration of 2.72 log_{10} gene copies per ng of DNA and showed cross reactivity with chicken (7/10), cow (3/10), duck (1/3), dog (2/10), and goose (1/3) fecal DNA samples identifying it as the least specific (69.5%). The BacHum marker had the highest specificity (80.4%) among the tested human-associated markers, along with HF183 Taqman. The BacHum assay had a sensitivity of 73.3% (6/10 human feces and 5/5 sewage samples) at an average concentration of 3.19 log_{10} copies per ng of DNA and was detected (above LOD) in three different host fecal DNA samples – chicken (6/10), cow (1/10), and dog (2/10). Similar to BacHum, the HF183 Taqman marker was highly specific (80.4%) among human-associated assays and was found in 73.3% of target sources (6/10 human feces and 5/5 sewage samples) at an average concentration of 3.63 log_{10} copies per ng of DNA. However, HF183 Taqman marker was found in only two different host fecal DNA samples, chicken (7/10) and dog (2/10). The final human-associated assay, Hum2 was the least sensitive marker and was detected in only 53% of samples of human origin (7/10 human feces and 1/5 sewage samples) at an average concentration of 2.52 log_{10} copies per ng of DNA. It was also detected in chicken (4/10), cow (2/10), pig (2/10), dog (1/10), and goose (1/3) fecal DNA samples, making it less specific (78%). In general, chicken (40–70%) and dog fecal samples (10–20%) had cross-reactivity with all of the human-associated assays. Overall, HF183 Taqman was the only assay that did not exhibit any cross-reactivity with cattle or swine fecal DNA samples, while HF183 SYBR, Hum2, and BacHum showed cross-reactivity with either cattle or swine fecal DNA samples (**Table 3**).

Performance of Animal Associated MST Assays

The performance of the swine associated assay (Pig-2-Bac) was evaluated with 10 pig fecal samples and the target was found in 90% of samples (9/10) at an average concentration of 3.03 log_{10} copies per ng of DNA (**Table 4**). The Pig-2-Bac marker was highly specific (95%) and it had a low level of cross-reactivity with cow fecal samples (2/10). BacCow marker was found in 100% of cattle fecal samples (10/10) at an average concentration of 2.81 log_{10} copies per ng of DNA (**Table 4**), but showed some cross-reactivity with pig (2/10) and chicken (2/10) fecal DNA samples, although not found in any of the human fecal DNA samples at above LOD levels, yielding a specificity value of 77%.

The avian associated MST assays performed very distinctively on the tested fecal DNA samples (**Table 4**). The AV4143 marker was found in 100% of chicken fecal samples but was also detected in human (1/10) and cow (2/10) fecal DNA. The mean concentration of AV4143 marker was 4.13 $\log_{10}$ copies per ng of DNA in chicken feces. Those human and cow samples for which there was cross reactivity comprised ca. 3 log-fold fewer gene copies than chicken feces. The GFD markers were only detected in 7 of the 10 chicken feces samples and cross-reacted with dog fecal DNA samples (3/10). The mean concentration of GFD markers was 2.20 $\log_{10}$ copies per ng of fecal DNA sample, so ca. 100-fold less than AV4143.

Assessment of Microbial Quality of Tiaoxi River Water and Sediments

Enumeration of Fecal Coliforms in Water Samples

FC count data was used for an initial assessment of fecal contamination at these sampling locations and the results reported in our previous study (Vadde et al., 2018). The FC counts are interpreted according to US EPA standards (USEPA, 2012), and elevated levels of FC (>250 CFU/100 ml) were detected at 15 locations (1–6, 8, 10, 12–16, 20, and 21) on one or more occasions (**Figure 2**). In general, the FC counts were higher during summer, which could be correlated with the warm (optimal) weather supporting acclimatization of FC bacteria; a rainfall event that occurred the day before the sampling may have led to transport of fecal matter and proliferation of FC bacteria (Heaney et al., 2015). Based on the elevated levels of FC, 15 out of 25 locations were considered as preliminary hotspots of fecal contamination and were selected for further quantification of MST fecal markers and pathogenic bacterial genes in DNA extracted from water and sediment samples. The FC counts (range and mean) along with physico-chemical analysis results for 25 sampling locations monitored during 2014 to 2015 is provided in **Supplementary Table S6**.

Quality Assurance of Extracted DNA and Performance of qPCR Assays

DNA samples tested for PCR inhibition did not show any major difference in concentration values (based on mean Cp and percentage of coefficient of variation) for undiluted and 1:4 diluted DNA extracts, indicating that the samples were free of potential PCR inhibitors. The range and compiled values of amplification efficiencies and linear range of quantification for all qPCR assays are provided in **Supplementary Table S7**. The average Cp value for all negative controls (NTC) was >38, and samples were repeat tested if the average Cp value of NTCs was <38.

Detection Frequency and Concentration of MST Markers in Water and Sediment Samples

Data on the presence and distribution of MST markers in water and sediment samples at 15 sampling locations, determined by qPCR, are presented in **Table 5**. Since these monitoring locations selected for the MST study were presumed hot spots of fecal contamination (based on FC count), the total *Bacteroidales* marker was detected in all water and sediment samples at the 15 locations. In water samples, the mean concentration of total *Bacteroidales* marker was 6.22 $\log_{10}$ gene copies/100 ml with concentrations ranging from 4.62 to 7.63 $\log_{10}$ gene copies/100 ml (**Figure 3A**). For sediment, the mean concentration was 6.11 $\log_{10}$ gene copies/gram and concentrations ranged from 4.37 to 7.82 $\log_{10}$ gene copies/gram (**Figure 4A**). Significant statistical variation in total *Bacteroidales* concentrations among different locations was observed for both water ($P > 0.015$) and sediment samples ($P > 0.003$). In relative terms, the total *Bacteroidales* concentration was high during winter for both water and sediment samples. Based on the quantification of total *Bacteroidales*, the water samples from location 16 and sediment samples from location 15 were found to be the most fecally polluted, regardless of the fecal source (human versus animal species). Locations 15 and 16 are suburban areas, which are close to a WWTP. For the host associated MST

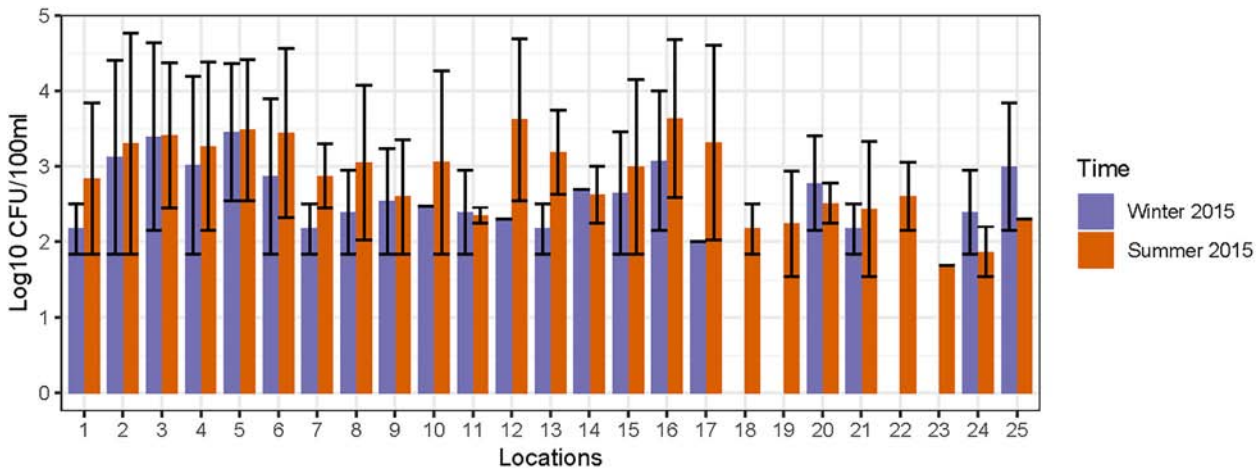

FIGURE 2 | Concentration of fecal coliforms observed in different sampling locations of Tiaoxi River.

TABLE 5 | Detection frequencies of MST markers in water and sediment samples of Tiaoxi River, Taihu watershed (2014–2015).

Sample type	No. of samples tested (*n*)	No. of positive samples (%)[a]			
		Total *Bacteroidales*	Human associated markers	Swine associated markers	Avian associated markers
Water					
Autumn	15	15 (100%)	15 (100%)	10 (66%)	13 (86%)
Winter	15	15 (100%)	15 (100%)	13 (86%)	15 (100%)
Summer	15	15 (100%)	14 (93%)	15 (100%)	13 (86%)
Total	**45**	**45 (100%)**	**44 (97%)**	**38 (84%)**	**40 (89%)**
Sediment					
Autumn	15	15 (100%)	13 (86%)	6 (40%)	–[b]
Winter	15	15 (100%)	11 (73%)	8 (53%)	–[b]
Summer	15	15 (100%)	15 (100%)	15 (100%)	4 (26.7%)
Total	**45**	**45 (100%)**	**39 (86%)**	**29 (64%)**	**4 (8.9%)**

[a] *Limit of detection (LOD) as cutoff.* [b] *Below detection limits.*

marker analysis in water samples, human-associated markers were the most frequently detected (97%), followed by avian (89%) and swine (84%). In sediment samples, human-associated MST marker was detected more often (86%), followed by swine (64%). The avian markers were positive for several sediment samples but were always below the LOD.

The human-associated marker, HF183 Taqman, was detectable at most of the locations tested in water samples (44/45) in all three seasons with a mean concentration of 3.75 $\log_{10}$ gene copies/100 ml (range 2.91–5.6 $\log_{10}$ gene copies/100 ml) (**Figure 3B**). For sediment samples, the HF183 Taqman was detected with high frequency (39/45) at concentrations ranging from 3.8 to 5.6 $\log_{10}$ gene copies/gram (mean 3.91 $\log_{10}$ gene copies/gram) (**Figure 4B**). During the summer, human-associated markers were detected at a higher prevalence in water and sediment samples, probably due to the runoff water received from heavy rainfall (349 and 268 mm in July and August 2015) that occurred before summer sampling (NBSC, 2016). There was a statistically significant difference in the prevalence of human markers in the sediment samples ($P > 0.004$) but not in the water samples. Based on the HF183 Taqman assay, water samples collected from locations 12 and 16, and sediment samples collected from location 15 had the highest concentration of human-associated marker during the three seasons. Location 12 is very close to Huzhou city and as stated above, locations 15 and 16 are suburban areas close to a WWTP, and the sampling was carried out at the junction of Tiaoxi River and a canal that enters Taihu Lake (Vadde et al., 2018) (**Supplementary Table S2**).

With respect to swine fecal contamination, the swine associated marker was detected less often in water (38/45) and sediment samples (29/45) than human markers. The mean concentration of swine marker in water samples was 2.96 $\log_{10}$ gene copies/100 ml (range 2.77–5.56 $\log_{10}$ gene copies/100 ml) (**Figure 3C**). The mean concentration of swine markers in sediment samples was 3.75 $\log_{10}$ gene copies/gram (range 3.6–4.7 $\log_{10}$ gene copies/gram) (**Figure 4C**). The variation in the concentration of swine markers detected in water ($P > 0.001$) and sediment samples ($P > 0.001$) was statistically significant. Higher concentrations of swine associated marker were observed in water samples at location 1 during summer and in sediment samples at location 10 during winter. The samples at location 1 were collected 1 km inside the Taihu Lake from the junction with the Tiaoxi River, and runoff during the summer was probably a contributory factor. Location 10 was close to a rural area where the agricultural input to the river upstream was likely to enhance the swine marker content.

The avian associated fecal pollution was found to be the second dominant host associated fecal pollution in the Tiaoxi River water samples. The avian markers were detected in 89% of water samples (40/45) at concentrations of 2.30–5.56 $\log_{10}$ gene copies/100 ml (mean 2.70 $\log_{10}$ gene copies/100 ml) (**Figure 3D**). There was no significant statistical variation for avian marker concentration in water samples across different locations of the study area. For sediment samples, the avian markers were detected in only four of the 15 samples collected in the summer season. During the autumn and winter seasons, although some samples were positive for the avian MST assay, they were below the LOD limits. The highest avian marker concentration was observed at location 6 for both water and sediment samples. Location 6 is in a suburban area near Qijia village, where several swine and poultry farms are located.

Concentration of Pathogen Bacterial Genes in Water and Sediment Samples

Data on the presence and distribution of gene markers for five bacterial pathogens are presented in **Table 6**. Considering detected but not quantifiable (DNQs) as positive samples, the most commonly detected pathogens in water and sediment samples, respectively, were *Campylobacter jejuni* (62% and 53%) and *Shigella* spp. (60% and 91%), followed by STEC (55% and 51%) and pathogenic *Leptospira* spp. (33% and 13%). The *E. coli* O157:H7 marker was detected only in sediment samples (11%). The concentrations of marker genes of bacterial pathogens detected in water and sediment samples at each location are provided in **Supplementary Table S8**. Using the LOQ as the selection criterion, *Campylobacter jejuni* (*mapA*) was present in a quantifiable range in 20 out of 45 water samples (2.31–2.88 $\log_{10}$ gene copies/100 ml) and 13 of 45 sediment samples (3.30–3.86 $\log_{10}$ gene copies/gram) (**Figure 5**). The highest *mapA* gene concentration was observed in water samples collected at location 16, and in sediment samples collected at location 20 (**Supplementary Table S8**). In the case of *Shigella* spp., although the *ipaH* gene was detected in several samples, it was quantifiable in only two out of 45 water samples (locations 3 and 12) with concentrations of 2.32 and 2.35 $\log_{10}$ gene copies/100 ml, respectively. In sediments, the *ipaH* gene was quantified in 14 samples with concentrations ranging 3.32–3.47 $\log_{10}$ gene copies/gram (**Figure 5**) and the highest concentration was observed at location 12. Similarly, the *stx2* (Shiga toxin-producing *E. coli*) was quantified in only 2 out of

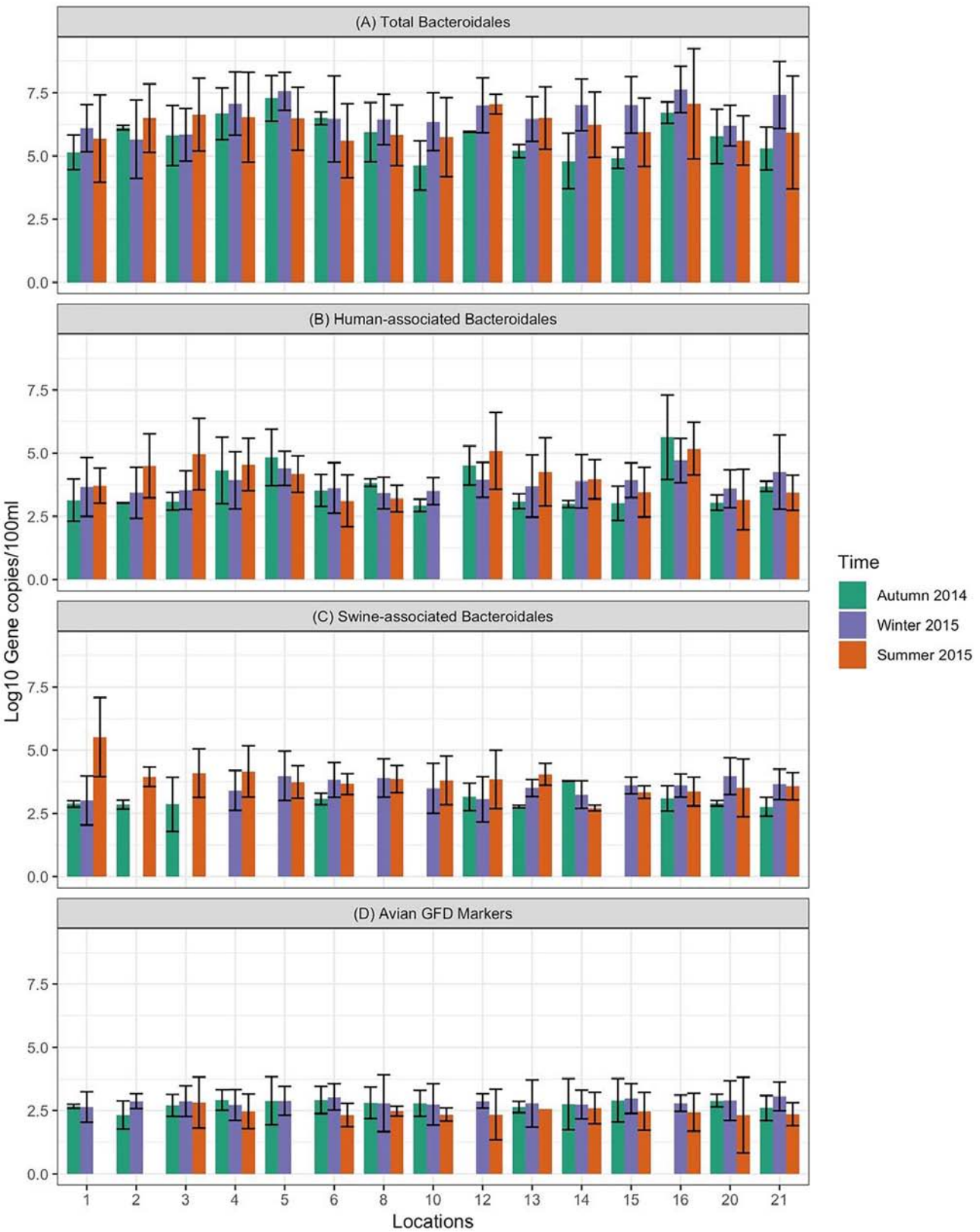

FIGURE 3 | Concentration of MST fecal markers quantified in water samples at different sampling locations of Tiaoxi River. **(A)** Total *Bacteroidales*; **(B)** human-associated *Bacteroidales*; **(C)** swine-associated *Bacteroidales,* and **(D)** avian-associated MST marker.

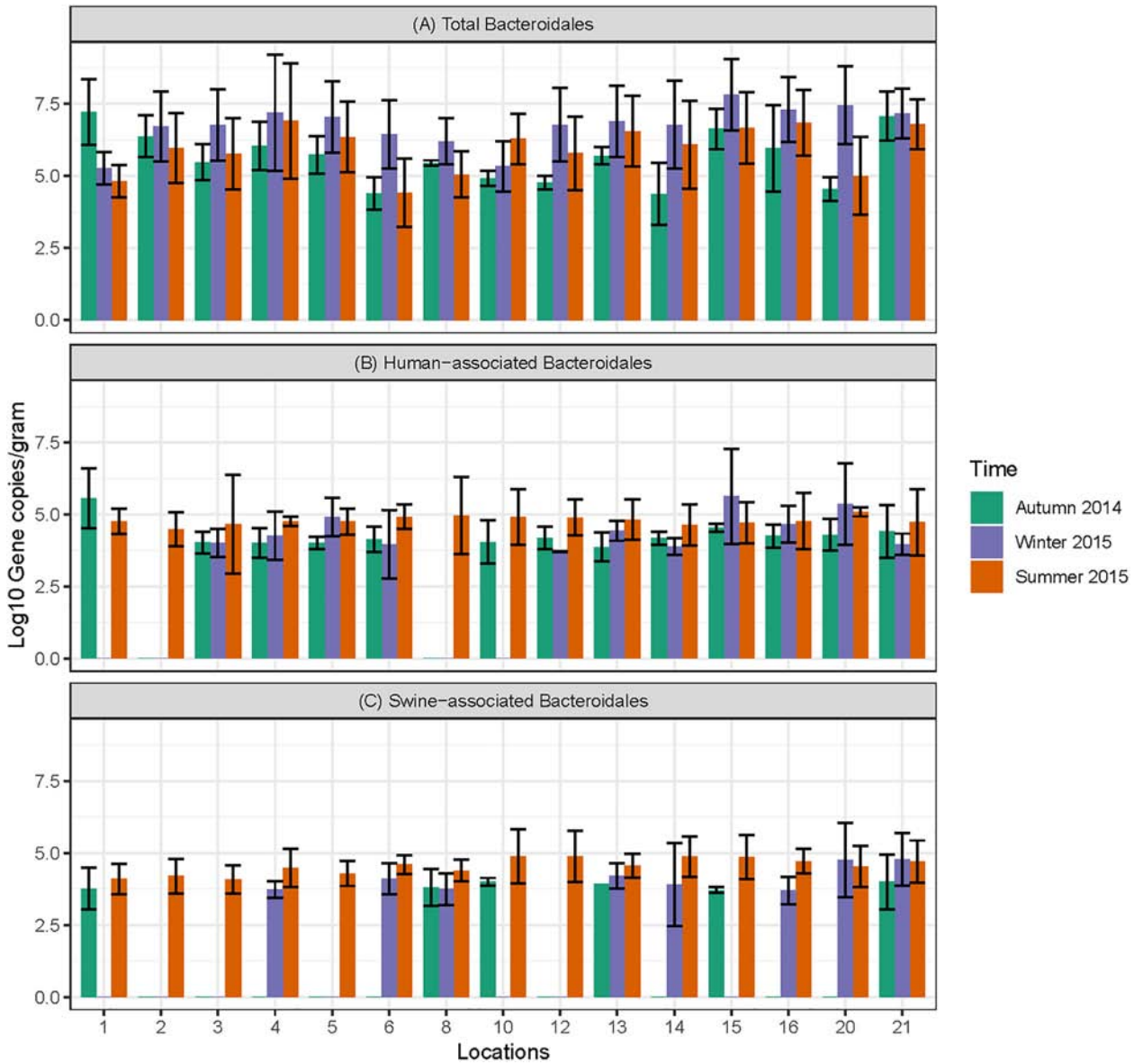

FIGURE 4 | Concentration of MST markers quantified in sediment samples at different sampling locations in Tiaoxi River. **(A)** Total *Bacteroidales*; **(B)** human-associated *Bacteroidales*; **(C)** swine-associated *Bacteroidales*.

45 water samples (locations 5 and 21) with a concentration of 2.31 and 2.42 $\log_{10}$ gene copies/100 ml, respectively. In sediments, it was quantified in 14 out of 45 samples with a concentration range of 3.32–3.65 $\log_{10}$ gene copies/gram (**Figure 5**) and the highest concentration of *stx2* genes was observed at location 14. The *LipL32* gene (Pathogenic *Leptospira* spp.) was quantified in 15 out of 45 water samples with the concentration ranging from 2.43 to 3.13 $\log_{10}$ gene copies/100 ml, with the highest levels recorded at location 21. The *LipL32* gene was quantified in 6 (out of 45) sediment samples at a concentration of 3.32–3.65 $\log_{10}$ gene copies/gram (**Figure 5**) and highest concentrations were observed at location 20. The *eae* gene of *E. coli* O157:H7 was quantified in only three sediment samples collected in autumn 2014 with a concentration of 3.32–4.03 $\log_{10}$ gene copies/gram and the highest concentration recorded at location 20 (**Supplementary Table S8**).

Correlation Between FC, MST Markers, and Genes of Bacterial Pathogens

All the correlations in this study were considered as significant only when Rho(r) and p-values were >0.5 and <0.05, respectively (Steele et al., 2018). The concentrations of FC (FIB) were positively correlated with BacUni ($r = 0.667$ and $p < 0.01$) and HF183 Taqman ($r = 0.572$ and $p < 0.05$) but not with Pig-2-Bac and GFD markers (**Table 7**), indicating that the common source of fecal pollution is effluents from WWTP or human waste

TABLE 6 | Detection frequencies of bacterial pathogen marker genes in water and sediment samples of Tiaoxi River, Taihu watershed (2014–2015).

Sample type	No. of samples tested (*n*)	No. of positive samples[a]				
		Leptospira (*LipL32*)	*Campylobacter* (*mapA*)	*Shigella* (*ipaH*)	*STEC* (*stx2*)	*EHEC O157:H7* (*eae*)
Water						
Autumn	15	5 (33%)	4 (26.6)	15 (100%)	0	0
Winter	15	10 (66%)	9 (60%)	8 (53%)	12 (80%)	0
Summer	15	0	15 (100%)	4 (26.6)	12 (80%)	0
Total	**45**	**15 (33%)**	**28 (62%)**	**27 (60%)**	**25 (55%)**	**0**
Sediment						
Autumn	15	0	6 (40%)	15 (100%)	11 (73%)	5 (33%)
Winter	15	6	10 (66%)	12 (80%)	3 (20%)	0
Summer	15	0	8 (53%)	14 (97%)	9 (60%)	0
Total	**45**	**6 (13%)**	**24 (53%)**	**41 (91%)**	**23 (51%)**	**5 (11%)**

[a] *DNQ's (detected but not quantifiable) recorded as positive samples.*

entry into the river. The FC did not show correlation with any of the genes of bacterial pathogens tested in this study, which is in agreement with previous studies (Bradshaw et al., 2016; Zhang Q. et al., 2016); FC points to the potential risk of exposure to pathogens but does not demonstrate their specific presence. The BacUni marker showed a strong positive correlation with HF183 Taqman ($r = 0.832$ and $p < 0.01$), suggesting humans as the major contributor to the total *Bacteroidales* content. BacUni also showed positive correlation with *stx2* gene ($r = 0.6$ and $p < 0.05$). HF183 Taqman showed negative correlation with GFD marker ($r = -0.582$ and $p < 0.05$) and positive correlation with *stx2* gene ($r = 0.593$ and $p < 0.05$). Since there are multiple fecal sources (such as pig, cow, and poultry) of *stx2* gene presence in the environment, it is difficult to draw conclusions on the *stx2* gene correlation with BacUni and HF183 Taqman. No significant correlation was observed for Pig-2-Bac and GFD markers with the marker genes of bacterial pathogens addressed in this study.

DISCUSSION

Evaluation of MST qPCR Assays for Their Applicability at Taihu Lake/Tiaoxi River Watershed

Overall, this is a comprehensive study evaluating the performance of existing universal, human and animal associated MST qPCR assays for their applicability to ascertain host-associated fecal pollution in the Taihu Lake/Tiaoxi River watershed, China.

Among universal/total *Bacteroidales* MST qPCR assays, the high sensitivity of the BacUni (Universal *Bacteroidales*) marker for human and animal feces, excluding avian sources, has frequently been reported in Asian countries such as India (Odagiri et al., 2015) and Singapore (Nshimyimana et al., 2017), and also in the United States (Kildare et al., 2007), and Kenya (Jenkins et al., 2009). The GenBac3 general *Bacteroidales* assay is the most widely used assay in the United States for quantifying *Bacteroidales* in environmental samples (Shanks et al., 2009; Ervin et al., 2013). In our study, both BacUni and GenBac3 showed 100% sensitivity to fecal samples but the BacUni assay amplified higher copies per ng of DNA than the GenBac3 assay in all of the tested samples. We conclude that the BacUni assay is more suitable for quantification of total *Bacteroidales* in the Taihu watershed, China; Odagiri et al. (2015) also reported that the BacUni marker quantified higher copy numbers than GenBac3 in fecal DNA samples tested in Odisha, India. The ability of human-associated markers to identify human fecal sources as distinct from other sources in an aquatic environment is vital to the MST approach. Variations, due for example to the impact of dietary patterns on gut microbiomes (Wu et al., 2011) or geographical differences (Yatsunenko et al., 2012), could significantly affect the performance of MST assays and this has been supported by several validation studies across different countries in recent years (Jenkins et al., 2009; Reischer et al., 2013; Odagiri et al., 2015; Boehm et al., 2016; He et al., 2016; Nshimyimana et al., 2017; Malla et al., 2018). Therefore, it is important to evaluate the performance of human fecal markers prior to application. Here, with the exception of the HF183 SYBR assay, all of the human-associated assays showed lower sensitivity (53–73%) than expected (81–100%). This reduced sensitivity range could well be due to the geographical variability in human gut microbiomes (Yatsunenko et al., 2012). The HF183 SYBR assay, which performed well in Bangladesh (Ahmed et al., 2010) and in Singapore as a human sewage indicator (Nshimyimana et al., 2014), showed less specificity in our study. Our results on the specificity of this assay are more in line with previous studies conducted in India (Odagiri et al., 2015) and Nepal (Malla et al., 2018). Although the remaining three assays are less sensitive compared to HF183 SYBR, they are more specific. The BacHum and HF183 Taqman assays showed relatively more specificity (80.4%), followed by Hum2 with 72.5% specificity. All of the human target assays gave some level of cross-reactivity with other fecal samples, with

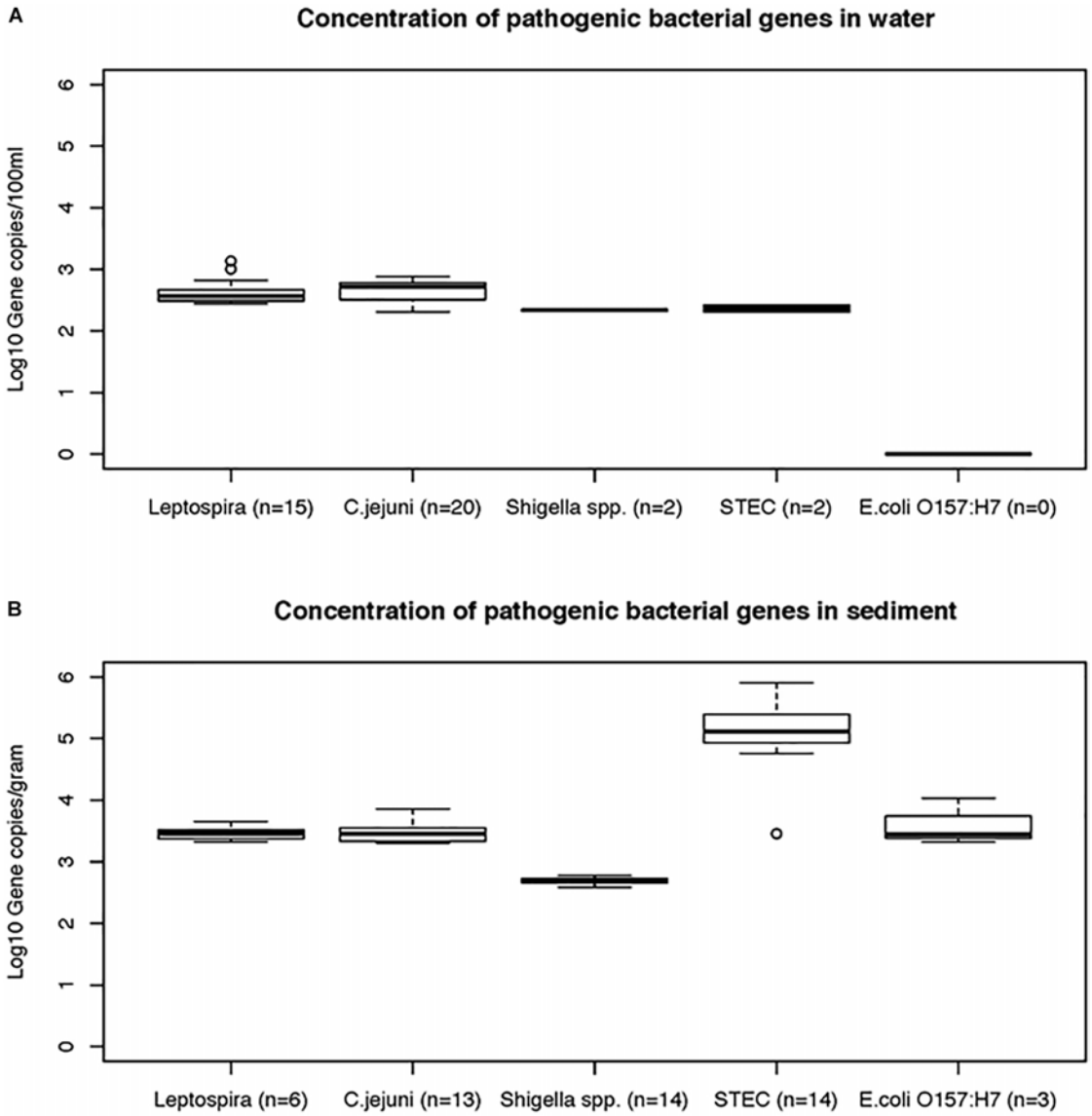

FIGURE 5 | The concentrations (mean and standard deviations) of genes of bacterial pathogens detected in water **(A)** and sediment samples **(B)** of Tiaoxi River.

the highest levels recorded in chickens (**Table 3**). The high cross-reactivity with chicken fecal samples by human-associated markers has been described in earlier studies directed in South Asia (Odagiri et al., 2015; Nshimyimana et al., 2017). The occurrence of the HF183 marker in dogs and chickens has also been reported previously, with the HF183 forward primers with Bac708 reverse primer picking up a target sequence in chicken fecal samples (Gourmelon et al., 2007; Ahmed et al., 2012). The BacHum assay's cross-reactivity with chicken fecal DNA has also been indicated previously in several studies (Reischer et al., 2013; Odagiri et al., 2015; Nshimyimana et al., 2017). With the exception of HumM2, none of the markers exhibited cross-reactivity with pig fecal DNA, which is encouraging as pigs are major livestock animals in Zhejiang province (Taihu watershed region). An assay that showed zero cross-reactivity to pig fecal DNA and highly sensitive to sewage samples would be considered as very suitable for source tracking in the Taihu watershed region. In this study, HF183 Taqman and BacHum assays showed the same accuracy, but HF183 Taqman was found to be the more suitable human-associated fecal maker than BacHum as it amplified DNA from all of the sewage samples with higher abundance and did not show any cross-reactivity with pig and cattle fecal samples (**Table 3**). The HF183 Taqman's cross-reactivity to chicken fecal samples can be negated by employing avian associated assays, such as GFD assay, in tandem to verify the existence of true human fecal pollution. An evaluation study carried out in Singapore (Nshimyimana et al., 2017) indicated similar sensitivity and specificity for HF183 Taqman to that reported here, though that study recommended another human-associated

TABLE 7 | Correlation between FC, MST markers and pathogenic bacterial marker genes.

	Correlation coefficient								
	FC	**BacUni**	**HF183Taq**	**Pig-2-Bac**	**GFD**	***LipL32***	***mapA***	***ipaH***	***stx2***
FC	1	0.667**	0.572*	−0.234	−0.27	−0.248	0.095	−0.361	0.397
BacUni		1	0.832**	−0.036	−0.396	−0.04	−0.018	−0.168	0.600*
HF183Taq			1	−0.061	−0.582*	−0.265	0.1	−0.121	0.593*
Pig-2-Bac				1	−0.268	0.346	0.5	0.068	−0.421
GFD					1	−0.095	0	0.057	−0.275
LipL32						1	−0.251	−0.225	0.207
mapA							1	0.379	−0.286
ipaH								1	−0.018
stx2									1

***Correlation is significant at 0.01 level (two-tailed). *Correlation is significant at 0.05 level (two-tailed).*

assay, B. theta (Taqman), for source tracking of human fecal and sewage in Singapore. The inconsistencies in the performance of *Bacteroidales* assays in regions other than the originally developed have been reported elsewhere (Layton et al., 2013; Reischer et al., 2013; Boehm et al., 2016).

The swine associated marker, Pig-2-Bac, has broadly been evaluated and used for MST studies across different countries, including China and Nepal (Jia et al., 2014; Arfken et al., 2015; He et al., 2016; Malla et al., 2018). He et al. (2016) validated the Pig-2-Bac assay on target and non-target fecal samples of Taihu watershed region and reported that it was more sensitive and specific than mitochondrial DNA based swine markers. They have also applied the Pig-2-Bac marker for identifying swine fecal pollution in the Taige River of Taihu watershed. Jia et al. (2014) used Pig-2-Bac assay for quantification of swine fecal markers in Hongqi River, Yongan River, and Taige River. The results of the swine associated assay in our study are in agreement with the findings of He et al. (2016), and the suitability of the Pig-2-Bac assay for identifying contamination by pig fecal sources at Taihu watershed is confirmed. The BacCow marker, which was originally developed to detect fecal source of cow or cattle origin (Kildare et al., 2007), has shown cross-reactivity with fecal samples collected from other ruminants (e.g., deer) and non-ruminants such as horse, pig, dog, and chicken in a California based validation study leading to its reclassification as ruminant-associated marker (Raith et al., 2013). Similar findings were reported in evaluation studies conducted in Australia and Europe, indicating that this assay had cross-reactivity with non-targets such as chicken, goose, dog, pig, and duck (Ahmed et al., 2013; Reischer et al., 2013). In a validation study conducted in India, BacCow markers were reported to be found in all types of composite livestock/domestic animal feces (cow, buffalo, goat, sheep, dog, and chicken) but not in tested human samples and it was recommended that the BacCow assay could be used to detect fecal pollution by livestock/domestic animals (Odagiri et al., 2015). More recently, BacCow was detected in all fecal samples tested including human origin (composite sewage) in a validation study conducted in Nepal (Malla et al., 2018). In order to check the true specificity and sensitivity of BacCow, this study was conducted with individual fecal samples instead of composite fecal samples. Here, we detected BacCow in all of the cattle fecal samples tested but found some cross-reactivity with pig (2/10) and chicken (2/10) samples in agreement with the findings of Ahmed et al. (2013) and Reischer et al. (2013). Since the BacCow marker was not identified in all of the livestock/domestic fecal samples tested, it is not applicable in the Taihu watershed as a livestock/domestic animal fecal source-tracking marker.

The ability to draw conclusions on the microbial flora in avian fecal samples is still ambiguous worldwide, making it difficult to develop reliable qPCR assays for the specific detection of avian fecal contaminations (Ohad et al., 2016). This could be due to variation in food intake by the avian sources regionally (Ahmed et al., 2016a). Though *Bacteroides* and its closely related organisms are commonly used for identifying the source of fecal contamination for human and animals (Bernhard and Field, 2000; Layton et al., 2006; Kildare et al., 2007), previous studies revealed that *Bacteroides* are rarely present in avian sources (Lu et al., 2009). The phylum level mapping of avian fecal samples showed that Firmicutes, Proteobacteria, and Fusobacteria are the main phyla (Lu et al., 2009). *Bacteroidales* members were not frequently reported in avian gut or excreta, and they were found to be nearly absent in a few studies (Zhu et al., 2002) or they were identified in varying frequencies in other studies (Scupham et al., 2008). Therefore, MST markers targeting avian fecal markers are still limited (Fremaux et al., 2010; Green et al., 2012; Ohad et al., 2016). We found that the AV4143 assay targeting *Lactobacillus* showed higher sensitivity and specificity than the GFD assay targeting *Helicobacter* spp. However, GFD markers were not detected in human fecal samples making this assay very suitable for application in the Taihu watershed as it can reliably differentiate chicken and human fecal samples. The GFD assay was similarly validated in Australia, Bangladesh, New Zealand, and North America with similar results for sensitivity and specificity (Ahmed et al., 2016b; Boehm et al., 2016). Overall, BacUni, HF183 Taqman, Pig-2-Bac, and GFD markers are recommended here, for tracking total and host-associated fecal contamination in the Taihu watershed region. The results also reinforce the importance of regional MST validation studies prior to their application in a new geographical region.

Application of Evaluated MST qPCR Assays to Track the Source of Fecal Pollution in Tiaoxi River

Fecal pollution of surface waters is a serious concern to the aquatic ecosystem and human health. In this study, fecal coliform counts were higher than suggested limits at 15 out of 25 monitoring locations, and increased concentrations were observed during the summer season. Acclimatization of existing FC bacteria to warm temperatures or entry of fresh feces from different sources such as human, animal or sewage into the surface water due to runoff from rainfall event occurred prior to sampling could have elevated the levels of FC during summer (Sidhu et al., 2012). Therefore, MST was conducted to assess the presence of fresh fecal pollution in the Tiaoxi River and to determine the fecal sources at these locations. In general, the distribution of MST markers among different locations correlated well with the land use pattern and results indicated that there was a mixed input of fecal pollution at several locations. Presence of Total *Bacteroidales* markers with high frequency in water and sediment samples at all fifteen locations (**Figures 3A**, **4A**) shows possible fresh fecal source entry and transportation to other locations within the study area (Marti et al., 2013). Human-associated markers were consistently identified (in both water and sediment) in most of the sampling locations during three occasions (**Figures 3B**, **4B**). Except for summer season (July/August 2015) where a rainfall event (∼349/268 mm) occurred, autumn (October 2014) and winter (January/February 2015) were dry seasons (with only 32 and 66 mm precipitation) indicating that fecal contamination at these locations might not be merely through runoff but could be due to direct discharge of sewer and septic waste (Ohad et al., 2015). The detection of *Shigella* spp. that solely originate from human fecal sources at several locations also points to human fecal contamination in the studied area. High levels of human-associated markers were observed in water samples at locations 3, 5, 12, and 16 and in sediment samples at location 15 on one or more occasions. The higher levels of human-associated markers observed in water samples at locations 5 and 16 and sediment samples at 15 could be associated with effluents from WWTP located near these locations (Zheng et al., 2017). The higher levels of human-associated markers in water samples at location 3 (rural area) and 12 (urban area) that does not have agricultural or effluent entry from WWTP (Vadde et al., 2018) (**Supplementary Table S2**), indicates that the major source of human-associated markers at these locations could be sewage (Kapoor et al., 2015).

Swine farming is the dominant livestock-based agricultural activity in Zhejiang province. The swine associated marker was frequently detected in water samples collected at locations 6, 12, 13, 20, and 21 and sediment samples collected in locations 13 and 21 (**Figures 3C**, **4C**). The results obtained were consistent with the land use pattern as these locations have active pig-farming operations. Location 6 is near Qijia village where commercial and household backyard pig and poultry farms were observed during the sampling. On the upstream side of location 13, WWTP and active pig farming (**Supplementary Table S9**) were found near to this location (Zheng et al., 2017). Locations 20 and 21 were close to Changxing port, which has several farms for pigs and poultry (**Supplementary Table S7**). The only possible explanation for the consistent detection of swine associated markers at location 12 is the transport of bacteria from location 13, as the distance between two locations is ∼1 km. In China, both backyard and commercial based poultry farming are common and the existence of such farms nearby leads to the release of poultry feces into the watershed (Zhuang et al., 2017). The provincial government of Zhejiang had concerns over the illegal discharge of poultry wastes into the watershed and has recently initiated monitoring control measures (Zheijiang, 2016). The avian associated marker quantification results prove that poultry fecal pollution was high in the study area as markers were detected in 89% of water samples (40/45) (**Figure 3D**). Based on the GFD assay, water samples collected at locations 6, 15, 20, and 21 (**Figure 3D**) and sediments (summer season) collected at locations 6 and 20 (data not shown here) had high levels of avian markers. Active commercial and backyard poultry farming was observed at these locations (locations 6, 20, and 21) and results correlate well with the land use pattern (**Supplementary Tables S2**, **S9**) (Vadde et al., 2018). Although the avian associated marker quantification results were positive for sediment samples collected from several locations in autumn and winter, the quantities were below the detection limit, i.e., LOD. Overall, the human associated *Bacteroidales* MST marker was the most frequently detected host-associated MST marker in the sediment samples, highlighting the presence of human fecal pollution in the Tiaoxi River. The survival and persistence of *Bacteroidales* associated MST markers in sediment samples, which could act as a non-point source of fecal pollution, has previously been reported (Kim and Wuertz, 2015). However, recent studies have reported that the HF183 Taqman marker showed limited persistence (<7 days) in freshwater sediments and suggested that it could be a reliable marker to detect recent fecal input into freshwater sediment, although these studies also cautioned that the decay of this marker in a different geographical setting could be influenced by various factors such as organic matter and nutrients (Zimmer-Faust et al., 2017; Ahmed et al., 2019). Overall, MST results obtained in the present study indicate the potential occurrence of pathogens at these locations, which was followed up with in-depth monitoring of host-associated pathogens.

Detection of Pathogenic Bacterial Gene Markers to Assess the Potential Health Risk Posed by Tiaoxi River

Although MST is a promising technique for identifying the source of fecal contamination, a combination of a fecal indicator organism enumeration, MST, and associated waterborne pathogenic bacterial gene marker quantification, provides more reliable information on water quality and associated health risks in the watershed. Such studies provide valuable information to water quality management authorities, taking tangible actions to reduce pollution in contaminated waters.

Among the bacterial pathogens monitored, *Campylobacter jejuni* was found to be the most frequently detected pathogen in the study area (**Table 6**). *C. jejuni* originates primarily from chicken and other avian feces (Lund et al., 2004) and although high frequency of *C. jejuni* detection could be indicative of high avian fecal contamination, this organism can survive for up to 4 months in the environment (Murphy et al., 2006). *C. jejuni* was frequently detected in water and sediment samples at locations 4, 6, 8, and 13 and the concentrations were higher at locations 6 and 13 on one or more occasions, indicating that these locations could pose significant health risks. *Campylobacter jejuni* infective doses for human gastroenteritis have been reported to be as low as 500 cells (Ahmed et al., 2009). Globally, *Shigella* spp. are among the major bacterial causes of diarrhea; they are considered as one of the top four groups of pathogens that causes moderate to severe diarrhea in the children of Africa and South Asia (Huynh et al., 2015). *Shigella sonnei* is the most commonly recovered species in infected patients of the United States, while in Asia and developing countries, *S. dysenteriae* and *S. flexneri* were the major causative species (Wu et al., 2009). In the present study, the *Shigella* marker gene, *ipaH,* was detected in 68 (75.6%) of the 90 water and sediment samples tested (**Table 6**). Humans are considered as the common and natural reservoirs for *Shigella* spp. (Ishii et al., 2013) and the presence of these bacteria indicates human fecal contamination (Oster et al., 2014). As the *ipaH* gene occurs in 5–10 copies in plasmid and genomic DNA of *Shigella* spp. (Greenberg et al., 2010), only *Shigella* spp. detected in water and sediment samples at locations 3 and 12 were found to be at higher concentrations and may pose a potential human health risk. Monitoring of *Shigella* and *Campylobacter* spp. is a useful tool for watershed managers/monitoring agencies as these organisms are associated with specific sources (host associated). Shiga toxin-producing *E. coli* (STEC) can cause gastrointestinal disease leading to mild or severe bloody diarrhea (Haack et al., 2015) and they originate from multiple sources or reservoirs (Beutin et al., 2008). Here, although STEC was detected in nearly 50% of water samples tested in the study area (**Table 6**), only locations 5 and 21 had higher concentrations indicating significant human health risk at these locations. Pathogenic *Leptospira* species cause leptospirosis by colonization of the renal tubules of infected reservoir hosts such as dogs, rats and, cattle, and leptospires enter the aquatic environment via urine (Monahan et al., 2008). Pathogenic *Leptospira* spp. have a high infective dose due to the acid sensitivity of the bacteria (Ganoza et al., 2010). Therefore, the pathogenic *Leptospira* quantified in the present study may not be of significant human health risks, although the higher concentrations were frequently detected at locations 20 and 21. *E. coli* O157:H7 (*eae* gene) was not detected in any of the water samples, but detected at low frequency (33%) in sediment samples (during autumn season) (**Figure 5**). It has been reported that cattle are the main reservoir for *E. coli* O157:H7 (Ahmed et al., 2009) and the results presented here are consistent with the paucity of cattle farming in the watershed area (NBSC, 2015). Overall, the quantification of the genes of bacterial pathogens in water and sediment samples indicate that *C. jejuni* and STEC are the major concerns for human health risk in a few specific locations of the study area. Furthermore, the bacterial pathogen quantification results correlate with the findings of host associated fecal markers, demonstrating the potential of MST in predicting the presence of pathogenic organisms and the concomitant risk to human health.

CONCLUSION

In summary, our MST qPCR validation study demonstrates that BacUni, HF183 Taqman, Pig-2-Bac, and GFD assays are the most suitable for differentially identifying and monitoring human and animal fecal contamination in the Taihu watershed. In the case of fecal pollution monitoring at the Tiaoxi River, 15 out of 25 monitoring locations were identified as hotspots of fecal contamination based on FC enumeration, and samples collected from those 15 locations were further used for the quantification of MST and pathogenic bacterial gene markers. The total *Bacteroidales* marker was detected in all of the water and sediment samples at these 15 monitoring locations, confirming the presence of fecal contamination. Although human-associated markers were frequently detected at several locations, locations 3, 12, and 16 had high concentrations on one or more occasions, indicating that they are major human fecal contaminated sites of the Tiaoxi River region. The swine associated marker was frequently detected in samples from locations 13 and 21 and the avian associated marker was detected with high concentrations at locations 6, 15, 20, and 21, matching the land use pattern and pointing to the entry of swine and avian fecal sources to the Tiaoxi River. Among five bacterial pathogens monitored, *Campylobacter jejuni* was frequently detected at locations that are primarily polluted with avian fecal material (locations 4, 6, 8, and 13) and high concentrations were detected at locations 6 and 13 (on one or more occasions) indicating that these sites pose potential human health risks. Similarly, *Shigella* spp. were frequently detected at higher concentrations in two locations (locations 3 and 12) that are highly contaminated with human fecal sources, and the Shiga toxin-producing *E. coli* (STEC) at two locations (locations 5 and 21), which are contaminated with either human or pig fecal sources. The bacterial pathogen quantification results correlate with the findings of host-associated fecal markers, and the data generated here are valuable for water quality monitoring authorities responsible for minimizing the health risks associated with pathogens, by identifying sites where intervention is required.

ETHICS STATEMENT

Ethical approval for this study was provided by XJTLU Research Ethics Committee (EXT-16-07-01).

AUTHOR CONTRIBUTIONS

RS, AM, and RR conceived and designed the experiments. RS and KV carried out the field sampling. KV performed the

experiments and data analyses and prepared the manuscript with the directions of his supervisors RS, AM, and RR. RS and AM contributed to the revision of the manuscript.

FUNDING

The authors would like to acknowledge the Natural Science Foundation of Jiangsu Province (Grant No. BK20141211), Natural Science Foundation of the Jiangsu Higher Education Institutions of China (Grant No. 13KJB180022), Suzhou Industrial Park Supplement Fund and Xi'an Jiaotong-Liverpool University (XJTLU) for financial support. Financial support to KV was provided through the Postgraduate Research Scholarship (PGRS-12-01-08) awarded by XJTLU.

ACKNOWLEDGMENTS

The authors would like to thank the Department of Biological Sciences, XJTLU and Suzhou Institute for Advanced Study, University of Science and Technology (USTC) for providing facilities and Long Cao, Shen Li, and Tianma Yuan for their help with the field sampling. The authors are very grateful to Praveena Sekar for preparing the Graphical Abstract in this paper.

SUPPLEMENTARY MATERIAL

The Supplementary Material for this article can be found online at: https://www.frontiersin.org/articles/10.3389/fmicb.2019.00699/full#supplementary-material

REFERENCES

Ahmed, W., Hamilton, K. A., Gyawali, P., Toze, S., and Haas, C. N. (2016a). Evidence of avian and possum fecal contamination in rainwater tanks as determined by microbial source tracking approaches. *Appl. Environ. Microbiol.* 82, 4379–4386. doi: 10.1128/AEM.00892-16

Ahmed, W., Harwood, V. J., Nguyen, K., Young, S., Hamilton, K., and Toze, S. (2016b). Utility of Helicobacter spp. associated GFD markers for detecting avian fecal pollution in natural waters of two continents. *Water Res.* 88, 613–622. doi: 10.1016/j.watres.2015.10.050

Ahmed, W., Masters, N., and Toze, S. (2012). Consistency in the host specificity and host sensitivity of the *Bacteroides* HF183 marker for sewage pollution tracking. *Lett. Appl. Microbiol.* 55, 283–289. doi: 10.1111/j.1472-765X.2012.03291.x

Ahmed, W., Sawant, S., Huygens, F., Goonetilleke, A., and Gardner, T. (2009). Prevalence and occurrence of zoonotic bacterial pathogens in surface waters determined by quantitative PCR. *Water Res.* 43, 4918–4928. doi: 10.1016/j.watres.2009.03.041

Ahmed, W., Sritharan, T., Palmer, A., Sidhu, J. P., and Toze, S. (2013). Evaluation of bovine feces-associated microbial source tracking markers and their correlations with fecal indicators and zoonotic pathogens in a Brisbane, Australia, reservoir. *Appl. Environ. Microbiol.* 79, 2682–2691. doi: 10.1128/AEM.03234-12

Ahmed, W., Yusuf, R., Hasan, I., Goonetilleke, A., and Gardner, T. (2010). Quantitative PCR assay of sewage-associated *Bacteroides* markers to assess sewage pollution in an urban lake in Dhaka, Bangladesh. *Can. J. Microbiol.* 56, 838–845. doi: 10.1139/W10-070

Ahmed, W., Zhang, Q., Kozak, S., Beale, D., Gyawali, P., Sadowsky, M. J., et al. (2019). Comparative decay of sewage-associated marker genes in beach water and sediment in a subtropical region. *Water Res.* 149, 511–521. doi: 10.1016/j.watres.2018.10.088

APHA (2005). *Standard Methods for the Examination of Water and Wastewater*, 21st Edn. Washington, DC: American Public Health Association.

Arfken, A. M., Song, B., and Mallin, M. A. (2015). Assessing hog lagoon waste contamination in the Cape Fear Watershed using Bacteroidetes 16S rRNA gene pyrosequencing. *Appl. Microbiol. Biotechnol.* 99, 7283–7293. doi: 10.1007/s00253-015-6784-x

Bernhard, A. E., and Field, K. G. (2000). A PCR assay To discriminate human and ruminant feces on the basis of host differences in *Bacteroides*-Prevotella genes encoding 16S rRNA. *Appl. Environ. Microbiol.* 66, 4571–4574. doi: 10.1128/AEM.66.10.4571-4574.2000

Best, E. L., Powell, E. J., Swift, C., Grant, K. A., and Frost, J. A. (2003). Applicability of a rapid duplex real-time PCR assay for speciation of Campylobacter jejuniand Campylobacter colidirectly from culture plates. *FEMS Microbiol. Lett.* 229, 237–241. doi: 10.1016/S0378-1097(03)00845-0

Beutin, L., Kruger, U., Krause, G., Miko, A., Martin, A., and Strauch, E. (2008). Evaluation of major types of Shiga toxin 2E-producing *Escherichia coli* bacteria present in food, pigs, and the environment as potential pathogens for humans. *Appl. Environ. Microbiol.* 74, 4806–4816. doi: 10.1128/AEM.00623-08

Boehm, A. B., Wang, D., Ercumen, A., Shea, M., Harris, A. R., Shanks, O. C., et al. (2016). Occurrence of host-associated fecal markers on child hands, household soil, and drinking water in rural Bangladeshi households. *Environ. Sci. Technol. Lett.* 3, 393–398. doi: 10.1021/acs.estlett.6b00382

Bradshaw, J. K., Snyder, B. J., Oladeinde, A., Spidle, D., Berrang, M. E., Meinersmann, R. J., et al. (2016). Characterizing relationships among fecal indicator bacteria, microbial source tracking markers, and associated waterborne pathogen occurrence in stream water and sediments in a mixed land use watershed. *Water Res.* 101, 498–509. doi: 10.1016/j.watres.2016.05.014

Bustin, S. A., Benes, V., Garson, J. A., Hellemans, J., Huggett, J., Kubista, M., et al. (2009). The MIQE guidelines: minimum information for publication of quantitative real-time PCR experiments. *Clin. Chem.* 55, 611–622. doi: 10.1373/clinchem.2008.112797

Byappanahalli, M. N., Shively, D. A., Nevers, M. B., Sadowsky, M. J., and Whitman, R. L. (2003). Growth and survival of *Escherichia coli* and enterococci populations in the macro-alga Cladophora (Chlorophyta). *FEMS Microbiol. Ecol.* 46, 203–211. doi: 10.1016/S0168-6496(03)00214-9

Ervin, J. S., Russell, T. L., Layton, B. A., Yamahara, K. M., Wang, D., Sassoubre, L. M., et al. (2013). Characterization of fecal concentrations in human and other animal sources by physical, culture-based, and quantitative real-time PCR methods. *Water Res.* 47, 6873–6882. doi: 10.1016/j.watres.2013.02.060

Fan, L., Shuai, J., Zeng, R., Mo, H., Wang, S., Zhang, X., et al. (2017). Validation and application of quantitative PCR assays using host-specific Bacteroidales genetic markers for swine fecal pollution tracking. *Environ. Pollut.* 231, 1569–1577. doi: 10.1016/j.envpol.2017.09.047

Field, K. G., and Samadpour, M. (2007). Fecal source tracking, the indicator paradigm, and managing water quality. *Water Res.* 41, 3517–3538. doi: 10.1016/j.watres.2007.06.056

Fremaux, B., Boa, T., and Yost, C. K. (2010). Quantitative real-time PCR assays for sensitive detection of Canada goose-specific fecal pollution in water sources. *Appl. Environ. Microbiol.* 76, 4886–4889. doi: 10.1128/AEM.00110-10

Ganoza, C. A., Matthias, M. A., Saito, M., Cespedes, M., Gotuzzo, E., and Vinetz, J. M. (2010). Asymptomatic renal colonization of humans in the Peruvian Amazon by Leptospira. *PLoS Negl. Trop. Dis.* 4:e612. doi: 10.1371/journal.pntd.0000612

Gourmelon, M., Caprais, M. P., Segura, R., Le Mennec, C., Lozach, S., Piriou, J. Y., et al. (2007). Evaluation of two library-independent microbial source tracking methods to identify sources of fecal contamination in French estuaries. *Appl. Environ. Microbiol.* 73, 4857–4866. doi: 10.1128/AEM.03003-06

Green, H. C., Dick, L. K., Gilpin, B., Samadpour, M., and Field, K. G. (2012). Genetic markers for rapid PCR-based identification of gull, Canada goose, duck, and chicken fecal contamination in water. *Appl. Environ. Microbiol.* 78, 503–510. doi: 10.1128/AEM.05734-11

Green, H. C., Haugland, R. A., Varma, M., Millen, H. T., Borchardt, M. A., Field, K. G., et al. (2014). Improved HF183 Quantitative Real-Time PCR assay for characterization of human fecal pollution in ambient surface water samples. *Appl. Environ. Microbiol.* 80, 3086–3094. doi: 10.1128/AEM.04137-13

Greenberg, J., Price, B., and Ware, A. (2010). Alternative estimate of source distribution in microbial source tracking using posterior probabilities. *Water Res.* 44, 2629–2637. doi: 10.1016/j.watres.2010.01.018

Griffith, J. F., Cao, Y., Mcgee, C. D., and Weisberg, S. B. (2009). Evaluation of rapid methods and novel indicators for assessing microbiological beach water quality. *Water Res.* 43, 4900–4907. doi: 10.1016/j.watres.2009.09.017

Haack, S. K., Duris, J. W., Kolpin, D. W., Fogarty, L. R., Johnson, H. E., Gibson, K. E., et al. (2015). Genes indicative of zoonotic and swine pathogens are persistent in stream water and sediment following a swine manure spill. *Appl. Environ. Microbiol.* 81, 3430–3441. doi: 10.1128/AEM.04195-14

Hagedorn, C., and Liang, X. (2011). Current and future trends in fecal source tracking and deployment in the Lake Taihu Region of China. *Phys. Chem. Earth* 36, 352–359. doi: 10.1016/j.pce.2010.03.031

Harwood, V. J., Wiggins, B., Hagedorn, C., Ellender, R. D., Gooch, J., Kern, J., et al. (2003). Phenotypic library-based microbial source tracking methods: efficacy in the California collaborative study. *J. Water Health* 1, 153–166. doi: 10.2166/wh.2003.0018

He, X. W., Liu, P., Zheng, G. L., Chen, H. M., Shi, W., Cui, Y. B., et al. (2016). Evaluation of five microbial and four mitochondrial DNA markers for tracking human and pig fecal pollution in freshwater. *Sci. Rep.* 6:35311. doi: 10.1038/srep35311

Heaney, C. D., Myers, K., Wing, S., Hall, D., Baron, D., and Stewart, J. R. (2015). Source tracking swine fecal waste in surface water proximal to swine concentrated animal feeding operations. *Sci. Total Environ.* 511, 676–683. doi: 10.1016/j.scitotenv.2014.12.062

Huynh, A., Mcgrath, C., Johnson, D., and Burrell, L. M. (2015). *Shigella* sonnei bacteraemia occurring in a young man with shigellosis. *BMJ Case Rep.* 2015:bcr2014208875. doi: 10.1136/bcr-2014-208875

Ibekwe, A. M., Watt, P. M., Grieve, C. M., Sharma, V. K., and Lyons, S. R. (2002). Multiplex Fluorogenic Real-Time PCR for Detection and Quantification of *Escherichia coli* O157:H7 in Dairy Wastewater Wetlands. *Appl. Environ. Microbiol.* 68, 4853–4862. doi: 10.1128/AEM.68.10.4853-4862.2002

Ishii, S., Segawa, T., and Okabe, S. (2013). Simultaneous quantification of multiple food- and waterborne pathogens by use of microfluidic quantitative PCR. *Appl. Environ. Microbiol.* 79, 2891–2898. doi: 10.1128/AEM.00205-13

Jenkins, M. W., Tiwari, S., Lorente, M., Gichaba, C. M., and Wuertz, S. (2009). Identifying human and livestock sources of fecal contamination in Kenya with host-specific Bacteroidales assays. *Water Res.* 43, 4956–4966. doi: 10.1016/j.watres.2009.07.028

Jia, S., He, X., Bu, Y., Shi, P., Miao, Y., Zhou, H., et al. (2014). Environmental fate of tetracycline resistance genes originating from swine feedlots in river water. *J. Environ. Sci. Health B* 49, 624–631. doi: 10.1080/03601234.2014.911594

Kapoor, V., Pitkanen, T., Ryu, H., Elk, M., Wendell, D., and Domingo, J. W. S. (2015). Distribution of human-specific bacteroidales and fecal indicator bacteria in an urban watershed impacted by sewage pollution, determined using RNA-and DNA-based quantitative PCR assays. *Appl. Environ. Microbiol.* 81, 91–99. doi: 10.1128/AEM.02446-14

Kildare, B. J., Leutenegger, C. M., Mcswain, B. S., Bambic, D. G., Rajal, V. B., and Wuertz, S. (2007). 16S rRNA-based assays for quantitative detection of universal, human-, cow-, and dog-specific fecal Bacteroidales: a Bayesian approach. *Water Res.* 41, 3701–3715. doi: 10.1016/j.watres.2007.06.037

Kim, M., and Wuertz, S. (2015). Survival and persistence of host-associated Bacteroidales cells and DNA in comparison with *Escherichia coli* and Enterococcus in freshwater sediments as quantified by PMA-qPCR and qPCR. *Water Res.* 87, 182–192. doi: 10.1016/j.watres.2015.09.014

Layton, A., Mckay, L., Williams, D., Garrett, V., Gentry, R., and Sayler, G. (2006). Development of *Bacteroides* 16S rRNA gene TaqMan-based real-time PCR assays for estimation of total, human, and bovine fecal pollution in water. *Appl. Environ. Microbiol.* 72, 4214–4224. doi: 10.1128/AEM.01036-05

Layton, B. A., Cao, Y. P., Ebentier, D. L., Hanley, K., Balleste, E., Brandao, J., et al. (2013). Performance of human fecal anaerobe-associated PCR-based assays in a multi-laboratory method evaluation study. *Water Res.* 47, 6897–6908. doi: 10.1016/j.watres.2013.05.060

Lu, J., Santo Domingo, J. W., Hill, S., and Edge, T. A. (2009). Microbial diversity and host-specific sequences of Canada goose feces. *Appl. Environ. Microbiol.* 75, 5919–5926. doi: 10.1128/AEM.00462-09

Lund, M., Nordentoft, S., Pedersen, K., and Madsen, M. (2004). Detection of Campylobacter spp. in chicken fecal samples by real-time PCR. *J. Clin. Microbiol.* 42, 5125–5132. doi: 10.1128/JCM.42.11.5125-5132.2004

Lv, H., Xu, Y., Han, L., and Zhou, F. (2015). Scale-dependence effects of landscape on seasonal water quality in Xitiaoxi catchment of Taihu Basin. China. *Water Sci. Technol.* 71, 59–66. doi: 10.2166/wst.2014.463

Malla, B., Ghaju Shrestha, R., Tandukar, S., Bhandari, D., Inoue, D., Sei, K., et al. (2018). Validation of host-specific Bacteroidales quantitative PCR assays and their application to microbial source tracking of drinking water sources in the Kathmandu Valley, Nepal. *J. Appl. Microbiol.* 125, 609–619 doi: 10.1111/jam.13884

Marti, R., Gannon, V. P. J., Jokinen, C., Lanthier, M., Lapen, D. R., Neumann, N. F., et al. (2013). Quantitative multi-year elucidation of fecal sources of waterborne pathogen contamination in the South Nation River basin using Bacteroidales microbial source tracking markers. *Water Res.* 47, 2315–2324. doi: 10.1016/j.watres.2013.02.009

Mieszkin, S., Furet, J. P., Corthier, G., and Gourmelon, M. (2009). Estimation of pig fecal contamination in a river catchment by real-time PCR using two pig-specific Bacteroidales 16S rRNA genetic markers. *Appl. Environ. Microbiol.* 75, 3045–3054. doi: 10.1128/AEM.02343-08

Monahan, A. M., Callanan, J. J., and Nally, J. E. (2008). Proteomic analysis of Leptospira interrogans shed in urine of chronically infected hosts. *Infect. Immun.* 76, 4952–4958. doi: 10.1128/IAI.00511-08

Murphy, C., Carroll, C., and Jordan, K. N. (2006). Environmental survival mechanisms of the foodborne pathogen Campylobacter jejuni. *J. Appl. Microbiol.* 100, 623–632. doi: 10.1111/j.1365-2672.2006.02903.x

Napier, M. D., Haugland, R., Poole, C., Dufour, A. P., Stewart, J. R., Weber, D. J., et al. (2017). Exposure to human-associated fecal indicators and self-reported illness among swimmers at recreational beaches: a cohort study. *Environ. Health* 16:103. doi: 10.1186/s12940-017-0308-3

NBSC (2015). *National Bureau of Statistics of China*. Available at: http://www.stats.gov.cn/english/statisticaldata/annualdata/ (accessed April 26, 2016).

NBSC (2016). *National Bureau of Statistics of China [Online]*. Available at: http://www.stats.gov.cn/tjsj/ndsj/2016/indexeh.htm (accessed June 6, 2018).

Nshimyimana, J. P., Cruz, M. C., Thompson, R. J., and Wuertz, S. (2017). Bacteroidales markers for microbial source tracking in Southeast Asia. *Water Res.* 118, 239–248. doi: 10.1016/j.watres.2017.04.027

Nshimyimana, J. P., Ekklesia, E., Shanahan, P., Chua, L. H., and Thompson, J. R. (2014). Distribution and abundance of human-specific *Bacteroides* and relation to traditional indicators in an urban tropical catchment. *J. Appl. Microbiol.* 116, 1369–1383. doi: 10.1111/jam.12455

Odagiri, M., Schriewer, A., Hanley, K., Wuertz, S., Misra, P. R., Panigrahi, P., et al. (2015). Validation of Bacteroidales quantitative PCR assays targeting human and animal fecal contamination in the public and domestic domains in India. *Sci. Total Environ.* 502, 462–470. doi: 10.1016/j.scitotenv.2014.09.040

Ohad, S., Ben-Dor, S., Prilusky, J., Kravitz, V., Dassa, B., Chalifa-Caspi, T., et al. (2016). The Development of a Novel qPCR assay-set for identifying fecal contamination originating from domestic fowls and waterfowl in israel. *Front. Microbiol.* 7:145. doi: 10.3389/fmicb.2016.00145

Ohad, S., Vaizel-Ohayon, D., Rom, M., Guttman, J., Berger, D., Kravitz, V., et al. (2015). Microbial source tracking in adjacent karst springs. *Appl. Environ. Microbiol.* 81, 5037–5047. doi: 10.1128/AEM.00855-15

Oster, R. J., Wijesinghe, R. U., Haack, S. K., Fogarty, L. R., Tucker, T. R., and Riley, S. C. (2014). Bacterial pathogen gene abundance and relation to recreational water quality at seven Great Lakes beaches. *Environ. Sci. Technol.* 48, 14148–14157. doi: 10.1021/es5038657

Qin, B., Xu, P., Wu, Q., Luo, L., and Zhang, Y. (2007). Environmental issues of Lake Taihu. China. *Hydrobiologia* 581, 3–14. doi: 10.1007/s10750-006-0521-5

Raith, M. R., Kelty, C. A., Griffith, J. F., Schriewer, A., Wuertz, S., Mieszkin, S., et al. (2013). Comparison of PCR and quantitative real-time PCR methods for the characterization of ruminant and cattle fecal pollution sources. *Water Res.* 47, 6921–6928. doi: 10.1016/j.watres.2013.03.061

Reischer, G. H., Ebdon, J. E., Bauer, J. M., Schuster, N., Ahmed, W., Astrom, J., et al. (2013). Performance characteristics of qPCR assays targeting human- and ruminant-associated bacteroidetes for microbial source tracking across sixteen countries on six continents. *Environ. Sci. Technol.* 47, 8548–8556. doi: 10.1021/es304367t

Ridley, C. M., Jamieson, R. C., Hansen, L. T., Yost, C. K., and Bezanson, G. S. (2014). Baseline and storm event monitoring of Bacteroidales marker concentrations and enteric pathogen presence in a rural Canadian watershed. *Water Res.* 60, 278–288. doi: 10.1016/j.watres.2014.04.039

Saxena, G., Bharagava, R. N., Kaithwas, G., and Raj, A. (2015). Microbial indicators, pathogens and methods for their monitoring in water environment. *J. Water Health* 13, 319–339. doi: 10.2166/wh.2014.275

Schriewer, A., Goodwin, K. D., Sinigalliano, C. D., Cox, A. M., Wanless, D., Bartkowiak, J., et al. (2013). Performance evaluation of canine-associated Bacteroidales assays in a multi-laboratory comparison study. *Water Res.* 47, 6909–6920. doi: 10.1016/j.watres.2013.03.062

Scupham, A. J., Patton, T. G., Bent, E., and Bayles, D. O. (2008). Comparison of the cecal microbiota of domestic and wild turkeys. *Microb. Ecol.* 56, 322–331. doi: 10.1007/s00248-007-9349-4

Seurinck, S., Defoirdt, T., Verstraete, W., and Siciliano, S. D. (2005). Detection and quantification of the human-specific HF183 *Bacteroides* 16S rRNA genetic marker with real-time PCR for assessment of human faecal pollution in freshwater. *Environ. Microbiol.* 7, 249–259. doi: 10.1111/j.1462-2920.2004.00702.x

Shanks, O. C., Atikovic, E., Blackwood, A. D., Lu, J., Noble, R. T., Domingo, J. S., et al. (2008). Quantitative PCR for detection and enumeration of genetic markers of bovine fecal pollution. *Appl. Environ. Microbiol.* 74, 745–752. doi: 10.1128/AEM.01843-07

Shanks, O. C., Kelty, C. A., Sivaganesan, M., Varma, M., and Haugland, R. A. (2009). Quantitative PCR for genetic markers of human fecal pollution. *Appl. Environ. Microbiol.* 75, 5507–5513. doi: 10.1128/AEM.00305-09

Sidhu, J. P. S., Hodgers, L., Ahmed, W., Chong, M. N., and Toze, S. (2012). Prevalence of human pathogens and indicators in stormwater runoff in Brisbane. Australia. *Water Res.* 46, 6652–6660. doi: 10.1016/j.watres.2012.03.012

Steele, J. A., Blackwood, A. D., Griffith, J. F., Noble, R. T., and Schiff, K. C. (2018). Quantification of pathogens and markers of fecal contamination during storm events along popular surfing beaches in San Diego. California. *Water Res.* 136, 137–149. doi: 10.1016/j.watres.2018.01.056

Stoddard, R. A., Gee, J. E., Wilkins, P. P., Mccaustland, K., and Hoffmaster, A. R. (2009). Detection of pathogenic Leptospira spp. through TaqMan polymerase chain reaction targeting the LipL32 gene. *Diagn. Microbiol. Infect. Dis.* 64, 247–255. doi: 10.1016/j.diagmicrobio.2009.03.014

Tambalo, D. D., Fremaux, B., Boa, T., and Yost, C. K. (2012). Persistence of host-associated Bacteroidales gene markers and their quantitative detection in an urban and agricultural mixed prairie watershed. *Water Res.* 46, 2891–2904. doi: 10.1016/j.watres.2012.02.048

USEPA (2012). *United States Environmental Protection Agency. Water: Monitoring & Analysis. [Online]*. Washington, DC: USEPA

Vadde, K., Wang, J., Cao, L., Yuan, T., Mccarthy, A., and Sekar, R. (2018). Assessment of Water Quality and Identification of Pollution Risk Locations in Tiaoxi River (Taihu Watershed). China. *Water* 10:183. doi: 10.3390/w10020183

Wang, L., Li, Y., and Mustaphai, A. (2007). Rapid and simultaneous quantitation of *Escherichia coli* 0157:H7, *Salmonella*, and *Shigella* in ground beef by multiplex real-time PCR and immunomagnetic separation. *J. Food Prot.* 70, 1366–1372. doi: 10.4315/0362-028X-70.6.1366

Wu, C. H., Huang, L. T., Huang, I. F., Liu, J. W., Chen, J. B., Liang, C. D., et al. (2009). Acute non-outbreak shigellosis: ten years experience in southern Taiwan. *Chang Gung Med. J.* 32, 59–65.

Wu, G. D., Chen, J., Hoffmann, C., Bittinger, K., Chen, Y. Y., Keilbaugh, S. A., et al. (2011). Linking long-term dietary patterns with gut microbial enterotypes. *Science* 334, 105–108. doi: 10.1126/science.1208344

Yatsunenko, T., Rey, F. E., Manary, M. J., Trehan, I., Dominguez-Bello, M. G., Contreras, M., et al. (2012). Human gut microbiome viewed across age and geography. *Nature* 486, 222–227. doi: 10.1038/nature11053

Zhang, Q., Eichmiller, J. J., Staley, C., Sadowsky, M. J., and Ishii, S. (2016). Correlations between pathogen concentration and fecal indicator marker genes in beach environments. *Sci. Total Environ.* 573, 826–830. doi: 10.1016/j.scitotenv.2016.08.122

Zhang, Y., Shi, K., Zhou, Y., Liu, X., and Qin, B. (2016). Monitoring the river plume induced by heavy rainfall events in large, shallow, Lake Taihu using MODIS 250m imagery. *Remote Sens. Environ.* 173, 109–121. doi: 10.1016/j.rse.2015.11.020

Zheijiang, G. O. (2016). *Zhejiang Scrutinizes Livestock, Poultry Pollution [Online]. Government of Zheijiang*. Available: http://english.zj.gov.cn/art/2016/4/27/art_5798_2098514.html (accessed April 26, 2016).

Zheng, J., Gao, R., Wei, Y., Chen, T., Fan, J., Zhou, Z., et al. (2017). High-throughput profiling and analysis of antibiotic resistance genes in East Tiaoxi River. China. *Environ. Pollut.* 230, 648–654. doi: 10.1016/j.envpol.2017.07.025

Zhu, X. Y., Zhong, T., Pandya, Y., and Joerger, R. D. (2002). 16S rRNA-based analysis of microbiota from the cecum of broiler chickens. *Appl. Environ. Microbiol.* 68, 124–137. doi: 10.1128/AEM.68.1.124-137.2002

Zhuang, F. F., Li, H., Zhou, X. Y., Zhu, Y. G., and Su, J. Q. (2017). Quantitative detection of fecal contamination with domestic poultry feces in environments in China. *AMB Express* 7:80. doi: 10.1186/s13568-017-0379-0

Zimmer-Faust, A. G., Thulsiraj, V., Marambio-Jones, C., Cao, Y., Griffith, J. F., Holden, P. A., et al. (2017). Effect of freshwater sediment characteristics on the persistence of fecal indicator bacteria and genetic markers within a Southern California watershed. *Water Res.* 119, 1–11. doi: 10.1016/j.watres.2017.04.028

Conflict of Interest Statement: The authors declare that the research was conducted in the absence of any commercial or financial relationships that could be construed as a potential conflict of interest.

Copyright © 2019 Vadde, McCarthy, Rong and Sekar. This is an open-access article distributed under the terms of the Creative Commons Attribution License (CC BY). The use, distribution or reproduction in other forums is permitted, provided the original author(s) and the copyright owner(s) are credited and that the original publication in this journal is cited, in accordance with accepted academic practice. No use, distribution or reproduction is permitted which does not comply with these terms.

frontiers in Microbiology

ORIGINAL RESEARCH
published: 14 May 2019
doi: 10.3389/fmicb.2019.00996

Bacterial Community 16S rRNA Gene Sequencing Characterizes Riverine Microbial Impact on Lake Michigan

Cindy H. Nakatsu[1], Muruleedhara N. Byappanahalli[2†] and Meredith B. Nevers[2‡]*

[1] Department of Agronomy, Purdue University, West Lafayette, IN, United States, [2] Great Lakes Science Center, United States Geological Survey, Chesterton, IN, United States

Restoration of degraded aquatic habitats is critical to preserve and maintain ecosystem processes and economic viability. Effective restoration requires contaminant sources identification. Microbial communities are increasingly used to characterize fecal contamination sources. The objective was to determine whether nearshore and adjacent beach bacterial contamination originated from the Grand Calumet River, a highly urbanized aquatic ecosystem, and to determine if there were correlations between pathogens/feces associated bacteria in any of the samples to counts of the pathogen indicator species *Escherichia coli*. Water samples were collected from the river, river mouth, nearshore, and offshore sites along southern Lake Michigan. Comparisons among communities were made using beta diversity distances (weighted and unweighted Unifrac, and Bray Curtis) and Principal Coordinate Analysis of 16S rRNA gene Illumina sequence data that indicated river bacterial communities differed significantly from the river mouth, nearshore lake, and offshore lake samples. These differences were further supported using Source Tracker software that indicated nearshore lake communities differed significantly from river and offshore samples. Among locations, there was separation by sampling date that was associated with environmental factors (e.g., water and air temperature, water turbidity). Although about half the genera (48.1%) were common to all sampling sites, linear discriminant analysis effect size indicated there were several taxa that differed significantly among sites; there were significant positive correlations of feces-associated genera with *E. coli* most probable numbers. Results collectively highlight that understanding microbial communities, rather than relying solely on select fecal indicators with uncertain origin, are more useful for developing strategies to restore degraded aquatic habitats.

Keywords: microbial communities, freshwater lake, 16S rRNA gene, hydrodynamic model, *Escherichia coli*

OPEN ACCESS

Edited by:
Raju Sekar,
Xi'an Jiaotong-Liverpool University, China

Reviewed by:
Jianjun Wang,
Nanjing Institute of Geography and Limnology (CAS), China
Paola Grenni,
Istituto di Ricerca sulle Acque (IRSA), Italy
Christopher Staley,
University of Minnesota, United States

****Correspondence:***
Cindy H. Nakatsu
cnakatsu@purdue.edu
orcid.org/0000-0003-0663-180X

[†]orcid.org/0000-0001-5376-597X
[‡]orcid.org/0000-0001-6963-6734

Specialty section:
This article was submitted to Aquatic Microbiology, a section of the journal Frontiers in Microbiology

Received: *25 November 2018*
Accepted: *18 April 2019*
Published: *14 May 2019*

Citation:
Nakatsu CH, Byappanahalli MN and Nevers MB (2019) Bacterial Community 16S rRNA Gene Sequencing Characterizes Riverine Microbial Impact on Lake Michigan. Front. Microbiol. 10:996. doi: 10.3389/fmicb.2019.00996

INTRODUCTION

Aquatic microbial contamination by pollutants derived from anthropogenic sources is a problem across the United States and worldwide; control of this contamination and restoration of degraded habitats can cost millions of dollars and considerable on-the-ground effort by water and land managers (Great Lakes Interagency Task Force, 2016; Steinman et al., 2017). Traditionally, indicator bacteria, such as *Escherichia coli* and/or enterococci, have been used to monitor potential

contamination of recreational waters (U.S. EPA, 1986). Often, these bacteria are not adequate to identify contamination sources because they can originate from a variety of warm-blooded animals and from environmental sources (Byappanahalli and Ishii, 2011). This lack of specificity has led to the development of other methods, such as detection of source-host bacterial indicators (see Field and Samadpour, 2007).

Microbial source tracking has been used in recent years to identify specific sources of fecal contamination through the use of targeted genetic markers (Harwood et al., 2014). Genetic markers have been used to indicate microbial contamination from humans, birds, dogs, and other animals (Harwood et al., 2014). This targeted approach is useful for identifying and mitigating microbial contamination if there is a dominant contamination source, but restoration becomes more complicated if there are multiple sources (Byappanahalli and Ishii, 2011; Nevers et al., 2014).

With the uncertainty associated with indicator bacteria and microbial source tracking, as well as the need to refine specificity of source identification, particularly in instances of legal obligation, better characterization of pollutant sources contributing to fecal contamination and associated links to sources is needed. In the past 2–3 decades, molecular techniques targeting the 16S rRNA gene and other genetic markers have been developed to characterize and analyze microbial communities from a variety of habitats including soil and water (Konopka et al., 1999; Nakatsu, 2007; Tanaka et al., 2014). More recently, the decrease in cost of next-generation high throughput sequencing technology has enabled the use of metagenomic approaches (targeted and non-targeted) to differentiate sources of aquatic microbial contamination (Newton et al., 2013; Cloutier et al., 2015; Newton et al., 2015). The depth of information acquired by using these advanced molecular genetic approaches provides a means to characterize microbial composition, distribution, and transportation pathways in the environment and to relate them to understand pollution mechanisms (Newton et al., 2013; Halliday et al., 2014).

Through federal programs (e.g., The Beach Act of 2000; Great Lakes Restoration Initiative, 2009-current; International Joint Commission, 2012), federal-state partnerships have been established to decrease contamination sources and the effects of contamination on these lake ecosystems; among these contamination concerns are beach closings due to high concentrations of indicator bacteria such as *E. coli*. The objective of this study was to determine if samples with elevated levels of *E. coli* were correlated with potential pathogens or other fecal indicator bacteria in the microbial community. A 16S rRNA gene targeted high throughput sequencing approach was used to determine microbial community structure and composition. The objectives were (1) to determine the similarity of nearshore and offshore lake microbial communities to the adjacent riverine water source and (2) to determine the incidence and correlation of pathogens/feces associated species in the aquatic microbiome to the pathogen indicator species *E. coli* counts. The results will help to illuminate the association of shoreline and riverine bacterial communities and the potential contribution of bacteria originating from the Grand Calumet River in northern Indiana. The outcome of this work will contribute to determining the critical role of microbial communities in these degraded ecosystems and to aid in developing and assessing effective strategies for management and restoration of these environments.

MATERIALS AND METHODS

Study Area

The study area is located in northern Indiana along the southern shore of Lake Michigan of the Laurentian Great Lakes. The focal point of the area is the Grand Calumet River, which has been highly urbanized during industrialization of the early 20th century. The Grand Calumet River flows into Lake Michigan through the channelized Indiana Ship Canal, and the entire river and associated shoreline is considered an "Area of Concern" by the International Joint Commission on boundary waters between the United States and Canada and therefore the focus of significant restoration efforts.

Sample Collection

Sampling sites were located in the Grand Calumet River at Columbus Drive (GCR), at the mouth of the river (GCM), at offshore locations north (GCN) and east (GCE) of the peninsula that lies between the river mouth and Jeorse Park, and at three nearshore locations: Jeorse Park (JP), East Chicago, IN; Whihala Beach (WH), Whiting, IN; and 63rd Street Beach (63rd), Chicago, IL (**Figure 1**; Byappanahalli and Nevers, 2019).

Water samples (∼1.5 L) were collected in triplicate during three independent events in the summer of 2015. Two dates were during dry weather conditions (8/12, 9/1) and one date was

FIGURE 1 | Sampling locations along the southern shore of Lake Michigan. Latitude and longitude for the study locations are as follows: 63rd, 41.782209/–87.572926; WH, 41.685118/–87.492282; GCR, 41.6394/–87.471276; GCM, 41.68719002/–87.43974003; GCN, 41.69217/–87.41554995; GCE, 41.66712/–87.40494006; and JP, 41.650478/–87.433551.

after a rainfall event (9/21). The seven locations represented four sources: river (9 samples), river mouth (9 samples), nearshore (27 samples), and offshore (18 samples), for a total of 63 samples. Water from GCR was collected by tossing a sterile collection bucket from the bridge crossing at Columbus Drive; offshore surface water samples (GCM, GCN, GCE) were collected from a boat by dipping a sterile 1-L collection bottle below the surface; and nearshore samples (JP, WH, 63rd) were collected by dipping a 1-L collection bottle below the surface in 45-cm deep water. All samples were stored on ice directly after collection for return to the laboratory for processing within 6 h of collection.

DNA Extraction

Upon return to the laboratory samples were concentrated by vacuum filtration first through a 5.0 μm nitrocellulose (Millipore) then 0.2 μm nitrocellulose filter (Millipore) then stored at −80°C until DNA extraction. Total genomic DNA from each 0.2 μm filter was extracted using the MoBio PowerWater kit according to the manufacturer's instructions. Nucleic acid quality (i.e., 260/280 ratio) was measured with a Nanodrop 1000 spectrophotometer (Thermo Fisher Scientific, Wilmington, DE, United States). DNA concentrations for all samples were measured by fluorometric quantitation using a Qubit® instrument and High Sensitivity dsDNA HS Assay kit (Thermo Fisher Scientific, Waltham, MA, United States); and purified DNA extracts were stored at −80°C until used.

Illumina 16S rRNA Gene Sequencing

The 16S rRNA gene in water DNA extracts was PCR-amplified using primers targeting the V3-V4 region (343-forward TAC GGR AGG CAG CAG and 804-reverse CTA CCR GGG TAT CTA ATC C) (Liu et al., 2008; Nossa et al., 2010). Primers with dual index tags were used to differentiate multiple samples in a single run following the manufacturer's (Illumina, San Diego, CA, United States) suggested step out protocol (Gloor et al., 2010). Reactions were carried out using ∼10 ng of template DNA in Q5® High Fidelity DNA Polymerase 2X master mix (New England Biolabs). PCR amplicons were purified using AxyPrepMag PCR clean-up kit (Axygen Scientific) and quantified using a Nanodrop 3000 fluorospectrophotometer after staining with the QuantiFluor dsDNA System (Promega). Equimolar amounts of amplicons from each sample were combined and sent to the Purdue Genomics Core Facility for 2 × 250 paired end sequencing using a MiSeq Illumina system. Sequence reads were pre-processed to remove primer tags and low-quality sequences, and paired end reads were merged using PANDAseq software (Masella et al., 2012).

16S rRNA Gene Sequence Analysis

Sequences were analyzed using the QIIME pipeline (version 1.9.1) (Caporaso et al., 2010). Operational taxonomic units (OTUs) were picked using the "pick_open_otus" option in QIIME (Rideout et al., 2014) that uses a 97% sequence similarity threshold, the uclust method (Edgar, 2010) for clustering, sequence alignment using PyNAST (Caporaso et al., 2010), and taxonomic assignment to the Greengenes data set version 13_5 (McDonald et al., 2012) using the RDP classifier (Wang et al., 2007). The lowest number of reads among the samples, 24,890, was chosen to rarefy datasets to use equal number of reads for all community comparisons. Beta-diversity measures were calculated using phylogenetic Unifrac distances (weighted and un-weighted) (Lozupone et al., 2011) and non-phylogenetic distance (Bray Curtis). Alpha-diversity measurements were used for richness and evenness (Shannon diversity), richness (ChaoI index, observed-species), Faith's phylogenetic diversity (PD whole tree) and Good's coverage to assess the completeness of OTU representation in each sample. Venn diagrams illustrating genera common to all samples was produced using the Venny program (Oliveros, 2007/2015).

The SourceTracker (Knights et al., 2011) plugin in QIIME 1.9.1 was used to predict if river samples were significant contributors of OTUs to offshore or nearshore sites. Default conditions of the program were used after filtering out OTUs that were present in less than 1% of samples. This method used relative proportion of genera present to estimate the probability that the river was a significant source of microbes into the lake.

Quantification of Indicator Bacteria

Water samples were analyzed for *E. coli* using the IDEXX Colilert-18 and Quanti-Tray 2000 method (IDEXX Laboratories, Westbrook, Maine), a defined substrate technology (Edberg et al., 1991). Generally, 100 ml of water was analyzed; excessively turbid samples were diluted as needed before analysis. Results are calculated as most probable number (MPN)/100 mL (Byappanahalli and Nevers, 2019).

Hydrometeorological Measurements

Ambient conditions were measured at the time of sample collection: water and air temperature (°C, H-B Instrument, Trappe, PA, United States), current speed (U.S. EPA, 2008) and direction (eastward, westward, float method), wind direction and speed (m/s, SKYTECH, Weatherhawk, Logan, UT, United States), wave height (inches, meter stick), rainfall (<24 h, <48, <72, and >72 prior to sample collection), and cloud cover (percent scale). Bird counts were recorded, as well as general beach conditions, including amount of debris, trash, and *Cladophora* algae. Water samples were analyzed for turbidity in the laboratory (2100N, Hach, Loveland, CO, United States) (Byappanahalli and Nevers, 2019).

Hydrologic data, including water temperature (°C), specific conductance (μs/cm), pH, DO (mg/L), and turbidity (FNU) at East Chicago, IN (Jeorse Park, 04092788) and Jackson Park, IL (63rd, 04092440) were extracted from the United States Geological Survey National Water Information System (2018) database for use in the analysis (United States Geological Survey, 2018).

In addition, at 63rd, hydrometeorological data were collected from a multi-parameter weather station (Vaisala WXT520) installed on a light post (30') at the beach and a data buoy (NexSens CB-100) installed in the swimming area (∼1.5 m depth). Data obtained from the weather station included measurements of wind direction and speed (m/s), air temperature (°C), rainfall (cm), solar radiation (LI-COR sensor; LI-200), relative humidity (%), and barometric pressure (mm/Hg).

Data obtained from the buoy included turbidity (NTU, FTS sensor, DTS-12), wave height (m) and wave period (seconds) (NexSens Accustage pressure transducer; OEM, Keller America), and water temperature (°C).

Statistical Analyses

Significant differences in beta diversity among communities were determined using 999 permutations of PERMANOVA (Anderson, 2001); then, PERMDISP (permutational analysis of multivariate dispersions) (Anderson, 2006) was used to ensure significant differences were not due to differences in dispersion. Differences in alpha diversity metrics were determined using non-parametric *t*-tests with 999 permutations. Additionally, potential biomarkers differentiating collection sites was determined using LEfSE (linear discriminate analysis effect size) (Segata et al., 2012). LEfSE is a three-step process in which non-parametric Krustal Wallis is performed to first identify taxa that differed significantly among sources, then for these taxa, pairwise Wilcoxon rank-sum test is performed and finally linear discriminant analysis (LDA) is used to estimate the effect size and biological consistency within groups being tested. Data output are taxa with LDA greater than 2.0 at any taxonomic level that is discriminating.

Correlations between genera and *E. coli* contamination levels were determined using Spearman's Rho. Associations among relative abundances of genera in each sample and all measured environmental factors (water temperature, air temperature, turbidity, dissolved oxygen, and *E. coli* MPN) as well as water source (river, river mouth, nearshore, or offshore) were determined using canonical correspondence analysis (CCA) (Ter Braak, 1986; Ter Braak and Verdonschot, 1995). Significantly different correlations were calculated using a Monte Carlo test with 999 permutations. Hydrometeorological data were sub-divided into: 1, low; 2, medium; 3, medium/high; and 4, high for analysis. This was accomplished using the visual binning method in SPSS version 23 (SPSS, 2014); cut points for binning were made using the ±1 SD option. All other statistics were performed using the Paleontological Statistics package version 3.01 (PAST software[1]) or software available in QIIME. Differences were considered significant if $p \leq 0.05$ with multiple comparisons using 999 permutations.

RESULTS AND DISCUSSION

One of the primary needs before initiating beach restoration for recreational use is to determine sources of fecal contamination in nearshore areas. Depending on the findings, remedial strategies can then be employed to reduce or mitigate those sources contributing to water quality; for instance, gull deterrence using trained dogs and physical modifying structures (e.g., breakwalls) to improve water circulation and dissipation of contaminants at shallow, embayed beaches are a few examples of management actions to restore water quality (Ge et al., 2012; Nevers et al., 2018).

[1]http://folk.uio.no/ohammer/past/index.html

The sampling locations for this study were specifically chosen because the shorelines had traditionally suffered from elevated levels of fecal indicator bacteria (*E. coli*) leading to frequent beach closures (Byappanahalli et al., 2015; Nevers et al., 2018). Specifically, the Grand Calumet River and associated shoreline is an area designated for intensive restoration efforts under a bi-national agreement between the United States and Canada (International Joint Commission, 2012). Nearshore water quality at Jeorse Park has steadily deteriorated between 2005 and until recently, as evidenced by increased *E. coli* levels exceeding the state recreational water quality standard for safe swimming (Byappanahalli et al., 2015; Nevers et al., 2018). Early efforts in source tracking have identified shorebirds and human fecal contamination at these beaches. Unknown are the relative inputs of point (river) and other non-point (shoreline) sources.

Illumina sequencing results produced an abundant number of reads for bacterial communities across the sites. The 63 water samples collected from seven locations on three dates produced a total of 5,136,926 paired-end reads after quality filtering and merging. There was an average of 81,538 ± 63,981 reads per sample, ranging from 7,050 to 396,284 reads. The sample with the lowest read (a river sample from the first sampling date) was excluded from community analyses, and the remaining 62 samples were rarified to 24,890 reads per sample, with a Goods coverage of 0.96 (±0.01 SD), ranging from 0.94 to 0.98.

Alpha Diversity Differences Among Sites

In terms of alpha diversity, rarefaction curves indicated Shannon diversity reached saturation in all samples (**Supplementary Figure S1A**) and was beginning to level off using other indices (e.g., phylogenetic diversity, PD whole tree **Supplementary Figure S1B**). The Shannon index, a measure of richness and evenness, was statistically higher for river mouth samples compared to the other sources (**Figure 2A**). Whereas, PD whole tree, which only accounts for species richness, indicated the phylogenetic diversity was statistically higher in lake nearshore samples compared to lake offshore, river and river mouth samples (**Figure 2B**). This could indicate more complex input sources to the nearshore community because of coastal processes likely mediated by (a) hydrometeorological events, previously seen for *E. coli* in nearshore waters (Ge et al., 2012), (b) exchanges between shoreline sources, and (c) interactions between nearshore and offshore communities.

Beta Diversity Differences Among Sites and Dates

Beta diversity analysis of the 16S rRNA gene sequences indicated that the bacterial community in the Grand Calumet River was the least similar to the communities along the shoreline or offshore. The PCoA plots of beta diversity distances among samples from the four water sources illustrate that the main separation was between the river samples and all other sources (**Figure 3A**). The first three axes of Bray Curtis distances accounted for ∼74% of the variation with the river samples separated from the other sources along the first axis (PCoA 1 = 54.5%). This difference was statistically significant based on

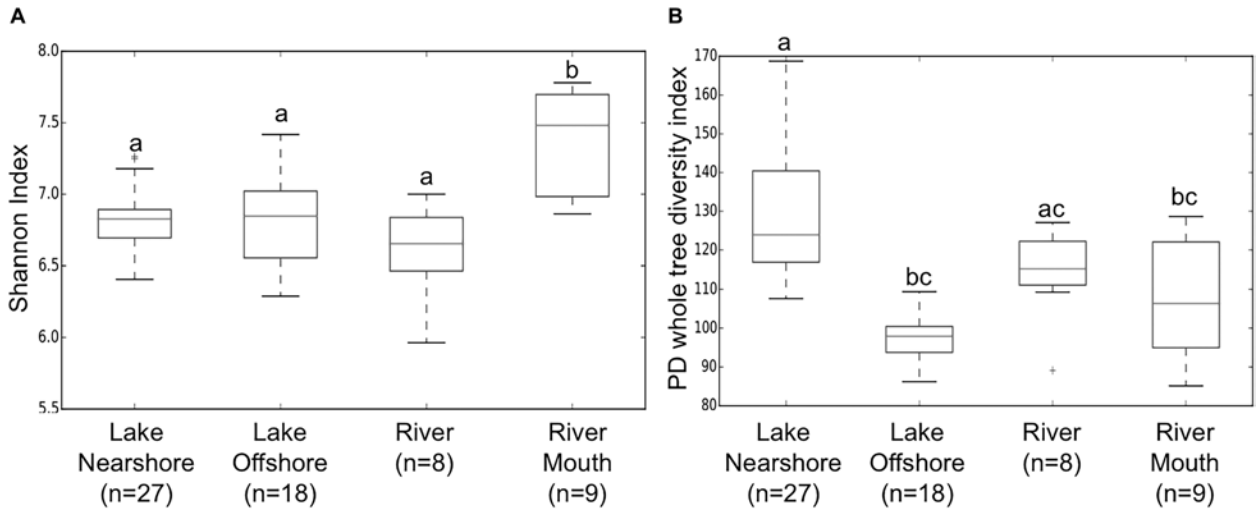

FIGURE 2 | Boxplots of means and SD (standard deviations) of within sample (alpha) diversity indices **(A)** Shannon (richness and evenness) and **(B)** PD whole tree (Faith's Diversity, phylogenetic richness) of samples from different water sources. Non-parametric two sample *t*-test with 999 permutations with significant differences $p < 0.02$ illustrated by different letters above bars.

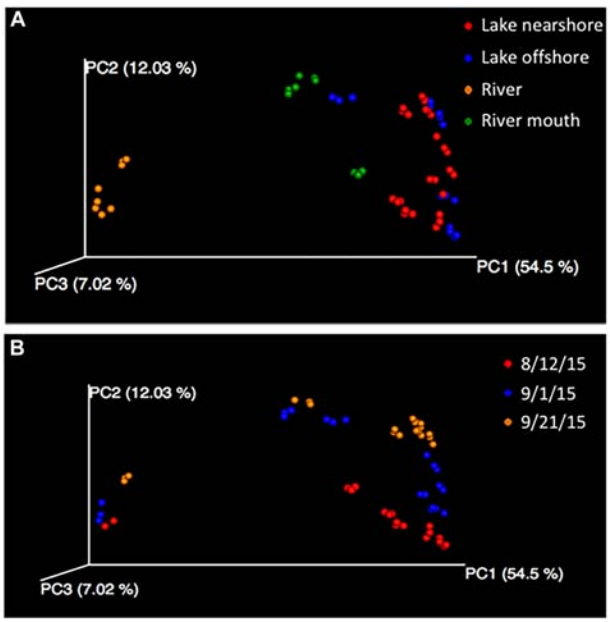

FIGURE 3 | Principal coordinate analysis (PCoA) of Bray Curtis dissimilarity metrics of samples labeled according to the **(A)** water sources and by **(B)** sampling date. Differences among microbial communities are significant, PERMANOVA and ANOSIM $P = 0.001$ and meets the assumption of dispersion homogeneity because PERMDISP is not significant.

PERMANOVA ($P = 0.001$) and ANOSIM ($R = 0.598$, $P = 0.001$) and not significant due to dispersion (PERMDISP $P = 0.41$). If the samples were differentiated into the seven sampling locations, the differences remained significant. Using distances based on phylogenetic relationship of community members (weighted and unweighted Unifrac) yielded similar statistically significant results (data not shown). Similarity between samples collected at the mouth of the river and offshore samples indicates that perhaps river flow is minimal, with an extensive mixing zone in the river mouth. This suggests that during the three sampling periods between August and September 2015, bacterial contribution from the river to the lake was minimal. These findings support previous research that much of the Jeorse Park (JP) nearshore microbial contamination, which has led to recreational beach closures, is from local, non-point sources (e.g., birds, *Cladophora* algae) with few anthropogenic contributions (e.g., combined sewer outflows) from the river (Byappanahalli et al., 2015; Nevers et al., 2018). This indicates that mitigation strategies for this shoreline will likely differ from those initiated for other riverine habitats in the Grand Calumet River corridor.

The date of sampling was also significantly different ($P = 0.001$) although community differences were less pronounced than between water types (**Figure 3**). Factors that differed by sampling dates were rain events, temperature and dissolved oxygen (**Supplementary Table S5**). While collection dates targeted one rain event (9/21) to compare it to two dry weather events, there was no difference in collection dates that could be attributed to rain rather than the other factors that differed among the three dates. Interestingly, combined sewer overflow was recorded at the Hammond Sanitary District on 9/21[2], but the volume of water released was likely insufficient to impact the shoreline microbial communities. The similarity of community composition in the river between sampling dates and dissimilarity with the shoreline communities may result from a combination of frequent combined sewage overflows and low river flow, respectively.

[2]http://www.hammondsd.com/cso-discharge-activity-maps/

Microbial Taxa Represented

There were 50 phyla (**Supplementary Table S1**) represented in the 16S rRNA gene sequences, and >90% of the relative abundance could be attributed to three phyla: Proteobacteria (45.6 ± 5.9%), Actinobacteria (26.8 ± 8.9%), and Bacteroidetes (22.8 ± 6.1%) (mean ± SD). These findings are consistent with other studies suggesting the dominance of these three phyla in freshwater systems (Newton et al., 2011; Mou et al., 2013). Among the remaining phyla, those representing >0.1% included the Chloroflexi (0.9 ± 0.9%), Cyanobacteria (1.5 ± 1.3%), Firmicutes (0.3 ± 0.3%), and Verrucomicrobia (0.7 ± 0.6%); 0.9 ± 0.4% was not assigned to a phylum. Of the remaining phyla, 25 represent currently tentative phyla likely lacking in cultivated isolates needed for classification. Dominance of a few taxa was found at all taxonomic levels of classification. For example, there was a total of 786 genera assignments, of which 23 (∼3% of total genera) had a mean relative proportion >1% (mean of all samples) and accounted for 85.6 ± 4.0% of the community. The majority, 505 (64%), could not be assigned to a genus or is currently listed as a candidate genus.

One of the major advantages of using targeted metagenomic techniques, such as the 16S rRNA gene sequencing, is that they are culture-independent and can theoretically recover almost all bacterial taxa in any habitat. However, despite rapid advancements in this area, most bacterial species in communities remain to be identified (Locey and Lennon, 2016). A general lack of cultured organisms with sequencing information (in NCBI and other databases) essentially limits taxonomic identification from the sequenced data.

Taxa Differences Among Sites

Venn diagrams illustrate the total number of genera shared among samples as well as the percentage of the total number of genera. About one third (284 genera, 36.1%) of the total genera identified were common to all samples (**Figure 4A**). They represent an average of more than 60% of the relative proportion of genera in these samples. Shared genera, such as Actinobacteria ACK-M1, likely represent those common to aquatic ecosystems (Newton et al., 2011; Mou et al., 2013). Only an additional 1.3% more genera were common to the river and river mouth samples only (**Figure 4A**), indicating there are very few unique genera from the river flowing into the lake microbial community, perhaps because of low river flow and minimal mixing. The combined nearshore sites had the greatest number of unique genera (19.1%). A comparison of the number of genera common among the river and individual nearshore sampling sites (**Figure 4B**), and river and offshore sites (**Figure 4C**) showed 41.4 and 41.2%, respectively, were shared. The nearshore sites had unique genera ranging from 2.6 to 10.1%. This could be the result of high variation among the nearshore collection sites: 63rd (an urban beach) is located much further north of the other two sites, and JP and WH are situated on opposite sides of a large constructed industrial peninsula. There are likely different sources of microbial communities, potentially arising from beach sand (Solo-Gabriele et al., 2016; Staley and Sadowsky, 2016) and the nuisance shoreline alga *Cladophora* (Zulkifly et al., 2012; Whitman et al., 2014a; Chun et al., 2017), and the relative locations of 63rd and JP further isolates exchange along the shoreline (Ge et al., 2012; Byappanahalli et al., 2015).

Potential for Grand Calumet River to Contribute to Nearshore Microbial Communities

Since the Venn diagrams only illustrated the presence and absence of genera at each study site, additional analysis was conducted using SourceTracker that accounts for the relative proportions of each OTU. SourceTracker estimated that the highest possible contributions of river water to the river mouth, offshore, and nearshore (combined) (**Table 1**) or nearshore sites, 63rd, WH, JP (individually) (**Table 1**) were on the first sampling date (8/12/15). Krustal Wallis test indicated that there was an overall significant difference ($p < 0.002$) in contributions from the river; however, pairwise comparisons only showed that nearshore was significantly different from river mouth and offshore. Analysis specifically of the river to nearshore sites indicated significantly higher contribution to 63rd on 8/12/15; alternately, 63rd and WH had significantly lower contribution than JP on 9/1/15 (**Table 1**).

The program LEfSE was used to identify the taxa that differed among the different sampling sites and to determine if any of these genera were potentially pathogens or indicators of potential fecal contamination. LEfSE analysis identified significant differences in taxa among sample sources (river, nearshore and offshore) at all levels of taxonomic classification, and also in comparisons of sampling sites and sampling dates. Comparisons of sample sources (river, nearshore and offshore) indicated there were 233 taxa with LDA effect sizes greater than 2.0 (**Supplementary Table S2**). The most taxa differences were in the river samples (96 taxa) followed by river mouth (63 taxa), nearshore (55 taxa) and offshore (42 taxa). Examination of taxa with LDA effect sizes greater than 4.0 at the lowest level of classification showed that most belonged to taxa yet to be classified (**Figure 5A**). Taxa that could be classified to the genus level were *Flavobacterium, Polynucleobacter*, and *Fluviicola* in the river samples and various unclassified taxa in the other water sources (**Figure 5A**); *Polynucleobacter* has been shown to be widespread in streams associated with human/anthropogenic activities (Hosen et al., 2017).

When the sources were split into specific sites there were 313 taxa with LDA effect sizes greater than 2.0 (**Supplementary Table S3**). The most taxa differences were in the river samples (84 taxa) followed by the JP nearshore site (76 taxa), river mouth (63 taxa), then nearshore site 63 (36 taxa), offshore site GCE (34 taxa), GCN (12 taxa) and the nearshore site WH (9 taxa). In this comparison there were no taxa identified that are considered indicators of fecal contamination, therefore the data was reanalyzed to include only the nearshore samples. A comparison focusing on just the nearshore sites including GCM (river mouth) indicates GCM has more taxa that differ significantly with LDA effect sizes greater than 3.0 at the lowest level of classification (**Figure 5B**; taxa LDA >2.0 **Supplementary Table S4**). Most of the differing taxa in GCM samples belonged to

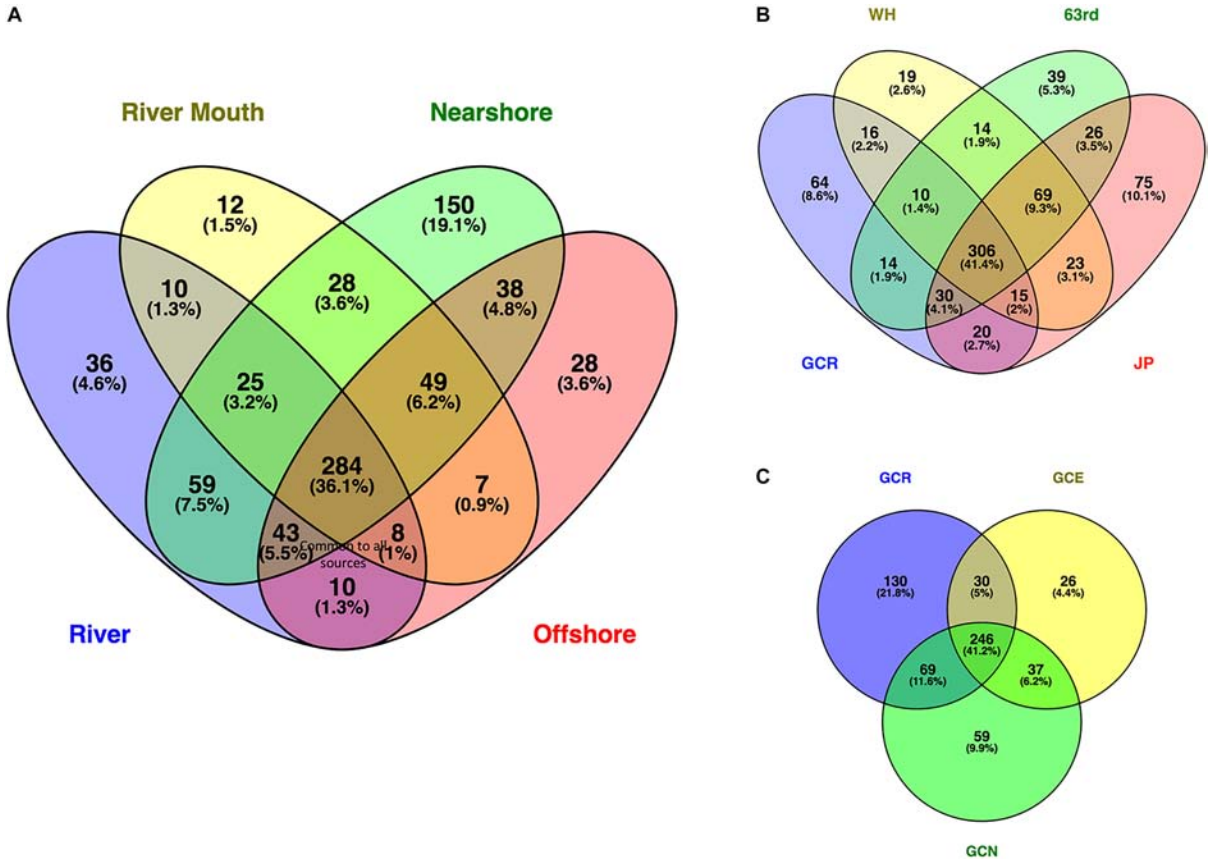

FIGURE 4 | Venn diagram illustrating shared and unique genera among **(A)** water sources, **(B)** river and nearshore sites, and **(C)** river, river mouth, and lake offshore sites. Sampling sites in **(A,B)** represented by nearshore locations Jeorse Park (JP), Whihala beach (WH), and 63rd Street Beach (63) in Chicago, Grand Calumet River (GCR), mouth of the river (GCM), offshore sites north (GCN) and east (GCE). Calculations and illustrations were determined using the Venny program (Oliveros, 2007–2015).

TABLE 1 | Estimation of Grand Calumet River as a potential source† of bacterial populations (mean percentages ± standard error of mean) on three sampling dates for (A) Lake communities as sink‡, or (B) Specific nearshore communities as sink§.

	A			B		
Date	**River mouth**	**Lake nearshore**	**Lake offshore**	**JP**	**WH**	**63**
8/12/15	83.7 ± 0.4%^{ab}	81.1 ± 1.1%^{a}	76.2 ± 0.9%^{ab}	79.6 ± 1.5%^{ab}	79.9 ± 2.2%^{ab}	84.0 ± 1.0%^{a}
9/1/15	80.7 ± 0.4%^{ab}	71.9 ± 0.8%^{b}	73.5 ± 2.1%^{ab}	74.2 ± 0.9%^{ab}	69.4 ± 1.1%^{b}	72.0 ± 0.6%^{b}
9/21/15	79.3 ± 0.3%^{b}	78.7 ± 0.7%^{a}	76.0 ± 0.8%^{ab}	77.1 ± 0.3%^{ab}	77.4 ± 0.3%^{ab}	81.6 ± 0.4%^{ab}

†*Source contribution estimated using SourceTracker (Knights et al., 2011) plugin in QIIME 1.9.1 (Caporaso et al., 2010) using default conditions.* ‡*Sinks are river mouth, nearshore, and offshore samples a (n = 3, 9, 6 per sampling date, respectively), Krustal Wallis (P = 0.00003).* §*Sinks are three nearshore beaches: Jeorse Park (JP), Whihala (WH), and 63rd Street (63) in Chicago, Krustal Wallis (P = 0.004). Different superscripts letters in the tables indicate significant difference of pairwise comparisons by date using Dunn's post hoc test with Bonferroni correction.*

the phylum Proteobacteria whereas in the JP samples they were mainly in the Bacteroidetes and a mixture of Proteobacteria and Actinobacteria in the site 63rd and WH samples. Bacteroidetes are a common phylum in fecal samples but since the taxa that differed are not classified to the genus level it is not possible to speculate if they are feces associated. However, at LDA 2.0 unclassified Enterobacteriaceae are significant in the JP sample (**Supplementary Table S4**). This group associated with fecal contamination. Of the nearshore site JP had the highest frequency of elevated *E. coli* MPN values (**Supplementary Table S5**). This indicates that targeted metagenomic analysis can provide additional data of fecal contamination.

Microbial Community and *E. coli*

Although the incidences of elevated *E. coli* MPN values were limited, correlation analysis indicated that there were positive correlations with other biomarkers and bacterial genera commonly reported from fecal samples. There were

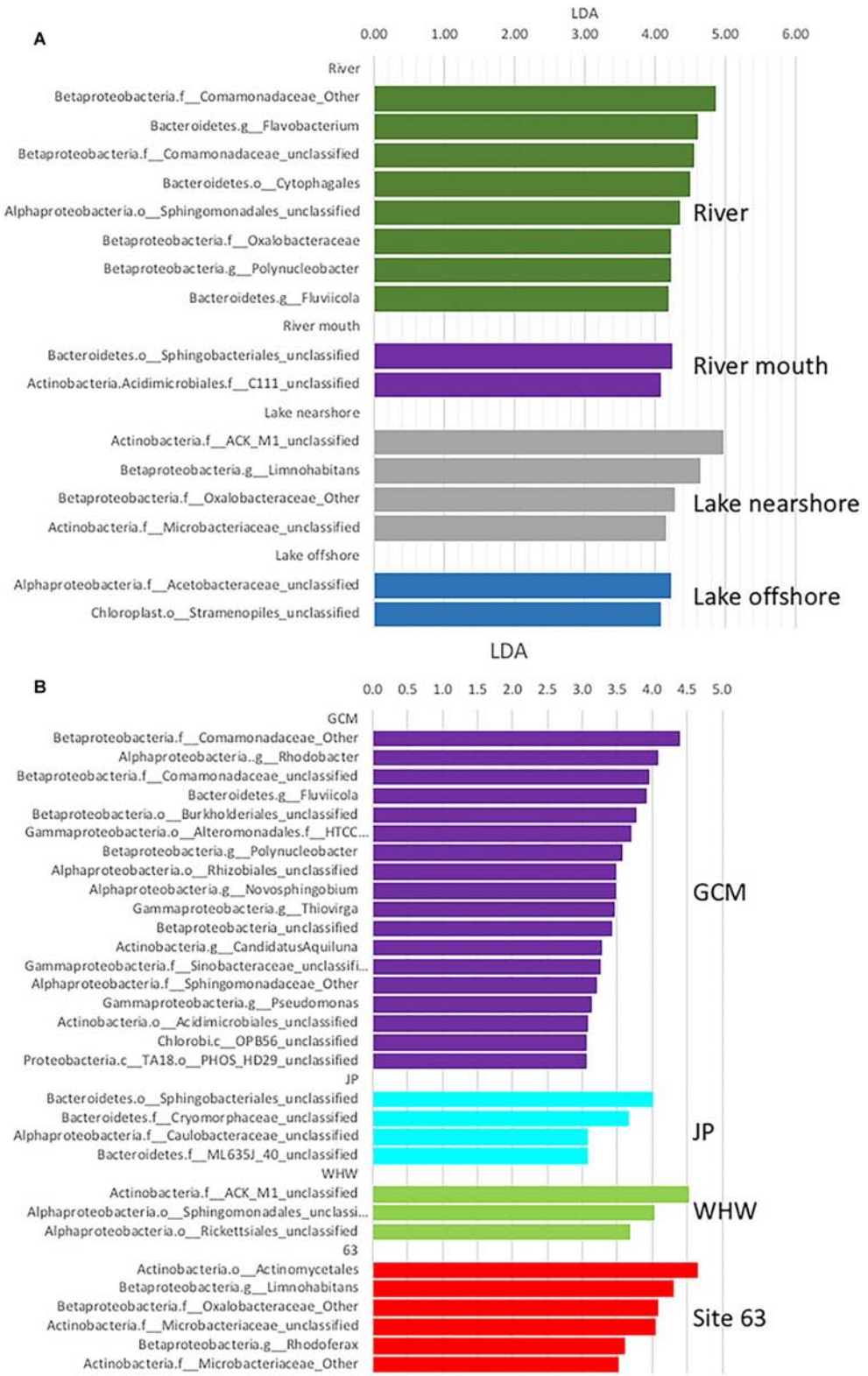

FIGURE 5 | Linear Discriminate Analysis Effect Size (LEfSE) analysis of microbial communities from the various **(A)** water sources and **(B)** nearshore collection sites and river mouth. Only taxa that differed significantly ($p < 0.05$) with LDA effect sizes greater than 4.0 in **(A)** and 3.0 in **(B)** are illustrated in the histograms. Taxa names include phylum followed by lowest taxonomic assignment available. Nearshore beaches include Jeorse Park (JP), Whihala (WH), and 63rd Street (63) in Chicago, and mouth of the Calumet River (GCM).

few samples that had elevated *E. coli* (>235 CFU/MPN per 100 ml) that would lead to closures of recreational waters (**Supplementary Table S5**; U.S. EPA, 2012). Spearman Rho analysis of bacterial taxa relative abundances and *E. coli* MPN (sorted into bins) indicated there were 52 genera with significant positive correlations and 1 negative correlation (**Supplementary Table S6**). Notable is the positive correlation with several genera in the phylum Firmicutes that are associated with fecal contamination, *Enterococcus*, *Blautia*, *Faecalibacterium*, *Clostridium*, *Collinsella*, and *Selenomonas* as well as *Bacteroides* from the phylum Bacteroidetes.

Enterococcus (Wheeler et al., 2002) and *Bacteroides* (Bernhard and Field, 2000) are often used as fecal indicator species, and more recently, *Blautia* (Koskey et al., 2014; Eren et al., 2015) and *Dialister* (Jeong et al., 2011) have also been proposed as indicator species. A species within *Clostridium* (*C. perfringens*) has been suggested as a reliable indicator of water quality in tropical areas (Fujioka and Shizumura, 1985; Fujioka et al., 1997), where traditional indicators such as *E. coli*, and enterococci, are commonly found in the environment (Byappanahalli and Ishii, 2011). *Collinsella*, *Blautia*, and *Faecalibacterium*, are examples of commonly found members of gut microbiomes that correlated with *E. coli* MPNs. With the availability of high throughput sequencing technology, others have suggested that community analysis may be an additional means to assess water quality and can be applied to microbial source tracking (Newton et al., 2013; Henry et al., 2016).

The influence of physical conditions on overall microbial community was also examined (**Figure 6**) using CCA. Factors corresponding to the differences in the bacterial communities were water type (river water being most distant from lake) along the first axis explaining 64.3% of the variation; sampling time, water temperatures and dissolved oxygen along the second axis (14.3%) (**Figure 6A**); and *E. coli* MPN and turbidity along the third and fourth axes (**Figure 6B**) (100 permutations, $p < 0.01$). The influence of water type describing the microbial community is like the finding of beta diversity analysis due to differences of the river community to the other water types (**Figure 3A**). A secondary factor was the difference in communities with sampling time (**Figure 3B**) that was shown by CCA to be influenced by increasing dissolved oxygen and decreasing water temperatures (**Figures 6A,B**). The *E. coli* MPN corresponded to the three river samples collected on the third sampling date after rainfall (**Figure 6B**). This suggests that both shoreline sources (e.g., gulls, runoff, nearshore sand-water interactions) and large-scale processes (e.g., waves, currents, lake turnover), as well as time of year, are likely to influence changes in community along the shoreline. The relative impact of these factors could have inter-annual variation. Integration of physical modeling and multiple years of data could help resolve some of these interactions.

Implications for Mitigation Strategies

After the recognition that aquatic systems have become degraded, it is essential to develop strategies to restore compromised ecosystems through appropriate remedial actions and in many instances, those actions tend to be site-specific. For instance, at the study locations, nonpoint sources of microbial contamination by shoreline birds (gulls), has been previously identified as a major contributing factor using microbial source tracking and gull deterrence activities have significantly improved shoreline water quality in recent years (Nevers et al., 2018). Similarly, the periodic presence of the human marker *Bacteroides* HF183 (Byappanahalli et al., 2015) has been a cause of concern for the potential significant human health threat; previously, the Grand Calumet River was the presumptive source of any human contamination. Results presented here, however, indicate that the river, even following a rain event, was likely not impacting shoreline bacterial communities. There may, therefore,

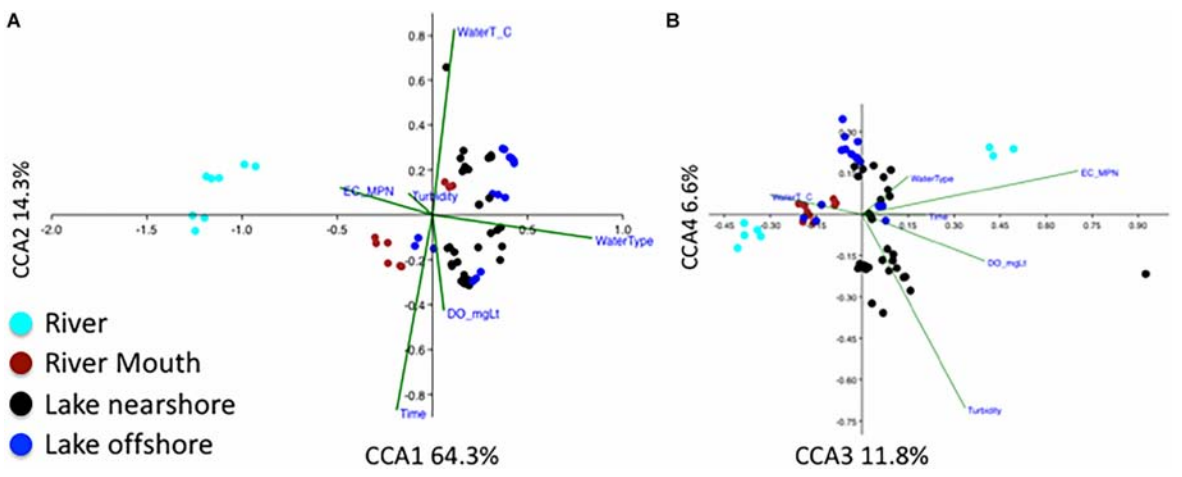

FIGURE 6 | Canonical correspondence analysis (CCA) of relative abundance of bacterial genera, water type (river, river mouth, nearshore, and offshore), *Escherichia coli* most probable number (ECMPN), and the environmental variables water temperature (WaterT_C), water turbidity (Turbidity_FNU), dissolved oxygen in mgL^{-1} (DOmgLt) and sampling date (time). **(A)** CCA1 and 2 explain 64.3 and 14.4% and **(B)** CCA3 and CCA4 explain 11.8 and 6.6% of the total constrained variation, respectively. Number of samples $n = 63$, overall $P = 0.001$.

be additional sources of human contamination currently unknown impacting these shoreline locations. At Jeorse Park and 63rd, the shoreline configuration has also been identified as contributing to the persistence of bacterial contamination due to the tendency toward accumulation and the decrease in circulation (Ge et al., 2012; Byappanahalli et al., 2015). Because the river is not the major exogenous source of microbes into the nearshore lake sites, efforts to curtail river flow toward recreational beach areas would not be a sufficient means to decrease beach closures. Efforts toward identifying and mitigating shoreline or nonpoint sources, such as decreasing gull presence (Nevers et al., 2018) and reducing other contributions (e.g., shoreline algae Whitman et al., 2014b), would likely have a greater impact on eliminating beach closures. By incorporating emerging technologies, such as the microbiome, into water quality monitoring programs will be helpful to study long-term changes and underlaying factors that influence these changes which are difficult to elucidate with traditional monitoring programs.

To summarize using a targeted 16S rRNA gene sequencing approach to analyze aquatic microbial communities demonstrated it is possible (1) to identify sources of contamination using a consortium of microbes as an index of pollutant sources rather than using one or two traditional indicators (e.g., *E. coli*, enterococci) often used in monitoring programs. Using this approach, we were able to show that the Grand Calumet River had minimal influence on shoreline water quality at the study sites, indicating that the sources contributing to high *E. coli* levels (e.g., at JP, WH) were more likely internal (e.g., shoreline birds, sand, *Cladophora*) with an intermittent contamination from GCR. (2) The data gathered from this research will be useful to management agencies, such as U.S. EPA and Indiana Department of Environmental Management, for addressing water quality restoration efforts currently under implementation at the study locations. An example will be delisting shorelines as impaired for beneficial use such as recreation. This can begin the process to modify acceptable approaches by government agencies to identify microbially contaminated locations to implement effective mitigation.

AUTHOR CONTRIBUTIONS

All authors wrote and approved the final version of the manuscript. MN and MB conceived the project. MB, MN, and CN performed the sample designing, contributed to methodology, and wrote the manuscript. CN analyzed the data.

FUNDING

Funding was provided to the USGS through the Great Lakes Restoration Initiative and USGS agreement G15AC00427, and to Purdue University from the USDA National Institute of Food and Agriculture Hatch grant IND010825.

ACKNOWLEDGMENTS

We thank P. Ryan Jackson, Kasia Kelly, Dawn Shively, Ashley Spoljaric, and Paul Buszka, USGS and Stephanie Grebinoski, Purdue University for the collection of samples and for help during sample processing. The Purdue Genomics Core Facility at Purdue University performed sequencing and the Purdue Bioinformatics Core kindly provided servers to run the bioinformatics analyses.

SUPPLEMENTARY MATERIAL

The Supplementary Material for this article can be found online at: https://www.frontiersin.org/articles/10.3389/fmicb.2019.00996/full#supplementary-material

FIGURE S1 | Rarefaction curves of alpha diversity measures **(A)** Shannon Diversity and **(B)** PD whole tree (Faith's Phylogenetic Diversity). Each line represents a single sample.

TABLE S1 | Relative proportion of phyla represented in Lake Michigan water sample.

TABLE S2 | LEfSe results of a comparison of different Lake Michigan water sources, taxa at all levels with LDA > 2.0 are listed.

TABLE S3 | LEfSe results of a comparison of Lake Michigan sampling sites, taxa at all levels with LDA > 2.0 are listed GCR.

TABLE S4 | LEfSe results of a comparison of only the nearshore Lake Michigan sampling sites, taxa at all levels with LDA > 2.0 are listed.

TABLE S5 | Environmental conditions and *E. coli* most probable numbers (MPN) in triplicate samples from each sampling location on three collection dates.

TABLE S6 | Significant Spearman rho correlations *E. coli* most probable numbers (MPN) binned and relative abundances of bacteria at genus level.

REFERENCES

Anderson, M. J. (2001). A new method for non-parametric multivariate analysis of variance. *Austral Ecol.* 26, 32–46. doi: 10.1111/j.1442-9993.2001.01070.pp.x

Anderson, M. J. (2006). Distance-based tests for homogeneity of multivariate dispersions. *Biometrics* 62, 245–253. doi: 10.1111/j.1541-0420.2005.00440.x

Bernhard, A. E., and Field, K. G. (2000). A PCR assay to discriminate human and ruminant feces on the basis of host differences in *Bacteroides*-Prevotella genes encoding 16S rRNA. *Appl. Environ. Microbiol.* 66, 4571–4574. doi: 10.1128/aem.66.10.4571-4574.2000

Byappanahalli, M. N., and Ishii, S. (2011). "Environmental sources of fecal bacteria," in *Fecal Bacteria*, eds M. J. Sadowsky and R. L. Whitman (Washington, DC: ASM Press), 93–110. doi: 10.1128/9781555816865.ch5

Byappanahalli, M. N., and Nevers, M. B. (2019). *16S rRNA Gene Sequencing and E. coli for Shorelines and the Grand Calumet River, Indiana, 2015*. Reston: U.S. Geological Survey Data Release. doi: 10.5066/P92JWFUR

Byappanahalli, M. N., Nevers, M. B., Whitman, R. L., Ge, Z., Shively, D., Spoljaric, A., et al. (2015). Wildlife, urban inputs, and landscape configuration are responsible for degraded swimming water quality at an embayed beach. *J. Great Lakes Res.* 41, 156–163. doi: 10.1016/j.jglr.2014.11.027

Caporaso, J. G., Kuczynski, J., Stombaugh, J., Bittinger, K., Bushman, F. D., Costello, E. K., et al. (2010). QIIME allows analysis of high-throughput community sequencing data. *Nat. Methods* 7, 335–336.

Chun, C. L., Peller, J. R., Shively, D., Byappanahalli, M. N., Whitman, R. L., Staley, C., et al. (2017). Virulence and biodegradation potential of dynamic microbial

communities associated with decaying Cladophora in Great Lakes. *Sci. Total Environ.* 574, 872–880. doi: 10.1016/j.scitotenv.2016.09.107

Cloutier, D. D., Alm, E. W., and Mclellan, S. L. (2015). Influence of land use, nutrients, and geography on microbial communities and fecal indicator abundance at Lake Michigan beaches. *Appl. Environ. Microbiol.* 81, 4904–4913. doi: 10.1128/AEM.00233-15

Edberg, S. C., Allen, M. J., and Smith, D. B. (1991). Defined substrate technology method for rapid and specific simultaneous enumeration of total coliforms and *Escherichia coli* from water: collaborative study. *J. Assoc. Off. Anal. Chem.* 74, 526–529.

Edgar, R. C. (2010). Search and clustering orders of magnitude faster than BLAST. *Bioinformatics* 26, 2460–2461. doi: 10.1093/bioinformatics/btq461

Eren, A. M., Sogin, M. L., Morrison, H. G., Vineis, J. H., Fisher, J. C., Newton, R. J., et al. (2015). A single genus in the gut microbiome reflects host preference and specificity. *ISME J.* 9, 90–100. doi: 10.1038/ismej.2014.97

Field, K. G., and Samadpour, M. (2007). Fecal source tracking, the indicator paradigm, and managing water quality. *Water Res.* 41, 3517–3538.

Fujioka, R. S., Roll, B., and Byappanahalli, M. N. (1997). "Appropriate recreational water quality standards for Hawaii and other tropical regions based on concentrations of *Clostridium perfringens*," in *Proceedings of the Water Environment Federation 70th Annual Conference and Exposition*, Chicago, 405–411.

Fujioka, R. S., and Shizumura, L. K. (1985). *Clostridium perfingens*, a reliable indicator of stream water quality. *J. Water Pollut. Control Fed.* 57, 986–992.

Ge, Z., Whitman, R. L., Nevers, M. B., Phanikumar, M. S., and Byappanahalli, M. N. (2012). Nearshore hydrodynamics as loading and forcing factors for *Escherichia coli* contamination at an embayed beach. *Limnol. Oceanogr.* 57, 362–381.

Gloor, G. B., Hummelen, R., Macklaim, J. M., Dickson, R. J., Fernandes, A. D., Macphee, R., et al. (2010). Microbiome profiling by Illumina sequencing of combinatorial sequence-tagged PCR products. *PLoS One* 5:e15406. doi: 10.1371/journal.pone.0015406

Great Lakes Interagency Task Force (2016). *Great Lakes Restoration Imitative: Report to Congress and the President*. Washington, D.C: Environmental Protection Agency.

Halliday, E., Mclellan, S. L., Amaral-Zettler, L. A., Sogin, M. L., and Gast, R. J. (2014). Comparison of bacterial communities in sands and water at beaches with bacterial water quality violations. *PLoS One* 9:e90815. doi: 10.1371/journal.pone.0090815

Harwood, V. J., Staley, C., Badgley, B. D., Borges, K., and Korajkic, A. (2014). Microbial source tracking markers for detection of fecal contamination in environmental waters: relationships between pathogens and human health outcomes. *FEMS Microbiol. Rev.* 38, 1–40. doi: 10.1111/1574-6976.12031

Henry, R., Schang, C., Coutts, S., Kolotelo, P., Prosser, T., Crosbie, N., et al. (2016). Into the deep: evaluation of source tracker for assessment of faecal contamination of coastal waters. *Water Res.* 93, 242–253. doi: 10.1016/j.watres.2016.02.029

Hosen, J. D., Febria, C. M., Crump, B. C., and Palmer, M. A. (2017). Watershed urbanization linked to differences in stream bacterial community composition. *Front. Microbiol.* 8:1452. doi: 10.3389/fmicb.2017.01452

International Joint Commission (2012). *The Great Lakes Water Quality Agreement*. Available at: https://binational.net/2012/09/05/2012-glwqa-aqegl/

Jeong, J. Y., Park, H. D., Lee, K. H., Weon, H. Y., and Ka, J. O. (2011). Microbial community analysis and identification of alternative host-specific fecal indicators in fecal and river water samples using pyrosequencing. *J. Microbiol.* 49, 585–594. doi: 10.1007/s12275-011-0530-6

Knights, D., Kuczynski, J., Charlson, E. S., Zaneveld, J., Mozer, M. C., Collman, R. G., et al. (2011). Bayesian community-wide culture-independent microbial source tracking. *Nat. Methods* 8, 761–793. doi: 10.1038/nmeth.1650

Konopka, A., Bercot, T., and Nakatsu, C. (1999). Bacterioplankton community diversity in a series of thermally stratified lakes. *Microb. Ecol.* 38, 126–135.

Koskey, A. M., Fisher, J. C., Eren, A. M., Ponce-Terashima, R., Reis, M. G., Blanton, R. E., et al. (2014). Blautia and Prevotella sequences distinguish human and animal fecal pollution in Brazil surface waters. *Environ. Microbiol. Rep.* 6, 696–704. doi: 10.1111/1758-2229.12189

Liu, Z. Z., Desantis, T. Z., Andersen, G. L., and Knight, R. (2008). Accurate taxonomy assignments from 16S rRNA sequences produced by highly parallel pyrosequencers. *Nucleic Acids Res.* 36:e120. doi: 10.1093/nar/gkn491

Locey, K. J., and Lennon, J. T. (2016). Scaling laws predict global microbial diversity. *Proc. Natl. Acad. Sci. U.S.A.* 113, 5970–5975. doi: 10.1073/pnas.1521291113

Lozupone, C., Lladser, M. E., Knights, D., Stombaugh, J., and Knight, R. (2011). UniFrac: an effective distance metric for microbial community comparison. *ISME J.* 5, 169–172.

Masella, A. P., Bartram, A. K., Truszkowski, J. M., Brown, D. G., and Neufeld, J. D. (2012). PANDAseq: PAired-eND Assembler for Illumina sequences. *BMC Bioinform.* 13:31.

McDonald, D., Price, M. N., Goodrich, J., Nawrocki, E. P., Desantis, T. Z., Probst, A., et al. (2012). An improved greengenes taxonomy with explicit ranks for ecological and evolutionary analyses of bacteria and archaea. *ISME J.* 6, 610–618. doi: 10.1038/ismej.2011.139

Mou, X., Jacob, J., Lu, X., Robbins, S., Sun, S., and Ortiz, J. D. (2013). Diversity and distribution of free-living and particle-associated bacterioplankton in Sandusky Bay and adjacent waters of Lake Erie Western Basin. *J. Great Lakes Res.* 39, 352–357.

Nakatsu, C. H. (2007). Soil microbial community analysis using denaturing gradient gel electrophoresis. *Soil Sci. Soc. Am. J.* 71, 562–571.

Nevers, M. B., Byappanahalli, M. N., Edge, T. A., and Whitman, R. L. (2014). Beach science in the great lakes. *J. Great Lakes Res.* 40, 1–14. doi: 10.1016/j.jglr.2013.12.011

Nevers, M. B., Byappanahalli, M. N., Shively, D., Buszka, P. M., Jackson, P. R., and Phanikumar, M. S. (2018). Identifying and eliminating sources of recreational water quality degradation along an urban coast. *J. Environ. Qual.* 47, 1042–1050. doi: 10.2134/jeq2017.11.0461

Newton, R. J., Bootsma, M. J., Morrison, H. G., Sogin, M. L., and Mclellan, S. L. (2013). A microbial signature approach to identify fecal pollution in the waters off an urbanized coast of Lake Michigan. *Microb. Ecol.* 65, 1011–1023. doi: 10.1007/s00248-013-0200-9

Newton, R. J., Jones, S. E., Eiler, A., Mcmahon, K. D., and Bertilsson, S. (2011). A guide to the natural history of freshwater lake bacteria. *Microbiol. Mol. Biol. Rev.* 75, 14–49. doi: 10.1128/MMBR.00028-10

Newton, R. J., Mclellan, S. L., Dila, D. K., Vineis, J. H., Morrison, H. G., Eren, A. M., et al. (2015). Sewage reflects the microbiomes of human populations. *mBio* 6, e2574–e2514. doi: 10.1128/mBio.02574-14

Nossa, C. W., Oberdorf, W. E., Yang, L. Y., Aas, J. A., Paster, B. J., Desantis, T. Z., et al. (2010). Design of 16S rRNA gene primers for 454 pyrosequencing of the human foregut microbiome. *World J. Gastroenterol.* 16, 4135–4144.

Oliveros, J. C. (2007/2015). *Venny. An Interactive Tool for Comparing Lists With Venn's Diagrams*. Available at: http://bioinfogp.cnb.csic.es/tools/venny/index.html (accessed April 03, 2019).

Rideout, J. R., He, Y., Navas-Molina, J. A., Walters, W. A., Ursell, L. K., Gibbons, S. M., et al. (2014). Subsampled open-reference clustering creates consistent, comprehensive OTU definitions and scales to billions of sequences. *PeerJ* 2:e545. doi: 10.7717/peerj.545

Segata, N., Waldron, L., Ballarini, A., Narasimhan, V., Jousson, O., and Huttenhower, C. (2012). Metagenomic microbial community profiling using unique clade-specific marker genes. *Nat. Methods* 9, 811–814. doi: 10.1038/nmeth.2066

Solo-Gabriele, H. M., Harwood, V. J., Kay, D., Fujioka, R. S., Sadowsky, M. J., Whitman, R. L., et al. (2016). Beach sand and the potential for infectious disease transmission: observations and recommendations. *J. Marine Biolog. Assoc. U.K.* 96, 101–120.

SPSS (2014). *SPSS, Version 23*. Armonk, NY: IBM Corp., SPSS Inc.

Staley, C., and Sadowsky, M. J. (2016). Regional similarities and consistent patterns of local variation in beach sand bacterial communities throughout the Northern Hemisphere. *Appl. Environ. Microbiol.* 82, 2751–2762. doi: 10.1128/AEM.00247-16

Steinman, A. D., Cardinale, B. J., Munns, W. R., Ogdahl, M. E., Allan, J. D., Angadi, T., et al. (2017). Ecosystem services in the Great Lakes. *J Great Lakes Res.* 43, 161–168.

Tanaka, T., Kawasaki, K., Daimon, S., Kitagawa, W., Yamamoto, K., Tamaki, H., et al. (2014). A hidden pitfall in the preparation of agar media undermines microorganism cultivability. *Appl. Environ. Microbiol.* 80, 7659–7666. doi: 10.1128/AEM.02741-14

Ter Braak, C. J. F. (1986). Canonical correspondence analysis - A new eigenvector technique for multivariate direct gradient analysis. *Ecology* 67, 1167–1179.

Ter Braak, C. J. F., and Verdonschot, P. F. M. (1995). Canonical correspondence analysis and related multivariate methods in aquatic ecology. *Aquat. Sci.* 57, 255–289.

U. S. EPA (1986). *Ambient Water Quality Criteria*. Washington, D. C: U.S. Environmental Protection Agency. Available at: http://www.epa.gov/waterscience/beaches/1986crit.pdf

U.S. EPA (2008). *Great Lakes Beach Sanitary Survey User Manual.* Washington, DC: U.S. Environmental Protection Agency, Office of Water.

U. S. EPA (2012). *Recreational Water Quality Criteria", in: Water Quality Standards Handbook*. Washington, D.C: US EPA. Available at: https://www.epa.gov/wqs-tech/water-quality-standards-handbook

United States Geological Survey (2018). *National Water Information System Data Available on the World Wide Web (USGS Water Data for the Nation)*. Reston: USGS. Available at: https://waterdata.usgs.gov/nwis

Wang, Q., Garrity, G. M., Tiedje, J. M., and Cole, J. R. (2007). Naive Bayesian classifier for rapid assignment of rRNA sequences into the new bacterial taxonomy. *Appl. Environ. Microbiol.* 73, 5261–5267.

Wheeler, A. L., Hartel, P. G., Godfrey, D. G., Hill, J. L., and Segars, W. I. (2002). Potential of *Enterococcus faecalis* as a human fecal indicator for microbial source tracking. *J. Environ. Qual.* 31, 1286–1293.

Whitman, R. L., Byappanahalli, M. N., Spoljaric, A. M., Przybyla-Kelly, K., Shively, D. A., and Nevers, M. B. (2014a). Evidence for free-living *Bacteroides* in cladophora along the shores of the Great Lakes. *Aquat. Microb. Ecol.* 72, 119–128.

Whitman, R. L., Harwood, V. J., Edge, T. A., Nevers, M. B., Byappanahalli, M., Vijayavel, K., et al. (2014b). Microbes in beach sands: integrating environment, ecology and public health. *Rev. Environ. Sci. Bio Technol.* 13, 329–368.

Zulkifly, S., Hanshew, A., Young, E. B., Lee, P., Graham, M. E., Graham, M. E., et al. (2012). The epiphytic microbiota of the globally widespread macroalga *Cladophora glomerata* (*Chlorophyta, Cladophorales*). *Am. J. Bot.* 99, 1541–1552. doi: 10.3732/ajb.1200161

Conflict of Interest Statement: The authors declare that the research was conducted in the absence of any commercial or financial relationships that could be construed as a potential conflict of interest.

Copyright © 2019 Nakatsu, Byappanahalli and Nevers. This is an open-access article distributed under the terms of the Creative Commons Attribution License (CC BY). The use, distribution or reproduction in other forums is permitted, provided the original author(s) and the copyright owner(s) are credited and that the original publication in this journal is cited, in accordance with accepted academic practice. No use, distribution or reproduction is permitted which does not comply with these terms.

frontiers in Microbiology

ORIGINAL RESEARCH
published: 04 June 2019
doi: 10.3389/fmicb.2019.01229

The DNRA-Denitrification Dichotomy Differentiates Nitrogen Transformation Pathways in Mountain Lake Benthic Habitats

Carlos Palacin-Lizarbe[1], Lluís Camarero[2†], Sara Hallin[3‡], Christopher M. Jones[3§], Joan Cáliz[2‖], Emilio O. Casamayor[2¶] and Jordi Catalan[1,4#]*

[1] Centro de Investigación Ecológica y Aplicaciones Forestales, Cerdanyola del Vallès, Spain, [2] Center for Advanced Studies of Blanes, (CEAB–CSIC), Girona, Spain, [3] Department of Forest Mycology and Plant Pathology, Swedish University of Agricultural Sciences, Uppsala, Sweden, [4] Consejo Superior de Investigaciones Científicas, Cerdanyola del Vallès, Spain

OPEN ACCESS

Edited by:
Haihan Zhang,
Xi'an University of Architecture and Technology, China

Reviewed by:
Marja Tiirola,
University of Jyväskylä, Finland
Katharina Kujala,
University of Oulu, Finland

****Correspondence:***
Carlos Palacin-Lizarbe
cpalacli7@gmail.com
orcid.org/0000-0002-1572-6053
[†]orcid.org/0000-0003-4271-8988
[‡]orcid.org/0000-0002-9069-9024
[§]orcid.org/0000-0002-2723-6019
[‖]orcid.org/0000-0001-5714-7431
[¶]orcid.org/0000-0001-7074-3318
[#]orcid.org/0000-0002-2934-4013

Specialty section:
This article was submitted to Aquatic Microbiology, a section of the journal Frontiers in Microbiology

Received: *15 January 2019*
Accepted: *16 May 2019*
Published: *04 June 2019*

Citation:
Palacin-Lizarbe C, Camarero L, Hallin S, Jones CM, Cáliz J, Casamayor EO and Catalan J (2019) The DNRA-Denitrification Dichotomy Differentiates Nitrogen Transformation Pathways in Mountain Lake Benthic Habitats. Front. Microbiol. 10:1229. doi: 10.3389/fmicb.2019.01229

Effects of nitrogen (N) deposition on microbially-driven processes in oligotrophic freshwater ecosystems are poorly understood. We quantified guilds in the main N-transformation pathways in benthic habitats of 11 mountain lakes along a dissolved inorganic nitrogen gradient. The genes involved in denitrification (*nirS*, *nirK*, *nosZ*), nitrification (archaeal and bacterial *amoA*), dissimilatory nitrate reduction to ammonium (DNRA, *nrfA*) and anaerobic ammonium oxidation (anammox, *hdh*) were quantified, and the bacterial 16S rRNA gene was sequenced. The dominant pathways and associated bacterial communities defined four main N-transforming clusters that differed across habitat types. DNRA dominated in the sediments, except in the upper layers of more productive lakes where *nirS* denitrifiers prevailed with potential N_2O release. Loss as N_2 was more likely in lithic biofilms, as indicated by the higher *hdh* and *nosZ* abundances. Archaeal ammonia oxidisers predominated in the isoetid rhizosphere and rocky littoral sediments, suggesting nitrifying hotspots. Overall, we observed a change in potential for reactive N recycling via DNRA to N losses via denitrification as lake productivity increases in oligotrophic mountain lakes. Thus, N deposition results in a shift in genetic potential from an internal N accumulation to an atmospheric release in the respective lake systems, with increased risk for N_2O emissions from productive lakes.

Keywords: denitrification, DNRA, lithic biofilms, mountain lake, nitrogen deposition, remote ecosystems, sediment, 16S

INTRODUCTION

According to the planetary boundaries framework (Rockström et al., 2009), anthropogenic alteration of the nitrogen (N) cycle is one of the major challenges facing the Earth system. Human activities have at least doubled the levels of reactive N (N_r) available in the biosphere (Erisman et al., 2011), resulting in deposition of N_r in or near heavily populated areas as well as remote ecosystems (Catalan et al., 2013). In the context of global change, remote ecosystems — defined here as being affected by atmospheric processes rather than direct human action in catchment areas — can be particularly informative about potential large-scale changes in the Earth system

(Catalan et al., 2013). Alpine lakes of the Northern hemisphere and subarctic regions are examples of remote ecosystems that have been exposed to increased N_r deposition during the last decades (Holtgrieve et al., 2011; Camarero, 2017), triggering a nutrient imbalance in these freshwater systems which are otherwise known to have low nutrient availability (Catalan et al., 2006). While alpine and subarctic lakes are often considered important sensors of global change (Smol, 2012), there is minimal understanding of how increased N_r availability affects microbially-driven N-cycle pathways in these ecosystems (McCrackin and Elser, 2010; Palacin-Lizarbe et al., 2018).

The N cycle is best described as a modular and complex network of biological N-transformation reactions carried out by metabolically versatile communities of microorganisms (Graf et al., 2014; Kuypers et al., 2018), whose overall composition largely determines whether N_r is lost, via denitrification or anammox, or retained in the system via dissimilatory nitrate reduction to ammonium (DNRA). Within lakes, benthic habitats are known as hotspots of N cycling due to steep redox gradients in the sediments and biofilms (Melton et al., 2014). Furthermore, the presence and composition of macrophytes also influence the biogeochemistry of the sediment (Gacia et al., 2009). In particular, isoetid species oxygenate the sediment and may promote coupled nitrification-denitrification (Vila-Costa et al., 2016). However, the effect of increased N deposition on the N-cycling microbial communities, and the factors controlling their distribution are poorly understood in mountain lakes.

Our study aims to investigate how the distribution of microbial communities in general and those that drive different N-transformation pathways changes across a range of different benthic habitats in mountain lakes that have been affected by enhanced N deposition in the absence of significant acidification (Camarero and Catalan, 1998). We hypothesise that benthic habitat type and lake productivity together determines the fate of deposited N and that increased productivity will promote pathways resulting in N_r loss. Lakes at lower altitudes tend to be more productive, particularly if they are small since the productive period is longer (Catalan et al., 2009) and phosphorus loading to the lake increases as the catchment is more vegetated (Kopàček et al., 2011). In the Pyrenees, more than 70% of the lakes are considered ultraoligotrophic based on total phosphorus (TP; <150 nM), whereas 22 and 6% are oligotrophic and mesotrophic, respectively (Catalan et al., 2006). In general, more productive oligotrophic mountain lakes exhibit low dissolved inorganic nitrogen (DIN) concentrations due to higher consumption of excess N from atmospheric loading by primary producers (Camarero and Catalan, 2012). We therefore selected lakes to establish a DIN gradient and sampled lithic biofilms, sediments with elodeid, isoetid and helophyte macrophytes, and littoral and deep non-vegetated sediments (**Figure 1**). We then characterised the N-functional pathways by quantifying the abundances of key N-functional genes involved in denitrification, nitrification, DNRA and anammox pathways (**Table 1**). We also determined the bacterial community composition in the benthic habitats and linked these to the functional guilds using a multivariate approach combined with indicator species analyses. The environment was characterised by including proximal (benthic) and more distal (lake) descriptors to capture potential drivers acting at different spatial scales (Wallenstein et al., 2006; Battin et al., 2016).

MATERIALS AND METHODS

Sampling Location and Habitat Description

The lakes are located in the central region of the Pyrenees mountain range within the Aigüestortes i Estany de Sant Maurici National Park (**Table 2** and **Figure 1**). All lakes are dimictic and ultra-oligotrophic (TP < 150 nM) except for Bassa de les Granotes, which is classified as oligotrophic (150 < TP < 300 nM; Catalan et al., 1993) with a circumneutral pH (∼7; Vila-Costa et al., 2014). All main benthic habitats in the lakes were considered (**Figure 1**), although certain habitats were present in only a few lakes (**Table 2** and **Supplementary Table S1**). Plan Lake is particularly rich in macrophytes, including isoetids (*Isoetes setacea, I. palustris,* and *Subularia aquatica*), elodeids (*Myriophyllum alterniflorum, Potamogeton alpinus,* and *P. berchtoldii*) and the helophyte *Carex rostrata* (Gacia et al., 1994). Sampling was carried out during the ice-free period (June–November) of 2013 and 2014, with a total of 30 sites and 226 samples analysed.

Water, Lithic Biofilm, and Sediment Characterisation

The overlying water, sediments and lithic biofilms were characterised using physical, chemical and biological variables (**Supplementary Table S1**). The temperature of the overlying water was measured at the time of sampling. For chemical analyses, water samples were filtered through a pre-combusted (4 h at 450°C) GF/F glass fibre philtre. Nitrate and sulphate were determined by capillary electrophoresis using a Quanta 4000 (Waters) instrument. Ammonium and nitrite were determined by colourimetric methods in a segmented-flow autoanalyser (AA3HR, Seal), using the Berthelot reaction for ammonium (Bran+Luebbe method G-171-96) and the Griess reaction for nitrite (Bran+Luebbe method G-173-96). Dissolved organic carbon (DOC) was measured by catalytic combustion to CO_2 and detection by IR spectroscopy in a TOC5000 (Shimadzu) analyser.

Lithic biofilms were sampled collecting several cobbles (ø ∼10 cm) from different sites of the lake. Cobbles were scraped entirely (upper and lower sides) with clean metal brushes and washed with deionized water and pooling together the collected material. Biofilm subsamples were collected on 0.2-μm pore polycarbonate membranes for DNA analysis, and triplicate volumes were filtered through a pre-combusted and pre-weighted GF/F glass fibre philtre for chemical and physical analyses. Sediment cores (ø 6.35 cm) were collected with a gravity corer (Glew, 1991) around the deepest point of each lake or manually by scuba diving for the littoral sediments. The cores were sliced in three sections (0–0.5, 0.5–2, and 2–4 cm) to capture the oxic and the nitrate reduction zones (Melton et al., 2014).

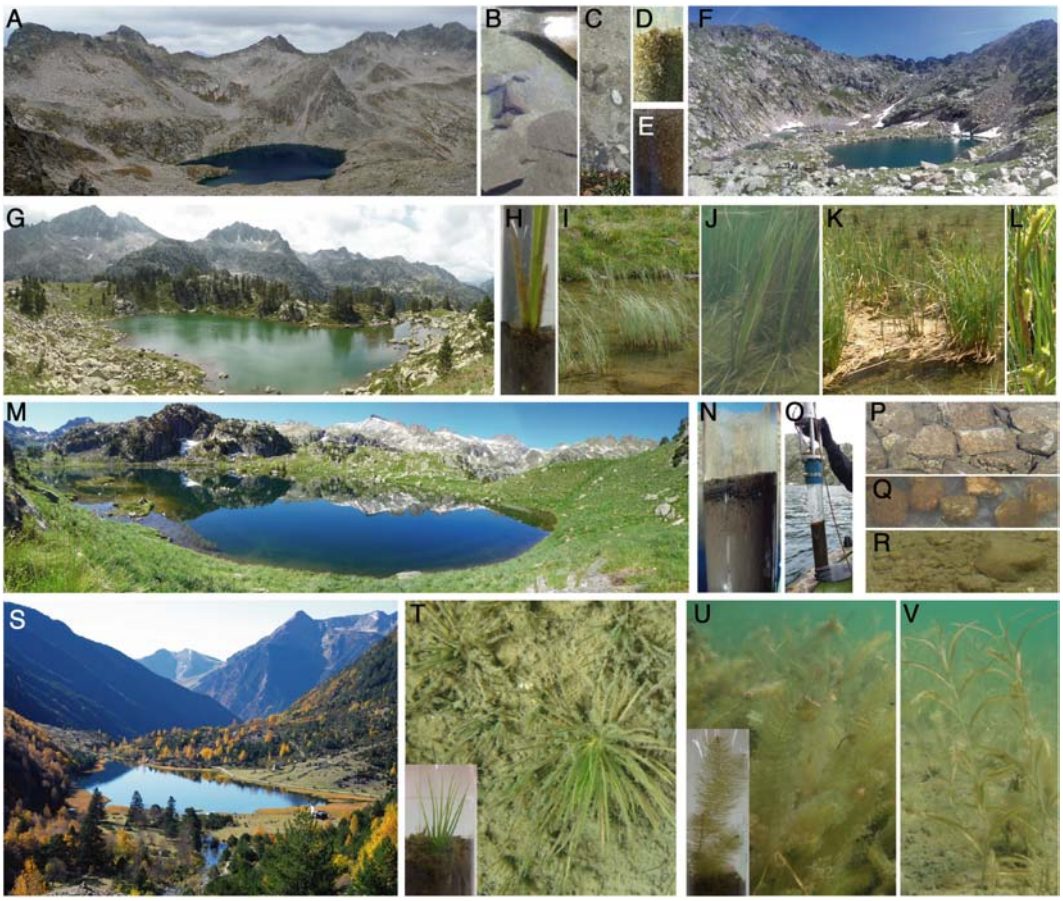

FIGURE 1 | Examples of the lakes and habitats studied. Lakes: Contraix **(A)**, Gelats de Bergús **(F)**, Bassa de les Granotes **(G)**, Plan **(M)**, and Llebreta **(S)**. Benthic habitats: sediments near the deepest point of the lake (non-vegetated) **(N,O)**; littoral sediments from beds of isoetids [*Isoetes lacustris* **(T)**] and elodeids [*Myriophyllum alterniflorum* **(U)**, *Potamogeton alpinus* **(V)**] macrophytes, helophyte (*Carex rostrata*) belts **(H–L)** and rocky areas **(B–E)**; and lithic biofilms from littoral cobbles **(P–R)**.

For total carbon (C) and N and isotopic composition, ca. 5 mg of the freeze-dried sample was placed with a catalyst (Va_2O_5) in tin capsules, and the analyses were performed by the University of California Davis Stable Isotope Facility. Organic matter (OM) content was determined using the loss on ignition (LOI) procedure (Heiri et al., 2001). The median grain size of the sediment was determined by laser diffraction (Mastersizer, 2000, Malvern Instruments Ltd, United Kingdom), using freeze-dried sediment rehydrated in distilled water and introduced into the sample dispersion unit (Hydro 2000 G, Malvern Instruments Ltd, United Kingdom) after adding hexametaphosphate and sonicating to avoid aggregates. Laser obscuration was between 10–20% and the measuring range between 0.02 and 2000 μm.

TABLE 1 | N-functional genes accounted for in this study.

Gene	Enzyme	Pathway	Reaction	Process type
amoA	Ammonium monooxygenase	Nitrification	Ammonium oxidation to hydroxylamine	Aerobic
nirS	Nitrite reductase (cytochrome-cd1)	Denitrification	Nitrite reduction to nitric oxide	Anaerobic
nirK	Nitrite reductase (copper-based)			
nosZ	Nitrous oxide reductase	Denitrification	Nitrous oxide reduction to dinitrogen	Anaerobic
nrfA	Nitrite reductase (formate-dependent)	DNRA	Nitrite reduction to ammonium	Anaerobic
hdh	Hydrazine dehydrogenase	Anammox	Hydrazine oxidation to dinitrogen	Anaerobic

DNA Extraction and Quantitative PCR of 16S rRNA and N Cycle Genes

DNA was extracted from 0.33 ± 0.06 g of sediment or lithic biofilm using the FastDNA® Spin Kit for Soil (MP Biomedical) following the manufacturer's instructions. The extracted DNA was quantified using the Qubit® fluorometer (Thermo Fisher Scientific Inc.).

Quantitative real-time PCR (qPCR) was used to quantify functional genes encoding enzyme involved in N-cycle pathways

TABLE 2 | Site location, habitats studied and characteristics sorted by the dissolved inorganic nitrogen (DIN) concentration.

Lake (Abbreviation)	Vegetation belt	Habitats Studied[a]	Latitude (N)	Longitude (E)	Altitude (m a.s.l.)	Area (ha)	Catchment (ha)	Depth[b] (m)	Renewal time (months)	TP[c] (nM)	DIN[d] (μM)
Redon de Vilamòs (R)	Alpine	I	42.78078	0.76233	2209	0.6	12	5	1.7	NA	1.2
Plan (P)	Subalpine	D, I, E, C, L	42.62248	0.9307	2188	5	23	9	15.1	102	1.7 ± 0.9
Bassa de les Granotes (G)	Alpine	D, L	42.5733	0.97124	2330	0.7	3	5	9.9	292	2.4 ± 0.7
Redó Algüestortes (RA)	Subalpine	D, L	42.58216	0.95949	2117	6.3	325	11	1.6	76	8.5 ± 0.9
Gelat de Bergús (GB)	Alpine	D, R, L	42.59106	0.96331	2493	1.4	24	8	2.3	42	8.8 ± 3.3
Llong (Lo)	Montane	D, R, L	42.57431	0.95063	2000	7.1	1111	13	0.6	89	10.3 ± 11.6
Bergús (B)	Alpine	D, L	42.58947	0.95717	2449	6.2	126	50	3.9	44	17.1 ± 11.3
Llebreta (Le)	Montane	D, C, R, L	42.55083	0.89031	1620	8	5438	12	0.1	89	17.9 ± 2.7
Contraix (C)	Alpine	D, R, L	42.58874	0.91861	2572	9.3	100	59	9.9	49	18.0 ± 1.3
Redon (RC)	Alpine	D, R, L	42.64208	0.77951	2235	24.1	153	73	36	58	23.5 ± 19.6
Pòdo (Po)	Alpine	D, L	42.60307	0.93906	2450	4.6	33	25	9.4	75	25.2 ± 14.7

[a]*D, sediments in the deepest point of the lake; I, isoetid littoral sediments; E, elodeid littoral sediments; C, Carex rostrata belts littoral sediments; R, rocky areas littoral sediments, L, lithic biofilms from littoral cobbles.* [b]*Maximum water column depth.* [c]*Total phosphorus (Camarero and Catalan, 2012).* [d]*DIN concentration (sum of nitrate, nitrite and ammonium) in the overlying water.*

(**Table 1** and **Supplementary Table S2**), as well as the bacterial 16S rRNA gene. All qPCR reactions were performed in duplicate in a total reaction volume of 20 μL using DyNAmo Flash SYBR Green qPCR kit (Thermo Fisher Scientific Inc.), 0.1% Bovine Serum Albumin, 0.5–1.0 μM of each primer and 15 ng DNA on the Biorad CFX Connect Real-Time System. Primers (Rotthauwe et al., 1997; Hallin and Lindgren, 1999; Lopez-Gutierrez et al., 2004; Mohan et al., 2004; Throbäck et al., 2004; Henry et al., 2006; Schmid et al., 2008; Tourna et al., 2008; Jones et al., 2013; Welsh et al., 2014), amplification protocols and resulting efficiencies for each assay are listed in **Supplementary Table S3**. Potential inhibition of the PCR reactions was checked by amplifying a known amount of the pGEM-T plasmid (Promega) with the plasmid-specific T7 and SP6 primers added to the DNA extracts and non-template controls. No inhibition of the amplification reactions was detected with the amount of template DNA used. Standard curves for each assay were generated by serial dilutions of linearized plasmids with cloned fragments of the respective gene. Standard curves were linear (R^2 = 0.997 ± 0.003) in the range used, and amplification efficiency was 90% for the 16S rRNA gene and 65–88% for the functional genes (**Supplementary Table S3**). Melting curve profiles were inspected, and final products were run on an agarose gel to confirm amplicon size. Non-template controls resulted in negligible values.

Sequencing of the 16S rRNA Gene, Sequence Processing and OTU Clustering

The diversity and structure of total bacterial and archaeal communities were determined by targeting the V3-V4 region of the 16S rRNA gene (Takahashi et al., 2014). Amplicon libraries for each sample were generated using a two-step protocol (Berry et al., 2011). First, PCR products were generated in duplicate 20 μL reactions per sample using 16S rRNA primer constructs that included Nextera adapter sequences, with reactions consisting of Phusion PCR mastermix (Thermo Fisher Scientific), 0.5 μg μL^{-1} BSA, 0.25 μM of each primer and 10 ng extracted DNA. Thermal cycling was performed for 25 cycles, and cycling conditions and primer sequences are listed in **Supplementary Table S3**. The resulting PCR products were pooled and purified using the AMPure bead purification kit, and 3 μL of the purified product was used as template in the second PCR using barcodes. Duplicate 30 μL reactions were performed for each sample, with similar reagent concentrations as in the first step except for the use of 0.2 μM final primer concentrations. PCR was performed according to **Supplementary Table S3**. Products were pooled, bead purified, followed by equimolar pooling and sequencing performed by Microsynth AG (Balgach, Sweden) using the Illumina MiSeq platform with v3 chemistry (2 × 300 bp paired-end reads).

Paired-end reads were merged using PEAR (Zhang et al., 2013) and dereplicated and clustered into operational taxonomic units (OTUs) at a cut-off of 3% identity using UPARSE (Edgar, 2013). The final dataset comprised 13069 OTUs after removal of chimaeras and singletons, with 83% of the quality filtered sequence pool mapped back to OTUs. Taxonomic assignment

was carried out with the RDP classifier (Wang et al., 2007) against the SILVA reference database (release 119) (Quast et al., 2013). Sequences classified as mitochondria or chloroplasts were excluded. The original OTU table was rarefied (100 random subsampling) to 10660 sequences per sample. The sequences are available in the NCBI Sequence Read Archive (PRJNA494630).

Statistical Methods

All multivariate, clustering and correlation analyses were performed using R (R Core Team, 2017). Comparisons of gene abundances between habitat types were performed using Kruskal–Wallis (KW) and Wilcoxon–Mann–Whitney (WMW) tests. Principal component analysis (PCA) and Redundancy analysis (RDA) using Hellinger distances (Borcard et al., 2011) were used to investigate the unconstrained ordination of the relative abundances of the N-functional genes studied (PCA) and of the bacterial community composition (PCA), and the relationship between the relative abundance of the N-functional genes and the environmental conditions (RDA), as well as between the overall bacterial community composition and the relative abundance of the N-functional genes (RDA). Hereafter, we refer to the PCAs as gene-PCA (gen-PCA) and community-PCA (com-PCA), and to the RDAs as gene-environment-RDA (gen-env-RDA) and community-gene-RDA (com-gen-RDA), respectively. In the analyses, functional gene abundances were standardised to total 16S rRNA gene copy numbers. Taxa < 5% occurrence (3453 of the total 13069 OTUs) were excluded from the bacterial community composition analysis (com-PCA and com-gen-RDA), and values for nitrate, nitrite, ammonium and sulphate were log-transformed in the gen-env-RDA. In the RDAs, forward selection was used to identify a minimum set of significant explanatory variables ($p < 0.05$; Blanchet et al., 2008), which exhibited low collinearity (variance inflation factors well below 10). Permutation tests of the resulting ordinations showed significant pseudo-F values ($p < 0.05$, $n = 1000$) for the main explanatory axes in each ordination — first to third axes in the gen-env-RDA, and first to fifth axes in the com-gen-RDA.

A structure of four sample clusters was present in both RDAs. Consequently, we used the samples scores of the three main axes of the com-gen-RDA as coordinates in four-group k-means clustering. We looked for indicative OTUs of each cluster performing a multi-level pattern analysis using the *multipatt* function from the *indicspecies* R package (Cáceres and Legendre, 2009), considering site group combinations, and the entire OTU set (13069) as the community data table. For each OTU, the method provides an indicator value (IndVal) of each cluster or a joint set of them. We accepted as significant indicator taxa those with adjusted p-value < 0.001, using the false discovery rate method to calculate the adjusted p-value (Storey et al., 2004).

RESULTS

Genetic Potentials

The sum of the N-functional gene copies per dry weight of sediment increased with OM ($r = 0.42$, $p < 0.001$, **Figure 2A**) but with a large scattering. Individual gene abundances were highly positively correlated among them (**Figure 2B**). However, the correlation structure markedly simplified when standardising by the 16S rRNA copy number in each sample (**Figure 2C**), showing that the *nrfA* pool was weekly related to the rest of N-functional gene pools. The sum of the N-functional gene copies accounted for an average of 15 ± 8% (mean ± SD) of bacterial 16S rRNA gene copies across all samples (**Supplementary Figure S1**). Maximum values of 52% were found in the lower sediment layer (2–4 cm) near the isoetid rhizosphere, while minimum values of 2% were observed in lithic biofilms. Hereafter, unless otherwise indicated, we report the N-functional gene abundance standardised to total bacterial 16S rRNA gene copies.

The *nirS* and *nrfA* genes showed the highest relative abundances, up to 33 and 18% of total 16S gene copies, respectively. The abundance of *nirS* was approximately 50-fold greater than *nirK* across all lakes, with the highest numbers detected in the more productive lakes (R, P and G, **Table 2** and **Figures 3A,B**). The abundance of *nirK* genes exhibited an overall trend of increasing abundance with lake DIN levels (**Figure 3B**), opposed to that observed for *nirS*. Higher *nrfA* abundance was observed in the sediments of the deepest part of the lakes (**Figure 3E**), while abundances in the elodeid sediments were significantly higher than those of the isoetids (KW test, $p = 0.028$). Closer inspection of the macrophyte sediment profiles showed a significant *nrfA* increase deeper in the elodeid sediments ($r = 0.85$, $p < 0.001$; **Supplementary Figure S2A**), while no trend was observed in the isoetid sediments.

The *amoA* gene of ammonia-oxidising archaea (AOA) was more abundant than the bacterial (AOB) counterpart. No obvious trend was observed for either AOA or AOB abundance across the lake DIN gradient. Although the average total abundance of ammonia oxidisers across all lakes was low relative to those of 16S rRNA genes (0.87 ± 2.66% and 0.05 ± 0.14% for AOA and AOB, respectively), several lakes showed AOA and AOB proportions of 57 and 23% of the total N-functional gene abundance. The highest AOA abundance was observed in the lower sediment layers of the isoetid rhizosphere and rocky littoral sediments of high-altitude lakes in the alpine belt, that is, those located above treeline (**Figure 3G**). Abundances of AOA were significantly higher in isoetid than elodeid sediments (KW test, $p < 0.001$), and increased with depth in the former ($r = 0.64$, $p = 0.001$; **Supplementary Figure S2B**). All habitats of the highest altitude lakes (GB and C lakes, **Table 2** and **Figure 3H**) showed a relatively high abundance of AOB copies compared to the same habitats in lakes at lower elevations.

The gene variants of the nitrous oxide reductase, *nosZ* clade I and II, as well as the *hdh* gene associated with the anammox pathway, exhibited low relative abundances (**Figures 3C,D,F**). The abundance of clade I *nosZ* genes was typically higher (∼7-fold on average) than that of clade II *nosZ* across all lakes and habitats. The lithic biofilm habitats of Contraix, the most elevated lake, showed the highest abundance of *nosZ* clade I genes (**Figure 3C**), while *nosZ* clade II abundances were higher in the rocky littoral sediments of alpine lakes (**Figure 3D**). Relative abundances of *hdh* were higher in the lithic biofilms (**Figure 3F**), with no obvious relationship with DIN levels across the lakes.

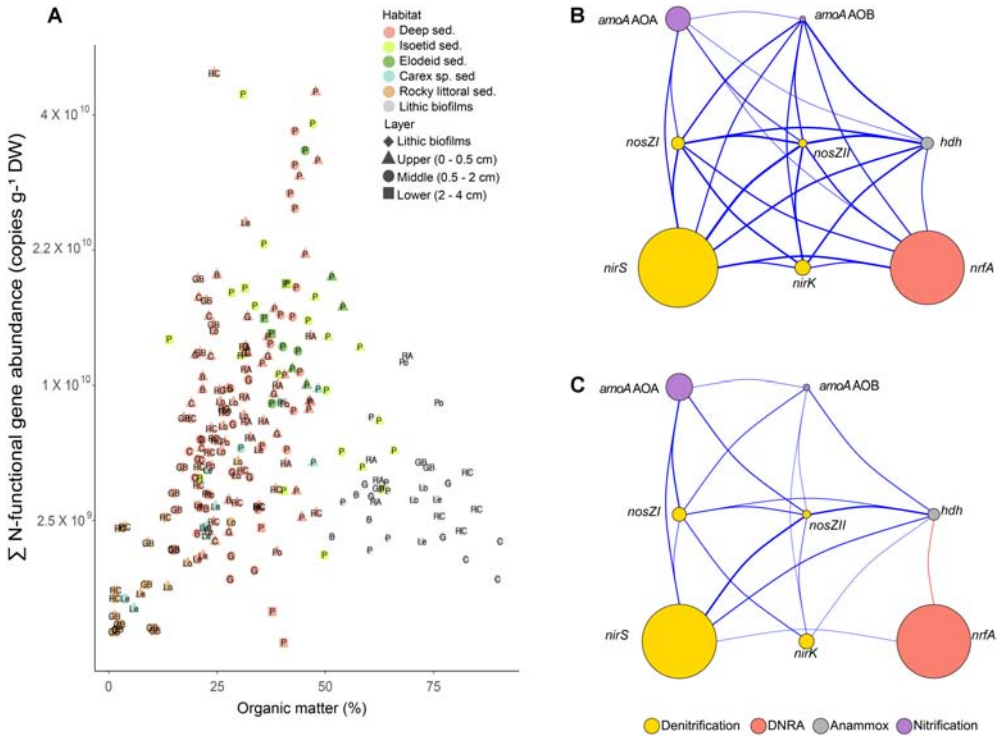

FIGURE 2 | (A) Sum of the accounted N-functional gene copies g^{-1} of dry weight (DW) against the percentage of organic matter (OM). Labels are the Lake abbreviations (see **Table 2**). Note that *Y*-axis has a square root scale. **(B,C)** Correlation structure of N-transforming gene abundances in mountain lake benthic habitats. N-functional gene abundances are in gene copies g^{-1} DW **(B)** or standardised to the 16S rRNA gene copies **(C)** (**Supplementary Table S2**). The nodes symbolise the genes whose colour and size indicate their associated pathway and abundance, respectively. Link width is proportional to the coefficient values of significant associations ($p < 0.05$), and blue and red colours indicate positive and negative Spearman's correlations, respectively.

N-Functional Genes and the Environment

The constrained ordination of N-*functional* gene abundances identified three distinct gradients explaining 54% of the total variation across habitats and lakes (**Figure 4**). A similar result was obtained in a non-constrained analysis (**Supplementary Figure S3**), indicating that the main environmental drivers were captured by the constrained analysis. The main variation of benthic N-cycling genetic potentials was across a *nirS* vs *nrfA* abundance gradient (**Figure 4**). The *nirS*-rich samples corresponded to those from shallow and productive lakes (R, P, and G, **Table 2** and **Supplementary Figures S4A,B**), specifically the upper sediments in all habitats and sediments near the roots of isoetids. These sites were associated with higher temperature, DNA content, isotopic signatures, DOC content, and C and N content, as well as coarser granulometry (**Supplementary Figure S5**) and lower C/N and nitrate/nitrite ratios (**Figure 4**). In contrast, *nrfA* rich environments occurred in the deep parts of the deep lakes, the lower layers of all sediments (except the isoetid rhizosphere) and the littoral sediments of the montane belt lakes (**Table 2** and **Supplementary Figures S4A,B**). Sulphate, ammonium, nitrate and nitrite concentrations were higher in these sites compared to those associated with *nirS*. The same *nirS*-*nrfA* main axis was also found if only samples from the deep habitat were included in the analysis.

The gen-env-RDA second axis of variation discriminated between sediments and lithic biofilms. The latter characterised by higher abundances of *nirK*, *nosZI*, *nosZII*, *hdh* and AOB (**Figure 4A**). The rocky littoral sediments of Lake Contraix separated from the other sediment samples (**Supplementary Figure S4A**). These sites shared relatively high concentrations of nitrate, nitrite and sulphate in the overlying water, high OM content, and particular isotopic signatures (high $\delta^{13}C$ and low $\delta^{15}N$). Finally, the third axis of variation was associated with the AOA abundance (**Figure 4B**) and resulted in the segregation of the majority of the isoetid sediments from the other habitats. The sites with the highest abundance of AOA were located close to the isoetid rhizosphere and in the rocky littoral sediments of the alpine lakes (**Supplementary Figure S4B** and **Table 2**). These samples showed high $\delta^{15}N$ values and likely corresponded to more oxygenated sediments (**Figure 4B**).

N-Functional Genes and the Associated Microbial Community

The ordination of the OTU composition constrained by the N-functional gene abundances resulted in a pattern of four distinct sample clusters (**Figure 5**), similar to that obtained in an unconstrained ordination (**Supplementary Figure S6**). The four clusters consisted of samples associated with a high relative abundance of *nrfA*, *nirS*, AOA, or a combination of the rest of

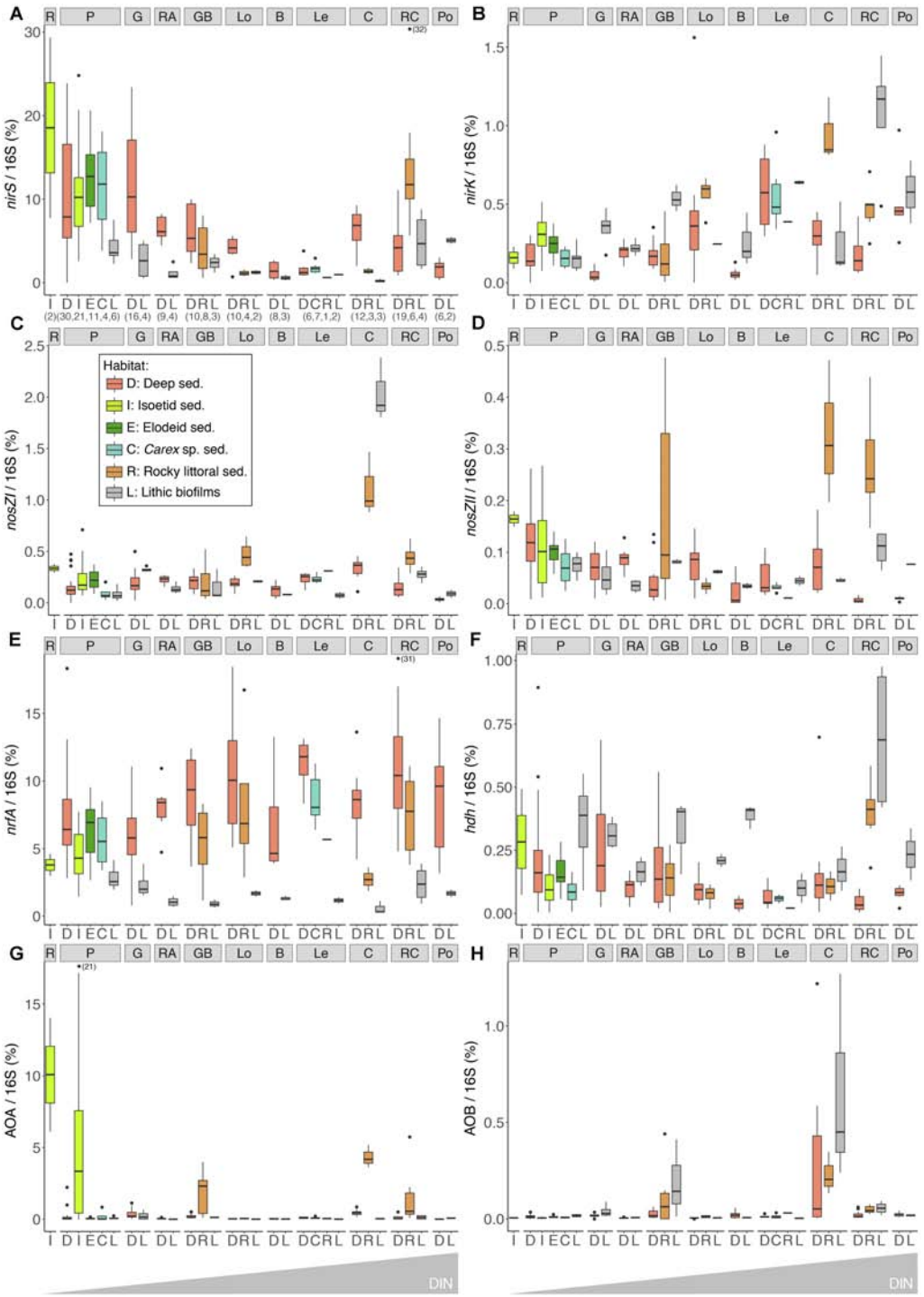

FIGURE 3 | Abundances of *nirS* **(A)**, *nirK* **(B)**, *nosZ*I **(C)**, *nosZII* **(D)**, *nrfA* **(E)**, *hdh* **(F)**, archaeal *amoA* **(G)**, and bacterial *amoA* **(H)** standardised to the 16S rRNA gene copies in different lakes and habitats. Numbers in brackets in the *X*-axis indicated the samples analysed. Boxplots depict the interquartile range (box), median value (line), 1.5x interquartile (whiskers), and outliers (points). Lakes are arranged from left to right by increasing water-column DIN level (see **Table 2** for lake abbreviations and characteristics).

the targeted genes. Classification of samples into the four clusters using *k*-means followed by indicator species analysis resulted in approximately 29% of OTUs being identified as exclusively associated with samples from a single cluster (**Figure 6** and **Supplementary Tables S4, S5**). Approximately 12 % of OTUs were significant indicators of the AOA sample cluster and found

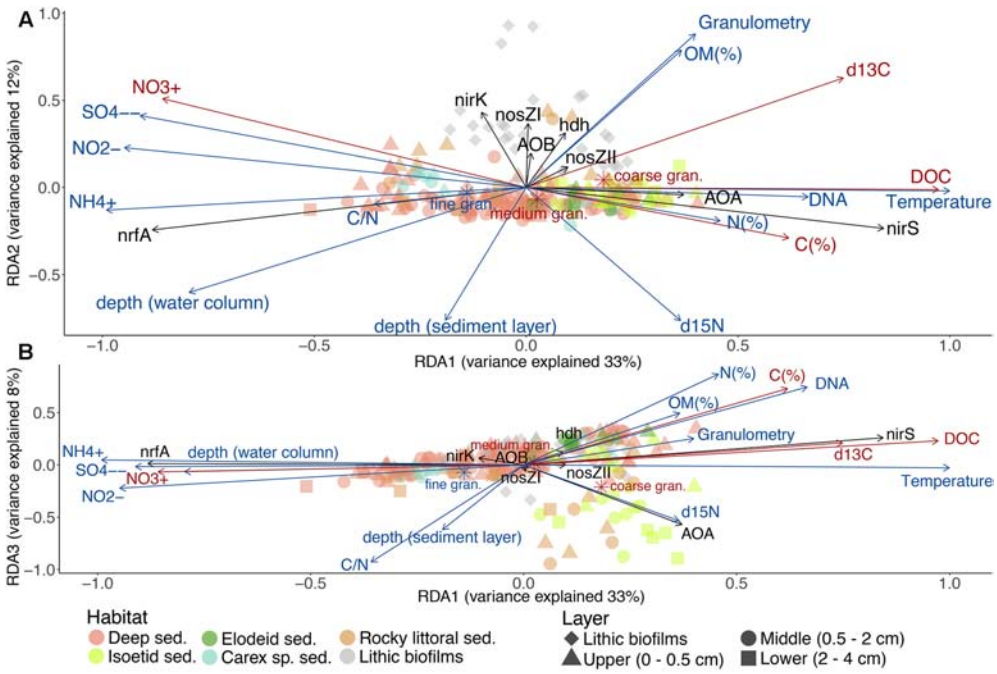

FIGURE 4 | RDA based on N-functional gene abundances (response variables, black arrows) and the environmental variables (explanatory variables, blue arrows). Red arrows represent the unselected environmental variables in the previous forward selection. Triplots of the 1st and 2nd **(A)** or of the 1st and 3rd **(B)** main gradients. See **Supplementary Figures S4A,B** for samples scores. The axes sizes are proportional to the explained variation.

across a wide range of different bacterial taxa. By contrast, 6% of OTUs were significant indicators of the mixed N-transformation cluster, with large numbers of indicators concentrated within the phyla Cyanobacteria, Bacteroidetes, and Planctomycetes, as well as Alpha- and Betaprotoebacteria classes. Similarly, 6% of OTUs were associated with samples in the *nrfA* cluster and were classified into Firmicutes, Bacteroidetes, Actinobacteria, and Chloroflexi phyla, and Epsilon- and Deltaproteobacterial classes. Finally, 4% of OTUs were exclusive indicators of samples in the *nirS* cluster and were found across a large number of bacterial taxa, similar to the AOA sample cluster.

DISCUSSION

The DNRA-Denitrification Gradient

The gradient of *nrfA* to *nirS* dominance was the main pattern of variation in the N-transforming microbial communities of the benthic habitats. From an ecosystem perspective, this gradient indicates a shift from habitats with a higher potential for internal N_r cycling via DNRA, and thus retention of N_r in the system, to those in which loss of N_r from the lake is more likely through denitrification. The environments with the lowest ratios of denitrifying to DNRA nitrite reductase genes were characterised by variables indicating refractory OM with high C/N, lower oxygen diffusion and lower redox potentials. This was particularly the case in the deepest part of the deep lakes (maximum depth $\geq$ 25 m) and in the deeper regions of the reduced elodeid sediments. In agreement with our result, previous work in a tropical high-altitude oligotrophic lake has shown *nrfA* abundance to be highest in the deepest part of the hypolimnion with anoxic conditions during late stratification (Pajares et al., 2017), and more reduced conditions favoured DNRA over denitrification in Australian estuaries (Kessler et al., 2018). Increased C/N ratio may favour DNRA over denitrification (Kraft et al., 2014).

The highest genetic potential for denitrification, based on *nirS* abundance, was detected in shallower and less oligotrophic lakes, where DIN levels were lower in the water column due to higher primary productivity. These lakes also have lower C/N ratios (**Supplementary Table S1**). Generally, lake autochthonous OM is fresher and of higher quality (e.g., lower C/N), and is a substantial proportion of total OM in lakes with a lower ratio of the catchment to the lake area. This fresh OM can be used as electron donors for denitrifiers, as demonstrated in several aquatic ecosystems [eutrophic lakes (Chen et al., 2012; Gardner et al., 2017), streams (Barnes et al., 2012; Stelzer et al., 2014), wetlands (Dodla et al., 2008), and oceans (Van Mooy et al., 2002)]. Oxygen levels in upper sediments of shallow and productive lakes likely fluctuate to a greater degree than those observed in habitats dominated by DNRA, thereby favouring organisms with facultative anaerobic respiration pathways such as denitrification (Wittorf et al., 2016; Chen J. et al., 2017). The *nirS* denitrifiers along the DNRA-denitrification gradient were associated with *nosZ* clade II N_2O reduction and AOA communities involved in ammonia oxidation, whereas denitrifier communities present in lithic biofilms dominated by *nirK*-types were associated with *nosZ* clade I N_2O reduction and AOB. These patterns indicate

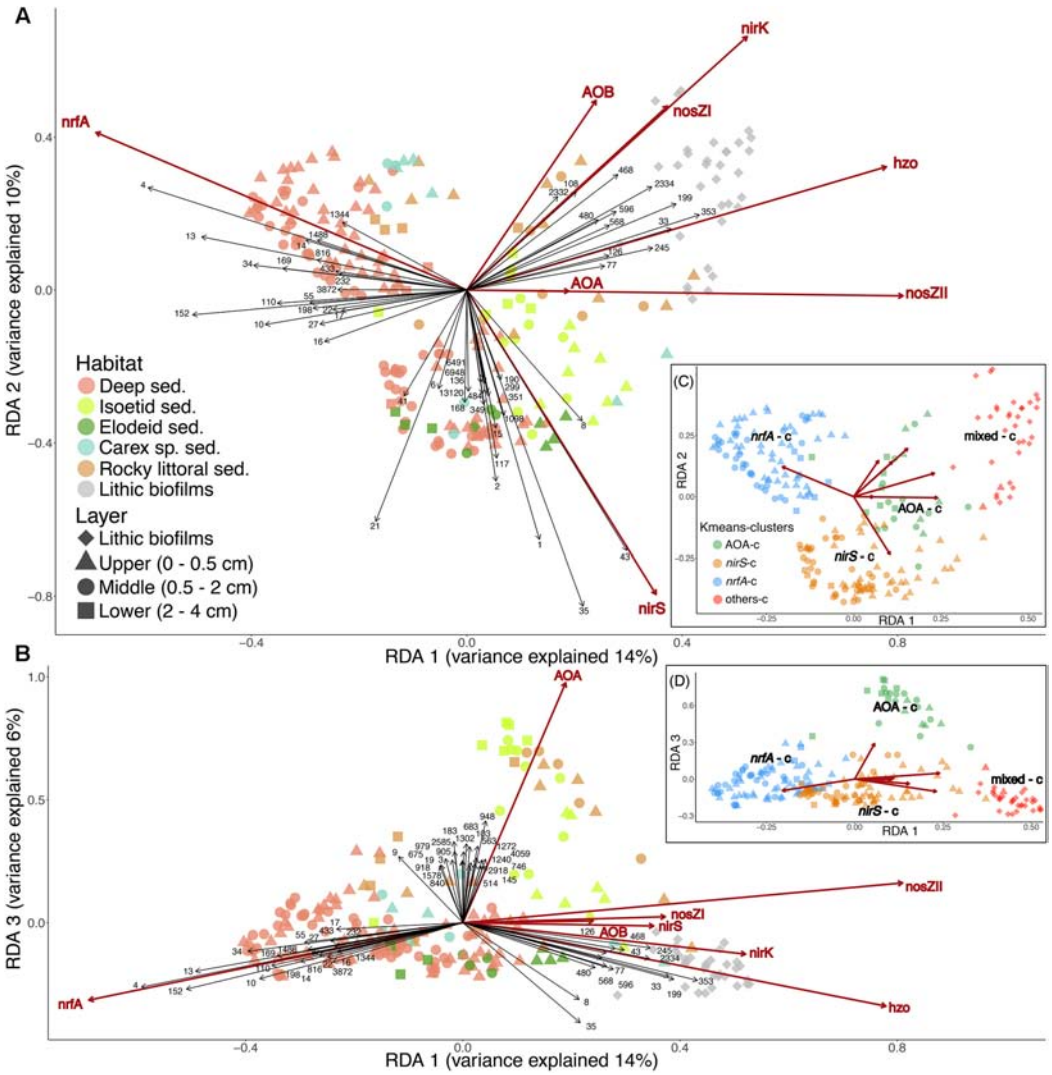

FIGURE 5 | RDA with the OTUs abundance (response variables) and the abundance of the N-functional genes (explanatory variables, red arrows). Triplots of the 1st and 2nd **(A)** or the 1st and 3rd **(B)** main gradients. Only the most influential OTUs for each gradient are shown (black arrows and ID, **Supplementary Table S6**). Clusters are resulting from the k-means analysis with the sample scores of the three main RDA gradients (Subplots C and D). See **Supplementary Figures S4C,D** for samples scores. The axes sizes are proportional to the explained variation.

that different N transformation networks developed in these habitats even when in both cases exhibited potential for linked nitrification and denitrification.

The overall high proportion of denitrifying nitrite versus nitrous oxide reductase genes (∼30 *nir*:*nosZ* ratio on average) suggests a dominance of partial denitrification, especially in productive habitats dominated by *nirS* denitrifier communities (i.e., *nirS*-cluster showed *nir*:*nosZ* higher ratios compared to the other clusters, WMW test, $p < 0.01$). This observation agrees with Castellano-Hinojosa et al. (2017) who found high N_2O/N_2 emissions in a productive, shallow warm Mediterranean mountain lake, as well as Myrstener et al. (2016) who demonstrated that addition of nitrate, phosphorus and labile C to sediments from a boreal lake resulted in higher relative N_2O production compared to addition of nitrate alone. Other studies have shown that higher *nir*:*nosZ1* ratios in the sediments of boreal lakes were associated with hypolimnion N_2O excess, as well as increased phosphate and nitrate concentrations (Saarenheimo et al., 2015a). Thus, productive sites could favour partial denitrifiers that survive anoxic periods. Before arriving to the atmosphere, N_2O might be consumed in the hypolimnion of deep lakes. *NosZ*-harbouring bacteria have been found in the hypolimnion of boreal lakes (Peura et al., 2018). However, in the sediments studied, the higher *nir*:*nosZ* ratios were found in shallower lakes. in which N_2O may easily reach the atmosphere (Dore et al., 1998). Further studies accounting for real N_2O emissions could corroborate our conjecture.

Nitrite-dependent anaerobic methane oxidation (N-DAMO, Simon and Klotz, 2013) is a potential alternative to DNRA, denitrification and anammox nitrite consumption. N-DAMO

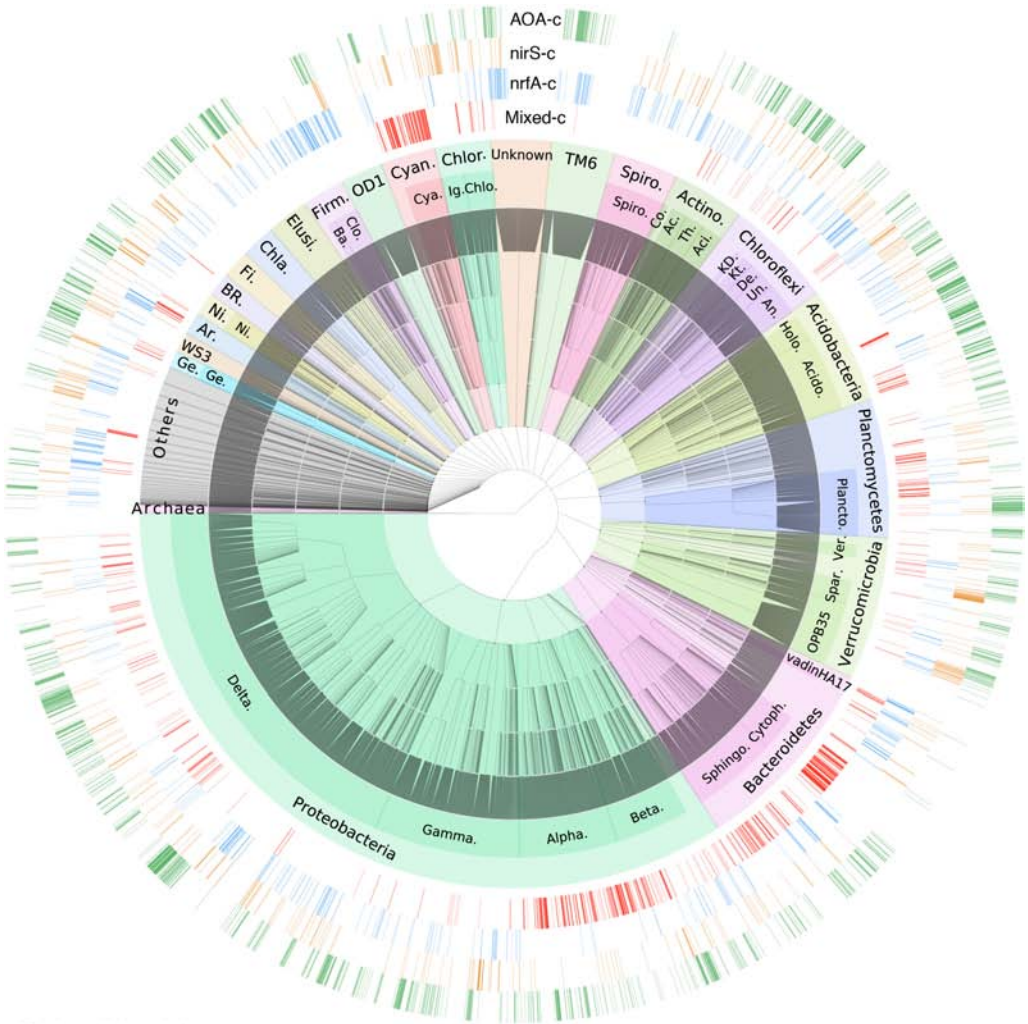

Phylum Abbreviations

Actino.: Actinobacteria	Spiro.: Spirochaetae	TM6.: Cand. division TM6	Chlor.: Chlorobi
Cyano.: Cyanobacteria	OD1.: Cand. division OD1	Firmi.: Firmicutes	Elusi.: Elusimicrobia
Chla.: Chlamydiae	Fi.: Fibrobacteres	BR.: Cand. division BRC1	Ni.: Nitrospirae
Ar.: Armatimonadetes	WS3.: Cand. division WS3	Ge.: Gemmatimonadetes	

Class Abbreviations

Delta.: Deltaproteobacteria	Gamma.: Gammaproteobacteria	Alpha.: Alphaproteobacteria	Beta.: Betaproteobacteria
Sphingo.: Sphingobacteriia	Cytoph.: Cytophagia	OPB35: OPB35 soil group	Sparto.: Spartobacteria
Ver.: Verrucomicrobiae	Plancto.: Planctomycetacia	Acido.: Acidobacteria	Holo.: Holophagae
An.: Anaerolineae	Un.: Uncultured	De.: Dehalococcoidia	Kt.: Ktedonobacteria
KD.: KD4.96	Aci.: Acidimicrobiia	Th.: Thermoleophilia	Ac.: Actinobacteria
Co.: Coriobacteriia	Spiro.: Spirochaetes	Chlo.: Chlorobia	Ig.: Ignavibacteria
Cya.: Cyanobacteria	Clo.: Clostridia	Ba.: Bacilli	Ni.: Nitrospira
Ge.: Gemmatimonadetes			

FIGURE 6 | Hierarchical taxonomic classification of OTUs found in all surveyed lakes. Major bacterial phyla are indicated by shaded areas, while dominant classes within each phylum are labelled. External rings show OTUs that are exclusive indicators (adjusted-$p < 0.001$) of each of the four N-transformation functional sample clusters, as delimited by the dominant N-functional gene abundances.

has been found as a key driver of methane oxidation in nitrate-rich lakes (Deutzmann et al., 2014) and reduced sandy riverbeds (Shen et al., 2019). In these habitats, bacteria related to Candidatus *Methylomirabilis oxyfera*, known to perform this pathway, were abundant. In our study, we detected only two OTUs of low relative abundance (0.02%) classified as Candidatus *Methylomirabilis*. Nonetheless, OTUs belonging to the genus *Methylocaldum* were more abundant (∼0.3%), and were significant indicators of the '*nirS*' cluster. These findings are similar to those of a survey of methane oxidation in Indian reservoirs (Naqvi et al., 2018), where low relative abundance of NC10 bacteria capable of N-DAMO (0.003–0.022%) was found; whereas Type I aerobic methanotrophs, which include *Methylocaldum* and other

members of the Methylococcaceae family, were predominant and co-occurred with a diverse community of potential *nirS* type denitrifiers. Other Methylococcaceae are partial denitrifying aerobic methanotrophs with N_2O as the end product (Kits et al., 2015a,b). Overall, these results, added to the high ratio of *nir* to *nosZ* gene abundance, suggest that N_2O emissions are the most likely endpoint of nitrite reduction in *nirS*-cluster sediments, independent of the pathway. Further studies are required to elucidate the importance and distribution of methane dependent processes in mountain lakes and to evaluate their role as a bypass of partial denitrification.

The Idiosyncratic Lithic Biofilms

Microbial N-transforming guilds in the lithic biofilms differentiate from those in the sediments. Gene abundance results indicate a complex N-transformation structure in this habitat, consisting of processes demanding both oxic and anoxic conditions, which suggest highly structured microbial communities in relatively short spatial distances. The idiosyncratic nature of the guild composition (e.g., *nosZI*, *hdh*, *nirK*) declines as the productivity of the lake increases; *nirS* becomes more prominent compared to *nirK,* and the N-transforming communities are more similar to the upper sediments. The high abundance of *nirS* differs from the dominance of *nirK* previously found in another study of epilithic biofilms from a subset of the same lakes. A main difference between the two studies is that in Vila-Costa et al. (2014) only sampled the upper side of the cobbles, whereas we sampled both sides. Differences in ammonia oxidisers between the upper (light-side) and lower (dark-side) sides of cobbles have been previously reported (Merbt et al., 2017). The higher relative abundance of *hdh* and *nosZ* genes indicates that N loss in the form of N_2 could be higher in the lithic biofilms compared to the other benthic habitats in the studied lakes.

Archaeal Nitrification Hotspots

The positive $\delta^{15}N$ signals observed in samples from the lower sediment layers of the isoetid rhizosphere and the rocky littoral sediments of the alpine lakes support the view of them as nitrification hotspots (Mariotti et al., 1981), likely performed by AOA as suggested by the *amoA* gene abundance. Nitrification in rocky littoral sediments could be quantitatively more relevant than the isoetid rhizosphere given that rocky littorals occupy large areas in alpine lakes. Nevertheless, the archaeal *amoA* densities observed in the lower isoetid sediment layer were nearly 100-fold higher than in the rocky sediment samples with the highest AOA abundance. Sediments close to the roots of isoetids are episodically well-oxygenated due to the release of oxygen through roots during photosynthetic periods (Sand-Jensen et al., 1982), which increases the interface between oxidised and reduced sediments where the NH_4^+ oxidation occurs. Intensive nitrification would result in high NO_3^- accumulation in the sediment porewater (maxinun 2 mM; Catalan et al., 1994). However, this is likely transient as the NO_3^- concentration in the overlying water column was negligible, suggesting a close coupling of nitrification and denitrification in this habitat (Vila-Costa et al., 2016). Indeed, there was a positive correlation ($r = 0.68$, $p < 0.001$) between nitrification and denitrification gene abundances in the isoetid sediments of Plan lake. Lakes at a higher altitude, Contraix and Gelats de Bergús, also showed significant correlations between nitrification and denitrification gene abundances for deep and littoral habitats ($r = 0.48$, $p = 0.02$ and $r = 0.44$, $p = 0.08$, respectively), suggesting that nitrification and denitrification are also linked in the nitrification hotspots.

Linking the Taxonomic Distribution and Functional Potential

Each of the four main N-transforming communities consists of a highly diverse and distinct consortium of co-occurring bacterial taxa, based on the large number of indicator OTUs detected. However, taxonomic classification does not necessarily predict functioning, as different prokaryotic traits may be conserved at different phylogenetic depths (Martiny et al., 2015). While ammonia oxidation and anammox capacities are restricted to only a few lineages, denitrification and DNRA are widely distributed across the phylogeny (Graf et al., 2014; Welsh et al., 2014). Thus, many of the indicator OTUs identified are likely not directly involved in each N-transformation pathway. However, the high degree of similarity observed between unconstrained and functional gene-constrained OTU-based ordinations indicates that shifts in the genetic potential of different N-transformation processes are tightly linked to changes in the overall prokaryotic community structure, which itself is shaped by differences in environmental conditions across habitats.

Links between taxonomic composition and functional potential has been observed in previous works in lakes based on metagenomes or sequencing of functional genes. The occurrence of several proteobacterial families, in particular, Rhodobacteraceae (Alphaproteobacteria), Methylococcaceae (Gammaproteobacteria), and Burkholderiales, Comamonadaceae and Rhodocyclaceae (Betaproteobacteria) has been shown to be strongly associated with denitrification gene presence or abundance (Vila-Costa et al., 2014; Peura et al., 2015; Saarenheimo et al., 2015b; Castellano-Hinojosa et al., 2017; Chen R. et al., 2017). These taxa were also highly abundant in samples within the *nirS*-denitrifier and mixed functional gene communities, which included *nirK*-type denitrifiers. Moreover, metagenomic studies of boreal lakes water columns have identified *nosZ* sequences originating from Myxococcales (Deltaproteobacteria) and Sphingobacteriaceae (Bacteroidetes) in the hypolimnion near the oxycline (Peura et al., 2015, 2018). Many organisms within these families are known to possess the clade II variant of the *nosZ* gene (Hallin et al., 2018). Accordingly, a large proportion of indicator OTUs for the mixed N-cycling communities, which includes the clade II *nosZ* variant, were also classified as belonging to these families. The 4th most abundant genus in the studied lakes is *Anaeromyxobacter*, one member of this Deltaproteobacteria genus is *A. dehalogenans* a chemodenitrifier, an organism that combines chemical chemodenitrification reactions and enzymatic reaction(s) to reduce NO_3^- to N_2O or N_2, without

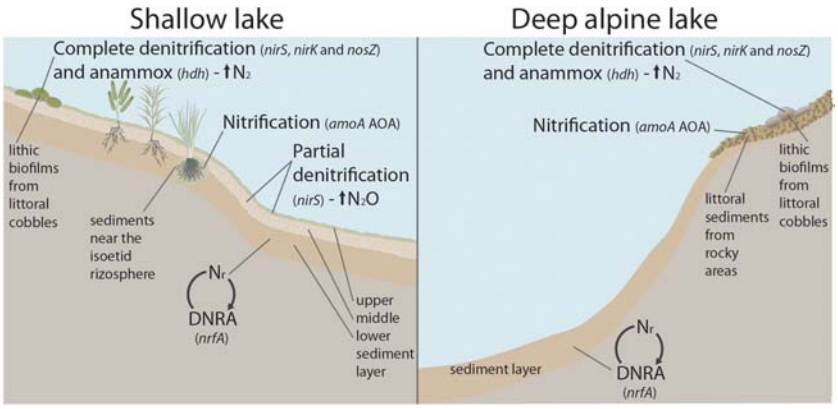

FIGURE 7 | Conceptual sketch of a shallow, mountain lake with macrophytes **(left)**, and a deep alpine lake **(right)**. The benthic habitats with the genetic potential for the dominant N-cycling process(es) and fate of N (N_r recycling, or N_2 and N_2O emission) are indicated. The dominant N functional gene(s) in each habitat are shown in italics. Abbreviations: N_r, reactive nitrogen; AOA, ammonia-oxidising archaea; anammox, anaerobic ammonium oxidation; DNRA, dissimilatory nitrate reduction to ammonium.

having denitrifying nitrite reductases codified by *nirS* or *nirK*, also performs DNRA and Fe-reduction (Onley et al., 2018). *Rhodoferax* (Beta-) and *Desulfomonile* (Delta-) possible chemodenitrifiers (Onley et al., 2018) were also common genus present. There are other eubacteria non-proteobacteria taxa also carrying denitrifying genes (Graf et al., 2014) present in our samples (e.g., Actinobacteria).

Operational taxonomic units associated with samples in the *nrfA* cluster were classified as Firmicutes, Epsilon- and Deltaproteobacteria (Campylobacterales and *Anaeromyxobacter*, *Desulfovibrio,* and *Geobacter*, respectively), Bacteroidetes (Bacteroidia), Actinobacteria (Coriobacterales and Corynebacterales) and Chloroflexi (Anaerolineaceae), all these taxa include microbes that are known to carry *nrfA* (Welsh et al., 2014).

Regarding the ammonia oxidisers, the primers used in the 16S rRNA sequencing mainly target bacteria, but also pick up Euryarchaeota (Takahashi et al., 2014). Therefore, OTUs assigned to Thaumarchaeota were not detected, although AOA hotspots could be identified based on qPCR data. Nitrosomonadaceae was the most common AOB, with 89 OTUs classified as being similar to uncultured members of this family. *Nitrospirae* was the only identified nitrite oxidising bacteria (NOB) in our samples. There was a likely coupling between AOA and NOB, as suggested by the correlation between archaeal *amoA* genes and the relative abundance of Nitrospirae members in general, and *Nitrospira* in particular, in the AOA-cluster samples (r = 0.65, p = 0.0005; r = 0.47, p = 0.02, respectively). This coupling has previously also been found in grasslands (Simonin et al., 2015), agricultural soils (Jones and Hallin, 2019), and sediments of an Andean mountain lake (Parro et al., 2019). Comammox *Nitrospira* could be important in the nitrifying hotspots found in the present study, as suggested by previous studies in other surface-attached oligotrophic habitats (Kits et al., 2017; Pjevac et al., 2017; Fowler et al., 2018). For anaerobic ammonia oxidation, OTUs belonging to the "*Candidatus* Anammoximicrobium" (Khramenkov et al., 2013) was the only taxa present with demonstrated anammox capacity. However, more bacteria within the numerous uncultured Planctomycetes detected in our samples could potentially perform anammox.

CONCLUSION

The N-transforming guild composition in benthic habitats of mountain lakes is complex and deeply embedded in the overall prokaryotic community. There is a high positive correlation among all the genes, and they all generally increase with OM. The dominant pathways change depending on the habitat and productivity of the lake (**Figure 7**). The fate of nitrite is the main diverging point differentiating the N-transforming guilds. The genetic potential for DNRA dominate in the deep part of the lakes and the lower sediment layers, which indicates recycling of the N_r. By contrast, the denitrifying *nirS* nitrite reduction potential prevails in the upper layer of the sediments in the shallow, warmer and more productive lakes, which indicates a loss of N_r. Emissions of N_2O and N_2 are likely spatially segregated within lakes, with lithic biofilms being candidates for preferential N loss as N_2 as they show a more balanced gene abundance of nitrous oxide reductases (*nosZ*I+II) and anammox (*hdh*) in relation to NO-forming nitrite reductases (*nirS*+*nirK*). The more productive and *nirS*-dominated habitats may be a main source of N_2O because of the striking excess of this gene over the ones of the final steps of complete denitrification unless another bypass process is relevant (e.g., N-DAMO). There may be two types of nitrifying-denitrifying coupled community types in the benthic habitats of mountain lakes. The first is based on nitrification by AOA coupled to Nitrospirae (NOB) and denitrification by *nirS*-denitrifiers, with hotspots in the rocky littoral sediments of the lakes above treeline and the sediments near the isoetid rhizosphere. The second includes AOB coupled to *nirK*-type denitrifiers reducing nitrite and *nosZ*I-N_2O reduction in the lithic biofilms. Overall, our results point out two types of potential

response to high atmospheric N deposition in these lakes. In highly oligotrophic lakes, there will be an accumulation of N_r because of the predominance of internal N_r recycling via DNRA. In less oligotrophic lakes, generally with macrophyte growth, the N_r deposition loads may be more effectively directed toward N gas release to the atmosphere via denitrification.

ETHICS STATEMENT

The authors declare that the present study does not involve human or animals, that they have all the licenses, and that they follow all the rules for sampling in the Aigüestortes National Park.

AUTHOR CONTRIBUTIONS

CP-L and JCat contributed to the study design. LC and CP-L carried out sampling. CP-L, CJ, and JCal carried out the lab work and data analysis. JCat, SH, LC, and EC contributed to reagents, materials, and analysis tools. CP-L and JCat wrote the manuscript. All authors substantially contributed to commenting and revising it.

FUNDING

The Spanish Government provided funds through the Ministerio de Educación as a predoctoral fellowship to CP-L (FPU12–00644) and research grants of the Ministerio de Economia y Competitividad: NitroPir (CGL2010–19737), DARKNESS (CGL2012-32747), LACUS (CGL2013–45348-P), TRANSFER (CGL2016–80124-C2-1-P). The REPLIM grant (INRE - INTERREG Programme. EUUN – European Union. EFA056/15) and the ALTER-NET Mobility Scheme supported the final writing.

ACKNOWLEDGMENTS

We thank the authorities of the Aigüestortes and Estany de Sant Maurici National Park for sampling facilities in protected areas and support.

SUPPLEMENTARY MATERIAL

The Supplementary Material for this article can be found online at: https://www.frontiersin.org/articles/10.3389/fmicb.2019.01229/full#supplementary-material

REFERENCES

Barnes, R. T., Smith, R. L., and Aiken, G. R. (2012). Linkages between denitrification and dissolved organic matter quality, Boulder Creek watershed, Colorado. *J. Geophys. Res.* 117:G01014.

Battin, T. J., Besemer, K., Bengtsson, M. M., Romani, A. M., and Packmann, A. I. (2016). The ecology and biogeochemistry of stream biofilms. *Nat. Rev. Microbiol.* 14, 251–263. doi: 10.1038/nrmicro.2016.15

Berry, D., Ben Mahfoudh, K., Wagner, M., and Loy, A. (2011). Barcoded primers used in multiplex amplicon pyrosequencing bias amplification. *Appl. Environ. Microbiol.* 77, 7846–7849. doi: 10.1128/AEM.05220-11

Blanchet, F. G., Legendre, P., and Borcard, D. (2008). Forward selection of explanatory variables. *Ecology* 89, 2623–2632. doi: 10.1890/07-0986.1

Borcard, D., Gillet, F., and Legendre, P. (2011). *Numerical Ecology with R*. New York, NY: Springer.

Cáceres, M. D., and Legendre, P. (2009). Associations between species and groups of sites: indices and statistical inference. *Ecology* 90, 3566–3574. doi: 10.1890/08-1823.1

Camarero, L. (2017). "Atmospheric chemical loadings in the high mountain: current forcing and legacy pollution," in *High Mountain Conservation in a Changing World*, eds J. Catalan, J. Ninot, and M. M. Aniz (New York, NY: Springer), 325–341. doi: 10.1007/978-3-319-55982-7_14

Camarero, L., and Catalan, J. (1998). A simple model of regional acidification for high mountain lakes: application to the Pyrenean lakes (north-east Spain). *Water Res.* 32, 1126–1136. doi: 10.1016/s0043-1354(97)00291-1

Camarero, L., and Catalan, J. (2012). Atmospheric phosphorus deposition may cause lakes to revert from phosphorus limitation back to nitrogen limitation. *Nat. Commun.* 3:1118. doi: 10.1038/ncomms2125

Castellano-Hinojosa, A., Correa-Galeote, D., Carrillo, P., Bedmar, E. J., and Medina-Sánchez, J. M. (2017). Denitrification and biodiversity of denitrifiers in a high-mountain Mediterranean lake. *Front. Microbiol.* 8:1911. doi: 10.3389/fmicb.2017.01911

Catalan, J., Ballesteros, E., Gacia, E., Palau, A., and Camarero, L. (1993). Chemical-composition of disturbed and undisturbed high-mountain lakes in the Pyrenees: a reference for acidified sites. *Water Res.* 27, 133–141. doi: 10.1016/0043-1354(93)90203-t

Catalan, J., Barbieri, M. G., Bartumeus, F., Bitušík, P., Botev, I., Brancelj, A., et al. (2009). Ecological thresholds in European alpine lakes. *Freshw. Biol.* 54, 2494–2517. doi: 10.1111/j.1365-2427.2009.02286.x

Catalan, J., Camarero, L., De Quijano, D. D., Felip, M., Pla, S., Ventura, M., et al. (2006). High mountain lakes: extreme habitats and witnesses of environmental changes. *Limnetica* 25, 551–584.

Catalan, J., Camarero, L., Gacia, E., Ballesteros, E., and Felip, M. (1994). Nitrogen in the Pyrenean lakes (Spain). *Hydrobiologia* 274, 17–27. doi: 10.1007/978-94-017-2095-3_3

Catalan, J., Pla-Rabes, S., Wolfe, A. P., Smol, J. P., Ruhland, K. M., Anderson, N. J., et al. (2013). Global change revealed by palaeolimnological records from remote lakes: a review. *J. Paleolimnol.* 49, 513–535. doi: 10.1007/s10933-013-9681-2

Chen, J., Hanke, A., Tegetmeyer, H. E., Kattelmann, I., Sharma, R., Hamann, E., et al. (2017). Impacts of chemical gradients on microbial community structure. *ISME J.* 11, 920–931. doi: 10.1038/ismej.2016.175

Chen, R., Deng, M., He, X., and Hou, J. (2017). Enhancing nitrate removal from freshwater pond by regulating carbon/nitrogen ratio. *Front. Microbiol.* 8:1712. doi: 10.3389/fmicb.2017.01712

Chen, X., Yang, L., Xiao, L., Miao, A., and Xi, B. (2012). Nitrogen removal by denitrification during cyanobacterial bloom in Lake Taihu. *J. Freshw. Ecol.* 27, 243–258. doi: 10.1080/02705060.2011.644405

Deutzmann, J. S., Stief, P., Brandes, J., and Schink, B. (2014). Anaerobic methane oxidation coupled to denitrification is the dominant methane sink in a deep lake. *Proc. Natl. Acad. Sci. U.S.A.* 111, 18273–18278. doi: 10.1073/pnas.1411617111

Dodla, S. K., Wang, J. J., Delaune, R. D., and Cook, R. L. (2008). Denitrification potential and its relation to organic carbon quality in three coastal wetland soils. *Sci. Total Environ.* 407, 471–480. doi: 10.1016/j.scitotenv.2008.08.022

Dore, J. E., Popp, B. N., Karl, D. M., and Sansone, F. J. (1998). A large source of atmospheric nitrous oxide from subtropical North Pacific surface waters. *Nature* 396, 63–66. doi: 10.1038/23921

Edgar, R. C. (2013). UPARSE highly accurate OTU sequences from microbial amplicon reads. *Nat. Methods* 10, 996–998. doi: 10.1038/nmeth.2604

Erisman, J. W., Galloway, J., Seitzinger, S., Bleeker, A., and Butterbach-Bahl, K. (2011). Reactive nitrogen in the environment and its effect on climate change. *Curr. Opin. Environ. Sustain.* 3, 281–290. doi: 10.1016/j.cosust.2011.08.012

Fowler, S. J., Palomo, A., Dechesne, A., Mines, P. D., and Smets, B. F. (2018). Comammox nitrospira are abundant ammonia oxidizers in diverse groundwater-fed rapid sand filter communities. *Environ. Microbiol.* 20, 1002–1015. doi: 10.1111/1462-2920.14033

Gacia, E., Ballesteros, E., Camarero, L., Delgado, O., Palau, A., Riera, J. L., et al. (1994). Macrophytes from lakes in the eastern pyrenees: community composition and ordination in relation to environmental factors. *Freshw. Biol.* 32, 73–81. doi: 10.1111/j.1365-2427.1994.tb00867.x

Gacia, E., Chappuis, E., Lumbreras, A., Riera, J. L., and Ballesteros, E. (2009). Functional diversity of macrophyte communities within and between Pyrenean lakes. *J. Limnol.* 68, 25–36.

Gardner, W. S., Newell, S. E., Mccarthy, M. J., Hoffman, D. K., Lu, K., Lavrentyev, P. J., et al. (2017). Community biological ammonium demand: a conceptual model for Cyanobacteria blooms in eutrophic lakes. *Environ. Sci. Technol.* 51, 7785–7793. doi: 10.1021/acs.est.6b06296

Glew, J. (1991). Miniature gravity corer for recovering short sediment cores. *J. Paleolimnol.* 5, 285–287. doi: 10.1007/BF00200351

Graf, D. R. H., Jones, C. M., and Hallin, S. (2014). Intergenomic comparisons highlight modularity of the denitrification pathway and underpin the importance of community structure for N2O emissions. *PLoS One* 9:e114118. doi: 10.1371/journal.pone.0114118

Hallin, S., and Lindgren, P. E. (1999). PCR detection of genes encoding nitrile reductase in denitrifying bacteria. *Appl. Environ. Microbiol.* 65, 1652–1657.

Hallin, S., Philippot, L., Löffler, F. E., Sanford, R. A., and Jones, C. M. (2018). Genomics and ecology of novel N2O-reducing microorganisms. *Trends Microbiol.* 26, 43–55. doi: 10.1016/j.tim.2017.07.003

Heiri, O., Lotter, A. F., and Lemcke, G. (2001). Loss on ignition as a method for estimating organic and carbonate content in sediments: reproducibility and comparability of results. *J. Paleolimnol.* 25, 101–110.

Henry, S., Bru, D., Stres, B., Hallet, S., and Philippot, L. (2006). Quantitative detection of the nosZ gene, encoding nitrous oxide reductase, and comparison of the abundances of 16S rRNA, narG, nirK, and nosZ genes in soils. *Appl. Environ. Microbiol.* 72, 5181–5189. doi: 10.1128/aem.00231-06

Holtgrieve, G. W., Schindler, D. E., Hobbs, W. O., Leavitt, P. R., Ward, E. J., Bunting, L., et al. (2011). A coherent signature of anthropogenic nitrogen deposition to remote watersheds of the northern hemisphere. *Science* 334, 1545–1548. doi: 10.1126/science.1212267

Jones, C. M., Graf, D. R., Bru, D., Philippot, L., and Hallin, S. (2013). The unaccounted yet abundant nitrous oxide-reducing microbial community: a potential nitrous oxide sink. *ISME J.* 7, 417–426. doi: 10.1038/ismej.2012.125

Jones, C. M., and Hallin, S. (2019). Geospatial variation in co-occurrence networks of nitrifying microbial guilds. *Mol. Ecol.* 28, 293–306. doi: 10.1111/mec.14893

Kessler, A. J., Roberts, K. L., Bissett, A., and Cook, P. L. (2018). Biogeochemical controls on the relative importance of denitrification and dissimilatory nitrate reduction to ammonium in estuaries. *Glob. Biogeochem. Cycles* 32, 1045–1057. doi: 10.1029/2018gb005908

Khramenkov, S. V., Kozlov, M. N., Kevbrina, M. V., Dorofeev, A. G., Kazakova, E. A., Grachev, V. A., et al. (2013). A novel bacterium carrying out anaerobic ammonium oxidation in a reactor for biological treatment of the filtrate of wastewater fermented sludge. *Microbiology* 82, 628–636. doi: 10.1134/s002626171305007x

Kits, K. D., Campbell, D. J., Rosana, A. R., and Stein, L. Y. (2015a). Diverse electron sources support denitrification under hypoxia in the obligate methanotroph Methylomicrobium album strain BG8. *Front. Microbiol.* 6:1072. doi: 10.3389/fmicb.2015.01072

Kits, K. D., Klotz, M. G., and Stein, L. Y. (2015b). Methane oxidation coupled to nitrate reduction under hypoxia by the Gammaproteobacterium Methylomonas denitrificans, sp. nov. type strain FJG1. *Environ. Microbiol.* 17, 3219–3232. doi: 10.1111/1462-2920.12772

Kits, K. D., Sedlacek, C. J., Lebedeva, E. V., Han, P., Bulaev, A., Pjevac, P., et al. (2017). Kinetic analysis of a complete nitrifier reveals an oligotrophic lifestyle. *Nature* 549, 269–272. doi: 10.1038/nature23679

Kopàček, J., Hejzlar, J., Vrba, J., and Stuchlík, E. (2011). Phosphorus loading of mountain lakes: terrestrial export and atmospheric deposition. *Limnol. Oceanogr.* 56, 1343–1354. doi: 10.4319/lo.2011.56.4.1343

Kraft, B., Tegetmeyer, H. E., Sharma, R., Klotz, M. G., Ferdelman, T. G., Hettich, R. L., et al. (2014). The environmental controls that govern the end product of bacterial nitrate respiration. *Science* 345, 676–679. doi: 10.1126/science.1254070

Kuypers, M. M. M., Marchant, H. K., and Kartal, B. (2018). The microbial nitrogen-cycling network. *Nat. Rev. Microbiol.* 16, 263–276. doi: 10.1038/nrmicro.2018.9

Lopez-Gutierrez, J. C., Henry, S., Hallet, S., Martin-Laurent, F., Catroux, G., and Philippot, L. (2004). Quantification of a novel group of nitrate-reducing bacteria in the environment by real-time PCR. *J. Microbiol. Methods* 57, 399–407. doi: 10.1016/j.mimet.2004.02.009

Mariotti, A., Germon, J., Hubert, P., Kaiser, P., Letolle, R., Tardieux, A., et al. (1981). Experimental determination of nitrogen kinetic isotope fractionation: some principles; illustration for the denitrification and nitrification processes. *Plant Soil* 62, 413–430. doi: 10.1007/bf02374138

Martiny, J. B., Jones, S. E., Lennon, J. T., and Martiny, A. C. (2015). Microbiomes in light of traits: a phylogenetic perspective. *Science* 350:aac9323. doi: 10.1126/science.aac9323

McCrackin, M. L., and Elser, J. J. (2010). Atmospheric nitrogen deposition influences denitrification and nitrous oxide production in lakes. *Ecology* 91, 528–539. doi: 10.1890/08-2210.1

Melton, E. D., Stief, P., Behrens, S., Kappler, A., and Schmidt, C. (2014). High spatial resolution of distribution and interconnections between Fe- and N-redox processes in profundal lake sediments. *Environ. Microbiol.* 16, 3287–3303. doi: 10.1111/1462-2920.12566

Merbt, S. N., Bernal, S., Proia, L., Martí, E., and Casamayor, E. O. (2017). Photoinhibition on natural ammonia oxidizers biofilm populations and implications for nitrogen uptake in stream biofilms. *Limnol. Oceanogr.* 62, 364–375. doi: 10.1002/lno.10436

Mohan, S. B., Schmid, M., Jetten, M., and Cole, J. (2004). Detection and widespread distribution of the nrfA gene encoding nitrite reduction to ammonia, a short circuit in the biological nitrogen cycle that competes with denitrification. *FEMS Microbiol. Ecol.* 49, 433–443. doi: 10.1016/j.femsec.2004.04.012

Myrstener, M., Jonsson, A., and Bergstrom, A. K. (2016). The effects of temperature and resource availability on denitrification and relative N2O production in boreal lake sediments. *J. Environ. Sci.* 47, 82–90. doi: 10.1016/j.jes.2016.03.003

Naqvi, S. W. A., Lam, P., Narvenkar, G., Sarkar, A., Naik, H., Pratihary, A., et al. (2018). Methane stimulates massive nitrogen loss from freshwater reservoirs in India. *Nat. Commun.* 9:1265. doi: 10.1038/s41467-018-03607-z

Onley, J. R., Ahsan, S., Sanford, R. A., and Löffler, F. E. (2018). Denitrification by Anaeromyxobacter dehalogenans, a common soil bacterium lacking the nitrite reductase genes nirS and nirK. *Appl. Environ. Microbiol.* 84:e1985-17. doi: 10.1128/AEM.01985-17

Pajares, S., Merino-Ibarra, M., Macek, M., and Alcocer, J. (2017). Vertical and seasonal distribution of picoplankton and functional nitrogen genes in a high-altitude warm-monomictic tropical lake. *Freshw. Biol.* 62, 1180–1193. doi: 10.1111/fwb.12935

Palacin-Lizarbe, C., Camarero, L., and Catalan, J. (2018). Denitrification temperature dependence in remote, cold, and N-poor lake sediments. *Water Resour. Res.* 54, 1161–1173. doi: 10.1002/2017wr021680

Parro, V., Puente-Sánchez, F., Cabrol, N. A., Gallardo-Carreño, I., Moreno-Paz, M., Blanco, Y., et al. (2019). Microbiology and nitrogen cycle in the benthic sediments of a glacial oligotrophic deep andean lake as analog of ancient martian lake-beds. *Front. Microbiol.* 10:929. doi: 10.3389/fmicb.2019.00929

Peura, S., Buck, M., Aalto, S. L., Morales, S. E., Nykanen, H., and Eiler, A. (2018). Novel autotrophic organisms contribute significantly to the internal carbon cycling potential of a boreal lake. *mBio* 9, e916–e918. doi: 10.1128/mBio.00916-18

Peura, S., Sinclair, L., Bertilsson, S., and Eiler, A. (2015). Metagenomic insights into strategies of aerobic and anaerobic carbon and nitrogen transformation in boreal lakes. *Sci. Rep.* 5:12102. doi: 10.1038/srep12102

Pjevac, P., Schauberger, C., Poghosyan, L., Herbold, C. W., Van Kessel, M., Daebeler, A., et al. (2017). AmoA-targeted polymerase chain reaction primers for the specific detection and quantification of comammox Nitrospira in the environment. *Front. Microbiol.* 8:1508. doi: 10.3389/fmicb.2017.01508

Quast, C., Pruesse, E., Yilmaz, P., Gerken, J., Schweer, T., Yarza, P., et al. (2013). The SILVA ribosomal RNA gene database project: improved data processing and web-based tools. *Nucleic Acids Res.* 41, D590–D596. doi: 10.1093/nar/gks1219

Rockström, J., Steffen, W., Noone, K., Persson, A., Chapin, F. S. III, Lambin, E. F., et al. (2009). A safe operating space for humanity. *Nature* 461, 472–475.

Rotthauwe, J. H., Witzel, K. P., and Liesack, W. (1997). The ammonia monooxygenase structural gene amoA as a functional marker: molecular fine-scale analysis of natural ammonia-oxidizing populations. *Appl. Environ. Microbiol.* 63, 4704–4712.

R Core Team (2017). *R: A Language and Environment for Statistical Computing*. Available at: http://www.r-project.org (accessed May 22, 2019).

Saarenheimo, J., Rissanen, A. J., Arvola, L., Nykanen, H., Lehmann, M. F., and Tiirola, M. (2015a). Genetic and environmental controls on nitrous oxide accumulation in lakes. *PLoS One* 10:e0121201. doi: 10.1371/journal.pone.0121201

Saarenheimo, J., Tiirola, M., and Rissanen, A. J. (2015b). Functional gene pyrosequencing reveals core proteobacterial denitrifiers in boreal lakes. *Front. Microbiol.* 6:674. doi: 10.3389/fmicb.2015.00674

Sand-Jensen, K., Prahl, C., and Stokholm, H. (1982). Oxygen release from roots of submerged aquatic macrophytes. *Oikos* 38, 349–354.

Schmid, M. C., Hooper, A. B., Klotz, M. G., Woebken, D., Lam, P., Kuypers, M. M. M., et al. (2008). Environmental detection of octahaem cytochrome c hydroxylamine/hydrazine oxidoreductase genes of aerobic and anaerobic ammonium-oxidizing bacteria. *Environ. Microbiol.* 10, 3140–3149. doi: 10.1111/j.1462-2920.2008.01732.x

Shen, L.-D., Ouyang, L., Zhu, Y., and Trimmer, M. (2019). Active pathways of anaerobic methane oxidation across contrasting riverbeds. *ISME J.* 13, 752–766.

Simon, J., and Klotz, M. G. (2013). Diversity and evolution of bioenergetic systems involved in microbial nitrogen compound transformations. *Biochim. Biophys. Acta* 1827, 114–135. doi: 10.1016/j.bbabio.2012.07.005

Simonin, M., Le Roux, X., Poly, F., Lerondelle, C., Hungate, B. A., Nunan, N., et al. (2015). Coupling between and among ammonia oxidizers and nitrite oxidizers in grassland mesocosms submitted to elevated CO2 and nitrogen supply. *Microb. Ecol.* 70, 809–818. doi: 10.1007/s00248-015-0604-9

Smol, J. P. (2012). A planet in flux: how is life on Earth reacting to climate change? *Nature* 483, S12–S15.

Stelzer, R., Scott, J. T., Bartsch, L. A., and Parr, T. (2014). Particulate organic matter quality influences nitrate retention and denitrification in stream sediments: evidence from a carbon burial experiment. *Biogeochemistry* 119, 387–402. doi: 10.1007/s10533-014-9975-0

Storey, J. D., Taylor, J. E., and Siegmund, D. (2004). Strong control, conservative point estimation and simultaneous conservative consistency of false discovery rates: a unified approach. *J. R. Stat. Soc. B Met.* 66, 187–205. doi: 10.1111/j.1467-9868.2004.00439.x

Takahashi, S., Tomita, J., Nishioka, K., Hisada, T., and Nishijima, M. (2014). Development of a prokaryotic universal primer for simultaneous analysis of Bacteria and Archaea using next-generation sequencing. *PLoS One* 9:e105592. doi: 10.1371/journal.pone.0105592

Throbäck, I. N., Enwall, K., Jarvis, Å, and Hallin, S. (2004). Reassessing PCR primers targeting nirS, nirK and nosZ genes for community surveys of denitrifying bacteria with DGGE. *FEMS Microbiol. Ecol.* 49, 401–417. doi: 10.1016/j.femsec.2004.04.011

Tourna, M., Freitag, T. E., Nicol, G. W., and Prosser, J. I. (2008). Growth, activity and temperature responses of ammonia-oxidizing archaea and bacteria in soil microcosms. *Environ. Microbiol.* 10, 1357–1364. doi: 10.1111/j.1462-2920.2007.01563.x

Van Mooy, B., Keil, R., and Devol, A. (2002). Impact of suboxia on sinking particulate organic carbon: enhanced carbon flux and preferential degradation of amino acids via denitrification. *Geochim. Cosmochim. Acta* 66, 457–465. doi: 10.1016/s0016-7037(01)00787-6

Vila-Costa, M., Bartrons, M., Catalan, J., and Casamayor, E. O. (2014). Nitrogen-cycling genes in epilithic biofilms of oligotrophic high-altitude lakes (Central Pyrenees, Spain). *Microb. Ecol.* 68, 60–69. doi: 10.1007/s00248-014-0417-2

Vila-Costa, M., Pulido, C., Chappuis, E., Calviño, A., Casamayor, E. O., and Gacia, E. (2016). Macrophyte landscape modulates lake ecosystem-level nitrogen losses through tightly coupled plant-microbe interactions. *Limnol. Oceanogr.* 61, 78–88. doi: 10.1002/lno.10209

Wallenstein, M. D., Myrold, D. D., Firestone, M., and Voytek, M. (2006). Environmental controls on denitrifying communities and denitrification rates: insights from molecular methods. *Ecol. Appl.* 16, 2143–2152. doi: 10.1890/1051-0761(2006)016%5B2143:ecodca%5D2.0.co;2

Wang, Q., Garrity, G. M., Tiedje, J. M., and Cole, J. R. (2007). naive bayesian classifier for rapid assignment of rRNA sequences into the new bacterial taxonomy. *Appl. Environ. Microbiol.* 73, 5261–5267. doi: 10.1128/aem.00062-07

Welsh, A., Chee-Sanford, J. C., Connor, L. M., Loffler, F. E., and Sanford, R. A. (2014). Refined NrfA phylogeny improves PCR-based nrfA gene detection. *Appl. Environ. Microbiol.* 80, 2110–2119. doi: 10.1128/AEM.03443-13

Wittorf, L., Bonilla-Rosso, G., Jones, C. M., Backman, O., Hulth, S., and Hallin, S. (2016). Habitat partitioning of marine benthic denitrifier communities in response to oxygen availability. *Environ. Microbiol. Rep.* 8, 486–492. doi: 10.1111/1758-2229.12393

Zhang, J., Kobert, K., Flouri, T., and Stamatakis, A. (2013). PEAR: a fast and accurate Illumina paired-end read mergeR. *Bioinformatics* 30, 614–620. doi: 10.1093/bioinformatics/btt593

Conflict of Interest Statement: The authors declare that the research was conducted in the absence of any commercial or financial relationships that could be construed as a potential conflict of interest.

Copyright © 2019 Palacin-Lizarbe, Camarero, Hallin, Jones, Cáliz, Casamayor and Catalan. This is an open-access article distributed under the terms of the Creative Commons Attribution License (CC BY). The use, distribution or reproduction in other forums is permitted, provided the original author(s) and the copyright owner(s) are credited and that the original publication in this journal is cited, in accordance with accepted academic practice. No use, distribution or reproduction is permitted which does not comply with these terms.

frontiers in Microbiology

ORIGINAL RESEARCH
published: 02 July 2019
doi: 10.3389/fmicb.2019.01448

Decoupling the Dynamics of Bacterial Taxonomy and Antibiotic Resistance Function in a Subtropical Urban Reservoir as Revealed by High-Frequency Sampling

*Peiju Fang[1,2], Feng Peng[1,2], Xiaofei Gao[1,2], Peng Xiao[1] and Jun Yang[1]**

[1] Aquatic Ecohealth Group, Key Laboratory of Urban Environment and Health, Institute of Urban Environment, Chinese Academy of Sciences, Xiamen, China, [2] University of Chinese Academy of Sciences, Beijing, China

Aquatic environments serve as important reservoirs of antibiotic resistance genes (ARGs), but the information on the high-resolution temporal pattern of ARGs in waterbodies is extremely limited. In this study, the weekly dynamics of ARGs and their relationships with microbial taxonomic communities and environmental variables were analyzed in a subtropical urban reservoir over the period of 1 year using high-throughput approaches. In total, 197 ARGs and 10 mobile genetic elements (MGEs) were detected. The results showed that the bacterial community had a seasonal pattern, while ARGs composition did not exhibit seasonality, thereby indicating the asynchrony or decoupling of temporal patterns of microbial taxonomy and function. More importantly, bacterial abundance and community diversity were more strongly correlated with 17 measured environmental variables than ARGs (36 significant correlations for OTUs, 11 for ARGs). However, stochastic processes appeared to have a minor role in the structuring of the ARG profiles, but a more important role in the structuring of bacterial taxonomic communities. Furthermore, we found that precipitation and turbidity were significantly correlated with the richness and diversity of ARGs, suggesting that multiple environmental factors influence the composition and dynamics of ARGs in complex ways. MGEs were abundant and showed significant positive correlations with ARGs, indicating a plausible influence of MGEs on the variation of ARGs. This is the first study which provides an overview of high-resolution dynamics of ARGs in a subtropical waterbody. Our results improve the understanding of microbial processes and mechanisms of ARGs at fine temporal scale, and offer empirical data of use in the monitoring, assessment and management of the urban water environments.

Keywords: antibiotic resistance genes, bacterioplankton, microbial community, high-resolution temporal pattern, subtropical reservoir

OPEN ACCESS

Edited by:
Haihan Zhang,
Xi'an University of Architecture and Technology, China

Reviewed by:
Wenguang Xiong,
South China Agricultural University, China
Yihui Ban,
Wuhan University of Technology, China

***Correspondence:**
Jun Yang
jyang@iue.ac.cn

Specialty section:
This article was submitted to Aquatic Microbiology, a section of the journal Frontiers in Microbiology

Received: *03 April 2019*
Accepted: *11 June 2019*
Published: *02 July 2019*

Citation:
Fang P, Peng F, Gao X, Xiao P and Yang J (2019) Decoupling the Dynamics of Bacterial Taxonomy and Antibiotic Resistance Function in a Subtropical Urban Reservoir as Revealed by High-Frequency Sampling. Front. Microbiol. 10:1448. doi: 10.3389/fmicb.2019.01448

INTRODUCTION

In aquatic ecosystems many studies have been carried out on nitrogen, phosphorus, and microbial community (Yang et al., 2012; Zhang et al., 2019), however various "emerging" pollutants including antibiotics and antibiotic resistance genes (ARGs) have been rapidly drawing increased attention from the public and government (Pruden et al., 2006; Zhu et al., 2017; Yang et al., 2018).

Antibiotics, first discovered by Sir Alexander Fleming in 1928, were regarded as panacea for any microbial infections (World Health Organization [WHO], 2014). However, with the emerging problem of antibiotic resistance, antibiotic resistant bacteria (ARB) and ARGs have been identified as a significant issue, posing a serious threat to the health of humans and the environment (Pruden et al., 2006; Berendonk et al., 2015). Antibiotic resistance is ancient (D'Costa et al., 2011), but with the continuous increase in discharge of overused antibiotics, the development, spread, and enrichment of ARGs has accelerated globally (Laxminarayan, 2014), and heavy metal has been reported to play an important role in the enrichment of antibiotic resistance by co-selection mechanisms (Stepanauskas et al., 2006). More importantly, ARGs can be exchanged and transferred among environmental bacteria, pathogens and non-pathogens via horizontal gene transfer (HGT) carried out by mobile genetic elements (MGEs) (Kruse and Sørum, 1994; Martínez et al., 2015). Aquatic environments are considered to be significant reservoirs of both ARB and ARGs, providing ideal settings for the occurrence and dissemination of ARGs (Marti et al., 2014). Due to long-term misuse and overuse of antibiotics by human, urban water often contains diverse ARGs at high levels (Xu et al., 2016), which may pose high risk to human health during the interaction with receivers. Therefore, ARGs occurrence and their temporal dynamics in the aquatic environment have become an important issue in environmental science (Yang et al., 2018).

Microbial communities can vary between environments, and play an important role in drive global biogeochemical cycling, but it is not well known how variation in taxonomic composition relates to function (Louca et al., 2016). Previous studies reported that bacterial community composition closely correlates with ARG profiles and controls the transfer of ARGs in antibiotic-rich environments (e.g., soil, urban wastewater, and sewage sludge) (Forsberg et al., 2014; Su et al., 2015), but the contribution of microbial community shifts to antibiotic resistance function variations in natural waterbodies with low and medium antibiotic concentrations remains largely unknown, especially at a fine temporal scale. Furthermore, microbial communities have been reported to exhibit seasonal variability in the environment (Treusch et al., 2009), and high-frequency sampling analysis could reveal and disentangle detailed temporal dynamics of bacterial community (Lindh et al., 2015). Previous studies have assessed the temporal variation of ARGs and supported the occurrence of seasonal variations of ARGs based on only two or four sampling time points in 1 year (An et al., 2018; Zheng et al., 2018). However, research on the dynamics of ARGs in urban water environment, and their relationship to microbial taxonomic community and environmental factors based on high-frequency time series is still lacking.

Revealing the mechanisms that drive the variation of microbial communities and ARG profiles are major challenges. It has been shown that microbial communities are simultaneously shaped by stochastic (neutral) and deterministic processes (Sloan et al., 2006; Logares et al., 2013). The neutral model is a stochastic process that develops community through births, death and immigration, can successfully predict microbial community assembly dynamics (Hubbell, 2001). However, the neutral model cannot completely descript the community assembly without deterministic process such as environmental factors and competition (Sloan et al., 2006; Ofiţeru et al., 2010). Both stochastic (neutral) and deterministic processes need to be considered when investigating the assembly of microbial communities and ARG profiles, but there is still a lack of studies on the contribution of both processes in structuring ARG profiles (Zhu et al., 2017; Guo et al., 2018).

The urban reservoir in this study is located in a rapidly urbanizing area of Xiamen, it receives numerous pollutants from surrounding housing estates by point and non-point source pollutions. However, this urban reservoir is the most important landscape waterbody in the Jimei district, so the ARB and ARGs in the water may pose ecological risk in the interaction with inhabitants and tourists. In this study, we simultaneously investigated the dynamics of bacterial OTUs and ARGs in the urban reservoir using high-throughput qPCR and 16S rRNA gene sequencing on a weekly basis over a 1-year period. We aimed to (1) characterize the temporal dynamics of both bacterial taxonomic community and antibiotic resistance gene profiles; (2) reveal the relationships between bacterial taxonomic composition and antibiotic resistance function at different levels of taxonomic resolution; and (3) explore the community assembly processes and mechanisms shaping the ARGs composition dynamics. Additionally, we hypothesize that the temporal patterns of microbial OTUs and ARGs are asynchronous, and their temporal patterns are influenced by different processes and mechanisms. To our best knowledge, this is the first study to analyze a high-resolution time series of bacterial OTUs and ARGs communities in urban water environments. Therefore, this study may provide a fundamental data for evaluating the ecological risks of ARGs in urban water environment and offer useful information for government and policy maker.

MATERIALS AND METHODS

Study Area and Sample Collection

All samples were collected once a week from September 2016 to August 2017 in station G (24°36′ N, 118°04′ E) of Xinglinwan Reservoir, which is situated in the Houxi River watershed, Xiamen city, Fujian province, southeast China (**Supplementary Figure S1**). In total, 51 samples were collected in this study. Several stormwater and wastewater inlets were found near the station G along the reservoir shoreline within a distance of 1000 m. The Xinglinwan Reservoir is a subtropical eutrophic urban reservoir, and is characterized by high turbidity and low water transparency. It has multiple functions in flood control, aquaculture and tourism, exerting a great impact on the surrounding residents.

Surface waters were collected in a sterile container from the top 0.5 m water, immediately transported to laboratory and kept in the dark until pre-treatment within 0.5 h. In order to remove the influence of large plankton and particles, samples were pre-filtered through a 200 μm mesh, and then filtered through

0.22 μm polycarbonate membranes (47 mm diameter, Millipore, Billerica, MA, United States) using a vacuum filtration system. To ensure the sufficient microorganisms, the filtrated water volume ranged from 200 to 500 mL for all samples, because we kept a similar filtrating time (about 50 min) for each of membranes. The membranes were placed in sterilized tubes and stored at −80°C until DNA extraction.

Environmental Parameters

A total of 17 environmental variables were determined in this study (**Supplementary Figure S2**). The comprehensive trophic state index (TSIc) were calculated according to Yang et al. (2012). Water temperature (WT), pH, dissolved oxygen (DO), turbidity, electrical conductivity (EC), salinity, and oxidation reduction potential (ORP) were measured *in situ* with a Hydrolab DS5 multiparameter water quality analyzer (Hach Company, Loveland, CO, United States). Chlorophyll *a* concentrations were quantified by PHYTO-PAM Phytoplankton Analyzer (Heinz Walz GmbH, Eichenring, Germany). Total carbon (TC), total organic carbon (TOC), total nitrogen (TN), ammonium nitrogen (NH_4-N), nitrate nitrogen (NO_3-N), nitrite nitrogen (NO_2-N), total phosphorus (TP), and phosphate phosphorus (PO_4-P) were measured according to the standard methods described in our previous study (Liu et al., 2013). The precipitation data referred to the cumulative rainfall during the last week before the sampling day, and the data were collected from the Xiamen Meteorological Bureau.

DNA Extraction and High-Throughput Sequencing

Total DNA was directly extracted from each membrane using the FastDNA SPIN Kit (MP Biomedical, Santa Ana, CA, United States) according to the manufacturer's protocol, and subsequently the concentration and quality of the DNA were determined using a NanoDrop 1000 spectrophotometer (Thermo Fisher Scientific, Waltham, MA, United States).

To investigate the bacterial taxonomic community, the V3-V4 hypervariable regions of the 16S rRNA gene were amplified, purified, and quantified according to our previous procedure (Guo et al., 2018). The PCR products were pooled and sequenced on the Illumina Miseq platform (Illumina, Inc., San Diego, CA, United States) using a paired-end (2 × 250 bp) sequencing strategy. All the raw sequences were quality-controlled using MOTHUR v1.39.0 (Schloss et al., 2009). The unoise3 pipeline was used to pick operational taxonomy units (OTUs) at 3% dissimilarity level (Edgar, 2010). OTU sequences were taxonomically classified by USEARCH (sintax) against the Greengenes database (DeSantis et al., 2006). All eukaryotic, chloroplast, archaeal, mitochondrial and unknown sequences were removed from the data set. Finally, all sequences were normalized to 50,014 sequences for each of 51 samples, and these sequences were clustered into 9834 OTUs.

The raw data for 16S rRNA gene analysis in this study have been deposited in the NCBI sequence read archive (SRA) database under the BioProject number PRJNA510463 and the accession number SRP173857.

High-Throughput Quantitative PCR (HT-qPCR)

High-throughput quantitative PCR was performed to detect the abundance of ARGs using the Wafergen SmartChip real-time qPCR platform (Wafergen Biosystems, Fremont, CA, United States). A total of 296 primer sets targeting 285 resistance genes, 8 transposase genes, the class I integron-integrase gene (*intI*), the clinical class 1 integron-integrase gene (*cIntI*), and 16S rRNA gene were used. These primer sets and PCR reaction protocols were listed in our previous studies (Guo et al., 2018; Liu et al., 2018). Three technical replicates were performed for each sample, and non-template negative control was also included for each primer set. The absolute abundance of ARGs and MGEs was calculated by normalizing their abundance to the absolute 16S rRNA gene copy number, which was estimated by real-time quantitative PCR (Ouyang et al., 2015) as described below.

Real-Time Quantitative PCR (qPCR)

Real-time quantitative PCR was used to quantify the absolute copy number of 16S rRNA genes in all samples. It was performed on a Lightcycler 480 instrument (Roche, Basel, Switzerland). The 20 μL reaction contained 10 μL 2× LightCycler 480 SYBR Green I Master Mix (Roche, Basel, Switzerland), 7 μL nuclease-free PCR-grade water, 2 μL diluted DNA, and 0.5 μM of each primer. The reactions were performed in triplicate with negative controls. The following thermal cycling conditions were used: initial incubation at 95°C for 5 min, followed by 40 cycles of 95°C for 15 s, 60°C for 1 min, and 72°C for 15 s.

A six-point calibration curve was generated from 10-fold dilutions for an external standard calculation. The melting curves were used to analyze the specificity of PCR products, and PCR efficiency ranged from 96 to 105% in this study.

Statistics

The Bray-Curtis similarity was calculated using PRIMER v7.0 (Clarke and Gorley, 2015), and non-linear regression of time lag with community similarity was analyzed to reveal the temporal patterns of bacterial OTUs and ARGs communities. The non-linear regression was the fit to the sinusoidal curve to explore the seasonality in SigmaPlot v12.0 (Systat Software Inc., Chicago, IL, United States). The diversity indexes were calculated using the vegan package in R v3.3.1. The SIMPER analysis was performed to identify the contribution of bacterial OTUs and ARGs to the temporal variation of communities or profiles (Clarke and Gorley, 2015).

Spearman's and Pearson's correlations were calculated using SPSS v20.0 (IBM Corp, Armonk, NY, United States), and the Mantel test was performed in an R environment with the vegan package. Further, a Procrustes test was conducted with the vegan package in R environment to explore the synchronicity of bacterial OTUs communities and ARG profiles (Forsberg et al., 2014). Network analysis was used to reveal Spearman correlations between ARGs and bacterial taxa with the picante package in R v3.3.1, and the correlation coefficients $|\rho| > 0.6$ between microbial taxa and ARGs, and $|\rho| > 0.4$ between MGEs and

ARGs, were considered at $P < 0.01$. Network information was generated by the Gephi v8.2 and Cytoscape v3.6.1.

In addition, we used redundancy analysis (RDA) to explore the relationship between environmental factors and the compositions of bacterial OTUs and ARGs subtypes. We further used partial redundancy analysis (pRDA) to evaluate the relative contribution of bacterial taxonomic community, environment variables and MGEs to the ARG profiles of all samples by R v3.3.1 with the vegan package. To reveal the assembly processes underlying both bacterial OTUs and ARGs compositions, we used the neutral community model, which can evaluate the importance of stochastic processes in explaining the assembly of bacterial taxonomic and functional communities (Sloan et al., 2006). This model predicts the relationship between the frequency at which taxa occur in a set of local communities (in this case, bacterial OTUs and ARGs at one sampling point) and their abundance across the wider metacommunity (bacterial OTUs and ARGs sampled over a year). The neutral models were performed in R v3.3.1 using the Hmisc, stats4, and minpack.lm packages.

RESULTS

Dynamics of Environmental Variables, Bacterial OTUs, and ARGs Compositions

The major physicochemical variables exhibited a great change over time (**Supplementary Figure S3**). Comprehensive TSIc varied from middle eutrophic level to hypereutrophic level, and nutrient concentrations were high throughout the study period, with higher value in 2017 than 2016. Water temperature ranged from 15 to 35°C during the 1-year sampling. Higher precipitation values were recorded in September 2016 and June 2017.

We found 197 unique ARGs and 10 MGEs in this study, and the ARGs covered almost all major classes of antibiotics commonly used. The number of ARGs detected in each sample varied from 18 to 74, representing three major resistance mechanisms including antibiotic deactivation (53.8%), cellular protection (28.6%), and efflux pump (16.9%) (**Supplementary Figure S4**). The absolute abundance of ARGs ranged from 4.03×10^6 copies/L to 3.72×10^9 copies/L (mean ± s.e. = $4.55 \times 10^8 \pm 1.11 \times 10^8$), while the absolute abundance of MGEs varied from 6.62×10^5 copies/L to 1.84×10^9 copies/L ($1.92 \times 10^8 \pm 5.28 \times 10^7$). The Shannon-Wiener index of bacteria ranged from 4.95 to 7.58 (**Supplementary Figure S5**). The bacterial community was dominated by Actinobacteria, Proteobacteria and Cyanobacteria, while Proteobacteria was the most abundant phylum in September and October (36.1% ± 2.5%, $n = 8$), and Actinobacteria dominated the bacterial community most of the time (37.9% ± 1.7%, $n = 43$).

Time series analysis indicated relative stability at bacterial phylum and ARG type level, but very rapid or abrupt fluctuations among both bacterial OTUs and ARG subtypes (**Figure 1**). The relative abundance of ARG subtypes exhibited distinct variations across the year at weekly intervals (**Figure 1D**). For example, the relative abundance of *qacEΔ1-02* (multidrug resistance gene) varied from 0 to 0.5 and its relative abundance changed almost every week. Time-lag regression analysis showed that the bacterial community displayed a good fit to a sinusoidal curve (**Figure 1E**), but ARG profiles failed to fit such a curve (**Figure 1F**); indicating that bacterial community composition exhibited seasonality while ARGs composition did not. The general variation of ARG similarity was narrower compared to the bacterial taxonomic community (**Supplementary Figure S6**), suggesting that the compositions of resistomes were more stable. Additionally, SIMPER analysis indicated that Proteobacteria contributed most to the variation within the microbial community (31.86%), while beta-lactamase resistance gene contributed most to the variation of ARGs (23.41%) (**Supplementary Table S1**). Furthermore, Procrustes test revealed asynchrony or decoupling between bacterial ARGs and OTUs communities ($r = 0.347$, $P < 0.01$, **Figure 2A**). However, the Pearson's correlation indicated a significant but weak relationship between bacterial ARGs and OTUs communities (**Figure 2B**).

Co-occurrence Patterns Between Bacterial Taxonomic Community and Antibiotic Resistome

Network analysis was performed to reveal the significant and robust correlations between ARG subtypes and bacterial OTUs. The whole network consisted of 1,547 nodes and 2,139 edges, and showed a modularity index of 0.762. Aminoglycoside resistance genes had the most edges (489) with bacterial taxa, followed by tetracycline (474), MLSB (454), and beta-lactamase (318) resistance genes (**Figures 3A,B**). Meanwhile, Proteobacteria, Bacteroidetes, Firmicutes, and TM7 were significantly correlated with most ARGs. The co-occurrence network showed that the hubs of all modules were ARGs (**Supplementary Figure S7A**), indicating the important roles of ARGs in the network.

We also used Mantel tests to evaluate the relationships between bacterial phyla and ARG types. Similar to the results of the network analysis, most ARGs were significantly and strongly correlated with Bacteroidetes, Firmicutes, and Proteobacteria (**Supplementary Table S2**). However, sulfonamide resistance genes did not show any significant correlation with the bacterial community, and MGEs only significantly correlated with Chloroflexi, Firmicutes, and TM7.

Relationships Between Environmental Factors, Bacterial OTUs, and ARGs

Mantel tests showed aminoglycoside, beta-lactamase, MLSB, tetracycline, and vancomycin resistance genes were significantly correlated with precipitation (**Supplementary Table S3**). RDA further indicated that water temperature, chlorophyll *a*, salinity, total carbon, TOC, total nitrogen, nitrate nitrogen, and total phosphorus were significantly correlated with the β-diversity of the bacterial community, while salinity, total carbon, nitrate nitrogen, total phosphorus, and precipitation were strongly correlated with ARGs compositions, suggesting that nutrients were key factors that influence the dynamics of

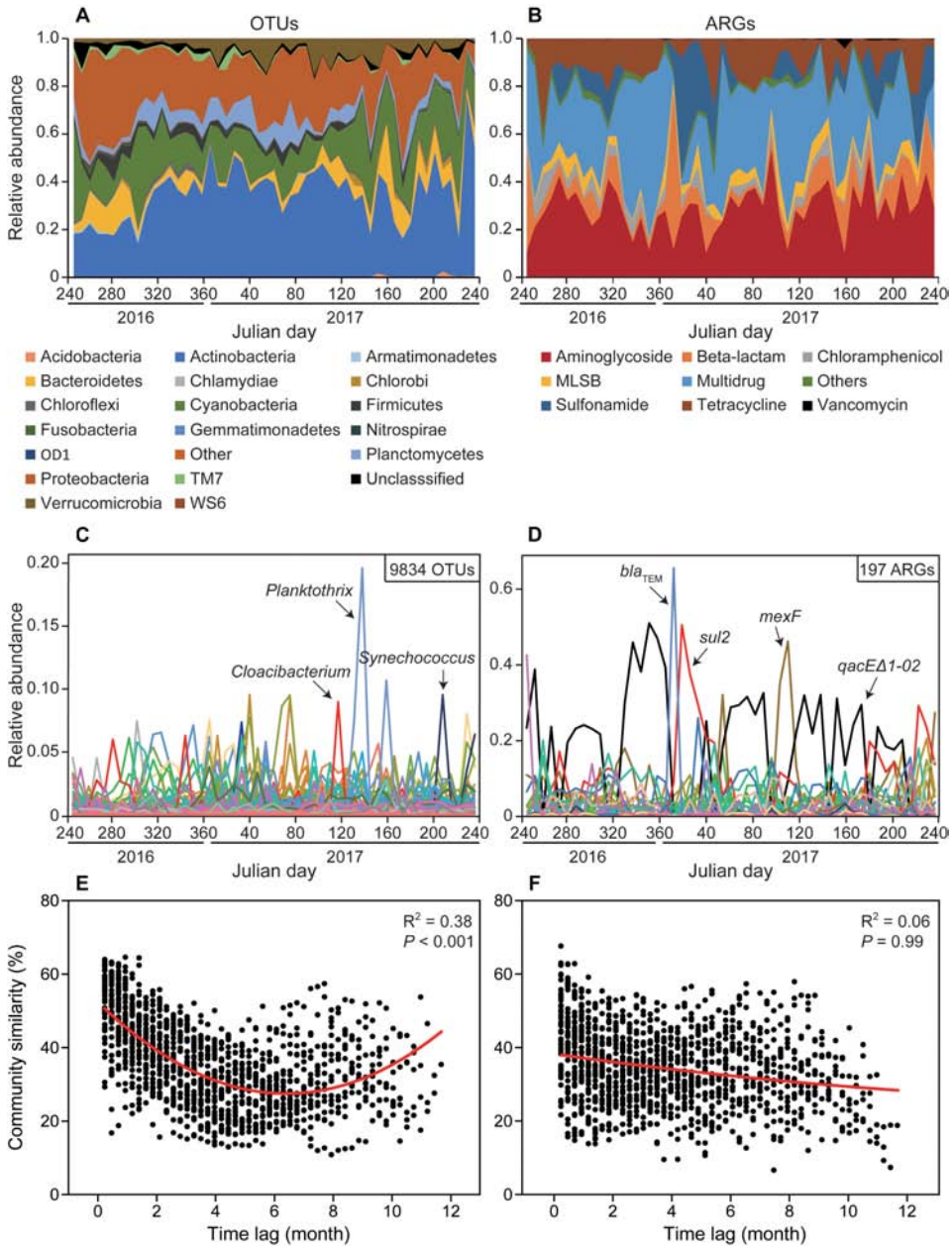

FIGURE 1 | Contrasting dynamics of bacterioplankton OTUs and antibiotic resistance genes (ARGs) from September 2016 to August 2017 in Xinglinwan Reservoir. Although relative abundances of bacteria at phylum level **(A)** and ARG at type level **(B)** appeared to be relatively stable, the relative abundances of bacterioplankton OTUs **(C)** and ARG subtypes **(D)** varied extensively and rapidly. Time-lag regression analysis showing temporal dynamics of bacterial community **(E)** and ARG profiles **(F)**. The red lines represent non-linear regression model fit to month lag versus Bray-Curtis similarity (%), and only bacterial community results in a good fit of a sinusoidal curve, indicating only bacterial community has the evidence of seasonality.

both ARGs and bacterial communities (**Figure 4**). We found that the bacterial community (R^2 = 0.365) showed a much better fitted to the neutral model (**Figure 4**) than ARGs (R^2 = 0.079), indicating that stochastic process played an important role in microbial community assembly but not in the resistome profiles.

The absolute abundance of ARGs was positively correlated with total carbon and TOC, while ARGs richness was significantly and positively correlated with turbidity and precipitation (**Figure 5A**). Additionally, turbidity and precipitation also exhibited a positive correlation with richness and α-diversity of bacterial community, but were not significantly correlated with 16S rRNA gene abundance (**Figure 5A**). Partial redundancy analysis showed that the bacterial community, MGEs and environmental factors separately explained 19.23, 19.87, and 9.4% of the variation of ARG profiles, respectively. Interaction between

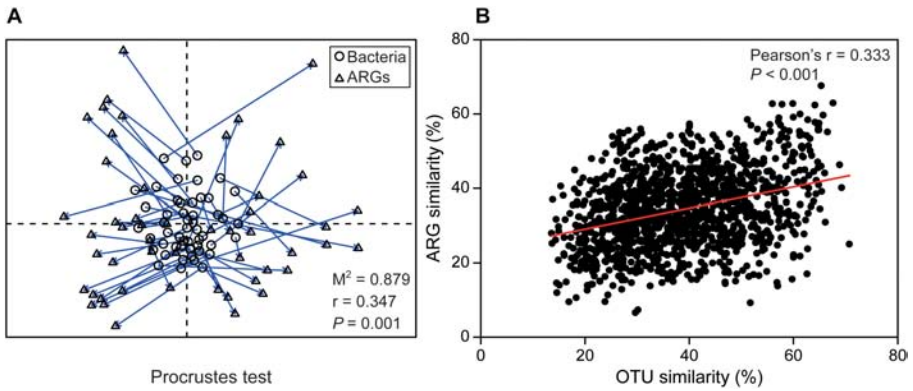

FIGURE 2 | The relationships between bacterial community and ARG profiles. **(A)** Procrustes test of the significant correlation between ARG composition and bacterial community composition based on Bray-Curtis similarity metrics (M^2 = 0.879, r = 0.347, P = 0.001, 999 permutations). **(B)** The significant but weak correlation between bacterial taxonomic community similarity and ARG profiles similarity.

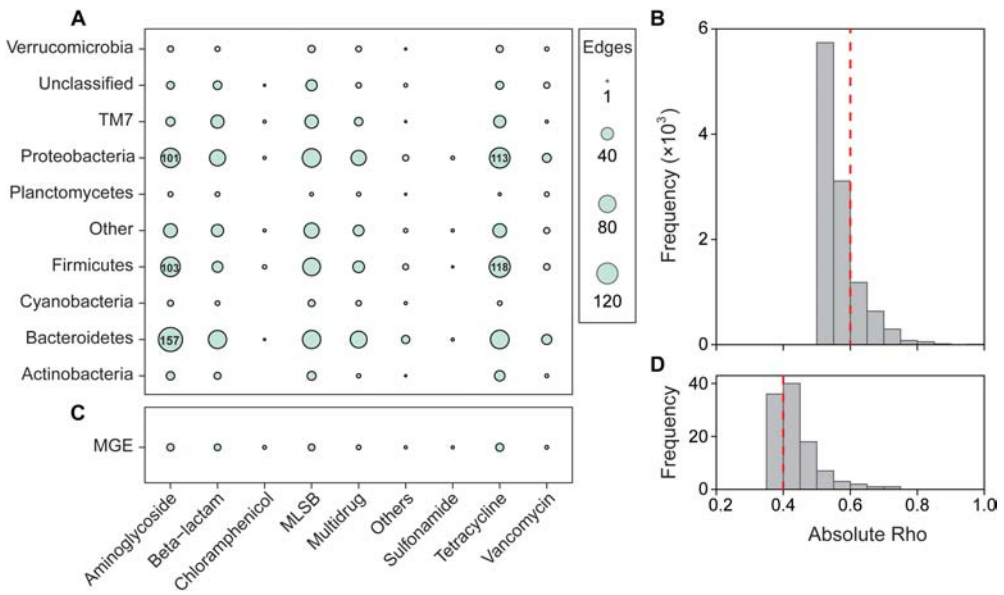

FIGURE 3 | Significant correlation among bacterial OTUs, ARGs, and MGEs. Classification of nodes within the network depicting the co-occurrence patterns of microbial taxa and ARGs **(A)**, MGEs and ARGs **(C)**. Other, other bacterial phyla; others, other ARGs. The Spearman's absolute rho was calculated at OTU and ARG subtype levels, and the number of edges was summarized at phylum and type levels, respectively. The edges correspond to a strong (Spearman's $|\rho| > 0.6$ for microbial taxa and ARGs, Spearman's $|\rho| > 0.4$ for MGEs and ARGs) and significant ($P < 0.01$) correlation between nodes. Frequency distributions of correlation coefficients between ARGs and microbial taxa **(B)** and between ARGs and MGEs **(D)** at $P < 0.01$.

all variables explained 4.63% of the variation, and 42.49% of the variation was unexplained.

Correlations Between ARGs and MGEs

The absolute abundance of ARGs was positively correlated with MGEs (**Supplementary Figure S8**), and the normalized abundance of MGEs was significantly correlated with the richness and normalized abundance of ARGs (**Supplementary Table S4**). The network analysis further indicated that aminoglycoside, beta-lactamase, MLSB, and tetracycline resistance genes were significantly correlated with MGEs (**Figures 3C,D**), and the co-occurrence pattern revealed that *Tp614* and *tnpA-03* play the most important roles in the network (**Supplementary Figure S7B**). However, the integrase gene *intI-1* only showed a significant correlation with multidrug and vancomycin resistance genes (**Supplementary Table S5**), but the absolute abundance of transpose gene *tnpA-05* showed a strong correlation to all ARG types except vancomycin resistance genes (**Supplementary Table S6**). Additionally, the transposase genes *IS613*, *tnpA-03*, *tnpA-04,* and *tnpA-07* also showed a significant correlation with some types of ARGs. Partial redundancy analysis showed that 19.87% of the variation of ARG profiles was explained by MGEs (**Figure 5B**), indicating that MGEs were an important contributor to the change

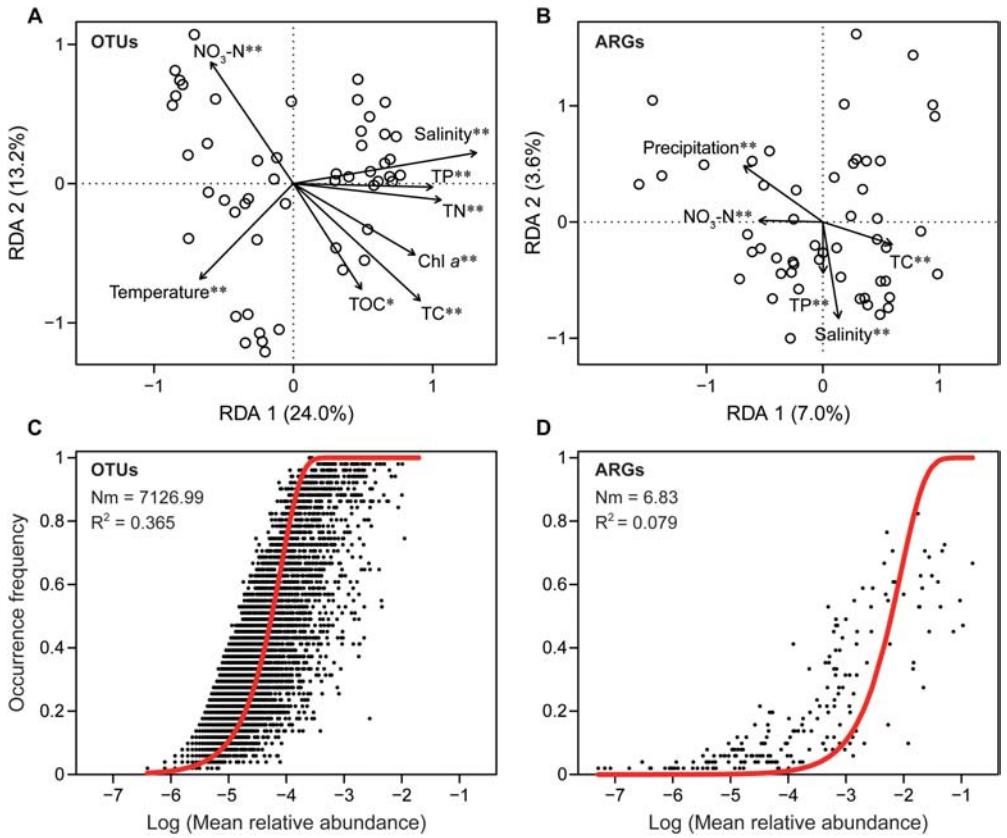

FIGURE 4 | The different assembly mechanisms of bacterial community (taxonomy) and ARG profiles (function). Redundancy analysis (RDA) showing the significant relationship between environmental factors and bacterial community **(A)**, environmental factors and ARGs **(B)**. Chl *a*, chlorophyll *a*; TC, total carbon; TOC, total organic carbon; TN, total nitrogen; NO_3-N, nitrate nitrogen; TP, total phosphorus. Only factors with significant correlation were included. $^*P < 0.05$; $^{**}P < 0.01$. Fit of neutral model for bacterial taxonomic **(C)** and ARG functional **(D)** communities. Red lines represent the best fit to the neutral model. Nm indicates metacommunity size times immigration, R^2 indicates the fit to the neutral model.

of ARG profiles during our study period. These results suggested that MGEs played a crucial role in the change, accumulation and dissemination of ARGs in this urban landscape reservoir.

DISCUSSION

The Contrasting Temporal Patterns Between Bacterial OTUs and ARGs

Our high-frequency time series-based study revealed clear differences in the temporal patterns of microbial communities and ARG profiles, along with the decoupling of the temporal dynamics of bacterial taxonomy and antibiotic resistance function in an urban waterbody. The composition of ARG subtypes varied frequently over the year but was relatively stable at the ARG type level. None of the ARG subtypes was present in all 51 samples, and no distinct seasonal patterns in ARG profiles could be determined, but microbial taxonomic community had significant seasonal pattern.

ARGs in this urban reservoir were detected at relatively high abundance and richness. The diversity of ARGs in this study was greater than that reported from Chinese suburban/rural lakes/reservoirs (Liu et al., 2018). The high abundance and richness in this waterbody may be driven by the combined human activities of sewage discharge and agricultural/urban runoff, as it is generally known that these activities increase the number of ARGs in waterbodies (Zhu et al., 2017; Ahmed et al., 2018; Liu et al., 2018). Moreover, aminoglycoside and multidrug resistance genes dominated the abundance of ARGs in this study, while aminoglycoside and beta-lactamase resistance genes dominated the types or richness of ARGs. In contrast, Jia et al. (2017) found in swine wastewater and downstream water that tetracycline and aminoglycoside resistance genes were the dominant ARGs, perhaps due to the different antibiotic selection pressures in different environments. However, the primer limitation of this study may result in the bias of detected ARGs, as the PCR-based method only covered limited number of ARG types. Additionally, a majority of ARGs investigations have been carried out in municipal wastewater treatment plants. An et al. (2018) showed significant changes of ARG profiles based on samples just collected in February and August, while another study based on monthly samples for 1 year did not find obvious seasonal variation in methicillin-resistant gene although it varied between

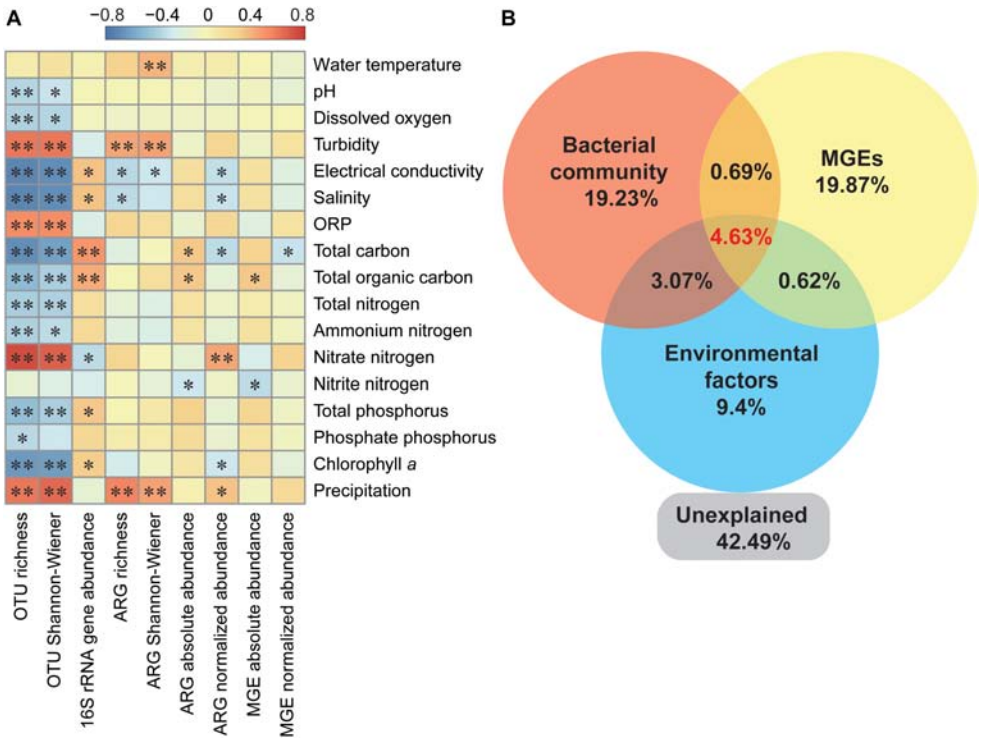

FIGURE 5 | Variation of ARG profiles explained by different ecological variables. **(A)** Spearman's correlation between bacterial OTUs, ARGs, MGEs, and environmental parameters. ORP, oxidation reduction potential. $^{*}P < 0.05$; $^{**}P < 0.01$. **(B)** Partial redundancy analysis illustrating the effects of bacterial community (relative abundance of ten major phyla), MGEs and environment factors on ARGs distribution pattern. Environmental factors referred to significant correlated factors, including salinity, total carbon, nitrate nitrogen, total phosphorus, and precipitation.

months and sampling sites (Börjesson et al., 2009). Yang et al. (2013) suggested that some types of ARGs in activated sludge showed seasonal fluctuations during a 4-year investigation, while most types of ARGs did not show seasonal fluctuations, but these results were based on samples collected only in summer and winter. However, according to our study, ARG subtypes were extremely dynamic and some of them frequently showed rises and falls over short-time periods (i.e., in just one week) but did not show seasonal pattern, so the previous low-frequency based studies may not completely and effectively reflect actual seasonal dynamic patterns of ARGs at fine temporal scale. Overall, our study based on high-frequency sampling over long timescales provide better understanding of the detailed temporal pattern of ARG profiles.

Our data revealed that some bacterial OTUs (e.g., *Planktothrix*) fluctuated rapidly, while major phyla remained stable at a broad taxonomic level. The microbial community showed an obviously seasonal variation and a trend of resilience during 1 year (12 months). In the microbial community, Proteobacteria and Actinobacteria were the dominant phyla, consistent with previous studies in drinking water system (Jia et al., 2015) and rivers (Jia et al., 2017). Additionally, the high relative percentage of Cyanobacteria was previously reported to have significant impacts on the variation of ARGs (Guo et al., 2018). Wang et al. (2018) showed that Proteobacteria, Actinobacteria and Cyanobacteria in the environment can carry some ARGs, confirming the high normalized abundance of ARGs and the vital roles of these bacteria in the dissemination of ARGs. Furthermore, we found a significant seasonality in the microbial taxonomic community, and the Procrustes test indicated the asynchronous temporal patterns between microbial OTUs and ARGs compositions (**Figure 2**). Previous studies have shown that ARGs strongly correlate with microbial communities in antibiotic-rich environments including human gut (Feng et al., 2018) and landfill leachate (Zhao et al., 2018). Recently, Ma et al. (2017) indicated that ARGs and bacterial communities did not show a strong correlation in drinking water, which is similar to the result of our study under low or medium antibiotic pressure. Altogether, the weak correlation between ARGs and bacterial communities in this study may be due to the relatively low antibiotic and heavy metal selection pressure in the natural environment.

The Co-occurrence Pattern of Bacterial OTUs and ARGs

Previous studies have confirmed that network analysis is a useful and reliable method to decipher the co-occurrence patterns between bacterial taxa and ARG subtypes, and to track potential hosts of ARGs (Barberán et al., 2012; Li et al., 2015; Ma et al., 2017; Feng et al., 2018). The module hubs in the network function as keystone of the module (Faust and Raes, 2012). All

module hubs in our co-occurrence network were affiliated to ARGs, implying that ARGs were important in maintaining the structure of the network and that HGT of ARGs was frequent among bacteria in the microbial community. The high frequency of aminoglycoside resistance genes in the network may be due to their high abundance and richness in the community. However, the abundance and richness of tetracycline resistance genes were relatively low in our studied system, but they connected tightly with various bacterial taxa. This suggests that the tetracycline resistance genes were shared among multiple bacterial taxa (Li et al., 2015). An increasing number of studies have reported the widespread distribution of tetracycline resistance genes (Czekalski et al., 2014; Zhou et al., 2017), as this antibiotic has been widely used in China (Hvistendahl, 2012).

In the co-occurrence network, Proteobacteria, Bacteroidetes and Firmicutes were the most prevalent phyla. These taxa were predicted as possible ARG hosts, and/or they originated from a similar source including upstream wastewater and surface runoff, suggesting the potential dissemination risk of ARGs with these taxa. In fact, Proteobacteria include a wide variety of pathogens and occur frequently as opportunistic pathogens, and have been found in soils that contained almost all major ARG types (Forsberg et al., 2014). Moreover, Jang et al. (2018) found that Bacteroidetes can be potential hosts of the *intI-1* gene. In this study, Bacteroidetes were significantly correlated to all major ARG types except sulfonamide resistance genes (**Figure 3** and **Supplementary Table S2**), suggesting the potential transmission of ARGs to human pathogenic bacteria. The Firmicutes were strongly correlated to aminoglycoside resistance genes in sewage sludge (Su et al., 2015), and the ARGs were shown to frequently switch hosts from Firmicutes to other bacterial phyla (Wang et al., 2017). In our study, Firmicutes were not the dominant bacteria but may carry diverse ARGs and further cause ARGs pollution to different environments or ecosystems. Nevertheless, the co-occurrence patterns revealed by this study were based on correlation, so the exact ARG carrying host and transmission pathway of ARGs need to be verified by further study.

Assembly Mechanisms Driving the Dynamics of ARGs

Our results indicated that the variation in ARGs could be explained by the bacterial community, MGEs and environmental factors. Environmental factors including salinity, total carbon, nitrate nitrogen, total phosphorus and precipitation influenced the temporal variation of ARGs, while precipitation was the strongest factor. A recent study reported that nutrients explained a large part of ARGs variation and that the nutrients combined with other factors could drive the distribution of ARGs (Zhao et al., 2017). The seasonal stormwater runoff induced by rainfall can increase the absolute abundance of ARGs and MGEs in an aquatic environment (Chen et al., 2019) and could influence the ARGs load through increased input from runoff and soil resuspension (Di Cesare et al., 2017). In accordance with previous studies, we found that precipitation displayed a significant influence on the ARG composition and structure, and was positively correlated with the richness and normalized abundance of ARGs, supporting the view that rainfall contributed to the loading of ARGs in the river and reservoir waters in urban region. In addition, rainfall significantly influenced pathogenic bacterial abundance because stormwater was able to significantly contribute to the occurrence and elevated concentration of pathogenic bacteria in subtropical waters (Ahmed et al., 2018). Our results further showed that turbidity was strongly correlated to richness and diversity of bacteria and ARGs. A turbidity increase is normally associated with rainfall-induced contamination, suspended particulate matter and sediment disturbance. This may further drive changes in bacterial community and ARG profiles. It has been demonstrated that turbidity was significantly correlated to bacterial diversity, reiterating the influence of runoff on the bacterial community (Peter and Sommaruga, 2016). Taken together, our results indicated that precipitation had both direct and indirect effects on bacterial taxonomic communities and resistomes, supporting the idea that stormwater with agriculture/urban runoff, with contaminants from the urban region could increase loadings of bacterial ARGs thereby increasing the risk of ARGs dissemination (Garner et al., 2017). In contrast, we did not find any significant relationship between water temperature and the ARGs composition or abundance, corroborating the fact that the ARGs in this subtropical urban reservoir did not have a significant seasonal pattern. This is inconsistent with a previous finding that water temperature was a potential factor driving the dynamics of ARG profiles (Zheng et al., 2018), and this inconsistency may be attributed to a difference in sampling frequency and climate conditions, as the range of temperature was narrower in this subtropical reservoir compared to other studies in temperate zone. In the Zheng et al. (2018) study, water samples were only collected in March, June, September, and December, and their river showed a wider temperature range than our studied reservoir. In our study, the 42.49% of ARGs variance remained unexplained, may partly be due to the environmental factors that were not considered, such as anthropogenic factors and the co-selection of antibiotics and heavy metals (Stepanauskas et al., 2006; Liu et al., 2018; Chen et al., 2019).

The bacterial community has been identified as one of the key drivers that shape the ARG profiles in antibiotic-rich environments (Forsberg et al., 2014; Su et al., 2015). However, our results of pRDA, Procrustes test and Spearman's relationship all showed that microbial community was weakly correlated with ARG profiles. More interestingly, our results indicated that the neutral process played a more important role in the assembly of microbial taxonomic communities than in ARG profiles, as the neutral model only explained a minor part (7.9%) of the variation in ARG profiles. Therefore, dispersal and stochastic processes appeared to have more influence on bacterial taxonomic communities compared to ARG profiles. This may be one of the reasons why microbial OTUs and ARGs communities exhibited a decoupling change over 1 year. These results indicated that the vertical transmission

(mother-to-child transmission) of ARGs in this environment may not play a leading role.

Our study showed that MGEs could partly explain the variation of ARG profiles in the urban reservoir, and the absolute abundance of MGEs showed a significant and positive correlation with ARGs. Further, MGEs that were always abundant in our samples, could potentially enhance the probability of HGT of ARGs. Previous studies reported that environmental contaminants at low concentration have a potential role in the dissemination of ARGs by promoting HGT, such as antibiotic and non-antibiotic pharmaceuticals (Andersson and Hughes, 2014; Wang et al., 2019). In this study, the rainfall combined with possible contaminants and MGEs may largely facilitate the proliferation and spread of ARGs among different bacterial taxa. These results suggest that MGEs played an important role in the temporal variation of ARGs in the urban waterbody, implying the potential risk that the ARGs may be transferred by MGEs from aquatic environments to human pathogens (Martínez et al., 2015).

CONCLUSION

Our weekly study revealed the asynchronous succession patterns of bacterial taxonomic communities and ARG profiles, indicating a decoupling dynamic between bacterial taxonomy and function on a temporal scale in a subtropical urban reservoir. The bacterial taxonomic community was significantly correlated with water temperature and exhibited seasonality, while ARG profiles was strongly correlated with precipitation and did not show distinct seasonality. Precipitation had both direct and indirect effects on the temporal patterns of bacterial community and ARG profiles, reflecting the effect of stormwater runoff on temporal dynamics of ARG profiles. The diversity and composition of bacterial taxonomic communities appeared to be more responsive to environmental variables than ARGs, and the composition of ARG profiles appeared to be governed less by stochastic processes. Additionally, MGEs were positively correlated with ARGs and had significant contribution to the variation of ARGs community, suggesting the potential risk of HGT. This study may help to better understand the temporal dynamic of ARG profiles in urban water environments at fine temporal scale, and highlight that further high-frequency and long-term time series research should be undertaken to reveal the specific drivers and deep mechanisms of ARGs assembly and dynamics.

DATA AVAILABILITY

The raw data for 16S rRNA gene analysis in this study have been deposited in the NCBI SRA database under the BioProject number PRJNA510463 and the accession number SRP173857.

AUTHOR CONTRIBUTIONS

JY designed the experiments. PF, FP, and XG carried out the sample collection and determined the environmental parameters. PF, FP, and PX conducted the PCR, high-throughput qPCR, high-throughput sequencing, and bioinformatics. PF and JY wrote the first draft of the manuscript. All authors contributed to and have approved the final manuscript.

FUNDING

This work was funded by the Strategic Priority Research Program of the Chinese Academy of Sciences (XDA23040302), the National Natural Science Foundation of China (91851104), the Key Laboratory of Urban Environment and Health, Chinese Academy of Sciences (KLUEH-C-201801), and the Xiamen Municipal Bureau of Science and Technology (3502Z20172024 and 3502Z20171003).

ACKNOWLEDGMENTS

We thank Prof. David M. Wilkinson for his comments on the manuscript.

SUPPLEMENTARY MATERIAL

The Supplementary Material for this article can be found online at: https://www.frontiersin.org/articles/10.3389/fmicb.2019.01448/full#supplementary-material

REFERENCES

Ahmed, W., Zhang, Q., Lobos, A., Senkbeil, J., Sadowsky, M. J., Harwood, V. J., et al. (2018). Precipitation influences pathogenic bacteria and antibiotic resistance gene abundance in storm drain outfalls in coastal sub-tropical waters. *Environ. Int.* 116, 308–318. doi: 10.1016/j.envint.2018.04.005

An, X. L., Su, J. Q., Li, B., Ouyang, W. Y., Zhao, Y., Chen, Q. L., et al. (2018). Tracking antibiotic resistome during wastewater treatment using high throughput quantitative PCR. *Environ. Int.* 117, 146–153. doi: 10.1016/j.envint.2018.05.011

Andersson, D. I., and Hughes, D. (2014). Microbiological effects of sublethal levels of antibiotics. *Nat. Rev. Microbiol.* 12, 465–478. doi: 10.1038/nrmicro3270

Barberán, A., Bates, S. T., Casamayor, E. O., and Fierer, N. (2012). Using network analysis to explore co-occurrence patterns in soil microbial communities. *ISME J.* 6, 343–351. doi: 10.1038/ismej.2011.119

Berendonk, T. U., Manaia, C. M., Merlin, C., Fatta-Kassinos, D., Cytryn, E., Walsh, F., et al. (2015). Tackling antibiotic resistance: the environmental framework. *Nat. Rev. Microbiol.* 13, 310–317. doi: 10.1038/nrmicro3439

Börjesson, S., Melin, S., Matussek, A., and Lindgren, P. E. (2009). A seasonal study of the mecA gene and *Staphylococcus aureus* including methicillin-resistant *S. aureus* in a municipal wastewater treatment plant. *Water Res.* 43, 925–932. doi: 10.1016/j.watres.2008.11.036

Chen, Y., Su, J. Q., Zhang, J., Li, P., Chen, H., Zhang, B., et al. (2019). High-throughput profiling of antibiotic resistance gene dynamic in a drinking water

river-reservoir system. *Water Res.* 149, 179–189. doi: 10.1016/j.watres.2018.11.007

Clarke, K. R., and Gorley, R. N. (2015). *PRIMER v7: User Manual/Tutorial*. Plymouth: PRIMER-E Ltd.

Czekalski, N., Diez, E. G., and Bürgmann, H. (2014). Wastewater as a point source of antibiotic-resistance genes in the sediment of a freshwater lake. *ISME J.* 8, 1381–1390. doi: 10.1038/ismej.2014.8

D'Costa, V. M., King, C. E., Kalan, L., Morar, M., Sung, W. W. L., Schwarz, C., et al. (2011). Antibiotic resistance is ancient. *Nature* 477, 457–461. doi: 10.1038/nature10388

DeSantis, T. Z., Hugenholtz, P., Larsen, N., Rojas, M., Brodie, E. L., Keller, K., et al. (2006). Greengenes, a chimera-checked 16S rRNA gene database and workbench compatible with ARB. *Appl. Environ. Microbiol.* 72, 5069–5072. doi: 10.1128/AEM.03006-05

Di Cesare, A., Eckert, E. M., Rogora, M., and Corno, G. (2017). Rainfall increases the abundance of antibiotic resistance genes within a riverine microbial community. *Environ. Pollut.* 226, 473–478. doi: 10.1016/j.envpol.2017.04.036

Edgar, R. C. (2010). Search and clustering orders of magnitude faster than BLAST. *Bioinformatics* 26, 2460–2461. doi: 10.1093/bioinformatics/btq461

Faust, K., and Raes, J. (2012). Microbial interactions: from networks to models. *Nat. Rev. Microbiol.* 10, 538–550. doi: 10.1038/nrmicro2832

Feng, J., Li, B., Jiang, X., Yang, Y., Wells, G. F., Zhang, T., et al. (2018). Antibiotic resistome in a large-scale healthy human gut microbiota deciphered by metagenomic and network analyses. *Environ. Microbiol.* 20, 355–368. doi: 10.1111/1462-2920.14009

Forsberg, K. J., Patel, S., Gibson, M. K., Lauber, C. L., Knight, R., Fierer, N., et al. (2014). Bacterial phylogeny structures soil resistomes across habitats. *Nature* 509, 612–616. doi: 10.1038/nature13377

Garner, E., Benitez, R., von Wagoner, E., Sawyer, R., Schaberg, E., Hession, W. C., et al. (2017). Stormwater loadings of antibiotic resistance genes in an urban stream. *Water Res.* 123, 144–152. doi: 10.1016/j.watres.2017.06.046

Guo, Y. Y., Liu, M., Liu, L. M., Liu, X., Chen, H. H., and Yang, J. (2018). The antibiotic resistome of free-living and particle-attached bacteria under a reservoir cyanobacterial bloom. *Environ. Int.* 117, 107–115. doi: 10.1016/j.envint.2018.04.045

Hubbell, S. P. (2001). *The Unified Neutral Theory of Biodiversity and Biogeography (MPB-32)*. Princeton, NJ: Princeton University Press.

Hvistendahl, M. (2012). China takes aim at rampant antibiotic resistance. *Science* 336, 795–795. doi: 10.1126/science.336.6083.795

Jang, H. M., Kim, Y. B., Choi, S., Lee, Y., Shin, S. G., Unno, T., et al. (2018). Prevalence of antibiotic resistance genes from effluent of coastal aquaculture, South Korea. *Environ. Pollut.* 233, 1049–1057. doi: 10.1016/j.envpol.2017.10.006

Jia, S., Shi, P., Hu, Q., Li, B., Zhang, T., and Zhang, X. X. (2015). Bacterial community shift drives antibiotic resistance promotion during drinking water chlorination. *Environ. Sci. Technol.* 49, 12271–12279. doi: 10.1021/acs.est.5b03521

Jia, S., Zhang, X. X., Miao, Y., Zhao, Y., Ye, L., Li, B., et al. (2017). Fate of antibiotic resistance genes and their associations with bacterial community in livestock breeding wastewater and its receiving river water. *Water Res.* 124, 259–268. doi: 10.1016/j.watres.2017.07.061

Kruse, H., and Sørum, H. (1994). Transfer of multiple drug resistance plasmids between bacteria of diverse origins in natural microenvironments. *Appl. Environ. Microbiol.* 60, 4015–4021.

Laxminarayan, R. (2014). Antibiotic effectiveness: balancing conservation against innovation. *Science* 345, 1299–1301. doi: 10.1126/science.1254163

Li, B., Yang, Y., Ma, L., Ju, F., Guo, F., Tiedje, J. M., et al. (2015). Metagenomic and network analysis reveal wide distribution and co-occurrence of environmental antibiotic resistance genes. *ISME J.* 9, 2490–2502. doi: 10.1038/ismej.2015.59

Lindh, M. V., Sjöstedt, J., Andersson, A. F., Baltar, F., Hugerth, L. W., Lundin, D., et al. (2015). Disentangling seasonal bacterioplankton population dynamics by high-frequency sampling. *Environ. Microbiol.* 17, 2459–2476. doi: 10.1111/1462-2920.12720

Liu, L. M., Su, J. Q., Guo, Y. Y., Wilkinson, D. M., Liu, Z. W., Zhu, Y. G., et al. (2018). Large-scale biogeographical patterns of bacterial antibiotic resistome in the waterbodies of China. *Environ. Int.* 117, 292–299. doi: 10.1016/j.envint.2018.05.023

Liu, L. M., Yang, J., Yu, X. Q., Chen, G. J., and Yu, Z. (2013). Patterns in the composition of microbial communities from a subtropical river: effects of environmental, spatial and temporal factors. *PLoS One* 8:e81232. doi: 10.1371/journal.pone.0081232

Logares, R., Lindström, E. S., Langenheder, S., Logue, J. B., Paterson, H., Laybourn-Parry, J., et al. (2013). Biogeography of bacterial communities exposed to progressive long-term environmental change. *ISME J.* 7, 937–948. doi: 10.1038/ismej.2012.168

Louca, S., Parfrey, L. W., and Doebeli, M. (2016). Decoupling function and taxonomy in the global ocean microbiome. *Science* 353, 1272–1277. doi: 10.1126/science.aaf4507

Ma, L., Li, B., Jiang, X. T., Wang, Y. L., Xia, Y., and Li, A. D. (2017). Catalogue of antibiotic resistome and host-tracking in drinking water deciphered by a large scale survey. *Microbiome* 5:154. doi: 10.1186/s40168-017-0369-0

Marti, E., Variatza, E., and Balcazar, J. L. (2014). The role of aquatic ecosystems as reservoirs of antibiotic resistance. *Trends Microbiol.* 22, 36–41. doi: 10.1016/j.tim.2013.11.001

Martínez, J. L., Coque, T. M., and Baquero, F. (2015). What is a resistance gene? Ranking risk in resistomes. *Nat. Rev. Microbiol.* 13, 116–123. doi: 10.1038/nrmicro3399

Ofiţeru, I. D., Lunn, M., Curtis, T. P., Wells, G. F., Criddle, C. S., Francis, C. A., et al. (2010). Combined niche and neutral effects in a microbial wastewater treatment community. *Proc. Natl. Acad. Sci. U.S.A.* 107, 15345–15350. doi: 10.1073/pnas.1000604107

Ouyang, W. Y., Huang, F. Y., Zhao, Y., Li, H., and Su, J. Q. (2015). Increased levels of antibiotic resistance in urban stream of Jiulongjiang River, China. *Appl. Microbiol. Biotechnol.* 99, 5697–5707. doi: 10.1007/s00253-015-6416-5

Peter, H., and Sommaruga, R. (2016). Shifts in diversity and function of lake bacterial communities upon glacier retreat. *ISME J.* 10, 1545–1554. doi: 10.1038/ismej.2015.245

Pruden, A., Pei, R., Storteboom, H., and Carlson, K. H. (2006). Antibiotic resistance genes as emerging contaminants: studies in northern Colorado. *Environ. Sci. Technol.* 40, 7445–7450. doi: 10.1021/es060413l

Schloss, P. D., Westcott, S. L., Ryabin, T., Hall, J. R., Hartmann, M., Hollister, E. B., et al. (2009). Introducing mothur: open-source, platform-independent, community-supported software for describing and comparing microbial communities. *Appl. Environ. Microbiol.* 75, 7537–7541. doi: 10.1128/AEM.01541-09

Sloan, W. T., Lunn, M., Woodcock, S., Head, L. M., Nee, S., and Curtis, T. P. (2006). Quantifying the roles of immigration and chance in shaping prokaryote community structure. *Environ. Microbiol.* 8, 732–740. doi: 10.1111/j.1462-2920.2005.00956.x

Stepanauskas, R., Glenn, T. C., Jagoe, C. H., Tuckfield, R. C., Lindell, A. H., King, C. J., et al. (2006). Coselection for microbial resistance to metals and antibiotics in freshwater microcosms. *Environ. Microbiol.* 8, 1510–1514. doi: 10.1111/j.1462-2920.2006.01091.x

Su, J. Q., Wei, B., Ouyang, W. Y., Huang, F. Y., Zhao, Y., Xu, H. J., et al. (2015). Antibiotic resistome and its association with bacterial communities during sewage sludge composting. *Environ. Sci. Technol.* 49, 7356–7363. doi: 10.1021/acs.est.5b01012

Treusch, A. H., Vergin, K. L., Finlay, L. A., Donatz, M. G., Burton, R. M., Carlson, C. A., et al. (2009). Seasonality and vertical structure of microbial communities in an ocean gyre. *ISME J.* 3, 1148–1163. doi: 10.1038/ismej.2009.60

Wang, C., Dong, D., Strong, P. J., Zhu, W., Ma, Z., Qin, Y., et al. (2017). Microbial phylogeny determines transcriptional response of resistome to dynamic composting processes. *Microbiome* 5, 1–15. doi: 10.1186/s40168-017-0324-0

Wang, J. H., Lu, J., Zhang, Y. X., Wu, J., Luo, Y., and Liu, H. (2018). Metagenomic analysis of antibiotic resistance genes in coastal industrial mariculture systems. *Bioresour. Technol.* 253, 235–243. doi: 10.1016/j.biortech.2018.01.035

Wang, Y., Lu, J., Mao, L., Li, J., Yuan, Z., Bond, P. L., et al. (2019). Antiepileptic drug carbamazepine promotes horizontal transfer of plasmid-borne multi-antibiotic resistance genes within and across bacterial genera. *ISME J.* 13, 509–522. doi: 10.1038/s41396-018-0275-x

World Health Organization [WHO] (2014). *Antimicrobial Resistance: Global Report on Surveillance 2014*. Geneva: World Health Organization.

Xu, L., Ouyang, W., Qian, Y., Su, C., Su, J., and Chen, H. (2016). High-throughput profiling of antibiotic resistance genes in drinking water treatment plants and

distribution systems. *Environ. Pollut.* 213, 119–126. doi: 10.1016/j.envpol.2016.02.013

Yang, J., Yu, X. Q., Liu, L. M., Zhang, W. J., and Guo, P. Y. (2012). Algae community and trophic state of subtropical reservoirs in southeast Fujian, China. *Environ. Sci. Pollut. Res.* 19, 1432–1442. doi: 10.1007/s11356-011-0683-1

Yang, Y., Li, B., Ju, F., and Zhang, T. (2013). Exploring variation of antibiotic resistance genes in activated sludge over a four-year period through a metagenomic approach. *Environ. Sci. Technol.* 47, 10197–10205. doi: 10.1021/es4017365

Yang, Y., Song, W., Lin, H., Wang, W., Du, L., and Xing, W. (2018). Antibiotics and antibiotic resistance genes in global lakes: a review and meta-analysis. *Environ. Int.* 116, 60–73. doi: 10.1016/j.envint.2018.04.011

Zhang, H., Feng, J., Chen, S., Zhao, Z., Li, B., Wang, Y., et al. (2019). Geographical patterns of *nirS* gene abundance and *nirS*-type denitrifying bacterial community associated with activated sludge from different wastewater treatment plants. *Microb. Ecol.* 77, 304–316. doi: 10.1007/s00248-018-1236-7

Zhao, R., Feng, J., Yin, X., Liu, J., Fu, W., Berendonk, T. U., et al. (2018). Antibiotic resistome in landfill leachate from different cities of China deciphered by metagenomic analysis. *Water Res.* 134, 126–139. doi: 10.1016/j.watres.2018.01.063

Zhao, Z., Wang, J., Han, Y., Chen, J., Liu, G., Lu, H., et al. (2017). Nutrients, heavy metals and microbial communities co-driven distribution of antibiotic resistance genes in adjacent environment of mariculture. *Environ. Pollut.* 220, 909–918. doi: 10.1016/j.envpol.2016.10.075

Zheng, J., Zhou, Z., Wei, Y., Chen, T., Feng, W., and Chen, H. (2018). High-throughput profiling of seasonal variations of antibiotic resistance gene transport in a peri-urban river. *Environ. Int.* 114, 87–94. doi: 10.1016/j.envint.2018.02.039

Zhou, Y., Niu, L., Zhu, S., Lu, H., and Liu, W. (2017). Occurrence, abundance, and distribution of sulfonamide and tetracycline resistance genes in agricultural soils across China. *Sci. Total Environ.* 599, 1977–1983. doi: 10.1016/j.scitotenv.2017.05.152

Zhu, Y. G., Zhao, Y., Li, B., Huang, C. L., Zhang, S. Y., Yu, S., et al. (2017). Continental-scale pollution of estuaries with antibiotic resistance genes. *Nat. Microbiol.* 2:16270. doi: 10.1038/nmicrobiol.2016.270

Conflict of Interest Statement: The authors declare that the research was conducted in the absence of any commercial or financial relationships that could be construed as a potential conflict of interest.

Copyright © 2019 Fang, Peng, Gao, Xiao and Yang. This is an open-access article distributed under the terms of the Creative Commons Attribution License (CC BY). The use, distribution or reproduction in other forums is permitted, provided the original author(s) and the copyright owner(s) are credited and that the original publication in this journal is cited, in accordance with accepted academic practice. No use, distribution or reproduction is permitted which does not comply with these terms.

frontiers in Microbiology

ORIGINAL RESEARCH
published: 10 July 2019
doi: 10.3389/fmicb.2019.01521

The Relative Abundance of Benthic Bacterial Phyla Along a Water-Depth Gradient in a Plateau Lake: Physical, Chemical, and Biotic Drivers

Kaiyuan Wu[1,2†], Wenqian Zhao[2,3†], Qian Wang[2], Xiangdong Yang[2], Lifeng Zhu[3], Ji Shen[2], Xiaoying Cheng[1] and Jianjun Wang[2,4*]*

[1]School of Environment and Civil Engineering, Jiangnan University, Wuxi, China, [2]State Key Laboratory of Lake Science and Environment, Nanjing Institute of Geography and Limnology, Chinese Academy of Sciences, Nanjing, China, [3]School of Biological Sciences, Nanjing Normal University, Nanjing, China, [4]University of Chinese Academy of Sciences, Beijing, China

OPEN ACCESS

Edited by:
Haihan Zhang,
Xi'an University of Architecture and Technology, China

Reviewed by:
Jie Wang,
China Agricultural University, China
Man Kit Cheung,
The Chinese University of Hong Kong, China

***Correspondence:**
Xiaoying Cheng
chengxiaoysytu@163.com
Jianjun Wang
jjwang@niglas.ac.cn

†These authors have contributed equally to this work

Specialty section:
This article was submitted to Aquatic Microbiology, a section of the journal Frontiers in Microbiology

Received: 30 April 2019
Accepted: 18 June 2019
Published: 10 July 2019

Citation:
Wu K, Zhao W, Wang Q, Yang X, Zhu L, Shen J, Cheng X and Wang J (2019) The Relative Abundance of Benthic Bacterial Phyla Along a Water-Depth Gradient in a Plateau Lake: Physical, Chemical, and Biotic Drivers. Front. Microbiol. 10:1521. doi: 10.3389/fmicb.2019.01521

Water-depth biodiversity gradient, one of the typical biogeographical patterns on Earth, is understudied for bacteria in freshwater ecosystems, and thus left the underlying mechanisms poorly understood especially for benthic bacteria. Here, we investigated the water-depth distribution of surface sediment bacterial phyla and their driving factors in Lake Lugu, a plateau lake in Southwest China. Our results revealed that the relative abundance of 11 dominant bacterial phyla showed various water-depth patterns, such as increasing, decreasing, hump-shaped, and U-shaped patterns. These patterns across phyla were consistent with their different niche positions of water depth, while the occupancy-abundance relationships were not dependent on phylum attributes. Consistently, phylum abundance was best explained by water depth; other physical and chemical factors, such as metal ion concentrations, SiO_2, and pH, can also explain the variations in some bacterial phyla. Chemical variables were the main drivers of the dominant bacterial phyla. However, biotic variables also showed substantial importance for some phyla, such as Planctomycetes, Actinobacteria, and WS3. This work could provide new insights into the general water-depth patterns and underlying mechanisms of the relative abundance of bacterial phyla in freshwater ecosystems.

Keywords: bacteria, phyla, relative abundance, water depth, biotic effects, abiotic effects

INTRODUCTION

Biogeographical patterns of biodiversity along gradients, such as those of latitude, elevation, and water depth, are among the most widely studied topics in ecology (Zintzen et al., 2017), and researchers have described the latitudinal and elevational patterns in biodiversity in a variety of ecosystems across the globe (Fuhrman et al., 2008; Wang et al., 2011; Shi et al., 2014). Similar to the more commonly studied latitudinal and elevational gradients, water-depth gradient show complex changes in various environmental attributes and thus impose strong

environmental filtering on the aquatic microbial community (Bryant et al., 2012). The phylogenetic and physiological diversity of microbial phyla, especially those of bacteria, is considerably greater than that of animal and plant phyla (Prosser et al., 2007; Yeh et al., 2019). Furthermore, benthic bacteria play an important role in organic matter transformation and in the biogeochemical cycling of major elements such as nitrogen, phosphorus, sulfur, and iron (Martins et al., 2011; Cheng et al., 2014). Knowledge of benthic bacterial phyla distribution in aquatic ecosystems is of great significance and can provide novel perspectives regarding water-depth biodiversity patterns among microorganisms and their potential drivers and further contribute to the sustainable management of water resources. Nonetheless, as most studies focus on marine waters (Agogue et al., 2011; Bryant et al., 2012; Walsh et al., 2016), the general patterns and driving mechanisms of bacterial communities along water-depth gradients have been less studied for freshwater ecosystems.

In recent years, the niche position and niche breadth hypotheses have been used to investigate how niche characteristics account for species distribution and abundance (Brandle and Brandl, 2001). Among these two referenced niche parameters, niche position indicates the availability of habitat and resources (Teittinen et al., 2018). Some species have marginal niche positions at the very edges of the environmental ranges, while other species have nonmarginal niche positions that exist under average environmental conditions (Vilmi et al., 2019). Niche position, rather than niche breadth, is the chief predictive factor of species distributions, such as those of stream insects (Heino and de Mendoza, 2016). In addition, previous research has provided strong evidence that the occupancy and abundance relationships of species tend to be positively and often strongly linked with each other in a variety of ecosystems (Gaston et al., 2000; Foggo et al., 2007; Zuckerberg et al., 2009). Niche position could be a strong predictor of species variation in terms of occupancy and abundance. For instance, niche position is negatively associated with mean abundance in diatom and macroinvertebrate species, and the occupancy-abundance relationship clearly differs across taxonomic groups (Vilmi et al., 2019). At the community level, niche position and occupancy are related to the abundance distribution, but whether such a relationship exists at phylum level remains unexplored.

Traditional niche-based theory asserts that the relative abundances of species are determined by abiotic and biotic factors, such as environmental conditions, habitat heterogeneity, and species interactions (Dumbrell et al., 2010; Liao et al., 2016). Most studies have shown that local environmental conditions, such as physical and chemical attributes, can affect microbial community composition and species diversity in lake ecosystems and the biogeochemical processes they mediate (Staley et al., 2015; Qin et al., 2016). The bacterial community can be shaped by a variety of environmental factors, such as water depth, nitrogen, phosphorus, pH, and pollution (Brown et al., 2009; Haller et al., 2011; Song et al., 2012; Liu et al., 2015b; Zhang et al., 2019). In addition, biotic interactions could also affect microbial community structure. However, rarely considered are the important ecological processes associated with biotic variables, such as the community composition and diversity of other organisms that feed on bacteria (Langenheder et al., 2017). Ecosystems are constructed around interaction webs, such as predation, mutualism, competition, and host-parasite interactions, that connect every species to many others at an array of spatial scales (Estes et al., 2011; Amin et al., 2012). For example, viral abundance is typically strongly correlated with bacterial abundance in marine systems (Clasen et al., 2008; Hanson et al., 2017). In the soil, fungi and bacteria have an effect on the formation of each other's community structure (Singh et al., 2009). Moreover, biotic attributes such as the composition of other taxonomic groups are generally better predictors of species diversity in streams than other environmental variables (Johnson and Hering, 2010).

Here, we explored the water-depth patterns and underlying drivers of the relative abundance of bacterial phyla in the surface sediments of Lake Lugu, a typical deep plateau lake system located in Southwest China. This lake has a water depth of 93.5 m and an area of 50.5 km^2. We had the four following objectives. First, we examined the water-depth patterns in terms of the relative abundance of benthic bacterial phyla. Second, we expected that niche positions at the phylum and species levels are related and also the relationship between the occupancy and abundance of each phylum. Finally, we explored the main factors driving the above water-depth patterns in bacterial phyla and further quantified the relative importance of physical, chemical, and biological drivers.

MATERIALS AND METHODS

Study Region

The studied Lake Lugu, with an elevation of 2,685 m, is located in the Yunnan Province, Southwest China (27°41′–27°45′N, 100°45′–100°50′E). It is one of the deepest freshwater plateau lakes in the region. This lake has spatial characteristics that include high connectivity and a small area, allowing species to be freely distributed at different locations with no apparent barriers to dispersal. Macrophytes were partly absent from the lake, allowing for the collection of surface sediments in shallow waters. In August 2010, we collected 37 surface sediment (~0–1 cm) samples along the water-depth gradient from 0 to 93.5 m. At each site, three sediment cores with a 6-cm diameter were retrieved for surface sediments. The sample collection process was described in detail in a previous study (Wang et al., 2012b).

Bacterial Community Analysis

Bacterial analyses were performed according to the previous literature (Wang et al., 2012a). Briefly, genomic DNA was extracted from surface sediment samples using the phenol chloroform method (Zhou et al., 1996). Bacterial tag-encoded FLX amplicon pyrosequencing was conducted as described previously (Dowd et al., 2008). Bacterial 16S rRNA genes were amplified using the 27F primer (5′ GAG TTT GAT CNT GGC TCA G 3′) with the 454 Life Sciences A sequencing adapter, and the modified 519R primer (5′ GTN TTA CNG

CGG CKG CTG 3′) with a 8-bp barcode sequence and the 454 Life Sciences B sequencing adapter. The PCR amplification of a single 35 cycle was performed in a ABI9700 thermocycler (ABI, Foster City, USA) using the program 95°C for 2 min; 25 cycles of 95°C for 30 s, 55°C for 30 s, 72°C for 30 s; 72°C for 5 min; finally kept at 10°C. Triplicate positive PCR products were pooled and purified with AxyPrep DNA Gel Extraction Kit (Axygen, USA). Amplicon sequencing was performed based upon the manufacturer protocols (Roche Applied Science, Indianapolis, IN) for Titanium sequencing on FLX-titanium platform (Dowd et al., 2008). The purified amplicons were pooled at equal molality, and then sequenced using a Roche 454 FLX pyrosequencer (Roche, Switzerland).

All 16S rRNA pyrosequencing reads were analyzed using QIIME, version 1.9.0 (Caporaso et al., 2010b). We imported barcoded 16S rRNA gene sequences and removed the primers, demultiplexed reads, and then filtered them according to Phred quality scores. Quality criteria were a minimum sequence length of 200 bp, a maximum sequence length of 900 bp, and a minimum average quality score of 25. With such quality control, we allowed few ambiguous bases or mismatches in the primer sequence and no barcode errors, and a maximum homopolymer length of 6 bp.

Sequences were denoised with the Denoiser algorithm (Reeder and Knight, 2010), clustered into operational taxonomic units (OTUs) at 97% similarity level with the seed-based UCLUST algorithm (Edgar, 2010). We used the longest sequence in a cluster as the representative sequence for that OTU. Singletons, i.e., OTUs with only one read in the entire dataset, were removed and chimeras were excluded using ChimeraSlayer (Haas et al., 2011). After chimeras were removed *via* ChimeraSlayer, representative sequences from each OTU were aligned to the Greengenes v13.8 imputed core reference alignment (DeSantis et al., 2006) using PyNAST (Caporaso et al., 2010a). The taxonomic identity of each representative sequence was determined using the RDP Classifier (Wang et al., 2007) and chloroplast and archaeal sequences were removed. Before the subsequent analysis, bacterial community were rarefied at 1,139 sequences to avoid the variation in abundance or sampling intensity biased. The generated sequences can be found in figshare (https://doi.org/10.6084/m9.figshare.8052788).

Abiotic and Biotic Variables

We evaluated several environmental characteristics important to the biological community in the surface water of 0.5 m and bottom water near the sediment-water interface at each site (**Supplementary Table S1**). We analyzed the temperature, pH, conductivity, total nitrogen, total phosphorus, dissolved oxygen (DO), HCO_3^- concentration (HCO_3·water), and silica of the surface water, and measured the temperature, pH, conductivity, and DO of the bottom water. In addition, the surface sediment total phosphorus, loss-on-ignition (LOI), water content, grain size, porosity, and the metal ion concentrations were measured. The measured metal ions included Al, Ba, Be, Ca, Co, Cr, Cu, Fe, Li, K, Mg, Mn, Na, Ni, Pb, Sr., Ti, V, and Zn. The grain size was divided into five classes: <4, 4–16, 16–32, 32–64, and >64 μm. A detailed description of the methods for the measurement and calculation of the abiotic variables was described in a previous study (Wang et al., 2012b).

In terms of the biotic variables, diatoms and chironomids were classified and identified to the lowest possible taxonomic level (typically to the species level) as shown in previous studies (Wang et al., 2012b; Zhang et al., 2013). We used the following biotic factors as predictor variables: (1) the chlorophyll *a* concentration of the surface and bottom water, (2) the biomass of diatoms and chironomids, and (3) the richness of diatoms and chironomids. The concentration of chlorophyll *a* was the representative of the phytoplankton biomass. The biomass of diatoms and chironomids was indicated by the number of diatoms per gram of wet sediment and the count of head capsules per gram of wet sediment, respectively.

Statistical Analyses

First, we only included the highly abundant bacterial phyla by considering species occurrence percentages larger than 85%. We explored the relationships between water depth and the relative abundance of bacterial phyla with linear or quadratic models. The most appropriate model was selected based on the lowest value of Akaike's information criterion (Yamaoka et al., 1978).

Second, we calculated the niche position of the water depth for both the species and phylum levels. For each species or phylum, we estimated the weighted water-depth position by averaging the product of their water-depth values and their abundances across all samples (Wang et al., 2013). We selected the linear or quadratic model based on the lower value of Akaike's information criterion and explored the relationship of niche position between the phylum and species levels. In practice, the proportion of sites was considered as "occupancy," and the mean abundance at occupied sites was considered as "abundance." The relationship between the occupancy and abundance of bacterial phyla was examined by linear or quadric models, and the better model was selected based on the lower value of Akaike's information criterion (Yamaoka et al., 1978).

Third, to identify the important factors affecting each phylum, we applied random forest model (Feld et al., 2016) and redundancy analysis (RDA). Statistical dependence between the explanatory variables was assessed using Pearson's correlation coefficients, and variables with high correlation coefficients (Pearson $r > 0.7$) were excluded from the models. By performing principal component analysis, the 19 metal ion concentrations were reduced to the first two axes of the principal components analysis, which thus represented the environmental variables that reflected the geochemical factors. This process was performed to decrease the degrees of freedom so that they were lower than the number of sampled sites. The other measured variables were used as environmental variables without principal component analysis. For the random forest analysis, we used techniques such as cross-validation to prune the 2,000 trees to an optimal size (Prasad et al., 2006). The importance of a predictor variable was determined by its frequency of selection weighted by a measure of improvement of the model given each split and averaged across all trees (contributions were scaled to sum to 100).

Furthermore, RDA was used to examine the potential explanatory variables of community composition at the phylum level. We used RDA with Hellinger-transformed abundance data of the bacterial community, as this transformation makes complex data with numerous zero values more suitable for the analysis with linear methods (Legendre and Gallagher, 2001).

Finally, we applied variation partitioning to quantify the relative importance of the main environmental drivers using linear model (Anderson and Cribble, 1998; Legendre, 2008). We categorized the explanatory variables into three groups: physical, chemical, and biological components. The physical component included water depth, conductivity of surface water, porosity, and grain size. The chemical component included surface water pH, total phosphorus, total nitrogen, SiO_2 and HCO_3, bottom water DO and pH, and surface sediment LOI, grain size, PC1 and PC2 of metals. For biological component, we considered the richness and biomass of diatoms and chironomids, and chlorophyll *a* of surface and bottom water. We generated three explanatory matrix models and estimated the proportions of variation in the relative abundance of the bacterial phyla explained by these three components. For each component, significant explanatory variables were selected by forward selection against the Hellinger-transformed abundance phylum data with 9,999 permutations.

We did not apply more statistical analyses because it is a challenge to differentiate the direct or indirect effects of underlying drivers on the relative abundance of bacterial phyla based on field observations. These above analyses were conducted with vegan V2.5-5 (Oksanen et al. 2013) and randomForestSRC V2.9.0 (Ishwaran and Kogalur 2014) in the R environment.

RESULTS

In total, we selected 11 major bacterial phyla based on their relative abundance, including Proteobacteria, Nitrospirae, Chlorobi, Chloroflexi, and Bacteroidetes. Among these phyla, Proteobacteria was the most dominant, followed by Bacteroidetes, Chloroflexi, and Nitrospirae (**Table 1**). The relative abundance of most phyla, seven out of 11, exhibited significant ($p < 0.05$) and clear water-depth patterns (**Figure 1**), such as increasing, decreasing, hump-shaped, and U-shaped trends. For example, the relative abundance of Bacteroidetes decreased with water depth, while that of Nitrospirae increased toward deep water (**Figure 1**). In addition, Acidobacteria, Planctomycetes, and

TABLE 1 | Abbreviations for the abundant phyla.

Phyla	Abbrev.	Relative abundance (%)
Proteobacteria	PRO	35.80
Bacteroidetes	BAC	10.06
Chloroflexi	CHF	9.58
Nitrospirae	NIT	8.85
Acidobacteria	ACI	5.39
Planctomycetes	PLA	4.35
Chlorobi	CHB	3.69
Actinobacteria	ACT	3.22
Verrucomicrobia	VER	3.06
WS3	WS3	0.87
Gemmatimonadetes	GEM	0.83

The Table includes the most abundant bacterial phyla that together contributed up to 85% of the total sequence read. Relative abundance represents the average value of each phylum across all sites.

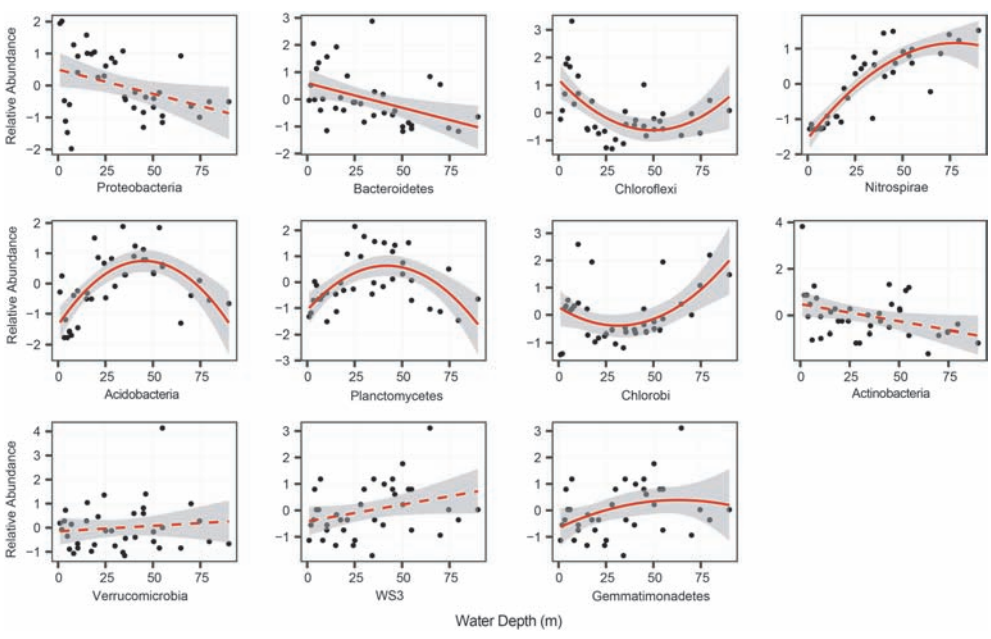

FIGURE 1 | The relative abundance of bacterial phyla along the water-depth gradient. The relationships between water depth and relative abundance were modeled with linear and quadratic models. The better model was selected based on the lower value of Akaike's information criterion. For better visualization, species relative abundance was scaled as mean = 0 and SD = 1.

Gemmatimonadetes showed hump-shaped trends along the water-depth gradient (**Figure 1**). Interestingly, the phototrophic phyla Chlorobi and Chloroflexi showed U-shaped patterns.

At the phylum level, the niche position of water depth showed great variations, ranging from 26 to 48 m (**Figure 2A**). The phylum-level niche positions had significant ($p < 0.05$) positive correlations with those at the species level (**Figure 2A**). For the whole bacterial community, there was a significant relationship between occupancy and abundance (**Figure 2B**). This is consistent with the finding at the phylum level, which also showed rather strong and positive occupancy-abundance relationships (**Figure 2B**). However, there were no clear differences among phyla in terms of the relationship of occupancy and mean abundance.

The random forest analyses showed that water depth was the strongest variable correlating with the relative abundance of the most bacterial phyla. Other environmental variables, such as metal ion concentrations, SiO_2, pH, total phosphorus, DO, and conductivity also have important effects on bacterial phyla (**Figure 3A**). Interestingly, biological factors such as chironomid richness and chlorophyll *a* concentration were also important for some bacterial phyla (**Figure 3A**). Such findings were confirmed by RDA, which shows that water depth was the strongest factor ($p < 0.001$) related to the distribution of bacterial phyla, while biological attributes, such as diatoms biomass, also showed significant ($p = 0.038$) correlations (**Figure 3B**).

In the variation partitioning analyses with the three variable components, the pure effect of chemical component was the higher for bacterial phyla rather than the pure effects of physical and biological components. The relative abundance of most phyla, such as Planctomycetes (29.9%), WS3 (22.1%), and Verrucomicrobia (21.0%), was well explained by the pure

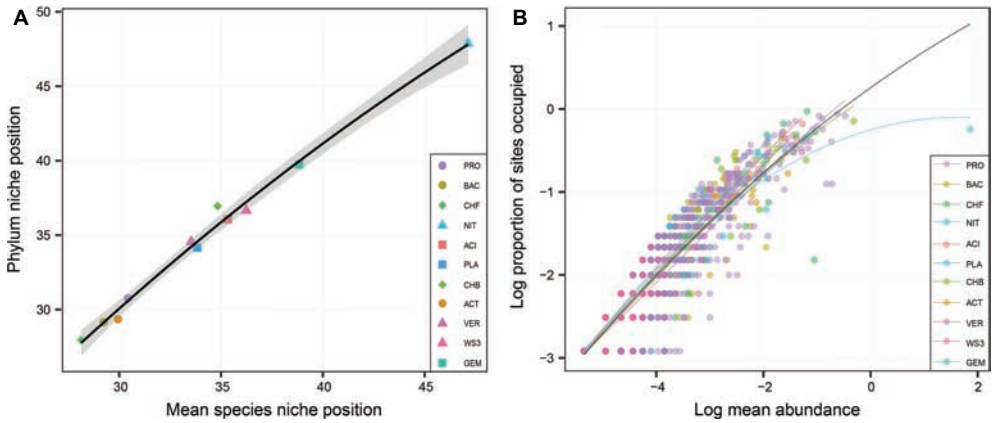

FIGURE 2 | The relationship of niche position between the phylum and species levels **(A)**, and the relationships between the occupancy and abundance of each phylum **(B)**. The shapes in **(A)** represent various distributional patterns: ■, hump-shaped pattern; ●, decreasing pattern; ▲, increasing pattern; ♦, U-shaped pattern. **(B)** Relationships between occupancy and mean local abundance for bacterial phyla. The points in **(B)** represent the different species. Linear or quadratic models were selected according to a lower value of Akaike's information criterion.

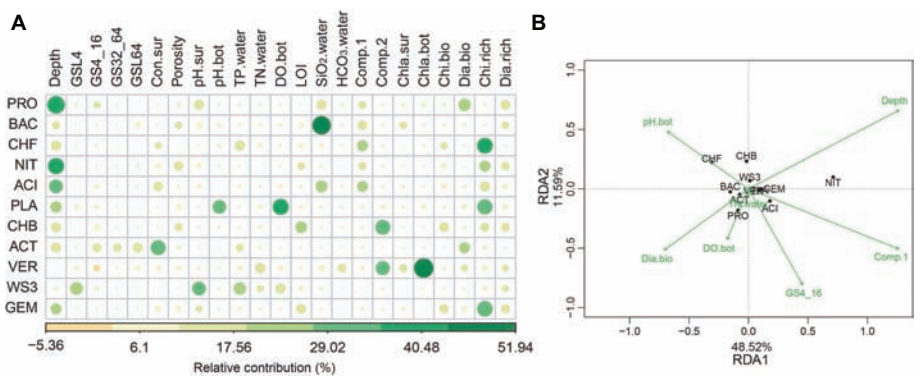

FIGURE 3 | The abiotic and biotic factors related to the relative abundance of bacterial phyla. These factors were identified with random forest **(A)** and redundancy analysis (RDA, **B**). For abiotic factors, we considered water depth (depth), total phosphorus (TP.water), total nitrogen (TN.water), conductivity (Con.sur) and concentrations of HCO_3^- (HCO_3-water) and SiO_2 (SiO_2-water), pH (pH.bot and pH.sur), dissolved oxygen (DO.bot), sediment porosity, loss-on-ignition (LOI), the first two axes of metal ion principal component analysis (Comp.1 and Comp.2) and grain size. Grain size: <4 μm (GSL4), 4–16 μm (GS4_16), 32–64 μm (GS32_64), and > 64 μm (GSL64). Biotic factors included the biomass (Dia.bio and Chi.bio) and richness (Dia.rich and Chi,rich) of diatoms and chironomids, and chlorophyll *a* (Chla.bot and Chla.sur). For RDA, the abiotic variables were automatically selected based on Monte Carlo permutation tests (999 permutations).

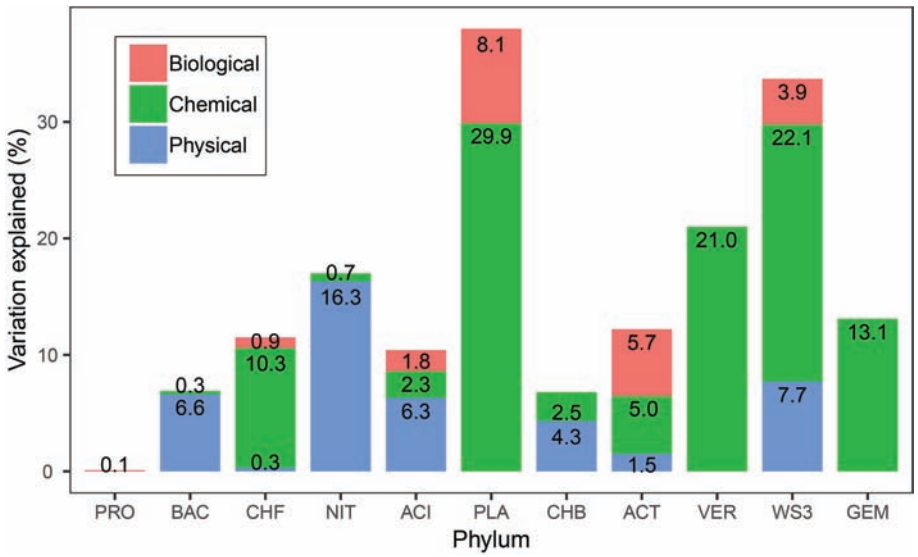

FIGURE 4 | The proportion of the variance in bacterial phylum relative abundance explained by physical, chemical, and biological variables. For simplicity, the pure effects of the three components in predicting the relative abundance are shown, but not the joint effects or unexplained variances. An alternative version of this figure showing the unique and shared variance of each group can be found in **Supplementary Figure S1**.

effect of chemical component. This is especially true for Verrucomicrobia and Gemmatimonadetes, which were only explained by the pure effect of chemical component (**Figure 4**). Physical and biological variables had effects on seven and six bacterial phyla, respectively. For Nitrospirae, physical variables were especially important, which explained 16.3% of its variation. The pure effect of biotic variables accounted for 8.1% variations of the relative abundance of Planctomycetes. For Proteobacteria, only 0.1% was explained by biological variables. Four bacterial phyla can be explained by the combination of pure effects of biological, chemical, and physical variables.

DISCUSSION

A long-standing task in ecology has been to explain biological distribution patterns and the drivers underlying these patterns. In recent years, the water-depth patterns of microbial community distribution have been extensively investigated in aquatic systems. However, most studies have focused on marine environments (Smith and Brown, 2002; Wang et al., 2013), while few studies have been conducted in freshwater ecosystems, such as lake sediments (Haglund et al., 2003; De Wever et al., 2005; Yu et al., 2014). The main aim of our study was to explore the distributional patterns of bacterial abundance at the phylum level and to analyze the abiotic and biotic variables explaining these patterns. Our results highlight four main findings. First, the bacterial phyla exhibited various patterns along the water-depth gradient, some of which are rarely reported, such as the hump-shaped and U-shaped patterns. Second, the occurrence of these patterns across phyla might be explained by the variation in their niche positions, while the occupancy-abundance relationships were not dependent on phylum attributes. Third, among all measured exploratory variables, water depth was the most important predictor of the relative abundance of bacterial phyla. Finally, although the environmental variables were shown to have pivotal roles in terms of the relative abundance of bacterial phyla, biotic variables could also substantially explain the abundance of some phyla, such as Planctomycetes, Actinobacteria, and WS3.

Proteobacteria was the most dominant phyla in the sediments of this lake, followed by Bacteroidetes, Chloroflexi, and Nitrospirae. This is consistent with previous studies that Proteobacteria and Bacteroidetes are the most abundant phyla in sediments (Diao et al., 2017). These phyla have frequently been shown to dominate freshwater bacterial communities (Dai et al., 2016). At present, investigations of the spatial pattern of bacterial relative abundance in freshwater lake sediments indicate that bacterial abundance shows clear spatial variations (Bouzat et al., 2013; Liu et al., 2015a). However, the distributional patterns of bacterial abundance along water-depth gradients, especially among bacterial phyla, have been less explored. Bacterial abundance generally decreases with water depth in freshwater systems (Liu et al., 2016). Our results reveal various water-depth patterns in terms of the relative abundance of bacterial phyla, among which some patterns have been rarely reported so far. For instance, there were significantly ($p < 0.05$) decreasing patterns for Bacteroidetes, increasing patterns for Nitrospirae, and hump-shaped patterns for Acidobacteria, Planctomycetes, and Gemmatimonadetes. The decreasing and increasing water-depth patterns of the relative abundance of bacterial phyla are consistent with the patterns found in earlier studies along other environmental gradients, such as elevations. For instance, the relative abundance of Actinobacteria, Bacteroidetes, and Deltaproteobacteria increases with elevation in stream biofilms, while that of Alphaproteobacteria decreases with elevation (Wang et al., 2012a). However, the U-shaped patterns of Chlorobi and Chloroflexi

were unexpected because such patterns are extremely rarely observed in nature, and these two phyla have phototrophic capability (Gupta, 2010). The two phyla are commonly present in the surface waters and bottom waters of deep lakes and oceans (Newton et al., 2011). The phylum Chlorobi is resistant to very low light conditions (Freed et al., 2019) and primarily exists in the anoxic aquatic environment of stratified lakes (Gupta, 2010). Chloroflexi, however, contains both photosynthetic and nonphotosynthetic members (Bryant and Frigaard, 2006), but metabolic insights suggest that a primarily heterotrophic lifestyle boosted by light-driven energy generation *via* aerobic anoxygenic phototrophy occurs in some groups (Mehrshad et al., 2018). It should be noted that alternative explanations may be needed for such U-shaped patterns of Chlorobi and Chloroflexi.

These water-depth patterns may be explained by the niche positions of the bacterial phyla. Consistent with the various water-depth patterns of relative abundance, the niche position also obviously differed among phyla. For instance, the phyla with decreasing water-depth patterns had a lower niche position, while those with increasing and hump-shaped patterns had a higher niche position. In other words, niche position may have a certain impact on bacterial phylum distributional patterns. This phenomenon has also been reported for other taxonomic groups, such as the distribution of stream insects, the predictability of which depends on niche position (Heino and de Mendoza, 2016). Furthermore, niche position could be an important predictor of the regional occupancy and local abundance of diatoms and insects, such as those in streams (Rocha et al., 2018). However, the occupancy-abundance relationship showed a relatively similar trend for all phyla. This result may have occurred because of the taxonomic relatedness among bacteria, as taxonomic relatedness has only minor influence on occupancy and abundance, as observed among the diatoms and macroinvertebrates across a set of lakes (Heino and Tolonen, 2018). Hence, the occupancy-abundance relationship could not explain the variation in water-depth patterns across phyla.

Physicochemical variables were important in explaining the relative abundance of bacterial phyla along the water-depth gradient. Among them, water depth was the most important environmental factor affecting the relative abundance of bacterial phyla in this lake ecosystem, which is consistent with previous studies showing that water depth has important effects on bacterial community composition (Yokokawa et al., 2010; Zhang et al., 2015). However, water depth could also be associated with many other physiochemical variables, including temperature, pressure, productivity, and nutrient availability (Smith and Brown, 2002; Bryant et al., 2012). It seems that water depth is only a proxy for multiple physiochemical variables, and we cannot completely exclude the influence of other environmental and biological factors on the vertical distribution of bacterial phyla.

In addition, some other environmental factors, such as metal ion concentrations, SiO_2, pH, total phosphorus, and conductivity, were also related to some bacterial phyla abundance in our study. This is in line with the finding that species are filtered by environmental factors and reproduce more under more suitable conditions (Schei et al., 2012; Alofs and Jackson, 2015). For instance, sediment bacterial abundance in freshwater plateau lakes could be influenced by pH and conductivity (Xiong et al., 2012; Liu et al., 2016), and ion concentrations are an important factor controlling bacterial community composition in lake system (Liu et al., 2014). Environmental variables, such as pH and silicate silicon, are important for the composition of the bacterial community in lake sediments, such as those in an Arctic lake area (Wang et al., 2016).

However, we also found that biotic variables were important in accounting for the relative abundance of bacterial phyla. For example, biotic variables explained 8.1, 5.7, 3.9, and 1.8% of the variation in Planctomycetes, Actinobacteria, WS3, and Acidobacteria, respectively. In particular, the relative abundance of Proteobacteria was only explained by biological variables of 0.1%, indicating that additional abiotic and biotic interactions are involved. Biotic variables, such as chlorophyll *a*, and chironomid richness, were identified to be important for the abundance of some bacterial phyla. This is in line with previous findings that biotic interactions can affect species distributions and alter biodiversity patterns (Alofs and Jackson, 2015; Sarker et al., 2018). Bacterial abundances within the lakes are positively correlated with chlorophyll *a* (Lee and Bong, 2008; Liu et al., 2016). In aquatic ecosystems, phytoplankton excrete dissolved organic matter, such as extracellular organic carbon, which may be an important source of bacterial growth. Phytoplankton and bacteria also compete for common inorganic phosphorus resources (Aota and Nakajima, 2001). Bacteria and benthic diatoms have a mutually beneficial effect in terms of promoting microalgae growth and maintaining the bacterial community (Jauffrais et al., 2017). For example, in marine environments, the bacterial abundance and community structure largely depend on the growth and physiological status of diatoms (Grossart et al., 2005), and bacteria can also control algal populations by inhibiting the growth of diatoms or by the active lysis of algal cells (Paul and Pohnert, 2011). Moreover, experimental evidence has shown that bacterial communities and chironomid larvae have a symbiotic relationship (Kuncham et al., 2017), chironomids can influence bacterial densities by grazing, and bacterial densities can in turn be related to variation in larval chironomids density (Schmid and Schmid-Araya, 2010).

CONCLUSION

In summary, we found that the relative abundance of bacterial phyla showed various water-depth patterns, such as hump-shaped and U-shaped trends. The niche position of each phylum was significantly different, which is consistent with their abundance distribution patterns. The occupancy-abundance relationship did not show differences among phyla, and niche position could be one of the predictors of the distribution of bacterial phyla. We further found that water depth was the predominant driver of the relative abundance of bacterial phyla. The relative abundance was influenced mainly by chemical variables, while the pure effect of biological variables was also important for some phyla, such as Planctomycetes, Actinobacteria, and WS3. We provided new evidence regarding the important role of

biological variables in explaining the variation in bacterial communities from the perspective of the relative abundance of bacterial phyla.

DATA AVAILABILITY

The datasets generated for this study can be found in figshare, https://doi.org/10.6084/m9.figshare.8052788.

AUTHOR CONTRIBUTIONS

JW conceived the idea and performed the bioinformatic analyses. JW, XY, and QW provided physiochemical and biological data. KW led the statistical analyses with the contributions from WZ and JW and wrote the first draft of the manuscript. KW, JW, and WZ finished the manuscript with the contributions from JS, LZ, and XC. All the authors contributed substantially to the study.

FUNDING

The work was financially supported by the Program of Global Change and Mitigation (2017YFA0605200), CAS Strategic Pilot Science and Technology (XDB31000000), CAS Key Research Program of Frontier Sciences (QYZDB-SSW-DQC043), NSFC Science Fund for Creative Research Groups (41621002), and NSFC (41571058, 41871048, 91851117).

ACKNOWLEDGMENTS

We are grateful to X. Chen, M. Yao, and Z. Hu for field sampling.

SUPPLEMENTARY MATERIAL

The Supplementary Material for this article can be found online at: https://www.frontiersin.org/articles/10.3389/fmicb.2019.01521/full#supplementary-material

REFERENCES

Agogue, H., Lamy, D., Neal, P. R., Sogin, M. L., and Herndl, G. J. (2011). Water mass-specificity of bacterial communities in the North Atlantic revealed by massively parallel sequencing. *Mol. Ecol.* 20, 258–274. doi: 10.1111/j.1365-294x.2010.04932.x

Alofs, K. M., and Jackson, D. A. (2015). The abiotic and biotic factors limiting establishment of predatory fishes at their expanding northern range boundaries in Ontario, Canada. *Glob. Chang. Biol.* 21, 2227–2237. doi: 10.1111/gcb.12853

Amin, S. A., Parker, M. S., and Armbrust, E. V. (2012). Interactions between diatoms and bacteria. *Microbiol. Mol. Biol. Rev.* 76, 667–684. doi: 10.1128/mmbr.00007-12

Anderson, M., and Cribble, N. (1998). Partitioning the variation among spatial, temporal and environmental components in a multivariate data set. *Aust. J. Ecol.* 23, 158–167.

Aota, Y., and Nakajima, H. (2001). Mutualistic relationships between phytoplankton and bacteria caused by carbon excretion from phytoplankton. *Ecol. Res.* 16, 289–299. doi: 10.1046/j.1440-1703.2001.00396.x

Bouzat, J. L., Hoostal, M. J., and Looft, T. (2013). Spatial patterns of bacterial community composition within Lake Erie sediments. *J. Great Lakes Res.* 39, 344–351. doi: 10.1016/j.jglr.2013.03.003

Brandle, M., and Brandl, R. (2001). Distribution, abundance and niche breadth of birds: scale matters. *Glob. Ecol. Biogeogr.* 10, 173–177. doi: 10.1046/j.1466-822x.2001.00213.x

Brown, M. V., Philip, G. K., Bunge, J. A., Smith, M. C., Bissett, A., Lauro, F. M., et al. (2009). Microbial community structure in the North Pacific ocean. *ISME J.* 3, 1374–1386. doi: 10.1038/ismej.2009.86

Bryant, D. A., and Frigaard, N. U. (2006). Prokaryotic photosynthesis and phototrophy illuminated. *Trends Microbiol.* 14, 488–496. doi: 10.1016/j.tim.2006.09.001

Bryant, J. A., Stewart, F. J., Eppley, J. M., and Delong, E. F. (2012). Microbial community phylogenetic and trait diversity declines with depth in a marine oxygen minimum zone. *Ecology* 93, 1659–1673. doi: 10.1890/11-1204.1

Caporaso, J. G., Bittinger, K., Bushman, F. D., DeSantis, T. Z., Andersen, G. L., and Knight, R. (2010a). PyNAST: a flexible tool for aligning sequences to a template alignment. *Bioinformatics* 26, 266–267. doi: 10.1093/bioinformatics/btp636

Caporaso, J. G., Kuczynski, J., Stombaugh, J., Bittinger, K., Bushman, F. D., Costello, E. K., et al. (2010b). QIIME allows analysis of high-throughput community sequencing data. *Nat. Methods* 7, 335–336. doi: 10.1038/nmeth.f.303

Cheng, W., Zhang, J. X., Wang, Z., Wang, M., and Xie, S. G. (2014). Bacterial communities in sediments of a drinking water reservoir. *Ann. Microbiol.* 64, 875–878. doi: 10.1007/s13213-013-0712-z

Clasen, J. L., Brigden, S. M., Payet, J. P., and Suttle, C. A. (2008). Evidence that viral abundance across oceans and lakes is driven by different biological factors. *Freshw. Biol.* 53, 1090–1100. doi: 10.1111/j.1365-2427.2008.01992.x

Dai, Y., Yang, Y., Wu, Z., Feng, Q., Xie, S., and Liu, Y. (2016). Spatiotemporal variation of planktonic and sediment bacterial assemblages in two plateau freshwater lakes at different trophic status. *Appl. Microbiol. Biotechnol.* 100, 4161–4175. doi: 10.1007/s00253-015-7253-2

De Wever, A., Muylaert, K., Van Der Gucht, K., Pirlot, S., Cocquyt, C., Descy, J. P., et al. (2005). Bacterial community composition in Lake Tanganyika: vertical and horizontal heterogeneity. *Appl. Environ. Microbiol.* 71, 5029–5037. doi: 10.1128/AEM.71.9.5029-5037.2005

DeSantis, T. Z., Hugenholtz, P., Larsen, N., Rojas, M., Brodie, E. L., Keller, K., et al. (2006). Greengenes, a chimera-checked 16S rRNA gene database and workbench compatible with ARB. *Appl. Environ. Microbiol.* 72, 5069–5072. doi: 10.1128/aem.03006-05

Diao, M., Sinnige, R., Kalbitz, K., Huisman, J., and Muyzer, G. (2017). Succession of bacterial communities in a seasonally stratified lake with an anoxic and sulfidic hypolimnion. *Front. Microbiol.* 8:15. doi: 10.3389/fmicb.2017.02511

Dowd, S. E., Sun, Y., Wolcott, R. D., Domingo, A., and Carroll, J. A. (2008). Bacterial tag–encoded FLX amplicon pyrosequencing (bTEFAP) for microbiome studies: bacterial diversity in the ileum of newly weaned salmonella-infected pigs. *Foodborne Pathog. Dis.* 5, 459–472. doi: 10.1089/fpd.2008.0107

Dumbrell, A. J., Nelson, M., Helgason, T., Dytham, C., and Fitter, A. H. (2010). Relative roles of niche and neutral processes in structuring a soil microbial community. *ISME J.* 4, 337–345. doi: 10.1038/ismej.2009.122

Edgar, R. C. (2010). Search and clustering orders of magnitude faster than BLAST. *Bioinformatics* 26, 2460–2461. doi: 10.1093/bioinformatics/btq461

Estes, J. A., Terborgh, J., Brashares, J. S., Power, M. E., Berger, J., Bond, W. J., et al. (2011). Trophic downgrading of planet earth. *Science* 333, 301–306. doi: 10.1126/science.1205106

Feld, C. K., Segurado, P., and Gutierrez-Canovas, C. (2016). Analysing the impact of multiple stressors in aquatic biomonitoring data: a 'cookbook' with applications in R. *Sci. Total Environ.* 573, 1320–1339. doi: 10.1016/j.scitotenv.2016.06.243

Foggo, A., Bilton, D. T., and Rundle, S. D. (2007). Do developmental mode and dispersal shape abundance-occupancy relationships in marine macroinvertebrates? *J. Anim. Ecol.* 76, 695–702. doi: 10.1111/j.1365-2656.2007.01245.x

Freed, S., Robertson, S., Meyer, T., and Kyndt, J. (2019). Draft whole-genome sequence of the green sulfur photosynthetic bacterium *Chlorobaculum* sp. strain 24CR, isolated from the carmel river. *Microbiol. Resour. Announc.* 8, 1–2. doi: 10.1128/MRA.00116-19

Fuhrman, J. A., Steele, J. A., Hewson, I., Schwalbach, M. S., Brown, M. V., Green, J. L., et al. (2008). A latitudinal diversity gradient in planktonic marine bacteria. *Proc. Natl. Acad. Sci. USA* 105, 7774–7778. doi: 10.1073/pnas.0803070105

Gaston, K. J., Blackburn, T. M., Greenwood, J. J. D., Gregory, R. D., Quinn, R. M., and Lawton, J. H. (2000). Abundance-occupancy relationships. *J. Appl. Ecol.* 37, 39–59. doi: 10.1046/j.1365-2664.2000.00485.x

Grossart, H. P., Levold, F., Allgaier, M., Simon, M., and Brinkhoff, T. (2005). Marine diatom species harbour distinct bacterial communities. *Environ. Microbiol.* 7, 860–873. doi: 10.1111/j.1462-2920.2005.00759.x

Gupta, R. S. (2010). Molecular signatures for the main phyla of photosynthetic bacteria and their subgroups. *Photosynth. Res.* 104, 357–372. doi: 10.1007/s11120-010-9553-9

Haas, B. J., Gevers, D., Earl, A. M., Feldgarden, M., Ward, D. V., Giannoukos, G., et al. (2011). Chimeric 16S rRNA sequence formation and detection in Sanger and 454-pyrosequenced PCR amplicons. *Genome Res.* 21, 494–504. doi: 10.1101/gr.112730.110

Haglund, A. L., Lantz, P., Tornblom, E., and Tranvik, L. (2003). Depth distribution of active bacteria and bacterial activity in lake sediment. *FEMS Microbiol. Ecol.* 46, 31–38. doi: 10.1016/s0168-6496(03)00190-9

Haller, L., Tonolla, M., Zopfi, J., Peduzzi, R., Wildi, W., and Pote, J. (2011). Composition of bacterial and archaeal communities in freshwater sediments with different contamination levels (Lake Geneva, Switzerland). *Water Res.* 45, 1213–1228. doi: 10.1016/j.watres.2010.11.018

Hanson, A., Berges, J., and Young, E. (2017). Virus morphological diversity and relationship to bacteria and chlorophyll across a freshwater trophic gradient in the Lake Michigan watershed. *Hydrobiologia* 794, 93–108. doi: 10.1007/s10750-016-3084-0

Heino, J., and De Mendoza, G. (2016). Predictability of stream insect distributions is dependent on niche position, but not on biological traits or taxonomic relatedness of species. *Ecography* 39, 1216–1226. doi: 10.1111/ecog.02034

Heino, J., and Tolonen, K. T. (2018). Ecological niche features override biological traits and taxonomic relatedness as predictors of occupancy and abundance in lake littoral macroinvertebrates. *Ecography* 41, 2092–2103. doi: 10.1111/ecog.03968

Ishwaran, H., and Kogalur, U. (2014). RandomForestSRC: Random forests for survival, regression and classification (RF-SRC). R package version 1.

Jauffrais, T., Agogue, H., Gemin, M.-P., Beaugeard, L., and Martin-Jezequel, V. (2017). Effect of bacteria on growth and biochemical composition of two benthic diatoms Halamphora coffeaeformis and Entomoneis paludosa. *J. Exp. Mar. Biol. Ecol.* 495, 65–74. doi: 10.1016/j.jembe.2017.06.004

Johnson, R. K., and Hering, D. (2010). Spatial congruency of benthic diatom, invertebrate, macrophyte, and fish assemblages in European streams. *Ecol. Appl.* 20, 978–992. doi: 10.1890/08-1153.1

Kuncham, R., Sivaprakasam, T., Puneeth Kumar, R., Sreenath, P., Nayak, R., Thayumanavan, T., et al. (2017). Bacterial fauna associating with chironomid larvae from lakes of Bengaluru city, India - A 16s rRNA gene based identification. *Genom. Data* 12, 44–48. doi: 10.1016/j.gdata.2017.03.001

Langenheder, S., Wang, J. J., Karjalainen, S. M., Laamanen, T. M., Tolonen, K. T., Vilmi, A., et al. (2017). Bacterial metacommunity organization in a highly connected aquatic system. *FEMS Microbiol. Ecol.* 93, 1–9. doi: 10.1093/femsec/fiw225

Lee, C. W., and Bong, C. W. (2008). Bacterial abundance and production, and their relation to primary production in tropical coastal waters of Peninsular Malaysia. *Mar. Freshw. Res.* 59, 10–21. doi: 10.1071/MF07099

Legendre, P. (2008). Studying beta diversity: ecological variation partitioning by multiple regression and canonical analysis. *J. Plant Ecol.* 1, 3–8. doi: 10.1093/jpe/rtm001

Legendre, P., and Gallagher, E. D. (2001). Ecologically meaningful transformations for ordination of species data. *Oecologia* 129, 271–280. doi: 10.1007/s004420100716

Liao, J. Q., Cao, X. F., Zhao, L., Wang, J., Gao, Z., Wang, M. C., et al. (2016). The importance of neutral and niche processes for bacterial community assembly differs between habitat generalists and specialists. *FEMS Microbiol. Ecol.* 92, 1–10. doi: 10.1093/femsec/fiw174

Liu, K., Liu, Y., Jiao, N., Zhu, L., Wang, J., Hu, A., et al. (2016). Vertical variation of bacterial community in Nam Co, a large stratified lake in central Tibetan Plateau. *Anton. Leeuw. Int. J. Gen. Mol. Microbiol.* 109, 1323–1335. doi: 10.1007/s10482-016-0731-4

Liu, Y. Q., Priscu, J. C., Yao, T. D., Vick-Majors, T. J., Michaud, A. B., Jiao, N. Z., et al. (2014). A comparison of pelagic, littoral, and riverine bacterial assemblages in Lake Bangongco, Tibetan Plateau. *FEMS Microbiol. Ecol.* 89, 211–221. doi: 10.1111/1574-6941.12278

Liu, S., Ren, H. X., Shen, L. D., Lou, L. P., Tan, G. M., Zheng, P., et al. (2015b). pH levels drive bacterial community structure in sediments of the Qiantang river as determined by 454 pyrosequencing. *Front. Microbiol.* 6:7. doi: 10.3389/fmicb.2015.00285

Liu, L.-X., Xu, M., Qiu, S., and Shen, R.-C. (2015a). Spatial patterns of benthic bacterial communities in a large lake. *Int. Rev. Hydrobiol.* 100, 97–105. doi: 10.1002/iroh.201401734

Martins, G., Terada, A., Ribeiro, D. C., Corral, A. M., Brito, A. G., Smets, B. F., et al. (2011). Structure and activity of lacustrine sediment bacteria involved in nutrient and iron cycles. *FEMS Microbiol. Ecol.* 77, 666–679. doi: 10.1111/j.1574-6941.2011.01145.x

Mehrshad, M., Salcher, M. M., Okazaki, Y., Nakano, S., Simek, K., Andrei, A. S., et al. (2018). Hidden in plain sight-highly abundant and diverse planktonic freshwater Chloroflexi. *Microbiome* 6:13. doi: 10.1186/s40168-018-0563-8

Newton, R. J., Jones, S. E., Eiler, A., McMahon, K. D., and Bertilsson, S. (2011). A guide to the natural history of freshwater lake bacteria. *Microbiol. Mol. Biol. Rev.* 75, 14–49.

Oksanen, J., Blanchet, F. G., Kindt, R., Legendre, P., Minchin, P. R., O'Hara, R., et al. (2013). Package 'vegan'. Community ecology package, version 2.

Paul, C., and Pohnert, G. (2011). Interactions of the algicidal bacterium Kordia algicida with diatoms: regulated protease excretion for specific algal lysis. *PLoS One* 6:8. doi: 10.1371/journal.pone.0021032

Prasad, A. M., Iverson, L. R., and Liaw, A. (2006). Newer classification and regression tree techniques: bagging and random forests for ecological prediction. *Ecosystems* 9, 181–199. doi: 10.1007/s10021-005-0054-1

Prosser, J. I., Bohannan, B. J. M., Curtis, T. P., Ellis, R. J., Firestone, M. K., Freckleton, R. P., et al. (2007). Essay - the role of ecological theory in microbial ecology. *Nat. Rev. Microbiol.* 5, 384–392. doi: 10.1038/nrmicro1643

Qin, Y., Hou, J., Deng, M., Liu, Q., Wu, C., Ji, Y., et al. (2016). Bacterial abundance and diversity in pond water supplied with different feeds. *Sci. Rep.* 6, 1–13. doi: 10.1038/srep35232

Reeder, J., and Knight, R. (2010). Rapidly denoising pyrosequencing amplicon reads by exploiting rank-abundance distributions. *Nat. Methods* 7, 668–669. doi: 10.1038/nmeth0910-668b

Rocha, M. P., Bini, L. M., Siqueira, T., Hjort, J., Gronroos, M., Lindholm, M., et al. (2018). Predicting occupancy and abundance by niche position, niche breadth and body size in stream organisms. *Oecologia* 186, 205–216. doi: 10.1007/s00442-017-3988-z

Sarker, S., Al-Noman, M., Basak, S. C., and Islam, M. M. (2018). Do biotic interactions explain zooplankton diversity differences in the Meghna river estuary ecosystems of Bangladesh? *Estuar. Coast. Shelf Sci.* 212, 146–152. doi: 10.1016/j.ecss.2018.07.012

Schei, F. H., Blom, H. H., Gjerde, I., Grytnes, J. A., Heegaard, E., and Saetersdal, M. (2012). Fine-scale distribution and abundance of epiphytic lichens: environmental filtering or local dispersal dynamics? *J. Veg. Sci.* 23, 459–470. doi: 10.1111/j.1654-1103.2011.01368.x

Schmid, P. E., and Schmid-Araya, J. M. (2010). Scale-dependent relations between bacteria, organic matter and invertebrates in a headwater stream. *Fundam. Appl. Limnol.* 176, 365–375. doi: 10.1127/1863-9135/2010/0176-0365

Shi, L.-L., Mortimer, P. E., Slik, J. W. F., Zou, X.-M., Xu, J., Feng, W.-T., et al. (2014). Variation in forest soil fungal diversity along a latitudinal gradient. *Fungal Divers.* 64, 305–315. doi: 10.1007/s13225-013-0270-5

Singh, B. K., Dawson, L. A., Macdonald, C. A., and Buckland, S. M. (2009). Impact of biotic and abiotic interaction on soil microbial communities and functions: a field study. *Appl. Soil Ecol.* 41, 239–248. doi: 10.1016/j.apsoil.2008.10.003

Smith, K. F., and Brown, J. H. (2002). Patterns of diversity, depth range and body size among pelagic fishes along a gradient of depth. *Glob. Ecol. Biogeogr.* 11, 313–322. doi: 10.1046/j.1466-822x.2002.00286.x

Song, H., Li, Z., Du, B., Wang, G., and Ding, Y. (2012). Bacterial communities in sediments of the shallow Lake Dongping in China. *J. Appl. Microbiol.* 112, 79–89. doi: 10.1111/j.1365-2672.2011.05187.x

Staley, C., Gould, T. J., Wang, P., Phillips, J., Cotner, J. B., and Sadowsky, M. J. (2015). Species sorting and seasonal dynamics primarily shape bacterial communities in the Upper Mississippi River. *Sci. Total Environ.* 505, 435–445. doi: 10.1016/j.scitotenv.2014.10.012

Teittinen, A., Weckstrom, J., and Soininen, J. (2018). Cell size and acid tolerance constrain pond diatom distributions in the subarctic. *Freshw. Biol.* 63, 1569–1578. doi: 10.1111/fwb.13186

Vilmi, A., Tolonen, K. T., Karjalainen, S. M., and Heino, J. (2019). Niche position drives interspecific variation in occupancy and abundance in a highly-connected lake system. *Ecol. Indic.* 99, 159–166. doi: 10.1016/j.ecolind.2018.12.029

Walsh, E. A., Kirkpatrick, J. B., Rutherford, S. D., Smith, D. C., Sogin, M., and D'hondt, S. (2016). Bacterial diversity and community composition from seasurface to subseafloor. *ISME J.* 10, 979–989. doi: 10.1038/ismej.2015.175

Wang, Q., Garrity, G. M., Tiedje, J. M., and Cole, J. R. (2007). Naive Bayesian classifier for rapid assignment of rRNA sequences into the new bacterial taxonomy. *Appl. Environ. Microbiol.* 73, 5261–5267. doi: 10.1128/aem.00062-07

Wang, J., Shen, J., Wu, Y., Tu, C., Soininen, J., Stegen, J. C., et al. (2013). Phylogenetic beta diversity in bacterial assemblages across ecosystems: deterministic versus stochastic processes. *ISME J.* 7, 1310–1321. doi: 10.1038/ismej.2013.30

Wang, J., Soininen, J., He, J., and Shen, J. (2012a). Phylogenetic clustering increases with elevation for microbes. *Environ. Microbiol. Rep.* 4, 217–226. doi: 10.1111/j.1758-2229.2011.00324.x

Wang, J., Soininen, J., Zhang, Y., Wang, B., Yang, X., and Shen, J. (2011). Contrasting patterns in elevational diversity between microorganisms and macroorganisms. *J. Biogeogr.* 38, 595–603. doi: 10.1111/j.1365-2699.2010.02423.x

Wang, Q., Yang, X., Hamilton, P. B., and Zhang, E. (2012b). Linking spatial distributions of sediment diatom assemblages with hydrological depth profiles in a plateau deep-water lake system of subtropical China. *Fottea* 12, 59–73. doi: 10.5507/fot.2012.005

Wang, N. F., Zhang, T., Yang, X., Wang, S., Yu, Y., Dong, L. L., et al. (2016). Diversity and composition of bacterial community in soils and lake sediments from an arctic lake area. *Front. Microbiol.* 7:9. doi: 10.3389/fmicb.2016.01170

Xiong, J. B., Liu, Y. Q., Lin, X. G., Zhang, H. Y., Zeng, J., Hou, J. Z., et al. (2012). Geographic distance and pH drive bacterial distribution in alkaline lake sediments across Tibetan Plateau. *Environ. Microbiol.* 14, 2457–2466. doi: 10.1111/j.1462-2920.2012.02799.x

Yamaoka, K., Nakagawa, T., and Uno, T. (1978). Application of Akaike's information criterion (AIC) in the evaluation of linear pharmacokinetic equations. *J. Pharmacokinet. Biopharm.* 6, 165–175. doi: 10.1007/BF01117450

Yeh, C.-F., Soininen, J., Teittinen, A., and Wang, J. (2019). Elevational patterns and hierarchical determinants of biodiversity across microbial taxonomic scales. *Mol. Ecol.* 28, 86–99. doi: 10.1111/mec.14935

Yokokawa, T., De Corte, D., Sintes, E., and Herndl, G. J. (2010). Spatial patterns of bacterial abundance, activity and community composition in relation to water masses in the eastern Mediterranean Sea. *Aquat. Microb. Ecol.* 59, 185–195. doi: 10.3354/ame01393

Yu, Z., Yang, J., Amalfitano, S., Yu, X. Q., and Liu, L. M. (2014). Effects of water stratification and mixing on microbial community structure in a subtropical deep reservoir. *Sci. Rep.* 4, 1–7. doi: 10.1038/srep05821

Zhang, E. L., Cao, Y. M., Langdon, P., Wang, Q., Shen, J., and Yang, X. D. (2013). Within-lake variability of subfossil chironomid assemblage in a large, deep subtropical lake (Lugu lake, Southwest China). *J. Limnol.* 72, 117–126. doi: 10.4081/jlimol.2013.e10

Zhang, J., Yang, Y., Zhao, L., Li, Y., Xie, S., and Liu, Y. (2015). Distribution of sediment bacterial and archaeal communities in plateau freshwater lakes. *Appl. Microbiol. Biotechnol.* 99, 3291–3302. doi: 10.1007/s00253-014-6262-x

Zhang, L., Zhao, T. T., Shen, T. T., and Gao, G. (2019). Seasonal and spatial variation in the sediment bacterial community and diversity of Lake Bosten, China. *J. Basic Microbiol.* 59, 224–233. doi: 10.1002/jobm.201800452

Zhou, J. Z., Bruns, M. A., and Tiedje, J. M. (1996). DNA recovery from soils of diverse composition. *Appl. Environ. Microbiol.* 62, 316–322

Zintzen, V., Anderson, M. J., Roberts, C. D., Harvey, E. S., and Stewart, A. L. (2017). Effects of latitude and depth on the beta diversity of New Zealand fish communities. *Sci. Rep.* 7, 1–10. doi: 10.1038/s41598-017-08427-7

Zuckerberg, B., Porter, W. F., and Corwin, K. (2009). The consistency and stability of abundance-occupancy relationships in large-scale population dynamics. *J. Anim. Ecol.* 78, 172–181. doi: 10.1111/j.1365-2656.2008.01463.x

Conflict of Interest Statement: The authors declare that the research was conducted in the absence of any commercial or financial relationships that could be construed as a potential conflict of interest.

Copyright © 2019 Wu, Zhao, Wang, Yang, Zhu, Shen, Cheng and Wang. This is an open-access article distributed under the terms of the Creative Commons Attribution License (CC BY). The use, distribution or reproduction in other forums is permitted, provided the original author(s) and the copyright owner(s) are credited and that the original publication in this journal is cited, in accordance with accepted academic practice. No use, distribution or reproduction is permitted which does not comply with these terms.

frontiers in Microbiology

ORIGINAL RESEARCH
published: 11 July 2019
doi: 10.3389/fmicb.2019.01583

Highly Diverse Aquatic Microbial Communities Separated by Permafrost in Greenland Show Distinct Features According to Environmental Niches

Malin Bomberg[1], Lillemor Claesson Liljedahl[2], Tiina Lamminmäki[3] and Anne Kontula[3]*

[1] VTT Technical Research Centre of Finland Ltd., Espoo, Finland, [2] Svensk Kärnbränslehantering AB, Solna, Sweden, [3] Posiva Oy, Eurajoki, Finland

OPEN ACCESS

Edited by:
Petra M. Visser, University of Amsterdam, Netherlands

Reviewed by:
Malak Tfaily, Pacific Northwest National Laboratory (DOE), United States
Jiri Barta, University of South Bohemia in České Budějovice, Czechia
Sarah J. Fansler, Pacific Northwest National Laboratory (DOE), United States

***Correspondence:**
Malin Bomberg
malin.bomberg@vtt.fi

Specialty section:
This article was submitted to Aquatic Microbiology, a section of the journal Frontiers in Microbiology

Received: *29 January 2019*
Accepted: *25 June 2019*
Published: *11 July 2019*

Citation:
Bomberg M, Claesson Liljedahl L, Lamminmäki T and Kontula A (2019) Highly Diverse Aquatic Microbial Communities Separated by Permafrost in Greenland Show Distinct Features According to Environmental Niches. Front. Microbiol. 10:1583. doi: 10.3389/fmicb.2019.01583

The Greenland Analog Project (GAP) study area in the vicinity of Kangarlussuaq, Western Greenland, was sampled for surface water and deep groundwater in order to determine the composition and estimate the metabolic features of the microbial communities in water bodies separated by permafrost. The sampling sites comprised a freshwater pond, talik lake, deep anoxic groundwater, glacier ice and supraglacial river, meltwater river and melting permafrost active layer. The microbial communities were characterized by amplicon sequencing of the bacterial and archaeal 16S rRNA genes and fungal ITS1 spacer. In addition, bacterial, archaeal and fungal numbers were determined by qPCR and plate counts, and the utilization pattern of carbon and nitrogen substrates was determined with Biolog AN plates and metabolic functions were predicted with FAPROTAX. Different sample types were clearly distinguishable from each other based on community composition, microbial numbers, and substrate utilization patterns, forming four groups, (1) pond/lake, (2) deep groundwater, (3) glacial ice, and (4) meltwater. Bacteria were the most abundant microbial domain, ranging from 0.2–1.4 $\times$ 10^7 16S rRNA gene copies mL^{-1} in pond/lake and meltwater, 0.1−7.8 $\times$ 10^6 copies mL^{-1} in groundwater and less than 10^4 copies mL^{-1} in ice. The number of archaeal 16S and fungal 5.8S rRNA genes was generally less than 6.0 $\times$ 10^3 and 1.5 $\times$ 10^3, respectively. N_2-fixing and methane-oxidizing Actinomycetes, Bacteroidetes and Verrucomicrobia were the dominant microorganisms in the pond/lake samples, whereas iron reducing *Desulfosporosinus* sp. dominated the deep anaerobic groundwater. The glacial ice was inhabited by Cyanobacteria, which were mostly Chloroplast-like. The meltwater contained methano- and methylotrophic Proteobacteria, but had also high relative abundances of the nano-sized Parcubacteria. The archaea composed approximately 1% of the 16S rRNA gene pool in the pond/lake samples with nano-sized Woesearchaeota as the dominating taxon, while in the other sample types archaea were almost negligent. Fungi were also most common in the pond/lake communities, were zoospore-forming Chytridiomycetes dominated. Our results show

highly diverse microbial communities inhabiting the different cold Greenlandic aqueous environments and show clear segregation of the microbial communities according to habitat, with distinctive dominating metabolic features specifically inhabiting defined environmental niches and a high relative abundance of putatively parasitic or symbiotic nano-sized taxa.

Keywords: deep biosphere, nitrogen fixation, iron reduction, photosynthesis, groundwater, metabolic profile

INTRODUCTION

Arctic environments are highly susceptible to the effects of global climate change. The effects can be seen as increased glacier melt and glacier thinning, melting of the permafrost to greater depths and increased generation of melt water (Hanna et al., 2008). The permafrost has a major impact on hydrology in Arctic regions since it separates the surface water from the deep subsurface water, providing to two from each other separate water environments (e.g., White et al., 2007; Bosson et al., 2013; Kane et al., 2013). However, in specific spots or areas called taliks, flow between surface and deep subsurface water may be possible because the ground remains unfrozen below these taliks throughout the year.

Warming of the arctic has a profound effect on arctic lake ecosystems. Even a few degrees raise in temperature may increase the open water period of arctic lakes, which may result in greater primary production rates (Vincent et al., 2009). Greater primary production is followed by increase (blooms) in biota consuming the primary produced compounds, which affect the light penetration to deeper water layers and eventually increases the amount of dead biomass sinking to the bottom of the lake where it is decomposed and causes alterations in the oxygen levels of the lake (Scheffer and Carpenter, 2003). Decreasing light penetration would also lead to decrease in the original rate of primary production, turning the lakes from CO_2 sinks to CO_2 sources (Mariash et al., 2018). Increased organic matter could severely change the food web composition in oligotrophic lakes from mostly bacteria driven in oligotrophic water to microbial eukaryotic driven with increasing organic carbon content (Cotner and Biddanda, 2002; Mariash et al., 2018). Heterotrophic bacteria have been shown to dominate the microbial communities in oligotrophic aquatic environments, such as arctic lakes, where they have crucial roles in the mineralization of primary produced organic compounds as well as recycling of carbon (reviewed by Cotner and Biddanda, 2002). In oligotrophic lakes the organic carbon is generally dissolved, in comparison to eutrophic lakes, where the organic carbon is bound in particulate matter (Biddanda et al., 2001).

Bioavailable nitrogen is introduced to the ecosystem through nitrogen fixation. In Svalbard tundra and lake sediment the availability of ammonia, nitrate, organic carbon and organic nitrogen were strong drivers for the diversity of the bacterial communities (Wang et al., 2016). In Greenlandic tundra soil, moisture was the main factor driving the nitrogen fixation, but increasing soil temperature had a negative effect on the nitrogen fixation rate (Rousk et al., 2018). Nevertheless, bedrock may also be a significant source of nitrogen compounds in aquatic ecosystems as different types of rock, e.g., metasedimentary rock types, may contain significant (up to 1 g kg^{-1}) concentrations of nitrogen (Holloway and Dahlgren, 2002). In tundra ponds in Alaska, phosphorus was the more critically limiting nutrient, whereas nitrogen was constantly supplied from the bottom sediment (Alexander et al., 1989). Severe phosphorus limitation was also reported for two lakes in SW Greenland, especially in spring (Brutemark et al., 2006). A study on more than 50 lakes and other surface water types (supraglacial and subglacial meltwater) in the Kangarlussuaq area also reported severe P and N limitations in the water (Henkemans, 2016). Thus, oligotrophic lakes are highly susceptible to increased input of nitrogen and phosphorus, which may lead to increased growth of the algal communities and this may lead to an elevation in the nitrogen and phosphorus concentrations in the water resulting from decaying biomass (Ogbebo et al., 2009).

The motivation for studying the microbial communities in aquatic environments above and below the permafrost in Greenland is connected to the safety of deep geological repositories (DGRs) for high-level radioactive waste. DGRs are designed to keep the spent nuclear fuel isolated from the surface biosphere on a time scale of hundreds of thousands of years. Over this time frame, glacial conditions are expected in northern latitudes, such as the Nordic countries and Canada (e.g.,SKB, 2011; Posiva, 2012). A thick ice cover may influence groundwater flow due to increased ice load. Melt water from the ice may also penetrate in to the bedrock environment bringing nutrients and oxygen down to repository depths (e.g., SKB, 2011; Posiva, 2012). Greenland with its ice sheet and permafrost was used as an analogous environment in the Greenland Analog Project (GAP) to investigate the hydrological, hydrogeological and geochemical processes that a nordic DGR can experience during glacial conditions resembling the retreat phase of a glacial cycle (Claesson Liljedahl et al., 2016; Harper et al., 2016). The aims were to investigate how and if the surface waters influence the deep groundwater using both geochemical and microbiological tools. In addition, we aimed to characterize the composition of arctic microbial communities in different aquatic environments and estimate the metabolic potential of these communities in order to gain more information on the little studied arctic microbial flora. Our hypotheses were; (1) the deep subsurface microbial communities are distinctly different from the surface water communities, and (2) the different environment types contain defined, environment-specific communities, even though the environments may be in direct contact with each other, such as the inflow to the Talik lake and the Talik lake water.

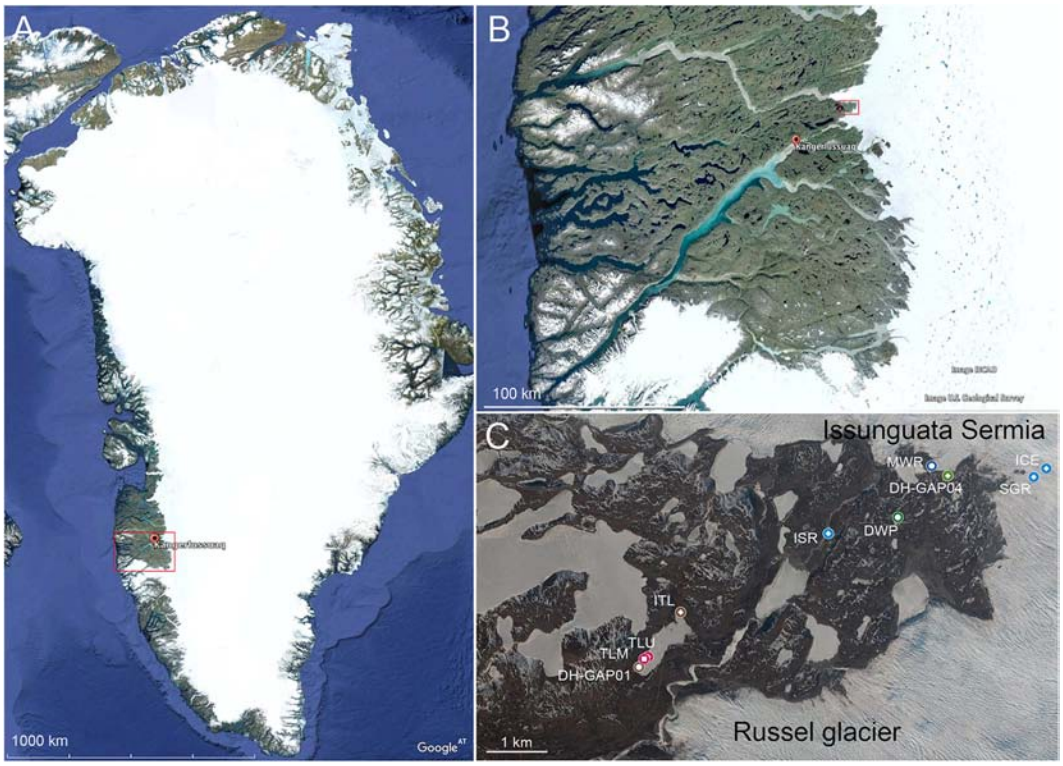

FIGURE 1 | The study area is located on the west coast of Greenland **(A)** in the Kangarlussuaq area **(B)**, which is indicated by the red square in **A**. The sampling area **(C)** is indicated by a red square in **B**. The sampling sites are indicated by colored symbols in **C**. The sample codes are explained in **Table 1**. The white bar in the lower left corner of the figures represent 1000, 100, and 1 km in **A**, **B**, and **C**, respectively. DWP, drill water pond; TLU, talik lake up; TLM, talik lake mid; DH-GAP01, drillhole DH-GAP01; DH-GAP04, drillhole DH-GAP04; ICE, glacial ice from Issunguata Sermia; SGR, Supra Glacial River; MWR, melt water river directly below the glacier; ISR, Issunguata Sermia River; ITL, inflow to Talik lake. Maps from Google Earth 2017.

MATERIALS AND METHODS

Site Description

The Kangerlussuaq area is situated on the west coast of Greenland, approximately 50 km north of the Arctic circle. Local bedrock belongs to the Nagssugtoqidian Orogen area, which is composed of 1800–1900 Ma old Archaean ortho-gneisses containing minor amounts of amphibolite and metasedimentary rocks, that have undergone metamorphosis during the Palaeo-Proterozoic (van Gool et al., 2002; Garde and Marker, 2010). The nearest ice tongues of the Greenland Ice Sheet (GrIS) are situated only 20 km east of the Kangerlussuaq village (**Figure 1**). Here the ice sheet terminates on land at a distance of 150 km from the coast. The mean annual air temperature is −5.1°C and the annual precipitation 173 mm for the period 1977–2011 (Cappelen, 2018). The two main outlet glaciers in the area are Isunnguata Sermia and the Russell glacier (**Figure 1**). In the GAP study area, the ice sheet thickness reaches approximately 1500 m with a mean value of approximately 800 m (Lindbäck et al., 2014). The ice flow is generally in the direction from east to west with a mean surface velocity of the 150 m/year. The outlet glaciers here are land-terminated and isolated from marine influence.

The vegetation consists of dwarf-shrub heath, which grow lower and less dense with increasing altitude and proximity to the ice sheet. The ice sheet melt season, with surface melt and runoff, lasts from May to September, during which time the ice sheet loses 3–4 m of thickness. The climate in the study area in low Arctic continental with continuous permafrost and is highly impacted by the presence of the GrIS. The study area is described in detail in Claesson Liljedahl et al. (2016) and Harper et al. (2016).

Surface waters (glacial ice and meltwaters, melt water ponds, lakes, rivers) and subsurface waters (deep groundwater) have been extensively studied in the Kangarlussuaq area (Henkemans, 2016). The waters are typically highly nitrogen deficient with nitrate concentrations generally below the detection limit of 0.2 mg L^{-1}. The surface waters are furthermore severely depleted in phosphorus, with P concentrations generally below 10 μg L^{-1}. However, the deep groundwater from three different sections (described below) of borehole and DH-GAP04 was shown to contain 42–4320 μg L^{-1} P, although the concentration of P in groundwater from borehole DH-GAP01 was below 10 μg L^{-1}.

A total of 12 different samples, representing lake and pond water (samples DWP, TLU, TLM), deep subsurface water (samples DH-GAP01, DH-GAP04.up/.mid/.low) and ice and meltwater (samples ICE, SGR, MWR, ISR, and ITL) were collected during September 6–14, 2014 (**Table 1** and **Figure 1**) when the permafrost is thinnest. The Talik lake area, from where

TABLE 1 | Sampling sites, dates and coordinates of the study and explanations to the abbreviations (Code) in **Figure 1**.

Code	Name	Description	Sampling date	Coordinates (UTM 22 WGS84)
DWP	Drill water pond	Pond used as water source for DH-drilling GAP04. Sample from 0–20 cm depth.	8.9.2014	N 7448270 E 0539892 z 427 m
TLU	Talik lake Upper layer	Talik Lake by DH-GAP01, 0–20 cm	11.9.2014	N7445789, E0535645, z 384 m
TLM	Talik Lake Middle layer	Talik Lake by DH-GAP01, 10 m depth	11.9.2014	N 7445751, E 0535581, z 334 m
DH-GAP01	Drillhole #01 of the Greenland Analog Project	DH-GAP01 borehole, borehole section 129–191 m	6.9.2014	N 7445607, E 0535489
DH-GAP04.up	Drillhole #04 of the Greenland Analog Project upper sample	DH-GAP04 borehole	12.9.2014	N 7449004, E 0540732
DH-GAP04.mid	Drillhole #04 of the Greenland Analog Project middle sample	DH-GAP04 borehole	13.9.2014	N 7449004, E 0540732
DH-GAP04.low	Drillhole #04 of the Greenland Analog Project lower sample	DH-GAP04 borehole	14.9.2014	N 7449004, E 0540732
ICE	Glacial ice	Isunnguata Sermia	10.9.2014	N 7449156, E 0542424, z 517 m
SGR	Supra glacial river	Isunnguata Sermia	10.9.2014	N 7449007, E 0542209, z 489 m
MWR	Melt water river	Discharge directly below Isunnguata Sermia glacier at DH-GAP04	9.9.2014	N 7449170, E 0540460, z 403 m
ISR	Isunnguata Sermia river	Downriver after meltwater pond	14.9.2014	N 7447968, E 0538703
ITL	Inflow to Talik lake	Infiltration of permafrost active layer meltwater into Talik Lake	12.9.2014	N 7446570, E 0536194, z 384 m

samples ITL, TLU, TLM, and DH-GAP01 originate is situated at an elevation of 369 m above sea level (masl) measured from the lake surface, and approximately 800 m from the ice sheet margin. The lake has a surface area of 0.37 km^2 and a catchment area of 1.56 km^2 and a maximum depth of 29.9 m. The catchment area is dominated by glacial till and glaciofluvial deposits overlain by eolian silt and fine sand. Water flows into the lake from the melting active layer of the permafrost and may also be influenced by the under lying groundwater (Johansson et al., 2015).

Drill hole DH-GAP01 was drilled in 2009. It is situated 20 m from the lake and was drilled at an angle to reach below the lake. The drill hole has a length of 221 m and reaches a vertical depth of 191 m below land surface. It was drilled using sodium fluorescein ($C_2OH_{10}Na_2O_5$) spiked water from the Talik lake. An inflatable packer is installed at 129 m vertical depth below land surface (drill hole length 150 m), allowing for sample collection from 129 – 191 m vertical depth, yielding a sampling section with a volume of 174 L. Sample intake and sensors for *in situ* pressure, temperature and electric conductivity (EC) are located at 161 m borehole length (138 m vertical depth) (Kontula et al., 2016). The lithology of this section consists mostly of felsic gneiss, with inclusions of intermediate gneiss at drill hole length 110–130 m and mafic gneiss below 180 m (Pere, 2014). Fractures are frequent and the fracture filling mineral is pyrite. The groundwater is anaerobic.

Drill hole DH-GAP04 is situated just at the margin of the Isunnguata Sermia outlet glacier (**Figure 1**). This drill hole was drilled in June 2011, has a length of 687 m and reaches a vertical depth of 645 m below land surface. Water from the Drill Water Pond (DWP), a small pond situated at approximately 1 km southwest of DH-GAP04, spiked with sodium fluorescein, was used as drilling water. Two inflatable packers are installed dividing the drill hole into three sections. The packers are installed at vertical depths of 561 and 571 m below land surface (drill hole lengths 593.5 and 605.5 m, respectively), isolating a 44 L section (DH-GAP04.mid) including two fracture zones (Harper et al., 2016). The section above the upper packer (DH-GAP04.up) extends from the base of the permafrost at 400 m depth to the upper packer, forming a 840 L drill hole section with groundwater inflow from 3 fracture systems (borehole length 548, 551, and 584 m, vertical depth 518, 522, 554 m, respectively), with a sample intake, EC and *in situ* pressure sensors installed at 541 m borehole length (512 m vertical depth). The lower section (DH-GAP04.low) has a volume of approximately 350 L containing 3 weak fractures at 638, 670, and 682 m drill hole length, equal to 604, 632, and 644 m vertical depth. Sample intake, EC and *in situ* pressure sensors are located within 2 m of the lower packer (Kontula et al., 2016). The lithology of the DH-GAP04 drill hole was intermediate gneiss at the sampling depths (Pere, 2014). The fracture filling mineral is gypsum at the depth of sampling. For more details on boreholes DH-GAP01 and DH-GAP04, see e.g., Pere (2014), Harper et al. (2016), Kontula et al. (2016). The groundwater is anaerobic.

Sampling for Chemistry

The temperature, pH and conductivity of the water samples were measured immediately in the field with a portable pH, conductivity and temperature meter (Oakton), with exception of the ice sample, which was thawed in the laboratory before measurement. Sodium fluorescein had been added to the drilling fluid when the drill holes were drilled in order to monitor the possible contamination of the deep groundwater by the drilling fluid. By purging the drill holes and allowing them to fill with groundwater from the fracture zones, the sodium fluorescein concentration and thus the drilling fluid impact eventually decreases. Samples for measuring the fluorescein content were collected into plastic bottles and wrapped in aluminum foil in order to protect the fluorescein from deterioration. Water samples for analysis of anions were collected as such directly in to unused factory-clean plastic bottles (Nalgene) and were filtered in the laboratory prior to analysis through

0.45 μm pore-size cellulose acetate filters. Samples for cationic analyses were filtered in the field through 0.45 μm pore-size cellulose acetate filters in to factory-clean plastic bottles (Nalgene) and acidified with ultra-clean nitric acid that had been rinsed three times with filtered sample water before sample collection. The anaerobic samples from DH-GAP01 and DH-GAP04 samples were collected anaerobically under nitrogen atmosphere. The samples for geochemical analyses were sent to Teollisuuden Voima Oyj (TVO), Finland, where the cations were analyzed with ICP-OES (iCAP 6500 Thermo Fisher Scientific). Anions (Br, Cl, F, NO_3, and SO_4) were analyzed with ion chromatography (DIONEX ICS-200). The alkalinity of the samples was determined with titrimetric analysis (Metrohm 905 Titrando) and the concentration of HCO_3 was calculated from this analysis. Non-purgeable organic carbon (NPOC) and Dissolved inorganic carbon (DIC) were filtered through 0.45 μm pore-size cellulose acetate filters and analyzed with a TOC analyzer at TVO with Shimadzu TOC-V CPH. Chemical analyses were done from three subsamples of each sample.

Samples for Microbiology

Water samples were collected in triplicate from each sampling site. The biomass from the water samples was collected on to Sterivex^{TM} filter units using a peristaltic pump equipped with sterile silicone tubing. The samples on the filters were immediately fixed with 5 mL MoBio LifeGuard^{TM} solution in order to preserve the nucleic acids and placed on coolers in a cooling box for a maximum time of 6 h until the samples could be placed in a freezer at −20°C. The samples were transported frozen from Greenland to Finland for processing.

In addition, two parallel 50 mL water samples were collected from each site into sterile, oxygen-free glass infusion bottles equipped with an air tight butyl rubber stopper (Bellco) and aluminum crimp cap. The water samples were collected in sterile syringes equipped with a hypodermic needle. The water samples were inserted into the sealed bottle by pushing the needle through the rubber stopper. These live water samples were kept refrigerated at 4°C and transported on ice to Finland. The storage time before processing, due to logistical necessity, was at most 2 weeks.

Estimation of Number of Cultivable Microorganisms

Nutrient agar, TSA and R2A (Sigma) agar plates for cultivation of heterotrophic microorganisms were prepared from ready media mixes according to the manufacturer's recommendations. In addition, autotrophic microorganisms were targeted using modified Medium 72 agar plates[1] without methanol. A ten-fold dilution series was prepared from each sample in sterile 0.9% NaCl solution. Aliquots of 100 μl of the undiluted sample, 10^{-1} and 10^{-2} dilutions were spread on duplicate agar plates in a laminar flow hood. The agar plates were incubated at +1°C (+/−1°C) and the appearance of colonies was checked for weekly.

[1]http://bccm.belspo.be/catalogs/lmg-media-details?CultureMediaID=72

Biolog AM

The capacity of the indigenous microbial flora of the different water samples for hydrolyzing carbon and nitrogen compounds was tested on Biolog AM 96-well plates (Biolog, Hayward, CA, United States) intended also for anaerobic microorganisms. The Biolog AM plates were prepared in an anaerobic cabinet in order to protect the plates and the samples from oxygen. The sealed sample bottles were opened in an anaerobic cabinet and aliquots 100 μl sample water were pipetted into each well on four parallel Biolog AM plates per sample. Two of the four plates were inserted into anaerobic pouches equipped with an oxygen indicator in order to maintain anoxic conditions during incubation, and two of the plates were incubated in ambient atmosphere. The Biolog AM plates were kept at 10°C and checked weekly for changes in color in the wells.

Nucleic Acid Isolation

For DNA extraction the Sterivex filter units were opened in a laminar flow hood using sterilized pliers. The membranes were removed with sterile scalpels and tweezers and put in 15 mL sterile screw cap cone tubes (Corning) for DNA extraction. DNA was extracted from the filters using the NucleoSpin Soil DNA isolation kit (Macherey-Nagel, Germany). First the beads from one bead tube were inserted to the cone tube containing the Sterivex^{TM} membrane and two reaction volumes of SL1 buffer was added to the tube, and the sealed tubes were horizontally shaken using a vortex shaker for 10 min. After 5 min centrifugation at 4000 rpm in an Eppendorf 5810R table top centrifuge the supernatant was collected and the extraction procedure continued as recommended by the manufacturer. The DNA was eluted in 50 μl of buffer SE and the DNA concentrations were measured using a Nanodrop 1000 spectrophotometer (Thermo Fisher Scientific). The mean DNA concentrations for the different sample types varied between 4.0 ± 1.0 ng μl^{-1} in DH-GAP04-UP to 10.2 ± 6.8 ng μl^{-1} in ITL. The extracted DNA was stored at −80°C.

Estimation of Microbial Community Size by Quantitative PCR

The size of the microbial community in the different sampling sites was estimated by bacterial and archaeal 16S rRNA gene qPCR as described in Bomberg et al. (2016). The fungal community sizes were estimated targeting the fungal 5.8 rRNA gene using a TaqMan approach, using primers 5.8F1 and 5.8R1 and probe 5.8P1 (Haugland and Vesper, 2002) as described in Rajala et al. (2016).

Amplicon Library Preparation

The amplification libraries for high throughput sequencing with Ion Torrent PGM were prepared by PCR from the DNA samples. Bacterial 16S genes were amplified with primers S-D-Bact-0341-b-S-17/S-D-Bact-0785-a-A-21 (Herlemann et al., 2011), targeting the variable region V3-V4 region of the 16S rDNA gene, archaeal 16S genes with primers S-D-Arch-0349-a-S-17/S-D-Arch-0787-a-A-20 (Klindworth et al., 2013), targeting the V4 region of the gene and fungal internal transcribed spacer (ITS) gene

markers with primer pair ITS1 and ITS2 targeting the fungal ITS1 region (White et al., 1990; Gardes and Bruns, 1993). PCR amplification was performed in parallel 25 μl reactions for every sample containing 1× MyTaq™ Red Mix (Bioline, London, United Kingdom, 20 pmol of each primer, up to 25 μl molecular-biology-grade water (Sigma) and 2 μl of template. The PCR program consisted of an initial denaturation step at 95°C for 3 min, 35 cycles for bacteria and fungi and 40 cycles for archaea of 15 s at 95°C, 15 s at 50°C, and 15 s at 72°C. A final elongation step of 30 s was performed at 72°C. The PCR products were verified with agarose gel electrophoresis. Amplicons were sent to Ion Torrent sequencing with PGM equipment (Bioser, Oulu, Finland) and amplicons were purified before sequencing by the staff at Bioser. The sequences have been submitted to the European Nucleotide Archive (ENA) under Study Accession Number PRJEB30970.

Sequence Processing and Analysis

The fastq sequence files obtained from Ion Torrent sequencing were first converted to fasta and qual files using the QIIME v. 1.9 software (Caporaso et al., 2010) and the sequence analysis was continued using the mothur software, v. 1.33.4 (Schloss et al., 2009). Adapters, barcodes and primers were removed and the sequence reads were trimmed to a minimum length of 250 nucleotides using mothur. No barcode differences, no ambiguous nucleotides and a maximum of 8 nucleotide homopolymers were allowed. A qwindowaverage of 25 and a qwindowsize of 50 were used on the PGM read data in order to remove erroneous reads from the data set. Chimeric sequence reads were removed with Chimera Slayer in mothur using the Silva 128 database as template (Quast et al., 2012). A phylip distance matrix was built according to the aligned sequences using the dist.seqs command in mothur with a cutoff value of 0.03. Sequence reads were clustered in to operational taxonomic units (OTU) sharing 97% identity within each OTU. The OTUs were classified against the Silva.seed_v128 database in mothur using the wang classification method. Functional profiles for the bacterial and archaeal communities were predicted using FAPROTAX (Louca et al., 2016).

ITS1 sequences were analyzed using the QIIME v 1.9 software. Adapters, barcodes and primers were removed from the sequence reads, and chimeric sequence reads were removed from the dataset with the USEARCH algorithm (Edgar, 2010) by *de novo* detection and through similarity searches against the UNITE reference dataset (Version sh_refs_qiime_ver7_dynamic_s_20.11.2016_dev) (Kõljalg et al., 2013; Unite Community, 2017; Nilsson et al., 2018) with fungal sequences. Sequences that failed to hit the sequence database with a minimum of 60% sequence identity were discarded as sequencing errors. The open reference strategy in QIIME was used for OTU picking and taxonomic classification of the sequences.

Alpha-diversity measures (number of OTUs detected in the dataset – observed OTUs, estimated number of OTUs that could in total be detected in the environment from which the data set originates – Chao1 OTU richness, and the Shannon diversity index describing the OTU richness and evenness of OTU distribution in the examined environment) were calculated based on the absolute number of sequence reads per OTU using the Phyloseq package in R (McMurdie and Holmes, 2013; R Development Core Team, 2018) and visualized using ggplot2. The similarity of the archaeal, bacterial and fungal communities between the different sample sites was tested by principal coordinate analysis (PCoA) using the Phyloseq package in R using the Bray-Curtis dissimilarity model. Eigen values for the variance explained by the PCoA dimensions were calculated on 999 random repeats.

Significant difference between the mean number of bacterial and archaeal 16S rRNA gene copies, fungal 5.8S rRNA copies and colony forming units (cfu) per mL sample water was tested using one-way ANOVA, Tukey's Q test and Kruskal-Wallis test using the PAST3 software (Hammer et al., 2009). In addition, the differences between microbial communities above and below the permafrost and between different sample types was tested with PERMANOVA using the Bray-Curtis dissimilarity model and 9999 permutations in PAST3.

RESULTS

Chemical Parameters of the Samples

The pH of the different water samples varied between 6.3 in the ICE sample (measured from molten ice in the laboratory) and 8.7 in the DH-GAP04.mid sample (**Table 2**). The conductivity (EC) of the water was highest, 3.71 mS/cm, in the DH-GAP04.low sample and lowest in the ICE and melt water samples. The deep subsurface DH-GAP04.up, .mid, and .low samples had the highest salinity, total concentration of sulfur and sulfate, while the pond and lake water contained the highest concentrations of dissolved inorganic carbon (DIC), bicarbonate and non-purgeable organic carbon (NPOC) (**Table 2**).

Microbial Biomass

The number of bacterial and archaeal 16S rRNA gene copies, fungal 5.8S rRNA gene copies and number of colony forming units (cfu) varied greatly between the different sample types (**Figure 2**). The concentration of bacterial 16S rRNA genes varied between 1.5×10^7 mL^{-1} in TLM and 1.4×10^4 mL^{-1} in DH-GAP04.low, while the concentration of archaeal 16S rRNA genes was highest in MWR, 1.2×10^4 and lowest in ICE, 1.5×10^1 mL^{-1}. The fungal 5.8S rRNA gene concentration was highest, 3.2×10^3 in TLM and lowest, 5.0 mL^{-1}, in DH-GAP04.low. The amount of culturable microorganisms varied on NA between 2.7×10^1 in TLM and 2.9×10^5 cfu mL^{-1} in DH-GAP04.mid, on TSA between 7.5×10^1 in MWR and 2.6×10^5 cfu mL^{-1} in DH-GAP04.mid, and on R2A between 2.6×10^2 in TLU and 2.6×10^5 cfu mL^{-1} in DH-GAP04.mid. No microbial colonies were obtained from the ICE sample. No colonies were detected on the modified M72 medium targeting autotrophs.

The highest concentration of bacterial 16S rRNA genes and fungal 5.8S rRNA genes correlated positively and significantly ($r > 0.8$, $p < 0.02$ and $r > 0.6$, $p < 0.02$ for bacteria and fungi, respectively) with the highest concentrations of DIC and bicarbonate. The highest number of cfu:s obtained on TSA

TABLE 2 | The chemical characteristics of the sampled water.

Sample	unit	DWP	TLU	TLM	DH-GAP01	DH-GAP04.up	DH-GAP04.mid	DH-GAP04.low	ICE	SGR	MWR	ISR	ITL
pH (field)		8.4	8.3	8.4	8.6	8.5	8.7	8.2	6.3*	8.1	7.5	7.4	6.9
Temperature (field)	°C	6.7	7.4	6.4	7.0	11.3	10.5	10.6	–	0.4	0.4	6.8	3.4
Conductivity (field)	mS/cm	0.18	0.19	0.19	0.82	2.68	2.66	3.71	0.00*	0.00	0.02	0.19	0.17
Gran titration, HCl consumption	mmol/L	1.5	1.6	1.6	n.a.	0.21	0.23	0.31	<0.03	<0.03	0.09	0.07	0.41
NPOC	mg/L	16	7.0	7.0	n.a.	4.6	4.0	0.8	6.9	<0.3	0.5	0.7	21
DIC	mg/L	16	17	17	n.a.	2.2	2.3	3.2	0.3	<0.3	1.1	0.9	4.8
Charge balance DIC	%	7.06	7.02	7.20	3.73	−0.39	−1.15	−1.14	−10.02	100.00	12.53	11.74	6.48
Charge balance HCO_3	%	2.17	1.86	2.02	3.73	−0.44	−1.21	−1.19	1.90	−31.11	13.04	13.44	6.12
Nitrogen total	mg/L	1.1	0.49	0.50	n.a.	0.50	0.27	0.053	0.042	0.052	0.30	0.34	1.1
Nitrate	mg/L	<0.4	<0.4	<0.4	<0.4	<0.4	<0.4	<0.4	<0.4	<0.4	<0.4	<0.4	<0.4
Iron	mg/L	0.11	0.009	0.020	0.027	0.024	0.018	0.056	0.064	0.017	0.15	0.15	0.24
Sulfur total	mg/L	2.1	1.3	1.3	120	460	440	660	<0.3	<0.3	0.72	0.79	14
Sulfate	mg/L	6.0	3.5	3.5	370	1410	1370	1990	<0.1	<0.1	2.1	2.3	41
TDS	mg/L	144	148	148	568	2195	2147	3123	2	1	13	12	108
Aluminum	µg/L	6	2	8	10	27	9	3	26	14	150	150	97
Bicarbonate	mg/L	92	98	98	n.a.	13	14	19	1.2	0.6	5.5	4.3	25
Bromid, Br	mg/L	<0.1	<0.1	<0.1	0.2	1.2	1.3	2.1	<0.1	<0.1	0.3	<0.1	<0.1
Fluorid, F	mg/L	0.2	0.3	0.3	0.6	0.2	0.2	0.1	<0.1	<0.1	<0.1	<0.1	0.1
Potassium	mg/L	5.2	6.2	6.2	2.0	4.1	6.7	5.5	<0.1	<0.1	0.4	0.4	1.4
Calsium	mg/L	14	15	15	99	370	330	430	<0.2	<0.2	1.9	1.7	14
Chloride,	mg/L	8.5	8.6	8.5	7.7	100	110	170	<0.2	<0.2	<0.2	0.3	4.6
Magnesium	mg/L	10	9.9	9.9	3.3	25	31	60	0.01	0.03	0.38	0.40	7.5
Sodium,	mg/L	7.0	6.6	6.6	74	260	270	430	0.3	<0.2	0.4	0.3	4.7
SiO_2	mg/L	0.70	0.45	0.46	8.1	5.4	6.4	7.9	0.09	0.29	1.9	1.6	8.8
Strontium	mg/L	0.05	0.05	0.05	2.6	6.5	6.3	8.2	0.01	0.01	0.02	0.02	0.05
Sodium fluorescein	mg/L	n.d.	n.d.	n.d.	<1	76	67	2.6	n.d.	n.d.	n.d.	n.d.	n.d.

* *measured in the laboratory, n.a., not available; n.d., not determined.*

correlated positively and significantly ($r > 0.59$, $p < 0.05$) with the highest concentration of Ca, S_{tot}, Sr, SO_4, and TDS, and the highest number of cfu:s on R2A correlated positively and significantly ($r > 0.6$, $p < 0.04$) with the highest concentration of Ca.

Alpha Diversity

The number of bacterial, archaeal and fungal sequences varied in the samples between 3.0×10^3–7.9×10^3, 1.0×10^1–8.6×10^3 and 3.0×10^3–7.9×10^3, respectively (**Supplementary Table S1** and **Supplementary Figure S1**). The highest number of observed bacterial OTUs (1.5×10^3) was observed in MWR, while the lowest number ($2.2–4.5 \times 10^2$) were detected in the deep subsurface samples and ITL. Nevertheless, the highest number of Chao1 estimated bacterial OTUs (4.6×10^3) was estimated for the ITL sample and the lowest for the deep subsurface samples. The ITL bacterial community also had the highest Shannon diversity index of 8.8 while the lowest Shannon diversity indices 3.6–6.1) were calculated for the deep subsurface samples and ICE.

The number of archaeal observed OTUs was highest in the DWP, MWR, ISR and ITL ($8.8 \times 10^2 - 1.2 \times 10^3$) and lowest in the deep subsurface and ICE, where the number of archaeal sequences was also low. The highest number of Chao1 estimated archaeal OTUs was also detected in DWP. The Shannon diversity index was highest in the lake/pond samples and MWR, ISR, and ITL and lowest in the deep subsurface and ICE samples.

The highest number of fungal ITS OTUs was observed in the lake/pond samples and MWR, ISR and ITL, while the lowest OTU numbers were obtained from the deep subsurface samples, ICE and SGR. The same was seen in the Chao1 estimations, with the exception that DH-GAP01 and ICE were also estimated to contain approximately 1.0×10^3 OTUs. The Shannon index for the fungal communities was above 4 in all other samples except TLU and the deep subsurface samples.

Bacterial Community

The bacterial community profiles differed greatly between the pond/lake, deep subsurface and ice/melt water samples. Altogether 52 bacterial Phyla were detected (**Figure 3A**). Nevertheless, specific bacterial phyla clearly dominated in the different habitats. In the pond/lake samples (DWP, TLU, and TLM), the majority of the bacterial communities consisted of Actinobacteria (**Figure 3A**), especially taxa belonging to the family Sporichthyaceae (unidentified Sporichthyaceae

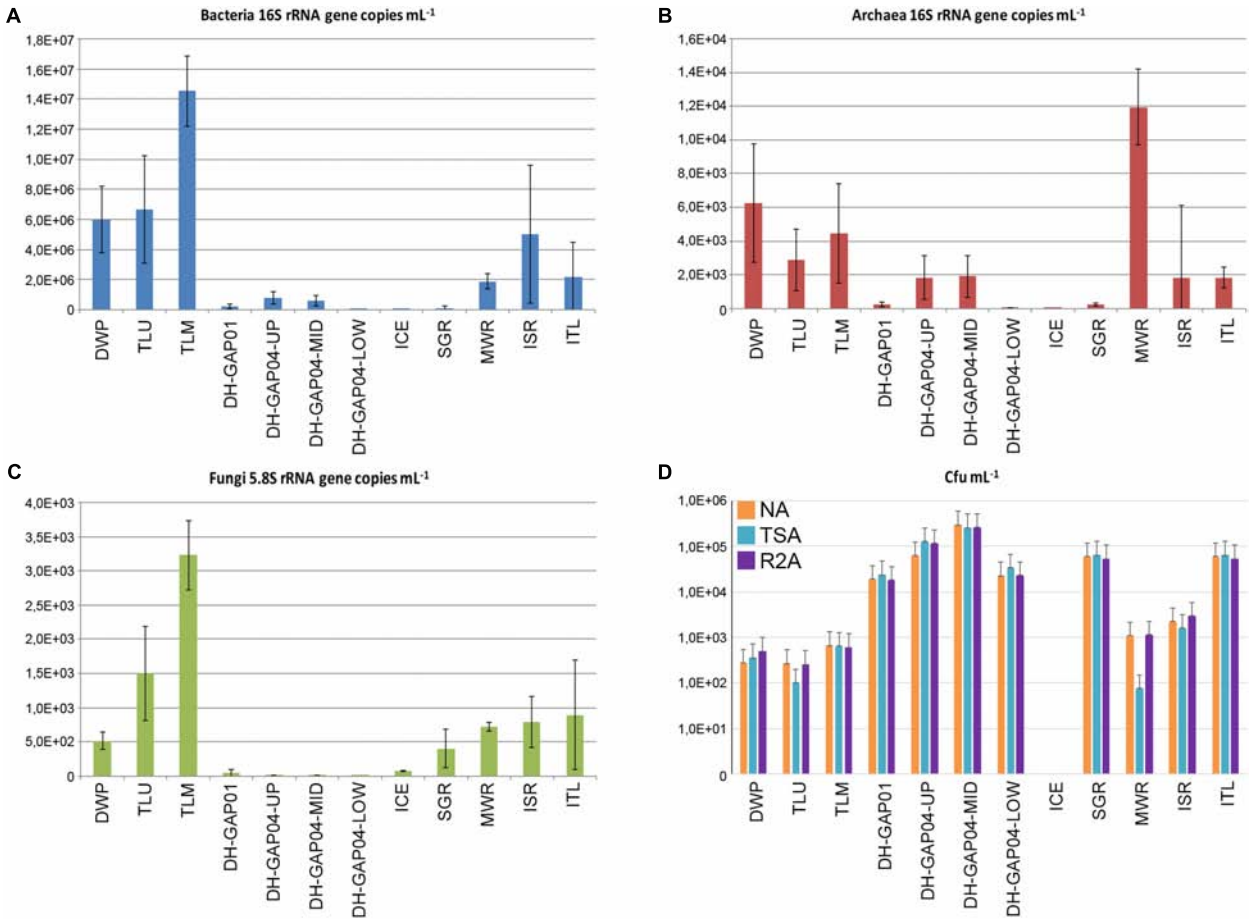

FIGURE 2 | The mean abundance of **(A)** bacteria, **(B)** archaea, **(C)** fungi estimated by quantifying the bacterial and archaeal 16S rRNA gene copies and the fungal 5.8S rRNA gene copies mL^{-1} sample water. **(D)** The mean number of colony forming units (cfu) mL^{-1} in the different water samples grown on Nutrient Agar (NA), Tryptic Soy AgR (TSA) and R2A agar. The error bars show standard deviation. In **(A–C)** the number of biological replicants was 3, of which 3 individual qPCR reactions were performed for each replicant. In **(D)** the mean number of cfu is based on dilution series including 4–6 plates per sample.

15–26% and hgcl clade 18 – 28% of the bacterial 16S rRNA gene sequence reads, **Supplementary Figure S2A**), and Candidate genus *Planktophila* (4.8 – 8.2%). In addition, the Talik lake samples (TLU and TLM) contained a large proportion of Verrucomicrobia sequences belonging to the genus *Methylacidiphilum* (11–12%) (**Supplementary Figure S2B**). Alphaproteobacteria belonging to the SAR11 clade were present as a major group in the Talik lake (9.4 – 11.4%) and as a small fraction (1.4%) also in the DWP sample.

In the deep subsurface samples, the major bacterial constituent was Firmicutes belonging to the genus *Desulfosporosinus* (23 – 61% of the sequence reads, **Supplementary Figure S2C**), and the DH-GAP04 samples also contained Thermoanaerobacterales bacteria classified as family SRB2 (13 – 37% of the sequence reads). Nevertheless, DH-GAP01 also contained 3% deltaproteobacteria belonging to the *Desulfovibrio*, 5.1 and 7.2% alphaproteobacteria belonging to *Janthinobacteria* and *Undibacteria*, respectively (**Supplementary Figure S3A**).

The bacterial community of the ICE consisted mostly of Cyanobacteria (63.5 – 76.6%) (**Figure 3A**) and proteobacteria belonging to the *Polaromnas* (10%) (**Supplementary Figure S3B**).

Proteobacteria were the most abundant bacteria in SGR, MWR and ISR (46 – 67%, **Supplementary Figure S3B**). Betaproteobacteria of the genera *Albiferax* and *Polaromonas* were detected in all three sample types (4.8 – 9% and 1.1–7.4%, respectively). However, SGR had a large proportion of *Massilia* (12.7%) and *Undibacterium* (20.6%), while MWR and ISR had *Rhodoferax* (1.2 – 4.2%) and *Methanotenera* 6.3 – 8.8%). In addition, MWR and ISR had between 10.7 – 17% *Methylobacter* sequences. Actinobacteria belonging to the Candidate genus *Planktophila* were present at a relative abundance of 6.1 – 7.1% in these two samples.

In the ITL sample, the majority of the bacterial sequences belonged to Parcubacteria (13.5 – 62% of all bacterial sequence reads) (**Figure 3A**), of which approximately 15% (of all bacterial sequence reads) belonged to a genus of the *Candidatus* class Nomurabacteria and an 10% to an unidentified Parcubacteria genus. Proteobacteria (19 – 50% of the sequence reads) belonged mostly to Methylobacter (6.4%) (**Supplementary Figure S3D**).

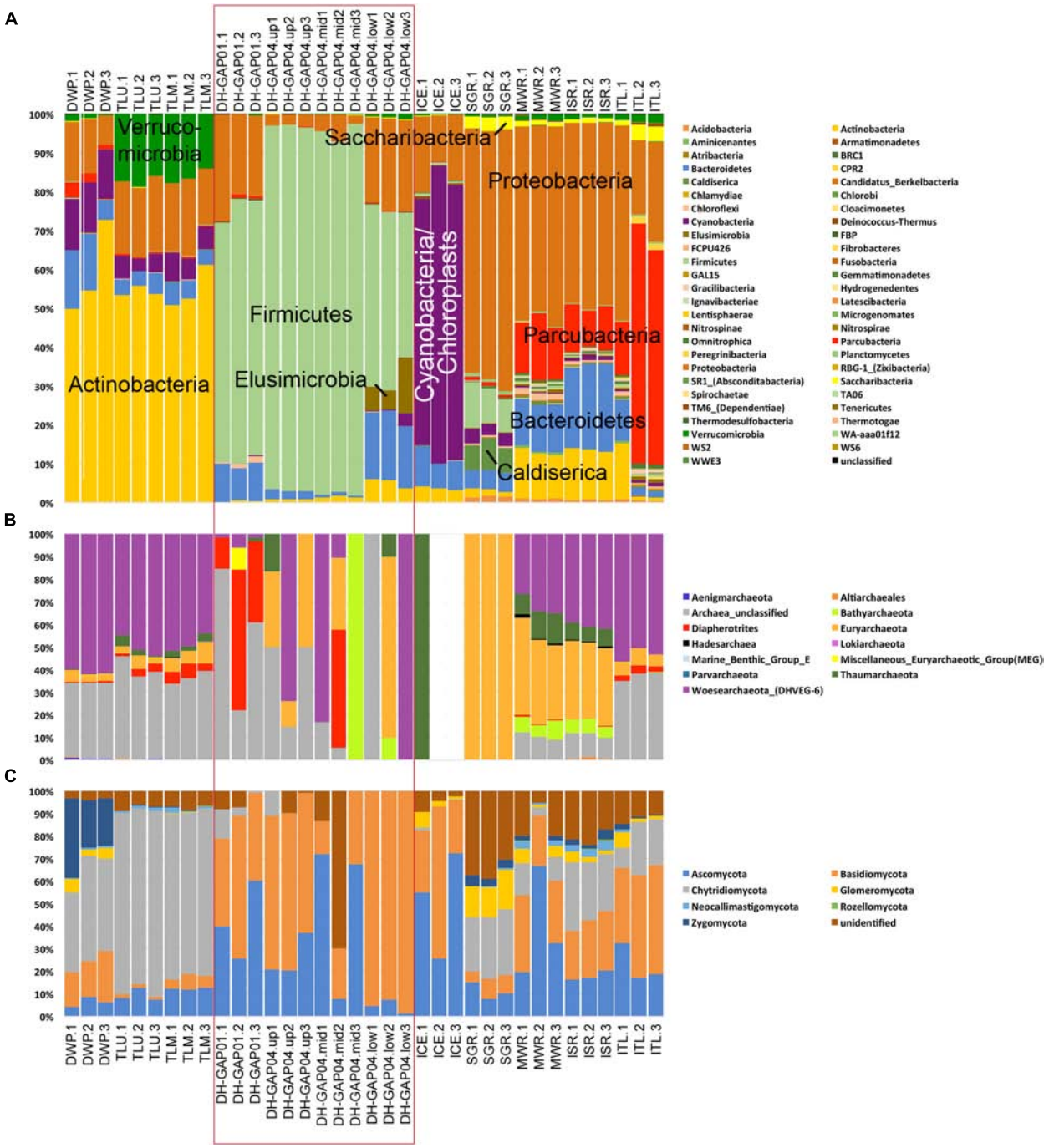

FIGURE 3 | The relative abundance of **(A)** bacterial, **(B)** archaeal, and **(C)** fungal phyla identified in the different samples. Note that each sampling site is represented by three biological replicates. The deep subsurface samples are indicated with a red rectangle, the pond/lake samples are presented to the left and the ice and melt water samples to the right of the rectangle for clarity. The bacteria with the highest relative abundances are indicated in **A**.

Bacteroidetes bacteria were present in all samples to some extent, 0.6 – 22%, most of which were Flavobacteria (**Figure 3** and **Supplementary Figure S2D**).

The difference in the bacterial communities could also be seen in the PCoA plots (**Figure 4A**), where the lake/pond samples fall to the lower right corner of the plot and the DH-GAP04 samples to the lower left. The bacterial community of the lake/pond samples are most strongly affected by the concentration of inorganic carbon (DIC, HCO_3) and buffering capacity (HCl consumption), while the deep subsurface bacterial communities are affected by salinity, sulfate and total Sulfur concentrations. Most of the ITL, MWR, and ISR cluster to the top of the plot, in

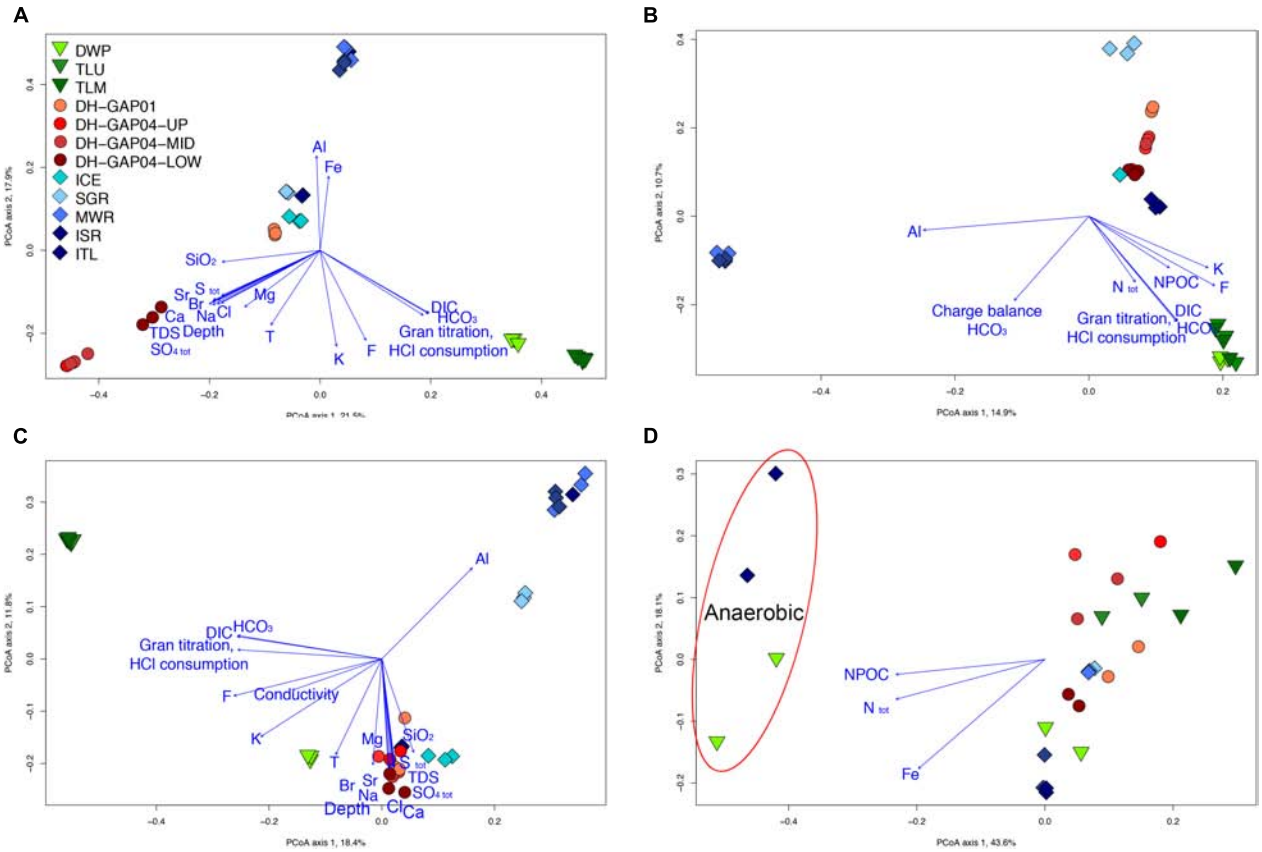

FIGURE 4 | Principal coordinates analysis plots of the **(A)** bacterial, **(B)** archaeal, **(C)** fungal communities, and **(D)** the hydrolysis patterns of substrates in the Biolog AN tests. The key to the samples in all figures is found in **A**. In **D**, the anaerobic Biolog AN tests are indicated with a red oval in the upper left quadrant. Only physicochemical parameters with $p < 0.0001$ **(A–C)** and $p < 0.001$ **(D)** were plotted.

the same direction as the concentration of Fe and Al, and the ICE and SGR samples to the middle. Interestingly, the DH-GAP01 samples also fall to the middle of this plot.

The two-way PERMANOVA analysis showed that the bacterial communities of the deep subsurface samples differed significantly ($p = 0.0001$) from the bacterial communities in water samples from above the permafrost. The bacterial communities identified from each sample type, i.e., lake/pond, deep subsurface, and ice and meltwater, also differed significantly ($p = 0.0001$) from each other.

Archaeal Diversity

Archaea were numerous only in the surface samples, but not in the DH-GAP01 or DH-GAP04 samples, or in ICE (**Figure 2B**). Altogether 13 archaeal phyla were detected, of which Woesearchaeota showed the highest relative abundance (**Figure 3B** and **Supplementary Figure 4A**). Although the archaea were not abundant in the deep drillhole samples, the most common archaea in DH-GAP01 was Ianiarchaeum (37.3%). The DH-GAP04 samples contained Woesearchaeota (24.7 – 33.3%) and *Methanoperedens* (3.3 – 31.5%) (**Supplementary Figure S4B**). In addition, DH-GAP04.mid had Nanoarchaeum (17.5%) and Bathyarchaeota (33.3%), and DH-GAP04.low had 16.7% *Methanoregula*. The archaeal community of the SGR the archaeal community consisted solely of Euryarchaeota, of which *Methanosaeta* contributed with 37.4% and *Methanospherula* with 58.7%. MWR and ISR contained a rich archaeal community, consisting of the euryarchaeotes *Methanoregula* (17.5 – 19.1%), *Methanoperedens* (5.2 – 7.3%), *Methanosaeta* (3.3 – 5.1%) and TMEG (3.1 – 3.5%), and also Woesearchaeota (31.7 – 40.6%), Thaumarchaeota (6.7 – 13.3%) and Bathyarchaeota (4.8 – 8.5%). The ITL archaeal community was similar to that of the pond/lake communities, containing 53.3% Bathyarchaeota. In all samples, except ICE and SGR, between 10 – 56% of the sequence reads belonged to unidentified Archaea. No archaeal sequences were obtained from the ICE sample.

The archaeal communities divide in to four distinct groups in the PCoA analysis (**Figure 4B**). The lake/pond samples form a cluster to the lower right corner of the plot, together with the highest concentration of inorganic and organic carbon (NPOC), total N concentration and buffering capacity of the water, while the MWR and ISR cluster together to the left of the plot. The SGR archaeal community cluster to the upper right of the plot while the deep subsurface samples fall in to a loose group to the middle right of the graph. The ITL samples appear to fall closer to the deep subsurface samples, but this is most likely a bias due

to the low number of archaeal sequences obtained from the deep subsurface samples.

The two-way PERMANOVA analysis showed that the archaeal identified from samples above and below the permafrost, as well as between different sample types (lake/pond, deep subsurface, and ice and meltwater) differed significantly ($p = 0.0001$).

Fungal Diversity

The fungal communities consisted of up to eight different fungal phyla. In the pond/lake samples, the fungal communities were dominated with Chytridiomycota (35.5 – 82.4% of all fungal ITS sequence reads in these samples) (**Figure 3C**), most of which (23.0 – 45.5% of the total number of fungal ITS reads) belonged to unidentified Chytridiomycota (**Supplementary Figure S5A**). In addition, the chytridiomycotal communities consisted of Powellomyces in all pond/lake samples (9.7 – 19.5%), and Spizellomyces (13.6 – 14.5%) in the Talik lake samples. DWP had also Zygomycota belonging to the *Ramicandelaber* (25.3%) and Basidiomycota (15.4 – 22.7%) belonging to different genera of the class Tremellomycetes (11.7%) (**Supplementary Figure S5C**). Neocallimastigomycota were represented by Orphinomyces in the lake/pond samples and by Anaeromyces in the metl water samples (**Supplementary Figure S5D**). The deep subsurface samples, as well as the ICE, contained mostly Ascomycota (20.2 – 72.5%) and Basidiomycota (22.3 – 69.9%), with the exception of the DH-GAP04.low samples, where Ascomycetes were only 1.4 – 7.2%, but Basidiomycetes contributed with 92.6 – 98.6%. In the deep subsurface samples (except DH-GAP04.low) *Cladosporium* was present in all samples (5.9 – 23.4%) (**Supplementary Figure S6A**). In addition, DH-GAP01 contained a number of Ascomycetes genera, such as an uncultured Helotiales (9.2%), *Phaeosphaeria* (6.2%), *Phaeococcomyces* (4.9%), and *Comoclathris* (4.7%), DH-GAP04.mid contained unidentified Herpotrichiellaceae (41.3%) and the ICE sample *Aspergillus* (4.4%) and unidentified Dothideomycetes (5.0%), in addition to numerous genera present at lower relative abundances (**Supplementary Figures S6A–D**). In contrast, Basidiomycetes belonging to the *Cryptococcus* were present at relative abundances of 5.6 to 22.3% in the ICE and all deep subsurface samples, except in DH-GAP04.mid, while the genus *Naganisha* was present in the DH-GAP04 and the ICE samples at relative abundances between 6.4 and 30.0, but at only 1.1% in the DH-GAP1 sample (**Supplementary Figure S7**). In addition, DH-GAP01 contained 7.9% *Collybia* and 17.4% *Mrakiella* and DH-GAP04.up *Hydnum* (5.2%), *Glaciozyma* (14.7%) and all deep subsurface samples and the ICE sample contained 1.5 – 5.3% *Malassezia* sequences (**Supplementary Figures S7A–D**).

SGR, MWR, ISR, and ITL had the highest diversity of fungal phyla and contained Ascomycota (7.7 – 66.7%), Basidiomycota (5.0 – 48.2%), Chytridiomycota (4.0 – 30.4%), Glomeromycota (0.9 – 17.5%) and a great deal on sequences of unidentified fungi (**Supplementary Figure S3C**). The main Ascomycetes groups present in all these samples belonged to Cladosporium (2.2 – 4.7%) and unidentified Helotiales (1.0 – 8.5%) (**Supplementary Figures S6A,C**). The Basidiomycetes in these samples consisted of *Rhodotorula* (1.8 – 4.8%) and unidentified Microbotrymycetes (1.6 – 3.3%), with the exception of SGR (**Supplementary Figure S7B**). In addition, ITL contained a high relative abundance of *Cronartium* (16.5%) (**Supplementary Figure S7B**). All the melt water samples, especially SGR, contained a high relative abundance of sequences affiliating with groups of the Glomeraceae (2.9 – 14.5%) not present in the other sample types (**Supplementary Figure S5B**).

The fungal communities followed the trend of the bacterial and archaeal communities in the PCoA analysis (**Figure 4C**). The TLU and TLM samples grouped together and the SGR, MWR and ISR formed a cluster of their own. The DH-GAP01, DH-GAP04, ICE and, surprisingly, ITL samples clustered together in the direction of salinity, sulfate and total S concentrations, while the DWP samples fell into a separate group closer to the deep subsurface samples than the other lake samples.

In accordance to the bacterial and archaeal communities, also the fungal communities identified from samples above and below the permafrost, as well as between different sample types (lake/pond, deep subsurface, and ice and meltwater) differed significantly ($p = 0.0001$) from each other when tested with two-way PERMANOVA.

Metabolic Profiles

The Biolog AM 96-well substrate plates were used to screen the capacity to utilize different carbon and nitrogen substrates. Substrate hydrolysis was recorded in the oxic tests in all other samples, but ICE (**Figure 5**). In the anoxic tests, substrates were hydrolyzed only by DWP and ITL communities. Between 32 and 86 of the 95 different substrates were hydrolyzed aerobically (**Figure 5**). The least number of substrates, 32 and 38, were hydrolyzed by the TLU and DH-GAP04.mid communities, respectively. The highest number of substrates, 80 and 86, were hydrolyzed by the ISR and ITL communities, respectively. In the anaerobic tests, 19 and 28 substrates were hydrolyzed by the ITL and DWP communities, respectively. The two-way PERMANOVA showed that the substrate utilization patterns were distinctly different in the surface water samples (lake/pond, ice and meltwater) compared to the deep subsurface samples ($p = 0.0009$), as well as between the different sample types (lake/pond, ice and meltwater, deep subsurface) ($p = 0.0001$) and the anaerobic vs. aerobic substrate utilization ($p = 0.0001$). In the PCoA analyses the anaerobic DWP and ITL samples clustered together as a separate group from the rest, with the DWP in the direction of the total N, NPOC and Fe concentrations (**Figure 4D**). The aerobic samples clustered to the lower half of the plot with the samples with the lowest number of hydrolyzed substrates in the left part of the cluster and to the right the samples with the highest number of hydrolyzed substrates. The greatest difference in substrate utilization was observed in the utilization pattern of carbohydrates, as the melt water communities were able to hydrolyze almost all tested substrates, while only D-Cellobiose, beta-Cyclodextrin, Dextrin, alpha-D-Glucose, Maltose, Maltotriose, L-Rhamnose, Sucrose and D-trehalose were hydrolyzed in at least 50% of the reactions from the lake/pond samples, and D-Cellobiose, beta-Cyclodextrin, L-Fructose, D-Galactose, alpha-D-Glucose, Maltose, D-Melibiose, L-Rhamnose, Sucrose and D-trehalose were used in at least 50% of the tests of the deep subsurface samples. Gentibiose was hydrolyzed anaerobically in DWP, but not aerobically. Carboxylic acids were generally hydrolyzed in all sample types,

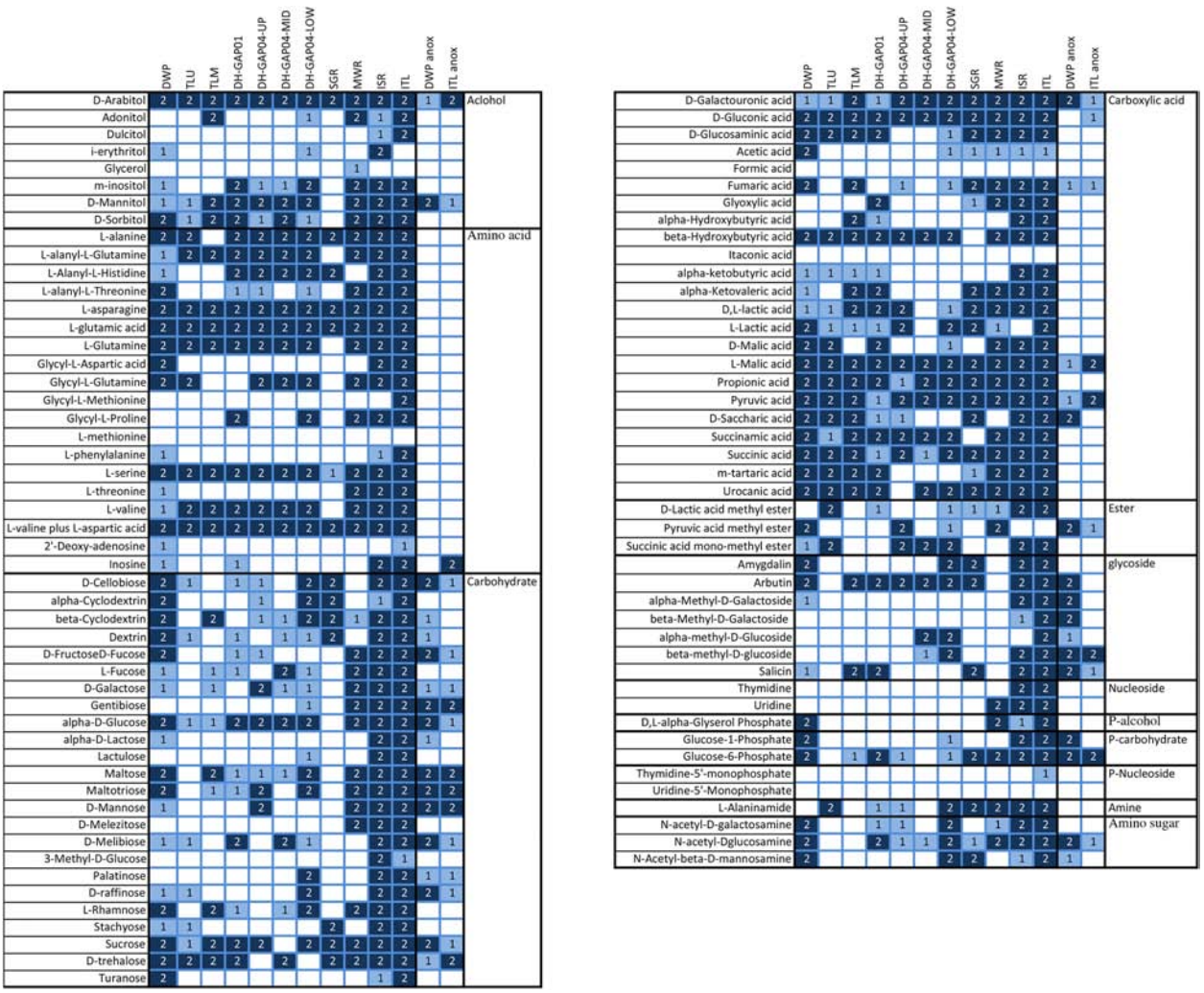

FIGURE 5 | The hydrolysis of substrates on the Biolog AN tests. All tests were done on duplicate test plates. The color coding in the figure indicates whether the hydrolysis occurred on only 1 (light blue) or on both (dark blue) plates. The samples with anaerobic hydrolysis are indicated with anox.

but interestingly, formic acid was not used in any sample. Acetate was used in the DWP, but not in the Talik lake samples. In addition, acetate was sporadically used in the meltwater sample type, but not in the deep subsurface environment, with the exception of one of the replicate reactions from DH-GAP04-LOW. D-Galacturonic acid, D-Glucuronic acid, L-Malic acid, Propionic acid, Pyruvic acid, and Succinic acid were used in all samples, of which D-Galacturonic acid, L-Malic acid and Pyruvic acid were also hydrolyzed anaerobically in DWP and ITL. Beta-hydroxybutyric acid, Succinamic acid, and Urocanic acid was used in all but one sample. Of the alcohols, D-Arabitol was used by all communities, also anaerobically in DWP and ITL. Of the amino acids, L-asparagine, L-glutamic acid, L-serine, and L-valine plus L-aspartic acid were utilized aerobically in all samples, while Glycyl-L-Proline was used only in two of four deep subsurface samples and the MWR, ISR, and ITL. L-Threonine was generally only used in the MWR, ISR, and ITL. Glycosides were sporadically used in all samples, but arbutin was especially popular and used by all, except the TLU and MWR. Interestingly, all tested glycosides, except Amygdalin, was used was used anaerobically in DWP. In contrast, Amygdalin was hydrolyzed aerobically in DWP. Thymidine and Uridine was used only in the melt water samples MWR, ISR and ITL, and only aerobically. DL-alpha-Glyserol Phosphate was used only in DWP, MWR, ISR, and ITL. Glucose-6-Phosphate was used in all sample types, although in a lesser degree in the Talik lake and the DH-GAP04 samples. The amino sugars N-acetyl-D-galactosamine and *N*-acetyl-D-glucosamine were used to some degree in all sample types, but not in the Talik lake. *N*-acetyl-D-glucosamine was also hydrolyzed anaerobically in DWP and ITL.

The FAPTOTAX predictions showed that chemoheterotrophy was the most common metabolic strategy in all identified bacterial communities, with the exception of the ICE, where chloroplasts and photosynthesis was most common (**Figure 6A** and **Supplementary Table S2**). Fermentation, sulfate and sulfur respiration were also prominent in the deep subsurface

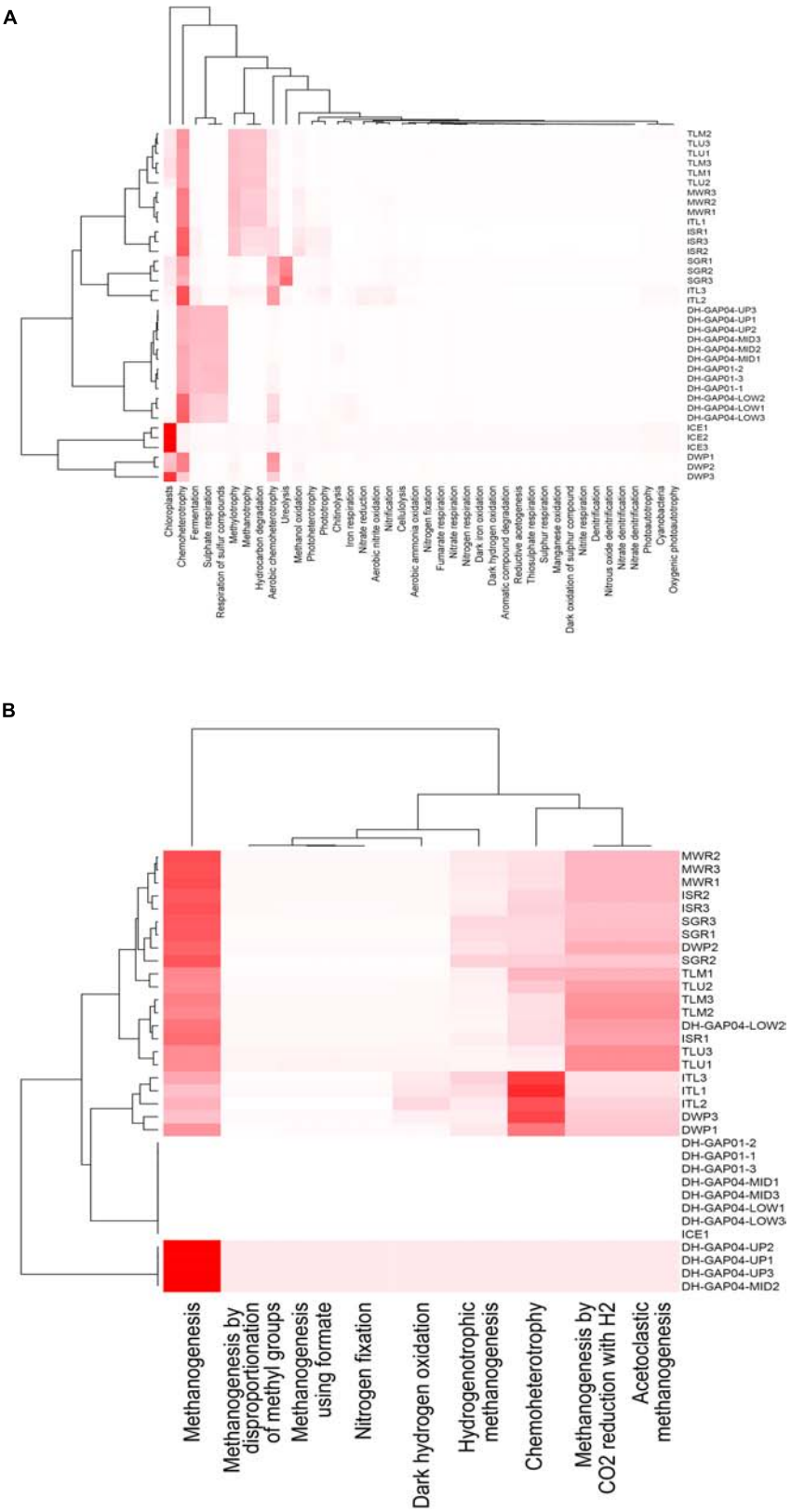

FIGURE 6 | Heatmap cluster based on the relative functional abundance predictions of the **(A)** bacterial and **(B)** archaeal communities based on FAPROTAX. The cladograms were calculated using the Bray-Curtis dissimilarity model in phyloseq.

communities, whereas methylotrophy, methanotrophy and hydrocarbon degradation were prominent metabolic strategies in the Talik lake (TLU and TLM) communities and in the melt water communities (MWR, ISR, and ITL). Ureolysis, in addition to chemoheterotrophy, was the most prominent metabolic strategy in the SGR, although this was not seen in the ICE or the MWR samples. In the archaeal communities, aceticlastic and CO_2-reducing-H_2-oxidizing methanogenesis was the most common predicted metabolic strategy (**Figure 6B** and **Supplementary Table S3**). However, in the DWP and ITL, chemoheterotrophy was more prominent in the archaeal communities than methanogenesis.

DISCUSSION

We discovered a surprisingly wide microbial diversity in the permanently cold aquatic environments of western Greenland, ranging from glacier ice and melt water to river, lake and permafrost active layer melt water and deep groundwater from below the permafrost (**Figure 1**). The microbial communities clustered into 3 – 4 more or less distinct community types according to the different habitat types, namely lake/pond (DWP, TLU, and TLM), deep groundwater (DH-GAP01 and DH-GAP04 samples) and the melt water samples (SGR, MWR, and ISR) with ICE and ITL often grouping with different samples, depending on the analysis (**Figure 4**). Adams et al. (2014) showed that the bacterial communities in the inflow, lake water, and outflow of a lake system differed significantly from each other. The authors suggested that the environmental parameters and the prevailing microbial communities had a greater role in determining the microbial community composition than the input of new organisms from inflow water. It has been shown that the deep subsurface water of the Kangarlussuaq area of Greenland originates from glacier melt water (Claesson Liljedahl et al., 2016). However, the microbial communities inhabiting the deep groundwater differ greatly in composition from the communities in the water above the permafrost layer.

Lake/Pond

Bacteria

The lake/pond samples (DWP, TLU, and TLM) were mostly affected by the concentration of DIC and the alkalinity (**Figure 4A**). Controversially, they contained high proportions, between 50.7 and 72.7%, of usually nitrogen-fixing Actinomycetes, such as *Planktophila*, typical in alkaline lakes (Jezbera et al., 2009) and *Frankiales*. According to the FAPROTAX analysis, these bacteria are responsible for the chemoheterotrophy in the lake. Bacteroidetes were also abundant in these samples, which also contribute to the chemoheterotrophy predicted in the bacterial communities (**Figure 6A** and **Supplementary Table S2**). *Flavobacteria*-like bacteria (also belonging to the Bacteroidetes) generally co-occur with periods of high heterotrophic activity and growth, and they have the ability to adapt to high-nutrient conditions (Newton and McMahon, 2011). Such conditions may have been prevailing in the lake ecosystem at the time of our sampling campaign, as we visited the site at the end of the growth season. Nitrogen fixation was not predicted by the FAPROTAX analysis for the Actinomycetes or Bacteroidetes phyla, but whole genome sequences of species belonging to the phylum Bacteroidetes (Inoue et al., 2015) have contained genes for nitrogen fixation.

Cyanobacteria were present in all lake/pond samples, but in the DWP their relative abundance was especially high. The Cyanobacteria were mostly similar to chloroplasts, indicating the importance of phytoplankton as primary producers in this ecosystem. The Talik lake samples, TLU and TLM, also contained a high relative abundance of methane-oxidizing Verrucomicrobia belonging to the novel *Methylacidiphilum* genus (Khadem et al., 2012), which also fixes nitrogen. The known *Methylacidiphilum* strains are extremely acidophilic, growing at pH as low as 1. However, in our study, approximately 12% of the bacterial sequences detected in the Talik lake samples (TLU and TLM) belonged to this genus, indicating a broader pH tolerance by this genus, or the presence of a novel type of *Methylacidiphilum*. This was also supported by the FAPROTAX predictions, which identified the *Methylacidiphilum* as both a methanotroph and a methylotroph (**Figure 6A** and **Supplementary Table S2**).

Archaea

The archaeal communities in the lake/pond samples were most affected by the concentration of organic carbon (NPOC), total N, inorganic carbon (DIC and HCO_3) and alkalinity (**Figure 4B**). Woesearchaeota were the most prominent archaeal lineage present in the lake/pond (DWP, TLU, and TLM) samples. This novel archaeal phylum was first detected in deep sea hydrothermal vents (DHVEG-6, Takai and Horikoshi, 1999), but has since then been shown to be wide spread in aquatic environments. Woesearchaeota were for example found to be frequent and abundant archaeal inhabitants of oligotrophic, high-altitude lake water in the Pyrenees (Ortiz-Alvarez and Casamayor, 2016). Ortiz-Alvarez and Casamayor (2016) also suggested that the Woesearchaeota preferred environmental conditions that also promoted high bacterial diversity, which might explain why the organic carbon, total N and inorganic carbon concentrations affected the archaeal community in this habitat. Interestingly, the Woesearchaea live in aquatic habitats covering a pH range of at least 4.4 – 10.1 as reported by Ortiz-Alvarez and Casamayor (2016). Castelle et al. (2015) showed in a study of single cell genome re-construction that the Woesearchaea have very small genomes completely lacking genes for several common metabolic pathways, such as glycolysis/gluconeogenesis, and appears to have only partial pathways for the biosynthesis of nucleotides and amino acids. It has been proposed that this group of archaea live symbiotic/parasitic lives. Between 33.4 and 40.4% of the archaeal sequences in the lake/pond samples belonged to yet unidentified archaea. Due to novel high throughput sample handling and sequencing techniques the number of genomes of uncultured archaeal lineages are expanding almost exponentially (Adams et al., 2014). Thus, the genes contained in these new genomes as well as the functions and metabolic properties or phylogenetic affiliations of the genomes of the uncultured archaea may not yet be defined, which is reflected in the databases. Due to their novelty, Woesearchaea have not yet been included in the latest version of the FAPROTAX database.

Fungi

The fungal community did not appear to be affected by organic or inorganic carbon concentrations, nor by nitrogen concentration, only by salinity and sulfate concentrations (**Figure 4C**). The main fungal component in the lake/pond (DWP, TLU, and TLM) samples belonged to the zoospore-forming Chytridiomycota. These fungi are typical aquatic inhabitants and are important decomposers of recalcitrant material, thus contributing to the nutrient cycle by releasing more easily digestible compounds from e.g., plant cell walls to the general microbial community. In addition, the DWP contained a high proportion of saprobic *Ramicandelaber* fungi belonging to the Zygomycetes phylum (Ogawa et al., 2001). These fungi were quite recently described and are generally found in soil, but now also in aquatic habitats. It is possible that the DWP, being small and shallow, is more profoundly influenced by the surrounding soil than the Talik lake, thus having a surplus of Ramicandelaber. However, the active layer melt water infiltrating into the Talik lake (ITL) did not have a high relative abundance of these fungi, which suggests that the *Ramicandelaber* is not originating from the soil. Or, it may also be possible that the soil surrounding the DWP differs from the soil in the vicinity of the Talik lake. The Talik lake environment have been glacier free for longer than the DWP, which may affect the chemical composition of the soil, which could be less favorable for the Ramicandelaber fungi compared to the younger soil surrounding the DWP.

The lake/pond samples had the highest concentration of bacterial 16S rRNA and fungal 5.8S rRNA genes but the lowest cfu concentrations. The TLU and TLM also showed among the lowest number of utilized substrates in the Biolog AM tests.

Deep Subsurface Environment

Bacteria

The bacterial community of the deep groundwater (DH-GAP01, DH-GAP04.up/.mid/.low) consisted mostly of Firmicutes (37.2 – 94.3%), which in contrast were almost absent in the surface water samples. The *Desulfosporosinus* genus had the highest relative abundance, with exception of DH-GAP04.low, contributing with up to 61% of the bacterial 16S rRNA gene sequences in these samples. The other significant firmicutes group belonging to the SRB2 cluster of the Thermoanaerobacterales family, contributed with 13.3 – 37.2% of the bacterial sequences in DH-GAP04 samples, but was absent in DH-GAP01. *Desulfosporosinus* species are known sulfate reducers with the capacity to also reduce Fe(III), nitrate, elemental sulfur ant thiosulfate (Pester et al., 2012; Sánchez-Andrea et al., 2015). The Thermoanaerobacterales SRB2 cluster is also highly likely sulfate reducers, although many Thermoanaerobacterales species do not reduce sulfate (e.g., Slobodkina et al., 2017). *Desulfosporosinus* species also have a broad range of possible electron donors and may even turn to fermentation in the absence of reducible electron acceptors (Sánchez-Andrea et al., 2015). The FAPROTAX predictions supported this as the *Desulfosporosinus* were the predominant bacteria deemed capable of fermentation, sulfate and sulfur compound respiration (**Figure 6A** and **Supplementary Table S2**). This makes the *Desulfosporosinus* very versatile bacteria able to survive in the harsh conditions of the arctic deep subsurface. Nixon et al. (2017) showed that *Desulfosporosinus* were important iron reducers in sub glacial arctic sediments, and this taxon appears to be wide spread in arctic anaerobic environments around the globe (Blanco et al., 2012). However, the FAPROTAX predictions did not show iron reduction for the *Desulfosporosinus*, neither did the deep subsurface community appear to be influenced by iron (**Figure 4A**). Instead, the samples containing the highest relative abundance of Desulfosporosinus were also most affected by the concentration of sulfate and total Sulfur.

Archaea

The archaea in the deep subsurface environments contributed with approximately 1% of the 16S rRNA gene pool. The main archaeal groups detected were the Ianarchaeum (DH-GAP01, DH-GAP04.mid), the Woesearchaeota (mainly DH-GAP04.up/.mid/.low) and the Bathyarchaeota (mainly DH-GAP04.mid). Ianarchaea, like the Woesearchaea, are minimal microbial cells dependent on other microbial species to support their growth (Golyshina et al., 2017). Nanorchaeota have been shown to grow together with specific *Thermoplasma* species in samples and cultures derived from acidic streamers, but in the deep Greenlandic subsurface groundwater the Nanorchaeota did not co-occur with any *Thermoplasma*. Due to the low abundance of archaea in these habitats, it is possible that these interactions were not seen because we worked close to the detection limit of the archaea. Bathyarchaeota, found in the DH-GAP04.mid and DH-GAP04.low samples have recently been described as a new archaeal phylum, formerly known as the Miscellaneous Crenarchaeotic Group, MCG (Evans et al., 2015). Based on single cell genome analyses this group of archaea have the necessary genes for methanogenesis, revealing that methanogenesis may be more widely spread among archaeal groups than previously thought. In addition, the fact that these archaea live in deep groundwater with an ambient temperature of 0–2°C may also suggest psychrophilic methanogenesis by these archaea.

Fungi

The fungal community in the deep subsurface samples was almost negligent. It should be considered, however, that the qPCR standard used for the estimation of fungal biomass is based on number of spores, and that spores may have several rRNA gene operons per genome. Nevertheless, the fungal communities were most affected by salinity and sulfate concentrations (**Figure 4C**).

Cladosporium was present in all samples (5.9 – 12.0 %), except DH-GAP04.low. This fungus is commonly found as a constituent of indoor mold communities and as parasites and pathogens of fungi and plants, respectively. Because the fungal community in the deep subsurface samples were very scarce, it is possible that the *Cladosporium* sequences in these samples are derived from contaminants. Nevertheless, these samples also contained different kinds of fungi previously detected in arctic environments, such as the Helotiales (Walker et al., 2011), Phaeococcomyces black yeast growing on rock surfaces (Gadd, 2007) and a variety of decomposer fungi (Singh and Singh, 2012). Despite their low abundance in the deep subsurface water, these

fungi may be important decomposers in biofilms on rock surfaces in the subsurface environments. In addition, fungi weather rock releasing important nutrients for the use by the rest of the microbial community. Fossils of filamentous fungal structures have recently been revealed from deep subsurface rock (Bengtson et al., 2017). The heterotrophic anaerobic fungi inhabiting the anoxic deep subsurface release hydrogen through their metabolism, thus also supporting other microbial growth (Drake and Ivarsson, 2018). It has also been shown in igneous crystalline deep rock environments that there is a coupling between the anaerobic, rock-weathering fungi and sulfate reducing bacteria (Drake et al., 2017).

The deep subsurface waters had (together with ICE and SGR) the lowest number of bacterial and archaeal 16S rRNA and fungal 5.8S rRNA genes in this study, with the exception of the number of archaea in DH-GAP04.up and DH-GAP04.mid, where the archaeal number was approximately the same as in ISR and ITL. In contrast to the low gene copy numbers, the highest numbers of bacterial colonies were detected in DH-GAP04.up and DH-GAP04.mid, despite these samples being anoxic. The microbial communities hydrolyzed between 33 and 53 of the 95 substrates provided on the Biolog plate, similarly to the lake/pond communities. In addition to the sulfate reducing bacteria and the fastidious archaea, a subpopulation of heterotrophic aerobic bacteria inhabited this ecosystem.

Ice and Melt Water

Bacteria

The glacial ICE had a surprisingly high number of bacterial 16S rRNA gene copies, 4.8×10^4 mL^{-1}. The population consisted mostly of Cyanobacteria, more exactly to Chloroplasts, which may originate from ice algae. Tanaka et al. (2016) found a large population of green algae and cyanobacteria in Siberian glaciers and showed that the biomass of algae increased with increasing temperature. Algae and cyanobacteria are primary producers, i.e., produce carbon compounds in their photosynthesis. In addition, these microorganisms fix atmospheric nitrogen. The produced carbon and nitrogen compounds are released in to the melt water and may be carried long distances from the point of primary production. Kohlbach et al. (2016) showed that the substrates produced by ice algae sustain ecological (macrobiota) key species in the Arctic Ocean, where the ice algae contribute with up to 25% of the primary produced carbon. This carbon strongly affects food webs in this ecosystem. In our study, the effect may be seen in the increase of microbial 16S rRNA gene copy numbers in the MWR and ISR, which are down flow from the glacier.

Proteobacteria was the most abundant bacterial phylum in the SGR, MWR and ISR, with beta- and gammaproteobacterial types as the most common. Psychrotrophic *Polaromonas* (1.1 – 7.4%) (Mattes et al., 2008; Darcy et al., 2011) and iron and manganese reducing *Albidiferax* (4.8 – 9.0%) (Lu et al., 2013; Akob et al., 2014; Kaden et al., 2014) were detected in all samples. The MWR and ISR also contained iron reducers belonging to the *Rhodoferax* (1.2 – 4.2%) (Kaden et al., 2014), some of which have been shown to be psychrotolerant and facultatively anaerobic (Finneran et al., 2003). This is well in agreement with the chemical parameters, as the bacterial communities in MWR, ISR and ITL were most strongly affected by the concentration of iron (**Figure 4A**). The *Rhodoferax* also contributed the majority of the phototrophy predicted to be present in the ISR and ITL (**Figure 6A** and **Supplementary Table S2**). Interestingly, the MWR and the ISR had a high relative abundance of methylotrophic bacteria belonging to the *Methylotenera* (6.3 – 8.8%) and *Methylobacter* (10.7 – 17.0%). *Methylobacter* species frequently been detected in arctic environments (Wartiainen et al., 2006). Although generally aerobic, *Methylobacter* species have been shown to perform anaerobic methane oxidation in sub-arctic lake sediments and to closely associate with iron reducers (Martinez-Cruz et al., 2017) and *Methylotenera* have also been shown to perform methane oxidation in arctic lake sediment (He et al., 2012). In addition, ISR had 5.4% of the 16S rRNA gene sequences belonging to *Crenotrix*, which have recently been shown to oxidize methane aerobically, but also anaerobically while reducing nitrate (Oswald et al., 2017). The FAPROTAX predictions also identified the *Methylotenera*, *Methylobacter,* and *Crenotrix* as the main methylotrophs in these samples (**Figure 6A** and **Supplementary Table S2**). *Undibacterium*, a genus ubiquitously found in aquatic (Chen et al., 2017) and soil (Li et al., 2017) environments was detected at high relative abundance (20.6%) only in SGR. *Massilia,* which contributed with a significant portion (12.7%) of the bacterial 16S rRNA gene pool in SGR, have been found in soil environments and especially as colonizers of plant roots (Ofek et al., 2012). *Massilia* could also play a significant role in the cycling of nitrogen compounds in the melting surface environment on glaciers, as they were predicted to be the main ureolytic microorganisms in the SGR (**Figure 6A** and **Supplementary Table S2**). Urea may be released from the decomposition of nitrogenous organic matter (Berman et al., 1999), which in this case could originate from the abundant Cyanobacteria found in the ICE. Our results indicate a more widespread distribution of habitats for this bacterium.

The MWR and ISR contained a high relative abundance of Parcubacteria (9.2 – 17.2%), which is a novel bacterial superphylum. These bacteria have reduced genome sizes, leading to limited metabolic capabilities, and they strongly rely on fermentation for their energy demand (León-Zayas et al., 2017). They are adapted to oxidative stress and they have genes for nitrate reduction. Due to their reduced metabolic capabilities in addition to the presence of genes for several adhesion and attachment proteins, it is assumed that they lead either symbiotic or parasitic lifestyles, but the assumption leans more toward symbiotic (Nelson and Stegen, 2015). The Bacteroidetes and Actinomycetes communities in these samples consisted of similar genera as in the lake/pond samples and were responsible for the chemoheterotrophic cycling of nutrients (**Figure 6A** and **Supplementary Table S2**). In the ITL samples, Parcubacteria dominated the bacterial communities with a relative abundance of up to 62.0%. The Proteobacteria were the second most abundant bacterial phylum, and also in ITL, *Methylobacter* contributed with 6.4% of the bacterial 16S rRNA gene sequences, indicating their important role in the oxidation of methane and

methylated compounds in this environment (**Figure 6A** and **Supplementary Table S2**).

Archaea

The ICE had hardly any archaea according to the qPCR and only a few sequences from one ICE sample replicate, all belonging to the *Nitrosoarchaeum*, were obtained. The SGR had 2.5×10^2 mL^{-1} archaeal 16S rRNA gene copies consisting almost exclusively of methanogens belonging to the *Methanosaeta* (37.3%) and *Methanospherula* (58.7%). The MWR had the highest abundance of Archaea measured in this study, with up to 1.2×10^4 mL^{-1} archaeal 16S rRNA gene copies. The ISR had 1 order of magnitude less archaea, but the archaeal community structure in the MWR and ISR were very similar. The majority of the archaea belonged to the earlier mentioned Woesearchaeota. Methanogens belonging to the *Methanoregula* (17.5 – 19.1%) and *Methanosaeta* (3.3 – 5.1%) were also prominent. However, ammonia oxidizing *Nitrosoarchaeum* (Li et al., 2016) (5.9 – 8.2%) and anaerobic methane oxidizing *Methanoperedens* (formerly known as ANME-2D archaea) contributed with 5.2 – 7.3% of the archaeal 16S rRNA gene sequences. Putative methanogenic Bathyarchaeota (Evans et al., 2015) were also present in these samples (5.8 – 6.9%). This further implies that the methane and nitrogen cycling microbiota are important parts of the microbial communities of the melting arctic (**Figure 6B** and **Supplementary Table S3**). The ITL archaeal community was similar to that of the lake/pond samples.

Fungi

The fungal community in the ICE sample consisted of only 7.9×10^1 mL^{-1} spore equivalents. In the SGR, MWR, ISR and ITL the fungal communities were over 10 times larger. Yeasts, such as *Cryptococcus* and *Rhodotorula* (Basidiomycetes) have previously been found in subglacial ice of high Arctic glaciers (Butinar et al., 2007), and the authors reported up to 4.0×10^3 cfu mL^{-1} melt ice. Other yeasts, such as *Microbotryomyces*, were also found in these samples. Genera of the Glomeraceae were abundant and found exclusively in this group of samples. This phylum contains fungi that grow only in symbiotic mycorrhizal relationships with plants. They may have ended up in these environments as spores or sloughed off from plant roots from the surrounding terrestrial habitats. The rust fungus *Cronartium* was only detected in ITL, probably because the melt water from the active layer of the permafrost runs through shrub vegetated soil, from where the rust has infected the plants. Fungi belonging to the *Anaeromyces* were found only in the SGR, MWR, ISR, and ITL samples, but only at low relative abundances. Nevertheless, this fungus is obligately anaerobic (Breton et al., 1990), but in our samples found in aerobic habitats.

The number of cfu in the SGR, MWR, ISR and ITL samples were in the range of the deep subsurface samples, but the number of bacterial 16S rRNA gene copies and fungal 5.8S rRNA gene copies were 1 order of magnitude higher, with exception for the bacteria in the SGR. The ISR and ITL microbial communities hydrolyzed the highest number of substrates in the Biolog AM test, indicating a high metabolic variety of the microbial communities in these samples. The lack of autotrophically growing bacteria also support the dominance of heterotrophic strategies in the high Arctic aquatic systems.

SUMMARY

The microbial communities in the different habitat types differed both in taxonomical and metabolic characteristics. The most important microbial process in the lake/pond environment at the time of sampling was chemoheterotrophy. These heterotrophic bacteria have key positions in the degradation of organic matter and nutrient cycling in oligotrophic aquatic environments. Nitrogen fixation capacity was predicted to be low, according to the metabolic predictions, indicating that the bioavailable nitrogen is cycled through the breakdown of biomass, but may also originate from geological deposits in the host rock. The primary producing phytoplankton are also important key species because they provide photosynthetically produced carbon for the use of the rest of the microbial community. The relatively high abundance of fungi in the lake/pond environments also indicate that dead biomass needs to be recycled. Methane released from the anaerobic sediments in the lake/pond environment is oxidized by the methylotrophic Verrucomicrobia.

The deep subsurface biosphere functions mostly through sulfate or iron reduction or fermentation. Thus, the both the microbial community composition as well as the metabolic profiles of the communities in the deep subsurface differ from the microbial communities of the surface biosphere.

The algae of the glacial ice are important primary producers for the whole aquatic system as the ice melts. These algae release photosynthetically produced carbon compounds and nitrogen compounds from their nitrogen fixation, which is then transported away from the glacier. They may also function as a nitrogen source in the melt water through biomass breakdown. The melt water streams are rich in methane oxidizing bacterial and archaeal types, which may function together with iron reducing bacteria when oxidizing methane. The high relative abundance of methane oxidizers and iron reducers in the melt water streams may thus decrease the general methane emissions from arctic aquatic environments.

Most of the archaea and some of the bacteria detected in this study affiliated with newly described groups, which have extremely small genomes. It is still debated whether these microorganisms are symbionts or parasites. However, their high abundance in cold arctic aquatic environments may mean that they are symbionts. By serving as symbionts to larger microorganisms, these micro-archaea and –bacteria may provide their hosts with specific enhancement or advantage for better survival in these conditions. These small genome-size microorganisms appear to have in common the capacity for fermentation coupled with the release of hydrogen, which may aid the host.

Fungi and yeast degrade organic macromolecules in arctic conditions by secretion of cold-adapted enzymes. They also weather rock, which releases important mineral nutrients, and release hydrogen, which is a preferred energy source for many

microorganisms. Thus, fungi contribute strongly to nutrient cycling in these environments.

CONCLUSION

In conclusion, our results demonstrate that the different water types (lake/pond, deep subsurface, ice and melt water) differ from each other both by chemical and biological measurements, despite the fact that a great part of the waters originate from glacier melt water. The infiltration of water from one habitat type to the other, does not affect the microbial communities as much as the environmental conditions of the habitat do. For example, the harsh conditions in the subsurface below the permafrost does not support survival of most of the aerobic surface microorganisms. However, some cultivable aerobic microorganisms survive in the anaerobic deep subsurface, although in the deep subsurface conditions, they form a minority of the microbial community.

AUTHOR CONTRIBUTIONS

MB, AK, and TL conceived the study and performed the sampling. MB did the microbiology work and analyses. AK and TL were responsible for the chemistry data. LC gave valuable background information of the site and prepared the deep boreholes for sampling. MB wrote the manuscript. AK, TL, and LC commented on the manuscript.

FUNDING

This work was supported by the Academy of Finland (MB, Grant No. 261220), Posiva Oy and Svensk Kärnbränslehantering AB.

ACKNOWLEDGMENTS

Birgitta Kalinowski (SKB) is thanked for critical review of the manuscript.

SUPPLEMENTARY MATERIAL

The Supplementary Material for this article can be found online at: https://www.frontiersin.org/articles/10.3389/fmicb.2019.01583/full#supplementary-material

REFERENCES

Adams, H. E., Crump, B. C., and Kling, G. W. (2014). Metacommunity dynamics of bacteria in an arctic lake: the impact of species sorting and mass effects on bacterial production and biogeography. *Front. Microbiol.* 5:82. doi: 10.3389/fmicb.2014.00082

Akob, D. M., Bohu, T., Beyer, A., Beyer, A., Schäffner, F., Händel, M., et al. (2014). Identification of Mn(II)-oxidizing bacteria from a low-pH contaminated former uranium mine. *Appl. Environ. Microbiol.* 80, 5086–5097. doi: 10.1128/AEM.01296-14

Alexander, V., Whalen, S. C., and Klingensmith, K. M. (1989). "Nitrogen cycling in arctic lakes and ponds," in *High Latitude Limnology*, eds W. F. Vincent and J. C. Ellis-Evans (Dordrecht: Springer), 165–172. doi: 10.1007/bf00031619

Bengtson, S., Rasmussen, B., Ivarsson, M., Muhling, J., Broman, C., Marone, F., et al. (2017). Fungus-like mycelial fossils in 2.4-billion-year-old vesicular basalt. *Nat. Ecol. Evol.* 1:0141. doi: 10.1038/s41559-017-0141

Berman, T., Béchemin, C., and Maestrini, S. Y. (1999). Release of ammonium and urea from dissolved organic nitrogen in aquatic ecosystems. *Aquat. Microb. Ecol.* 16, 295–302. doi: 10.3354/ame016295

Biddanda, B., Ogdahl, M., and Cotner, J. (2001). Dominance of bacterial metabolism in oligotrophic relative to eutrophic waters. *Limnol. Oceanogr.* 46, 730–739. doi: 10.4319/lo.2001.46.3.0730

Blanco, Y., Prieto-Ballesteros, O., Gómez, M. J., Moreno-Paz, M., García-Villadangos, M., Rodríguez-Manfredi, J. A., et al. (2012). Prokaryotic communities and operating metabolisms in the surface and the permafrost of Deception Island (Antarctica). *Environ. Microbiol.* 14, 2495–2510. doi: 10.1111/j.1462-2920.2012.02767.x

Bomberg, M., Lamminmäki, T., and Itävaara, M. (2016). Microbial communities and their predicted metabolic characteristics in deep fracture groundwaters of the crystalline bedrock at Olkiluoto. Finland. *Biogeosciences* 13, 6031–6047. doi: 10.5194/bg-13-6031-2016

Bosson, E., Selroos, J.-O., Stigsson, M., Gustafsson, L.-G., and Destouni, G. (2013). Exchange and pathways of deep and shallow groundwater in different climate and permafrost conditions using the Forsmark site, Sweden, as an example catchment. *Hydrogeol. J.* 21, 225–237. doi: 10.1007/s10040-012-0906-7

Breton, A., Bernalier, A., Dusser, M., Fonty, G., Gaillard-Martinie, B., and Guillot, J. (1990). Anaeromyces mucronatus nov. gen., nov. sp. A new strictly anaerobic rumen fungus with polycentric thallus. *FEMS Microbiol. Lett.* 70, 177–182. doi: 10.1111/j.1574-6968.1990.tb13974.x

Brutemark, A., Rengefors, K., and Anderson, N. J. (2006). An experimental investigation of phytoplankton nutrient limitation in two contrasting low arctic lakes. *Polar Biol.* 29, 487–494. doi: 10.1007/s00300-005-0079-0

Butinar, L., Spencer-Martins, I., and Gunde-Cimerman, N. (2007). Yeasts in high Arctic glaciers: the discovery of a new habitat for eukaryotic microorganisms. *Antonie Van Leeuwenhoek.* 91, 277–289. doi: 10.1007/s10482-006-9117-3

Caporaso, J. G., Kuczynski, J., Stombaugh, J., Bittinger, K., Bushman, F. D., Costello, E. K., et al. (2010). QIIME allows analysis of high-throughput community sequencing data. *Nat. Methods* 7, 335–336. doi: 10.1038/nmeth.f.303

Cappelen, J. (2018). *Weather and Climate Data from Greenland 1958-2011-Observation Data with Description*. Copenhagen: Danish Meteorological Institute.

Castelle, C. J., Wrighton, K. C., Thomas, B. C., Hug, L. A., Brown, C. T., Wilkins, M. J., et al. (2015). Genomic expansion of domain archaea highlights roles for organisms from new phyla in anaerobic carbon cycling. *Curr. Biol.* 25, 690–701. doi: 10.1016/j.cub.2015.01.014

Chen, W.-M., Hsieh, T.-Y., Young, C.-C., and Sheu, S.-Y. (2017). Undibacterium amnicola sp. nov., isolated from a freshwater stream. *Int. J. Syst. Evol. Microbiol.* 67, 5094–5101. doi: 10.1099/ijsem.0.002422

Claesson Liljedahl, L., Kontula, A., Harper, J., Näslund, J. O., Selroos, J. O., Pitkänen, P., et al. (2016). *The Greenland Analogue Project: Final Report. Tech. Rep. SKB TR-14-13*. Stockholm: Svensk Kärnbränslehantering.

Cotner, J. B., and Biddanda, B. A. (2002). Small players, large role: microbial influence on biogeochemical processes in pelagic aquatic ecosystems. *Ecosystems* 5, 105–121. doi: 10.1007/s10021-001-0059-3

Darcy, J. L., Lynch, R. C., King, A. J., Robeson, M. S., and Schmidt, S. K. (2011). Global distribution of polaromonas phylotypes - evidence for a highly successful dispersal capacity. López-García P, ed. *PLoS One* 6:e23742. doi: 10.1371/journal.pone.0023742

Drake, H., and Ivarsson, M. (2018). The role of anaerobic fungi in fundamental biogeochemical cycles in the deep biosphere. *Fungal Biol. Rev.* 32, 20–25. doi: 10.1016/J.FBR.2017.10.001

Drake, H., Ivarsson, M., Bengtson, S., Heim, C., Siljeström, S., Whitehouse, M. J., et al. (2017). Anaerobic consortia of fungi and sulfate reducing bacteria in deep granite fractures. *Nat. Commun.* 8:55. doi: 10.1038/s41467-017-00094-6

Edgar, R. C. (2010). Search and clustering orders of magnitude faster than BLAST. *Bioinformatics* 26, 2460–2461. doi: 10.1093/bioinformatics/btq461

Evans, P. N., Parks, D. H., Chadwick, G. L., Robbins, S. J., Orphan, V. J., Golding, S. D., et al. (2015). Methane metabolism in the archaeal phylum Bathyarchaeota revealed by genome-centric metagenomics. *Science* 350, 434–438. doi: 10.1126/science.aac7745

Finneran, K. T., Johnsen, C. V., and Lovley, D. R. (2003). *Rhodoferax ferrireducens* sp. nov., a psychrotolerant, facultatively anaerobic bacterium that oxidizes acetate with the reduction of Fe(III). *Int. J. Syst. Evol. Microbiol.* 53, 669–673. doi: 10.1099/ijs.0.02298-0

Gadd, G. M. (2007). Geomycology: biogeochemical transformations of rocks, minerals, metals and radionuclides by fungi, bioweathering and bioremediation. *Mycol. Res.* 111, 3–49. doi: 10.1016/J.MYCRES.2006.12.001

Garde, A. A., and Marker, M. (2010). *Geological Map of Greenland, 1: 500 000, Kangerlussuaq/Søndre Strømfjord Nuussuaq, Sheet 3*. Copenhagen: Geological Survey of Denmark and Greenland.

Gardes, M., and Bruns, T. D. (1993). ITS primers with enhanced specificity for basidiomycetes - application to the identification of mycorrhizae and rusts. *Mol. Ecol.* 2, 113–118. doi: 10.1111/j.1365-294X.1993.tb00005.x

Golyshina, O. V., Toshchakov, S. V., Makarova, K. S., Gavrilov, S. N., Korzhenkov, A. A., La Cono, V., et al. (2017). 'ARMAN'archaea depend on association with euryarchaeal host in culture and in situ. *Nat. Commun.* 8:60. doi: 10.1038/s41467-017-00104-7

Hammer, Ø, Harper, D. A. T., and Ryan, P. D. (2009). *Paleontological Statistics. Ver, 1.92*.

Hanna, E., Huybrechts, P., Steffen, K., Cappelen, J., Huff, R., Shuman, C., et al. (2008). Increased runoff from melt from the greenland ice sheet: a response to global warming. *J. Clim.* 21, 331–341. doi: 10.1175/2007JCLI1964.1

Harper, J., Brown, J., Hubbard, A., Doyle, S., Fitzpatrick, A., and Ruskeeniemi, T. (2016). *The Greenland Analogue Project: Data and Processes. Posiva Working Report 2016-37*. Stockholm: Svensk Kärnbränslehantering AB.

Haugland, R., and Vesper, S. (2002). *Method of Identifying and Quantifying Specific Fungi and Bacteria*. Available at: http://www.google.com/patents?hl=en&lr=&vid=USPAT6387652&id=fb0KAAAAEBAJ&oi=fnd&dq=Method+for+identifying+and+quantifying+specific+fungi+and+bacteria&printsec=abstract (accessed November 6, 2018).

He, R., Wooller, M. J., Pohlman, J. W., Catranis, C., Quensen, J., Tiedje, J. M., et al. (2012). Identification of functionally active aerobic methanotrophs in sediments from an arctic lake using stable isotope probing. *Environ. Microbiol.* 14, 1403–1419. doi: 10.1111/j.1462-2920.2012.02725.x

Henkemans, E. (2016). *Geochemical Characterization of Groundwaters, Surface Waters and Water-Rock Interaction in an Area of Continuous Permafrost Adjacent to the Greenland Ice Sheet. Kangerlussuaq, Southwest Greenland*. Waterloo: University of Waterloo.

Herlemann, D. P., Labrenz, M., Jürgens, K., Bertilsson, S., Waniek, J. J., and Andersson, A. F. (2011). Transitions in bacterial communities along the 2000 km salinity gradient of the Baltic Sea. *ISME J.* 5:1571. doi: 10.1038/ismej.2011.41

Holloway, J. M., and Dahlgren, R. A. (2002). Nitrogen in rock: occurrences and biogeochemical implications. *Glob. Biogeochem. Cycles* 16, 65–71.

Inoue, J., Oshima, K., Suda, W., Setubal, J. C., and Dixon, R. (2015). Distribution and evolution of nitrogen fixation genes in the phylum ⁢>bacteroidetes&It;/i>. *Microbes Environ.* 30, 44–50. doi: 10.1264/jsme2.ME14142

Jezbera, J., Sharma, A. K., Brandt, U., Doolittle, W. F., and Hahn, M. W. (2009). '*Candidatus* Planktophila limnetica', an actinobacterium representing one of the most numerically important taxa in freshwater bacterioplankton. *Int. J. Syst. Evol. Microbiol.* 59, 2864–2869. doi: 10.1099/ijs.0.010199-0

Johansson, E., Gustafsson, L.-G., Berglund, S., Lindborg, T., and Destouni, G. (2015). Data evaluation and numerical modeling of hydrological interactions between active layer, lake and talik in a permafrost catchment. Western Greenland. *J. Hydrol.* 527, 688–703. doi: 10.1016/J.JHYDROL.2015.05.026

Kaden, R., Sproer, C., Beyer, D., and Krolla-Sidenstein, P. (2014). *Rhodoferax saidenbachensis* sp. nov., a psychrotolerant, very slowly growing bacterium within the family Comamonadaceae, proposal of appropriate taxonomic position of *Albidiferax ferrireducens* strain T118T in the genus *Rhodoferax* and emended description of the genus *Rhodoferax*. *Int. J. Syst. Evol. Microbiol.* 64(Pt 4), 1186–1193. doi: 10.1099/ijs.0.054031-0

Kane, D. L., Yoshikawa, K., and McNamara, J. P. (2013). Regional groundwater flow in an area mapped as continuous permafrost, NE Alaska (USA). *Hydrogeol. J.* 21, 41–52. doi: 10.1007/s10040-012-0937-0

Khadem, A. F., Pol, A., Wieczorek, A. S., Jetten, M. S. M., and Op den Camp, H. J. M. (2012). Metabolic regulation of "Ca. *Methylacidiphilum Fumariolicum*" SolV cells grown under different nitrogen and oxygen limitations. *Front. Microbiol.* 3:266. doi: 10.3389/fmicb.2012.00266

Klindworth, A., Pruesse, E., Schweer, T., Peplies, J., Quast, C., Horn, M., et al. (2013). Evaluation of general 16S ribosomal RNA gene PCR primers for classical and next-generation sequencing-based diversity studies. *Nucleic Acids Res.* 41:e1. doi: 10.1093/nar/gks808

Kohlbach, D., Graeve, M., Lange, B. A., David, C., Peeken, I., and Flores, H. (2016). The importance of ice algae-produced carbon in the central Arctic Ocean ecosystem: food web relationships revealed by lipid and stable isotope analyses. *Limnol. Oceanogr.* 61, 2027–2044. doi: 10.1002/lno.10351

Kõljalg, U., Nilsson, R. H., Abarenkov, K., Tedersoo, L., Taylor, A. F., Bahram, M., et al. (2013). Towards a unified paradigm for sequence-based identification of fungi. *Mol. Ecol.* 22, 5271–5277. doi: 10.1111/mec.12481

Kontula, A., Pitkänen, P., Claesson Liljedahl, L., Näslund, J.-O., Selroos, J.-O., and Puigdomenech, I. (2016). *The Greenland Analogue Project: Final Report. Posiva Working Report 2016-17*. Available at: http://www.posiva.fi/files/4295/POSIVA_2016-17.pdf (accessed August 2016).

León-Zayas, R., Peoples, L., Biddle, J. F., Podell, S., Novotny, M., Cameron, J., et al. (2017). The metabolic potential of the single cell genomes obtained from the challenger deep, mariana trench within the candidate superphylum *P arcubacteria* (OD 1). *Environ. Microbiol.* 19, 2769–2784. doi: 10.1111/1462-2920.13789

Li, B., Chen, H., Li, N., Wu, Z., Wen, Z., Xie, S., et al. (2017). Spatio-temporal shifts in the archaeal community of a constructed wetland treating river water. *Sci. Total Environ.* 605, 269–275. doi: 10.1016/j.scitotenv.2017.06.221

Lindbäck, K., Pettersson, R., Doyle, S. H., Helanow, C., Jansson, P., Kristensen, S. S., et al. (2014). High-resolution ice thickness and bed topography of a land-terminating section of the Greenland Ice Sheet. *Earth Syst. Sci. Data* 6, 331–338. doi: 10.5194/essd-6-331-2014

Li, X., Chang, X., Zhang, Y., Liu, Z., Da, X., Kim, M., et al. (2016). *Undibacterium arcticum* sp. nov., isolated from arctic alpine soil. *Int. J. Syst. Evol. Microbiol.* 66, 2797–2802. doi: 10.1099/ijsem.0.001056

Louca, S., Parfrey, L. W., and Doebeli, M. (2016). Decoupling function and taxonomy in the global ocean microbiome. *Science* 353, 1272–1277. doi: 10.1126/science.aaf4507

Lu, S., Chourey, K., Reiche, M., Nietzsche, S., Shah, M. B., Neu, T. R., et al. (2013). Insights into the structure and metabolic function of microbes that shape pelagic iron-rich aggregates (iron snow). *Appl. Environ. Microbiol.* 79, 4272–4281. doi: 10.1128/AEM.00467-13

Mariash, H. L., Cazzanelli, M., Rautio, M., Hamerlik, L., Wooller, M. J., and Christoffersen, K. S. (2018). Changes in food web dynamics of low Arctic ponds with varying content of dissolved organic carbon. *Arct. Antarct. Alpine Res.* 50:S100016.

Martinez-Cruz, K., Leewis, M. C., Herriott, I. C., Sepulveda-Jauregui, A., Anthony, K. W., Thalasso, F., et al. (2017). Anaerobic oxidation of methane by aerobic methanotrophs in sub-Arctic lake sediments. *Sci. Total Environ.* 607, 23–31. doi: 10.1016/j.scitotenv.2017.06.187

Mattes, T. E., Alexander, A. K., Richardson, P. M., Munk, A. C., Han, C. S., Stothard, P., et al. (2008). The genome of *Polaromonas* sp. strain JS666: insights into the evolution of a hydrocarbon-and xenobiotic-degrading bacterium, and features of relevance to biotechnology. *Appl. Environ. Microbiol.* 74, 6405–6416. doi: 10.1128/AEM.00197-08

McMurdie, P. J., and Holmes, S. (2013). phyloseq: an R package for reproducible interactive analysis and graphics of microbiome census data. *PLoS One* 8:e61217. doi: 10.1371/journal.pone.0061217

Nelson, W. C., and Stegen, J. C. (2015). The reduced genomes of parcubacteria (OD1) contain signatures of a symbiotic lifestyle. *Front. Microbiol.* 6:71. doi: 10.3389/fmicb.2015.0071

Newton, R. J., and McMahon, K. D. (2011). Seasonal differences in bacterial community composition following nutrient additions in a eutrophic lake. *Environ. Microbiol.* 13, 887–899. doi: 10.1111/j.1462-2920.2010.02387.x

Nilsson, R. H., Larsson, K. H., Taylor, A. F. S., Bengtsson-Palme, J., Jeppesen, T. S., Schigel, D., et al. (2018). The UNITE database for molecular identification of

fungi: handling dark taxa and parallel taxonomic classifications. *Nucleic Acids Res.* 47, D259–D264. doi: 10.1093/nar/gky1022

Nixon, S. L., Telling, J. P., Wadham, J. L., and Cockell, C. S. (2017). Viable cold-tolerant iron-reducing microorganisms in geographically diverse subglacial environments. *Biogeosciences* 14, 1445–1455. doi: 10.5194/bg-14-1445-2017

Ofek, M., Hadar, Y., and Minz, D. (2012). Ecology of root colonizing Massilia (*Oxalobacteraceae*). Vinatzer BA, ed. *PLoS One* 7:e40117. doi: 10.1371/journal.pone.0040117

Ogawa, Y., Hayashi, S., Degawa, Y., and Yaguchi, Y. (2001). Ramicandelaber, a new genus of the Kickxellales, Zygomycetes. *Mycoscience* 42, 193–199. doi: 10.1007/BF02464137

Ogbebo, F. E., Evans, M. S., Waiser, M. J., Tumber, V. P., and Keating, J. J. (2009). Nutrient limitation of phytoplankton growth in Arctic lakes of the lower Mackenzie River Basin, northern Canada. *Can. J. Fish. Aquat. Sci.* 66, 247–260. doi: 10.1139/f08-202

Ortiz-Alvarez, R., and Casamayor, E. O. (2016). High occurrence of *Pacearchaeota* and *Woesearchaeota* (Archaea superphylum DPANN) in the surface waters of oligotrophic high-altitude lakes. *Environ. Microbiol. Rep.* 8, 210–217. doi: 10.1111/1758-2229.12370

Oswald, K., Graf, J. S., Littmann, S., Tienken, D., Brand, A., Wehrli, B., et al. (2017). Crenothrix are major methane consumers in stratified lakes. *ISME J.* 11:2124. doi: 10.1038/ismej.2017.77

Pere, T. (2014). *Geological Logging of the Greenland Analogue Project Drill Cores DH-GAP01, 03 and 04. Posiva Working Report 2013-59*. Available at:http://www.posiva.fi/files/3808/WR_2013-59.pdf (accessed August 2014).

Pester, M., Brambilla, E., Alazard, D., Rattei, T., Weinmaier, T., Han, J., et al. (2012). Complete genome sequences of *Desulfosporosinus orientis* DSM765T, *Desulfosporosinus youngiae* DSM17734T, *Desulfosporosinus meridiei* DSM13257T, and *Desulfosporosinus acidiphilus* DSM22704T. *J. Bacteriol.* 194, 6300–6301. doi: 10.1128/JB.01392-12

Posiva (2012). *Safety Case for the Disposal of Spent Nuclear Fuel at Olkiluoto. Formulation of Radionuclide Release Scenarios 2012. Posiva 2012-08*. Eurajoki: Posiva Oy.

Quast, C., Pruesse, E., Yilmaz, P., Gerken, J., Schweer, T., Yarza, P., et al. (2012). The SILVA ribosomal RNA gene database project: improved data processing and web-based tools. *Nucleic Acids Res.* 41, D590–D596. doi: 10.1093/nar/gks1219

R Development Core Team (2018). *R: A Language and Environment for Statistical Computing*. Vienna: R Foundation for StatisticalComputing.

Rajala, P., Bomberg, M., Huttunen-Saarivirta, E., Priha, O., Tausa, M., and Carpén, L. (2016). Influence of chlorination and choice of materials on fouling in cooling water system under brackish seawater conditions. *Materials* 9:475. doi: 10.3390/ma9060475

Rousk, K., Sorensen, P. L., and Michelsen, A. (2018). What drives biological nitrogen fixation in high arctic tundra: moisture or temperature? *Ecosphere* 9:e02117. doi: 10.1002/ecs2.2117

Sánchez-Andrea, I., Stams, A. J., Hedrich, S., Ňancucheo, I., and Johnson, D. B. (2015). *Desulfosporosinus acididurans* sp. nov.: an acidophilic sulfate-reducing bacterium isolated from acidic sediments. *Extremophiles* 19, 39–47. doi: 10.1007/s00792-014-0701-6

Scheffer, M., and Carpenter, S. R. (2003). Catastrophic regime shifts in ecosystems: linking theory to observation. *Trends Ecol. Evol.* 18, 648–656. doi: 10.1016/j.tree.2003.09.002

Schloss, P. D., Westcott, S. L., Ryabin, T., Hall, J. R., Hartmann, M., Hollister, E. B., et al. (2009). Introducing mothur: open-source, platform-independent, community-supported software for describing and comparing microbial communities. *Appl. Environ. Microbiol.* 75, 7537–7541. doi: 10.1128/AEM.01541-09

Singh, P., and Singh, S. M. (2012). Characterization of yeast and filamentous fungi isolated from cryoconite holes of Svalbard. *Arct. Polar Biol.* 35, 575–583. doi: 10.1007/s00300-011-1103-1

SKB (2011). *Long Term Safety for the Final Repository for Spent Nuclear Fuel at Forsmark. Main Report of the SR-Site Project. SKB TR-11-01*. Stockholm: Svensk Kärnbränslehantering AB.

Slobodkina, G. B., Baslerov, R. V., Novikov, A. A., Bonch-Osmolovskaya, E. A., and Slobodkin, A. I. (2017). *Thermodesulfitimonas autotrophica* gen. nov., sp. nov., a thermophilic, obligate sulfite-reducing bacterium isolated from a terrestrial hot spring. *Int. J. Syst. Evol. Microbiol.* 67, 301–305. doi: 10.1099/ijsem.0.001619

Takai, K., and Horikoshi, K. (1999). Genetic diversity of archaea in deep-sea hydrothermal vent environments. *Genetics* 152, 1285–1297.

Tanaka, S., Takeuchi, N., Miyairi, M., Fujisawa, Y., Kadota, T., Shirakawa, T., et al. (2016). Snow algal communities on glaciers in the Suntar-Khayata Mountain Range in eastern Siberia. *Russia. Polar Sci.* 10, 227–238. doi: 10.1016/j.polar.2016.03.004

Unite Community (2017). *UNITE Mothur Release*. London: UNITE Community.

van Gool, J. A., Connelly, J. N., Marker, M., and Mengel, F. C. (2002). The Nagssugtoqidian Orogen of West Greenland: tectonic evolution and regional correlations from a West Greenland perspective. *Can. J. Earth Sci.* 39, 665–686. doi: 10.1139/e02-027

Vincent, W. F., Whyte, L. G., Lovejoy, C., Greer, C. W., Laurion, I., Suttle, C. A., et al. (2009). Arctic microbial ecosystems and impacts of extreme warming during the international polar year. *Polar Sci.* 3, 171–180. doi: 10.1016/j.polar.2009.05.004

Walker, J. F., Aldrich-Wolfe, L., Riffel, A., Barbare, H., Simpson, N. B., Trowbridge, J., et al. (2011). Diverse Helotiales associated with the roots of three species of Arctic Ericaceae provide no evidence for host specificity. *New Phytol.* 191, 515–527. doi: 10.1111/j.1469-8137.2011.03703.x

Wang, N. F., Zhang, T., Yang, X., Wang, S., Yu, Y., Dong, L. L., et al. (2016). Diversity and composition of bacterial community in soils and lake sediments from an arctic lake area. *Front. Microbiol.* 7:1170. doi: 10.3389/fmicb.2016.01170

Wartiainen, I., Hestnes, A. G., McDonald, I. R., and Svenning, M. M. (2006). *Methylobacter tundripaludum* sp. nov., a methane-oxidizing bacterium from Arctic wetland soil on the Svalbard islands, Norway (78 N). *Int. J. Syst. Evol. Microbiol.* 56, 109–113. doi: 10.1099/ijs.0.63728-0

White, D., Hinzman, L., Alessa, L., Cassano, J., Chambers, M., Falkner, K., et al. (2007). The arctic freshwater system: changes and impacts. *J. Geophys. Res. Biogeosci.* 112:G04S54. doi: 10.1029/2006JG000353

White, T. J., Bruns, T., Lee, S., and Taylor, J. (1990). "Amplification and direct sequencing of fungal ribosomal RNA genes for phylogenetics," in *PCR Protocols: a Guide to Methods and Applications*, eds M. A. Innis, D. H. Gelfand, J. J. Sninsky, and T. J. White (New York, NY: Academic Press), 315–322. doi: 10.1016/b978-0-12-372180-8.50042-1

Conflict of Interest Statement: MB was employed by the VTT Technical Research Centre of Finland, Ltd., and received partial funding from the SKB and Posiva Oy during the study. LC was employed by the Svensk Kärnbränslehantering AB. TL and AK were employed by the Posiva Oy during the time of the study. The funding from the SKB and Posiva Oy was received in order to produce the manuscript. The authors declare that the research was conducted with highest academic integrity and without commercial interests.

Copyright © 2019 Bomberg, Claesson Liljedahl, Lamminmäki and Kontula. This is an open-access article distributed under the terms of the Creative Commons Attribution License (CC BY). The use, distribution or reproduction in other forums is permitted, provided the original author(s) and the copyright owner(s) are credited and that the original publication in this journal is cited, in accordance with accepted academic practice. No use, distribution or reproduction is permitted which does not comply with these terms.

frontiers in Microbiology

ORIGINAL RESEARCH
published: 31 July 2019
doi: 10.3389/fmicb.2019.01714

Temperature Response of Planktonic Microbiota in Remote Alpine Lakes

Yiming Jiang[1,2], Haiying Huang[1,2], Tianli Ma[1,2], Jinlong Ru[1,2], Stephan Blank[3], Rainer Kurmayer[3] and Li Deng[1,2]**

[1] Institute of Virology, Helmholtz Zentrum München, German Research Center for Environmental Health, Neuherberg, Germany, [2] Institute of Virology, Technical University of Munich, Munich, Germany, [3] Research Department for Limnology, Mondsee, University of Innsbruck, Innsbruck, Austria

Alpine lakes are considered pristine freshwater ecosystems and sensitive to direct and indirect changes in water temperature as induced by climate change. The bacterial plankton constitutes a key component in the water column and bacterial metabolic activity has direct consequences for water quality. In order to understand bacterial response to global temperature rise in five alpine lakes located in the Austrian Alps (1700–2188 m a.S.L.) water temperature was compared within a decadal period. Depth-integrated samples were characterized in community composition by 16S rDNA deep-amplicon sequencing early [56 ± 16 (SD) days after ice break up] and later (88 ± 16 days) in the growing season. Within the 10 years period, temperature rise was observed through reduced ice cover duration and increased average water temperature. During the early growing season, the average water temperature recorded between circulation in spring until sampling date (WAS), and the day of autumn circulation, as well as chemical composition including dissolved organic carbon influenced bacterial community composition. In contrast, only nutrients (such as nitrate) were found influential later in the growing season. Metabolic theory of ecology (MTE) was applied to explain the dependence of taxonomic richness on WAS in mathematical terms. The calculated activation energy exceeded the frequently reported prediction emphasizing the role of WAS during early growing season. Accordingly, the relative abundance of predicted metabolism related genes increased with WAS. Thus, the dominant influence of temperature after ice break up could be explained by overall climate change effects, such as a more intense warming in spring and an overall higher amplitude of temperature variation.

Keywords: high mountain lakes, climate change, growing seasons, nutrient level, metabarcoding, richness, activation energy

OPEN ACCESS

Edited by:
Haihan Zhang,
Xi'an University of Architecture and Technology, China

Reviewed by:
Jianyin Huang,
University of South Australia, Australia
Presentación Carrillo,
University of Granada, Spain

***Correspondence:**
Rainer Kurmayer
rainer.kurmayer@uibk.ac.at
Li Deng
li.deng@helmholtz-muenchen.de

Specialty section:
This article was submitted to Aquatic Microbiology, a section of the journal Frontiers in Microbiology

Received: *13 April 2019*
Accepted: *11 July 2019*
Published: *31 July 2019*

Citation:
Jiang Y, Huang H, Ma T, Ru J, Blank S, Kurmayer R and Deng L (2019) Temperature Response of Planktonic Microbiota in Remote Alpine Lakes. Front. Microbiol. 10:1714. doi: 10.3389/fmicb.2019.01714

INTRODUCTION

Climate change, which is mainly caused by anthropogenic activities, is a global issue. Since 1850, the Earth's surface temperature has increased by 0.76°C, and it is expected to increase by another 1.1–6.4°C by the end of this century (Stocker, 2014). Ongoing climate change has been shown to cause a rapid change in ecological communities, thereby threatening ecosystem functioning and services (Jassey et al., 2013). Mountain regions are suffering more from warming than the global

average (Beniston et al., 1997; Sommaruga-Wögrath et al., 1997; Parker et al., 2008). Over the past century, the annual average temperature in the Alps has risen by about 2°C, which is on average twice as high as estimated for the northern hemisphere (Djukic et al., 2013; Weckström et al., 2016). The alpine lake ecosystem is affected by global climate change through thawing of ice, melting of frozen soils, altered snow packing, shortened ice cover duration, and increasing summer water temperatures, thereby affecting biodiversity and functioning of water cycles and the microclimate (Holzapfel and Vinebrooke, 2005; Parker et al., 2008). Traditionally mountain lake ecosystems are highly sensitive to global warming, functioning as sentinels of climate change (Kamenik et al., 2001; Adrian et al., 2009; Williamson et al., 2009). Although various studies have documented the responses of plant and animal biodiversity to temperature, less studies have examined microbial responses to climate warming (Zhou et al., 2016; Guo et al., 2018).

One current challenge is to determine how environmental parameters (in)directly related by climate change affect the structure and diversity of the microbiota in lakes. Various factors have been elucidated, for example, studies have shown that climate warming impacts on alpine's lake bacterioplankton community structure through affecting the turbidity shift along with the glacier retreat (Peter and Sommaruga, 2016), or through changing the surrounding soil characteristics (Rofner et al., 2017). Besides, it is well established that temperature is a key driver in microbiota biodiversity construction, as temperature directly regulates metabolic rates and biochemical processes (Gillooly et al., 2001; Brown et al., 2004; Zhou et al., 2016). The metabolic theory of ecology (MTE) addresses the relationships between ecosystem properties, body size, and metabolism (Brown et al., 2004). The dependence of species richness on temperature is based on the energetic equivalence rule (Allen et al., 2002), assuming that the total energy flux of a population per unit area does not depend on body size. It is predicted that at higher temperature, each species has fewer individuals (because of faster growth) but the total number of individuals is the same. In other words, with increasing temperature the richness is increasing, since more species are present. Although the MTE was established for macroorganisms in the last decade, for the microbiota in soil this relationship has also been found (Zhou et al., 2016).

In this study we compared average water temperatures and ice cover duration observed during two summers in lakes located in the alpine zone of the Austrian Alps to records from 10 years earlier. We expected that based on the general understanding of climate change water temperature should show an increase in relation to corresponding air temperature while ice cover duration should decline. In a second step, we aimed to understand how the microbiota in alpine lakes respond to the temperature changes and other environmental factors occurring seasonally during two consecutive years. We hypothesized that besides water temperature regional factors influenced by the geology in the catchment (e.g., Kamenik et al., 2001) should be of major influence. In a third step MTE was applied to explain the dependence of taxonomic richness on the bacterial metabolic activity. We expected the so-called activation energy E_a (calculated from the slope between temperature and taxa richness) in a range of the previously observed and more frequently reported −0.65 prediction equivalent to a Q_{10} of ∼2.5 (Stegen et al., 2009; Zhou et al., 2016). Taking into account the overall climate change scenario on temperature rise in the Alps we speculate on the role of climate change effects.

MATERIALS AND METHODS

Study Sites and Topographic Parameters

Five alpine lakes in the "Niedere Tauern" region of the eastern Alps, Austria (Weckström et al., 2016) [Unterer Giglachsee (GIG), Moaralmsee (MOA), Oberer Landschitzsee (OLA), Twenger Almsee (TWA), and Wirpitschsee (WIR)], were selected as sampling sites (**Figure 1A**). The lakes were located along an altitude gradient ranging between 1700 and 2120 m above sea level (a.S.L.) in the alpine zone either above the treeline (WIR) or above the timberline (others). MOA was the smallest lake with an area of 2.1 ha and max depth of 5.9 m; the lake area and max depth of other lakes were 3.1–16.8 ha and 8–33.6 m, respectively (**Table 1**). Maps of the five lakes were generated with R using package "ggmap". In addition, meteorological data recorded from four relevant stations were used to compare changes in temperature and to analyze the potential influence of precipitation on the observed microbiota community composition: Sonnblick (3109 m a SL), Rudolfshütte (2317 m), Schmittenhöhe (1956 m), Obertauern (1772 m).

Sampling

Depth-integrated water samples were taken in the years 2010 and 2011 during (i) early stage of the growing season, i.e., in July 26–56 ± 17–82 (min–mean ± SD–max) days after ice break up, and (ii) later stage of the growing season, i.e., in August 69–88 ± 16–116 days after ice break up. Depth-integrated samples were taken based on the maximum depth of each lake, i.e., were integrated by subsampling every meter in MOA, OLA, and WIR, every two meters in GIG, and every three meters in TWA (**Figure 1B** and **Table 1**). To minimize changes occurring during transport, samples (1.5–2 L) were prefiltered immediately on the shore using a hand vacuum pump through previously autoclaved glass fiber filters (GF/C) to remove eukaryotic algae and particle-associated bacteria. An aliquot of 100 mL of each sample was fixed using formaldehyde (2% v/v final concentration) and used for bacterial cell counting by DAPI staining according to standard conditions (Porter and Feig, 1980). One to three milliliters were filtered onto polycarbonate membrane filters (0.2 μm, Nuclepore Track-Etch membrane, Whatman, Dassel, Germany) and microbes were counted using epifluorescence microscopy at 1000-fold magnification (Axioplan, Zeiss, Oberkochen, Germany). Cyanobacteria were differentiated using autofluorescence. The glass fiber prefiltered water samples were filtered onto previously autoclaved nitrocellulose membranes (NC, pore diameter: 0.2 μm, Whatman, 1–2.1 L) using low-vacuum filtration (<0.4 bar), and the filters were transferred into Eppendorf

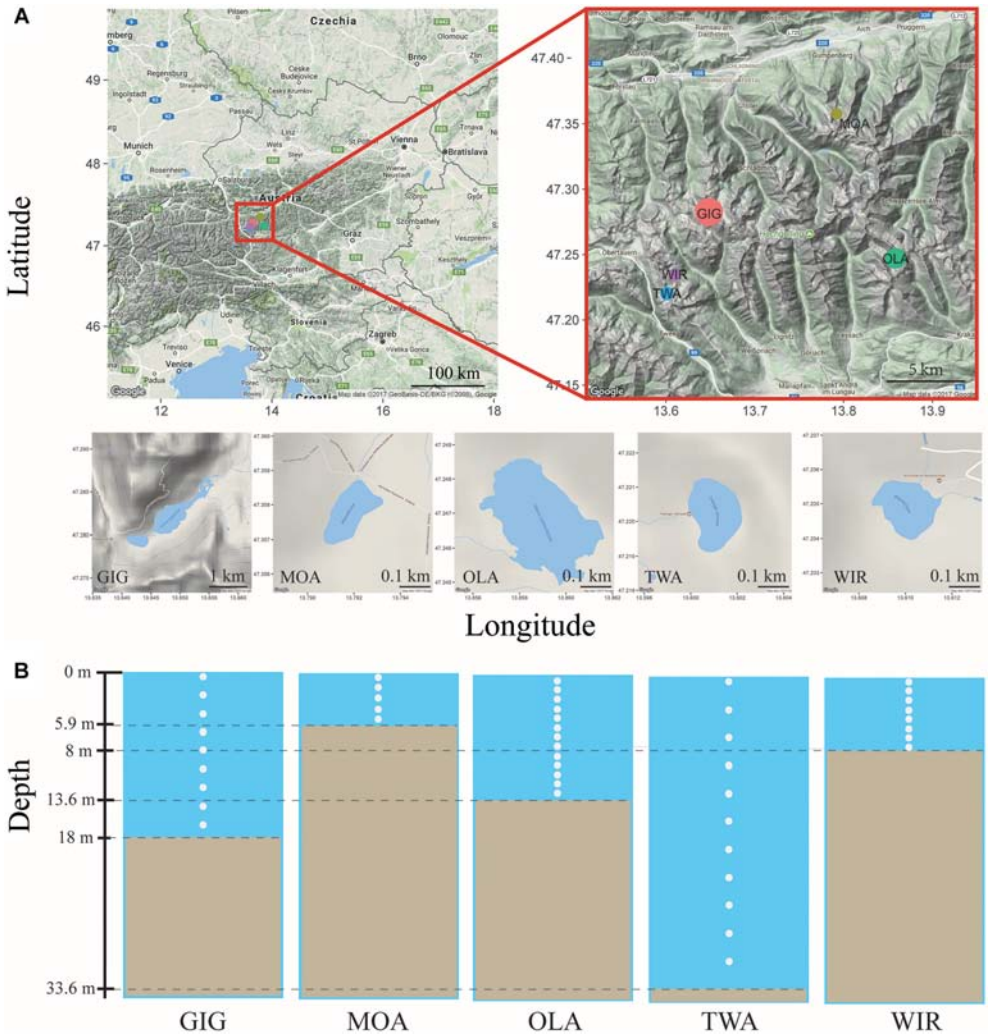

FIGURE 1 | (A) Map of study area and the five alpine lakes in the "Niedere Tauern" region of the Austrian Alps. **(B)** Depth-integrated sampling of water column. The subsamples were taken at every 1 m (MOA, OLA, and WIR), every 2 m (GIG), or every 3 m (TWA) from surface. The maps were generated with "ggmap" in R, a package based on Google Maps.

tubes, immediately frozen in dry ice, and stored at −20°C until DNA extraction.

Environmental Parameters

Water temperature was recorded at 2.5 m-depth in 2-h intervals between 26 September 1998 and 26 September 1999 (Schmidt et al., 2004) and in 4-h intervals between 1 September 2009 and 28 August 2012 using thermistors (MINILOG, Vemco Ltd., Bedford, NS, Canada). For each year and each lake, the calendar dates of spring mixing and autumn mixing were estimated by visual examination of individual temperature curves as described previously (Schmidt et al., 2004; Kamenik and Schmidt, 2005). The calendar day of circulation in autumn (CiA) was calculated from the date when the water temperature decreased to 4°C, while the calendar day of circulation in spring (CiS) was calculated from the first date when water temperature exceeded 4°C. The duration of ice cover (ICD) was calculated from the number of days in between CiA and CiS (Schmidt et al., 2004). The annual average water temperature (YAWT) over the entire year (including both the ice-free and ice-covered periods) and the average water temperature during the period between the calendar day of circulation in spring until the sampling date (WAS) were calculated.

Conductivity (Cond.) and pH were determined in the field using a multiprobe (YSI6920, YSI Environmental, Yellow Springs, OH, United States). The depth-integrated samples for chemical analyses were kept cool and analyzed within 2 days and included the following: Sulfate (SO_4^{2-}), chloride (Cl^-), ammonium (NH_4^+), sodium (Na^-), potassium (K^+), magnesium (Mg^{2+}), calcium (Ca^{2+}), total phosphorus (TP), dissolved organic carbon (DOC), nitrate (NO_3^-), dissolved nitrogen (DN), and dissolved reactive silica (DRSi), were determined as described previously (Kamenik et al., 2001; Schmidt et al., 2004).

TABLE 1 | Environmental characteristics (mean ± SD) for five alpine lakes.

Lake		Unterer Giglachsee GIG	Moaralmsee MOA	Oberer Landschitzsee OLA	Twenger Almsee TWA	Wirpitschsee WIR
Altitude	(m a.s.l)	1922	1825	2067	2118	1700
Lake area	(ha)	16.8	2.13	8.8	3.11	2.72
Max depth	(m)	18	6	14	33	8
YAWT (2010–2011)		5.43	4.90	6.06	5.34	6.41
YAWT (1998–1999)		5.25	4.46	5.05	4.61	5.34
ICD (2010–2011)		221.5	205	222	232.5	193
ICD (1998–1999)		221	223	224	240	209
Conductivity		74.15 ± 0.52^{b}	28.83 ± 2.1^{c}	14.15 ± 0.67^{d}	72.4 ± 1.36^{b}	85.25 ± 2.16^{a}
pH		7.5 ± 0.42^{a}	6.95 ± 0.58^{ab}	6.19 ± 0.39^{b}	7.36 ± 0.09^{a}	7.46 ± 0.61^{a}
Alkalinity	(μeq/L)	607.5 ± 12.29^{b}	186.75 ± 11.18^{d}	70.5 ± 3.87^{e}	552.75 ± 5.74^{c}	724.75 ± 27.44^{a}
NO_3^-	(μM)	0.23 ± 0.09^{d}	3.13 ± 0.17^{a}	1.04 ± 0.04^{c}	0.03 ± 0.03^{d}	2.52 ± 0.37^{b}
SO_4^{2-}	(μM)	60.63 ± 0.73^{b}	29.06 ± 2.08^{d}	21.67 ± 0.73^{e}	76.35 ± 2.92^{a}	52.71 ± 0.21^{c}
Cl^-	(μM)	5.07 ± 0.28^{a}	3.94 ± 1.13^{ab}	3.1 ± 0.85^{b}	4.23 ± 0.56^{ab}	5.63 ± 1.13
NH_4^+	(μM)	0.24 ± 0.1	0.22 ± 0.2	0.17 ± 0.1	0.18 ± 0.07	0.26 ± 0.05
Na^+	(μM)	19.13 ± 0.43^{b}	21.3 ± 0.87^{b}	13.04 ± 1.3^{c}	19.13 ± 0.43^{b}	25.22 ± 1.74^{a}
K^+	(μM)	3.59 ± 0.26^{c}	7.44 ± 0.51^{a}	7.18 ± 0.26^{a}	4.62 ± 0.26^{b}	5.13 ± 0.77^{b}
Mg^{2+}	(μM)	90.91 ± 2.06^{b}	11.52 ± 0.41^{d}	5.76 ± 0^{e}	121.76 ± 2.47^{a}	69.11 ± 2.06
Ca^{2+}	(μM)	271.75 ± 4^{b}	112.75 ± 5.5^{d}	49.5 ± 3.75^{e}	224.75 ± 3.25^{c}	347.75 ± 12.75^{a}
TP	(μM)	0.14 ± 0.04^{a}	0.1 ± 0.02^{a}	0.08 ± 0.01^{b}	0.11 ± 0.03^{a}	0.08 ± 0.03
DOC	(μg/L)	858 ± 71.82^{a}	444.75 ± 64.55^{bc}	631 ± 44.79^{bc}	590.25 ± 40.14^{bc}	407 ± 179.25^{c}
DN	(μg/L)	73.5 ± 16.86	209 ± 9.83	109.25 ± 14.38	218.5 ± 194.01	244.5 ± 127.25
DRSi	(μM)	0.08 ± 0.03	0.08 ± 0.03	10.84 ± 0.48	11.43 ± 2.22	17.84 ± 1.17
Chl a	(μg/L)	1.98 ± 0.34^{a}	0.44 ± 0.72^{b}	0.43 ± 0.26^{b}	0.85 ± 0.61^{ab}	0.35 ± 0.05^{b}
Bacteria	(Counts/ml)	$2.28 \times 10^{6} \pm 5.17 \times 10^{5a}$	$7.39 \times 10^{5} \pm 2.42 \times 10^{5b}$	$7.47 \times 10^{5} \pm 3.05 \times 10^{5b}$	$1.89 \times 10^{6} \pm 5.42 \times 10^{5ab}$	$9.14 \times 10^{5} \pm 3.44 \times 10^{5b}$
Cyanobacteria	(Counts/ml)	$1.05 \times 10^{5} \pm 8.93 \times 10^{4a}$	$9.63 \times 10^{2} \pm 2.79 \times 10^{2b}$	$4.71 \times 10^{2} \pm 1.62 \times 10^{2b}$	$1.17 \times 10^{4} \pm 7.81 \times 10^{3b}$	$2.93 \times 10^{3} \pm 2.61 \times 10^{3b}$
Sampling Date*	2010	W3Jul/W3Aug	W3Jul/W3Aug	W3Jul/W4Aug	W2Jul/W4Aug	W2Jul/W4Aug
	2011	W5Jul/W3Aug	W1Jul/W3Aug	W2Jul/W3Aug	W5Jul/W4Aug	W1Jul/W1Aug

*(i) Superscripts indicate significant difference among lakes ($p < 0.05$). (ii) *W... means the week of sampling in July or August.*

The concentration of chlorophyll a (Chl a) was determined from depth-integrated sample aliquots filtered on GF/C filters and stored frozen until extraction using hot ethanol (International Organisation of Standardization [ISO], 1992).

DNA Extraction

DNA was extracted and purified from bacteria collected on NC filters (as described above) using a NucleoSpin® Soil DNA purification kit (MACHEREY-NAGEL GmbH & Co. KG, Düren, Germany) according to the manufacturer's protocols. The quality and quantity of DNA were measured using a NanoDrop® ND-1000 Spectrophotometer (Thermo Fisher Scientific, Waltham, MA, United States). The amount of total extracted DNA ranged from 5–143 ng/μl (mean 32 ± 7 (SE) ng/μl), and the DNA was stored at −20°C.

Bacterial 16S rRNA Gene Amplification and 454 Sequencing

One hundred nanograms of purified genomic DNA from each sample were used as the template for PCR amplification. The V3-V6 hypervariable regions of the bacterial small-subunit (16S) rRNA genes were amplified with primers 338F (5′-ACT CCT ACG GGA GGC AGC AG-3′) (Weisburg et al., 1991) and 1046R (5′-CGA CAG CCA TGC ANC ACC T-3′) (Sogin et al., 2006) resulting in 726 bp of product size (*E. coli*, Access. No. U00096). In addition, the 5′ end of the forward primer was tagged with the Roche 454 pyrosequencing adapter "A" (5′-CGT ATC GCC TCC CTC GCG CCA TCA G-3′) as well as a unique 10 bp barcode sequence. For the reverse primer another adapter "B" (5′-CTA TGC GCC TTG CCA GCC CGC TCA G-3′) was used (Palmer et al., 2012). PCR amplification was performed in a total volume of 50 μL containing one-unit Phusion High-Fidelity DNA-Polymerase (Finnzymes Oy, Espoo, Finland), 10 μL buffer HF (5×), 1 μL of 10 mM of each dNTP, and 2.5 μL of primers (10 pmol μL^{-1}). After an initial denaturation at 98°C for 30 s, there were 25 cycles of (1) 98°C for 10 s, (2) 67.8°C for 20 s, and (3) 72°C for 30 s, and a final extension at 72°C for 1 min. For each sample four PCR amplicons were generated, cut out from the agarose gel in the expected size range (800 bp), purified using the QIAquick gel extraction kit (Qiagen, Hilden, Germany), and pooled for the emPCR reaction. A standard concentration of 5 ng/μl was sequenced from both directions using 454 titanium chemistry (GS Junior, Roche, Basel, Switzerland) installed at the Red Cross Transfusion Service of Upper Austria (Linz, Austria). Four amplicons were sequenced in four regions each separated by 4-region gaskets, loading approximately 3,100,000 amplicon-coated beads per run and recovering a combined total of 800,000 sequence tags (Deng et al., 2017).

Processing of Pyrosequencing Data and Statistics

Sequencing analysis was performed with the Quantitative Insights Into Microbial Ecology (QIIME, version 1.9.0) toolkit (Caporaso et al., 2010). Both forward (V4 region) and reverse (V6 region) sequences were processed and used as technical replicates. The clean reads were generated by *split_libraries.py* with default parameters (sequence length: 200–1000 bp, and average qual score: 25) to remove the potential adapters and primers and performing *identify_chimeric_seq.py* and *filter_fasta.py* to remove the chimeric sequences. After that, the clean reads were clustered to operational taxonomic units (OTUs) using an open reference strategy at the 97% similarity level (Stackebrandt et al., 2002; DeSantis et al., 2006). Subsequently, a representative sequence of each OTU was picked and assigned to a taxonomy based on the Greengenes Database (DeSantis et al., 2006).

Venn diagrams were constructed using jvenn (Bardou et al., 2014), and Circos plots were performed with R (Version 3.2.1). Variation in planktonic microbiota composition (beta-diversity) among samples was visualized via non-metric multidimensional scaling (NMDS) ordination based on Bray-Curtis dissimilarity matrices, while similarity of beta-diversity was tested via Analysis of Similarities (ANOSIM) using 999 permutations and Bray-Curtis distance. Both NMDS and ANOSIM were performed using the "vegan" package in R (Dixon, 2003). PCA and RDA were sequentially applied to relate OTUs abundance to the climatic and physico-chemical variables using CANOCO (version 4.5), Ter Braak and Smilauer, 2002: In a first step, since many of the environmental variables were autocorrelated, a Principal Component Analysis (PCA) was performed on the Pearson correlation matrix. Only the environmental variables that correlated most with PCA ordination axes 1-4 were kept for subsequent ordination analysis. These axes included monthly average water temperature (MAWT), YAWT, WAS, CiA, pH, Cl^-, DOC, NO_3^- for the early growing season, and maximum depth, WAS, NO_3^-, K^+, Ca^{2+}, TP, DOC, and DN for the late growing season. In a second step, from this subset of non-redundant variables redundancy analysis (RDA) using forward selection procedure was applied to select for the statistically significant environmental variables ($p < 0.05$). The potential dependence within consecutive samples taken repeatedly from the same lake was accounted for by including the sampling date as a covariate. Ordination biplots were constructed with CanoDraw. Alpha-diversity indices including richness (Chao1 and S_{obs}, indicating estimated and observed OTUs) and diversity (Shannon-Weaver index and Simpson index) were calculated with packages "vegan" and "OTUtable" (Dixon, 2003). The richness indices Chao1 and S_{obs} were included into the model of MTE (Brown et al., 2004) with command *lm()*. MTE addresses the relationship between organismal metabolism and temperature using the formula (Alcaraz, 2016):

$$ln(S_{chao1\ or\ obs}) = a - E_a \times \frac{1}{kT} \quad (1)$$

where k is Boltzmann's constant (8.62×10^{-5} eV/K), and T is the absolute temperature in Kelvin (K). E_a is the activation energy, which equals the inverse of the slope calculated from the linear regression, and a is the intercept of the same linear regression.

To address the influence of water temperature more directly, functional genes (PFGs), such as metabolic genes, were predicted from the 16S rDNA derived OTUs using Phylogenetic Investigation of Communities by Reconstruction of States (PICRUSt, version 1.1.3) according to the Metagenome

Prediction Tutorial (Langille et al., 2013) and related to the same units as applied for MTE. Mantel test, Pearson correlation, AIC value and significance analysis were performed with R. Specifically, Mantel test was used to estimate the correlation between the composition of bacterioplankton and environmental parameters with the package "vegan," while Pearson correlation was used to investigate the environmental parameters and alpha-diversity indices correlation with the function *cor()*. AIC (Akaike information criterion) values were generated with the function *AIC()* to evaluate the goodness of fit to the linear regression. Significant differences of alpha-diversity indices among lakes were tested using one-way ANOVA ($p < 0.05$).

RESULTS

Climate Change Effects and Environmental Parameters

The lakes had an average ice cover duration of 200 ± 18.7 (SD) days per year and maximum water temperature of 17.8°C (**Supplementary Figures S1a,b**). When comparing the two time periods 1998–1999 and 2009–2011 a trend of warming was observed. In particular, YAWT increased during the past decade by less than 1°C (**Table 1**). The measured increase in water temperature was related to increasing air temperatures as recorded from meteorological stations during the same observation period (see also Weckström et al., 2016). Compared with 1998–1999, ICDs in 2010–2011 were reduced by 11–37 days (**Table 1**). The shorter ICDs correlated significantly with the calendar day of spring mixing (R^2 = 0.92), but not with the calendar day of autumn mixing (R^2 = 0.007) (**Supplementary Figures S1c,d**). Consequently, the shorter ICD could be explained by an earlier ice break up in spring rather than by later ice formation in autumn.

The low concentrations of nutrients and Chl a in the study lakes indicated that all the five lakes were oligotrophic. The physico-chemical characteristics differed significantly among lakes because of differences in the geology of the various catchments (Kamenik et al., 2001), (**Table 1**). For example, OLA was slightly acidic (pH 6.3), while MOA was neutral (pH 7), and GIG, TWA, and WIR were slightly alkaline (pH 7.3–7.5). Furthermore, water chemistry such as NO_3^-, SO_4^{2-}, Cl^-, Na^+, K^+, Mg^{2+}, Ca^{2+}, TP, DOC, and DRSi, differed significantly between lakes ($p < 0.05$, **Table 1**). During the study period, physico-chemical variables in each lake were found rather stable (**Supplementary Table S1**). Correlation analysis showed that environmental parameters were interrelated, e.g., in the early growing season, Cl^- showed high correlation with NH^{4+}, Na^+, K^+, Mg^{2+}, Ca^{2+}, and TP (**Supplementary Table S2**). Not surprisingly, biological characteristics were found more variable. For example, cyanobacteria abundance ranged from 5.7×10^2 to 2.3×10^5 cells/ml. When compared with the early growing season, the bacterial abundance were found increased at the later stage of the growing season, i.e., in lake GIG, bacterial abundance was $1.78–1.94 \times 10^6$ cells/ml in the early growing season but ranged from $2.51–2.90 \times 10^6$ cells/ml in the late growing season. Altogether the results suggest that although study lakes differed in local influence, an on average minor, albeit significant increase in water temperature has become visible such as by reduced ice over duration.

Composition of the Microbiota in the Alpine Lakes

After denoising, 161 943 sequences were obtained clustering into 13 050 OTUs as defined by the 97% identity threshold. The OTUs were assigned to 36 phyla. Among these, 14 phyla occurred in all 5 lakes and were considered core phyla. *Proteobacteria* were dominant, with relative abundances in the range of 48–75%. *Actinobacteria*, *Cyanobacteria*, *Bacteroidetes*, and *Firmicutes* were abundant with proportions of 3.1–26.7, 3.7–28.7, 6.9–19.7, and 0–8%, respectively (**Supplementary Figures S2a,b**). There were 11 pan phyla that occurred in one lake only and in lowest proportion (<0.01%, **Supplementary Figure S2**), i.e., the phyla WS5 in GIG; *Armatimonadetes*, *Fusobacteria* and SR1 in MOA; GN02 and OP11 in OLA; AD3 and AB3 in TWA; GN04, AC1 and an unknown phylum in WIR. The relative abundances of the dominant phyla varied by season, i.e., in the early growing season, the most abundant phyla included *Proteobacteria* (58.8%), *Cyanobacteria* (16.2%), *Actinobacteria* (10.6%), *Bacteroidetes* (6.4%), *Firmicutes* (5.3%), and *Acidobacteria* (1.2%), while in the late growing season, the dominant phyla were composed of *Proteobacteria* (61.8%), *Bacteroidetes* (17.2%), *Actinobacteria* (14.2%), and *Cyanobacteria* (5.7%) (**Supplementary Figures S2c,d**).

NMDS analysis revealed a higher similarity of microbiota composition among lakes (**Figure 2A**), but higher variability between growing seasons (**Figure 2B**). Notably the microbiota showed higher variability in the early growing season (**Figure 2C**) than during the late growing season (**Figure 2D**). In the early growing season, planktonic microbiota structure was found significantly related to WAS, DOC, CiA, and Cl^-, explaining 18.4% of the total inertia in OTU distribution as revealed by ordination analysis (**Figure 3A**). The influence of time dependence (included as a covariate) was found small and both the first axis and all four axes were statistically significant (Monte Carlo permutation tests, $n = 499$, $p = 0.006$, $p = 0.002$). Canonical axis 1 and 2 explained 6.5 and 5% of total OTU variation based on variables WAS and DOC vs. CiA and Cl^-. In contrast, during the later growing season, only one variable (NO_3^-) explained 6.9% of the total OTU variation (**Figure 3B**). Using permutation analysis including time dependence as covariate the first axis was found marginally significant (p = 0.088). Correspondingly, Mantel tests revealed that for the early growing season, climatic parameters such as WAS and CiA, and nutrient concentrations were related to microbiota assembly. During later growing season, only nutrient concentrations, such as NO_3^- and TP were related to the microbial composition (**Table 2**). It is concluded that the microbiota composition during early growing season significantly depended on temperature and nutrients. In contrast during later season the influence of water temperature

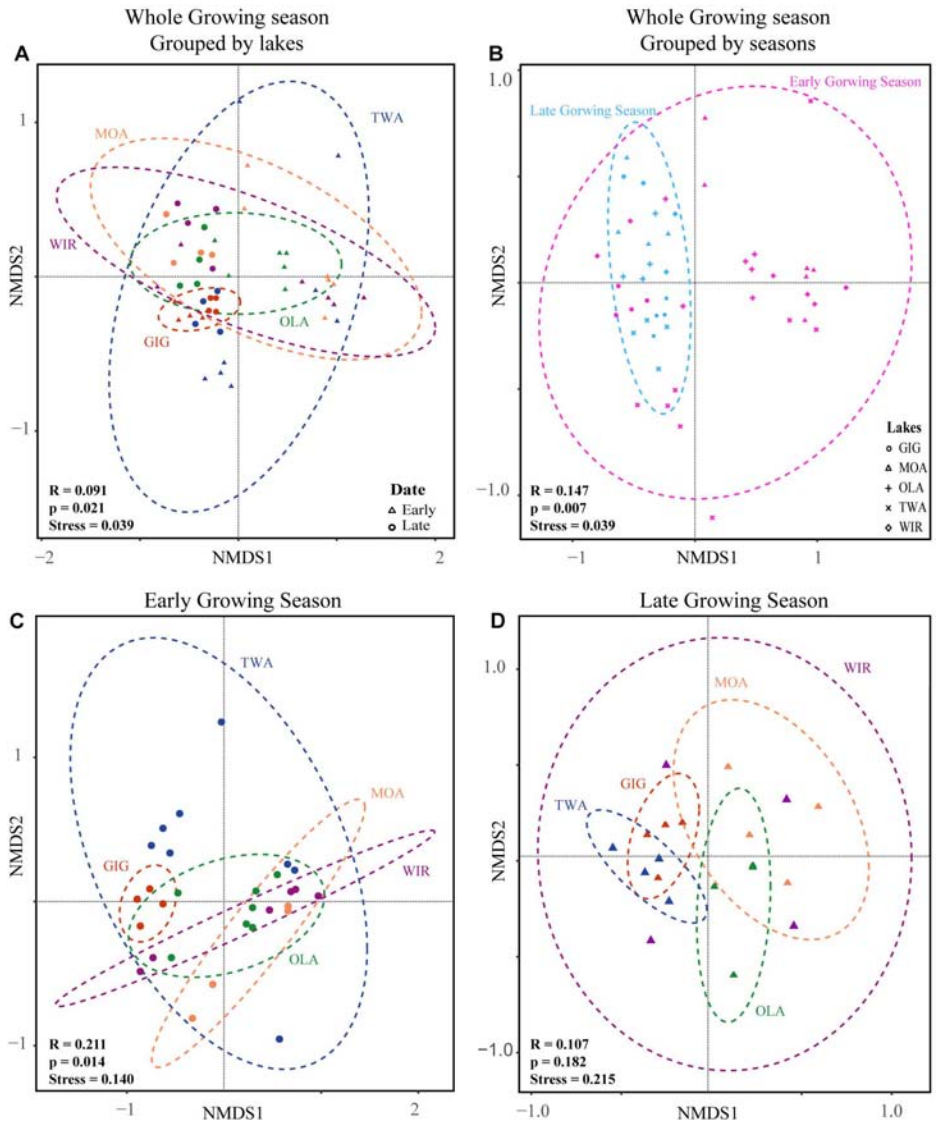

FIGURE 2 | Non-metric multidimensional scaling (NMDS) plots of beta-diversity recorded from five alpine lakes using the Bray-Curtis matrix. **(A)** NMDS plots for individual lakes. **(B)** NMDS plots for samples from early and late growing season. **(C)** NMDS plots for individual lakes in the early growing season. **(D)** NMDS plots for individual lakes in the late growing season. Ellipses represent 95% confidence intervals ($p < 0.05$). ANOSIM (indicated by R and p values) revealed a significant dissimilarity between groups of individual lakes or growing seasons ($p < 0.05$).

became less visible, while inorganic nutrients still played a significant role.

Richness and Diversity of Microbiota in Alpine Lakes

Both richness and diversity differed spatially more among lakes in the early growing season, but less in the late growing season (**Figure 4** and **Supplementary Figure S3** and **Supplementary Table S3**). Seasonally α-diversity differed significantly between the two growing seasons, i.e., both richness and diversity indices were higher in the late growing season than in the early growing season ($p < 0.01$, **Figure 4** and **Supplementary Figure S3**). Richness correlated with lake area, water temperature (WAS) and nutrients during the early growing season (**Table 3**). However, in the late growing season, correlation was found generally decreased and only ICD and CiA correlated with richness (**Table 3**). In contrast, diversity was significantly related to altitude, lake area, maximum depth, ICD, and CiA/CiS as well as nutrients. Using the same environmental variables as used for ordination analysis stepwise multiple regression included WAS, MAWT, pH, NO_3^-, Cl^-, YAWT for the prediction of richness indicator Chao1 (multiple $R^2 = 0.88$, $p < 0.001$) and MAWT, pH, WAS, Cl^-, NO_3^-, and YAWT for S_{obs} (multiple $R^2 = 0.92$, $p < 0.001$), (**Supplementary Table S4**). Vice versa for the prediction of diversity indices stepwise multiple regression included the variables CiA, MAWT, YAWT, WAS, pH, NO_3^-,

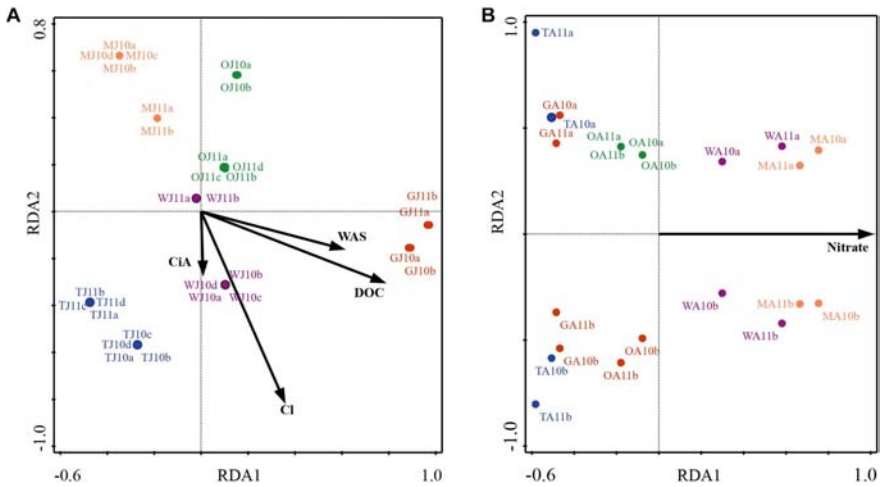

FIGURE 3 | Redundancy analysis (RDA) of planktonic microbiota composition in five alpine lakes during the early growing season **(A)** and the late growing season **(B)**. The first characters indicates the lake name (G: GIG, M: MOA, O: OLA; T: TWA; W: WIR), and the second character indicates the sampling period (J: July, early stage of growing season, A: August, later stage of growing season).

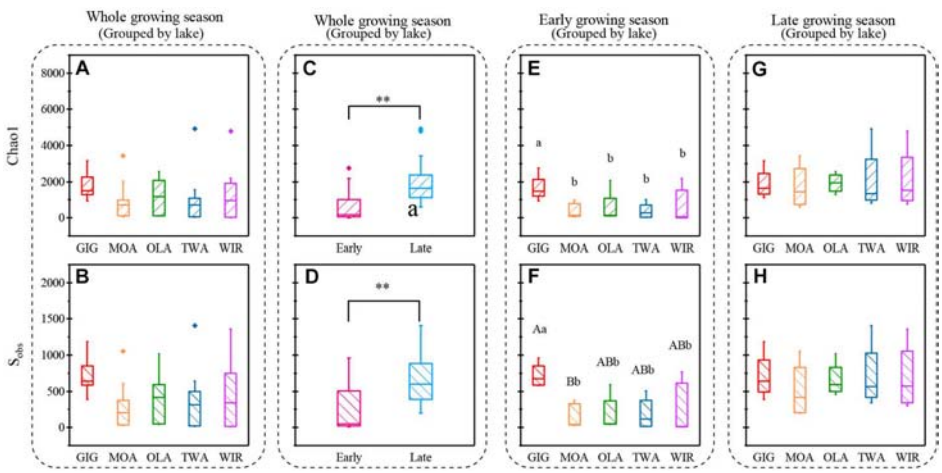

FIGURE 4 | Indices of richness (a,c,e,g Chao1, b,d,f,h, S_{obs}) recorded from planktonic microbiota for five alpine lakes **(A–D)** during the entire study period, **(E,F)** during early growing season, **(G,H)** during late growing season. Lowercase letters and * indicate that subgroups differ ($p < 0.05$), while uppercase letters and ** indicate that subgroups differ at ($p < 0.01$).

Cl^-, DOC for Shannon (multiple $R^2 = 0.96$, $p < 0.001$) and CiA, MAWT, YAWT, WAS, NO_3^-, Cl^- for Simpson (multiple $R^2 = 0.86$, $p < 0.001$ (**Supplementary Table S4**). It is concluded that besides lake morphometry, climatic variables related to water temperature and nutrients were influential to richness and diversity.

Relationship Between Metabolic Activity and Temperature

Since multivariate ordination analysis revealed a significant influence of WAS and CiA on OTU abundance (**Figure 3**) and richness and diversity were found significantly related to water temperature (**Table 2** and **Supplementary Table S4**) in the early growing season, we were interested to see to which extent MTE predicts higher richness and diversity with increasing water temperature. According to MTE only WAS (but not YAWT) was found significantly negatively related to richness in the early growing season (**Figure 5** and **Supplementary Figure S4**). The activation energy as calculated from the inverse slope of the regression curve varied from −3.8 eV for Chao1 and −3.7 eV for S_{obs} exceeding the theoretical estimate for E_a of −0.65 eV (Brown et al., 2004). Notably in the later growing season the observed slopes were closer to the more frequently reported −0.65 prediction. In conclusion, while water temperature played an apparent role for metabolic activity during the period from ice break up to the first sampling date, this factor got less important later in the year.

TABLE 2 | Correlations between the planktonic microbiota composition in five alpine lakes and various environmental variables.

Early growing season			Late growing season		
Factor	$r_{(M)}$	***p***	**Factor**	$r_{(M)}$	***p***
WAS	**0.25**	**0.002**	Max depth	0.19	0.01
CiA	**0.27**	**0.002**	WAS	0.13	0.06
MAWT	0.08	0.061	**NO_3^-**	**0.25**	**0.01**
YAWT	0.15	0.006	Ca^{2+}	−0.02	0.56
Climate related variables	**0.21**	**0.001**	K^+	0.09	0.10
pH	0.14	0.004	**TP**	**0.22**	**0.02**
NO_3^-	0.19	0.003	DOC	0.13	0.04
Cl^-	0.19	0.003	DN	0.14	0.03
DOC	0.18	0.002	**Nutrients**	**0.20**	**0.01**
Nutrients	**0.21**	**0.001**			

Climate variables included WAS, CiA, MAWT, YAWT; Nutrients for the early growing season included NO_3^-, Cl^-, and DOC; Nutrients for the late growing season included NO_3^-, Ca^{2+}, K^+, TP, DOC, and DN.

Functional Gene Prediction

To investigate the highlighted influence of water temperature more directly, functional genes (PFGs), such as metabolic genes, were predicted from the 16S rDNA derived OTUs using PICRUSt. Five groups of functional genes were predicted which included metabolism, environmental information processing, genetic information processing, others and unclassified. On average, metabolism related genes contributed the largest proportion that varied between and within habitats (**Figure 6A**). The natural logarithm of relative abundance of metabolism related genes [ln(PFGs-M)] was negatively related with 1/(kWAS) (**Figure 6B**) in the early growing season and also during the later growing season (**Figure 6C**). In summary, besides planktonic microbiota richness and diversity also metabolic genes increased proportional in response to water temperature supporting the more direct role of temperature variation in the study lakes.

DISCUSSION

Microbiota in Remote Alpine Lakes

Microorganisms in alpine lakes are exposed to extreme environmental pressures such as high radiation, low temperature, short growing season, and low food availability (Sommaruga, 2001; Rose et al., 2009). Not surprisingly bacterial abundance, cyanobacterial abundance, and concentration of Chl a (**Table 1**)

TABLE 3 | Pearson correlation coefficients between environmental variables and α-diversity indices recorded from planktonic microbiota composition in five alpine lakes.

	Early growing stage				Late growing stage			
	Chao1	**S_{ob}**	**Shannon**	**Simpson**	**Chao1**	**S_{ob}**	**Shannon**	**Simpson**
Altitude	−0.08	−0.05	**0.4***	**0.43***	0	0.06	**0.48***	0.41
Lake area	**0.5****	**0.56****	**0.44***	0.24	−0.03	0.08	0.01	−0.15
Max depth^L	−0.05	0.04	**0.44***	**0.48****	0.05	0.13	**0.75*****	**0.62****
ICD	−0.38*	−0.35	0.24	**0.43***	**−0.51***	**−0.5***	0.21	0.4
CiA^E	0.39*	**0.42***	**0.4***	0.2	**0.6****	**0.72*****	**0.5***	0.09
CiS	−0.29	−0.25	0.36*	**0.5****	−0.39	−0.36	0.34	**0.44***
MAWT^E	0.08	0.12	0	−0.13	−0.03	0.12	0.28	0.07
YAWT^E	−0.01	−0.07	−0.3	−0.24	0.02	0.01	0.07	−0.02
WAS^{EL}	**0.55****	**0.6*****	**0.47****	0.19	−0.02	0.13	0.27	0.03
WT	0.12	0.16	0.03	−0.11	−0.14	−0.01	0.35	0.19
Conductivity	0.17	0.26	0.13	0.11	0.06	0.11	0.42	0.28
pH^E	−0.22	−0.16	−0.26	−0.25	−0.03	0.04	0.29	0.25
Alkalinity	0.2	0.29	0.12	0.09	0.08	0.13	0.39	0.24
NO_3^{-EL}	−0.14	−0.22	**−0.55****	**−0.53****	0.03	−0.08	**−0.59****	**−0.44***
SO_4^{2-}	0.05	0.16	0.31	0.34	0.04	0.1	**0.63****	**0.5***
Cl^{-E}	−0.06	0.02	−0.33	−0.35	0.17	0.17	−0.09	−0.18
NH_4^+	0.23	0.39*	0.15	−0.13	0.32	0.33	−0.25	−0.3
Na^+	−0.09	−0.04	−0.32	−0.26	−0.03	−0.09	−0.19	−0.1
K^{+L}	−0.32	**−0.44***	**−0.48****	−0.38*	0.03	−0.06	**−0.48***	−0.33
Mg^{2+}	0.09	0.2	0.36	0.37*	0.09	0.16	**0.67****	**0.5***
Ca^{2+L}	0.2	0.28	0.03	−0.01	0.09	0.14	0.28	0.14
TP^L	−0.19	−0.07	−0.05	0.05	−0.34	−0.34	−0.02	0.13
DOC^{EL}	**0.51****	**0.59*****	**0.61*****	**0.43***	0.24	0.36	0.23	−0.03
DN^L	**−0.46****	**−0.52****	**−0.47****	−0.09	−0.36	−0.39	−0.17	0.06
DRSi	−0.37*	**−0.43***	**−0.57*****	−0.39*	−0.16	−0.3	**−0.5***	−0.23

Statistical significance threshold ($p < 0.05$, **$p < 0.01$, ***$p < 0.005$). ^{E}parameters of the early growing season, ^{L}parameters of the late growing season (as selected through PCA).*

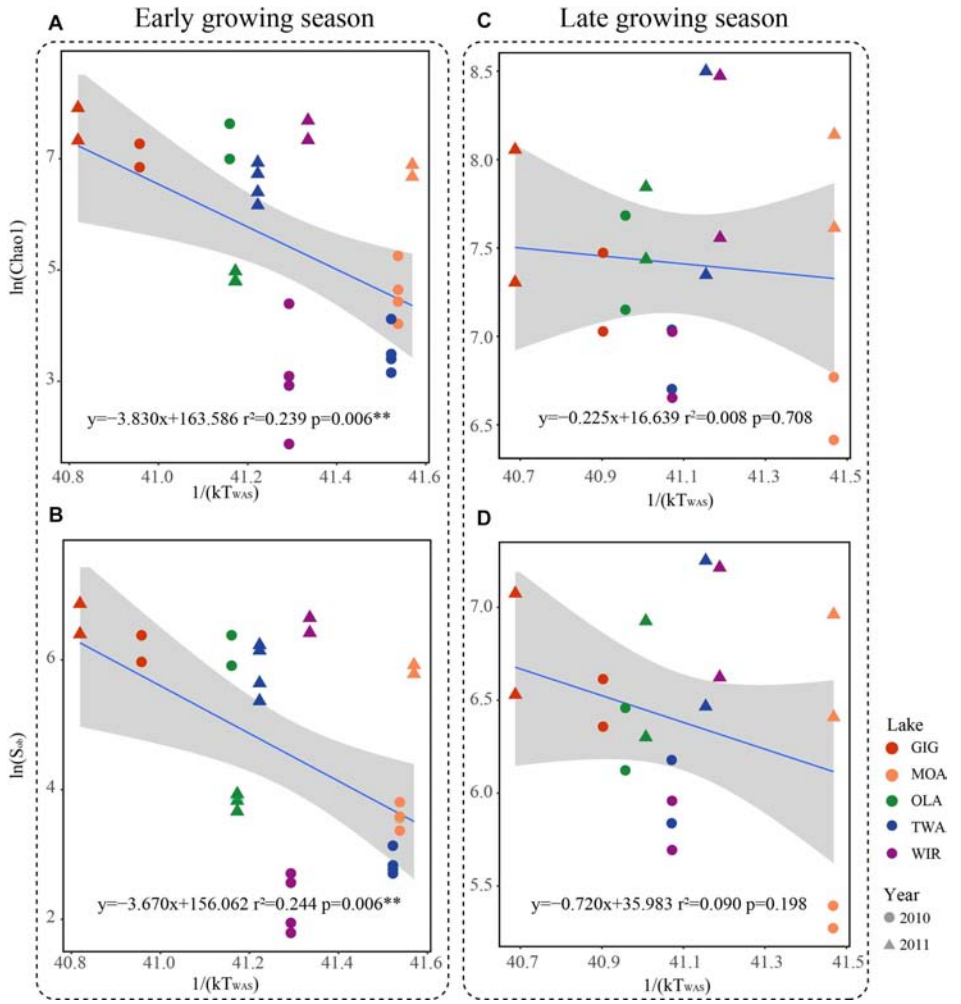

FIGURE 5 | Relationships between taxonomic richness of microbiota in five alpine lakes and average water temperature after circulation in spring (WAS) in Kelvin ($1/(KT_{(WAS)})$). **(A)** Relationship between Chao1 and $1/(KT_{(WAS)})$ in the early growing season. **(B)** Relationship between S_{obs} and $1/(KT_{(WAS)})$ in the early growing season. **(C)** Relationship between Chao1 and $1/(KT_{(WAS)})$ in the late growing season. **(D)** Relationship between S_{obs} and $1/(KT_{(WAS)})$ in the late growing season.

were lower than corresponding values in lowland lakes (Clasen et al., 2008) which is mostly because of lower trophic conditions and shorter vegetation times (Weckström et al., 2016). However, the abundances were in accordance with the microbial abundances reported for cold environments such as high altitude lakes in the Himalayan region (Sommaruga and Casamayor, 2009), the Qinghai-Tibet Plateau lakes (bacterial abundance ranged from 1.59×10^5 to 3.37×10^5 cells mL^{-1}) and lakes in the Mount Everest region (Nepal, bacterial abundance ranged from 2.4×10^5 to 1.15×10^6 cells mL^{-1}) (Liu et al., 2009; Sommaruga and Casamayor, 2009; Liu et al., 2011). The observed Chao1 and S_{obs} indices were similar to those reported for the bacterial community in lakes on Yunnan Plateau, while Shannon was lower (Chao1: 802∼2638, S_{obs}: 579∼2005, average Shannon: 8.44; Zhang et al., 2015). The dominant phyla in the study lakes included *Proteobacteria*, *Actinobacteria*, *Cyanobacteria*, and *Bacteroidetes*, which accounted for 75–99.8% of the relative abundance, which is similar to the findings in Tibetan lakes and Nepal lakes (Sommaruga and Casamayor, 2009; Xiong et al., 2012). In contrast, abundances of other phyla, such as *Verrucomicrobia* and *Planctomycetes*, that have been reported frequently in lowland lakes (Newton et al., 2011; Gies et al., 2014; Zhang et al., 2015), were less abundant. In this study there was less difference spatially among lakes in composition or in diversity detected by NMDS or ANOVA when compared with seasonal variation (**Figures 2**, **4**), indicating generally high similarity in structure and diversity of the alpine microbial communities at the spatial scale.

Microbiota in Alpine Lakes and the Influence of Temperature

In this study, evidence showed that temperature and/or nutrients were drivers shaping the microbiota in the alpine lakes, which highlighted the potential sentinel role of alpine lakes for climate change related changes, i.e., after the ice break up during the

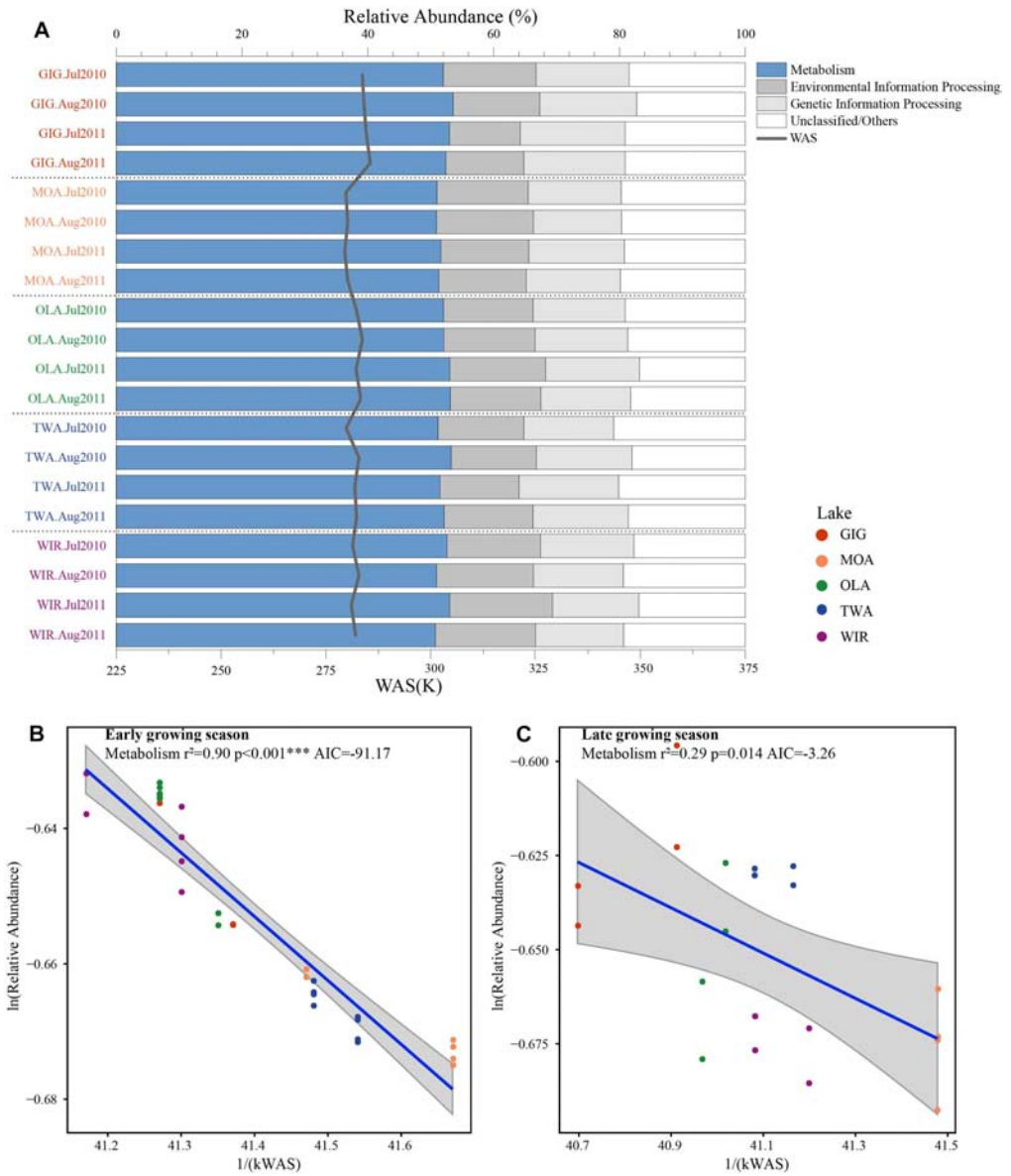

FIGURE 6 | (A) Relative abundance of predicted functional genes in five alpine lakes and **(B)** relative abundance of metabolism related genes as a function of WAS in Kelvin ($1/(KT_{(WAS)})$) during early growing season and **(C)** later growing season.

early growing season (**Figure 3** and **Table 2**). Both temperature and nutrients impact on the microbiota assembly directly and indirectly. For example, the nutrient level shapes microbiota both directly through bottom up regulation and indirectly through regulating the composition of the predators (Bouvy et al., 2011). Temperature after ice break up was shown to be a relevant factor determining microbial composition. Since about two dozen of environmental variables were found correlated in ordination analysis, the individual highlighted variables should be interpreted with caution although an indirect and direct increased temperature effect seems plausible. Direct effects would be related to higher metabolic activity and higher energy flux as outlined above. Indirect effects of increased temperature would include interactions among organisms in the lake food web, animal behavior, life histories, species interactions and ecosystem carbon cycling (Kraemer et al., 2017). Predator prey relations between zooplankton and bacteria (Kammerlander et al., 2016), bacteria and bacteria, such as *Cytophaga* vs. *Cyanobacteria*, and the viruses (Suttle, 2007; Bouvy et al., 2011; Martins et al., 2018) are also known as factors driving the assembly of microbiota in lakes. Besides direct effects it is known that the biomass and composition of plants are regulating the composition and diversity of planktonic bacteria in lowland lakes (Zeng et al., 2012) and may influence the seasonality of the pelagic microbiota in the alpine lakes as well. It seems possible that under increased terrestrial run off conditions during

snow melt the influence from the catchment becomes more visible and contributes to the observed dependence of richness on temperature conditions. Terrestrial runoff can introduce organic matter and nutrients from soils in the catchment thereby structuring planktonic microbiota composition (Crump et al., 2012). In order to test the possibility that the richness or diversity may be influenced by run-off through rainfall or snow melting the precipitation recorded twice a day at two meteorological stations (Schmittenhöhe, 1956 m a SL, Obertauern, 1772 m) were compared for both seasonal periods. Average rainfall in 12 h was calculated from ice break up to the respective sampling date. In general, slightly higher average rainfall was recorded in the later season, i.e., in early vs. late growing season 2.1 ± 0.2 vs. 2.4 ± 0.2 mm rainfall in 12 h were recorded for Obertauern, and 2.5 ± 0.4 vs. 3.5 ± 0.2 mm rainfall in 12 h were recorded at Schmittenhöhe. In addition, the maxima of rainfall which were recorded varied between 22.1 vs. 24.1 mm during the early and late growing season for Obertauern, and 20.2 vs. 27.8 mm, respectively, for Schmittenhöhe. Thus, run-off influence on microbiota composition was considered stable when compared between both early and late growing periods.

Richness of Alpine Planktonic Microbiota and the Influence of Water Temperature After Ice Break Up

Metabolic Theory of Ecology is a linear mechanistic approach addressing the correlation between metabolism of individuals, the population growth rate, the number of taxa and temperature. It underlines the role of temperature on the metabolic rate and taxon richness (Gillooly et al., 2001; Brown et al., 2004; Zhou et al., 2016). In general, for bacterial communities a few studies reported a significant dependence of richness vs. the inverse of annual average temperature. With their impressive example from soil Zhou et al. (2016) list numerous directly and indirect factors, mainly by annual average temperature, not at least by the influence of higher plant organisms. However, in this study, we found that the annual average temperature (YAWT) did not contribute significantly as explanatory variable in alpine lakes (**Supplementary Figure S4**) which would rather argue against a potential influence related to specific habitat characteristics (e.g., so called under cooled lakes, Thompson et al., 2005). On the contrary to YAWT, WAS showed significant correlation with richness (**Figure 5**), indicating the potential of water temperature to regulate the microbial metabolic rate in the early growing season after ice break up. Additionally, the significant correlation between the WAS and proportion of metabolic genes (**Figure 6**) implies that bacteria contributing to metabolic activity increased along with temperature. Notably, activation energy (E_a), as calculated from the slope and reflecting the metabolic rate, was −3.83 for Chao1 and −3.67 for S_{obs} exceeding the more frequent estimate five times (Brown et al., 2004) (**Figure 5**). In other words, the influence of temperature was more visible when compared with microbiota analyzed from lower altitudes. Compared with lowland lakes the microbiota in alpine lakes suffers from a shorter growing season that typically lasts from June to October (Parker et al., 2008). It might be speculated that during the early period after ice break up energy limitation of metabolic growth is the dominant factor while availability of nutrients or light availability is of minor importance. It is generally known that colder (arctic and alpine) habitats are warming faster than warmer places and warming phases in spring become more intense. The water phase in colder places might show steeper increases and perhaps higher amplitudes for a given time window when compared with habitats less affected by climate change. Steeper increases or decreases in temperature for a certain time period might explain the rather steep slopes observed in the early growing phase after ice break up. Vice versa after a certain temperature threshold is exceeded the limiting role of temperature gets less important as the seasonal vegetation period proceeds and nutrients and perhaps biotic factors become more relevant.

CONCLUSION

Within the 10 years period climate change was visible through reduced ice cover duration and increased average water temperature. While WAS and CiA, as well as nutrients and DOC, had a significant influence on bacterial community composition during the early growing season, only nutrients (such as nitrate) were found influential later in the growing season. In other words, the limiting role of temperature became overruled by limiting nutrients later in the growing season. MTE could explain the dependence of taxonomic richness on bacterial metabolic activity in mathematical terms. Interestingly the activation energy exceeded the MTE predicted estimate by far emphasizing the dominant role of temperature during early growing season. In contrast later in the growing season a less significant MTE dependency could be observed. The dominant influence of temperature after ice break up could be explained by overall climate change effects, such as a more intense warming in spring and an overall higher amplitude of temperature variation.

DATA AVAILABILITY

The datasets generated for this study can be found in NCBI Raw Sequence Read Archive (SRA), SRP181537.

AUTHOR CONTRIBUTIONS

RK and SB collected the samples and the metadata as well as extracted DNA and performed the sequencing. YJ, LD, RK, and HH analyzed and interpreted the data, and drafted the manuscript. YJ performed most of the bioinformatic and statistical analyses. JR assisted in bioinformatic analysis. YJ and HH constructed the figures and tables. TM uploaded the sequences. All authors approved the final version of the manuscript for submission and agreed to be accountable for the work.

ACKNOWLEDGMENTS

Johannes Pröll, Norbert Niklas, and Christian Gabriel (Red Cross Transfusion Service of Upper Austria Linz) performed

the sequencing. Josef Franzoi and Roland Psenner (University of Innsbruck) performed the chemical analysis. For the study period ZAMG (Zentralanstalt für Meteorologie and Geodynamik) provided meteorological data on temperature and precipitation from four stations. We would like to thank Ali Hassan Ali Elbehery for bioinformatic support and Judith Feichtmayer for correcting an earlier draft of the manuscript. We also thank the two reviewers for their critical suggestions improving the manuscript. YJ, HH, TM, and JR were supported by the Chinese Scholarship Council (CSC). The sampling and the data acquisition were funded by the Nationalkomitee Alpenforschung of the Austrian Academy of Sciences, project DETECTIVE (DEcadal deTECTion of biodIVErsity in alpine lakes) to RK.

SUPPLEMENTARY MATERIAL

The Supplementary Material for this article can be found online at: https://www.frontiersin.org/articles/10.3389/fmicb.2019.01714/full#supplementary-material

REFERENCES

Adrian, R., O'reilly, C. M., Zagarese, H., Baines, S. B., Hessen, D. O., Keller, W., et al. (2009). Lakes as sentinels of climate change. *Limnol. Oceanogr.* 54, 2283–2297.

Alcaraz, M. (2016). Marine zooplankton and the metabolic theory of ecology: is it a predictive tool? *J. Plankton Res.* 38, 762–770. doi: 10.1093/plankt/fbw012

Allen, A. P., Brown, J. H., and Gillooly, J. F. (2002). Global biodiversity, biochemical kinetics, and the energetic-equivalence rule. *Science* 297, 1545–1548. doi: 10.1126/science.1072380

Bardou, P., Mariette, J., Escudié, F., Djemiel, C., and Klopp, C. (2014). jvenn: an interactive venn diagram viewer. *BMC Bioinformatics* 15:293. doi: 10.1186/1471-2105-15-293

Beniston, M., Diaz, H., and Bradley, R. (1997). Climatic change at high elevation sites: an overview. *Clim. Change* 36, 233–251.

Bouvy, M., Bettarel, Y., Bouvier, C., Domaizon, I., Jacquet, S., Le Floc'h, E., et al. (2011). Trophic interactions between viruses, bacteria and nanoflagellates under various nutrient conditions and simulated climate change. *Environ. Microbiol.* 13, 1842–1857. doi: 10.1111/j.1462-2920.2011.02498.x

Brown, J. H., Gillooly, J. F., Allen, A. P., Savage, V. M., and West, G. B. (2004). Toward a metabolic theory of ecology. *Ecology* 85, 1771–1789. doi: 10.1890/03-9000

Caporaso, J. G., Kuczynski, J., Stombaugh, J., Bittinger, K., Bushman, F. D., Costello, E. K., et al. (2010). QIIME allows analysis of high-throughput community sequencing data. *Nat. Methods* 7, 335–336.

Clasen, J. L., Brigden, S. M., Payet, J. P., and Suttle, C. A. (2008). Evidence that viral abundance across oceans and lakes is driven by different biological factors. *Freshwater Biol.* 53, 1090–1100. doi: 10.1111/j.1365-2427.2008.01992.x

Crump, B. C., Amaral-Zettler, L. A., and Kling, G. W. (2012). Microbial diversity in arctic freshwaters is structured by inoculation of microbes from soils. *ISME J.* 6, 1629. doi: 10.1038/ismej.2012.9

Deng, L., Sweetlove, M., Blank, S., Obbels, D., Verleyen, E., Vyverman, W., et al. (2017). *Bioinformatics analysis for NGS amplicon sequencing. Molecular Tools for the Detection and Quantification of Toxigenic Cyanobacteria*. Hoboken, NJ: John Wiley & Sons

DeSantis, T. Z., Hugenholtz, P., Larsen, N., Rojas, M., Brodie, E. L., Keller, K., et al. (2006). Greengenes, a chimera-checked 16S rRNA gene database and workbench compatible with ARB. *Appl. Environ. Microbiol.* 72, 5069–5072. doi: 10.1128/aem.03006-05

Dixon, P. (2003). VEGAN, a package of R functions for community ecology. *J. Vegetation Sci.* 14, 927–930. doi: 10.1111/j.1654-1103.2003.tb02228.x

Djukic, I., Zehetner, F., Watzinger, A., Horacek, M., and Gerzabek, M. H. (2013). In situ carbon turnover dynamics and the role of soil microorganisms therein: a climate warming study in an alpine ecosystem. *FEMS Microbiol. Ecol.* 83, 112–124. doi: 10.1111/j.1574-6941.2012.01449.x

Gies, E. A., Konwar, K. M., Beatty, J. T., and Hallam, S. J. (2014). Illuminating microbial dark matter in meromictic Sakinaw Lake. *Appl. Environ. Microbiol.* 80, 6807–6818. doi: 10.1128/AEM.01774-14

Gillooly, J. F., Brown, J. H., West, G. B., Savage, V. M., and Charnov, E. L. (2001). Effects of size and temperature on metabolic rate. *Science* 293, 2248–2251. doi: 10.1126/science.1061967

Guo, X., Feng, J., Shi, Z., Zhou, X., Yuan, M., Tao, X., et al. (2018). Climate warming leads to divergent succession of grassland microbial communities. *Nat. Clim. Change* 8, 813. doi: 10.1038/s41558-018-0254-2

Holzapfel, A. M., and Vinebrooke, R. D. (2005). Environmental warming increases invasion potential of alpine lake communities by imported species. *Glob. Change Biol.* 11, 2009–2015.

Jassey, V. E., Chiapusio, G., Binet, P., Buttler, A., Laggoun-Défarge, F., Delarue, F., et al. (2013). Above-and belowground linkages in Sphagnum peatland: climate warming affects plant-microbial interactions. *Glob. Change Biol.*. 19, 811–823. doi: 10.1111/gcb.12075

Kamenik, C., and Schmidt, R. (2005). Chrysophyte resting stages: a tool for reconstructing winter/spring climate from Alpine lake sediments. *Boreas* 34, 477–489. doi: 10.1080/03009480500231468

Kamenik, C., Schmidt, R., Kum, G., and Psenner, R. (2001). The influence of catchment characteristics on the water chemistry of mountain lakes. *Arctic Antarctic Alpine Res.* 33, 404–409. doi: 10.1080/15230430.2001.12003448

Kammerlander, B., Koinig, K. A., Rott, E., Sommaruga, R., Tartarotti, B., Trattner, F., et al. (2016). Ciliate community structure and interactions within the planktonic food web in two alpine lakes of contrasting transparency. *Freshwater Biol.* 61, 1950–1965. doi: 10.1111/fwb.12828

Kraemer, B. M., Chandra, S., Dell, A. I., Dix, M., Kuusisto, E., Livingstone, D. M., et al. (2017). Global patterns in lake ecosystem responses to warming based on the temperature dependence of metabolism. *Glob. Change Biol.* 23, 1881–1890. doi: 10.1111/gcb.13459

Langille, M. G., Zaneveld, J., Caporaso, J. G., Mcdonald, D., Knights, D., Reyes, J. A., et al. (2013). Predictive functional profiling of microbial communities using 16S rRNA marker gene sequences. *Nat. Biotechnol.* 31, 814–821. doi: 10.1038/nbt.2676

Liu, Y., Yao, T., Jiao, N., Tian, L., Hu, A., Yu, W., et al. (2011). Microbial diversity in the snow, a moraine lake and a stream in Himalayan glacier. *Extremophiles* 15, 411. doi: 10.1007/s00792-011-0372-5

Liu, Y., Yao, T., Zhu, L., Jiao, N., Liu, X., Zeng, Y., et al. (2009). Bacterial diversity of freshwater alpine lake Puma Yumco on the tibetan plateau. *Geomicrobiol. J.* 26, 131–145. doi: 10.1080/01490450802660201

Martins, P. D., Danczak, R. E., Roux, S., Frank, J., Borton, M. A., Wolfe, R. A., et al. (2018). Viral and metabolic controls on high rates of microbial sulfur and carbon cycling in wetland ecosystems. *Microbiome* 6, 138. doi: 10.1186/s40168-018-0522-4

Newton, R. J., Jones, S. E., Eiler, A., Mcmahon, K. D., and Bertilsson, S. (2011). A guide to the natural history of freshwater lake bacteria. *Microbiol. Mol. Biol. Rev.* 75, 14–49. doi: 10.1128/MMBR.00028-10

Palmer, K., Biasi, C., and Horn, M. A. (2012). Contrasting denitrifier communities relate to contrasting N2O emission patterns from acidic peat soils in arctic tundra. *ISME J.* 6, 1058. doi: 10.1038/ismej.2011.172

Parker, B. R., Vinebrooke, R. D., and Schindler, D. W. (2008). Recent climate extremes alter alpine lake ecosystems. *Proc. Nat. Acad. Sci.* 105, 12927–12931. doi: 10.1073/pnas.0806481105

Peter, H., and Sommaruga, R. (2016). Shifts in diversity and function of lake bacterial communities upon glacier retreat. *ISME J.* 10, 1545. doi: 10.1038/ismej.2015.245

Porter, K. G., and Feig, Y. S. (1980). The use of DAPI for identifying and counting aquatic microflora 1. *Limnol. Oceanogr.* 25, 943–948. doi: 10.4319/lo.1980.25.5.0943

Rofner, C., Peter, H., Catalán, N., Drewes, F., Sommaruga, R., and Pérez, M. T. (2017). Climate−related changes of soil characteristics affect bacterial community composition and function of high altitude and latitude lakes. *Glob. Change Biol.* 23, 2331–2344. doi: 10.1111/gcb.13545

Rose, K. C., Williamson, C. E., Schladow, S. G., Winder, M., and Oris, J. T. (2009). Patterns of spatial and temporal variability of UV transparency in Lake Tahoe, California−Nevada. *J Geophys. Res.: Biogeosci.* 114:G00D03.

Schmidt, R., Kamenik, C., Lange-Bertalot, H., and Rolf, K. (2004). *Fragilaria* and *Staurosira* (*Bacillariophyceae*) from sediment surfaces of 40 lakes in the Austrian Alps in relation to environmental variables, and their potential for palaeoclimatology. *J Limnol.* 63, 171–189.

Sogin, M. L., Morrison, H. G., Huber, J. A., Welch, D. M., Huse, S. M., Neal, P. R., et al. (2006). Microbial diversity in the deep sea and the underexplored "rare biosphere". *Proc. Nat. Acad. Sci.* 103, 12115–12120. doi: 10.1073/pnas.0605127103

Sommaruga, R. (2001). The role of solar UV radiation in the ecology of alpine lakes. *J. Photochem. Photobiol. B Biol.* 62, 35–42. doi: 10.1016/s1011-1344(01)00154-3

Sommaruga-Wögrath, S., Koinig, K. A., Schmidt, R., Sommaruga, R., Tessadri, R., and Psenner, R. (1997). Temperature effects on the acidity of remote alpine lakes. *Nature* 387, 64. doi: 10.1038/387064a0

Sommaruga, R., and Casamayor, E. O. (2009). Bacterial 'cosmopolitanism'and importance of local environmental factors for community composition in remote high−altitude lakes. *Freshwater Biol.* 54, 994–1005. doi: 10.1111/j.1365-2427.2008.02146.x

Stackebrandt, E., Frederiksen, W., Garrity, G. M., Grimont, P. A., Kämpfer, P., Maiden, M. C., et al. (2002). Report of the ad hoc committee for the re-evaluation of the species definition in bacteriology. *Int. J. Syst. Evolut. Microbiol.* 52, 1043–1047. doi: 10.1099/ijs.0.02360-0

International Organisation of Standardization [ISO] (1992). *Water Quality: Measurement of Biochemical Parameters: Spectrometric Determination of the Chlorophyll-a Concentration*. Geneva: International Organization for Standardization.

Stegen, J. C., Enquist, B. J., and Ferriere, R. (2009). Advancing the metabolic theory of biodiversity. *Ecol. Lett.* 12, 1001–1015. doi: 10.1111/j.1461-0248.2009.01358.x

Stocker, T. (2014). *Climate Change 2013: the Physical Science Basis: Working Group I Contribution to the Fifth Assessment Report of the Intergovernmental Panel on Climate Change*. Cambridge: Cambridge University Press.

Suttle, C. A. (2007). Marine viruses—major players in the global ecosystem. *Nat. Rev. Microbiol.* 5, 801. doi: 10.1038/nrmicro1750

Ter Braak, C., and Smilauer, P. (2002). *CANOCO Reference Manual and CanoDraw for Windows user's gude: Software for Canonical Community Ordination (Version 4.5)*. Ithaca, NY: Scientific Report

Thompson, R., Kamenik, C., and Schmidt, R. (2005). Ultra-sensitive alpine lakes and climate change. *J. Limnol.* 64, 139–152. doi: 10.1016/j.scitotenv.2016.05.079

Weckström, K., Weckström, J., Huber, K., Kamenik, C., Schmidt, R., Salvenmoser, W., et al. (2016). Impacts of climate warming on Alpine lake biota over the past decade. *Arctic Antarctic Alpine Res.* 48, 361–376. doi: 10.1657/aaar0015-058

Weisburg, W. G., Barns, S. M., Pelletier, D. A., and Lane, D. J. (1991). 16S ribosomal DNA amplification for phylogenetic study. *J. Bacteriol.* 173, 697–703. doi: 10.1128/jb.173.2.697-703.1991

Williamson, C. E., Saros, J. E., and Schindler, D. W. (2009). Sentinels of change. *Science* 323, 887–888.

Xiong, J., Liu, Y., Lin, X., Zhang, H., Zeng, J., Hou, J., et al. (2012). Geographic distance and pH drive bacterial distribution in alkaline lake sediments across Tibetan Plateau. *Environ. Microbiol.* 14, 2457–2466. doi: 10.1111/j.1462-2920.2012.02799.x

Zeng, J., Bian, Y., Xing, P., and Wu, Q. L. (2012). Macrophyte species drive the variation of bacterioplankton community composition in a shallow freshwater lake. *Appl. Environ. Microbiol.* 78, 177–184. doi: 10.1128/AEM.05117-11

Zhang, J., Yang, Y., Zhao, L., Li, Y., Xie, S., and Liu, Y. (2015). Distribution of sediment bacterial and archaeal communities in plateau freshwater lakes. *Appl. Microbiol. Biotechnol.* 99, 3291–3302. doi: 10.1007/s00253-014-6262-x

Zhou, J., Deng, Y., Shen, L., Wen, C., Yan, Q., Ning, D., et al. (2016). Temperature mediates continental-scale diversity of microbes in forest soils. *Nat. Commun.* 7, 12083. doi: 10.1038/ncomms12083

Conflict of Interest Statement: The authors declare that the research was conducted in the absence of any commercial or financial relationships that could be construed as a potential conflict of interest.

Copyright © 2019 Jiang, Huang, Ma, Ru, Blank, Kurmayer and Deng. This is an open-access article distributed under the terms of the Creative Commons Attribution License (CC BY). The use, distribution or reproduction in other forums is permitted, provided the original author(s) and the copyright owner(s) are credited and that the original publication in this journal is cited, in accordance with accepted academic practice. No use, distribution or reproduction is permitted which does not comply with these terms.

frontiers in Microbiology

ORIGINAL RESEARCH
published: 04 September 2019
doi: 10.3389/fmicb.2019.02016

The Community Structure of Picophytoplankton in Lake Fuxian, a Deep and Oligotrophic Mountain Lake

Xiaoli Shi[1]†, Shengnan Li[2]†, Huabing Li[1], Feizhou Chen[1] and Qinglong Wu[1]*

[1] State Key Laboratory of Lake Science and Environment, Nanjing Institute of Geography and Limnology, Chinese Academy of Sciences, Nanjing, China, [2] Hunan Institute of Agro-Environment and Ecology, Hunan Academy of Agricultural Sciences, Changsha, China

Spatial and seasonal dynamics of picophytoplankton were investigated by flow cytometry over a year in Lake Fuxian, a deep and oligotrophic mountain lake in southwest China. The contribution of picophytoplankton to the total Chl-*a* biomass and primary production were 50.1 and 66.1%, respectively. Picophytoplankton were mainly composed of phycoerythrin-rich picocyanobacteria (PE-cells) and photosynthetic picoeukaryotes (PPEs). PPEs were dominant in spring, reaching a maximum cell density of 3.0×10^4 cell mL^{-1}, while PE-cells were prevalent in other seasons. PE-cell abundance was relatively similar throughout the year, except for a decrease in summer during the stratification period, when nutrient concentration was low. High-throughput sequencing results from the sorted samples revealed that *Synechococcus* was the major PE-cell type, while Chrysophyceae, Dinophyceae, Chlorophyceae, Eustigmatophyceae, and Prymnesiophyceae were equally important PPEs. In spring, PPEs were mainly composed of Chlorophyceae and Trebouxiophyceae, while in summer, their dominance was replaced by that of Chrysophyceae and Prymnesiophyceae. Eustigmatophyceae and Chlorophyceae became the major PPEs in autumn, and Dinophyceae became the most abundant in winter. Single cells of *Microcystis* were usually detected in summer in the south, suggesting the deterioration of the water quality in Lake Fuxian.

Keywords: photosynthetic picoeukaryotes, picocyanobacteria, Lake Fuxian, community structure, seasonal succession

OPEN ACCESS

Edited by:
Haihan Zhang,
Xi'an University of Architecture and Technology, China

Reviewed by:
Robert McKay,
University of Windsor, Canada
Michel Jean Denis,
UMR7294 Institut Méditerranéen d'Océanographie (MIO), France

***Correspondence:**
Xiaoli Shi
xlshi@niglas.ac.cn

† These authors have contributed equally to this work

Specialty section:
This article was submitted to Aquatic Microbiology, a section of the journal Frontiers in Microbiology

Received: *03 April 2019*
Accepted: *19 August 2019*
Published: *04 September 2019*

Citation:
Shi X, Li S, Li H, Chen F and Wu Q (2019) The Community Structure of Picophytoplankton in Lake Fuxian, a Deep and Oligotrophic Mountain Lake. Front. Microbiol. 10:2016. doi: 10.3389/fmicb.2019.02016

INTRODUCTION

Picophytoplankton (0.2–3 μm), comprising picocyanobacteria and photosynthetic picoeukaryotes (PPEs), are ubiquitous and important components of aquatic ecosystems. They contribute to 10–90% of the total plankton biomass and production in oceans and freshwaters (Stockner et al., 2000; Callieri, 2007). Picophytoplankton constitute an important energy resource in the aquatic microbial loop, and thus, are important in the biogeochemical processes (Cotner and Biddanda, 2002). Their contributions to the total biomass and production of plankton decline systematically with lakes of higher trophic status (Vörös et al., 1998; Bell and Kalff, 2001; Callieri et al., 2007). Environmental factors, such as water temperature, light limitation, nutrients and biotic factors, including grazing and viral-induced lysis, are all regarded as important factors controlling

picophytoplankton abundances (Stockner and Shortreed, 1989; Lefranc et al., 2005; Lepère et al., 2006; Mózes et al., 2006; Callieri et al., 2012; Li et al., 2016).

The understanding of the taxonomy and dynamics of picophytoplankton is largely enriched due to the developments in molecular biology (Callieri, 2007; Lepère et al., 2010; Li et al., 2017; Zhang et al., 2019). *Synechococcus* is the most abundant photosynthetic prokaryotes living in oceans and lakes, and their relative abundance among the total autotrophic biomass increases with decreasing trophic state in aquatic systems (Bell and Kalff, 2001; Callieri, 2007). In fact, freshwater *Synechococcus* strains were polyphyletic and cannot be considered a natural taxon (Callieri, 2017). In contrast, studies regarding PPEs were mainly focused on marine ecosystems during recent decades and to a lesser extent in lacustrine environments (Li et al., 2017). In recent years, the combination of flow cytometric sorting and high-throughput sequencing has allowed progress in understanding the diversity and composition of PPEs in eutrophic shallow lakes (Li et al., 2017; Shi et al., 2018). However, the PPEs community composition in oligotrophic and deep lakes has rarely been investigated, especially in China.

In addition, previous studies related to picophytoplankton in freshwater lakes have mostly focused on temperate lakes. The seasonal cycle of picocyanobacteria populations has been studied in temperate lakes of all trophic types, and a diverse successional patterns have been noted (Weisse, 1988; Weisse and Kenter, 1991; Callieri and Stockner, 2002; Winder, 2009). There is relatively scarce information on the abundance and population dynamics of picophytoplankton in tropical freshwater systems. In fact, subtropical water ecosystems are different from temperate ecosystems in many aspects, e.g., temperature, light and the food web (Bonilla et al., 2016; Iglesias et al., 2017). The aim of the present study is to expand our knowledge of the abundance and composition of the picophytoplankton community in warm subtropical and deep oligotrophic lakes.

MATERIALS AND METHODS

Study Site Description

Lake Fuxian is a subtropical and oligotrophic freshwater lake located in central Yunnan Province (24°17′-37′N, 102° 49′-57′E, altitude 1721 m, surface area 212 km^2, volume 189 × 10^8 m^3). It is the second deepest lake in China, with maximum and average depths of 155 and 89.7 m, respectively. The water retention time of Lake Fuxian is ∼167 years. The annual average rainfall is 951.4 cm. Lake Fuxian is considered warm-monomictic, with mixing during the cool dry season and thermal stratification from May to September.

Environmental Variables

Water samples from 50 cm depth were collected in March, July, October and December of 2015 at 5 sites along a N-S axis of the lake (**Figure 1**). Water temperature (T), pH, dissolved oxygen (DO), total dissolved solids (TDS), nephelometric turbidity units (NTU),conductivity (COND) and oxidation-reduction potential (ORP) were determined *in situ* using a multiparameter water quality probe (YSI 6600, Yellow Springs, OH, United States). A Secchi disk (SD) was used to measure the water transparency *in situ*. Water samples were collected in sterile bottles and transported immediately to the laboratory near shore on ice for further analysis. Total nitrogen (TN) and total phosphorous (TP) nitrate-nitrogen (NO_3^--N), ammonium-nitrogen (NH_4^+-N), and orthophosphate (PO_4^{3-}-P), and dissolved organic carbon (DOC) were determined as described before (Li et al., 2016). Subsamples used for flow cytometric analysis were fixed with paraformaldehyde (1% final concentration, 10% PBS, pH 7.5), quick-frozen with liquid nitrogen, and then kept at −80°C until analysis.

Pigment Analysis

Chlorophyll *a* (Chl-*a*) was estimated as a proxy of size-fractionated phytoplankton biomass. The large planktonic size fraction was firstly collected under a gentle vacuum on 3 μm Millipore Isopore™ membrane filters (Merck Millipore Ltd., Tullagreen, Carrigtwohill Co., Cork, IRL). Subsamples of the filtrate representing the pico-planktonic size fraction were further filtered through 0.2 μm Millipore Isopore™ membrane filters. The different size-fractionated biomass were summed to calculate the total phytoplankton biomass. The Chl-*a* of the membrane filters were extracted overnight in 90% acetone and determined spectrometrically as described in Yan et al. (2004). Water samples collected directly on GF/C glass fiber filters (1.2 μm pore size; Whatman, Maidstone, England, United Kingdom) were used for phycocyanin analysis, which were extracted in Tris buffer (0.05 M, pH 7.0) and measured spectrofluorometrically as described in Yan et al. (2004)

Primary Production Measurement

Primary production was determined as described in Li et al. (2015). Briefly, the oxygen production based on light-dark bottle incubation was determined to represent the plankton production. The 22-mL Perkin-Elmer headspace vials (Jansson et al., 2012) were filled with either integrated water samples representing the whole phytoplankton or filtrates representing the pico-planktonic size fraction. The vials were then submerged in waters near shore and incubated for 4 h under light and dark conditions. A micro fiberoptic oxygen transmitter with an oxygen sensor (PreSens Micro TX3, Germany) was used to determine the oxygen concentrations at the start and end of the incubation. The gross community production was determined by calculating the difference between bottles, assuming respiration to be the same in the light and dark bottles. All analyses were performed in triplicates.

Flow Cytometric Analysis

The frozen samples were thawed on ice and then filtered through a 48 μm pore-sized sieve as pretreatment to eliminate large particles (such as metazoan zooplankton and algal aggregates) and to avoid blocking the nozzle. A FACSJazz^{SE} flow cytometer (Becton Dickinson, United States) equipped with two lasers emitting at 488 nm and 640 nm, respectively, was used for the analysis. Full details of the discrimination and counting of different picophytoplankton

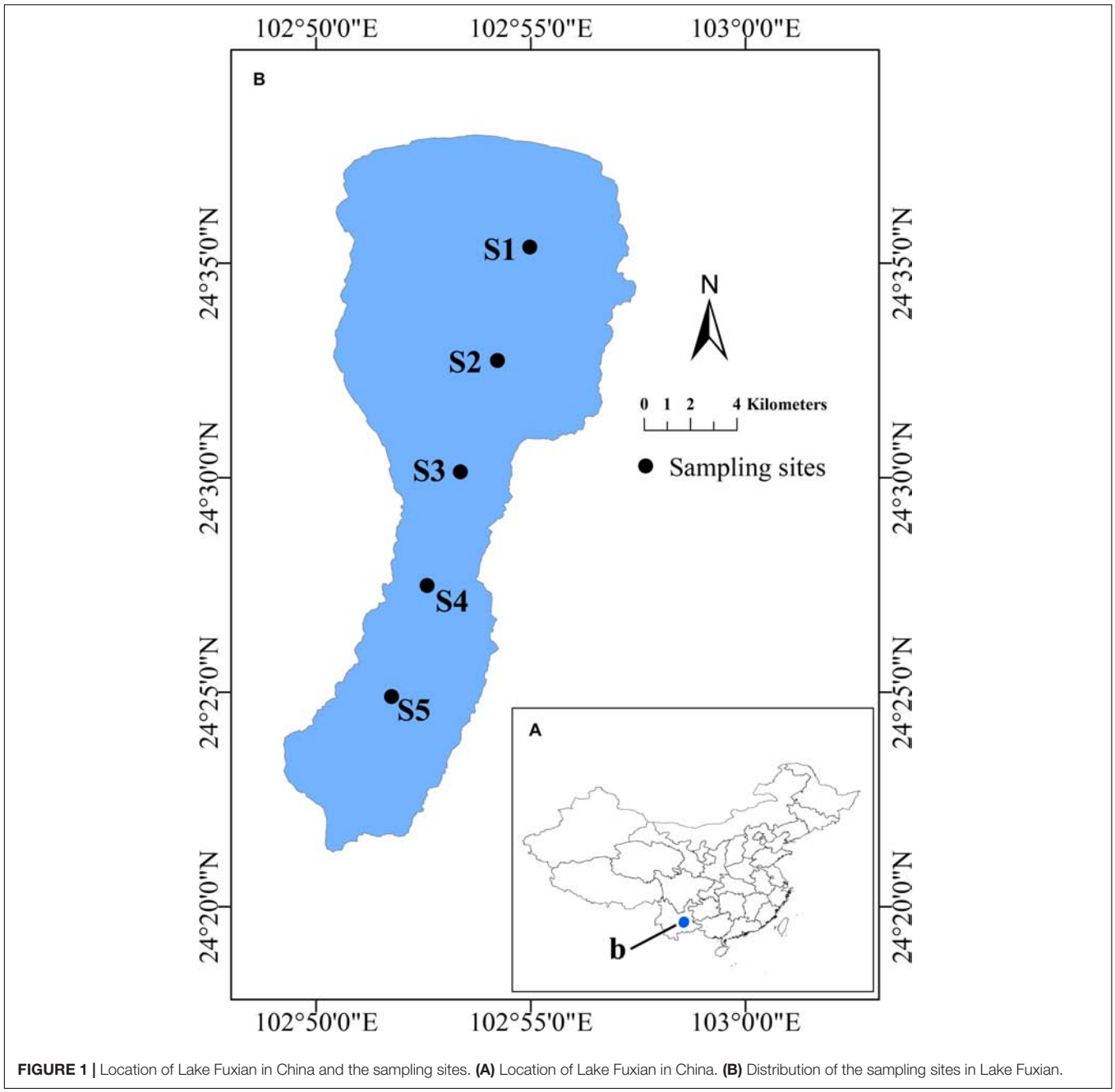

FIGURE 1 | Location of Lake Fuxian in China and the sampling sites. **(A)** Location of Lake Fuxian in China. **(B)** Distribution of the sampling sites in Lake Fuxian.

groups can be found in Li et al. (2015). Two groups of picophytoplankton, photosynthetic picoeukaryotes (PPEs) and phycoerythrin-rich picocyanobacteria (PE-cells), were clearly distinguished by the flow cytometry. They were also detected frequently during the investigation (**Supplementary Figure 1**). PPEs were identified with higher forward scattering (FSC) signals and far-red autofluorescence from Chl-*a*, while PE-cells were with lower FSC and rich phycoerythrin (PE) fluorescence (**Supplementary Figure 1**). PPEs and PE-cells (100,000 to 150,000 cells) were sorted in enrichment mode directly into Eppendorf tubes containing 180 μL of lysis buffer (Tris-HCl, pH 8; EDTA-Na_2 2 mM; Triton X-100, 1.2%) (Marie et al., 2010; Shi et al., 2018). They were stored at −20°C until DNA extraction.

DNA Extraction, PCR, and Pyrosequencing

DNA was extracted from the sorted samples using the DNeasy Blood and Tissue Extraction Kit (Qiagen, Germany) as modified by Marie et al. (2010). The V4 region of 16S rDNA was amplified using the cyanobacteria specific primers CYA 781R(a) 5′-GAC TAC TGG GGT ATC TAA TCC CAT T-3′ and CYA 781R(b) 5′-GAC TAC AGG GGT ATC TAA TCC CTT-3′. The V4 region

of the 18S rDNA was amplified using the universal eukaryote primers Ek-NSF573 (5′-CGCGGTAATTCCAGCTCCA-3′) and Ek-NSR951 (5′-TTGGYRAATGCTTTCGC-3′) (Mangot et al., 2013). The amplicons were purified using the PCR purification kit (Agencourt AMPure XP, Beckman) following the manufacturer's instructions. They were subjected to paired-end sequencing on an Illumina MiSeq platform. The subsequent sequence processing and taxonomic affiliation were described in Shi et al. (2019). Singletons were removed before further analysis. Sequences have been deposited at NCBI under BioProject number PRJNA534173.

Data Analysis

All of the statistical analyses and visualizations were implemented in the R environment (version 3.2.1[1]). The relationships between the environmental variables and the abundances of the picophytoplankton groups were assessed by Spearman correlations. The sequence data were Hellinger-transformed before further multiple statistical analyses to decrease the effect of rare species (Legendre and Gallagher, 2001). The correlations between the environmental factors and PPE community composition were explored using a Redundancy analysis (RDA).

RESULTS

Physical and Chemical Characteristics

The main physical and chemical parameters in Lake Fuxian were monitored in 4 months representing different seasons in 2015. The mean, minimum and maximum values recorded for each variable are listed in **Table 1**. As a typical subtropical lake, the water temperature of Lake Fuxian showed a small variation throughout the year, ranging between 15°C and 23°C. As Lake Fuxian is an oligotrophic lake, the nutrient concentrations are relatively low. The TP and TN concentrations were approximately 0.01 and 0.3 mg L^{-1}, respectively.

[1]http://www.r-project.org

TABLE 1 | The key environmental factors among different seasons of Lake Fuxian in 2015.

	Spring	Summer	Autumn	Winter
T (°C)	15.1 ± 0.4	21.9 ± 2.8	20.7 ± 2.4	16.3 ± 0.0
pH	8.53 ± 0.02	8.33 ± 0.69	9.30 ± 0.38	8.98 ± 0.74
NTU	5.39 ± 3.21	30.71 ± 1.44	16.75 ± 2.34	23.53 ± 7.07
ORP (mV)	236.20 ± 70.08	50.30 ± 25.52	1.23 ± 11.75	−4.78 ± 16.27
Cond (mS cm^{-1})	0.27 ± 0.00	0.31 ± 0.01	0.30 ± 0.01	0.27 ± 0.00
DO (mg L^{-1})	9.77 ± 0.45	7.81 ± 1.22	6.80 ± 2.53	8.39 ± 0.06
DOC (PPM)	4.53 ± 1.75	15.86 ± 8.70	6.91 ± 1.69	6.96 ± 1.72
TN (mg L^{-1})	0.33 ± 0.11	0.22 ± 0.07	0.34 ± 0.07	0.39 ± 0.04
TP (mg L^{-1})	0.02 ± 0.00	0.01 ± 0.00	0.01 ± 0.00	0.02 ± 0.00
NO_3-N (mg L^{-1})	0.06 ± 0.06	0.04 ± 0.04	0.10 ± 0.03	0.10 ± 0.06
PO_4-P (μg L^{-1})	1.00 ± 0.58	3.22 ± 0.91	2.11 ± 0.65	3.83 ± 1.43
NH_4-N (mg L^{-1})	0.04 ± 0.01	0.03 ± 0.01	0.06 ± 0.05	0.02 ± 0.01

The values are listed as mean ± sd.

Picophytoplankton Biomass, Production and Abundances

The total phytoplankton Chl-*a* concentration was quite low in Lake Fuxian, with the average level being 2.63 μg L^{-1}. The Chl-*a* biomass of picophytoplankton was highest in spring, with an average of 2.47 μg L^{-1}, whereas it maintained at a relatively low level in the other three seasons and reached its minimum in winter, with an average of 0.70 μg L^{-1} (**Figure 2A**). Likewise, the proportion of picophytoplankton to total phytoplankton Chl-*a* concentrations was lowest in winter, with an average of 36.3%, and highest in summer, with an average of 58.6% (**Figure 1A**). In addition, picophytoplankton also contributed greatly to the total phytoplankton primary production in Lake Fuxian (**Figure 2B**). Picophytoplankton production showed a similar dynamic with its Chl-*a* biomass and was highest in spring, with an average of 0.52 mg O_2 L^{-1} h^{-1}, followed by autumn and winter. Unfortunately, the primary production data in summer were missing due to a malfunction. The total phytoplankton primary production was clearly dominated by picophytoplankton, with its contributions being over 50% during most of the investigated year (**Figure 2B**).

Based on the flow cytometric scatter and fluorescence signals, two major picophytoplankton groups were identified in Lake Fuxian: PPEs and PE-cells (**Supplementary Figure 1**). These two groups were detected throughout the whole year at all sampling sites. The abundance of total picophytoplankton fluctuated throughout the year, and the highest levels were also achieved in spring, with approximately 3.0×10^4 cells mL^{-1} (**Figure 3**). The dynamics of PE-cells and PPE abundances were similar to total abundances with concentrations ranging from 0.5 to 1.5×10^3 cells mL^{-1} and 0.2 to 1.8×10^3 cells mL^{-1}, respectively. PE-cells dominated picophytoplankton in abundance in most of the seasons except in spring (**Figure 3**).

Relationships Between Picophytoplankton Abundances and Environmental Factors

The Spearman correlation analyses showed that the abundances of PPEs and PE-cells showed significant relationships with many environmental variables (**Table 2**). Specifically, PPE abundance was significantly negatively correlated with PO_4-P and positively correlated with Cond and DO concentrations, whereas PE-cell abundance showed little significance with those factors but was significantly positively correlated with TN and NO_3-N concentrations. In addition, PPE and PE-cell abundances exhibited similar correlations with other environmental factors (**Table 2**).

The Community Structure of Picocyanobacteria

A total of 1,502,233 sequences were retrieved for the 16S rRNA from GenBank, over 99% of which were associated with cyanobacteria and grouped into 44 OTUs. *Synechococcus*

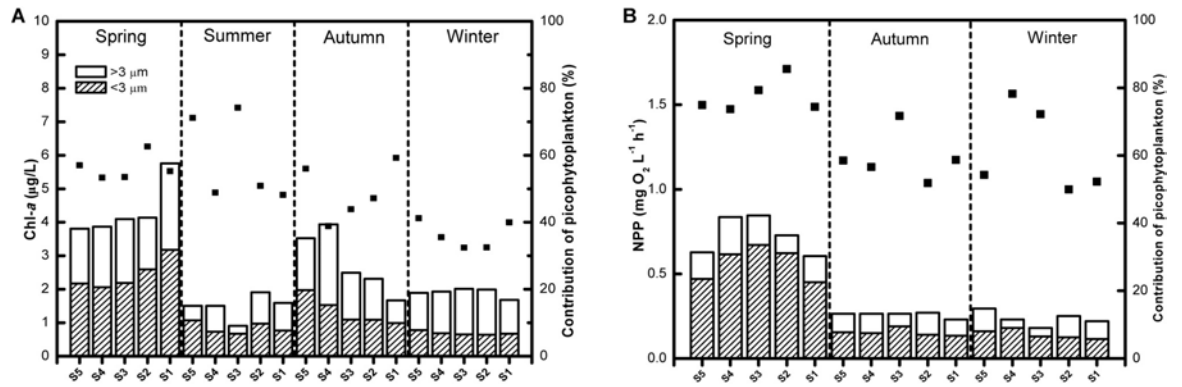

FIGURE 2 | (A) The size fractioned Chl-*a* concentrations (the columns) and the contribution of picophytoplankton to total phytoplankton Chl-*a* (the points) in Lake Fuxian. **(B)** The size fractioned net primary production (NPP, the columns) and the contribution of picophytoplankton to total phytoplankton primary production (the points) in Lake Fuxian.

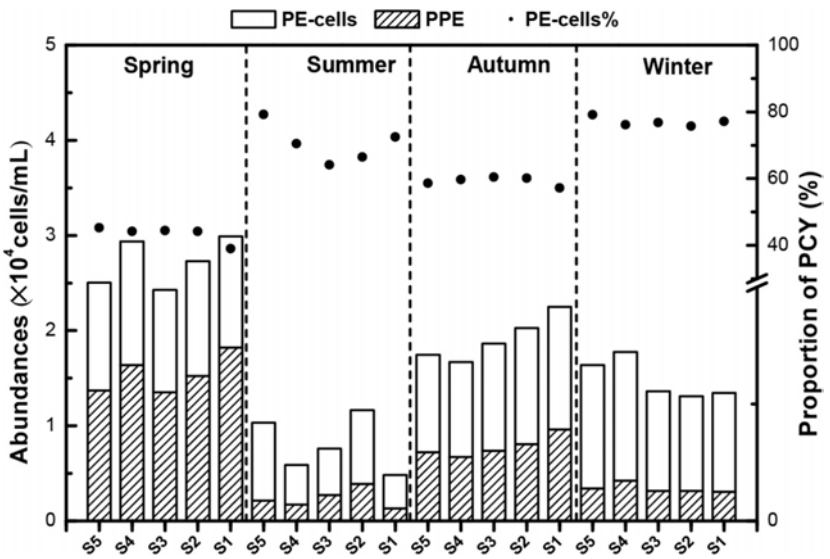

FIGURE 3 | The abundances of photosynthetic picoeukaryotes (PPEs) and picocyanobacteria (PCY) in different seasons in Lake Fuxian. The points indicated the contributions of PCY to total picophytoplankton abundances.

turned out to be the most dominant cyanobacteria genus in Lake Fuxian, which accounted for 77.0% of the total cyanobacterial sequences. Unfortunately, the identification of cluster for the representative OTUs were not achieved, since the sequence of 400 bp is too short to build up a robust phylogenetic tree with high bootstrap values. In summer, at Station S1, 80.3% of the cyanobacteria sequences were related to unclassified Chloroplast, while only 18.1% of sequences belonged to *Synechococcus*. At Station S5, the majority of sequences were associated with *Microcystis*. In autumn and winter, more than 90% of cyanobacterial sequences were all linked to *Synechococcus* (**Figure 4**).

The Community Structure of PPEs

The diversity of PPEs was described based on a total of 730,293 quality-filtered reads grouped into 480 OTUs. Interestingly, the number of sequences affiliated with PPEs was quite low, and over 50% of the sequences were affiliated with non-pigmented picoeukaryotes. PPEs contributed to 37.87% of the total reads and represented only 165 OTUs. The taxonomic composition of the PPEs retrieved from Lake Fuxian is shown in **Table 3**. About 9.54% of the sequences were not assigned to any known PPE assemblages and were identified as unclassified PPEs in the present study. When compared at a high taxonomic level (i.e., class), Dinophyceae, Chrysophyceae, Chlorophyceae, Eustigmatophyceae, and Haptophyceae represented most of the PPE diversity in Lake Fuxian. In spring, PPEs were mainly composed of Chlorophyceae and Trebouxiophyceae, while in summer, their dominance was replaced by that of Chrysophyceae and Haptophyceae. Eustigmatophyceae and Chlorophyceae became the major PPEs in autumn, and Dinophyceae became the most abundant in winter (**Figure 5**).

TABLE 2 | The correlations between environmental factors and the abundance of picophytoplankton.

	PPEs	PE-cells
T	−0.489,**	−0.539**
pH	−0.172	0.135
ORP	−0.485**	−0.607**
Cond	0.768**	0.262
DO	0.368*	0.153
NTU	−0.865**	−0.748**
DOC	−0.453**	−0.519**
TN	0.201	0.572**
TP	0.375*	0.358*
NO_3-N	−0.047	0.370*
PO_4-P	−0.690**	−0.293
NH_4-N	0.284	0.28

*P value <0.01, **P value <0.05.

TABLE 3 | Taxonomic composition of putative photosynthetic picoeukaryotes retrieved in Lake Fuxian.

	Numbers		Percentages (%)	
	OTUs	Reads	OTUs	Reads
Bacillariophyta	**10**	**7377**	**2.08**	**1.01**
Bacillariophyceae	2	3279	0.42	0.45
Coscinodiscophyceae	7	2812	1.46	0.39
Fragilariophyceae	1	1286	0.21	0.18
Chlorophyta	**59**	**46555**	**12.29**	**6.37**
Chlorophyceae	38	37821	7.92	5.18
Mamiellophyceae	6	2371	1.25	0.32
Pedinophyceae	1	12	0.21	0.00
Trebouxiophyceae	8	6275	1.67	0.86
Ulvophyceae	3	19	0.63	0.00
Unassigned	3	57	0.63	0.01
Chrysophyceae	**43**	**75481**	**8.96**	**10.34**
Cryptophyta	**11**	**1303**	**2.29**	**0.18**
Dictyochophyceae	**4**	**1383**	**0.83**	**0.19**
Dinophyceae	**27**	**82869**	**5.63**	**11.35**
Eustigmatophyceae	**3**	**27259**	**0.63**	**3.73**
Haptophyceae	**2**	**27229**	**0.42**	**3.73**
Synurophyceae	**6**	**7128**	**1.25**	**0.98**
Unassigned	**22**	**69642**	**4.58**	**9.54**
Sum	**187**	**346226**	**38.96**	**47.41**

During the investigated year, the top 10 most abundant PPE OTUs detected in Lake Fuxian were mainly affiliated with Dinophyceae (OTU197, OTU194, OTU262, OTU267), Chlorophyceae (OTU203 and OTU23), Chrysophyceae (OTU80), Eustigmatophyceae (OTU14), Haptophyceae (OTU190) and Synurophyceae (OTU87). Specifically, the four dominant Dinophyceae OTUs were all affiliated with uncultured eukaryotes according to the BLAST results (**Table 4**). Except for Eustigmatophyceae OTU4, the other 5 dominant OTUs were all aligned to known species with high identity.

The Relationship of PPE Community Structure and Environmental Factors

Based on the DCA analysis, the length of the first axis was 2.43; thus, we used the RDA analysis to investigate the correlation between the PPE communities and environmental factors, which showed a significant correlation (p = 0.008). After a forward selection based on the variance inflation factor (VIF) values, six factors, including DOC, TN, T, DO, NTU and PO_4, were retained and entered into the model. The first two axes explained 20.36% and 12.59% of the PPE community variances, respectively, in Lake Fuxian (**Figure 6**). The results indicated that the samples from the same season tended to cluster together; specifically, spring and autumn samples were closer to each other and exhibited more similar PPE community compositions.

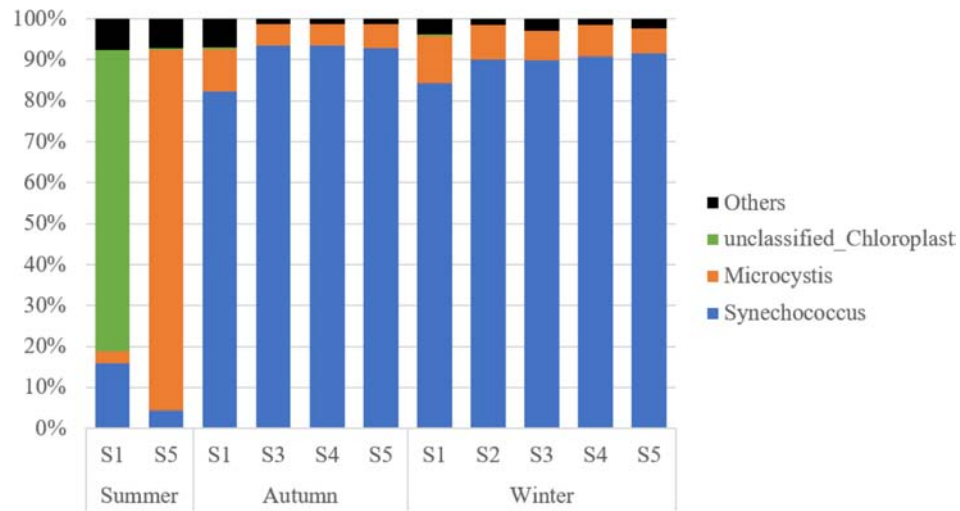

FIGURE 4 | The taxonomic composition of PE-cells from the sorted samples in Lake Fuxian.

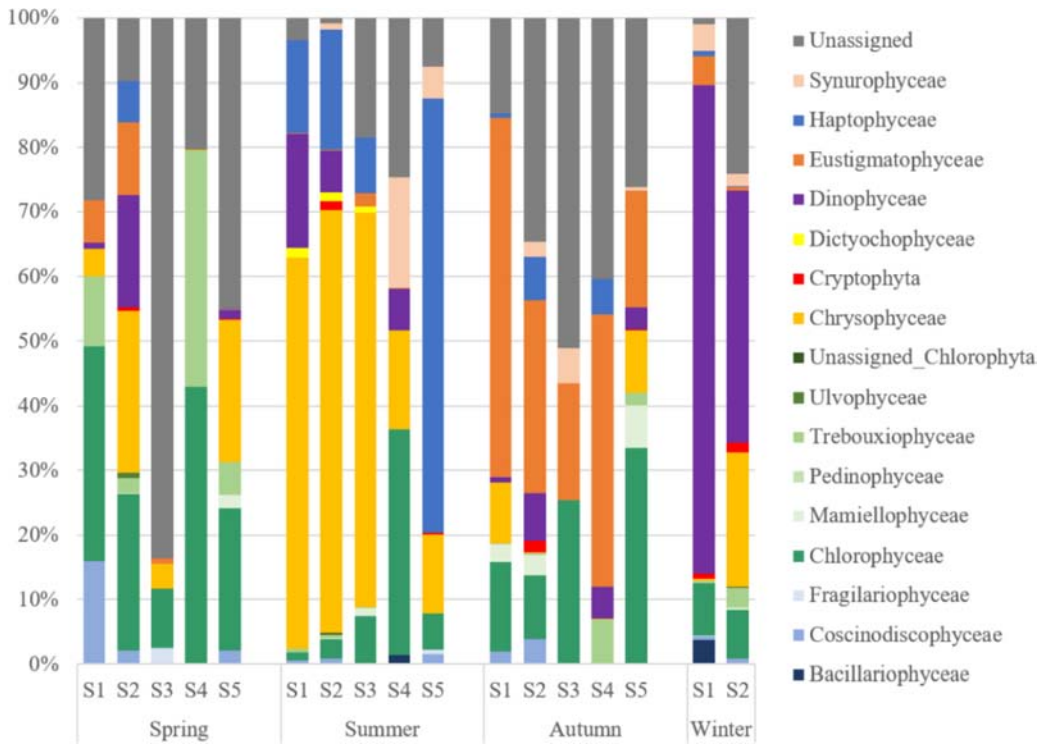

FIGURE 5 | The taxonomic composition at class level of PPEs from the sorted samples in Lake Fuxian.

TABLE 4 | Taxa of the 10 most abundant PPEs OTUs in Lake Fuxian, 2016.

OTU ID	Reads (%)	Class	Blast closest relative (identity)	Accession number
OTU80	8.38	Chrysophyceae	*Dinobryon sociale* (100%)	MK464020.1
OTU197	7.57	Dinophyceae	Uncultured eukaryote (99.71%)	JF317691.1
OTU190	3.73	Haptophyceae	*Chrysochromulina parva* (100%)	MH206612.1
OTU14	3.55	Eustigmatophyceae	*Eustigmatophyceae* sp. (87.29%)	KF757253.1
OTU203	1.64	Chlorophyceae	*Tetradesmus obliquus* (100%)	MK541731.1
OTU194	1.05	Dinophyceae	Uncultured eukaryote (100%)	JF317773.1
OTU262	0.80	Dinophyceae	Uncultured eukaryote (100%)	MG418714.1
OTU87	0.77	Synurophyceae	*Poterioochromonas malhamensis* (100%)	MH536661.1
OTU267	0.60	Dinophyceae	Uncultured eukaryote (99.71%)	JF317733.1
OTU233	0.51	Chlorophyceae	*Volvox aureus* (100%)	LC086362.1

DISCUSSION

The Contribution of Picophytoplankton in Lake Fuxian

Different populations of picophytoplankton in Lake Fuxian were identified based on their FSC (a proxy for cell size) signals and predominant pigments autofluorescence through flow cytometry. They were composed of phycoerythrin-rich prokaryotic and eukaryotic picophytoplankton. The relative proportion of picophytoplankton to total phytoplankton increases with decreasing trophic status of aquatic systems (Callieri, 2007; Ivanikova et al., 2007; Sterner, 2010; Shi et al., 2018). Unicellular picocyanobacteria and picoeukaryotes can outcompete the large phytoplankton in the ultraoligotrophic extreme of the trophic gradient (Suttle and Harrison, 1988; Suttle et al., 1988). One of the advantages of small cell size in low nutrient environments is that these organisms are less limited by molecular diffusion of nutrients because of the increase of the surface-to-volume ratio (Raven, 1998). Furthermore, better acclimation of picophytoplankton than that of the larger phytoplankton (>3 μm) to low-temperature and low-light winter environment was also confirmed by their higher maximum photosynthetic rate and light utilization parameter (Somogyi et al., 2016). Picophytoplankton concentrations in Lake Fuxian were in the 10^4 cells mL^{-1} range during the investigated year, which were lower than that in the oligotrophic tropical lakes and eutrophic subtropical lakes, being in the 10^5 cells mL^{-1} range (Sarmento et al., 2008; Li et al., 2016). The

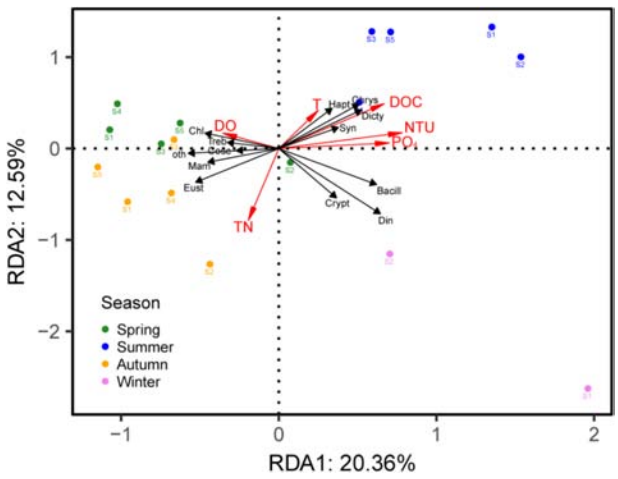

FIGURE 6 | RDA triplots of samples, environmental parameters and the main taxa of PPEs in Lake Fuxian. Bacill, Bacillariophyceae; Cosc, Coscinodiscophyceae; Chl, Chlorophyceae; Mam, Mamiellophyceae; Treb, Trebouxiophyceae; Chrys, Chrysophyceae; Crypt, Cryptophyceae; Dicty, Dictyochophyceae; Din, Dinophyceae; Eust, Eustigmatophyceae; Hapt, Haptophyta; Syn, Synurophyceae; oth, other PPEs.

model of picophytoplankton contribution to total production in freshwater is largely based on results from a study of eight New Zealand lakes (Petersen, 1991). In a trophic gradient, expressed as increasing Chl-*a* concentration from 0.57–103 μg L^{-1}, Petersen found an inverse relationship between picoplankton contribution to total carbon fixation and lake trophic state. In the present study in Lake Fuxian, which is an oligotrophic lake with low TN and TP concentrations, the mean contribution of picophytoplankton to total Chl-*a* biomass and primary production were 36.3% and 66.1%, respectively, which was significantly higher than that in the eutrophic lakes, Lake Taihu and Lake Chaohu (Li et al., 2016).

Picocyanobacteria Dominate Picophytoplankton Abundances in Lake Fuxian

The present study showed that picocyanobacteria were prevalent in Lake Fuxian in most seasons. The prokaryotic structure of the picocyanobacteria cells provides them with the minimum costs for metabolism, and this factor has been considered as the main reason for their success in oligotrophic conditions (Weisse and Kenter, 1991). Besides, the ability to adapt to low-P conditions by accessing multiple forms of organic P also contributed to their success in oligotrophic conditions (Kutovaya et al., 2013; Callieri, 2017). In a 4-year study of picophytoplankton communities in Lake Maggiore, the abundance of picocyanobacteria gradually increased as the lake's nutrient loads declined (Stockner, 1991). Lake typology and morphogenesis are also key factors influencing the picophytoplankton. Picocyanobacterial development was favored by the stability of the vertical structure of the lakes and by a high hydrological retention time. Large, deep lakes generally constitute preferred environments for the succession of picocyanobacteria (Stockner, 1991). In temperate lakes, the seasonal cycle of picocyanobacteria usually showed a bimodal pattern. They firstly peaked in spring or early summer, corresponding to the start of stratification, followed by a second peak during autumn (Stockner et al., 2000). In Lake Fuxian, picocyanobacteria showed equal abundances in winter as in spring and autumn because the temperature in winter is as high as 16°C in the subtropical region. The relatively low cell density in summer corresponded to the low nutrient concentration during the stratification period because our results showed that picocyanobacteria abundance was significantly positively correlated with TN and NO_3-N concentrations.

The Chroococcales order has been considered as polyphyletic, with disperse clades among Cyanobacteria, based on phylogenetic analysis of the 16S rDNA sequences (Urbach et al., 1998). However, *Synechococcus* and *Cyanobium* are the two genera dominate the prokaryotic picophytoplankton in freshwater (Komárek, 1996). Our results indicated that *Synechococcus* was the major picocyanobacteria in Lake Fuxian in autumn and winter. Freshwater *Synechococcus* strains have developed the production of pigments to exploit various underwater light niches, thus being successful in different light fields along trophic gradients of lakes (Callieri, 2017). In summer, many sequences affiliated with *Microcystis*, which is a typical bloom species, were retrieved in Station S5. In fact, single *Microcystis* cells were also detected by flow cytometry in the late spring and autumn in the highly eutrophic lakes, Lake Chaohu and Lake Taihu (Li et al., 2016), and thus, the detection of *Microcystis* suggests a potential deterioration of water quality in Lake Fuxian. The water quality of Lake Fuxian is shown to be consistently good but is threatened by increasing pollution, as shown by the increasing trend of pollutants over the past 25 years (Chen et al., 2019). Since Lake Fuxian is designated as a drinking water conservation area, it is critical to take actions for pollution control.

PPEs Community Structure in Lake Fuxian

Factors controlling PPE distribution differed markedly from those affecting picocyanobacteria both in space and time, largely because of their different nutritional and light requirements and potential growth rates (Weisse and Kenter, 1991). PPEs are often approximately one order of magnitude less abundant than picocyanobacteria, and in temperate regions, they tend to show a single population peak during spring isothermal mixing and early thermal stratification (Stockner, 1991; Fogg, 1995). Our results were consistent with this pattern, with PPEs in Lake Fuxian showing their peak abundances in spring.

To date, the community structure of PPEs in oligotrophic lakes has been little known. A previous study of Lake Pavin revealed that Chrysophyceae and Cryptophyta were major small pigmented eukaryotes (Lepère et al., 2006). However, classical methods using cloning and sequencing of the 18S rRNA genes in filtered water samples could cause an underestimation of PPEs because universal eukaryotic primers are heavily biased toward heterotrophs (Shi et al., 2009). Flow cytometric sorting

has been proven to be a key advance in analyzing the PPEs community, and this approach produced a notable reduction in the contribution of heterotrophic groups within 18S rRNA gene clone libraries and allowed the recovery of several novel lineages (Shi et al., 2009).

Consistent with the presence of Chrysophyceae (Lepère et al., 2006), we also revealed the dominances of Dinophyceae, Eustigmatophyceae, Chlorophyceae and Haptophyceae in Lake Fuxian. In comparison, the PPE community structure was mainly composed of Chlorophyceae and Bacillariophyceae in eutrophic lakes (Li et al., 2017; Shi et al., 2018, 2019). Therefore, freshwater ecosystems with various trophic states contain different PPE community structures. Research from marine ecosystems also showed that PPE community structure can be quite different in regions with different trophic statuses. In oligotrophic water, Prasinophyceae (IX), clades of marine Chrysophyceae and Haptophyta dominated, whereas in the coastal region, groups with cultivated representatives such as *Mamiellales* prevailed (Shi et al., 2009). In addition, the community of PPEs in Lake Fuxian also exhibited a seasonal dynamic and were dominated by various taxa in different seasons. The RDA analysis indicated that the dominance of PPE taxa in different seasons was significantly correlated with environmental changes, which indicated that these PPE taxa can occupy different ecological niches.

The most abundant OTU in Lake Fuxian was affiliated with *Dinobryon sociale*. *Dinobryon* has been reported to be present in oligotrophic lakes and has high affinity for low ambient concentrations of inorganic phosphate and a capacity to absorb organically bound phosphate (Lehman, 1976; Dokulil and Skolaut, 1991). A bloom of *Dinobryon sociale* was recorded in Lake Balaton in 1993, caused by the release of resting cysts from sediment to the water by a coastal dredging operation (Reynolds et al., 1993). Four OTUs were associated with Dinophyceae, contributing approximately 10% of the total reads. Dinophyceae was widely present in the oligotrophic mountain lakes of the northern and southern slopes of the eastern Alps (Tolotti et al., 2003). Another dominant OTU belongs to *Chrysochromulina parva*. This is a common species in oligotrophic lakes that is mixotrophic and has potential toxicity (Parke et al., 1962; Hansen et al., 1994; Queimaliños, 2002). One potential advantage of mixotrophy is the acquisition of nitrogen and phosphorus from particulate food when concentrations of dissolved nutrients are low (Sanders et al., 2000). Consistent with our results, Eustigmatophyceae was reported to be a common member of the phytoplankton community in Lake Baikal and occurred throughout the year (Fietz et al., 2010). Chlorophyceae, including *Volvox aureus* and *Tetradesmus obliquus,* is widely distributed in the freshwater ecosystem, and the latter is considered a promising green microalgae for sustainable production of biofuels (Di et al., 2017).

In summary, picophytoplankton was a major contributor to phytoplankton biomass and primary production in Lake Fuxian, a deep and oligotrophic mountain lake in the southwest China. PPEs were dominant in spring, while phycoerythrin-rich *Synechococcus* was prevalent in other seasons. PPEs community composition exhibited a seasonal variation. In spring, PPEs were mainly composed of Chlorophyceae and Trebouxiophyceae, while in summer, their dominance was replaced by that of Chrysophyceae and Prymnesiophyceae. Eustigmatophyceae and Chlorophyceae became the major PPEs in autumn, and Dinophyceae became the most abundant in winter. Furthermore, single *Microcystis* cells were also detected in the lake in summer, suggesting the deterioration of the water quality in Lake Fuxian.

DATA AVAILABILITY

The datasets generated for this study have been deposited at NCBI under BioProject number PRJNA534173.

AUTHOR CONTRIBUTIONS

XS conceived and designed the experiments. SL and HL performed the experiments. SL analyzed the data. FC and QW contributed reagents, materials, and analysis tools. XS and SL wrote the manuscript.

FUNDING

This research was supported by the National Natural Science Foundation of China (31670462, 31800388, and 31730013), the State Key Laboratory of Lake Science and Environment (No. 2018SKL008), and the Chinese Academy of Sciences (qyzdj-ssw-dqc030). The Project of 135 program of NIGLAS (NIGLAS2018GH03) also financially sponsored the research.

SUPPLEMENTARY MATERIAL

The Supplementary Material for this article can be found online at: https://www.frontiersin.org/articles/10.3389/fmicb.2019.02016/full#supplementary-material

REFERENCES

Bell, T., and Kalff, J. (2001). The contribution of picophytoplankton in marine and freshwater systems of different trophic status and depth. *Limnol. Oceanogr.* 46, 1243–1248. doi: 10.4319/lo.2001.46.5.1243

Bonilla, S., Gonzalez-Piana, M., Soares, M. C. S., Huszar, V. L. M., Becker, V., Somma, A., et al. (2016). The success of the cyanobacterium *Cylindrospermopsis raciborskii* in freshwaters is enhanced by the combined effects of light intensity and temperature. *J. Limnol.* 75, 606–617. doi: 10.4081/jlimnol.2016.1479

Callieri, C. (2007). Picophytoplankton in freshwater ecosystems: the importance of small-sized phototrophs. *Freshw. Rev.* 1, 1–28. doi: 10.1608/frj-1.1.1

Callieri, C. (2017). Synechococcus plasticity under environmental changes. *FEMS Microbiol. Lett.* 364:fnx229. doi: 10.1093/femsle/fnx229

Callieri, C., Cronberg, G., and Stockner, J. G. (2012). "Freshwater picocyanobacteria: single cells, microcolonies and colonial forms," in *Ecology*

of Cyanobacteria II: *Their Diversity in Time and Space*, 2nd Edn, ed. B. A. Whitton, (Berlin: Springer), 229–269. doi: 10.1007/978-94-007-3855-3_8

Callieri, C., Modenutti, B., Queimalinos, C., Bertoni, R., and Balseiro, E. (2007). Production and biomass of picophytoplankton and larger autotrophs in Andean ultraoligotrophic lakes: differences in light harvesting efficiency in deep layers. *Aquat. Ecol.* 41, 511–523. doi: 10.1007/s10452-007-9125-z

Callieri, C., and Stockner, J. G. (2002). Freshwater autotrophic picoplankton: a review. *J. Limnol.* 61, 1–14.

Chen, J., Lyu, Y., Zhao, Z., Liu, H., Zhao, H., and Li, Z. (2019). Using the multidimensional synthesis methods with non-parameter test, multiple time scales analysis to assess water quality trend and its characteristics over the past 25 years in the Fuxian Lake, China. *Sci. Total Environ.* 655, 242–254. doi: 10.1016/j.scitotenv.2018.11.144

Cotner, J. B., and Biddanda, B. A. (2002). Small players, large role: microbial influence on biogeochemical processes in pelagic aquatic ecosystems. *Ecosystems* 5, 105–121. doi: 10.1007/s10021-001-0059-3

Di, C. F., Pagnanelli, F., Wijffels, R. H., and Van der Veen, D. (2017). Quantification of Acutodesmus obliquus (Chlorophyceae) cell size and lipid content heterogeneity at single cell level. *J. Phycol.* 54, 187–197. doi: 10.1111/jpy.12610

Dokulil, M. T., and Skolaut, C. (1991). Aspects of phytoplankton seasonal succession in Mondsee, Austria, with particular reference to the ecology of Dinobryon Ehrenb. *Internationale Vereinigung für Theoretische und Angewandte Limnologie: Verhandlungen* 24, 968–973. doi: 10.1080/03680770.1989.11898892

Fietz, S., Bleiß, W., Hepperle, D., Koppitz, H., Krienitz, L., and Nicklisch, A. (2010). First record of *Nannochloropsis limnetica* (Eustigmatophyceae) in the autotrophic picoplankton from Lake Baikal. *J. Phycol.* 41, 780–790. doi: 10.1111/j.0022-3646.2005.04198.x

Fogg, G. E. (1995). Some comments on picoplankton and its importance in the pelagic ecosystem. *Aquat. Microb. Ecol.* 9, 33–39. doi: 10.3354/ame009033

Hansen, L. R., Kristiansen, J., and Rasmussen, J. V. (1994). Potential toxicity of the freshwater *Chrysochromulina* species *C. parva* (Prymnesiophyceae). *Hydrobiologia* 287, 157–159. doi: 10.1007/bf00010731

Iglesias, C., Meerhoff, M., Johansson, L. S., Gonzalez-Bergonzoni, I., Mazzeo, N., Pablo Pacheco, J., et al. (2017). Stable isotope analysis confirms substantial differences between subtropical and temperate shallow lake food webs. *Hydrobiologia* 784, 111–123. doi: 10.1007/s10750-016-2861-0

Ivanikova, N. V., Popels, L. C., McKay, R. M. L., and Bullerjahn, G. S. (2007). Lake superior supports novel clusters of cyanobacterial picoplankton. *Appl. Environ. Microbiol.* 73, 4055–4065. doi: 10.1128/aem.00214-7

Jansson, M., Karlsson, J., and Jonsson, A. (2012). Carbon dioxide supersaturation promotes primary production in lakes. *Ecol. Lett.* 15, 527–532. doi: 10.1111/j.1461-0248.2012.01762.x

Komárek, J. (1996). Towards a combined approach for the taxonomy and species delimitation of picoplanktic cyanoprokaryotes. *Algol. Stud.* 83, 377–401. doi: 10.1127/algol_stud/83/1996/377

Kutovaya, O. A., McKay, R. M. L., and Bullerjahn, G. S. (2013). Detection and expression of genes for phosphorus metabolism in picocyanobacteria from the Laurentian Great Lakes. *J. Great Lakes Res.* 39, 612–621. doi: 10.1016/j.jglr.2013.09.009

Lefranc, M., Thenot, A., Lepere, U., and Debroas, D. (2005). Genetic diversity of small eukaryotes in lakes differing by their trophic status. *Appl. Environ. Microbiol.* 71, 5935–5942. doi: 10.1128/aem.71.10.5935-5942.2005

Lehman, J. T. (1976). Ecological and nutritional studies on dinobryon ehrenb.: seasonal periodicity and the phosphate toxicity problem. *Limnol. Oceanogr.* 21, 646–658. doi: 10.4319/lo.1976.21.5.0646

Legendre, P., and Gallagher, E. D. (2001). Ecologically meaningful transformations for ordination of species data. *Oecologia* 129, 271–280. doi: 10.1007/s004420100716

Lepère, C., Boucher, D., Jardillier, L., Domaizon, I., and Debroas, D. (2006). Succession and regulation factors of small eukaryote community. composition in a lacustrine ecosystem (Lake pavin). *Appl. Environ. Microbiol.* 72, 2971–2981. doi: 10.1128/aem.72.4.2971-2981.2006

Lepère, C., Masquelier, S., Mangot, J.-F., Debroas, D., and Domaizon, I. (2010). Vertical structure of small eukaryotes in three lakes that differ by their trophic status: a quantitative approach. *ISME J.* 4, 1509–1519. doi: 10.1038/ismej.2010.83

Li, S., Bronner, G., Lepère, C., Kong, F., and Shi, X. L. (2017). Temporal and spatial variations in the composition of freshwater photosynthetic picoeukaryotes revealed by MiSeq sequencing from flow cytometry sorted samples. *Environ. Microbiol.* 19, 2286–2300. doi: 10.1111/1462-2920.13724

Li, S., Shi, X., Lepère, C., Liu, M., Wang, X., and Kong, F. (2016). Unexpected predominance of photosynthetic picoeukaryotes in shallow eutrophic lakes. *J. Plankton Res.* 38, 830–842. doi: 10.1093/plankt/fbw042

Li, S., Zhou, J., Wei, L., Kong, F., and Shi, X. (2015). The effect of elevated CO2 on autotrophic picoplankton abundance and production in a eutrophic lake (Lake Taihu, China). *Mar. Freshw. Res.* 67, 3179–3190.

Mangot, J. F., Domaizon, I., Taib, N., Marouni, N., Duffaud, E., Bronner, G., et al. (2013). Short-term dynamics of diversity patterns: evidence of continual reassembly within lacustrine small eukaryotes. *Environ. Microbiol.* 15, 1745–1758. doi: 10.1111/1462-2920.12065

Marie, D., Shi, X. L., Rigaut-Jalabert, F., and Vaulot, D. (2010). Use of flow cytometric sorting to better assess the diversity of small photosynthetic eukaryotes in the English channel. *FEMS Microbiol. Ecol.* 72, 165–178. doi: 10.1111/j.1574-6941.2010.00842.x

Mózes, A., Présing, M., and Vörös, L. (2006). Seasonal dynamics of picocyanobacteria and picoeukaryotes in a large shallow lake (Lake Balaton, Hungary). *Int. Rev. Hydrobiol.* 91, 38–50. doi: 10.1002/iroh.200510844

Parke, M., Lund, J. W. G., and Manton, I. (1962). Observations on the biology and fine structure of the type species of *Chrysochromulina* (*C. parva* Lackey) in the English Lake District. *Arch. Mikrobiol.* 42, 333–352. doi: 10.1007/bf00409070

Petersen, R. (1991). Carbon-14 uptake by picoplankton and total phytoplankton in Eight New Zealand Lakes. *Int. Rev. Hydrobiol.* 76, 631–641. doi: 10.1002/iroh.19910760413

Queimaliños, C. (2002). The role of phytoplanktonic size fractions in the microbial food webs in two north Patagonian lakes (Argentina). *Internationale Vereinigung für theoretische und angewandte Limnologie: Verhandlungen* 28, 1236–1240. doi: 10.1080/03680770.2001.11902651

Raven, J. A. (1998). The twelfth tansley lecture. small is beautiful: the picophytoplankton. *Funct. Ecol.* 12, 503–513. doi: 10.1046/j.1365-2435.1998.00233.x

Reynolds, C. S., Padisák, J., and Kóbor, I. (1993). A localized bloom of *Dinobryon sociale* in Lake Balaton: some implications for the perception of patchiness and the maintenance of species richness. *Abstracta Bot.* 17, 251–260.

Sanders, R. W., Berninger, U. G., Lim, E. L., Kemp, P. F., and Caron, D. A. (2000). Heterotrophic and mixotrophic nanoplankton predation on picoplankton in the Sargasso Sea and on Georges Bank. *Mar. Ecol. Prog.* 192, 103–118. doi: 10.3354/meps192103

Sarmento, H., Unrein, F., Isumbisho, M., Stenuite, S., Gasol, J. M., and Descy, J. P. (2008). Abundance and distribution of picoplankton in tropical, oligotrophic Lake Kivu, eastern Africa. *Freshw. Biol.* 53, 756–771. doi: 10.1111/j.1365-2427.2007.01939.x

Shi, X., Li, S., Fan, F., Zhang, M., Yang, Z., and Yang, Y. (2019). Mychonastes dominates the photosynthetic picoeukaryotes in Lake Poyang, a river-connected lake. *FEMS Microbiol. Ecol.* 95:fiy211. doi: 10.1093/femsec/fiy211

Shi, X., Li, S., Liu, C., Zhang, M., and Liu, M. (2018). Community structure of photosynthetic picoeukaryotes differs in lakes with different trophic statuses along the middle-lower reaches of the Yangtze River. *FEMS Microbiol. Ecol.* 94:fiy011. doi: 10.1093/femsec/fiy011

Shi, X. L., Marie, D., Jardillier, L., Scanlan, D. J., and Vaulot, D. (2009). Groups without cultured representatives dominate eukaryotic picophytoplankton in the oligotrophic South East Pacific Ocean. *PLoS One* 4:e7657. doi: 10.1371/journal.pone.0007657

Somogyi, B., Felföldi, T., Katalin, V.-B., Boros, E., Pálffy, K., and Vörös, L. (2016). The role and composition of winter picoeukaryotic assemblages in shallow Central European great lakes. *J. Great Lakes Res.* 42, 1420–1431. doi: 10.1016/j.jglr.2016.10.003

Sterner, R. W. (2010). In situ-measured primary production in Lake Superior. *J. Great Lakes Res.* 36, 139–149. doi: 10.1016/j.jglr.2009.12.007

Stockner, J., Callieri, C., and Cronberg, G. (2000). "Picoplankton and other non-bloom-forming cyanobacteria in lakes," in *The Ecology of Cyanobacteria*, eds B. A. Whitton, and M. Potts, (Dordrecht: Kluwer Academic Publishers), 195–231. doi: 10.1007/0-306-46855-7_7

Stockner, J. G. (1991). Autotrophic picoplankton in freshwater ecosystems: the view from the summit. *Internationale Revue der gesamten Hydrobiologie und Hydrographie* 76, 483–492. doi: 10.1002/iroh.19910760402

Stockner, J. G., and Shortreed, K. S. (1989). Algal picoplankton production and contribution to food-webs in oligotrophic British Columbia lakes. *Hydrobiologia* 173, 151–166. doi: 10.1007/bf00015525

Suttle, C. A., and Harrison, P. J. (1988). Ammonium and phosphate uptake kinetics of size-fractionated plankton from an oligotrophic freshwater lake. *J. Plankton Res.* 418, 343–346.

Suttle, C. A., Stockner, J. G., Shortreed, K. S., and Harrison, P. J. (1988). Time-courses of size-fractionated phosphate uptake: are larger cells better competitors for pulses of phosphate than smaller cells? *Oecologia* 74, 571–576. doi: 10.1007/BF00380055

Tolotti, M., Thies, H., and Cantonati, M. (2003). Flagellate algae (Chrysophyceae, Dinophyceae, Cryptophyceae) in 48 high mountain lakes of the Northern and Southern slope of the Eastern Alps: biodiversity, taxa distribution and their driving variables. *Hydrobiologia* 502, 331–348. doi: 10.1007/978-94-017-2666-5_27

Urbach, E., Scanlan, D. J., Distel, D. L., Waterbury, J. B., and Chisholm, S. W. (1998). Rapid diversification of marine picophytoplankton with dissimilar light-harvesting structures inferred from sequences of *Prochlorococcus* and *Synechococcus* (Cyanobacteria). *J. Mol. Evol.* 46, 188–201. doi: 10.1007/pl00006294

Vörös, L., Callieri, C., Balogh, K. V., and Bertoni, R. (1998). Freshwater picocyanobacteria along a trophic gradient and light quality range. *Hydrobiologia* 370, 117–125. doi: 10.1007/978-94-017-2668-9_10

Weisse, T. (1988). Dynamics of autotrophic picoplankton in lake constance. *J. Plankton Res.* 10, 1179–1188. doi: 10.1093/plankt/10.6.1179

Weisse, T., and Kenter, U. (1991). Ecological characteristics of autotrophic picoplankton in a prealpine lake. *Int. Rev. Hydrobiol.* 76, 493–504. doi: 10.1002/iroh.19910760403

Winder, M. (2009). Photosynthetic picoplankton dynamics in Lake Tahoe: temporal and spatial niche partitioning among prokaryotic and eukaryotic cells. *J. Plankton Res.* 31, 1307–1320. doi: 10.1093/plankt/fbp074

Yan, R., Kong, F., and Han, X. (2004). Analysis of the recruitment of the winter survival algae on the sediments of Lake Taihu by fluorometry. *J. Lake Sci.* 16, 164–169. doi: 10.18307/2004.0210

Zhang, H., Feng, J., Chen, S., Zhao, Z., Li, B., Wang, Y., et al. (2019). Geographical patterns of nirS gene abundance and nirS-type denitrifying bacterial community associated with activated sludge from different wastewater treatment plants. *Microb. Ecol.* 77, 304–316. doi: 10.1007/s00248-018-1236-7

Conflict of Interest Statement: The authors declare that the research was conducted in the absence of any commercial or financial relationships that could be construed as a potential conflict of interest.

Copyright © 2019 Shi, Li, Li, Chen and Wu. This is an open-access article distributed under the terms of the Creative Commons Attribution License (CC BY). The use, distribution or reproduction in other forums is permitted, provided the original author(s) and the copyright owner(s) are credited and that the original publication in this journal is cited, in accordance with accepted academic practice. No use, distribution or reproduction is permitted which does not comply with these terms.

frontiers in Microbiology

ORIGINAL RESEARCH
published: 10 September 2019
doi: 10.3389/fmicb.2019.02081

Metatranscriptomic Analyses of Diel Metabolic Functions During a *Microcystis* Bloom in Western Lake Erie (United States)

Emily J. Davenport[1,2†], Michelle J. Neudeck[1†], Paul G. Matson[1], George S. Bullerjahn[1], Timothy W. Davis[1], Steven W. Wilhelm[3], Maddie K. Denney[4], Lauren E. Krausfeldt[3], Joshua M. A. Stough[3], Kevin A. Meyer[2,5], Gregory J. Dick[5], Thomas H. Johengen[2], Erika Lindquist[6], Susannah G. Tringe[6] and Robert Michael L. McKay[1,7]*

[1] Department of Biological Sciences, Bowling Green State University, Bowling Green, OH, United States, [2] Cooperative Institute for Great Lakes Research (CIGLR), University of Michigan, Ann Arbor, MI, United States, [3] Department of Microbiology, The University of Tennessee, Knoxville, Knoxville, TN, United States, [4] Graduate School of Genome Science and Technology, The University of Tennessee, Knoxville, Knoxville, TN, United States, [5] Department of Earth and Environmental Sciences, University of Michigan, Ann Arbor, MI, United States, [6] U.S. Department of Energy Joint Genome Institute, Walnut Creek, CA, United States, [7] Great Lakes Institute for Environmental Research, University of Windsor, Windsor, ON, Canada

OPEN ACCESS

Edited by:
Petra M. Visser,
University of Amsterdam, Netherlands

Reviewed by:
Maureen Coleman,
The University of Chicago, United States
Chenlin Hu,
University of Houston, United States

***Correspondence:**
George S. Bullerjahn
bullerj@bgsu.edu

[†] These authors have contributed equally to this work

Specialty section:
This article was submitted to Aquatic Microbiology, a section of the journal Frontiers in Microbiology

Received: 16 April 2019
Accepted: 23 August 2019
Published: 10 September 2019

Citation:
Davenport EJ, Neudeck MJ, Matson PG, Bullerjahn GS, Davis TW, Wilhelm SW, Denney MK, Krausfeldt LE, Stough JMA, Meyer KA, Dick GJ, Johengen TH, Lindquist E, Tringe SG and McKay RML (2019) Metatranscriptomic Analyses of Diel Metabolic Functions During a Microcystis Bloom in Western Lake Erie (United States). Front. Microbiol. 10:2081. doi: 10.3389/fmicb.2019.02081

This study examined diel shifts in metabolic functions of *Microcystis* spp. during a 48-h Lagrangian survey of a toxin-producing cyanobacterial bloom in western Lake Erie in the aftermath of the 2014 Toledo Water Crisis. Transcripts mapped to the genomes of recently sequenced lower Great Lakes *Microcystis* isolates showed distinct patterns of gene expression between samples collected across day (10:00 h, 16:00 h) and night (22:00 h, 04:00 h). Daytime transcripts were enriched in functions related to Photosystem II (e.g., *psbA*), nitrogen and phosphate acquisition, cell division (*ftsHZ*), heat shock response (*dnaK*, *groEL*), and uptake of inorganic carbon (*rbc*, *bicA*). Genes transcribed during nighttime included those involved in phycobilisome protein synthesis and Photosystem I core subunits. Hierarchical clustering and principal component analysis (PCA) showed a tightly clustered group of nighttime expressed genes, whereas daytime transcripts were separated from each other over the 48-h duration. Lack of uniform clustering within the daytime transcripts suggested that the partitioning of gene expression in *Microcystis* is dependent on both circadian regulation and physicochemical changes within the environment.

Keywords: *Microcystis*, metatranscriptomics, microcystin, cyanobacterial blooms, Lake Erie

INTRODUCTION

Cyanobacterial harmful algal blooms (cHABs), dominated primarily by *Microcystis*, have recurred annually in the open waters of western Lake Erie since the mid-1990s (Brittain et al., 2000; Steffen M.M. et al., 2014) with blooms increasing in severity and duration over the past decade (Michalak et al., 2013; Bullerjahn et al., 2016). Within a bloom, a subset of strains of *Microcystis* spp. are capable of producing microcystins, which are known hepatotoxins and potential tumor promoters

(Falconer, 1994; Fan et al., 2014). Consequently, within the western Lake Erie watershed, cHABs result in increased costs for water treatment and are responsible for economic declines related to tourism, property values, and recreational fisheries (Bingham et al., 2015; Wolf and Klaiber, 2017).

Microcystis spp. can dominate late summer phytoplankton communities due to a variety of adaptive strategies. Cells over-winter in the sediments where they can be recruited to surface waters during the summer as light availability and temperatures increase (Brunberg and Blomqvist, 2003; Rinta-Kanto et al., 2009; Kitchens et al., 2018). *Microcystis* can also promote and tolerate the formation of pH extremes that preclude the growth of competing eukaryotes (Krausfeldt et al., 2019). Buoyancy resulting from gas vesicles allows cells to control their position in the water column, thus shaping light and nutrient availability (Reynolds et al., 1987; Brookes and Ganf, 2001). The genomic architecture of *Microcystis aeruginosa* is thought to be "plastic" due to horizontal gene transfer as well as the activity of transposases and restriction modification enzymes encoded within its genome (Kaneko et al., 2007; Frangeul et al., 2008; Steffen M. et al., 2014; Meyer et al., 2017). These functions are presumed to generate genetic diversity within the cyanobacterial population via deletion, duplication and/or acquisition of genes from the endemic community into the genome. Together, these mechanisms offer adaptive strategies to maintain competitive dominance (Humbert et al., 2013). *Microcystis* spp. also possess a variety of genes and pathways to compete for light and nutrients, including uptake systems for various nitrogen and carbon species (Valladares et al., 2002; Badger and Price, 2003). Increasing temperatures are also favorable for growth of *M. aeruginosa*, whose optimum growth temperature (>25°C) is typically higher than that of other phytoplankton species (Reynolds, 2006; Jöhnk et al., 2008). In many lakes, increasing temperatures consistent with climate change will likely strengthen vertical stratification thereby reducing mixing and allowing phytoplankton growth at the surface to remain undisturbed, promoting formation of surface blooms (Huisman and Hulot, 2005; Paerl and Huisman, 2008).

A critical adaptation of bloom-forming phytoplankton is the regulation of processes according to diel light availability. Circadian oscillators are genetic regulators of expression operating at a period of about 24 h. The circadian "clock" functions as a regulator that anticipates daily environmental changes that can shape cell metabolism. Circadian rhythms function as a constant, entrained by cycles of light/dark, independent of temperature effects (Bünning, 1973; Pittendrigh, 1981; Johnson and Hastings, 1986; Sweeney, 2013). These functions were initially observed in eukaryotes and thought to occur only within *Eukarya* (Konopka and Benzer, 1971), until their discovery in cyanobacteria (Kondo et al., 1993; Lorne et al., 2000). The *kaiABC* gene cluster and its physiological outputs within cyanobacteria have been shown to specifically control the rhythmicity of cell functions (Ishiura et al., 1998; reviewed in Welkie et al., 2019). The photosynthetic nature of cyanobacteria presumes the circadian pacemaker will initiate expression of some genes to anticipate dawn to maximize daytime functions such as photosynthetic light harvesting. Other physiological functions have been shown to yield maximum expression at subjective midday (Kucho et al., 2005). The cyanobacteria clock controls global gene expression by regulating the activity of all promoters (Liu et al., 1995; Xu et al., 2003; Labiosa et al., 2006).

Multiple cellular functions within cyanobacteria are coupled to circadian rhythms, including nutrient acquisition and assimilation, amino acid uptake, respiration, carbohydrate synthesis, replication, and cell division (Chen et al., 1991; Kramer et al., 1996; Golden et al., 1997; Ishiura et al., 1998). While fluctuating environmental conditions (light, temperature, pH, nutrient availability) may invoke stress responses, it is important to understand the mechanisms and range of circadian control that may mask or overlay expression resulting from transient stress. Indeed, patterns of gene expression under changing conditions of light, temperature and nutrient starvation are distinct from those under global circadian control. With respect to cHAB events, it is important to differentiate these two patterns (Labiosa et al., 2006; Penn et al., 2014). Additionally, diel patterns of expression can exist in cyanobacteria in the absence of a circadian clock (Holtzendorff et al., 2008). Whereas this study alone cannot sort out what functions are regulated by KaiABC, this work, along with future studies, can begin to understand the interplay of environmental cues and the circadian pacemaker.

This study queried expression of key metabolic functions to understand the ecophysiology of a *Microcystis* spp. bloom over the course of diel cycles. Specifically, a metatranscriptomic approach was undertaken to study temporal changes in the metabolic functions of an August 2014 *Microcystis* spp.-dominated bloom. Just 3 weeks prior, this event resulted in a "do not drink" order issued for Toledo, OH due to detection of microcystins in the finished water supply above the 1 $\mu g\ L^{-1}$ World Health Organization (WHO) drinking water advisory (Bullerjahn et al., 2016; Steffen et al., 2017). Metatranscriptome analyses paired with environmental metadata provided insight into factors related to bloom success and toxicity, along with a better understanding of bloom metabolism throughout the day and night, particularly with regard to photosynthesis, nutrient assimilation and microcystin production. Overall, this information can help inform the development of new strategies toward prediction of bloom toxigenicity and mitigation of bloom events.

MATERIALS AND METHODS

Sample Collection

A 48-h Lagrangian survey of the 2014 *Microcystis* bloom was conducted in western Lake Erie in late August 2014. Our study was designed to track the bloom over diel cycles using a drifter with GPS capabilities deployed near the Toledo water intake. Over the course of the survey, the drifter moved roughly 2 km through water depths varying from 10–15 m (**Figure 1**). Samples were collected at 6-h intervals beginning on August 26, at 22:00 h, producing two sets of triplicate samples from 22:00 h (samples 1S, 5S), one set of triplicates at 04:00 h (2S), and two sets of triplicates at 10:00 h (3S, 6S), and 16:00 h (4S, 7S). A sample for 04:00 h over the second diel cycle was not

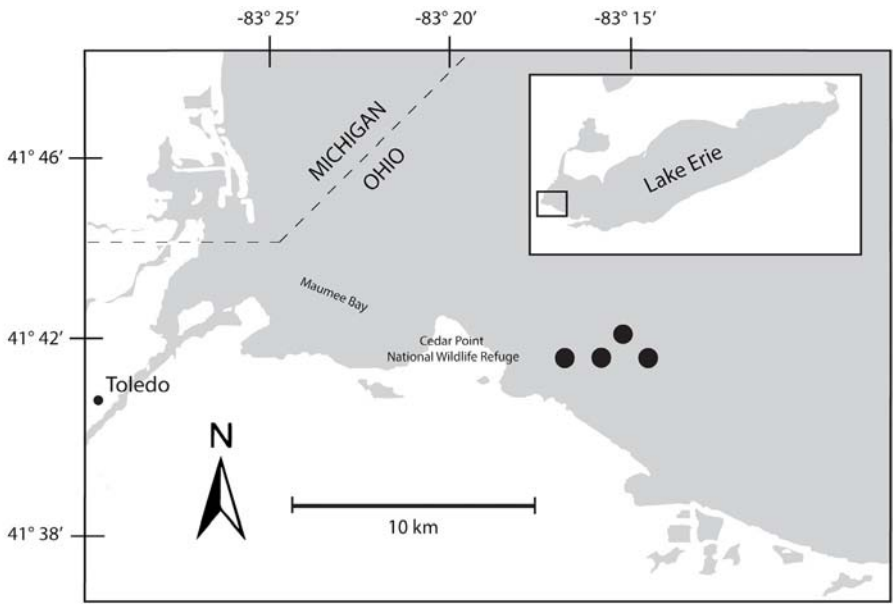

FIGURE 1 | Map of Maumee Bay, western basin of Lake Erie indicating movements of bloom during 48-h survey. The seven sampling events were mapped to the four sites indicated on the map.

collected due to adverse weather that precluded sampling. At each sampling time point, triplicate water samples for chlorophyll and nutrients were collected adjacent to the drifter by hand casting a Niskin bottle to a depth of 1 m. Biomass from each water sample was collected onto Sterivex cartridge filters (0.22 μm; EMD Millipore, Billerica, MA, United States) using a peristaltic pump. Filters were immediately stored in liquid nitrogen upon field collection followed by transfer to −80°C until RNA extraction.

Physico-Chemical Measurements

Chlorophyll-*a* (chl *a*) biomass was measured by concentrating lake water on a glass fiber filter (GF/F, 47 mm diameter, Whatman, Maidstone, United Kingdom) at low vacuum pressure under low light conditions and stored at −20°C until extraction. Samples were extracted with N, N-dimethylformamide and analyzed by fluorescence with a 10AU fluorometer (Turner Designs, Sunnyvale, CA, United States; Speziale et al., 1984).

Phycocyanin concentrations were measured by concentrating lake seston on a glass fiber filter (GF/F, 47 mm diameter, Whatman). Sodium phosphate buffer (pH 6.8; Ricca Chemical, Batesville, IN, United States) was added to the filter and phycocyanin was extracted using two freeze-thaw cycles followed by sonication. Relative fluorescence was measured using a Turner AquaFluor (Sunnyvale, CA, United States) and converted to phycocyanin concentration using a series of dilutions of a commercial standard (Sigma-Aldrich, St. Louis, MO, United States; Horváth et al., 2013). For total phosphorus (TP), duplicate 50 mL aliquots of whole lake water were collected into acid-washed glass culture tubes and stored at 4°C until analysis within 1 week. For dissolved nutrients, duplicate whole water samples were collected in a triple rinsed (ultrapure water) 20 mL syringe and filtered through 0.22 μm nominal pore-size nylon filters into 15 mL collection tubes that were stored at −20°C until analysis. Dissolved inorganic nitrogen (DIN) and phosphate concentrations were determined using standard automated colorimetric procedures as modified by Davis and Simmons (1979) on a QuAAtro Continuous Flow Analyzer (SEAL Analytical, Inc., Mequon, WI, United States) according to methods detailed by the manufacturer and in compliance with United States. EPA Methods 365.4, 350.1, and 353.1. TP and total dissolved phosphorus (TDP) used the same analysis following a persulfate digestion adapted from Menzel and Corwin (1965). Particulate microcystins were measured by filtering whole lake water onto a 3-μm pore-size polycarbonate membrane and kept at −20°C until analysis. Particulate microcystins were extracted from samples using a combination of physical and chemical lysis techniques. All samples were resuspended in 1 mL molecular grade water (pH 7; Sigma-Aldrich) and subjected to three freeze-thaw cycles before the addition of the QuikLyse reagents (Abraxis LLC, Warminster, PA, United States) per the manufacturer's instructions. The samples were then centrifuged for 5 min at 2×10^3 *g* to pellet cellular debris. The concentrations of microcystins (reported as microcystin-LR equivalents) were measured using a microcystin enzyme-linked immunosorbent assay (Abraxis LLC) following methods standardized by the manufacturer (Fischer et al., 2001). This assay is congener-independent and detects the ADDA moiety, a shared moiety among microcystins. The detection limit of the assay was 0.04 μg L^{-1}.

Nucleic Acid Extraction and Sequencing

RNA was extracted from a single Sterivex cartridge from each sampling time using the PowerWater DNA Isolation Kit

for Sterivex (Qiagen, Carlsbad, CA, United States), modified for RNA using manufacturer's protocols. To improve RNA yield, Sterivex®cartridges were vortexed for 5 min longer than recommended each time and all wash buffers were allowed to sit for 1 min before vacuum extraction through the binding column. DNase treatment was performed as recommended in the protocol using the On-Spin Column DNase kit (QIAGEN). This protocol was optimized by allowing the DNase solution to sit for an extra 15 min than recommended. RNA was checked for DNA contamination by PCR with universal 16S primers (27F and 1522R). Any additional DNase treatments required were performed using the Turbo DNase kit (Ambion, Austin, TX, United States). rRNA was removed from 1 μg of total RNA using Ribo-Zero rRNA Removal Kit (Epicenter, Madison, WI, United States). Stranded cDNA libraries were generated using the TruSeq Stranded Total RNA LT kit (Illumina, Inc., San Diego, CA, United States). The rRNA depleted RNA was fragmented and reversed transcribed using random hexamers and Superscript II reverse transcriptase (Invitrogen, Carlsbad, CA, United States) followed by second strand synthesis. The fragmented cDNA was treated with end-pair, A-tailing, adapter ligation, and eight cycles of PCR. The prepared libraries were quantified using a KAPA Library Quantification kit (Kapa Biosystems, Wilmington, MA, United States) and run on a LightCycler 480 real-time PCR instrument (Roche Diagnostics Corp., Indianapolis, IN, United States). The quantified libraries were then multiplexed with other libraries, and the pool of libraries was then prepared for sequencing on the Illumina HiSeq sequencing platform utilizing a HiSeq Cluster kit, v4 (Illumina^{TM}), and Illumina's cBot instrument to generate a clustered flow cell for sequencing. Sequencing of the flow cell was performed on the Illumina HiSeq2500 sequencer using a TruSeq SBS sequencing kit, v4, following a 2 × 150 indexed run recipe (Mavromatis et al., 2009). Metatranscriptomes obtained were accessed and downloaded through the Integrated Microbial Genomes platform (IMG) developed by U.S. DOE Joint Genome Institute (JGI) (Markowitz et al., 2012, 2014) and the JGI genome portals (Nordberg et al., 2014). Raw unassembled metagenomic sequence data were uploaded to the online server MG-RAST (Meyer et al., 2008) for assembly attribute data, phylogenetic, and functional analysis.

Bioinformatics and Statistical Analysis

Analyses and visualization of data were performed using CLC Genomics Workbench v 12.0.2 (Qiagen CLC Bio). Sequences were imported utilizing the Illumina High-Throughput Sequencing Import function. Low-quality reads and failed reads were automatically removed. The reads were trimmed with a quality limit of 0.05 and an ambiguous base limit of 2. Automatic read-through adapter trimming was performed. RNA-Seq Analysis was performed using the raw reads of the seven diel transcriptomes against the following genomes: *M. aeruginosa* LE3 from Lake Erie (Brittain et al., 2000; Meyer et al., 2017), *Synechococcus elongatus* PCC 6301, *Sulfurimonas denitrificans* DSM 1251, *Desulfovibrio magneticus* RS-1, *Anabaena cylindrica* PCC 7122, *Aphanizomenon flos-aquae* NIES-81, *Klebsiella pneumoniae* 1158, and *Burkholderia pseudomallei* K96243, and an annotated genome of *Planktothrix agardhii* from Lake Erie obtained from Greg Dick at the University of Michigan. RNASeq parameters were: one reference sequence per transcript, mismatch cost of 2, insertion cost of 3, deletion cost of 3, length fraction of 0.8, similarity fraction of 0.8. Data output of expression values were calculated as Transcripts Per Million mapped reads (TPM) through RNA-Seq function to normalize within each sample and manually normalized across all samples with a ratio to the housekeeping gene *gyrB* TPM.

Principal Component Analysis (PCA) was performed using the CLC Genomics Workbench (Qiagen CLC Bio) to assess relationships between diel samples with regards to expression. TPM gene expression plots were created in R 3.5.1 (R Core Team, 2018) using the packages tidyr 0.8.2 (Wickham and Henry, 2018) and ggplot2 v3.1.0 (Wickham, 2016). Raw sequences are available from the NCBI sequence read archive under SRP117911, SRP117914, SRP117915, SRP117922, SRP128942, SRP128945, and SRP128954.

RESULTS

Survey Physico-Chemical Properties

The bloom tracked a southwesterly course traveling nearly 2 km over the 48-h survey in late August (**Figure 1**). Whereas winds originated from S/SW leading up to buoy deployment and initial bloom tracking, wind direction switched in the early morning of August 27 and remained E/NE with daily averages of 5–6 knots for the remainder of the survey (weather data from KPCW: Erie-Ottawa International Airport; KTDZ: Toledo Executive Airport). Western Lake Erie is shallow (Z_{mean} = 7.4 m) and characterized as polymictic. Whereas buoyancy afforded by gas vesicles helped to maintain *Microcystis* colonies near the surface, wind gusts up to nine knots over the course of the survey likely promoted mixing as was predicted using a Lagrangian particle tracking model (Rowe et al., 2016) applied to the same geographic area preceding the early August 2014 cHAB at the Toledo water intake (Steffen et al., 2017). Increases in chl *a* biomass of 75% and more than a doubling of phycocyanin (PC) indicated that cyanobacterial biomass was increasing over the survey (**Figure 2**). Molar ratios of dissolved inorganic nitrogen to dissolved inorganic phosphorus (DIN:DIP) showed only minor variation around Redfield stoichiometry (N:P = 16:1; dashed line) during the first 18 h of sampling (**Figure 2**). The system then shifted to P-deficiency (N:P ∼ 40–60) during day 2 of the survey. Particulate microcystins, were initially between 1 and 2 μg L^{-1}, but reached as high as 5 μg L^{-1} toward the end of the survey (**Figure 2**). Archived weather reports from KPCW and KTDZ confirmed skies to be clear leading up to the start of the survey and switching to variable cloud cover during the morning hours of day 2[1]. Irradiance both days were similar (**Supplementary Figure S1**), yielding maximum PAR at the nearby Toledo intake crib of 1542 μmol quanta

[1]https://flightaware.com/live/airport/KPCW/weather

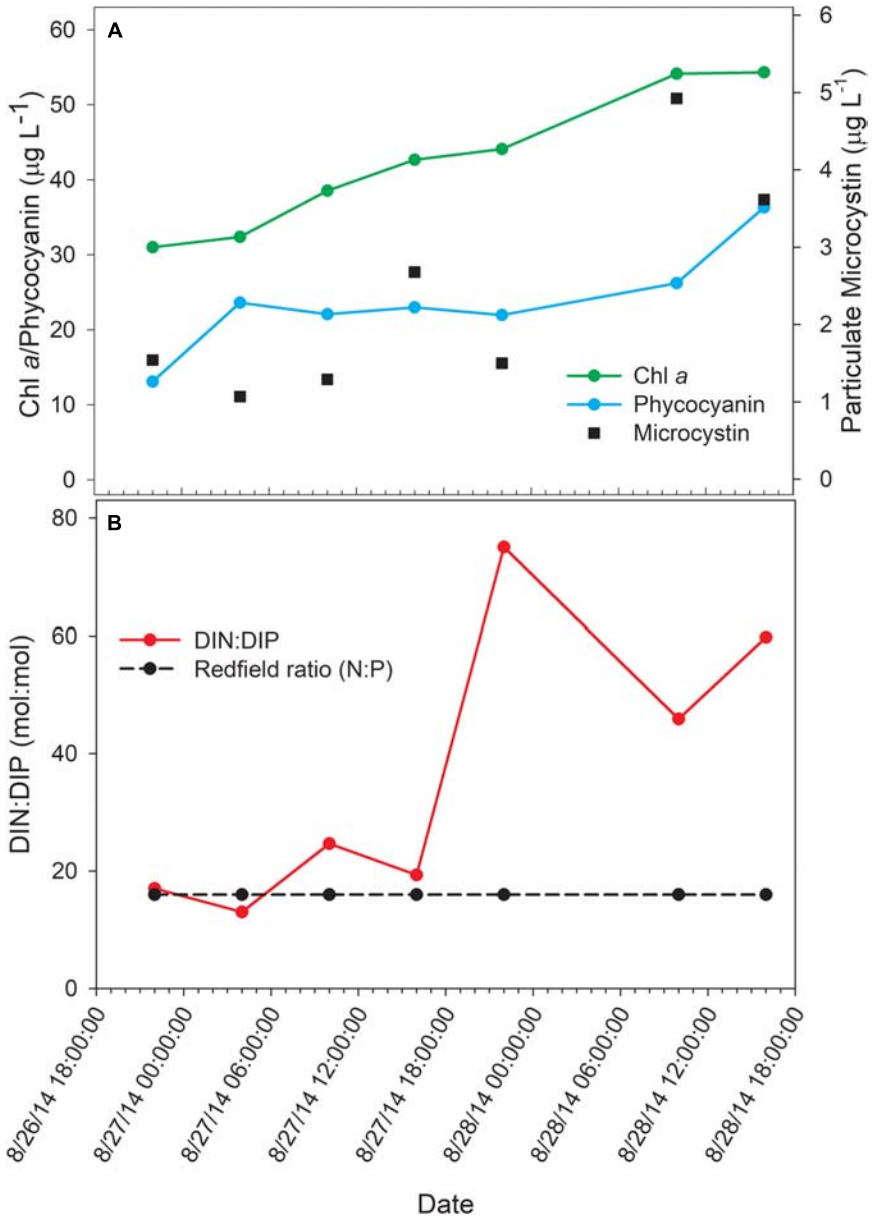

FIGURE 2 | Physico-chemical water data over the course of the 48-h Lagrangian study. **(A)** Photopigment and microcystin toxin concentrations; **(B)** dissolved inorganic nitrogen and phosphorus ratios.

$m^{-2}s^{-1}$ on August 27 and 1573 μmol quanta $m^{-2}s^{-1}$ on August 28[2].

Phylogenetic Classification of Transcripts

Seven metatranscriptomes were produced from the Western Lake Erie water samples (1.97 Gbp assembled) with read counts ranging from 109,124 to 570,660 per sample. rRNA accounted for ∼1% of the assembled metatranscriptomes. Fifty seven percent of the mRNA was annotated as encoding known proteins, the remaining ∼40% encoded unknown proteins. Of the predicted proteins, ∼70% were assigned to functional categories. Less than 5% of reads (per transcriptome) failed quality control tests.

Taxonomic analysis derived from MG-RAST showed reads dominated by *Bacteria* (∼70% of all reads) and *Eukaryota* (∼30%). *Archaea* and viral reads represented <1% of all transcripts. Of the *Bacteria* reads, *Cyanobacteria* (22–35%), *Proteobacteria* (16–37%), and *Bacteroidetes* (17–40%) were prominently represented in each metatranscriptome (**Figure 3**). The *Bacteroidetes* were dominated by the classes *Cytophagia* (∼30% of *Bacteroidetes* reads), *Flavobacteria* (∼30%), and *Sphingobacteria* (∼25%), whereas β-*Proteobacteria* were the

[2]http://lees.geo.msu.edu/research/sensor_net.html

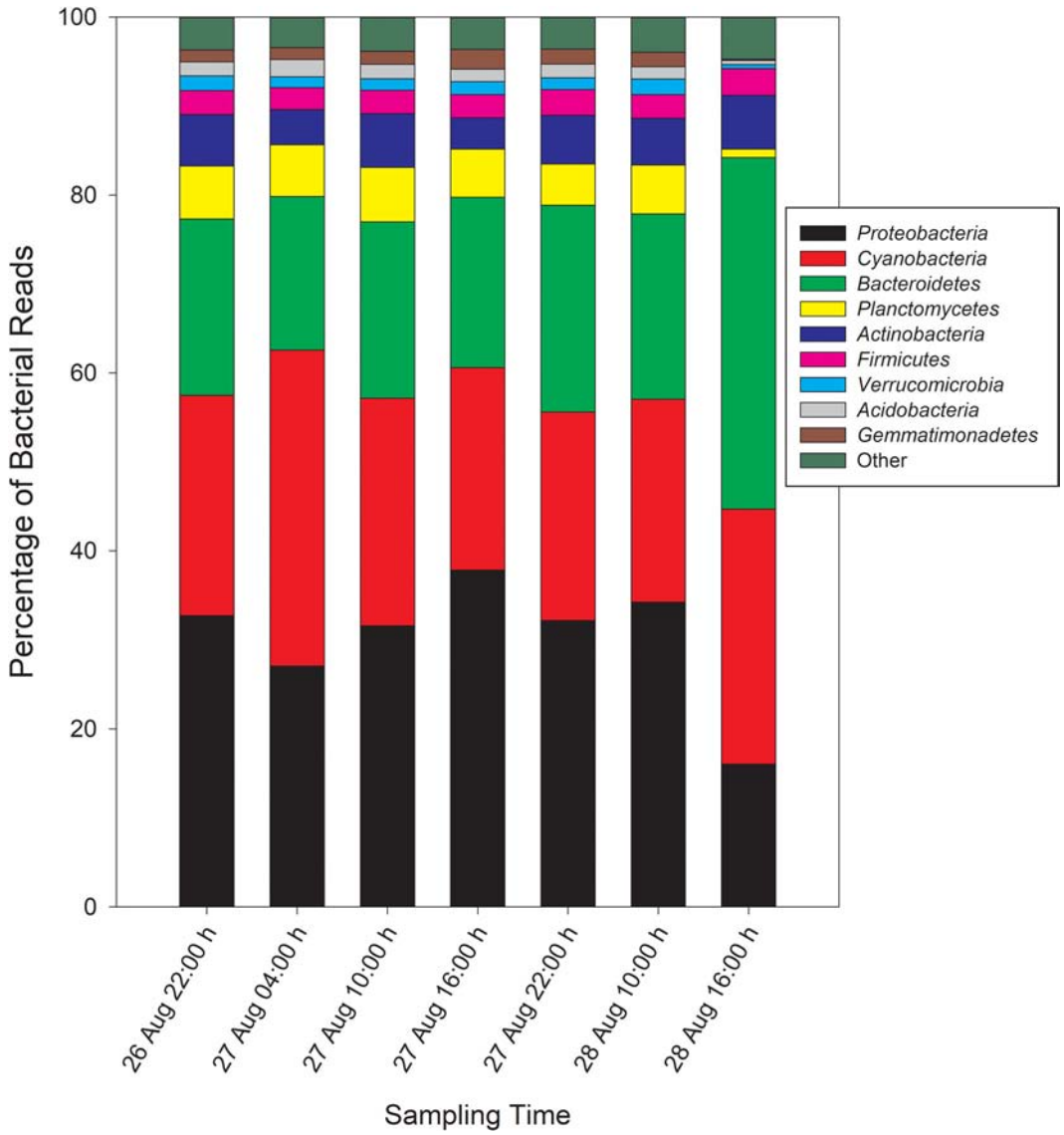

FIGURE 3 | Phylogenetic breakdown of transcripts over the course of the 48-h sampling period – community composition by phyla. "Other" refers to bacterial reads that could not be unambiguously assigned to a phylum.

most abundant proteobacterial reads (∼40%) followed by α-*Proteobacteria* (∼30%), γ-*Proteobacteria* (∼15%), and δ-*Proteobacteria* (**Figure 4**). Of the *Cyanobacteria*, ∼65% were order *Chroococcales*. *Microcystis* was the dominant genus, contributing half of the *Chroococcales* population. Classes *Nostocales* and *Oscillatoriales* contributed one-third of the *Cyanobacteria*, namely genera *Nostoc* and *Dolichospermum* within the *Nostocales*.

Differential Relative Abundance of *Microcystis* spp. Transcripts

The microcystin toxin-producing *Microcystis* LE3 genome isolated from Lake Erie was recruited to annotate metatranscriptomes to increase transcript coverage compared to publicly available *Microcystis* genomes currently available in the National Center for Biotechnology Information (GenBank assembly accession numbers GCA_000010625.1, GCA_000981785.2, GCA_001704955.2, GCA_002095975.1). PCA of differential expression and transcript abundance partitioned the seven transcriptomes into two general day and night groups (**Figure 5**). Variability within the day and night sample groups likely reflect day-to-day and hour-by-hour changes in nutrient and light availability, resulting in changes in gene expression patterns.

Highly Transcribed Genes

Supplementary Table S1 summarizes the most transcripts at each time point. In all samples, tmRNA transcripts were uniformly

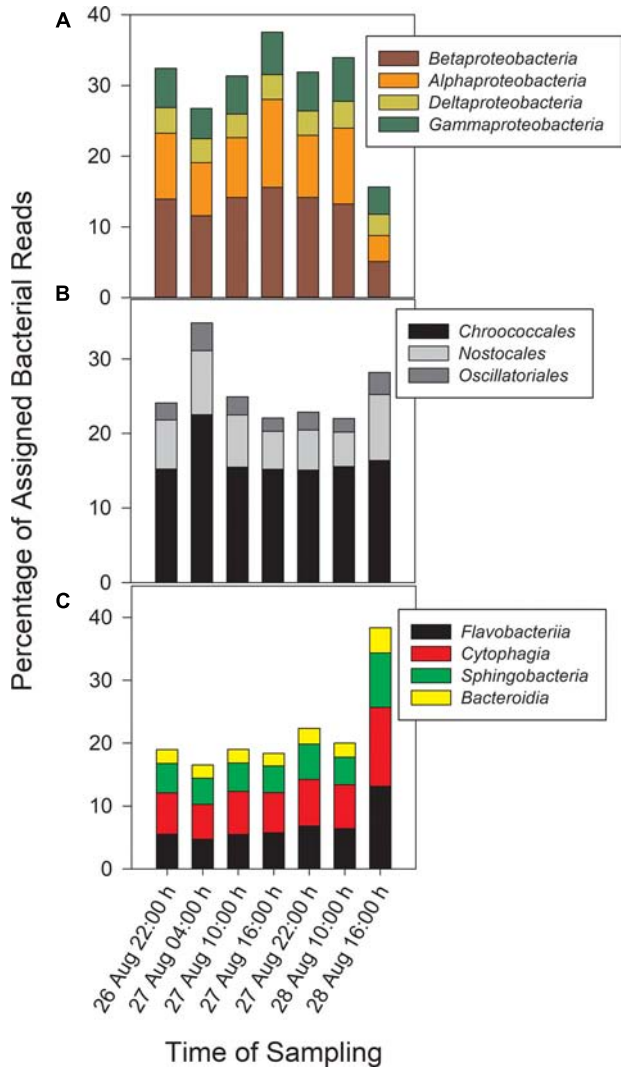

FIGURE 4 | Abundances of *Proteobacteria* **(A)** and *Cyanobacteria* **(B)** reads by order and *Bacteroidetes* reads **(C)** by class.

the most abundant, indicating active mechanisms were in place ensuring translational fidelity (Takada et al., 2002). Whereas many of the highly transcribed genes encoded gene products of unknown function, gas vesicle genes (*gvp*) were highly transcribed at all time points, and high light inducible (*hli*) and *psbA* transcripts were abundant by day, reflecting their role in Photoprotection, turnover and repair of Photosystem II (Kulkarni and Golden, 1994; Hutin et al., 2003). Genes encoding Hsp20 were highly transcribed by day and phycobilisome transcripts (*cpcAB*) were abundant in night samples.

Photosynthesis – Light Reactions

Gene transcripts associated with antenna function, Photosystems I and II (PSI, PSII) and the cytochrome b_6/f complex were assessed and revealed that relative abundance of phycobilisome (*cpc, apc*) and PSI (*psaA-L*) transcripts compared to *gyrB* increased primarily at night (**Figures 6A,B,E**). Conversely, PSII (*psb*), b_6/f complex (*petA-D*), ferredoxin and plastocyanin (*petEFH*) transcript abundance increased by day, yielding maximum relative abundance at 10:00 h (**Figures 6C,D,F**). *psbA*, encoding the PSII D1 protein, was analyzed separately due to its very high relative daytime expression due to high rates of DI protein turnover (**Supplementary Table S1**), and *psbA* expression matched the daytime pattern of other PSII-associated genes.

Photosynthesis – Ci Assimilation

Genes associated with Rubisco (*rbcLSX*) showed higher relative transcript abundance at night (04:00 h) during the first day of sampling and a pronounced minimum by the next afternoon (16:00 h), but during Day 2, the pattern was less distinct, as relative transcript abundance proceeded throughout the daytime hours (**Figure 7**). *bicA* transcripts were detected at low levels during the day, but with an inconsistent pattern from Day 1 to Day 2 that may reflect variation in bicarbonate availability.

Nutrient Acquisition

In general, transcription of nutrient acquisition functions was more active during the daytime hours. Genes encoding functions associated with N acquisition and N-responsive gene regulation yielded different patterns of transcript abundance. Whereas transcripts associated with the GS-GOGAT pathway and ammonium uptake (*amt, glnAN, glsE, gltBD, icd*) had a peak relative abundance in the afternoon (16:00 h), urea transporters and urease showed a more variable pattern and comparatively low relative expression throughout the two day period (**Figures 8A,C,E**). Relative transcript abundance for genes encoding nitrate and nitrite reduction also followed a daytime pattern, peaking at 16:00 h on Day 1 (**Figure 8B**). By contrast, transcripts detected associated with phosphorus acquisition and uptake (*pho, pst*) exhibited no clear diel pattern (**Figure 8D**).

Cell Division

Relative abundance of transcripts encoding the septation ring protein FtsZ and cell division function FtsH peak during the day on both days, indicating that cell division likely followed later during the daytime hours (**Figure 9**). Proxy measurements for bloom biomass suggested that the bloom was expanding at the time of the sampling (**Figure 2**), and the pattern of *fts* transcription reflects active growth of *Microcystis* during this time.

Microcystin Synthesis and Stress Responses

Relative expression of the *mcy* genes was very low and was elevated only during the afternoon of Day 2. Microcystin measured during the course of the sampling show a pattern of increased toxin, trending toward highest concentrations during morning of the second day (**Figure 10**).

Stress response genes examined included those involved in heat shock (*groEL, dnaK*), phycobilisome stability (*nblA*) and high light stress (*hliA*). Unsurprisingly, given increased daytime

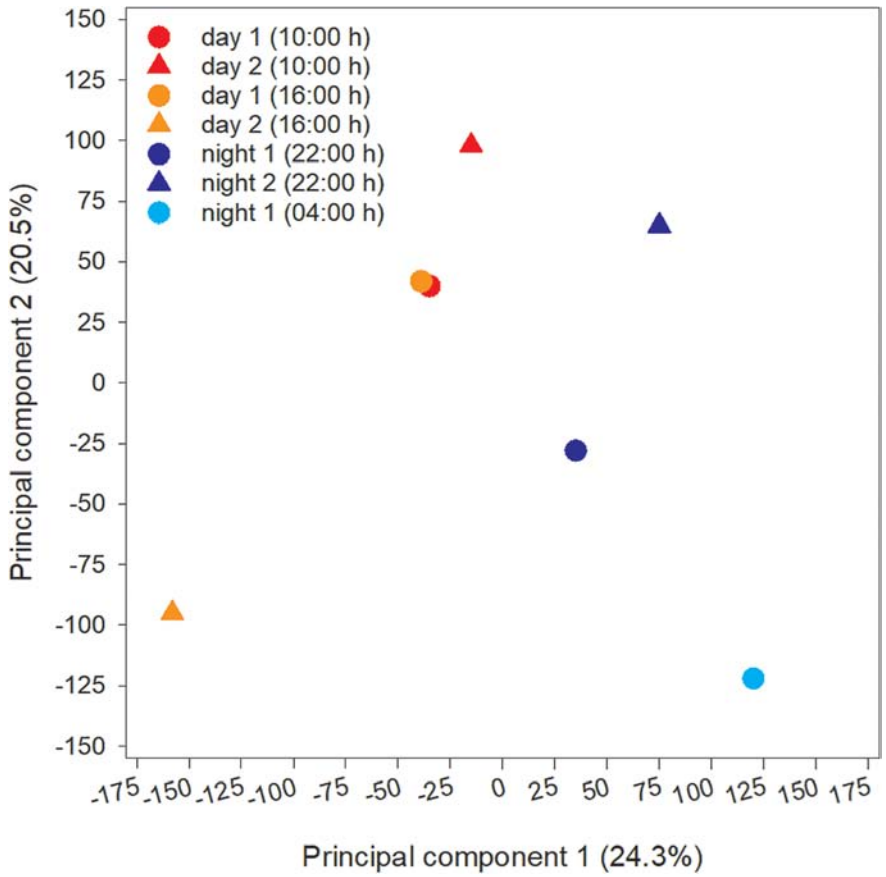

FIGURE 5 | Principal Component Analysis (PCA) of transcripts obtained from each time point during the study.

temperature, photosynthetic oxygen production and daytime irradiance, all genes showed increased relative transcription at 10:00 h and 16:00 h (**Figure 11**).

DISCUSSION

Metatranscriptomes spanning two diel cycles were produced from a toxic cyanobacterial bloom in western Lake Erie during late August 2014. The survey described here coincided with a mid-bloom phase with the bloom persisting through October (Steffen et al., 2017). A Lagrangian approach was adopted to ensure that a common patch of biomass was sampled over the 48-h experiment. In this way, changes in relative abundance of transcripts could be attributed to either diel patterns or changing physico-chemical conditions but not to sampling of different bloom populations. Taxonomic analysis of recruited transcripts showed *Microcystis* spp. to dominate cyanobacterial reads during the survey consistent with independent surveys of the western basin conducted during August 2014 (Berry et al., 2017; Steffen et al., 2017).

Cyanobacteria are known to regulate gene expression under circadian influences (Golden et al., 1997). The intent of this study was to identify cellular processes within a *Microcystis* bloom that show diel patterns of expression. PCA of *Microcystis* transcriptomes revealed grouping of samples based upon time of collection (i.e., "day" and "night"). Variability amongst day samples as shown by PCA (**Figure 5**) suggested circadian rhythms were not the sole determiner of expression, rather transient environmental changes may have contributed to differing transcript accumulation. A summary of transcriptional activity throughout the diel cycle is presented in **Figure 12**.

Reflecting the demands of a phototrophic lifestyle, photosynthesis-related functions for the dark and light reactions were detected at all time points. Photosynthesis functions appear to partition so that PSII-dependent O_2 evolution peaks in mid-afternoon, as has been observed in laboratory studies (Garczarek et al., 2001; Mackenzie and Morse, 2011). Expression of genes involved in the cyt b_6/f complex follow this same pattern. However, PSI genes were preferentially expressed at night, peaking at 22:00 h. Given the variability of the timing of PSI gene expression in N-fixing cyanobacteria (del Carmen Muñoz-Marin et al., 2019), and that degradation of PSI occurs during the night in *Crocosphaera watsonii* WH8501 (Masuda et al., 2018), nighttime expression of *psa* genes in *Microcystis* may be a genus-specific trait.

Consistent with modest nitrogen depletion during the first 18 h as revealed by nutrient stoichiometry, expression of

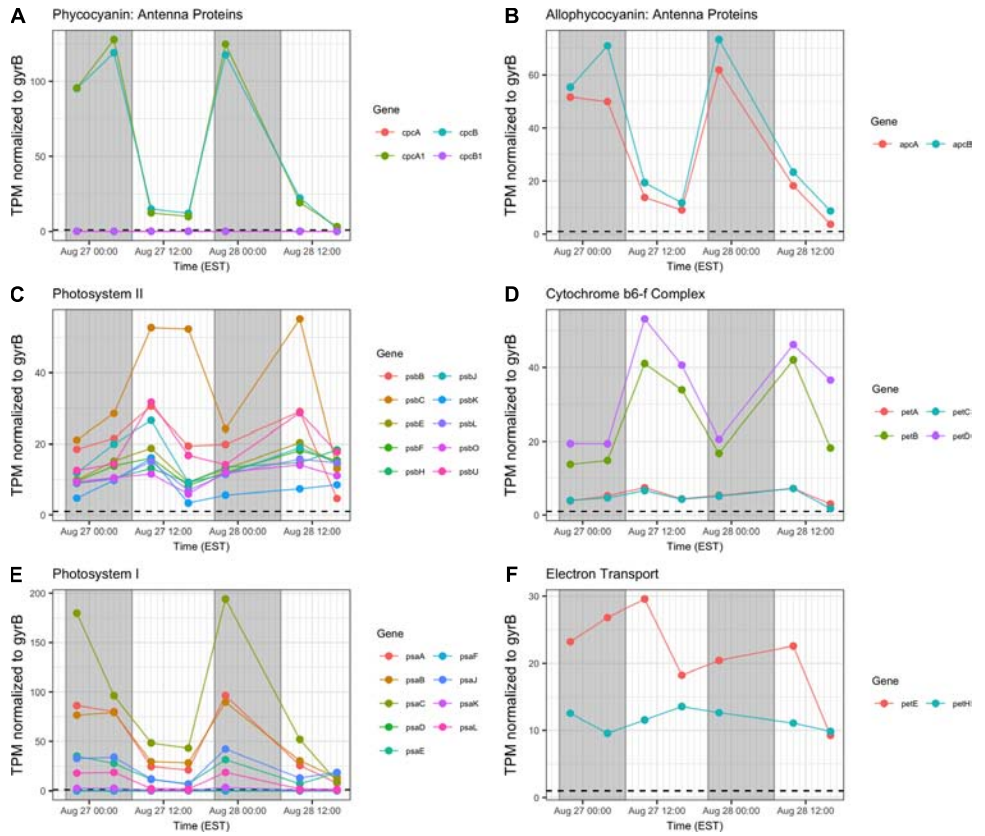

FIGURE 6 | Diel transcriptional patterns of *Microcystis* photosynthesis genes. **(A,B)** Phycobilisome subunits; **(C)** Photosystem II; **(D)** cytochrome b_6/f; **(E)**, Photosystem I; **(F)**, ferredoxin and plastocyanin. Gray shading indicates time periods between sunset and sunrise.

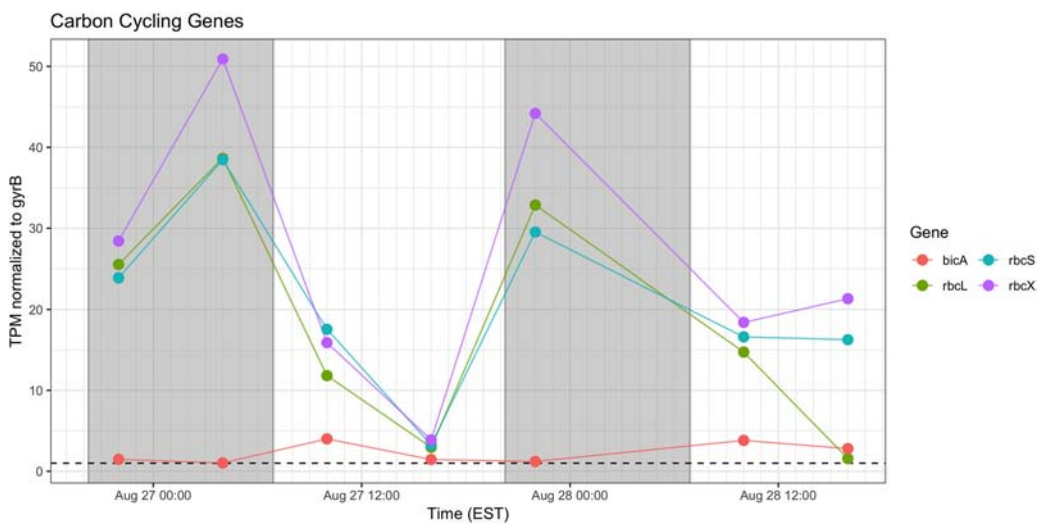

FIGURE 7 | Diel transcriptional patterns of *Microcystis* inorganic carbon acquisition genes. Gray shading indicates time periods between sunset and sunrise.

nitrogen assimilation genes was detected, as has been reported previously for western Lake Erie (Harke and Gobler, 2013, 2015; Steffen M. et al., 2014; Steffen et al., 2017). In the present survey, expression of nitrogen metabolism genes may reflect both transient nitrogen availability as well as circadian control. Indeed, elevated transcript abundance for *glnA* at the conclusion of sampling on Day 2 (16:00 h) may suggest environmental stresses resulting in reduced N bioavailability

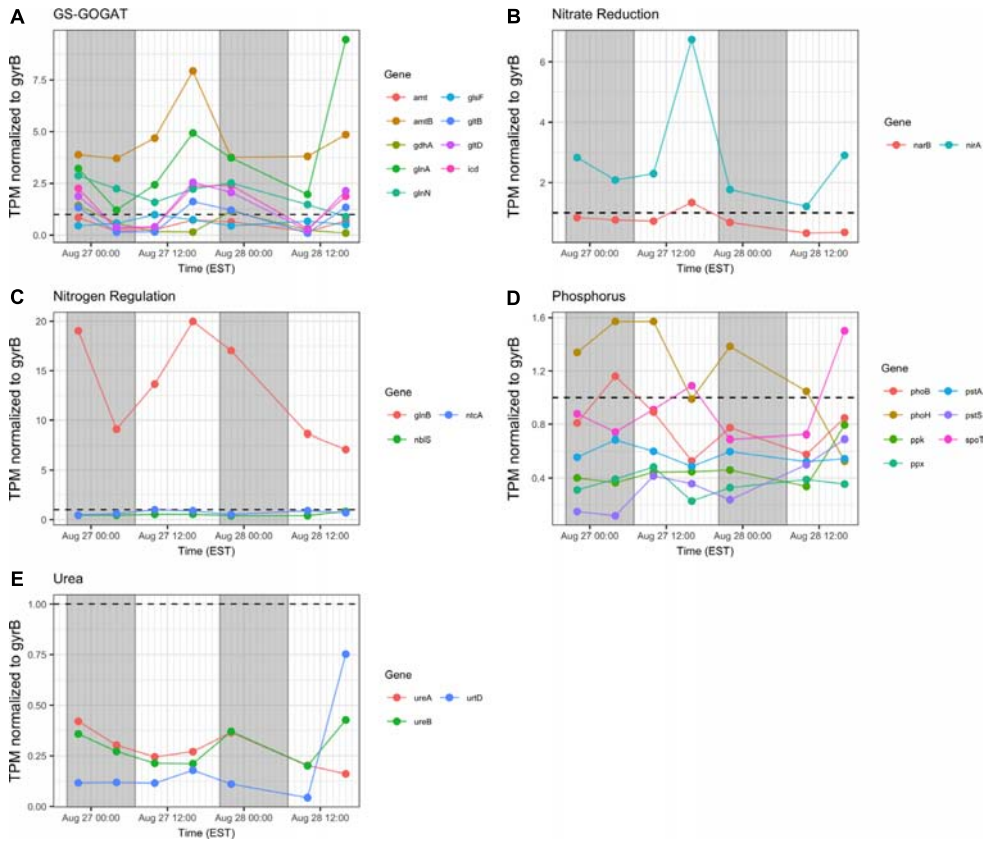

FIGURE 8 | Transcriptional patterns of *Microcystis* nutrient assimilation genes. **(A)** GS-GOGAT pathway; **(B)** nitrite reductase; **(C)** N regulation genes; **(D)** phosphorus assimilation; **(E)** urea assimilation. Gray shading indicates time periods between sunset and sunrise.

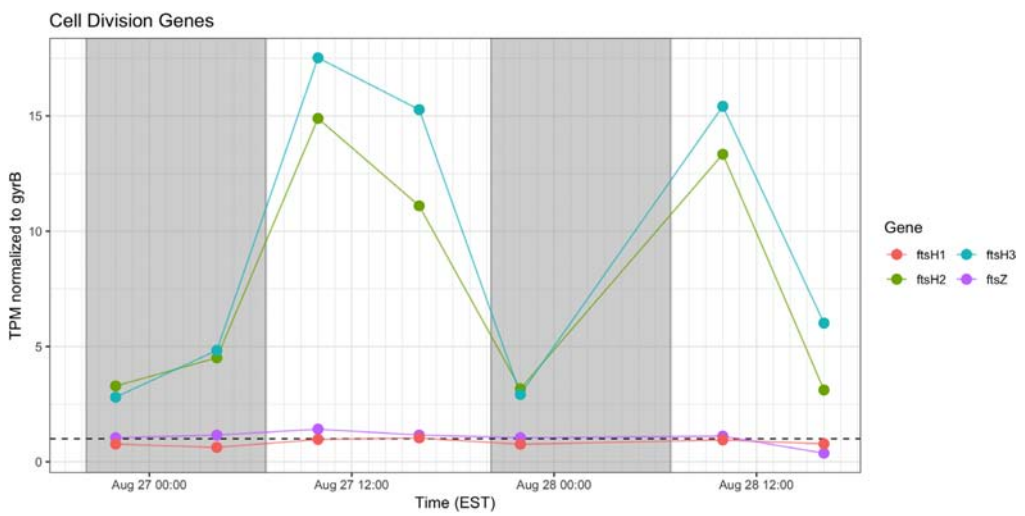

FIGURE 9 | Transcriptional patterns of *Microcystis* cell division genes *ftsH* and *ftsZ*. Gray shading indicates time periods between sunset and sunrise.

(**Figure 8**). However, the increasing DIN/DIP ratio over the course of the survey indicated a greater demand for P. Transcripts related to nitrogen assimilation that accumulated during the day included *narB* and *nirA* (encoding nitrate and nitrite reductase) and *glnA* (encoding glutamine synthetase), indicating active mechanisms of nitrogen assimilation and synthesis of amino acids in daylight (Mérida et al., 1991; Kramer et al., 1996; Marzluf, 1997; Wyman, 1999; Flores and Herrero, 2005). Overall,

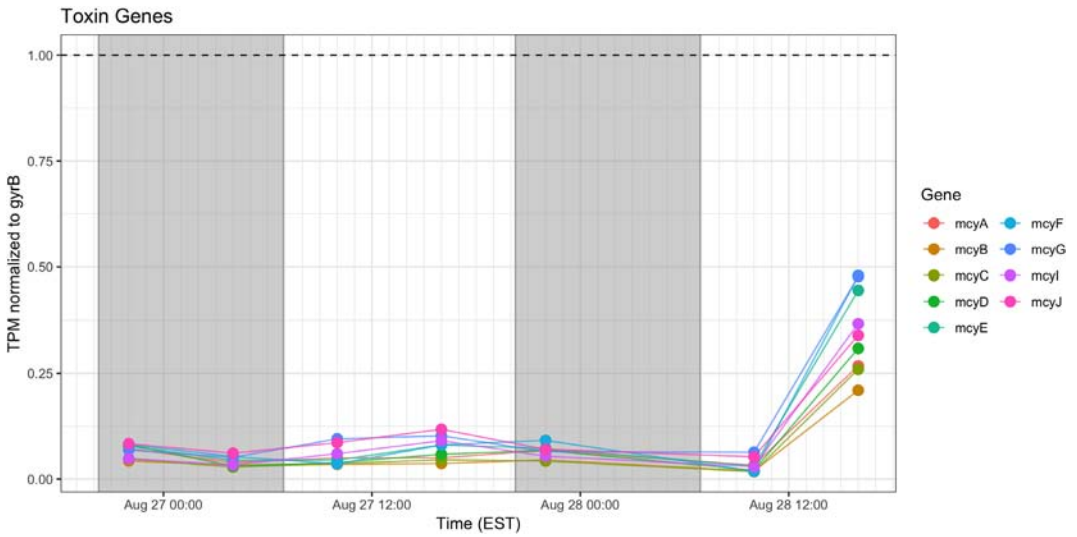

FIGURE 10 | Transcriptional patterns of *Microcystis* microcystin biosynthesis genes. Gray shading indicates time periods between sunset and sunrise.

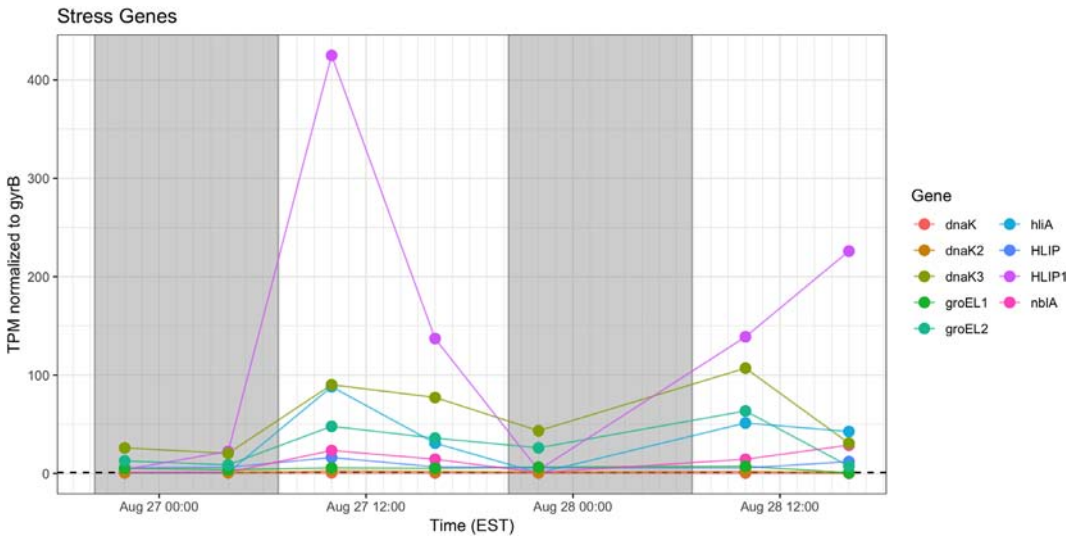

FIGURE 11 | Transcriptional patterns of *Microcystis* stress response genes (heat shock, high light, phycobilisome stability). Gray shading indicates time periods between sunset and sunrise.

nitrogen metabolism transcripts exhibited increases in relative abundances during the light period. Since nitrate reduction is an ATP-dependent process, nitrate assimilation may be regulated by day so that it is temporally aligned with daytime photosynthetic energy generation.

Regarding phosphate uptake, Penn et al. (2014) described highest transcription of alkaline phosphatase (*pho*) and phosphate transported (*pst*) genes during the day in a *Microcystis* bloom event, in this study, no such pattern is seen. Such differences may also be due to transient changes in P availability during the course of each survey. Indeed, analysis of dissolved nutrients over the course of the survey revealed a pronounced shift in dissolved N:P ratio (**Figure 2**).

Cyanobacteria are known to contain multiple inorganic carbon uptake genes and pathways, facilitating variable responses to availability of carbon for photoautotrophic growth (Sandrini et al., 2014, 2015). A growing concern in bloom formation and mitigation is the response of cHAB species to increasing atmospheric CO_2 (Verspagen et al., 2014; Visser et al., 2016). Whereas C fixation genes were preferentially expressed at night, carbon concentrating mechanism transcripts did not appear to express distinct diel patterns (data not shown). The relative transcript abundance of Rubisco genes in the predawn hours of Day 1 and elevated expression throughout Day 2 is in partial agreement with Wyman (1999) examining *rbcL* expression in natural populations of marine *Synechococcus*, and

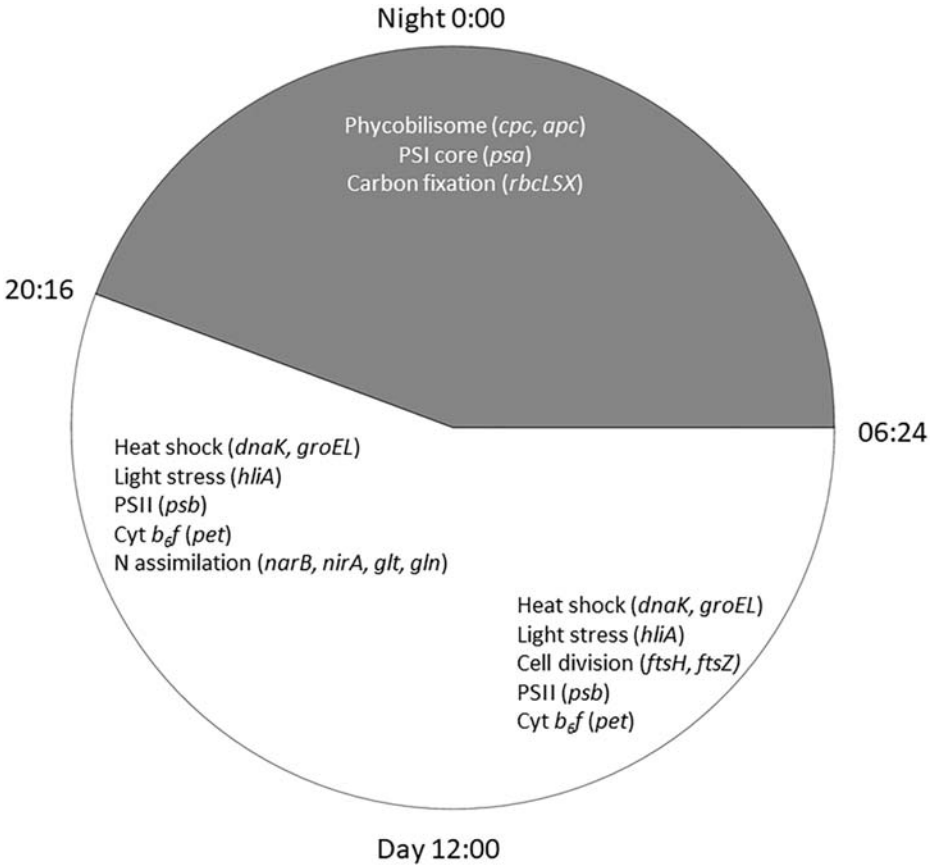

FIGURE 12 | Summary of significant *Microcystis* functions expressed during the 24 h cycle in the Toledo, 2014 bloom event. Lines of the clock indicate sunrise at 0654 h and sunset at 2016 h on August 26, 2014.

Straub et al. (2011), who documented a decline in *rbc* expression during daytime in culture experiments with *M. aeruginosa* PCC 7806. The data in this study are in some agreement with the findings of Sandrini et al. (2016) who demonstrated similar variable diel responses during a bloom event, in which *bicA* transcription was also correlated to bicarbonate concentration.

As expected, given environmental changes through the day, a diel pattern exists regarding transcript abundance for genes encoding stress and cell division proteins. *Synechococcus* cells have shown a specific gating of cell division independent of the circadian clock in avoidance of peak irradiance exposure (Mori et al., 1996). In agreement with this observation, relative transcript abundance for the ATP-binding *ftsH* and septation gene *ftsZ* increased during the morning, suggesting cell division at midday or in the afternoon (**Figure 9**). Relative abundance of the heat shock chaperones *dnaK*, *groEL* and high-light inducible gene *hliA* all peak during the day (**Figure 11**), similar to previous reports (Aoki et al., 1995).

Microcystin biosynthesis gene (*mcy*) transcript levels were very low (**Figure 10**), although transcripts were modestly higher during Day 2. Other studies have indicated toxin production to occur early in the night in a tropical bloom event (Penn et al., 2014) or as a daytime function in a culture experiment (Straub et al., 2011). Further complicating the issue is the observation that microcystin production is elevated at lower temperatures (Peng et al., 2018). Furthermore, previous studies that have examined the western Lake Erie *Microcystis* blooms have shown that toxin concentrations increase and *mcy* genes are significantly upregulated when the ambient communities are experimentally exposed to elevated nitrogen concentrations and high light, especially during August and September (Chaffin et al., 2018). Due to the low level of expression, it remains impossible within our data set to separate diel and light-driven effects on toxin production from the subtle effects of minor temperature fluctuations on both toxin gene transcription and toxin biosynthesis (Peng et al., 2018). However, what is known is that changes in toxic to non-toxic *Microcystis* strain ratios can be significantly influenced by physiochemical parameters such as nutrients and temperature (Davis et al., 2009, 2010) and that the shift in the toxic: non-toxic ratio will likely lead to changes in bloom toxin concentrations (O'Neil et al., 2012; Gobler et al., 2016). As such, both changes in gene expression and *Microcystis* community composition need to be taken into account when determining the relationship between the toxin concentration and the molecular underpinnings of production.

Examining the relative transcript abundance for the genes analyzed in the study reveals a marked increase in relative transcript abundance for a few genes (e.g., *rbcS, rbcX, glnA, mcyA-J*) at the final time point (16:00 h on Day 2). This increase likely indicated a change in environmental conditions on the second day. The nutrient profile shifted toward P deficiency on the 28th (**Figure 2**), suggesting the onset of modest nutrient stress, but light stress was likely not a factor given the similar peak irradiances measured at the Toledo water intake crib during both days (**Supplementary Figure S1**). This documented change in gene expression remains unexplained, but since the sample passed QA/QC at JGI it was not due to changes in transcript composition due to rRNA contamination or RNA degradation (data not shown). High abundance of viral reads were also not detected.

CONCLUSION

Lake Erie experiences annual cHAB events, and these events will continue as eutrophication intensifies (Watson et al., 1997; Michalak et al., 2013). In light of concerns over the safety of water resources and human health, there is an urgent need to elucidate the factors influencing cHAB formation, proliferation, and maintenance, to better inform prevention and mitigation strategies. Toward this goal, the present study used a metatranscriptomic approach to investigate metabolic function of a Lake Erie *Microcystis* bloom over diel cycles. Lab studies have found the genomes of *Microcystis* to be highly plastic and adaptable to the environment, increasing their competitive ability (Meyer et al., 2017). Previous investigations report the presence of circadian regulation of gene expression in cyanobacteria (Kondo et al., 1993; Golden et al., 1997). The circadian clock has been shown to enhance the fitness of the species within the microbial community. Paired with a highly adaptive genome, *Microcystis* has the potential to be very successful. Our analysis indicates that Lake Erie *Microcystis* likely utilizes efficient organization of gene expression to maintain productivity, such as utilization of a variety of nutrient species throughout a diel cycle (CO_2, bicarbonate, nitrate, ammonium), cell division and, if a toxic genotype, the production of microcystins. Our results suggest that although diel patterns are detectable, environmental cues also influence regulation, as supported by PCA analysis. The next step of this analysis is to study the metabolism of the global microbial community. In doing so, those results paired with this analysis of *Microcystis* spp. will provide insights into factors leading to the natural mitigation of a bloom, and how the surrounding consortium of heterotrophs and phages interact and influence both cHAB success and decline. Indeed, a role for *Microcystis* phage infection was suggested in constraining this same bloom 3 weeks earlier in Lake Erie, yielding shifts in microcystin toxin from an intracellular particulate fraction to the soluble phase (Steffen et al., 2017). Conversely, recent work invokes the Black Queen Hypothesis (Morris et al., 2012) in demonstrating a role for catalase produced by bloom-associated heterotrophs in protecting *Microcystis* from oxidative stress thus promoting bloom success (Greg Dick, personal communication).

DATA AVAILABILITY

The datasets generated for this study can be accessed from NCBI SRA, SRP117911, SRP117914, SRP117915, SRP117922, SRP128942, SRP128945, and SRP128954.

AUTHOR CONTRIBUTIONS

ED conducted the field sampling, initial analysis of the assembled reads, and wrote the Introduction and Materials and Methods sections. MN and PM analyzed the relative transcript abundance at each diel timepoint. MD, LK, and JS isolated RNA and processed the metatrascriptomic data from JGI. KM, GD, TD, SW, and RM developed the Lagrangian sampling plan. GB helped to devise the study, analyzed the metadata, and wrote the Results and Discussion sections. TJ led the field sampling and provided all field metadata. ST and EL processed the RNAs for sequencing.

FUNDING

GB was supported by NOAA's Ohio Sea Grant College Program, R/ER-104 (jointly with RMLM) and by funding from the NIH (1P01ES028939-01) and NSF (OCE-1840715) to the Great Lakes Center for Fresh Waters and Human Health, Bowling Green State University. SW was supported by the National Science Foundation (IOS-1451528). The work conducted by the U.S. DOE Joint Genome Institute, a DOE Office of Science User Facility, was supported by the Office of Science of the U.S. DOE under Contract No. DE-AC02-05CH11231. GD and KM were supported by grants from the University of Michigan Office for Research MCubed program and the Erb Family Foundation made through the University of Michigan Water Center. Additional funding was provided to the Cooperative Institute for Great Lakes Research (CIGLR) through the NOAA Cooperative Agreement with University of Michigan (NA17OAR4320152). This is CIGLR contribution number 1147.

ACKNOWLEDGMENTS

We thank Taylor Tuttle for assistance with sampling. We thank the captain and crew of the NOAA Great Lakes Environmental Research Laboratory for the research vessel used in this study. We would also like to thank Sunit Jain (Second Genome, South San Francisco, CA, United States) for initial quality control and assembly of *Microcystis* genomes, and Paul Den Uyl for extracting DNAs from *Microcystis* cultures for sequencing.

SUPPLEMENTARY MATERIAL

The Supplementary Material for this article can be found online at: https://www.frontiersin.org/articles/10.3389/fmicb.2019.02081/full#supplementary-material

REFERENCES

Aoki, S., Kondo, T., and Ishiura, M. (1995). Circadian expression of the dnaK gene in the cyanobacterium *Synechocystis* sp. strain PCC 6803. *J. Bacteriol.* 177, 5606–5611. doi: 10.1128/jb.177.19.5606-5611.1995

Badger, M., and Price, G. D. (2003). CO2 concentrating mechanisms in cyanobacteria: molecular components, their diversity and evolution. *J. Exp. Bot.* 54, 609–622. doi: 10.1093/jxb/erg076

Berry, M. A., Davis, T. W., Cory, R. M., Duhaime, M. B., Johengen, T. H., Kling, G. W., et al. (2017). Cyanobacterial harmful algal blooms are a biological disturbance to western lake erie bacterial communities. *Environ. Microbiol.* 19, 1149–1162. doi: 10.1111/1462-2920.13640

Bingham, M., Sinha, S. K., and Lupi, F. (2015). *Economic Benefits of Reducing Harmful Algal Blooms in Lake Erie*. Report No. 66. Gainesville, FL: Environmental Consulting & Technology, Inc.

Brittain, S. M., Wang, J., Babcock-Jackson, L., Carmichael, W. W., Rinehart, K. L., and Culver, D. A. (2000). Isolation and characterization of microcystins, cyclic heptapeptide hepatotoxins from a lake erie strain of *Microcystis aeruginosa*. *J. Great Lakes Res.* 26, 241–249. doi: 10.1016/s0380-1330(00)70690-3

Brookes, J., and Ganf, G. (2001). Variations in the buoyancy response of *Microcystis aeruginosa* to nitrogen, phosphorus and light. *J. Plankton Res.* 23, 1399–1411. doi: 10.1093/plankt/23.12.1399

Brunberg, A. K., and Blomqvist, P. (2003). Recruitment of *Microcystis* (Cyanophyceae) from lake sediments: the importance of littoral inocula. *J. Phycol.* 39, 58–63. doi: 10.1046/j.1529-8817.2003.02059.x

Bullerjahn, G. S., McKay, R. M., Davis, T. W., Baker, D. B., Boyer, G. L., D'Anglada, L. V., et al. (2016). Global solutions to regional problems: collecting global expertise to address the problem of harmful cyanobacterial blooms. A lake erie case study. *Harmful Algae* 54, 223–238. doi: 10.1016/j.hal.2016.01.003

Bünning, E. (1973). *Physiological Clocks; Circadian Rhythms and Biological Chronometry*. London: English Universities Press, 258.

Chaffin, J. D., Davis, T. W., Smith, D. J., Baer, M. M., and Dick, G. J. (2018). Interactions between nitrogen form, loading rate and light intensity on *Microcystis* and *Planktothrix* growth and microcystin production. *Harmful Algae* 73, 84–97. doi: 10.1016/j.hal.2018.02.001

Chen, T. H., Chen, T. L., Huang, L., and Huang, T. (1991). Circadian rhythm in amino acid uptake by *Synechococcus* RF-1. *Plant Physiol.* 97, 89–104.

Davis, C. O., and Simmons, M. S. (1979). *Water Chemistry and Phytoplankton Field and Laboratory Procedures*. Special Report No. 70. Ann Arbor, MI: Great Lakes Research Division, University of Michigan.

Davis, T. W., Berry, D. L., Boyer, G. L., and Gobler, C. J. (2009). The effects of temperature and nutrients on the growth and dynamics of toxic and non-toxic strains of *Microcystis* during cyanobacteria blooms. *Harmful Algae* 8, 715–725. doi: 10.1016/j.hal.2009.02.004

Davis, T. W., Harke, M. J., Marcoval, M. A., Goleski, J., Orano-Dawson, C., Berry, D. L., et al. (2010). Effects of nitrogenous compounds and phosphorus on the growth of toxic and non-toxic strains of *Microcystis* during cyanobacterial blooms. *Aquat. Microb. Ecol.* 61, 149–162. doi: 10.3354/ame01445

del Carmen Muñoz-Marin, M., Shilova, I. N., Shi, T., Farnelid, H., Cabello, A. M., and Zehr, J. P. (2019). The transcriptional cycle is suited to daytime N2 fixation in the unicellular cyanobacterium "*Candidatus Atelocyanobacterium thalassa*" (UCYN-A). *MBio* 10:e02495-e18. doi: 10.1128/mBio.02495-18

Falconer, I. R. (1994). "Health problems from exposure to cyanobacteria and proposed safety guidelines for drinking and recreational water," in *Detection Methods for Cyanobacterial Toxins*, eds G. A. Codd, T. M. Jefferies, C. W. Keevil, and P. Potter (Cambridge: Royal Society of Chemistry), 3–10. doi: 10.1533/9781845698164.1.3

Fan, H., Cai, Y., Xie, P., Xiao, W., Chen, J., Ji, W., et al. (2014). Microcystin-LR stabilizes c-myc protein by inhibiting protein phosphatase 2A in HEK293 cells. *Toxicology* 319, 69–74. doi: 10.1016/j.tox.2014.02.015

Fischer, W. J., Garthwaite, I., Miles, C. O., Ross, K. M., Aggen, J. B., Chamberlin, A. R., et al. (2001). Congener-independent immunoassay for microcystins and nodularins. *Environ. Sci. Technol.* 35, 4849–4856. doi: 10.1021/es011182f

Flores, E., and Herrero, A. (2005). Nitrogen assimilation and nitrogen control in cyanobacteria. *Biochem. Soc. Trans.* 33, 164–167. doi: 10.1042/bst0330164

Frangeul, L., Quillardet, P., Castets, A. M., Humbert, J. F., Matthijs, H. C. P., Cortez, D., et al. (2008). Highly plastic genome of *Microcystis aeruginosa* PCC7806, a ubiquitous toxic freshwater cyanobacterium. *BMC Genomics* 9:274. doi: 10.1186/1471-2164-9-274

Garczarek, L., Partensky, F., Irlbacher, H., Holtzendorff, J., Babin, M., Mary, I., et al. (2001). Differential expression of antenna and core genes in *Prochlorococcus* PCC 9511 (Oxyphotobacteria) grown under a modulated light–dark cycle. *Environ. Microbiol.* 3, 168–175. doi: 10.1046/j.1462-2920.2001.00173.x

Gobler, C. J., Burkholder, J. M., Davis, T. W., Harke, M. J., Johengen, T., Stow, C. A., et al. (2016). The dual role of nitrogen supply in controlling the growth and toxicity of cyanobacterial blooms. *Harmful Algae* 54, 87–97. doi: 10.1016/j.hal.2016.01.010

Golden, S. S., Ishiura, M., Johnson, C. H., and Kondo, T. (1997). Cyanobacterial circadian rhythms. *Ann. Rev. Plant Physiol. Plant Mol. Biol.* 48, 327–354.

Harke, M. J., and Gobler, C. J. (2013). Global transcriptional responses of the toxic cyanobacterium, *Microcystis aeruginosa*, to nitrogen stress, phosphorus stress, and growth on organic matter. *PLoS One* 8:e69834. doi: 10.1371/journal.pone.0069834

Harke, M. J., and Gobler, C. J. (2015). Daily transcriptome changes reveal the role of nitrogen in controlling microcystin synthesis and nutrient transport in the toxic cyanobacterium, *Microcystis aeruginosa*. *BMC Genomics* 16:1068. doi: 10.1186/s12864-015-2275-9

Holtzendorff, J., Partensky, F., Mella, D., Lennon, J.-F., Hess, W. R., and Garczarek, L. (2008). Genome streamlining results in loss of robustness of the circadian clock in the marine cyanobacterium *Prochlorococcus marinus* PCC 9511. *J. Biol. Rhyth.* 23, 187–199. doi: 10.1177/0748730408316040

Horváth, H., Kovács, A. W., Riddick, C., and Présing, M. (2013). Extraction methods for phycocyanin determination in freshwater filamentous cyanobacteria and their application in a shallow lake. *Eur. J. Phycol.* 48, 278–286. doi: 10.1080/09670262.2013.821525

Huisman, J., and Hulot, F. D. (2005). "Population dynamics of harmful cyanobacteria," in *Harmful Cyanobacteria*, eds J. Huisman, H. C. P. Matthijis, and P. M. Visser (New York, NY: Springer), 143–176. doi: 10.1007/1-4020-3022-3_7

Humbert, J. F., Barbe, V., Latifi, A., Calteau, A., Coursin, T., Lajus, A., et al. (2013). A tribute to disorder in the genome of the bloom-forming freshwater cyanobacterium *Microcystis aeruginosa*. *PLoS One* 8:e70747. doi: 10.1371/journal.pone.0070747

Hutin, C., Nussaume, L., Moise, N., Moya, I., Kloppstech, K., and Havaux, M. (2003). Early light-induced proteins protect *Arabidopsis* from photooxidative stress. *Proc. Natl. Acad. Sci. U.S.A.* 100, 4921–4926. doi: 10.1073/pnas.0736939100

Ishiura, M., Kutsuna, S., Aoki, S., Iwasaki, H., Andersson, C., Tanabe, A., et al. (1998). Expression of a gene cluster kaiABC as a circadian feedback process in cyanobacteria. *Science* 281, 1519–1523. doi: 10.1126/science.281.5382.1519

Jöhnk, K. D., Huisman, J., Sharples, J., Sommeijer, B., Visser, P. M., and Stroom, J. M. (2008). Summer heat waves promote blooms of harmful cyanobacteria. *Glob. Change Biol.* 14, 495–512. doi: 10.1111/j.1365-2486.2007.01510.x

Johnson, C. H., and Hastings, J. W. (1986). The elusive mechanism of the circadian clock: the quest for the chemical basis of the biological clock is beginning to yield tantalizing clues. *Am. Sci.* 74, 29–37.

Kaneko, T., Nakajima, N., Okamota, S., Suzuki, I., Tanabe, Y., Tamaoki, M., et al. (2007). Complete genomic structure of the bloom-forming toxic cyanobacterium *Microcystis aeruginosa* NIES-843. *DNA Res.* 14, 247–256. doi: 10.1093/dnares/dsm026

Kitchens, C. M., Johengen, T. H., and Davis, T. W. (2018). Establishing spatial and temporal patterns in *Microcystis* sediment seed stock viability and their relationship to subsequent bloom development in western lake erie. *PLoS One* 13:e0206821. doi: 10.1371/journal.pone.0206821

Kondo, T., Strayer, C., Kulkarni, R., Ishiura, W., Golden, S., and Johnson, C. (1993). Circadian rhythms in prokaryotes: luciferase as a reporter of circadian gene expression in cyanobacteria. *Proc. Nat. Acad. Sci. U.S.A.* 90, 5672–5676. doi: 10.1073/pnas.90.12.5672

Konopka, R., and Benzer, S. (1971). Clock mutants of *Drosophila melanogaster*. *Proc. Nat. Acad. Sci. U.S.A.* 68, 2112–2116. doi: 10.1073/pnas.68.9.2112

Kramer, J., Wyman, M., Zehr, J., and Capone, D. (1996). Diel variability in transcription of the structural gene for glutamine synthetase (glnA) in natural populations of the marine diazotrophic cyanobacterium *Trichodesmium thiebautii*. *FEMS Microbiol. Ecol.* 21, 187–196. doi: 10.1016/s0168-6496(96)00055-4

Krausfeldt, L. E., Farmer, A. T., Gonzalez, H. C., Zepernick, B. N., Campagna, S. R., and Wilhelm, S. W. (2019). Urea is both a carbon and nitrogen source for *Microcystis aeruginosa*: tracking 13C incorporation at bloom pH conditions. *Front. Microbiol.* 10:1064. doi: 10.3389/fmicb.2019.01064

Kucho, K., Okamoto, K., Tsuchiya, Y., Nomura, S., Nango, M., Kanehisa, M., et al. (2005). Global analysis of circadian expression in the cyanobacterium *Synechocystis* sp. strain PCC 6803. *J. Bacteriol.* 187, 2190–2199. doi: 10.1128/jb.187.6.2190-2199.2005

Kulkarni, R. D., and Golden, S. S. (1994). Adaptation to high light intensity in *Synechococcus* sp. strain PCC 7942: regulation of three psbA genes and two forms of the D1 protein. *J. Bacteriol.* 176, 959–965. doi: 10.1128/jb.176.4.959-965.1994

Labiosa, R., Arrigo, K., Tu, C., Bhaya, D., Bay, S., Grossman, A., et al. (2006). Examination of diel changes in global transcript accumulation in *Synechocystis* (Cyanobacteria). *J. Phycol.* 42, 622–636. doi: 10.1111/j.1529-8817.2006.00217.x

Liu, Y., Tsinoremas, N., Johnson, C. H., Lebedeva, N., Golden, S. S., Ishiura, M., et al. (1995). Circadian orchestration of gene expression in cyanobacteria. *Genes Dev.* 9, 1469–1478. doi: 10.1101/gad.9.12.1469

Lorne, J., Scheffer, J., Lee, A., Painter, M., and Miao, V. (2000). Genes controlling circadian rhythm are widely distributed in cyanobacteria. *FEMS Microbiol. Lett.* 189, 129–133. doi: 10.1016/s0378-1097(00)00237-8

Mackenzie, T. D., and Morse, D. (2011). Circadian photosynthetic reductant flow in the dinoflagellate *Lingulodinium* is limited by carbon availability. *Plant Cell Environ.* 34, 669–680. doi: 10.1111/j.1365-3040.2010.02271.x

Markowitz, V., Chen, I., Chu, K., Szeto, E., Palaniappan, K., Pillay, M., et al. (2014). IMG/M4 version of the integrated metagenome comparative analysis system. *Nucl. Acids Res.* 42, 568–573.

Markowitz, V., Chen, I., Palaniappan, K., Chu, K., Szeto, E., Grechkin, Y., et al. (2012). IMG: the integrated microbial genomes database and comparative analysis system. *Nucl. Acids Res.* 40, 115–122.

Marzluf, G. A. (1997). Genetic regulation of nitrogen metabolism in the fungi. *Microbiol. Mol. Biol. Rev.* 61, 17–32.

Masuda, T., Bernat, G., Beckova, M., Kotabova, E., Lawrenz, E., Lukes, M., et al. (2018). Diel regulation of photosynthetic activity in the unicellular diazotrophic cyanobacterium *Crocosphaera watsonii* WH8501. *Environ. Microbiol.* 20, 546–560. doi: 10.1111/1462-2920.13963

Mavromatis, K., Ivanova, N. N., Chen, I. M. A., Szeto, E., Markowitz, V. M., and Kyrpides, N. C. (2009). The DOE-JGI standard operating procedure for the annotations of microbial genomes. *Stand Genomics Sci.* 1:63. doi: 10.4056/sigs.632

Menzel, D. W., and Corwin, N. (1965). The measurement of total phosphorus liberated in seawater based on the liberation of organically bound fractions by persulfate oxidation. *Limnol. Oceanogr.* 10, 280–288.

Mérida, A., Candau, P., and Florencio, F. J. (1991). Regulation of glutamine synthetase activity in the unicellular cyanobacterium *Synechocystis* sp. strain PCC 6803 by the nitrogen source: effect of ammonium. *J. Bacteriol.* 173, 4095–4100. doi: 10.1128/jb.173.13.4095-4100.1991

Meyer, F., Paarmann, D., D'Souza, M., Olson, R., Glass, E. M., Kubal, M., et al. (2008). The metagenomics RAST server – a public resource for the automatic phylogenetic and functional analysis of metagenomes. *BMC Bioinformatics* 9:386. doi: 10.1186/1471-2105-9-386

Meyer, K. A., Davis, T. W., Watson, S. B., Denef, V. J., Berry, M. A., and Dick, G. J. (2017). Genome sequences of lower Great Lakes *Microcystis* sp. reveal strain-specific genes that are present and expressed in western lake erie blooms. *PLoS One* 12:e0183859. doi: 10.1371/journal.pone.0183859

Michalak, A. M., Anderson, E. J., Beletsky, D., Boland, S., Bosch, N. S., Bridgeman, T. B., et al. (2013). Record-setting algal bloom in lake erie caused by agricultural and meteorological trends consistent with expected future conditions. *Proc. Natl. Acad. Sci. U.S.A.* 110, 6448–6452. doi: 10.1073/pnas.1216006110

Mori, T., Binder, B., and Johnson, C. H. (1996). Circadian gating of cell division in cyanobacteria growing with average doubling times of less than 24 hours. *Proc. Nat. Acad. Sci. U.S.A.* 93, 10183–10188. doi: 10.1073/pnas.93.19.10183

Morris, J. J., Lenski, R. E., and Zinser, E. R. (2012). The black queen hypothesis: evolution of dependencies through adaptive gene loss. *MBio* 3:e00036-e12. doi: 10.1128/mBio.00036-12

Nordberg, H., Cantor, M., Dusheyko, S., Hua, S., Poliakov, A., and Shabalov, I. (2014). The genome portal of the department of energy joint genome institute: 2014 updates. *Nucl. Acids Res.* 42, D26–D31. doi: 10.1093/nar/gkt1069

O'Neil, J. M., Davis, T. W., Burford, M. A., and Gobler, C. J. (2012). The rise of harmful cyanobacteria blooms (CHABs): the potential roles of eutrophication and climate change. *Harmful Algae* 14, 313–334. doi: 10.1016/j.hal.2011.10.027

Paerl, H., and Huisman, J. (2008). Blooms like it hot. *Science* 320, 57–58. doi: 10.1126/science.1155398

Peng, G., Martin, R. M., Dearth, S. P., Sun, X., Boyer, G. L., Campagna, S. R., et al. (2018). Seasonally relevant cool temperatures interact with N chemistry to increase microcystins produced in lab cultures of *Microcystis aeruginosa* NIES-843. *Environ. Sci. Technol.* 52, 4127–4136. doi: 10.1021/acs.est.7b06532

Penn, K., Wang, J., Fernando, S., and Thompson, J. (2014). Secondary metabolite gene expression and interplay of bacterial functions in a tropical freshwater cyanobacterial bloom. *ISME J.* 8, 1866–1878. doi: 10.1038/ismej.2014.27

Pittendrigh, C. S. (1981). *Handbook of Behavioral Neurobiology: Biological Rhythms*, ed. J. Aschoff (New York, NY: Plenum Press), 57–80.

R Core Team (2018). *R: A Language and Environment for Statistical Computing*. Vienna: R Foundation for Statistical Computing.

Reynolds, C., Oliver, R., and Walsby, A. (1987). Cyanobacterial dominance: the role of buoyancy regulation in dynamic lake environments. *New Zealand J. Mar. Fresh. Res.* 21, 379–390. doi: 10.1080/00288330.1987.9516234

Reynolds, C. S. (2006). *Ecology of Phytoplankton*. Cambridge: Cambridge University Press, 55.

Rinta-Kanto, J. M., Saxton, M. A., DeBruyn, J. M., Smith, J. L., Marvin, C. H., Krieger, K. A., et al. (2009). The diversity and distribution of toxigenic *Microcystis* spp. in present day and archived pelagic and sediment samples from lake erie. *Harmful Algae* 8, 385–394. doi: 10.1016/j.hal.2008.08.026

Rowe, M. D., Anderson, E. J., Wynne, T. T., Stumpf, R. P., Fanslow, D. L., Kijanka, K., et al. (2016). Vertical distribution of buoyant *Microcystis* blooms in a Lagrangian particle tracking model for short-term forecasts in lake erie. *J. Geophys. Res.* 121, 5296–5314. doi: 10.1002/2016jc011720

Sandrini, G., Jakupovic, D., Matthijs, H., and Huisman, J. (2015). Strains of the harmful cyanobacterium *Microcystis aeruginosa* differ in gene expression and activity of inorganic carbon uptake systems at elevated CO2 levels. *Appl. Environ. Microbiol.* 81, 7730–7739. doi: 10.1128/AEM.02295-15

Sandrini, G., Matthijs, H., Verspagen, J., Muyzer, G., and Huisman, J. (2014). Genetic diversity of inorganic carbon uptake systems causes variation in CO2 response of the cyanobacterium *Microcystis*. *ISME J.* 8, 589–600. doi: 10.1038/ismej.2013.179

Sandrini, G., Tann, R. P., Schuurmans, J. M., van Beusekom, S. A., Matthijs, H. C., and Huisman, J. (2016). Diel variation in gene expression of the CO2-concentrating mechanism during a harmful algal bloom. *Front. Microbiol.* 7:551. doi: 10.3389/fmicb.2016.00551

Speziale, B. J., Schreiner, S. P., Giammatteo, P. A., and Schindler, J. E. (1984). Comparison of N,N-dimethyl-formamide, dimethylsulfoxide, and acetone for extraction of phytoplankton chlorophyll. *Can. J. Fish. Aquat. Sci.* 41, 1519–1522. doi: 10.1139/f84-187

Steffen, M., Dearth, S., Dill, B., Zhou, L., Larsen, K., Campagna, S., et al. (2014). Nutrient driven transcriptional changes that maintain metabolic homeostasis but alter genome architecture in *Microcystis*. *ISME J.* 8, 2080–2092. doi: 10.1038/ismej.2014.78

Steffen, M. M., Belisle, B. S., Watson, S. B., Boyer, G. L., and Wilhelm, S. W. (2014). Status, causes and consequences of cyanobacterial blooms in lake erie. *J. Great Lakes Res.* 40, 215–225. doi: 10.1016/j.jglr.2013.12.012

Steffen, M. M., Davis, T. W., McKay, R. M., Bullerjahn, G. S., Krausfeldt, L. E., Stough, J. M. A., et al. (2017). Ecophysiological examination of the lake erie *Microcystis* bloom in 2014: linkages between biology and the water supply shutdown of Toledo, Ohio. *Environ. Sci. Technol.* 20, 6745–6755. doi: 10.1021/acs.est.7b00856

Straub, C., Quillardet, P., Vergalli, J., Tandeau de Marsac, N., and Humbert, J. F. (2011). A day in the life of *Microcystis aeruginosa* strain PCC 7806 as revealed by a transcriptomic analysis. *PLoS One* 6:e16208. doi: 10.1371/journal.pone.0016208

Sweeney, B. M. (2013). *Rhythmic Phenomena in Plants*. Cambridge, MA: Academic Press, 171.

Takada, K., Hanawa, K., Lee, S. G., Himeno, H., and Muto, A. (2002). The structure and function of tmRNA. *Nucleic Acids Res. Suppl.* 2, 65–66.

Valladares, A., Montesinos, M., Herrero, A., and Flores, E. (2002). An ABC-type, high affinity urea permease identified in cyanobacteria. *Mol. Microbiol.* 43, 703–715. doi: 10.1046/j.1365-2958.2002.02778.x

Verspagen, J., Van de Waal, D., Finke, J., Visser, P., Van Donk, E., and Huisman, J. (2014). Rising CO2 levels will intensify phytoplankton blooms in eutrophic and hypereutrophic lakes. *PLoS One* 9:e104325. doi: 10.1371/journal.pone.0104325

Visser, P. M., Verspagen, J. M. H., Sandrini, G., Stal, L. J., Matthijs, H. C. P., and Davis, T. W. (2016). How rising CO2 and global warming may stimulate harmful cyanobacterial blooms. *Harmful Algae* 54, 145–159. doi: 10.1016/j.hal.2015.12.006

Watson, S. B., McCauley, E., and Downing, J. A. (1997). Patterns in phytoplankton taxonomic composition across temperate lakes of differing nutrient status. *Limnol. Oceanogr.* 42, 487–495. doi: 10.4319/lo.1997.42.3.0487

Welkie, D. G., Rubin, B. E., Diamond, S., Hood, R. D., Savage, D. F., and Golden, S. S. (2019). A hard day's night: cyanobacteria in diel cycles. *Trends Microbiol.* 27, 231–242. doi: 10.1016/j.tim.2018.11.002

Wickham, H. (2016). *ggplot2: Elegant Graphics for Data Analysis*. New York, NY: Springer-Verlag.

Wickham, H., and Henry, L. (2018). *tidyr: Easily Tidy Data with 'Spread()' and 'Gather()' Functions. R Package Version 0.8.3*.

Wolf, D., and Klaiber, H. A. (2017). Bloom and bust: toxic algae's impact on nearby property values. *Ecol. Econ.* 135, 209–221. doi: 10.1016/j.ecolecon.2016.12.007

Wyman, M. (1999). Diel rhythms in ribulose-1,5-bisphosphate carboxylase/oxygenase and glutamine synthetase gene expression in a natural population of marine picoplanktonic cyanobacteria (*Synechococcus* spp.). *Appl. Environ. Microbiol.* 65, 3651–3659.

Xu, Y., Mori, T., and Johnson, C. H. (2003). Cyanobacterial circadian resonance energy transfer (BRET) system: application to interacting circadian clock proteins. *Proc. Nat. Acad. Sci. U.S.A.* 96, 151–156. doi: 10.1073/pnas.96.1.151

Conflict of Interest Statement: The authors declare that the research was conducted in the absence of any commercial or financial relationships that could be construed as a potential conflict of interest.

Copyright © 2019 Davenport, Neudeck, Matson, Bullerjahn, Davis, Wilhelm, Denney, Krausfeldt, Stough, Meyer, Dick, Johengen, Lindquist, Tringe and McKay. This is an open-access article distributed under the terms of the Creative Commons Attribution License (CC BY). The use, distribution or reproduction in other forums is permitted, provided the original author(s) and the copyright owner(s) are credited and that the original publication in this journal is cited, in accordance with accepted academic practice. No use, distribution or reproduction is permitted which does not comply with these terms.

frontiers in Microbiology

ORIGINAL RESEARCH
published: 25 September 2019
doi: 10.3389/fmicb.2019.02202

Evidence for the Primary Role of Phytoplankton on Nitrogen Cycle in a Subtropical Reservoir: Reflected by the Stable Isotope Ratios of Particulate Nitrogen and Total Dissolved Nitrogen

*Yangyang Cai[1,2], Yingjie Cao[1,2] and Changyuan Tang[1,2,3]**

[1] School of Environmental Sciences and Engineering, Sun Yat-sen University, Guangzhou, China, [2] Guangdong Provincial Key Laboratory of Environmental Pollution Control and Remediation Technology, Sun Yat-sen University, Guangzhou, China, [3] School of Geography and Planning, Sun Yat-sen University, Guangzhou, China

Knowledge about the primary factor controlling stable isotope ratios of particulate nitrogen ($\delta^{15}N_{PN}$) and total dissolved nitrogen ($\delta^{15}N_{TDN}$) in a subtropical reservoir can improve the understanding of regional and global nitrogen cycles. Taking Lianhe Reservoir as a representative subtropical reservoir, we studied the spatial and temporal distributions of $\delta^{15}N_{PN}$ and$\delta^{15}N_{TDN}$ and their relationships with the surrounding physicochemical factors and phytoplankton. The results showed that variations in $\delta^{15}N_{PN}$ and $\delta^{15}N_{TDN}$ followed seasonal thermal cycles. The values of $\delta^{15}N_{TDN}$ were inversely proportional to those of $\delta^{15}N_{PN}$. PCA showed that phytoplankton cell density and pH were the primary drivers of the variation of $\delta^{15}N_{PN}$ (45.2%). The primary factors influencing $\delta^{15}N_{TDN}$ were Chl *a* and phytoplankton cell density, which both indicated phytoplankton biomass. We also determined that the dominant species was *Microcystis densa* during the thermal stratification period and *Staurodesmus aristiferus* during the mixing period. Laboratory experiments showed that $\delta^{15}N_{PN}$ values in both *M. densa* (from 19.5 to 14.6‰) and *S. aristiferus* (from 19.4 to 16.0 ‰) media decreased significantly as the algal cells grew. Furthermore, the $\delta^{15}N_{TDN}$ values increased from 4.9 to 7.9‰ and from 4.7 to 6.9‰ in *M. densa* and *S. aristiferus* media, respectively, when the $\delta^{15}N_{PN}$ values decreased. These experimental results were consistent with field investigation results and indicated that variations in $\delta^{15}N_{PN}$ and $\delta^{15}N_{TDN}$ were mainly controlled by phytoplankton cell density, especially the cell density of the dominant species, in both the thermal stratification and mixing periods. The results also suggested that cell density, not phytoplankton species, was the key factor regulating the distribution of nitrogen stable isotopes. These results together indicated that phytoplankton cell density is the primary factor in the regulation of nitrogen stable isotope composition and that its influence is greater than that of other physical and chemical factors. This study provided detailed information supporting the primary role of phytoplankton in the nitrogen geochemical cycle and improved the understanding of biochemical processes in natural subtropical reservoirs.

Keywords: phytoplankton, nitrogen stable isotope, subtropical reservoirs, nitrogen cycle, microbial ecology

OPEN ACCESS

Edited by:
Haihan Zhang,
Xi'an University of Architecture and Technology, China

Reviewed by:
Sang Heon Lee,
Pusan National University, South Korea
Ming Li,
Northwest A& F University, China

****Correspondence:***
Changyuan Tang
tangchy3@mail.sysu.edu.cn;
abbeycai@sina.com

Specialty section:
This article was submitted to Aquatic Microbiology, a section of the journal Frontiers in Microbiology

Received: *17 July 2019*
Accepted: *09 September 2019*
Published: *25 September 2019*

Citation:
Cai Y, Cao Y and Tang C (2019) Evidence for the Primary Role of Phytoplankton on Nitrogen Cycle in a Subtropical Reservoir: Reflected by the Stable Isotope Ratios of Particulate Nitrogen and Total Dissolved Nitrogen. Front. Microbiol. 10:2202. doi: 10.3389/fmicb.2019.02202

INTRODUCTION

Nitrogen pollution has become a serious environmental problem in aquatic ecosystems worldwide (Smith and Schindler, 2009). Large amounts of industrial, agricultural, and urban nitrogen pollutants are discharged into rivers, reducing water quality (Bu et al., 2011; Chen et al., 2019). These increased nitrogen loadings in rivers flow into lakes and reservoirs, causing algal biomass development, and even algal blooms (Dodds et al., 2009; Gao et al., 2018). Sewage pollutants heavy in nitrogen in wastewater treatment plants are removed by denitrifying bacteria (Zhang et al., 2019). The microbial community in aquatic ecosystems is closely related to nitrogen migration and transformation.

The nitrogen stable isotope ratio ($\delta^{15}N$) is an effective tool for studying the nitrogen (N) cycle in aquatic systems. $\delta^{15}N$ is also used as a tracer for detecting the distribution of pollutants and the amplification of biological effects on pollutants. $\delta^{15}N$ can produce an integrative picture of chemical and biochemical N transformations (Waser et al., 1998; Granger et al., 2004). Therefore, the N stable isotope ratios of particulate nitrogen ($\delta^{15}N_{PN}$) and total dissolved nitrogen ($\delta^{15}N_{TDN}$) can be used to assess nitrogen sources and various nitrogen cycling processes, such as nitrification and denitrification, the uptake of nitrogen by phytoplankton and even food chains and biological webs (Lehmann et al., 2004; Hadas et al., 2009). There are different $\delta^{15}N$ compositions in rivers, lakes, reservoirs and marine regions, because of characteristic living organisms and inanimate matter. Many studies have suggested that variations in $\delta^{15}N_{PN}$ and $\delta^{15}N_{TDN}$ are associated with thermal and hydrological characteristics, trophic states, nitrogen sources, N_2 fixation, and phytoplankton abundance (Altabet, 2006; Gu et al., 2006, Gu, 2009; Gu and Schelske, 2010; Hou et al., 2013). However, the key factors that control variations in $\delta^{15}N_{PN}$ and $\delta^{15}N_{TDN}$ are not well understood. Clear and strong evidence for phytoplankton directly regulating the distribution of $\delta^{15}N_{PN}$ and $\delta^{15}N_{TDN}$ is still needed.

Phytoplankton, responsible for the primary productivity in aquatic systems, uptakes and assimilates nitrogen for photosynthesis and the biosynthesis of macromolecules, such as proteins, nucleic acids, and chlorophyll (Gao et al., 2018). These processes influence the nitrogen stable isotope composition in the water column (Needoba and Harrison, 2004). Sachs et al. (1999) showed that when nitrogen is sufficient in water column, algal cells preferentially absorb ^{14}N, increasing the proportion of $^{15}N_{TDN}$ and decreasing the proportion of $^{15}N_{PN}$. However, when nitrogen is exhausted, algae preferentially absorb ^{15}N, which weakens the fractionation of nitrogen stable isotopes. Nutrient supply, light intensity, phytoplankton species and nitrogen type are suggested to affect the $^{15}N/^{14}N$ uptake of phytoplankton (Waser et al., 1999; Doi et al., 2004). However, the effect of phytoplankton biomass on the absorption of ^{15}N in a subtropical reservoir is still unclear.

In contrast to natural rivers and lakes, subtropical reservoirs are artificial aquatic systems with unique hydrological characteristics that experience the thermal stratification and mixing periods. Many subtropical reservoirs with similar hydrological and biochemical environments have experienced large-scale algal blooms, especially cyanobacterial blooms (**Table 1**). Lianhe Reservoir, located in a subtropical marine monsoon climate region, has also experienced a large outbreak of cyanobacteria. The temporal and spatial distributions of nitrogen in reservoirs are different from those before outbreaks because of the absorption and assimilation by large amounts of phytoplankton. The $\delta^{15}N_{PN}$ and $\delta^{15}N_{TDN}$ in the water column also change. Many studies have indicated the important role of phytoplankton in varying $\delta^{15}N_{PN}$ and $\delta^{15}N_{TDN}$ in rivers, lakes and marine areas (Sugimoto et al., 2014; Liu et al., 2017; Kharbush et al., 2019). However, the trends in $\delta^{15}N_{PN}$ and $\delta^{15}N_{TDN}$ in subtropical reservoirs might be less predictable than those listed above (Hou et al., 2013). Therefore, with Lianhe Reservoir as a classic example of a subtropical reservoir, it is necessary to study the relationship between phytoplankton cell density and seasonal variations in $\delta^{15}N_{PN}$ and $\delta^{15}N_{TDN}$. Our hypothesis is that phytoplankton cell density was the primary key factor controlling the temporal and spatial distributions of $\delta^{15}N_{PN}$ and $\delta^{15}N_{TDN}$ in subtropical reservoirs.

To comprehensively test our hypothesis, we carried out field surveys and laboratory experiments. The objective was to explore whether phytoplankton cell density plays a primary role in nitrogen migration and transformation that is more important than the roles of other physical and chemical factors. To fulfill our objective, we (1) investigated temporal and spatial variations in $\delta^{15}N_{PN}$ and $\delta^{15}N_{TDN}$, the phytoplankton community, and other physical, chemical and biological factors in Lianhe Reservoir; (2) analyzed the relationships between $\delta^{15}N_{PN}$, $\delta^{15}N_{TDN}$, phytoplankton and other physicochemical factors; and (3) used experiments to show that phytoplankton cell density was the key factor affecting variations in $\delta^{15}N_{PN}$ and $\delta^{15}N_{TDN}$. These results provide detailed information supporting the important role of phytoplankton in the nitrogen geochemical cycle and improve the understanding of the biochemical processes in subtropical reservoirs.

MATERIALS AND METHODS

Study Area

Lianhe Reservoir (23°17′57.2″N and 113°55′8.8″E), located in Guangdong Province, South China, is a typical canyon-shaped reservoir in the subtropical marine monsoon region (**Figure 1**). The catchment area is 110.8 km^2 with plenty of rainfall and heat in summer, and warmth and dryness in winter. The annual average rainfall and temperature is 1932.7 mm and 21.8°C, respectively. The dam was built in the southwest part of the study area in the 1970s, forming the reservoir with a surface area of 3.33 km^2 and a storage capacity of 8.2×10^7 m^3. Lianhe Reservoir serves multiple purposes, including irrigation, hydroelectric power generation, flood control, and especially drinking water supply.

The hills surrounding the reservoir are covered with pine and spruce on the east side and eucalyptuses on the other sides. A small river K (stations Y2) flows into the reservoir. Another small river M (station Y4) flows into the reservoir from Daogutian village (**Figure 1**).

TABLE 1 | Comparing the water temperature (WT, °C), dissolved oxygen (DO, mg l^{-1}), NO_3^--N (mg l^{-1}), NH_4^+-N (mg l^{-1}), total nitrogen (TN, mg l^{-1}), total phosphorus (TP, mg l^{-1}), and dominant algae during the thermal stratification period between the Lianhe Reservoir and other subtropical reservoirs.

Reservoirs	WT	DO	NO_3^--N	NH_4^+-N	TN	TP	Dominant algae	Location	References
Lianhe	30.5	8.4	1.3	0.3	3.8	0.07	Cyanobacteria	China	–
Salto Grande	27	7.5	–	–	2.9	0.02	Cyanobacteria	Aragentina	O'Farrell et al., 2012
Caxias	30.4	7.6	0.4	0.1	1.41	0.01	Cyanobacteria	Brazil	Wojciechowski et al., 2017
Chopim	29.2	7.1	0.4	0.1	1.28	0.04	Cyanobacteria		
Tingxi	30	5	2	0.1	5.5	0.14	Cyanobacteria	China	Lv et al., 2014
Shidou	33.1	5.4	0.05	0.03	5.5	0.02	Cyanobacteria		Yang et al., 2012
Bantou	32.3	5.3	0.01	0.03	6.1	0.03	Cyanobacteria		
Fengtou	31.2	4.9	5.7	0.1	6.5	0.03	Cyanobacteria		

Field Sampling and Methods

Water samples of Lianhe Reservoir were taken from stations X1 to X5 each month in 2017 (**Figure 1**). Because the depths at stations X1 and X2 were very shallow (<1.3 m), only surface (0.5 m) water (1000 ml) was collected there. Stations X3 and X5 were located in the deepest parts of the reservoir, with a depth of approximately 30 m, and station X5 was also near the dam where the water intake was positioned. Therefore, water samples (1000 ml) at the surface and 3, 5, 7, 10, 13, 15, 17, 20, 25, and 30 m below the surface were collected. The water at station X4 had a depth of approximately 16 m, and water samples (1000 ml) at 0.5, 5, 10, and 15 m below the surface were collected. The water columns at stations Y2 and Y4 were very shallow (<1.5 m), therefore, only surface water was collected there.

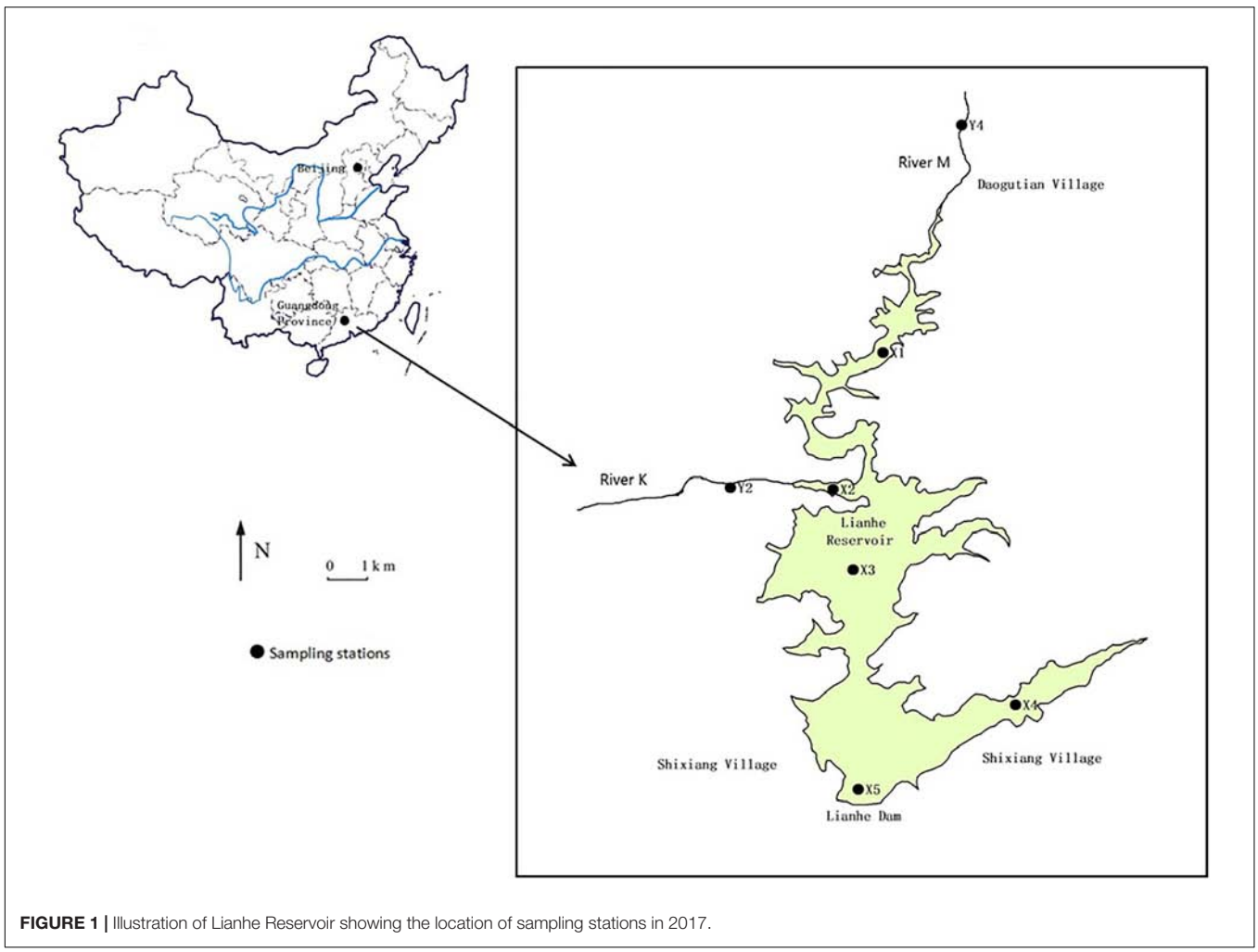

FIGURE 1 | Illustration of Lianhe Reservoir showing the location of sampling stations in 2017.

The water temperature, pH and dissolved oxygen (DO) profiles were measured *in situ* using a multi-parameter water quality meter EXO2 (YSI, United States). Water samples for chemical and isotope analysis were collected in pre-sterilized 1 l polyethylene bottles in triplicate from these stations. The samples were transported to the laboratory as soon as possible and stored at 4°C. Before analysis, the water samples were filtered through pre-combusted (450°C, 2 h) GF/F filters.

Water samples for determining the phytoplankton species were collected in triplicate in 1 l polyethylene bottles. The samples were collected from the surface to a depth of 30 m in the reservoir. The samples of phytoplankton were preserved with acidic Lugol's iodine solution (2% final concentration) *in situ* for later enumeration using a sedimentation technique. Phytoplankton samples were stored in polypropylene vials at 4°C before taxonomical analysis.

Quantitative zooplankton samples were collected as a 5 l water samples at each station from the surface to a depth of 30 m in the reservoir. Samples were filtered through a mesh of 64 μm to form an integrated sample. Vertical hauls were also made with 64 and 113 μm meshes. These zooplankton samples were preserved with 4% formaline and stored in polypropylene vials at 4°C before taxonomical analysis.

Total nitrogen (TN), NO_3^--N, and NH_4^+-N analyses were carried out using standard combined persulfate digestion methods for water quality (American Public Health Association [APHA] et al., 1989). The chlorophyll *a* (Chl *a*) concentrations were determined by a spectrofluorometer (Hitachi U-2810, United States) after extraction in 90% ethanol and filtering with glass microfiber filters (Whatman GF/F) (Pápista et al., 2002).

The phytoplankton samples were settled for 48 h by adding Lugol's solution, and gradually enriched to 10 ml. The cell density was measured with a Sedgwick-Rafter counting chamber under a fluorescence microscope at 200–400× magnification (Olympus, Japan). At least 100 individual cells from every abundant taxon were counted in each sample. Phytoplankton species were identified, as suggested by Hu and Wei (2006).

The identification of zooplankton was carried out by qualified Aquatic Biology Center (Jinan University, Guangzhou). The samples were counted (75× magnification) and taxonomically identified (150× magnification) as Rotifera, Cladocera, and Copepoda species (Wang, 1961; Chiang and Du, 1979; Shen, 1979), using a stereo microscope (Nikon, Japan).

Algal Strain and Culture Conditions

Strains of *Microcystis densa* (No. MD-1) and *Staurodesmus aristiferus* (No. SA-1) were isolated from the water column of Lianhe Reservoir in July and January 2017, respectively, and were maintained in the algal collection at the School of Environmental Science and Technology, Sun Yat-sen University, China.

Prior to the experiment, the cultures were re-inoculated three times during the exponential phase in BG-11 media (Stanier et al., 1971) and had final nitrogen concentrations of approximately 4 mg l^{-1}. The cultures were maintained at 28 ± 1°C for *M. densa* and at 15 ± 1°C for *S. aristiferus*, in a light dark cycle of 12:12 with an irradiation of 100 μmol photons m^{-2} s^{-1}. Antibiotics including penicillin G and streptomycin sulfate, were used to exclude bacterial contamination 48 h before the next inoculation (Guillard, 1973). The cultures were checked for bacterial contamination by 4′,6-diamidino-2-phenylindole (DAPI) (Sigma) staining at regular intervals by microscopic inspection.

Laboratory Experiments

The initial cell densities of *M. densa* and *S. aristiferus* in the media were both ∼4.5 × 10^5 cells ml^{-1}. NO_3^--N was added as the substrate with final concentrations of ∼1.4 mg N l^{-1}. To simulate actual field conditions as much as possible, the treatments were incubated at 28 ± 1°C for *M. densa* and at 15 ± 1°C for *S. aristiferus* with an irradiation of 100 μmol photons m^{-2} s^{-1}. These conditions were consistent with the actual water temperature and light intensity recorded in the field. These treatments were performed in triplicate.

Samples for the cell counts were obtained daily with fixation in a 2% acid Lugol's solution. Cell density was measured with a Sedgwick-Rafter counting chamber under a light inverted microscope (Olympus, Japan). The specific growth rates (μ, d^{-1}) of *M. densa* and *S. aristiferus* were calculated according to the following equation:

$$\mu = \frac{\ln N_2 - \ln N_1}{t_2 - t_1} \quad (1)$$

where N_2 and N_1 were the cell densities at respective time, t_2 and t_1.

Samples for the Chl *a* and NO_3^--N analyses were obtained daily in triplicate. Fifty ml Chl *a* samples were determined by a spectrofluorometer (Hitachi U-2810, United States) after extraction in 90% ethanol and filtering with glass microfiber filters (Whatman GF/F) (Pápista et al., 2002). Hundred ml NO_3^--N samples were filtered through pre-combusted (450°C, 2 h) GF/F filters and measured according to the APHA method (1989).

Stable Isotope Ratios for the PN and TDN Analyses

One liter and 250 ml water samples were required for $\delta^{15}N_{PN}$ measurements of the field and laboratory water samples, respectively. The samples were filtered through precombusted (450°C, 2 h) GF/F filters. After drying at 60°C for 48 h, the cell particulate samples for $\delta^{15}N_{PN}$ were scraped off the membrane with a small blade. The samples were stored in tin capsules for measurement.

One liter and 250 ml water samples were also filtered through precombusted (450°C, 2 h) GF/F filters for $\delta^{15}N_{TDN}$ measurements of the field and laboratory samples, respectively. These water samples for $\delta^{15}N_{TDN}$ were freeze-dried at −80°C for 72 h to a powder and stored in tin capsules for measurement.

Three sediment cores were taken at each station in the reservoir for $\delta^{15}N_{PN}$ measurements using a Mackereth corer (Mackereth, 1969). These sediments were retrieved from a depth of 0 ∼ 5 cm (Glew et al., 2001). Three replicate sediment cores were composited into one sample. After sampling, the cores were subsampled in the laboratory at 1 cm intervals. These sediment

samples were freeze-dried at −80°C for 72 h. The dried sediment samples were then ground in an agate grinder and sieved through a 0.149 mm mesh, and stored in tin capsules until isotope analysis.

All $\delta^{15}N_{PN}$ and $\delta^{15}N_{TDN}$ samples were measured by continuous flow isotope ratio mass spectrometry using a Flash 2000 elemental analyzer coupled to a Thermo Fisher Delta Plus XP IRMS (Thermo Fisher, United States). The results were expressed in the delta notation as follows:

$$\delta^{15}N(‰) = [\left(\frac{\frac{^{15}N}{^{14}N_{sample}}}{\frac{^{15}N}{^{14}N_{reference}}}\right) - 1] \times 10^3 \quad (2)$$

The $\delta^{15}N_{PN}$ measurements were calibrated against the international standard of atmospheric N_2. The standard deviation (S.D.) for the analytical standards was approximately ± 0.2‰.

Statistical Analysis

A one-way ANOVA with a Tukey test was performed to compare the differences and correlations among each parameter. A *P*-value < 0.05 was regarded as significant and <0.01 as highly significant for all tests. Principal component analysis (PCA) was used to determine the environmental variables that explain the largest per cent variance in $\delta^{15}N_{PN}$ and $\delta^{15}N_{TDN}$. Prior to the analysis, untransformed data in all cases were tested for normality and homogeneity of variation. Statistical analyses was performed using the SPSS 19.0 statistical package for personal computers (SPSS, United States).

RESULTS

Spatial and Temporal Variations in the Hydrographic and Biogeochemical Properties Within the Reservoir

Thermal stratification occurred from March to November (the thermal stratification period) and was absent in December, January and February (the mixing period) when the vertical temperature difference in the water column was small (**Figure 2**, WT). During the thermal stratification period, the water temperature (WT) was high, ranging from 27.3 ± 0.1 to 32.2 ± 0.1°C in the epilimnion but approximately 9.3 ± 0.2 to 12.4 ± 0.1°C in the hypolimnion. The thermocline was at a depth of approximately 20 m. During the mixing period, the WT was approximately 10°C in the whole water column.

The pH values were significantly higher during the thermal stratification period than during the mixing period ($p < 0.05$) (**Figure 2**, pH). The values from the surface to a depth of 6 m (7.2 ± 0.3 ∼ 9.2 ± 0.2) were significantly higher than those in other layers during the thermal stratification period, indicating a distinct stratified state ($p < 0.05$). The pH values (approximately 6.9 ± 0.3) were not stratified during the mixing period.

In the surface of the water column, the DO content was sufficient, ranging from 5.9 ± 0.4 to 11.2 ± 0.2 mg l^{-1}. During the thermal stratification period, the epilimnion was even hypersaturated at times (from 8.5 ± 0.3 to 10.5 ± 0.2 mg l^{-1}), but the DO content was below 2.5 ± 0.2 mg l^{-1} in the hypolimnion. Especially from June to November, DO concentrations in the

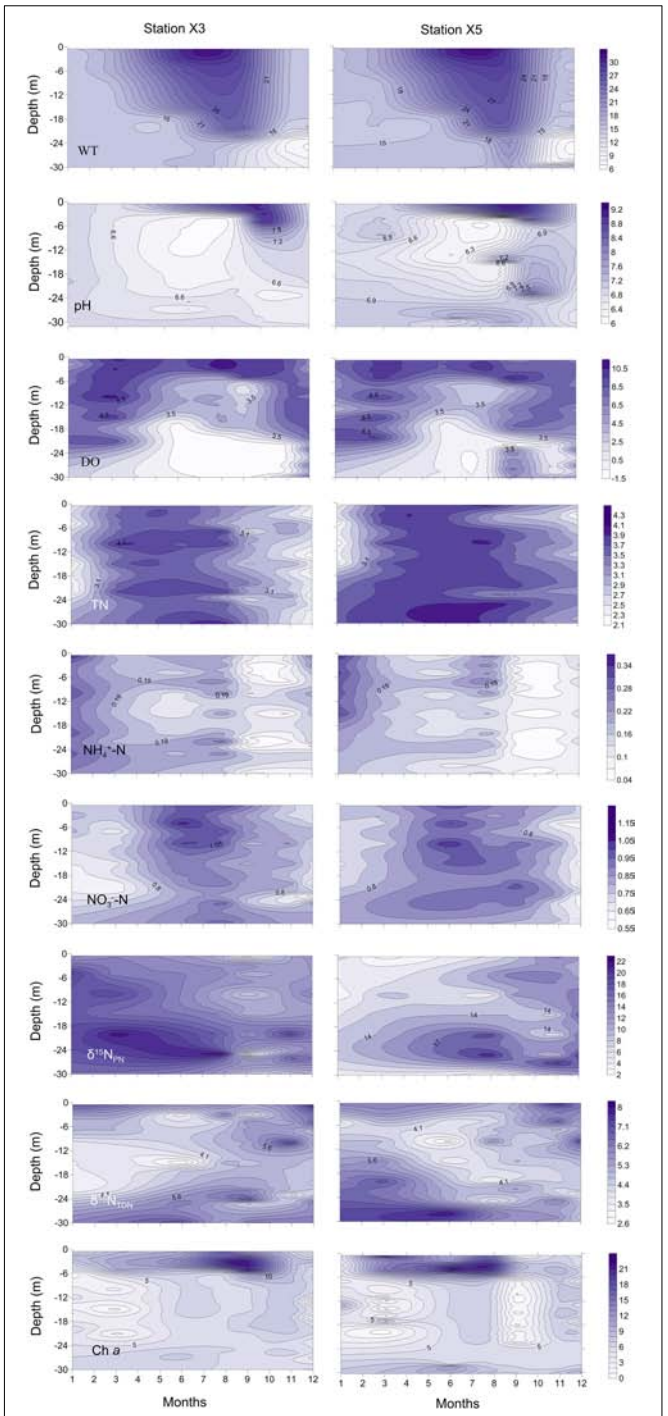

FIGURE 2 | Vertical profiles of the water temperature (WT, °C), pH, dissolved oxygen (DO, mg l^{-1}), total nitrogen (TN, mg l^{-1}), ammonia (NH_4^+-N, mg l^{-1}), nitrate (NO_3^--N, mg l^{-1}), particulate nitrogen stable isotope ratios ($\delta^{15}N_{PN}$, ‰), total dissolved nitrogen stable isotope ratios ($\delta^{15}N_{TDN}$, ‰) and chlorophyll *a* (Chl *a*, μg l^{-1}) at stations X3 and X5 in 2017 in the Lianhe Reservoir.

hypolimnion can be as low as 0 mg l^{-1}, forming an anoxic closed region. The oxycline occurred within the thermocline at a depth of approximately 16–20 m. DO was relatively abundant at the bottom during the mixing period. Vertical DO stratification was not obvious (**Figure 2**, DO).

The concentrations of TN were not vertically stratified year round (**Figure 2**, TN). The concentrations were approximately 3.1 ± 0.4 to 4.3 ± 0.2 mg l^{-1} during the thermal stratification period and 2.1 ± 0.3 to 3.1 ± 0.1 mg l^{-1} during the mixing period. TN concentrations during the thermal stratification period were higher than those during the mixing period ($p < 0.05$).

The concentrations of NO_3^--N were much higher than the concentrations of NH_4^+-N, indicating that NO_3^--N is the primary source of inorganic nitrogen in the reservoir (**Figure 2**, NO_3^--N and NH_4^+-N). The NO_3^--N concentration during the thermal stratification period was approximately 0.75 ± 0.01 ∼ 1.20 ± 0.01 mg l^{-1}, which was significantly higher than that (0.55 ± 0.02 ∼ 0.75 ± 0.01 mg l^{-1}) during the mixing period (**Figure 2**, NO_3^--N) ($p < 0.05$). The highest concentrations of NH_4^+-N (0.34 ± 0.03 mg l^{-1}) were detected in January, while the lowest concentrations (0.04 ± 0.01 mg l^{-1}) occurred from September to November (**Figure 2**, NH_4^+-N). Neither the NO_3^--N nor the NH_4^+-N concentrations changed significantly with depth ($p > 0.05$).

During the thermal stratification period, the vertical profile of $\delta^{15}N_{PN}$ varied dramatically (**Figure 2**, $\delta^{15}N_{PN}$). The $\delta^{15}N_{PN}$ values in the hypolimnion (16.3 ± 0.3 ∼ 22.7 ± 0.5‰) were significantly higher than those in the epilimnion (2.0 ± 0.1 ∼ 16.4 ± 0.3‰) ($p < 0.05$). During the mixing period, the $\delta^{15}N_{PN}$ value varied little with depth (**Figure 2**, $\delta^{15}N_{PN}$).

The values of $\delta^{15}N_{TDN}$ were significantly lower than the values of $\delta^{15}N_{PN}$ ($p < 0.05$), ranging from 2.6 ± 0.3 to 8.0 ± 0.4‰ (**Figure 2**, $\delta^{15}N_{TDN}$). The $\delta^{15}N_{TDN}$ values were approximately 5.2 ± 0.2 ∼ 7.9 ± 0.1‰ at the surface and approximately 4.6 ± 0.2 ∼ 8.0 ± 0.4‰ at the bottom. The average value of $\delta^{15}N_{TDN}$ during the mixing period (3.7 ± 0.3‰) was higher than that during the thermal stratification period (6.1 ± 0.1‰) (**Figure 2**, $\delta^{15}N_{TDN}$).

Chl *a*, a common pigment in phytoplankton cells, is often used as an environmental index to characterize phytoplankton biomass. The Chl *a* concentration was high (6.1 ± 0.2 ∼ 22.3 ± 0.2 μg l^{-1}) from the surface water to a depth of 6 m, where most phytoplankton gathered (**Figure 2**, Chl *a*). The average concentration of Chl *a* during the thermal stratification period (12.3 ± 0.4 μg l^{-1}) was higher than that during the mixing period (4.6 ± 0.2 μg l^{-1}). The Chl *a* concentration was distributed evenly in the vertical direction during the mixing period (**Figure 2**, Chl *a*).

Phytoplankton Community and the Dominant Species

A total of 87 and 80 phytoplankton species were identified during the thermal stratification and mixing periods, respectively (**Supplementary Table S1**). *M. densa* and *S. aristiferus* were the dominant species during the thermal stratification and mixing periods in 2017, respectively (**Table 2**). During the mixing period, the maximum cell density of *S. aristiferus* was 6.3 ± 0.2 × 10^5 cells ml^{-1} in the surface water (January 2017). However, during the thermal stratification period, the maximum cell density of *M. densa* was 9.6 ± 0.2 × 10^5 cells ml^{-1} and occurred in the epilimnion, while *S. aristiferus* was still the dominant species in the hypolimnion, with a maximum cell density of 1.4 ± 0.1 × 10^5 cells ml^{-1} (August, 2017). The total cell densities of phytoplankton during the thermal stratification period were much higher than those during the mixing period (**Table 2**). The cell densities of dominant species accounted for 77 to 93% of the total cell densities of phytoplankton (**Table 2**).

Zooplankton Community

A total of 4 rotifera, 3 cladocera and 2 copepoda species were found during the thermal stratification period (**Supplementary Table S2**). During the mixing period, there were 7 Rotifera, 3 Cladocera and 3 Copepoda species in the reservoir (**Supplementary Table S2**). Zooplankton densities varied from 2 to 19 ind. l^{-1} and 7 to 27 ind. l^{-1} during thermal stratification and mixing periods, respectively, indicating that zooplankton were more abundant during the mixing period.

$\delta^{15}N_{PN}$ Values in Rivers and Sediments

The $\delta^{15}N_{PN}$ values from the surface water at stations X1 and X2 and the stations in rivers (Y2 and Y4) are also shown in **Table 3**. The $\delta^{15}N_{PN}$ values at X1 and X2, the two stations in the reservoir that were the closest to the river shore, varied from 4.9 ± 0.4 to 7.4 ± 0.2‰ and from 4.5 ± 0.3 to 6.9 ± 0.7‰, respectively. The $\delta^{15}N_{PN}$ values at Y2 and Y4, the two stations in the rivers and close to the reservoir, ranged from 1.4 ± 0.3 to 5.7 ± 0.3‰ and from 4.2 ± 0.4 to 5.7 ± 0.4‰, respectively. The $\delta^{15}N_{PN}$ values from the rivers (Y2 and Y4) were much lower than those at reservoir stations X1 and X2 (**Table 3**).

The $\delta^{15}N_{PN}$ values of sediments at different depths at stations X1 ∼ X5 were also measured (**Table 4**). There were small differences in these $\delta^{15}N_{PN}$ values among depths and stations ($p > 0.05$). The average value of $\delta^{15}N_{PN}$ was 3.0 ± 0.5 ‰. However, the $\delta^{15}N_{PN}$ values in the sediment (2.3 ± 0.2 ∼ 3.8 ± 0.2‰) were much lower than those in the bottom of the water column, especially at station X3 ($p < 0.05$).

The Relationships Between $\delta^{15}N_{PN}$, $\delta^{15}N_{TDN}$ and Phytoplankton in the Field

The $\delta^{15}N_{PN}$ values in the reservoir were negatively correlated with the $\delta^{15}N_{TDN}$ and Chl *a* concentrations (**Figures 3A–D**) and positively correlated with the TN concentrations (**Figures 3E,F**) in both the thermal stratification and mixing periods. These results indicate that phytoplankton biomass is potentially the primary factor affecting the variations in $\delta^{15}N_{PN}$ in the reservoir.

PCA of $\delta^{15}N_{PN}$, $\delta^{15}N_{TDN}$ and the associated environmental variables revealed three principal components (PCs) with eigenvalues greater than 1.0 (**Table 5**). The first principal component (PC1) for $\delta^{15}N_{PN}$ included phytoplankton cell densities and pH, and explained 45.2% of the variance in the dataset. The second principal component (PC2) for $\delta^{15}N_{PN}$ included DO, TN and Chl *a*, and explained 26.3% of the variance.

TABLE 2 | Dominant species of phytoplankton and their cell densities/total cell densities of phytoplankton ($\times 10^5$ cells ml^{-1}) at stations X3 and X5 at a water layer depth of 0.5, 10, and 20 m during thermal stratification (e.g., August) and mixing periods (e.g., January) in 2017 at Lianhe Reservoir.

Depth (m)	Mixing period (e.g., January)		Thermal stratification period (e.g., August)	
	X3	X5	X3	X5
0.5	*S. aristiferus* (6.3 ± 0.2/7.3 ± 0.3)	*S. aristiferus* (5.2 ± 0.3/5.7 ± 0.4)	*M. densa* (9.6 ± 0.2/10.3 ± 0.3)	*M. densa* (8.9 ± 0.3/9.7 ± 0.4)
10	*S. aristiferus* (3.1 ± 0.2/3.8 ± 0.2)	*S. aristiferus* (1.7 ± 0.1/2.2 ± 0.2)	*M. densa* (3.2 ± 0.1/3.7 ± 0.3)	*M. densa* (2.6 ± 0.1/2.8 ± 0.1)
25	*S. aristiferus* (1.3 ± 0.1/1.4 ± 0.1)	*S. aristiferus* (1.0 ± 0.0/1.3 ± 0.1)	*S. aristiferus* (1.3 ± 0.1/1.5 ± 0.1)	*S. aristiferus* (1.4 ± 0.1/1.7 ± 0.0)

The values are the mean ± SD (n = 3).

TABLE 3 | Seasonal variations of particulate nitrogen stable isotope ratios ($\delta^{15}N_{PN}$, ‰) in surface water of stations X1 and X2 in the reservoir, and stations Y2 and Y4 in the nearby rivers in 2017.

Months	X1	X2	Y2	Y4
January	6.9 ± 0.3	5.6 ± 0.6	5.2 ± 0.3	5.4 ± 0.5
February	7.0 ± 0.3	5.4 ± 0.1	4.8 ± 0.4	4.8 ± 0.9
March	7.4 ± 0.2	6.1 ± 0.3	5.5 ± 0.5	5.7 ± 0.4
April	6.2 ± 0.4	5.1 ± 0.2	4.4 ± 0.1	4.2 ± 0.3
May	5.9 ± 0.3	4.7 ± 0.4	3.2 ± 0.2	4.7 ± 0.4
June	5.7 ± 0.6	4.5 ± 0.3	1.4 ± 0.3	5.4 ± 0.6
July	5.7 ± 0.3	5.2 ± 0.4	2.3 ± 0.2	4.3 ± 0.2
August	6.0 ± 0.4	5.7 ± 0.3	4.1 ± 0.4	4.4 ± 0.2
September	4.9 ± 0.4	6.9 ± 0.7	5.7 ± 0.3	4.2 ± 0.4
October	5.0 ± 0.4	6.5 ± 0.8	2.8 ± 0.3	4.8 ± 0.7
November	6.1 ± 0.2	5.3 ± 0.2	4.4 ± 0.3	5.5 ± 0.2
December	6.7 ± 0.4	5.7 ± 0.3	2.5 ± 0.4	4.7 ± 0.6

The values are the mean ± SD (n = 3).

TABLE 4 | Nitrogen stable isotope ratios ($\delta^{15}N_{PN}$, ‰) at different depths of sediments at stations X1, X2, X3, X4, and X5 in Lianhe Reservoir.

Depths (cm)	X1	X2	X3	X4	X5
1	3.4 ± 0.3	2.7 ± 0.2	2.4 ± 0.2	2.7 ± 0.4	2.5 ± 0.3
2	3.0 ± 0.5	2.9 ± 0.3	3.2 ± 0.4	2.4 ± 0.2	2.3 ± 0.2
3	2.8 ± 0.4	3.1 ± 0.3	3.3 ± 0.1	3.8 ± 0.2	2.6 ± 0.1
4	3.2 ± 0.1	3.3 ± 0.3	3.6 ± 0.2	3.5 ± 0.2	2.7 ± 0.2
5	2.4 ± 0.1	2.8 ± 0.1	2.5 ± 0.1	3.4 ± 0.1	3.3 ± 0.2

The values are the mean ± SD (n = 3).

The third principal component (PC3) included NO_3^--N and WT, and explained 18.1% of the variance (**Table 5**). These three PCs together accounted for 89.6% of the variation for $\delta^{15}N_{PN}$ (**Figure 4A**). For $\delta^{15}N_{TDN}$, PC1 contained $\delta^{15}N_{PN}$ and Chl *a*, and explained 34.1% of the variance. PC2 contained phytoplankton cell density, NO_3^--N and TN, and explained 26.2% of the variance. PC3 contained WT, DO, and NH_4^+-N and explained 15.9% of the variance (**Table 5**). These three PCs together accounted for 76.2% of the variance in $\delta^{15}N_{TDN}$ (**Figure 4B**). However, $\delta^{15}N_{PN}$ and $\delta^{15}N_{TDN}$ were interacted with each other. $\delta^{15}N_{PN}$ can not be considered as a factor influencing $\delta^{15}N_{TDN}$. Moreover, both Chl *a* (represents phytoplankton biomass) and phytoplankton cell density indicated the phytoplankton abundance. Therefore, these two factors were equally important for variations in $\delta^{15}N_{TDN}$. These results showed that phytoplankton cell density was the primary factor controlling the variations in $\delta^{15}N_{PN}$ and $\delta^{15}N_{TDN}$.

Variations in $\delta^{15}N_{PN}$ and $\delta^{15}N_{TDN}$ in Cultures of *M. densa* and *S. aristiferus*

Both *M. densa* and *S. aristiferus* grew well, and the cell densities peaked on Days 5 ∼ 6 in the experiments (**Figures 5A,B**). The maximum cell density of *M. densa* was $6.9 \pm 0.5 \times 10^6$ cells l^{-1}, while that of *S. aristiferus* was $7.8 \pm 0.4 \times 10^6$ cells l^{-1}. Both *M. densa* and *S. aristiferus* cells entered the stationary phase after Day 7 and decreased in number after Day 17. The specific growth rates of *M. densa* decreased on Day 4, while that of *S. aristiferus* decreased on Day 5 (**Figures 5C,D**).

The $\delta^{15}N_{PN}$ values were negatively correlated with the Chl *a* concentration (**Figure 6A**) and positively correlated with the nitrogen concentrations (**Figure 6B**) in the cultures. Similar trends were found in the field (**Figure 3**), indicating that variations in $\delta^{15}N_{PN}$ in the reservoir were mainly determined by phytoplankton cell density, especially the dominant species cell density.

The values of $\delta^{15}N_{TDN}$ in the cultures of both *M. densa* and *S. aristiferus* increased (**Figures 7A,B**). In the stationary phase on Day 13, the maximum value of $\delta^{15}N_{TDN}$ was 7.9 ± 0.3‰ in the culture of *M. densa*, while that in the culture of *S. aristiferus* was 6.9 ± 0.2‰. However, the $\delta^{15}N_{PN}$ value decreased continuously and reached its lowest value on Day 11: 14.6 ± 0.3‰ in *M. densa* cultures and 16.0 ± 0.1‰ in *S. aristiferus* cultures (**Figures 7C,D**) indicating that the continuous growth of both *S. aristiferus* and *M. densa* can directly reduce $\delta^{15}N_{PN}$ and increase $\delta^{15}N_{TDN}$.

DISCUSSION

Factors Affecting Variations in $\delta^{15}N_{PN}$ and $\delta^{15}N_{TDN}$

In general, nitrogen in reservoirs can be divided into exogenous nitrogen, including that entering via atmospheric deposition

TABLE 5 | Principal components and eigenvalues for $\delta^{15}N_{PN}$ and $\delta^{15}N_{TDN}$ in Lianhe Reservoir based on the analysis using monthly values at each depth of stations X1 ∼ X5 in 2017.

	Component	Variables	Eigenvalues		
			Total	% of Variance	Cumulative%
$\delta^{15}N_{PN}$	1	Phytoplankton cell density, pH	2.9	45.2	45.2
	2	Chl *a*, TN, DO	1.7	26.3	75.1
	3	NO_3^-, WT	1.3	18.1	89.6
$\delta^{15}N_{TDN}$	1	$\delta^{15}N_{PN}$, Chl *a*	2.7	34.1	34.1
	2	NO_3^-, TN, phytoplankton cell density	2.1	26.2	60.3
	3	WT, DO, NH_4^+	1.3	15.9	76.2

and rivers, and endogenous nitrogen, which originates from denitrification, sediments and biological processes. These nitrogen sources influence variations in $\delta^{15}N_{PN}$ and $\delta^{15}N_{TDN}$ in reservoirs to different degrees.

Exogenous Factors

Nitrogen pollutants in the air, mainly nitrate and nitrite, enter the surface water of the reservoir by wet deposition. Because the nitrogen isotope fractionation in the atmosphere is different from that in the water column, atmospheric deposition changes the variation in $\delta^{15}N$ in the water column. However, the $\delta^{15}N_{TDN}$ values in the surface water of Lianhe Reservoir ranged from $4.5 \pm 0.3 \sim 7.4 \pm 0.2$‰, which are much different from of the values for wet deposition (Xiao and Liu, 2002; Elliott et al., 2007). This result indicated that nitrogen from atmospheric deposition made little contribution to the nitrogen stable isotope composition in Lianhe Reservoir.

Particulate matter from the shore can be washed into the reservoir via rivers during heavy rain events. However, our results showed that the $\delta^{15}N_{PN}$ in the rivers near the reservoir (stations Y2 and Y4) was lower than that in the surface water at the junctions of Lianhe Reservoir and the nearby rivers (stations X1 and X2) (**Table 3**). If nitrogen from rivers is the major controller of variation in $\delta^{15}N_{PN}$ in Lianhe Reservoir, the river $\delta^{15}N_{PN}$ value should be greater than or equal to the values in the reservoir. However, our investigation showed the opposite, suggesting that the effects of nitrogen from rivers on the variations in the $\delta^{15}N_{PN}$ values in the reservoir were not large as expected.

Endogenous Factors

Isotopic fractionation occurs during nitrogen migration and transformation. Sugimoto et al. (2010, 2014) suggested that the value of $\delta^{15}N_{PN}$ is principally determined by the dissolved inorganic nitrogen (DIN) concentration. Hou et al. (2013) suggested that TN is the primary driver of the change in $\delta^{15}N_{PN}$. However, in our study, the vertical profiles of TN, NO_3^--N, and NH_4^+-N changed little, but particulate and dissolved nitrogen stable isotope fractionation had already occurred (**Figure 2**). PCA revealed that the effects of TN, NO_3^--N, and NH_4^+-N on both $\delta^{15}N_{PN}$ and $\delta^{15}N_{TDN}$ were not significant (**Table 5**). Obviously, nitrogen concentration might affect the variations in $\delta^{15}N_{PN}$ and $\delta^{15}N_{TDN}$, but it was not the critical controlling factor.

Debris from shore or sediment is generally considered an important source of $\delta^{15}N_{PN}$, especially in deep water (Hamilton et al., 2001; Wollheim et al., 2001). However, in Lianhe Reservoir, the $\delta^{15}N_{PN}$ values in the sediments were all lower than those in the water column (**Tables 3, 4**). Furthermore, we observed a large proportion of algal cells in particulate matter (PM) under a microscope. Therefore, we believe that Lianhe Reservoir is a phytoplankton-dominated PM subtropical reservoir. Other surveys have also shown that lakes or reservoirs with strong solar radiation and thermal stratification of the water body are usually phytoplankton-dominated PM pools (Gu, 2009). Lianhe Reservoir, located in southern China, is exposed to intense solar radiation. The water column in the reservoir thermally stratifies in summer. Therefore, the main source of PM is not the debris but phytoplankton cells.

Sediments contributed a low $\delta^{15}N_{PN}$ level ($2.3 \pm 0.2 \sim 3.6 \pm 0.2$‰) in Lianhe Reservoir, which was significantly lower than the $\delta^{15}N_{PN}$ in the bottom water ($p < 0.05$) (**Figure 2** and **Table 4**). This difference suggested that the denitrification between sediment and the water column at the bottom was not strong. Other studies have shown that the $\delta^{15}N_{PN}$ values resulting from denitrificatin in sediments are approximately $14 \sim 38$‰ (Casciotti et al., 2003), which were very different from the values obtained in this study. We speculate that the reason for this result is that reservoirs are semiartificial water bodies. The reservoir management station dredges every year, and the community of denitrobacteria in the sediment is destroyed. Furthermore, sedimentary denitrification had a minimal effect on the vertical variations in $\delta^{15}N_{PN}$ during the thermal stratification period because transport limited the overall rate, resulting in a low isotopic fractionation potential (Hadas et al., 2009). However, we cannot rule out the possibility that the remineralization of organic nitrogen and subsequent nitrification might have contributed to $\delta^{15}N_{TDN}$ in the reservoir during the mixing period, which requires further study.

Biochemical processes must be considered when studying the variations in nitrogen stable isotopes in reservoirs. In our study, although the distribution of $\delta^{15}N_{PN}$ differed greatly between the thermal stratification and mixing periods, $\delta^{15}N_{PN}$ still showed a strong correlation with phytoplankton cell density in both the field investigation and laboratory experiments (**Figures 4**, **6**). PCA showed that variations in $\delta^{15}N_{PN}$ and $\delta^{15}N_{TDN}$ were principally determined by phytoplankton cell density (**Table 5**). These results suggested that phytoplankton cell density was the key factor controlling nitrogen stable isotope composition. Phytoplankton biological effects are a primary factor in the N cycle of subtropical reservoirs, and their effects are much greater than those of other physical and chemical factors.

The laboratory experimental results showed that the $\delta^{15}N_{PN}$ values decreased and the $\delta^{15}N_{TDN}$ values increased in both *M. densa* and *S. aristiferus* cultures (**Figure 7**). To simulate the natural dynamics, phytoplankton were cultured at different WT, and the results were consistent with those of our field investigation. Because of the different culture temperatures,

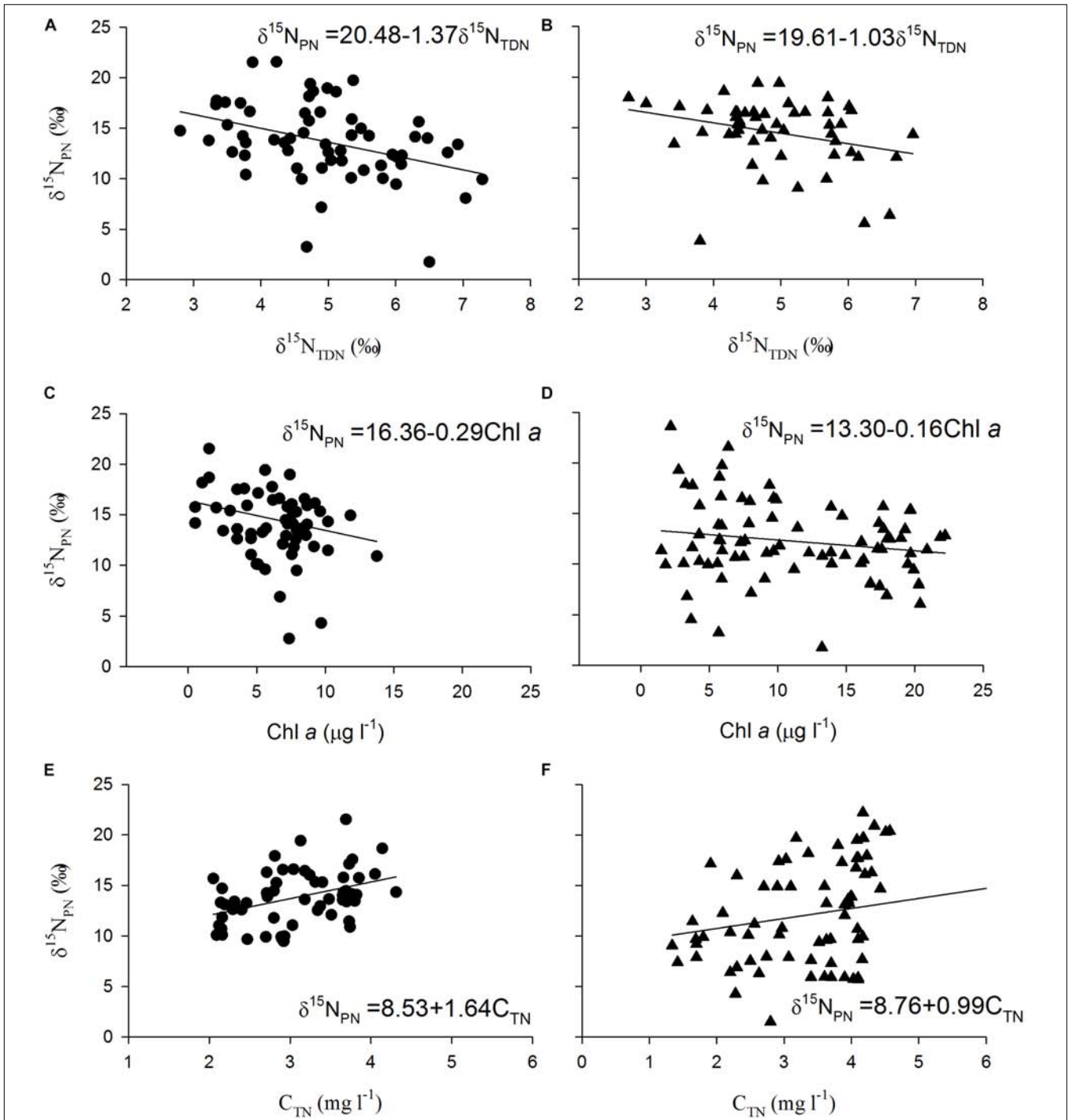

FIGURE 3 | Scatter plots of particulate nitrogen stable isotope ratios ($\delta^{15}N_{PN}$, ‰) against total dissolved nitrogen stable isotope ratios ($\delta^{15}N_{TDN}$, ‰) during **(A)** mixing and **(B)** thermal stratification periods, Chlorophyll *a* (Chl *a*) during **(C)** mixing and **(D)** thermal stratification periods, and total nitrogen (C_{TN}) during **(E)** mixing and **(F)** thermal stratification periods as well as their fitted curves in every depth at stations X1 ∼ X5 in Lianhe Reservoir in 2017.

we could not compare the nitrogen fractionation effects between these two dominant species, but the results still suggested that both of these dominant species could regulate the assignment of ^{15}N between particular nitrogen and total dissolved nitrogen. Based on the fact that both of these dominant species had the same regulatory capacity, this ^{15}N assignment mechanism seemed to be closely related to only cell density, not phytoplankton species. Furthermore, dominant species accounted for 77–93% of the total phytoplankton (**Table 2**). Therefore, dominant species are an important indicator of total

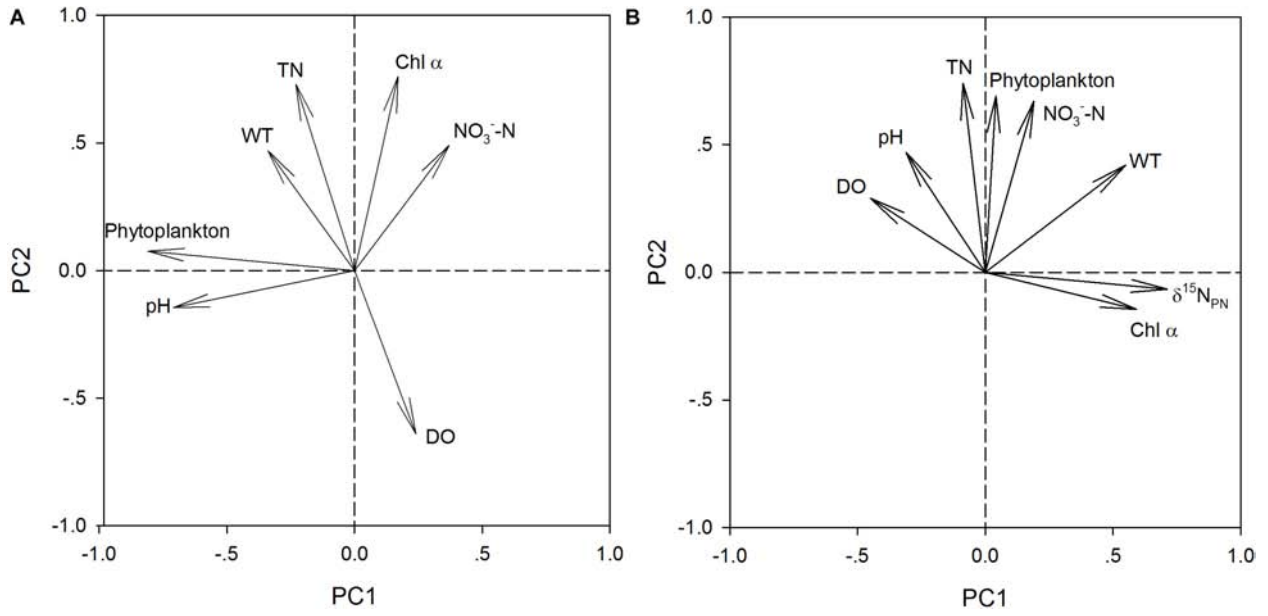

FIGURE 4 | Principal component 1 (PC1) versus principal component 2 (PC2) for $\delta^{15}N_{PN}$ **(A)** and $\delta^{15}N_{TDN}$ **(B)** using monthly values at eat depth of stations X1 ~ X5 in the Lianhe Reservoir in 2017.

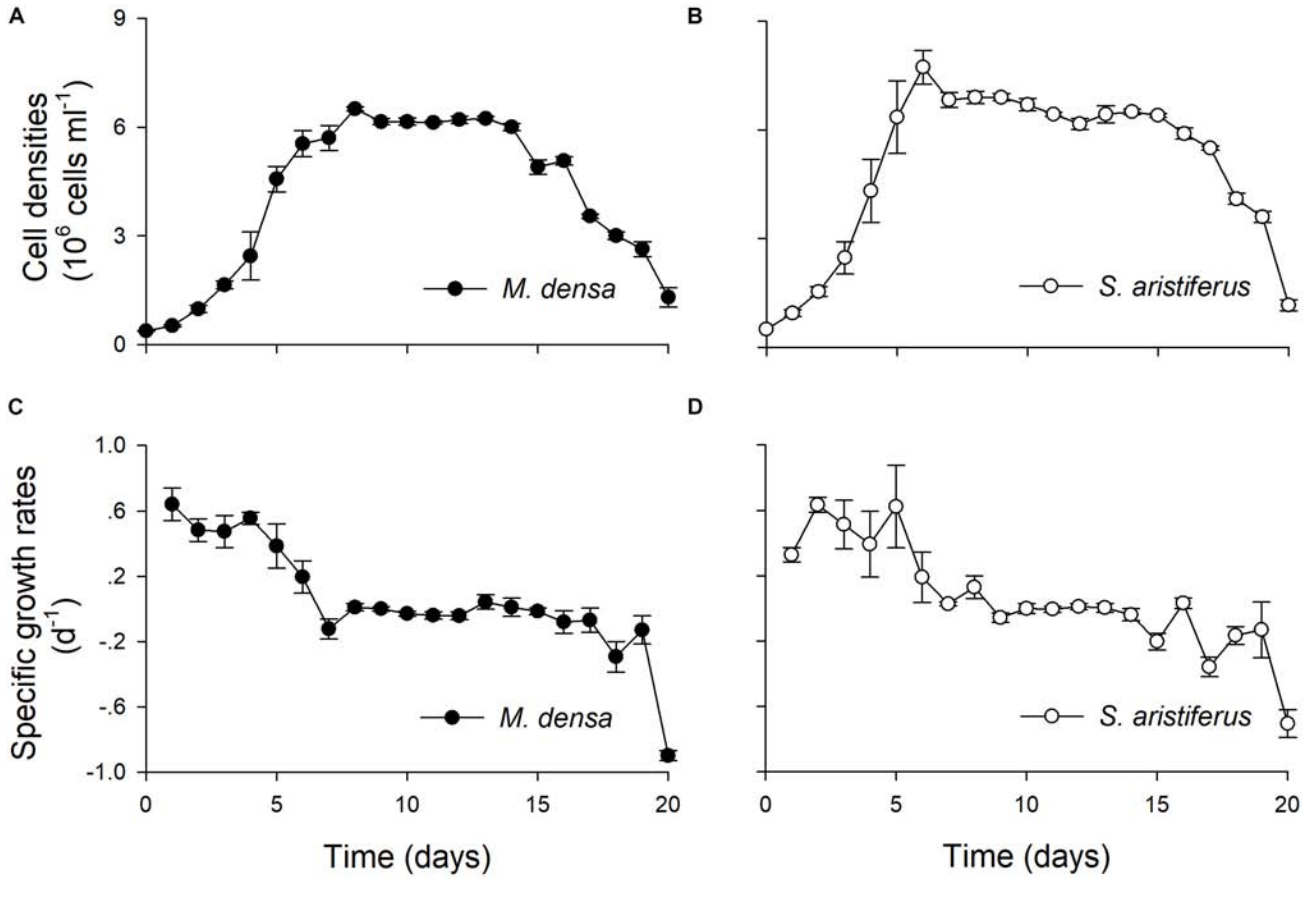

FIGURE 5 | The growth of *M. densa* and *S. aristiferus* during treatment with NO_3^--N. **(A)** Cell densities of *M. densa*. **(B)** Cell densities of *S. aristiferus*. **(C)** Specific growth rates of *M. densa*. **(D)** Specific growth rates of *S. aristiferus*. The values are the mean ± SD (n = 3).

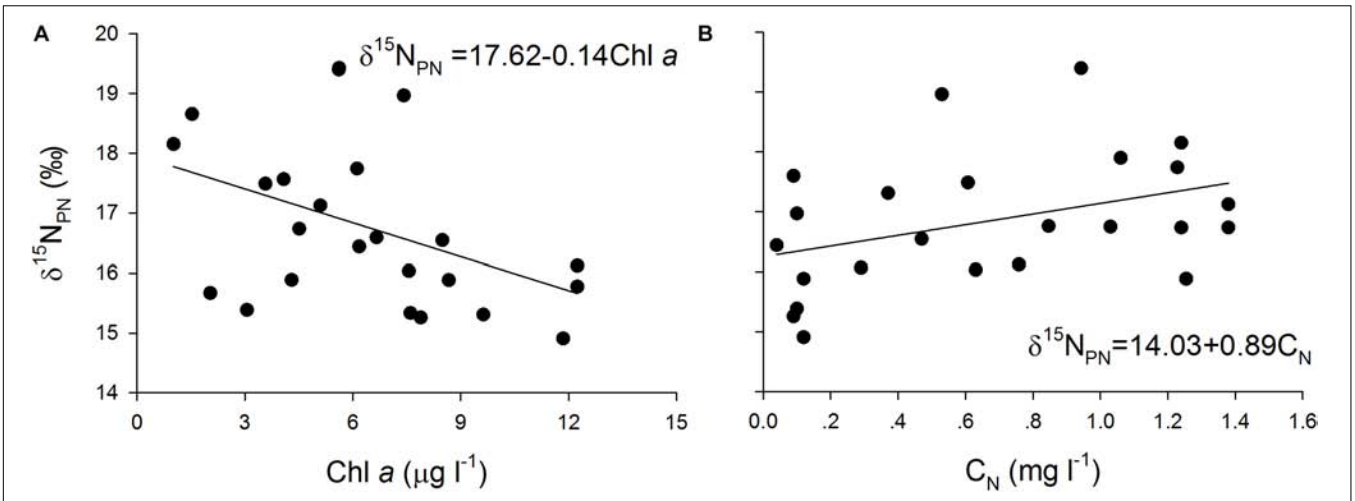

FIGURE 6 | Scatter plots of particulate nitrogen stable isotope ratios ($\delta^{15}N_{PN}$, ‰) against **(A)** Chlorophyll *a* (Chl *a*, μg l^{-1}) and **(B)** NO_3^--N (C_N, mg l^{-1}) and their fitted curves in the batch cultures.

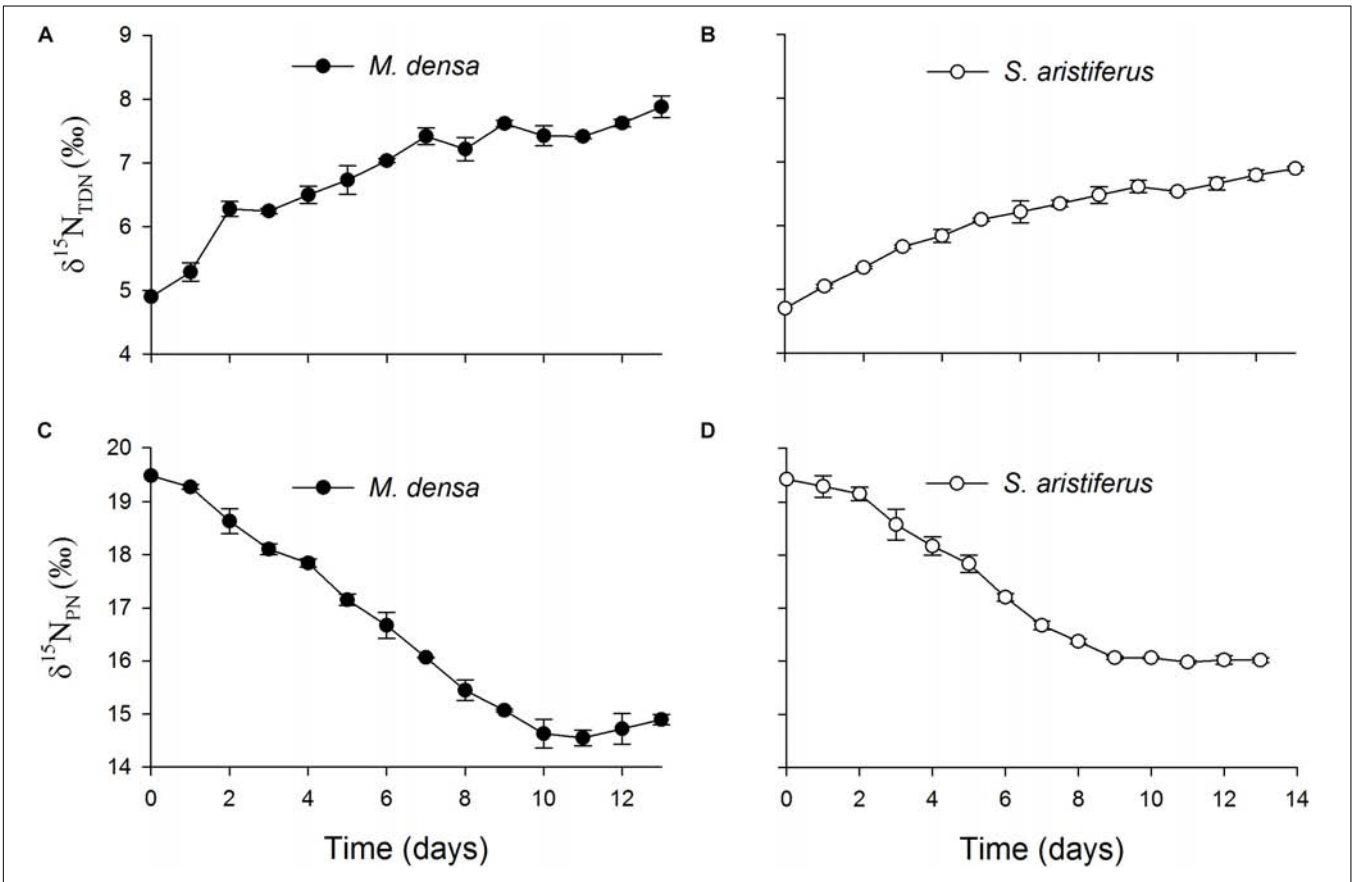

FIGURE 7 | The variation of the total dissolved nitrogen stable isotope ratios ($\delta^{15}N_{TDN}$) in the batch cultures of **(A)** *M. densa* and **(B)** *S. aristiferus*, and the particulate nitrogen stable isotope ratios ($\delta^{15}N_{PN}$) in the batch cultures of **(C)** *M. densa* and **(D)** *S. aristiferus*. The values are the mean ± SD (n = 3).

phytoplankton that can be used to evaluate the effect of biological processes on the N cycle.

Zooplankton play a mediating role in the food web of aquatic ecosystems, and excess zooplankton puts predation pressure on phytoplankton (Boyce et al., 2010; De Stasio et al., 2018; Sitta et al., 2018). When zooplankton biomass is low, phytoplankton will proliferate rapidly (Paerl et al., 2011; Er et al., 2018). In our study, 9 and 13 species of zooplankton

were found during the thermal stratification and mixing periods, respectively (**Supplementary Table S2**). The number of species and the biomass of zooplankton in Lianhe Reservoir were significantly lower than those in other subtropical reservoirs (Lin et al., 2003). On the other hand, phytoplankton cell density could reach up to $10.3 \pm 0.3 \times 10^5$ cells ml^{-1} (**Table 2**) and the predation pressure from zooplankton seemed to not have an effect. Therefore, in the plankton community, phytoplankton accounted for an overwhelming proportion of both species and biomass. Zooplankton could surely also regulate the spatial and temporal distribution of $\delta^{15}N$. However, the proportion of zooplankton in Lianhe Reservoir was so small that it did not play an important role in controlling $\delta^{15}N_{PN}$ and $\delta^{15}N_{TDN}$.

Compared to the $\delta^{15}N_{PN}$ values determined in other studies (Fogg et al., 1998; Kendall, 1998; Russell et al., 1998; Mayer et al., 2002; Vuorio et al., 2006; Bateman and Kelly, 2007; Finlay et al., 2007; Hales et al., 2007; Singleton et al., 2007; Lee et al., 2008; Xue et al., 2009; Doi et al., 2010; Titlyanov et al., 2011; Ólafsson et al., 2013), the $\delta^{15}N_{PN}$ values in Lianhe Reservoir were within the range of $\delta^{15}N_{PN}$ values from phytoplankton, which was approximately 3 ∼ 22‰ (**Figure 8**). This finding also supported our hypothesis that phytoplankton cell density was the primary factor controlling the temporal and spatial distributions of $\delta^{15}N_{PN}$ in a subtropical reservoir.

Implications for Biochemical Processes

Laboratory experiments showed that $\delta^{15}N_{PN}$ values were inversely proportional to $\delta^{15}N_{TDN}$ values (**Figure 9**). Interestingly, in the growth stationary phase, $\delta^{15}N_{TDN}$ in the media still increased while $\delta^{15}N_{PN}$ remained relatively constant (red circles in **Figure 9**). This result indicated that the amount of nitrogen is sufficient for algal cells, which no longer take up nitrogen from the ambient environment. Conversely, algal cells released nitrogen to maintain a balance of intracellular and extracellular nitrogen.

Excessive nitrogen flows into the reservoir and sinks to the bottom, which increases the nitrogen budget year by year. Denitrification is generally considered the major process that removes this excess nitrogen, especially in deep lakes and reservoirs (Han et al., 2014; Zhou et al., 2018). At the anoxic bottom during the thermal stratification period, NO_3^--N reduction to NO_2^--N, N_2O, and even N_2 is accomplished by the denitrifying bacterial community (Saunders and Kalff, 2001; Zhang et al., 2019). Generally, the ambient environment at the dark and anoxic bottom is not suitable for phytoplankton. Surprisingly, we found biomass of phytoplankton at the bottom (**Table 2**). As mentioned above, these phytoplankton not only take up nitrogen but also continuously excrete excess nitrogen into the water column to maintain metabolism stability (**Figure 9**). That is, in addition to denitrification causing nitrogen loss, there is a process for nitrogen accumulation by phytoplankton. There was no significant difference in the NO_3^--N vertical concentration even during the thermal stratification period (**Figure 2**), which also supported our deduction. These two opposing pathways maintain the nitrogen balance at the bottom of the reservoir.

Areas with industrial production, urban wastes, and fishing are enriched in $\delta^{15}N_{TDN}$ and can carry $\delta^{15}N_{TDN}$ signatures as high as 20‰ (Bedard-Haughn et al., 2003; Leavitt et al., 2006; Hou et al., 2013). However, in the middle water layer (18 ∼ 24 m below the surface) of Lianhe Reservoir, the phytoplankton biomass was low. Additionally, it is difficult for river runoff, rainfall and bottom denitrification to influence the physicochemical processes of this water layer during the thermal stratification period. Moreover, there is also less human activity around the reservoir. Therefore, we speculated that the low $\delta^{15}N_{TDN}$ value in this layer is close to the background value of $\delta^{15}N_{TDN}$ in natural subtropical reservoirs. Surely, the value of $\delta^{15}N_{TDN}$ is also associated with dissolved inorganic and organic nitrogen. Expanding the scope of investigation

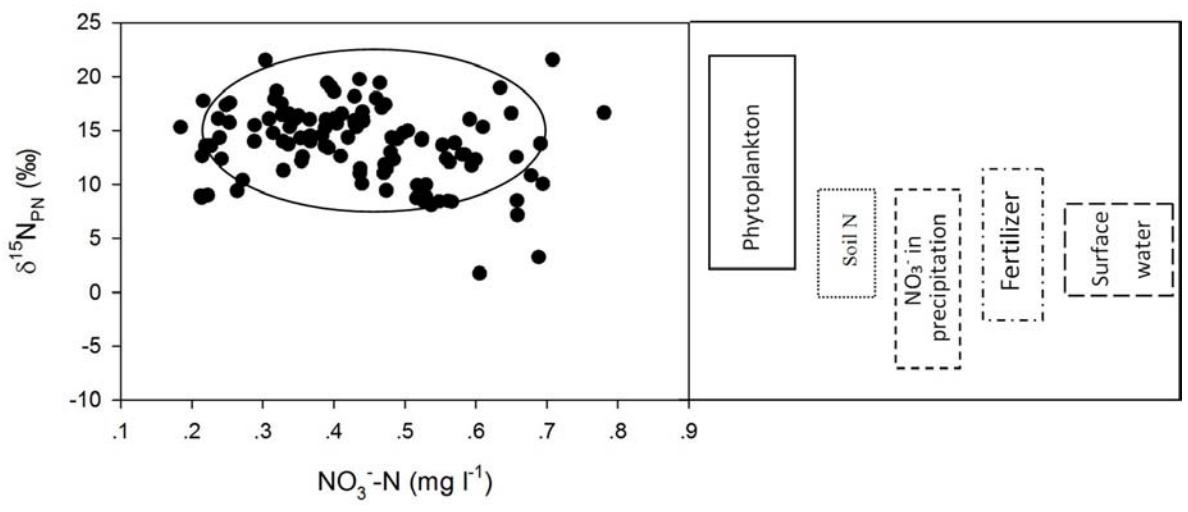

FIGURE 8 | Scatter plots of $\delta^{15}N_{PN}$ (‰) against NO_3^--N (mg l^{-1}) and the range of $\delta^{15}N_{PN}$ values from different sources.

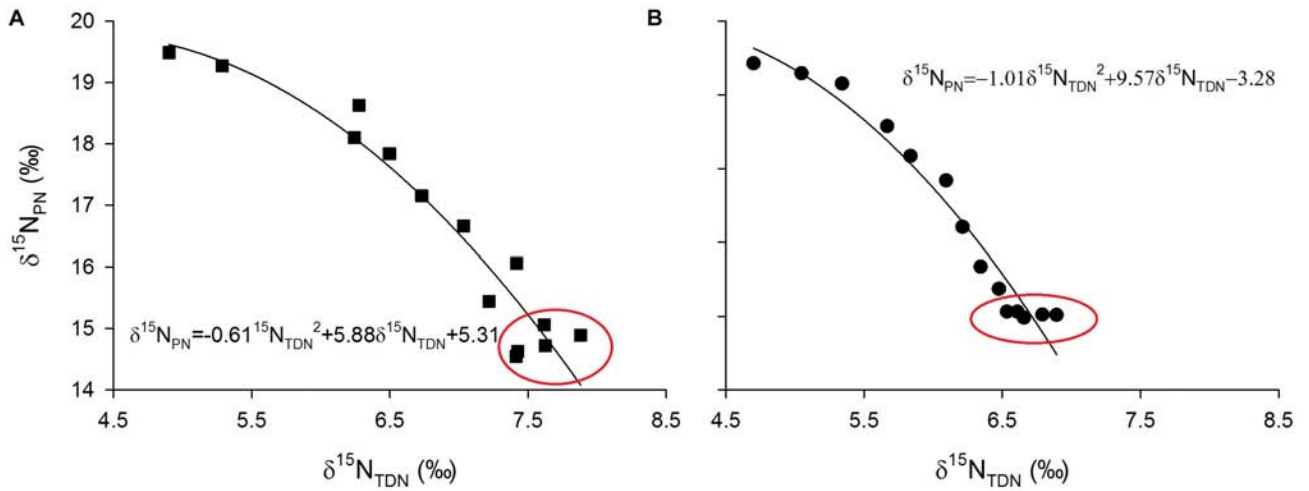

FIGURE 9 | Scatter plots of particulate nitrogen stable isotope ratios ($\delta^{15}N_{PN}$, ‰) against total dissolved nitrogen stable isotope ratios ($\delta^{15}N_{PN}$, ‰) and their fitted curves for *M. densa* **(A)** and *S. aristiferus* **(B)** cultures.

in further studies is needed to characterize the background $\delta^{15}N_{TDN}$ signature in natural subtropical reservoirs. However, we believe that the $\delta^{15}N_{TDN}$ value of this water layer can provide a reference for determining the natural background value of $\delta^{15}N_{TDN}$.

Biochemical Characteristics of Subtropical Reservoirs

The Thermal Stratification Period

The depth of the reservoir and intense solar radiation cause a discrepancy in the vertical heat budget during the thermal stratification period. This discrepancy represents a thermocline separating WT in the epilimnion and hypolimnion, leading to the vertical heterogeneity in the biomass and species composition of phytoplankton. The WT in the epilimnion is higher than that in the other layers, especially the surface temperature, which is close to the air temperature. However, the temperature drops sharply in the thermocline, while the temperature in the hypolimnion stays cool year round (**Figure 10A**).

Because of strong water-vapor exchange at the surface and photosynthesis by phytoplankton, the DO level in the epilimnion is always sufficient and sometimes even supersaturated. However, an anoxic environment is formed because of the lack of oxygen supplementation and phytoplankton respiration in the hypolimnion. There is also an oxycline that usually accompanies the thermocline (**Figure 10A**).

Due to relatively high temperature and optimum light intensity in the epilimnion, the abundant phytoplankton aggregate for photosynthesis. The dominant species in this layer are thermophilic species, such as *M. densa*. In the thermocline, temperature and light intensity decrease rapidly, and many species cannot endure the severe change in this layer. Therefore, the phytoplankton biomass in the thermocline is less than that in the epilimnion. Even fewer species gather in the hypolimnion, a totally dark anoxic zone. The phytoplankton community structure is mainly composed of psychrophilic species, such as *S. aristiferus*. The cells of dead phytoplankton in the upper layer will be decomposed into many fragments or mineralized into particulates down in the hypolimnion. These fragments and particulates further release nitrogen. Phytoplankton living in the hypolimnion also contributes some nitrogen through metabolism. However, the thermocline prevents the penetration of this nitrogen into the epilimnion, resulting in nitrogen accumulation in the hypolimnion (**Figure 10A**).

Nitrogen concentrations, such as the TN, NO_3^--N, and NH_4^+-N, were higher during the thermal stratification period than during the mixing period. These types of nitrogen have less vertical variation. However, $\delta^{15}N_{PN}$ and $\delta^{15}N_{TDN}$ are vertically stratified. Depending on high phytoplankton cell density, the $\delta^{15}N_{PN}$ value decreases in the epilimnion, while the $\delta^{15}N_{TDN}$ value increases. In contrast, there are higher $\delta^{15}N_{PN}$ and lower $\delta^{15}N_{TDN}$ in the hypolimnion than in the epilimnion due to the lower phytoplankton cell density in the former. Dentrification also occurs in the hypolimnion, removing excessive NO_3^--N and balancing the nitrogen budget (**Figure 10A**).

The Mixing Period

The thermocline disappears during the mixing period. Water density is homogeneous in the vertical direction, resulting in well-mixed water and vertical movement of materials (**Figure 10B**). Water-vapor exchange still occurs, and there is also sufficient oxygen in the surface water. DO can be transported vertically, forming a homogenous distribution throughout the water column (**Figure 10B**).

WT cool in the surface water, but solar radiation is still intense. Therefore, many phytoplankton gather in the upper water, and the dominant species changes to a psychrophilic species (*S. aristiferus*). Fewer phytoplankton live at the bottom than in the upper water, which is the same pattern as in the thermal stratification period. The dominant species remain those

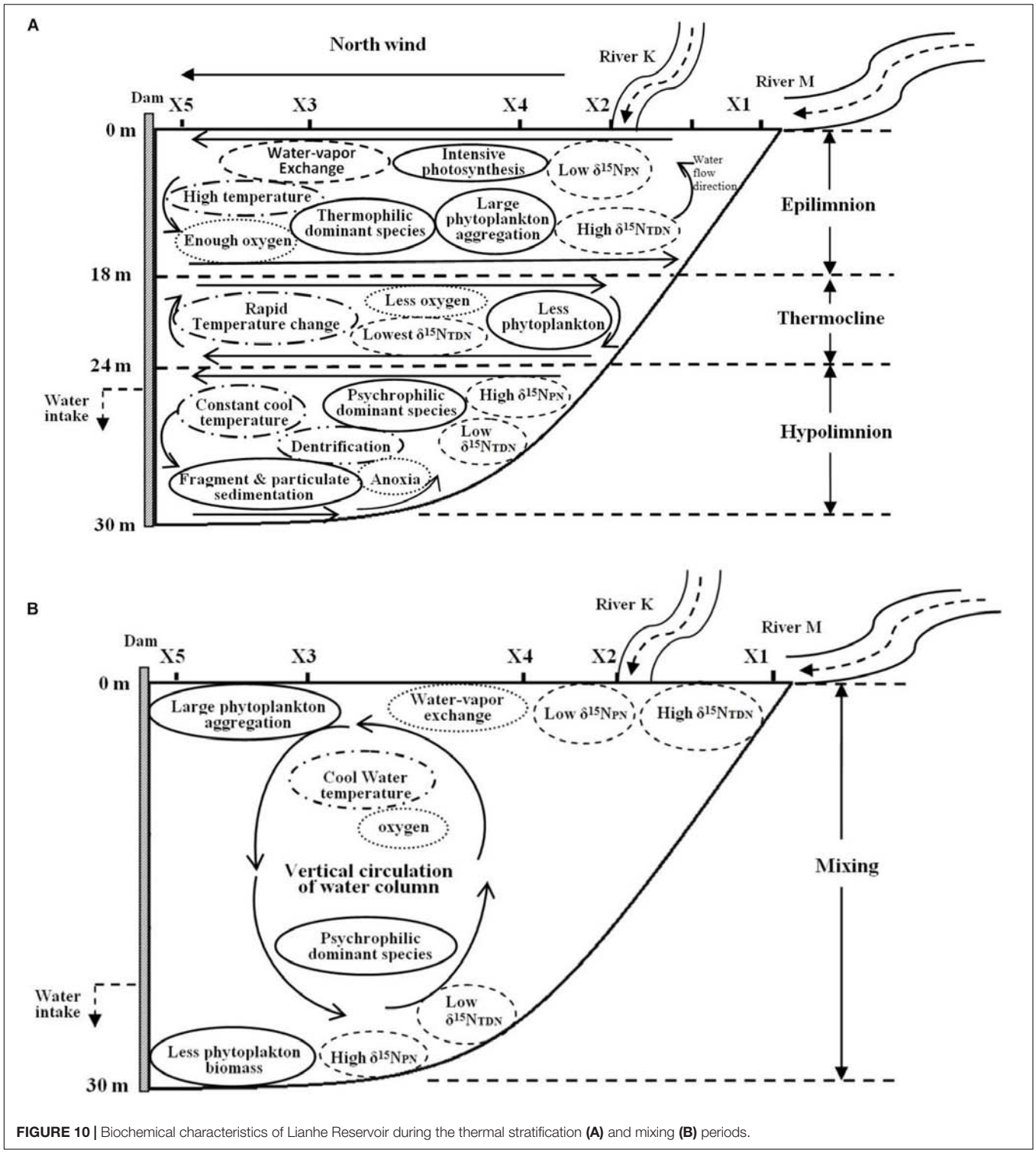

FIGURE 10 | Biochemical characteristics of Lianhe Reservoir during the thermal stratification **(A)** and mixing **(B)** periods.

that prefer to live in cool water. Due to the strong vertical water mixing, particulates and fragments generated from dead algal cells are distributed evenly along the vertical profile.

The concentrations of TN, NO_3^--N, and NH_4^+-N are lower in the mixing period than in the thermal stratification period and are still distributed uniformly throughout the water column. Vertical variations in $\delta^{15}N_{PN}$ and $\delta^{15}N_{TDN}$ are the same in the mixing and the thermal stratification periods, with lower $\delta^{15}N_{PN}$ and higher $\delta^{15}N_{TDN}$ in the upper waters and higher $\delta^{15}N_{PN}$ and lower $\delta^{15}N_{TDN}$ at the bottom (**Figure 10B**). Obviously, variations in $\delta^{15}N_{PN}$ and $\delta^{15}N_{TDN}$ are less affected by water movement and WT than by phytoplankton cell density, which dominates.

DATA AVAILABILITY STATEMENT

The raw data supporting the conclusions of this manuscript will be made available by the authors, without undue reservation, to any qualified researcher.

AUTHOR CONTRIBUTIONS

YaC designed the study, carried out the field and indoor experiments, analyzed the results, and drafted the manuscript. CT reviewed and edited the original draft of the manuscript. YiC participated in the field sampling and data interpretation. All authors read and approved the final manuscript.

FUNDING

This research was supported by the National Natural Science Foundation of China (grant number 41877470) and the Natural Science Foundation of Guangdong Province, China (No. 2017A030313229).

ACKNOWLEDGMENTS

We thank the editor and reviewers for their insightful comments and suggestions. We are thankful to Prof. Tao Jiang and Prof. Kun Li for their advice on sampling. We acknowledge Zewen Pan, Shuyuan Wang, and Jingsi Cui for assistance with sampling in this study.

SUPPLEMENTARY MATERIAL

The Supplementary Material for this article can be found online at: https://www.frontiersin.org/articles/10.3389/fmicb.2019.02202/full#supplementary-material

REFERENCES

Altabet, M. (2006). "Isotopic tracers of the marine nitrogen cycle: present and past," in *Marine Organic Matter: Biomarkers, Isotopes and DNA. The Handbook of Environmental Chemistry*, ed. J. K. Volkman, (Heidelberg: Springer), 251–293. doi: 10.1007/698_2_008

American Public Health Association [APHA], American Water Works Association [AWWA] and Water Environment Federation [WEF] (1989). *Standard Methods for the Examination of Water and Wastewater*. Washington DC: APHA.

Bateman, A. S., and Kelly, S. D. (2007). Fertilizer nitrogen isotope signatures. *Isot. Environ. Health Stud.* 43, 237–247. doi: 10.1080/10256010701550732

Bedard-Haughn, A., Van Groenigen, J., and Van Kessel, C. (2003). Tracing 15N through landscapes: potential uses and precautions. *J. Hydrol.* 272, 175–190. doi: 10.1016/s0022-1694(02)00263-9

Boyce, D. G., Lewis, M. R., and Worm, B. (2010). Global phytoplankton decline over the past century. *Nature* 466, 591–596. doi: 10.1038/nature09268

Bu, H., Meng, W., and Zhang, Y. (2011). Nitrogen pollution and source identification in the haicheng river basin in northeast China. *Sci. Total Environ.* 409, 3394–3402. doi: 10.1016/j.scitotenv.2011.05.030

Casciotti, K. L., Sigman, D. M., and Ward, B. B. (2003). Linking diversity and stable isotope fractionation in ammonia-oxidizing bacteria. *Geomicrobiol. J.* 23, 335–353. doi: 10.1080/01490450303895

Chen, X., Strokal, M., Kroeze, C., Ma, L., Shen, Z., Wu, J., et al. (2019). Seasonality in river export of nitrogen: a modelling approach for the Yangtze River. *Sci. Total Environ.* 671, 1282–1292. doi: 10.1016/j.scitotenv.2019.03.323

Chiang, S. C., and Du, N. S. (1979). *Freshwater Cladocera*. Beijing: Science Press.

De Stasio, B. T., Beranek, A. E., and Schrimpf, M. B. (2018). Zooplankton-phytoplankton interactions in Green Bay, Lake Michigan: lower food web responses to biological invasions. *J. Great Lakes Res.* 44, 910–923. doi: 10.1016/j.jglr.2018.05.020

Dodds, W. K., Bouska, W. W., Eitzmann, J. L., Pilger, T. J., Pitts, K. L., Reiley, A. J., et al. (2009). Eutrophication of US freshwaters: analysis of potential economic damages. *Environ. Sci. Technol.* 43, 12–19. doi: 10.1021/es801217q

Doi, H., Kikuchi, E., and Shikano, S. (2010). Differences in nitrogen and carbon stable isotopes between phanktonic and benthic microalgae. *Limnology* 11, 185–192. doi: 10.1007/s10201-009-0297-1

Doi, H., Kikuchi, E., Shikano, S., and Takagi, S. (2004). A study of the nitrogen stable isotope dynamics of phytoplankton in a simple natural ecosystem. *Aquat. Microb. Ecol.* 36, 285–291. doi: 10.3354/ame036285

Elliott, E. M., Kendall, C., Wankel, S. D., Burns, D. A., Boyer, E. W., Harlin, K., et al. (2007). Nitrogen isotopes as indicators of NO(x) source contributions to atmospheric nitrate deposition across the midwestern and northeastern United States. *Environ. Sci. Technol.* 41, 7661–7667. doi: 10.1021/es070898t

Er, H. H., Lee, L. K., Lim, Z. F., Teng, S. T., Leaw, C. P., and Lim, P. T. (2018). Responses of phytoplankton community to eutrophication in Semerak Lagoon (Malaysia). *Environ. Sci. Pollut. Res. Int.* 25, 22944–22962. doi: 10.1007/s11356-018-2389-0

Finlay, J. C., Sterner, R. W., and Kumar, S. (2007). Isotopic evidence for in-lake production of accumulating nitrate in Lake Superior. *Ecol. Appl.* 17, 2323–2332. doi: 10.2307/40061931

Fogg, G. E., Rolston, D. E., Decker, D. L., Louie, D. T., and Grismer, M. E. (1998). Spatial variation in nitrogen isotope values beneath nitrate contamination sources. *Ground Water* 36, 418–426. doi: 10.1111/j.1745-6584.1998.tb02812.x

Gao, G., Xia, J., Yu, J., and Zeng, X. (2018). Physiological response of a red tide alga (*Skeletonema costatum*) to nitrate enrichment, with special reference to inorganic carbon acquisition. *Mar. Environ. Res.* 133, 15–23. doi: 10.1016/j.marenvres.2017.11.003

Glew, J. R., Smol, J. P., and Last, W. M. (2001). "Sediment cores collecteion and extrusion," in *Tracking Environmental Changes Using Lake Sediments*, eds W. M. Last, and J. P. Smol, (Dordrecht: Kluwer Academic), 73–106.

Granger, J., Sigman, D. M., Needoba, J. A., and Harrison, P. J. (2004). Coupled nitrogen and oxygen isotope fractionation of nitrate during assimilation by cultures of marine phytoplankton. *Limnol. Oceanogr.* 49, 1763–1773. doi: 10.4319/lo.2004.49.5.1763

Gu, B. (2009). Variations and controls of nitrogen stable isotopes in particulate organic matter of lakes. *Oecologia* 160, 421–431. doi: 10.2307/40310089

Gu, B., Chapman, A. D., and Schelske, C. L. (2006). Factors controlling seasonal variations in stable isotope composition of particulate organic matter in a soft water eutrophic lake. *Limnol. Oceanogr.* 51, 2837–2848. doi: 10.4319/lo.2006.51.6.2837

Gu, B., and Schelske, C. L. (2010). Patterns and controls of nitrogen stable isotopes of particulate organic matter in subtropical lakes. *Annales de Limnol.* 46, 1–7. doi: 10.1051/limn/2010005

Guillard, R. R. L. (1973). "Methods for microflagellates and nanoplankton," in *Handbook of Phycological Methods: Culture Methods and Growth Measurements*, ed. J. R. Stein, (Cambridge: Cambridge University Press), 69–85.

Hadas, O., Altabet, M. A., and Agnihotri, R. (2009). Seasonally varying nitrogen isotope biogeochemistry of particulate organic matter in Lake Kinneret, Israel. *Limnol. Oceanogr.* 54, 75–85. doi: 10.4319/lo.2009.54.1.0075

Hales, H. C., Ross, D. S., and Lini, A. (2007). Isotopic signature of nitrate in two contrasting watersheds of Brush Brook, Vermont, USA. *Biogeochemistry* 84, 51–66. doi: 10.1007/s10533-007-9074-6

Hamilton, S. K., Tank, J. L., Raikow, D. F., Wollheim, W. M., Peterson, B. J., and Webster, J. R. (2001). Nitrogen uptake and transformation in a midwestern U. S. stream: a stable isotope enrichment study. *Biogeochemistry* 54, 297–340. doi: 10.2307/1469360

Han, H., Lu, X., Burger, D. F., Joshi, U. M., and Zhang, L. (2014). Nitrogen dynamics at the sediment-water interface in a tropical reservoir. *Ecol. Eng.* 73, 146–153. doi: 10.1016/j.ecoleng.2014.09.016

Hou, W., Gu, B., Lin, Q., Gu, J., and Han, B. (2013). Stable isotope composition of suspended particulate organic matter in twenty reservoirs from Guangdong, Southern China: implications for pelagic carbon and nitrogen cycling. *Water Res.* 47, 3610–3623. doi: 10.1016/j.watres.2013.04.014

Hu, H., and Wei, Y. (2006). *The Freshwater Algae of China– Systematics, Taxonomy and Ecology*. Beijing: Science Press.

Kendall, C. (1998). "Tracing sources and cycling of nitrate in catchments," in *Isotope Traces in Catchment Hydrology*, eds C. Kendall, and J. J. McDonnel, (Amsterdam: Elsevier), 519–576. doi: 10.1016/b978-0-444-81546-0.50023-9

Kharbush, J. J., Smith, D. J., Powers, M., Vanderploeg, H. A., Fanslow, D., Robinson, R. S., et al. (2019). Chlorophyll nitrogen isotope values track shifts between cyanobacteria and eukaryotic algae in a natural phytoplankton community in Lake Erie. *Org. Geochem.* 128, 71–77. doi: 10.1016/j.orggeochem.2018.12.006

Leavitt, P. R., Brock, C. S., Ebel, C., and Patoine, A. (2006). Landscape-scale effects of urban nitrogen on a chain of freshwater lakes in central North America. *Limnol. Oceanogr.* 51, 2262–2277. doi: 10.4319/lo.2006.51.5.2262

Lee, K. S., Bong, Y. S., Lee, D., Kim, Y., and Kim, K. (2008). Tracing the sources of nitrate in the Han River watersheds in Korea, using δ15N-NO3- values. *Sci. Total Environ.* 395, 117–124. doi: 10.1016/j.scitotenv.2008.01.058

Lehmann, M. F., Sigman, D. M., and Berelson, W. M. (2004). Couping the 15N/14N and 18O/16O of nitrate as a constraint on benthic nitrogen cycling. *Mar. Chem.* 88, 1–20. doi: 10.1016/j.marchem.2004.02.001

Lin, Q., Duan, S., Hu, R., and Han, B. (2003). Zooplankton distribution in tropical reservoirs, South China. *Internat. Rev. Hydrobiol.* 88, 602–613. doi: 10.1002/iroh.200310625

Liu, S., Altabet, M. A., Zhao, L., Larkum, J., Song, G., Zhang, G., et al. (2017). Tracing nitrogen biogeochemistry during the beginning of a spring phytoplankton bloom in the Yellow Sea using couped nitrate nitrogen and Oxygen isotope ratios. *Biogeosciences* 122, 2490–2508. doi: 10.1002/2016JG003752

Lv, H., Yang, J., Liu, L., Yu, X., Yu, Z., and Chiang, P. (2014). Temperature and nutrients are significant drivers of seasonal shift in phytoplankton community from a drinking water reservoir, subtropical China. *Environ. Sci. Pollut. Res.* 21, 5917–5928. doi: 10.1007/s11356-014-2534-3

Mackereth, F. J. H. (1969). A short core sampler for subaqueous deposits. *Limnol. Oceanogr.* 14, 145–151. doi: 10.4319/lo.1969.14.1.0145

Mayer, B., Boyer, E. W., Goodale, C., Jaworski, N. A., Breemen, N. V., Howarth, R. W., et al. (2002). Sources of nitrate in rivers draining sisteen watersheds in the northeastern U.S: isotope constraints. *Biogeochemistry* 57/58, 171–197. doi: 10.1023/A:1015744002496

Needoba, J. A., and Harrison, P. J. (2004). Influence of low light and a light: dark cycle on NO3- uptake, intracellular NO3-, and nitrogen isotope fractionation by marine phytoplankton. *J. Phycol.* 40, 505–516. doi: 10.1111/j.1529-8817.2004.03171.x

O'Farrell, I., Bordet, F., and Chaparro, G. (2012). Bloom forming cyanobacterial complexes co-occurring in a subtropical large reservoir: validation of dominant eco-strategies. *Hydrobiologia* 698, 175–190. doi: 10.1007/s10750-012-1102-4

Ólafsson, E., Aarnio, K., Bonsdorff, E., and Arroyo, N. L. (2013). Fauna of the green alga *Cladophora glomerata* in the Baltic Sea: density, diversity, and algal decomposition stage. *Mar. Biol.* 160, 2353–2362. doi: 10.1007/s00227-013-2229-1

Paerl, H. W., Xu, H., McCarthy, M. J., Zhu, G., Qin, B., Li, Y., et al. (2011). Controlling harmful cyanobacterial blooms in a hyper-eutrophic lake (Lake Taihu, China): the need for a dual nutrient (N & P) management. *Water Res.* 45, 1973–1983. doi: 10.1016/j.watres.2010.09.018

Pápista, É., Ács, É., and Böddi, B. (2002). Chlorophyll-a determination with ethanol-a critical test. *Hydrobiologia* 485, 191–198. doi: 10.1023/A:1021329602685

Russell, K. M., Galloway, J. N., Macko, S. A., Moody, J. L., and Scudlark, J. R. (1998). Sources of nitrogen in wet deposition to the Chesapeake Bay region. *Atmos. Environ.* 32, 2453–2465. doi: 10.1016/s1352-2310(98)00044-2

Sachs, J. P., Repeta, D. J., and Goericke, R. (1999). Nitrogen and carbon isotopic ratios of chlorophyll from marine phytoplankton. *Geochim. Cosmochim. Acta* 63, 1431–1441. doi: 10.1016/S0016-7037(99)00097-6

Saunders, D. L., and Kalff, J. (2001). Nitrogen retention in wetlands, lakes and rivers. *Hydrobiologia* 443, 205–212. doi: 10.1023/A:1017506914063

Shen, C. J. (1979). *Freshwater Copepoda*. Beijing: Science Press.

Singleton, M. J., Esser, B. K., Moran, J. E., Hudson, G. B., McNab, W. W., and Harter, T. (2007). Saturated zone denitrification: potential for natural attenuation of nitrate contamination in shallow groundwater under dairy operations. *Environ. Sci. Technol.* 41, 759–765. doi: 10.1021/es061253g

Sitta, K. A., Reed, M., Mortensen, R., Doll, C., Callahan, T., and Greenfield, D. (2018). The influences of nitrogen form and zooplankton grazing on phytoplankton assemblages in two coastal southeastern system. *Limnol. Oceanogr.* 63, 2523–2544. doi: 10.1002/lno.10957

Smith, V. H., and Schindler, D. W. (2009). Eutrophication science: where do we go from here? *Trends Ecol. Evol.* 24, 145–152. doi: 10.1016/j.tree.2008.11.009

Stanier, R. Y., Kunisawa, R., Mandel, M., and Cohen-Bazire, G. (1971). Purification and properties of unicellular blue-green algae (order *Chroococcales*). *Bacteriol. Rev.* 35, 171–205. doi: 10.1016/0003-9861(71)90363-8

Sugimoto, R., Kasai, A., Miyajima, T., and Fujita, K. (2010). Modeling of phytoplankton production is Ise Bay, Japan: use of nitrogen isotopes to identify the dissolved inorganic nitrogen sources. *Estuar Coast. Shelf Sci.* 86, 476–492. doi: 10.1016/j.ecss.2009.10.011

Sugimoto, R., Sato, T., Yoshida, T., and Tominaga, O. (2014). Using stable nitrogen isotopes to evaluate the relative importance of external and internal nitrogen loadings on phytoplankton production in a shallow eutrophic lake (Lake Mikata, Japan). *Limnol. Oceanogr.* 59, 37–47. doi: 10.4319/10.2014.59.1.0037

Titlyanov, E. A., Kiyashk, S. I., Titlyanova, T. V., Van Huyen, P., and Yakovleva, I. M. (2011). Identifying nitrogen sources for macroalgal growth in variously polluted coastal areas of southern Vietnam. *Botanica Marina* 54, 367–376. doi: 10.1515/bot.2011.041

Vuorio, K., Meili, M., and Sarvala, J. (2006). Taxon-specific variation in the stable isotopic signatures (δ13C and δ15N) of lake phytoplankton. *Freshw. Biol.* 51, 807–822. doi: 10.1111/j.1365-2427.2006.01529.x

Wang, J. J. (1961). *Freshwater Rotatoria Sinica*. Beijing: Science Press.

Waser, N. A. D., Harrison, P. J., Nielsen, B., and Calvert, S. E. (1998). Nitrogen isotope fractionation during the uptake and assimilation of nitrate, nitrite, ammonium, and urea by a marine diatom. *Limnol. Oceanogr.* 43, 215–224. doi: 10.4319/lo.1998.43.2.0215

Waser, N. A. D., Yu, D. Z., Yin, K., Nielsen, B., Harrison, P. J., and Calvert, S. E. (1999). Nitrogen isotopic fractionation during a simulatd diatom spring bloom: importance of N-starvatopm om controlling fractionation. *Mar. Ecol. Prog. Ser.* 179, 291–296. doi: 10.3354/meps179291

Wojciechowski, J., Heino, J., Bini, L. M., and Padial, A. A. (2017). Temporal variation in phytoplankton beta diversity patterns and metacommunity structures across subtropical reservoirs. *Freshw. Biol.* 62, 751–766. doi: 10.1111/fwb.12899

Wollheim, W. M., Peterson, B. J., Deegan, L. A., Hobbie, J. E., Hooker, B., Bowden, W. B., et al. (2001). Influence of stream size on ammonium and suspended particulate nitrogen processing. *Limnol. Oceanogr.* 46, 1–13. doi: 10.4319/lo.2001.46.1.0001

Xiao, H.-Y., and Liu, C.-Q. (2002). Sources of nitrogen and sulfur in wet deposition at Guiyang, southwest China. *Atmos. Environ.* 36, 5121–2130. doi: 10.1016/s1352-2310(02)00649-0

Xue, D., Botte, J., De Baets, B., Accoe, F., Nestler, A., Taylor, P., et al. (2009). Present limitations and future prospects of stable isotope methods for nitrate source identification in surface- and groundwater. *Water Res.* 43, 1159–1170. doi: 10.1016/j.watres.2008.12.048

Yang, J., Yu, X., Liu, L., Zhang, W., and Guo, P. (2012). Algae community and trophic state of subtropical reservoirs in southeast Fujian, China. *Environ. Sci. Pollut. Res.* 19, 1432–1442. doi: 10.1007/s11356-011-0683-1

Zhang, H., Feng, J., Chen, S., Zhao, Z., Li, B., Wang, Y., et al. (2019). Geographical patterns of *nirS* gene abundance and *nirS*-type denitrifying bacterial community associated with activated sludge from different wastewater plants. *Microb. Ecol.* 77, 304–316. doi: 10.1007/s00248-018-1236-7

Zhou, S., Xia, C., Huang, T., Zhang, C., and Fang, K. (2018). Seasonal variation of potential denitrification rate and enhanced denitrification performance via water-lifting aeration technology in a stratified reservoir-A case study of Zhoucun reservoir. *Chemosphere* 211, 1123–1136. doi: 10.1016/s1001-0742(09)60205-9

Conflict of Interest: The authors declare that the research was conducted in the absence of any commercial or financial relationships that could be construed as a potential conflict of interest.

Copyright © 2019 Cai, Cao and Tang. This is an open-access article distributed under the terms of the Creative Commons Attribution License (CC BY). The use, distribution or reproduction in other forums is permitted, provided the original author(s) and the copyright owner(s) are credited and that the original publication in this journal is cited, in accordance with accepted academic practice. No use, distribution or reproduction is permitted which does not comply with these terms.

frontiers in Microbiology

ORIGINAL RESEARCH
published: 04 October 2019
doi: 10.3389/fmicb.2019.02257

Effects of Habitat Partitioning on the Distribution of Bacterioplankton in Deep Lakes

*Nico Salmaso**

Research and Innovation Centre, Fondazione Edmund Mach, San Michele all'Adige, Italy

In deep lakes, many investigations highlighted the existence of exclusive groups of bacteria adapted to deep oxygenated and hypoxic and anoxic hypolimnia. Nevertheless, the extent of bacterial strain diversity has been much less scrutinized. This aspect is essential for an unbiased estimation of genetic variation, biodiversity, and population structure, which are essential for studying important research questions such as biogeographical patterns, temporal and spatial variability and the environmental factors affecting this variability. This study investigated the bacterioplankton community in the epilimnetic layers and in the oxygenated and hypoxic/anoxic hypolimnia of five large and deep lakes located at the southern border of the Alps using high throughput sequencing (HTS) analyses (16S rDNA) and identification of amplicon sequence variants (ASVs) resolving reads differing by as little as one nucleotide. The study sites, which included two oligomictic (Garda and Como) and three meromictic lakes (Iseo, Lugano, and Idro) with maximum depths spanning from 124 to 410 m, were chosen among large lakes to represent an oxic-hypoxic gradient. The analyses showed the existence of several unique ASVs in the three layers of the five lakes. In the case of cyanobacteria, this confirmed previous analyses made at the level of strains or based on oligotyping methods. As expected, the communities in the hypoxic/anoxic monimolimnia showed a strong differentiation from the oxygenated layer, with the exclusive presence in single lakes of several unique ASVs. In the meromictic lakes, results supported the hypothesis that the formation of isolated monimolimnia sustained the development of highly diversified bacterial communities through ecological selection, leading to the establishment of distinctive biodiversity zones. The genera identified in these layers are well-known to activate a wide range of redox reactions at low O_2 conditions. As inferred from 16S rDNA data, the highly diversified and coupled processes sustained by the monimolimnetic microbiota are essential ecosystem services that enhance mineralization of organic matter and formation of reduced compounds, and also abatement of undesirable greenhouse gasses.

Keywords: deep lakes, meromixis, bacterioplankton, biodiversity, habitat partitioning, amplicon sequence variants, high throughput sequencing

OPEN ACCESS

Edited by:
Petra M. Visser,
University of Amsterdam, Netherlands

Reviewed by:
Vincent J. Denef,
University of Michigan, United States
Didier Debroas,
Université Clermont Auvergne, France

***Correspondence:**
Nico Salmaso
nico.salmaso@fmach.it

Specialty section:
This article was submitted to Aquatic Microbiology, a section of the journal Frontiers in Microbiology

Received: *17 May 2019*
Accepted: *17 September 2019*
Published: *04 October 2019*

Citation:
Salmaso N (2019) Effects of Habitat Partitioning on the Distribution of Bacterioplankton in Deep Lakes. Front. Microbiol. 10:2257. doi: 10.3389/fmicb.2019.02257

INTRODUCTION

In deep lakes, seasonal differences in vertical water density gradients driven by water temperature and salinity are a key feature in the control of stratification dynamics and patterns (Wetzel, 2001; Kallf, 2002). In holomictic lakes, the cooling of surface waters in the coldest months is sufficient to trigger the complete circulation and vertical homogenization of the water column every year.

Within this typology, oligomictic lakes mix only irregularly. Conversely, in meromictic lakes, circulation in the winter months affects only the upper portion (mixolimnion) of the water column, whereas the deeper stratum of water (monimolimnion) is perennially separated from the surface by a steep salinity gradient (the chemolimnion) (Wetzel, 2001). As a consequence of complete isolation and oxidation of sinking particulate organic matter, in meromictic lakes the monimolimnion is almost (<1–2 mg L^{-1}) or completely depleted of oxygen, causing low redox potential conditions. The monimolimnion is often rich in phosphorus and reduced nitrogen compounds. Conversely, while reduced substances accumulate in the monimolimnion, biota in the surface illuminated layers and dark mixolimnion may be deprived of essential nutrients (Humayoun et al., 2003).

Depending on the lake physiography, illumination and nutrients, different communities develop in the epilimnion of lakes, including well-diversified photosynthetic cyanobacteria populations (Newton et al., 2011; Salmaso et al., 2018a). In the epilimnion and hypolimnion of holomictic lakes, and in the oxygenated mixolimnetic layers of meromictic lakes, the metabolic activities of microorganisms can rely on a sufficient replenishment of oxygen. In depleted-O_2 layers, microorganisms have to switch electron acceptors from oxygen to other compounds such as nitrate, manganese, iron, sulfate, and carbon dioxide (Stumm and Morgan, 1996; Humayoun et al., 2003). In the metalimnion of relatively shallower meromictic lakes, oxygen diffusing down from the surface and sulfide diffusing up from the hypolimnion, provide a niche for photosynthetic and non-photosynthetic sulfur-oxidizing bacteria (Storelli et al., 2013; Bush et al., 2017). As a result, several studies based on classical culture-independent approaches showed the occurrence of specific bacterioplankton populations exclusively occurring in the oxygenated (Urbach et al., 2001; Pollet et al., 2011; Okazaki and Nakano, 2016) and hypoxic/anoxic hypolimnia (De Wever et al., 2008; Casamayor et al., 2012; Mori et al., 2013; Kubo et al., 2014). A number of investigations, based on the application of high throughput sequencing (HTS) approaches, identified a high operational taxonomic unit (OTU) richness in the hypolimnetic layers shaped by oxygen availability (Garcia et al., 2013; Llirós et al., 2014; Kurilkina et al., 2016). Nevertheless, insights into the richness and spatial extension/distribution of bacteria in large and deep lakes remain largely to be explored (Rinke et al., 2013).

The lakes Garda, Maggiore, Como, Iseo, Lugano, and Idro are part of the group of deep lakes located at the southern border of the Alps [deep southern perialpine lakes (DSL) (Ambrosetti and Barbanti, 1992)]. Owing to their different maximum depths, deep mixing dynamics and oxygenation patterns, these lakes are excellent sites to study the selection of bacterial populations along oxic-hypoxic and light gradients. In a selection of these lakes, including both oligomictic and meromictic typologies, the application of CARD-FISH showed more pronounced differences in the vertical profile of prokaryoplankton than those observed between spring and summer (Hernández-Avilés et al., 2018). These changes were interpreted as caused by the physical and chemical differences between the epilimnetic and deep hypolimnetic layers. However, it was not possible to test the extent of these effects on the whole community biodiversity and the potential ecological selection of taxa adapted to specific lakes and layers.

Thanks to the vertical partition of the water layers, ecological selection in deep lakes has the potential to lead to the development of communities composed of different populations adapted to different local habitats. In this perspective, the work aims to clarify the extent and pattern in the bacterial community diversification and how this diversification may be explained by environmental variations. A specific objective of this work is to characterize the bacterioplankton community composition (BCC) in the upper and oxygenated layers, dark oxygenated layers, and deep hypoxic layers of DSL, quantifying the influence of light and oxygen concentrations (as a proxy of redox conditions) on the potential selection of specific bacterial lineages. A specific emphasis will be given to Cyanobacteria. This group of bacteria is widely represented with several adaptations in many aquatic and terrestrial ecosystems (Jungblut et al., 2010; Whitton, 2012; Jasser et al., 2013). Moreover, many species belonging to this phylum are able to develop huge blooms (Reynolds and Walsby, 1975; Bullerjahn and Post, 2014; Davis et al., 2019), producing a wide variety of toxic compounds that can strongly deteriorate the quality of water resources used for drinking and bathing purposes (Meriluoto et al., 2017a,b). Cyanobacteria are an issue also for the DSL where they are represented by several toxigenic species producing either hepatotoxins (microcystins; *Planktothrix rubescens* and *Microcystis aeruginosa*) or neurotoxins (anatoxins; *Tychonema bourrellyi*) (Cerasino et al., 2017).

MATERIALS AND METHODS

Study Sites

The lakes included in this work are located at the southern border of the Alps (**Figure 1**). The status of investigations in this selection of lakes and in the other large and deep lakes surrounding the Alpine chain has been reviewed by Salmaso et al. (2018b, and references therein). In this regard, in the Alpine region, an operational demarcation of large and deep lakes was defined by surface (S), maximum depth (z_m), and volume (V) values set at S 10 km^2, z_m 50 m, and V 0.5 km^3. The two largest lakes included in this work, i.e., Garda and Como, are oligomictic and oligo-mesotrophic; they have surface and maximum depths of 368 and 146 km^2, and 350 and 410 m, respectively. The two last complete vertical circulation events were between 2004 (Garda) and 2005–2006 (Garda and Como) (Rogora et al., 2018). Since then, hypolimnetic oxygen concentrations were above 7 mg L^{-1}. Lakes Iseo, Lugano, and Idro are meromictic and characterized by a trophic state between mesotrophy and meso-eutrophy; water surface and maximum depths are 62, 28 and 11 km^2, and 251, 288, and 124 m, respectively (Ambrosetti and Barbanti, 1992). In lakes Iseo and Lugano a larger overturn with hypolimnetic (<150 m) O_2 concentrations increasing up to 8 and 2.5 mg L^{-1}, respectively, was observed in 2006 and, partially, 2005 (Rogora et al., 2018); hypoxia and anoxia conditions restored immediately after 2–4 years. In Lake Idro, low oxygenation from 60 to 100 m and anoxia from 100 m to the bottom were documented since

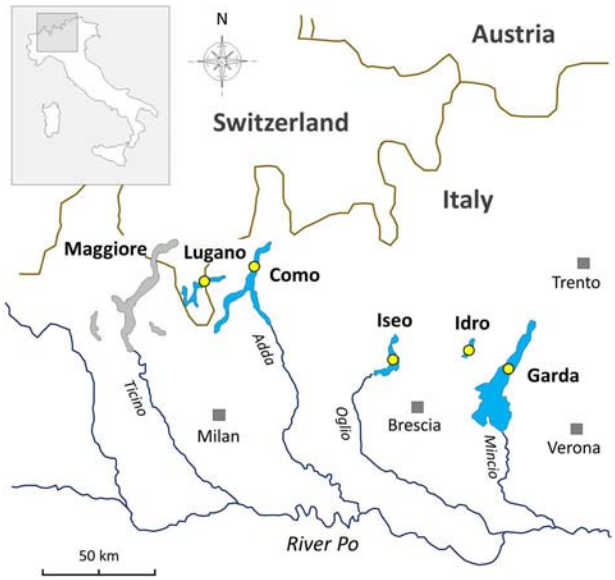

FIGURE 1 | Geographical location of the deep southern perialpine lakes (DSL) investigated in this work. The yellow circles indicate the sampling points.

1969 (Viaroli et al., 2018). Meromixis in lakes Iseo, Lugano, and Idro was triggered by a number of related factors, including the smaller water volumes compared to the other oligomictic lakes, geographical location sheltered from winds (Lugano, Idro), water warming (Lepori and Roberts, 2015; Pareeth et al., 2017), eutrophication and enhanced calcite precipitation, and supply of dissolved minerals from groundwater springs (Idro) (Rogora et al., 2018; Salmaso et al., 2018b; Viaroli et al., 2018).

Sampling and Laboratory Measurements

Samplings and measurements were carried out in 2016 during the stratification period in the deepest zones of the lakes Garda (5 July), Iseo (29 August), Lugano (northern basin, 21 June) and Idro (23 August); in Lake Como (14 June), samplings were carried out at the station of Dervio, in the northern basin (z_{max} = 270 m). The sampling stations in lakes Garda, Como, and Iseo are part of the Italian and European Long Term Ecological Research network (LTER[1,2]). Constant volumes of water were collected in each layer with a 5 L Niskin bottle for successive subsampling. Vertical profiles of temperature and oxygen were carried out using underwater probes (Idronaut, Seacat-Seabird, WTW probes). In the upper layers, samples were collected at 0, 10, 20, 40, and 60 m. Additional samples were collected, every 50 m or less, in the hypolimnetic layers (see **Figure 2**). The overall number of samples collected in the five lakes was 11 (Garda), 9 (Como), 9 (Iseo), 10 (Lugano), and 7 (Idro). Conductivity (at 20°C), pH, nitrogen compounds (NO_3-N, NH_4-N), total phosphorus (TP), soluble reactive phosphorus (SRP), reactive silica (Si), alkalinity and major ions (Ca, Mg, Na, K, Cl, and sulfate) were determined in a single laboratory (FEM) using standard analytical procedures (APHA-AWWA-WEF, 2005; Cerasino and Salmaso, 2012).

[1]http://www.lteritalia.it

[2]http://www.lter-europe.net/

DNA Extraction and Amplification

For HTS analyses, aliquots of water were filtered through 25 mm polycarbonate Isopore membranes (Merck) with 0.2 μm pore size. Filtered volumes ranged between around 500 and 1000 mL, depending on the quantity of suspended particles, and until near-clogging of the filters. Filters were stored at −20°C until DNA extraction with MO BIO PowerWater® DNA Isolation Kit (MO BIO Laboratories, Qiagen, United States). DNA concentrations, measured with a NanoDrop ND-8000 (Thermo Fisher Scientific, Inc., Waltham, MA, United States), ranged between 5 and 46 ng μL^{-1}. PCR amplification of bacterial sequences was carried out by targeting a ∼ 460-bp fragment of the 16S rRNA gene variable regions V3–V4 using the specific bacterial primer set 341F (5′-CCTACGGGNGGCWGCAG-3′) and 805Rmod (5′-GACTACNVGGGTWTCTAATCC-3′) with overhang Illumina adapters. The final barcoded library was sequenced on an Illumina® MiSeq (PE300) platform. A detailed description of procedures is reported in Salmaso et al. (2018a). Sequences in FASTQ format were deposited to the European Nucleotide Archive (ENA) with study Accession No. PRJEB33405.

Bioinformatic Pipelines and Downstream Analyses

Sequences were analyzed using the DADA2 package 1.10 (Callahan et al., 2016a) in R 3.5.1 (R Core Team, 2018) and Bioconductor 3.8 (Huber et al., 2015). The DADA2 algorithm is more sensitive and more specific than common bioinformatic pipelines based on the OTU identification, and resolves amplicon sequence variants (ASVs) that differ by as little as one nucleotide (Callahan et al., 2017). The results are exact ASVs that replace the traditional OTUs obtained by pipelines that cluster reads using subjective fixed global clustering threshold (generally 97%) or local thresholds (Swarm method) (Nguyen et al., 2016). Taxonomic assignment was carried out using the RDP naive Bayesian classifier method described in Wang et al. (2007) and the SILVA v. 132 ribosomal reference database (Quast et al., 2013; Glöckner et al., 2017) with a 80% minimum bootstrap confidence threshold. The corresponding general tree was built after alignment of sequences and phylogenetic analysis carried out using the R packages DECIPHER 2.10 and phangorn 2.4.0 (Callahan et al., 2016b), respectively. The workflow and intermediate steps are illustrated in the **Supplementary Methods**. After the application of the DADA2 pipeline, a total of 3514 ASVs were obtained, with an average sequence length of 417 bp. The number of reads per sample ranged between 13448 and 48922 (mean ± SD, 30809 ± 8790).

The ASVs abundance table, taxonomy, DNA reads and environmental data were imported into the R package phyloseq 1.28.0 (McMurdie and Holmes, 2013). Chloroplasts, mitochondria, unclassified/non-bacterial sequences were removed from the original dataset, obtaining 3298 ASVs. After inspection of the distribution of sample sequencing depth, the ASVs table was rarefied without replacement to 13367 sequences

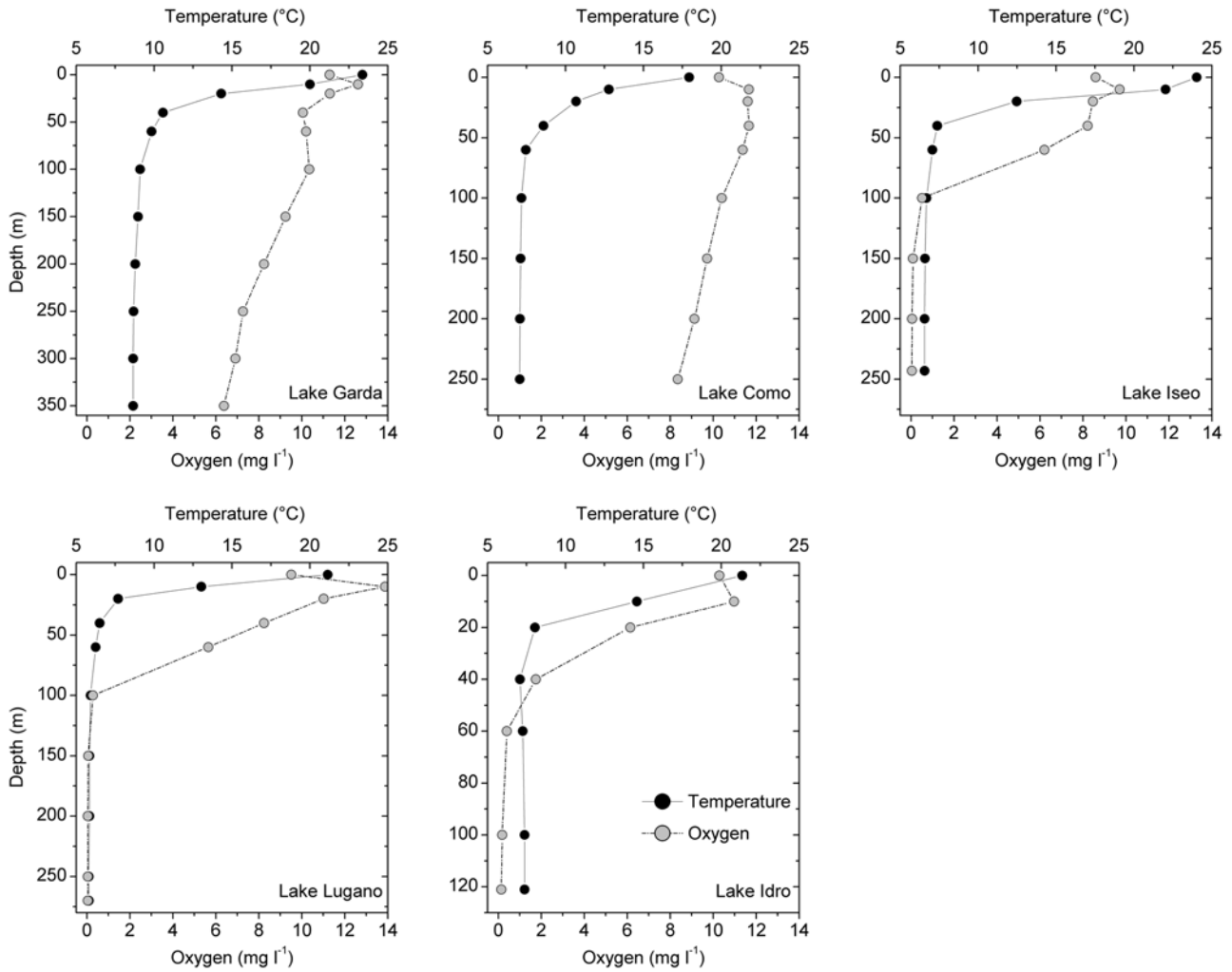

FIGURE 2 | Vertical measurements of water temperatures and oxygen concentrations in the two oligomictic (Garda and Como) and three meromictic (Iseo, Lugano, and Idro) lakes at discrete depths. Vertical scales are identical in lakes Como, Iseo, and Lugano. Samples for the determination of other chemical compounds and for HTS analyses were collected at the same depths.

per sample, obtaining a final table with 3216 ASVs. Alpha diversity (observed ASVs, Chao1 index, and Shannon diversity) and beta-diversity (Bray and Curtis) were computed following Salmaso et al. (2018a). Differences in alpha diversity between samples and layers were estimated using the Kruskal–Wallis rank sum test (KW). Ordination of samples was carried out by non-metric multidimensional scaling (NMDS) computed on a Bray and Curtis (BC) dissimilarity matrix, and vector fitting procedures (Salmaso et al., 2018a). Differences in bacterial composition between groups of samples were tested using PERMANOVA computed on the same BC distance matrix used in NMDS, with 9999 bootstraps and function adonis in R vegan 2.5.5 package (Oksanen et al., 2018).

Correlations between environmental variables and the bacterial community in the 5 lakes and selected layers were calculated by computing Mantel tests (Legendre and Legendre, 1998; Oksanen et al., 2018). The environmental distance matrix was computed using a set of standardized environmental variables (temperature, pH, conductivity, O_2, SRP, NO_3-N, NH_4-N, Si, Alk, SO_4). A second distance matrix was computed including only a subset of variables linked to stratification (water temperature) and major chemical gradients (pH, O_2, NH_4-N). The bacterial dissimilarity matrix was computed using the same methods used in NMDS. The significance of the statistic was evaluated by 9999 permutations of rows and columns of the dissimilarity matrix.

The differential distribution of taxa along the vertical oxygen gradient was tested using DESeq2 1.22.1 package in R (Love et al., 2014). Computations were carried out on the original (non-rarefied and un-normalized) abundance ASV table. Additionally, for every *k* species (or higher level taxonomy), the observed optimum environmental levels of oxygen were estimated by computing the average values – weighted by the corresponding abundances values – of the O_2 concentrations in

the corresponding samples where the *k* species were identified. Species optima (u_k), and species tolerances (t_k), were computed using standard approaches (ter Braak and van Dame, 1989) (R script in **Supplementary Code**).

The distribution of ASVs in the selected phylum Cyanobacteria was evaluated by mapping abundances on a phylogenetic tree built, after aligning sequences with MAFFT 7.427 (Katoh and Standley, 2013), using phyML 3.1 (Guindon et al., 2010) and the R package phyloseq. Potentially poorly aligned positions and divergent regions of the alignment were checked using Gblocks (Talavera and Castresana, 2007). The DNA substitution model (GTR + I + G) was selected after calling PhyML 3.1 with the phymltest function in the R package ape (Paradis, 2012; Salmaso et al., 2016). Only taxa identified at least at the genus level were included in the analysis. The outgroup was chosen from non-photosynthetic Cyanobacteria (NCY, Melainabacteria, unclassified taxa belonging to the order Caenarcaniphilales; Soo et al., 2014), after previous verification of their position in the general phylogenetic tree.

RESULTS

Vertical Physical and Chemical Gradients

The five lakes showed steep surface temperature gradients up to 40–50 m (Garda, Como, Iseo) and 20 m (Lugano, Idro) (**Figure 2**). Dissolved oxygen concentrations in the two oligomictic lakes (Garda and Como) showed only a minor vertical decrease, ranging between 6 and 13 mg L^{-1}. In the meromictic lakes, O_2 concentrations between 5.7 and 6.2 mg L^{-1} were measured up to the depths of 60 m (Iseo and Lugano) and 20 m (Idro). Below 60 m, O_2 concentrations in these three lakes were always below 0.5 mg L^{-1}. Based on the stratification patterns and O_2 concentrations, three layers were identified. In the five lakes, the upper oxygenated and productive layer included sampling depths between the surface and 20 m ("epi_oxy"; 15 samples); the dark oxygenated layers included all the hypolimnetic sampling depths in the oligomictic lakes (Garda and Como), and the depths at 40 and 60 m in lakes Iseo and Lugano ("hyp_oxy"; 18 samples); the third layer included the deep, dark and hypoxic sampling depths in the three meromictic lakes, below 100 m (Iseo and Lugano) and 40 m (Idro) ("hyp_hypox"; 13 samples).

The vertical gradients of oxygen were paralleled by similar changes in the vertical distribution of nitrate and ammonium nitrogen (**Supplementary Figure 1**). In lakes Garda and Como, NO_3-N begun to increase after the first 20–30 m, up to around 320 μg L^{-1} (Garda) and 750 μg L^{-1} (Como) in the deep layers; conversely, NH_4-N was generally below 20 μg L^{-1}. Apart from the increase of nitrate up to 20–50 m, both NO_3-N and NH_4-N in the three meromictic lakes showed opposite vertical patterns (**Supplementary Figure 1**). In lakes Garda, Como and Iseo, TP concentrations at the surface (0–20 m) were between 7 and 9 μg L^{-1}, whereas in lakes Lugano and Idro values were 20 and 12 μg L^{-1}, respectively. In the deep layers (>20 m), TP reached the highest concentrations in the meromictic lakes (averages between 88 and 204 μg L^{-1}). All the five lakes showed vertical decreasing values of pH and vertical increasing values of conductivity, Si, Alk, Ca, and Mg. In particular, the hypolimnion of the meromictic lakes showed low-medium pH (range: 7.4–8.3), high conductivity values (229–454 μS cm^{-1}), and high concentrations of calcium (37–71 mg L^{-1}) and alkalinity (117–209 mg L^{-1}) and, especially in Lake Idro, sulfate (7.6–86 mg L^{-1}), magnesium (7.2–20 mg L^{-1}), and silica (0.8–5.4 mg L^{-1}). Corresponding ranges in lakes Garda and Como were: pH, 7.4–8.2; conductivity, 169–240 μS cm^{-1}; calcium, 25–39 mg L^{-1}; alkalinity, 71–134 mg L^{-1}; sulfate, 11–27 mg L^{-1}; magnesium, 5.6–8.5 mg L^{-1}; silica, 0.3–2.3 mg L^{-1}. Differences in the distribution of Cl, Na, and K (i.e., conservative ions, or ions not susceptible of chemical precipitation) in the oligomictic and meromictic lakes were less apparent.

Alpha Diversity

The number of ASVs in the 5 lakes was generally comparable (**Figure 3A**; KW, $P = 0.32$). The median number of ASVs per lake was between 243 (Idro) and 316 (Como). Chao1 values closely followed the observed number of ASVs. Compared to Lake Como, the Shannon diversity in the other lakes showed a larger dispersion and lower values (KW, $P = 0.04$). The number of ASVs was higher in the oxygenated hypolimnion (median 344) than in the other two layers (251–261) (**Figure 3B**; KW, $P < 0.01$). Shannon diversity was higher in the oxygenated layers (**Figure 3B**; KW, $P < 0.01$).

Distribution of Bacterioplankton

The most abundant bacterioplankton phyla were Proteobacteria, Actinobacteria, Bacteroidetes, Chloroflexi, Planctomycetes, Verrucomicrobia, Cyanobacteria, and Epsilonbacteraeota. The relative contributions of these groups along with those of eight other phyla contributing with a minor fraction of reads are reported in **Figure 4**. In the two oligomictic lakes Garda and Como, differences in the vertical distribution of the main phyla were less apparent compared to the three meromictic lakes, and mostly limited to particular groups such as the Chloroflexi (family Anaerolineaceae) and Actinobacteria (*hgcI clade*, *CL500-29 marine_group*). Other dominant taxa in the two oligomictic lakes included Proteobacteria (*Ralstonia*, *Limnohabitans*), Bacteroidetes (*Fluviicola*, *Flavobacterium*), and Planctomycetes (*CL500-3*), whereas photosynthetic Cyanobacteria were mostly represented by *Tychonema bourrellyi*. In lakes Garda and Como, the dominant orders almost coincided (10 out of 12; **Supplementary Figure 2**).

The three meromictic lakes showed a strong increase of Proteobacteria in the upper and/or deep hypolimnion. Lake Idro had a peculiar presence of Epsilonbacteraeota (formerly Epsilonproteobacteria, Proteobacteria) at higher depths. Differences in the bacterial composition in the hypoxic layers were already apparent at the order level (**Supplementary Figure 2**). In Lake Iseo, the surface sample showed a lower abundance of Proteobacteria and Actinobacteria, and a greater fraction of Cyanobacteria (*Dolichospermum lemmermannii*) and Planctomycetes (family Gemmataceae) (**Figure 4**). In the trophogenic layers, a further important contribution of Oxyphotobacteria (*Pseudanabaena*) was found in Lake Lugano.

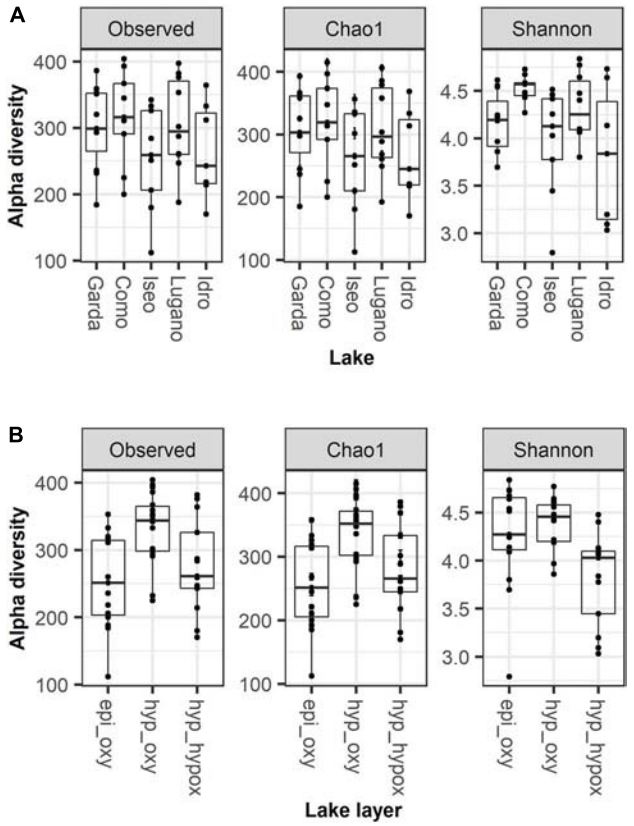

FIGURE 3 | Alpha diversity estimates in **(A)** the 5 lakes and **(B)** the three main water layers; epi_oxy, oxygenated upper layers (0–20 m); hyp_oxy, oxygenated hypolimnion; hyp_hypox, hypoxic/anoxic hypolimnion; the three layers are defined as in the text. Boxes report the median and hinges as 25th and 75th quartiles.

The number of ASVs exclusively present in the single lakes overshadowed those common in two or more lakes (**Supplementary Figure 3A**). Differences were even more amplified considering the distribution in the three main lake layers (**Supplementary Figure 3C**); the hyp_hypox layer included the larger fraction of exclusive ASVs. Differences between layers were apparent also considering the two oligomictic lakes (**Supplementary Figure 3E**). Nevertheless, most of the differences were due to the occurrence of rarest ASVs, as shown in **Supplementary Figures 3B,D,F**, which included only the more common species selected after filtering out rarest ASVs that did not appear more than 10 times in at least two samples (995 ASVs).

Relationship With Environmental Variables

Differences in the bacterial community in the 5 lakes and 3 main water layers were well-exemplified in the configurations obtained by NMDS (final stress, 0.09) (**Figure 5A**). Samples collected in the oxygenated upper layers, in the deep oxygenated layers, and in the deep hypoxic layers were grouped into three different zones (PERMANOVA, $P < 0.001$). A closer inspection of sites in the three layers allowed to identify differences in the positioning of samples belonging to the different lakes (PERMANOVA, $P < 0.001$), due to, e.g., the position of the samples of Lake Garda in the left area of the configuration, and to the three meromictic lakes, which showed a clear separation of the respective samples in the deep hypoxic hypolimnion (**Figure 5A**). The separation of samples was followed by a different positioning of ASVs (**Figure 5B**), which, in the case of the deep hypoxic layers, showed a clear grouping near the three meromictic lakes, suggesting the existence of peculiar deep communities. This was supported by the greater ASVs average dissimilarities between the samples of the deep hypoxic layers across lakes compared to the epi_oxy and hyp_oxy layers (**Supplementary Figure 4**).

Besides O_2, samples in the upper oxygenated layers were characterized by higher temperature values and pH, whereas the deep oxygenated layers had higher concentrations of NO_3-N, Cl, Na, and K (**Figure 5A**). Especially in Lake Idro, the deep hypoxic layers showed higher conductivity values, and higher concentrations of NH_4-N, TP, SRP, Si, sulfate, alkalinity, Ca, and Mg. The vector fitting analysis carried out including the dominant phyla listed in **Figure 4**, confirmed the close association between different bacterial groups and specific water layers (**Figure 5C**), such as, among others, Proteobacteria and Epsilonbacteraeota in the deep hypoxic layers, and Cyanobacteria in the upper illuminated layers.

The correlations between the environmental variables and the community structure were highly significant considering both the pooled data (5 lakes and layers; **Table 1A**), and the single lakes (**Table 1B**) and layers (**Table 1C**) separately. In general, though characterized by lower r values, all the correlations based on the group of 4 variables were equally significant (epi_oxy, $P < 0.05$) or highly significant (lakes, and the layers hyp_oxy and hyp_hypox; $P < 0.001$).

Characterization of the Dominant Genera Along the Oxygenation Gradient

Differential prevalence of taxa in one of the three reference water layers (epi_oxy, hyp_oxy, and hyp_hypox) was evaluated testing their abundances in one selected layer compared to the remaining layers (**Table 2** and **Supplementary Table 1**). The analysis has been carried out at the level of genus, including results significant at least at $P < 0.05$, and with a log2 fold change (Love et al., 2014) > 4. As expected, all the genera in the epi_oxy layer were aerobic and adapted to metabolic functions requiring O_2 (u_k optima ranges of O_2 between 8.7 and 11.9 mg L^{-1}; **Supplementary Table 1**), and/or potentially associated with human and animal hosts (**Table 2A**). Besides *Dolichospermum*, the most abundant genus in this group was *Flavobacterium*, which was present with a sizeable relative number of reads also in the oxygenated hypolimnion. A number of families with u_k-O_2 ranging between 9.0 and 11.2 mg L^{-1} tested positive for their prevalence in the epilimnetic layers (**Table 2A**). As expected, genera characteristics of the hyp_oxy layer (**Table 2B**) mostly inhabited the two oligomictic lakes Garda and Como, with a very limited presence in the three meromictic lakes. The O_2 optima range for this group of taxa was 7.1–9.7 mg L^{-1}.

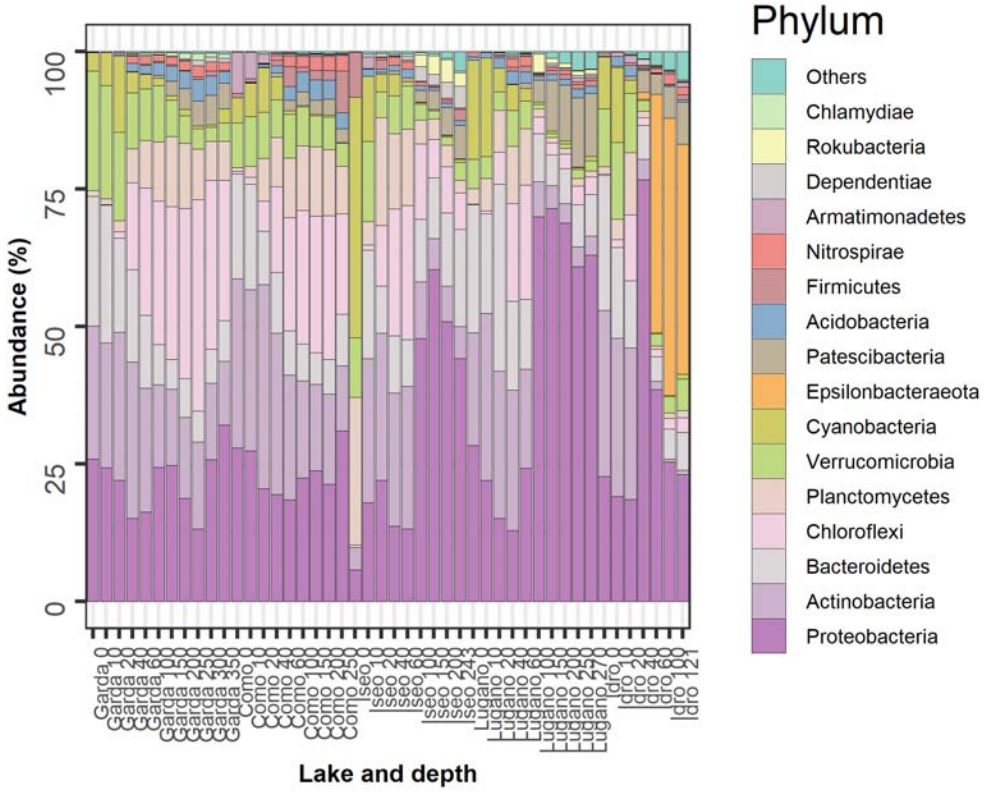

FIGURE 4 | Temporal development of the 16 more abundant phyla in the 5 lakes. Samples are coded by the name of the lake and depth (meters). The bars report the percentage contributions on the sample totals. The bacterial groups were selected identifying, for each lake, the 12 more abundant phyla. The high fraction of cyanobacteria at the surface of Lake Iseo was caused by a higher development of *Dolichospermum lemmermannii*.

The deep and hypoxic layers showed a number of classifiable genera typically present in the three meromictic lakes (**Table 2C**). Consistently with the distribution of ASVs at the phylum level (**Figure 4**), many genera belonged to the Proteobacteria, mostly Delta- and Betaproteobacteria, and Epsilonbacteraeota, as well as to other less represented phyla. u_k-O_2 ranged between 0.05 and 1.4 mg L^{-1}. The taxa identified belonged to genera that are known to be strictly or facultative anaerobic, or microaerobic, and linked to a wide variety of redox reactions at low O_2 conditions. Most genera belonging to the class Deltaproteobacteria were associated with sulfate reduction reactions, with *Desulfomonile* and *Desulfurivibrio* in lakes Idro and Lugano, *Desulfobacca* in both lakes, and *Desulfatirhabdium* in the three meromictic lakes. Along with other members of the Desulfobulbaceae, *Desulfurivibrio* is known also to perform disproportionation of elemental sulfur to sulfide and sulfate (Poser et al., 2013). A variety of oxidation processes under anaerobic and/or microaerobic conditions was carried out by a wide array of bacterial groups. Processes included methane oxidation (families Methylomonaceae, Methylomirabilaceae) and ammonium oxidation (*Candidatus* Anammoximicrobium); besides part of the family Rhodocyclaceae, denitrification can be performed by a wide array of microbial groups (including methanotrophs and methylotrophs). Other processes connected with known phenotypic characters included H_2-utilization in syntrophic association (*Syntrophus*) and, particularly in Lake Idro, sulfide (and hydrogen) oxidation at the expense of nitrate (*Sulfuricurvum* and *Sulfurimonas*). *Sulfurimonas* have been shown not only to use sulfide as electron donors but also for example thiosulfate or elemental sulfur. In Lake Lugano, *Gallionella* included iron-oxidizing bacteria requiring at least a certain amount of O_2. Further genera belonging to the less abundant phyla were linked to the mineralization of a wide variety of organic matter, including complex carbohydrates, cellulose, proteinaceous C, and organic acids (**Table 2**). Though it is difficult to clearly associate prevalent chemical functions to specific genera of bacteria (most of them are associated to multiple chemical transformations), the above descriptions provide an indication about the specialization of biologically mediated chemical processes in oxygen depleted hypolimnetic waters. Compared to the oxygenated layers, a few families emerged as typical monimolimnetic groups. Excluding the Methylophilaceae (u_k-O_2, 4.5) the optimum range of O_2 of "monimolimnetic" families was between 0.06 and 1.45 mg L^{-1}.

Variability of ASVs

The reads identified at the genus level were characterized by a very variable number of ASVs, due to variability in how many ASVs were nested within each genus. In a number of genera,

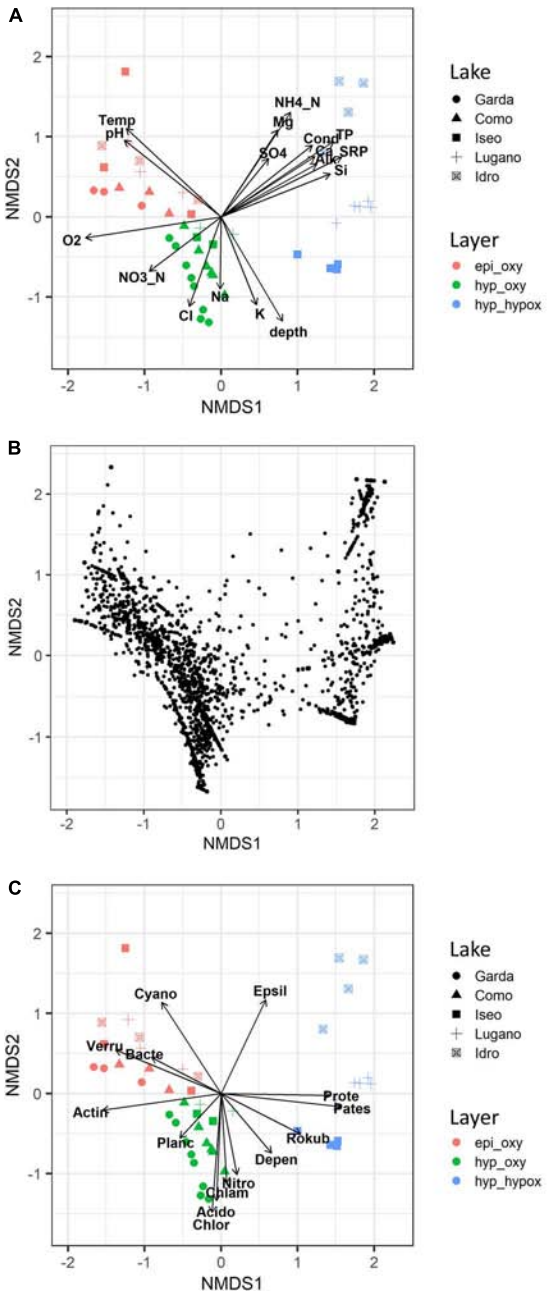

FIGURE 5 | Non-metric multidimensional scaling (NMDS) ordination (stress = 0.09) of samples based on the bacterioplankton composition; samples are coded by lake name (symbols) and layer (colors). **(A)** Vector fitting of significant ($P < 0.01$) environmental variables: Temp, water temperature; Cond, water conductivity; O_2, dissolved oxygen; SRP, soluble reactive phosphorus; TP, total phosphorus; NO_3_N, nitrate nitrogen; NH_4_N, ammoniacal nitrogen; Si, reactive silica; Alk, alkalinity; SO_4, sulfate; depth, sampling depth; other major ions are indicated by the element name. **(B)** Ordination of ASVs. **(C)** Vector fitting of significant ($P < 0.01$) dominant phyla: Acido, Acidobacteria; Actin, Actinobacteria; Bacte, Bacteroidetes; Chlam, Chlamydiae; Chlor, Chloroflexi; Cyano, Cyanobacteria; Depen, Dependentiae; Epsil, Epsilonbacteraeota; Nitro, Nitrospirae; Pates, Patescibacteria; Planc, Planctomycetes; Prote, Proteobacteria; Rokub, Rokubacteria; Verru, Verrucomicrobia. epi_oxy, 0–20 m layer; hyp_oxy, oxygenated hypolimnion; hyp_hypox, hypoxic/anoxic hypolimnion.

TABLE 1 | Association of the bacterial community structure with environmental factors based on **(A)** all the lakes and layers, **(B)** single lakes, and **(C)** single layers.

A

Lake/layers	Factor	Mantel *r*	*P*
ALL	10 var	0.72	<0.001
ALL	4 var	0.75	<0.001

B

Lake	Factor	Mantel *r*	*P*
Garda	10 var	0.93	<0.001
Como	10 var	0.89	<0.001
Iseo	10 var	0.78	<0.001
Lugano	10 var	0.89	<0.001
Idro	10 var	0.91	<0.001
Garda	4 var	0.86	<0.001
Como	4 var	0.86	<0.001
Iseo	4 var	0.71	<0.001
Lugano	4 var	0.82	<0.001
Idro	4 var	0.87	<0.001

C

Layer	Factor	Mantel *r*	*P*
epi_oxy	10 var	0.41	<0.05
hyp_oxy	10 var	0.58	<0.001
hyp_hypox	10 var	0.73	<0.001
epi_oxy	4 var	0.33	<0.05
hyp_oxy	4 var	0.50	<0.001
hyp_hypox	4 var	0.58	<0.001

The analyses were carried out by applying Mantel tests using Bray and Curtis dissimilarity matrices for ASVs abundances, and Euclidean distance matrices for groups of standardized environmental variables. Significance was assessed with 9999 permutations. The four variables include temperature, O_2, pH and NH_4-N; the 10 variables include, additionally, conductivity, SRP, NO_3-N, Si, alkalinity and SO_4.

such as *Flavobacterium*, the variability in ASVs was very high (61) and, considering the high number of species potentially included in this genus, not straightforward to interpret (mean sequence similarity in the 61 ASVs was 94%). For this genus, it was actually possible to assign a species name to only a low fraction of ASVs, i.e., *F. pectinovorum*, *F. succinicans*, *F. paronense*, *F. chungnamense/koreense*, and *F. terrigena*, each one present with only one sequence variant. Most of the different variants were mostly present in 2 or 3 lakes, only rarely 5 (figure not shown).

A similar distribution characterized other genera, such as those included in Cyanobacteria (**Figure 6**). The largest group in this phylum was represented by 15 ASVs classified within the picocyanobacteria (0.8–1.4 μm), namely *Cyanobium* PCC-6307. The similarity between each pair of aligned sequences assigned to this taxon ranged between 94.8 and 99.8%. Of these, only one ASV was present in the 5 lakes, whereas the majority (8) was found in one or several samples in one unique lake (**Figure 6**). The distribution of the *Cyanobium* strain present in the five lakes showed significant differences (KW, $P < 0.001$), with a number of reads greater in Lake Garda. Conversely, the

TABLE 2 | Differential distribution of genera along the vertical oxygen gradient.

Family	Genus	Ga	Co	Is	Lu	Id	epi_ oxy	hyp_ oxy	hyp_ hypox	Notes
A										
Acetobacteraceae	*Roseomonas*		+	+	+	+		+	+	Aerobic. Associated with human infections
Rhodobacteraceae	*Pseudorhodobacter*	+	+		+	+	+			Aerobic chemoorganotrophic
Sphingomonadaceae	*Sandarakinorhabdus*		+			+		+		cf. *limnophyla*; aerobic, bacteriochlorophyll-a
Burkholderiaceae	*Lautropia*	+		+		+		+		Mostly aerobic; human oral cavity and respiratory tract
Burkholderiaceae	*Polaromonas*			+		+		+		Aerobic, psychrophilic/psychotolerant
Microbacteriaceae	*Candidatus*_Aquiluna	+		+		+		+		Aerobic; photoheterotroph
Microbacteriaceae	*Candidatus*_Planktoluna		+		+	+	+			Aerobic; cf. sp. *difficilis*
Flavobacteriaceae	*Flavobacterium*			+					+	Widespread. Mostly aerobic.
Nostocaceae	*Dolichospermum*	+				+		+	+	*D. lemmermannii*; photosynthetic
Leptospiraceae	*Leptospira*	+	+	+		+	+			Includes pathogenic species
B										
Beijerinckiaceae	*Methylocystis*	+								Oxidizes methane; fixes N_2
Clade_I	Clade_Ia		+	+						Includes *Pelagibacter ubique*
Alteromonadaceae	*Rheinheimera*		+	+	+		+		+	Aerobic, chemoheterotrophic
Nitrosomonadaceae	MND1			+	+	+	+		+	
Solibacteraceae s.g.3	*Bryobacter*	+	+		+			+		Abundant within soils
Solibacteraceae s.g.3	*Candidatus*_Solibacter	+	+	+	+	+	+	+		Aerobic, mesophilic
Iamiaceae	*Iamia*	+	+	+	+					Similar clones isolated from Lake Bourget
Chthonomonadaceae	*Chthonomonas*	+	+	+	+			+		Includes obligately thermophilic species
Saprospiraceae	*Haliscomenobacter*									Utilization of complex carbon sources
Gemmataceae	*Gemmata*	+		+	+		+			Strictly aerobic
C										
Desulfobacteraceae	*Desulfatirhabdium*				+	+				Sulfate-reducing; anaerobic
Desulfobacteraceae	*Desulfobacula*			+	+				+	Sulfate-reducing; anaerobic
Desulfobacteraceae	Sva0081_sediment_g.	+		+	+	+		+	+	Sulfate-reducing; anaerobic
Desulfobulbaceae	*Desulfurivibrio*									Sulfate-reducing; anaerobic; perform S disproportionation
Syntrophaceae	*Desulfobacca*							+		Sulfate-reducing; anaerobic
Syntrophaceae	*Desulfomonile*						+			Sulfate-reducing; anaerobic
Syntrophaceae	*Syntrophus*			+		+				Syntrophic association with H_2-utilizing bacteria
Gallionellaceae	*Gallionella*									Includes iron-oxidizing bacteria living in low O_2
Methylophilaceae	*Methylotenera*	+					+			Denitrifying methylotroph
Rhodocyclaceae	*Dechloromonas*				+				+	Able to grow under anoxic conditions; dentrification
Rhodocyclaceae	*Denitratisoma*					+		+		Denitrifying bacterium
Rhodocyclaceae	*Sterolibacterium*							+		Denitrifying; O_2 or NO_3 as terminal electron acceptor
Rhodocyclaceae	*Sulfuritalea*	+			+	+		+		Oxidation of reduced sulfur compounds and hydrogen under anoxic conditions
Methylomonaceae	*Crenothrix*	+		+						Methane-oxidizing bacteria (O_2 and O_2-low conditions)
Methylomonaceae	*Methyloglobulus*			+	+	+		+	+	Microaerobic, methane-oxidizing bacterium
Methylomonaceae	pLW-20						+	+		
Thiovulaceae	*Sulfuricurvum*			+	+					Sulfide oxidation at the expense of nitrate; also thiosulfate or elemental sulfur as electron donors
Thiovulaceae	*Sulfurimonas*			+						Sulfide oxidation at the expense of nitrate; use H_2

(Continued)

TABLE 2 | Continued

C

Family	Genus	Ga	Co	Is	Lu	Id	epi_ oxy	hyp_ oxy	hyp_ hypox	Notes
Paludibacteraceae	*Paludibacter*				+	+	+			Anaerobic chemo-organotrophic
Prolixibacteraceae	BSV13									Isolated from anoxic soils
Parachlamydiaceae	*Candidatus* Protochlamydia		+	+	+		+	+	+	Intracellular symbionts
Anaerolineaceae	GWD2-49-16					+				Includes anaerobic species
Anaerolineaceae	*Longilinea*				+					Chemoheterotrophic, anaerobic
Anaerolineaceae	*Pelolinea*				+	+			+	Anaerobic, chemoorganotrophic
Family_XIII	*Anaerovorax*			+	+	+			+	Strictly anaerobic chemoorganotrophic
Kiritimatiellaceae	MSBL3			+						The family includes bacteria found in anoxic environments
Pirellulaceae	*Candidatus* Anammoximicrobium					+				Ammonium oxidation under anaerobic conditions
Methylomirabilaceae	*Candidatus* Methylomirabilis							+		Methane oxidation under anaerobic conditions
Methylomirabilaceae	Sh765B-TzT-35				+	+				
Opitutaceae	*Opitutus*? (*Cephaloticoccus*)				+	+				Anaerobe; chemo-organotrophic metabolism
Pedosphaeraceae	ADurb.Bin063-1			+	+	+			+	

*Taxa recorded with higher abundances (DESeq2, $P < 0.05$) in **(A)** the epilimnetic and **(B)** the hypolimnetic oxygenated layers, and **(C)** the hypoxic and anoxic monimolimnia. Cumulative relative abundances are highlighted as: +, 0% < reads < 1%; light gray, 1% ≤ reads < 5%; dark gray, reads ≥ 5%. For each layer in **(A–C)**, families with abundances significantly different from the other two layers were reported in bold ($P < 0.01$) and italic ($P < 0.05$). Ga, Garda; Co, Como; Is, Iseo; Lu, Lugano; Id, Idro. epi_oxy, oxygenated upper layers (0–20 m); hyp_oxy, oxygenated hypolimnion; hyp_hypox, hypoxic/anoxic hypolimnion. Family and genus names are based on the SILVA 132 taxonomy. The complete taxonomic table and additional information are reported in **Supplementary Table 1**. The bacteria listed in the table are known to present a wide array of adaptations and metabolic functions; only a few of the most characteristics are reported under the column "Notes."*

second more abundant strain present in four lakes did not show apparent differences (KW, $P < 0.1$, excluding Lake Lugano). At the species level, the two *Planktothrix* NIVA CYA 15 were assigned to the complex *P. agardhii/rubescens*. These two ASVs were distinguished by two sequence variants (AG). After a BLAST analysis, the more abundant ASV, (A), which was identified in all the lakes with the exclusion of Lake Idro, showed 100% similarity with many *P. rubescens/P. agardhii* sequences, including those previously associated to *P. rubescens* in the largest lakes south of the Alps (Salmaso et al., 2016). The distribution of this variant showed significant differences among lakes (KW, $P < 0.001$), with higher abundances in Lake Lugano. The second variant (G; lakes Garda, Iseo, and Lugano) was previously identified in Lake Garda using HTS approaches (Salmaso et al., 2018a). The sequence of the most abundant member of Nostocaceae (*Aphanizomenon* NIES 81), fully coincided (BLAST, 100%) with that of *Dolichospermum lemmermannii* (lakes Garda, Iseo, and Idro); the identification was confirmed also by previous observations carried out in all the DSL using a polyphasic approach (e.g., Capelli et al., 2017), and by further classification of reads using EzBioCloud (Yoon et al., 2017) and SILVA 132. The less abundant taxon among Nostocaceae coincided (99%) with *Aphanizomenon flos-aquae* (lakes Lugano and Idro). *Tychonema* sequences were identified, with one unique abundant oligotype, in lakes Como, Garda, and Iseo.

In this work, the new established group of non-photosynthetic Cyanobacteria was identified only in the three meromictic lakes, both in the oxygenated and hypoxic layers (Class Melainabacteria, orders Caenarcaniphilales, Gastranaerophilales, and Vampirovibrionales) and in the hypoxic layers (Class Sericytochromatia). The identity of the ASV attributed to Sericytochromatia was confirmed using a further downstream classification in SILVA 132, and evaluation of its position in the general phylogenetic tree. Considering the overall means, the relative abundances of NCY on the total of Cyanobacteria was however low, with maximum contributions < 6% in Melainabacteria and < 1% in Sericytocromatia.

The most impressive differences in the ASVs composition characterized the populations inhabiting the deep hypoxic/anoxic layers. Focusing on the most abundant taxa of **Table 2C**, all the genera were represented by at least one ASV exclusively present in one lake (**Table 3**). The high proportion of bases in common between each pair of sequences suggested that most of these genera, which were unclassified at the species level, were composed of the same or very closely related species. In several cases, only a very few ASVs were shared between two or more than one lake. It is worth to highlight the presence of unique ASVs of *Methylotenera* and *Crenothrix*, not shared with the meromictic lakes, in the two oligomictic lakes Garda and Como.

DISCUSSION

This work demonstrated the existence of a clear link between the vertical partition of water layers and the ecological selection of different bacterial populations and groups adapted to different local habitats. The BCC showed a large and significant divergence in the three main water layers that were identified on the basis

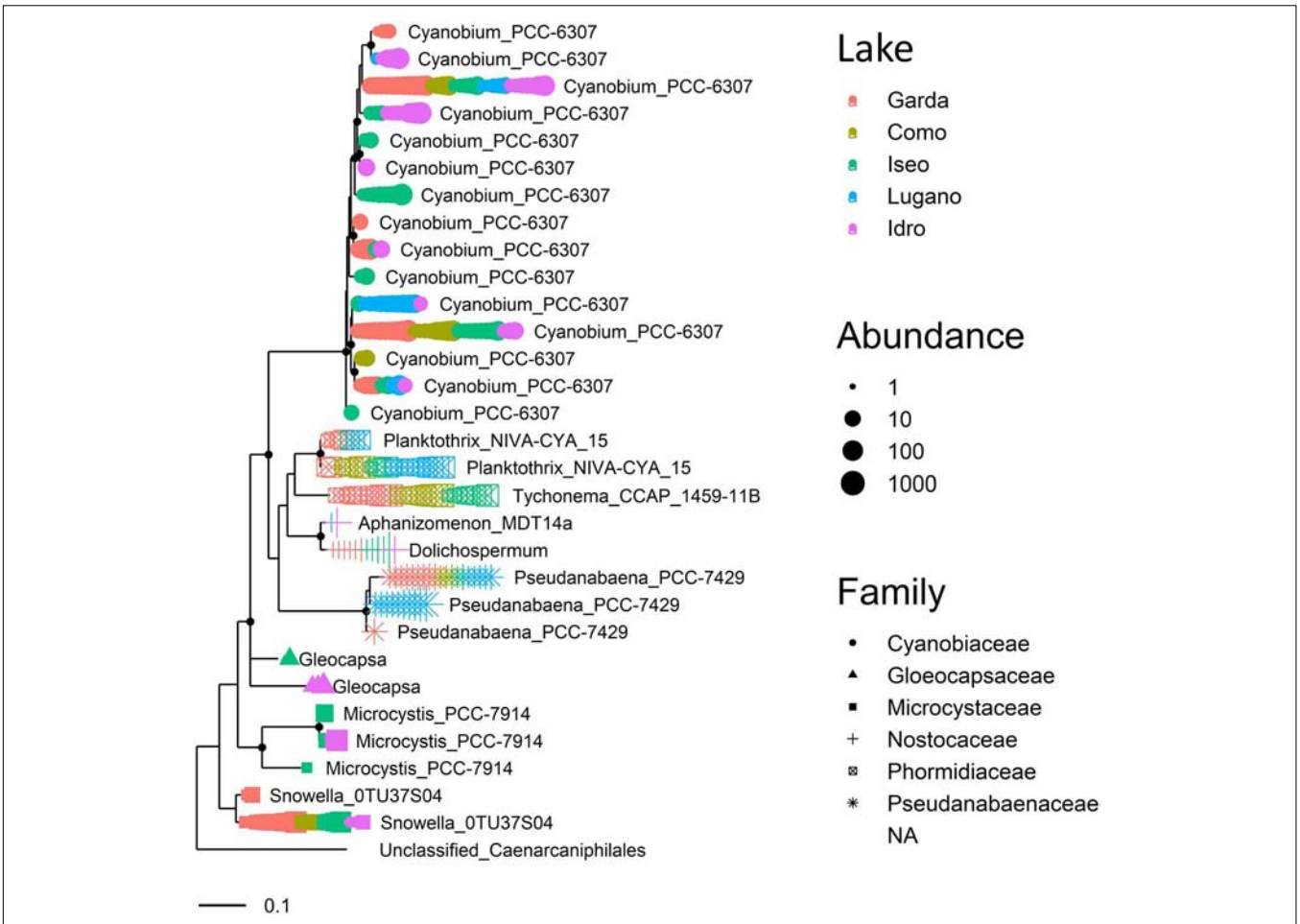

FIGURE 6 | Maximum likelihood (ML) rooted topology of cyanobacteria identified at least at the genus level in the 5 lakes based on alignment of 16S rRNA gene fragments; the tree is rooted by an outgroup member of non-photosynthetic cyanobacteria (unclassified Caenarcaniphilales, Melainabacteria). Each symbol on the tip of the tree corresponds to a single sample; different symbols and colors correspond to the cyanobacterial families (with the exclusion of the outgroup, "NA") and to the 5 lakes, respectively; the size of symbols is scaled according to abundance. The small black filled circles at the nodes indicate corresponding branch support aLRT-SH-like (Anisimova and Gascuel, 2006) values > 0.85.

of the oxygen concentrations and the main vertical physical and chemical gradients, namely the upper and oxygenated layers, dark oxygenated layers, and deep hypoxic layers. The differentiation was detected at different taxonomic levels and was linked to the ecological selection of different taxa adapted to perform a variety of metabolic functions constrained and driven by the availability of oxygen (as a proxy of redox conditions) and chemical compounds. Further, the higher sequence resolution to marker gene surveys provided by the oligotyping approach allowed to identify several exclusive ASVs present in single lakes and/or specific water layers and depths. After a brief examination of the elements that should be taken into account when analyzing ASVs, these aspects will be addressed in the next sections.

Interpretation of Oligotyping Results

The interpretation of data based on the identification of 16S rDNA oligotypes has to take into account several potential limitations intrinsic in the restricted sensitivity of this marker to resolve ecological and evolutionary variation between closely related lineages (Berry et al., 2017). The elucidation of ASVs diversity has to take into account the multicopy nature and intragenomic variability of the 16S rRNA gene (Větrovský and Baldrian, 2013; Stoddard et al., 2015; Callahan et al., 2017). Nevertheless, polymorphic sites in intragenomic 16S rRNA genes are scarce and occur at a much lower frequency than between 16S rRNA genes of different species (Espejo and Plaza, 2018). ASVs cannot be confused with species or clones (Dijkshoorn et al., 2000), rather they represent different oligotypes (Eren et al., 2013) of the same or different species and clones. As highlighted by Berry et al. (2017), the hypothesis that 16S rDNA oligotypes represent ecotypes or species like groups is still largely untested. Further, interpretation of ecological differentiation (differential traits) based on 16S rDNA oligotypes requires great care because many bacterial functional traits are not phylogenetically conserved (Martiny et al., 2013). For example, the investigations carried out in Lake Erie and several Michigan inland lakes showed that *Microcystis* 16S rDNA oligotypes were

TABLE 3 | Number of ASVs in the genera identified with higher abundances in the hypoxic and anoxic hypolimnia (**Table 2C**); only the most abundant genera (cumulative abundances > 1%) and with more than one ASVs have been included.

Genus	ASVs	% sim	Iseo	Lugano	Idro	More lakes
Desulfatirhabdium	3-3	99.1		2		1, Is_Lu_Id
Desulfurivibrio	3-3	99.4			3	
Desulfobacca	17-17	97.2[(a)]		9	8	
Desulfomonile	7-7	96.8			7	
Syntrophus	8-8	95.4		6	1	1, Is_Lu
Methylotenera	7-7	96.7		4		1, Is_Lu_Id – 1, Co_Lu_Id – 1, Ga_Co
Sterolibacterium	9-9	95.4	3	5		1, Lu_Is
Sulfuritalea	10-10	97.7	5	2		1, Is_Lu_Id – 1, Is_Id – 1, Ga
Crenothrix	8-8	94.4	1	1		3, Lu_Id – 2, Is_Id – 1, Ga_Co
pLW-20	7-7	98.6		3		4, Is_Lu_Id
Sulfuricurvum	4-4	96.2		1	2	1, Is_Id
Sulfurimonas	3-3	99.3			2	1, Is_Id
Paludibacter	14-13	97.4	5		4	4, Is_Id - 1, Is_Lu
BSV13	17-16	94.6	7	3	4	2, Is_Lu_Id - 1, Is_Id
GWD2-49-16	2-2	98.5		1		1, Lu_Id
Longilinea	2-2	92.1			1	1, Lu_Id
MSBL3	11-10	97.2[(b)]	1	5	3	1, Lu_Id - 1, Is_Id
C. Methylomirabilis	3-3	97.5	2			1, Is_Lu
Opitutus? (*Cephaloticoccus*)	2-2	98.1				1, Is_Lu_Id - 1, Is_Lu

"ASVs" reports the number of sequence variants identified on the original and rarefied tables, respectively. "% sim" reports the mean percentage DNA base similarity among ASVs; [(a,b)] excluding two and one, respectively, singular and very rare sequences in Lake Lugano. The number of exclusive ASVs in the lakes refers to determinations made on the original table; "More lakes" reports the number of ASVs shared between two or more lakes; oligomictic lakes are highlighted in light gray. Abbreviations as in ***Table 2****.*

not monophyletic and that they could not be used to infer toxicity (Berry et al., 2017).

At evolutionary time scales, the 16S rRNA gene has intrinsic limitations when the aim is to look at fine scale genetic differentiation because its molecular evolutionary rate is very slow (Ochman et al., 1999; Bahl et al., 2011; Dvořák et al., 2012; Segawa et al., 2018). Nevertheless, substitution rates in the 16S rRNA genes are highly variable across bacterial species, strongly depending on the life strategies and habitats. For example, rates of 16S rRNA gene evolution are higher in cultures or obligate pathogens and symbionts due to smaller population sizes and increased levels of genetic drift (Kuo and Ochman, 2009). However, these rates are still not within the ecological timescales of common limnological investigations, including the analyzed dataset. Therefore, from an evolutionary perspective, the 16S rRNA gene may not resolve more recent evolutionary diversification within a lineage (Berry et al., 2017).

Environmental Drivers and BCC Distribution

The bacterial communities in the DSL showed a different distribution in the single lakes and water layers. A distinguishing element in the NMDS configuration was well-represented by the presence of clusters of ASVs in correspondence the hypoxic layers of the three meromictic lakes.

Differences in the bacterial community structure were significantly associated with the main environmental variables. Based on the Mantel tests, besides the whole group of physical and chemical variables, bacteria showed a strong link with a subgroup of variables particularly representatives of the main physical and chemical gradients that contribute to differentiate the deep oligomictic and meromictic DSL, i.e., besides thermal gradients, pH, O_2, and NH_4-N (Garibaldi et al., 1997; Mosello and Giussani, 1997; Viaroli et al., 2018). These results supported the view that significant ecological processes contributed to assemble different bacterial communities adapted to different ecological conditions. Compared to the oxygenated layers, the association between BCC and environmental variables was even more pronounced in the deep hypoxic layers of the three meromictic lakes, highlighting the existence of a strong environmental filtering and peculiar deep habitats. These results were fully consistent with the identification by DESeq2 of specific groups of taxa inhabiting the oxygenated layers (epi-oxy and hyp_oxy) in the five lakes and the hypoxic layers (hyp_hypox) in the three meromictic lakes (see next sections).

The identification of genera typical of the three water layers was fully consistent with the corresponding optima (u_k) for oxygen, which, in the hypoxic/anoxic layers, and in the oxygenated layers, were between 0.05 and 1.4 mg L^{-1}, and 7.1 and 11.9 mg L^{-1}, respectively. These optima values allowed to quantify the O_2 concentration requirements of distinct taxa developing in distinct strata. At the same time, these values can contribute to compare, on a quantitative basis, the oxygen niche of the same group of taxa in other aquatic systems.

Diversity and Quantitative Importance and Ecophysiology of Representative Bacteria in the Three Lake Layers

The significance of the presence of 16S rDNA oligotypes in specific water layers (**Table 2**) was supported by a high number of ASVs characterized by cumulative relative abundances greater than 1 and 5%. The establishment of distinct bacterial genera in distinct layers allowed inferring a variety of metabolic processes. Although the 16S rRNA gene do not intrinsically provide evidence on microbial metabolism, this information has been widely used to identify metabolisms associated with related phenotyped strains (Bowman and Ducklow, 2015). Besides direct approaches (physiology and metabolomics), more detailed information on metabolic and functional profiles should rely on other sequencing techniques, such as shotgun metagenomic sequencing (Ortiz-Estrada et al., 2019).

Species localized at the surface were well-known to belong to groups living in oxygenated environments. Among these, Flavobacteria are known to include commensal and opportunistic pathogens (Crump et al., 2001). Though a few species of *Flavobacterium* may grow weakly under micro- and anaerobic conditions, many species are obligately aerobic and occurring in a variety of terrestrial and aquatic environments, and food (Betts, 2006). Other typical taxa at the surface included genera potentially associated with human and animal hosts (e.g., *Roseomonas* and *Lautropia*), as well as aerobic, anoxygenic (such as *Sandarakinorhabdus*; Gich and Overmann, 2006) and oxygenic (Cyanobacteria; Whitton, 2012) phototrophic bacteria. In the oxygenated hypolimnion, Anaerolineales (unclassified Anaerolineaceae) contributed for a great fraction to the bacterial community. A recent growing number of investigations confirmed the presence of this group (specifically the CL500-11 lineage) in the oxygenated hypolimnia of lakes (Urbach et al., 2007; Okazaki et al., 2013, 2018). CL500-11 was identified using CARD-FISH also in the hypolimnion of Lake Garda (Okazaki et al., 2018). In the oxygenated hypolimnion of Lake Michigan, Denef et al. (2016) showed an important role played by this taxon in nitrogen-rich DOM mineralization. Up to now, only a few species have been isolated and included in the class Anaerolineae, all of which showed anaerobic growth (Okazaki et al., 2013), as the three genera identified in the anoxic hypolimnion (**Table 2C**). Overall, the characteristics of this class and corresponding lower taxonomical levels will require a better characterization.

In the three meromictic lakes, the presence of peculiar species (**Supplementary Figure 3**) was particularly apparent in the hypoxic/anoxic hypolimnia. In the DSL, the unique assemblages in the deep layers were the result of the ecological selection of bacteria adapted to low redox conditions. The high relative abundance of sulfate reducing bacteria in Lake Idro can be linked to the replenishment of calcium sulfate from subsurface springs (Viaroli et al., 2018). The presence of several methane oxidizing bacteria in the hypoxic layers was indicative of an important methanotrophic activity. In freshwater lakes, methanotrophs are mostly part of aerobic Gamma- and Alpha-proteobacteria (such as *Methylocystis* in oxygenated hypolimnia; **Table 2B**). In the hypoxic/anoxic layers of lakes Iseo and Lugano, an important methanotroph was *Candidatus* Methylomirabilis. This genus includes species that are known to oxidize methane using a unique pathway of denitrification that tentatively produces N_2 and O_2 from nitric oxide (NO) (Graf et al., 2018). Selected species, such as *Ca.* M. limnetica were found to bloom in the anoxic layers of the deep stratified Lake Zug, suggesting a niche for NC10 bacteria in the methane and nitrogen cycle (Graf et al., 2018). A further important methanotroph able to develop with oxygen as well as under oxygen-deficient conditions in lakes Lugano and Idro was *Crenothrix*. Oswald et al. (2017) demonstrated that an important fraction of upward-diffusing methane in stratified freshwater lakes was oxidized by *Crenothrix polyspora*. Overall, methane-oxidizing bacteria are a major biological sink of CH_4, protecting Earth against the effects of this strong greenhouse gas. Conversely, during mineralization of organic matter, the production of methane in anoxic conditions is due to anaerobic Archaea (not analyzed in this work). Methanogenesis represents the largest biogenic source of methane on Earth (Vanwonterghem et al., 2016). Though documented also in the upper well-oxygenated layers (Grossart et al., 2011; Bogard et al., 2014), methanogenesis is the cause of significant production and accumulations of CH_4 in hypoxic and anoxic hypolimnia (Brock, 1985). *Candidatus* Anammoximicrobium, a bacterium capable of ammonium oxidation under anaerobic conditions in the presence of nitrite (Khramenkov et al., 2013) was detected in lakes Lugano and Idro. Nevertheless, high concentrations of ammonium in these two lakes could suggest that anammox activity is negligible (or at least at levels that do not consume the ammonium pool) or that nitrite, not measured, is limiting. Denitrification processes were exemplified by the presence of two denitrifying genera in lakes Iseo and Lugano: *Denitratisoma* and *Sterolibacterium*; these bacteria were shown to be able to use also O_2 as terminal electron acceptor (Tarlera and Denner, 2003; Fahrbach et al., 2006). The phylum Epsilonbacteraeota included two among the most abundant monimolimnetic organisms, i.e., *Sulfurimonas* and *Sulfuricurvum*. Both oxidize sulfide at the expense of nitrate (Haaijer et al., 2012); their high abundance in Lake Idro can be coupled to high sulfate concentrations and reduction. Further, *Sulfurimonas* species can grow with a variety of electron donors and acceptors, including O_2 as an electron acceptor for selected species (Han and Perner, 2015). Overall, the observation that anoxic hypolimnia harbor putative sulfur cycling groups not present in polymictic hypolimnia, which are more frequently oxygenated, was confirmed also in smaller lakes (z_m = 5–22 m) (Linz et al., 2017).

Besides large and deep lakes (Kurilkina et al., 2016; Salmaso et al., 2018a), the high diversity of deep layers documented in the DSL is also consistent with previous results obtained in a group of medium size (z_m < 30 m) stratified lakes, which showed a higher number of unique OTUs in the hypolimnia than epilimnia (Schmidt et al., 2016). A few of the most representative taxa identified in the DSL were common to the more abundant genera found recently in other two meromictic (Lake Pavin, z_m = 92 m) and dimictic (Lake Aydat, z_m = 12 m) perialpine lakes (Keshri et al., 2018). Besides the core microbiome typical of one or both lakes (*clade hgcI* and *CL500-29 marine group*, *Limnohabitans*), the most represented genera in the anoxic

zone were *Syntrophus, Methylotenera, Gallionella, Sulfurimonas, Desulfurivibrio,* and *Sulfuritalea*. These genera were mostly present in the meromictic lakes included in this work, further confirming how predominant vertical environmental gradients can affect the environmental filtering of bacterial communities.

Identification and Distribution of ASVs and Genera in Lakes and Water Layers

The identification of genera in **Tables 2**, **3** cannot be considered exhaustive because, in the analyzed dataset, only the 40 and <4% of taxa were classified at least at the genus and species level, respectively. Besides highlighting the limitations of techniques based on amplicon sequencing based on short reads (Poretsky et al., 2014; Ranjan et al., 2016), the high fraction of unclassified taxa at the lower taxonomic ranks contributed partly to confirm the existence of a fraction of diversity still not described in taxonomic databases (Menzel et al., 2015, 2016; Sunagawa et al., 2015). This incompleteness is mostly due to the limits of classical culture-based approaches in the estimation of environmental biodiversity (Lloyd et al., 2018; Overmann et al., 2019). Due to current fast technological developments, the detection of uncultured environmental "species" using metagenome-assembled genomes (MAGs) is expected to grow exponentially, calling for an update of present nomenclatural approaches (Oren and Garrity, 2018; Rosselló-Móra and Whitman, 2019). A paradigmatic example is provided by the recent discovery of non-photosynthetic cyanobacteria in a wide variety of environments (Di Rienzi et al., 2013; Soo et al., 2017) and in the perialpine lakes (Salmaso et al., 2018a; Monchamp et al., 2019). Excluding one isolated species (Soo et al., 2015), NCY are presently recognized and described from MAGs (Glöckner et al., 2017), without being formally described in the nomenclatural systems of prokaryotes (ICP) and algae fungi and plants (ICN) (Komárek et al., 2014; cf. Guiry and Guiry, 2019), and without clear described ecological roles and functions (but see Soo et al., 2015). On the other side, the taxonomic annotations in databases from predictions from sequences rather than authoritative assignments based on studies of type strains or isolates are not free of complications (Edgar, 2018).

A few classified genera included a high number of ASVs. At the genus level, though characterized by a high dispersion, the association between abundances and ASVs diversity was highly significant (Spearman $\rho = 0.68$, $P < 0.001$), highlighting the general relationship between sequencing depth and ASVs numbers. This was exemplified by the high number of ASVs in the genera identified with higher abundances in the hypoxic and anoxic hypolimnia (**Table 3**) and in the phylum Cyanobacteria. In this group, the higher number of ASVs was found in the smallest cell−size Cyanobacteria (*Cyanobium*), i.e., the fraction roughly corresponding to the picocyanobacteria (Jasser and Callieri, 2017). The high diversity of this functional fraction was recognized, using oligotyping methods (Eren et al., 2013), also in previous investigations carried out in Lake Garda (Salmaso et al., 2018a). In the case of Cyanobacteria investigated in previous studies, such as *Planktothrix rubescens* (D'Alelio et al., 2013; Salmaso et al., 2016), it was possible to confirm the existence of two sequence variants already identified in Lake Garda using oligotyping methods (Salmaso et al., 2018a). Conversely, filaments of *Tychonema bourrellyi* were identified with only one ASV, and only in the lakes where their presence was for the first time discovered using microscopical and phylogenetic methods (Shams et al., 2015; Salmaso et al., 2016). The appearance of this cryptogenic (*sensu* Kokociński et al., 2017) species was documented, for the first time in Lake Maggiore in 2004–2005. Since then, excluding lakes Lugano and Idro, *Tychonema* showed an increasing emergence in all the DSL. The discovery of *Tychonema* in the largest DSL was cause of concern, because of the ability of this species to produce neurotoxins (anatoxins; Shams et al., 2015; Cerasino et al., 2016). Analogously, the unique ASV detected in the populations of the bloom forming *Dolichospermum lemmermannii* (**Figure 6**) was consistent with the equivalence of 16S rDNA sequences in strains previously isolated in lakes Garda, Como, Iseo, and Lugano (Capelli et al., 2017).

While the presence of specialized bacterial communities in the monimolimnia of the three meromictic lakes was widely expected, the existence of groups of different ASVs was less obvious. Though not independent on the denoising strategy used (Nearing et al., 2018), the extent of ASVs differentiation was however apparent for several genera and species. A few dominant genera as well as ASVs were exclusively found in the deep layers of only one or two meromictic lakes. Considering the high 16S rDNA base similarity, most of the ASVs could represent strains belonging to the same species. The uneven distribution of taxa does not have a clear-cut explanation. Starting from the assumption that no barriers can prevent the migration of hypolimnetic inhabitants between the hypolimia of different lakes, the results of this study suggest that the exclusive (or dominant) presence of genera and species can be explained by ecological selection due to differences in environmental conditions in different lakes and strata.

The results obtained in this work have to be considered representative of the stratification period. As previously demonstrated, in large lakes BCC in the trophogenic layers can show strong temporal fluctuations following the temperate seasonal climate patterns (Salmaso et al., 2018a). Therefore, differences are expected to be mainly manifest in the layers mostly affected by climatic fluctuations and mixing dynamics, i.e., the surface layers, whereas the BCC in the more stable and not or only partially mixed deep hypolimnia should be less affected. Nevertheless, considering that at present the range of seasonal variation of BCC in the deepest layers is unknown, this speculation must be considered as a hypothesis to be verified on the basis of the investigations currently underway on a seasonal basis.

CONCLUSION

The establishment of meromixis in deep lakes opens the way to the creation of new isolated, dark, hypoxic and anoxic

habitats, drastically changing the biogeochemical gradients and processes along the water column. In the deep meromictic lakes south of the Alps, the formation of habitats completely segregated for long periods of time sustained the ecological selection and development of diversified bacterial communities. The highly diversified and coupled processes sustained by the monimolimnetic microbiota are essential ecosystem services that enhance mineralization of organic matter and formation of reduced compounds, and also abatement of undesirable greenhouse gasses. Though much less marked, the presence of distinctive populations was substantiated, confirming previous works (Denef et al., 2016; Okazaki et al., 2017, 2018), also in the oxygenated hypolimnia. Finally, though ASVs does not necessarily reflect phylogenetically consistent populations (Berry et al., 2017), this study confirms the utility of oligotyping based methods for distinguishing sequence types along ecological gradients. ASVs have an intrinsic biological meaning as a DNA sequence (Callahan et al., 2017). In perspective, their use will contribute providing a more solid basis to compare biodiversity in a wide spectrum of habitat types, including large lakes.

DATA AVAILABILITY STATEMENT

The datasets generated for this study can be found in the European Nucleotide Archive (ENA) with study accession PRJEB33405.

AUTHOR CONTRIBUTIONS

NS was involved in all aspects of the manuscript; see Acknowledgments for technical support.

ACKNOWLEDGMENTS

Investigations were carried out in the framework of the LTER (Long Term Ecological Research) Italian network, site Southern Alpine lakes, IT08-000-A (http://www.lteritalia.it/), with the support of G. Franzini and colleagues (ARPA Veneto), F. Buzzi (ARPA Lombardia), and B. Leoni (University of Milan Bicocca). I would like to express my gratitude to my colleagues in FEM, Hydrobiology, in particular Adriano Boscaini and the technical staff, for their support in the field and/or laboratory activities, and Leonardo Cerasino for water chemical analyses (FEM, Hydrochemistry platform). Special thanks are due to M. Pindo (FEM, Computational Biology) for HTS analyses. I am grateful to the reviewers for critically reading the manuscript and suggesting substantial improvements.

SUPPLEMENTARY MATERIAL

The Supplementary Material for this article can be found online at: https://www.frontiersin.org/articles/10.3389/fmicb.2019.02257/full#supplementary-material

REFERENCES

Ambrosetti, W., and Barbanti, L. (1992). Physical limnology in Italy: an historical overview. *Mem. dell'Istituto Ital. di Idriobiologia* 50, 37–59.

Anisimova, M., and Gascuel, O. (2006). Approximate likelihood-ratio test for branches: a fast, accurate, and powerful alternative. *Syst. Biol.* 55, 539–552. doi: 10.1080/10635150600755453

APHA-AWWA-WEF (2005). *Standard Methods for the Examination of Water and Wastewater*, 21st Edn. Washington, D.C: American Public Health Association/American Water Works Association/Water Environment Federation.

Bahl, J., Lau, M. C. Y., Smith, G. J. D., Vijaykrishna, D., Cary, S. C., Lacap, D. C., et al. (2011). Ancient origins determine global biogeography of hot and cold desert cyanobacteria. *Nat. Commun.* 2:163. doi: 10.1038/ncomms1167

Berry, M. A., White, J. D., Davis, T. W., Jain, S., Johengen, T. H., Dick, G. J., et al. (2017). Are oligotypes meaningful ecological and phylogenetic units? A case study of *Microcystis* in Freshwater Lakes. *Front. Microbiol.* 8:365. doi: 10.3389/fmicb.2017.00365

Betts, G. (2006). "Other spoilage bacteria," in *Food Spoilage Microorganisms*, eds C. de and W. Blackburn (Cambridge: Woodhead Publishing), 668–693. doi: 10.1533/9781845691417.5.668

Bogard, M. J., Del Giorgio, P. A., Boutet, L., Chaves, M. C. G., Prairie, Y. T., Merante, A., et al. (2014). Oxic water column methanogenesis as a major component of aquatic CH4 fluxes. *Nat. Commun.* 5:5350. doi: 10.1038/ncomms6350

Bowman, J. S., and Ducklow, H. W. (2015). Microbial communities can be described by metabolic structure: a general framework and application to a seasonally variable, depth-stratified microbial community from the coastal West Antarctic Peninsula. *PLoS One* 10:e0135868. doi: 10.1371/journal.pone.0135868

Brock, T. D. (1985). *A Eutrophic Lake - Lake Mendota*. Madison, WIS: Springer Science.

Bullerjahn, G. S., and Post, A. F. (2014). Physiology and molecular biology of aquatic cyanobacteria. *Front. Microbiol.* 5:359. doi: 10.3389/fmicb.2014.00359

Bush, T., Diao, M., Allen, R. J., Sinnige, R., Muyzer, G., and Huisman, J. (2017). Oxic-anoxic regime shifts mediated by feedbacks between biogeochemical processes and microbial community dynamics. *Nat. Commun.* 8:789. doi: 10.1038/s41467-017-00912-x

Callahan, B. J., McMurdie, P. J., and Holmes, S. P. (2017). Exact sequence variants should replace operational taxonomic units in marker-gene data analysis. *ISME J.* 11, 2639–2643. doi: 10.1038/ismej.2017.119

Callahan, B. J., McMurdie, P. J., Rosen, M. J., Han, A. W., Johnson, A. J. A., and Holmes, S. P. (2016a). DADA2: high-resolution sample inference from Illumina amplicon data. *Nat. Methods* 13, 581–583. doi: 10.1038/nmeth.3869

Callahan, B. J., Sankaran, K., Fukuyama, J. A., McMurdie, P. J., and Holmes, S. P. (2016b). Bioconductor workflow for microbiome data analysis: from raw reads to community analyses. *F1000Res.* 5:1492. doi: 10.12688/f1000research.8986.2

Capelli, C., Ballot, A., Cerasino, L., Papini, A., and Salmaso, N. (2017). Biogeography of bloom-forming microcystin producing and non-toxigenic populations of *Dolichospermum lemmermannii* (Cyanobacteria). *Harmful Algae* 67, 1–12. doi: 10.1016/j.hal.2017.05.004

Casamayor, E. O., Llirós, M., Picazo, A., Barberán, A., Borrego, C. M., and Camacho, A. (2012). Contribution of deep dark fixation processes to overall CO2 incorporation and large vertical changes of microbial populations in stratified karstic lakes. *Aquat. Sci.* 74, 61–75. doi: 10.1007/s00027-011-0196-5

Cerasino, L., Capelli, C., and Salmaso, N. (2017). A comparative study of the metabolic profiles of common nuisance cyanobacteria in southern perialpine lakes. *Adv. Oceanogr. Limnol.* 8, 22–32. doi: 10.4081/aiol.2017.6381

Cerasino, L., and Salmaso, N. (2012). Diversity and distribution of cyanobacterial toxins in the Italian subalpine lacustrine district. *Oceanol. Hydrobiol. Stud.* 41, 54–63. doi: 10.2478/s13545-012-0028-9

Cerasino, L., Shams, S., Boscaini, A., and Salmaso, N. (2016). Multiannual trend of microcystin production in the toxic cyanobacterium *Planktothrix rubescens* in Lake Garda (Italy). *Chem. Ecol.* 32, 492–506. doi: 10.1080/02757540.2016.1157175

Crump, E. M., Perry, M. B., Clouthier, S. C., and Kay, W. W. (2001). Antigenic characterization of the fish pathogen *Flavobacterium psychrophilum*. *Appl. Environ. Microbiol.* 67, 750–759. doi: 10.1128/AEM.67.2.750-759.2001

D'Alelio, D., Salmaso, N., and Gandolfi, A. (2013). Frequent recombination shapes the epidemic population structure of *Planktothrix* (Cyanoprokaryota) in Italian subalpine lakes. *J. Phycol.* 49, 1107–1117. doi: 10.1111/jpy.12116

Davis, T. W., Stumpf, R., Bullerjahn, G. S., McKay, R. M. L., Chaffin, J. D., Bridgeman, T. B., et al. (2019). Science meets policy: a framework for determining impairment designation criteria for large waterbodies affected by cyanobacterial harmful algal blooms. *Harmful Algae* 81, 59–64. doi: 10.1016/j.hal.2018.11.016

De Wever, A., Van Der Gucht, K., Muylaert, K., Cousin, S., and Vyverman, W. (2008). Clone library analysis reveals an unusual composition and strong habitat partitioning of pelagic bacterial communities in Lake Tanganyika. *Aquat. Microb. Ecol.* 50, 113–122. doi: 10.3354/ame01157

Denef, V. J., Mueller, R. S., Chiang, E., Liebig, J. R., and Vanderploeg, H. A. (2016). Chloroflexi CL500-11 populations that predominate deep-lake hypolimnion bacterioplankton rely on nitrogen-rich dissolved organic matter metabolism and C1 compound oxidation. *Appl. Environ. Microbiol.* 82, 1423–1432. doi: 10.1128/AEM.03014-5

Di Rienzi, S. C., Sharon, I., Wrighton, K. C., Koren, O., Hug, L. A., Thomas, B. C., et al. (2013). The human gut and groundwater harbor non-photosynthetic bacteria belonging to a new candidate phylum sibling to Cyanobacteria. *eLife* 2:e01102. doi: 10.7554/eLife.01102

Dijkshoorn, L., Ursing, B. M., and Ursing, J. B. (2000). Strain, clone and species: comments on three basic concepts of bacteriology. *J. Med. Microbiol.* 49, 397–401. doi: 10.1099/0022-1317-49-5-397

Dvořák, P., Hašler, P., and Poulíčková, A. (2012). Phylogeography of the *Microcoleus vaginatus* (Cyanobacteria) from three continents - a spatial and temporal characterization. *PLoS One* 7:e40153. doi: 10.1371/journal.pone.0040153

Edgar, R. (2018). Taxonomy annotation and guide tree errors in 16S rRNA databases. *PeerJ* 6:e5030. doi: 10.7717/peerj.5030

Eren, A. M., Maignien, L., Sul, W. J., Murphy, L. G., Grim, S. L., Morrison, H. G., et al. (2013). Oligotyping: differentiating between closely related microbial taxa using 16S rRNA gene data. *Methods Ecol. Evol.* 4, 1111–1119. doi: 10.1111/2041-210X.12114

Espejo, R. T., and Plaza, N. (2018). Multiple Ribosomal RNA operons in bacteria; Their concerted evolution and potential consequences on the rate of evolution of their 16S rRNA. *Front. Microbiol.* 9:1232. doi: 10.3389/fmicb.2018.01232

Fahrbach, M., Kuever, J., Meinke, R., Kämpfer, P., and Hollender, J. (2006). *Denitratisoma oestradiolicum* gen. nov., sp. nov., a 17 β-oestradiol-degrading, denitrifying betaproteobacterium. *Int. J. Syst. Evol. Microbiol.* 56, 1547–1552. doi: 10.1099/ijs.0.63672-0

Garcia, S. L., Salka, I., Grossart, H. P., and Warnecke, F. (2013). Depth-discrete profiles of bacterial communities reveal pronounced spatio-temporal dynamics related to lake stratification. *Environ. Microbiol. Rep.* 5, 549–555. doi: 10.1111/1758-2229.12044

Garibaldi, L., Brizzio, M. C., Mezzanotte, V., Varallo, A., and Mosello, R. (1997). Water chemistry and trophic level evolution of Lake Iseo. *Doc. dell'Istituto Ital. di Idrobiol.* 61, 135–151.

Gich, F., and Overmann, J. (2006). *Sandarakinorhabdus limnophila* gen. nov., sp. nov., a novel bacteriochlorophyll a-containing, obligately aerobic bacterium isolated from freshwater lakes. *Int. J. Syst. Evol. Microbiol.* 56, 847–854. doi: 10.1099/ijs.0.63970-0

Glöckner, F. O., Yilmaz, P., Quast, C., Gerken, J., Beccati, A., Ciuprina, A., et al. (2017). 25 years of serving the community with ribosomal RNA gene reference databases and tools. *J. Biotechnol.* 261, 169–176. doi: 10.1016/J.JBIOTEC.2017.06.1198

Graf, J. S., Mayr, M. J., Marchant, H. K., Tienken, D., Hach, P. F., Brand, A., et al. (2018). Bloom of a denitrifying methanotroph, "*Candidatus* Methylomirabilis limnetica", in a deep stratified lake. *Environ. Microbiol.* 20, 2598–2614. doi: 10.1111/1462-2920.14285

Grossart, H.-P., Frindte, K., Dziallas, C., Eckert, W., and Tang, K. W. (2011). Microbial methane production in oxygenated water column of an oligotrophic lake. *Proc. Natl. Acad. Sci.* 108, 19657–19661. doi: 10.1073/pnas.1110716108

Guindon, S., Dufayard, J.-F., Lefort, V., Anisimova, M., Hordijk, W., and Gascuel, O. (2010). New algorithms and methods to estimate maximum-likelihood phylogenies: assessing the performance of PhyML 3.0. *Syst. Biol.* 59, 307–321. doi: 10.1093/sysbio/syq010

Guiry, M. D., and Guiry, G. M. (2019). *AlgaeBase. World-Wide Electronic Publication*. Galway: National University of Ireland.

Haaijer, S. C. M., Crienen, G., Jetten, M. S. M., and Op den Camp, H. J. M. (2012). Anoxic iron cycling bacteria from an iron sulfide- and nitrate-rich freshwater environment. *Front. Microbiol.* 3:26. doi: 10.3389/fmicb.2012.00026

Han, Y., and Perner, M. (2015). The globally widespread genus *Sulfurimonas*: versatile energy metabolisms and adaptations to redox clines. *Front. Microbiol.* 6:989. doi: 10.3389/fmicb.2015.00989

Hernández-Avilés, J. S., Callieri, C., Bertoni, R., Morabito, G., Leoni, B., Lepori, F., et al. (2018). Prokaryoplankton and phytoplankton community compositions in five large deep perialpine lakes. *Hydrobiol* 824, 71–92. doi: 10.1007/s10750-018-3586-z

Huber, W., Carey, V. J., Gentleman, R., Anders, S., Carlson, M., Carvalho, B. S., et al. (2015). Orchestrating high-throughput genomic analysis with Bioconductor. *Nat. Methods* 12, 115–121. doi: 10.1038/nmeth.3252

Humayoun, S. B., Bano, N., and Hollibaugh, J. T. (2003). Depth distribution of microbial diversity in mono lake, a meromictic soda lake in California. *Appl. Environ. Microbiol.* 69, 1030–1042. doi: 10.1128/AEM.69.2.1030-1042.2003

Jasser, I., and Callieri, C. (2017). "Picocyanobacteria – the smallest cell-size cyanobacteria," in *Handbook on Cyanobacterial Monitoring and Cyanotoxin Analysis*, eds J. Meriluoto, L. Spoof, and G. A. Codd (Chichester: Wiley), 19–27. doi: 10.1002/9781119068761.ch3

Jasser, I., Królicka, A., Jakubiec, K., and Chróst, R. J. (2013). Seasonal and spatial diversity of picocyanobacteria community in the Great Mazurian Lakes derived from DGGE analyses of ITS region of rDNA and cpcBAIGS [corrected] markers. *J. Microbiol. Biotechnol.* 23, 739–749. doi: 10.4014/jmb.1208.08002

Jungblut, A. D., Lovejoy, C., and Vincent, W. F. (2010). Global distribution of cyanobacterial ecotypes in the cold biosphere. *ISME J.* 4, 191–202. doi: 10.1038/ismej.2009.113

Kallf, J. (2002). *Limnology*. Upper Saddle River, NJ: Prentice-Hall, Inc.

Katoh, K., and Standley, D. M. (2013). MAFFT multiple sequence alignment software version 7: improvements in performance and usability. *Mol. Biol. Evol.* 30, 772–780. doi: 10.1093/molbev/mst010

Keshri, J., Pradeep Ram, A. S., Nana, P. A., and Sime-Ngando, T. (2018). Taxonomical resolution and distribution of bacterioplankton along the vertical gradient reveals pronounced spatiotemporal patterns in contrasted temperate freshwater lakes. *Microb. Ecol.* 76, 372–386. doi: 10.1007/s00248-018-1143-y

Khramenkov, S. V., Kozlov, M. N., Kevbrina, M. V., Dorofeev, A. G., Kazakova, E. A., Grachev, V. A., et al. (2013). A novel bacterium carrying out anaerobic ammonium oxidation in a reactor for biological treatment of the filtrate of wastewater fermented sludge. *Microbiology* 82, 628–636. doi: 10.1134/S002626171305007X

Kokociński, M., Akçaalan, R., Salmaso, N., Stoyneva-Gärtner, M. P., and Sukenik, A. (2017). "Expansion of alien and invasive Cyanobacteria," in *Handbook on Cyanobacterial Monitoring and Cyanotoxin Analysis*, eds J. Meriluoto, L. Spoof, and G. A. Codd (Chichester: Wiley), 28–39. doi: 10.1002/9781119068761.ch4

Komárek, J., Kaštovský, J., Mareš, J., and Johansen, J. R. (2014). Taxonomic classification of cyanoprokaryotes (cyanobacterial genera) 2014, using a polyphasic approach. *Preslia* 86, 295–335.

Kubo, K., Kojima, H., and Fukui, M. (2014). Vertical distribution of major sulfate-reducing bacteria in a shallow eutrophic meromictic lake. *Syst. Appl. Microbiol.* 37, 510–519. doi: 10.1016/j.syapm.2014.05.008

Kuo, C. H., and Ochman, H. (2009). Inferring clocks when lacking rocks: the variable rates of molecular evolution in bacteria. *Biol. Direct* 4:35. doi: 10.1186/1745-6150-4-35

Kurilkina, M. I., Zakharova, Y. R., Galachyants, Y. P., Petrova, D. P., Bukin, Y. S., Domysheva, V. M., et al. (2016). Bacterial community composition in the water column of the deepest freshwater Lake Baikal as determined by next-generation sequencing. *FEMS Microbiol. Ecol.* 92:fiw094. doi: 10.1093/femsec/fiw094

Legendre, P., and Legendre, L. (1998). *Numerical Ecology*, 2nd English Edn. Amsterdam: Elsevier Science.

Lepori, F., and Roberts, J. J. (2015). Past and future warming of a deep European lake (Lake Lugano): what are the climatic drivers? *J. Great Lakes Res.* 41, 973–981. doi: 10.1016/j.jglr.2015.08.004

Linz, A. M., Crary, B. C., Shade, A., Owens, S., Gilbert, J. A., Knight, R., et al. (2017). Bacterial community composition and dynamics spanning five years in freshwater Bog Lakes. *mSphere* 2:e00169-17. doi: 10.1128/mSphere.00169-17

Llirós, M., Inceoğlu, Ö, García-Armisen, T., Anzil, A., Leporcq, B., Pigneur, L.-M., et al. (2014). Bacterial community composition in three freshwater reservoirs of different alkalinity and trophic status. *PLoS One* 9:e116145. doi: 10.1371/journal.pone.0116145

Lloyd, K. G., Steen, A. D., Ladau, J., Yin, J., and Crosby, L. (2018). Phylogenetically novel uncultured microbial cells dominate earth microbiomes. *mSystems* 3:e0055-18. doi: 10.1128/msystems.00055-18

Love, M. I., Huber, W., and Anders, S. (2014). Moderated estimation of fold change and dispersion for RNA-seq data with DESeq2. *Genome Biol.* 15:550. doi: 10.1186/s13059-014-0550-8

Martiny, A. C., Treseder, K., and Pusch, G. (2013). Phylogenetic conservatism of functional traits in microorganisms. *ISME J.* 7, 830–838. doi: 10.1038/ismej.2012.160

McMurdie, P. J., and Holmes, S. (2013). Phyloseq: an R package for reproducible interactive analysis and graphics of microbiome census data. *PLoS One* 8:e61217. doi: 10.1371/journal.pone.0061217

Menzel, P., Gudbergsdóttir, S. R., Rike, A. G., Lin, L., Zhang, Q., Contursi, P., et al. (2015). Comparative metagenomics of eight geographically remote terrestrial hot springs. *Microb. Ecol.* 70, 411–424. doi: 10.1007/s00248-015-0576-9

Menzel, P., Ng, K. L., and Krogh, A. (2016). Fast and sensitive taxonomic classification for metagenomics with Kaiju. *Nat. Commun.* 7:11257. doi: 10.1038/ncomms11257

Meriluoto, J., Blaha, L., Bojadzija, G., Bormans, M., Brient, L., Codd, G. A., et al. (2017a). Toxic cyanobacteria and cyanotoxins in European waters – recent progress achieved through the CYANOCOST Action and challenges for further research. *Adv. Oceanogr. Limnol.* 8, 161–178. doi: 10.4081/aiol.2017.6429

Meriluoto, J., Spoof, L., and Codd, G. A. (eds) (2017b). *Handbook on Cyanobacterial Monitoring and Cyanotoxin Analysis*, 1st Edn. Chichester: Wiley.

Monchamp, M. E., Spaak, P., and Pomati, F. (2019). Long term diversity and distribution of non-photosynthetic cyanobacteria in peri-alpine lakes. *Front. Microbiol.* 10:3344. doi: 10.3389/fmicb.2018.03344

Mori, Y., Kataoka, T., Okamura, T., and Kondo, R. (2013). Dominance of green sulfur bacteria in the chemocline of the meromictic Lake Suigetsu, Japan, as revealed by dissimilatory sulfite reductase gene analysis. *Arch. Microbiol.* 195, 303–312. doi: 10.1007/s00203-013-0879-5

Mosello, R., and Giussani, G. (1997). Recent evolution of water quality of deep southern Alpine lakes (in Italian). *Doc. Ist. Ital. di Idrobiol.* 61, 1–228.

Nearing, J. T., Douglas, G. M., Comeau, A. M., and Langille, M. G. I. (2018). Denoising the denoisers: an independent evaluation of microbiome sequence error-correction approaches. *PeerJ* 6:e5364. doi: 10.7717/peerj.5364

Newton, R. J., Jones, S. E., Eiler, A., McMahon, K. D., and Bertilsson, S. (2011). A guide to the natural history of freshwater lake bacteria. *Microbiol. Mol. Biol. Rev.* 75, 14–49. doi: 10.1128/MMBR.00028-10

Nguyen, N. P., Warnow, T., Pop, M., and White, B. (2016). A perspective on 16S rRNA operational taxonomic unit clustering using sequence similarity. *NPJ Biofilms Microbiomes* 2:6004. doi: 10.1038/npjbiofilms.2016.4

Ochman, H., Elwyn, S., and Moran, N. A. (1999). Calibrating bacterial evolution. *Proc. Natl. Acad. Sci.* 96, 12638–12643. doi: 10.1073/pnas.96.22.12638

Okazaki, Y., Fujinaga, S., Tanaka, A., Kohzu, A., Oyagi, H., and Nakano, S. I. (2017). Ubiquity and quantitative significance of bacterioplankton lineages inhabiting the oxygenated hypolimnion of deep freshwater lakes. *ISME J.* 11, 2279–2293. doi: 10.1038/ismej.2017.89

Okazaki, Y., Hodoki, Y., and Nakano, S. I. (2013). Seasonal dominance of CL500-11 bacterioplankton (phylum Chloroflexi) in the oxygenated hypolimnion of Lake Biwa. *Japan. FEMS Microbiol. Ecol.* 83, 82–92. doi: 10.1111/j.1574-6941.2012.01451.x

Okazaki, Y., and Nakano, S. I. (2016). Vertical partitioning of freshwater bacterioplankton community in a deep mesotrophic lake with a fully oxygenated hypolimnion (Lake Biwa, Japan). *Environ. Microbiol. Rep.* 8, 780–788. doi: 10.1111/1758-2229.12439

Okazaki, Y., Salcher, M. M., Callieri, C., and Nakano, S. (2018). The broad habitat spectrum of the CL500-11 lineage (Phylum Chloroflexi), a dominant bacterioplankton in oxygenated hypolimnia of deep freshwater Lakes. *Front. Microbiol.* 9:2891. doi: 10.3389/fmicb.2018.02891

Oksanen, J., Blanchet, F. G., Friendly, M., Kindt, R., Legendre, P., McGlinn, D., et al. (2018). *vegan: Community Ecology Package.* 285. Available at: https://cran.r-project.org/package=vegan (accessed July 24, 2019).

Oren, A., and Garrity, G. M. (2018). Uncultivated microbes - In need of their own nomenclature? *ISME J.* 12, 309–311. doi: 10.1038/ismej.2017.188

Ortiz-Estrada, ÁM., Gollas-Galván, T., Martínez-Córdova, L. R., and Martínez-Porchas, M. (2019). Predictive functional profiles using metagenomic 16S rRNA data: a novel approach to understanding the microbial ecology of aquaculture systems. *Rev. Aquac.* 11, 234–245. doi: 10.1111/raq.12237

Oswald, K., Graf, J. S., Littmann, S., Tienken, D., Brand, A., Wehrli, B., et al. (2017). *Crenothrix* are major methane consumers in stratified lakes. *ISME J.* 11, 2124–2140. doi: 10.1038/ismej.2017.77

Overmann, J., Huang, S., Nübel, U., Hahnke, R. L., and Tindall, B. J. (2019). Relevance of phenotypic information for the taxonomy of not-yet-cultured microorganisms. *Syst. Appl. Microbiol.* 42, 22–29. doi: 10.1016/j.syapm.2018.08.009

Paradis, E. (2012). *Analysis of Phylogenetics and Evolution with R*, 2nd Edn. New York, NY: Springer.

Pareeth, S., Bresciani, M., Buzzi, F., Leoni, B., Lepori, F., Ludovisi, A., et al. (2017). Warming trends of perialpine lakes from homogenised time series of historical satellite and in-situ data. *Sci. Total Environ.* 578, 417–426. doi: 10.1016/j.scitotenv.2016.10.199

Pollet, T., Tadonléké, R. D., and Humbert, J. F. (2011). Spatiotemporal changes in the structure and composition of a less-abundant bacterial phylum (Planctomycetes) in two perialpine lakes. *Appl. Environ. Microbiol.* 77, 4811–4821. doi: 10.1128/AEM.02697-10

Poretsky, R., Rodriguez-R, L. M., Luo, C., Tsementzi, D., and Konstantinidis, K. T. (2014). Strengths and limitations of 16S rRNA gene amplicon sequencing in revealing temporal microbial community dynamics. *PLoS One* 9:e93827. doi: 10.1371/journal.pone.0093827

Poser, A., Lohmayer, R., Vogt, C., Knoeller, K., Planer-Friedrich, B., Sorokin, D., et al. (2013). Disproportionation of elemental sulfur by haloalkaliphilic bacteria from soda lakes. *Extremophiles* 17, 1003–1012. doi: 10.1007/s00792-013-0582-0

Quast, C., Pruesse, E., Yilmaz, P., Gerken, J., Schweer, T., Yarza, P., et al. (2013). The SILVA ribosomal RNA gene database project: improved data processing and web-based tools. *Nucleic Acids Res.* 41, D590–D596. doi: 10.1093/nar/gks1219

R Core Team (2018). *R: A language and Environment for Statistical Computing*. Vienna: R Foundation for Statistical Computing.

Ranjan, R., Rani, A., Metwally, A., McGee, H. S., and Perkins, D. L. (2016). Analysis of the microbiome: advantages of whole genome shotgun versus 16S amplicon sequencing. *Biochem. Biophys. Res. Commun.* 469, 967–977. doi: 10.1016/j.bbrc.2015.12.083

Reynolds, C. S., and Walsby, A. E. (1975). Water-Blooms. *Biol. Rev.* 50, 437–481. doi: 10.1111/j.1469-185X.1975.tb01060.x

Rinke, C., Schwientek, P., Sczyrba, A., Ivanova, N. N., Anderson, I. J., Cheng, J.-F., et al. (2013). Insights into the phylogeny and coding potential of microbial dark matter. *Nature* 499, 431–437. doi: 10.1038/nature12352

Rogora, M., Buzzi, F., Dresti, C., Leoni, B., Lepori, F., Mosello, R., et al. (2018). Climatic effects on vertical mixing and deep-water oxygenation in the deep subalpine lakes in Italy. *Hydrobiologia* 824, 33–50. doi: 10.1007/s10750-018-3623-y

Rosselló-Móra, R., and Whitman, W. B. (2019). Dialogue on the nomenclature and classification of prokaryotes. *Syst. Appl. Microbiol.* 42, 5–14. doi: 10.1016/j.syapm.2018.07.002

Salmaso, N., Albanese, D., Capelli, C., Boscaini, A., Pindo, M., and Donati, C. (2018a). Diversity and cyclical seasonal transitions in the bacterial community in a large and deep Perialpine Lake. *Microb. Ecol.* 76, 125–143. doi: 10.1007/s00248-017-1120-x

Salmaso, N., Anneville, O., Straile, D., and Viaroli, P. (2018b). European large perialpine lakes under anthropogenic pressures and climate change: present status, research gaps and future challenges. *Hydrobiologia* 824, 1–32. doi: 10.1007/s10750-018-3758-x

Salmaso, N., Cerasino, L., Boscaini, A., and Capelli, C. (2016). Planktic *Tychonema* (Cyanobacteria) in the large lakes south of the Alps: phylogenetic assessment and toxigenic potential. *FEMS Microbiol. Ecol.* 92:fiw155. doi: 10.1093/femsec/fiw155

Schmidt, M. L., White, J. D., and Denef, V. J. (2016). Phylogenetic conservation of freshwater lake habitat preference varies between abundant bacterioplankton phyla. *Environ. Microbiol.* 18, 1212–1226. doi: 10.1111/1462-2920.13143

Segawa, T., Takeuchi, N., Fujita, K., Aizen, V. B., Willerslev, E., and Yonezawa, T. (2018). Demographic analysis of cyanobacteria based on the mutation rates estimated from an ancient ice core. *Heredity* 120, 562–573. doi: 10.1038/s41437-017-0040-3

Shams, S., Capelli, C., Cerasino, L., Ballot, A., Dietrich, D. R., Sivonen, K., et al. (2015). Anatoxin-a producing *Tychonema* (Cyanobacteria) in European waterbodies. *Water Res.* 69, 68–79. doi: 10.1016/j.watres.2014.11.006

Soo, R. M., Hemp, J., Parks, D. H., Fischer, W. W., and Hugenholtz, P. (2017). On the origins of oxygenic photosynthesis and aerobic respiration in Cyanobacteria. *Science* 355, 1436–1440. doi: 10.1126/science.aal3794

Soo, R. M., Skennerton, C. T., Sekiguchi, Y., Imelfort, M., Paech, S. J., Dennis, P. G., et al. (2014). An expanded genomic representation of the phylum cyanobacteria. *Genome Biol. Evol.* 6, 1031–1045. doi: 10.1093/gbe/evu073

Soo, R. M., Woodcroft, B. J., Parks, D. H., Tyson, G. W., and Hugenholtz, P. (2015). Back from the dead; the curious tale of the predatory cyanobacterium *Vampirovibrio chlorellavorus*. *PeerJ* 3:e968. doi: 10.7717/peerj.968

Stoddard, S. F., Smith, B. J., Hein, R., Roller, B. R. K., and Schmidt, T. M. (2015). rrnDB: improved tools for interpreting rRNA gene abundance in bacteria and archaea and a new foundation for future development. *Nucleic Acids Res.* 43, D593–D598. doi: 10.1093/nar/gku1201

Storelli, N., Peduzzi, S., Saad, M. M., Frigaard, N. U., Perret, X., and Tonolla, M. (2013). CO2 assimilation in the chemocline of Lake Cadagno is dominated by a few types of phototrophic purple sulfur bacteria. *FEMS Microbiol. Ecol.* 84, 421–432. doi: 10.1111/1574-6941.12074

Stumm, W., and Morgan, J. J. (1996). "Aquatic chemistry: chemical equilibria and rates in natural waters," in *Environmental Science and Technology: A Wiley-Interscience Series of Texts and Monographs*, 3rd Edn, eds J. L. Schnoor and A. Zehnder (New York, NY: John Wiley & sons).

Sunagawa, S., Coelho, L. P., Chaffron, S., Kultima, J. R., Labadie, K., Salazar, G., et al. (2015). Structure and function of the global ocean microbiome. *Science* 348:1261359. doi: 10.1126/science.1261359

Talavera, G., and Castresana, J. (2007). Improvement of phylogenies after removing divergent and ambiguously aligned blocks from protein sequence alignments. *Syst. Biol.* 56, 564–577. doi: 10.1080/10635150701472164

Tarlera, S., and Denner, E. B. M. (2003). *Sterolibacterium denitrificans* gen. nov., sp. nov., a novel cholesterol-oxidizing, denitrifying member of the β-Proteobacteria. *Int. J. Syst. Evol. Microbiol.* 53, 1085–1091. doi: 10.1099/ijs.0.02039-0

ter Braak, C. J. F., and van Dame, H. (1989). Inferring pH from diatoms: a comparison of old and new calibration methods. *Hydrobiologia* 178, 209–223. doi: 10.1007/BF00006028

Urbach, E., Vergin, K. L., Larson, G. L., and Giovannoni, S. J. (2007). Bacterioplankton communities of Crater Lake, OR: dynamic changes with euphotic zone food web structure and stable deep water populations. *Hydrobiologia* 574, 161–177. doi: 10.1007/s10750-006-0351-5

Urbach, E., Vergin, K. L., Young, L., Morse, A., Larson, G. L., and Giovannoni, S. J. (2001). Unusual bacterioplankton community structure in ultra-oligotrophic Crater Lake. *Limnol. Oceanogr.* 46, 557–572. doi: 10.4319/lo.2001.46.3.0557

Vanwonterghem, I., Evans, P. N., Parks, D. H., Jensen, P. D., Woodcroft, B. J., Hugenholtz, P., et al. (2016). Methylotrophic methanogenesis discovered in the archaeal phylum Verstraetearchaeota. *Nat. Microbiol.* 1:16170. doi: 10.1038/nmicrobiol.2016.170

Větrovský, T., and Baldrian, P. (2013). The variability of the 16S rRNA gene in bacterial genomes and its consequences for bacterial community analyses. *PLoS One* 8:e57923. doi: 10.1371/journal.pone.0057923

Viaroli, P., Azzoni, R., Bartoli, M., Iacumin, P., Longhi, D., Mosello, R., et al. (2018). Persistence of meromixis and its effects on redox conditions and trophic status in Lake Idro (Southern Alps, Italy). *Hydrobiologia* 824, 51–69. doi: 10.1007/s10750-018-3767-9

Wang, Q., Garrity, G. M., Tiedje, J. M., and Cole, J. R. (2007). Naive Bayesian classifier for rapid assignment of rRNA sequences into the new bacterial taxonomy. *Appl. Environ. Microbiol.* 73, 5261–5267. doi: 10.1128/AEM.00062-7

Wetzel, R. G. (2001). *Limnology, Lake and River Ecosystems*. San Diego, CA: Academic Press.

Whitton, B. A. (ed.) (2012). *Ecology of Cyanobacteria II Their Diversity in Space and Time*, 2nd Edn. Dordrecht: Springer.

Yoon, S.-H., Ha, S.-M., Kwon, S., Lim, J., Kim, Y., Seo, H., et al. (2017). Introducing EzBioCloud: a taxonomically united database of 16S rRNA and whole genome assemblies. *Int. J. Syst. Evol. Microbiol.* 67, 1613–1617. doi: 10.1099/ijsem.0.001755

Conflict of Interest: The author declares that the research was conducted in the absence of any commercial or financial relationships that could be construed as a potential conflict of interest.

Copyright © 2019 Salmaso. This is an open-access article distributed under the terms of the Creative Commons Attribution License (CC BY). The use, distribution or reproduction in other forums is permitted, provided the original author(s) and the copyright owner(s) are credited and that the original publication in this journal is cited, in accordance with accepted academic practice. No use, distribution or reproduction is permitted which does not comply with these terms.

frontiers in Microbiology

ORIGINAL RESEARCH
published: 15 October 2019
doi: 10.3389/fmicb.2019.02376

Discovery of High Abundances of Aster-Like Nanoparticles in Pelagic Environments: Characterization and Dynamics

Jonathan Colombet[1†], Hermine Billard[1†], Bernard Viguès[1†], Stéphanie Balor[2], Christelle Boulé[3], Lucie Geay[3], Karim Benzerara[4], Nicolas Menguy[4], Guy Ilango[1], Maxime Fuster[1], François Enault[1], Corinne Bardot[1], Véronique Gautier[5], Angia Sriram Pradeep Ram[1] and Télesphore Sime-Ngando[1]*

[1] Laboratoire Microorganismes: Génome et Environnement, Université Clermont Auvergne, UMR CNRS 6023, Aubière, France, [2] Plateforme de Microscopie Électronique Intégrative (METI), Centre de Biologie Intégrative (CBI), Université Paul Sabatier Toulouse III, CNRS, Toulouse, France, [3] Centre Technologique des Microstructures (CTμ), Université Claude Bernard Lyon 1, Villeurbanne, France, [4] Institut de Minéralogie, de Physique des Matériaux, et de Cosmochimie, Sorbonne Universités, UMR CNRS 7590, Université Pierre et Marie Curie Paris 06, Muséum National d'Histoire Naturelle, Institut de Recherche pour le Développement-Unité Mixte de Recherche 206, Paris, France, [5] Plateforme GENTYANE, UMR INRA 1095 GDEC, Université Clermont Auvergne, Site de Crouel, Clermont Ferrand, France

OPEN ACCESS

Edited by:
Petra M. Visser,
University of Amsterdam, Netherlands

Reviewed by:
Serena Rasconi,
INRA UMR1347 Agroécologie, France
Nina Sofia Atanasova,
University of Helsinki, Finland

***Correspondence:**
Jonathan Colombet
jonathan.colombet@uca.fr

[†]These authors have contributed equally to this work

Specialty section:
This article was submitted to Aquatic Microbiology, a section of the journal Frontiers in Microbiology

Received: 28 June 2019
Accepted: 30 September 2019
Published: 15 October 2019

Citation:
Colombet J, Billard H, Viguès B, Balor S, Boulé C, Geay L, Benzerara K, Menguy N, Ilango G, Fuster M, Enault F, Bardot C, Gautier V, Pradeep Ram AS and Sime-Ngando T (2019) Discovery of High Abundances of Aster-Like Nanoparticles in Pelagic Environments: Characterization and Dynamics. Front. Microbiol. 10:2376. doi: 10.3389/fmicb.2019.02376

This study reports the discovery of Aster-Like Nanoparticles (ALNs) in pelagic environments. ALNs are pleomorphic, with three dominant morphotypes which do not fit into any previously defined environmental entities [i.e., ultramicro-prokaryotes, controversed nanobes, and non-living particles (biomimetic mineralo-organic particles, natural nanoparticles or viruses)] of similar size. Elemental composition and selected-area electron diffraction patterns suggested that the organic nature of ALNs may prevail over the possibility of crystal structures. Likewise, recorded changes in ALN numbers in the absence of cells are at odds with an affiliation to until now described viral particles. ALN abundances showed marked seasonal dynamics in the lakewater, with maximal values (up to $9.0 \pm 0.5 \times 10^7$ particles·mL^{-1}) reaching eight times those obtained for prokaryotes, and representing up to about 40% of the abundances of virus-like particles. We conclude that (i) aquatic ecosystems are reservoirs of novel, abundant, and dynamic aster-like nanoparticles, (ii) not all virus-like particles observed in aquatic systems are necessarily viruses, and (iii) there may be several types of other ultra-small particles in natural waters that are currently unknown but potentially ecologically important.

Keywords: pleomorphic nanoparticles, femtoplankton, femtoplanktonic diversity, aquatic ecosystems, aquatic ecology

INTRODUCTION

Recent advances in environmental and nanoparticle sciences have helped to reveal an unexpected diversity of living and non-living femto-entities (0.02–0.2 μm as defined for femtoplankton by Sieburth et al., 1978) in the environment. Previously considered to be mainly composed of viruses (Sieburth et al., 1978), the successive discovery in significant abundance, and in various environments, of mysterious nanobes (Folk, 1993; McKay et al., 1996; Sillitoe et al., 1996; Uwins et al., 1998), extracellular vesicles (EVs) (Soler et al., 2015; Biller et al., 2017),

ultramicro-prokaryotes (Duda et al., 2012; Brown et al., 2015; Hug et al., 2016; Ortiz-Alvarez and Casamayor, 2016; Wurch et al., 2016; Castelle et al., 2018; Ghuneim et al., 2018), and biomimetic mineralo-organic particles (BMOPs) (Wu et al., 2016), has significantly increased the complexity within the environmental fraction of femto-entities.

Contrary to viruses or EVs, controversed nanobes, some of which could be affiliable to BMOPs, and ultramicro-prokaryotes, including recently discovered CPR (*Candidate Phyla Radiation*) and DPANN (*Diapherotrites, Parvarchaeota, Aenigmarchaeota, Nanoarchaeota, Nanohaloarchaea*), have the ability to develop outside a host (Benzerara et al., 2003, 2006; Martel and Young, 2008; Raoult et al., 2008; Wu et al., 2016). Nanobes exhibit diverse morphotypes: coccoid, amiboid, ovoid or filamentous shapes (Folk, 1993; McKay et al., 1996; Sillitoe et al., 1996; Uwins et al., 1998). Among them, only ultramicro-prokaryotes are clearly affiliated to living organisms according to the volumetric criteria advanced by the National Research Council (1999), i.e., the theoretical minimal cell volume (TMCV) sufficient to house nucleic acids and the associated biosynthetic machinery is at 0.008 μm^3. Though these new entities were described in natural environments, relatively little is known about their ecological significance. Available data however suggests a significant impact on the biogeochemical cycles. EVs are potentially involved in cell communication, competition and survival of bacteria (Liu et al., 2019). Interactions between ultramicro-prokaryotes and other micro-organisms communities may shape natural microbiome function (Castelle et al., 2018). Likewise, BMOPs incorporate trace elements and proteins suggesting that these entities may play a role in the circulation and availability of minerals and organic molecules in the environment (Wu et al., 2016). Characterizing the femtoplankton biomass and the diversity of its representatives seems crucial to our understanding of the functioning of aquatic ecosystems.

In this study, we report the discovery of abundant and seasonally-fluctuating populations of "Aster-Like Nanoparticles" (ALNs) in a freshwater lake of Massif Central (France), with volumes lower than TMCV. ALNs display typical and unique morphological features. Physical-chemical aspects, pleomorphism, flow cytometry and growth analyses of ALNs are presented and compared to distinctive features of living or not-living particles of similar size. Preliminary attempts to evidence DNA-based heredity support are reported.

MATERIALS AND METHODS

Study Sites and Sample Collection

Samples were collected at the surface of an artificial and highly eutrophic freshwater lake (surface area 1.2 ha, maximum depth 2.5 m) near Neuville in the French Massif Central (45°44'24"N; 3°27'39"E; 465 m altitude). Part of the samples were immediately fixed with 1% (v/v) formaldehyde and stored at 4°C until analysis (see below). Unfixed samples were transported at 4°C to the laboratory and treated within two h (see below). *In situ* dynamics of ALNs were monitored in 11 fixed samples collected between November 2016 and January 2018. **Table 1** lists the physical-chemical characteristics of the water analyzed once, in February 2017.

TABLE 1 | Physical–chemical characteristics of the lakewater on February 2017.

Parameters	Values
Water temperature, °C	4
pH	7.4
Total carbon, $mg{\cdot}L^{-1}$	16
Total phosphorous, $mg{\cdot}L^{-1}$	0.28
Un-ionized ammonia, $mg{\cdot}L^{-1}$	<0.05
Alkali concentration, °F	0
Complete alkali concentration, °F	27.65
Kjeldahl nitrogen, $mg{\cdot}L^{-1}$	3.3
Overall nitrogen, $mg{\cdot}L^{-1}$	4
Ammonium, $mg{\cdot}L^{-1}$	0.12
Carbonate, $mg{\cdot}L^{-1}$	Below limit of detection
Chloride, $mg{\cdot}L^{-1}$	12.5
Nitrate, $mg{\cdot}L^{-1}$	3.1
Orthophosphate, $mg{\cdot}L^{-1}$	0.05
Nitrite, $mg{\cdot}L^{-1}$	0.05
Total potassium, $mg{\cdot}L^{-1}$	9.6
Total sodium, $mg{\cdot}L^{-1}$	3.1
Total calcium, $mg{\cdot}L^{-1}$	9.1
Total magnesium, $mg{\cdot}L^{-1}$	1.7

Detection of ALNs was also conducted on surface microlayer samples of 16 selected geographical stations (namely HL1 to HL16) from the Ha Long Bay (Vietnam). Details on these samples and their environment were provided in a previous work (Pradeep Ram et al., 2018). ALNs were quantified on electronic microscopy grids prepared as mentioned below.

ALN, Prokaryote, and Virus-Like Particle (VLP) Counts and Imaging

ALNs in fixed samples were collected by centrifugation at 15,000 *g* for 20 min at 14°C directly onto 400-mesh electron microscopy copper grids covered with carbon-coated Formvar film (Pelanne Instruments, Toulouse, France). Particles were over-contrasted using uranyl salts as described elsewhere (Borrel et al., 2012). ALNs were counted by transmission electron microscopy (TEM) using a Jeol 1200EX microscope (JEOL, Akishima, Tokyo, Japan) at 80 kV and x50,000 magnification. Grids were scanned before counting to check that ALNs were randomly distributed. A defined area of the grid was then randomly selected for counting ALNs. Counts of ALNs were converted into ALNs per milliliter using a conversion factor deduced from control grids prepared with pre-determined concentrations of viruses. Direct magnifications ranging from x50,000 to x150,000 were required for morphological characterization of the particles. Volume of the ALN particles was computed by considering the radial arms as cylinders (extrapolation validated by cryo-TEM and SEM imaging; see below) and the central core as a sphere. Ultra-thin (20-nm thickness) sections were obtained and imaged as previously described (Kéraval et al., 2016). Counts of prokaryotes

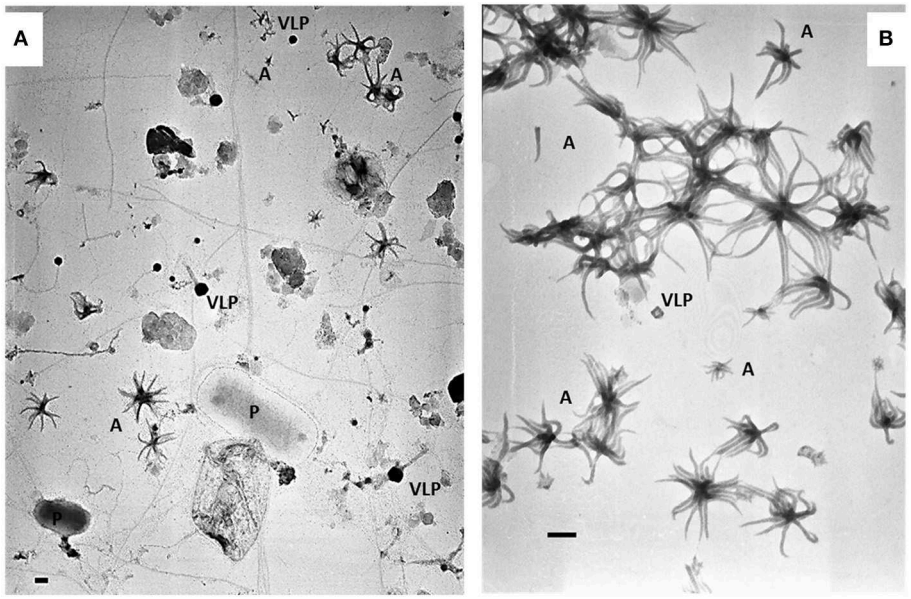

FIGURE 1 | Electromicrographs showing heterogeneity of pelagic communities **(A)** in lakewater collected on March 15th 2017 and ALN-enriched culture **(B)** obtained from this sampling. P, prokaryote; VLP, virus-like particle; A, ALNs. Scale bars = 100 nm.

and VLPs from fixed samples were performed by flow cytometry as described elsewhere (Brussaard, 2004) using a BD FACS Calibur cytometer (BD Sciences, San Jose, CA) equipped with an air-cooled laser, delivering 15 mW at 488 nm with the standard filter set-up.

Experimental Design

Enrichment and Culture of ALNs

The sample with the highest density of ALNs collected on March 15th 2017 was used for enrichment and culture of ALNs. Within two h after sampling, 20 L of raw lake water was filtered through a 25-μm-pore-size nylon mesh and filtrates were immediately concentrated by tangential-flow ultrafiltration using a Kross-Flow system (Spectrum, Breda, The Netherlands) equipped with a 0.2-μm cut-off cartridge. Aliquots of this concentrated 0.2 μm−25 μm fraction were sequentially centrifuged at 8,000 *g*, 10,000 *g* (pellets discarded) then 12,000 *g* for 20 min each time at 14°C. ALNs contained in the supernatant of this last run were cultivated at 4°C in the dark with a regular supply of culture medium. To obtain this culture medium, ultra-filtrate < 0.2 μm of the initial lake sample was filtered through a 30 KDa cut-off cartridge and autoclaved. **Figure 1** shows ALN cultures obtained through this procedure compared to the raw samples. The pellet obtained at 12,000 *g* was suspended in distilled/deionized sterile water (DDW), centrifuged at 10,000 *g*, and the supernatant was directly frozen to−20°C for microscopic and flow cytometry analyses of Enriched-ALNs (E-ALNs).

Detailed procedure of experimental design and analyses is provided in supplementary materials (**Figure S1**).

Growth Monitoring

As state above, ALN cultures were enriched by sequential centrifugations at 8,000 *g*, 10,000 *g* (pellets discarded) then 12,000 *g* for 20 min each time at 14°C. For growth monitoring, this was followed by successive filtrations of the highest-speed supernatant through 0.45-μm and 0.2-μm filters (Sartorius, Göttingen, Germany) to obtain ALN-enriched but prokaryote-free medium. This filtrate (<0.2-μm) was diluted 10-folds in the culture medium (see above) and incubated in triplicate over a 36-day period at 4°C in the dark, then 12 uneven subsamples were taken and formaldehyde-fixed before counts. Absence of prokaryotes at the start and end of the growth monitoring period was checked by flow cytometry, transmission electron microscopy and plate count agar spreading incubated at 4°C and 20°C during 4 weeks.

Susceptibility to Chemical or Physical Agents

To address the question of the living nature of the ALNs we examined their susceptibility to various chemical (lysozyme, antibiotics) or physical (heat) agents. Lysozyme is an antimicrobial enzyme that destructs Gram + bacteria cell wall by peptidoglycan hydrolysis (Manchenko, 1994) and which can also act against viruses (Cisani et al., 1984; Lee-Huang et al., 2005). Antibiotics treatments used in this study are all known to block replication processes of bacteria DNA or protein synthesis (Engle et al., 1982; Dar et al., 2007). Novobiocin is principally active against Gram+ bacteria, gentamycin against Gram- bacteria and norfloxacin has a broad-spectrum bactericidal action. Heat shock above 85°C was used owing to the irreversible physiological damage caused by this treatment to biological entities (Mackey et al., 1991).

Prokaryote-free ALN fractions prepared as described under the '*growth monitoring*' section were separately treated with 2 mg/mL lysosyme (1 h at room temperature), submitted to heat-shock (1 h at 90°C) or supplemented with antibiotics (50 μg/mL norfloxacin in sterile DDW; 10 μg/mL gentamycin in sterile

DDW or 250 μg/mL novobiocin in sterile DDW) (all chemicals from Sigma-Aldrich, Saint-Quentin-Fallavier, France). Treated samples were incubated for 20 days in the dark at 4°C. To test the efficiencies of these biocide treatments, we used two treated "control fractions": ALN-free bacteria cultures isolated from lake Neuville and grown on the same culture medium as ALNs, and 0.2 μm filtered ALN-free but ultrafiltration-enriched VLP water lake. This second control fraction was obtained from Lake Pavin where ALNs are undetectable over the year. Biocide effects of treatments were determined by direct comparison of treated vs. untreated samples at day 20. ALN, prokaryote and femtoplanktonic communities were performed on formaldehyde-fixed samples at the end of the incubations as previously described. All tests were carried out in triplicates.

Cryo-Transmission Electron Microscopy (Cryo-TEM) Specimen Preparation and Imaging

For cryo-TEM, 3 μL of unfixed suspensions containing ALNs were deposited onto glow-discharged Lacey Carbon 200-mesh grids and loaded into the thermostatic chamber of a Leica EM-GP automatic plunge freezer, set at 20°C, and 95% humidity. Excess solution was blotted for 1" with a Whatman filter paper No. 1, and the grid was immediately flash-frozen in liquid ethane cooled at−185°C. Specimens were then transferred onto a Gatan 626 cryo-holder, and cryo-TEM was carried out on a Jeol 2100 microscope, equipped with a LaB_6 cathode and operating at 200 kV, under low-dose conditions. Images were acquired using SerialEM software (Mastronarde, 2005), with defocus ranging of 1,000 nm, on a Gatan US4000 CCD camera. This device was placed at the end of a GIF Quantum energy filter (Gatan Inc., Pleasanton, CA), operated in zero-energy-loss mode, with a slit width of 25 eV. Images were recorded at a magnification corresponding to the calibrated pixel size of 1.80Å or 0.89Å.

Scanning Electron Microscopy (SEM) Specimen Preparation and Imaging

A fixed suspension (1% (v/v) formaldehyde) containing ALNs was deposited by filtration on 0.2-μm-pore-size filters (Whatman, Maidstone, UK), post-fixed with 1% osmium tetroxide, rinsed, and dehydrated through increasing concentrations of ethanol and then of hexamethyldisilasane. Following Cu sputter coating, dry filters were observed and imaged using a Zeiss Merlin Compact SEM operating at 2, 3 or 5 kV (Zeiss, Oberkochen, Germany).

Energy-Filtered Transmission Electron Microscopy (EFTEM) and Electron Energy Loss Spectroscopy (EELS) Analyses

Observations of unfixed samples were carried out using a Jeol 2010F transmission electron microscope operating at 200 kV, equipped with a field emission gun, an high-resolution ultra-high-radiation (UHR) pole piece, a STEM device which allows Z-contrast imaging in the high-angular annular dark-field (HAADF) mode, and a GIF 200 Gatan energy filter. EFTEM elemental mapping of C, N, O and Ca was performed on entire ALN using the 3-window technique (Hofer et al., 1997). The 3-window technique requires three energy-filtered images: two positioned before the ionization edge (pre-edge images), which serve to calculate the background, and one positioned just after the edge (post-edge image). Calculated background image was subtracted from the post-edge image to give an elemental map, in which changes in background shape were taken into account. Maps were calculated for C, N and O K-edges and Ca $L_{2,3}$ edges using a 20-eV-wide (for C) or 30-eV-wide (for N, O, Ca) energy window for pre-edge and post-edge. Zero-loss images were obtained by selecting elastically scattered electrons only. EELS spectra were acquired using a dispersion of 0.2 eV/channel to record spectra in the range 270–600 eV. Energy resolution was 1.3 eV as measured by the full width at half maximum of the zero-loss peak. Dwell time was optimized to acquire sufficient signal intensity and limit beam damage. Spectra were corrected from plural scattering using the Egerton procedure available with the EL/P program (Gatan).

Nucleic Acid Staining, Membrane Markers, and Flow Cytometry (FC) Analyses and Sorting of ALNs

Unfixed suspensions containing ALNs were thawed at 4°C and diluted in 0.02-μm-filtered Tris EDTA buffer prior to FC analyses. Analyses were performed using four nucleic acid dyes [SYBR Green I (Invitrogen S7563, Paisley, UK), SYBR Gold (Invitrogen S11494), propidium iodide (PI) (Sigma-Aldrich P4864) and DAPI (Sigma-Aldrich 32670)] and two lipophilic membrane markers [FM4-64 (Molecular Probes T13320, Eugene, OR) and PKH26 (Sigma-Aldrich P9691)]. ALNs were i) stained at 80°C for 10 min with SYBR Green I or SYBR Gold as described in Brussaard (2004); ii) pre-heated at 80°C for 10 min then stained with 10 $\mu g \cdot mL^{-1}$ PI or 1 $\mu g \cdot mL^{-1}$ DAPI for 10 min in the dark. Nucleic acids were also stained without heating. Staining with FM4-64 (5 $\mu g \cdot mL^{-1}$) and PKH26 (1/500 diluted from commercial solution) was carried out in the dark for 10 min at room temperature. All experimental conditions were reproduced in triplicates. Triplicates of 0.2 μm ALN-free filtrated water lake (i.e., enriched VLPs water from lake Pavin) and cultivated bacteria from lake Neuville were used for biological controls. Cytometric analysis was performed on a BD FACSAria Fusion SORP flow cytometer (BD Biosciences) equipped with a 70-μm nozzle. Laser and filter configuration was as follows: DAPI was excited by a 355-nm UV laser, fluorescence was collected with a 410 long pass (LP) and a 450/50 band pass (BP). SYBR Green I and SYBR Gold were excited at 488 nm and fluorescence was collected with a 502 LP and a 530/30 BP. PI and FM4-64 were excited at 561 nm and fluorescence was collected with a 600 LP and a 610/20 BP for PI, and with a 685 LP and a 710/50 BP for FM4-64. PKH26 was excited at 561 nm and fluorescence was collected with a 582/15 BP. Targeted particles were visualized on a "marker fluorescence vs. side scatter" dotplot. Data were acquired and processed using FACSDivA 8 software (BD Biosciences). Characterization of ALNs and VLPs from samples processed for cytometric analyses was carried out by TEM as previously described. Plots were compared

with those of a similarly-processed VLPs community obtained from Lake Pavin (see site description in Borrel et al., 2012) on October 24th 2017. FC sorting was performed on samples stained with SYBR Green I in un-heated conditions for optimal preservation of ALNs morphology and reliable morphotype diagnosis. Commonly described "viral fractions" (Brussaard, 2004) were gated on SYBR Green I fluorescence and sorted out using the continuous "Purity" mode. 0.5-μm fluorescent beads (Polysciences, Warrington, PA) served as control sorted fraction. Particles from sorted gates were re-analyzed by FC and identified and counted by TEM.

Genomic Analyses

Nucleic Acids Extraction and Amplification

Genomic DNA was extracted from unfixed suspensions containing ALNs obtained as described in the section "*Growth monitoring*". The sample was harvested by centrifugation at 12,000 g for 20 min at 14°C. The pellet was resuspended in 500 μl of sterile DDW and mixed with 600 ml of saturated phenol (pH 8.0). Then, two cycles of freezing in a liquid nitrogen bath (15 min) and thawing in a 100°C water bath (5 min) were conducted. The sample was mixed with 750 μL of chloroform and centrifuged at 14,000 g for 20 min at 4°C. Thereafter, the aqueous layer was transferred to another fresh 1.5 ml microtube and mixed with same volume of cold absolute ethanol and 3 M sodium acetate. The nucleic acid pellet obtained by centrifugation at 14,000 g for 20 min at 4°C was washed twice with ice-cold 70% ethanol and pelleted again. The pellet was resuspended in 50 μL of deionized water. Total extracted DNA was randomly amplified by Whole Genome Amplification (WGA) with GenomiPhi V2 kit (GE Healthcare, Chicago, Illinois, USA).

Library Preparation and Sequencing

Single-molecule Real-time long reads sequencing was performed with a PacBio Sequel Sequencer (Pacific Biosciences, Menlo Park, CA, USA). The SMRTBell library was prepared using a DNA Template Prep Kit 1.0, following the "procedure and checklist for greater than 10 kb template using AMPure PB beads" protocol. Genomic DNA(1,7 ug) was slightly sheared using a Covaris g-Tube (Covaris, UK) generating DNA fragments of approximately 20 kb. A Fragment Analyzer (Agilent Technologies, Santa Clara, CA, USA) assay was used to assess the fragment size distribution. Sheared genomic DNA was carried into the first enzymatic reaction to remove single-stranded overhangs followed by treatment with repair enzymes to repair any damages that may be present on the DNA backbone. A blunt-end ligation reaction followed by exonuclease treatment was conducted to generate the SMRT Bell template. Two AMPure PB beads 0.45X purifications, and one at 0.4X were used to obtain the final library. The SMRTBell library was quality inspected and quantified on a Fragment Analyzer (Agilent Technologies) and a Qubit fluorimeter with Qubit dsDNA HS reagent Assay kit (Life Technologies). A ready-to-sequence SMRTBell Polymerase Complex was created using a Binding Kit 2.1 (PacBio) and the primer V4, the diffusion loading protocol was used, according to the manufacturer's instructions. The PacBio Sequel instrument was programmed to load and sequenced the sample on PacBio SMRT cells v2.0 (Pacific Biosciences), acquiring one movie of 600 min per SMRTcell and generate 8 Gb of bases and an insert N50 at 7.75Kb.

Sequence Assembly and Annotation

The 1,930,845 raw PacBio reads (4.1 Kb in average) were assembled using the SMRT Analysis software and the Hierarchical Genome Assembly Process (HGAP) workflow (Chin et al., 2013). This procedure includes pre-assembly error correction, assembly and polishing. The circular nature of HGAP derived contigs was assessed via the dot-plotting tool Gepard (Krumsiek et al., 2007) and circular genome sequences were derived through an alignment approach and manual curation. The 5,162 corrected long reads (12.6 Kb in average) produced after the pre-assembly error correction process were utilized to determine the coverage of each contig using BLASTn (threshold of 90% on the identity percent) (Altschul et al., 1997). These corrected reads and contigs were compared using BLASTn to the SILVA 16S rRNA gene reference database (version 132) (Quast et al., 2013). The 233 contigs were also compared to the UniProt (February 2019) (UniProt Consortium, 2019) protein database using Diamond (sensitive mode) (Buchfink et al., 2015). Gene-calling was performed on contigs through the Prodigal software (Hyatt et al., 2010) and proteins were also compared to Uniprot using Diamond. Genomic data are presented in **Supplementary Data Sheet 1**.

RESULTS

Morphological Analyses

The ALN shape corresponds to arm-like segments which extend radially from a unique core structure. Three dominant morphotypes emerged on the basis of size and number of arms. The first morphotype displayed 4 to 10 arms connected to a delta-shaped tail with a mean length of 110 ± 18 nm and an average volume of 0.000055 μm^3 (**Figures 2A–F**). The second morphotype consisted of forms with 11-arms that were consistently observed within the ALN population (**Figures 2G–K**). They were clearly distinct from the first morphotype by their length (333 ± 28 nm) and volume (mean value: 0.00057 μm^3). Some appeared endowed with a singular bud-like appendix that seemed to arise from the center of symmetry of the particle. This appendix is thicker and slightly longer than the radial arms (**Figures 2I–K**). Finally, the third ALN morphotype corresponds to a sub-population that was composed of 20 arms (**Figures 2L–P**). These 20-armed forms constituted the lengthiest (439 ± 39 nm) and the most voluminous (0.0014 μm^3) ALNs identified in our samples. Their arms displayed characteristic tapered shapes, were frequently associated by pairs (**Figure 2P**), and there was no indication for supernumerary outgrowths as seen in other ALN morphotypes.

Standard, scanning, and cryo-transmission electron microscopy (cryo-TEM) indicated that the arms of ALN particles project from a central core (**Figures 3A–D**). This core displayed high and homogeneous electron density, while the arms showed differential contrasts depending on the plane

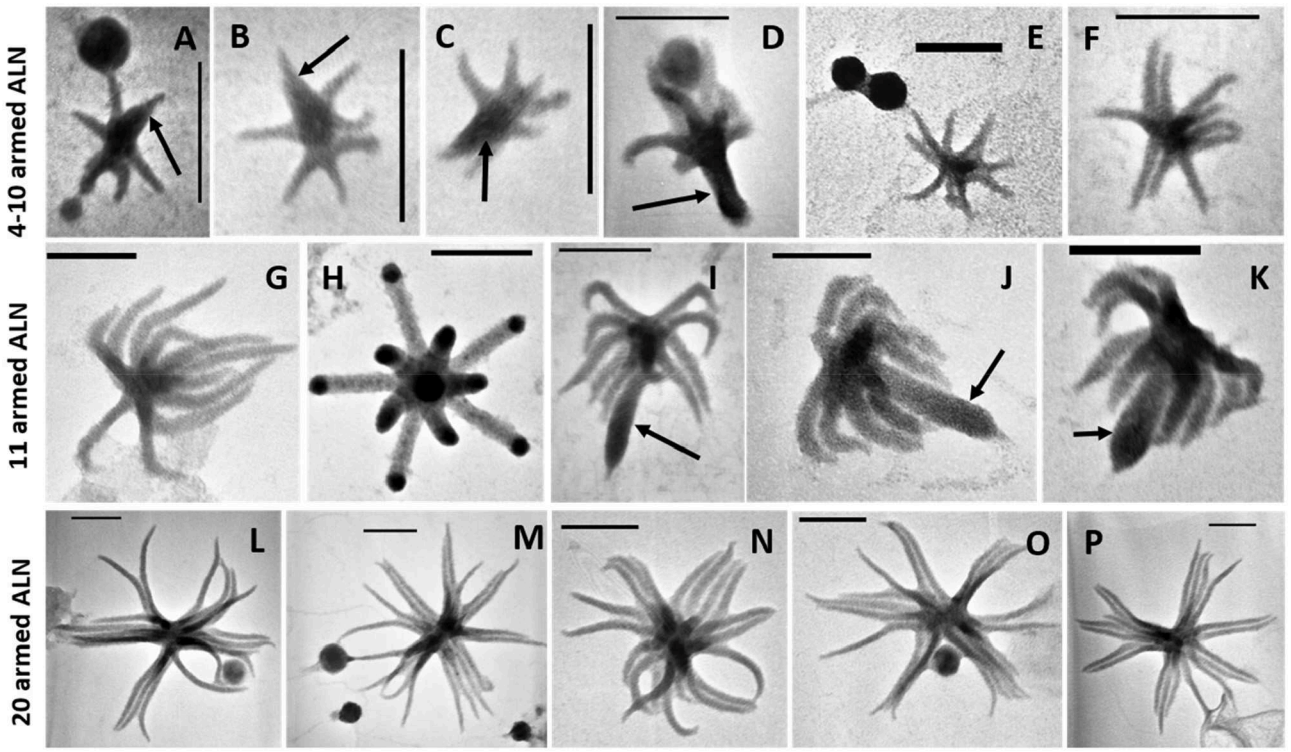

FIGURE 2 | Transmission electron microscopy (TEM) micrographs of different morphotypes of aster-like nanoparticles (ALNs). **(A–F)** 4–10-armed forms with some **(A–D)** presenting a few arms articulated around a delta-shaped excrescence (arrows). **(G–K)** 11-armed forms and their budding 11-armed variants **(I–K)** with elongated and swollen bud-like excrescences (arrows). **(L–P)** 20-armed forms. Scale bars = 100 nm.

of the section. Arms appeared as hollow structures when viewed in sagittal sections (**Figure 3C**). Cryo-TEM of whole specimens allowed direct comparison between the central core, the radial arms and the supernumerary appendix of the 11-armed morphotypes (**Figures 3D,E**). All areas showed a similar dot-pattern, which was more conspicuous in the case of the central-core/appendix complex. Branched chains formed by these elementary components might account for the higher electron contrast and apparent rigidity of the supernumerary appendix compared to the slacker aspect of radial arms.

Descriptively, ALNs are pleomorphic nanoparticles with a reduced biovolume ($<0.0014\ \mu m^3$) exhibiting 4 to 20 radial arms organized around a unique central core.

Elementary Analysis

Energy-filtered transmission electron microscopy and electron energy loss spectroscopy (EELS) analyses performed on entire ALNs indicated that these nanoparticles were mostly composed of carbon, oxygen, calcium and nitrogen (**Figures 4A,B**). Trace amounts of potassium were also identified in association with the particles. EELS spectra at the C K-edge and Ca $L_{2,3}$-edges of ALNs were significantly different from those of Ca-carbonates used as reference (**Figure 4C**) as they did not show a peak at 290 eV indicative of $1s \rightarrow \pi^*$ electronic transitions in carbonates and a much lower Ca/C ratio. Likewise, selected-area electron diffraction of ALNs revealed an amorphous structure (K.B. personal communication).

Elemental composition and selected-area electron diffraction patterns thus suggest that ALNs are presumably formed of organic components, indicating that their organic nature may prevail over the possibility of mineral structures.

Flow Cytometry Analysis

Flow cytometry (FC) analyses were performed on enriched-ALNs fraction (E-ALNs, *see Materials and methods*) composed of 96% ALNs and 4% of VLPs (**Figure 1B**) ascertained by TEM observation and counting.

No fluorescence signal was obtained using lipophilic markers FM4-64 or PKH26. Different nucleic acid dyes were tested, including DAPI, PI, SYBR Green I, SYBR Gold. While labeling with DAPI (a weakly permeant AT selective dye) and PI (impermeant nucleic acid intercalating dye) were unsuccessful, the SYBR dyes (permeant cyanine dyes), which are more sensitive compounds with high penetrating capacities, allowed to separate distinctive populations from E-ALN samples. As shown in **Figure 5A**, three populations termed P1, P2, and P3 were reproducibly split on the basis of SYBR Green I signal intensity and side scatter. Because ALNs were shown to be thermo-sensitive, heating was omitted in the protocol used for SYBR labeling. TEM indicated ALNs with familiar shapes in all sorted gates excepted in P4 gate that exclusively contained beads used as a control for sorting quality control (**Figure 5B**). Absence of ALNs in P4 indicated a non-random but differential sorting of the nanoparticles using the selected sorting gates. This was confirmed by TEM analyses of ALNs from the three sorting

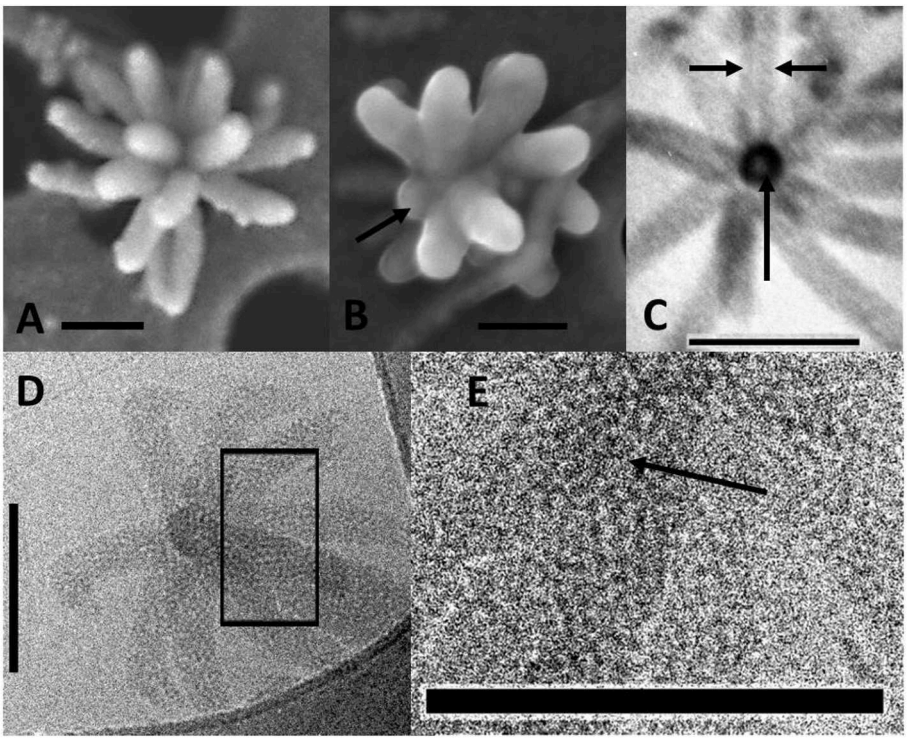

FIGURE 3 | Electromicrographs of aster-like nanoparticles (ALNs). **(A,B)** Scanning electron microscopy (SEM) micrographs showing ALNs with multiple full-grown radial arms **(A)** or a mix of emerging (arrow) and full-grown arms **(B)**. **(C)** TEM micrograph of an ultra-thin section of an ALN. Sagittal sections of arms reveal a tubular appearance with electron light area enclosed by a wall-like structure (arrows). **(D,E)** Cryo-TEM micrographs. **(D)** Radial arms display a similar mottled appearance. **(E)** Magnified view of the box selected from the previous image revealing circular substructures (arrow). Scale bars = 100 nm.

gates (**Figure 5B**). The sub-population from P3 gate provided the strongest SYBR signal, and consisted of large ALN morphotypes, i.e., 20-armed, budding 11-armed, and 11-armed morphotypes. The smaller ALNs (4–10 armed forms) were mostly concentrated in gates P1 and P2 together with virus-like particles and similar-sized particles of undetermined nature (VLPs).

Interference between ALNs and VLPs in FC particle quantification was evaluated using thermo-sensitivity property of ALNs compared to VLPs. This was achieved through comparative analysis of E-ALNs and a VLP community used as an ALN-free control, submitted or not to heating (**Figure 5C**). Heat induced a significant increase of counted VLPs in P2 (from 4.8 ± 0.7 to $8.2 \pm 1.1 \times 10^6$ mL^{-1}) and P3 (from 1.7 ± 0.2 to $2.0 \pm 0.3 \times 10^6$ mL^{-1}) populations sorted from the ALN-free control. Heating of P2 and P3 sorted from E-ALNs resulted in the opposite effect, i.e., a decrease in number of recorded events (P2: from 5.8 ± 0.6 to $4.2 \pm 0.4 \times 10^6$ mL^{-1}; P3: from 1.8 ± 0.2 to $0.9 \pm 0.1 \times 10^6$ mL^{-1}).

Overall, ALNs are positively labeled with SYBR nucleic acid dyes and interfere with VLPs quantification when using fluorescence based methods.

Nucleic Acid Detection

Detection of nucleic acid was performed on fraction composed of >99% ALNs and <1% of VLPs ascertained by TEM and obtained as described in section '*growth monitoring*'.

No reads or contigs were similar to a prokaryotic 16S rRNA sequence. All the 233 contigs were shorter than 6 Kb except one contig of 11,258 bp. Almost all contigs could be unambigously affiliated to small single-stranded DNA viruses, 213 being affiliated to the Microviridae family and 16 to CRESS DNA viruses (circular Rep-encoding ssDNA viruses) (**Figure 6**). Two contigs had no similarity to Uniprot proteins and one contig was similar to a bacterial DNA-directed DNA polymerase (49.5 amino acid identity on 94 residues), but these contigs were all very short (1,300, 115, and 290 bp, respectively). Although the largest contig of 11,258 bp had no obvious affiliation, its characteristics are similar to known viruses that infect prokaryotes: (i) short genes (23 protein coding genes, 442 bp long in average), (ii) no strand switching and (iii) only 4 proteins out of 23 being similar to a protein of Uniprot (3 similar to proteins from unaffiliated phages and one to an archaeal protein, all four proteins having an unknown function).

Based on our genomic analyses and on the methodology used presence of nucleic acids in ALNs is not proved.

Susceptibility to Chemical or Physical Agents

Effects of various life-inhibiting treatments were tested on ALNs, and on ALN-free prokaryotes and femtoplanktonic communities used as control after 20-day incubations.

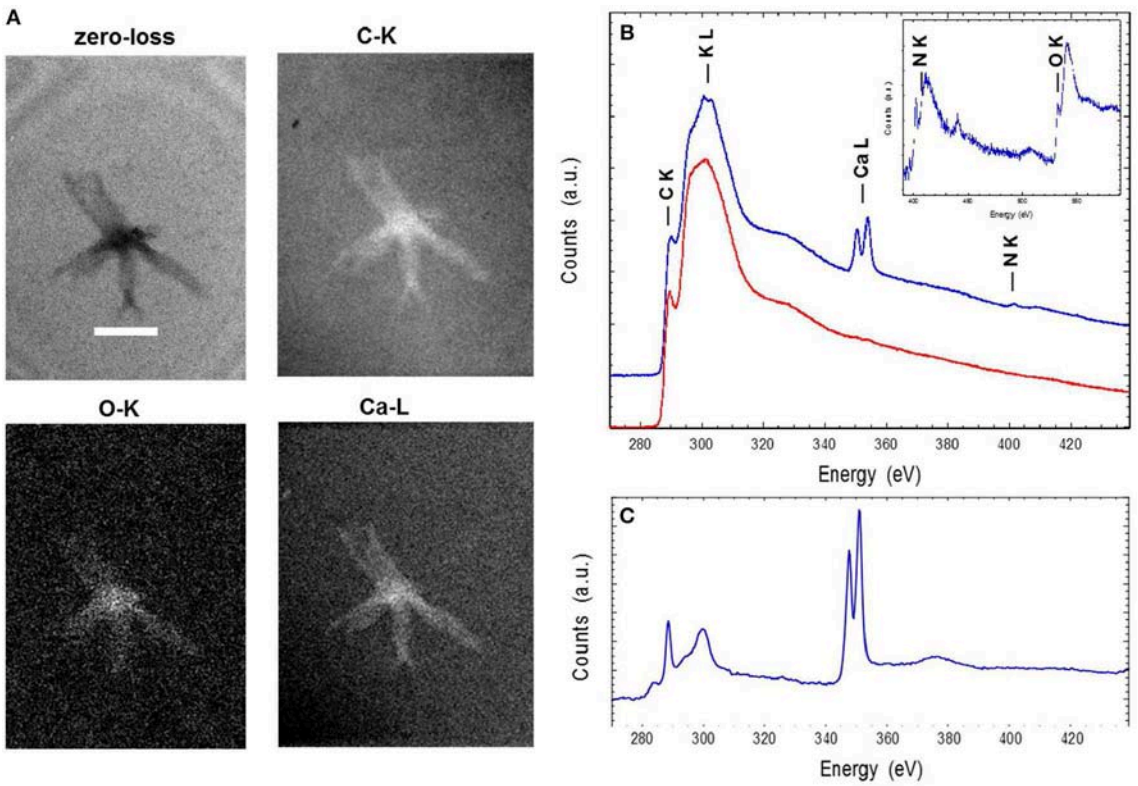

FIGURE 4 | Energy-filtered transmission electron microscopy (EFTEM) **(A)** and electron energy loss spectroscopy (EELS) analyses **(B,C)** of aster-like nanoparticles (ALNs). **(A)** Zero-loss image and EFTEM C, O, and Ca maps of an ALN. Scale bar=200 nm. **(B)** EELS spectra of an ALN particle (blue) and formvar (red). Insert: close-up of the background-normalized spectrum of an ALN particle at the N and O K-edges. **(C)** EELS spectra of a reference calcite crystal at the C K-edge and the Ca L2,3-edges. The relative intensities at the C K-edge and Ca L2,3 edges correlate with C/Ca atomic ratio.

Dramatic effects on total ALNs (T test, $p < 0.05$) were observed (**Figure 7**) after heating 1 h at 90°C or lysozyme (2 mg/mL) treatments (80 ± 12% and 51 ± 19% loss after 20 day incubation), and in the presence of the norfloxacin (50 μg/mL) and novobiocin (250 μg/mL) antibiotics (85 ± 7% and 58 ± 8%, respectively). Gentamycin antibiotic treatment had a smaller effect on the nanoparticles (41 ± 17% loss; $p = 0.05$). The losses were more pronounced following heating, lysozyme, norfloxacin, novobiocin and gentamycin treatments for the 4–10–armed form (96 ± 1, 53 ± 15, 89 ± 5, 61 ± 8, 41 ± 14%, respectively) compared to the 11–armed forms (0 ± 10, 37 ± 4, 66 ± 2, 53 ± 1, 12 ± 4%, respectively).

Lysozyme treatment leaded to a rise of prokaryotes (58%) suggesting that this ALN-free fraction was mostly composed of Gram – species. The complete loss of ALN-free femtoplanktonic communities (99%) showed the strong antiviral activity of this enzyme (Cisani et al., 1984; Lee-Huang et al., 2005). As expected prokaryotic "control fraction" displayed drastic loss in response to heat, norfloxacin, gentamicin and novobiocin (100%, 100%, 57%, 41%, respectively) (**Figure 7**).

Clearly, ALNs are susceptible to the life-inhibiting treatments. It seems also worth noting that responses to the treatments differed depending on the morphotypes. For example, 11-armed morphotypes proved much more resilient than others, while the 4–10-armed appeared more sensitive to the treatments.

In vitro Monitoring

ALN population fluctuates over a 36-day period in prokaryote-free medium (PFM) at 4°C (**Figure 8**). A transient rise of abundance was evident from day 0 to day 1 (multiplication factor MF=3.6). The population then appeared relatively stable from day 1 to day 15 before a marked decrease up to day 20, preceding a second rise period from day 20 to day 29 (MF=3.3), then a second decline phase up to day 36. All these fluctuations with time were statistically significant (**Figure 8**). Quantification of ALN morphotypes in PFM revealed that 4–10-armed and 11-armed morphotypes fluctuate inversely over time (**Figure 8**, Spearman's r=-0.86, $p < 0.001$). These fluctuations were positively (4–10-armed forms) or negatively (11-armed forms) correlated to total ALN population (Spearman's $r = 0.66$ and $r = -0.82$, respectively, $p < 0.05$). The proportion of the smallest ALN forms (predominant morphotype at day 0) increases concomitantly with total number of ALNs but decreases as the abundance of total ALNs returns to baseline (day 0, day 20, and day 36). Inversely, the proportion of 11-armed forms increases during phases of total ALN decline (days 20, day 36). Throughout the

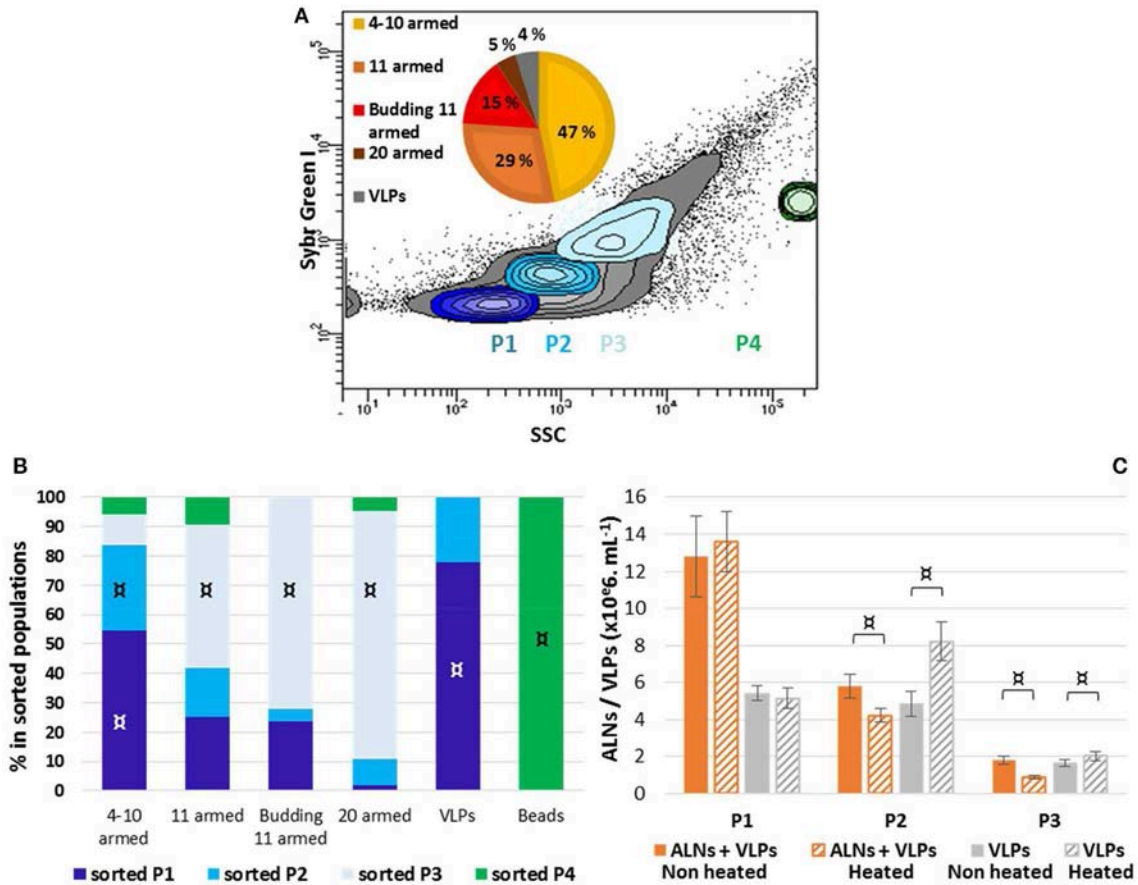

FIGURE 5 | Flow cytometry analysis of aster-like nanoparticle-enriched preparations (E-ALNs). **(A)** Gating of three distinctive populations (P1, P2, P3) of SYBR Green-stained E-ALNs. Heating was omitted during the staining procedure, and beads (0.5 μm) were used as control fraction (P4). The gray area in scatter plot including in P1, P2, and P3 commonly represents VLP fractions (see Brussaard, 2004). A pie chart shows the relative proportions of ALNs morphotypes attested by TEM. **(B)** Distribution of ALNs morphotypes and beads in the four FACS-sorted fractions counted by TEM. **(C)** Cytometry counts of P1, P2, and P3 gated fractions compared to counts obtained when heating was included in the SYBR Green staining procedure, and to counts of particles in ALNs-free viral community stained in heat-driven conditions. Mean values from triplicate and standard errors are plotted. Significant representativeness of morphotypes in sorted populations **(B)** is indicated by symbols: ¤ (Fisher's exact test on a contingency table, $p < 0.01$). Significant differences between "non-heated" and "heated" conditions **(C)** are indicated by an symbol ¤ (Student *T*-test, $p < 0.05$).

incubation period, we were not able to detect any prokaryotic cells using different approaches: flow cytometry, transmission electron microscopy, and plate count agar spreading.

The above incubation monitoring show that the abundance of ALNs can change significantly over time in the absence of cellular entities, with different patterns registered in contrasted morphotype categories. The mechanisms under these changes remain unclear in the absence of a detectable genomic support.

Ecosystemic Monitoring

Analysis of natural samples collected over a 13-month period in an eutrophic lake of the French Massif Central revealed high ALN abundances characterized by marked seasonal fluctuations (**Figure 9**). The maximal density reached a value of 9.0 ± 0.5 × 10^7 mL^{-1} (March 15th 2017). ALN abundances were up to 8-fold higher than those obtained for FC-counted prokaryotes and represented up to 39% of the total FC-counted VLPs in corresponding samples. ALN abundances increased with season from autumn to spring (MF=60). Prokaryote abundances fluctuated slowly from 0.8 ± 0.1 to 2.1 ± 0.4 × 10^7 mL^{-1}, while VLPs ranged from 2.0 ± 0.2 to 48.4 ± 1.5 × 10^7 particles mL^{-1}. For both communities, highest values were recorded in spring and in autumn, respectively (**Figure S2**). ALN abundance was not correlated to those of prokaryotes or VLPs.

At the morphotype level, we observed a high dominance of 11-armed forms which averaged 79 ± 16% of the total abundance over the 13-month sampling period (**Figure 9**). The 4–10 and 20-armed forms appeared in much smaller proportions (mean values = 10 ± 11% and 11 ± 11%, respectively). Proportions of these two forms were inversely correlated with those of 11-armed forms over time (Spearman's r=-0.77 and r=-0.73, respectively, $p < 0.05$). Proportions of budding 11-armed forms and 11-armed forms devoid of bud-like appendix were also negatively correlated to each other (Spearman's r=-0.91, $p < 0.01$). Budding

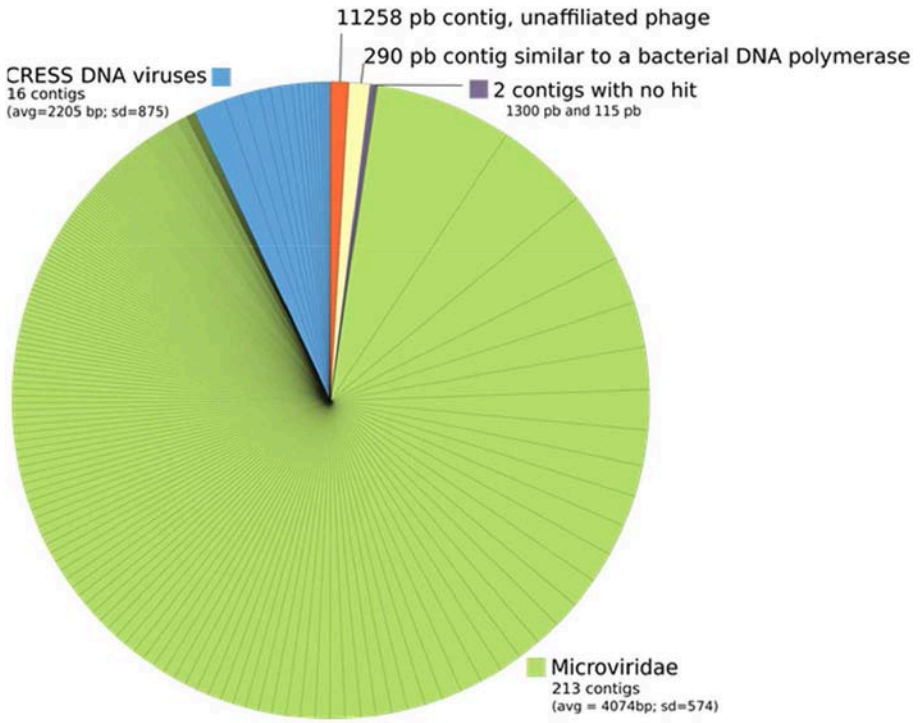

FIGURE 6 | Taxonomic affiliation of the 233 contigs from ALN-enriched DNA templates. Each piece of the pie corresponds to a contig and its size is proportional to the number of reads that were associated to this contig.

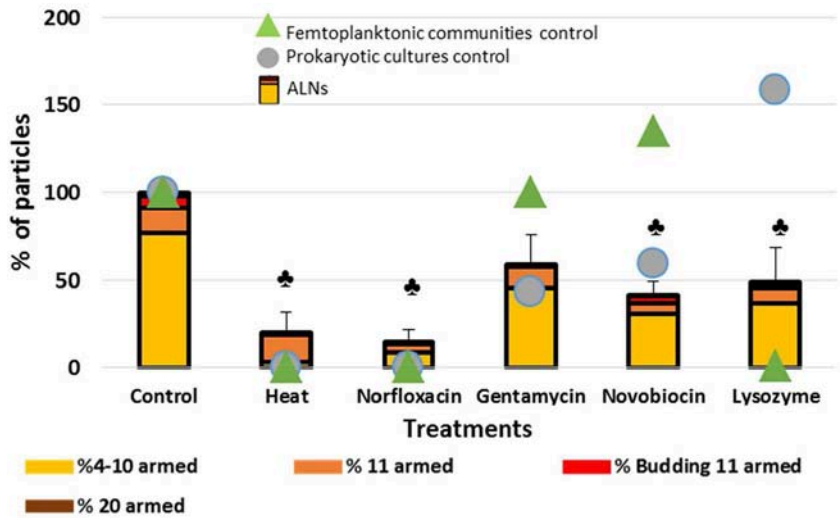

FIGURE 7 | Sensitivity of the particles to heat, antibiotics or lysosyme treatments. Effects of treatments by heat, antibiotics and lysosyme were assessed compared to untreated controls at day 20. Results are expressed as the percentage of ALNs which have resisted to treatments and continued to develop compared to control after a 20-day incubation. ALN-free prokaryotic cultures and femtoplanktonic communities (0.2 μm filtrated water from an eutrophic lake) were used as controls. Mean values from triplicate and standard errors are plotted. Significant differences with control are indicated by symbol ♣ (*T*-test, $p < 0.05$).

forms accounted for the highest proportions at the onset and throughout the increasing phase of total ALNs, but then disappeared with the decline in the total ALN abundance. ALNs were exclusively composed of 11-armed morphotypes a few months after their population was stabilized at its lowest level.

Detection of ALNs conducted on surface microlayer of 16 selected geographical stations (namely HL1 to HL16) from Ha Long Bay (Vietnam) show a high spatial heterogeneity with values ranging from undetectable to 3.4×10^4 mL^{-1} (**Figure 10A**). The dynamics of ALNs and bacteria were

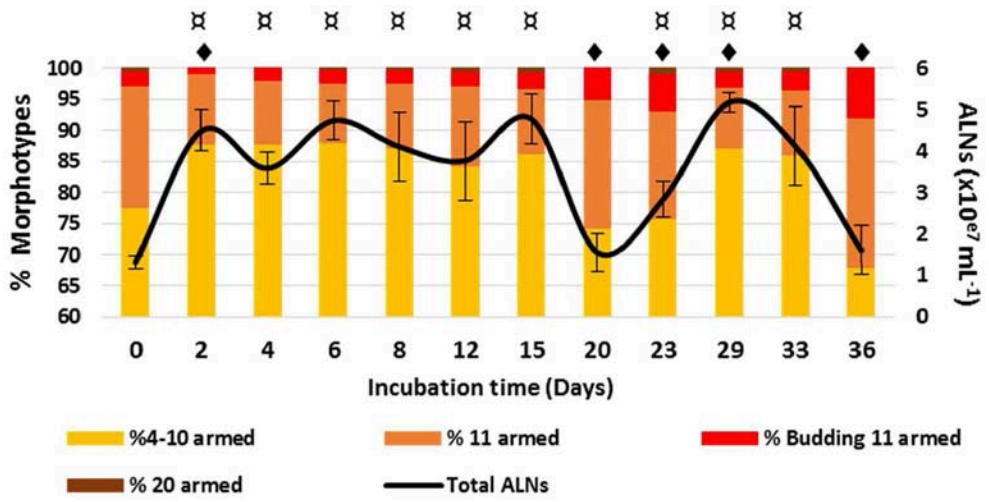

FIGURE 8 | Development monitoring of aster-like nanoparticles (ALNs) in prokaryote-free medium. Temporal variations of ALNs abundances and ratios (in %) of different morphotypes over a 36-day period. Mean values from triplicate and standard errors are plotted. Significant differences between ALNs abundance at t (n) and t (0) and between ALNs abundance at t (n) and t (n-1) are indicated by symbols ¤ and ♦, respectively (*T*-test, $p < 0.05$).

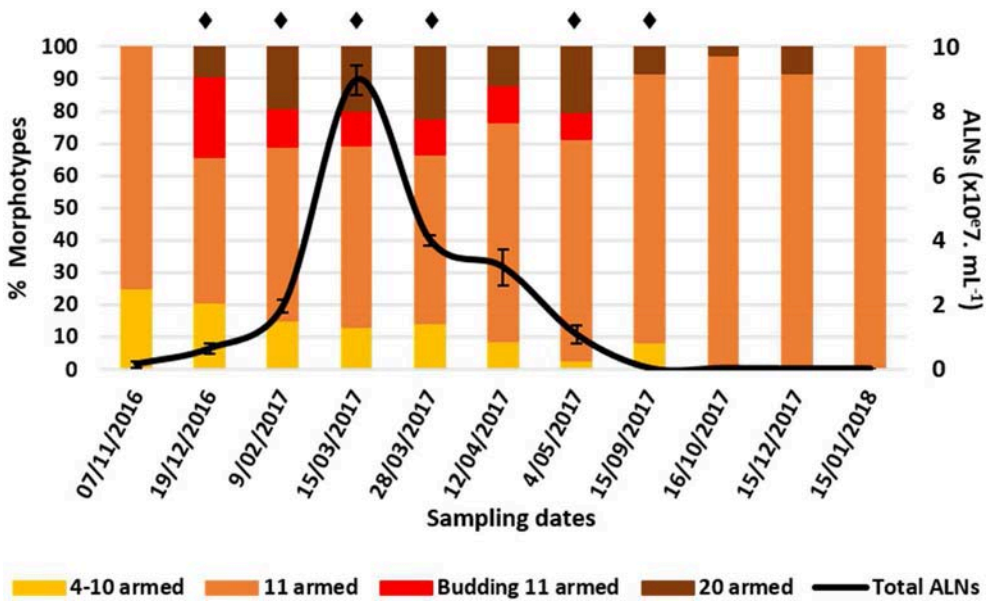

FIGURE 9 | Abundance of aster-like nanoparticles (ALNs) *in situ* (Neuville-France) and ratios (in %) of different morphotypes over a 15-month period. Note the peak of abundance between late December 2017 and mid-March 2017 and the return to low-density populations within a few months. Mean values from triplicate and standard errors are plotted. Significant differences between ALNs abundance and the previous time are indicated by asterisks ♦ (Student *T*-test, $p < 0.05$).

significantly correlated (Spearman's r = 0.81, $p < 0.01$, **Figure 10B**). No reliable correlation could be established between ALNs and physico-chemical variables (**Figure 10B**).

ALNs show seasonal and ecosystemic fluctuations probably induced by environmental parameters. Proportions of each recorded morphotype shift according to seasonal dynamics.

DISCUSSION

ALNs Are Original Pleomorphic Nanoparticles

Here we report the discovery of 'Aster-Like Nanoparticles' (ALNs) in lakewater. These pleomorphic entities, exhibit

A

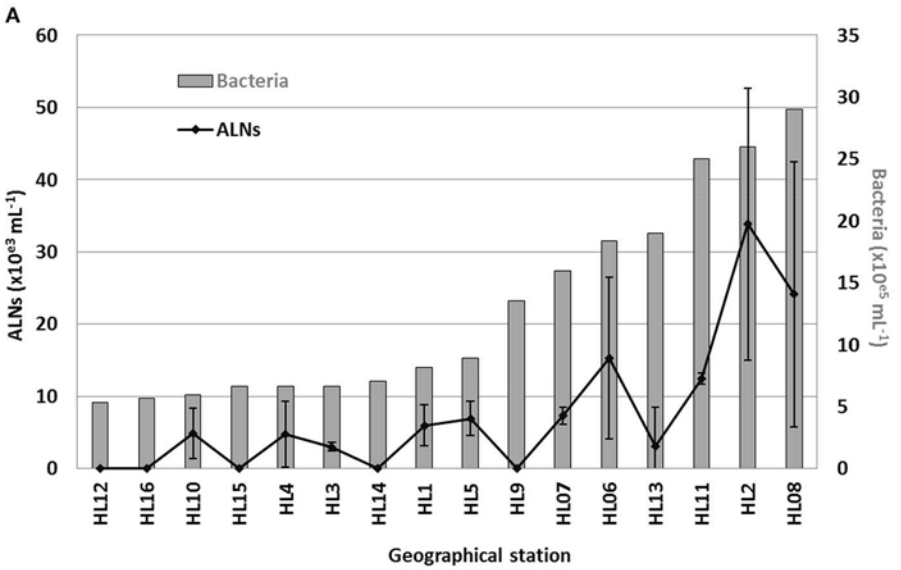

B

	Biological parameters				Physico-chemical parameters									
	VA	BA	BP	FIC	TEMP	SAL	Turb.	DOC	TPC	TPN	NO_3+NO_2-N	NH_4-N	PO_4-P	SiO_2
ALNs	**0.85 ***	**0.81 ***	0.59	0.62	-0.46	-0.33	-0.3	0.28	0.72	0.73	0.09	0.18	0.5	0.66

FIGURE 10 | (A) Distribution of aster-like nanoparticles (ALNs) and bacteria abundances in 16 selected stations of a tropical coastal ecosystem (Ha Long Bay-Vietnam), and **(B)** analyses of correlations (Spearman's product-moment correlation coefficient) between ALNs and environmental parameters which compile all sampling points. All details on Ha Long Bay (Vietnam) environment are available from Pradeep Ram et al. (2018). Level of significance: $^*p < 0.001$. VA, viral abundance; BA, bacterial abundance; BP, bacterial production; FIC, frequency of infected cells; TEMP, temperature; SAL, salinity; Turb, turbidity; DOC, dissolved organic carbon; TPC, total particulate carbon; TPN, total particulate nitrogen in the bulk sample.

puzzling aster-like shapes with arm-like processes that project from a central core (**Figure 3**). All morphotypes exhibit shapes that distinguish ALNs from previously established groups of nanoparticles, including ultramicro-prokaryotes (Duda et al., 2012; Castelle et al., 2018; Ghuneim et al., 2018), controversed nanobes (Folk, 1993; Sillitoe et al., 1996; Uwins et al., 1998; Aho and Kajander, 2003; Yaghobee et al., 2015), biomimetic mineralo-organic particles (BMOPs) (Wu et al., 2016), viruses (King et al., 2018) or extracellular vesicles (EVs) (Soler et al., 2015; Biller et al., 2017). Their mean length ranges from 110 ± 18 nm (4–10-armed morphotype) to 439 ± 39 nm (20-armed morphotype). Volumetric estimates of all ALN types indicated values (averaging 0.000055 μm^3, 0.00057 μm^3, and 0.0014 μm^3 for 4–10, 11, and 20-armed morphotypes respectively) that were significantly lower compared to the smallest known prokaryotes (Ghuneim et al., 2018) and to the Theoretical Minimal Cell Volume (TMCV). Nanobes, BMOPs, viruses (excepted giant viruses) and EVs are the sole examples of entities comparable to ALNs in terms of numerical volume. The composition (mostly carbon, oxygen, calcium and nitrogen with trace amounts of potassium) and the amorphous structure revealed by electronic microscopy (**Figure 4**) point out that ALN are possible organic particles (Uwins et al., 1998; Benzerara et al., 2003), or at least that their organic content may prevailed over their mineral composition known from mineral forming nanobes (Kajander et al., 2003), BMOPs or "natural nanoparticles" (Wu et al., 2016; Griffin et al., 2018), partly or totally composed of minerals.

ALN volumes were largely under the theoretical minimal cell volume (TMCV) required to house nucleic acids and the associated biosynthetic machinery required for a self-sufficient form of life (National Research Council, 1999). Use of the TMCV established there is 20 years ago to define compatibility with living nature must be however considered with caution. Indeed, recent advances in microbiology and virology have revealed existence of nanosized prokaryotes with biovolumes close to the TMCV. Giant viruses were reported as well. Genomic analysis of nanosized prokaryotes revealed a limited sub-cellular organization coupled with a significant reduction of biosynthetic and energy conservation pathways (Castelle et al., 2018; Ghuneim et al., 2018). Meanwhile, exceptionally large viruses were discovered that contain DNA encoding proteins involved in mRNA translation (Schulz et al., 2017; Abrahão et al., 2018). These discoveries have reopened the debate on the origin and the definition of life. In the absence of scientific consensus on what the TMCV should be exactly, it would be perhaps premature to make the conclusion that ALNs cannot be living particles with the only criteria being their exceptionally small size. Various experimental approaches were developed to address this issue (see below).

The ability of ALNs to develop in the absence of cells (**Figure 8**) provides additional entry points to discuss the nature

of these particles compared to viruses or extracellular vesicles (EVs). It seems worthwhile to underline, at this point, that host-independent morphogenesis is quite unusual in viral world or for EVs, although extracellular morphological plasticity has been reported for ATV viruses *(Acidianius Two-tailed Virus)* that infect archaeons living in particularly harsh aquatic environments (Häring et al., 2005; Prangishvili et al., 2006). ALN morphotype fluctuations that happen in the absence of cells seem at odds with a viral nature of ALNs if viewed as gradual assembly/disassembly processes within a single particle having a pleomorphic lifestyle. However, the alternative, i.e., convergence of otherwise unrelated nanoparticles, toward an "aster-shaped" morphology must also be considered. In this case, morphotype fluctuations could merely reflect survival capabilities of unrelated particles in the absence of cells. Clearly, further studies are required to elucidate morphotype fluctuations related to the exact nature of ALNs.

Sensitivity to a wide range of antibiotics was used as a critical point to establish the non-living nature of biomimetic particles (Raoult et al., 2008). The abundance of ALNs was dramatically affected by biocide agents (norfloxacin, novobiocin, lysozyme or heat shock) (**Figure 7**). These results could suggest ALNs as self-sufficient forms of life. Differential responses of ALN morphotypes to the multiple damaging treatments should also be considered. 4–10-armed forms appeared more affected than the 11-armed forms, suggesting possibility of more resilient morphotypes within the population of nanoparticles. Comparisons of ALN responses to those of other populations used as controls did not however permit to draw more definite conclusions indicative of the living or non-living nature of these particles.

More basically, the ability of ALN populations to persist in the absence of cells and the sensibility of the particles to biocide agents both raise the question of the existence of endogenous nucleic acids. Hypothesis of an heredity support is also supported by the reoccurrence of different ALN morphotypes whatever was the environmental context or season (see below) and the recurrent radial symmetry of the particles which might reflect a developmental relationship between morphotypes. Flow cytometry (FC) plotting and subsequent TEM analysis of the sorted ALNs provided preliminary insights in this topic. The cytometry step was assessed using permeant cyanine SYBR dyes. These stains preferentially bind to double-stranded DNA, but can also stain single-stranded DNA and RNA with variable efficiency. TEM analyses of sorted fractions showed that SYBR Green I and side scatter signal intensities were morphotype-dependent and allowed to establish a positive correlation between the complexity of morphotypes and the intensity of fluorescence emitted by the particles (**Figure 5**). Assuming that FC-detected SYBR-staining is indicative for the presence of nucleic acids encased in the nanoparticle (core structure?), highly enriched ALN cultures (0.2 μm filtered) appeared as suitable material from which putative DNA could be directly extracted and characterized at the molecular level. Whole genome sequencing was then developed using the same DNA template. 16S rRNA genes have not been identified as part of the 233 contigs assembled through this approach (**Figure 6**). Assuming that DNA extraction and amplification were efficient, our data suggests that ALNs lack a detectable genomic features and translation machinery of prokaryotes. The great majority of contigs delivered by whole genome analysis were affiliated to the microviridae, a family of bacteriophages with a single-stranded DNA genome. However, microviridae contigs must be viewed as assemblies of sequence fragments from remnants of viral populations initially comprised in the lake water sample. According to these results, we were not able to demonstrate the presence of nucleic acids in ALNs. Extraction and non-specific amplification efficiencies of nucleic acids are strongly linked to the nature of the particle. Development of a specific protocol to purified ALN enriched-cultures will be a critical point as soon as the exact nature of ALNs will be determined.

Overall, our data on the atypical morphology, the reduced biovolume, the suspected dominant organic nature, the sensibility to biocide treatments, and the ability to develop in the absence of cells indicate than ALNs are new femto-entities which, at the moment, cannot be classified in any known category of femto-entities previously described in environmental samples.

Ecological Significance of ALNs

Our discovery of ALNs and the existence of other ultra-small non-viral particles raise the ecological question of the accuracy of the "VLP" (i.e., virus-like-particles) fraction in aquatic ecosystems. Commonly used to designate free-occurring viruses, the acronym VLP is also synonymous of "known and yet unknown viral aquatic particles" especially as standardized FC methodologies include heat-driven procedures particularly efficient for detection of viral particles that are, otherwise, refractory or weakly responsive to SYBR-staining (Brussaard, 2004). Interference between ALNs and VLPs in FC particle quantification and successful sorting of largest morphotypes (**Figure 5**), indicate that ALNs must be viewed as atypical nanoparticles comprised in the VLP fraction. Events recorded from ALNs may lead to overestimate the viral load when analyzing viromes in aquatic ecosystems by counting SYBR-stained particles which is the methodology currently used for optimal detection of viruses by flow cytometry (Weinbauer, 2004). Experimental bias generated by overlapping of fluorescent signals produced by viruses and by other types of nanoparticles encompassed within the viral population was previously assessed in the case of EVs which constitute regular components of VLP fractions in natural environment (Soler et al., 2008, 2015; Forterre et al., 2013). Comparative studies between ecological groups comprising viral communities should therefore be interpreted with caution when pleomorphic nanoparticles such as ALNs occur in samples, notably when seasonal variations favor temporary bloom or predominance of one ALN morphotype over others.

Ecological significance of ALNs was approached by *in situ* seasonal and ecosystemic analyses. Seasonal analyses in a French eutrophic lake revealed a marked seasonal dynamic in ALN abundances from $8.0 \pm 3.8 \times 10^4$ to $9.0 \pm 0.5 \times 10^7$ mL^{-1} (**Figure 9**) and suggest a tight control of the environmental parameters on ALNs. Relative proportions of each morphotype

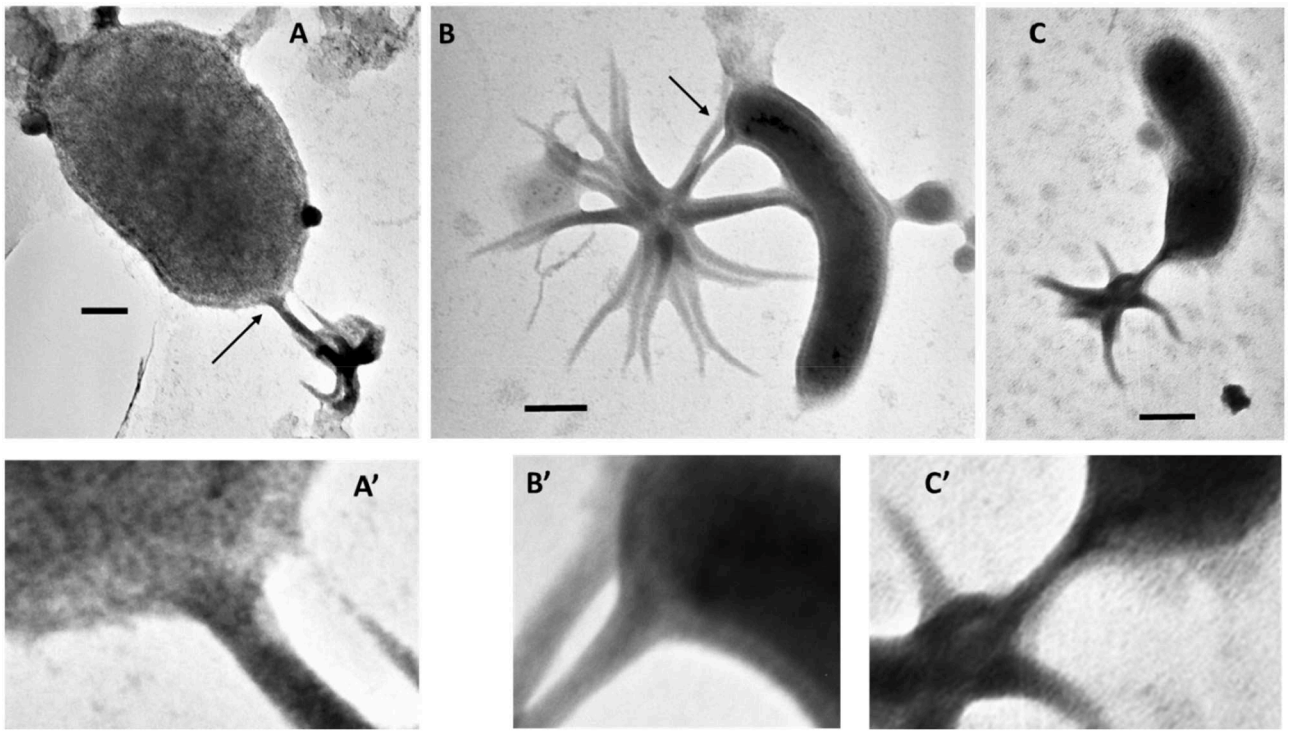

FIGURE 11 | (A–C), Electromicrographs documenting a putative interaction between aster-like nanoparticles (ALNs) and microbial cells. **(A'–C')** are magnified views of sections indicated by arrows in **(A–C)**. Note the close contact between arms of the ALNs and the microbial cells. Scale bars = 100 nm.

shifted concomitant to fluctuations in total ALN abundance. 11-armed form appeared the alone form in condition of the lowest density of ALNs, suggesting that this peculiar form could be more resistant to adverse environmental factors than others forms. Inverted correlation between 11-armed forms and the others forms, also noted when ALNs were maintained for 36 days in prokaryote-free lake water (in laboratory condition) suggests that these forms may be of importance in maintaining a permanent pool of ALNs in lake water and in promoting propagation of the nanoparticles when growth conditions become more favorable. This assumption is only possible assuming that pleomorphism arises from inter-conversion between morphotypes. The idea that morphotypes described in this study all develop from the same "stem entity" is not demonstrated and remains a fundamental question to be addressed in the future. The importance of ALN degeneration or starvation controlled by environmental factors, which can differently affect the abundances of ALN morphotypes in both controlled and *in situ* conditions, must also be addressed. Such a regulative function by environmental factors has been reported in the case of ultramicro-bacteria (Duda et al., 2012) and in the case of *Phaeodactylum tricornutum*, a 10 μm sized diatom (He et al., 2014).

Identification of ALNs in a tropical estuarine system and in Saloum river in Senegal (J.C. unpublished data) shows a pan-geographic distribution and adaptability of ALNs. This property prompted us to explore the environmental parameters potentially affecting ALN dynamics at the spatial scale. This was achieved on 16 selected geographical stations from Ha long bay estuary in Vietnam, a highly spatially contrasted environment previously characterized by Pradeep Ram et al. (2018). This spatial survey indicated significant coupling between ALN and prokaryote abundances (**Figure 10**). No reliable correlation could be established with physico-chemical variables of the bay environment. In contrast, no closed relation between ALNs and prokaryote abundances was recorded at the seasonal scale in the French Lake. However, in this environment, ALNs displayed limited pleomorphism and abundance changes in cell-free medium compared to *in situ* analyses (multiplication factor of 3.6 in cell-free medium compared to 60 in French Lake). These data suggests that microbial communities may help promoting the nanoparticle dynamics. Interestingly, more detailed observations of microbial communities collected from eutrophic lakes revealed arm-mediated contacts between ALNs and bacteria (**Figure 11**). The role of microbial communities in the control of ALNs and the functional significance of the observed contacts between ALNs and bacteria are still unclear. Further ecological studies of these puzzling nanoparticles should be placed in the context of ecosystemic relationships between ALNs and prokaryotes as well as between ALNs and other biological or physic-chemical components.

Seasonal and spatial dynamics are a characteristic of aquatic microbial communities which regulate energy and matter flows in aquatic systems (Weinbauer, 2004; Diao et al., 2017). To our knowledge, long-term ongoing researches on the ecology

and population dynamics of nanobes or non-living particles are currently lacking. This precludes any comparison with our ALN studies. Nevertheless, our observations clearly raise the question of the ecological importance of ALNs in the functioning of aquatic ecosystems. Although reduced on a unit scale, the biomass of total ALNs during bloom periods is likely to mobilize circulating mineral and organic nutrients at the expense (competition?) of other microbial communities of aquatic ecosystems. In addition, direct interplay with bacteria (**Figure 11**) could significantly influence the energy and material flows mediated by the prokaryotic compartments.

CONCLUSION

This study shows, for the first time, that aquatic ecosystems may contain abundant and dynamic nanoparticles of a novel type with ecological potentialities, especially in meso- and eutrophic waters which are predilection sites for ALN detection. Tough the question of the living or non-living nature of ALNs remains unresolved at this time, their original features re-open the debate on the minimal cell volume for a self-sufficient form of life. Experiments are in progress to explore the exact nature of ALNs and identify biotic and abiotic factors involved in regulation of their dynamics in microcosm and environmental conditions. In this context, an upcoming challenge will be to obtain mass cultures of ALN particles grown in VLP-, EV- and prokaryote-free medium. Clearly, we have describe novel types of environmental nanoparticles that, as the most ecological outcome, emphasize that not all virus-like particles observed in aquatic systems are necessarily viruses and that there may be several types of other ultra-small particles in natural waters that are currently unknown but potentially ecologically important.

DATA AVAILABILITY STATEMENT

The datasets generated for this study are available on request to the corresponding author.

AUTHOR CONTRIBUTIONS

JC and HB performed the experiments and the flow cytometric analyses. JC performed the transmission electron microscopy analyses. SB performed the cryo-transmission electron microscopy analysis. ChB and LG performed the scanning electron microscopy analysis. KB and NM performed the EFTEM and EELS analyses. JC, GI, MF, and AP analyzed samples from Ha Long Bay. FE, CoB, and VG realized genomic analyses. JC, HB, TS-N, and BV designed the research and wrote the manuscript. All authors have read, commented, and approved the final version of the manuscript.

FUNDING

FE was supported by the EUed Horizon 2020 Framework Programme for Research and Innovation (Virus-X, project no. 685778). This study is a contribution to the C NO LIMIT project funded by the Interdisciplinary Mission of the French National Center of Scientific Research (CNRS) Program X-life, 2018 edition. Funding for sampling at Halong Bay was obtained through the French-Vietnamese Hubert Curien Partnership (Contract No. 23971TK) and the Ministry of Science and Technology of Vietnam (Contract No. 46/2012/HD-NDT).

ACKNOWLEDGMENTS

This study was supported by the CYSTEM platform UCA-PARTNER (University of Clermont Auvergne UCA), Clermont-Ferrand, France) and the Microorganisms: Genome and Environment laboratory (LMGE, UMR6023 CNRS-UCA, Clermont-Ferrand, France). This work also benefitted from the assistance of the Multiscale Electron imaging platform (METi) at the CBI (Toulouse, France), from the Technological Center for Microstructures (CTμ) (Villeurbanne, France) and from the GENTYANE Sequencing Platform (Clermont-Ferrand, France). The authors thank the UCA Centre Imagerie Cellulaire Santé (UCA, Clermont-Ferrand) for help with microscopy intercalibration. We thank Anne Catherine Lehours (LMGE) and Guillaume Borrel (BECM, Institut Pasteur, Paris, France) for helpful comments and discussions on the manuscript and Matthieu Legendre (IGS, UMR7256 Aix Marseille Université-CNRS, Marseille, France) for his assistance with the assembly of the sequence data. We also thank the two reviewers for their comments and suggestions which greatly increased the quality of this manuscript.

SUPPLEMENTARY MATERIAL

The Supplementary Material for this article can be found online at: https://www.frontiersin.org/articles/10.3389/fmicb.2019.02376/full#supplementary-material

Supplementary Data Sheet 1 | Contigs from ALN-enriched DNA templates.

REFERENCES

Abrahão, J., Silva, L., Silva, L. S., Khalil, J. Y. B., Rodrigues, R., Arantes, T., et al. (2018). Tailed giant Tupanvirus possesses the most complete translational apparatus of the known virosphere. *Nat. Commun.* 9:749. doi: 10.1038/s41467-018-03168-1

Aho, K., and Kajander, E. O. (2003). Pitfalls in detection of novel nanoorganisms. *J. Clin. Microbiol.* 41, 3460–3461. doi: 10.1128/JCM.41.7.3460-3461.2003

Altschul, S. F., Madden, T. L., Schäffer, A. A., Zhang, J., Zhang, Z., Miller, W., et al. (1997). Gapped BLAST and PSI-BLAST: a new generation of protein database search programs. *Nucleic Acids Res.* 25, 3389–3402. doi: 10.1093/nar/25.17.3389

Benzerara, K., Menguy, N., Guyot, F., Dominici, D., and Gillet, P. (2003). Nanobacteria-like calcite single crystals at the surface of the Tatahouine meteorite. *Proc. Natl. Acad. Sci. U.S.A.* 100, 7438–7442. doi: 10.1073/pnas.0832464100

Benzerara, K., Miller, V. M., Barell, G., Kumar, V., Miot, J., Brown, G. E. Jr., et al. (2006). Search for microbial signatures within human and microbial

calcifications using soft X-ray spectromicroscopy. *J. Investig. Med*. 54, 367–379. doi: 10.2310/6650.2006.06016

Biller, S. J., McDaniel, L. D., Breitbart, M., Rogers, E., Paul, J. H., and Chisholm, S. W. (2017). Membrane vesicles in sea water: heterogeneous DNA content and implications for viral abundance estimates. *ISME J.* 11, 394–404. doi: 10.1038/ismej.2016.134

Borrel, G., Joblin, K., Guedon, A., Colombet, J., Tardy, V., Lehours, A. C., et al. (2012). *Methanobacterium lacus sp*. nov., isolated from the profundal sediment of a freshwater meromictic lake. *Int. J. Syst. Evol. Microbiol*. 62, 1625–1629. doi: 10.1099/ijs.0.034538-0

Brown, C. T., Hug, L. A., Thomas, B. C., Sharon, I., Castelle, C. J., Singh, A., et al. (2015). Unusual biology across a group comprising more than 15% of domain Bacteria. *Nature* 523, 208–211. doi: 10.1038/nature14486

Brussaard, C. P. (2004). Optimization of procedures for counting viruses by flow cytometry. *Appl. Environ. Microbiol*. 70, 1506–1513. doi: 10.1128/AEM.70.3.1506-1513.2004

Buchfink, B., Xie, C., and Huson, D. H. (2015). Fast and sensitive protein alignment using DIAMOND. *Nat. Methods*. 12, 59–60. doi: 10.1038/nmeth.3176

Castelle, C. J., Brown, C. T., Anantharaman, K., Probst, A. J., Huang, R. H., and Banfield, J. F. (2018). Biosynthetic capacity, metabolic variety and unusual biology in the CPR and DPANN radiations. *Nat. Rev*. 16, 629–645. doi: 10.1038/s41579-018-0076-2

Chin, C. S., Alexander, D. H., Marks, P., Klammer, A. A., Drake, J., Heiner, C., et al. (2013). Nonhybrid, finished microbial genome assemblies from long-read SMRT sequencing data. *Nat. Methods*. 10, 563–569. doi: 10.1038/nmeth.2474

Cisani, G., Varaldo, P. E., Ingianni, A., Pompei, R., and Satta, G. (1984). Inhibition of herpes simplex virus-induced cytopathic effect by modified hen egg-white lysozymes. *Curr. Microbiol.* 10, 35–40. doi: 10.1007/BF01576045

Dar, M. A., Sharma, A., Mondal, N., and Dhar, S. K. (2007). Molecular cloning of apicoplast-targeted *Plasmodium falciparum* DNA gyrase genes: unique intrinsic ATPase activity and ATP-independent dimerization of Pf GyrB subunit. *Eukaryot. Cell* 6, 398–412. doi: 10.1128/EC.00357-06

Diao, M., Sinnige, R., Kalbitz, K., Huisman, J., and Muyzer, G. (2017). Succession of bacterial communities in a seasonally stratified lake with an anoxic and sulfidic hypolimnion. *Front. Microbiol.* 8:2511. doi: 10.3389/fmicb.2017.02511

Duda, V. I., Suzina, N. E., Polivtseva, V. N., and Boronin, A. M. (2012). Ultramicrobacteria: formation of the concept and contribution of ultramicrobacteria to biology. *Microbiology* 81, 379–390. doi: 10.1134/S0026261712040054

Engle, E. C., Manes, S. H., and Drlica, K. (1982). Differential effects of antibiotics inhibiting gyrase. *J. Bacteriol*. 149, 92–98.

Folk, R. L. (1993). SEM imaging of bacteria and nanobacteria in carbonate sediments and rocks. *J. Sediment Res*. 63, 990–999. doi: 10.1306/D4267C67-2B26-11D7-8648000102C1865D

Forterre, P., Soler, N., Krupovic, M., Marguet, E., and Ackermann, H. W. (2013). Fake virus particles generated by fluorescence microscopy. *Trends Microbiol.* 21, 1–5. doi: 10.1016/j.tim.2012.10.005

Ghuneim, L. J., Jones, D. L., Golyshin, P. N., and Golyshina, O. V. (2018). Nano-sized and filterable bacteria and archaea: biodiversity and function. *Front. Microbiol.* 9:1971. doi: 10.3389/fmicb.2018.01971

Griffin, S., Masood, M. I., Nasim, M. J., Sarfraz, M., Ebokaiwe, A. P., Schäfer, K. H., et al. (2018). Natural nanoparticles: a particular matter inspired by nature. *Antioxidants* 7:3. doi: 10.3390/antiox7010003

Häring, M., Vestergarrd, G., Rachel, R., Chen, L., Garret, R. A., and Prangishvili, D. (2005). Virology: independent virus development outside a host. *Nature* 436, 1101–1102. doi: 10.1038/4361101a

He, L., Han, X., and Yu, Z. (2014). A Rare *Phaeodactylum tricornutum* cruciform morphotype: culture conditions, transformation and unique fatty acid characteristics. *PLoS ONE* 9:e93922. doi: 10.1371/journal.pone.0093922

Hofer, F., Grogger, W., Kothleitner, G., and Warbichler, P. (1997). Quantitative analysis of EFTEM elemental distribution images. *Ultramicroscopy* 67, 83–103. doi: 10.1016/S0304-3991(96)00106-4

Hug, L. A., Baker, B. J., Anantharaman, K., Brown, C. T., Probst, A. J., Castelle, C. J., et al. (2016). A new view of the tree of life. *Nat. Microbiol.* 1:16048. doi: 10.1038/nmicrobiol.2016.48

Hyatt, D., Chen, G. L., Locascio, P. F., Land, M. L., Larimer, F. W., and Hauser, L. J. (2010). Prodigal: prokaryotic gene recognition and translation initiation site identification. *BMC Bioinformatics* 11:119. doi: 10.1186/1471-2105-11-119

Kajander, E. O., Ciftcioglu, N., Aho, K., and Garcia-Cuerpo, E. (2003). Characteristics of Nanobacteria and their possible role in stone formation. *Urol. Res*. 31, 47–54. doi: 10.1007/s00240-003-0304-7

Kéraval, B., Lehours, A. C., Colombet, J., Amblard, C., Alvarez, G., and Fontaine, S. (2016). Soil carbon dioxide emissions controlled by an extracellular oxidative metabolism identifiable by its isotope signature. *Biogeosciences* 13, 6353–6362. doi: 10.5194/bg-13-6353-2016

King, A. M. Q., Lefkowitz, E. J., Mushegian, A. R., Adams, M. J., Dutilh, B. E., Gorbalenya, A. E., et al. (2018). Changes to taxonomy and the international code of virus classification and nomenclature ratified by the International Committee on Taxonomy of Viruses (2018). *Arch. Virol*. 163, 2601–2631. doi: 10.1007/s00705-018-3847-1

Krumsiek, J., Arnold, R., and Rattei, T. (2007). Gepard: a rapid and sensitive tool for creating dotplots on genome scale. *Bioinformatics* 23, 1026–1028. doi: 10.1093/bioinformatics/btm039

Lee-Huang, S., Maiorov, V., Huang, P. L., Ng, A., Lee, H. C., Chang, Y. T., et al. (2005). Structural and functional modeling of human lysozyme reveals a unique nonapeptide, HL9, with anti-HIV activity. *Biochemistry* 44, 4648–4655. doi: 10.1021/bi0477081

Liu, Y., Smid, E. J., Abee, T., and Notebaart, R. A. (2019). Delivery of genome editing tools by bacterial extracellular vesicles. *Microb. Biotechnol*. 12, 71–73. doi: 10.1111/1751-7915.13356

Mackey, B. M., Miles, C. A., Parsons, S. E., and Seymour, D. A. (1991). Thermal denaturation of whole cells and cell components of *Escherichia coli* examined by differential scanning calorimetry. *J. Gen. Microbiol*. 137, 2361–2374. doi: 10.1099/00221287-137-10-2361

Manchenko, G. P. (1994). *Handbook of Detection of Enzymes on Electrophoresis Gels*. Boca Raton, FL: CRC Press; Taylor & Francis Group.

Martel, J., and Young, J. D. (2008). Purported nanobacteria in human blood as calcium carbonate nanoparticles. *Proc. Natl. Acad. Sci. U.S.A.* 105, 5549–5554. doi: 10.1073/pnas.0711744105

Mastronarde, D. N. (2005). Automated electron microscope tomography using robust prediction of specimen movements. *J. Struct. Biol*. 152, 36–51. doi: 10.1016/j.jsb.2005.07.007

McKay, D. S., Gibson, E. K., and Thomas-Keprta, K. L. (1996). Search for past life on Mars: possible relic biogenic activity in martian meteorite ALH84001. *Science* 273, 924–930. doi: 10.1126/science.273.5277.924

National Research Council (1999). *Size Limits of Very Small Microorganisms: Proceedings of a Workshop*. Washington, DC: The National Academies Press.

Ortiz-Alvarez, R., and Casamayor, E. O. (2016). High occurrence of Pacearchaeota and Woesearchaeota (Archaea superphylum DPANN) in the surface waters of oligotrophic high-altitude lakes. *Environ. Microbiol. Rep*. 8, 210–217. doi: 10.1111/1758-2229.12370

Pradeep Ram, A. S., Mari, X., Brune, J., Torréton, J. P., Chu, V. T., Raimbault, P., et al. (2018). Bacterial-viral interactions in the sea surface microlayer of a black carbon-dominated tropical coastal ecosystem (Halong Bay, Vietnam). *Elem. Sci. Anth*. 6, 2–19. doi: 10.1525/elementa.276

Prangishvili, D., Vestergaard, G., Häring, M., Aramyo, R., Basta, T., Rachel, R., et al. (2006). Structural and genomic properties of the hyperthermophilic archeal virus ATV with an extracellular stage of reproductive cycle. *J. Mol. Biol*. 359, 1203–1216. doi: 10.1016/j.jmb.2006.04.027

Quast, C., Pruesse, E., Yilmaz, P., Gerken, J., Schweer, T., Yarza, P., et al. (2013). The SILVA ribosomal RNA gene database project: improved data processing and web-based tools. *Nucleic Acids Res*. 41, D590–D596. doi: 10.1093/nar/gks1219

Raoult, D., Drancourt, M., Azza, S., Nappez, C., Guieu, R., Rolain, J. M., et al. (2008). Nanobacteria are mineralo fetuin complexes. *PLoS Pathog*. 4:e41. doi: 10.1371/journal.ppat.0040041

Schulz, F., Yutin, N., Ivanova, N. N., Ortega, D. R., Lee, T. K., Vierheilig, J., et al. (2017). Giant viruses with an expanded complement of translation system components. *Science* 356, 82–85. doi: 10.1126/science.aal4657

Sieburth, J.,Mc, N., Smetacek, V., and Lenz, J. (1978). Pelagic ecosystem structure: heterotrophic compartments of the plankton and their relationship to plankton size fractions. *Limnol. Oceanogr*. 23, 1256–1263. doi: 10.4319/lo.1978.23.6.1256

Sillitoe, R. H., Folk, R. L., and Saric, N. (1996). Bacteria as mediators of copper sulfide enrichment during weathering. *Science* 272, 1153–1155. doi: 10.1126/science.272.5265.1153

Soler, N., Kruprovic, M., Marguet, E., and Forterre, P. (2015). Membrane vesicles in natural environments: a major challenge in viral ecology. *ISME J.* 9, 793–796. doi: 10.1038/ismej.2014.184

Soler, N., Marguet, E., Verbavatz, J. M., and Forterre, P. (2008). Virus-like vesicles and extracellular DNA produced by hyperthermophilic archaea of the order Thermococcales. *Res. Microbiol.* 159, 390–399. doi: 10.1016/j.resmic.2008.04.015

UniProt Consortium (2019). UniProt: a worldwide hub of protein knowledge. *Nucleic Acids Res.* 47, D506–D515. doi: 10.1093/nar/gky1049

Uwins, P. J., Webb, R. I., and Taylor, A. P. (1998). Novel nano-organisms from Australian sandstones. *Am. Mineral.* 83, 1541–1550. doi: 10.2138/am-1998-11-1242

Weinbauer, M. G. (2004). Ecology of prokaryotic viruses. *FEMS Microbiol. Rev.* 28, 127–181. doi: 10.1016/j.femsre.2003.08.001

Wu, C. Y., Martel, J., Wong, T. Y., Young, D., Liu, C. C., Lin, C. W., et al. (2016). Formation and characteristics of biomimetic mineralo-organic particles in natural surface water. *Sci. Rep.* 6:28817. doi: 10.1038/srep28817

Wurch, L., Giannone, R. J., Belisle, B. S., Swift, C., Utturkar, S., Hettich, R. L., et al. (2016). Genomics-informed isolation and characterization of a symbiotic Nanoarchaeota system from a terrestrial geothermal environment. *Nat. Commun.* 7:12115. doi: 10.1038/ncomms12115

Yaghobee, S., Mojtaba, B., Samiei, N., and Jahedmanesh, N. (2015). What are the nanobacteria? *Biotechnol. Biotechnol. Equip.* 29, 826–833. doi: 10.1080/13102818.2015.1052761

Conflict of Interest: The authors declare that the research was conducted in the absence of any commercial or financial relationships that could be construed as a potential conflict of interest.

Copyright © 2019 Colombet, Billard, Viguès, Balor, Boulé, Geay, Benzerara, Menguy, Ilango, Fuster, Enault, Bardot, Gautier, Pradeep Ram and Sime-Ngando. This is an open-access article distributed under the terms of the Creative Commons Attribution License (CC BY). The use, distribution or reproduction in other forums is permitted, provided the original author(s) and the copyright owner(s) are credited and that the original publication in this journal is cited, in accordance with accepted academic practice. No use, distribution or reproduction is permitted which does not comply with these terms.

frontiers in Microbiology

ORIGINAL RESEARCH
published: 16 October 2019
doi: 10.3389/fmicb.2019.02375

Widespread Dominance of Kinetoplastids and Unexpected Presence of Diplonemids in Deep Freshwater Lakes

Indranil Mukherjee[1†], Yoshikuni Hodoki[1], Yusuke Okazaki[2], Shohei Fujinaga[1], Kako Ohbayashi[1,3] and Shin-ichi Nakano[1]*

[1] Center for Ecological Research, Kyoto University, Otsu, Japan, [2] Bioproduction Research Institute, National Institute of Advanced Industrial Science and Technology, Tsukuba, Japan, [3] Department of General Systems Studies, The University of Tokyo, Tokyo, Japan

OPEN ACCESS

Edited by:
Raju Sekar, Xi'an Jiaotong-Liverpool University, China

Reviewed by:
Purificacion Lopez-Garcia, Centre National de la Recherche Scientifique (CNRS), France
Weida Gong, The University of North Carolina at Chapel Hill, United States

***Correspondence:**
Indranil Mukherjee
indranilmukherjee04@yahoo.com

†Present address:
Indranil Mukherjee, Biology Centre, Czech Academy of Sciences, Institute of Hydrobiology, České Budejovice, Czechia

Specialty section:
This article was submitted to Aquatic Microbiology, a section of the journal Frontiers in Microbiology

Received: *11 July 2019*
Accepted: *30 September 2019*
Published: *16 October 2019*

Citation:
Mukherjee I, Hodoki Y, Okazaki Y, Fujinaga S, Ohbayashi K and Nakano S-i (2019) Widespread Dominance of Kinetoplastids and Unexpected Presence of Diplonemids in Deep Freshwater Lakes. Front. Microbiol. 10:2375. doi: 10.3389/fmicb.2019.02375

Kinetoplastid flagellates are generally abundant in the deep sea and recently they were even found to be dominant in the hypolimnion of a deep freshwater lake. Therefore, to understand the distribution of kinetoplastids in deep freshwater lakes, we have collected vertical samples from five lakes in Japan. The abundance of kinetoplastids was enumerated by Catalyzed Reporter Deposition-Fluorescence *in situ* Hybridization, and the diversity was determined by 18S amplicon sequencing using universal eukaryote and kinetoplastid-specific primers. Kinetoplastids were abundant in the deep waters of all the lakes, contributing up to 53.6% of total nanoeukaryotes. Despite this significant contribution, kinetoplastids remain undetected by amplicon sequencing using universal primers that are widely used in eukaryotic diversity studies. However, they were detected with specific primers, and the communities were characterized by both ubiquitous and lake-specific unique OTUs. Oligotyping of a ubiquitous and dominant OTU revealed the presence of lake-specific sequence types (oligotypes). Remarkably, we also detected diplonemids (a sister group of kinetoplastids and considered to be specific in the marine habitat) using kinetoplastid-specific primers, showing their presence in freshwaters. Underestimation of kinetoplastids and diplonemids using universal primers indicates that euglenozoan flagellates are overlooked in diversity studies worldwide. The present study highlighted the importance of kinetoplastids in the hypolimnion of deep lakes, thereby indicating their role in material cycling in deep waters.

Keywords: 18S amplicon sequencing, CARD-FISH, deep lakes, diplonemids, flagellates, hypolimnion, kinetoplastids

INTRODUCTION

Diversity studies in microbial eukaryotes conducted recently by various molecular techniques have shown immense diversity of protists (Moon-van der Staay et al., 2001; Moreira and Lopez-Garcia, 2002; Grossmann et al., 2016) and identified several important lineages. Several of these recently reported lineages were previously unknown when the studies were mainly culture-based and employed light microscopy for identification (Massana et al., 2006; de Vargas et al., 2015).

However, the universal eukaryote primers commonly used to understand the diversity of these organisms often underestimate several lineages owing to the divergent nature of their 18S rRNA gene (Berney et al., 2004; Simpson et al., 2006; Bochdanksy and Huang, 2010). This might not create a serious problem if minor groups are underestimated, but can display a different picture of the ecosystem processes if abundant groups are ignored.

One particular flagellate group, kinetoplastids, have regularly been undetected in nearly all the diversity studies in microbial eukaryotes using molecular techniques (Von der Heyden and Cavalier-Smith, 2005; Vaerewijck et al., 2008; Mukherjee et al., 2015). Kinetoplastids are among the most cosmopolitan flagellates in aquatic environments (Patterson and Larsen, 1991; Arndt et al., 2000) with high diversity (Von der Heyden and Cavalier-Smith, 2005). An important aspect of kinetoplastid phylogeny is the massive evolutionary change of their 18S rRNA gene, due to which they are found at the base of the eukaryotic phylogenetic trees (Simpson et al., 2006; Janouškovec et al., 2017; Strassert et al., 2019). Kinetoplastids, along with diplonemids and euglenids belong to the phylum Euglenozoa (Cavalier-Smith, 1981), where the free-living and occasionally parasitic group diplonemids are their closest relatives (Lara et al., 2009). The euglenozoans diverged from other eukaryotes (Moreira et al., 2004; Vlcek et al., 2010) and are known as basal eukaryotes (Cavalier-Smith, 2009).

Class Kinetoplastea consists of parasitic, uniflagellate trypanosomatids and free-living, biflagellate bodonids (Vickerman, 1976). Trypanosomatids are well studied owing to their medical importance, whereas bodonids have received limited attention (Simpson et al., 2006). Bodonids are heterotrophic and are often found to dominate in cultures. Owing to their opportunistic nature, several stains have been cultured and a few laboratory studies have been conducted to understand their ecology (Caron, 1987; Boenigk and Arndt, 2000; Zubkov and Sleigh, 2000). Although these flagellates are cosmopolitan with high diversity they are considered to have lower abundance in the aquatic ecosystems (Arndt et al., 2000). Recent studies reported that owing to the mismatches in their 18S rRNA gene the commonly used universal eukaryote primers and probes do not target kinetoplastids (Bochdanksy and Huang, 2010; Mukherjee et al., 2015). This has led to their underestimation in diversity and abundance-based studies worldwide and is likely the reason for there being fewer reports on them in natural environments in such studies. This group has recently attracted some interest among researchers as using specific primers and Catalyzed Reporter Deposition-Fluorescence *In Situ* Hybridization (CARD-FISH) probes kinetoplastids were reported to have high abundance and diversity in the deep sea (López-García et al., 2003; Edgcomb et al., 2011; Morgan-Smith et al., 2011, 2013; Salani et al., 2012) and also from the hypolimnion of a freshwater deep holomictic lake (Mukherjee et al., 2015). The results from these studies suggest that kinetoplastid flagellates mainly inhabit the deep waters of both oceans and lakes. However, limited studies from the deep waters of freshwater lakes have restricted our understanding of the hypolimnion kinetoplastid communities, therefore indicating the need for further studies to understand the importance of these less-studied flagellates, especially from the deeper waters of freshwater lakes.

Owing to the water mixing patterns in freshwater deep holomictic lakes, where water column is mixed in some seasons and remain stratified in other seasons, the microbial communities in different depths undergo community assembly and re-assembly. This seasonal community variation in different depths presents an interesting ecosystem to understand the ecology of these microorganisms. However there are only a few studies on freshwater deep lakes, and the microbial communities in the hypolimnion waters are poorly understood (Okazaki and Nakano, 2016; Mukherjee et al., 2017). The limited number of studies that have been conducted on the oxygenated hypolimnion of freshwater deep lakes have studied bacterial community, where they reported the dominance of hypolimnion-specific bacterial lineages (Urbach et al., 2001; Callieri et al., 2015; Okazaki et al., 2017; Mehrshad et al., 2018; Andrei et al., 2019). Information about the protist communities in hypolimnion waters is poorly known. However, the limited information available about the protist communities in the oxygenated hypolimnion waters of some deep holomictic lakes also indicates the dominance of hypolimnion-specific lineages (Lepère et al., 2010; Mukherjee et al., 2015, 2017).

To understand the abundance and distribution of kinetoplastids in deep freshwater lakes, we took water samples of various depths from five deep freshwater lakes in Japan (**Figure 1**) with oxygenated hypolimnion during summer stratification (**Table 1**). The abundance of kinetoplastids was examined using group-specific CARD-FISH probes and their detailed community composition was analyzed by 18S rRNA gene amplicon sequencing with universal eukaryote and kinetoplastid-specific primers. Moreover, oligotyping was conducted on ubiquitous kinetoplastid OTU to understand whether geographically isolated deep waters of freshwater lakes exhibit sequence variation among the OTUs.

MATERIALS AND METHODS

Study Site and Sampling

Samples were collected from five monomictic deep freshwater lakes in Japan with oxygenated hypolimnion (**Figure 1** and **Table 1**). Samples from various depths covering the epilimnion and hypolimnion were taken once from one station in each lake (except for Lake Biwa where sampling was conducted twice) during the thermal stratification period (**Figure 2A** and **Table 1**). Sampling in Lake Biwa was conducted from station Ie-1 (a long-term limnological survey station of Kyoto University, Japan) and from a station located at the deepest part for all the other lakes. Samples were collected with a 5 liter Niskin sampler (General Oceanics, Miami, United States) and the hydrographic structure was determined with a conductivity-temperature-depth profiler (911 plus, Sea Bird Electronics, Inc., United States) for Lake Biwa and with a Rinko profiler (ASTD 102, JFE Advantech Co., Ltd., Japan) for the other lakes. The concentration of chlorophyll *a* was measured simultaneously using the CTD and Rinko profiler (**Supplementary Figure S1A** and **Table 1**). Samples were

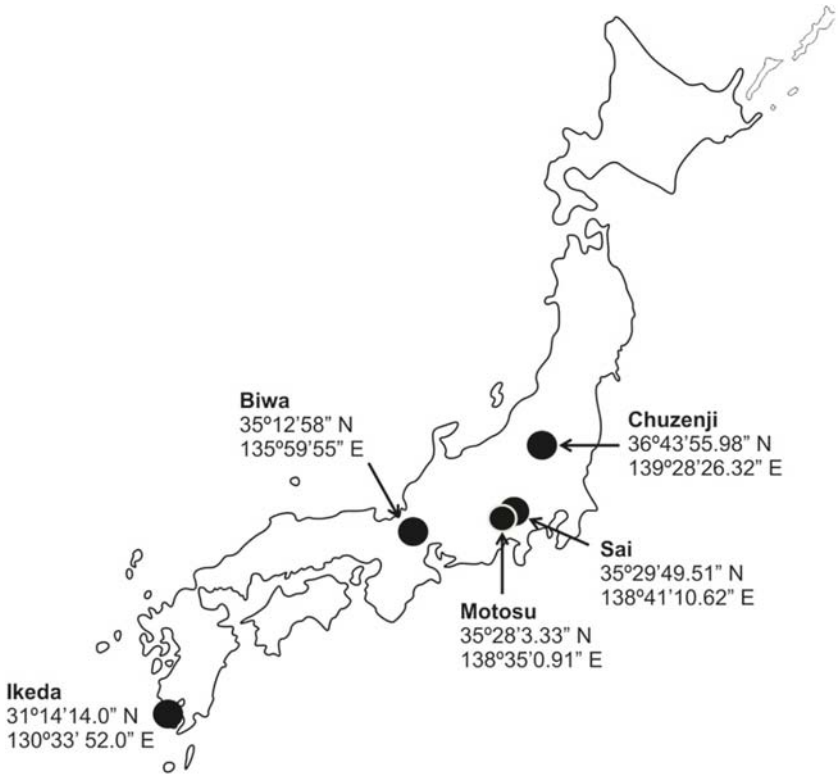

FIGURE 1 | Map of Japan with the location of the sampled lakes.

TABLE 1 | Characteristics and sampling information of each lake.

Lake	Trophic status	Surface area (km^2)	Z max (m)	Sampling month and year	Mean bacterial abundance ($\times 10^6$ cells ml^{-1})	Mean conc. (till 30 m) of chlorophyll *a* ($\mu g\ l^{-1}$)
Biwa	Mesotrophic	674.0	104	August and November 2014	2.0 ± 1.3	0.8 ± 0.5
Chuzenji	Oligotrophic	11.62	161	August 2014	1.3 ± 0.6	0.8 ± 0.4
Motosu	Oligotrophic	4.7	121	October 2014	0.7 ± 0.1	0.5 ± 0.9
Sai	Oligotrophic	2.1	74	October 2014	1.4 ± 0.4	1.1 ± 0.7
Ikeda	Mesotrophic	11.0	200	July 2015	2.8 ± 3.2	1.9 ± 1.5

collected in clean plastic bottles, which were rinsed three times with sample water before collection and were kept cool and dark in an icebox and transported to the laboratory within a few hours of collection.

Total Bacteria Count

Samples were fixed immediately after collection with glutaraldehyde (1% final concentration) and stored at 4°C until filtration. A 1 ml water sample was filtered through a polycarbonate membrane filter (pore size 0.2 μm, diameter 25 mm, Advantec), and stained with 4, 6-diamidino-2-phenylindole (DAPI) (Porter and Feig, 1980). The bacterial cells were observed under UV light with an epi-fluorescent microscope (Olympus BX- 50, Japan). Duplicate counts from each sample were counted at 1000 × magnification from 20 randomly chosen fields (a minimum of 300 cells were counted) (**Supplementary Figure S1B** and **Table 1**).

DNA Extraction and Pyrosequencing

In Lake Biwa, owing to the relatively high abundance of kinetoplastids in the hypolimnion from August and November and also in the epilimnion from August (Mukherjee et al., 2015), DNA samples were collected from both the epilimnion and hypolimnion in August and only from the hypolimnion in November (**Table 2**). DNA samples from the four other lakes were collected from one depth in the hypolimnion (**Table 2**). Water samples were pre-filtered just after collection using a 20-μm mesh plankton net to exclude bigger organisms. One to two liters (500 ml for Lake Ikeda) of water samples were filtered with a 0.8 μm polycarbonate filter (47 mm diameter, Costar) at low vacuum (7.5 cm Hg) and immediately frozen at −30°C until analysis. DNA was extracted using a Power Soil DNA isolation and purification kit (MoBio laboratories, Carlsbad, CA, United States) and quantified using a Nanodrop ND-1000 spectrophotometer (NanoDrop

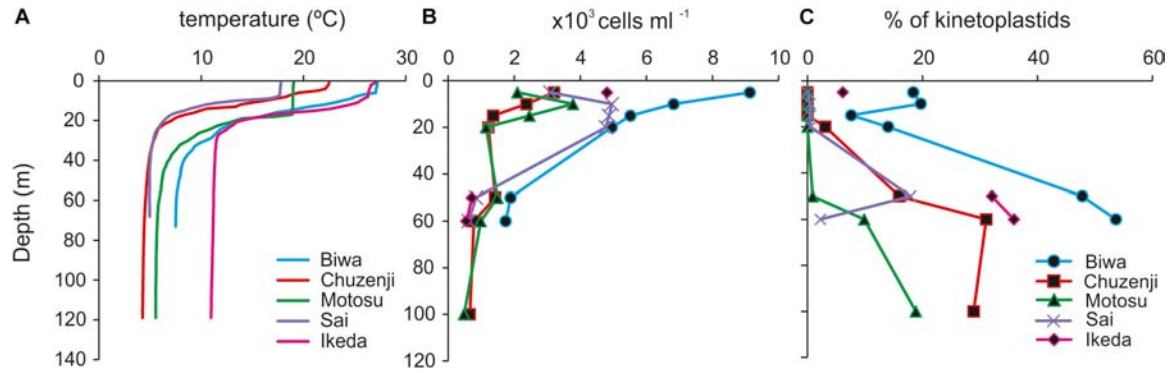

FIGURE 2 | Vertical profile of **(A)** temperature; **(B)** abundance of nanoeukaryotes; **(C)** percentage contribution of kinetoplastids to total nanoeukaryotes in the studied lakes. Sampling depths are indicated by symbols. Sampling depths of each lake covering the epilimnion and hypolimnion are: Biwa (5, 10, 15, 20, 50, and 60 m), Chuzenji (5, 10, 15, 20, 50, 60, and 100 m), Motosu (5, 10, 15, 20, 50, 60, and 100 m), Sai (5, 10, 20, 50, and 60 m), and Ikeda (5, 50 and 60 m).

TABLE 2 | Details of individual libraries with kinetoplastid-specific primers.

Sample	Depth (m)	No. of OTUs	Unique OTUs	Euglenozoan sequences	Shannon diversity	Richness S.chao1
Biwa Epi	5	6	1	458	2.07	17
Biwa Aug Hypo	60	15	3	1558	1.09	24.33
Biwa Nov Hypo	60	19	10	1036	0.95	25.33
Chuzenji	70	5	1	2555	0.78	4.0
Motosu	100	1	0	181	0.08	3.0
Sai	65	4	0	293	0.63	5.0
Ikeda	50	8	2	286	1.72	9.0

Biwa Epi, Lake Biwa epilimnion; Biwa Aug Hypo, Lake Biwa August hypolimnion; Biwa Nov Hypo, Lake Biwa November hypolimnion.

Technologies, Inc., Wilmington, DE, United States). Separate polymerase chain reactions (PCR) were conducted for general eukaryotes and kinetoplastids. PCR was conducted using universal eukaryote primers TAReuk454FWD1 (5′-CCAGCA(G/C)C(C/T)GCGGTAATTCC-3′) and TAReukREV3 (5′-ACTTTCGTTCTTGAT(C/T)(A/G)A-3′) to amplify the V4 region of the 18S rRNA gene of all eukaryotes (Stoeck et al., 2010). Samples from Lake Ikeda were not used for the analysis of the total eukaryotic community. The kinetoplastid 18S rRNA gene was amplified using kinetoplastid-specific primers, kineto14F (Von der Heyden and Cavalier-Smith, 2005) and Kin500R (Scheckenbach et al., 2005) to amplify the V1 and V2 variable regions. Adapters for the 454 pyrosequencer were attached to both the forward and reverse primers and sample-specific barcode tags were attached only to the forward primers. PCRs were performed in 25 μl of reaction volume with a Blend Taq PCR kit (Toyobo, Osaka, Japan). The PCR conditions for the universal eukaryote primers were: initial denaturation at 98°C for 30 s, 10 cycles (98°C for 10 s, 53°C for 30 s, and 72°C for 2 s), then 15 similar cycles with a 48°C annealing temperature, and a final extension at 72°C for 10 min (Massana et al., 2015). The PCR conditions for the Kinetoplastid-specific primers were 94°C for 5 min, 35 cycles (94°C for 30 s, 69°C for 36 s, and 72°C for 4.5 min), and a final extension at 72°C for 10 min (Von der Heyden and Cavalier-Smith, 2005). For the Lake Ikeda samples, owing to the lower concentration of kinetoplastid template DNA, the number of PCR cycles was increased to 40. Amplicons were checked using agarose gel electrophoresis and DNA was purified using an UltraClean PCR Clean-Up kit (MoBio Laboratories, Carlsbad, CA, United States). Samples were quantified using a Nanodrop ND-1000 spectrophotometer (NanoDrop Technologies, Inc., Wilmington, DE, United States). The samples were pooled to have uniform DNA concentration in each sample and were sent to Macrogen, Japan for pyrosequencing using a Roche 454 GS-FLX titanium system (Macrogen Japan Corp. Kyoto, Japan). The sequence data were submitted to the DDBJ Sequence Read Archive (DRA) database and are available under the Bio-project accession number: PRJDB6819.

Pyrotag Processing

The processing and quality control of the sequencing data were conducted using UPARSE (Edgar, 2013). Sequences were de-multiplexed using the bar code identifier in the forward primer. A chimera check was conducted with UCHIME (Edgar et al., 2011) using *de novo* and reference-based chimera searches against the PR2 database (Guillou et al., 2013). Pyrotags were trimmed to have 300 bp of a good quality sequence, and pyrotags with less than 200 bp lengths were excluded from further analysis. OTUs were then clustered with 97% similarity with USEARCH (Edgar, 2010). Classification of each OTU was conducted against the SILVA reference database[1]. The unknown OTUs were separately

[1]www.arb-silva.de/

classified to their closest relatives with BLAST searches against the NCBI nucleotide collection (nt) database[2].

Oligotyping

Oligotyping was conducted to understand the intra-diversity within a particular OTU by analyzing the single nucleotide variation, excluding the sequencing errors based on Shannon entropy values (Eren et al., 2013). The dominant kinetoplastid OTU was selected for oligotyping following the author's instructions[3]. The quality filtered FASTA files of the individual reads in each OTU generated by the UPARSE pipeline were aligned using online aligner SINA 1.2.11 (Pruesse et al., 2012). Gaps in the aligned sequences were eliminated and sequences were trimmed using the scripts "o-trim-uninformative-columns-from-alignment" and "o-smart-trim" scripts, respectively. The most informative column with the highest entropy value was chosen from several rounds of oligotyping until all oligotypes with >100 reads exceeded the purity score of 0.90.

Phylogenetic Analysis

Phylogenetic analysis was conducted with 18S rRNA gene sequence of diplonemids closely related to the diplonemid OTU obtained in the present study and also with the sequences of cultured diplonemids. Kinetoplastids and other euglenozoan sequences were considered as an outgroup. Sequences were aligned using MAFFT (LINSI) (Katoh and Toh, 2010) and a maximum likelihood tree was inferred using IQ-TREE (-m GTR + I + G4) with standard bootstraps (-b 100) (Nguyen et al., 2014).

CARD-FISH

Water samples were pre-filtered through a 20-μm mesh plankton net and fixed in a 2% final concentration of formaldehyde (freshly prepared by filtering through 0.2 μm syringe filter) for at least 3–4 h before filtration. 50 ml of epilimnion and 100 ml of hypolimnion samples were filtered through polycarbonate filters (pore size 0.8 μm, diameter 25 mm, Advantec), rinsed twice with 1X PBS and twice with MilliQ water, air dried and frozen at −20°C until further processing.

CARD-FISH was performed according to the method described in Mukherjee et al. (2015). The filters were embedded in 0.1% low-gelling-point agarose and cut into eight sections, which were hybridized at 35°C for 12 h with a 0.5 μg ml^{-1} probe concentration and a 30% concentration of formamide. The probes (**Supplementary Table S1**) were purchased from Thermo Electron Co. (Ulm, Germany). Counting was performed using an Olympus BX50 epifluorescence microscope under 1000 × magnification at blue/UV excitation. For the kinetoplastids, either 100 microscopic fields were counted, or when the densities were low the complete filter piece was screened per sample. The total eukaryotes were counted simultaneously with the kinetoplastid cells by DAPI staining under UV excitation.

[2]https://blast.ncbi.nlm.nih.gov/Blast.cgi?PROGRAM=blastn&PAGE_TYPE=BlastSearch&LINK_LOC=blasthome

[3]http://merenlab.org/software/oligotyping/

Statistical Analysis

Coverage-based rarefaction (Chao and Jost, 2012) was conducted before diversity analysis, where the reads were discarded from each sample until the coverage was 97%, or slope of the rarefaction curve was >0.03, which was the minimum value recorded among the samples. To compare the kinetoplastid communities in the studied lakes, cluster analysis was computed on the rarefied data on a Bray-Curtis similarity matrix using the 'Vegan' R package. Subsequently, kinetoplastid diversity in different samples was compared with a diversity index analysis (Shannon) using the 'Vegan R package' (Oksanen et al., 2013). Venn diagram was plotted to compare the OTUs of Lake Biwa samples using the 'Venn diagram' package for R. All the analyses were computed in R environment[4] (R Development Core Team, 2013). The distance between kinetoplastid communities in the studied lakes were estimated by an unconstrained ordination analysis, Detrended Correspondence Analysis (DCA) using Canoco v5.0 program package (Ter Braak and Smilauer, 2012) on the rarefied data.

RESULTS

Physico-Chemical Parameters

The water columns from all the studied lakes were thermally stratified with the thermocline located at 20–30 m (**Figure 2A**). The epilimnion temperature of Lakes Biwa and Ikeda were relatively higher at 27°C, whereas the temperatures in the other lakes were 23°, 19° and 18°C in Lakes Chuzenji, Motosu and Sai, respectively. The hypolimnion of Lake Ikeda had the highest temperature of 11°C, followed by 8°, 6°, 5° and 4°C in Lakes Biwa, Motosu, Sai and Chuzenji, respectively. All the lakes had oxygenated hypolimnion except for Lake Ikeda, which has an anoxic hypolimnion near the bottom waters (ca. 200 m). Therefore, hypolimnion samples from Lake Ikeda were taken from the oxygenated layers (50 and 70 m).

Abundance of Nanoeukaryotes and Kinetoplastids

A high abundance of nanoeukaryotes was found in the epilimnion of all the lakes, where the highest abundance of 9.1×10^3 cells ml^{-1} was found at 5 m in Lake Biwa (**Figure 2B**). The abundance of nanoeukaryotes reduced with the increase in depth and the lowest abundance was found at 100 m in Lake Motosu (0.5×10^3 cells ml^{-1}). In the epilimnion, kinetoplastid flagellates were detected only from Lake Biwa and Lake Ikeda (**Figure 2C**). The abundance of kinetoplastids was 1.7×10^3 cells ml^{-1} and 1.3×10^3 cells ml^{-1} and contributed up to 18 and 20% of total nanoeukaryotes at 5 and 10 m, respectively in Lake Biwa, and the abundance in Lake Ikeda was 2.9×10^2 cells ml^{-1}, and contributed 6% of total nanoeukaryotes (**Figure 2C**). The contribution of kinetoplastids increased with the increase in depth in all lakes, and they were the dominant members of total nanoeukaryotes in the hypolimnion. The highest abundance of

[4]www.r-project.org

kinetoplastids was detected from the hypolimnion of Lake Biwa with the maximum abundance of 9.3×10^2 cells ml^{-1} at 70 m, contributing up to 54% of total nanoeukaryotes. Similarly, the abundance of kinetoplastids in the hypolimnion of Lake Ikeda was 2.3×10^2 cells ml^{-1} at 50 m and 2.0×10^2 cells ml^{-1} at 70 m, contributing up to 32 and 36% of total nanoeukaryotes, respectively. The maximum abundance of kinetoplastids in the hypolimnion of other lakes was 2.4×10^2 cells ml^{-1} (31% of total nanoeukaryotes) in Lake Chuzenji, 1.5×10^2 cells ml^{-1} (18% of total nanoeukaryotes) in Lake Sai and 9.1×10^1 cells ml^{-1} (19% of total nanoeukaryotes) in Lake Motosu.

Diversity of Kinetoplastid and Other Euglenozoan Flagellates

A total of 9610 raw reads were obtained with the universal eukaryote primers, from which 7946 sequences remained after quality filtration. Various group of microbial eukaryotes were detected using the universal primers, where Cryptophyta and Dinophyta dominated the epilimnion and hypolimnion communities, respectively, in all the lakes based on the sequence abundance (**Figure 3A**). However, the major groups were evenly distributed in each lake based on the number of OTUs observed in each group (**Figure 3B**). Several OTUs specific to epilimnion and hypolimnion with a significant contribution were also detected. Although they had a high abundance, no sequences affiliated to kinetoplastids were detected from any lakes using the universal primers. However, kinetoplastids were readily detected from all the lakes using kinetoplastid-specific primers (**Figure 4**). Seven samples with kinetoplastid-specific primers produced 9017 raw reads, which yielded 7449 pyrotags after quality filtering. A total of 58 OTUs were obtained, where 17 OTUs were unique to each environment (**Table 2**). OTUs affiliated to eukaryotes other than the Euglenozoans, were not considered for further analysis. In the Shannon diversity index the highest diversity was observed in the epilimnion of Lake Biwa, followed by Lake Ikeda (**Table 2**). However, the richness (S.chao1) was the highest in the hypolimnion of Lake Biwa followed by the epilimnion of Lake Biwa (**Table 2**).

Six OTUs of kinetoplastids were obtained from the epilimnion sample, where the dominant OTU (OTU_5) was closely related to *Rhynchomonas nasuta* (**Figure 4** and **Supplementary Table S2**). Interestingly, the second dominant OTU was affiliated to *Diplonema* sp. (OTU_4), followed by OTU_3, which was closely related to *Azumiobodo hoyamushi*. OTU_15, which was closely related to *Neobodo designis* was only detected from the epilimnion of Lake Biwa, though it was not among the dominant representatives. Two samples were analyzed from the hypolimnion of Lake Biwa to understand the community of the dominant kinetoplastids. Both the samples representing 60 m from August and November showed high number of OTUs with 15 and 19 OTUs, respectively (**Table 2**). The kinetoplastid community in both the samples was similar with the dominant OTU (OTU_1) being closely related to *Bodo saltans* (**Figure 4** and **Supplementary Table S2**). The OTU affiliated to *Diplonema* sp. (OTU_4), which had a significant contribution in the epilimnion was also dominant in the hypolimnion community. Five out of the six epilimnion kinetoplastid OTUs were present in both the hypolimnion samples (**Figure 5**). Compared with the epilimnion OTUs, the hypolimnion showed a high number of unique OTUs with 3 in August and 10 in November. The dominant hypolimnion OTU (OTU_1), which contributed 78% and 82% of total sequences in August and November, was not detected from the epilimnion sample.

OTU_1 was also predominant in the hypolimnion of Lakes Chuzenji, Motosu and Sai (**Figure 4**), contributing 63%, 100% and 23% of total sequence abundance, respectively. However, this OTU was not detected in the hypolimnion of Lake Ikeda. The dominant OTU in the hypolimnion of Lake Ikeda (OTU_7) was closely related to *B. saltans*, contributing 34% of total sequence abundance. The OTU closely related to *Diplonema* sp., that was found in the epilimnion and hypolimnion of Lake Biwa was also detected in the hypolimnion of Lake Ikeda (OTU_4) with a significantly high contribution (25% of total sequence abundance). In phylogenetic analysis, the diplonemid OTU was separated from the marine clones and majority of the cultured diplonemids. However, this OTU was closely related to two diplonemid isolates from the sea around Japan (**Figure 6**). The Lake Biwa epilimnion kinetoplastid community had the closest similarity with the hypolimnion community of Lake Ikeda (**Figure 4**), though the similarity was low and the distance was high (**Supplementary Figure S2**). In contrast, the kinetoplastid community of the Lake Biwa hypolimnion showed a high similarity to the hypolimnion community of Lakes Chuzenji and Motosu (**Figure 4** and **Supplementary Figure S2**).

Presence of Ubiquitous and Unique OTUs in Each Lake

The most ubiquitous OTU in the present study was OTU_3, which was closely related to *Azumiobodo hoyamushi* and which was detected in all the samples, except for those from Lake Motosu (**Figure 4** and **Supplementary Table S2**). Another ubiquitous OTU (OTU_1), which was closely related to *Bodo saltans* was found in the hypolimnion of all the lakes, except for Lake Ikeda. Three out of the five lakes showed the presence of unique OTUs confined to each environment (**Table 2**), where the hypolimnion of Lake Biwa had the highest number of unique OTUs (**Table 2**). The exceptions were Lakes Sai and Motosu, which were inhabited by four and one kinetoplastid OTUs, respectively. The OTUs unique to Lake Biwa (the major ones-OTU_ 5, 10, 13 and 15), Lake Chuzenji (OTU_2) and Lake Ikeda (OTU_7 and 17) had significant contributions to the total kinetoplastid community (**Supplementary Table S2**). Moreover, several of these unique OTUs and also OTUs obtained from the hypolimnion of all the lakes had less similarity with the closest sequences in the database (**Supplementary Table S2**).

Oligotyping of the Dominant OTU

Oligotyping of OTU_1, which was dominant in the hypolimnion of four of the five studied lakes (**Figure 7A**), revealed five oligotypes (GA, G-, UA, AA and A-) (**Figure 7B** and

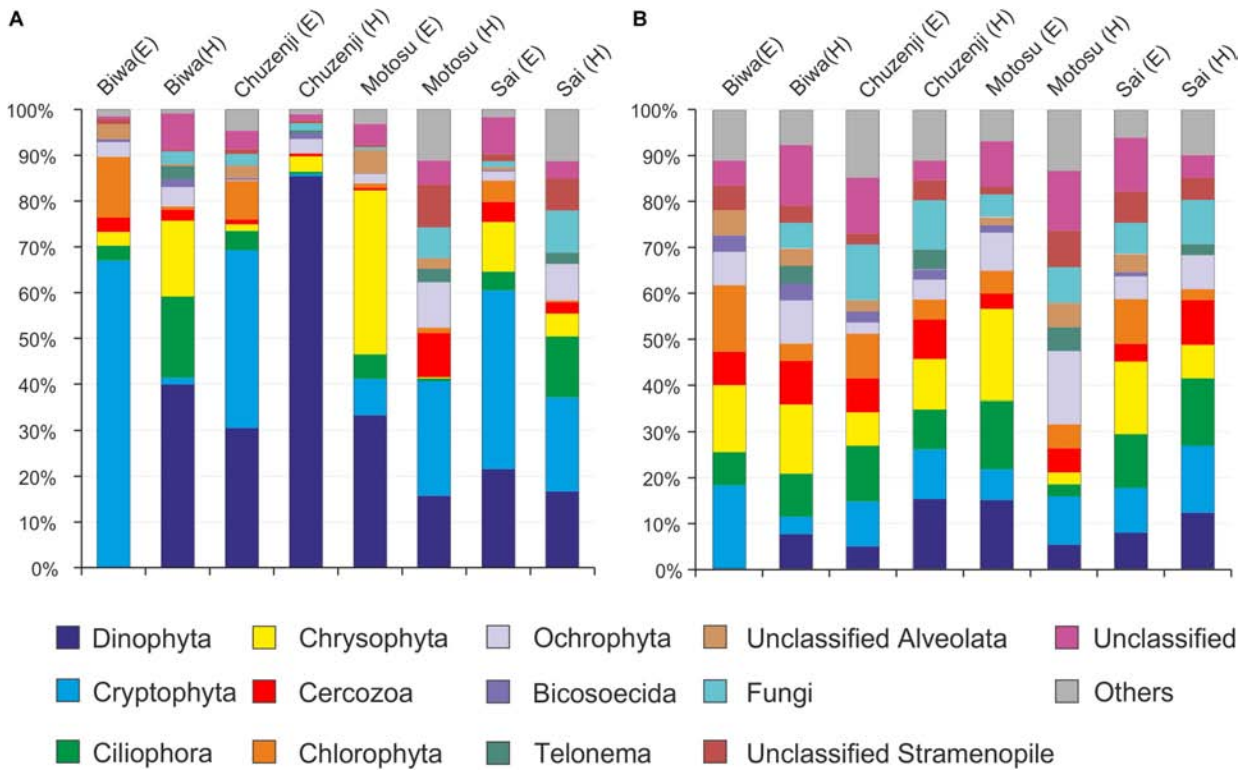

FIGURE 3 | Diversity of nanoeukaryotes in Japanese deep freshwater lakes using universal primers, **(A)** sequence abundance of each OTU and **(B)** OTU abundance (number of OTUs).

Supplementary Figure S3). Each lake consisted of three oligotypes, and the oligotype UA was found in all lakes. Lakes Biwa and Motosu shared the same oligotypes, with oligotype GA the dominant representative. Similarly, oligotypes of Lakes Chuzenji and Sai were the same with oligotype AA being the dominant representative.

DISCUSSION

The abundance of nanoeukaryotes in the studied lakes (**Figure 2B**) corroborates the results from studies of other deep lakes of the world (Lepère et al., 2010). However, the present study is the first to analyze the abundance and diversity of kinetoplastids in deep freshwater lakes to understand their importance in the hypolimnion waters, which will lead to understanding their ecological role in the freshwater food web. The results of the present study along with the previous studies show that kinetoplastids are important eukaryotes in the hypolimnion of freshwater lakes (Steinberg et al., 1983; Mukherjee et al., 2015), suggesting their importance in matter cycling in deep waters. The dominance of kinetoplastids in the oxygenated hypolimnion of Japanese deep lakes (**Figure 2C**) and kinetoplastid-like flagellates in some European deep lakes (Steinberg et al., 1983) indicate the possible dominance of this previously underestimated group in the deep freshwater lakes of the world.

Distribution of Kinetoplastid and Other Euglenozoan Flagellates in Deep Freshwater Lakes

The diversity of a particular group of flagellates is poorly understood and the present study is the first to understand the detailed diversity of a flagellate group using amplicon sequencing. The kinetoplastid communities in the hypolimnion were similar among all the lakes, except for Lake Ikeda (**Figure 4** and **Supplementary Figure S2**), probably due to the relatively warmer water in its hypolimnion (**Figure 2A**). The communities of the studied lakes were characterized by the presence of both ubiquitous and unique lake-specific OTUs (**Figure 4** and **Table 2**). Identical OTUs of eukaryotic microorganisms were reported from geographically distant sampling stations in oceans (Atkins et al., 2000; Massana et al., 2004). Moreover, dominant and identical kinetoplastid OTUs were also reported from the deep waters of geographically distant parts of the Atlantic Ocean as oceanic waters are interconnected and allow extensive gene flow (Salani et al., 2012) and also owing to the high dispersal potential of the microorganisms, which can overcome geographical and environmental barriers (Finlay, 2002). Even though freshwater lakes are isolated environments, the same genotype of flagellates was reported and isolated from freshwaters of geographically distant countries (Boenigk et al., 2005). Therefore, the presence of ubiquitous OTUs, with some dominant, in the hypolimnion of the studied lakes suggests that

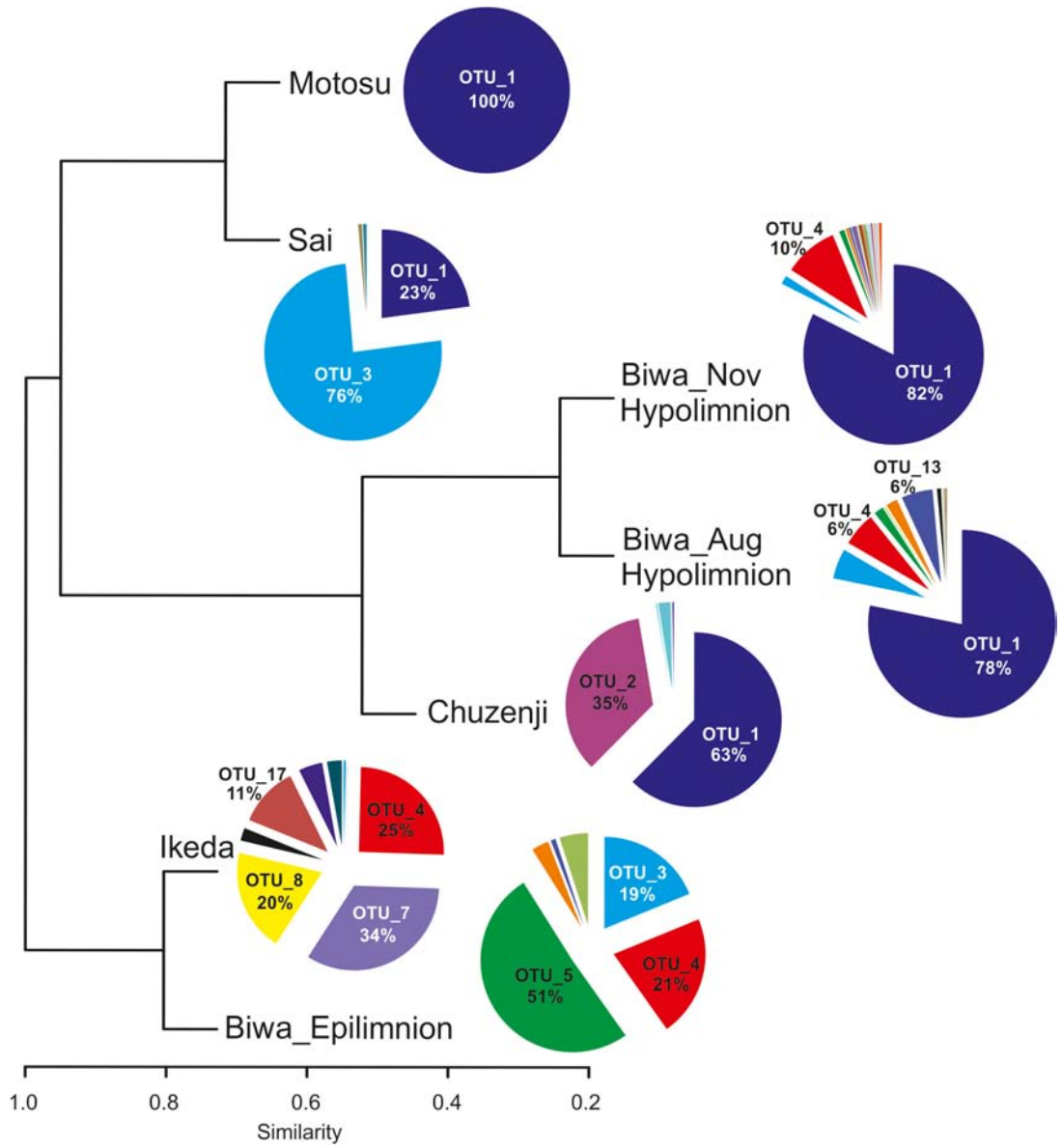

FIGURE 4 | Diversity of kinetoplastids and other euglenozoan flagellates in Japanese deep freshwater lakes using kinetoplastid-specific primers (based on sequence abundance of each OTU). The cluster dendrogram is based on a Bray-Curtis similarity matrix.

dispersal also play a major role in shaping the community of geographically distant freshwater lakes that have similar physico-chemical characteristics.

Detection of unique lake-specific OTUs (**Figure 4** and **Table 2**) was an interesting finding, as these OTUs were not minor taxa and had significant contribution to the kinetoplastid community. However, deeper sequencing and temporal data collection are necessary to conclude about their lake-specificity. Nevertheless, low similarity of these OTUs along with the other hypolimnion OTUs with the related sequences in the database (**Supplementary Table S2**) indicates that these taxa are potentially new. Near full-length sequences of the dominant hypolimnion kinetoplastids obtained from the present study using clone library analysis and Sanger sequencing, also showed low similarity with the closely related sequences in the database (data not shown).

Detection of one OTU of diplonemids from both Lake Biwa and Ikeda using kinetoplastid-specific primers reveal the close similarity between the two sister groups (Lukeš et al., 2005). No diplonemid OTU was detected using the universal eukaryote primers (**Figure 3**), indicating that the commonly used universal primers also underestimate diplonemids. Diplonemids are considered as marine flagellates (Lukeš et al., 2015; Tashyreva et al., 2018) and are especially associated with sediments (López-García et al., 2007). Recently, this group has attracted significant interest due to their high abundance and diversity in global oceans, especially in the deep waters (Lara et al., 2009;

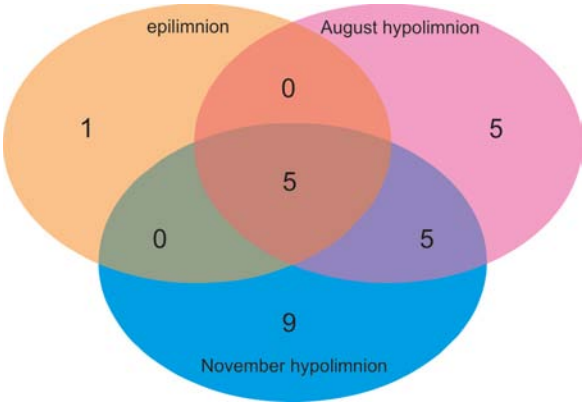

FIGURE 5 | Venn diagram showing the OTU sharing of kinetoplastid flagellates among the epilimnion and hypolimnion of Lake Biwa.

de Vargas et al., 2015; Flegontova et al., 2016). To the best of our knowledge, diplonemids are not reported from freshwaters and this is the first report on their presence in freshwater lakes. The diplonemid OTU of the present study has less similarity with the marine diplonemids, indicating that freshwater diplonemids are new (**Figure 6**). However, the relatively close similarity with two marine diplonemid isolates from sea around Japan indicates some evolutionary link between the freshwater and marine diplonemids, which are geographically closely distributed. The detection of diplonemids with a significant contribution in the freshwater lakes and their un-detection using universal eukaryote primers indicates their hidden distribution in freshwater deep lakes.

Dynamic Community Composition of Kinetoplastid Flagellates in Lake Biwa

Kinetoplastids were found to be dominant in the hypolimnion of Lake Biwa throughout the stratified period (Mukherjee et al., 2015). Although, the overall community in the two hypolimnion samples of Lake Biwa was similar (**Figure 4**), high OTU richness (**Table 2**) and the presence of several distinct OTUs showed a variation in the community composition among the less represented OTUs (**Figures 4**, **5**). A study from Lake Fuschlsee has also observed highly variable protist community compositions in the epilimnion, primarily due to the variations in the less represented taxa (Nolte et al., 2010). Flagellate communities in the hypolimnion are known to fluctuate based on the season (Mukherjee et al., 2017), and the fluctuations in the present study were also found within a single group in the stable hypolimnion waters. This indicates that due to the seasonal variation in the hypolimnion communities, the kinetoplastid communities in the studied lakes may also change, especially among the less represented members. Thus, seasonal changes in the individual communities must be studied to understand the community dynamics in more detail.

Intra-Diversity Within the Dominant OTU

Oligotyping has been conducted in environmental prokaryotic communities to understand the sequence variation within particular OTUs among different environments (Eren et al., 2013; Magnabosco et al., 2014; Newton and McLellan, 2015; Kleindienst et al., 2016; Okazaki et al., 2017). This is the first study in microbial eukaryotes to conduct oligotyping to reveal the intra-diversity within an OTU and their distribution in different lakes. We detected five oligotypes of the dominant hypolimnion OTU with shared and restricted representatives in particular lakes (**Figure 7**) indicating the role of both dispersal and local environmental conditions in sequence variation in deep waters. However, the distribution pattern of the oligotypes among the lakes hints at the possibility of environmental selection or geographic isolation in playing the major role in structuring the community of microbial eukaryotes, as the shared oligotype was not dominant and the dominant oligotypes were not shared among all the lakes. However, the reason behind the presence of similar oligotypes between Lakes Biwa-Motosu and Chuzenji-Sai is not clear. Nevertheless, intra-diversity within OTUs and their distribution pattern shows interesting information about the adaptation of oligotypes in different lakes, which are otherwise missed when only OTUs are considered. This pattern was well represented in freshwater bacterioplankton communities where oligotypes of ubiquitous bacterial lineages specific to each environment were present in eutrophic and oligotrophic waters (Newton and McLellan, 2015). Thus, oligotyping is an essential tool and more studies on microbial eukaryotes are needed to understand the intra-diversity within the OTUs of ubiquitous lineages from different trophic levels or from isolated environments or environments separated by geographic distance. In the present study oligotyping was conducted at OTU levels, separated at 97% cut-off. Although the cut-off was 97%, the similarity among the sequences in OTU1 (OTU used for oligotyping in the present study) was still more than 99% (the commonly used OTU level cutoff in microbial eukaryotic diversity studies).

Undetection of Euglenozoan Flagellates in Diversity Studies Using Universal Primers

Kinetoplastids were overlooked in clone libraries by commonly used universal eukaryote primers (Mukherjee et al., 2015), and in the present study these flagellates were also overlooked using amplicon sequencing with another commonly used universal eukaryote primer pair (Stoeck et al., 2010) (**Figure 3**). Therefore, the frequently used universal primers employed to study the diversity of microbial eukaryotes (Massana et al., 2015; Pernice et al., 2016) overlook an important group, irrespective of the sequencing platform used. Moreover, undetection of diplonemids in the present study by the universal primers indicate the underestimation of Euglenozoans in diversity studies worldwide due to their highly divergent 18S rRNA gene (Simpson et al., 2006; Bochdanksy and Huang, 2010; Mukherjee et al., 2015). A recent study has reported that similar to kinetoplastids, diplonemids also have mismatches in the conserved region of the 18S rRNA gene (Bochdansky et al., 2017). This indicates that the contributions of several important groups in the ecosystem

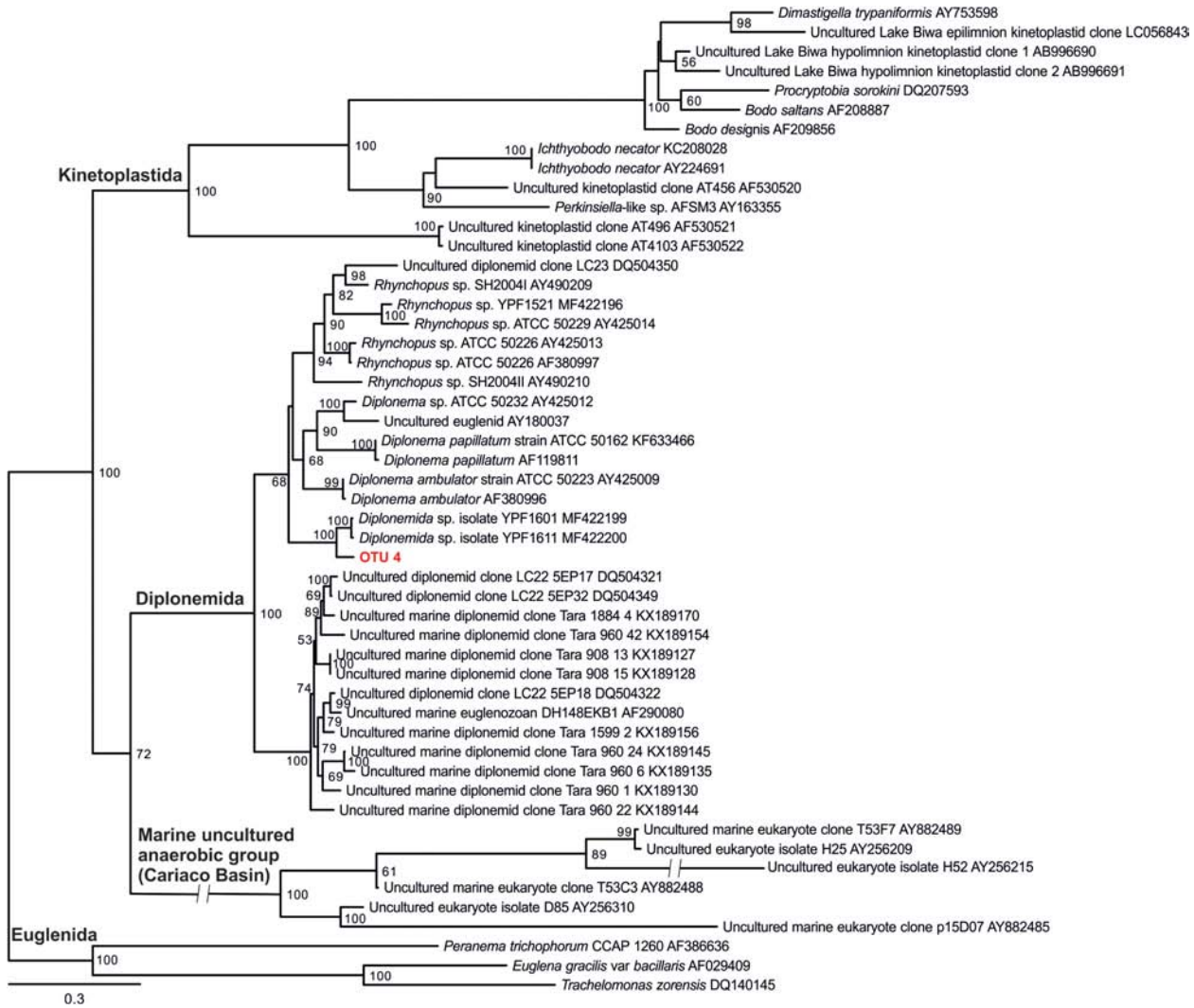

FIGURE 6 | 18s rRNA gene phylogenetic tree of diplonemid from freshwater deep lakes of Japan with 28 sequences of cultured and environmental sequences of marine diplonemids. The diplonemid OTU obtained from the present study (OTU 4) is highlighted in bold and red color. Kinetoplastids and other euglenozoan sequences were considered as outgroup. ML tree was inferred with standard bootstraps (-b 100). Scale bar = 0.3 substitution per site.

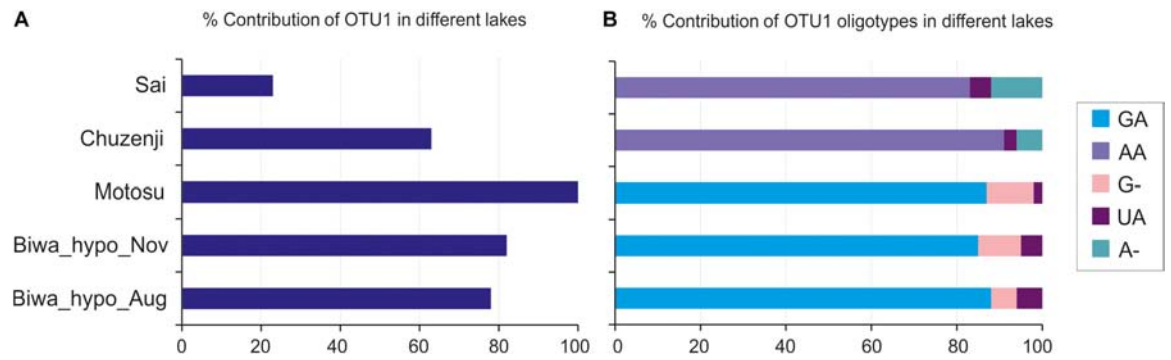

FIGURE 7 | Oligotyping of the dominant kinetoplastid OTU (OTU_1). **(A)** Percentage contribution of OTU_1 in the hypolimnion of studied lakes; **(B)** Percentage contribution of OTU_1 oligotypes. GA, AA, G-, UA and A- represent the detected oligotypes.

are overlooked owing to their underestimation by the universal primers. One of the limitations of the present study is that we could not collect seasonal samples from each lake to be able to understand the fluctuations in the community in detail. Thus, seasonal studies in particular groups should be conducted to understand the dynamics and importance of individual groups.

CONCLUSION

The use of 18S amplicon sequencing in the present study helped to unravel the detailed diversity of a dominant group of flagellates in various deep freshwater lakes. High diversity of a particular group and presence of oligotypes within an OTU suggest that flagellate communities are complex and more studies are required with a focus on individual groups. The results of the present study suggest the need for further studies to understand the probable dominance of these cosmopolitan flagellates in the hypolimnion of other deep lakes of the world. The complete ignorance of kinetoplastid flagellates with universal primers even with high amplicon sequencing indicates the global ignorance of an important group. Moreover, detection of diplonemids from freshwater lakes shows their presence in freshwaters and indicates the underestimation of euglenozoan flagellates in molecular diversity studies. Studies on particular groups are necessary due to the limitation of universal primers in being able to target phylogenetically diverse groups and also to understand the importance of individual groups to better understand the ecosystem processes.

DATA AVAILABILITY STATEMENT

The datasets generated for this study can be found in the DDBJ Sequence Read Archive (DRA) database, Bio-project accession number: PRJDB6819.

AUTHOR CONTRIBUTIONS

IM, YH, and S-iN contributed to conception and design of the study. IM, YH, SF, and KO conducted the sampling. IM conducted the experiments. YH and KO helped in some analysis. IM, YO, and SF processed and analyzed the data. IM drafted the manuscript. All authors contributed to critical revisions and approved the final version of the manuscript.

FUNDING

This work was funded by the Environmental Research and Technology Development Fund (Grant Number 5-1607) of the Ministry of the Environment, Japan and JSPS KAKENHI (Grant Number 17K19289). This work was also partly supported by KAKENHI, Grants-in-Aid for Scientific Research (Grant Number 19H03302) from the Japan Society for the Promotion of Science. IM was supported by the Monbukagakusho Scholarship provided by the Japanese Ministry of Education, Culture, Sports, Science and Technology.

ACKNOWLEDGMENTS

We are thankful to the captains of the research vessel 'Hasu,' the late T. Koitabashi and Dr. Y. Goda, and also Prof. M. Sugiyama and Prof. Y. Ito for their assistance during the sample collection. We are also thankful to Dr. T. Shabarova for her help with DCA analysis using Canoco v5.0 program.

SUPPLEMENTARY MATERIAL

The Supplementary Material for this article can be found online at: https://www.frontiersin.org/articles/10.3389/fmicb.2019.02375/full#supplementary-material

REFERENCES

Andrei, A. Ş, Salcher, M. M., Mehrshad, M., Rychtecký, P., Znachor, P., and Ghai, R. (2019). Niche-directed evolution modulates genome architecture in freshwater *Planctomycetes*. *ISME J.* 13, 1056–1071. doi: 10.1038/s41396-018-0332-5

Arndt, H., Dietrich, D., Auer, B., Cleven, E.-J., Gräfenhan, T., Weitere, M., et al. (2000). "Functional diversity of heterotrophic flagellates in aquatic ecosystems," in *The Flagellates: Unity, Diversity and Evolution*, eds B. S. C. Leadbeater, and J. C. Green, (London: Taylor and Francis), 240–268.

Atkins, M. S., Teske, A. P., and Anderson, O. R. (2000). A survey of flagellate diversity at four deep-sea hydrothermal vents in the eastern Pacific Ocean using structural and molecular approaches. *J. Eukaryot. Microbiol.* 47, 400–411. doi: 10.1111/j.1550-7408.2000.tb00067.x

Berney, C., Fahrni, J., and Pawlowski, J. (2004). How many novel eukaryotic 'kingdoms'? Pitfalls and limitations of environmental DNA surveys. *BMC Biol.* 2:13. doi: 10.1186/1741-7007-2-13

Bochdanksy, A. B., and Huang, L. (2010). Re-evaluation of the EUK516 probe for the domain eukarya results in a suitable probe for the detection of Kinetoplastids, an important group of parasitic and free-living flagellates. *J. Eukaryot. Microbiol.* 57, 229–235. doi: 10.1111/j.1550-7408.2010.00470.x

Bochdansky, A. B., Clouse, M. A., and Herndl, G. J. (2017). Eukaryotic microbes, principally fungi and labyrinthulomycetes, dominate biomass on bathypelagic marine snow. *ISME J.* 11, 362–373. doi: 10.1038/ismej.2016.113

Boenigk, J., and Arndt, H. (2000). Comparative studies on the feeding behavior of two heterotrophic nanoflagellates: the filter feeding choanoflagellate Monosiga ovata and the raptorial feeding kinetoplastid Rhynchomonas nasuta. *Aquat. Microb. Ecol.* 22, 243–249. doi: 10.3354/ame022243

Boenigk, J., Pfandl, K., Stadler, P., and Chatzinotas, A. (2005). High diversity of the 'Spumella−like'flagellates: an investigation based on the SSU rRNA gene sequences of isolates from habitats located in six different geographic regions. *Environ. Microbiol.* 7, 685–697. doi: 10.1111/j.1462-2920.2005.00743.x

Callieri, C., Hernández-Avilés, S., Salcher, M. M., Fontaneto, D., and Bertoni, R. (2015). Distribution patterns and environmental correlates of *Thaumarchaeota abundance* in six deep subalpine lakes. *Aquat. Sci.* 78, 215–225. doi: 10.1007/s00027-015-0418-3

Caron, D. A. (1987). Grazing of attached bacteria by heterotrophic microflagellates. *Microb. Ecol.* 13, 203–218. doi: 10.1007/BF02024998

Cavalier-Smith, T. (1981). Eukaryote kingdoms: seven or nine? *Biosystems* 14, 461–481. doi: 10.1016/0303-2647(81)90050-2

Cavalier-Smith, T. (2009). Kingdoms protozoa and chromista and the eozoan root of the eukaryotic tree. *Biol. Lett.* 6, 342–345. doi: 10.1098/rsbl.2009.0948

Chao, A., and Jost, L. (2012). Coverage-based rarefaction and extrapolation: standardizing samples by completeness rather than size. *Ecology* 93, 2533–2547. doi: 10.1890/11-1952.1

de Vargas, C., Audic, S., Henry, N., Decelle, J., Mahé, F., Logares, R., et al. (2015). Eukaryotic plankton diversity in the sunlit ocean. *Science* 348, 1–12. doi: 10.1126/science.1261605

Edgar, R. C. (2010). Search and clustering orders of magnitude faster than BLAST. *Bioinformat* 26, 2460–2461. doi: 10.1093/bioinformatics/btq461

Edgar, R. C. (2013). UPARSE: highly accurate OTU sequences from microbial amplicon reads. *Nat. Methods* 10, 996–998. doi: 10.1038/nmeth.2604

Edgar, R. C., Haas, B. J., Clemente, J. C., Quince, C., and Knight, R. (2011). UCHIME improves sensitivity and speed of chimera detection. *Bioinformat* 27, 2194–2200. doi: 10.1093/bioinformatics/btr381

Edgcomb, V. P., Orsi, W., Breiner, H. W., Stock, A., Filker, S., Yakimov, M. M., et al. (2011). Novel active kinetoplastids associated with hypersaline anoxic basins in the eastern Mediterranean deep-sea. *Deep Sea Res. I Oceanogr. Res. Pap.* 58, 1040–1048. doi: 10.1016/j.dsr.2011.07.003

Eren, A. M., Maignien, L., Sul, W. J., Murphy, L. G., Grim, S. L., Morrison, H. G., et al. (2013). Oligotyping: differentiating between closely related microbial taxa using 16S rRNA gene data. *Methods Ecol. Evol.* 4, 1111–1119. doi: 10.1111/2041-210X.12114

Finlay, B. J. (2002). Global dispersal of free-living microbial eukaryote species. *Science* 296, 1061–1063. doi: 10.1126/science.1070710

Flegontova, O., Flegontov, P., Malviya, S., Audic, S., Wincker, P., de Vargas, C., et al. (2016). Extreme diversity of *Diplonemid eukaryotes* in the Ocean. *Curr. Biol.* 26, 3060–3065. doi: 10.1016/j.cub.2016.09.031

Grossmann, L., Jensen, M., Heider, D., Jost, S., Glücksman, E., Hartikainen, H., et al. (2016). Protistan community analysis: key findings of a large-scale molecular sampling. *ISME J.* 10, 2269–2279. doi: 10.1038/ismej.2016.10

Guillou, L., Bachar, D., Audic, S., Bass, D., Berney, C., Bittner, L., et al. (2013). The protist ribosomal reference database (PR2): a catalog of unicellular eukaryote small sub-unit rRNA sequences with curated taxonomy. *Nucleic Acids Res.* 41, D597–D604. doi: 10.1093/nar/gks1160

Janouškovec, J., Tikhonenkov, D. V., Burki, F., Howe, A. T., Rohwer, F. L., Mylnikov, A. P., et al. (2017). A new lineage of eukaryotes illuminates early mitochondrial genome reduction. *Curr. Biol.* 27, 3717–3724. doi: 10.1016/j.cub.2017.10.051

Katoh, K., and Toh, H. (2010). Parallelization of the MAFFT multiple sequence alignment program. *Bioinformatics* 26, 1899–1900. doi: 10.1093/bioinformatics/btq224

Kleindienst, S., Grim, S., Sogin, M., Bracco, A., Crespo-Medina, M., and Joye, S. B. (2016). Diverse, rare microbial taxa responded to the deepwater horizon deep-sea hydrocarbon plume. *ISME J.* 10, 400–415. doi: 10.1038/ismej.2015.121

Lara, E., Moreira, D., Vereshchaka, A., and López-García, P. (2009). Pan−oceanic distribution of new highly diverse clades of deep−sea *Diplonemids*. *Environ. Microbiol.* 11, 47–55. doi: 10.1111/j.1462-2920.2008.01737.x

Lepère, C., Masquelier, S., Mangot, J. F., Debroas, D., and Domaizon, I. (2010). Vertical structure of small eukaryotes in three lakes that differ by their trophic status: a quantitative approach. *ISME J.* 4, 1509–1519. doi: 10.1038/ismej.2010.83

López-García, P., Philippe, H., Gail, F., and Moreira, D. (2003). Autochthonous eukaryotic diversity in hydrothermal sediment and experimental microcolonizers at the mid-atlantic ridge. *Proc. Natl. Acad. Sci. U.S.A.* 100, 697–702. doi: 10.1073/pnas.0235779100

López-García, P., Vereshchaka, A., and Moreira, D. (2007). Eukaryotic diversity associated with carbonates and fluid–seawater interface in lost city hydrothermal field. *Environ. Microbiol.* 9, 546–554. doi: 10.1111/j.1462-2920.2006.01158.x

Lukeš, J., Flegontova, O., and Horák, A. (2015). *Diplonemids*. *Curr. Biol.* 25, R702–R704. doi: 10.1016/j.cub.2015.04.052

Lukeš, J., Hashimi, H., and Zíková, A. (2005). Unexplained complexity of the mitochondrial genome and transcriptome in kinetoplastid flagellates. *Curr. Gen.* 48, 277–299. doi: 10.1007/s00294-005-0027-0

Magnabosco, C., Tekere, M., Lau, M. C., Linage, B., Kuloyo, O., Erasmus, M., et al. (2014). Comparisons of the composition and biogeographic distribution of the bacterial communities occupying South African thermal springs with those inhabiting deep subsurface fracture water. *Front. Microbiol.* 5:679. doi: 10.3389/fmicb.2014.00679

Massana, R., Castresana, J., Balagué, V., Guillou, L., Romari, K., Groisillier, A., et al. (2004). Phylogenetic and ecological analysis of novel marine stramenopiles. *Appl. Environ. Microbiol.* 70, 3528–3534. doi: 10.1128/aem.70.6.3528-3534.2004

Massana, R., Gobet, A., Audic, S., Bass, D., Bittner, L., Boutte, C., et al. (2015). Marine protist diversity in European coastal waters and sediments as revealed by high−throughput sequencing. *Environ. Microbiol.* 17, 4035–4049. doi: 10.1111/1462-2920.12955

Massana, R., Terrado, R., Forn, I., Lovejoy, C., and Pedrós-Alió, C. (2006). Distribution and abundance of uncultured heterotrophic flagellates in the world oceans. *Environ. Microbiol.* 8, 1515–1522. doi: 10.1111/j.1462-2920.2006.01042.x

Mehrshad, M., Salcher, M. M., Okazaki, Y., Nakano, S. I., Šimek, K., Andrei, A. S., et al. (2018). Hidden in plain sight-highly abundant and diverse planktonic freshwater Chloroflexi. *Microbiome* 6:176. doi: 10.1186/s40168-018-0563-8

Moon-van der Staay, S. Y., De Wachter, R., and Vaulot, D. (2001). Oceanic 18S rDNA sequences from picoplankton reveal unsuspected eukaryotic diversity. *Nature* 409, 607–610. doi: 10.1038/35054541

Moreira, D., and Lopez-Garcia, P. (2002). The molecular ecology of microbial eukaryotes unveils a hidden world. *Trend Microbiol.* 10, 31–38. doi: 10.1016/s0966-842x(01)02257-0

Moreira, D., Lopez-Garcia, P., and Vickerman, K. (2004). An updated view of kinetoplastid phylogeny using environmental sequences and a closer outgroup: proposal for a new classification of the class *Kinetoplastea*. *Int. J. Syst. Evol. Microbiol* 54, 1861–1875. doi: 10.1099/ijs.0.63081-0

Morgan-Smith, D., Herndl, G. J., van Aken, H. M., and Bochdansky, A. B. (2011). Abundance of eukaryotic microbes in the deep subtropical North Atlantic. *Aquat. Microb. Ecol.* 65, 103–115. doi: 10.3354/ame01536

Morgan-Smith, D., Clouse, M. A., Herndl, G. J., and Bochdansky, A. B. (2013). Diversity and distribution of microbial eukaryotes in the deep tropical and subtropical North Atlantic Ocean. *Deep Sea Res Pt I Oceanogr. Res. Pap.* 78, 58–69. doi: 10.1016/j.dsr.2013.04.010

Mukherjee, I., Hodoki, Y., and Nakano, S. (2015). Kinetoplastid flagellates overlooked by universal primers dominate in the oxygenated hypolimnion of Lake Biwa, Japan. *FEMS Microbiol. Ecol.* 91:fiv083. doi: 10.1093/femsec/fiv083

Mukherjee, I., Hodoki, Y., and Nakano, S. (2017). Seasonal dynamics of heterotrophic and plastidic protists in the water column of Lake Biwa, Japan. *Aquat. Microb. Ecol.* 80, 123–137. doi: 10.3354/ame01843

Newton, R. J., and McLellan, S. L. (2015). A unique assemblage of cosmopolitan freshwater bacteria and higher community diversity differentiate an urbanized estuary from oligotrophic Lake Michigan. *Front. Microbiol.* 6:1028. doi: 10.3389/fmicb.2015.01028

Nguyen, L. T., Schmidt, H. A., von Haeseler, A., and Minh, B. Q. (2014). IQ-TREE: a fast and effective stochastic algorithm for estimating maximum-likelihood phylogenies. *Mol. Biol. Evol.* 32, 268–274. doi: 10.1093/molbev/msu300

Nolte, V., Pandey, R. V., Jost, S., Medinger, R., Ottenwälder, B., Boenigk, J., et al. (2010). Contrasting seasonal niche separation between rare and abundant taxa conceals the extent of protist diversity. *Mol. Ecol.* 19, 2908–2915. doi: 10.1111/j.1365-294X.2010.04669.x

Okazaki, Y., Fujinaga, S., Tanaka, A., Kohzu, A., Oyagi, H., and Nakano, S. (2017). Ubiquity and quantitative significance of bacterioplankton lineages inhabiting the oxygenated hypolimnion of deep freshwater lakes. *ISME J.* 11, 2279–2293. doi: 10.1038/ismej.2017.89

Okazaki, Y., and Nakano, S. I. (2016). Vertical partitioning of freshwater bacterioplankton community in a deep mesotrophic lake with a fully oxygenated hypolimnion (Lake Biwa. Japan). *Environ. Microbiol. Rep.* 8, 780–788. doi: 10.1111/1758-2229.12439

Oksanen, J., Blanchet, F. G., Kindt, R., Legendre, P., Minchin, P. R., O'Hara, R. B., et al. (2013). *Package 'vegan'. Community Ecology Package, Version 2.20*

Patterson, D. J., and Larsen, J. (1991). *Biology of Free-Living Heterotrophic Flagellates*. New York, NY: Oxford University Press.

Pernice, M. C., Giner, C. R., Logares, R., Perera-Bel, J., Acinas, S. G., Duarte, C. M., et al. (2016). Large variability of bathypelagic microbial eukaryotic communities across the world's oceans. *ISME J.* 10, 945–958. doi: 10.1038/ismej.2015.170

Porter, K. G., and Feig, Y. S. (1980). The use of DAPI for identifying and counting aquatic microflora. *Limnol. Oceanogr.* 25, 943–948. doi: 10.4319/lo.1980.25.5.0943

Pruesse, E., Peplies, J., and Glöckner, F. O. (2012). SINA: accurate high-throughput multiple sequence alignment of ribosomal RNA genes. *Bioinformatics* 28, 1823–1829. doi: 10.1093/bioinformatics/bts252

R Development Core Team (2013). *R: A Language and Environment for Statistical Computing*. Vienna: R Development Core Team.

Salani, F. S., Arndt, H., Hausmann, K., Nitsche, F., and Scheckenbach, F. (2012). Analysis of the community structure of abyssal kinetoplastids revealed similar communities at larger spatial scales. *ISME J.* 6, 713–723. doi: 10.1038/ismej.2011.138

Scheckenbach, F., Wylezich, C., Weitere, M., Hausmann, K., and Arndt, H. (2005). Molecular identity of strains of heterotrophic flagellates isolated from surface waters and deep-sea sediments of the South Atlantic based on SSU rDNA. *Aquat. Microb. Ecol.* 38, 239–247. doi: 10.3354/ame038239

Simpson, A. G. B., Stevens, J. R., and Lukeš, J. (2006). The evolution and diversity of kinetoplastid flagellates. *Trends Parasitol.* 22, 168–174. doi: 10.1016/j.pt.2006.02.006

Steinberg, V. C., Lenhart, B., and Klee, R. (1983). Bemerkungen zur okologie eines farblosen phytoflagellaten, *Phyllomitus apiculatus* Skuja (1948), *Cryptophyceae*. *Arch. Protistenk* 127, 307–317. doi: 10.1016/s0003-9365(83)80025-6

Stoeck, T., Bass, D., Nebel, M., Christen, R., Jones, M. D., Breiner, H.-W., et al. (2010). Multiple marker parallel tag environmental DNA sequencing reveals a highly complex eukaryotic community in marine anoxic water. *Mol. Ecol.* 19, 21–31. doi: 10.1111/j.1365-294X.2009.04480.x

Strassert, J. F., Jamy, M., Mylnikov, A. P., Tikhonenkov, D. V., and Burki, F. (2019). New phylogenomic analysis of the enigmatic phylum telonemia further resolves the eukaryote tree of life. *Mol. Biol. Evol.* 36, 757–765. doi: 10.1093/molbev/msz012

Tashyreva, D., Prokopchuk, G., Yabuki, A., Kaur, B., Faktorová, D., Votýpka, J., et al. (2018). Phylogeny and morphology of new *Diplonemids* from Japan. *Protist* 169, 158–179. doi: 10.1016/j.protis.2018.02.001

Ter Braak, C. J. F., and Smilauer, P. (2012). *Canoco Reference Manual and User's Guide: Software for Ordination, Version 5.0*. Ithaca, NY: Microcomputer Power, 496.

Urbach, E., Vergin, K. L., Young, L., Morse, A., Larson, G. L., and Giovannoni, S. J. (2001). Unusual bacterioplankton community structure in ultra-oligotrophic crater Lake. *Limnol. Oceanogr.* 46, 557–572. doi: 10.4319/lo.2001.46.3.0557

Vaerewijck, M. J. M., Sabbe, K., Baré, J., and Houf, K. (2008). Microscopic and molecular studies of the diversity of free-living protozoa in meat-cutting plants. *Appl. Environ. Microbiol.* 74, 5741–5749. doi: 10.1128/AEM.00980-08

Vickerman, K. (1976). "The Diversity of the Kinetoplastid Flagellates," In *Biology of the Kinetoplastida,* W.H.R Lumsden, and D.A. Evans, (London: Academic Press), 1–34, vol. 1.

Vlcek, C., Marande, W., Teijeiro, S., Lukeš, J., and Burger, G. (2010). Systematically fragmented genes in a multipartite mitochondrial genome. *Nucleic Acids Res.* 39, 979–988. doi: 10.1093/nar/gkq883

Von der Heyden, S., and Cavalier-Smith, T. (2005). Culturing and environmental DNA sequencing uncover hidden kinetoplastid biodiversity and a major marine clade within ancestrally freshwater Neobodo designis. *Int. J. Syst. Evol. Microbiol.* 55, 2605–2621. doi: 10.1099/ijs.0.63606-0

Zubkov, M. V., and Sleigh, M. A. (2000). Comparison of growth efficiencies of protozoa growing on bacteria deposited on surfaces and in suspension. *J. Eukaryot. Microbiol.* 47, 62–69. doi: 10.1111/j.1550-7408.2000.tb00012.x

Conflict of Interest: The authors declare that the research was conducted in the absence of any commercial or financial relationships that could be construed as a potential conflict of interest.

Copyright © 2019 Mukherjee, Hodoki, Okazaki, Fujinaga, Ohbayashi and Nakano. This is an open-access article distributed under the terms of the Creative Commons Attribution License (CC BY). The use, distribution or reproduction in other forums is permitted, provided the original author(s) and the copyright owner(s) are credited and that the original publication in this journal is cited, in accordance with accepted academic practice. No use, distribution or reproduction is permitted which does not comply with these terms.

frontiers in Microbiology

ORIGINAL RESEARCH
published: 16 October 2019
doi: 10.3389/fmicb.2019.02359

Annual Protist Community Dynamics in a Freshwater Ecosystem Undergoing Contrasted Climatic Conditions: The Saint-Charles River (Canada)

Perrine Cruaud[1,2,3], Adrien Vigneron[1,4,5], Marie-Stéphanie Fradette[1,2,3], Caetano C. Dorea[6], Alexander I. Culley[1,2,7], Manuel J. Rodriguez[3,8] and Steve J. Charette[1,2,9]*

[1] Institut de Biologie Intégrative et des Systèmes, Université Laval, Québec City, QC, Canada, [2] Département de Biochimie, de Microbiologie et de Bio-Informatique, Faculté des Sciences et de Génie, Université Laval, Québec City, QC, Canada, [3] CRAD, Université Laval, Québec City, QC, Canada, [4] Centre D'Études Nordiques, Université Laval, Québec City, QC, Canada, [5] Département de Biologie, Université Laval, Québec City, QC, Canada, [6] Department of Civil Engineering, University of Victoria, Victoria, BC, Canada, [7] Groupe de Recherche en Ecologie Buccale, Faculté de Médecine Dentaire, Université Laval, Québec City, QC, Canada, [8] École Supérieure D'aménagement du Territoire et de Développement Régional (ESAD), Université Laval, Québec City, QC, Canada, [9] Centre de Recherche de l'Institut Universitaire de Cardiologie et de Pneumologie de Québec, Québec City, QC, Canada

OPEN ACCESS

Edited by:
Haihan Zhang,
Xi'an University of Architecture and Technology, China

Reviewed by:
Jean-François Mangot,
Spanish National Research Council (CSIC), Spain
Thorsten Stoeck,
University of Kaiserslautern, Germany

***Correspondence:**
Perrine Cruaud
perrine.cruaud@gmail.com

Specialty section:
This article was submitted to Aquatic Microbiology, a section of the journal Frontiers in Microbiology

Received: 09 April 2019
Accepted: 27 September 2019
Published: 16 October 2019

Citation:
Cruaud P, Vigneron A, Fradette M-S, Dorea CC, Culley AI, Rodriguez MJ and Charette SJ (2019) Annual Protist Community Dynamics in a Freshwater Ecosystem Undergoing Contrasted Climatic Conditions: The Saint-Charles River (Canada). Front. Microbiol. 10:2359. doi: 10.3389/fmicb.2019.02359

Protists are key stone components of aquatic ecosystems, sustaining primary productivity and aquatic food webs. However, their diversity, ecology and structuring factors shaping their temporal distribution remain strongly misunderstood in freshwaters. Using high-throughput sequencing on water samples collected over 16 different months (including two summer and two winter periods), combined with geochemical measurements and climate monitoring, we comprehensively determined the pico- and nanoeukaryotic community composition and dynamics in a Canadian river undergoing prolonged ice-cover winters. Our analysis revealed a large protist diversity in this fluctuating ecosystem and clear seasonal patterns demonstrating a direct and/or indirect selective role of abiotic factors, such as water temperature or nitrogen concentrations, in structuring the eukaryotic microbial community. Nonetheless, our results also revealed that primary productivity, predatory as well as parasitism lifestyles, inferred from fine phylogenetic placements, remained potentially present over the annual cycle, despite the large seasonal fluctuations and the remodeling of the community composition under ice. In addition, potential interplays with the bacterial community composition were identified supporting a possible contribution of the bacterial community to the temporal dynamics of the protist community structure. Our results illustrate the complexity of the eukaryotic microbial community and provide a substantive and useful dataset to better understand the global freshwater ecosystem functioning.

Keywords: microbial eukaryotes, protists, freshwater, river, seasonal cycles, winter, bacterial communities

INTRODUCTION

Eukaryotic microorganisms are widespread, diverse and involved in global functioning of ecosystems (Sherr and Sherr, 1988; Caron et al., 2009; Worden et al., 2015; Debroas et al., 2017). As primary producers, global consumers or prey for larger microbial grazers and metazoans, they represent a key link in aquatic food webs (Sherr and Sherr, 1988; Arndt, 1993; Premke and Arndt, 2000; Šlapeta et al., 2005). However, they have received less attention than prokaryotes in microbial ecology (Simon et al., 2015; Debroas et al., 2017) and their diversity has been generally less investigated in freshwaters than in oceans (Nolte et al., 2010; Debroas et al., 2017). Therefore, there is a gap in the current knowledge of the distribution, biodiversity and temporal dynamics of these microorganisms in freshwater environments (Triadó-Margarit and Casamayor, 2012).

From autotrophy (photosynthesizers) to heterotrophy (predators feeding on other eukaryotic or prokaryotic organisms, decomposers, saprophytes, and parasites of other organisms), through mixotrophy, protists cover multiple ecological roles in ecosystems (Arndt et al., 2000; Zubkov and Tarran, 2008). While it was commonly accepted that some eukaryotic phyla were strictly photosynthetic or phagotrophic, numerous studies have demonstrated that many groups are actually more flexible in their nutritional capabilities than initially thought (Laval-Peuto and Febvre, 1986; McManus and Fuhrman, 1986; Stoecker and Silver, 1987; McManus et al., 2018). For example, photosynthetic capability *via* endosymbiotic associations or chloroplast retention (uptake of chloroplast from their prey, or kleptoplasty) has been observed in a broad range of eukaryotic lineages, such as ciliates, that were previously associated with a phagotrophic non-photosynthetic lifestyle (Stoecker and Silver, 1987; Dolan, 1992; Johnson, 2011; McManus et al., 2018) or dinoflagellates (Minnhagen et al., 2008; Hansen et al., 2016). Likewise, the loss of chloroplasts by lineages within commonly accepted photosynthetic groups has also been detected, such as the *Paraphysomonas*-clade within *Chrysophyceae* (Stramenopiles) (Caron et al., 1999; Boenigk et al., 2005; Scoble and Cavalier-Smith, 2014; Grossmann et al., 2016). Mixotrophy, defined as the combination of phagotrophy and photosynthesis in an individual cell, is increasingly recognized as an important trophic mode among aquatic eukaryotes and is likely the rule rather than the exception in microbial food webs (Caron et al., 1999; Stoecker et al., 2017; McManus et al., 2018; Stoecker and Lavrentyev, 2018). In addition, bacterivorous eukaryotes do not feed equally on all microorganisms. Some of them are considered generalists, feeding on a broad range of prey, while others are specialists, feeding on a narrow range of species (Haraguchi, 2018). Thus, each phagotrophic eukaryotic species might have different prey preferences affecting the microbial assemblage differently (Massana et al., 2009). Moreover, growth, grazing and photosynthesis rates as well as prey preferences could be greatly modulated depending on environmental factors such as temperature (Wilken et al., 2013), light (Millette et al., 2017) and nutrient availability (Urabe et al., 1999; Kamjunke et al., 2006; Stoecker and Lavrentyev, 2018) or presence/absence of some microbial lineages (Terrado et al., 2017), adding a supplementary layer of complexity in microeukaryote ecology.

While amplicon sequencing and "omic" analyses allow the identification of prokaryotic microorganisms as well as their functional and nutritional capabilities which might explain temporal and spatial dynamics (Logares et al., 2014; Lima-Mendez et al., 2015; Salcher et al., 2015; Samad and Bertilsson, 2017; Vigneron et al., 2018, 2019; Cruaud et al., 2019), these analyses do not yet allow as easily the assignment of functional roles to complex eukaryotic communities. Over the past few years, increasing efforts have been made to understand their ecological roles using extensive genome-level description and single-cell sequencing revealing genomic elements associated with bacterivorous or photosynthetic lifestyles (Roy et al., 2014; Seeleuthner et al., 2018). However, these studies are still scarce and challenged by the high eukaryotic genome size that leads to highly fragmented assemblies and incomplete genomes (Seeleuthner et al., 2018). Therefore, the understanding of the temporal dynamics of eukaryotic microorganisms and the underlying environmental drivers remains a real challenge in environmental microbial ecology.

Previous studies on freshwater environments showed that seasonal cycles characterized by both abiotic and biotic disturbances may influence the protist community composition and more broadly control the structure of all biota (Kalff and Knoechel, 1978; Carrias et al., 1998; Lepère et al., 2006; Zhao et al., 2011; Sommer et al., 2012; Jones et al., 2013; Simon et al., 2015). For its part, the Plankton Ecology Group (PEG) model propose a standard template to describe the successive stages of the phytoplankton and zooplankton biomasses in lake ecosystems. It also indicates potential factors driving these seasonal successions and emphasizes that further investigations at finer taxonomical level are required to complete this model (Sommer et al., 1986, 2012). Study of the temporal dynamics of eukaryotic microbial community composition in freshwater ecosystems experiencing large fluctuations in environmental parameters, that lead to marked changes in populations, can therefore contribute to a better understanding of the mechanisms driving the dynamics of these communities.

The Saint-Charles River, located in Quebec, Canada, experiences contrasted seasons with long freezing winters and relatively short temperate summers (Cruaud et al., 2019) and might therefore represent an interesting environment to investigate microeukaryotic ecology in freshwaters. The harsh climatic conditions of the region have been shown to induce an annual cycle of bacterial communities in this river with rapid successions of bacterial lineages (Cruaud et al., 2019). Bacterial communities detected during the warm season (WS) were typical of other freshwater ecosystems with high proportions of *Limnohabitans* and *Actinobacteria*, such as *Sporichthyaceae* hgcI/acI lineages, which are frequently reported as prey for eukaryotes (Grujcic et al., 2018; Piwosz et al., 2018; Šimek et al., 2018). By contrast, the bacterial communities changed during winter, with a notable increase in proportions of potential gammaproteobacterial methanotrophs (Cruaud et al., 2019), revealing a deep modification of the microbial ecosystem, with potential consequences on aquatic food webs.

The present study is therefore the eukaryotic counterpart of the bacterial community analysis conducted in the Saint-Charles River (Cruaud et al., 2019) and aim to better understand the dynamics of eukaryotic microbial communities in freshwater ecosystems and the underlying mechanisms of the global functioning of this river.

With these objectives, we have monitored the changes in the community structure of pico- and nanoplanktonic protists (i.e., small microbial eukaryotes of 0.22–20 μm diameter) in the Saint-Charles River water samples collected over 16 different months (including two summer and two winter periods) using massive sequencing of the 18S rRNA gene (rDNA). We then examined these results in the light of environmental parameters, such as geochemical measurements and climate monitoring. After an overall analysis of the entire protist community structure, we focused on a subset of 25 dominant eukaryotic OTUs that explained most of the community variation across samples. We investigated in detail the dynamics and potential trophic modes of these protists using phylogenetic analyses and looked for interplays between eukaryotic, bacterial microbial communities and environmental parameters.

MATERIALS AND METHODS

Sampling Sites and Methods

The Saint-Charles River, a major drinking water source in the Quebec city region, is evenly fed by the Saint-Charles Lake and two main tributaries (Jaune and Nelson Rivers) (**Figure 1**). The river flow of the Saint-Charles River is mainly controlled by flood gates at the Saint-Charles Lake dam to ensure adequate supply for the Loretteville Drinking Water Treatment Plant (DWTP – Quebec city, 11 km downstream of the dam) and a minimum ecological flow in the river. The Saint-Charles Lake is stratified during summer and winter and mixed during fall and spring turnovers (Boulé et al., 2010). The lake is ice-covered during winter and usually ice-free after mid-April or early May, before the spring turnover (APEL, 2015). The Saint-Charles River water samples were collected weekly or bimonthly at the raw water intake of the Loretteville DWTP (**Figure 1**) from May 2016 to June 2017 with two additional sampling on 31 January and 12 February 2018, representing a total of 34 sampling dates. The part of the Saint-Charles River from the dam to the DWTP is a river of order 5, with an average width of 22 m and is characterized by numerous meanders and wetlands (Brodeur et al., 2009). Raw water was collected at the DWTP before any chemical or physical treatments excepted a coarse screening at the water collection point. Water incoming at the DWTP cover a large part of the river water column (∼2 m depth) and could be considered as a representative sample of the full river water column at this point. Water was collected directly in three different sterile and nucleic acid-free 4-liter Cubitainers™ (replicates) then transported at 4°C to the laboratory, and processed within 2 h. The sampling strategy and experimental procedures used in this study were detailed in the previous work focusing on the bacterial communities of the Saint-Charles River (Cruaud et al., 2019). Briefly, 400 mL of each Cubitainers™ were first passed through a 20 μm mesh and then filtered through a 3 μm pore-size polycarbonate membrane filter (*large pore-size filter*) in line with a 0.22 μm Sterivex™ unit (*small pore-size filter*). To evaluate replicability of the protocol, filtrations were carried out in duplicate per Cubitainers™, leading in total to 204 large and 204 small pore-size filters.

The environmental metadata associated with the samples, including details on the geochemistry and climatic conditions, were previously analyzed in Cruaud et al. (2019), where further information about the measurement procedures can be found. Briefly, during the sampling period (May 2016 – February 2018), the Saint-Charles River experienced large water temperature variations from 0.7°C to 21.7°C (**Figure 1** and **Supplementary Table S1**). Snow was on the ground from 19 November 2016 to 26 April 2017 and for the two sampling dates in January and February 2018 (turquoise arrow on **Figure 1** and **Supplementary Table S1**). The winter period was characterized by an increase in nitrogen and nitrates/nitrites concentrations, reaching 0.88 mg $N.L^{-1}$ and 0.58 mg $N.L^{-1}$ on 23 February 2017, respectively (**Supplementary Table S1**). The sampling period was characterized by some significant rainfall events during spring, summer and autumn. Both snowmelt and rainfall events usually led to an increase in the river flow and to the opening of the floodgates to prevent flooding of the lakefront. These events also led to a decrease in alkalinity and conductivity (**Supplementary Table S1**).

DNA Extraction, DNA Amplifications and Sequencing

For each sampling date, nucleic acids were extracted from two *large pore-size filters* and two *small pore-size filters* coming from two different Cubitainers™ using the AllPrep DNA/RNA mini kit (QIAGEN) with modifications, as described in Cruaud et al. (2017b, 2019), for a total of 136 DNA samples. Eukaryotic 18S rRNA genes (rDNA) were amplified and sequenced following a two-step PCR library preparation as detailed in Cruaud et al. (2017a). During the first PCR step, the V4 region of the eukaryotic 18S rDNA was amplified by PCR using primers E572F and E1009R (Comeau et al., 2011). PCR conditions were the same as in Cruaud et al. (2019) with 35 cycles of amplification and a hybridization temperature of 55°C. Illumina MiSeq adaptors and barcodes were subsequently added during the second PCR step, then PCR products were pooled, purified and paired-end sequenced on an Illumina MiSeq sequencer using a V3 MiSeq sequencing kit (2 × 300 bp) at the IBIS sequencing platform (Université Laval, Canada). The raw sequencing data have been submitted to the NCBI database under BioProject accession number PRJNA486319.

Sequencing Analyses

Sequence quality controls were performed on the raw sequence dataset with FastQC v0.11.5 (Andrews, 2012). Paired-end reads were merged using FLASH v2.2.00 (Magoč and Salzberg, 2011) with default parameters and extended maximum overlap length (300). Afterward, CUTADAPT v1.12 (Martin, 2011) was used to remove primers and filter out sequences shorter

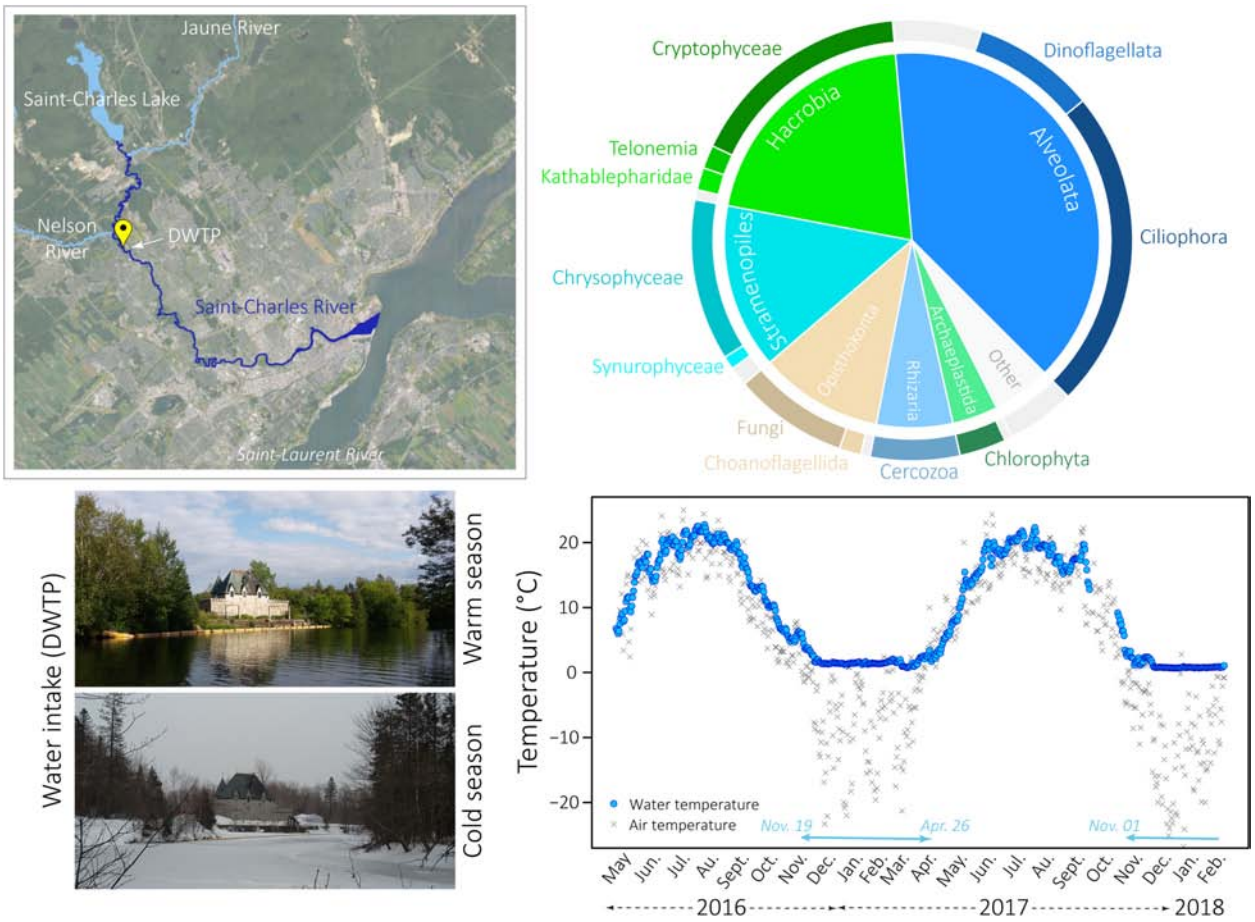

FIGURE 1 | Global eukaryotic microbial community in the Saint-Charles River. Top left: map of the Saint-Charles River showing the principal tributaries (Saint-Charles Lake and Jaune and Nelson Rivers) and the sampling location (DWTP) (QGIS software, v. 2.8.6-Wien, Geoindex + platform with geospatial data from Ville de Quebec held by the Library of the Université Laval). Bottom left: pictures of the Saint-Charles River taken at the sampling location during the warm and the cold season. Bottom right: daily measurements of air and water temperatures at the water intake from May 2016 to February 2018. Turquoise arrows at the bottom of the graph indicate the presence of snow on the ground. Top right: pie charts representing the average proportion of the main microbial eukaryotic communities detected in all samples.

than 350 bp. Sorted sequences were then dereplicated and clustered into Operational Taxonomic Units (OTUs, 97% similarity), then putative chimeric sequences and singletons were removed using VSEARCH v.2.3.4 (Rognes et al., 2016). Finally, taxonomic assignment of the reads was performed using the *Mothur* Bayesian classifier (Schloss et al., 2009), on the Protist Ribosomal Reference database (PR2, Version 4.10.0, March 2018,Guillou et al., 2013). Analysis scripts and documentations are available in a GitHub repository[1]. OTUs affiliated with *Bacteria*, *Archaea* or *Metazoa* were removed and results were normalized so that each sample contained the same number of sequences (5,053 normalized reads per sample corresponding to the lowest number of sequences in one sample for the large-pore size filters). Since eukaryotic communities from duplicate samples strongly clustered together in dendrogram analyses with Unweighted Pair Group Method with Arithmetic mean (UPGMA) (**Supplementary Figure S1**), an average relative proportion of each OTU was therefore calculated for each sampling date for the subsequent analyses.

Statistical Analyses

All statistical analyses (Bray–Curtis indexes, UPGMA, Non-metric MultiDimensional Scaling (NMDS) analyses, Non-Parametric Multivariate ANalysis Of VAriance (NP-MANOVA) Student *t*-tests and Pearson's correlation tables) were conducted using the software environment R (v. 3.4.4) and the RStudio toolkit (v.1.0.143) implemented with *Vegan* (Oksanen et al., 2007), *stringr* (Wickham, 2015), *dendextend* (Galili, 2015), *gplots* (Warnes et al., 2015), *plotrix* (Lemon, 2006), and *corrplot* (Wei et al., 2017) packages.

SIMilarity PERcentage analysis (SIMPER) was performed using the *Vegan* package on the entire OTU dataset, including sequences obtained from large and small pore-size filters. The

[1]https://github.com/CruaudPe/MiSeq_Multigenique

25 OTUs that explained the most of the dissimilarity observed between the eukaryotic community structures of cold and warm season samples were selected for further analyses.

Interplays among these 25 OTUs and between these 25 OTUs and the bacterial OTUs detected in proportions >1% for at least one sampling date in our previous study (Cruaud et al., 2019) were investigated using Pearson's correlation and local similarity (LS) analyses using the eLSA package (Ruan et al., 2006; Xia et al., 2011, 2016) with default parameters and no delay between sampling dates. While Pearson's correlation coefficients detect linear relationships between OTUs during the full sampling period, the LS method might capture non-linear associations, such as predator-prey interactions for which successive positive and negative covariance may exist over the course of the time (Ruan et al., 2006; Xia et al., 2011; Carr et al., 2019). Results were represented as networks using the software environment R implemented with the *igraph* package (Csardi and Nepusz, 2006). For both Pearson's correlation and LS networks, eukaryotic OTUs were defined as nodes and position of the nodes were determined using a same force-directed layout calculated with the Pearson's correlations (Fruchterman-Reingold layout algorithm, using the weight parameter defined with Pearson's correlation coefficient to increase the attraction/repulsion forces among nodes connected by higher coefficients). Connecting links (edges) represented the Pearson or LS scores with a p-value < 0.05. In addition, the bacterial OTUs sharing the highest Pearson and LS scores (p-value < 0.05) with eukaryotic OTUs (top 10 bacterial OTUs from both large and small pore-size filters) were represented around the eukaryotic networks. Correlations between two OTUs can indicate a predictive relationship that can be exploited whether or not these variables are causally related to one another. Thus, the results obtained through these analyses have to be interpreted with caution and were used in this study to search for hypothetical interactions, such as mutualism or competition, that might be experimentally tested in the future (Carr et al., 2019).

Phylogenetic Analyses

Five phylogenetic trees (for Stramenopiles, Cryptomonads, *Spirotrichea*, *Dinophyceae*, and *Perkinsea*) were constructed to assign a finer taxonomic affiliation than obtained with the comparison against PR2 database and to infer potential nutritional capabilities for the 25 OTUs selected by SIMPER analyses (**Supplementary Figures S2–S6**). Sequences were compared to the GenBank, EMBL, and DDBJ databases, using the NCBI BLAST search program (Altschul et al., 1990). A total of 453 sequences composed of BLAST hits of these OTUs, sequences from PR2 database and reference publications (>1,000 bp in length) (Shalchian-Tabrizi et al., 2008; Bråte et al., 2010b; Thamm et al., 2010; Remias et al., 2013; Fernandes et al., 2016; Piwosz et al., 2016) were downloaded and aligned with MAFFT 7.310 (Katoh and Standley, 2013). Sequences of the 25 selected OTUs were aligned with this reference alignment using the "-addfragments" options in the MAFFT package (Katoh and Frith, 2012). Phylogenetic trees were estimated using maximum likelihood methods performed with RAxML HPC v8 on XSEDE (CIPRES gateway) (Miller et al., 2010; Stamatakis, 2014), using a GTR model with among-site rate variation modeled by a discrete gamma approximation with four categories. GTRCAT approximation of models was used for ML bootstrapping (1,000 replicates). The phylogenetic trees were visualized and annotated according to reference publications and PR2 taxonomic affiliations using the iTOL online tool (Letunic and Bork, 2016). Sequences of these 25 OTUs were deposited in the GenBank nucleotide sequence database under accession numbers MK618733 – MK618757. Based on their phylogenetic proximity with known lineages and considering that proximity in biological evolution could potentially lead to similar trophic mode between organisms, we tentatively classified these OTUs into three potential nutritional strategies: phototrophy, heterotrophy and mixotrophy (**Supplementary Figures S2–S6** and **Supplementary Table S2**), with phototrophy including kleptoplasty, heterotrophy including grazing, predation and parasitism (the latter being distinguished from the heterotrophy in our figures) and mixotrophy gathering both phototrophy and heterotrophy in a same lineage. Since prediction of trophic modes based on 18S rRNA data can be challenging, only large categories of putative trophic modes were considered in this study.

RESULTS

Overall Protist Diversity and Community Composition

The protist diversity was characterized based on 18S rDNA amplicon sequencing from duplicate water samples collected on large (3 μm) and small (0.22 μm) pore-size filters over 2 years from the Saint-Charles River (**Figure 1**). We obtained a total of 611,413 quality-filtered reads (5,053 reads per sample) that grouped within 10,500 OTUs (97% similarity), with an average of 1,217 OTUs per sampling date. Most OTUs (98.2% of the OTUs) occurred at low abundance (<1% of the reads in all samples), however, predominant OTUs (>1% of the reads in at least one sample) represented the majority of sequences (73.8% of total sequences). Only 48 OTUs (0.5% of the OTUs) were highly abundant (>5% of the reads in at least one sample) representing on average 48.9% of the reads per sample.

Bray–Curtis dissimilarity indices (Bray and Curtis, 1957, ranging from 0: the two samples have the same microbial composition, to 1: the two samples do not share any OTU) were calculated between all pairs of samples. Based on these indices, UPGMA and NMDS analyses revealed a clear seasonal pattern (**Figure 2** and **Supplementary Figures S7, S8**). A significant difference of the eukaryotic community structure was detected between the cold and the WS (**Figure 2** and **Supplementary Figure S8**) (NP-MANOVA, p-value < 0.001) with 45.8 and 48.1% of the predominant OTUs that significantly differing between the two seasons, for the large and the small pore-size filters, respectively (t-test, p-value < 0.05). Only the samples collected on 08 November showed a divergent clustering between the large and the small pore-size filters (with the cold season (CS) for the large and with the WS for the small pore-size filters, **Supplementary Figure S7**). Thus, the samples collected from 24 May 2016 to 24 October 2016 and from 17 May 2017 to 15 June 2017 were thereafter referred as WS samples (water

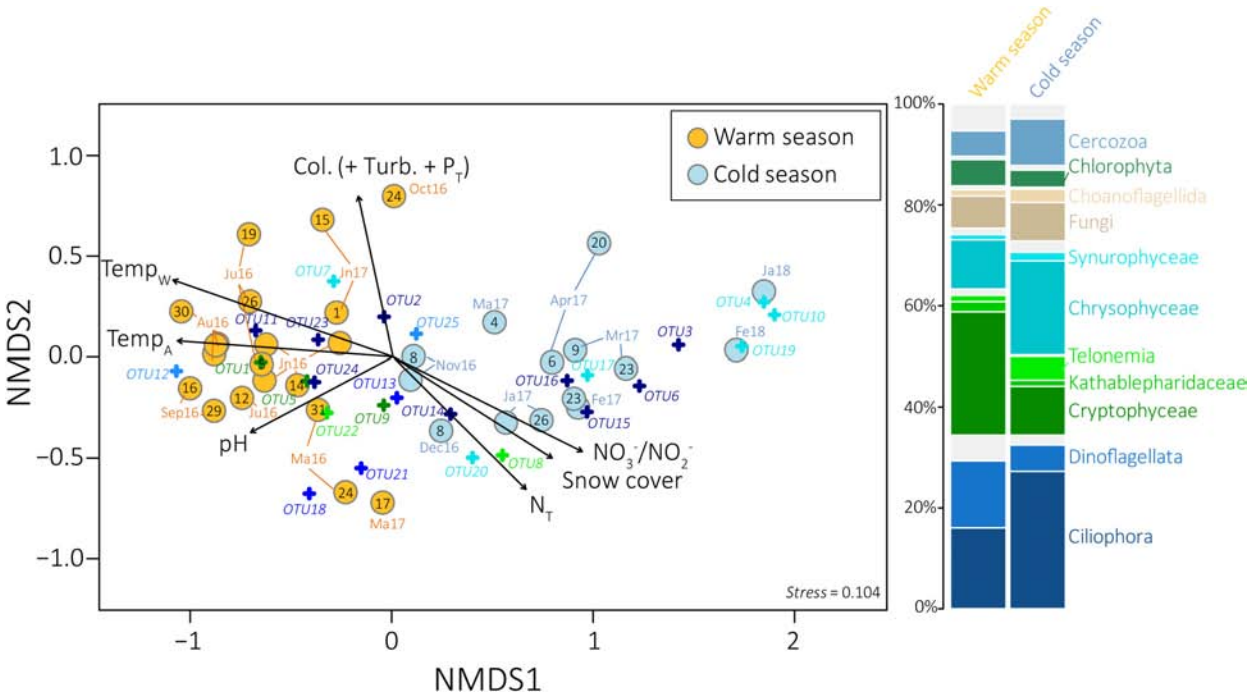

FIGURE 2 | Non-metric multidimensional scaling ordination plot derived from the Bray–Curtis dissimilarity measure between samples collected on the large pore-size filters. Seasons as defined in UPGMA dendrograms are indicated in yellow and blue for the warm and the cold season, respectively. Sampling dates are indicated in black. Fitted vectors (black arrows) were added to the ordinations for the most significant variables (*envfit*, p-value < 0.001). The length of the arrow is proportional to the correlation between ordination and environmental variable. The 25 eukaryotic OTUs selected by SIMPER analyses were also added to the ordination (cross). The stacked barplot on the right represents the average distribution of the main microbial eukaryotic communities detected in the samples collected during the warm (left) and the cold (rigth) season as defined by UPGMA dendrograms, for the large pore-size filters. P_T, Total phosphorus; Turb, Turbidity; Col, Apparent color; $Temp_W$, Water temperature; $Temp_A$, Air temperature; N_T, Total nitrogen, Mr, March; Ma, May; Jn, Juni; Jl, July.

temperature > 8°C, **Supplementary Table S1**), whereas the samples collected from 21 November 2016 to 04 May 2017 and the two sampling dates from January and February 2018 were associated to CS samples (**Supplementary Figure S7**, water temperature < 8°C). Bray–Curtis indices ranged from 0.98 between winter (31/01/2018) and summer (12/07/2016) samples to 0.33 between two summer samples (09/008/2016 and 16/08/2016) with an average of 0.75 over the year.

Ordination analyses of the eukaryotic community composition with environmental vector fitting suggest that water temperature and covarying factors, including air temperature, snow cover and nitrogen concentrations, as well as pH, apparent color, turbidity and phosphorus concentrations were among the main drivers of the community structure detected throughout the year (envfit, goodness of fit statistic r^2 = 0.86 for water temperature, 0.67 for air temperature, 0.61 for snow cover, 0.47 for nitrogen concentrations, 0.44 for pH, 0.42 for apparent color, 0.39 for phosphorus concentrations and 0.38 for turbidity, p-value < 0.001, **Figure 2**, **Supplementary Figure S8**, and **Supplementary Table S1**).

Overall, Alveolates (mainly *Ciliophora*, *Dinoflagellata*, and *Perkinsea*), *Hacrobia* (mainly *Cryptophyceae*, *Telonemia* and *Katablepharidophyta*), Stramenopiles (mainly *Chrysophyceae* and *Synurophyceae*), *Opisthokonta* (mainly *Fungi*), *Rhizaria* (mainly *Cercozoa*), and *Archaeplastida* (mainly *Chlorophyta*) were the most predominant groups detected in our samples, both on the large and the small pore-size filters (**Figure 1**). Higher proportions of *Ciliophora* and *Telonemia* were detected during the CS (**Figure 2** and **Supplementary Figure S11**) (t-test, p-value < 0.005, 27.2% in CS vs. 16.0% in WS and 4.6% in CS vs. 1.2% in WS, respectively, for the large pore-size filters, and 44.4% in CS vs. 20.9% in WS and 7.5% in CS vs. 3.8% in WS, respectively, for the small pore-size filters). *Chrysophyceae* were also detected in higher proportions during the CS but the difference was not statistically significant (**Figure 2**, 18.6% vs. 9.8% for the large pore-size filters and 14.2% vs. 7.5% for the small pore-size filters). In contrast, *Cryptophyta* and *Dinoflagellata* were detected in higher proportions during the WS (**Figure 2** and **Supplementary Figure S1**, t-test, p-value < 0.005, 24.3% vs. 9.7% and 13.3% vs. 5.2%, respectively, for the large pore-size filters and 24.3% vs. 9.7% and 9.6% vs. 2.1%, respectively, for the small pore-size filters).

Large Versus Small Pore-Size Filters

Results obtained from the large and the small pore-size filters were quite similar (**Figures 2**, **3**, **Supplementary Figures S7–S10**, and **Supplementary Table S2**). Many published works considered eukaryotic cells smaller than 3 μm as important component of the eukaryotic community (e.g., Medlin et al., 2006; Newbold et al., 2012; Marquardt et al., 2016). However,

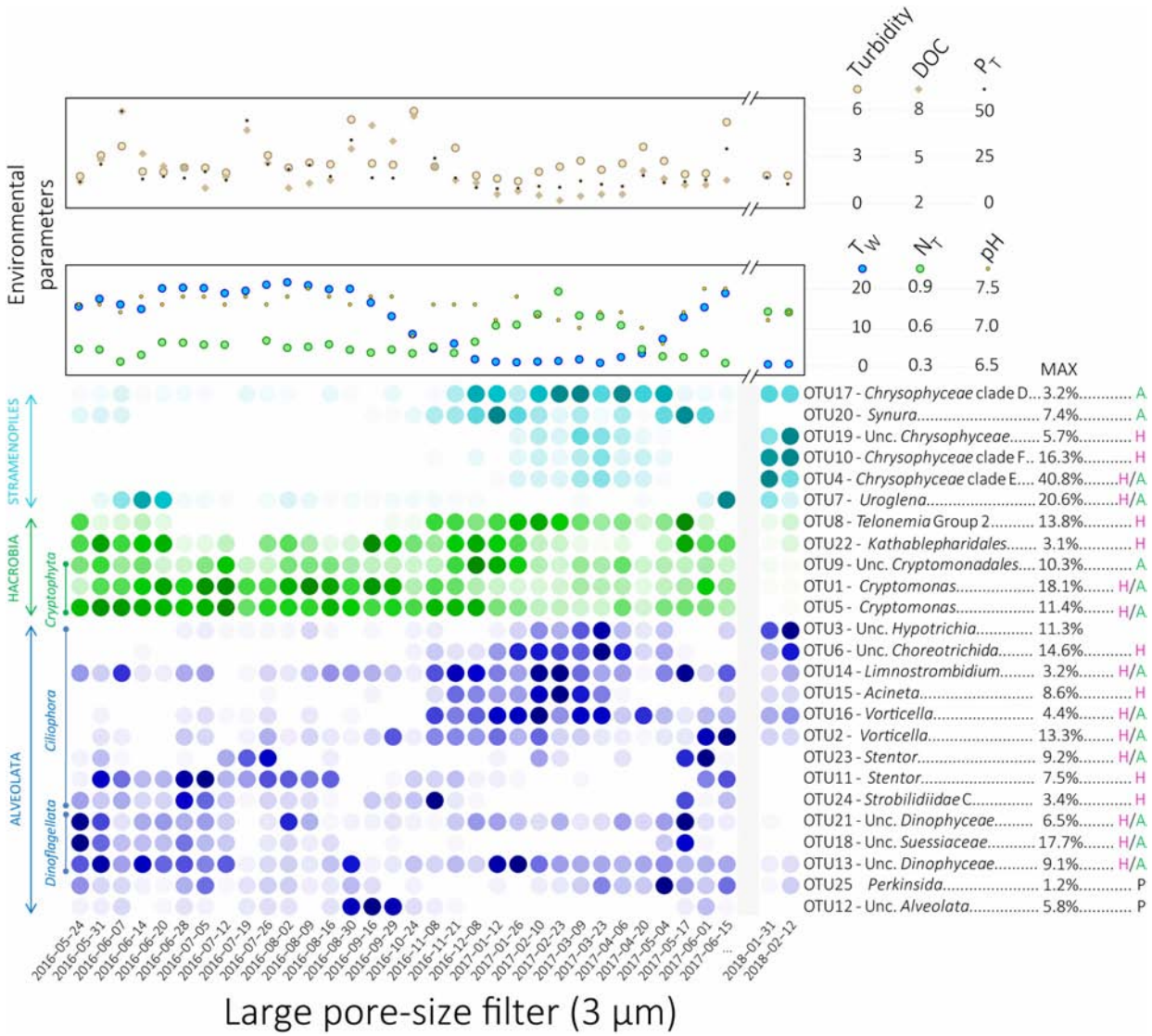

FIGURE 3 | Heatmap display of the relative proportions of the 25 OTUs selected by SIMPER analyses for the large pore-size filters. The color intensity represents the relative proportion of each OTU where dark colors represent high relative proportions and light colors represent low relative proportions. The darkest colors for the highest relative proportions were defined separately for each OTU. Letters to the right of OTU names represent potential nutritional capabilities for each OTU: green "A" for potential phototrophy, purple "H" for potential heterotrophy, "H/A" for potential mixotrophy and black "P" for potential parasitism. Variations of the environmental and physico-chemical parameters highlighted using *envfit* analyses for NMDS ordination are represented at the top of the heatmap. Unc, Unclassified; P_T, Total phosphorus, T_W, Water temperature; N_T, Total nitrogen.

a large number of sequences affiliated with organisms that are well known to be bigger than the pore-size of the large pore-size filters (e.g., ciliates and dinoflagellates) was detected on the small pore-size filters (0.2–3 µm). This observation could result from potential methodological bias maybe associated with filtration failures, although different bacterial communities were observed between small and large pore-size filters (Cruaud et al., 2019). It could also result from cell plasticity and disruption. Furthermore, low PCR amplifications and insufficient sequence numbers, leading to the removal of four samples from our datasets, were observed for the small pore-size filters. For these reasons, results from the two size fractions were not averaged or pooled to avoid assignment of the same weight for the large and the small pore-size filters in our dataset. Consequently, results for the small pore-size filters are presented as **Supplementary Files** (**Supplementary Figures S1, S7–S10**), while results for the large pore-size filters are presented in the main text.

Affiliations and Phylogenetic Placements of 25 Specific Protist OTUs

Based on SIMPER analyses, we identified 25 OTUs that explain most of the dissimilarity between seasons (39.4% of total number of sequences, cumulative contribution to the

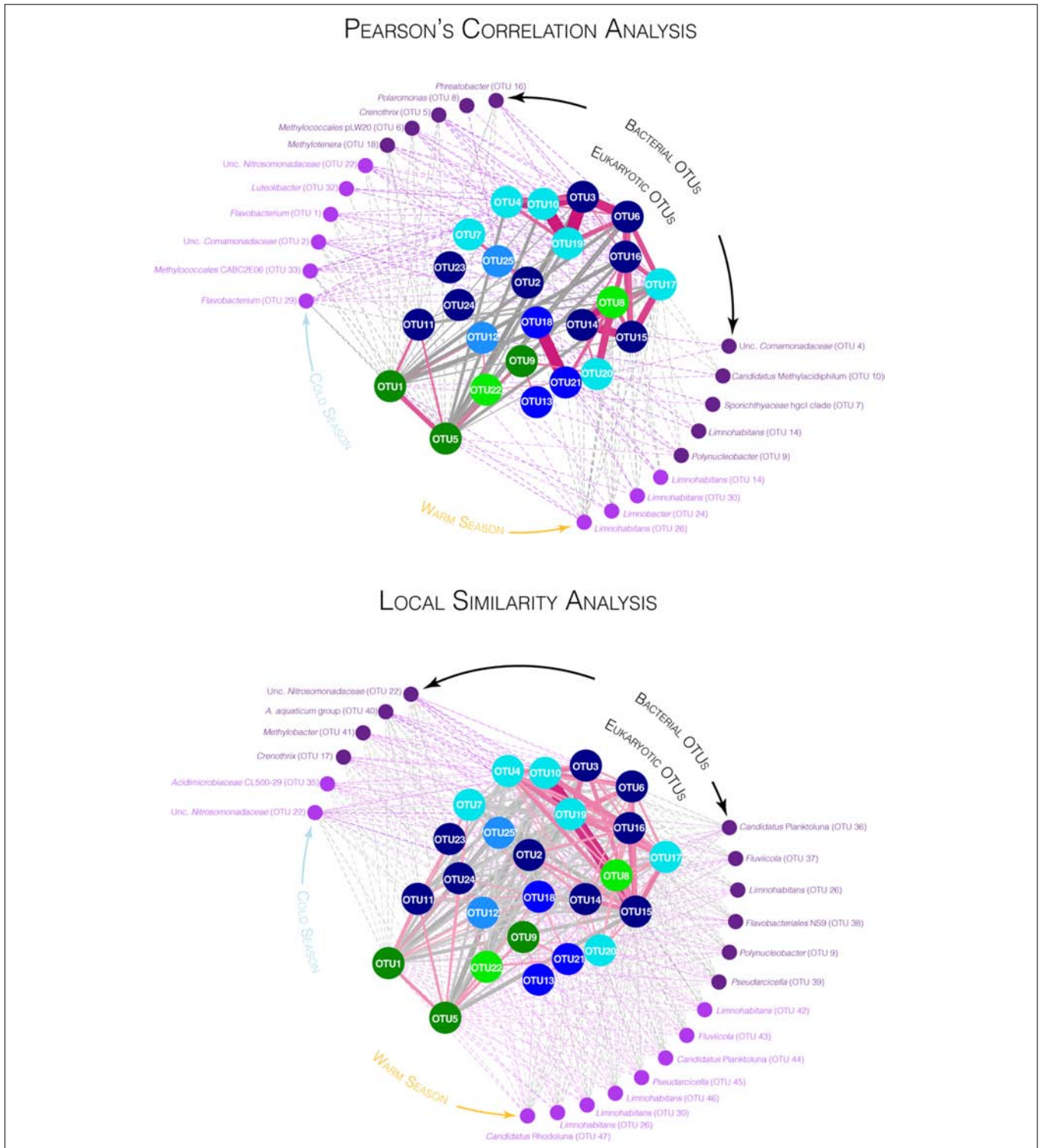

FIGURE 4 | Co-varying networks for the 25 OTUs selected by SIMPER analyses for the large pore size filters with bacterial OTUs detected on both large and small fractions. Networks were constructed based on the significant Pearson's correlation coefficients (PCC, top) and on the significant local similarity (LS) scores (bottom) between eukaryotic OTUs and between eukaryotic and bacterial OTUs (p-value < 0.05). Large nodes in the center of the networks represent eukaryotic OTUs (circle) with the same color code as in **Figure 3**. Small nodes at the periphery of the networks represent the top 10 bacterial OTUs detected on the large pore-size filters (dark purple) and the top 10 bacterial OTUs detected on the small pore-size filters (light purple) that shared the highest PCC (network on the top) or the highest LS scores (network on the bottom) with the 25 eukaryotic OTUs. Solid links (edges) represent correlation between eukaryotic OTUs and dashed links represent correlation between bacterial and eukaryotic OTUs. Pink links and gray links represent positive and negative correlations, respectively (darker and larger edges represent higher PCC or LS scores, detailed in **Supplementary Table S3**).

dissimilarity 38.6%). These OTUs, affiliated to Stramenopiles, *Hacrobia*, and *Alveolata*, were studied in detail (**Figures 3**, **4**, **Supplementary Figure S9**, and **Supplementary Table S2**). Phylogenetic trees (**Supplementary Figures S2–S6**) were used to (i) confirm taxonomic affiliations obtained with the PR2 database, (ii) identify phylogenetically close sequences and their isolation source, and (iii) to infer potential nutritional strategies depending on their phylogenetic placements.

Six OTUs affiliated with Stramenopiles were selected (**Supplementary Figure S2** and **Supplementary Table S2**). The OTUs 4, 7, 10, 17, and 19 were affiliated with *Chrysophyceae*. The OTU4 was close to the mixotrophic *Ochromonas tuberculata* (Bird and Kalff, 1986; Charvet et al., 2012; Stoecker and Lavrentyev, 2018) and the OTU7 was affiliated with the mixotroph *Uroglena americana* (Kimura and Ishida, 1985; Sandgren et al., 1995; Urabe et al., 1999) and formed a highly supported group with other sequences affiliated with *Uroglena* within the clade C of *Chrysophyceae*. The OTU10 was close to the colorless chrysomonads *Paraphysomonas* genus group (Caron et al., 1999; Scoble and Cavalier-Smith, 2014) and the OTU17 clustered with the *Hydrurus*-related algae (Klaveness and Lindstrøm, 2011; Remias et al., 2013) and other environmental clones isolated from high-mountain and arctic lakes in the *Hydrurus*-clade. Finally, the OTU19 formed a highly supported phylogenetic group with colorless *Spumella*-like flagellate JBC27 (Boenigk et al., 2005). Belonging to the *Synurophyceae*, the OTU20, affiliated with *Synura petersenii*, clustered with the highly supported group of the strict phototrophic *Synura* (Olefeld et al., 2018) (**Supplementary Figure S2** and **Supplementary Table S2**).

Five OTUs affiliated with *Hacrobia* were selected by SIMPER analyses (**Supplementary Figure S3** and **Supplementary Table S2**). Three OTUs were affiliated with *Cryptophyceae* (OTUs 1, 5, and 9), whereas one OTU was affiliated with *Telonemia* (OTU8) and another OTU with Kathablepharidales (OTU22). Two cryptophyte OTUs formed a highly supported group with the mixotrophic *Cryptomonas* (OTUs 1 and 5) (Tranvik et al., 1989; Choi et al., 2013). The third cryptophyte OTU, affiliated with unclassified *Cryptomonadales*, formed a highly supported phylogenetic group with potential phototrophic CRY2 lineage within the *Cryptophyceae* (OTU9) (Laza-Martínez et al., 2012). The OTU8 was affiliated with the heterotrophic predator lineage *Telonemia* (Klaveness et al., 2005; Bråte et al., 2010a) and the kathablepharid OTU22 formed a highly supported phylogenetic group with other uncultured freshwater eukaryotes within the kathablepharids, a group of predatory, heterotrophic biflagellates (Arndt et al., 2000) (**Supplementary Figure S3** and **Supplementary Table S2**).

Fourteen OTUs affiliated with *Alveolata* were selected (**Supplementary Figures S4–S6** and **Supplementary Table S2**). Nine OTUs were affiliated with *Ciliophora* (OTUs 2, 3, 6, 11, 14, 15, 16, 23, and 24), three were affiliated with *Dinoflagellata* (OTUs 13, 18, and 21), one was affiliated with *Perkinsida* (OTU25) and one OTU remained unclassified within the *Alveolata* (OTU12) according to the PR2 database. Among the *Ciliophora*, four OTUs were affiliated with *Spirotrichea* (OTUs 3, 6, 14, and 24). The OTU3 was affiliated with unclassified *Hypotrichia* and the OTU6 was affiliated with unclassified *Choreotrichida* [clustering with the highly supported group C of potential heterotrophs *Strobilidiidae* (Stoecker and Michaels, 1991)]. The OTU14, affiliated with *Limnostrombidium* within the *Strombidiida* lineage, might be able to switch from heterotrophy to phototrophy using ingested chloroplast (kleptoplasty (Stoecker and Silver, 1990; Dolan, 1992; Schoener and McManus, 2012). The last *Spirotrichea* OTU, the OTU24, grouped within the *Strobilidiidae* clade C composed of potentially heterotrophic lineages (Stoecker and Michaels, 1991) (**Supplementary Figure S4** and **Supplementary Table S2**). Two ciliates OTUs were affiliated with *Stentor*: the OTUs 11 and 23, close to *Stentor muelleri* and *Stentor* cf. *katashimai*, which are known to contain no symbiotic green algae (Gong et al., 2007; Thamm et al., 2010) (**Supplementary Table S2**). Two other ciliates OTUs, the OTU2, and the OTU16, were affiliated with potentially mixotrophic *Vorticella* (feeding on bacteria but usually containing *Chlorella*) (Dolan, 1992; Jacquet et al., 2005) (**Supplementary Table S2**). The last ciliate OTU, the OTU15, was affiliated with the potential heterotrophic *Acineta* (Dovgal and Pesic, 2007; Gazulha and Utz, 2016) (**Supplementary Table S2**). Among the OTUs affiliated with *Dinoflagellata*, the OTU18 was affiliated with unclassified *Suessiaceae* close to *Biecheleriopsis adriatica* while the OTU13 and the OTU21 were phylogenetically closed and affiliated with unclassified *Dinophyceae*. These OTUs were potential mixotrophic dinoflagellates (Hansen et al., 2007; Moestrup et al., 2009) (**Supplementary Figure S5** and **Supplementary Table S2**). The OTU25 was affiliated with *Perkinsida* within the PERK 12-17 clade among the parasitic lineage *Perkinsea* (Lepère et al., 2008; Bråte et al., 2010b; Chambouvet et al., 2014) (**Supplementary Figure S6** and **Supplementary Table S2**). Finally, the unclassified *Alveolata* OTU12 (based on PR2 database affiliation) shared 97% sequence similarity with sequences amplified from the oligo-mesotrophic Lake Pavin and identified as perkinsid based on Chambouvet et al. (2014). This OTU was thus included in the phylogenetic tree of perkinsid that confirmed its place close to the perkinsid OTU25 within the PERK12-17 clade (**Supplementary Figure S6** and **Supplementary Table S2**).

Temporal Variation of the 25 Selected Protist OTUs and Correlations With Biotic and Abiotic Factors

Temporal variations of the relative proportions of the 25 protist OTUs were analyzed in detail (**Figure 3** and **Supplementary Figure S9**). In addition, highest covariations between the relative proportions of these 25 OTUs based on Pearson's correlation and LS analyses were explored using networks (**Figure 4**, **Supplementary Figure S12**, and **Supplementary Table S3**). Correlations between relative proportions of eukaryotic and bacterial OTUs [details in Cruaud et al. (2019)] were also investigated and the highest correlations were represented on the same networks (**Figure 4**, **Supplementary Figure S13**, and **Supplementary Table S3**). Finally, correlations have been also searched between the 25 eukaryotic OTUs and environmental parameters (**Supplementary Figure S14**).

The eukaryotic OTUs were distributed in the networks according to a force-directed layout, clustering together the most

covariable OTUs (**Figure 4**). The OTUs 3, 4, 6, 8, 10, 14, 15, 16, 17, 19, and 20 were mainly detected during the CS while the other OTUs were detected throughout the year or mainly during the WS. Both the Pearson and the LS analyses showed higher covariation patterns between OTUs detected during the CS than between other OTUs. A larger number of significant correlations were detected with the LS analyses than with the Pearson's analyses (**Figure 4**) but some correlations detected with the Pearson analyses were also not identified with the LS analyses (**Figure 4**).

The *Chrysophyceae* OTU17 as well as the three *Ciliophora* OTUs 6, 15, and 16 were detected throughout the CS and showed similar pattern of variation (**Figures 2–4**, **Supplementary Figure S9**, and **Supplementary Table S3**). Covariations were detected between these eukaryotic OTUs and numerous bacterial OTUs detected during the CS such as *Crenothrix*, *Methylotenera*, unclassified *Comamonadaceae*, unclassified *Nitrosomonadaceae*, *Candidatus* Nitrotoga and *Methylococcales* pLW20 (**Figure 4**, **Supplementary Figure S13**, and **Supplementary Table S3**). These eukaryotic OTUs were positively correlated with environmental variables increasing during the winter season such as the snow cover and the nitrogen concentrations and were negatively correlated with environmental variables decreasing during the CS such as the air and the water temperatures (**Figure 2** and **Supplementary Figure S14**). Also mainly detected during the CS, relative proportions of the *Hypotrichia* OTU3 and the three *Chrysophyceae* OTUs 4, 10, and 19 showed similar variations reaching maximal proportions in March in winter 2017 and larger proportions during winter 2018 (up to 40.8% of the reads for the OTU4, **Figures 2–4**, **Supplementary Figures S9, S13,** and **Supplementary Table S3**). Covariations were detected with bacterial OTUs detected during the CS such as *Crenothrix*, *Methylococcales* CABC2E06, *Flavobacterium* or *Luteolibacter* (**Figure 4**, **Supplementary Figure S13,** and **Supplementary Table S3**). Although coefficients were lower, the eukaryotic OTUs 3, 4, 10, and 19 were also correlated with environmental variables that characterize the CS (**Figure 2** and **Supplementary Figure S14**). The *Telonemia* OTU8, the *Ciliophora* OTU14 and the *Synura* OTU20 also showed the highest proportions during the CS (**Figures 2, 3** and **Supplementary Figure S9**). However, these OTUs showed a slightly different pattern, reaching maximal proportions at the beginning of the CS as well as at the first date of the WS (17 May 2017, **Figures 3, 4** and **Supplementary Figures S9, S12**), sharing lower correlations with the bacterial OTUs detected during the CS (**Figure 4**, **Supplementary Figure S13**, and **Supplementary Table S3**). These three OTUs were slightly correlated with the environmental variables associated with the CS such as the decrease in temperatures and the increase in snow cover and nitrogen concentrations (**Figure 2** and **Supplementary Figure S14**). These three patterns (throughout the CS, higher proportions detected during the winter 2018 and beginning of the CS as well as the first date of the WS) were clearer on network build using Pearson's correlation analyses than using LS analyses where all eukaryotic OTUs detected during the CS were connected (**Figure 4**).

By contrast, covariations between the eukaryotic OTUs mainly detected during the WS were less obvious, each of them showing relatively different temporal patterns. Furthermore, only few correlations were detected with the environmental variables measured in this study (**Supplementary Figure S14**). Some of these eukaryotic OTUs (OTUs 1, 5, 11, 12, 18, and 21) were correlated with different bacterial OTUs mainly detected during the WS, such as *Sporichthyaceae* hgcI clade and *Limnohabitans* (**Figure 4**, **Supplementary Figure S13**, and **Supplementary Table S3**) The OTUs affiliated with *Cryptophyceae* and Katablepharidales (OTUs 1, 5, 9, and 22) were detected throughout the year but their relative proportions remained relatively low from February to May (**Figures 2–4** and **Supplementary Figure S9**). The *Cryptomonas* OTUs 1 and 5 were highly correlated with environmental parameters associated with the WS such as the increase in temperature and the decrease in snow cover (**Figure 2** and **Supplementary Figure S14**). The *Uroglena* OTU7 was the only OTU affiliated with Stramenopiles showing the highest relative proportions during the WS (**Figures 2, 3** and **Supplementary Figure S9**) but was also detected in significant proportions on 31 January 2018 (up to 12.35% for the small pore-size filters, **Figure 3** and **Supplementary Figure S9**). The distribution of the dinoflagellates OTUs 18 and 21 reached maximal relative proportions at the end of May (**Figure 3** and **Supplementary Figure S9**). These OTUs were highly correlated according to Pearson's correlation analyses, showing a global covariation along the entire time of our sampling period, while only a little correlation was found with the LS analyses, revealing different local dynamics (**Figure 4** and **Supplementary Table S3**), that preclude real relationship between these OTUs. In addition with the bacterial OTUs noted above, these two OTUs were correlated with a bacterial OTU affiliated with *Polynucleobacter* (**Figure 4**, **Supplementary Figure S13**, and **Supplementary Table S3**). The third dinoflagellate OTU (OTU13) fluctuated throughout the year (**Figure 3** and **Supplementary Figure S9**). The *Ciliophora* OTUs 2, 11, 23, and 24 showed higher relative proportions during the WS. Among them, the *Stentor* OTUs 11 and 23 reached maximal relative proportions at the beginning of the WS (May and June, **Figure 3** and **Supplementary Figure S9**) and the OTU11 was correlated with the increase in air and water temperatures (**Supplementary Figure S14**). The OTU24 reached maximal relative proportions on 28 June 2016 and high relative proportions on 08 November 2016 as well (**Figure 3** and **Supplementary Figure S9**). The *Perkinsida* OTU25 was detected intermittently throughout the year and mainly on the small pore-size filters with highest proportions on May 2017 (up to 12.6% on these filters, **Figure 3**, **Supplementary Figure S9**, and **Supplementary Table S2**). This OTU was highly correlated with a bacterial OTU affiliated with *Polaromonas* (**Figure 4**, **Supplementary Figure S13**, and **Supplementary Table S3**). This OTU was also correlated with the increase in river flow, the opening of the dam floodgates and the amount of rainfall 3 days before sampling (**Supplementary Figure S14**). Finally, the OTU12 was mainly detected on 3 sampling dates, in late summer 2016 (up to 19.8% for the small pore-size filters on 29 September, **Figure 3**, **Supplementary Figure S9**, and **Supplementary Table S2**) and was highly correlated with two bacterial OTUs mainly detected

during the WS and affiliated with *Sporichthyaceae* hgcI clade and *Candidatus* Methylacidiphilum (**Figure 4**, **Supplementary Figure S13**, and **Supplementary Table S3**) and with the increase of the dissolved organic carbon concentration in the water (**Supplementary Figure S14**).

DISCUSSION

Marked Seasonality of Overall Composition of Protist Communities

Using 18S rDNA sequencing, a high diversity of small eukaryotes was observed in the Saint-Charles River with members of all eukaryotic superphyla (**Figure 1**) and numerous rare OTUs. The eukaryotic microbial communities were dominated by *Alveolata*, *Hacrobia*, and Stramenopiles while *Opisthokonta*, *Rhizaria*, and *Chlorophyta* were detected in smaller proportions (**Figure 1**). If this result is consistent with many reports from freshwater ecosystems (Lefranc et al., 2005; Richards et al., 2005; Šlapeta et al., 2005; Triadó-Margarit and Casamayor, 2012; Taib et al., 2013; Simon et al., 2015), the large variation in 18S rRNA gene copy numbers among eukaryotic species and between growth phases [1 to highest estimates around 37,000 copies per cell in diatoms and 310,000 copies in ciliates (Prokopowich et al., 2003; Godhe et al., 2008; Gong et al., 2013)] might have led to overestimation of the relative abundance of some lineages compared to others, as previously mentioned (e.g., Mangot et al., 2009; Gong et al., 2013; Ren et al., 2018). We thus avoided as far as possible to compare relative proportions between the different lineages and focused on the dynamics of eukaryotic OTUs over months and seasons.

Eukaryotic communities showed a clear seasonal pattern with different communities between winter and summer (**Figure 2** and **Supplementary Figures S7, S8**), as a probable consequence of the contrasted environmental conditions. This pattern was repeated during the 2nd year of sampling, suggesting an annual eukaryotic community cycle, which is consistent with previous investigations on lakes (Nolte et al., 2010; Bock et al., 2014), ponds and brooks (Simon et al., 2015). This seasonal pattern was correlated with summer and winter-associated contrasting parameters such as air and water temperatures, snow cover and nitrogen concentrations and has also been observed for the bacterial communities of the Saint-Charles River (Cruaud et al., 2019). This suggests that both bacterial and eukaryotic communities undergo deep modifications of their community composition, reflecting the dramatically different seasonal and environmental conditions of the region (**Figure 2** and **Supplementary Table S1**) and confirming the structuring role of environmental selection in this ecosystem.

Ciliophora, *Chrysophyceae*, and *Telonemia* were detected in higher proportions during the CS, whereas *Cryptophyta* and *Dinoflagellata* were detected in higher proportions during the WS (**Figure 2** and **Supplementary Figure S11**). Although DNA might not directly indicate activity or viability of the cells and the fact that 18S rDNA relative proportions could not be considered as abundances due to different copy numbers and primer efficiency, the successive increases and decreases in relative proportions of specific eukaryotic lineages during the CS (**Supplementary Figure S10**) suggest that, despite the ice-cover and the very low water temperature during this season (**Figure 1** and **Supplementary Table S1**), at least a part of the eukaryotic microbial community could potentially be active and growing in the river and/or in the lake feeding the river. Furthermore, phylogenetic trees indicated that some 18S rRNA genes sequenced from winter samples clustered with sequences recovered from cold environments (ice, moutain lakes) (Klaveness and Lindstrøm, 2011; Charvet et al., 2012; Remias et al., 2013), supporting the viability of these lineages during the CS. This may reveal a potential better tolerance to cold conditions or different strategies for overwintering among these lineages. This change in microbial community composition was also observed for the bacterial community, with increasing proportion of potential methane and nitrogen cycling bacteria (e.g., bacterial OTUs 5, 6, 17, 18, 22, 33 and 41 in **Figure 4**) in winter, which was consistent with environmental conditions during this season. Together these results suggest that the winter season is probably not a dormant season for prokaryotic and eukaryotic microorganisms. However, we cannot exclude that a non-negligible part of the observed diversity may overwinter in a dormant or resting state (Sommer et al., 2012).

While *Ciliophora* are mainly considered as predators of bacteria (Lefranc et al., 2005; Richards and Bass, 2005) and *Cryptophyta* are assumed to be mainly photoautotrophic (Lepère et al., 2008; Grujcic et al., 2018), plastid-retention and true symbiosis with algal cell in *Ciliophora* as well as bacterivory in *Cryptophyta* have been also reported (Dolan, 1992; Stoecker et al., 2017; Grujcic et al., 2018; Stoecker and Lavrentyev, 2018), challenging the attribution of a consensus nutritional mode for these large groups. Therefore, we selected and analyzed in detail 25 predominant OTUs that fluctuated throughout the sampling period to investigate the freshwater microeukaryote ecology and the potential variations of nutritional mode throughout the annual cycle (**Figure 3** and **Supplementary Figure S3**).

Life in a River Covered by Ice

The CS was characterized by a broadly constant low water temperature and ice- and snow-cover on the river and on the upstream lake (**Figure 1** and **Supplementary Table S1**). These conditions are usually associated with limited atmospheric gas exchanges and reduced particulate inputs in the water (Catalan, 1992; Bertilsson et al., 2013; Hampton et al., 2017), as well as reduced macro- and mega-faunal predatory pressure, although zooplankton and fish predation may be high even in winter (Jeppesen et al., 2004; Sørensen et al., 2011; Sommer et al., 2012). Taxonomic comparison with known representatives of the selected OTUs that predominated during winter revealed that the potential for phototrophy and phagotrophy could occur in the river during the CS (**Figure 3**, **Supplementary Figure S3**, and **Supplementary Table S2**). Inhibition of photosynthesis at low temperatures has been previously reported (Murata, 1989; Anesi et al., 2016) but specific physiological adaptations have been proposed for lineages in cold ecosystems, such as the *Hydrurus*-clade that includes the OTU17 (**Supplementary Figure S5** and **Supplementary Table S2**)

(Klaveness and Lindstrøm, 2011; Remias et al., 2013), suggesting that eukaryotic primary productivity might be maintained under ice. During the CS, the bacterial communities also changed in the river (Cruaud et al., 2019), suggesting a modification of the potential prey availability. Eight predominant eukaryotic OTUs with heterotrophic or mixotrophic potential were positively correlated with various winter-associated bacterial lineages, such as *Crenothrix*, *Candidatus* Nitrotoga and *Methylococcales* pLW20 (Cruaud et al., 2019; **Figure 4**, **Supplementary Figure S13**, and **Supplementary Table S3**). While these correlations might indicate that the same or related environmental factors (e.g., temperature, nitrogen, **Figure 2**, **Supplementary Figure S14,** and **Supplementary Table S1**) drive bacterial and eukaryotic populations, it might also suggest potential variation in prey availability, supporting an influence of the bacterial community composition on heterotrophic eukaryotes and *vice versa* (Jezbera et al., 2005, 2006; Pernthaler, 2005; Massana et al., 2009; Šimek et al., 2013, 2018; Grujcic et al., 2018). Together these results suggest that winter conditions did not preclude the use of light for photosynthesis or the existence of a potential grazing pressure on bacterial communities and that important mechanisms could occur during this season as emphasized in the re-evaluation of the Plankton Group Ecology (PEG) model of seasonal succession of phytoplankton and zooplankton biomasses in lake ecosystems (Sommer et al., 2012). However, these conditions may select a different fraction of the eukaryotic community that is more adapted and competitive under winter conditions than lineages identified in summer, as previously reported (Brown et al., 2004; Gyllström et al., 2005).

Winter Comes Every Year but Each Winter Is Different

Although the overall community structure remained relatively similar during the two sampled winters (**Figure 2** and **Supplementary Figures S7, S8**), a group of covarying OTUs that were mainly detected in March during the winter 2017 showed very high proportions during the winter 2018 (OTU3 within the *Ciliophora* and OTUs 4, 10, and 19 within the *Stramenopiles*, **Figures 3, 4,** and **Supplementary Figure S9,** and **Supplementary Table S2**), highlighting potential changes in environmental conditions between winters. The winter 2018 was characterized by a particularly important mid-winter thaw in January (maximal air temperature 9.3°C on 12 January 2018, **Figure 1**), that led to an unusual increase in river flow and a massive flooding of the watershed. Such events could potentially result in nutrient inputs from the watershed. Furthermore, below freezing temperatures in the following days coupled with the residence time of the water in the lake [32 days in average (APEL, 2015)] could have allowed the persistence of the disturbance effect over a long period of time. Thus the difference observed in eukaryotic microbial community composition between the two winters might be explained by this mid-winter weather perturbation. Interestingly, while only a limited part of the protist community was impacted, the eukaryotic microbial community composition was more altered than the bacterial communities (Cruaud et al., 2019), suggesting differences in the response time or sensitivity between the eukaryotic and the bacterial communities to environmental changes. Based on their taxonomic proximity with known species, heterotrophic and mixotrophic lifestyles were inferred for the eukaryotic OTUs detected in high proportions during the winter 2018. Therefore, they might have been triggered directly by nutrient inputs from the watershed, boosted by potential increase of light penetration in the water, or indirectly activated through the predation of specific organic matter degrading bacteria, such as *Polynucleobacter* that was also detected in unusually high proportions during the winter 2018 (affiliated as *Polynucleobacter asymbioticus* on Silva release 128 Cruaud et al., 2019). This *Polynucleobacter* lineage, that was mainly detected in strong proportion during the WS, is known to exploit photodegradation products of humic substances (Hahn et al., 2012) and to be consumed by a wide range of bacterivorous eukaryotes (Grujcic et al., 2018). However, the emergence of *Polynucleobacter* in the winter 2018 was not associated with a simultaneous growth of summer bacterivorous eukaryotes, suggesting that environmental conditions (e.g., cold temperature) apply a stronger selection on bacterivorous eukaryotic lineages than the availability of bacterial prey.

Complex Temporal Dynamics During the Ice-Free Period

The relative proportions of the OTUs detected during the WS were more fluctuant than during the CS and only few correlations were detected among them (**Figure 4**, and **Supplementary Figure S12**, and **Supplementary Table S3**), suggesting a more complex temporal dynamic of the eukaryotic microbial community during this season. This results might be directly due to larger variations in environmental conditions (e.g., frequent rainfall events and runoff, water temperature fluctuating from 8°C to 23°C, changes in the watershed input such as pollen, leaf fall or erosion, **Figure 1** and **Supplementary Table S1**) that might provide a large variety of niche opportunities for eukaryotic microorganisms. The environmental conditions during the WS could also impact the potential bacterial prey community composition (Cruaud et al., 2019) and also change the predation by higher trophic levels (Sommer et al., 1986, 2012).

At the beginning of the WS, different OTUs, related to major identified groups (*Ciliophora*, *Hacrobia*, and *Stramenopiles*) were detected in higher proportions (OTUs 8, 14, 18, 20, 21, 22, 23, and 24 **Figure 3** and **Supplementary Figure S9**). While the *Telonemia* OTU8, the *Limnostrombidium* OTU14, the *Synura* OTU20 and the *Dinophyceae* OTU21 were detected throughout the CS and the *Suessiaceae* OTU18, the *Stentor* OTU23 and the *Strobilidiidae* OTU24 were rather detected in very low proportions during this season (CS), all these OTUs were characterized by a sudden increase in relative proportions on 17 May 2017 (**Figures 3, 4** and **Supplementary Figure S9**). This period could correspond to the spring bloom as described in the PEG model (Sommer et al., 1986, 2012). After the spring break up in mid-April, the Saint-Charles Lake, the main source of the Saint-Charles River, was totally ice-free in early May. At this period, water of the lake mix once the water temperature reach 4°C. The mixing of the lake, as well as the large water inputs produced by snow- and ice-melting in

spring, likely bring fresh nutrients which could intermittently fuel the eukaryotic community and enrich it with additional species from snow, ice, deeper waters of the lake or soil leaching. Thus, toward the end of winter, increasing water temperature, light and nutrient availability could allow the growth of fast-growing protists that overwintered in an active or a resting stage with early termination of the diapause phase (Sommer et al., 1986, 2012), as potentially illustrated by the OTUs described above and supporting that the growing season does not start from zero after the winter season (Sommer et al., 2012). Moreover, some of these OTUs were also detected in higher proportions at the beginning of the CS (OTUs 8, 14, 20, and 24). This period correspond to the fall turnover in the Saint-Charles Lake (Wetzel, 2001; Boulé et al., 2010), leading to the redistribution throughout the water column of the nutrients isolated in the hypolymnion during the summer season and potentially modifying the microbial community composition through nutrients or bacteria intake (Cruaud et al., 2019). By contrast with the WS, the beginning of the CS is not characterized by an increase in light supply and in water temperature, suggesting that these lineages might rather respond to an increase in nutrient availability or another confounding factor rather than an increase in light supply, as suggested as main starter for the spring bloom in the PEG model (Sommer et al., 1986, 2012).

After this early summer stage, we observed an increase in relative proportions of different OTUs, such as the *Cryptomonas* OTUs 1 and 5 and the *Stentor* OTU11 (**Figure 3** and **Supplementary Figure S9**). These OTUs were correlated with the increase in air and water temperatures (**Supplementary Figure S14**) and with the relative proportion of some bacterial lineages mainly detected during the WS, such as *Limnohabitans*, *Limnobacter* or *Sporichthyaceae* hgcI (**Figure 4**, **Supplementary Figure S13**, and **Supplementary Table S3**), which are known prey for bacterivorous eukaryotes (Šimek et al., 2013, 2018; Grujcic et al., 2018; Piwosz et al., 2018). These results suggest that these potentially mixotrophic or heterotrophic OTUs could be more competitive in the middle of summer and could be slower growing species than the OTUs detected in early summer as suggested in the PEG model (Sommer et al., 1986). In addition, other eukaryotic OTUs were detected more sporadically during the WS (*Uroglena* OTU7, Unc. *Alveolata* OTU12, and *Stentor* OTU23) or both during the warm and the CS (Unc. *Dinophyceae* OTU13) with few correlations with the main environmental parameters (**Supplementary Figure S14**). Punctual events, such as a transient increase in phosphorus (07 June 2016, 15 June 2017) or nitrogen concentrations (CS), could explain these kinds of temporal dynamics. Likewise, the OTU12 and the OTU25, affiliated with the parasitic lineage *Perkinsidea* (Lepère et al., 2008; Chambouvet et al., 2014) were also detected sporadically throughout the sampling period. Moreover, the *Perkinsida* OTU25 was strongly correlated with a bacterial OTU affiliated with *Polaromonas* (**Figure 4**, **Supplementary Figure S13**, and **Supplementary Table S3**), highlighting potential hosts for this *Perkinsidae* OTU. The detection of these parasitic lineages among the main protist lineages suggests an important role of parasitism in regulation of population dynamics in freshwater ecosystems, as previously suggested (Lefranc et al., 2005; Lepère et al., 2008; Sommer et al., 2012; Mangot et al., 2013).

Together, these results might indicate potential differences among protist lineages detected during the WS such as in generation times, resistance to grazing, susceptibility to infection by virulent parasites or sensitivity to nutrient and prey availability. According to the PEG model, the plankton community during the ice-free period follows successive stages starting from a phytoplankton spring bloom followed by the development of zooplankton in response to food availability. This growth of zooplankton leads to the decline of early summer lineages, which is known as the "clear water phase" (Sommer et al., 1986, 2012). Subsequently, food limitation and fish predation limit the zooplankton biomass allowing the increase of zooplankton preys (Sommer et al., 1986, 2012). Interestingly, the variations observed in our study in the protist community composition and diversity throughout the WS did not reveal clearly separated groups for these successive stages. Without any protist, zooplankton and other predators (e.g., fish) community quantifications, the stages of plankton biomass succession cannot be clearly distinguished in our dataset. However, our study suggests that beyond the total biomass changes, complex and numerous species replacements also occur in freshwater ecosystems during the WS.

CONCLUSION

Our study shows a pronounced seasonal clustering of eukaryotic microbial communities confirming the important role of environmental selection in freshwater ecosystems and the necessity of temporal series to comprehensively assess the biodiversity of these systems. Although all nutritional modes (autotrophy, heterotrophy, mixotrophy, and parasitism) were potentially identified throughout the year, complex patterns of distribution have been observed suggesting a large complexity of factors and interactions that could shape the temporal dynamics of the microbial eukaryotic community. While the modulation of grazing, photosynthesis and growth rates by water temperature could be an important variable controlling the annual dynamics of eukaryotic microbial populations, our results suggest that other factors such as the availability of specific bacterial and eukaryotic prey, variations in nutrients concentrations and the presence of various predators could also greatly influence the eukaryotic community composition warranting further investigations. Thus, understanding the underlying causes of eukaryotic microbial community temporal dynamics is highly complex and will require considerable efforts and an adequate way to understand this specific part of microbial ecology. However, such efforts are crucial considering the important impact of microbial eukaryotes on the global functioning of freshwater ecosystems.

DATA AVAILABILITY STATEMENT

The datasets generated for this study can be found in NCBI, PRJNA486319, MK618733 – MK618757.

AUTHOR CONTRIBUTIONS

PC, CD, AC, MR, and SC designed the study. PC and M-SF collected the samples. PC performed the laboratory work, sequencing data analyses, and statistical analyses. PC, AV, and SC analyzed and interpreted the results. PC and AV wrote the manuscript with revisions by SC, MR, CD, and AC.

FUNDING

This research project was supported by grants from the Natural Sciences and Engineering Research Council of Canada (NSERC), the Drinking Water Chair of Laval University (CREPUL), and Sentinel North. SC is a research scholar from the Fonds de Recherche du Québec en Santé.

ACKNOWLEDGMENTS

We thank the AD team, and especially Marianne Potvin, as well as all members of the Lab Charette for very helpful scientific discussions. We thank Alex Bernatchez and Morgane Mieli for sampling assistance. We would also like to thank the Ville de Québec and operators of the Loretteville Water Treatment Plant, with a special thanks to Louis Collin and François Proulx.

SUPPLEMENTARY MATERIAL

The Supplementary Material for this article can be found online at: https://www.frontiersin.org/articles/10.3389/fmicb.2019.02359/full#supplementary-material

REFERENCES

Altschul, S. F., Gish, W., Miller, W., Myers, E. W., and Lipman, D. J. (1990). Basic local alignment search tool. *J. Mol. Biol.* 215, 403–410. doi: 10.1016/S0022-2836(05)80360-2

Andrews, S., (2012). *FastQC: A Quality Control Application for High Throughput Sequence Data*. Available at: https://www.bioinformatics.babraham.ac.uk/projects/fastqc/ (accessed October 07, 2019).

Anesi, A., Obertegger, U., Hansen, G., Sukenik, A., Flaim, G., and Guella, G. (2016). Comparative analysis of membrane lipids in psychrophilic and mesophilic freshwater dinoflagellates. *Front. Plant Sci.* 7:524. doi: 10.3389/fpls.2016.00524

APEL (2015). *Suivi du lac Saint-Charles - Bilan des Campagnes 2011 à 2013*. Québec: Association pour la protection de l'environnement du lac Saint-Charles et des Marais du Nord.

Arndt, H. (1993). Rotifers as predators on components of the microbial web (bacteria, heterotrophic flagellates, ciliates)—a review. *Hydrobiologia* 83, 231–246. doi: 10.1007/978-94-011-1606-0_31

Arndt, H., Dietrich, D., Auer, B., Cleven, E.-J., Gräfenhan, T., Weitere, M., et al. (2000). "Functional diversity of heterotrophic flagellates in aquatic ecosystems," in *The Flagellates*, eds B. S. C. Leadbeater, and J. C. Green, (London: Taylor & Francis Ltd), 240–268.

Bertilsson, S., Burgin, A., Carey, C. C., Fey, S. B., Grossart, H.-P., Grubisic, L. M., et al. (2013). The under-ice microbiome of seasonally frozen lakes. *Limnol. Oceanogr.* 58, 1998–2012. doi: 10.4319/lo.2013.58.6.1998

Bird, D. F., and Kalff, J. (1986). Bacterial grazing by planktonic lake algae. *Science* 231, 493–495. doi: 10.1126/science.231.4737.493

Bock, C., Medinger, R., Jost, S., Psenner, R., and Boenigk, J. (2014). Seasonal variation of planktonic chrysophytes with special focus on Dinobryon. *Fottea* 14, 179–190. doi: 10.5507/fot.2014.014

Boenigk, J., Pfandl, K., Stadler, P., and Chatzinotas, A. (2005). High diversity of the 'Spumella-like'flagellates: an investigation based on the SSU rRNA gene sequences of isolates from habitats located in six different geographic regions. *Environ. Microbiol.* 7, 685–697. doi: 10.1111/j.1462-2920.2005.00743.x

Boulé, V., Vallières, C., Laflamme, V., Bouchard-Valentine, M., Jobin, P., Sauvageau, C., et al. (2010). *État de la Situation du Bassin Versant de la Prise d'eau de la Rivière St-Charles - Rapport Final*. Basel: Roche.

Bråte, J., Klaveness, D., Rygh, T., Jakobsen, K. S., and Shalchian-Tabrizi, K. (2010a). Telonemia-specific environmental 18S rDNA PCR reveals unknown diversity and multiple marine-freshwater colonizations. *BMC Microbiol.* 10:168. doi: 10.1186/1471-2180-10-168

Bråte, J., Logares, R., Berney, C., Ree, D. K., Klaveness, D., Jakobsen, K. S., et al. (2010b). Freshwater Perkinsea and marine-freshwater colonizations revealed by pyrosequencing and phylogeny of environmental rDNA. *ISME J.* 4, 1144–1153. doi: 10.1038/ismej.2010.39

Bray, J. R., and Curtis, J. T. (1957). An ordination of the upland forest communities of Southern Wisconsin. *Ecol. Monogr.* 27, 325–349. doi: 10.2307/1942268

Brodeur, C., Lewis, F., Huet-Alegre, E., Ksouri, Y., Leclerc, M.-C., and Viens, D. (2009). Portrait du bassin de la rivière Saint-Charles. *Conseil de bassin de la rivière Saint-Charles*, 9, 217–340.

Brown, J. H., Gillooly, J. F., Allen, A. P., Savage, V. M., and West, G. B. (2004). Toward a metabolic theory of ecology. *Ecology* 85, 1771–1789. doi: 10.1890/03-9000

Caron, D. A., Lim, E. L., Dennett, M. R., Gast, R. J., Kosman, C., and DeLong, E. F. (1999). Molecular phylogenetic analysis of the heterotrophic chrysophyte genus Paraphysomonas (Chrysophyceae), and the design of rRNA-targeted oligonucleotide probes for two species. *J. Phycol.* 35, 824–837. doi: 10.1046/j.1529-8817.1999.3540824.x

Caron, D. A., Worden, A. Z., Countway, P. D., Demir, E., and Heidelberg, K. B. (2009). Protists are microbes too: a perspective. *ISME J.* 3, 4–12. doi: 10.1038/ismej.2008.101

Carr, A., Diener, C., Baliga, N. S., and Gibbons, S. M. (2019). Use and abuse of correlation analyses in microbial ecology. *ISME J.* 1:177. doi: 10.1038/s41396-019-0459-z

Carrias, J., Amblard, C., Quiblier-Lloberas, C., and Bourdier, G. (1998). Seasonal dynamics of free and attached heterotrophic nanoflagellates in an oligomesotrophic lake. *Freshw. Biol.* 39, 91–101. doi: 10.1046/j.1365-2427.1998.00263.x

Catalan, J. (1992). Evolution of dissolved and particulate matter during the ice-covered period in a deep, high-mountain lake. *Can. J. Fish. Aquat. Sci.* 49, 945–955. doi: 10.1139/f92-105

Chambouvet, A., Berney, C., Romac, S., Audic, S., Maguire, F., De Vargas, C., et al. (2014). Diverse molecular signatures for ribosomally 'active' Perkinsea in marine sediments. *BMC Microbiol.* 14:110. doi: 10.1186/1471-2180-14-110

Charvet, S., Vincent, W. F., and Lovejoy, C. (2012). Chrysophytes and other protists in High Arctic lakes: molecular gene surveys, pigment signatures and microscopy. *Polar Biol.* 35, 733–748. doi: 10.1007/s00300-011-1118-7

Choi, B., Son, M., Kim, J. I., and Shin, W. (2013). Taxonomy and phylogeny of the genus cryptomonas (Cryptophyceae, Cryptophyta) from Korea. *Algae* 28, 307–330. doi: 10.4490/algae.2013.28.4.307

Comeau, A. M., Li, W. K. W., Tremblay, J. -É, Carmack, E. C., and Lovejoy, C. (2011). Arctic ocean microbial community structure before and after the 2007 record sea ice minimum. *PLoS One* 6:e27492. doi: 10.1371/journal.pone.0027492

Cruaud, P., Rasplus, J.-Y., Rodriguez, L. J., and Cruaud, A. (2017a). High-throughput sequencing of multiple amplicons for barcoding and integrative taxonomy. *Sci. Rep.* 7:41948. doi: 10.1038/srep41948

Cruaud, P., Vigneron, A., Fradette, M.-S., Charette, S. J., Rodriguez, M. J., Dorea, C. C., et al. (2017b). Open the SterivexTM casing: an easy and effective way to improve DNA extraction yields. *Limnol. Oceanogr. Methods* 15, 1015–1020. doi: 10.1002/lom3.10221

Cruaud, P., Vigneron, A., Fradette, M.-S., Dorea, C. C., Culley, A. I., Rodriguez, M. J., et al. (2019). Annual bacterial community cycle in a seasonally ice-covered

river reflects environmental and climatic conditions. *Limnol. Oceanogr.* doi: 10.1002/lno.11130

Csardi, G., and Nepusz, T. (2006). The igraph software package for complex network research. *InterJ. Compl. Syst.* 1695, 1–9.

Debroas, D., Domaizon, I., Humbert, J.-F., Jardillier, L., Lepère, C., Oudart, A., et al. (2017). Overview of freshwater microbial eukaryotes diversity: a first analysis of publicly available metabarcoding data. *FEMS Microbiol. Ecol.* 93. doi: 10.1093/femsec/fix023

Dolan, J. (1992). Mixotrophy in ciliates: a review of chlorella symbiosis and chloroplast retention. *Mar. Microb. Food Webs* 6, 115–132.

Dovgal, I. V., and Pesic, V. (2007). *Acineta persiensis* sp. n. (Ciliophora, Suctorea) — a new freshwater suctorian species from the water mites of the Genus Protzia (Acari, Hydrachnidia). *Вестник зоологии* 41, 165–167.

Fernandes, N. M., da Silva Paiva, T., da Silva-Neto, I. D., Schlegel, M., and Schrago, C. G. (2016). Expanded phylogenetic analyses of the class heterotrichea (Ciliophora, Postciliodesmatophora) using five molecular markers and morphological data. *Mol. Phylogenet. Evol.* 95, 229–246. doi: 10.1016/j.ympev.2015.10.030

Galili, T. (2015). dendextend: an R package for visualizing, adjusting and comparing trees of hierarchical clustering. *Bioinformatics* 31, 3718–3720. doi: 10.1093/bioinformatics/btv428

Gazulha, F. B., and Utz, L. R. P. (2016). *Occurrence of Suctorian Ciliates (Ciliophora, Suctoria) in a Polluted Creek in Southern Brazil*. Available at: https://zoociencias.ufjf.emnuvens.com.br/zoociencias/article/view/2878 (accessed February 7, 2019).

Godhe, A., Asplund, M. E., Härnström, K., Saravanan, V., Tyagi, A., and Karunasagar, I. (2008). Quantification of diatom and dinoflagellate biomasses in coastal marine seawater samples by real-time PCR. *Appl. Environ. Microbiol.* 74, 7174–7182. doi: 10.1128/AEM.01298-08

Gong, J., Dong, J., Liu, X., and Massana, R. (2013). Extremely high copy numbers and polymorphisms of the rDNA operon estimated from single cell analysis of oligotrich and peritrich ciliates. *Protist* 164, 369–379. doi: 10.1016/j.protis.2012.11.006

Gong, Y.-C., Yu, Y.-H., Zhu, F.-Y., and Feng, W.-S. (2007). Molecular phylogeny of stentor (Ciliophora: Heterotrichea) based on small subunit ribosomal RNA sequences. *J. Eukaryot. Microbiol.* 54, 45–48. doi: 10.1111/j.1550-7408.2006.00147.x

Grossmann, L., Bock, C., Schweikert, M., and Boenigk, J. (2016). Small but manifold – hidden diversity in "Spumella-like Flagellates.". *J. Eukaryot. Microbiol.* 63, 419–439. doi: 10.1111/jeu.12287

Grujcic, V., Nuy, J. K., Salcher, M. M., Shabarova, T., Kasalicky, V., Boenigk, J., et al. (2018). Cryptophyta as major bacterivores in freshwater summer plankton. *ISME J.* 12, 1668–1681. doi: 10.1038/s41396-018-0057-5

Guillou, L., Bachar, D., Audic, S., Bass, D., Berney, C., Bittner, L., et al. (2013). The protist ribosomal reference database (PR2): a catalog of unicellular eukaryote small sub-unit rRNA sequences with curated taxonomy. *Nucleic Acids Res.* 41, D597–D604. doi: 10.1093/nar/gks1160

Gyllström, M., Hansson, L.-A., Jeppesen, E., Criado, F. G., Gross, E., Irvine, K., et al. (2005). The role of climate in shaping zooplankton communities of shallow lakes. *Limnol. Oceanogr.* 50, 2008–2021. doi: 10.4319/lo.2005.50.6.2008

Hahn, M. W., Scheuerl, T., Jezberová, J., Koll, U., Jezbera, J., Šimek, K., et al. (2012). The passive yet successful way of planktonic life: genomic and experimental analysis of the ecology of a free-living Polynucleobacter population. *PLoS One* 7:e32772. doi: 10.1371/journal.pone.0032772

Hampton, S. E., Galloway, A. W. E., Powers, S. M., Ozersky, T., Woo, K. H., Batt, R. D., et al. (2017). Ecology under lake ice. *Ecol. Lett.* 20, 98–111. doi: 10.1111/ele.12699

Hansen, G., Daugbjerg, N., and Henriksen, P. (2007). *Baldinia anauniensis* gen. et sp. nov.: a 'new'dinoflagellate from Lake Tovel, N. Italy. *Phycologia* 46, 86–108. doi: 10.2216/PH06-23.1

Hansen, P. J., Ojamäe, K., Berge, T., Trampe, E. C. L., Nielsen, L. T., Lips, I., et al. (2016). Photoregulation in a kleptochloroplastidic dinoflagellate, *Dinophysis acuta*. *Front. Microbiol.* 7:785. doi: 10.3389/fmicb.2016.00785

Haraguchi, L. (2018). Phytoplankton community dynamic: a driver for ciliate trophic strategies. *Front. Mar. Sci.* 5:272. doi: 10.3389/fmars.2018.00272

Jacquet, V., Lair, N., Hoffmann, L., and Cauchie, H.-M. (2005). Spatio-temporal patterns of protozoan communities in a meso-eutrophic reservoir (Esch-sur-Sûre, Luxembourg). *Hydrobiologia* 551, 49–60. doi: 10.1007/s10750-005-4449-y

Jeppesen, E., Jensen, J. P., Søndergaard, M., Fenger-Grøn, M., Bramm, M. E., Sandby, K., et al. (2004). Impact of fish predation on cladoceran body weight distribution and zooplankton grazing in lakes during winter. *Freshw. Biol.* 49, 432–447. doi: 10.1111/j.1365-2427.2004.01199.x

Jezbera, J., Horňák, K., and Šimek, K. (2005). Food selection by bacterivorous protists: insight from the analysis of the food vacuole content by means of fluorescence in situ hybridization. *FEMS Microbiol. Ecol.* 52, 351–363. doi: 10.1016/j.femsec.2004.12.001

Jezbera, J., Horòák, K., and Šimek, K. (2006). Prey selectivity of bacterivorous protists in different size fractions of reservoir water amended with nutrients. *Environ. Microbiol.* 8, 1330–1339. doi: 10.1111/j.1462-2920.2006.01026.x

Johnson, M. D. (2011). The acquisition of phototrophy: adaptive strategies of hosting endosymbionts and organelles. *Photosynth. Res.* 107, 117–132. doi: 10.1007/s11120-010-9546-8

Jones, A. C., Liao, T. V., Najar, F. Z., Roe, B. A., Hambright, K. D., and Caron, D. A. (2013). Seasonality and disturbance: annual pattern and response of the bacterial and microbial eukaryotic assemblages in a freshwater ecosystem. *Environ. Microbiol.* 15, 2557–2572. doi: 10.1111/1462-2920.12151

Kalff, J., and Knoechel, R. (1978). Phytoplankton and their dynamics in oligotrophic and eutrophic lakes. *Annu. Rev. Ecol. Syst.* 9, 475–495. doi: 10.1146/annurev.es.09.110178.002355

Kamjunke, N., Henrichs, T., and Gaedke, U. (2006). Phosphorus gain by bacterivory promotes the mixotrophic flagellate *Dinobryon* spp. during re-oligotrophication. *J. Plankton Res.* 29, 39–46. doi: 10.1093/plankt/fbl054

Katoh, K., and Frith, M. C. (2012). Adding unaligned sequences into an existing alignment using MAFFT and LAST. *Bioinformatics* 28, 3144–3146. doi: 10.1093/bioinformatics/bts578

Katoh, K., and Standley, D. M. (2013). MAFFT multiple sequence alignment software version 7: improvements in performance and usability. *Mol. Biol. Evol.* 30, 772–780. doi: 10.1093/molbev/mst010

Kimura, B., and Ishida, Y. (1985). Photophagotrophy in Uroglena americana, Chrysophyceae. *Jpn. J. Limnol. Rikusuigaku Zasshi* 46, 315–318. doi: 10.3739/rikusui.46.315

Klaveness, D., and Lindstrøm, E.-A. (2011). Hydrurus foetidus (Chromista, Chrysophyceae): a large freshwater chromophyte alga in laboratory culture. *Phycol. Res.* 59, 105–112. doi: 10.1111/j.1440-1835.2010.00606.x

Klaveness, D., Shalchian-Tabrizi, K., Thomsen, H. A., Eikrem, W., and Jakobsen, K. S. (2005). Telonema antarcticum sp. nov., a common marine phagotrophic flagellate. *Int. J. Syst. Evol. Microbiol.* 55, 2595–2604. doi: 10.1099/ijs.0.63652-0

Laval-Peuto, M., and Febvre, M. (1986). On plastid symbiosis in Tontonia appendiculariformis (Ciliophora, Oligotrichina). *Biosystems* 19, 137–158. doi: 10.1016/0303-2647(86)90026-2

Laza-Martínez, A., Arluzea, J., Miguel, I., and Orive, E. (2012). Morphological and molecular characterization of Teleaulax gracilis sp. nov. and *T. minuta* sp. nov.(Cryptophyceae). *Phycologia* 51, 649–661. doi: 10.2216/11-044.1

Lefranc, M., Thénot, A., Lepère, C., and Debroas, D. (2005). Genetic diversity of small eukaryotes in lakes differing by their trophic status. *Appl. Environ. Microbiol.* 71, 5935–5942. doi: 10.1128/AEM.71.10.5935-5942.2005

Lemon, J. (2006). Plotrix: a package in the red light district of R. *R-News* 6, 8–12.

Lepère, C., Boucher, D., Jardillier, L., Domaizon, I., and Debroas, D. (2006). Succession and regulation factors of small eukaryote community composition in a lacustrine ecosystem (Lake Pavin). *Appl. Environ. Microbiol.* 72, 2971–2981. doi: 10.1128/AEM.72.4.2971-2981.2006

Lepère, C., Domaizon, I., and Debroas, D. (2008). Unexpected importance of potential parasites in the composition of the freshwater small-eukaryote community. *Appl. Environ. Microbiol.* 74, 2940–2949. doi: 10.1128/AEM.01156-07

Letunic, I., and Bork, P. (2016). Interactive tree of life (iTOL) v3: an online tool for the display and annotation of phylogenetic and other trees. *Nucleic Acids Res.* 44, W242–W245. doi: 10.1093/nar/gkw290

Lima-Mendez, G., Faust, K., Henry, N., Decelle, J., Colin, S., Carcillo, F., et al. (2015). Determinants of community structure in the global plankton interactome. *Science* 348:1262073. doi: 10.1126/science.1262073

Logares, R., Sunagawa, S., Salazar, G., Cornejo-Castillo, F. M., Ferrera, I., Sarmento, H., et al. (2014). Metagenomic 16S rDNA Illumina tags are a powerful alternative to amplicon sequencing to explore diversity and structure of

microbial communities. *Environ. Microbiol.* 16, 2659–2671. doi: 10.1111/1462-2920.12250

Magoč, T., and Salzberg, S. L. (2011). FLASH: fast length adjustment of short reads to improve genome assemblies. *Bioinformatics* 27, 2957–2963. doi: 10.1093/bioinformatics/btr507

Mangot, J.-F., Domaizon, I., Taib, N., Marouni, N., Duffaud, E., Bronner, G., et al. (2013). Short-term dynamics of diversity patterns: evidence of continual reassembly within lacustrine small eukaryotes. *Environ. Microbiol.* 15, 1745–1758. doi: 10.1111/1462-2920.12065

Mangot, J.-F., Lepère, C., Bouvier, C., Debroas, D., and Domaizon, I. (2009). Community structure and dynamics of small eukaryotes targeted by new oligonucleotide probes: new insight into the lacustrine microbial food web. *Appl. Environ. Microbiol.* 75, 6373–6381. doi: 10.1128/AEM.00607-09

Marquardt, M., Vader, A., Stübner, E. I., Reigstad, M., and Gabrielsen, T. M. (2016). Strong seasonality of marine microbial eukaryotes in a High-Arctic Fjord (Isfjorden, in West Spitsbergen, Norway). *Appl. Environ. Microbiol.* 82, 1868–1880. doi: 10.1128/AEM.03208-15

Martin, M. (2011). Cutadapt removes adapter sequences from high-throughput sequencing reads. *EMBnet J.* 17, 10–12. doi: 10.14806/ej.17.1.200

Massana, R., Unrein, F., Rodríguez-Martínez, R., Forn, I., Lefort, T., Pinhassi, J., et al. (2009). Grazing rates and functional diversity of uncultured heterotrophic flagellates. *ISME J.* 3, 588–596. doi: 10.1038/ismej.2008.130

McManus, G. B., and Fuhrman, J. A. (1986). Photosynthetic pigments in the ciliate Laboea strobila from long Island Sound, USA. *J. Plankt. Res.* 8, 317–327. doi: 10.1093/plankt/8.2.317

McManus, G. B., Liu, W., Cole, R. A., Biemesderfer, D., and Mydosh, J. L. (2018). *Strombidium rassoulzadegani*: a model species for chloroplast retention in Oligotrich Ciliates. *Front. Mar. Sci.* 5:205. doi: 10.3389/fmars.2018.00205

Medlin, L. K., Metfies, K., Mehl, H., Wiltshire, K., and Valentin, K. (2006). Picoeukaryotic plankton diversity at the helgoland time series site as assessed by three molecular methods. *Microb. Ecol.* 52, 53–71. doi: 10.1007/s00248-005-0062-x

Miller, M. A., Pfeiffer, W., and Schwartz, T. (2010). Creating the CIPRES science gateway for inference of large phylogenetic trees. *Gatew. Comput. Environ. Workshop GCE* 2010, 1–8. doi: 10.1109/GCE.2010.5676129

Millette, N. C., Pierson, J. J., Aceves, A., and Stoecker, D. K. (2017). Mixotrophy in Heterocapsa rotundata: a mechanism for dominating the winter phytoplankton. *Limnol. Oceanogr.* 62, 836–845. doi: 10.1002/lno.10470

Minnhagen, S., Carvalho, W. F., Salomon, P. S., and Janson, S. (2008). Chloroplast DNA content in *Dinophysis* (Dinophyceae) from different cell cycle stages is consistent with kleptoplasty. *Environ. Microbiol.* 10, 2411–2417. doi: 10.1111/j.1462-2920.2008.01666.x

Moestrup, Ø, Lindberg, K., and Daugbjerg, N. (2009). Studies on woloszynskioid dinoflagellates V. Ultrastructure of *Biecheleriopsis* gen. nov., with description of *Biecheleriopsis adriatica* sp. nov. *Phycol. Res.* 57, 221–237. doi: 10.1111/j.1440-1835.2009.00541.x

Murata, N. (1989). Low-temperature effects on cyanobacterial membranes. *J. Bioenerg. Biomembr.* 21, 61–75. doi: 10.1007/BF00762212

Newbold, L. K., Oliver, A. E., Booth, T., Tiwari, B., DeSantis, T., Maguire, M., et al. (2012). The response of marine picoplankton to ocean acidification. *Environ. Microbiol.* 14, 2293–2307. doi: 10.1111/j.1462-2920.2012.02762.x

Nolte, V., Pandey, R. V., Jost, S., Medinger, R., Ottenwaelder, B., Boenigk, J., et al. (2010). Contrasting seasonal niche separation between rare and abundant taxa conceals the extent of protist diversity. *Mol. Ecol.* 19, 2908–2915. doi: 10.1111/j.1365-294X.2010.04669.x

Oksanen, J., Kindt, R., Legendre, P., O'Hara, B., Stevens, M. H. H., Oksanen, M. J., et al. (2007). The vegan package. *Commun. Ecol. Pack.* 10, 631–637.

Olefeld, J. L., Majda, S., Albach, D. C., Marks, S., and Boenigk, J. (2018). Genome size of chrysophytes varies with cell size and nutritional mode. *Org. Divers. Evol.* 18, 163–173. doi: 10.1007/s13127-018-0365-7

Pernthaler, J. (2005). Predation on prokaryotes in the water column and its ecological implications. *Nat. Rev. Microbiol.* 3, 537–546. doi: 10.1038/nrmicro1180

Piwosz, K., Kownacka, J., Ameryk, A., Zalewski, M., and Pernthaler, J. (2016). Phenology of cryptomonads and the CRY1 lineage in a coastal brackish lagoon (Vistula Lagoon, Baltic Sea). *J. Phycol.* 52, 626–637. doi: 10.1111/jpy.12424

Piwosz, K., Shabarova, T., Tomasch, J., Šimek, K., Kopejtka, K., Kahl, S., et al. (2018). Determining lineage-specific bacterial growth curves with a novel approach based on amplicon reads normalization using internal standard (ARNIS). *ISME J.* 12:2640. doi: 10.1038/s41396-018-0213-y

Premke, K., and Arndt, H. (2000). Predation on heterotrophic flagellates by protists: food selectivity determined using a live-staining technique. *Arch. Für Hydrobiol.* 150, 17–28. doi: 10.1127/archiv-hydrobiol/150/2000/17

Prokopowich, C. D., Gregory, T. R., and Crease, T. J. (2003). The correlation between rDNA copy number and genome size in eukaryotes. *Genome* 46, 48–50. doi: 10.1139/g02-103

Remias, D., Jost, S., Boenigk, J., Wastian, J., and Lütz, C. (2013). Hydrurus-related golden algae (C hrysophyceae) cause yellow snow in polar summer snowfields. *Phycol. Res.* 61, 277–285. doi: 10.1111/pre.12025

Ren, K., Xue, Y., Rønn, R., Liu, L., Chen, H., Rensing, C., et al. (2018). Dynamics and determinants of amoeba community, occurrence and abundance in subtropical reservoirs and rivers. *Water Res.* 146, 177–186. doi: 10.1016/j.watres.2018.09.011

Richards, T. A., and Bass, D. (2005). Molecular screening of free-living microbial eukaryotes: diversity and distribution using a meta-analysis. *Curr. Opin. Microbiol.* 8, 240–252. doi: 10.1016/j.mib.2005.04.010

Richards, T. A., Vepritskiy, A. A., Gouliamova, D. E., and Nierzwicki-Bauer, S. A. (2005). The molecular diversity of freshwater picoeukaryotes from an oligotrophic lake reveals diverse, distinctive and globally dispersed lineages. *Environ. Microbiol.* 7, 1413–1425. doi: 10.1111/j.1462-2920.2005.00828.x

Rognes, T., Flouri, T., Nichols, B., Quince, C., and Mahé, F. (2016). VSEARCH: a versatile open source tool for metagenomics. *PeerJ* 4:e2584. doi: 10.7717/peerj.2584

Roy, R. S., Price, D. C., Schliep, A., Cai, G., Korobeynikov, A., Yoon, H. S., et al. (2014). Single cell genome analysis of an uncultured heterotrophic stramenopile. *Sci. Rep.* 4:4780. doi: 10.1038/srep04780

Ruan, Q., Dutta, D., Schwalbach, M. S., Steele, J. A., Fuhrman, J. A., and Sun, F. (2006). Local similarity analysis reveals unique associations among marine bacterioplankton species and environmental factors. *Bioinformatics* 22, 2532–2538. doi: 10.1093/bioinformatics/btl417

Salcher, M. M., Neuenschwander, S. M., Posch, T., and Pernthaler, J. (2015). The ecology of pelagic freshwater methylotrophs assessed by a high-resolution monitoring and isolation campaign. *ISME J.* 9, 2442–2453. doi: 10.1038/ismej.2015.55

Samad, M. S., and Bertilsson, S. (2017). Seasonal variation in abundance and diversity of bacterial methanotrophs in five temperate lakes. *Front. Microbiol.* 8:142. doi: 10.3389/fmicb.2017.00142

Sandgren, C. D., Smol, J. P., and Kristiansen, J. (1995). *Chrysophyte Algae: Ecology, Phylogeny and Development*. Cambridge: Cambridge University Press.

Schloss, P. D., Westcott, S. L., Ryabin, T., Hall, J. R., Hartmann, M., Hollister, E. B., et al. (2009). Introducing mothur: open-source, platform-independent, community-supported software for describing and comparing microbial communities. *Appl. Environ. Microbiol.* 75, 7537–7541. doi: 10.1128/AEM.01541-9

Schoener, D. M., and McManus, G. B. (2012). Plastid retention, use, and replacement in a kleptoplastidic ciliate. *Aquat. Microbiol. Ecol.* 67, 177–187. doi: 10.3354/ame01601

Scoble, J. M., and Cavalier-Smith, T. (2014). Scale evolution in Paraphysomonadida (Chrysophyceae): sequence phylogeny and revised taxonomy of Paraphysomonas, new genus Clathromonas, and 25 new species. *Eur. J. Protistol.* 50, 551–592. doi: 10.1016/j.ejop.2014.08.001

Seeleuthner, Y., Mondy, S., Lombard, V., Carradec, Q., Pelletier, E., Wessner, M., et al. (2018). Single-cell genomics of multiple uncultured stramenopiles reveals underestimated functional diversity across oceans. *Nat. Commun.* 9, 1–10. doi: 10.1038/s41467-017-02235-3

Shalchian-Tabrizi, K., Bråte, J., Logares, R., Klaveness, D., Berney, C., and Jakobsen, K. S. (2008). Diversification of unicellular eukaryotes: cryptomonad colonizations of marine and fresh waters inferred from revised 18S rRNA phylogeny. *Environ. Microbiol.* 10, 2635–2644. doi: 10.1111/j.1462-2920.2008.01685.x

Sherr, E., and Sherr, B. (1988). Role of microbes in pelagic food webs: a revised concept. *Limnol. Oceanogr.* 33, 1225–1227. doi: 10.4319/lo.1988.33.5.1225

Šimek, K., Grujčić, V., Hahn, M. W., Horòák, K., Jezberová, J., Kasalický, V., et al. (2018). Bacterial prey food characteristics modulate community growth

response of freshwater bacterivorous flagellates. *Limnol. Oceanogr.* 63, 484–502. doi: 10.1002/lno.10759

Šimek, K., Kasalický, V., Jezbera, J., Horňák, K., Nedoma, J., Hahn, M. W., et al. (2013). Differential freshwater flagellate community response to bacterial food quality with a focus on Limnohabitans bacteria. *ISME J.* 7:1519. doi: 10.1038/ismej.2013.57

Simon, M., López-García, P., Deschamps, P., Moreira, D., Restoux, G., Bertolino, P., et al. (2015). Marked seasonality and high spatial variability of protist communities in shallow freshwater systems. *ISME J.* 9, 1941–1953. doi: 10.1038/ismej.2015.6

Šlapeta, J., Moreira, D., and López-García, P. (2005). The extent of protist diversity: insights from molecular ecology of freshwater eukaryotes. *Proc. R. Soc. Lond. B Biol. Sci.* 272, 2073–2081. doi: 10.1098/rspb.2005.3195

Sommer, U., Adrian, R., De Senerpont Domis, L., Elser, J. J., Gaedke, U., Ibelings, B., et al. (2012). Beyond the plankton ecology group (PEG) model: mechanisms driving plankton succession. *Annu. Rev. Ecol. Evol. Syst.* 43, 429–448. doi: 10.1146/annurev-ecolsys-110411-160251

Sommer, U., Gliwicz, Z. M., Lampert, W., and Duncan, A. (1986). The PEG-model of seasonal succession of planktonic events in fresh waters. *Arch. Hydrobiol.* 106, 433–471.

Sørensen, T., Mulderij, G., Søndergaard, M., Lauridsen, T. L., Liboriussen, L., Brucet, S., et al. (2011). Winter ecology of shallow lakes: strongest effect of fish on water clarity at high nutrient levels. *Hydrobiologia* 664, 147–162. doi: 10.1007/s10750-010-0595-y

Stamatakis, A. (2014). RAxML version 8: a tool for phylogenetic analysis and post-analysis of large phylogenies. *Bioinformatics* 30, 1312–1313. doi: 10.1093/bioinformatics/btu033

Stoecker, D. K., Hansen, P. J., Caron, D. A., and Mitra, A. (2017). Mixotrophy in the marine plankton. *Annu. Rev. Mar. Sci.* 9, 311–335. doi: 10.1146/annurev-marine-010816-060617

Stoecker, D. K., and Lavrentyev, P. J. (2018). Mixotrophic plankton in the polar seas: a pan-arctic review. *Front. Mar. Sci.* 5:292. doi: 10.3389/fmars.2018.00292

Stoecker, D. K., and Michaels, A. E. (1991). Respiration, photosynthesis and carbon metabolism in planktonic ciliates. *Mar. Biol.* 108, 441–447. doi: 10.1007/BF01313654

Stoecker, D. K., and Silver, M. W. (1987). Chloroplast retention by marine planktonic ciliatesa. *Ann. N. Y. Acad. Sci.* 503, 562–565. doi: 10.1111/j.1749-6632.1987.tb40646.x

Stoecker, D. K., and Silver, M. W. (1990). Replacement and aging of chloroplasts in Strombidium capitatum (Ciliophora: Oligotrichida). *Mar. Biol.* 107, 491–502. doi: 10.1007/BF01313434

Taib, N., Mangot, J.-F., Domaizon, I., Bronner, G., and Debroas, D. (2013). Phylogenetic affiliation of SSU rRNA genes generated by massively parallel sequencing: new insights into the freshwater protist diversity. *PLoS One* 8:e58950. doi: 10.1371/journal.pone.0058950

Terrado, R., Pasulka, A. L., Lie, A. A.-Y., Orphan, V. J., Heidelberg, K. B., and Caron, D. A. (2017). Autotrophic and heterotrophic acquisition of carbon and nitrogen by a mixotrophic chrysophyte established through stable isotope analysis. *ISME J.* 11, 2022–2034. doi: 10.1038/ismej.2017.68

Thamm, M., Schmidt, S. L., and Bernhard, D. (2010). Insights into the phylogeny of the genus Stentor (Heterotrichea, Ciliophora) with special emphasis on the evolution of the macronucleus based on SSU rDNA data. *Acta Protozool.* 2010:149157.

Tranvik, L. J., Porter, K. G., and Sieburth, J. M. (1989). Occurrence of bacterivory in cryptomonas, a common freshwater phytoplankter. *Oecologia* 78, 473–476. doi: 10.1007/BF00378736

Triadó-Margarit, X., and Casamayor, E. O. (2012). Genetic diversity of planktonic eukaryotes in high mountain lakes (Central Pyrenees, Spain). *Environ. Microbiol.* 14, 2445–2456. doi: 10.1111/j.1462-2920.2012.02797.x

Urabe, J., Gurung, T. B., and Yoshida, T. (1999). Effects of phosphorus supply on phagotrophy by the mixotrophic alga Uroglena americana (Chrysophyceae). *Aquat. Microb. Ecol.* 18, 77–83. doi: 10.3354/ame018077

Vigneron, A., Cruaud, P., Mohit, V., Martineau, M.-J., Culley, A. I., Lovejoy, C., et al. (2018). Multiple strategies for light-harvesting, photoprotection, and carbon flow in high latitude microbial mats. *Front. Microbiol.* 9:2881. doi: 10.3389/fmicb.2018.02881

Vigneron, A., Lovejoy, C., Cruaud, P., Kalenitchenko, D., Culley, A., and Vincent, W. F. (2019). Contrasting winter versus summer microbial communities and metabolic functions in a Permafrost Thaw Lake. *Front. Microbiol.* 10:1656. doi: 10.3389/fmicb.2019.01656

Warnes, G. R., Bolker, B., Bonebakker, L., Gentleman, R., Liaw, W. H. A., Lumley, T., et al. (2015). *gplots: Various R Programming Tools for Plotting Data. R package version 2.17. 0*.

Wei, T., Simko, V., Levy, M., Xie, Y., Jin, Y., and Zemla, J. (2017). Package 'corrplot.'. *Statistician* 56, 316–324.

Wetzel, R. G. (2001). *Limnology: Lake and River Ecosystems*. Houston, TX: Gulf professional publishing.

Wickham, H. (2015). *Stringr: Simple, Consistent Wrappers for Common String Operations. R Package Version 1*.

Wilken, S., Huisman, J., Naus-Wiezer, S., and Donk, E. V. (2013). Mixotrophic organisms become more heterotrophic with rising temperature. *Ecol. Lett.* 16, 225–233. doi: 10.1111/ele.12033

Worden, A. Z., Follows, M. J., Giovannoni, S. J., Wilken, S., Zimmerman, A. E., and Keeling, P. J. (2015). Rethinking the marine carbon cycle: factoring in the multifarious lifestyles of microbes. *Science* 347:1257594. doi: 10.1126/science.1257594

Xia, L. C., Steele, J. A., Cram, J. A., Cardon, Z. G., Simmons, S. L., Vallino, J. J., et al. (2011). Extended local similarity analysis (eLSA) of microbial community and other time series data with replicates. *BMC Syst. Biol.* 5:S15. doi: 10.1186/1752-0509-5-S2-S15

Xia, Y., Wang, Y., Wang, Y., Chin, F. Y. L., and Zhang, T. (2016). Cellular adhesiveness and cellulolytic capacity in Anaerolineae revealed by omics-based genome interpretation. *Biotechnol. Biofuels* 9:111. doi: 10.1186/s13068-016-0524-z

Zhao, B., Chen, M., Sun, Y., Yang, J., and Chen, F. (2011). Genetic diversity of picoeukaryotes in eight lakes differing in trophic status. *Can. J. Microbiol.* 57, 115–126. doi: 10.1139/W10-107

Zubkov, M. V., and Tarran, G. A. (2008). High bacterivory by the smallest phytoplankton in the North Atlantic Ocean. *Nature* 225:193. doi: 10.1038/nature07236

Conflict of Interest: The authors declare that the research was conducted in the absence of any commercial or financial relationships that could be construed as a potential conflict of interest.

Copyright © 2019 Cruaud, Vigneron, Fradette, Dorea, Culley, Rodriguez and Charette. This is an open-access article distributed under the terms of the Creative Commons Attribution License (CC BY). The use, distribution or reproduction in other forums is permitted, provided the original author(s) and the copyright owner(s) are credited and that the original publication in this journal is cited, in accordance with accepted academic practice. No use, distribution or reproduction is permitted which does not comply with these terms.

frontiers in Microbiology

ORIGINAL RESEARCH
published: 30 October 2019
doi: 10.3389/fmicb.2019.02474

Enhanced Microbial Interactions and Deterministic Successions During Anoxic Decomposition of *Microcystis* Biomass in Lake Sediment

Yu-Fan Wu[1,4†], Peng Xing[2†], Shuangjiang Liu[1] and Qinglong L. Wu[2,3*]*

[1] State Key Laboratory of Microbial Resources, Institute of Microbiology, Chinese Academy of Sciences, Beijing, China, [2] State Key Laboratory of Lake Science and Environment, Nanjing Institute of Geography & Limnology, Chinese Academy of Sciences, Nanjing, China, [3] Sino-Danish Centre for Education and Research, University of Chinese Academy of Sciences, Beijing, China, [4] Technology Center of Zhangjiagang Customs, Zhangjiagang, China

Microcystis biomass remineralization after blooming represents a hotspot of nutrient recycling in eutrophic lakes. Because *Microcystis* blooms are massively deposited on lake sediments, resulting in anoxic conditions, it is important to understand the response and role of benthic microbial communities during the anoxic decomposition of *Microcystis* in freshwater lakes. In the present study, we employed a microcosm method, combined with high-throughput sequencing, functional prediction, and network analysis, to investigate microbial succession during the short-term (30 days) anaerobic decomposition of *Microcystis* in a eutrophic sediment. Continuous accumulation of CH_4 and CO_2 and increasing relative abundance of methanogens were observed during the incubation. The microbial community composition (MCC) significantly changed after addition of *Microcystis* biomass, with a shift in the community from a stochastic to a functional, deterministic succession. Families, including *Clostridiaceae*, *Rhodocyclaceae*, *Rikenellaceae*, *Peptostreptococcaceae*, *Syntrophomonadaceae*, *Lachnospiraceae*, and *Methanosarcinaceae*, were predominantly enriched and formed diverse substitution patterns, suggesting a synergistic action of these family members in the decomposition of *Microcystis* biomass. Importantly, intense species-to-species interactions and weak resistance to disturbance were observed in the microbial community after *Microcystis* biomass addition. Collectively, these results suggest that the addition of *Microcystis* induce phylogenetic clustering and structure instability in the sediment microbial community and the synergistic interactions among saprotrophic bacteria play a key role in *Microcystis* biomass remineralization.

Keywords: microbial interaction, deterministic succession, *Microcystis*, anoxic decomposition, *Clostridiaceae*

OPEN ACCESS

Edited by:
Petra M. Visser, University of Amsterdam, Netherlands

Reviewed by:
Gregory Dick, University of Michigan, United States
Diogo Antonio Tschoeke, Federal University of Rio de Janeiro, Brazil

***Correspondence:**
Peng Xing
pxing@niglas.ac.cn
Qinglong L. Wu
qlwu@niglas.ac.cn

† These authors have contributed equally to this work

Specialty section:
This article was submitted to Aquatic Microbiology, a section of the journal Frontiers in Microbiology

Received: *14 April 2019*
Accepted: *15 October 2019*
Published: *30 October 2019*

Citation:
Wu Y-F, Xing P, Liu S and Wu QL (2019) Enhanced Microbial Interactions and Deterministic Successions During Anoxic Decomposition of Microcystis Biomass in Lake Sediment. Front. Microbiol. 10:2474. doi: 10.3389/fmicb.2019.02474

INTRODUCTION

Cyanobacterial blooms have become a widespread phenomenon in freshwater habitats (Zhang et al., 2010; Zhai et al., 2013) as one of the harmful consequences of eutrophication, which mainly results from intensive human activities affecting freshwater lakes and reservoirs worldwide (Paerl et al., 2001). As the primary producer, *Cyanobacteria* contribute 0.05% of the global

carbon biomass, causing high product accumulation during blooms and making eutrophic lakes extremely active sites for the transport, transformation, and storage of a considerable amount of carbon and nutrients (Wilms et al., 2006). In bloom seasons, high microbial activity leads to oxygen depletion within the uppermost few millimeters of the sediment and even the overlying water (Karlson et al., 2008; Chen et al., 2010). In this scenario, accumulated bloom biomass is primarily mineralized through anaerobic processes in the surface sediment (Bastviken et al., 2008). Furthermore, anaerobic mineralization in the sediments contributes to massive CH_4 emission from inland water bodies on a global scale (Cole et al., 1994; Schink, 1997; Krinner, 2003; Bastviken et al., 2004a). Thus, it is important to comprehensively understand the microbial transformation process and relevant prerequisite conditions, constituting the basis for the estimation of local and global CH_4 contribution by anaerobic decomposition of cyanobacterial blooms in inland waters.

Some studies addressing the associated microbial communities during cyanobacterial blooms have been reported, mainly focusing on microbial community dynamics in freshwater environments during the blooms (Li et al., 2012) or bacterial communities associated with certain algae species (Shi et al., 2009). These studies have revealed the influence of algal blooms on the planktonic bacterial community and have also provided important information about the microorganisms involved in algal biomass transformation (Tang et al., 2015).

However, the knowledge of which and how microbes participate in the anaerobic degradation of cyanobacterial blooms in the eutrophic lakes and reservoirs is limited. On the one hand, the involvement of microbial taxa, as well as the interactions between them, are not clear; on the other hand, the limitations of analysis methods have hampered the investigations of the phylogenetic diversity (PD), composition, and dynamics of the microbial community participating in the decomposition of sedimentary algae. In general, the anaerobic decomposition of organic material includes sequential hydrolytic, homoacetogenic, and methanogenic processes (Schink, 1997). Non-representative microbial taxa have been identified for each key step during the anaerobic degradation of cyanobacterial biomass. However, such research has been lagging far behind the analogous research in artificial anaerobic digestion, such as in wastewater treatment plants, where the different types of microorganisms involved have been extensively studied (Li et al., 2014; Narihiro et al., 2015; Shu et al., 2015). Using ^{13}C-labeled *Spirulina* biomass and denaturing gradient gel electrophoresis (DGGE), Graue et al. (2012) found that *Psychrilyobacter atlanticus* and some *Propionigenium*-like taxa participated in *Spirulina* biomass anoxic degradation. *In situ Microcystis* scums were incubated for 90 days to simulate the degradation of *Microcystis* biomass in an anoxic water column, and subsequent T-RFLP analysis revealed the predominance of a few novel *Clostridium* spp. during this process (Xing et al., 2011). Shao et al. (2013) investigated the effect of *Microcystis* bloom decomposition on sediment bacterial communities using DGGE in the 100 L mesocosms. The relative abundance of *Bacteroidetes* and *Verrucomicrobia* strongly increased after 14 days. However, it is remarkable that (i) the scenarios of cyanobacterial biomass mineralization in anoxic sediments have been less touched in the available studies; (ii) because of being restricted by the resolution of fingerprinting methods, the important processes in decomposition and the associated microbial groups remain undefined; (iii) greenhouse gas effect of decomposition in the sediment, which is even crucial for the CH_4 formation in eutrophic aquatic environments, has not been studied well.

The objective of the present study was to determine how sediment microbial communities respond and participate in *Microcystis* anaerobic decomposition after the massive deposition of *Microcystis* into freshwater sediment. Microcosms with sediment slurry and supplemental *Microcystis* biomass under anoxic conditions were generated to examine the sediment microbial communities after incubation for 30 days. Illumina MiSeq sequencing was applied to the sequential samples to elucidate the differential patterns with high taxonomic resolution. To further depict the inherent response of the microbial community to *Microcystis* addition, the relationship among co-occurring species was evaluated, and the community function profiles were also predicted based on the structural data. We observed distinct microbial succession during the anoxic decomposition of *Microcystis* in freshwater sediment, characterized by enhanced species-species interaction and low resistance to disturbance. Such works are helpful for a better understanding of algae biomass transformation and greenhouse gas production, constituting the center of carbon cycling in eutrophic lakes.

MATERIALS AND METHODS

Microcosm Setup

The *Microcystis* strain used was *Microcystis* sp. FACH-B 7806 (obtained from Freshwater Algae Culture Collection at the Institute of Hydrobiology, Chinese Academy of Sciences). *Microcystis* biomass was collected in the lab, cultivated in BG11 medium[1] under a luminance of 1200 Lux and 12 h dark: 12 h light photoperiod for 15 days, then collected by centrifugation and dried using a freeze dryer (ALPHA 1-2, CHRIST, Osterode am Harz, Germany). The *Microcystis* powder was UV sterilized for 20 min and stored at −80°C before adding to the microcosms. The sediment slurry used for the anaerobic *Microcystis* biodegradation tests were collected from Meiliang Bay (31.28946° N, 120.812905° E) of Lake Taihu in October 2012. Prior to the experiment, the sediments (1–5 cm deep) were sieved using a 0.6-mm mesh to remove the macrofauna and debris and subsequently incubated at room temperature (20–25°C) for 2 weeks to decrease the organic carbon content.

More than 60 microcosms built up in the sterile 100-mL air-tight glass bottles (100-mL capacity; CNW Technologies GmbH, Düsseldorf, Germany), which were divided into two groups. Each bottle in the control group contained 12.5 g homogenized sediment slurry +10 mL of sterile water, and in the treatment group, 12.5 g homogenized sediment slurry +10 mL of sterile water +25 mg freeze-dried *Microcystis* biomass. All the bottles

[1]https://www.dsmz.de/microorganisms/medium/pdf/DSMZ_Medium1593.pdf

were sealed with rubber stoppers and aluminum seals and wrapped with a silver paper to keep them in the dark. The headspace in the bottles was vacuumed for 10 s and filled with purified N_2 gas four times to maintain the anoxic conditions. All the microcosms were incubated in an incubator at 25°C.

Sampling and Physicochemical Analyses

During the incubation, six bottles from the treatment group and two bottles from the control group were randomly selected at each time point of (0, 1, 3, 10, 17, 23, and 30) days. The headspace in each jar was sampled with a 500 μL syringe (Part Number/REF: 81256, HAMILTON, Romania) after vigorously shaking to remove the gas bubbles trapped in the sediment slurry. The concentrations of H_2, CO_2, and CH_4 in the headspace were measured on a gas chromatograph equipped with a packed column TDX-01 (Techcomp, Shanghai, China), a flame ionization detector (FID), and a thermal conductivity detector (TCD). The gas concentration was calibrated using H_2, CH_4, and CO_2 standards purchased from the National Institute of Metrology P. R. China Standard Gas Testing Center. The bottles were sacrificed after gas measurement. A pH meter (METTLER TOLEDO FE20, Shanghai, China) was used to measure the pH of the slurry.

Microbial Biomass Collection and DNA Extraction

The sediment slurry samples were collected and stored at −20°C after freeze-drying. Genomic DNA was extracted from 0.25 g of freeze-dried sediment slurry using the FastDNA SPIN Kit (MP Biomedicals, Santa Ana, CA, United States) according to the manufacturer's instructions. The genomic DNA was quantified using a spectrophotometer (GE, Pittsburgh, United States) and stored at −20°C until subsequent procedures.

Real-Time Quantitative PCR

The 16S rRNA genes of the total bacteria were quantified by real-time PCR using the primer set 341F and 534R (Bru et al., 2008). Total Archaea were quantified using the 16S rRNA gene primer set Arch 333F and Arch 554R (Suzuki et al., 2000). Methanogens were quantified using the primer set ME1 and mlas (Steinberg and Regan, 2008), which targets the *mcrA* gene. The PCR conditions were as described by Nunoura et al. (2006). To construct standard curves for quantitative PCR, the PCR products for the partial bacterial 16S rRNA (341F and 534R), archaeal 16S rRNA (Arch333F and Arch554R), and *mcrA* (ME1 and mlas) genes (**Supplementary Table S1**) were purified and cloned into the pMD18-T vector (Takara, Dalian, China), and subsequently transformed into *Escherichia coli* DH5α competent cells (Takara, Dalian, China). The successfully inserted plasmids were extracted using a Plasmid Mini-Prep Kit (Axygen Biosciences, Union City, CA, United States), and the concentrations were determined by spectrophotometry using a NanoVue (GE, Pittsburgh, United States). The standard curves were prepared from linearized plasmid serial dilutions of 10^0 to 10^8 gene copies directly calculated from the concentration of the extracted plasmid. Quantitative PCR was performed in a 20 μL reaction comprising 10 μL of SYBR Premix ExTaq™ (Takara, Dalian, China), 0.25 μM each primer, 1 μL of 1/10 diluted DNA, and RNase-free water. The thermocycling program for quantitative PCR comprised an initial cycle at 95°C for 30 s, followed by 40 cycles at 95°C for 5 s and 60°C for 34 s. All measurements were obtained in triplicate. The standard curves were used as the references to calculate the copy number of bacterial 16S rRNA, archaeal 16S rRNA, and methanogens *mcrA* genes (correlation coefficient r^2 = 0.993, 0.993, and 0.993, respectively). The efficiencies of the qPCR amplification for the bacteria, archaea, and *mcrA* were 105.8, 96.6, and 97.1%, respectively.

Illumina MiSeq Sequencing and Data Processing

Genomic DNA was extracted from six replicates in the treatment group and two replicates in the control group at (0, 1, 3, 10, 17, 23, and 30) days. To analyze the bacterial diversity during cultivation, the V4-V6 region of the bacterial 16S rRNA genes was amplified and sequenced on an Illumina MiSeq platform. The V4-V6 region of the 16S rRNA gene was amplified using the primers 515F (5′- GTGCCAGCMGCCGCGGTAA-3′) and 907R (5′- CCGTCAATTCCTTTRAGTTT-3′) (Zhou X. et al., 2015). PCR amplification was performed using an ABI GeneAmp® 9700 thermal cycler (Applied Biosystems, Waltham, MA, United States). The PCR reaction was performed in a 20-μL reaction volume containing 10 μL of Trans Start Fast pfu DNA Polymerase Super Mix (Trans Gen AP221-02), 0.2 μM of forward and reverse primers, and 10 ng of template DNA. The thermal cycling parameters were denaturation at 95°C for 1 min, followed by 30 cycles at 94°C for 10 s, 55°C for 30 s, and 72°C for 45 s, with a final step at 72°C for 5 min. The PCR products were analyzed on a 2% agarose gel, purified using the AxyPrep™ DNA Gel Extraction Kit (Axygen Biosciences, Union City, CA, United States) according to the manufacturer's instructions, and quantified using QuantiFluor™ -ST (Promega, Fitchburg, WI, United States). The purified amplicons were pooled in equal molar ratios and paired-end sequenced (2 × 250 bp) on an Illumina MiSeq platform according to the standard protocols of the Major Bio Co., Ltd. (Shanghai, China).

The raw sequencing reads were de-multiplexed, quality-filtered, and analyzed using QIIME v1.17 (Caporaso et al., 2010). Sequence quality management and operational taxonomic units (OTUs) analysis were conducted using the UPARSE pipeline according to Edgar (2013). Briefly, reads <250 bp, with an average quality score (Q score) of <25 in a sliding window of 50 bp, with mismatched primer sequences, or containing ambiguous bases (Ns) were removed from downstream analyses. Both the forward and reverse primers were truncated from the reads. Chimeric sequences were removed using USEARCH software (Edgar, 2010) based on the UCHIME algorithm (Edgar et al., 2011). After quality and chimera filtering, 1.73 million reads with an average read length of 395 bp in 56 samples were obtained. The lowest number of sequences was 13,628. Therefore, the sequences in the samples were randomly normalized to 13,628 prior to conducting subsequent analyses. All the reads

were clustered into OTUs at 97% pairwise identity using UCLUST (Edgar, 2013). Representative OTUs were aligned to the Greengenes database (gg_13_8_otus).

Community Diversity Analysis and Null Model Test

Alpha diversity was estimated according to the Shannon index, Chao1, observed species, and PD for all the samples by using QIIME v1.17. Beta diversity was based on Bray–Curtis algorithm of the OTU table to identify the clustering patterns in the microbial communities among the samples across the incubation times (R-vegan function vegdist). In addition, the null model Raup-Crick index (β_{RC}) was used to assess whether the null-expected number of shared species between any two communities was different from the observed number of shared species (Chase et al., 2011). The null community was generated by randomly shuffling the original community 199 times with the independent swap algorithm by holding the number of OTUs in each sample and the number of samples, in which each OTU appears constant. The PAST program (Hammer et al., 2001) was used for these analyses. Both the Bray–Curtis and Raup-Crick algorithms were visualized on the 2D non-metric multidimensional scaling (NMDS) plots using the program PRIMER v7 (Clarke and Gorley, 2015).

Microbial Functional Prediction and Network Construction

The functional profiles of the microbial communities were predicted by using PICRUSt (Phylogenetic Investigation of Communities by Reconstruction of Unobserved States[2]; Langille et al., 2013) based on our 16S rRNA data. The 6,763 close-reference OTUs were picked up with Greengenes 13.5 in Galaxy[3] and their functional profiles were predicted from the Kyoto Encyclopedia of Genes and Genomes (KEGG) pathways (Kanehisa et al., 2014). The average nearest sequenced taxon index (NSTI, 0.182 $\pm$ 0.02 SD) of these samples was near that reported for soil communities (0.17 $\pm$ 0.02) (Langille et al., 2013). To identify functional and metabolic subsystems, whose relative frequencies (rel. freq. %) in treatments differed significantly from that in control samples based on KEGG, two-sided Welch's *t*-test (*p*-value) was used in the STAMP v2.01 software (Parks et al., 2014).

Potential interactions between co-occurring microbial taxa in control and treatment were determined by molecular ecological networks (MENs), which were constructed by using a random matrix theory (RMT)-based approach on an open-accessible comprehensive pipeline (Molecular Ecological Network Analysis Pipeline, MENAP[4], Deng et al., 2012). In the construction of the MENs, data standardization, Spearman's correlation estimation, adjacency matrix determination by RMT-based approach, network characterization, module detection, eigengene network analysis, and network comparisons were accomplished in order (Zhou et al., 2010). For each network, 100 corresponding random networks were then generated with the same network size and an average number of links. A Z-test was applied to determine the differences in the indices between the constructed and random networks. Cytoscape 3.4.0 was used for the network visualization.

Statistical Analysis

One-way ANOVA was used to identify the statistical significance of the pH value within each group along the incubation time. The differences of alpha diversity index, as well as the q-PCR abundance of bacteria, archaea, and methanogens, between the control and treatment groups was evaluated by Independent-Samples *t*-test (SPSS v20.0) at a single time point. Heatmaps representing the relative sequence abundances of bacterial OTUs among the samples were constructed using the "pheatmap" and "gplots" packages. Significantly enriched microbial taxa during the treatment was evaluated by Independent-Samples *t*-test (SPSS v20.0) at each time point. The relationships between relative abundance and incubation time for each group were then explored with four models, linear, quadratic, exponential, and logarithmic regression. The best models were selected based on Akaike's information criterion (AIC, Bozdogan, 1987). Permutational multivariate analysis of variance (PERMANOVA) (Anderson, 2001) was performed using the adonis function in the Vegan package (R studio, version 2.14.1, R Development Core Team, 2011) to evaluate the two-sided effects of *Microcystis* addition and incubation time on microbial community dynamics. The correlation between methane concentration and methanogen abundance was measured by Pearson correlation coefficient (*r*-value, SPSS v20.0).

Deposition of DNA Sequences

All the DNA sequences retrieved from the control and treatment groups at different sampling times were deposited at the European Nucleotide Archive and can be found under the Accession number PRJEB21014[5].

RESULTS

Decomposition of *Microcystis* Biomass and CH_4/CO_2 Production

Production of CO_2 and CH_4 is an indicator of *Microcystis* decomposition, and they continuously accumulated after *Microcystis* addition, with final concentrations of 27.10 ± 2.28 μmol cm^{-3} sediment and 21.87 ± 2.29 μmol cm^{-3} sediment, respectively (**Figures 1A,B**). The CH_4 production exhibited a sigmoidal curve with a lag phase (from day 0 to day 7), an exponential phase (from day 7 to day 17), and a stationary phase (from day 23 to day 30). CO_2 rapidly accumulated from the beginning to the stationary phase (day 17) and remained stable throughout the experiment. In the control group, the production of CO_2 and CH_4 was not detectable. The addition of *Microcystis* biomass caused no significant pH difference in

[2]http://picrust.github.com

[3]http://huttenhower.sph.harvard.edu/galaxy/

[4]http://ieg2.ou.edu/MENA

[5]https://www.ncbi.nlm.nih.gov/bioproject/?term=PRJEB21014

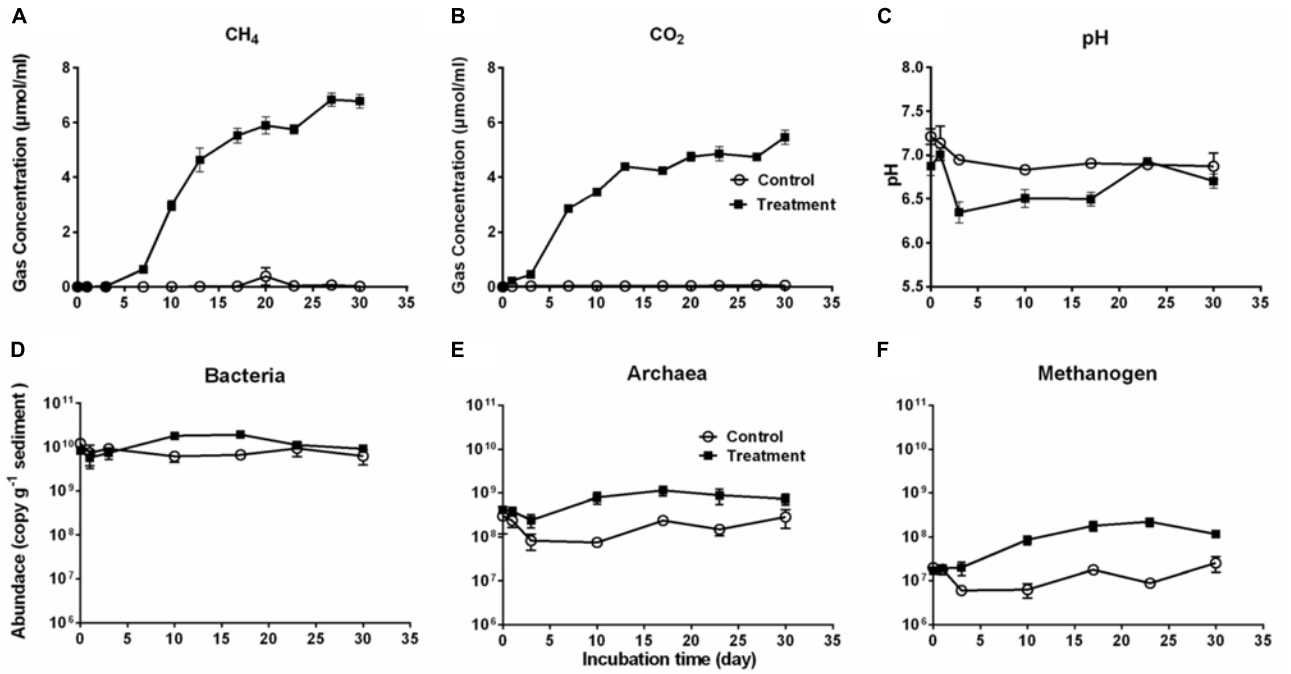

FIGURE 1 | The cumulative CH_4 **(A)** and CO_2 **(B)** production, pH **(C)** in the microcosms, and the abundances of Bacteria **(D)**, Archaea **(E)**, and Methanogens **(F)** during 30-day cultivation in the microcosm without (Control, open circles) or with (Treatment, solid squares) *Microcystis* addition. Microbial abundances were determined by qPCR method.

the treatment group (one-way ANOVA, $p > 0.5$), which seemed more stable (6.66–7.06) than the control (6.19–7.30) throughout the 30-day period (**Figure 1C**).

Accordingly, the bacterial abundance increased in the treatment group from day 1 to day 17, followed by a slight decrease, whereas it remained stable in the control group (**Figure 1D**). The abundance of Archaea and methanogens were significantly higher in the treatment group than in the control group (for both, Independent-Samples *t*-test, $p = 0.001$) (**Figures 1E,F**). As a subgroup of the total archaeal population, methanogens accounted for approximately 2–47% of the total Archaea. There was a close correlation between the abundance of methanogens and CH_4 production in the treatment group (Pearson's correlation $r = 0.88$, $p = 0.009$) but not in the control group (Pearson's correlation $r = -0.04$, $p = 0.931$).

Microbial Community Diversity

In total, 18,540 OTUs were detected and classified into 73 phyla and 1,011 genera. We observed significantly lower OTU numbers, Shannon index, and PD value in the treatment group than in the control group (**Table 1**). For the Chao1 estimates of microbial communities component, the treatment group was significantly lower than the control during the first 10 days of the incubation and then no significant difference was observed between the two groups (**Table 1**).

Non-metric multidimensional scaling analysis with whole samples revealed a clear separation of the microbial community composition (MCC) between the control and treatment groups (**Figure 2A**). The MCC in the treatment group significantly changed after *Microcystis* biomass addition (**Figure 2D** and **Supplementary Figure S1**, PERMANOVA, $F_{1,42} = 17.02$, $p < 0.001$), whereas in the control group, the MCC remained almost undisturbed (**Figure 2B**). Random sampling effects were primarily observed in the control samples during incubation, and there was no difference in β_{RC} before and after the incubation course (**Figures 2B,C**). However, the β_{RC} values of the treatment samples indicated that the MCC after *Microcystis* biomass addition was more similar to the start-point samples than expected by chance (**Figures 2D,E**). This observation suggests that the changes in β-diversity did not reflect the random influence of incubation on the microbial species and that the input organic matter provided a systematic ecological filter for the removal of some species from each community exposed to the substrate.

Microbial Succession During *Microcystis* Degradation

We observed systematic successions of the relative abundances of dominant OTUs (**Figure 3A**) during *Microcystis* degradation (**Figure 3B**). Based on the AIC test, microbial successions can be classified into three distinct types (**Figure 3C** and **Table 2**). (i) The type I group exhibited an exponential increase in abundance across time. Representative taxa included *Bacteroides*, *Syntrophomonas*, and unidentified genera from *Bacteroidales* and *Methanobacteriaceae*. (ii) The type II group exhibited a quadratic regression along time with positive

TABLE 1 | Comparison of microbial community diversity between microcosms without (Control) or with *Microcystis* (Treatment) addition during the incubation course.

	Observed OTUs		Shannon index		Chao1		PD	
Day	Control	Treatment	Control	Treatment	Control	Treatment	Control	Treatment
0	5654 (±808)	5277 (±420)	10.41 (±0.05)	9.42 (±0.31)	9571.52 (±1499.6)	9420.07 (±1563.9)	255.9 (±25.9)	246.8 (±18.37)
1	5150 (±110)	2242 (±245)**	10.33 (±0.001)	6.79 (±0.46)**	9084.26 (±47.2)	4524.54 (±143.5)**	243.0 (±4.5)	128.7 (±9.2)**
3	5324 (±823)	2435 (±607)**	10.30 (±0.16)	6.79 (±0.67)**	8739.55 (±2068.8)	4631.02 (±960.2)*	248.2 (±30.7)	135.9 (±25.5)**
10	5698 (±814)	2717 (±368)**	10.31 (±0.05)	7.22 (±0.58)**	11037.34 (±2743.7)	5489.47 (±736.8)**	259.9 (±27.1)	150.7 (±15.4)**
17	4722 (±95)	3239 (±509)*	10.13 (±0.05)	7.76 (±0.35)*	7656.56 (±343.8)	6261.16 (±1035.9)	223.9 (±5.2)	168.7 (±20.7)*
23	4917 (±690)	3021 (±497)*	10.36 (±0.09)	8.26 (±0.33)*	8028.89 (±743.8)	5284.65 (±1164.6)	231.7 (±26.5)	161.6 (±20.2)*
30	4644 (±314)	2823 (±464)*	10.13 (±0.001)	8.11 (±0.44)*	7695.61 (±299.5)	5088.86 (±809.4)	219.2 (±11.9)	152.7 (±18.6)*

*All data are listed as: mean (±SD). The statistical significance of Control and Treatment group was evaluated by the Independent-Samples t-test and statistical levels are indicated by asterisks of $p \leq 0.01$ (two asterisks, **), $p \leq 0.05$ (one asterisk, *) and $p > 0.05$ (no asterisk).*

binomial coefficients. Representative taxa included *Tepidibacter*, unidentified *Fusobacteriales*, *Lachnospiriaceae* and unidentified genera from *Clostridiaceae*. The relative abundance sharply increased after the addition of *Microcystis* and remained relatively stable during the incubation. (iii) The type III group exhibited a quadratic regression along time with negative binomial coefficients. Representative taxa included *Clostridium*, *Dechloromonas*, *Methanosarcina*, and *Hydrogenophaga*.

The differences in the MCC between the control and treatment groups were also significant at coarse taxonomic resolution. For example, at the phylum level, the relative abundances of the abundant phyla in the control group remained stable throughout the experiment. However, in the treatment group, the relative abundances of *Firmicutes* and *Bacteroidetes* immediately increased after *Microcystis* addition, whereas the relative abundances of *Proteobacteria* and *Cyanobacteria* (*Microcystis*) rapidly decreased (**Supplementary Figure S2**). At the family level, eight families in the treatment group, *Clostridiaceae*, *Lachnospiraceae*, *Peptostreptococcaceae*, *Ruminococcaceae*, *Veillonellaceae*, *Bacteroidaceae*, *Rikenellaceae*, and *Aeromonadaceae* immediately increased in abundance after *Microcystis* addition (**Figure 4**). Interestingly, five of these families belong to the same order of *Clostridiales*. The relative abundance of methanogens also steadily increased from 0.8% on day 0 to 3.8% on day 17 and remained stable thereafter (**Supplementary Figure S3**). In addition to the increasing abundance of methanogens, the families *Anaerolinaceae*, *Spirochaetaceae*, *Peptococcaceae*, and *Syntrophomonadaceae* also increased in abundance on day 17 (**Figure 4**).

Network Analyses and Community Functional Prediction

Based on the network analysis, 157 and 82 nodes were obtained from the control and Treatment, respectively. Positive correlations were predominant in both networks with rare negative correlations (**Figure 5**). The clustering coefficients and harmonic geodesic distance were significantly different from those of the corresponding random networks with the same network size and average number of links (**Table 3**), indicating that the MENs in both the control and the treatment showed small-world characteristics. In comparison with the control, MENs in the treatment generally had significantly higher connectivity, higher clustering efficiencies, and fewer modules (**Table 3**). Focusing on the microbial associations within the treatment group showed that three clusters were distinct in the treatment network (**Figure 5**). Cluster I, including OTUs affiliated with the phyla *Proteobacteria-Acidobacteria-Chloroflexi*, showed co-occurrence among most nodes within it, and Cluster II, including the phyla *Bacteroidetes-Firmicutes*, showed an overall negative connection with Cluster I. Furthermore, *Microcystis* formed a co-exclusive pattern with other bacterial taxa in Cluster II, and Cluster III, including methanogens, *Syntrophomonas* and *Longilinea*, was independent of Cluster I and II.

Functional prediction indicated that17 subpathways I belong to four major categories were significantly different between control and treatment (**Figure 6A**, $p < 0.01$). Nine of them were significantly enriched in the microcosms of the treatment group, including membrane transport, replication and repair, carbohydrate metabolism, amino acid metabolism, transcription, metabolism of cofactors and vitamins, nucleotide metabolism, enzyme families, and metabolism of other amino acids. The dynamics of relative frequencies along time are shown in **Figure 6B**. Five of the nine subpathways I belonged to the category metabolism. In subpathway II, we observed increased frequency of genes distributed in diverse pathways in the treatment group (**Supplementary Figure S4**). For example, within the carbohydrate metabolism, six metabolic pathways showed higher frequency in the treatment samples: fructose and mannose metabolism, galactose metabolism, starch and sucrose metabolism, the pentose phosphate pathway, pentose and glucuronate interconversions, and amino sugar and nucleotide sugar metabolism.

DISCUSSION

Efficient Production of CH_4 From Anoxic Decomposition of *Microcystis*

Blooming *Microcystis* form scum, which is massively deposited onto lake sediments, resulting in rapid oxygen depletion on the surface sediment (Xing et al., 2011). A positive correlation between the biomass of *Microcystis* and CH_4 production has

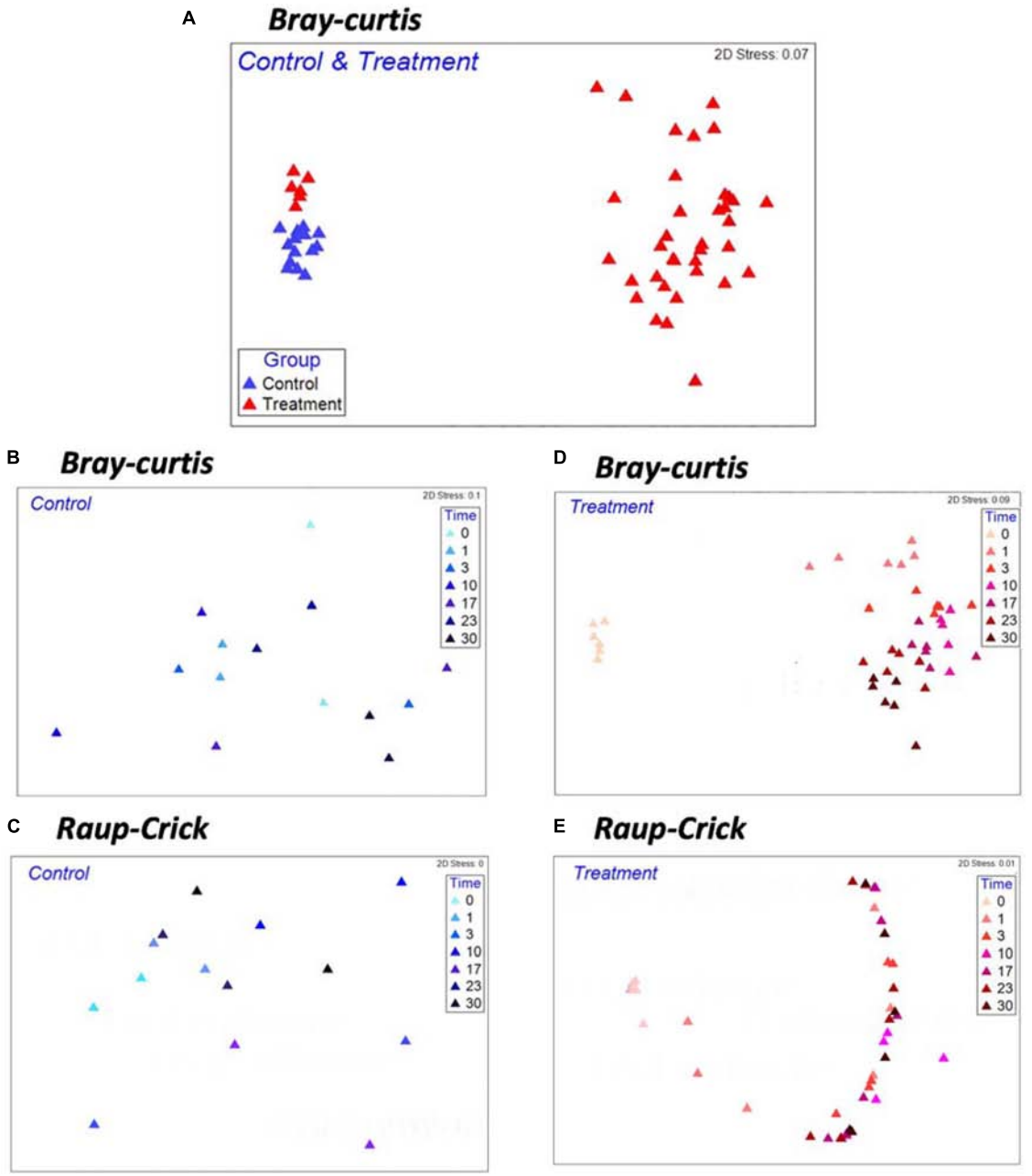

FIGURE 2 | Non-metric multi-dimensional scaling (NMDS) ordinations based on Bray–Curtis Index **(A,B,D)** and β_{RC} **(C,E)** for Control and Treatment examining the effects of *Microcystis* biomass addition on patterns of microbial community compositions. Each symbol in the NMDS plot represents a sample collected during the incubation.

been observed in the littoral zones of hypereutrophic Lake Taihu, suggesting that the biomass of *Microcystis* is actually transformed to CH_4 in the field (Wang et al., 2006). The observations of this study further demonstrated that sedimentary *Microcystis* blooms could enhance the accumulation of CO_2 and CH_4 in the anaerobic sediment, and this process occurred instantly after *Microcystis* biomass addition.

In the present study, approximately 14.56 mL of CH_4 (equivalent to 7.8 mg carbon, estimated with the gas density of 0.717 g/L at standard condition) was produced from the initial 25 mg dry-weight of *Microcystis* biomass (equivalent to 9.5 mg carbon with chemical formula $C_{106}H_{263}O_{110}N_{16}P$, molecular weight 3350 g/mol) during the 30-day anaerobic incubation, indicating an efficient transformation from algal organic carbon to greenhouse gases (~82.5% conversion efficiency). Based on water content of 99% in living *Microcystis* cells, 1 kg of wet algal biomass could be degraded with ~5.82 L of CH_4 gas production. In Lake Taihu, cyanobacterial blooms might reproduce at a

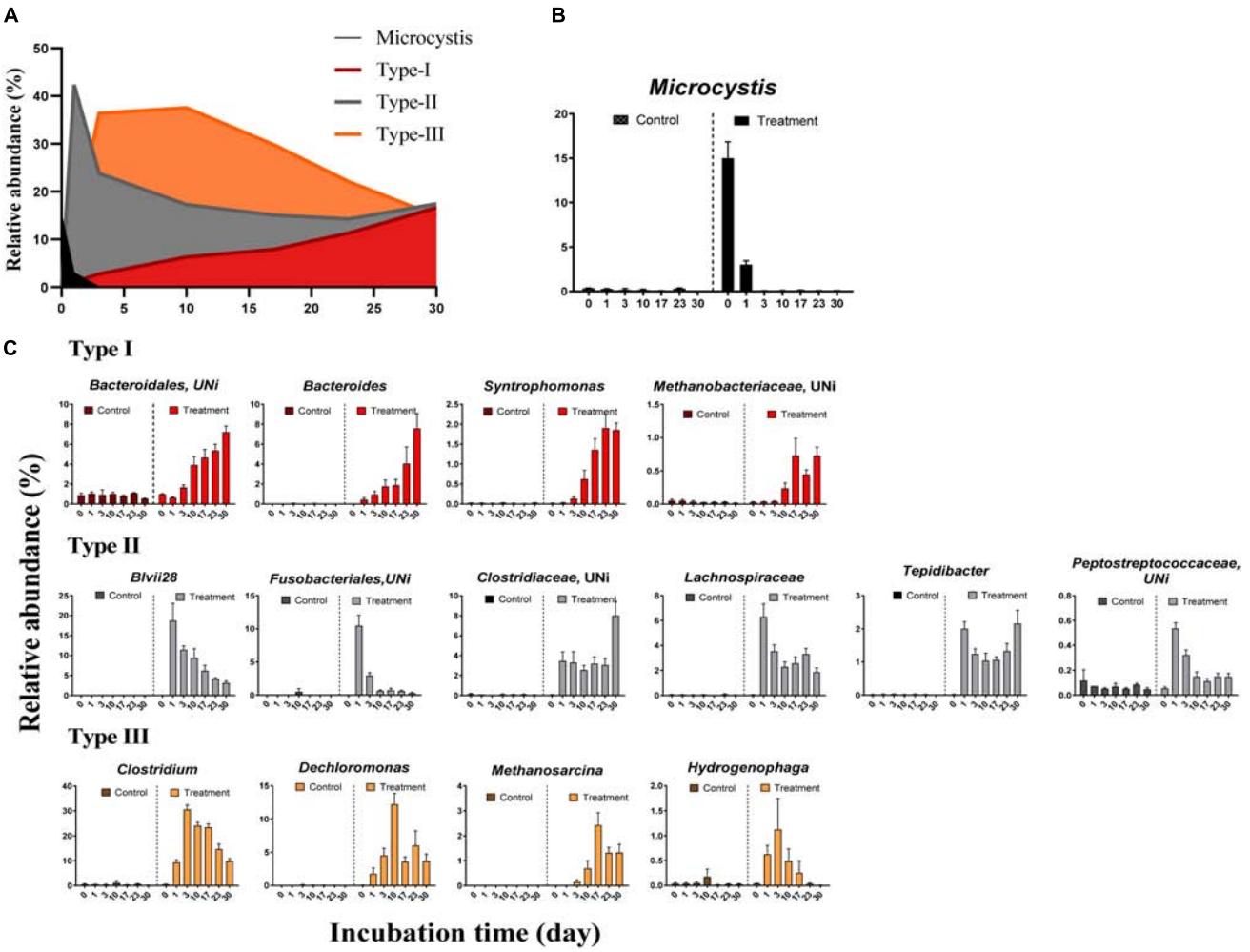

FIGURE 3 | The relative abundance of *Microcystis* and three distinct microbial groups during the incubation. **(A)** The overview of relative abundance of *Microcystis* and three bacterial groups in Treatment samples; **(B)** the decay of *Microcystis* along the time; **(C)** variation of the relative abundance for representative genera in each group. The colors in subfigure of **(C)** are corresponding to those in panel **(A)**.

TABLE 2 | The dynamics of the significantly enriched groups were simulated by the multiple regression models.

Group	Best models[a]	r^2	*p*-value	Equation	Constants
Bacteroidales	Exponential/linear/quadric	0.69	<0.001	Type I: Exponential $y = a \times e^{\wedge}T \pm b$	*a*:0.21, *b*:0.79
Bacteroides	Exponential/quadric	0.47	<0.001		*a*:0.22, *b*:−0.44
Methanobacteriaceae	Exponential/linear/quadric	0.40	<0.001		*a*:0.02, *b*:0.00
Syntrophomonas	Exponential/quadric	0.68	<0.001		*a*:0.07, *b*:−0.08
Clostridiaceae	Quadric/exponential	0.25	<0.01	Type II: Quadric $y = aT^2 \pm bT \pm c$	*a*:1.71, *b*:−6.28, *c*:7.59
Tepidibacter	Quadric	0.36	<0.001		*a*:0.60, *b*:−2.54, *c*:3.53
Blvii28	Logarithmic/linear/quadric	0.53	<0.001		*a*:0.57, *b*:−7.56, *c*:22.83
Fusobacteriales	Quadric	0.81	<0.001		*a*:2.36, *b*:−12.96, *c*:17.68
Lachnospiraceae	Quadric/logarithmic	0.48	<0.001		*a*:0.86, *b*:−4.79, *c*:8.97
Peptostreptococcaceae	Quadric	0.80	<0.001		*a*:0.09, *b*:−0.49, *c*:0.84
Clostridium	Quadric	0.74	<0.001	Type III: Quadric $y = aT^2 \pm bT \pm c$	*a*:−10.72, *b*:43.23, *c*:−13.44
Dechloromonas	Quadric	0.30	<0.01		*a*:−3.43, *b*:15.03, *c*:−7.73
Hydrogenophaga	Exponential/linear/quadric	0.21	<0.05		*a*:−0.34, *b*:0.67, *c*:−0.40
Methanosarcina	Linear/logarithmic/quadric	0.39	<0.001		*a*:−0.08, *b*:0.99, *c*:−0.81

[a]*The best models were selected based on the minimum Akaike's Information Criterion (AIC) value. If the difference of AIC value between two models <2, there is no difference in their performance. T in the equations means incubation time (days).*

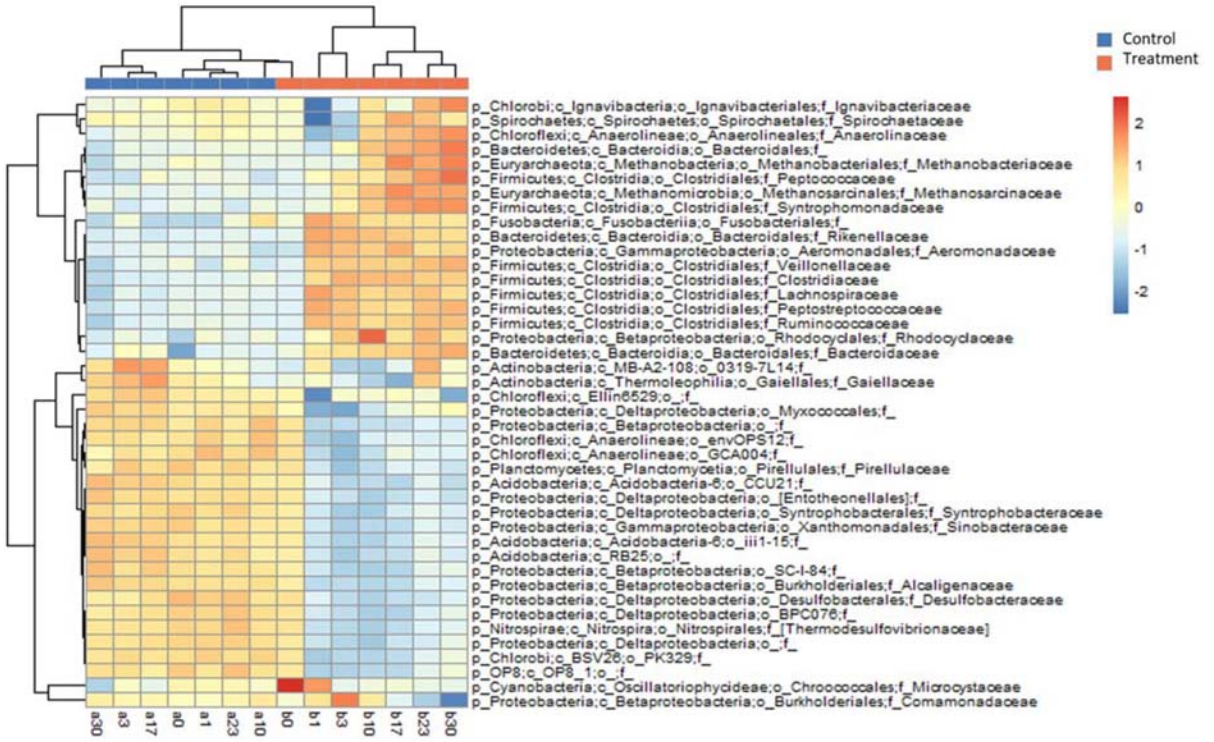

FIGURE 4 | Heatmap diagram showing relative abundances of the top 25 families selected from Control and Treatment (a total of 42 families). Upper dendrogram shows community similarity among samples and left dendrogram depicts clustering of families by co-occurrence.

rate of at least 0.25 million kilograms (weight wet) per year during the whole bloom season (personal communication with Dr. Hongtao Duan). In this case, 1.46 million liters of CH_4 (equivalent to 1043 kg) would be generated under anoxic or anaerobic conditions. Please note that this estimate does not take into account the contribution of other organic matter in sediments to the methane formation under anoxic and anaerobic conditions. The real lake ecosystems are much more complex and dynamic than the microcosms built up in this study; therefore, the conversion efficiency from cyanobacterial biomass to CH_4 needs to be further evaluated before its application. In any case, methane accounts for approximately 20% of the greenhouse effect (Wuebbles and Hayhoe, 2002; Sessions et al., 2009), significantly contributing to global warming. The present study evidently demonstrates that, under hypertrophic conditions, accumulated CH_4 induced by cyanobacterial blooms is an important component of methane budgets in local lakes as well as in the drainage basin (Bastviken et al., 2004b, 2008, 2011).

Distinct Microbial Succession During Anaerobic Degradation of *Microcystis*

Although decomposition of organic material under anaerobic conditions is generally assumed to include hydrolysis, acidogenesis, syntrophic acetogenesis, and methanogenesis (Schink, 2002), the composition and dynamics of the microbial communities involved in *Microcystis* biodegradation is far from well-documented. In the present study, we investigated the MCC based on Illumina Miseq sequencing, enabling the detection of the distinct pattern of microbial successions during *Microcystis* degradation.

During the hydrolysis phase, *Bacteroides* spp. and an unidentified genus in *Bacteroidales* continuously increased in abundance (type I group). The superb ability of these bacteria for degradation of polymers, particularly various types of polysaccharides (Wexler, 2007; Ravcheev et al., 2013), initiated flourishing during *Microcystis* degradation. The bacteria taxa belong to type II, such as the *Blvii28* group (*Rikenellaceae*), *Fusobacteriales, Lachnospiraceae*, and *Peptostreptococcaceae*, rapidly responded to *Microcystis* biomass addition and peaked at Day 1. Most of them were considered as hydrolytic fermenting bacteria in the degradation of complex polysaccharides (Tholozan et al., 1992; Bennett and Eley, 1993; Schink, 2002; Zhou L. et al., 2015). Some of the 16S rRNA sequences from *Blvii28* were highly similar (∼99% identity) with that of *Acetobacteroides hydrogenigenes*, which is involved in the conversion of carbohydrates to acetate and CO_2 (Su et al., 2014). *Clostridium* and *Dechloromonas* from the type III group also strongly increased in abundance during the initial days of incubation. Bacteria in the genus *Clostridium* are commonly known as hydrolytic (saccharolytic and proteolytic) and fermentative bacteria that can ferment various polysaccharides to volatile fatty acids, H_2, and CO_2 (Ruan et al., 2014; Deng et al., 2015). The importance of *Clostridium*

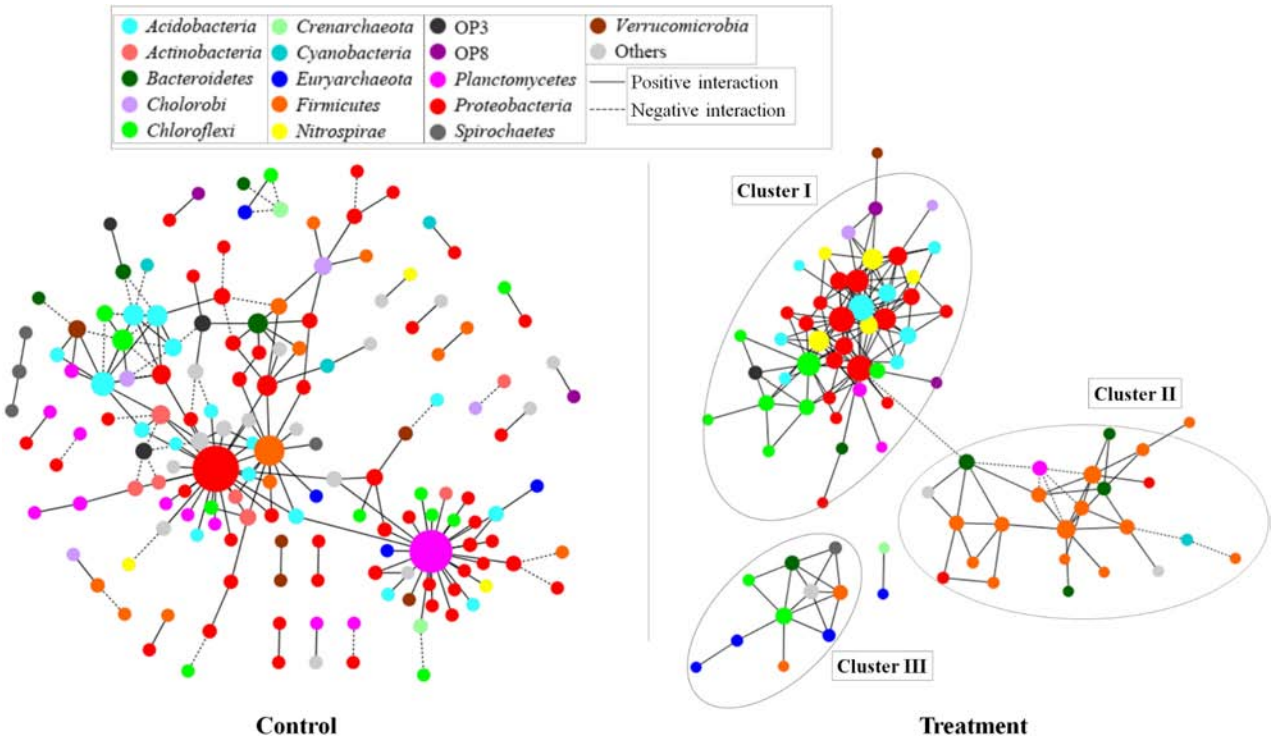

FIGURE 5 | Networks based on correlation analysis of co-occurring bacterial and archaeal genera in a 30-day incubation with (treatment) or without (control) *Microcystis* addition. A connection between nodes stands for a statistically significant positive (a Spearman's $\rho > 0.8$ and $p < 0.01$, red line) or negative (b Spearman's $\rho < -0.8$ and $p < 0.01$, blue line) correlation. The size of each node is proportional to the number of connections (that is, degree). The nodes were colored by taxonomy, the top 20 abundant phyla are shown in different colors and all the others were in gray.

species during the anaerobic degradation of organic material in freshwater environments has previously been identified (Mallet et al., 2004; Xing et al., 2011), and *Dechloromonas* is frequently detected in various degradation and nitrate reduction processes of monoaromatic compounds (Coates et al., 2001).

The increase in the abundance of syntrophic bacteria after Day 10 reflected the accumulation of fatty acid intermediates during *Microcystis* biomass decomposition. Syntrophic acetogens (in type I group), such as *Syntrophomonas*, was significantly promoted during *Microcystis* degradation, suggesting that these species are more likely to utilize the intermediates generated from *Microcystis* hydrolysis. *Syntrophomonas* species utilize a variety of fatty acids ranging from C4 to C8 or other longer fatty acids and coexist with butyrate-producing bacteria (McInerney et al., 1981, 2008).

Methanogens, such as *Methanobacteriaceae* and *Methanosarcina* species, were significantly enriched during the degradation. The most dominant *Methanosarcina* reached the highest abundance on day 17. Species within *Methanosarcina* can use all the methanogenic substrates, H_2 and CO_2, methanol, methylamine, methyl sulfides, and acetate, except for format (Galagan et al., 2002; Lambie et al., 2015). The increase in the abundance of these methanogens suggested that diverse substrates were available for CH_4 synthesis.

Overall, hydrolytic-fermenting bacteria (such as *Blvii28* group, *Clostridium*, and *Bacteroidales* species), syntrophic acetogens (*Syntrophomonas*), and methanogens (*Methanobacteriaceae* and *Methanosarcina*) were significantly enriched, and their succession patterns suggested that these microbial groups might

TABLE 3 | Topological properties of the empirical molecular ecological networks (MENs) for the control and treatment group and their associated random MENs.

	Group	Control	Treatment
Empirical networks	Similarity threshold (St)	0.86	0.86
	Network size (*n*)	157	82
	R^2 of power law	0.873	0.788
	Harmonic geodesic distance (HD)	2.127	2.768
	Average connectivity (avgK)	2.328	4.561
	Average clustering coefficient (avgCC)	0.127	0.373
	Modularity	0.729 (24)	0.581 (6)
	Transitivity (Trans)	0.105	0.36
Random networks	Harmonic geodesic distance (HD ± SD)	2.557 ± 0.262	2.915 ± 0.127
	Average clustering coefficient (avgCC ± SD)	0.042 ± 0.014	0.101 ± 0.019
	Modularity ± SD	0.646 ± 0.012	0.384 ± 0.012

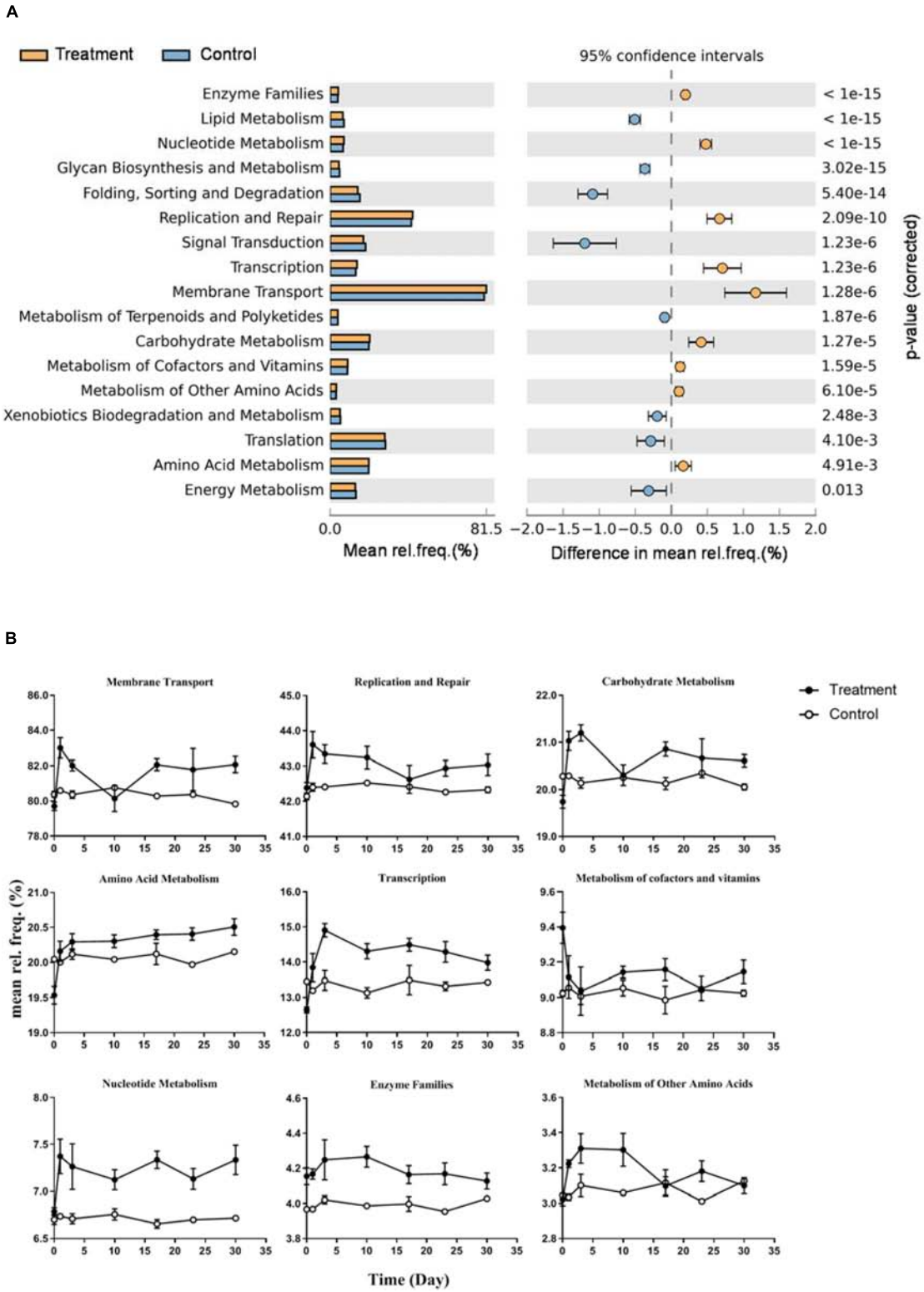

FIGURE 6 | Differences of predicted microbial community function between Control and Treatment throughout the incubation. **(A)** KEGG subpathway I with significant different relative frequency (rel. freq. %) picked up by STAMP with a two-sided Welch's *t*-test of a symptomatic confidence intervals (0.95). Subpathways overrepresented in the Treatment which have a positive value of proportions are indicated by orange filled circles and those overrepresented in the Control are indicated by blue filled circles. **(B)** Nine line charts showing specific dynamics of the overrepresented pathways in Treatment group (corresponding to orange filled circles in panel **A**) during the incubation.

possess unique substrate utilization preferences and could synergistically function during the degradation of *Microcystis*.

Predicted Community Function and Inter-Specific Connections

Studies have shown that ecosystem properties greatly depend on biodiversity due to differences in the functional characteristics of organisms present in the ecosystem (Bell et al., 2005; Hooper et al., 2005). Based on diversity-stability relationships (Naeem and Li, 1997), the lower α-diversity (Shannon and PD index) in the treatment group indicated a weaker anti-interference ability of the microbial community during *Microcystis* degradation. Moreover, good consistency was found between the realistic Bray–Curtis dissimilarity and the probabilistic β_{RC} index for the treatment, which suggested the relative importance of deterministic (niche-related) processes in their microbial community assembly. Therefore, the input of organic matter imposed as a systematic ecological filtering to enhance partial members with specific functional characteristics in the community (Zhang et al., 2018).

During the anaerobic decomposition of *Microcystis*, the relative frequency and dominance of metabolic pathways significantly varied at each phase, uncovering the non-overlapping niches of the functional groups in the process. Mannose is one of the most abundant mono-saccharides within the *Microcystis* cells (Jürgens et al., 1989). The relative frequency of fructose and mannose metabolism pathways was significantly higher in the treatment group, which suggested that mannose in the biomass could be effectively transformed during the decomposition. Not only that, the enriched amino acid metabolism and secreted peptidases suggested that *Microcystis* biomass could provide plenty of carbon and nitrogen sources for the co-existing microbiomes. Furthermore, the phosphotransferase system plays an important role in the transportation and phosphorylation of numerous mono-saccharides, disaccharides, amino sugars, and other sugar derivatives through the bacterial cell membrane (Deutscher et al., 2006). The higher frequency of the phosphotransferase system in the treatment group indicated the transportation of those small-molecule intermediates following initial extracellular hydrolysis.

In the ecological processes, microorganisms interact with each other and therefore form a complex network within the communities. MENs construction is an ideal way to characterize the species co-occurring pattern in an ecosystem. In general, positive links could be attributed to niche overlap or cross-feeding, and negative links could be attributed to competition or antagonism (Faust and Raes, 2012). In the present study, co-existing taxa in the treatment group was much more connected and clustered than those in the control group, which implied that the decomposition of *Microcystis* or utilization of *Microcystis* substrates required inter-specific cooperation among various functional groups. The lower modularity in treatment group indicated a less resistance of the system to disturbance. Therefore, the enhanced connection in the community might be an adaptive mechanism in response to massive disturbance, i.e., the organic matter impulse.

Taken together, the community dynamics, predicted functions and network analysis reflected the transition of the microbial communities toward a low diverse, high connected and high effective situation for the nutrient assimilation during algal carbon/nitrogen transformation.

DATA AVAILABILITY STATEMENT

The datasets generated for this study can be found in NCBI, https://www.ncbi.nlm.nih.gov/bioproject/?term=PRJEB21014.

AUTHOR CONTRIBUTIONS

Y-FW did the experiment and data analysis. PX provided most of the idea of data treatment and wrote the manuscript. SL and QW did the experiment design and revised the manuscript.

FUNDING

This study was supported by the National Natural Science Foundation of China (41621002, 31670505, and 31722008), Key Research Program of Frontier Sciences, CAS (Grant Number QYZDJ-SSW-DQC030), and the Youth Innovation Promotion Association of CAS (Grant Number 2014273).

SUPPLEMENTARY MATERIAL

The Supplementary Material for this article can be found online at: https://www.frontiersin.org/articles/10.3389/fmicb.2019.02474/full#supplementary-material

REFERENCES

Anderson, M. J. (2001). A new method for non-parametric multivariate analysis of variance. *Austral. Ecol.* 26, 32–46. doi: 10.1111/j.1442-9993.2001.01070.pp.x

Bastviken, D., Cole, J. J., Pace, M. L., and Tranvik, L. (2004a). Methane emissions from lakes: dependence of lake characteristics, two regional assessments, and a global estimate. *Global. Biogeochem. Cycles* 18:GB4009.

Bastviken, D., Persson, L., Odham, G., and Tranvik, L. (2004b). Degradation of dissolved organic matter in oxic and anoxic lake water. *Limnol. Oceanogr.* 49, 109–116. doi: 10.4319/lo.2004.49.1.0109

Bastviken, D., Cole, J. J., Pace, M. L., and Van de Bogert, M. C. (2008). Fates of methane from different lake habitats: connecting whole-lake budgets and CH4 emissions. *J. Geophys. Res.* 113:G02024.

Bastviken, D., Tranvik, L. J., Downing, J. A., Crill, P. M., and Enrich-Prast, A. (2011). Freshwater methane emissions offset the continental carbon sink. *Science* 331:50. doi: 10.1126/science.1196808

Bell, T., Newman, J. A., Silverman, B. W., Turner, S. L., and Lilley, A. K. (2005). The contribution of species richness and composition to bacterial services. *Nature* 436, 1157–1160. doi: 10.1038/nature03891

Bennett, K. W., and Eley, A. (1993). *Fusobacteria* - new taxonomy and related diseases. *J. Med. Microbiol.* 39, 246–254. doi: 10.1099/00222615-39-4-246

Bozdogan, H. (1987). Model selection and Akaike's Information Criterion (AIC): the general theory and its analytical extensions. *Psychometrika* 52, 345–370. doi: 10.1007/bf02294361

Bru, D., Martin-Laurent, F., and Philippot, L. (2008). Quantification of the detrimental effect of a single primer-template mismatch by real-time PCR using the 16S rRNA gene as an example. *Appl. Environ. Microbiol.* 74, 1660–1663. doi: 10.1128/AEM.02403-07

Caporaso, J. G., Kuczynski, J., Stombaugh, J., Bittinger, K., Bushman, F. D., Costello, E. K., et al. (2010). QIIME allows analysis of high-throughput community sequencing data. *Nat. Methods* 7, 335–336.

Chase, J. M., Kraft, N. J. B., Smith, K. G., Vellend, M., and Inouye, B. D. (2011). Using null models to disentangle variation in community dissimilarity from variation in α-diversity. *Ecosphere* 2, 1–11.

Chen, M., Chen, F., Xing, P., Li, H., and Wu, Q. L. (2010). Microbial eukaryotic community in response to *Microcystis* spp. bloom, as assessed by an enclosure experiment in lake Taihu. *FEMS Microbiol. Ecol.* 74, 19–31. doi: 10.1111/j.1574-6941.2010.00923.x

Clarke, K., and Gorley, R. N. (2015). *PRIMER v7: user Manual/Tutorial*. Plymouth: PRIMER-E Ltd, 269.

Coates, J. D., Chakraborty, R., Lack, J. G., O'Connor, S. M., Cole, K. A., Bender, K. S., et al. (2001). Anaerobic benzene oxidation coupled to nitrate reduction in pure culture by two strains of *Dechloromonas*. *Nature* 411, 1039–1043. doi: 10.1038/35082545

Cole, J. J., Caraco, N. F., Kling, G. W., and Kratz, T. K. (1994). Carbon-dioxide supersaturation in the surface waters of lakes. *Science* 265, 1568–1570. doi: 10.1126/science.265.5178.1568

Deng, L., Mori, Y., Sermsathanaswadi, J., Apiwatanapiwat, W., and Kosugi, A. (2015). Cellulose hydrolysis ability of a *Clostridium thermocellum* cellulosome containing small-size scaffolding protein CipA. *J. Biotechnol.* 212, 144–152. doi: 10.1016/j.jbiotec.2015.08.016

Deng, Y., Jiang, Y. H., Yang, Y. F., He, Z. L., Luo, F., and Zhou, J. Z. (2012). Molecular ecological network analyses. *BMC Bioinformatics* 13:113. doi: 10.1186/1471-2105-13-113

Deutscher, J., Francke, C., and Postma, P. W. (2006). How phosphotransferase system-related protein phosphorylation regulates carbohydrate metabolism in bacteria. *Microbiol. Mol. Biol. Rev.* 70, 939–1031. doi: 10.1128/mmbr.00024-06

Edgar, R. C. (2010). Search and clustering orders of magnitude faster than BLAST. *Bioinformatics* 26, 2460–2461. doi: 10.1093/bioinformatics/btq461

Edgar, R. C. (2013). UPARSE: highly accurate OTU sequences from microbial amplicon reads. *Nat. Methods* 10, 996–998. doi: 10.1038/nmeth.2604

Edgar, R. C., Haas, B. J., Clemente, J. C., Quince, C., and Knight, R. (2011). UCHIME improves sensitivity and speed of chimera detection. *Bioinformatics* 27, 2194–2200. doi: 10.1093/bioinformatics/btr381

Faust, K., and Raes, J. (2012). Microbial interactions: from networks to models. *Nat. Rev. Microbiol.* 10, 538–550. doi: 10.1038/nrmicro2832

Galagan, J. E., Nusbaum, C., Roy, A., Endrizzi, M. G., Macdonald, P., FitzHugh, W., et al. (2002). The genome of *M. acetivorans* reveals extensive metabolic and physiological diversity. *Genome Res.* 12, 532–542. doi: 10.1101/gr.223902

Graue, J., Engelen, B., and Cypionka, H. (2012). Degradation of cyanobacterial biomass in anoxic tidal-flat sediments: a microcosm study of metabolic processes and community changes. *ISME J.* 6, 660–669. doi: 10.1038/ismej.2011.120

Hammer, Ø, Harper, D. A., and Ryan, P. D. (2001). PAST: paleontological statistics software package for education and data analysis. *Palaeontol. Electron.* 4, 1–9.

Hooper, D. U., Chapin, F. S. III, Ewel, J. J., Hector, A., Inchausti, P., Lavorel, S., et al. (2005). Effects of biodiversity on ecosystem functioning: a consensus of current knowledge. *Ecol. Monogr.* 75, 3–35. doi: 10.1111/brv.12110

Jürgens, U. J., Martin, C., and Weckesser, J. (1989). Cell-wall constituents of Microcystis sp. PCC 7806. *FEMS Microbiol. Lett.* 53, 47–51. doi: 10.1016/0378-1097(89)90364-9

Kanehisa, M., Goto, S., Sato, Y., Kawashima, M., Furumichi, M., and Tanabe, M. (2014). Data, information, knowledge and principle: back to metabolism in KEGG. *Nucleic Acids Res.* 42, D199–D205. doi: 10.1093/nar/gkt1076

Karlson, A. M. L., Nascimento, F. J. A., and Elmgren, R. (2008). Incorporation and burial of carbon from settling cyanobacterial blooms by deposit-feeding macrofauna. *Limnol. Oceanogr.* 53, 2754–2758. doi: 10.4319/lo.2008.53.6.2754

Krinner, G. (2003). Impact of lakes and wetlands on boreal climate. *J. Geophys. Res.* 108:D16.

Lambie, S. C., Kelly, W. J., Leahy, S. C., Li, D., Reilly, K., McAllister, T. A., et al. (2015). The complete genome sequence of the rumen methanogen *Methanosarcina barkeri* CM1. *Stand. Genomic Sci.* 10:57. doi: 10.1186/s40793-015-0038-5

Langille, M. G., Zaneveld, J., Caporaso, J. G., McDonald, D., Knights, D., Reyes, J. A., et al. (2013). Predictive functional profiling of microbial communities using 16S rRNA marker gene sequences. *Nat. Biotechnol.* 31, 814–821. doi: 10.1038/nbt.2676

Li, H., Xing, P., and Wu, Q. L. (2012). Characterization of the bacterial community composition in a hypoxic zone induced by *Microcystis* blooms in lake Taihu. *China. FEMS Microbiol. Ecol.* 79, 773–784. doi: 10.1111/j.1574-6941.2011.01262.x

Li, Z., Haynes, R., Sato, E., Shields, M. S., Fujita, Y., and Sato, C. (2014). Microbial community analysis of a single chamber microbial fuel cell using potato wastewater. *Water Environ. Res.* 86, 324–330. doi: 10.2175/106143013x13751480308641

Mallet, C., Basset, M., Fonty, G., Desvilettes, C., Bourdier, G., and Debroas, D. (2004). Microbial population dynamics in the sediments of a eutrophic lake (Aydat. *Microb. Ecol.* 48, 66–77. doi: 10.1007/s00248-003-2017-4

McInerney, M. J., Bryant, M. P., Hespell, R. B., and Costerton, J. W. (1981). Syntrophomonas wolfei gen. nov. sp. nov, an anaerobic, syntrophic, fatty-acid oxidizing bacterium. *Appl. Environ. Microbiol.* 41, 1029–1039.

McInerney, M. J., Struchtemeyer, C. G., Sieber, J., Mouttaki, H., Stams, A. J. M., Schink, B., et al. (2008). Physiology, ecology, phylogeny, and genomics of microorganisms capable of syntrophic metabolism. *Ann. N. Y. Acad. Sci.* 1125, 58–72. doi: 10.1196/annals.1419.005

Naeem, S., and Li, S. B. (1997). Biodiversity enhances ecosystem reliability. *Nature* 390, 507–509. doi: 10.1038/37348

Narihiro, T., Kim, N. K., Mei, R., Nobu, M. K., and Liu, W. T. (2015). Microbial community analysis of anaerobic reactors treating soft drink wastewater. *PLoS One* 10:e0119131. doi: 10.1371/journal.pone.0119131

Nunoura, T., Oida, H., Toki, T., Ashi, J., Takai, K., and Horikoshi, K. (2006). Quantification of mcrA by quantitative fluorescent PCR in sediments from methane seep of the nankai trough. *FEMS Microbiol. Ecol.* 57, 149–157. doi: 10.1111/j.1574-6941.2006.00101.x

Paerl, H. W., Fulton, R. S., Moisander, P. H., and Dyble, J. (2001). Harmful freshwater algal blooms, with an emphasis on *Cyanobacteria*. *Sci. World J.* 1, 76–113. doi: 10.1100/tsw.2001.16

Parks, D. H., Tyson, G. W., Hugenholtz, P., and Beiko, R. G. (2014). STAMP: statistical analysis of taxonomic and functional profiles. *Bioinformatics* 30, 3123–3124. doi: 10.1093/bioinformatics/btu494

R Development Core Team (2011). *R: A Language and Environment for Statistical Computing*. Vienna: R Foundation for Statistical Computing.

Ravcheev, D. A., Godzik, A., Osterman, A. L., and Rodionov, D. A. (2013). Polysaccharides utilization in human gut bacterium *Bacteroides thetaiotaomicron*: comparative genomics reconstruction of metabolic and regulatory networks. *BMC Genomics* 14:873. doi: 10.1186/1471-2164-14-873

Ruan, Z., Wang, Y., Zhang, C., Song, J., Zhai, Y., Zhuang, Y., et al. (2014). Clostridium huakuii sp. nov., an anaerobic, acetogenic bacterium isolated from methanogenic consortia. *Int. J. Syst. Evol. Micr.* 64, 4027–4032. doi: 10.1099/ijs.0.062711-0

Schink, B. (1997). Energetics of syntrophic cooperation in methanogenic degradation. *Microbiol. Mol. Biol. Rev.* 61, 262–280.

Schink, B. (2002). Synergistic interactions in the microbial world. *Antonie Van Leeuwenhoek* 81, 257–261.

Sessions, A. L., Doughty, D. M., Welander, P. V., Summons, R. E., and Newman, D. K. (2009). The continuing puzzle of the great oxidation event. *Curr. Biol.* 19, R567–R574. doi: 10.1016/j.cub.2009.05.054

Shao, K., Gao, G., Chi, K., Qin, B., Tang, X., Yao, X., et al. (2013). Decomposition of *Microcystis* blooms: implications for the structure of the sediment bacterial community, as assessed by a mesocosm experiment in lake Taihu. *China J. Basic Microbiol.* 53, 549–554. doi: 10.1002/jobm.201100532

Shi, L., Cai, Y., Yang, H., Xing, P., Li, P., Kong, L., et al. (2009). Phylogenetic diversity and specificity of bacteria associated with *Microcystis aeruginosa* and other cyanobacteria. *J. Environ. Sci.* 21, 1581–1590. doi: 10.1016/s1001-0742(08)62459-6

Shu, D. T., He, Y. L., Yue, H., and Wang, Q. Y. (2015). Microbial structures and community functions of anaerobic sludge in six full-scale wastewater treatment

plants as revealed by 454 high-throughput pyrosequencing. *Bioresour. Technol.* 186, 163–172. doi: 10.1016/j.biortech.2015.03.072

Steinberg, L. M., and Regan, J. M. (2008). Phylogenetic comparison of the methanogenic communities from an acidic, oligotrophic fen and an anaerobic digester treating municipal wastewater sludge. *Appl. Environ. Microbiol.* 74, 6663–6671. doi: 10.1128/AEM.00553-08

Su, X. L., Tian, Q., Zhang, J., Yuan, X. Z., Shi, X. S., Guo, R. B., et al. (2014). Acetobacteroides hydrogenigenes gen. nov., sp. nov., an anaerobic hydrogen-producing bacterium in the family Rikenellaceae isolated from a reed swamp. *Int. J. Syst. Evol. Micr.* 64, 2986–2991. doi: 10.1099/ijs.0.063917-0

Suzuki, M. T., Taylor, L. T., and Delong, E. F. (2000). Quantitative analysis of small-subunit rRNA genes in mixed microbial populations. *Appl. Environ. Microbiol.* 66, 4605–4614. doi: 10.1128/aem.66.11.4605-4614.2000

Tang, X., Li, L., Shao, K., Wang, B., Cai, X., Zhang, L., et al. (2015). Pyrosequencing analysis of free-living and attached bacterial communities in meiliang bay. *Can. J. Microbiol.* 61, 22–31. doi: 10.1139/cjm-2014-0503

Tholozan, J. L., Touzel, J. P., Samain, E., Grivet, J. P., Prensier, G., and Albagnac, G. (1992). Clostridium neopropionicum sp. nov., a strict anaerobic bacterium fermenting ethanol to propionate through acrylate pathway. *Arch. Microbiol.* 157, 249–257. doi: 10.1007/bf00245158

Wang, H., Lu, J., Wang, W., Yang, L., and Yin, C. (2006). Methane fluxes from the littoral zone of hypertrophic Taihu lake. *J. Geophys. Res.* 111:D17109.

Wexler, H. M. (2007). *Bacteroides*: the good, the bad, and the nitty-gritty. *Clin. Microbiol. Rev.* 20, 593–621. doi: 10.1128/cmr.00008-07

Wilms, R., Kopke, B., Sass, H., Chang, T. S., Cypionka, H., and Engelen, B. (2006). Deep biosphere-related bacteria within the subsurface of tidal flat sediments. *Environ. Microbiol.* 8, 709–719. doi: 10.1111/j.1462-2920.2005.00949.x

Wuebbles, D. J., and Hayhoe, K. (2002). Atmospheric methane and global change. *Earth-Sci. Rev.* 57, 177–210. doi: 10.1016/s0012-8252(01)00062-9

Xing, P., Guo, L., Tian, W., and Wu, Q. L. (2011). Novel *Clostridium* populations involved in the anaerobic degradation of *Microcystis* blooms. *ISME J.* 5, 792–800. doi: 10.1038/ismej.2010.176

Zhai, C., Song, S., Zou, S., Liu, C., and Xue, Y. (2013). The mechanism of competition between two bloom-forming *Microcystis* species. *Freshw. Biol.* 58, 1831–1839. doi: 10.1093/jxb/erx027

Zhang, Q., Goberna, M., Liu, Y., Cui, M., Yang, H., Sun, Q., et al. (2018). Competition and habitat filtering jointly explain phylogenetic structure of soil bacterial communities across elevational gradients. *Environ. Microbiol.* 20, 2386–2396. doi: 10.1111/1462-2920.14247

Zhang, X. J., Chen, C., Ding, J., Hou, A., Li, Y., Niu, Z., et al. (2010). The 2007 water crisis in Wuxi. *J. Hazard. Mater.* 182, 130–135. doi: 10.1016/j.jhazmat.2010.06.006

Zhou, J., Deng, Y., Luo, F., He, Z., Tu, Q., and Zhi, X. (2010). Functional molecular ecological networks. *mBio* 1:e00169-10. doi: 10.1128/mBio.00169-10

Zhou, L., Fang, L., Sun, Y., Su, Y., and Zhu, W. (2015). Effects of the dietary protein level on the microbial composition and metabolomic profile in the hindgut of the pig. *Anaerobe* 38, 61–69. doi: 10.1016/j.anaerobe.2015.12.009

Zhou, X., Fornara, D., Wasson, E. A., Wang, D., Ren, G., Christie, P., et al. (2015). Effects of 44 years of chronic nitrogen fertilization on the soil nitrifying community of permanent grassland. *Soil Biol. Biochem.* 91, 76–83. doi: 10.1016/j.soilbio.2015.08.031

Conflict of Interest: The authors declare that the research was conducted in the absence of any commercial or financial relationships that could be construed as a potential conflict of interest.

Copyright © 2019 Wu, Xing, Liu and Wu. This is an open-access article distributed under the terms of the Creative Commons Attribution License (CC BY). The use, distribution or reproduction in other forums is permitted, provided the original author(s) and the copyright owner(s) are credited and that the original publication in this journal is cited, in accordance with accepted academic practice. No use, distribution or reproduction is permitted which does not comply with these terms.

frontiers in Microbiology

ORIGINAL RESEARCH
published: 07 November 2019
doi: 10.3389/fmicb.2019.02560

Trophic Status Is Associated With Community Structure and Metabolic Potential of Planktonic Microbiota in Plateau Lakes

Mengyuan Shen[1,2], Qi Li[1], Minglei Ren[3], Yan Lin[1], Juanping Wang[1], Li Chen[4], Tao Li[1]* and Jindong Zhao[1,2,5]*

[1] State Key Laboratory of Freshwater Ecology and Biotechnology, Institute of Hydrobiology, Chinese Academy of Sciences, Wuhan, China, [2] University of Chinese Academy of Sciences, Beijing, China, [3] State Key Laboratory of Lake Science and Environment, Nanjing Institute of Geography and Limnology, Chinese Academy of Sciences, Nanjing, China, [4] Yunnan Key Laboratory of Plateau Geographical Processes and Environment Change, School of Tourism and Geography, Yunnan Normal University, Kunming, China, [5] State Key Laboratory of Protein and Plant Genetic Engineering, College of Life Sciences, Peking University, Beijing, China

OPEN ACCESS

Edited by:
Petra M. Visser, University of Amsterdam, Netherlands

Reviewed by:
Jianjun Wang, Nanjing Institute of Geography and Limnology (CAS), China
Patricia M. Valdespino-Castillo, Lawrence Berkeley National Laboratory, United States

***Correspondence:**
Li Chen
chenli5311@163.com
Tao Li
litao@ihb.ac.cn

Specialty section:
This article was submitted to Aquatic Microbiology, a section of the journal Frontiers in Microbiology

Received: *04 July 2019*
Accepted: *23 October 2019*
Published: *07 November 2019*

Citation:
Shen M, Li Q, Ren M, Lin Y, Wang J, Chen L, Li T and Zhao J (2019) Trophic Status Is Associated With Community Structure and Metabolic Potential of Planktonic Microbiota in Plateau Lakes. Front. Microbiol. 10:2560. doi: 10.3389/fmicb.2019.02560

Microbes in various aquatic ecosystems play a key role in global energy fluxes and biogeochemical processes. However, the detailed patterns on the functional structure and the metabolic potential of microbial communities in freshwater lakes with different trophic status remain to be understood. We employed a metagenomics workflow to analyze the correlations between trophic status and planktonic microbiota in freshwater lakes on Yun-Gui Plateau, China. Our results revealed that microbial communities in the eutrophic and mesotrophic-oligotrophic lake ecosystems harbor distinct community structure and metabolic potential. Cyanobacteria were dominant in the eutrophic ecosystems, mainly driving the processes of aerobic respiration, fermentation, nitrogen assimilation, nitrogen mineralization, assimilatory sulfate reduction and sulfur mineralization in this ecosystem group. Actinobacteria, Proteobacteria (Alpha-, Beta-, and Gammaproteobacteria), Verrucomicrobia and Planctomycetes, occurred more often in the mesotrophic-oligotrophic ecosystems than those in the eutrophic ecosystems, and these taxa potentially mediate the above metabolic processes. In these two groups of ecosystems, a difference in the abundance of functional genes involved in carbohydrate metabolism, energy metabolism, glycan biosynthesis and metabolism, and metabolism of cofactors and vitamins significantly contribute to the distinct functional structure of microbiota from surface water. Furthermore, the microbe-mediated metabolic potentials for carbon, nitrogen and sulfur transformation showed differences in the two ecosystem groups. Compared with the mesotrophic-oligotrophic ecosystems, planktonic microbial communities in the eutrophic ecosystems showed higher potential for aerobic carbon fixation, fermentation, methanogenesis, anammox, denitrification, and sulfur mineralization, but they showed lower potential for aerobic respiration, CO oxidation, nitrogen fixation, and assimilatory

sulfate reduction. This study offers insights into the relationships of trophic status to planktonic microbial community structure and its metabolic potential, and identifies the main taxa responsible for the biogeochemical cycles of carbon, nitrogen and sulfur in freshwater lake environments.

Keywords: metagenomics, trophic status, taxonomic diversity, community structure, metabolic potential, planktonic microbiota, lake ecosystem, Cyanobacterial bloom

INTRODUCTION

The microbiota in aquatic ecosystems plays an important role in elemental cycling and global energy fluxes (Falkowski et al., 2008; Clark et al., 2018; Cronan, 2018). The relations between the taxonomic structure of microbial communities in aquatic environments and complex environmental factors such as trophic status (Llirós et al., 2014; Wan et al., 2017), seasons (Zhu et al., 2019), elevation gradient (Li H. et al., 2017), and salinity (Eiler et al., 2014) have been well studied. However, little is known about the correlations of these factors with community functions. Therefore, improving our knowledge about the link between taxonomy and function of microbial communities can contribute to a better understanding of the response mechanisms of microbiota to key environmental changes and gradients (Logue et al., 2015; Arora-Williams et al., 2018).

The Yun-Gui Plateau Lake Zone is the smallest of the five lake-zones in China (Ma et al., 2011). About half of the lakes in this zone, accounting for 90% of the lake area, are located in Yunnan Province which is a biodiversity hotspot (Zhou et al., 2019), and these lakes are sensitive areas for recording regional ecology and global climate change (Li et al., 2015). The plateau lake ecosystems are vulnerable and not easily restored once damaged because of the relatively low rate of water exchange and resilience, and the steep and little-developed lakeshores (Wang and Dong, 1998; Liao et al., 2016). In the past few decades, some of these lakes have been seriously damaged by intensification of human activities, leading to deterioration of water quality and degradation of ecosystem function (Li W. et al., 2017; Liu et al., 2017; Gao et al., 2018; Wu et al., 2019). Eutrophication is one of the biggest of such challenges; it changes the diversity and composition of lake organisms and poses a serious threat to ecosystem service function (Liu et al., 2012; Shi et al., 2016; Dong et al., 2018). To date, most studies have concentrated on microbial communities in sediment from Yun-Gui Plateau lakes with different trophic levels (Bai et al., 2012; Dai et al., 2016; Yang et al., 2017a,b). Only a few studies have focused on microbiota in lake surface waters, in which the microorganisms are more sensitive to lake eutrophication than those in sediment (Zeng et al., 2019). Bacterioplankton compositions in eutrophic Lake Dianchi (Wen et al., 2012; Dai et al., 2016; Han et al., 2016), mesotrophic Lake Erhai (Hu et al., 2013) and oligotrophic Lake Haixihai (Dai et al., 2016) were investigated by analyzing 16S rRNA gene sequences. Dai et al. (2016) and Han et al. (2016) demonstrated that trophic status may play important roles in shaping the taxonomic structure of bacterioplankton communities in the Yun-Gui Plateau freshwater lakes. Nevertheless, the relations of lake trophic status to the functional structure of the microbial communities and the ecological processes within freshwater systems have seldom been examined.

Because of decreased cost and increased throughput of sequencing technology (Neufeld, 2017; Quince et al., 2017), the powerful approach of metagenomics is now widely applied in studies of microbial communities from many diverse environments, including soil (Diamond et al., 2019), sediment (Vavourakis et al., 2018), hosts (Rothschild et al., 2018), seawater (Sunagawa et al., 2015), and freshwater (Arora-Williams et al., 2018). A curated set of metabolic marker genes was used to quantify the genetic potential for microbe-mediated biogeochemical cycles in a meromictic lake by Lauro et al. (2011). This method has since been widely used in different types of ecosystem, including salt marsh (Dini-Andreote et al., 2016), sediments (Hamilton et al., 2016), an estuary (Kieft et al., 2018), and a stratified euxinic lake (Llorens-Marès et al., 2015). Therefore, besides the characterization of community structure and reconstruction of genomes in individual samples, comparative analysis of the samples at multiple time points or of parallel samples across different environmental gradients using metagenomics facilitates the elucidation of complex microbial processes in the community, which are difficult to simulate in the laboratory.

In this study, we applied shotgun metagenomics to examine the taxonomic and functional structure of surface-water microbial communities from five freshwater lakes on the Yun-Gui Plateau. These lakes had four trophic levels: eutrophic, meso-eutrophic, oligo-mesotrophic and oligotrophic. The relative abundance of metabolic marker genes was used to assess the genetic potential for each conversion step of the carbon, nitrogen, and sulfur cycles in the freshwater lake ecosystems. We explored the links between microbial composition and metabolic potential, and inferred the response mechanisms of microbe-mediated carbon, nitrogen, and sulfur cycles to lake trophic-level changes. We addressed the following two questions: (a) How does trophic status relate to distinct taxonomic and functional structures of planktonic microbial communities? (b) To what extent is it related to trophic status that each conversion step of microbe-mediated biogeochemical cycling pathways?

MATERIALS AND METHODS

Study Sites and Sampling

To investigate the relationship of trophic status and the microbial communities in a plateau lake ecosystem, five lakes with different trophic status were selected in Yunnan Province, China

(**Supplementary Figure S1** and **Table 1**). Dianchi Lake (DCL) and Xingyun Lake (XYL) are eutrophic lakes, turbid with abundant algae (Yang et al., 2010; Gao et al., 2018). Erhai Lake (EL) has undergone alteration from mesotrophic to eutrophic conditions owing to excessive usage of chemical fertilizers and severe destruction of wetland vegetation along the lakeshore (Hu et al., 2014; Wang et al., 2015a). Fuxian Lake (FXL) is oligo-mesotrophic (Cui et al., 2008). Lugu Lake (LGL) is oligotrophic, and clear with abundant submerged plants (Liao et al., 2015). Water samples were collected from the surface layer (0–0.5 m depth) of each lake between June 2014 and September 2017. Our study focused on the planktonic microbes in water samples, and the methods of sample collection are described in **Supplementary Table S1** and **Supplementary Figure S2**. Two samples (DCL-1 and XYL-1) from eutrophic lakes during the algal bloom period were filtered to enrich the "Cyanobacteria-attached" fraction (CA, >64 μm) (Li et al., 2011), and the other samples were collected with mixed-size fractions (>0 μm, >0.2 μm, and 0.2–64 μm). The volume of water sampling water was determined by the abundance of the planktonic microbial community and the size-fraction of filtration to ensure sufficient biomass for metagenomic DNA extraction. Collected biomass was stored at −80°C until processing. The sampling dates, sampling locations and physicochemical properties of lake water are shown in **Table 1**. A flow diagram describing the data analysis process is shown in **Supplementary Figure S3**, and scripts used in this study are available in a public GitHub repository[1].

DNA Extraction, Sequencing, and Assembly

Total community DNA extraction was conducted following a modified phenol-chloroform method from Xie et al. (2016). Metagenome sequencing was performed on an Illumina Genome Analyzer IIx, and yielded > 40 GB per library (>276 M reads, 150 bp paired-end, insert size ∼300 bp). Reads from the same lake were then co-assembled with MEGAHIT assembler (Li et al., 2016) (v.1.1.1, with preset meta-large). Coding sequences (CDSs) were predicted using Prodigal v2.6.3 (-p meta) in all contigs > 500 bp long (Hyatt et al., 2012). In each sample, clean reads were aligned back to the contigs using Bowtie2 (Langmead and Salzberg, 2012) and counted by featureCounts (Smyth et al., 2013). The number of reads for each CDS was normalized to "transcripts per million" (TPM) as described elsewhere (Ribicic et al., 2018).

Taxonomic and Functional Assignment of Metagenome

Two main approaches were chosen for taxonomic annotation, involving assembly free and assembly based methods (Quince et al., 2017). The clean reads from each sample were classified for community composition analysis by using the assembly free approach. The Kaiju classifier (Menzel et al., 2016) was used to assign metagenomic reads against the subset of NCBI-NR protein database (bacteria, archaea, virus) (*E*-value 0.05). Then, the kaijuReport program was used to count the phylum-level, class-level, and order-level abundance of each sample. In addition, the predicted CDSs were taxonomically assigned to filter eukaryotic contamination by using the assembly based method. Diamond (Buchfink et al., 2015) was used to compare predicted protein sequences against the NR database (version Apr 2, 2019; blastp -f 100 -e 0.00001 –sensitive –top 3), and then the LCA algorithm in MEGAN6 (blast2lca -f DAA -m BlastP) was performed for CDSs to produce a taxonomic classification (Huson et al., 2016).

Functional analysis was performed based on microbial CDSs. The GhostKoala server[2] was used to functionally annotate each CDS by giving KEGG Orthology (KO) accession numbers (Kanehisa et al., 2016). Then, the annotated functional CDSs were extracted and assigned to KEGG metabolism of level 2 categories for subsequent distribution analysis of CDSs with metabolism. The TPM values of CDSs from the same functional category were added together.

The analysis of metabolic potential focused on three elemental biogeochemical cycles (carbon, nitrogen, and sulfur) for the four trophic lake types. To infer the genetic potential of each lake ecosystem, the relative abundance of metabolic marker genes (KO accession numbers) identified in previous studies was calculated as described elsewhere (Lauro et al., 2011; Llorens-Marès et al., 2015; Dini-Andreote et al., 2016; Hamilton et al., 2016; Kieft et al., 2018). In this study, 50 marker genes were used, representing 20 microbe-mediated elemental cycling processes (**Supplementary Table S2**).

Statistical Analysis

Phylum-level read count data matrices and functional abundance matrices were Hellinger-transformed, respectively. Unweighted pair group method with arithmetic mean (UPGMA) clustering analysis and principal coordinate analysis (PCoA) were used to display and compare the patterns of taxonomic structure and metabolic function among different samples. In addition, the significant variance ($P < 0.01$) between groups of samples was assessed by permutational multivariate analysis of variance (PERMANOVA). The correlation between taxonomic and functional composition was calculated by the Mantel test (9999 permutations). Similarity percentage (SIMPER) analysis determined the contributions from each metabolic function group to PERMANOVA reported differences. Based on the taxonomic annotation of the metagenomic reads results at the order-level, the alpha-diversity of each community was calculated using the 'diversity()' function.

Environmental data were normalized to *z*-scores before calculating distance. Euclidean distance was used for environmental data, and Bray-Curtis distance was used for compositional data. Based on these distance matrices, Mantel correlations between environmental data and taxonomic and functional compositional data were calculated, respectively. Furthermore, pairwise Pearson's correlation analysis was carried out to examine the relationship between environmental variables. Pearson's correlation analyses between all environmental factors and the relative abundances of the functional categories were

[1] https://github.com/shenmengyuan/Yun-Gui_plateau_lake

[2] www.kegg.jp/ghostkoala/

TABLE 1 | Description of the samples used in this study.

Sample ID		DCL-1	DCL-2	XYL-1	XYL-2	EL-1	EL-2	FXL-1	FXL-2	LGL-1	LGL-2
Physicochemical properties	Date	20160618	20170925	20160607	20170924	20140614	20170721	20151210	20170924	20160518	20170812
	Location	24.96°N 102.65°E	24.95°N 102.66°E	24.38°N 102.78°E	24.36°N 102.79°E	25.94°N 100.16°E	25.90°N 100.15°E	24.57°N 102.89°E	24.38°N 102.85°E	27.71°N 100.78°E	27.71-27.73°N 100.76-100.80°E
	WT (°C)	22.13	21.80	25.08	23.80	23.50	22.20	16.91	22.40	15.19	20.87
	PH	8.45	8.63	8.88	9.45	9.51	8.66	8.04	8.94	8.18	8.76
	TP (mg/L)	0.544	0.351	0.468	0.581	0.032*	0.031	0.022	0.020	0.024	0.013
	TN (mg/L)	5.815	4.816	5.181	4.151	0.57*	0.593	0.220	0.168	0.048	<0.103
Geographic information#	Lake	Lake Dianchi		Lake Xingyun		Lake Erhai		Lake Fuxian		Lake Lugu	
	Trophic status	Eutrophic		Eutrophic		Mesoeutrophic		Oligomesotrophic		Oligotrophic	
	Basin	The Yangtze River		The Pearl River		The Lancang River, Jinsha, and Yuanjiang Rivers		The Pearl River		The Yangtze River	
	Water level (m a.s.l.)	1887.4		1722		1971		1721		2690.75	
	Area (km^2)	308.6		34.7		249.8		211		48.25	
	Average water depth (m)	4.4		7		10.5		87		40.3	
	Maximum depth(m)	6		11		21.5		155		93.5	
	Volume (10^8 m^3)	11.69		1.84		25.31		189		19.53	
	Lake type	Shallow		Shallow		Shallow		Deep		Deep	
Metagenomic survey	Clean data (Gbps)	50.60	58.91	50.38	64.12	63.43	63.98	60.49	53.01	51.85	41.43
	Number of clean reads	337,333,394	392,760,680	335,888,304	427,445,344	422,842,886	426,528,358	403,286,044	353,402,296	345,656,552	276,184,372
	Number of contigs (>500 bps)	2,381,193		2,318,367		3,929,297		3,368,043		1,604,121	
	Number of predicted CDS	3,775,712		3,059,812		6,560,747		5,229,770		2,840,196	
	% Predicted CDS with taxonomic group assignment	60.22		44.12		57.69		40.85		58.89	
	% Predicted CDS with KOs assignment	26.45		20.66		27.24		20.23		27.91	
	Bacteria (%, based on reads from metagenomic data)	23.31	33.11	14.66	41.15	13.65	18.79	19.69	12.55	22.61	28.97
	Archaea (%, based on reads from metagenomic data)	0.04	0.02	0.01	0.01	0.02	0.03	0.03	0.02	0.03	0.02
	Viruses (%, based on reads from metagenomic data)	0.74	0.09	0.03	0.03	0.06	0.14	0.28	0.08	0.39	0.11

*TN, total nitrogen concentration (mg/L); TP, total phosphorus concentration (mg/L); WT, water temperature; *Data source: Cao et al. (2018). #Data source: Cui et al. (2008); Yang et al. (2010), Hu et al. (2014); Liao et al. (2015), Wang et al. (2015a,b), Ding et al. (2017); Gao et al. (2018).*

performed using the 'corr.test' function. Redundancy analysis (RDA) was performed to investigate the relationships between environmental variables and microbial communities. Based on Monte Carlo permutation tests (n = 999 permutations), only the significant environmental variables were accepted ($p < 0.05$) for RDA. In addition, to avoid col-linearity among environmental variables, high variance inflation factors (VIF > 20) were eliminated. Environmental variables significantly explaining community variations were selected by using forward model selection with the 'ordistep' function, and then the variance explained by each key variable was evaluated by variation partitioning. All of the above statistical analyses were performed using the vegan (Oksanen et al., 2019) and psych (Revelle, 2019) packages in R version 3.5.3.

STAMP software was used to test for differences in microbial community structure and relative abundance of KOs between groups, as described elsewhere (Castro-Nallar et al., 2015). White's non-parametric t-test in STAMP was applied to compare the relative abundance of phyla, orders and KOs between two groups of lake samples (White et al., 2009). A percentile bootstrapping method (10,000 replications) was used to estimated confidence intervals, and the false discovery rate (FDR) in multiple testing was corrected with the Storey's FDR method ($p < 0.05$) (Storey et al., 2004). The trophic preference KO lists were then uploaded to the online functional pathway mapping tool iPath3 (Interactive Pathways Explorer v3[3]) for visualization. KOs that differentially segregated across groups were identified from 50 metabolic marker genes by random forest analysis with Boruta feature selection (R package Boruta, maxRuns = 1000).

RESULTS

Diversity of Microbial Communities

On average, 372.13 million high-quality sequence reads with an average length of 150 bp were obtained from 10 samples from the five lakes with different trophic levels located on the Yun-Gui Plateau (**Table 1**). The taxonomic assignment of the microbial communities was performed using short reads-based methods. A minority of metagenomic reads could be classified (12–41%). The bacterial domain was the main taxonomic component of the microbial community in all lake samples.

A Bray–Curtis matrix of samples was used to generate a dendrogram using the UPGMA clustering method. The samples from the five lakes were classified into two groups (**Figure 1A**). Group I included the four samples from Dianchi Lake and Xingyun Lake. These two lakes were hypertrophic. Group II was a complex cluster, consisting of the six samples from EL, FXL, and LGL. PCoA showed that the classification of lake samples was highly consistent with that by UPGMA analysis (**Figure 1B**). Furthermore, the PCoA plot indicated that trophic status (eutrophic or mesotrophic-oligotrophic conditions) explained 75.73% of the change in beta-diversity, that was, the total variation in planktonic microbial community structure between groups (PERMANOVA, Pseudo-F = 15.867, $p < 0.01$). In addition, compared with the samples in Group II, the samples in Group I had lower taxonomic alpha-diversity (Wilcoxon test, $p < 0.01$) (**Figure 1C** and **Supplementary Table S3**).

Taxonomic Structure of Microbial Communities

Taxonomic annotation showed that the structural composition of the microbial community at the phylum level varied between Groups I and II (**Figure 1A** and **Supplementary Table S4a**). We compared the taxonomic structures of these two groups at the phylum-level (**Figure 1D** and **Supplementary Table S5a**). Hits to the bacterial phylum Cyanobacteria were more abundant in Group I metagenomic datasets (on average 73.26 ± 13.11%, q-value < 0.01, difference in mean proportions [DM] 62.65%) than in Group II datasets, and Actinobacteria were dominant in Group II (on average 28.07 ± 5.15%, q-value < 0.05, DM −26.22%). Other notable taxa in Group II were Alphaproteobacteria (on average 15.79 ± 5.32%, q-value < 0.05, DM −7.91%), Betaproteobacteria (on average 15.34 ± 2.32%, q-value < 0.05, DM −9.50%), Bacteroidetes (on average 10.58 ± 3.07%, q-value < 0.05, DM −5.77%), Verrucomicrobia (on average 7.02 ± 4.27%, q-value < 0.05, DM −6.77%), Planctomycetes (on average 3.97 ± 3.02%, q-value < 0.05, DM −3.00%), and Gammaproteobacteria (on average 3.95 ± 2.78%, q-value < 0.05, DM −2.32%).

Moreover, we also identified significant relative abundance differences between the groups at the order-level (**Supplementary Figure S4** and **Supplementary Table S4b**). Of the 209 orders recovered, 16 (7.66%) were overrepresented in one of the two groups (q-value < 0.05, absolute difference between means > 1%) (**Figure 1D** and **Supplementary Table S5b**). For example, we observed a higher proportion of reads affiliated to Chroococcales (phylum Cyanobacteria, q-value < 0.05, DM 73.79%) in Group I than in Group II; conversely, more metagenomic reads of Burkholderiales were detected in Group II than that in Group I (Betaproteobacteria, q-value < 0.05, DM −13.37%).

Functional Structure of Microbial Communities

Assembly of ∼213 Gbps metagenomic sequences yielded ∼14 M contigs (18 Gbps), and ∼24 M predicted CDSs (excluding eukaryotic CDSs) across the five sampled lakes. Between 40.85 and 60.22% of CDSs were assigned to a taxonomic group, and between 20.23 and 27.91% were annotated to KOs (**Table 1**). PCoA based on selected KOs involved in metabolism revealed a distinct separation of functional structures between Groups I and II (**Figure 2A**) (PERMANOVA, Pseudo-F = 18.358, $p < 0.01$), with a similar ordination pattern to the taxonomic structure (**Figure 1B**). Interestingly, there was a significant correlation between the functional and taxonomic structures inferred from metagenomic reads (Mantel's test, Pearson r = 0.964; $p < 0.001$).

Carbohydrate metabolism was the most abundant functional category, with relative abundance range from 22.31 to 25.34%

[3]https://pathways.embl.de/

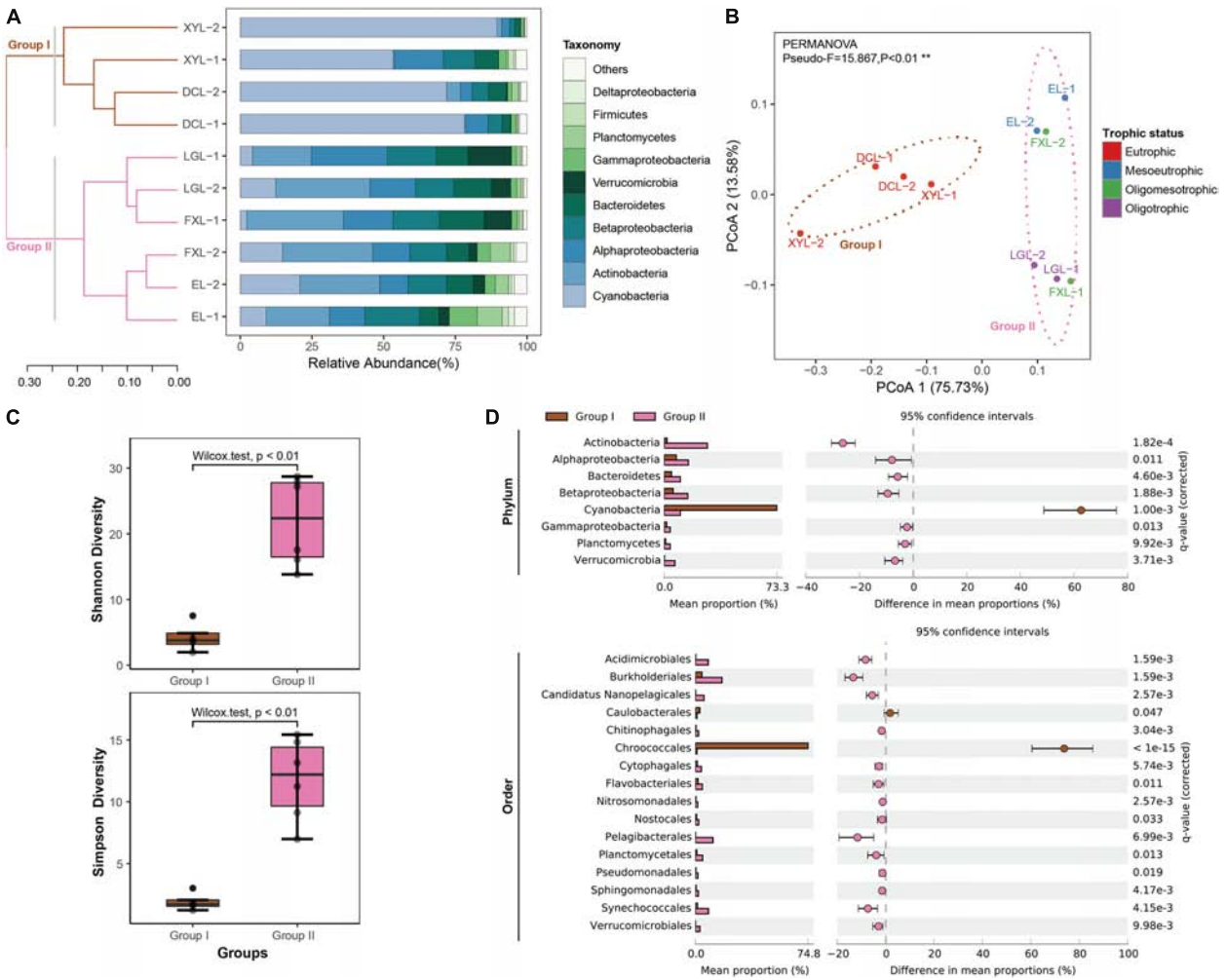

FIGURE 1 | Taxonomic structure and diversity of planktonic microbial communities in lakes exhibiting different trophic status. **(A)** The taxonomic structure across samples. The relative abundance of reads grouped at the phylum-level is shown for each metagenome library. Phyla with relative abundance not in the top ten are shown as "Other." Hierarchical clustering (UPGMA) based on Bray–Curtis dissimilarity matrices. See detailed information in **Supplementary Table S4a**. **(B)** PCoA based on complete taxonomic community profiles with 75% confidence ellipses (phylum-level taxonomic annotations). Significant clusters are indicated by dashed lines (PERMANOVA, 9999 permutations, $P < 0.01$). **(C)** Boxplots figure shows the range of different alpha diversity indices. The box represents the lower quartile, median, and upper quartile. See detailed information in **Supplementary Table S3**. **(D)** The extended error bar plot shows that phyla and orders significantly over−/−under-represented in Group I and Group II samples (see **Supplementary Tables S5a,b**). The difference in mean proportions and the corrected *p*-value of significance are also pointed out.

within samples (**Figure 2B**). The second most abundant functional category was amino acid metabolism (18.81–21.17%), followed by energy metabolism (13.25–18.41%). SIMPER analysis was performed to determine the categories making a significant contribution to the differences between groups. Based on the average abundance of functional categories in Groups I and II, we found that functional categories of carbohydrate metabolism, energy metabolism, glycan biosynthesis and metabolism, and metabolism of cofactors and vitamins (SIMPER ratio > 2.0%, FDR padj < 0.01) were different between Group I and Group II samples. A total of 1395 significantly different KOs were successfully mapped onto the KEGG reference metabolic pathway map (**Supplementary Figure S5** and **Supplementary Table S5c**), which indicated that the interrelation of the microbial taxa both within and between these various categories of metabolism deserves further study.

Correlations Between Environmental Factors and Community Composition

The environmental characteristics of the five lakes are displayed in **Table 1**. The five lakes involved in this study represented a wide range of trophic status, including oligotrophic, oligo-mesotrophic, meso-eutrophic and eutrophic ecosystems. They range from 0.048 to 5.815 mg/L total nitrogen (TN), and 0.013 to 0.581 mg/L total phosphorus (TP). Furthermore, TN was positively correlated with TP (Pearson's test $R^2 > 0.95, p < 0.001$) (**Figure 3A**). Water temperature (WT) and PH were positively

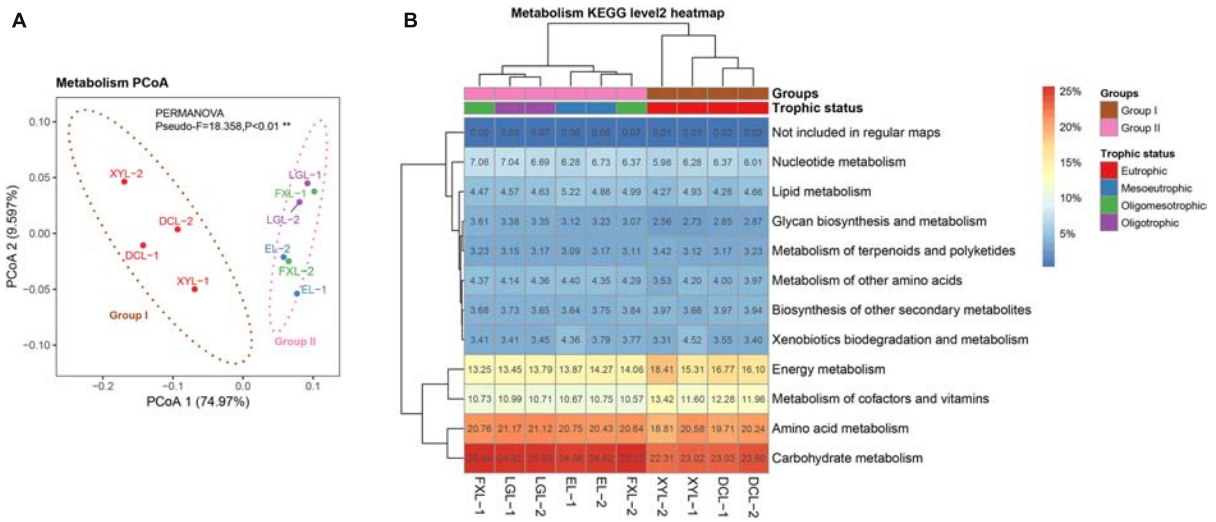

FIGURE 2 | Functional structure of planktonic microbial communities in lakes with different trophic status. **(A)** PCoA based on selected KOs involved in the metabolism pathway with 90% confidence ellipses. **(B)** Heatmap representing the functional clustering of the predicted CDS from the metagenomic data based on the KEGG categories of metabolism level 2. Hierarchical clustering (UPGMA) based on Bray–Curtis dissimilarity matrices.

correlated with TN and TP, and most of lake geography factors (average water depth, volume and water level) were negatively correlated with lake water quality factors (WT, PH, TN, and TP). It should be noted that the average water depth had a strong negative correlation with WT, TN and TP. Mantel tests indicated that TN and TP were strongly related to taxonomic and gene functional composition (Mantel's $R > 0.7$, $p < 0.01$) (**Figure 3A**).

In the RDA model (**Figure 3B**), environmental factors including TN, TP, WT and average water depth made significant contributions to the relationship between taxonomic composition and environment ($p < 0.05$), and the first axis (RDA1) explained 79.65% of the total variance for the planktonic microbial communities. TN and TP were positively associated with the proportion of Cyanobacteria, but they were negatively associated with the proportion of Actinobacteria, Proteobacteria (Alpha-, Beta-, and Gammaproteobacteria), Bacteroidetes, Planctomycetes and Verrucomicrobia. The results of variation partitioning further showed that TN and TP jointly explained 77.9% of the changes in community structure, among which TN and TP explained 67.7 and 75.5% of the community changes, respectively (**Figure 3B**). A heatmap showed Pearson's correlations between all environmental factors and the relative abundances of the functional categories with an important contribution to the differences between groups (**Figure 3C**). TN and TP were positively related to energy metabolism and metabolism of cofactors and vitamins ($p < 0.01$), while they were negatively related to carbohydrate metabolism and glycan biosynthesis and metabolism ($p < 0.01$).

Community Metabolic Potential

We used the TPM value of each marker genes present in the samples from the five lakes as proxies for the genetic potential of microbiota in different steps of the C, N, and S cycles. Among 50 marker genes, 17 were found to have a different distribution between the two groups (**Figure 4**). Furthermore, marker gene-level hierarchical analysis grouped the samples according to trophic state, which was consistent with the grouping results from other community annotations, including taxonomic classification and metabolism.

In the carbon cycle, in all lakes, the main pathway detected was aerobic respiration, by Cyanobacteria in Group I, and by Actinobacteria and Alphaproteobacteria in Group II (Group I: 41.84%; Group II: 62.79%; $p < 0.01$) (**Figure 5**, **Supplementary Figure S6**, and **Supplementary Table S6**). Aerobic carbon fixation through the Calvin cycle in Group I was mainly driven by Cyanobacteria, and the potential was higher than that in Group II where it was driven by Cyanobacteria and Betaproteobacteria ($p < 0.01$). In addition, fermentation in Group I was also driven by Cyanobacteria, and the potential was higher than that in Group II where it was driven by Planctomycetes ($p < 0.01$). The potential for CO oxidation in Group II, driven by Actinobacteria and Betaproteobacteria, was higher than that in Group I where it was mediated by Alphaproteobacteria ($p < 0.01$). Notably, low abundance methanogenesis marker genes from Euryarchaeota were detected only in Group I.

In the nitrogen cycle, there was no statistically significant difference in the genetic potential for metabolic processes between the two groups, but we could still observe some interesting results. Marker genes associated with the processes of N assimilation and mineralization accounted for the major proportion of nitrogen cycle genes in both groups (Group I: 65.25% and 29.43%; Group II: 70.87% and 25.34%, respectively) (**Figure 5**). In communities belonging to Group I, these processes were mainly driven by Cyanobacteria, whereas in Group II they were driven by Actinobacteria. The genetic potential for anammox and denitrification in Group I was higher than that in Group II, while the potential for nitrogen fixation and nitrate reduction in Group I was lower than that in Group II. There was

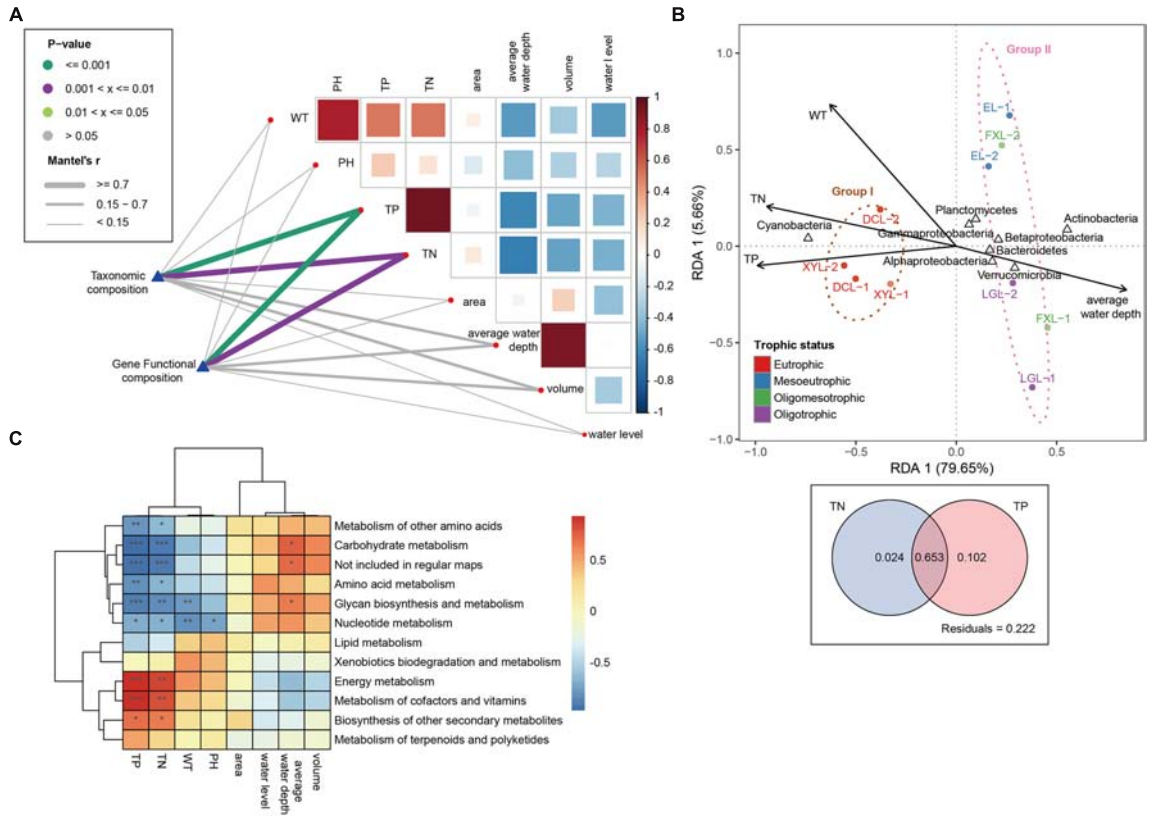

FIGURE 3 | Environmental drivers of community composition. **(A)** Pairwise comparisons of environmental factors are shown. The color gradients and box sizes represent Pearson's correlation coefficient, and red indicates a positive correlation and blue indicates a negative correlation. Taxonomic and functional (based on metabolism KEGG modules) community composition are related to each environmental factor by Mantel tests. Line width corresponds to the Mantel's r statistic for the corresponding distance correlations, and line color indicates the statistical significance based on 9999 permutations. **(B)** Redundancy analysis (RDA) is performed on the taxonomic profile (phylum level) and key environmental characteristics (WT, TN, TP, average water depth). Arrows indicate the correlation between environmental parameters and community structure. **(C)** Pearson's correlations between all environmental factors and the relative abundances of the different metabolism categories (***$p < 0.001$; **$p < 0.01$; *$p < 0.05$).

no obvious difference between groups in the potential for, and mediating-microbiota for, ammonification, nitrification, nitrate reduction and nitrite oxidation.

In the sulfur cycle, sulfur mineralization and assimilatory sulfate reduction processes had the highest genetic potential in all lakes. The genetic potential for assimilatory sulfate reduction in Group II was driven by Actinobacteria, and which was higher than that in Group I where it was mediated by Cyanobacteria ($p < 0.01$). Conversely, the potential for sulfur mineralization in Group I, mediated by Cyanobacteria, was higher than that in Group II, where it was mediated by Proteobacteria ($p < 0.01$).

DISCUSSION

Distinct Taxonomic Structure and Diversity of Communities in Each Ecosystem

In this study, the percentage of reads that could be taxonomically classified was relatively low. This is a reasonable outcome, explained by the incomplete information contained in reference databases and eukaryotic contamination in environmental metagenomes (Gori et al., 2011; Miller et al., 2019). Nevertheless, the annotation results reflect the composition of the microbial communities in the samples based on high-quality assignments.

Only a few studies have shown that there are remarkable differences in planktonic microbial community structure in freshwater lakes with different trophic status (Dai et al., 2016; Han et al., 2016; Hanson et al., 2017; Ji et al., 2018). In this study, we found that there were large differences in the taxonomic structures of the microbial communities from eutrophic (Group I) and mesotrophic-oligotrophic (Group II, the trophic level from mesotrophy to oligotrophy) freshwater ecosystems in the Yun-Gui Plateau. Moreover, our results suggested that the abundance of the phylum Cyanobacteria (order Chroococcales), which was dominant in eutrophic conditions, was significantly higher in eutrophic environments than that in mesotrophic-oligotrophic environments. In the mesotrophic-oligotrophic ecosystems, the phyla of Actinobacteria and Proteobacteria (Alpha-, Beta-, and Gammaproteobacteria) became dominant, indicating that they have a distinct preference for less eutrophic

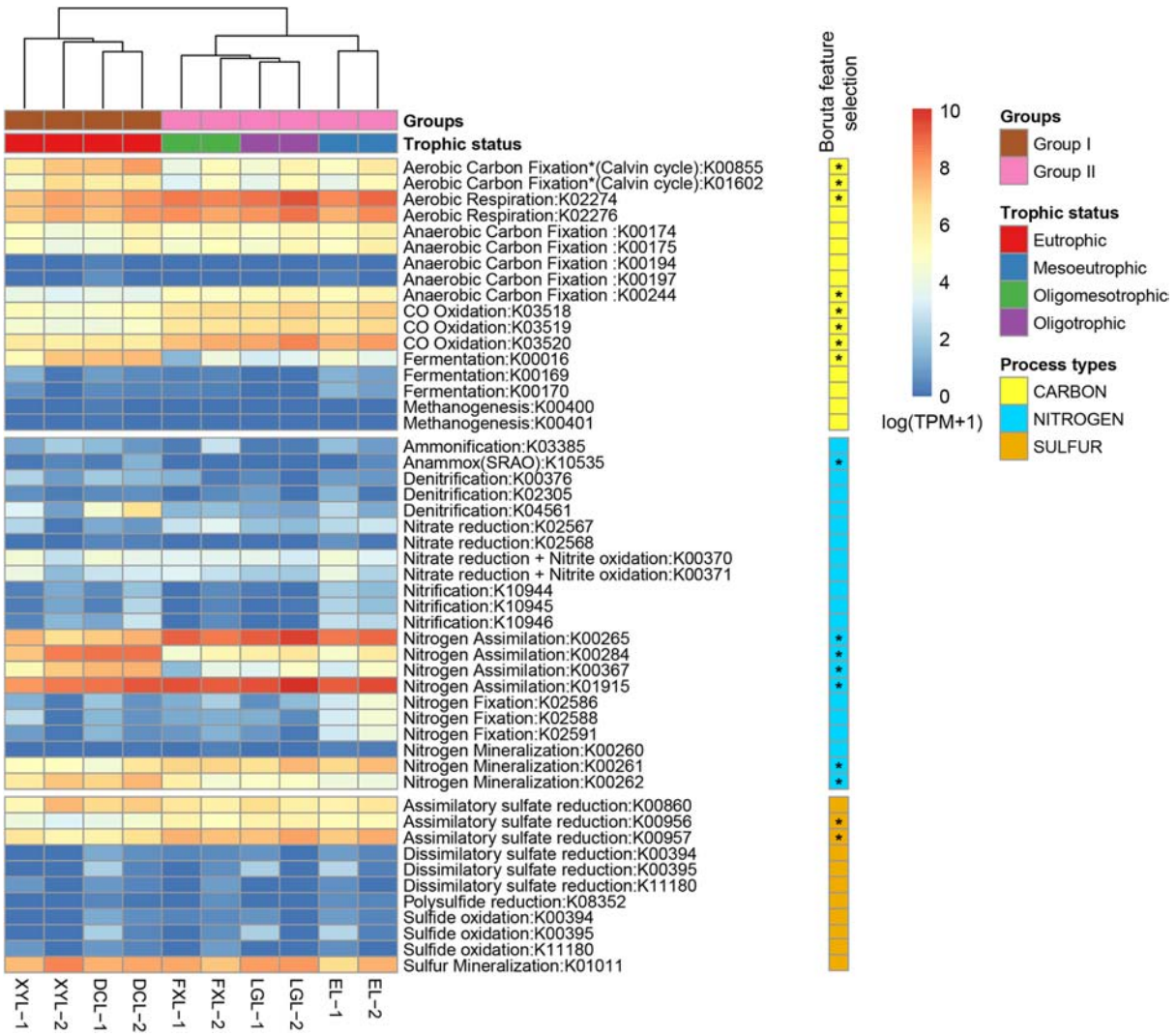

FIGURE 4 | Distribution of KOs involved in C, N, S cycle transformations in samples collected along the five Yun-Gui Plateau lakes. The heatmap displays the relative abundance [log2(TPM + 1)] of KOs across all samples. Hierarchical clustering (UPGMA) based on Bray–Curtis dissimilarity matrices. KOs that differentially segregated across groups are identified by random forest analysis with Boruta feature selection (1000 runs > 4).

conditions. Thus, we focused on the correlation between these key taxonomic groups and trophic status. The results of RDA revealed that the occurrence of the phylum Cyanobacteria correlated with trophic status (McMahon and Read, 2013), and the occurrence of Actinobacteria and Proteobacteria (Alpha-, Beta-, and Gammaproteobacteria) with less eutrophic states (Haukka et al., 2006; Ji et al., 2018). The co-occurrence of the key taxa and the particular trophic level indicates that each taxonomic group has unique characteristics in freshwater lake ecosystems. For example, Alphaproteobacteria are competitive in conditions of low nutrient/substrate utilization rate (Newton et al., 2011), and Cyanobacteria outcompete other planktonic microbes for nutrients in eutrophic systems (McMahon and Read, 2013).

Liu et al. (2012) reported that deeper lakes usually have better water quality than shallow lakes, and lake depth plays an important role in explaining the spatial dynamic of water quality in Yunnan Plateau. In our study, we observed the same findings that eutrophic ecosystems were shallow lakes and mesotrophic-oligotrophic ecosystems were deep lakes. It may be due to the deep lakes are associated with higher nutrient dilution ability than shallow lakes (Liu et al., 2012). The correlation analysis between environmental factors indicated that lake depth has significant relationships with TN and TP concentrations. Thus, we propose the average water depth of a lake can be used as a predictor of eutrophication. Additionally, previous studies have reported that the diversity pattern of planktonic bacterial communities in freshwater systems could be significantly correlated with TN and TP concentrations when subjected to eutrophication (Dai et al., 2016; Zeng et al., 2019), and this is consistent with the results of our RDA and variation partitioning. Although there were some differences in sampling time, location and size fraction of samples from the same lake in

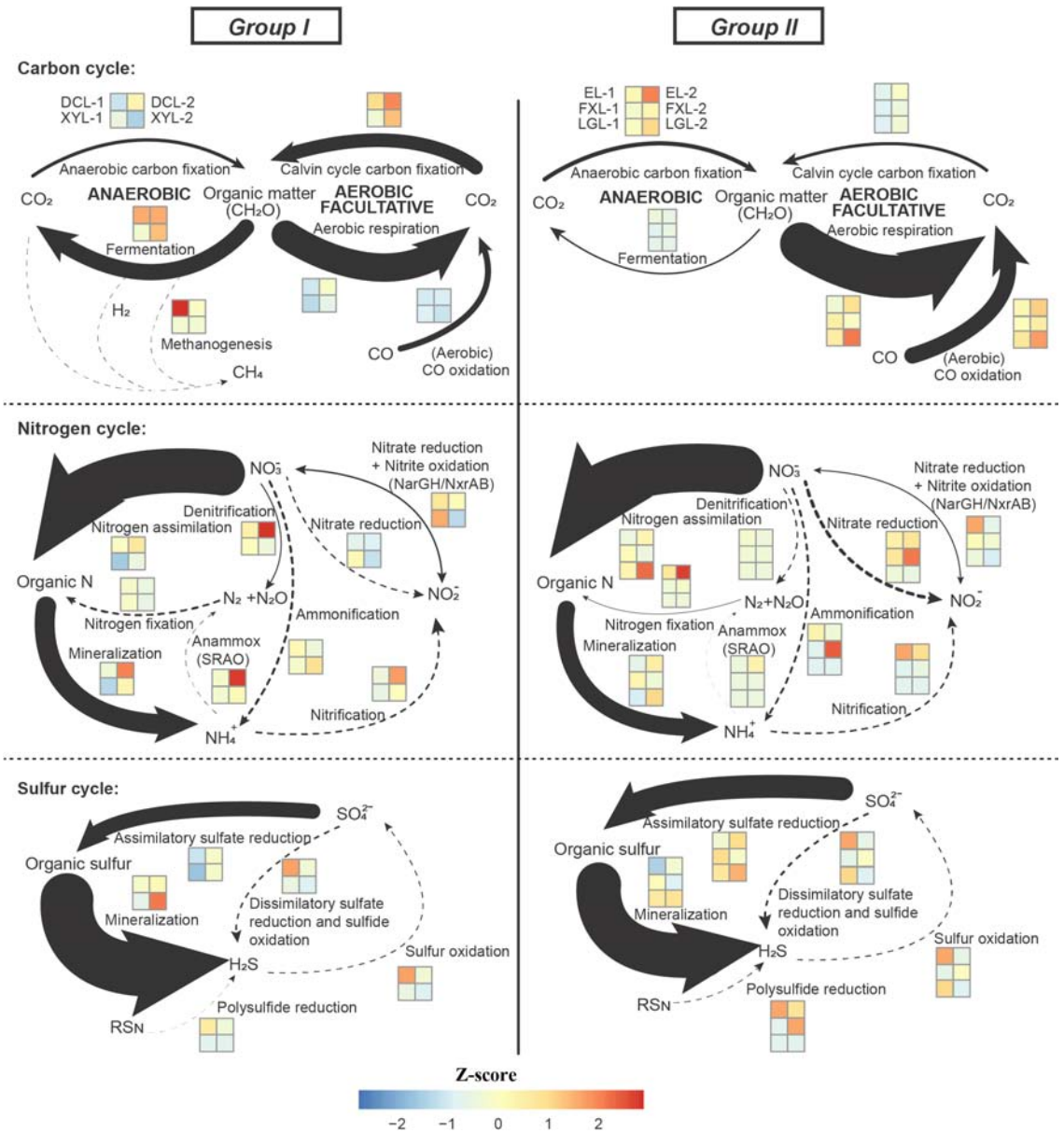

FIGURE 5 | Distribution of genes involved in the carbon, nitrogen and sulfur cycle. Genetic potential for several processes of the C, N, S cycle in the five Yun-Gui Plateau lakes using normalized marked genes. The genetic potentials for each conversion process are assessed based on the combination of these selected marker genes. For marker genes in the same process, the TPM values of genes with the same metabolic function are averaged, and the TPM values of genes with different metabolic functions are added. Arrow sizes are proportional to the genetic potential of the pathways (100% values of each cycle, see **Supplementary Table S6**). Dotted lines indicate that marked genes are rarely detected. Differences across trophic status are shown by *z*-score heatmap boxes indicated in each C/N/S transformation.

our study, the clustering of all samples still showed a significant pattern. Samples could be divided into two groups according to the trophic status of the lake. In addition, we observed that there were important differences in taxonomic alpha- and beta-diversity patterns across trophic gradients. Consequently, we conclude that the taxonomic diversity of planktonic microbial communities in freshwater lakes may be related to trophic status. Horner-Devine et al. (2003) observed that the diversity of planktonic bacteria exhibits a downward arched (parabolic) pattern along a gradient of primary productivity. Zeng et al. (2019) also found that the planktonic bacterial community has a positive quadratic relationship with the trophic level. Our results reflected a similar trend, that the alpha-diversity of planktonic microbiota in the eutrophic systems was significantly lower than that in mesotrophic-oligotrophic conditions, and within the mesotrophic-oligotrophic ecosystems, the alpha-diversity in the mesotrophic lake was higher than that in the oligotrophic lake.

Distinct Functional Structure of Communities in Each Ecosystem

Previous studies suggested that the functional structure of the microbial community is strongly associated with the taxonomic structure across the soil, estuary water and lake ecosystems (Dini-Andreote et al., 2016; Ren et al., 2017; Kieft et al., 2018). The profile of microbial community functions during a Cyanobacterial bloom in a eutrophic freshwater lake has been reported (Steffen et al., 2012; Chen et al., 2018). However, no comparative metagenomics study has been performed revealing the differences in microbial communities in lakes with different trophic status. Using metagenomic analysis, we observed a large difference in the functional structure of the planktonic microbial community between eutrophic and mesotrophic-oligotrophic freshwater ecosystems in the Yun-Gui Plateau lakes, which was strongly correlated with the differences in the taxonomic structures of the communities. By correlation analysis between environmental factors and functional categories, we found that the functional profiles of lakes with different trophic status were mainly correlated to TN and TP concentrations.

Our results showed that genes encoding carbohydrate metabolism and glycan biosynthesis and metabolism were abundant in mesotrophic-oligotrophic freshwater ecosystems, suggesting that microbial communities in surface water of mesotrophic-oligotrophic freshwater ecosystems may have higher utilization rates of organic carbon and higher carbon flux than those of eutrophic systems (Biddanda et al., 2001). Furthermore, genes involved in energy metabolism and cofactors and vitamin metabolism were abundant in the eutrophic ecosystems, which probably related to the high abundance of Cyanobacteria driving rapid energy conversion in this ecosystem and the need for heterotrophic bacteria to produce a large number of cofactors and vitamins (Tang et al., 2010; Li et al., 2018). Accordingly, we inferred that trophic status may contribute to changes in ecosystem function by driving the taxonomic and functional divergence of the microbial community.

Metabolic Potential of Communities in Each Ecosystem

Owing to variance in the overall functional potential distributions of microbial communities, it can be hypothesized that microbe-mediated biogeochemical cycles are ecosystem-specific, resulting in differences in genetic potential for carbon, nitrogen and sulfur cycling processes in the overlying water of freshwater lakes with different trophic states.

In our study, two high abundance metabolic processes, nitrogen assimilation and nitrogen mineralization, had equal potential across all lakes, indicating that differences in taxonomic composition do not influence the potential of the community to drive these processes. However, the relative abundance of markers of some processes was not constant between ecosystems. For instance, the potential for aerobic respiration and assimilatory sulfate reduction was relatively more abundant in the mesotrophic-oligotrophic freshwater ecosystems, while aerobic carbon fixation, fermentation and sulfur mineralization genes were relatively more abundant in the eutrophic freshwater ecosystems. Although lakes only account for a small fraction of the surface of the Earth (Chen et al., 2015), changes in these processes caused by trophic alteration in freshwater lakes may affect global biogeochemical cycles.

The phylum Cyanobacteria plays a crucial role as a primary producer in freshwater ecosystems, and it provides organic matter through photosynthesis to support the growth of various heterotrophic planktonic bacteria (Fujii et al., 2016). Therefore, it is reasonable that eutrophic ecosystems with a high abundance of Cyanobacteria have a stronger potential for aerobic carbon fixation. Furthermore, in shallow eutrophic lakes, the occurrence of algal blooms in summer not only provides abundant organic matter, but also forms a local dark and anaerobic environment in the overlying water. Stal and Moezelaar (1997) reported that in dark, anoxic conditions, Cyanobacteria use fermentation instead of aerobic respiration as an alternative means of energy generation. Hence, Cyanobacteria in eutrophic ecosystems drive fermentation processes to produce energy to compensate for the relatively low potential of aerobic respiration.

There have been few studies on CO oxidation in lake surface waters. CO in water mainly comes from photochemical degradation of Chromophoric/Colored dissolved organic matter (Stubbins, 2001), which is accelerated by nutrient accumulation (Zhang et al., 2010; Zhou et al., 2018a). Therefore, a eutrophic ecosystem should have more CO flux. However, the abundance of marker genes related to CO oxidation in the mesotrophic-oligotrophic freshwater ecosystems was higher than that in the eutrophic lakes, indicating that the CO oxidation potential in the mesotrophic-oligotrophic lakes was higher. This may be because of microorganisms need more efficient energy harvesting in conditions of low nutrition, and higher primary productivity can reduce the dependence of planktonic microorganisms on exogenous carbon in eutrophic waters. Furthermore, we found that methanogenesis was driven by Euryarchaeota in the eutrophic surface water of Dianchi Lake. Recent works have revealed that a large fraction of CH_4 oversaturation in aquatic environments is produced in oxygenated surface waters (Townsend-Small et al., 2016; Zhou et al., 2018b). Thus, we suspect that a local anaerobic environment caused by Cyanobacterial blooms in eutrophic lakes may promote the production of CH_4 in aerobic overlying water to some extent (Xing et al., 2012). Evans et al. (2017) reported that eutrophication causes lakes to transition from sinks to sources of carbon. Our data suggest carbon accumulation in the eutrophic lake because of increased carbon fixation potential relative to respiratory potential.

Wu et al. (2019) found that algal blooms could accelerate the nitrogen cycling rate. Our results showed that there was no dramatic divergence in the potential for N-cycle processes between the eutrophic and the mesotrophic-oligotrophic freshwater ecosystems, but there were some noteworthy differences in anammox, denitrification and nitrogen fixation. Rich organic matter produced by algal blooms can be converted into ammonia and nitrate for anammox and denitrification (Wu et al., 2019). Hence, we infer that there are high potentials

for these two processes in eutrophic ecosystems, which may be the result of an accelerated N-cycle within this ecosystem. In addition, the lower potential for nitrogen fixation in eutrophic ecosystems is the result of the presence of rich organic matter, while the higher potential for nitrogen fixation in the mesotrophic-oligotrophic ecosystems is most likely related to a lack of organic matter.

Although sulfur cycling in freshwater sediments and vertical water columns has been well studied (Cai et al., 2019; Ren et al., 2019), the genetic potential for sulfur transformation in surface waters of lakes with different trophic status has not been studied. With the death of a large number of Cyanobacteria in eutrophic lakes, the high content of sulfur-containing amino acids in their cells might be released (Lu et al., 2013), resulting in a water column enriched with organic sulfur. Our results showed that planktonic microbial communities in the eutrophic ecosystems exhibited less abundance of assimilatory sulfur reduction-related genes to produce organic sulfur; on the contrary, planktonic microbial communities in the eutrophic ecosystems exhibited higher potential for sulfur mineralization than those in the mesotrophic-oligotrophic environments, which may lead to the tendency of the eutrophic ecosystems to release H_2S gas.

CONCLUSION

Our research reports on the planktonic microbial communities of five plateau freshwater lakes with different trophic status, located in Yunnan, China. The trophic alterations caused by anthropogenic activities are not only related to microbial community composition, but also to the genetic potential for important carbon, nitrogen and sulfur biogeochemical cycling reactions mediated by microbes in the surface waters.

The overall differences in metabolic functions and the genetic potential for elemental cycling were strongly related to divergence in the taxonomic structure and diversity of the planktonic microbial communities. Energy metabolism and cofactors and vitamin metabolism had strong representation in the eutrophic ecosystems; carbohydrate metabolism and glycan biosynthesis and metabolism had strong representation in the mesotrophic-oligotrophic ecosystems. Moreover, the phylum Cyanobacteria, dominant in the eutrophic ecosystems, mainly mediated the processes of aerobic respiration, fermentation, nitrogen assimilation, nitrogen mineralization, assimilatory sulfate reduction and sulfur mineralization in this system. The phyla Actinobacteria and Proteobacteria (Alpha-, Beta-, and Gammaproteobacteria), Verrucomicrobia and Planctomycetes showed higher relative abundance in the mesotrophic-oligotrophic ecosystems than those in the eutrophic ecosystems. In the mesotrophic-oligotrophic ecosystems, aerobic respiration, nitrogen assimilation, nitrogen mineralization and assimilatory sulfate reduction were mainly mediated by the phylum Actinobacteria, sulfur mineralization was mainly driven by Alphaproteobacteria, and fermentation was mainly driven by Planctomycetes. Planktonic microbial communities in the eutrophic ecosystems had higher potential for aerobic carbon fixation, fermentation, methanogenesis, anammox, denitrification and sulfur mineralization than those in the mesotrophic-oligotrophic ecosystems. Besides, planktonic microbial communities in the mesotrophic-oligotrophic ecosystems had higher metabolic potentials for aerobic respiration, CO oxidation, nitrogen fixation and assimilatory sulfate reduction than those in the eutrophic ecosystems. Overall, trophic preference of some key taxonomic groups leads to communities with distinct taxonomy and functions, corresponding to ecosystem-specific carbon, nitrogen and sulfur cycles in Yun-Gui Plateau freshwater lakes characterized by different trophic status.

DATA AVAILABILITY STATEMENT

Metagenomics data sets have been deposited in the NCBI Short Read Archive (SRA) the Bioproject Number PRJNA548910 (accessions: SAMN12058482, SAMN12058483, SAMN12058484, SAMN12058485, SAMN12058486, SAMN120-58487, SAMN12058488, SAMN12058489, SAMN120-58490, SAMN12058491).

AUTHOR CONTRIBUTIONS

MS carried out the library preparation, sample sequencing, data analysis, and wrote the first draft of the manuscript. QL assisted in library preparation and sample sequencing. MR polished the manuscript. YL and JW helped the revision of the manuscript. LC performed the sample collection and filtration, and polished the manuscript. TL and JZ conceived the study and designed the experiments. All authors read and approved the final manuscript.

FUNDING

This research was supported by the National Natural Science Foundation of China (Grant No. 91851118), the Science and Technology Basic Resources Investigation Program of China (Grant No. 2017FY100300), the Key Research Program of the Chinese Academy of Sciences (Grant No. KFZD-SW-219), the State Key Laboratory of Freshwater Ecology and Biotechnology (Grant No. 2019FBZ01), and the National Key R&D Program of China (Grant No. 2018YFA0903100).

ACKNOWLEDGMENTS

The authors would like to thank the editors and the reviewers for the valuable suggestions to improve the manuscript.

SUPPLEMENTARY MATERIAL

The Supplementary Material for this article can be found online at: https://www.frontiersin.org/articles/10.3389/fmicb.2019.02560/full#supplementary-material

REFERENCES

Arora-Williams, K., Olesen, S. W., Scandella, B. P., Delwiche, K., Spencer, S. J., Myers, E. M., et al. (2018). Dynamics of microbial populations mediating biogeochemical cycling in a freshwater lake. *Microbiome* 6:165. doi: 10.1186/s40168-018-0556-557

Bai, Y., Shi, Q., Wen, D., Li, Z., Jefferson, W. A., Feng, C., et al. (2012). Bacterial communities in the sediments of Dianchi lake, a partitioned eutrophic waterbody in China. *PLoS One* 7:e37796. doi: 10.1371/journal.pone.0037796

Biddanda, B., Ogdahl, M., and Cotner, J. (2001). Dominance of bacterial metabolism in oligotrophic relative to eutrophic waters. *Limnol. Oceanogr.* 46, 730–739. doi: 10.4319/lo.2001.46.3.0730

Buchfink, B., Xie, C., and Huson, D. H. (2015). Fast and sensitive protein alignment using DIAMOND. *Nat. Methods* 12, 59–60. doi: 10.1038/nmeth.3176

Cai, W., Li, Y., Shen, Y., Wang, C., Wang, P., Wang, L., et al. (2019). Vertical distribution and assemblages of microbial communities and their potential effects on sulfur metabolism in a black-odor urban river. *J. Environ. Manage.* 235, 368–376. doi: 10.1016/j.jenvman.2019.01.078

Cao, J., Hou, Z., Li, Z., Chu, Z., Yang, P., and Zheng, B. (2018). Succession of phytoplankton functional groups and their driving factors in a subtropical plateau lake. *Sci. Total Environ.* 63, 1127–1137. doi: 10.1016/j.scitotenv.2018.03.026

Castro-Nallar, E., Bendall, M. L., Pérez-Losada, M., Sabuncyan, S., Severance, E. G., Dickerson, F. B., et al. (2015). Composition, taxonomy and functional diversity of the oropharynx microbiome in individuals with schizophrenia and controls. *PeerJ* 3:e1140. doi: 10.7717/peerj.1140

Chen, M., Zeng, G., Zhang, J., Xu, P., Chen, A., and Lu, L. (2015). Global landscape of total organic carbon, nitrogen and phosphorus in Lake Water. *Sci. Rep.* 5:15043. doi: 10.1038/srep15043

Chen, Z., Zhang, J., Li, R., Tian, F., Shen, Y., Xie, X., et al. (2018). Metatranscriptomics analysis of cyanobacterial aggregates during cyanobacterial bloom period in Lake Taihu, China. *Environ. Sci. Pollut. Res.* 25, 4811–4825. doi: 10.1007/s11356-017-0733-734

Clark, D. R., Ferguson, R. M. W., Harris, D. N., Matthews Nicholass, K. J., Prentice, H. J., Randall, K. C., et al. (2018). Streams of data from drops of water: 21st century molecular microbial ecology. *Wiley Interdiscip. Rev. Water* 5:e1280. doi: 10.1002/wat2.1280

Cronan, C. S. (2018). "Microbial biogeochemistry," in *Ecosystem Biogeochemistry: Element Cycling in the Forest Landscape*, ed. C. S. Cronan, (Cham: Springer International Publishing), 31–40. doi: 10.1007/978-3-319-66444-6_3

Cui, Y.-D., Liu, X.-Q., and Wang, H.-Z. (2008). Macrozoobenthic community of Fuxian Lake, the deepest lake of southwest China. *Limnologica* 38, 116–125. doi: 10.1016/j.limno.2007.10.003

Dai, Y., Yang, Y., Wu, Z., Feng, Q., Xie, S., and Liu, Y. (2016). Spatiotemporal variation of planktonic and sediment bacterial assemblages in two plateau freshwater lakes at different trophic status. *Appl. Microbiol. Biotechnol.* 100, 4161–4175. doi: 10.1007/s00253-015-7253-7252

Diamond, S., Andeer, P. F., Li, Z., Crits-Christoph, A., Burstein, D., Anantharaman, K., et al. (2019). Mediterranean grassland soil C–N compound turnover is dependent on rainfall and depth, and is mediated by genomically divergent microorganisms. *Nat. Microbiol.* 4, 1356–1367. doi: 10.1038/s41564-019-0449-y

Ding, C., Jiang, X., Xie, Z., and Brosse, S. (2017). Seventy-five years of biodiversity decline of fish assemblages in Chinese isolated plateau lakes: widespread introductions and extirpations of narrow endemics lead to regional loss of dissimilarity. *Divers. Distrib.* 23, 171–184. doi: 10.1111/ddi.12507

Dini-Andreote, F., Brossi, M. J., de, L., van Elsas, J. D., and Salles, J. F. (2016). Reconstructing the genetic potential of the microbially-mediated nitrogen cycle in a salt marsh ecosystem. *Front. Microbiol.* 7:902. doi: 10.3389/fmicb.2016.00902

Dong, J., Zhou, Q., Gao, Y., Gu, Q., Li, G., and Song, L. (2018). Long-term effects of temperature and nutrient concentrations on the phytoplankton biomass in three lakes with differing trophic statuses on the Yungui Plateau, China. *Ann. Limnol. - Int. J. Limnol.* 54:9. doi: 10.1051/limn/2017031

Eiler, A., Zaremba-Niedzwiedzka, K., Martínez-García, M., McMahon, K. D., Stepanauskas, R., Andersson, S. G. E., et al. (2014). Productivity and salinity structuring of the microplankton revealed by comparative freshwater metagenomics. *Environ. Microbiol.* 16, 2682–2698. doi: 10.1111/1462-2920.12301

Evans, C. D., Futter, M. N., Moldan, F., Valinia, S., Frogbrook, Z., and Kothawala, D. N. (2017). Variability in organic carbon reactivity across lake residence time and trophic gradients. *Nat. Geosci.* 10, 832–835. doi: 10.1038/ngeo3051

Falkowski, P. G., Fenchel, T., and Delong, E. F. (2008). The microbial engines that drive earth's biogeochemical cycles. *Science* 320, 1034–1039. doi: 10.1126/science.1153213

Fujii, M., Hirao, T., Kojima, H., and Fukui, M. (2016). "Planktonic bacterial communities in mountain lake ecosystems," in *Structure and Function of Mountain Ecosystems in Japan: Biodiversity and Vulnerability to Climate Change*, ed. G. Kudo, (Tokyo: Springer Japan), 145–169. doi: 10.1007/978-4-431-55954-2_7

Gao, C., Yu, J., Min, X., Cheng, A., Hong, R., and Zhang, L. (2018). Heavy metal concentrations in sediments from Xingyun lake, southwestern China: implications for environmental changes and human activities. *Environ. Earth Sci.* 77:666. doi: 10.1007/s12665-018-7840-7845

Gori, F., Folino, G., Jetten, M. S. M., and Marchiori, E. (2011). MTR: taxonomic annotation of short metagenomic reads using clustering at multiple taxonomic ranks. *Bioinformatics* 27, 196–203. doi: 10.1093/bioinformatics/btq649

Hamilton, T. L., Bovee, R. J., Sattin, S. R., Mohr, W., Gilhooly, W. P., Lyons, T. W., et al. (2016). Carbon and sulfur cycling below the chemocline in a meromictic lake and the identification of a novel taxonomic lineage in the FCB Superphylum, *Candidatus aegiribacteria*. *Front. Microbiol.* 7:598. doi: 10.3389/fmicb.2016.00598

Han, M., Gong, Y., Zhou, C., Zhang, J., Wang, Z., and Ning, K. (2016). Comparison and interpretation of taxonomical structure of bacterial communities in two types of lakes on Yun-Gui plateau of China. *Sci. Rep.* 6:30616. doi: 10.1038/srep30616

Hanson, A. M., Berges, J. A., and Young, E. B. (2017). Virus morphological diversity and relationship to bacteria and chlorophyll across a freshwater trophic gradient in the Lake Michigan watershed. *Hydrobiologia* 794, 93–108. doi: 10.1007/s10750-016-3084-0

Haukka, K., Kolmonen, E., Hyder, R., Hietala, J., Vakkilainen, K., Kairesalo, T., et al. (2006). Effect of nutrient loading on bacterioplankton community composition in Lake Mesocosms. *Microb. Ecol.* 51, 137–146. doi: 10.1007/s00248-005-0049-47

Horner-Devine, M. C., Leibold, M. A., Smith, V. H., and Bohannan, B. J. M. (2003). Bacterial diversity patterns along a gradient of primary productivity. *Ecol. Lett.* 6, 613–622. doi: 10.1046/j.1461-0248.2003.00472.x

Hu, C., Wang, S., Guo, L., and Xie, P. (2014). Effects of the proximal factors on the diel vertical migration of zooplankton in a plateau meso-eutrophic Lake Erhai, China. *J. Limnol.* 73, 375–386. doi: 10.4081/jlimnol.2014.684

Hu, M., Yanhui, L., Yuchun, W., Huaidong, Z., Yongding, L., and Gaofeng, Z. (2013). Phytoplankton and bacterioplankton abundances and community dynamics in Lake Erhai. *Water Sci. Technol. J. Int. Assoc. Water Pollut. Res.* 68, 348–356. doi: 10.2166/wst.2013.215

Huson, D. H., Beier, S., Flade, I., Górska, A., El-Hadidi, M., Mitra, S., et al. (2016). MEGAN community edition - interactive exploration and analysis of large-scale microbiome sequencing data. *PLoS Comput. Biol.* 12:e1004957. doi: 10.1371/journal.pcbi.1004957

Hyatt, D., LoCascio, P. F., Hauser, L. J., and Uberbacher, E. C. (2012). Gene and translation initiation site prediction in metagenomic sequences. *Bioinformatics* 28, 2223–2230. doi: 10.1093/bioinformatics/bts429

Ji, B., Qin, H., Guo, S., Chen, W., Zhang, X., and Liang, J. (2018). Bacterial communities of four adjacent fresh lakes at different trophic status. *Ecotoxicol. Environ. Saf.* 157, 388–394. doi: 10.1016/j.ecoenv.2018.03.086

Kanehisa, M., Sato, Y., and Morishima, K. (2016). BlastKOALA and GhostKOALA: KEGG tools for functional characterization of genome and metagenome sequences. *J. Mol. Biol.* 428, 726–731. doi: 10.1016/j.jmb.2015.11.006

Kieft, B., Li, Z., Bryson, S., Crump, B. C., Hettich, R., Pan, C., et al. (2018). Microbial community structure–function relationships in Yaquina Bay estuary reveal spatially distinct carbon and nitrogen cycling capacities. *Front. Microbiol.* 9:1282. doi: 10.3389/fmicb.2018.01282

Langmead, B., and Salzberg, S. L. (2012). Fast gapped-read alignment with Bowtie 2. *Nat. Methods* 9, 357–359. doi: 10.1038/NMETH.1923

Lauro, F. M., DeMaere, M. Z., Yau, S., Brown, M. V., Ng, C., Wilkins, D., et al. (2011). An integrative study of a meromictic lake ecosystem in Antarctica. *ISME J.* 5, 879–895. doi: 10.1038/ismej.2010.185

Li, D., Luo, R., Liu, C.-M., Leung, C.-M., Ting, H.-F., Sadakane, K., et al. (2016). MEGAHIT v1.0: a fast and scalable metagenome assembler driven by advanced methodologies and community practices. *Methods* 102, 3–11. doi: 10.1016/j.ymeth.2016.02.020

Li, H., Xing, P., Chen, M., Bian, Y., and Wu, Q. L. (2011). Short-term bacterial community composition dynamics in response to accumulation and breakdown of Microcystis blooms. *Water Res.* 45, 1702–1710. doi: 10.1016/j.watres.2010.11.011

Li, H., Zeng, J., Ren, L., Wang, J., Xing, P., and Wu, Q. L. (2017). Contrasting patterns of diversity of abundant and rare bacterioplankton in freshwater lakes along an elevation gradient. *Limnol. Oceanogr.* 62, 1570–1585. doi: 10.1002/lno.10518

Li, W., Zhong, J., Yuan, G., Fu, H., Fan, H., Ni, L., et al. (2017). Stoichiometric characteristics of four submersed macrophytes in three plateau lakes with contrasting trophic statuses. *Ecol. Eng.* 99, 265–270. doi: 10.1016/j.ecoleng.2016.11.059

Li, Q., Lin, F., Yang, C., Wang, J., Lin, Y., Shen, M., et al. (2018). A large-scale comparative metagenomic study reveals the functional interactions in six bloom-forming microcystis-epibiont communities. *Front. Microbiol.* 9:746. doi: 10.3389/fmicb.2018.00746

Li, R., Kraft, N. J. B., Yang, J., and Wang, Y. (2015). A phylogenetically informed delineation of floristic regions within a biodiversity hotspot in Yunnan, China. *Sci. Rep.* 5:9396. doi: 10.1038/srep09396

Liao, J., Zhao, L., Cao, X., Sun, J., Gao, Z., Wang, J., et al. (2016). Cyanobacteria in lakes on Yungui Plateau, China are assembled via niche processes driven by water physicochemical property, lake morphology and watershed land-use. *Sci. Rep.* 6:36357. doi: 10.1038/srep36357

Liao, M., Yu, G., Ventelä, A.-M., and Dong, X. (2015). Determining long-term trends of four fast-eutrophicated Lakes in China and Finland. *J. Agric. Sci.* 8, 39–54. doi: 10.5539/jas.v8n1p39

Liu, W., Li, S., Bu, H., Zhang, Q., and Liu, G. (2012). Eutrophication in the Yunnan Plateau lakes: the influence of lake morphology, watershed land use, and socioeconomic factors. *Environ. Sci. Pollut. Res.* 19, 858–870. doi: 10.1007/s11356-011-0616-z

Liu, Y., Chen, G., Hu, K., Shi, H., Huang, L., Chen, X., et al. (2017). Biological responses to recent eutrophication and hydrologic changes in Xingyun Lake, southwest China. *J. Paleolimnol.* 57, 343–360. doi: 10.1007/s10933-017-9952-9954

Llirós, M., Inceoğlu, Ö, García-Armisen, T., Anzil, A., Leporcq, B., Pigneur, L.-M., et al. (2014). Bacterial community composition in three freshwater reservoirs of different alkalinity and trophic status. *PLoS One* 9:e116145. doi: 10.1371/journal.pone.0116145

Llorens-Marès, T., Yooseph, S., Goll, J., Hoffman, J., Vila-Costa, M., Borrego, C. M., et al. (2015). Connecting biodiversity and potential functional role in modern euxinic environments by microbial metagenomics. *ISME J.* 9, 1648–1661. doi: 10.1038/ismej.2014.254

Logue, J. B., Findlay, S. E. G., and Comte, J. (2015). Editorial: microbial responses to environmental changes. *Front. Microbiol.* 6:1364. doi: 10.3389/fmicb.2015.01364

Lu, X., Fan, C., He, W., Deng, J., and Yin, H. (2013). Sulfur-containing amino acid methionine as the precursor of volatile organic sulfur compounds in algea-induced black bloom. *J. Environ. Sci.* 25, 33–43. doi: 10.1016/S1001-0742(12)60019-60019

Ma, R., Yang, G., Duan, H., Jiang, J., Wang, S., Feng, X., et al. (2011). China's lakes at present: number, area and spatial distribution. *Sci. China Earth Sci.* 54, 283–289. doi: 10.1007/s11430-010-4052-4056

McMahon, K. D., and Read, E. K. (2013). Microbial contributions to phosphorus cycling in Eutrophic Lakes and wastewater. *Annu. Rev. Microbiol.* 67, 199–219. doi: 10.1146/annurev-micro-092412-155713

Menzel, P., Ng, K. L., and Krogh, A. (2016). Fast and sensitive taxonomic classification for metagenomics with Kaiju. *Nat. Commun.* 7:11257. doi: 10.1038/ncomms11257

Miller, I. J., Rees, E. R., Ross, J., Miller, I., Baxa, J., Lopera, J., et al. (2019). Autometa: automated extraction of microbial genomes from individual shotgun metagenomes. *Nucleic Acids Res.* 47:e57. doi: 10.1093/nar/gkz148

Neufeld, J. D. (2017). Migrating SSU rRNA gene surveys to the metagenomics era. *Environ. Microbiol. Rep.* 9, 23–24. doi: 10.1111/1758-2229.12493

Newton, R. J., Jones, S. E., Eiler, A., McMahon, K. D., and Bertilsson, S. (2011). A guide to the natural history of freshwater lake bacteria. *Microbiol. Mol. Biol. Rev.* 75, 14–49. doi: 10.1128/MMBR.00028-10

Oksanen, J., Blanchet, F. G., Friendly, M., Kindt, R., Legendre, P., McGlinn, D., et al. (2019). *vegan: Community Ecology Package. R package vesion 2.5-3*. Available at: https://CRAN.R-project.org/package=vegan (accessed June 17, 2019).

Quince, C., Walker, A. W., Simpson, J. T., Loman, N. J., and Segata, N. (2017). Shotgun metagenomics, from sampling to analysis. *Nat. Biotechnol.* 35, 833–844. doi: 10.1038/nbt.3935

Ren, Z., Qu, X., Peng, W., Yu, Y., and Zhang, M. (2019). Functional properties of bacterial communities in water and sediment of the eutrophic river-lake system of Poyang Lake, China. *PeerJ* 7:e7318. doi: 10.7717/peerj.7318

Ren, Z., Wang, F., Qu, X., Elser, J. J., Liu, Y., and Chu, L. (2017). Taxonomic and functional differences between microbial communities in Qinghai Lake and its input streams. *Front. Microbiol.* 8:2319. doi: 10.3389/fmicb.2017.02319

Revelle, W. (2019). *psych: Procedures for Psychological, Psychometric, and Personality Research*. Available at: https://CRAN.R-project.org/package=psych (accessed June 17, 2019).

Ribicic, D., Netzer, R., Hazen, T. C., Techtmann, S. M., Drabløs, F., and Brakstad, O. G. (2018). Microbial community and metagenome dynamics during biodegradation of dispersed oil reveals potential key-players in cold Norwegian seawater. *Mar. Pollut. Bull.* 129, 370–378. doi: 10.1016/j.marpolbul.2018.02.034

Rothschild, D., Weissbrod, O., Barkan, E., Kurilshikov, A., Korem, T., Zeevi, D., et al. (2018). Environment dominates over host genetics in shaping human gut microbiota. *Nature* 555, 210–215. doi: 10.1038/nature25973

Shi, H., Chen, G., Lu, H., Wang, J., Huang, L., Wang, L., et al. (2016). Regional pattern of Bosmina responses to fish introduction and eutrophication in four large lakes from Southwest China. *J. Plankton Res.* 38, 443–455. doi: 10.1093/plankt/fbv118

Smyth, G. K., Shi, W., and Liao, Y. (2013). featureCounts: an efficient general purpose program for assigning sequence reads to genomic features. *Bioinformatics* 30, 923–930. doi: 10.1093/bioinformatics/btt656

Stal, L. J., and Moezelaar, R. (1997). Fermentation in cyanobacteria. *FEMS Microbiol. Rev.* 21, 179–211. doi: 10.1016/S0168-6445(97)00056-59

Steffen, M. M., Li, Z., Effler, T. C., Hauser, L. J., Boyer, G. L., and Wilhelm, S. W. (2012). Comparative metagenomics of toxic freshwater cyanobacteria bloom communities on two continents. *PLoS One* 7:e44002. doi: 10.1371/journal.pone.0044002

Storey, J. D., Taylor, J. E., and Siegmund, D. (2004). Strong control, conservative point estimation and simultaneous conservative consistency of false discovery rates: a unified approach. *J. R. Stat. Soc. Ser. B Stat. Methodol.* 66, 187–205. doi: 10.1111/j.1467-9868.2004.00439.x

Stubbins, A. P. (2001). *Aspects of aquatic CO photoproduction from CDOM*. Ph.D. Thesis. University of Newcastle-Upon-Tyne, Newcastle-upon-Tyne.

Sunagawa, S., Coelho, L. P., Chaffron, S., Kultima, J. R., Labadie, K., Salazar, G., et al. (2015). Structure and function of the global ocean microbiome. *Science* 348:1261359. doi: 10.1126/science.1261359

Tang, Y. Z., Koch, F., and Gobler, C. J. (2010). Most harmful algal bloom species are vitamin B1 and B12 auxotrophs. *Proc. Natl. Acad. Sci. U.S.A.* 107, 20756–20761. doi: 10.1073/pnas.1009566107

Townsend-Small, A., Disbennett, D., Fernandez, J. M., Ransohoff, R. W., Mackay, R., and Bourbonniere, R. A. (2016). Quantifying emissions of methane derived from anaerobic organic matter respiration and natural gas extraction in Lake Erie: methane emissions from Lake Erie. *Limnol. Oceanogr.* 61, S356–S366. doi: 10.1002/lno.10273

Vavourakis, C. D., Andrei, A.-S., Mehrshad, M., Ghai, R., Sorokin, D. Y., and Muyzer, G. (2018). A metagenomics roadmap to the uncultured genome diversity in hypersaline soda lake sediments. *Microbiome* 6:168. doi: 10.1186/s40168-018-0548-547

Wan, Y., Ruan, X., Zhang, Y., and Li, R. (2017). Illumina sequencing-based analysis of sediment bacteria community in different trophic status freshwater lakes. *MicrobiologyOpen* 6:e00450. doi: 10.1002/mbo3.450

Wang, S., and Dong, H. (1998). *Chinese Lake Catalogue (in Chinese)*. Beijing: Science Press.

Wang, S., Zhang, L., Ni, L., Zhao, H., Jiao, L., Yang, S., et al. (2015a). Ecological degeneration of the Erhai Lake and prevention measures. *Environ. Earth Sci.* 74, 3839–3847. doi: 10.1007/s12665-015-4433-4434

Wang, S., Zhao, Y., Jiao, L., Zhang, L., and Guo, W. (2015b). Characteristics of soluble organic nitrogen composition and sources in sediments from Erhai Lake in China and the effect on the water quality. *Environ. Earth Sci.* 74, 3849–3856. doi: 10.1007/s12665-015-4107-4102

Wen, D., Bai, Y., Shi, Q., Li, Z., Sun, Q., Sun, R., et al. (2012). Bacterial diversity in the polluted water of the Dianchi Lakeshore in China. *Ann. Microbiol.* 62, 715–723. doi: 10.1007/s13213-011-0311-319

White, J. R., Nagarajan, N., and Pop, M. (2009). Statistical methods for detecting differentially abundant features in clinical metagenomic samples. *PLoS Comput. Biol.* 5:e1000352. doi: 10.1371/journal.pcbi.1000352

Wu, S., Wu, Z., Liang, Z., Liu, Y., and Wang, Y. (2019). Denitrification and the controlling factors in Yunnan Plateau Lakes (China): exploring the role of enhanced internal nitrogen cycling by algal blooms. *J. Environ. Sci.* 76, 349–358. doi: 10.1016/j.jes.2018.05.028

Xie, M., Ren, M., Yang, C., Yi, H., Li, Z., Li, T., et al. (2016). Metagenomic analysis reveals symbiotic relationship among bacteria in microcystis-dominated community. *Front. Microbiol.* 7:56. doi: 10.3389/fmicb.2016.00056

Xing, P., Li, H., Liu, Q., and Zheng, J. (2012). Composition of the archaeal community involved in methane production during the decomposition of Microcystis blooms in the laboratory. *Can. J. Microbiol.* 58, 1153–1158. doi: 10.1139/w2012-097

Yang, Y., Dai, Y., Li, N., Li, B., Xie, S., and Liu, Y. (2017a). Temporal and spatial dynamics of sediment anaerobic ammonium oxidation (Anammox) bacteria in freshwater lakes. *Microb. Ecol.* 73, 285–295. doi: 10.1007/s00248-016-0872-z

Yang, Y., Li, N., Wang, W., Li, B., Xie, S., and Liu, Y. (2017b). Vertical profiles of sediment methanogenic potential and communities in two plateau freshwater lakes. *Biogeosciences* 14, 341–351. doi: 10.5194/bg-14-341-2017

Yang, Y.-H., Zhou, F., Guo, H.-C., Sheng, H., Liu, H., Dao, X., et al. (2010). Analysis of spatial and temporal water pollution patterns in Lake Dianchi using multivariate statistical methods. *Environ. Monit. Assess.* 170, 407–416. doi: 10.1007/s10661-009-1242-1249

Zeng, J., Jiao, C., Zhao, D., Xu, H., Huang, R., Cao, X., et al. (2019). Patterns and assembly processes of planktonic and sedimentary bacterial community differ along a trophic gradient in freshwater lakes. *Ecol. Indic.* 106:105491. doi: 10.1016/j.ecolind.2019.105491

Zhang, Y., Zhang, E., Yin, Y., van Dijk, M. A., Feng, L., Shi, Z., et al. (2010). Characteristics and sources of chromophoric dissolved organic matter in lakes of the Yungui Plateau, China, differing in trophic state and altitude. *Limnol. Oceanogr.* 55, 2645–2659. doi: 10.4319/lo.2010.55.6.2645

Zhou, Q., Wang, W., Huang, L., Zhang, Y., Qin, J., Li, K., et al. (2019). Spatial and temporal variability in water transparency in Yunnan Plateau lakes, China. *Aquat. Sci.* 81:36. doi: 10.1007/s00027-019-0632-635

Zhou, Y., Davidson, T. A., Yao, X., Zhang, Y., Jeppesen, E., de Souza, J. G., et al. (2018a). How autochthonous dissolved organic matter responds to eutrophication and climate warming: evidence from a cross-continental data analysis and experiments. *Earth-Sci. Rev.* 185, 928–937. doi: 10.1016/j.earscirev.2018.08.013

Zhou, Y., Xiao, Q., Yao, X., Zhang, Y., Zhang, M., Shi, K., et al. (2018b). Accumulation of terrestrial dissolved organic matter potentially enhances dissolved methane levels in Eutrophic Lake Taihu, China. *Environ. Sci. Technol.* 52, 10297–10306. doi: 10.1021/acs.est.8b02163

Zhu, C., Zhang, J., Nawaz, M. Z., Mahboob, S., Al-Ghanim, K. A., Khan, I. A., et al. (2019). Seasonal succession and spatial distribution of bacterial community structure in a eutrophic freshwater Lake, Lake Taihu. *Sci. Total Environ.* 669, 29–40. doi: 10.1016/j.scitotenv.2019.03.087

Conflict of Interest: The authors declare that the research was conducted in the absence of any commercial or financial relationships that could be construed as a potential conflict of interest.

The reviewer JW declared a shared affiliation, with no collaboration, with one of the authors, MR, to the handling Editor at time of review.

Copyright © 2019 Shen, Li, Ren, Lin, Wang, Chen, Li and Zhao. This is an open-access article distributed under the terms of the Creative Commons Attribution License (CC BY). The use, distribution or reproduction in other forums is permitted, provided the original author(s) and the copyright owner(s) are credited and that the original publication in this journal is cited, in accordance with accepted academic practice. No use, distribution or reproduction is permitted which does not comply with these terms.

frontiers in Microbiology

ORIGINAL RESEARCH
published: 14 May 2020
doi: 10.3389/fmicb.2020.00715

Impact of Electron Acceptor Availability on Methane-Influenced Microorganisms in an Enrichment Culture Obtained From a Stratified Lake

Sigrid van Grinsven[1]*, *Jaap S. Sinninghe Damsté*[1,2], *John Harrison*[3] and *Laura Villanueva*[1]

[1] Department of Marine Microbiology and Biogeochemistry, NIOZ Royal Netherlands Institute for Sea Research, Utrecht University, Utrecht, Netherlands, [2] Department of Earth Sciences, Faculty of Geosciences, Utrecht University, Utrecht, Netherlands, [3] School of the Environment, Washington State University Vancouver, Vancouver, WA, United States

Methanotrophs are of major importance in limiting methane emissions from lakes. They are known to preferably inhabit the oxycline of stratified water columns, often assumed due to an intolerance to atmospheric oxygen concentrations, but little is known on the response of methanotrophs to different oxygen concentrations as well as their preference for different electron acceptors. In this study, we enriched a methanotroph of the *Methylobacter* genus from the oxycline and the anoxic water column of a stratified lake, which was also present in the oxic water column in the winter. We tested the response of this *Methylobacter*-dominated enrichment culture to different electron acceptors, i.e., oxygen, nitrate, sulfate, and humic substances, and found that, in contrast to earlier results with water column incubations, oxygen was the preferred electron acceptor, leading to methane oxidation rates of 45–72 pmol cell^{-1} day^{-1}. Despite the general assumption of methanotrophs preferring microaerobic conditions, methane oxidation was most efficient under high oxygen concentrations (>600 μM). Low (<30 μM) oxygen concentrations still supported methane oxidation, but no methane oxidation was observed with trace oxygen concentrations (<9 μM) or under anoxic conditions. Remarkably, the presence of nitrate stimulated methane oxidation rates under oxic conditions, raising the methane oxidation rates by 50% when compared to oxic incubations with ammonium. Under anoxic conditions, no net methane consumption was observed; however, methanotroph abundances were two to three times higher in incubations with nitrate and sulfate compared to anoxic incubations with ammonium as the nitrogen source. Metagenomic sequencing revealed the absence of a complete denitrification pathway in the dominant methanotroph *Methylobacter*, but the most abundant methylotroph *Methylotenera* seemed capable of denitrification, which can possibly play a role in the enhanced methane oxidation rates under nitrate-rich conditions.

Keywords: methanotroph culture, nitrate, electron acceptor, *Methylobacter*, microaerobic, methane oxidation, oxygen concentration

OPEN ACCESS

Edited by:
Jonathan P. Zehr, University of California, Santa Cruz, United States

Reviewed by:
Yahai Lu, Peking University, China
John Quensen, Michigan State University, United States

***Correspondence:**
Sigrid van Grinsven
sigrid.van.grinsven@nioz.nl

Specialty section:
This article was submitted to Aquatic Microbiology, a section of the journal Frontiers in Microbiology

Received: *20 June 2019*
Accepted: *27 March 2020*
Published: *14 May 2020*

Citation:
van Grinsven S, Sinninghe Damsté JS, Harrison J and Villanueva L (2020) Impact of Electron Acceptor Availability on Methane-Influenced Microorganisms in an Enrichment Culture Obtained From a Stratified Lake. Front. Microbiol. 11:715. doi: 10.3389/fmicb.2020.00715

INTRODUCTION

Methane is the second most important greenhouse gas on earth, and a direct reduction in methane emissions is needed to keep global temperatures below the goal of 1.5°C above pre-industrial levels (Rogelj et al., 2018). Methanotrophy, the microbial conversion of methane to carbon dioxide, is a key process in limiting methane emissions from aquatic systems. Segarra et al. (2015) estimated the decrease in freshwater wetland emissions by methane oxidation to be up to 50%, while Martinez-Cruz et al. (2018) estimated that up to 34% of produced methane in lake sediments is consumed by methanotrophy. In marine systems, anaerobic oxidation of methane (AOM) is estimated to reduce methane emissions by 90% (Knittel and Boetius, 2009). A consortium of anaerobic methane-oxidizing archaea (ANME) and sulfate-reducing bacteria using sulfate as the electron acceptor for methane oxidation is responsible for this process (Boetius et al., 2000). In the water column of freshwater systems, these archaea are rarely detected, likely due to their zero tolerance to oxygen. Many anoxic lakes and reservoirs experience regular or irregular intrusions of oxygen, which make these systems less suitable habitats for ANME. Methane-oxidizing bacteria (MOB) are often detected in freshwater systems, at the oxic–anoxic interface and, more rarely, in the anoxic water column (e.g., Rudd and Hamilton, 1975; Harrits and Hanson, 1980; Biderre-Petit et al., 2011; Blees et al., 2014; Milucka et al., 2015; Oswald et al., 2016; Michaud et al., 2017). Although most methanotrophs require oxygen to oxidize methane, MOB are often assumed to prefer low-oxygen conditions over oxygen saturation. Several studies suggest an inhibitory effect of atmospheric oxygen concentrations on the methane oxidation rate (Rudd and Hamilton, 1975; Van Bodegom et al., 2001; Danilova et al., 2016; Thottathil et al., 2019). A few species of MOB have been described that could potentially use electron acceptors other than oxygen, such as nitrite (Ettwig et al., 2010) and nitrate (Kits et al., 2015; Oswald et al., 2017; Rissanen et al., 2018). Sulfate has also been suggested as an electron acceptor in freshwater sediments, but not in the water column (Schubert et al., 2011). Organic matter and humic substances, which are shown to be able to function as both an electron donor and acceptor (Lovley et al., 1996; Klüpfel et al., 2014; Valenzuela et al., 2019), have been suggested to play a role in AOM in lakes (Saxton et al., 2016; Reed et al., 2017), but have so far only been shown to impact aquatic AOM performed by ANME in marine (Scheller et al., 2016) and tropical wetland systems (Valenzuela et al., 2017, 2019).

Several studies (Murase and Frenzel, 2007; Jones and Grey, 2011; Sanseverino et al., 2012) have shown that methane-derived carbon is an important contributor to aquatic food webs on different scales. Many microbes cannot use methane and therefore depend on the conversion of methane-derived carbon by methanotrophs. Generally, methane-derived carbon is assumed to end up in methanotroph biomass or CO_2, the main reaction product of methane oxidation. However, under oxygen-limited conditions, MOB have been shown to excrete metabolites such as methanol, formaldehyde, formate, acetate, and succinate (Xin et al., 2004, 2007; Kalyuzhnaya et al., 2013; Gilman et al., 2017), which can be used by other members of the microbial community.

This study aims to expand the knowledge of how oxygen and other potential terminal electron acceptors affect methanotrophs, especially *Methylobacter*, which occur naturally in oxic, microoxic, and anoxic zones of stratified lake water columns. Previously, we showed that *Methylobacter* sp. is an important methanotroph in the seasonally stratified Lake Lacamas, and water column incubation experiments revealed that it is capable of methane oxidation under a variety of conditions (van Grinsven et al., 2019). Here, we describe the establishment of an enrichment culture dominated by *Methylobacter* and used it to evaluate the effects of the concentration of the potential electron acceptor (oxygen, nitrate, sulfate, and humic substances) on the methane oxidation rates and microbial community structure using 16S ribosomal RNA (rRNA) gene amplicon sequencing. Furthermore, the metabolic potential of selected microbial groups stimulated in the enrichment cultures was also determined by a metagenomic sequencing approach.

EXPERIMENTAL SETUP

Sample Collection

Suspended particulate matter samples were collected on 9 April 2018 from the center of Lacamas Lake, WA, USA (45.62N, 122.43W). Lacamas Lake is a seasonally stratified, hypereutrophic system with an average depth of 7.8 m and maximum depth of 19.8 m, which is on the Environmental Protection Agency list of impaired and threatened waters. It is monomictic, with stratification occurring yearly in May and a turnover mixing period from October to December. During sampling, the lake was not stratified, as determined using a Hydrolab DS5X sonde (Hach, Loveland, USA) with sensors for conductivity, temperature, dissolved oxygen, and pH. At the moment of sampling, the oxygen concentration was $>350\,\mu M$ throughout the water column, the temperature 4–8°C, and the methane concentration $<1\,\mu M$. Water was collected from 12 m depth using a VanDorn sampler, stored in carboys, and transported back to the lab, where it was filtered within 96 h over 47 mm 0.7 μm pore size glass fiber filters. Filters were stored in non-filtered lake water from 12 m depth and kept at 4°C until shipment and further processing.

Cultivation

The suspended particulate matter that was collected on the filters was scraped off and transferred under oxic conditions to 20 ml nitrate mineral salts (NMS) medium (Whittenbury et al., 1970) in a 120 ml acid-washed and autoclaved glass pressure bottle with butyl rubber stopper. A flow scheme is shown in **Figure S1**. Methane (1 ml, 99.99% pure) was added and the bottle was stored at 15°C in the dark. Every 2 weeks, the pressure bottle was opened under oxic conditions, and 2 ml of the cell-containing medium was transferred to 18 ml fresh sterile NMS medium in a sterile 120 ml glass pressure bottle with butyl stopper, after which 1 ml methane was added again. These steps were repeated every 2 weeks. After 8 weeks, the resulting enrichment culture was studied using catalyzed

reporter deposition fluorescence *in situ* hybridization (CARD-FISH) with probes MLB482 (targeting *Methylobacter*; Gulledge et al., 2001) and Creno445 (targeting *Crenothrix*; Oswald et al., 2017), following the protocol as described on https://www.arb-silva.de/fish-probes/fish-protocols. The medium was filtered over a 10 μm mesh glass fiber filter (Whatmann) to separate cell clusters from single cells, as illustrated in **Figure S1**. The cell material that remained on the filter was scraped off and transferred to a sterile 120 ml bottle with NMS media. The steps described above were repeated for this enrichment culture. The amount of biomass was increased by replicating the subculture in eight 500 to 1,000 ml glass bottles. After 8 weeks, the cells were harvested by centrifugation at 2,800 × *g* for 5 min. The supernatant was discarded and all biomass of the enrichment cultures was combined to create one uniform concentrated enrichment culture in NMS medium. Cell density was not measured. A 20 ml aliquot was used for DNA analysis.

Incubation Experiments With the Enrichment Culture

Two sets of incubation experiments were performed using the methanotroph enrichment culture. The first set of experiments was aimed at the response of *Methylobacter* to the electron acceptors nitrate (in the presence and absence of oxygen), sulfate, and humic substances and is referred to as the "electron acceptor experiments." The second set of experiments, referred to as the "O_2 concentration experiment," was set up to study the response of *Methylobacter* sp. to different oxygen concentrations. An overview of the experimental setup of these two experiments is provided in **Table S1**.

All experiments were performed in triplicate. "Electron acceptor experiments" were performed in 260 ml acid-washed and autoclaved glass bottles with butyl rubber stoppers, with a total volume of 210 ml media. The O_2 concentration experiments were performed in 120 ml bottles containing 70 ml media. The media of the "anoxic incubation" bottles and all bottles of the O_2 concentration experiments were prepared using boiled ultrapure water to minimize the initial oxygen concentration of the media. Each incubation bottle was inoculated with the same amount of concentrated enrichment culture. All media in the anoxic bottles was bubbled with nitrogen for 20 min to remove residual oxygen, after which the bottles were closed, crimp sealed, and the headspace was flushed and exchanged with N_2 gas using a GRInstruments (Wijk bij Duurstede, the Netherlands) automatic gas exchanger. Abiotic controls were set up identically to the bottles for the anoxic experiments, but were not inoculated with the concentrated enrichment culture. This resulted in a lower liquid volume and, therefore, in a methane concentration ±120 μM lower than that in the anoxic incubations.

All bottles were supplemented with 2.6 ml 100% methane (Sigma-Aldrich), shaken vigorously for 1 min to establish equilibrium between the gas and the water phase, and the methane concentration in the gas phase was subsequently measured by gas chromatography with flame ionization detection (GC-FID; Thermo Scientific Focus GC). The bottles were subsequently incubated at 15°C in the dark. Bottles were shaken at sampling moments.

Electron Acceptor Incubation Experiments

"Electron acceptor incubations" lasted 3 days for the oxic experiments and 33 days for the anoxic incubation experiments. Incubation experiments with nitrate (i.e., oxic and anoxic nitrate incubations) were performed with the same NMS medium that was used for cultivation, as described above, containing nitrate as the only nitrogen source (Whittenbury et al., 1970). Control, sulfate-supplemented, and humic-supplemented incubations of the electron acceptor experiments were performed with an AMS medium, containing ammonium rather than nitrate as the nitrogen source (1 g L^{-1} KNO_3 was replaced with 0.5 g L^{-1} NH_4Cl, as described by Whittenbury et al., 1970). As the enrichment culture used for inoculation was in the NMS media, relatively small amounts of nitrate were introduced into the control, sulfate-supplemented, and humic-supplemented incubation experiments. Anoxic nitrate-supplemented bottles of the electron acceptor experiments were amended with 0.3 g additional KNO_3 (in addition to the KNO_3 that was present in the NMS media). To the sulfate-supplemented bottles, 0.35 g Na_2SO_4 was added (target concentration, 0.012 M). The humic substance-supplemented bottles contained 1 g of commercially available humic acids mixture (Sigma-Aldrich). Methane concentrations in the headspace were measured by extracting 50 μl gas using a gas-tight syringe, daily during the first 4 days and irregularly after this initial phase. All methane analyses using a GC-FID were performed in triplicate. Methane oxidation rates were determined using linear regression analysis (Microsoft Excel version 16.16.10).

Upon termination of the experiment, all bottles were sampled for DNA by filtering the contents of the individual bottles over individual 47 mm 0.2 μm pore size polycarbonate filters. All samples were stored at −80°C until DNA was extracted by using the RNeasy Powersoil Total RNA extraction + DNA elution kits. DNA extracts were kept at −80°C until further processing.

O_2 Concentration Experiments

All experiments were performed with the NMS medium and the same concentrated culture used to inoculate the electron acceptor experiments, although 3 weeks were in between the start of the electron acceptor experiments and O_2 concentration experiments. All bottles of the O_2 concentration experiments were set up as anoxic bottles and left for 2 days after setup, after which the bottles were randomly divided into four groups, of which three received air injections. Bottles for the anoxic experiment received no injection, "trace oxygen" bottles received 20 μl air ([O_2] 7.5–9 μM), "microoxic" bottles received 160 μl air ([O_2] 23–30 μM), and "saturated oxygen" bottles received 5,000 μl air ([O_2] ±600 μM). The methane concentration in all bottles was measured on days 3 and 5, after which the "saturated oxygen" incubations were terminated. The "microoxic" and "trace oxygen" bottles received another air injection on days 6 and 13, identical to the volume of the first injections. On day 14, all incubations were terminated. DNA was sampled following the same procedure as described above, but extraction was done with the RNeasy Powersoil DNA extraction kit, after which the DNA extracts were kept at −80°C until further processing.

16S rRNA Gene Analysis

The general 16S rRNA archaeal and bacteria primer pair 515F and 806RB targeting the V4 region (Caporaso et al., 2012) was used for the 16S rRNA gene amplicon sequencing and analysis, as described in Besseling et al. (2018), with a melting temperature of 56°C. PCR products were gel purified using the QIAquick Gel-Purification kit (Qiagen), pooled, and diluted. Sequencing was performed by the Utrecht Sequencing Facility (Utrecht, the Netherlands) using an Illumina MiSeq sequencing platform (Caporaso et al., 2010). The 16S rRNA gene amplicon sequences were analyzed by the Cascabel pipeline (Asbun et al., 2019), including quality assessment by FastQC (Andrews, 2010), assembly of the paired-end reads with Pear (Zhang et al., 2014), library demultiplexing, operational taxonomic unit (OTU) clustering, and representative sequence selection ("longest" method) by diverse Qiime scripts (Caporaso et al., 2010). The OTU clustering algorithm was uclust (Edgar, 2010) with an identity threshold of 97% and assign taxonomy with BLAST (Altschul et al., 1990) by using the Silva 128 release as the reference database (https://www.arb-silva.de/; Quast et al., 2013). To compare the *Methylobacter* OTUs, we focused on OTUs with relative abundances >0.4% of the total 16S rRNA gene reads.

16S rRNA gene copies were quantified using quantitative PCR (qPCR) with the same primer pairs as used for amplicon sequencing (515F, 806RB). The qPCR reaction mixture (25 μl) contained 1 U of Pico Maxx high-fidelity DNA polymerase (Stratagene, Agilent Technologies, Santa Clara, CA), 2.5 μl of 10× Pico Maxx PCR buffer, 2.5 μl of 2.5 mM of each dNTP, 0.5 μl bovine serum albumin (20 mg ml^{-1}), 0.02 pmol μl^{-1} of primers, 10,000 times diluted SYBR Green® (Invitrogen) (optimized concentration), 0.5 μl of $MgCl_2$ (50 mM), and ultrapure sterile water. The cycling conditions for the qPCR reaction were the following: initial denaturation at 98°C for 30 s, 45 cycles of 98°C for 10 s, and 56°C for 20 s, followed by a plate read, 72°C for 30 s, and 80°C for 25 s. Specificity of the reaction was tested with a gradient melting temperature assay from 55 to 95°C, with 0.5°C increments of 5 s. The qPCR reactions were performed in triplicate with standard curves encompassing a range from 10^3 to 10^7 molecules μl^{-1}. qPCR efficiency for the 16S rRNA gene quantification was 103.7%, with $R^2 = 0.980$. For quantification of the microbial groups, we make the simplifying assumption that all microorganisms of the microbial community in Lacamas Lake contained a single 16S rRNA gene copy in their genome.

Representative sequences were extracted from the dataset and compared with closely related sequences by performing a phylogenetic analysis using the maximum likelihood method and the General Time-Reversible model in MEGA6 (Tamura et al., 2013). Additionally, the phylogenetic placement of the metagenome-assembled genome (MAG) LL-enrich-bin26 (**Table S2**), attributed to the *Methylobacter* genus, was further assessed and compared to the MAG bin63 of the *Methylobacter* clade 2 reported in van Grinsven et al. (2019) by using Phylosift (v. 1.0.1) (Darling et al., 2014) based on 34 marker genes, as described in van Grinsven et al. (2019). The 16S rRNA amplicon reads (raw data) have been deposited in the NCBI Sequence Read Archive (SRA) under BioProject number PRJNA598329, BioSamples SAMN13712582–SAMN13712612.

Metagenome Analysis

The sample that was selected for metagenomic sequencing originated from the 10 μm filtrate, (**Figure S1**). DNA was extracted as described above and used to prepare a TruSeq DNA nano-library, which was further sequenced with Illumina MiSeq 2 × 300 bp, generating over 46 million 2 × 300-bp paired-end reads. Data was analyzed with an in-house pipeline as described in van Grinsven et al. (2019). The binning of MAGs was performed with DAS Tool with penalty for duplicate marker genes and a megabin penalty of 0.3. Quality of the MAGs was assessed using CheckM v1.0.7 running the lineage-specific workflow (Parks et al., 2015). MAGs were annotated with Prokka v1.12 (Seemann, 2014) and by the Rapid Annotation using Subsystem Technology (RAST) pipeline v2.0 (Aziz et al., 2008). The annotation of key metabolic pathways was refined manually. In order to classify the MAGs according to their relative abundance in the sequenced sample, MetaBAT was run again by using the abundance estimation (total average depth, average abundance, or also called average coverage of each contig included in the bin) generated by MetaSPAdes and checked again with CheckM, as included in **Table S2**. The completeness and redundancy of the MAG bins was assessed by the DAS_Tool Package (Sieber et al., 2018). The taxonomic classification of the MAGs of interest was determined by using GTDB-Tk (v0.3.2; http://gtdb.ecogenomic.org) (**Table S2**). The metagenome of the sample specified in **Table S3** is available in NCBI under BioProject number PRJNA598329, BioSample SAMN13712974. The sequence raw data of the MAGs LL-enrich-bin26 and bin28 are deposited in NCBI under BioSample numbers SAMN13735002 and SAMN13735003, respectively.

RESULTS

The most abundant methanotroph of Lacamas Lake, a seasonally stratified lake, is a *Methylobacter* species; it was detected in the oxic water column in the winter and in the microoxic oxycline and the anoxic hypolimnion in the summer (van Grinsven et al., 2019). In order to be able to further study the response of this methanotroph to different concentrations of oxygen and other electron acceptors, an enrichment culture was established.

Enrichment Culture Microbial Community

The enrichment culture was dominated by gene sequences attributed to *Methylobacter* clade 2 (43%; **Figure 1**) (Smith et al., 2018), accompanied by 2.8% of *Methylomonas* sp. and 0.1% other methanotrophs, all part of the order Methylococcales (**Table 1**). The *Methylobacter* OTUs with the highest relative abundances were LLE-16S-2, LLE-16S-7, LLE-16S-8, LLE-16S-10, and LLE-16S-12 (**Table S4**). These OTUs form a phylogenetic subcluster of closely related sequences (i.e., 96–99% similarity; **Supplementary File 1**) in the *Methylobacter* clade 2 cluster (i.e., the Lacamas Lake OTU cluster; **Figure 1B**) together with the detected sequences in the Lacamas Lake water column (i.e., LL-16S-number). The most closely related cultured species was *Methylobacter tundripaludum* (**Figure 1A**).

Apart from *Methylobacter* sp., also bacteria of the genus *Methylotenera* were highly abundant in the enrichment culture.

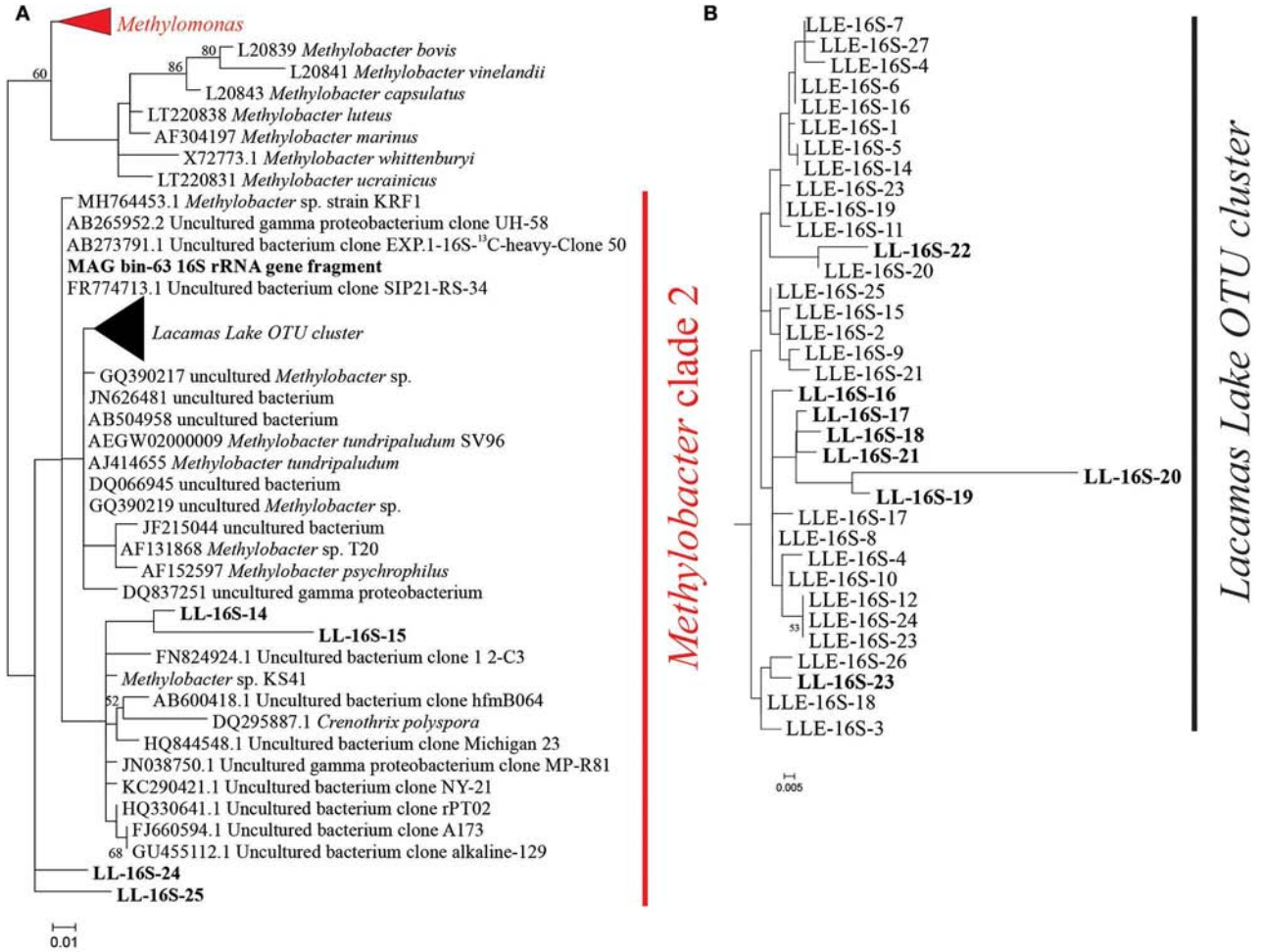

FIGURE 1 | (A) Phylogenetic 16S rRNA gene tree in which the representative sequences of the methanotrophic groups detected in the 16S rRNA gene amplicon sequencing analysis (i.e., *Methylomonas* and *Methylobacter*) of the incubation experiments are indicated in *red*. **(B)** Zoom in on the Lake Lacamas *Methylobacter* cluster as defined in the text. *LL-16S-number* sequences in *bold* represent operational taxonomic unit (OTU) sequences previously detected in the Lacamas Lake water column and the water column incubations as described in van Grinsven et al. (2019). *LLE-16S-number* sequences correspond to the *Methylobacter* OTU sequences detected in this study and are listed in **Table S4**. The *MAG bin63* 16S rRNA gene sequence corresponds to the 16S rRNA sequence of the most abundant MAG bin in a water column incubation experiment sample which was taxonomically assigned to *Methylobacter*, as described in van Grinsven et al. (2019). The phylogenetic analysis was restricted to the sequence fragment (~290 bp) obtained with the 16S rRNA amplicon sequencing analysis. Maximum likelihood estimation was performed using the General Time-Reversible model.

They represent 21% of the total 16S rRNA gene copies (**Table 1**). The detected OTUs classified as *Methylotenera* clustered with two uncultured bacterium clones; the most closely related cultured species was *Methylotenera versatilis* (**Figure 2**). Bacteria of the genus *Flavobacterium* were also relatively abundant in the enrichment culture (5.5%; **Table 2**), as well as members of the order Burkholderiales (8.3%; **Table 2**).

Metabolic Potential of the Main Microbial Components of the Enrichment Culture

In order to characterize the metabolic potential of the main microbial components of the enrichment culture, we performed metagenomic sequencing of a sample derived from the 10 μm filtrate (see **Figure S1**). *Methylobacter* sp. was less abundant than in the enrichment (i.e., 22 vs. 43% the total 16S rRNA gene reads). However, the distribution of the OTUs attributed to *Methylobacter* spp. in this sequenced sample was similar to that reported in the enrichment culture (**Table S4**). High relative abundances of *Methylotenera* (i.e., 24%) and *Methylomonas* (17%) were also evident (**Table S3**).

Metagenome sequencing resulted in three most abundant MAG bins affiliated to the methanotrophs *Methylobacter* sp. (i.e., LLE-enrich-bin26), *Methylomonas* sp. (i.e., LLE-enrich-bin27), and to the methylotroph *Methylotenera* sp. (i.e., LLE-enrich-bin28) (**Table S2**). Here, we focus on the metabolic characterization of the MAG bins affiliated to *Methylobacter* and *Methylotenera* due to their higher relative abundances in the enrichment culture (**Table 1**), specifically of the genetic potential

TABLE 1 | Relative abundance of 16S rRNA gene reads (% of total) attributed to methylotrophs and 16S rRNA copies per liter in the sample as determined using quantitative PCR.

	Sample		Electron acceptor experiment						O_2 concentration experiment			
	Starting lake water	*Methylobacter* sp. enrichment culture	Control, oxic	Nitrate, oxic	Control, anoxic	Nitrate, anoxic	Sulfate, anoxic	Humics, anoxic	Saturated	Microoxic	Trace	Anoxic
Methylobacter spp. (%)	0.6	43	44	38	11	25	19	1.6	23	21	19	20
Methylomonas spp. (%)	0.2	2.8	4.6	6.6	0.4	4.8	1.2	0.3	1.4	1.9	2	1.9
Other Methylococcales (%)	0.02	0.1	0.5	0.5	0.3	0.5	0.4	0.2	0.2	0.3	0.3	0.2
Methylotenera spp. (%)	1	21	15	22	13	17	14	14	12	11	13	11
Total 16S rRNA copies per liter	n.d.	n.d.	1.8×10^7	1.5×10^7	2.5×10^7	1.8×10^7	1.8×10^7	1.3×10^7	1.9×10^7	2.1×10^7	1.5×10^7	1.6×10^7
Methanotroph cells per liter[a]	n.d.	n.d.	4.3×10^6	3.3×10^6	1.5×10^6	2.6×10^6	1.9×10^6	0.1×10^6	2.3×10^6	2.4×10^6	1.6×10^6	1.7×10^6

n.d., not determined.

[a]*Calculated with assuming two copies of the 16S rRNA gene per Methylobacter cell, three copies per Methylomonas cell, and one copy per "other Methylococcales" cell.*

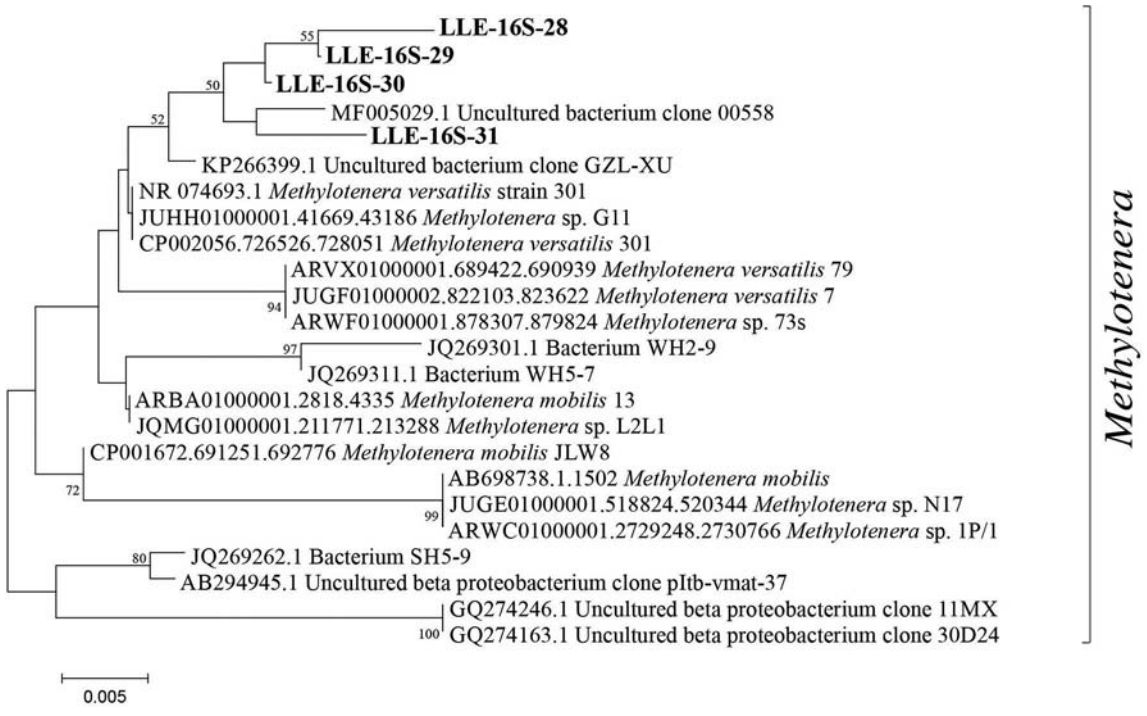

FIGURE 2 | Phylogenetic 16S rRNA gene tree with representative sequences of the operational taxonomic units (OTUs) classified as *Methylotenera*, indicated in *bold*. The phylogenetic analysis was restricted to the sequence fragment (~290 bp) obtained with the 16S rRNA amplicon sequencing analysis. Maximum likelihood estimation was performed using the General Time-Reversible model.

of the nitrogen and methane and carbon metabolism. The MAG LLE-enrich-bin26 is taxonomically classified as a *Methylobacter* sp. and harbors all the genes encoding for the particulate methane monooxygenase (pMMO; see **Supplementary File 2**), allowing for the conversion from methane to methanol, while the *Methylotenera* MAG LLE-enrich-bin28 lacks this gene (**Supplementary File 3**; **Figure 3**). The genes required for the further conversion from methanol to CO_2 are present in both MAGs (see **Figure 3**). Regarding the nitrogen metabolism pathways, both the *Methylobacter* and *Methylotenera*

TABLE 2 | Relative abundance of 16S rRNA gene reads (% of total) of other microbial groups discussed in the manuscript.

	Sample		Electron acceptor experiment						O_2 concentration experiment			
	Starting lake water	Enrichment culture	Control, oxic	Nitrate, oxic	Control, anoxic	Nitrate, anoxic	Sulfate, anoxic	Humics, anoxic	Saturated	Microoxic	Trace	Anoxic
Brevundimonas	0.1	0.5	0.6	0.5	15	3.2	10	1.3	2.2	3.2	3.1	3.5
Burkholderiaceae	15	8.3	12	6	11	11	10	30	9.5	10	10	10
Flavobacterium	1.5	5.5	4	5.4	18	10	16	16	12	14	16	14
Pseudomonas	0.2	0.1	0.3	0.2	3	2	1.3	5.9	0.5	1.1	1	0.9
Rhodocyclaceae	0.8	0.2	0.4	0.4	1.9	0.9	1.9	2.1	0.9	1.8	1.8	1.8
Sulfuritalea	0.4	0.2	0.2	0.2	1.0[a]	0.5	1.3	0.9	0.2	0.5	0.5	0.6

[a] *High standard deviation between triplicate incubations of 0.45%.*

LLE-enrich-bin26 and bin28 MAGs harbor the genes encoding for nitrate transporters, assimilatory nitrate reductase (Nas), nitrite reductase (NirBD) to ammonia and to nitric oxide (NirK), as well as the gene coding for the nitric oxide reductase (NorBC) to nitrous oxide (N_2O), but not the genes coding for the nitrous oxide reductase (NorZ) to dinitrogen gas (**Figure 3**).

Microbial Community Composition and Methane Consumption in Incubation Experiments With Different Electron Acceptors

Two sets of incubation experiments were performed using the methanotroph enrichment culture obtained. The first set of experiments was aimed at the response of *Methylobacter* sp. to the electron acceptors nitrate (in the presence and absence of oxygen), sulfate, and humic substances. In all oxic experiments, methane was consumed rapidly (**Figure 4**). The experiments were terminated within 2–3 days in anticipation of methane depletion. The net methane consumption rate of the incubation with nitrate was higher than that in the control incubation with ammonium (310 and 200 μmol L^{-1} day^{-1}, respectively). We estimated that the total number of methanotrophic bacteria in the oxic incubations was 3.3×10^6–4.3×10^6 cells L^{-1} (**Table 1**).

The methane turnover rate per cell is, therefore, estimated to be 45 and 72 pmol $cell^{-1}$ day^{-1} for the control and nitrate-amended oxic incubations, respectively. No net methane consumption could be detected under anoxic conditions, even with the addition of the alternative electron acceptors nitrate, sulfate, or humic substances (**Figure 4**). Nitrate concentration measurements showed no clear difference between the nitrate concentrations at the start and the end of the experiment (**Figure S2**), mainly due to large variations between the samples and the high starting concentrations.

The relative abundance of *Methylobacter* sp. was significantly higher ($p < 0.05$; **Table S5**) in the two oxic incubations of the electron acceptor experiment when compared to the anoxic incubations. The *Methylobacter* abundance in the oxic incubations (43 and 38% for the control and nitrate-supplemented, respectively; **Table 1**) was not significantly different due to substantial variations between replicates. The addition of different electron acceptors in the anoxic incubations changed the microbial community (**Tables 1**, **3**). The addition of nitrate or sulfate resulted into a significantly ($p < 0.05$; **Table S5**) higher *Methylobacter* abundance (25 and 18%, respectively; **Table 1**) compared to the anoxic control (11%; **Table 1**). *Methylobacter* OTUs LLE-16S-2 and LLE-16S-7 were the most abundant in the oxic incubations, similarly to the enrichment culture (**Table S4**). LLE-16S-12, which was highly abundant in the enrichment culture, became less dominant in the incubations. Similar to the oxic incubations, LLE-16S-2 and LLE-16S-7 were the most abundant *Methylobacter* OTUs in the anoxic control and nitrate incubations, with, in addition, a relatively high abundance of LLE-16S-9 (**Table S4**). The sequences closely related to *Methylotenera* (**Figure 2**) remained relatively abundant in all incubation experiments (14–29%; **Table 1**). Bacteria of the genera *Flavobacterium Brevundimonas* and *Pseudomonas* had higher relative abundances in the anoxic than in oxic incubations, both with and without nitrate, although *Brevundimonas* was more abundant in the anoxic incubations without nitrate (**Table 2**). *Brevundimonas* comprised 15 and 3% of the total microbial abundance in the anoxic control and nitrate-supplemented incubations, respectively. The genus *Sulfuritalea* was more abundant in the anoxic sulfate incubations (1.3%) than in nitrate incubations (0.5%; **Table 2**). The microbial community composition of the incubation with added humic substances was completely different compared to the other anoxic incubations (**Tables 1**, **2**), with remarkably high relative abundances of bacteria of the order Burkholderiales and the family Comamonadaccea (31 and 16%, respectively). The relative abundance of total archaeal 16S rRNA gene sequences was below 0.5% in all incubations.

Microbial Community Composition and Methane Consumption in Incubation Experiments With Different Oxygen Concentrations

The second set of incubation experiments performed with the *Methylobacter* sp. enrichment culture was aimed at the response of *Methylobacter* sp. to different oxygen conditions. We incubated the enrichment culture under saturated ($[O_2]$ >600 μM), microoxic ($[O_2]$ 23–30 μM), trace oxygen ($[O_2]$ 7.5–9 μM), and anoxic conditions.

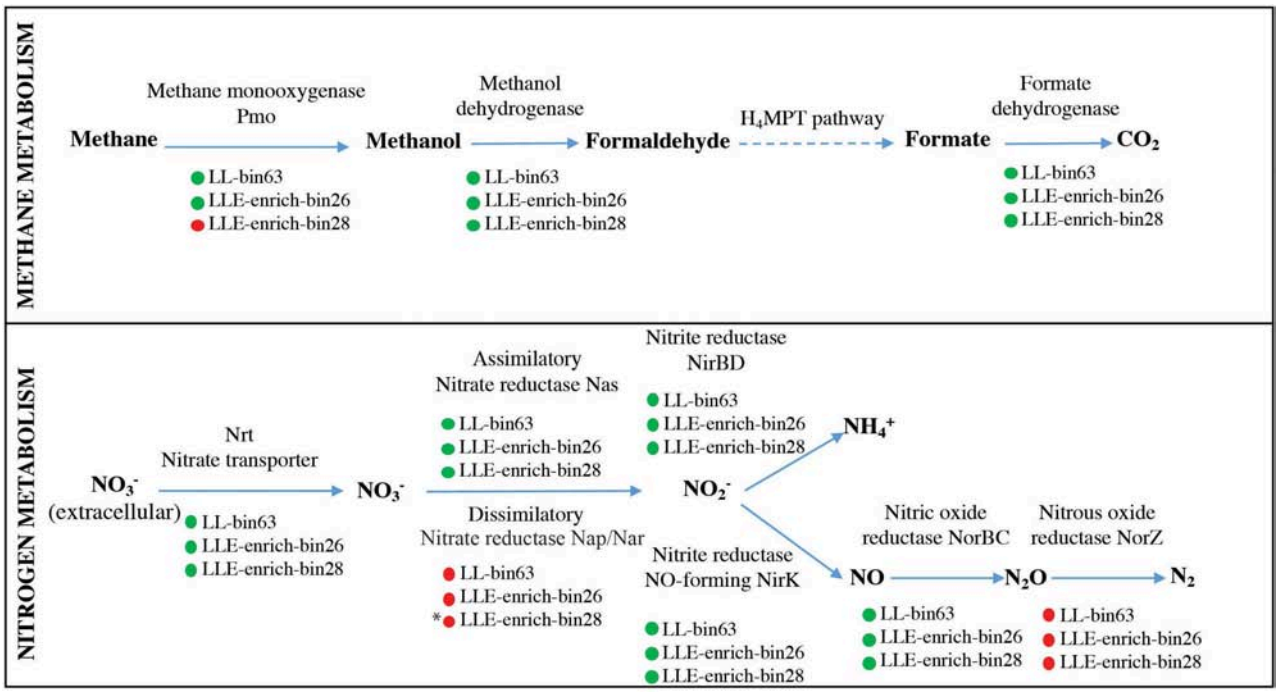

FIGURE 3 | Description of the genes present in the *Methylobacter* LLE-enrich-bin26 and *Methylotenera* LLE-enrich-bin28 regarding their methane and nitrogen metabolic pathways and comparison with the *Methylobacter* MAG LL-bin63 previously obtained from incubations with Lacamas Lake water samples (van Grinsven et al., 2019). *Green* and *red circles* indicate the presence/absence of the coding gene. * indicates that *Methylotenera* LLE-enrich-bin28 may have the potential to perform dissimilatory nitrate reduction in the absence of the *Nap/Nar* gene, as explained in the text.

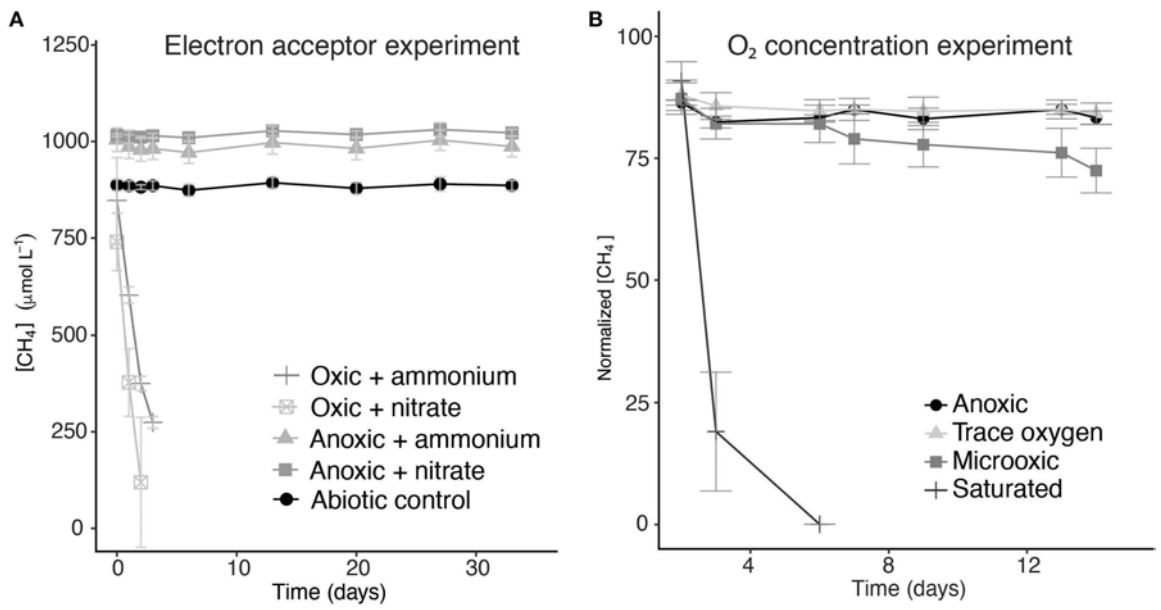

FIGURE 4 | Methane concentrations over time during the incubation experiments with different electron acceptors **(A)** and normalized methane concentrations in incubation experiments with different oxygen concentrations **(B)**. *Error bars* represent the standard error of triplicate incubations. The methane concentrations over time of the incubations to which sulfate and humic substances were added are not shown, but were very similar to the ammonium- and nitrate-supplemented anoxic incubations.

The methane consumption rates were two orders of magnitude higher under oxygen saturation condition than under microoxic conditions (520 and 6.4 μM day^{-1}, respectively). Under trace oxygen and anoxic conditions, no methane consumption was observed (**Figure 4B**). Based on the measured concentrations of methane and the estimated concentrations of oxygen in the vials, a ratio of methane and oxygen consumption was calculated. The oxygen concentration in the saturated oxygen incubations (±640 μM) was, assuming methanotrophy was the only process consuming oxygen, present in surplus and, thus, sufficient for a 2:1 molar ratio of oxygen/methane usage. In the microoxic incubation bottles, between 6 and 8 μmol of methane was consumed over the whole duration of the experiment. The amount of oxygen present in the microoxic incubations was estimated based on oxygen measurements and injected air volume, to be maximum 7.1 μmol, allowing for a maximum ratio of 1:1 in the oxygen/methane usage.

The relative abundance of the 16S rRNA gene sequences attributed to *Methylobacter* was highest in the incubation under saturated oxygen conditions (23%; **Table 1**), but the absolute abundances of all methanotrophs (including *Methylotenera*, *Methylomonas*, *Methylotenera*, or other Methylococcales) were not significantly different between the oxic, microoxic, trace, and anoxic experiments (1.6–2.3 × 10^6 cells L^{-1}; **Table 1**). Overall, the communities of the microoxic, suboxic, and anoxic incubations were similar, whereas the community under saturated oxygen conditions was significantly different, with lower relative abundances of all non-methanotrophic species, as listed in **Table 2**.

DISCUSSION

Lacamas Lake, the source of the material used for our enrichment culture, contained uncultured *Methylobacter* species thriving in the oxic and anoxic water columns as well as in the microoxic oxycline (van Grinsven et al., 2019). Incubations with water column samples revealed that these bacteria oxidized large amounts of methane (72 μM day^{-1}) under anoxic conditions in the stratified summer water column, stimulated by the addition of both nitrate and sulfate (van Grinsven et al., 2019), but were also naturally present in the oxic, methane-depleted winter water column. Phylogenetic analysis showed that the *Methylobacter* species of the Lacamas Lake summer and winter water columns and incubations grouped closely together with the *Methylobacter* species that dominated the enrichment culture (i.e., 96–99% similarity; **Figure 1**). *Methylobacter* and related methanotrophs have been previously detected in lakes, mostly under microoxic conditions ([O_2] ±60 μM) (Rudd and Hamilton, 1975; Harrits and Hanson, 1980; Oswald et al., 2016; Michaud et al., 2017), but also in anoxic environments, such as sediments or anoxic lake waters (Biderre-Petit et al., 2011; Milucka et al., 2015; Martinez-Cruz et al., 2017). Although most bacteria falling in the *Methylobacter* group are known as aerobic methanotrophs, it has recently been suggested that specific species contain the genomic potential to perform anaerobic methane oxidation, or methane oxidation under strong oxygen limitation, by coupling methane oxidation to nitrate reduction (Svenning et al., 2011; Smith et al., 2018) or by using a fermentation pathway (van Grinsven et al., 2019). Knowledge on the effect of other electron acceptors (i.e., sulfate and humic substances) on *Methylobacter* sp. is, however, lacking, and often the biochemical pathways involved in methanotrophy under anoxic conditions remain unclear (Biderre-Petit et al., 2011; Blees et al., 2014; Martinez-Cruz et al., 2017; Reed et al., 2017). Despite the increase in methane oxidation rates (from 9 to 72 μM day^{-1}) that was observed in anoxic Lacamas Lake incubations with the addition of nitrate, the genome of the dominant *Methylobacter* species did not encode all the genes required to perform denitrification, and its mechanisms for anaerobic methane oxidation therefore remain unclear (van Grinsven et al., 2019).

In the current study, we aimed to determine the preference of the *Methylobacter* species, and other methanotrophs present in Lacamas Lake, for oxygen concentrations and electron acceptors other than oxygen, such as nitrate, by means of laboratory incubations with an enrichment culture.

Methylobacter sp. in Water Column and Enrichment Culture Incubations

The *Methylobacter* OTU sequences detected in the enrichment culture obtained from Lacamas Lake were closely related to the sequences previously detected both in Lacamas Lake water column and incubation studies with lake water samples, as was confirmed by the 16S rRNA gene phylogeny (**Figure 1**). In addition, the *Methylobacter* MAG bin obtained from the enrichment culture (i.e., LLE-enrich-bin26) was also closely related to the *Methylobacter* MAG previously obtained in an incubation with Lacamas Lake water (i.e., LL-bin63) (van Grinsven et al., 2019; see **Figure S3**). Therefore, we conclude that the *Methylobacter* species obtained in the enrichment culture in this study are representative of those existing in Lacamas Lake and can thus be used to draw conclusions on their electron acceptor and oxygen preferences, which can be extrapolated to the conditions in the original system. Both the two *Methylobacter* MAGs coincided in their genetic potential to oxidize methane, perform mixed-acid fermentation from pyruvate to succinate and H_2 (**Figure S4**), as well as in harboring an incomplete denitrification pathway (**Figure 3**). Several methanotrophs contain parts of the denitrification pathway, but only few species have been shown to couple methane oxidation to denitrification (Smith et al., 2018). Based on its genetic potential, the *Methylobacter* species present in our incubation experiments could be capable of dissimilatory nitrite reduction, but as no nitrite was provided in the incubation experiments, we do not expect this pathway to be relevant for methane oxidation.

Methylotenera–Methylobacter Co-occurrence

Bacteria of the genus *Methylotenera*, which were highly abundant in our enrichment culture incubations (11–22%), have often been detected in co-occurrence with methanotrophs and have been shown to use reaction products of methanotrophy (Yu

and Chistoserdova, 2017), coupling methanol oxidation to nitrate reduction (Kalyuzhnaya et al., 2011). Their relative abundances increased not only in the enrichment culture but also in water column incubations with high methane oxidation rates (van Grinsven et al., 2019); an interaction between *Methylobacter* and *Methylotenera* species is, therefore, not unlikely. The *Methylotenera* MAG LLE-enrich-bin28 has the genomic potential to oxidize methanol (**Figure 3**), but lacks the *pmoA* gene necessary for the oxidation of methane. Its denitrification pathway seems incomplete as the gene encoding for the dissimilatory reduction of nitrate to nitrite (*Nap*/*Nar* gene) was missing. A mutant phenotype study on *Methylotenera mobilis*, however, demonstrated that the single subunit nitrate reductase (*Nap*), Mmol_1648, appears to be involved in both the assimilatory and dissimilatory denitrification pathways (Mustakhimov et al., 2013). The nitrate reductase (*Nas*) detected in our *Methylotenera* MAG LLE-enrich-bin28 was homologous to the nitrate reductase (*Nap*) of *M. mobilis*. The *Methylotenera* species detected in our incubations may therefore also be able to perform denitrification, similarly to the *Methylotenera* species that have been described in the literature before (*M. mobilis* and *M. versatilis*: Lapidus et al., 2011; Mustakhimov et al., 2013).

Role of Nitrate and Ammonium in Methane Oxidation

The methane oxidation rates of the oxic incubation experiments were higher than those observed previously in environmental studies (Eller et al., 2005; Schubert et al., 2010; Blees et al., 2014), but a proper comparison between an enrichment culture and environmental studies is difficult to make. The methane oxidation rates in the oxic incubations with nitrate were significantly higher than those in the ammonium control incubations (311 and 195 μmol L^{-1} day^{-1}, respectively), despite the fact that the methanotroph abundance was higher in the oxic control (8.6×10^6 copies L^{-1} in the control and 6.7×10^6 copies L^{-1} in the nitrate-amended incubations). Ammonium (NH_4^+), which was added to the control experiment as the nitrogen source, can lower the methanotrophic activity due to the structural similarity between CH_4 and NH_4^+, causing competitive inhibition (Bédard and Knowles, 1989). The affinity of the methane monooxygenase enzyme for CH_4 is, however, 600- to 1,300-fold higher than the affinity for NH_4^+, so we expect this effect to be of little influence. Generally, ammonium stimulates methanotroph growth and protein synthesis by providing bioavailable nitrogen (Bodelier et al., 2000), although recent research in soils found a decrease in methane oxidation rates after ammonium addition (Walkiewicz et al., 2018). Nitrate has also been suggested in earlier studies to inhibit methane oxidation under oxic conditions (Geng et al., 2017; Walkiewicz and Brzezinska, 2019), although the observed effect in those studies could have been due to the high salt concentrations, not specifically nitrate (Dunfield and Knowles, 1995), or due to the conversion of nitrate to nitrite (Roco et al., 2016), which is known to be an inhibitor of methane oxidation (Dunfield and Knowles, 1995; Hutsch, 1998).

As we consider ammonium inhibition unlikely, we assume a stimulating effect of nitrate on the oxic methane oxidation rate. As discussed above, the dominant *Methylobacter* species in both the enrichment cultures as well as the water column lack the genes for a complete denitrification pathway. A complete assimilatory nitrate reduction pathway was present, and nitrate can thus be used for protein synthesis, enhancing growth. Another possibility would, however, be an interaction with *Methylotenera*, which is likely capable of denitrification. *Methylotenera* could function as a syntrophic partner for *Methylobacter*, as has been observed in several methane-oxidizing bacteria and archaea (Boetius et al., 2000; Milucka et al., 2015; Krause et al., 2017). Whether such a partnership indeed exists in our incubation experiments requires more research.

Methylobacter sp. Under Oxygen Limitation

Surprisingly, in contrast to the water column incubation studies, in which methane oxidation by *Methylobacter* was the highest under oxygen-limiting conditions (van Grinsven et al., 2019), methane oxidation in incubations with the enrichment culture was the highest under oxygen-saturated conditions (**Figure 4B**). Methane oxidation under low-oxygen conditions (microoxic; O_2, 23–30 μM) occurred, but was much less efficient than the methanotrophy under oxygen saturation conditions. The oxygen concentration in the closed bottles was measured only at the start of the incubations, and the concentrations may thus have changed over the course of the experiments. Air was, however, injected into the microoxic and trace oxygen incubation bottles on days 2, 6, and 13 in order to prevent oxygen depletion. Despite being aerobes, methanotrophs are generally assumed to be (partially) inhibited by oxygen concentrations $>60\,\mu$M or at least stimulated by low-oxygen conditions (Rudd and Hamilton, 1975; Van Bodegom et al., 2001; Danilova et al., 2016; Walkiewicz et al., 2018; Thottathil et al., 2019; Walkiewicz and Brzezinska, 2019), resulting in a low methane oxidation efficiency at high oxygen concentrations. A recent study by Thottathil et al. (2019) stated that methane oxidation rates are only at 20% of their maximum value at oxygen saturation and that the fact that this oxygen inhibition is generally not considered for global models may offset the total methane oxidation potential calculations greatly, expressing the need for additional studies on the response of methanotrophs to different oxygen concentrations. Our data reveal that this general assumption about the oxygen inhibition of methanotrophy is not correct for the *Methylobacter* species present in this lake system.

The methane oxidation detected in the microoxic conditions may depend partially on a fermentative pathway, as was also suggested for methanotrophs in the Lacamas Lake water column (van Grinsven et al., 2019), with an energy yield too low for cell growth but supporting only cell maintenance. It, however, remains unclear why the *Methylobacter* cells in the trace oxygen and anoxic incubations, which possibly went into a dormant state, remain almost as abundant as the *Methylobacter* cells in the oxic and microoxic experiments, while no methane oxidation and, thus, no energy production seemed to take place in the first

two. Similarly, methanotrophs remained a substantial part of the community in the anoxic electron acceptor incubations despite no detectable methane oxidation, with higher *Methylobacter* abundances in the nitrate- and sulfate-amended incubations compared to the control (19 and 25%, 4.3×10^6 and 3.3×10^6 methanotroph cells per liter in the nitrate and sulfate incubations, respectively, while only 11%, 2.6×10^6 methanotroph cells per liter in the anoxic control). The DNA method used cannot distinguish between dead, dormant, or active cells, but the strong contrast between the nitrate and sulfate incubations, and the incubations with humic substances, in which a major reduction in *Methylobacter* relative abundance to 1.6% and a decrease in methanotroph abundance to 1×10^5 cells L^{-1} (**Table 1**) was observed, suggests that a difference between the treatments exists. Methanotrophs were shown to have an efficient survival mechanism under starvation in anoxic conditions compared to starvation under oxic conditions (Roslev and King, 1995), increasing their chance of survival under stress conditions.

Methane oxidation occurred directly after oxygen injection into the oxic and microoxic bottles (**Figure 4**), despite the fact that the cultures were under anoxic conditions for several days before the start of the experiment. It is unknown whether the cells were in a dormant state under anoxic conditions, but these results showed that no recovery time was needed, therefore implying a fast adaptation mechanism. This ability to rapidly adapt to anoxic or oxic conditions could be a strategy of methanotrophs living in dynamic environments, such as seasonally stratified water columns, allowing them to rapidly adapt to the changing conditions of their niche.

Fermentation-based methane oxidation, which could potentially be performed by *Methylobacter* under trace oxygen conditions, has been shown to occur under extremely low methane oxidation and growth rates (1.75 nmol min^{-1} mg^{-1} protein) (Kalyuzhnaya et al., 2013). Rates like these were below the detection limit of our methods, opening the possibility of low-rate methane oxidation in the trace oxygen incubations.

Methane Oxidation Under Anoxic Conditions

No methane oxidation was observed under the anoxic conditions in the *Methylobacter* enrichment culture obtained in this study despite *Methylobacter* being present and active under the anoxic conditions in the incubations performed with the water column samples (van Grinsven et al., 2019). Possibly, the anaerobic methane oxidation rates were too low to detect by our methods. Rates in anoxic lake waters have been reported to be in the range of 0.1–2.5 μM day^{-1} (Blees et al., 2014; Oswald et al., 2016). If comparable rates would occur in our anoxic incubations, the result would be a total decrease in methane of 3.2–80 μM over the full 32-day period, which would be difficult to detect given the large fluctuations between our measurements. The measured methane oxidation rates in the Lacamas Lake anoxic water column were, however, much higher (up to 45 μM day^{-1}) (van Grinsven et al., 2019). Simultaneous methane production, counteracting the decrease in the concentration of methane caused by oxidation, could also have masked methane consumption. Methane production in anoxic systems is commonly observed, both in environmental and culture studies (Reeburgh, 2007; Conrad et al., 2011; Grasset et al., 2018), and could be fueled by the reaction products of methane oxidation by *Methylobacter*, such as acetate or methanol (Oremland and Polcin, 1982). We did, however, not detect commonly known methane producers such as methanogenic archaea with the 16S rRNA gene diversity analysis.

Possibly, non-methanotrophic members of the microbial community, which are present in the natural community of the Lacamas Lake water column, are essential in mediating methane oxidation under anoxic conditions. These microbes may not have been selected in the oxic enrichment process used in this study. In this regard, Oswald et al. (2015) showed that methanotrophs in the anoxic hypolimnion of Lake Rotsee were dependent on phototrophic microorganisms for the production of oxygen to mediate their methane oxidation pathway. This pathway was not relevant in our incubations, which were performed in the dark, but a similar collaboration between a non-methanotrophic species and *Methylobacter* species may be essential in mediating methane oxidation under anoxic conditions. A possible candidate could be bacteria of the genus *Sulfuritalea*, which were abundant in the water column incubations in which anoxic methane oxidation was observed (van Grinsven et al., 2019), but which were only present in low relative abundance in the enrichment culture and the incubation experiments of the current study (**Table 2**). They could be potentially involved as a partner in anoxic methane oxidation due to their capabilities of nitrate reduction (Kojima and Fukui, 2011). In contrast, bacteria of the order Burkholderiales were abundant in both the water column incubations and the enrichment culture incubations, although they were most abundant in the enrichment incubations with humic substances, which actually contained the lowest abundance of methanotrophs (**Tables 1**, **2**). Another possibility could be the composition of the medium. The enrichment culture incubation experiments were performed on a rich media, including common trace metals and a vitamin solution. Certain compounds may, however, have been present in the lake water, which were missing in the medium. Lanthanides, part of the rare earth elements, have been shown to affect *Methylobacter* (Krause et al., 2017) and were not added to the enrichment medium. Possibly, compounds like these were lacking in the enrichment incubation experiments and limited anaerobic methane oxidation.

CONCLUSIONS

Studies have found methanotrophs at a wide range of locations and environmental conditions. Despite these observations, little is known about the drivers of the spatial distribution that is observed, while recent research stressed the importance of a correct representation of the nonlinear response of methane oxidation rates to oxygen concentrations (Thottathil et al.,

2019). The effect of nitrogen and oxygen concentrations on methanotrophs was shown to differ strongly between similar environments, likely due to the different organic carbon contents (Walkiewicz and Brzezinska, 2019), indicating that the relationships between the methane oxidation rates, methanotroph abundance, nitrogen source, and oxygen concentration are complicated and that more work is needed to understand these relationships. Our study shows that *Methylobacter* sp., a methanotroph often assumed to thrive under low-oxygen conditions, preferred high-oxygen conditions over a microoxic environment under laboratory conditions. When comparing this data with an environmental study with the same *Methylobacter* species, we, however, saw that the oxygen response of this species is dependent on factors we do not yet fully understand, potentially involving interactions with other non-methanotrophic microorganisms present in the same system. More research is therefore needed to reveal the pathways and microorganisms involved in the aerobic and anaerobic methane oxidation by this *Methylobacter* species.

DATA AVAILABILITY STATEMENT

The 16S rRNA amplicon reads (raw data) have been deposited in the NCBI Sequence Read Archive (SRA) under BioProject number PRJNA598329, BioSamples SAMN13712582-SAMN13712612. The metagenome of the sample specified in **Table S3** is available in NCBI under BioProject number PRJNA598329, BioSample SAMN13712974. The sequence raw data of the MAGs LL-enrich-bin-26, and bin-28 are deposited in NCBI under BioSample numbers SAMN13735002 and SAMN13735003, respectively.

AUTHOR CONTRIBUTIONS

SG designed and conducted the experiments under the supervision of LV and JS. LV and JH assisted in designing the experiment. SG and LV analyzed the data. SG wrote a first draft of the manuscript, to which all authors contributed in subsequent revisions.

FUNDING

This research was supported by the Soehngen Institute of Anaerobic Microbiology (SIAM) Gravitation grant (024.002.002) to JS and LV of the Netherlands Ministry of Education, Culture and Science (OCW) and the Netherlands Organisation for Scientific Research (NWO).

ACKNOWLEDGMENTS

We sincerely thank Keith Birchfield for sample collection and for taking care of the sample transport to the Netherlands. We thank Maartje Brouwer and Sanne Vreugdenhil for help with qPCR analysis, Alejandro Abdala, and Julia Engelmann for support with the bioinformatics analyses, and Jan van Ooijen of the NIOZ nutrient lab. Darci Rush was appreciated for her help in proofreading this manuscript.

SUPPLEMENTARY MATERIAL

The Supplementary Material for this article can be found online at: https://www.frontiersin.org/articles/10.3389/fmicb.2020.00715/full#supplementary-material

Figure S1 | Overview of experimental methods. The lake graphic represents Lacamas Lake, with on the left side the mixed winter water column, homogeneously low in methane and rich in oxygen, and on the right side the stratified summer water column, with a methane-rich oxygen-depleted deeper water layer and a methane-poor and oxygen-rich top water layer. Samples for this study were collected in the mixed winter water column, transferred onto nitrate mineral salts (NMS) media **(A)** and received methane. The enrichment culture was subcultured six times, by transferring culture to fresh media rich in methane in a 1:20 dilution, before using size separation **(B)** to increase the *Methylobacter* relative abundance. The particulate matter that remained on the 10 μm filter was scraped off and suspended in fresh media **(C)**. The resulting cultures were again subcultured six times **(D)**, and afterwards combined and concentrated to create one concentrated culture that was used to set up incubation experiments **(E)**. A sample for metagenomic sequencing was obtained via subculturing of the filtrate **(F)**. This metagenomic sequencing sample is described in **Table S3**. For more details, see the Experimental setup section.

Figure S2 | Nitrate concentration at the start and end of the electron acceptor incubation experiments. Error bars represent the standard error over triplicate incubations.

Figure S3 | Maximum likelihood phylogenetic tree based on 34 concatenated single-copy, protein-coding genes (following the method of Dombrowski et al., 2018) of the MAG bin LLE-enrich-bin26 and the MAGs as described in van Grinsven et al. (2019) (i.e., bin-63, bin-37, and bin-19).

Figure S4 | Predicted pathway for mixed-acid fermentation from pyruvate to succinate and H2 production in the *Methylobacter* LL-bin63 and *Methylobacter* LLE-enrich-bin26 (Green and red circles indicate presence/absence of the coding gene).

Table S1 | Overview of the media (AMS - ammonium mineral salts, NMS - nitrate mineral salts) used in the incubation experiments, and of the additions of methane, additional nitrate, sulfate or humic substances to the incubation experiments.

Table S2 | Characteristics of the most abundant MAGs detected in the sample derived from the 10 μm filtrate (**Figure S1**), which contained a high diversity in *methanotrophs* (i.e. 22% *Methylobacter* and 17% *Methylomonas*) and a high relative abundance of *Methylotenera* (i.e. 24%) based on 16S rRNA gene amplicon sequencing. Avg, average. Classification was inferred by GTDB-Tk as indicated in the material and methods.

Table S3 | Composition of the sample that was used for metagenome sequencing.

Table S4 | Relative abundance (%) of *Methylobacter* OTUs (>0.4% in at least one of the samples) in respect to the total 16S rRNA gene reads in the amplicon sequencing analysis for each incubation and for the enrichment sample used for the metagenomic sequencing.

Table S5 | P-value of t-tests between *Methylobacter* relative abundances of the three replicates per incubation type, indicating whether the difference in relative abundance between sample categories was statistically significant.

Supplementary File 1 | Rapid Annotation using Subsystem Technology (RAST) annotation of the MAG LLE-enrich-26 Methylobacter.

Supplementary File 2 | Rapid Annotation using Subsystem Technology (RAST) annotation of the MAG LLE-bin28 Methylotenera.

Supplementary File 3 | Percentage of similarity of the sequences included in the phylogenetic tree of **Figure 2**.

REFERENCES

Altschul, S. F., Gish, W., Miller, W., Myers, E. W., and Lipman, D. J. (1990). Basic local alignment search tool. *J. Mol. Biol.* 215, 403–410. doi: 10.1016/S0022-2836(05)80360-2

Andrews, S. (2010). *FastQC, a Quality Control Tool for High Throughput Sequence Data, Version 0.11.9*. Available online at: http://www.bioinformatics.babraham.ac.uk/projects/fastqc/ (accessed April 2019).

Asbun, A. A., Besseling, M. A., Balzano, S., Bleijswijk, J., Van, Witte, H., Villanueva, L., et al. (2019). Cascabel, a flexible, scalable and easy-to-use amplicon sequence data analysis pipeline. *BioRxiv*. 809384. doi: 10.1101/809384

Aziz, R. K., Bartels, D., Best, A. A., Dejongh, M., Disz, T., Edwards, R. A., et al. (2008). The RAST server, rapid annotations using subsystems technology. *BMC Genomics* 15, 1–15. doi: 10.1186/1471-2164-9-75

Bédard, C., and Knowles, R. (1989). Physiology, biochemistry, and specific inhibitors of CH4, NH4+, and CO oxidation by methanotrophs and nitrifiers. *Microbiol. Rev.* 53, 68–84. doi: 10.1128/MMBR.53.1.68-84.1989

Besseling, M. A., Hopmans, E. C., Christine Boschman, R., Sinninghe Damsté, J. S., and Villanueva, L. (2018). Benthic archaea as potential sources of tetraether membrane lipids in sediments across an oxygen minimum zone. *Biogeosciences* 15, 4047–4064. doi: 10.5194/bg-15-4047-2018

Biderre-Petit, C., Jézéquel, D., Dugat-Bony, E., Lopes, F., Kuever, J., Borrel, G., et al. (2011). Identification of microbial communities involved in the methane cycle of a freshwater meromictic lake. *FEMS Microbiol. Ecol.* 77, 533–545. doi: 10.1111/j.1574-6941.2011.01134.x

Blees, J., Niemann, H., Wenk, C. B., Zopfi, J., Schubert, C. J., Kirf, M. K., et al. (2014). Micro-aerobic bacterial methane oxidation in the chemocline and anoxic water column of deep south-Alpine Lake Lugano (Switzerland). *Limnol. Oceanogr.* 59, 311–324. doi: 10.4319/lo.2014.59.2.0311

Bodelier, P. L. E., Roslev, P., Henckel, T., and Frenzel, P. (2000). Stimulation by ammonium-based fertilizers of methane oxidation in soil around rice roots. *Nature*. 403, 421–424. doi: 10.1038/35000193

Boetius, A., Ravenschlag, K., Schubert, C. J., Rickert, D., Widdel, F., Gieseke, A., et al. (2000). A marine microbial consortium apparently mediating anaerobic oxidation of methane. *Nature.* 407, 623–626. doi: 10.1038/35036572

Caporaso, J. G., Kuczynski, J., Stombaugh, J., Bittinger, K., Bushman, F. D., Costello, E. K., et al. (2010). QIIME allows analysis of high-throughput community sequencing data. *Nat. Methods* 7, 335–336. doi: 10.1038/nmeth.f.303

Caporaso, J. G., Lauber, C. L., Walters, W. A., Berg-Lyons, D., Huntley, J., Fierer, N., et al. (2012). Ultra-high-throughput microbial community analysis on the Illumina HiSeq and MiSeq platforms. *ISME J.* 6, 1621–1624. doi: 10.1038/ismej.2012.8

Conrad, R., Noll, M., Claus, P., Klose, M., Bastos, W. R., and Enrich-Prast, A. (2011). Stable carbon isotope discrimination and microbiology of methane formation in tropical anoxic lake sediments. *Biogeosciences* 8, 795–814. doi: 10.5194/bg-8-795-2011

Danilova, O. V., Suzina, N. E., Van De Kamp, J., Svenning, M. M., Bodrossy, L., and Dedysh, S. N. (2016). A new cell morphotype among methane oxidizers, A spiral-shaped obligately microaerophilic methanotroph from northern low-oxygen environments. *ISME J.* 10, 2734–2743. doi: 10.1038/ismej.2016.48

Darling, A. E., Jospin, G., Lowe, E., Matsen, F. A., Bik, H. M., and Eisen, J. A. (2014). PhyloSift, Phylogenetic analysis of genomes and metagenomes. *PeerJ*. 9:e243. doi: 10.7717/peerj.243

Dombrowski, N., Teske, A. P., and Baker, B. J. (2018). Expansive microbial metabolic versatility and biodiversity in dynamic Guaymas Basin hydrothermal sediments. *Nat. communicat.* 9, 1–13.

Dunfield, P., and Knowles, R. (1995). Kinetics of inhibition of methane oxidation by nitrate, nitrite, and ammonium in a humisol. *Appl. Environ. Microbiol.* 61, 3129–3135. doi: 10.1128/AEM.61.8.3129-3135.1995

Edgar, R. C. (2010). Search and clustering orders of magnitude faster than BLAST. *Bioinformatics* 26, 2460–2461. doi: 10.1093/bioinformatics/btq461

Eller, G., Känel, L., Krüger, M., Ka, L., and Kru, M. (2005). Cooccurrence of aerobic and anaerobic methane oxidation in the water column of lake plußsee. *Appl. Environ. Microbiol.* 71, 8925–8928. doi: 10.1128/AEM.71.12.8925-8928.2005

Ettwig, K. F., Butler, M. K., Le Paslier, D., Pelletier, E., Mangenot, S., Kuypers, M. M. M., et al. (2010). Nitrite-driven anaerobic methane oxidation by oxygenic bacteria. *Nature* 464, 543–548. doi: 10.1038/nature08883

Geng, J., Cheng, S., Fang, H., Yu, G., Li, X., Si, G., et al. (2017). Soil nitrate accumulation explains the nonlinear responses of soil CO2 and CH4 fluxes to nitrogen addition in a temperate needle-broadleaved mixed forest. *Ecol. Indic.* 79, 28–36. doi: 10.1016/j.ecolind.2017.03.054

Gilman, A., Fu, Y., Hendershott, M., Chu, F., Puri, A. W., Smith, A. L., et al. (2017). Oxygen-limited metabolism in the methanotroph *Methylomicrobium buryatense* 5GB1C. *PeerJ* 5:e3945. doi: 10.7717/peerj.3945

Grasset, C., Mendonça, R., Villamor Saucedo, G., Bastviken, D., Roland, F., and Sobek, S. (2018). Large but variable methane production in anoxic freshwater sediment upon addition of allochthonous and autochthonous organic matter. *Limnol. Oceanogr.* 63, 1488–1501. doi: 10.1002/lno.10786

Gulledge, J., Ahmad, A., Steudler, P. A., Pomerantz, W. J., and Cavanaugh, C. M. (2001). Family- and genus-level 16S rRNA-targeted oligonucleotide probes for ecological studies of methanotrophic bacteria. *Appl. Environ. Microbiol.* 67, 4726–4733. doi: 10.1128/AEM.67.10.4726-4733.2001

Harrits, S. M., and Hanson, R. S. (1980). Stratification of aerobic methane-oxidizing organisms in Lake Mendota, Madison, Wisconsin. *Limnol. Oceanogr.* 25, 412–421. doi: 10.4319/lo.1980.25.3.0412

Hutsch, B. W. (1998). Methane oxidation in arable soil as inhibited by ammonium, nitrite, and organic manure with respect to soil pH. *Biology and Fertility of Soils*. 28, 27–35. doi: 10.1007/s003740050459

Jones, R. I., and Grey, J. (2011). Biogenic methane in freshwater food webs. *Freshw. Biol.* 56, 213–229. doi: 10.1111/j.1365-2427.2010.02494.x

Kalyuzhnaya, M. G., Beck, D. A. C., Vorobev, A., Smalley, N., Kunkel, D. D., Lidstrom, M. E., et al. (2011). Novel methylotrophic isolates from lake sediment, description of *Methylotenera versatilis* sp. nov. and emended description of the genus methylotenera. *Int. J. Syst. Evol. Microbiol.* 62, 106–111. doi: 10.1099/ijs.0.029165-0

Kalyuzhnaya, M. G., Yang, S., Rozova, O. N., Smalley, N. E., Clubb, J., Lamb, A., et al. (2013). Highly efficient methane biocatalysis revealed in a methanotrophic bacterium. *Nat. Commun.* 4, 1–7. doi: 10.1038/ncomms3785

Kits, K. D., Klotz, M. G., and Stein, L. Y. (2015). Methane oxidation coupled to nitrate reduction under hypoxia by the gammaproteobacterium *Methylomonas denitrificans*, sp. nov. type strain FJG1. *Environ. Microbiol.* 17, 3219–3232. doi: 10.1111/1462-2920.12772

Klüpfel, L., Piepenbrock, A., Kappler, A., and Sander, M. (2014). Humic substances as fully regenerable electron acceptors in recurrently anoxic environments. *Nat. Geosci.* 7, 195–200. doi: 10.1038/ngeo2084

Knittel, K., and Boetius, A. (2009). Anaerobic oxidation of methane, progress with an unknown process. *Annu. Rev. Microbiol.* 63, 311–334. doi: 10.1146/annurev.micro.61.080706.093130

Kojima, H., and Fukui, M. (2011). Sulfuritalea hydrogenivorans gen. nov., sp. nov., a facultative autotroph isolated from a freshwater lake. *Int. J. Syst. Evol. Microbiol.* 61, 1651–1655. doi: 10.1099/ijs.0.024968-0

Krause, S. M. B., Johnson, T., Karunaratne, Y. S., Fu, Y., Beck, D. A. C., Chistoserdova, L., et al. (2017). Lanthanide-dependent cross-feeding of methane-derived carbon is linked by microbial community interactions. *Proc. Natl. Acad. Sci. U. S. A.* 114, 358–363. doi: 10.1073/pnas.1619871114

Lapidus, A., Clum, A., LaButti, K., Kaluzhnaya, M. G., Lim, S., Beck, D. A. C., et al. (2011). Genomes of three methylotrophs from a single niche reveal the genetic and metabolic divergence of the methylophilaceae. *J. Bacteriol.* 193, 3757–3764. doi: 10.1128/JB.00404-11

Lovley, D. R., Coates, J. D., BluntHarris, E. L., Phillips, E. J. P., and Woodward, J. C. (1996). Humic substances as electron acceptors for microbial respiration. *Nature* 382, 445–448. doi: 10.1038/382445a0

Martinez-Cruz, K., Leewis, M. C., Herriott, I. C., Sepulveda-Jauregui, A., Anthony, K. W., Thalasso, F., et al. (2017). Anaerobic oxidation of methane by aerobic methanotrophs in sub-Arctic lake sediments. *Sci. Total Environ.* 607–608, 23–31. doi: 10.1016/j.scitotenv.2017.06.187

Martinez-Cruz, K., Sepulveda-Jauregui, A., Casper, P., Anthony, K. W., Smemo, K. A., and Thalasso, F. (2018). Ubiquitous and significant anaerobic oxidation of methane in freshwater lake sediments. *Water Res.* 144, 332–340. doi: 10.1016/j.watres.2018.07.053

Michaud, A. B., Dore, J. E., Achberger, A. M., Christner, B. C., Mitchell, A. C., Skidmore, M. L., et al. (2017). Microbial oxidation as a methane sink beneath the West Antarctic Ice Sheet. *Nat. Geosci.* 10, 582–586. doi: 10.1038/ngeo2992

Milucka, J., Kirf, M., Lu, L., Krupke, A., Lam, P., Littmann, S., et al. (2015). Methane oxidation coupled to oxygenic photosynthesis in anoxic waters. *ISME J.* 9, 1991–2002. doi: 10.1038/ismej.2015.12

Murase, J., and Frenzel, P. (2007). A methane-driven microbial food web in a wetland rice soil. *Eniron. Microbiol.* 9, 3025–3034. doi: 10.1111/j.1462-2920.2007.01414.x

Mustakhimov, I., Kalyuzhnaya, M. G., Lidstrom, M. E., and Chistoserdova, L. (2013). Insights into denitrification in *Methylotenera mobilis* from denitrification pathway and methanol metabolism mutants. *J. Bacteriol.* 195, 2207–2211. doi: 10.1128/JB.00069-13

Oremland, R. S., and Polcin, S. (1982). Methanogenesis and sulfate reduction, competitive and noncompetitive substrates in estuarine sediments. *Appl. Environ. Microbiol.* 44, 1270–1276. doi: 10.1128/AEM.44.6.1270-1276.1982

Oswald, K., Graf, J. S., Littmann, S., Tienken, D., Brand, A., Wehrli, B., et al. (2017). Crenothrix are major methane consumers in stratified lakes. *ISME J.* 11, 2124–2140. doi: 10.1038/ismej.2017.77

Oswald, K., Milucka, J., Brand, A., Hach, P., Littmann, S., Wehrli, B., et al. (2016). Aerobic gammaproteobacterial methanotrophs mitigate methane emissions from oxic and anoxic lake waters. *Limnol. Oceanogr.* 61, S101–S118. doi: 10.1002/lno.10312

Oswald, K., Milucka, J., Brand, A., Littmann, S., Wehrli, B., Kuypers, M. M. M., et al. (2015). Light-dependent aerobic methane oxidation reduces methane emissions from seasonally stratified lakes. *PLoS ONE* 10:e0132574. doi: 10.1371/journal.pone.0132574

Parks, D. H., Imelfort, M., Skennerton, C. T., Hugenholtz, P., and Tyson, G. W. (2015). CheckM, assessing the quality of microbial genomes recovered from isolates, single cells, and metagenomes. *Genome Res.* 25, 1043–1055. doi: 10.1101/gr.186072.114

Quast, C., Pruesse, E., Yilmaz, P., Gerken, J., Schweer, T., Yarza, P., et al. (2013). The SILVA ribosomal RNA gene database project, improved data processing and web-based tools. *Nucleic Acids Res.* 41, D590–D596. doi: 10.1093/nar/gks1219

Reeburgh, W. S. (2007). Oceanic methane biogeochemistry. *Chem. Rev.* 107, 486–513. doi: 10.1021/cr050362v

Reed, D. C., Deemer, B. R., van Grinsven, S., and Harrison, J. A. (2017). Are elusive anaerobic pathways key methane sinks in eutrophic lakes and reservoirs? *Biogeochemistry* 134, 29–39. doi: 10.1007/s10533-017-0356-3

Rissanen, A. J., Saarenheimo, J., Tiirola, M., Peura, S., Aalto, S. L., Karvinen, A., et al. (2018). Gammaproteobacterial methanotrophs dominate methanotrophy in aerobic and anaerobic layers of boreal lake waters. *Aquat. Microb. Ecol.* 81, 257–276. doi: 10.3354/ame01874

Roco, C. A., Bergaust, L. L., Shapleigh, J. P., and Yavitt, J. B. (2016). Reduction of nitrate to nitrite by microbes under oxic conditions. *Soil Biol. Biochem.* 100, 1–8. doi: 10.1016/j.soilbio.2016.05.008

Rogelj, J., Shindell, D., Jiang, K., Fifita, S., Forster, P., Ginzburg, V., et al. (2018). Mitigation pathways compatible with 1.5°C in the context of sustainable development. *Glob. Warm. 1.5°C. An IPCC Spec. Rep. [...] 2*. Available online at: https://www.ipcc.ch/sr15/chapter/chapter-2/

Roslev, P., and King, G. M. (1995). Aerobic and anaerobic starvation metabolism in methanotrophic bacteria. *Appl. Environ. Microbiol.* 61, 1563–1570. doi: 10.1128/AEM.61.4.1563-1570.1995

Rudd, J. W. M., and Hamilton, R. D. (1975). Factors controlling rates of methane oxidation and the distribution of the methane oxidizers in a small stratified lake. *Arch. Hydrobiol.* 75, 522–538.

Sanseverino, A. M., Bastviken, D., Sundh, I., Pickova, J., and Enrich-Prast, A. (2012). Methane carbon supports aquatic food webs to the fish level. *PLoS ONE* 7:e42723. doi: 10.1371/journal.pone.0042723

Saxton, M. A., Samarkin, V. A., Schutte, C. A., Bowles, M. W., Madigan, M. T., Cadieux, S. B., et al. (2016). Biogeochemical and 16S rRNA gene sequence evidence supports a novel mode of anaerobic methanotrophy in permanently ice-covered Lake Fryxell, Antarctica. *Limnol. Oceanogr.* 61, S119–S130. doi: 10.1002/lno.10320

Scheller, S., Yu, H., Chadwick, G. L., and Mcglynn, S. E. (2016). Artificial electron acceptors decouple archaeal methane oxidation from sulfate reduction. *Science* 351, 1754–1756. doi: 10.1126/science.aad7154

Schubert, C. J., Lucas, F. S., Durisch-Kaiser, E., Stierli, R., Diem, T., Scheidegger, O., et al. (2010). Oxidation and emission of methane in a monomictic lake (Rotsee, Switzerland). *Aquat. Sci.* 72, 455–466. doi: 10.1007/s00027-010-0148-5

Schubert, C. J., Vazquez, F., Loesekann-Behrens, T., Knittel, K., Tonolla, M., and Boetius, A. (2011). Evidence for anaerobic oxidation of methane in sediments of a freshwater system (Lago di Cadagno). *FEMS Microbiol. Ecol.* 76, 26–38. doi: 10.1111/j.1574-6941.2010.01036.x

Seemann, T. (2014). Prokka, rapid prokaryotic genome annotation. *Bioinfrormatics* 30, 2068–2069. doi: 10.1093/bioinformatics/btu153

Segarra, K. E. A., Schubotz, F., Samarkin, V., Yoshinaga, M. Y., Hinrichs, K., and Joye, S. B. (2015). High rates of anaerobic methane oxidation in freshwater wetlands reduce potential atmospheric methane emissions. *Nat. Commun.* 6, 1–8. doi: 10.1038/ncomms8477

Sieber, C. M. K., Probst, A. J., Sharrar, A., Thomas, B. C., Hess, M., Tringe, S. G., et al. (2018). Recovery of genomes from metagenomes via a dereplication, aggregation and scoring strategy. *Nat. Microbiol.* 3, 836–843. doi: 10.1038/s41564-018-0171-1

Smith, G. J., Angle, J. C., Solden, L. M., Daly, R. A., Johnston, M. D., Borton, M. A., et al. (2018). Members of the genus methylobacter are inferred to account for the majority of aerobic methane oxidation in oxic soils from a freshwater Wetland. *MBio* 9, 1–17. doi: 10.1128/mBio.00815-18

Svenning, M. M., Hestnes, A. G., Wartiainen, I., Stein, L. Y., Klotz, M. G., Kalyuzhnaya, M. G., et al. (2011). Genome sequence of the arctic methanotroph methylobacter tundripaludum SV96. *J. Bacteriol.* 193, 6418–6419. doi: 10.1128/JB.05380-11

Tamura, K., Stecher, G., Peterson, D., Filipski, A., and Kumar, S. (2013). MEGA6, molecular evolutionary genetics analysis version 6.0. *Mol. Biol. Evol.* 30, 2725–2729. doi: 10.1093/molbev/mst197

Thottathil, S. D., Reis, P. C. J., and Prairie, Y. T. (2019). Methane oxidation kinetics in northern freshwater lakes. *Biogeochemistry*. 143, 105–116. doi: 10.1007/s10533-019-00552-x

Valenzuela, E. I., Avendaño, K. A., Balagurusamy, N., Arriaga, S., Nieto-Delgado, C., Thalasso, F., et al. (2019). Electron shuttling mediated by humic substances fuels anaerobic methane oxidation and carbon burial in wetland sediments. *Sci. Total Environ.* 650, 2674–2684. doi: 10.1016/j.scitotenv.2018.09.388

Valenzuela, E. I., Prieto-dav,ó, A., López-lozano, N. E., García-gonzález, A. S., López, M. G., and Cervantes, J. (2017). Anaerobic methane oxidation driven by microbial reduction of natural organic matter in a tropical Wetland. *Appl. Environ. Microbiol.* 83, 1–15. doi: 10.1128/AEM.00645-17

Van Bodegom, P., Stams, F., Mollema, L., Boeke, S., and Leffelaar, P. (2001). Methane oxidation and the competition for oxygen in the rice rhizosphere. *Appl. Environ. Microbiol.* 67, 3586–3597. doi: 10.1128/AEM.67.8.3586-3597.2001

van Grinsven, S., Asbun, A. A., Julia, C., Harrison, J., and Villanueva, L. (2019). Methane oxidation in anoxic lake water stimulated by nitrate and sulfate addition. *Environ. Microbiol.* 22, 766–782. doi: 10.1111/1462-2920.14886

Walkiewicz, A., and Brzezinska, M. (2019). Interactive effects of nitrate and oxygen on methane oxidation in three different soils. *Soil Biol. Biochem.* 133, 116–118. doi: 10.1016/j.soilbio.2019.03.001

Walkiewicz, A., Brzezinska, M., and Bieganowski, A. (2018). Methanotrophs are favored under hypoxia in ammonium-fertilized soils. *Biol. Fertil. Soils* 54, 861–870. doi: 10.1007/s00374-018-1302-9

Whittenbury, R., Phillips, K. C., and Wilkinson, J. F. (1970). Enrichment, isolation and some properties of methane-utilizing bacteria. *J. Gen. Microbiol.* 61, 205–218. doi: 10.1099/00221287-61-2-205

Xin, J. Y., Cui, J. R., Niu, J. Z., Hua, S. F., Xia, C. G., Li, S., et al. (2004). Production of methanol from methane by methanotrophic bacteria. *Biocatal. Biotrans.* 22, 225–229. doi: 10.1080/10242420412331283305

Xin, J. Y., Zhang, Y. X., Zhang, S., Xia, C. G., and Li, S., Ben. (2007). Methanol production from CO2 by resting cells of the methanotrophic bacterium *Methylosinus trichosporium* IMV 3011. *J. Basic Microbiol.* 47, 426–435. doi: 10.1002/jobm.200710313

Yu, Z., and Chistoserdova, L. (2017). Communal metabolism of methane and the rare earth element switch. *J. Bacteriol.* 199:e00328. doi: 10.1128/JB.00328-17

Zhang, J., Kobert, K., Flouri, T., and Stamatakis, A. (2014). PEAR, a fast and accurate Illumina Paired-End reAd mergeR. *Bioinformatics* 30, 614–620. doi: 10.1093/bioinformatics/btt593

Conflict of Interest: The authors declare that the research was conducted in the absence of any commercial or financial relationships that could be construed as a potential conflict of interest.

Copyright © 2020 van Grinsven, Sinninghe Damsté, Harrison and Villanueva. This is an open-access article distributed under the terms of the Creative Commons Attribution License (CC BY). The use, distribution or reproduction in other forums is permitted, provided the original author(s) and the copyright owner(s) are credited and that the original publication in this journal is cited, in accordance with accepted academic practice. No use, distribution or reproduction is permitted which does not comply with these terms.

Advantages of publishing in Frontiers

OPEN ACCESS
Articles are free to read for greatest visibility and readership

FAST PUBLICATION
Around 90 days from submission to decision

HIGH QUALITY PEER-REVIEW
Rigorous, collaborative, and constructive peer-review

TRANSPARENT PEER-REVIEW
Editors and reviewers acknowledged by name on published articles

Frontiers
Avenue du Tribunal-Fédéral 34
1005 Lausanne | Switzerland

Visit us: www.frontiersin.org
Contact us: info@frontiersin.org | +41 21 510 17 00

REPRODUCIBILITY OF RESEARCH
Support open data and methods to enhance research reproducibility

DIGITAL PUBLISHING
Articles designed for optimal readership across devices

FOLLOW US
@frontiersin

IMPACT METRICS
Advanced article metrics track visibility across digital media

EXTENSIVE PROMOTION
Marketing and promotion of impactful research

LOOP RESEARCH NETWORK
Our network increases your article's readership